



Ni-Catalyzed Reductive Coupling Reactions to Forge sp^3 Carbon Linkages

Shangzheng Sun

ADVERTIMENT. L'accés als continguts d'aquesta tesi doctoral i la seva utilització ha de respectar els drets de la persona autora. Pot ser utilitzada per a consulta o estudi personal, així com en activitats o materials d'investigació i docència en els termes establerts a l'art. 32 del Text Refós de la Llei de Propietat Intel·lectual (RDL 1/1996). Per altres utilitzacions es requereix l'autorització prèvia i expressa de la persona autora. En qualsevol cas, en la utilització dels seus continguts caldrà indicar de forma clara el nom i cognoms de la persona autora i el títol de la tesi doctoral. No s'autoritza la seva reproducció o altres formes d'explotació efectuades amb finalitats de lucre ni la seva comunicació pública des d'un lloc aliè al servei TDX. Tampoc s'autoritza la presentació del seu contingut en una finestra o marc aliè a TDX (framing). Aquesta reserva de drets afecta tant als continguts de la tesi com als seus resums i índexs.

ADVERTENCIA. El acceso a los contenidos de esta tesis doctoral y su utilización debe respetar los derechos de la persona autora. Puede ser utilizada para consulta o estudio personal, así como en actividades o materiales de investigación y docencia en los términos establecidos en el art. 32 del Texto Refundido de la Ley de Propiedad Intelectual (RDL 1/1996). Para otros usos se requiere la autorización previa y expresa de la persona autora. En cualquier caso, en la utilización de sus contenidos se deberá indicar de forma clara el nombre y apellidos de la persona autora y el título de la tesis doctoral. No se autoriza su reproducción u otras formas de explotación efectuadas con fines lucrativos ni su comunicación pública desde un sitio ajeno al servicio TDR. Tampoco se autoriza la presentación de su contenido en una ventana o marco ajeno a TDR (framing). Esta reserva de derechos afecta tanto al contenido de la tesis como a sus resúmenes e índices.

WARNING. Access to the contents of this doctoral thesis and its use must respect the rights of the author. It can be used for reference or private study, as well as research and learning activities or materials in the terms established by the 32nd article of the Spanish Consolidated Copyright Act (RDL 1/1996). Express and previous authorization of the author is required for any other uses. In any case, when using its content, full name of the author and title of the thesis must be clearly indicated. Reproduction or other forms of for profit use or public communication from outside TDX service is not allowed. Presentation of its content in a window or frame external to TDX (framing) is not authorized either. These rights affect both the content of the thesis and its abstracts and indexes.



UNIVERSITAT
ROVIRA i VIRGILI

Ni-Catalyzed Reductive Coupling Reactions to Forge sp^3 Carbon Linkages

Shangzheng Sun



DOCTORAL THESIS
2020

Ni-Catalyzed Reductive Coupling Reactions to Forge sp^3 Carbon Linkages

Shangzheng Sun

Doctoral Thesis

Supervised by Prof. Ruben Martin Romo

Institute of Chemical Research of Catalonia (ICIQ)

Universitat Rovira i Virgili (URV)

Department of Analytical Chemistry & Organic Chemistry



UNIVERSITAT
ROVIRA i VIRGILI



Tarragona, 2020



UNIVERSITAT
ROVIRA i VIRGILI



FAIG CONSTAR que aquest treball, titulat “Ni-catalyzed reductive coupling reactions to forge sp^3 carbon linkages”, que presenta Shangzheng Sun per a l’obtenció del títol de Doctor, ha estat realitzat sota la meua direcció al Departament Institut Català d’Investigació Química. d’aquesta universitat.

HAGO CONSTAR que el presente trabajo, titulado “Ni-catalyzed reductive coupling reactions to forge sp^3 carbon linkages”, que presenta Shangzheng Sun para la obtención del título de Doctor, ha sido realizado bajo mi dirección en el Departamento Instituto Catalán de Investigación Química de esta universidad.

I STATE that the present study, entitled “Ni-catalyzed reductive coupling reactions to forge sp^3 carbon linkages”, presented by Shangzheng Sun for the award of the degree of Doctor, has been carried out under my supervision at the Department Institute of Chemical Research of Catalonia of this university.

TCAT P
Ruben Martin
Romo - DNI
38129823D

Firmado digitalmente
por TCAT P Ruben
Martin Romo - DNI
38129823D
Fecha: 2020.10.30
18:06:28 +01'00'

Tarragona, October 20th 2020

El/s director/s de la tesi doctoral
El/los director/es de la tesis doctoral
Doctoral Thesis Supervisor/s

List of Publications

1. **Shang-Zheng Sun**, Yaya Duan, Riccardo S. Mega, Rosie J. Somerville, Ruben Martin. Site-Selective 1,2-Dicarbofunctionalization of Vinyl Boronates via Dual Catalysis. *Angew. Chem. Int. Ed.* **2020**, *59*, 4370-4374.
 2. Daniel Janssen-Müller, Basudev Sahoo, **Shang-Zheng Sun**, Ruben Martin. Tackling Remote sp^3 C-H Functionalization via Ni-Catalyzed Chain-Walking Reactions. *Isr. J. Chem.* **2020**, *60*, 195-206.
 3. **Shang-Zheng Sun**, Ciro Romano, Ruben Martin. Site-Selective Catalytic Deaminative Alkylation of Unactivated Olefins. *J. Am. Chem. Soc.* **2019**, *141*, 16197-16201.
 4. **Shang-Zheng Sun**, Marino Borjesson, Raul Martin-Montero, Ruben Martin. Site-Selective Ni-Catalyzed Reductive Coupling of Alpha-Haloboranes with Unactivated Olefins. *J. Am. Chem. Soc.* **2018**, *140*, 12765-12769.
 5. **Shang-Zheng Sun**, Ruben Martin. Nickel-Catalyzed Umpolung Arylation of Ambiphilic-Bromoalkyl Boronic Esters. *Angew. Chem. Int. Ed.* **2018**, *57*, 3622-3625.
 6. Manuel van Gemmeren, Marino Borjesson, Andreu Tortajada, **Shang-Zheng Sun**, Keisho Okura, Ruben Martin. Switchable Site-Selective Catalytic Carboxylation of Allylic Alcohols with CO₂. *Angew. Chem. Int. Ed.* **2017**, *56*, 6558-6562.
-

Table Contents

Acknowledgements	5
Preface	9
Abbreviations & Acronyms	11
Abstract	13
Chapter 1. General Introduction	17
1.1 General Introduction.....	19
1.2 General Characteristics of Nickel Catalysts.....	22
1.3 Nickel Catalyzed Cross-Electrophile Coupling.....	23
1.3.1 Nickel Catalyzed Reductive Coupling of Organic Halides.....	23
1.3.2 Nickel-Catalyzed Decarboxylative Reductive Cross-Couplings.....	40
1.3.3 Nickel-Catalyzed Reductive Coupling of Unactivated sp^3 C–O Electrophiles.....	43
1.3.4 The Merger of Ni and Photoredox Dual Catalysis for Reductive Coupling Reactions.....	44
1.4 General Aim of This Thesis.....	48
1.5 References:.....	49
Chapter 2. Site-Selective Ni-Catalyzed Reductive Coupling of α-Haloboranes with Unactivated Olefins	63
2.1 General Introduction.....	65
2.2 Ni-Catalyzed Reductive Coupling of Olefins.....	66
2.2.1 Ni-Catalyzed anti-Markovnikov Hydrofunctionalization of Olefins.....	66
2.2.2 Ni-Catalyzed Markovnikov-Selective Hydrofunctionalization of Olefins.....	69
2.3 Remote sp^3 C–H Functionalization via Ni-Catalyzed Chain-Walking.....	72
2.3.1 Ni-Catalyzed Remote Arylation and Alkenylation of Olefins or Alkyl Halides.....	74
2.3.2 C_{sp^3} – C_{sp^3} Bonds Formation via Ni-Catalyzed Remote sp^3 C–H Alkylation of Olefins.....	79
2.3.3 Ni-Catalyzed Remote sp^3 C–H Acylation of Olefins or Alkyl Halides.....	82
2.3.4 Ni-Catalyzed Remote sp^3 C–H Carboxylation of Alkyl Halides and Alkenes.....	83
2.3.5 Ni-Catalyzed Remote C-Heteroatom Bonds Formation.....	85
2.4 General Aim of the Project.....	88
2.5 Ni-Catalyzed Reductive Alkylation of α -Haloboranes with Unactivated Olefins.....	89

2.5.1 Ni-Catalyzed Reductive Alkylation of α -Haloboranes with α -Olefins	89
2.5.2 Ni-Catalyzed Reductive Alkylation of α -Haloboranes with Internal Olefins	99
2.5.3 Iterative Platform for C–C Bond-Formations	105
2.5.4 Mechanism Experiments	106
2.5.5 Preliminary Enantioconvergent Coupling Reaction	109
2.6 Conclusions	110
2.7 References	111
2.8 Experimental Section	122
2.8.1 General Considerations	122
2.8.2 Optimization of the Reaction Conditions	123
2.8.3 Determination of the Major and Minor Regioisomers Employing Internal Olefins	123
2.8.4 Synthesis of Ligands and Starting Materials	129
2.8.5 Ni-Catalyzed Reductive Coupling with Terminal Olefins	137
2.8.6 Ni-Catalyzed Reductive Coupling with Internal Olefins	148
2.8.7 Gram Scale Reaction and Iterative C–C Bond Formations	157
2.8.8 Mechanistic Experiments	161
2.8.9 Preliminary Enantioconvergent Coupling Reaction	173
2.8.10 Bibliography of Known Compounds	180
2.8.11 NMR Spectra	181
Chapter 3. Site-Selective Ni-Catalyzed Deaminative Alkylation of Unactivated Olefins	275
3.1 General Introduction	277
3.2 Pyridinium Salts as Electrophiles in Cross-Coupling Reactions	278
3.2.1 Catalytic Deaminative Alkylation of (Hetero)Arenes with Pyridinium Salts	280
3.2.2 Catalytic Deaminative Alkylation Strategies for the Synthesis of Alkenes and Alkynes	284
3.2.3 Catalytic Deaminative Alkylation Strategies for the Formation of New C_{sp^3} – C_{sp^3} Bonds	287
3.2.4 Catalytic Deaminative Borylation of Alkyl Pyridinium Salts	290
3.2.5 Catalytic Deaminative Cross-Coupling of <i>N</i> -Aryl Pyridinium Salts	292
3.3 General Aim of the Project	293
3.4 Site-Selective Ni-Catalyzed Deaminative Alkylation of Unactivated Olefins	294
3.4.1 Catalytic Deaminative Alkylation of α -Olefins	294
3.4.2 Catalytic Deaminative Alkylation with Internal Olefins	302
3.4.3 Late-stage Functionalization	307
3.4.4 Unsuccessful Substrates	309
3.4.5 Synthetic Applications	310
3.4.6 Mechanistic Investigation	311

3.5 Conclusions	315
3.6 References	316
3.7 Experimental Section.....	326
3.7.1 General Considerations	326
3.7.2 Optimization of the Reaction Conditions.....	327
3.7.3 Synthesis of Ligands and Starting Materials	327
3.7.4 Ni-Catalyzed Deaminative Alkylation with Terminal Olefins.....	335
3.7.5 Ni-Catalyzed Deaminative Alkylation with Internal Olefins.....	345
3.7.6 Deaminative Alkylation in Late-Stage Functionalization.....	351
3.7.7 Large Scale Reaction and Synthetic Applications.....	360
3.7.8 Mechanistic Experiments	363
3.7.9 Bibliography	369
3.7.10 NMR Spectra	370
Chapter 4. Site-Selective 1,2-Dicarbonylfunctionalization of Vinyl Boronates through Dual Catalysis.....	443
4.1 General Introduction.....	445
4.2 Catalytic Dicarbonylfunctionalization of Vinyl Borons	446
4.2.1 Catalytic Difunctionalization of Vinyl Boron-ate Complex	446
4.2.2 Pd-Catalyzed Conjunctive Coupling of Vinyl Boron-ate Complex	447
4.2.3 Ni-Catalyzed Conjunctive Coupling of Vinyl Boron-ate Complex.....	450
4.2.4 Radical Induced Conjunctive Coupling of Vinyl Boron-ate Complex.....	453
4.2.5 Catalytic 1,2-Dicarbonylfunctionalization of Vinyl Boronates.....	455
4.3 Ni-Catalyzed Intermolecular Reductive Difunctionalization of Olefins	460
4.4 General Aim of the Project	465
4.5 Site-Selective 1,2-Dicarbonylfunctionalization of Vinyl Boronates through Dual Catalysis.....	466
4.5.1 Optimization of Reaction Conditions	466
4.5.2 Preparative Substrate Scope	473
4.5.3 Synthetic Applicability.....	477
4.5.4 Mechanistic Experiments	479
4.6 Conclusion.....	485
4.7 References	486
4.8 Experimental Section.....	494
4.8.1 General Considerations	494
4.8.2 General Procedure for Optimization of the Reaction Conditions.....	495
4.8.3 Synthesis of Starting Materials.....	496
4.8.4 Site-Selective 1,2-Dicarbonylfunctionalization of Vinyl Boronates	497
4.8.5 Gram Scale Reaction.....	515
4.8.6 Synthetic Applicability.....	516
4.8.7 Mechanistic Experiments	519

4.8.8 X-Ray Crystallography Data	528
4.8.9 Bibliography of Known Compounds	549
4.8.10 NMR Spectra	550
Chapter 5. Conclusion	609

Acknowledgements

The four years I spent at the Institute of Chemical Research of Catalonia (ICIQ) have been a very special time in my life. I feel very fortunate to have developed as a scientist in ICIQ, which offering high-quality educational programs to students.

First of all, I would like to express my deepest gratitude to my PhD advisor, **Prof. Ruben Martin**, for giving me opportunity to join his research group. I still remember that the first day when I joined ICIQ, I almost impossible to speak a complete sentence in English. Over the past four years, your persistent support and guidance have helped me grown up rapidly. Your passion, profound insight and abundant knowledge reserve have taught me how to be a scientist. I always feeling lucky and proud to have you as my supervisor. **Ruben!** I am not exaggerating, without your strong support, patience help and encouragement, I could not do my PhD such successful.

Secondly, I would also like to thank the members of the jury, **Prof. Ilan Marek**, **Prof. Marcos Garcia Suero** and **Prof. Josep Cornella** for accepting to be part of my examination committee.

Ingrid, thank for all help and support with all the administrative staff during my PhD. **Miriam**, **Sope** and **David**, thanks for all your tireless work to make the group running smoothly and efficiently. I would also like to thank **ICIQ Research Support Units**, without their help, my research would not be possible.

I would also like to acknowledge all the incredible project partner that I had worked with during last four years. **Dr. Marino Borjesson**, thank you for offering me to join the allyl alcohol project and teaching me to use all the lab equipment at the very beginning of my PhD, for helping me to carry out the α -haloboronates project. "Marchino", my best friend, thank you for always bringing me out to drink beers and for our nicely trip to Japan. **Andreu**, you are very friendly. Thank you for helping me improve my English at the first year of my PhD, for teaching me how to set up

reactions with CO₂, for bringing me to your birthday party, for driving me home so many times. **Rual**, my “Spanish teacher”, even though only taught me one word, the bad word I know in Spanish. You are also an awesome partner, thank you for your efforts to improve the enantioselectivity on α -haloboronates project. Another awesome partner is **Dr. Ciro Romano**, a very clever postdoctoral. I was enjoying to discussing chain-walking chemistry with you. I also feel lucky to have worked with **Dr. Yaya Duan**. You are one of the nicest persons I have ever met and you always show your willingness to help others. Good luck for your future! **Riccardo**, now Dr. Riccardo! It was a pleasure to work with you on conjunctive coupling project. Thank you for teaching me boron chemistry and photochemistry. A special thanks to **Rosie**, for your always encouraging words, for helping me corrected the drafts, for helping me grow crystals. **Laura**, I really appreciate you join my 1,1-difunctionalization project. Your focus and calm attitude made the project moving forward very much. I wish all the best for your PhD study. **Philipp**, you are the best master students I have ever met. Good luck with your PhD study in Vienna.

I would like to thank all the **current and past members of the Martin group**. I really enjoyed working together with you all. I am so grateful for everything I have learned from you guys.

Basu, thank you for being such a great friend, for teaching me basic chemistry, for going home together every night. I wish you all the best in your academia career. **Reddy**, my former desk mate, a hardworking postdoctoral. Thank you for leaving me many pyridinium salts before you left. **Paco**, an incredible postdoctoral I have ever met. Learned a lot from you. **Toni** and **Morgane**, thank you for being very nice lab mates. **Alica**, it was great to have you in our lab. I will never forget the games you made during our group retreat. Thank you for your kind help. **Eloisa**, thank you for all your kind help. **Georgios**, it was a great pleasure to have you as my desk mate. You brought happiness and laughter to the whole group. I hope the LED light is still working. **Bradley**, you are a very talent PhD in our lab. Thank you for always sharing your crazy chemistry ideas to me. **Daniel**, I really missed the BBQs at your house and the time when we went fishing with Marino. Good luck in your future! **Jessica**, **Victoria** and **Tiago**, you guys are so nice. Thank you for being lab mates. **Jacob** and **Chris**, I feel so lucky to have met you guys and really want to learn more

electrochemistry from you. **Craig**, thank you for being my friend, for sharing your organometallic knowledge to me. I will never forget all the times we had lunch in the Chinese restaurant. **Carlota**, you're so sweet and caring. I wish you all the best. **Dmitry**, it was a pleasure to have met you. Good luck with your PhD studies.

A very special thanks to the "Chinese Mafia" from Martin group! **Yangyang**, a sincere gratitude for you. I will never forget the first lunch you made for me when I just arrived Tarragona. Thank you sharing your experience and chemistry knowledge to me, for numerous discussions on chemistry, for helping me made α -haloboronates. I always feel lucky to being friend with you and **Yiting**. I hope you and **Yiting** enjoy life in New York. Looking forward to meet you there. **Hongfei**, it was awesome to have met you and to share apartment with you. I wish you have a great future! **Liang**, it was a great pleasure to have you in lab. I really enjoy chatting with you. Thank you for sharing your experience to me. **Juzeng**, it was a pleasure to meet you and work with you. **Fei**, you are so clever and hardworking. Thank you for taking over the project. **Xinyang** and **Wenjun**, now the most hardworking PhD students in our lab. I feel lucky to being friend with you guys. I am sure you will do great job during your PhD.

I also would like to express my deep appreciation to many friends in ICIQ for sharing their experience, for giving me support and encouragement all the time.

Of course, none of this would be possible without the love and support of my wonderful family. I love you all very much! to my parents, thank you for all that you have putt into my growth and education over the years. To my wife, **Wenjuan**, without your love, understanding and encouragements, I would not make this thesis possible. Although we have spent most of this time far from each other you have patiently and lovingly supported me. You never complain that I spent most time in the lab. I am so truly grateful to have you in my life. I love you!

Preface

The entirety of the work presented in this dissertation has been carried out at the Institute of Chemical Research of Catalonia (ICIQ) during the period of October 2016 to October 2020 under the supervision of Prof. Ruben Martin. The thesis contains five chapters: a general introduction, three research chapters, and the last chapter with a general conclusion of all the research work. Each of the research chapter includes a brief introduction and the aim of the respective topic, followed by a discussion of the experimental results, mechanistic analysis, conclusions, and experimental sections. The relevant references and their numbering are independently organized by chapters.

The first chapter deals with a general introduction of the background of the Ni-catalyzed cross-coupling reactions. A particularly focus is on the Ni-Catalyzed cross-electrophiles coupling reactions.

The second chapter, “*Site-Selective Ni-Catalyzed Reductive Coupling of α -Haloboranes with Unactivated Olefins*”, describes the site-selective alkylation of α -haloboranes with unactivated olefins, which allows for high chemo- and site-selective incorporating the alkylborane fragment into olefin feedstocks. Particularly, the use of internal olefins enables sp^3 C–C bond formation at remote sp^3 C–H site via a nickel catalyzed chain-walking event. The results of this chapter have been published in *J. Am. Chem. Soc.* **2018**, *140*, 12765–12769, in collaboration with Dr. Marino Borjesson and Rual Martin.

The third chapter, “*Site-Selective Catalytic Deaminative Alkylation of Unactivated Olefins*”, describes the deaminative alkylation of alkylamines with unactivated olefins. Our novel catalytic platform allows for forming the sp^3 – sp^3 linkages from both olefin functionalization and sp^3 C–N cleavage events. The synthetic utility could be explained by the context of the late-stage functionalization of drug-like molecules. The results of this chapter have been published in *J. Am. Chem. Soc.* **2019**, *141*, 16197-16201, in collaboration with Dr. Ciro Romano.

The fourth chapter, “*Site-Selective 1,2-Dicarbofunctionalization of Vinyl Boronates through Dual Catalysis*”, presents a modular, chemo- and region-selective

1,2-difunctionalization of vinyl boronates with readily available organic halides via nickel and photoredox dual catalysis. The results of this chapter have been published in *Angew. Chem. Int. Ed.* **2020**, *59*, 4370-4374, in collaboration with Dr. Yaya Duan, Dr. Riccardo Salvatore Mega and Dr. Rosie Somerville.

Abbreviations & Acronyms

4CzIPN = 2,4,5,6-Tetra(9H-carbazol-9-yl)isophthalonitrile
9-BBN = 9-Boracyclo[3.3.1]nonane
acac = Acetylacetonate
BDE = Bond dissociation energy
Boc = *tert*-Butyloxycarbonyl
Bpin = 4,4,5,5-Tetramethyl-1,3,2-dioxaboronic ester
bpy = 2,2'-Bipyridine
Cat. = Catalyst
COD = 1,5-Cyclooctadiene
dtbppy = 4,4'-Di-*tert*-butyl-2,2'-dipyridyl
DEMS = Diethoxymethylsilane
DMMS = Dimethoxymethylsilane
DFT = Density Functional Theory
DG = Directing group
DMAP = 4-Dimethylaminopyridine
DME = Ethylene glycol dimethyl ether
DMF = *N,N*-Dimethylformamide
DMPU = *N,N'*-Dimethylpropyleneurea
DMSO = Dimethyl sulfoxide
DABSO = 1,4-Diazabicyclo[2.2.2]octane bis(sulfur dioxide)
equiv = Equivalent
EDA = Electron-Donor-Acceptor
Int = Intermediate
LED = Light-emitting diode
MIDA: *N*-methyliminodiacetic acid
NHC = *N*-heterocyclic carbene
NHPI = *N*-(acyloxy)phthalimides
NMP = *N*-Methyl-2-pyrrolidone
PC = Photocatalyst
PMHS = Poly(methylhydrosiloxane)
rt (RT) = Room temperature
SCE = Saturated calomel electrode

SET = Single electron transfer

Ts = Tosyl

TBS = *tert*-butyldimethylsilyl

TDAE = Tetrakis(dimethylamino)ethylene

TEMPO = 2,2,6,6-Tetramethyl-1-piperidinyloxy

THF = Tetrahydrofuran

TMEDA = Tetrametiletildiamina

m = meta

o = ortho

p = para

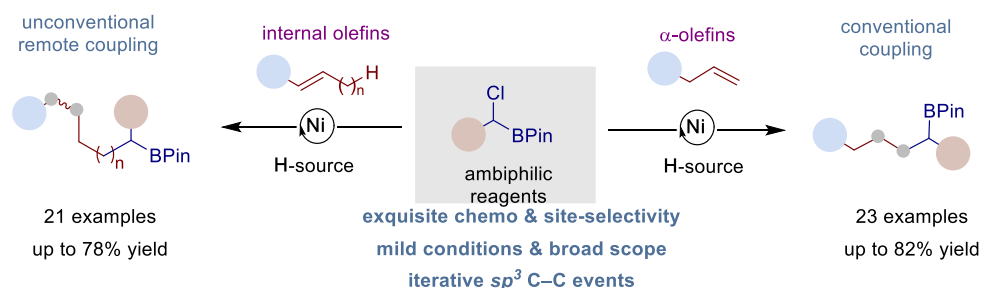
t = tert

Abstract

Metal-catalyzed C–C bond forming reactions have streamlined synthetic routes when assembling complex molecules. These methods are particularly important when incorporating unreactive saturated hydrocarbons, which are common motifs in petrochemicals and biologically relevant molecules. Recently, nickel-catalyzed reductive cross-coupling reactions have become a powerful alternative to traditional cross-coupling reactions for the formation of C–C bonds. Apart from the operational simplicity of these procedures, the wide commercial availability of electrophiles as compare to organometallic reagents, and the highly chemo-selectivity derived from the *in-situ* formation of transient organometallic species, make cross-electrophile coupling high attractive to synthetic chemists.

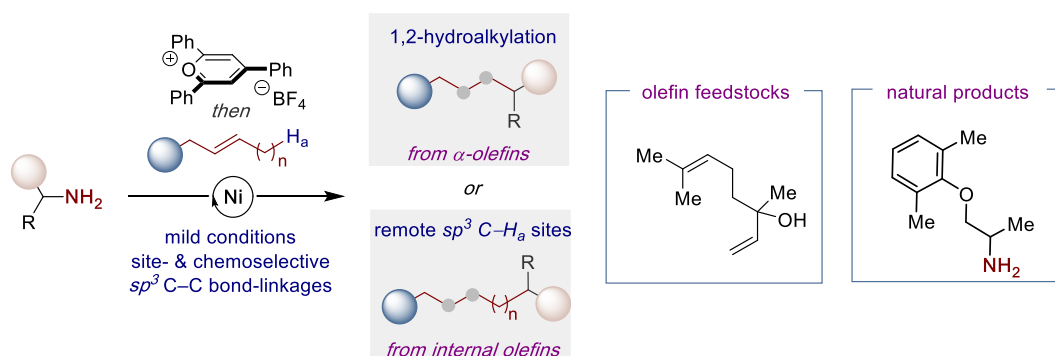
In line with our group interests in Ni-catalyzed cross-coupling reactions, we have decided to focus my doctoral studies on the development of sp^3 C–C bond forming reactions by means of nickel-catalyzed reductive cross-coupling.

Our first efforts were focused on the development of reductive alkylation of α -haloboronates with unactivated olefin feedstocks. Towards this goal, we developed a mild, chemo- and site-selective catalytic protocol that allows for incorporating an alkylboron fragment into unactivated olefins. The use of internal olefins enables C–C bond-formation at remote sp^3 C–H sites via nickel-catalyzed chain-walking process. Of particular importance was the ability to establish a platform to build up multiple sp^3 – sp^3 bonds in an iterative fashion from simple building blocks. Preliminary mechanistic studies rule out the boron stabilized radical addition to olefin, and instead suggest that a hydrometallation via Ni–H species precedes C–C bond formation with the corresponding α -chloroboronates.



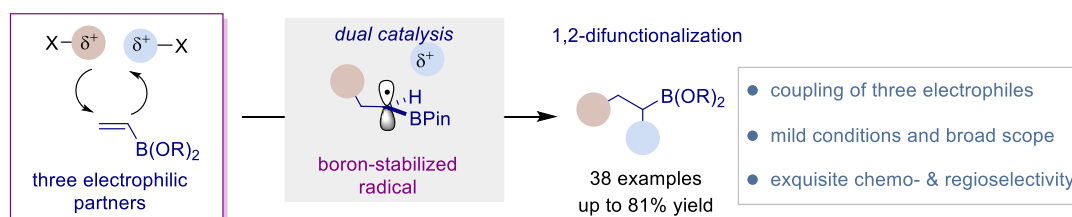
Scheme 1. Ni-Catalyzed site-selective reductive coupling of α -haloboronates with unactivated olefins

Following this development of nickel-catalyzed chain-walking process, we reported a site-selective catalytic deaminative alkylation of unactivated olefins that operates under mild conditions and is characterized by its wide substrate scope and exquisite site-selectivity profile. Particularly noteworthy is that this technique could also be employed in the context of ethylene derivatization and late-stage functionalization. This new platform offers new opportunities in both olefin functionalization and sp^3 C–N bond cleavage events and a complementary activation mode to existing sp^3 – sp^3 bond-forming events.



Scheme 2. Site-selective Ni-catalyzed deaminative alkylation of unactivated olefins

Our final efforts on sp^3 C–C bond formation were focused on the development of a regio-selective three electrophile cross-coupling by means of nickel/photoredox dual catalysis. In this work, we were able to develop a modular, chemo- and regio-selective 1,2-difunctionalization of simple vinyl boronates with readily available organic halides through a dual catalytic platform. Preliminary mechanistic studies and control experiments suggest that a tertiary alkyl radical undergoes addition to the vinyl boronates, forming a boron stabilized radical, then combines with oxidative addition species (ArNi(II)X). In a formal sense, our method serves as a testament to the viability of conducting a reductive cross-couplings of three different electrophilic partners in a synergistic manner.



Scheme 3. Site-selective 1,2-dicarbofunctionalization of vinyl boronates via dual catalysis

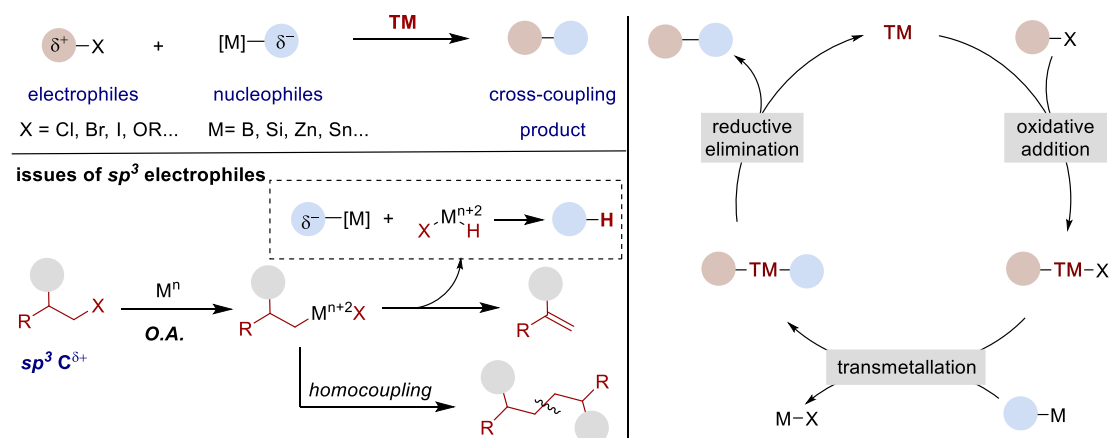
In conclusion, we have developed new methods for the construction of new sp^3 C–C bonds via nickel catalysis or nickel/photoredox dual catalysis under exceptionally mild conditions and with excellent chemo- and regio-selectivity profiles. These works were also supported by preliminary mechanistic investigations to understand how and why these reactions proceeded.

Chapter 1

General Introduction

1.1 General Introduction

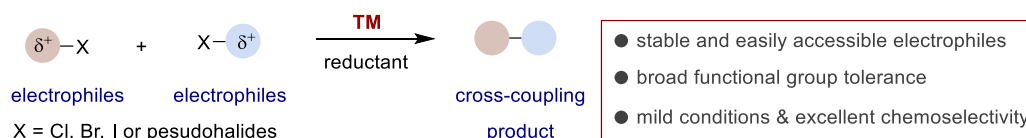
Over the past 50 years, metal-catalyzed cross-coupling reactions of organic electrophile with a nucleophilic (organometallic) reagent have revolutionized the way chemists build C–C and C–heteroatom bonds, thus allowing rapid assembly of molecular complexity in organic synthesis (Scheme 1.1, *top left*).¹ The high efficiency, mild conditions and broad functional group tolerance associated with these reactions have contributed to their widespread use in synthetic organic chemistry, both in academia and industry. The importance of the field was recognized by the 2010 Nobel Prize in Chemistry, which was awarded to Professors Richard F. Heck, Ei-ichi Negishi and Akira Suzuki, for their pioneering contribution in Pd-catalyzed cross-coupling reactions for the formation of C–C bonds.²



Scheme 1.1 Metal-catalyzed cross-coupling reactions

In general, the process of metal-catalyzed cross-coupling reactions started from oxidative addition of an electrophile to the low valent transition metal center, followed by transmetalation with the nucleophilic (organometallic) reagent, and, reductive elimination to form the new cross-coupling product (Scheme 1.1, *right*).¹ Despite advances realized, the coupling of sp^3 carbon fragments remains challenging.³ This is owing to the slow oxidative addition and transmetalation with alkyl electrophiles, where product formation competes with the formation of side-product through other competent pathways, such as homocoupling, β -hydride elimination or hydrogenation (Scheme 1.1, *bottom left*).^{1,3} Additionally, the organometallic reagents need to be prepared from corresponding organic(pseudo)halides by metalation reactions, with most of these organometallic compounds are air and moisture sensitive.

Therefore, the ideal approach would be the direct use of two electrophiles as coupling partners to form the same kind of C–C bonds. To this end, Ni-catalyzed reductive cross-electrophile couplings (reductive couplings) have recently emerged as powerful synthetic methods for the mild and selective construction of C–C bonds,⁴ in which two electrophilic partners can be combined in the presence of a stoichiometric reducing agent (Scheme 1.2). Compared to traditional metal catalyzed cross-coupling reactions, cross-electrophile-coupling shown significant advantages.⁴ Among the advantages of these methodologies are their experimental simplicity, the use of stable and easily accessible organic (pseudo)halides as opposed to reactive and possibly synthetically complex organometallic reagents, and the enhanced chemoselectivity that results from the mild conditions given by the formation of transient organometallic intermediates.



Scheme 1.2 Metal-catalyzed cross-electrophile-coupling (reductive-coupling) reactions

The earliest contribution on reductive coupling of two electrophiles can be dated back to 100 years ago when Wurtz⁵ found the sodium-mediated dimerization of alkyl halides and independently, Ullmann⁶ discovered the Cu-mediated homocoupling of aryl halides. However, these dimerization reactions are characterized by low dimerization efficiency and harsh reducing conditions, which limited their utilization in organic synthesis. The first Ni-catalyzed reductive coupling was reported as the Nozaki-Hiyama-Kishi reaction,^{7,8} which occurred by the addition of allyl- or vinyl halides to aldehyde via a Ni/Cr-catalytic system by using stoichiometric Mn(0) as reductant.⁹ Subsequently, the reductive coupling reactions were also developed by electrochemical processes.^{10,11,12,13} Metal catalyzed or mediated reductive coupling of electrophiles are among the earliest reactions, however, the development of this protocol is far behind classical cross-coupling reactions between electrophiles and nucleophiles.⁴

The major reason for this slow development is the difficulty in achieving high level of selectivity in cross-electrophile coupling reactions. Since the coupling partners used in cross-electrophile coupling reactions have similar reactivity and

typically compete as electrophiles during oxidative addition, this often lead to undesired homocoupling products instead of the formation of the targeted cross-coupled product.¹⁴ In recent years, the issues have been addressed with several strategies, such as **(I)** the addition of an excess of one reagent, **(II)** the electronic differentiation of the starting materials, **(III)** catalyst-substrate steric matching, **(IV)** the development of reactions that couple substrates for which oxidative addition occurs via two different mechanisms, such as through two-electron polar or radical pathways.¹⁵ Since these innovations, metal-catalyzed cross-electrophile coupling reactions have grown exponentially.⁴

Redox Couple	<i>E</i> vs SCE (V)
[Ni(bpy) ₃] ²⁺ /[Ni(bpy) ₃] ⁺	-1.24
Mg ²⁺ /Mg ⁰	-2.62
Mn ²⁺ /Mn ⁰	-1.44
Zn ²⁺ /Zn ⁰	-0.76
TDAE	-0.62

Scheme 1.3 Redox potentials of reductant couples

In the last decade, the intensive study of cross-electrophile coupling reactions have achieved significant breakthroughs in the selective formation of C–C bonds. Recent catalytic systems have been based on Co¹⁶ and Pd¹⁷ but most reports have been demonstrated with Ni catalysts. In these protocols, the reductant provides the necessary electrons to balance the redox equation of the reaction. Specifically, it reduces the transient catalytic metal-species within the catalytic cycle and affords reaction turnover. Moreover, it can also react directly with the substrate to *in-situ* and slowly generate the corresponding organometallic nucleophile via metal-insertion reactions. Common reducing agents employed in these transformations are zero-valent metals, such as Mn, Zn and Mg.⁴ In addition, organic reductants such as tetrakis(dimethylamino)ethylene (TDAE) can provide strong reducing power but are more expensive. The redox potentials of the commonly used reductant are listed in **Scheme 1.3**, which might provide a guidance in estimating the feasibility of reductive coupling reactions in many cases.¹⁸

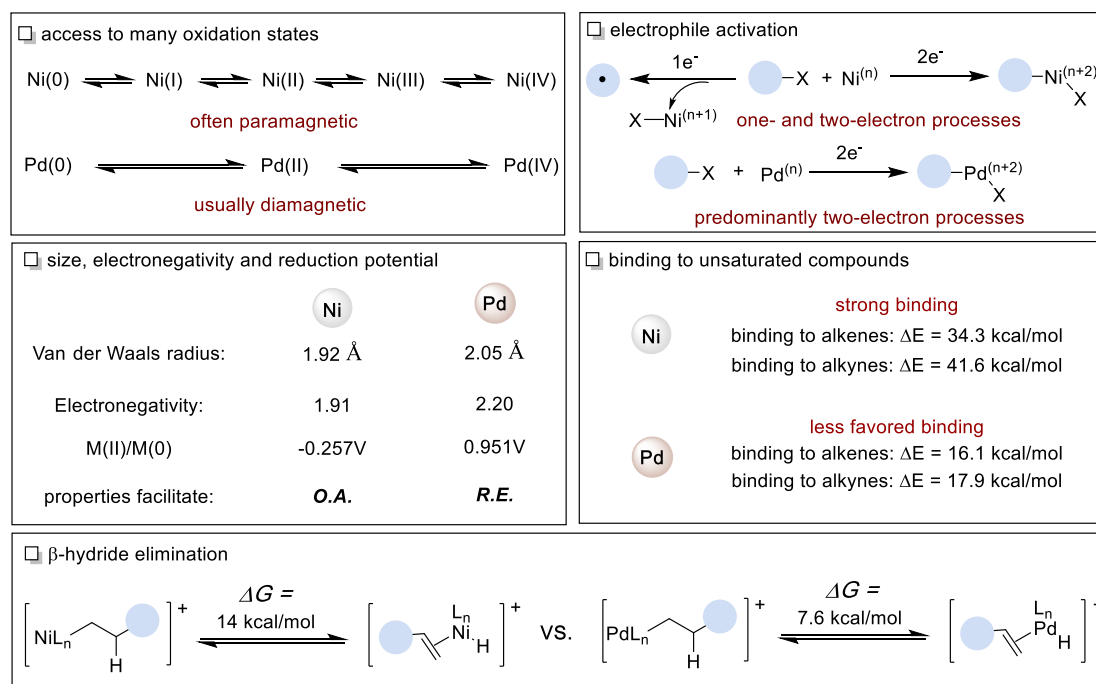
1.2 General Characteristics of Nickel Catalysts

Nickel belongs to the group 10 metals of the periodic table, and it is an inexpensive and earth-abundant alternative to precious metal catalysts, such as Pd, for cross-coupling reactions.¹⁹ Despite palladium catalysts being heavily investigated in cross-coupling reactions, the utilization of nickel predates Pd system,²⁰ with Sabatier awarded the 1912 Nobel Prize for the nickel-mediated hydrogenation of ethylene. Further progress in the field however has been overshadowed by the rapid developments of Pd catalysis. The slow development of nickel catalysis is perhaps due to the difficulties associated with controlling reactive organonickel species that contributed to the false impression of nickel catalysis not being suitable for synthetic applications. However, over the past decade, chemists have truly begun to understand the subtle differences and advantages that nickel can offer as a catalyst compared to palladium, thus leading to the explosive growth of Ni-catalyzed transformations.²¹

The differences between the general characteristics of nickel and palladium catalysts are highlighted in **Scheme 1.4**.^{19,21} First, nickel has a series of readily available oxidation states ranging from Ni(0) to Ni(IV),^{22,23,24,25} whereas Pd most commonly adopts Pd(0), Pd(II) and Pd(IV) oxidation states. Moreover, the open-shell Ni(I) and Ni(III) are more stable than Pd,²⁶ which is likely a result of higher pairing energy of Ni due to a more condensed electron cloud.²⁷ Therefore, Ni-catalyzed cross-coupling reactions are more likely to undergo Ni(I)/Ni(III) cycle or *single-electron-transfer* (SET) pathways when compared to Pd.²⁸ In addition, nickel has a lower reduction potential,²⁹ smaller atomic radius³⁰ and lower electronegativity³¹ than those of Pd. These properties allow for more facile oxidative addition with electron-rich Ni(0) to strong σ -bonds, such as C-F,³² C-N,³³ C-O³⁴ bonds. Furthermore, the more favored π -back donation from Ni compare to Pd, resulting in a stronger binding to alkenes and alkynes ($d-\pi^*$ back donation), and thus in the more facile activation of these motifs.^{19a} Finally, the β -hydride elimination of alkyl-Ni complex is slower than the corresponding alkyl-Pd species, when compared in the same ligand framework. This is owing to a weaker agostic interaction compared to Pd, and a more strained geometry in the transition state.^{35,36,37} Therefore, the use of traditionally challenging C_{sp^3} coupling partners can be employed with nickel catalysis. Taken together, nickel catalysis shows complementary reactivity to palladium, and has

Chapter 1.

seen tremendous success in the application and development of alternative transformations.



Scheme 1.4 General characteristics of nickel and palladium catalysts

1.3 Nickel Catalyzed Cross-Electrophile Coupling

Driven by the diversity of nickel catalysis in the activation of electrophiles, either via two-electron or single-electron pathways, allows for sequential activation of different electrophiles via different mechanisms which offers a method to control reaction selectivity. In recent years, nickel-catalyzed reductive cross-coupling reactions of electrophiles have become very important technique in organic synthesis, particularly in C–C bonds formation.⁴

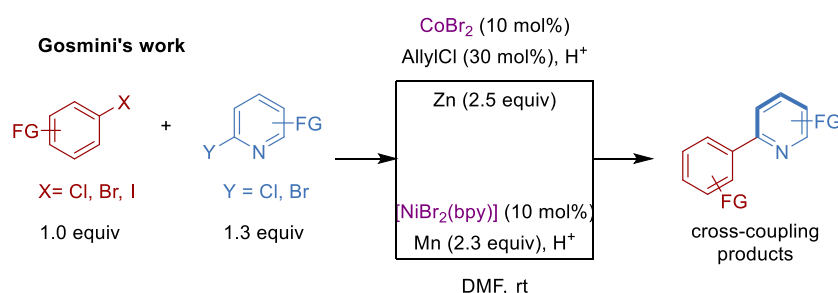
1.3.1 Nickel Catalyzed Reductive Coupling of Organic Halides

1.3.1.1 C_{sp^2} – C_{sp^2} Bonds Formation via Ni-Catalyzed Reductive Cross-Coupling

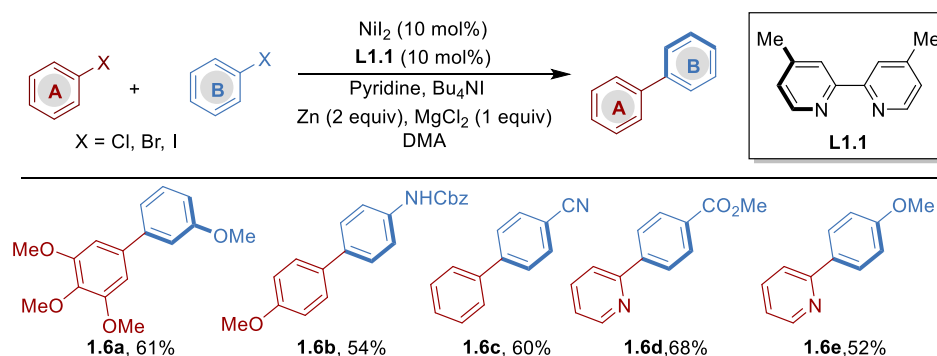
Biaryl units are often found as part of skeletons in natural products and have been intensively applied in several fields, including ligand design and material science. Since Ullmann reported the first copper mediated dimerization of aryl halides,⁶ a

number of methods have been developed for the construction of the biaryl skeletons. In particular, unsymmetrical biaryl compounds are generally prepared through conventional cross-coupling of electrophiles and nucleophiles.^{38,39,40} However, direct reductive coupling of two different aryl electrophiles, is generally less effective due to intrinsic poor chemoselectivity between two structurally similar aryl coupling partners.⁴¹

Following the early efforts on cobalt catalyzed reductive coupling of two aryl halides to form the unsymmetrical biaryls,⁴² Gosmini and co-workers extended this technique to nickel catalysis. In this case, a series of functionalized 2-arylpyridines were prepared by using $\text{NiBr}_2(\text{bpy})$ as the catalyst and stoichiometric Mn as reductant (Scheme 1.5).⁴³ Later on, Gong, Qian and co-workers reported a Ni-catalyzed reductive cross-coupling between two different aryl halides to prepare unsymmetrical biaryl compounds (Scheme 1.6).⁴⁴ The combination of NiI_2 , 4,4'-dimethyl-2,2'-bipyridine (**L1.1**), MgCl_2 and pyridine in DMA, using Zn as reductant, provided the biaryl compounds in moderate to good yield. The additive (MgCl_2) presumably activates the zinc powder by removing residual salts from its surface. The mild reaction conditions were shown to tolerate a range of functional groups such as esters, nitriles, ketones and the coupling of electron-deficient pyridyl and quinoline bromides with aryl halides that afforded the coupled products in good yields. The chemoselectivity in these methods varies from poor to excellent, largely rely on the electron-density difference between the two aryl coupling partners. In general, one of the aryl electrophiles need to be set in excess to improve the yields.

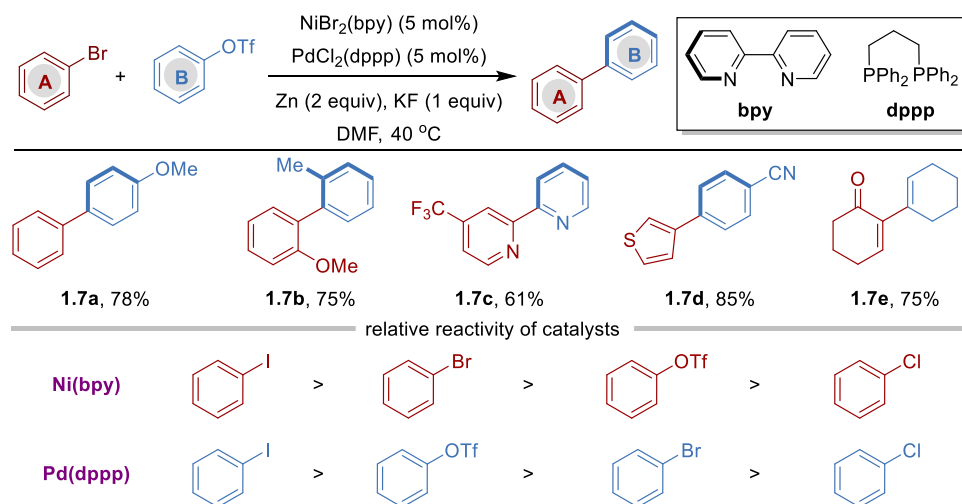


Scheme 1.5 Co(II)- and Ni(II)-catalyzed cross-reductive-coupling of aryl halides with heteroaryl halides

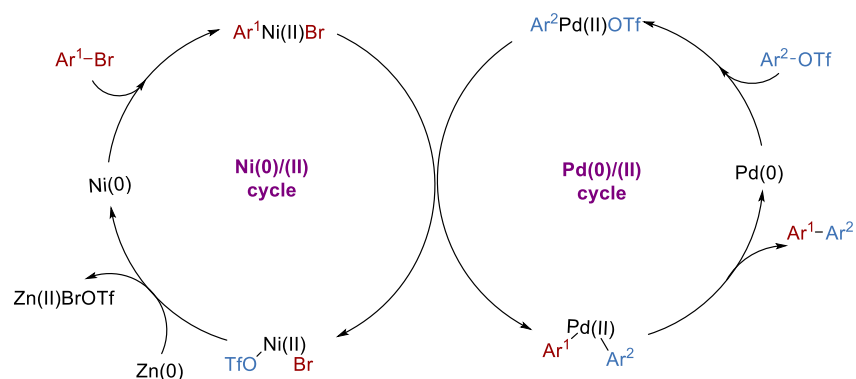


Scheme 1.6 Ni(II)-catalyzed cross-reductive-coupling of two different aryl halides

In 2015, Weix and co-workers made a remarkable breakthrough in achieving excellent chemoselectivity between two different aryl electrophiles. To achieve this selectivity, they employed a Pd/Ni dual catalytic system which enabled efficient coupling of aryl/vinyl bromides with aryl/vinyl triflates to generate unsymmetrical biaryls and dienes (Scheme 1.7).⁴⁵ The reaction is characterized by its mild conditions and excellent chemoselectivity. Key to access highly chemoselectivity is attributing the difference reactivities of aryl electrophiles with the different catalysts (Scheme 1.7, *bottom*).^{46,47,48} In this system, the aryl bromide undergoes selective oxidative addition with the Ni-bpy catalyst to generate a transient and reactive $\text{Ar}^1\text{Ni(II)Br}$ species, whilst the aryl triflate interacts exclusively with the Pd-dppp catalyst to provide a persistent $\text{Ar}^2\text{Pd(II)OTf}$ intermediate. Subsequent transmetalation between the $\text{Ar}^1\text{Ni(II)Br}$ and $\text{Ar}^2\text{Pd(II)OTf}$ intermediates affords $\text{Ar}^1\text{-Pd(II)-Ar}^2$ and Br-Ni(II)-OTf species. The following reductive elimination on the Pd center provide the cross-coupled biaryl products and regenerates Pd(0) (Scheme 1.8). Zn(0) acts as the terminal reductant to close the catalytic cycle, reducing Ni(II) back to Ni(0). Additionally, they found KF is essential to improve the selectivity and reaction rate. They proposed KF can reduce the amount of homocoupling by-products formed in nickel catalytic cycle; and can alter the oxidative addition selectivity for C-OTf bonds over C-X bonds through the formation of a palladium ‘ate’ complex. Very recently, the same group extended this strategy to 1,3-dienes formation via the cross-coupling of vinyl bromides with vinyl triflates.⁴⁹



Scheme 1.7 Pd/Ni dual catalyzed reductive-coupling of aryl halides with aryl triflates

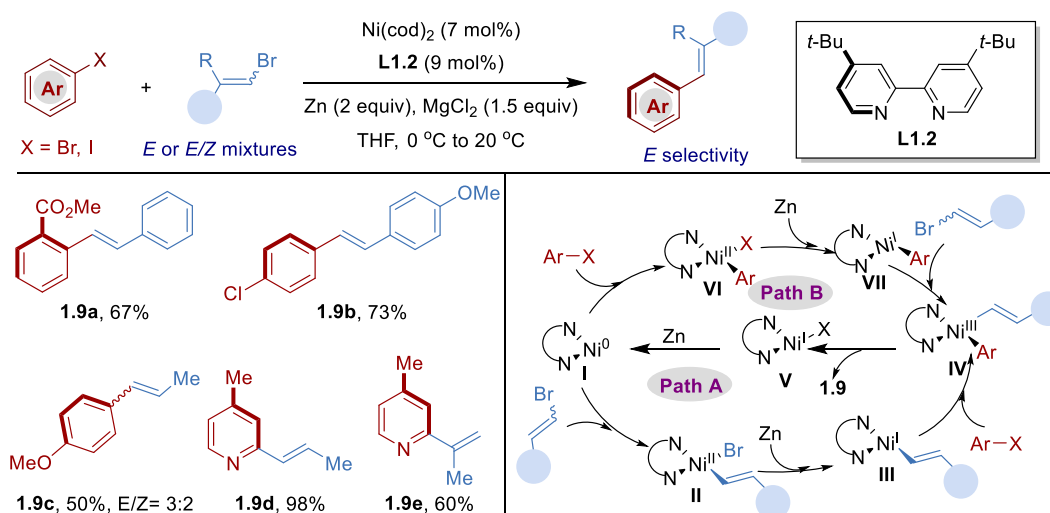


Scheme 1.8 Proposed mechanism of the Pd/Ni dual catalyzed reductive coupling

While Ni-catalyzed reductive cross-coupling of two aryl electrophiles or vinyl electrophiles have been developed, the coupling between aryl halides and vinyl halides are exceptionally rare. To meet this challenge, recently, Gong and co-workers were able to develop a Ni-catalyzed reductive cross-coupling of aryl halides with vinyl bromides, thus enabling to chemoselective construction of vinyl arenes (Scheme 1.9).⁵⁰ A wide range of functionalized aryl halides, including heteroaromatics and vinyl bromides were employed to yield *E*-selectivity vinyl arenes in good yield. Noteworthy, no cross-coupling product obtained when used pure (*Z*)-vinyl bromide as coupling partner. The authors proposed two different reaction pathways, **path A**: oxidative addition of vinyl-Br to Ni(0) to give vinyl-Ni(II)-Br intermediate **II**; or **path B**: oxidative addition of aryl halide to Ni(0) to form Ar-Ni(II)-X species **VI** (Scheme 1.9, *left*). Then SET reduction by Zn(0) generates the vinyl-Ni(I) intermediate (**III**) or ArNi(I) complex (**VII**). Subsequently oxidative addition of

Chapter 1.

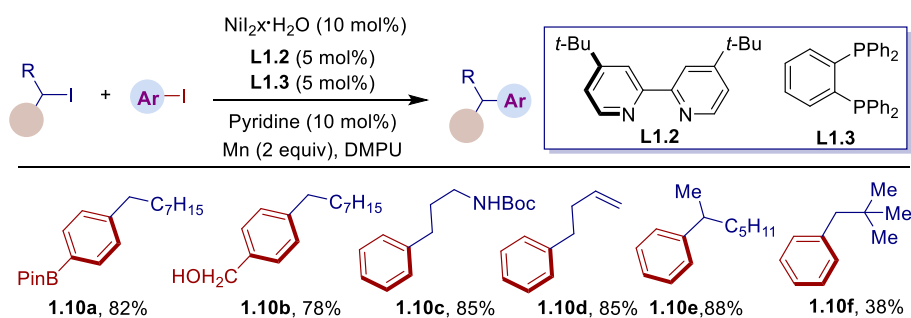
complex **III** or **VI** with the other coupling partner will form the Ar–Ni(III)–vinyl intermediate **IV**, which furnishes the cross-coupling product upon reductive elimination. Preliminary mechanistic studies and DFT calculations suggested that preferential oxidative addition of aryl halides to Ni(I)–vinyl is the key step (path A).



Scheme 1.9 Preparation of vinyl arenes by Ni-catalyzed reductive coupling of aryl halides with vinyl bromides

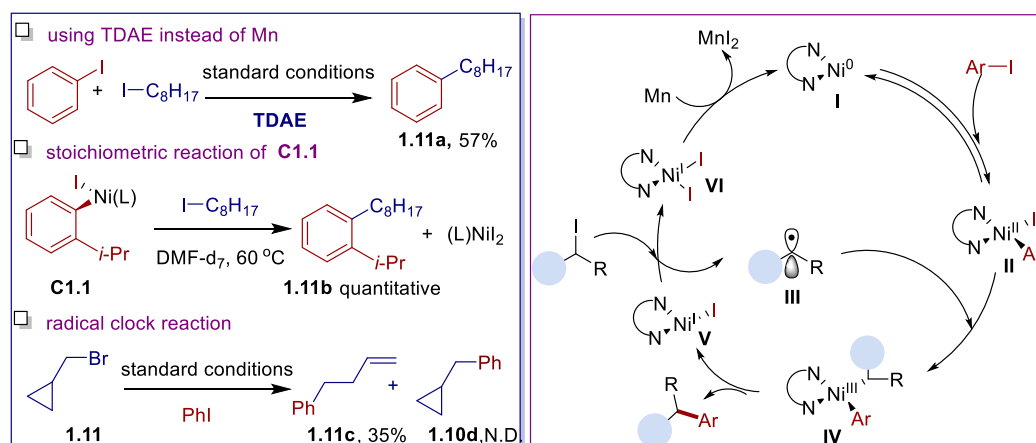
1.3.1.2 C_{sp2} – C_{sp3} Bonds Formation via Ni-Catalyzed Reductive Cross-Coupling

In 2010, Weix and co-workers reported a Ni-catalyzed C_{sp2} – C_{sp3} cross electrophile coupling of aryl iodides with alkyl iodides (Scheme 1.10).⁵¹ The authors found that the combination of $NiI_2 \cdot xH_2O$, dtbppy (**L1.2**), phosphine ligand (**L1.3**) and pyridine, with Mn(0) as reducing reagent were crucial for the reaction success. In this case, the reaction shows good functional group tolerance, even with substrates containing acidic proton, such as free hydroxyl groups. Not only primary alkyl halides, more steric hindered secondary alkyl halides were also able to undergo coupling with aryl iodides. Both the bipyridyl (**L1.2**) and phosphine (**L1.3**) ligands were required for achieve high yield and selectivity, and pyridine was included as an additive to inhibit β -hydride elimination in the alkyl species.



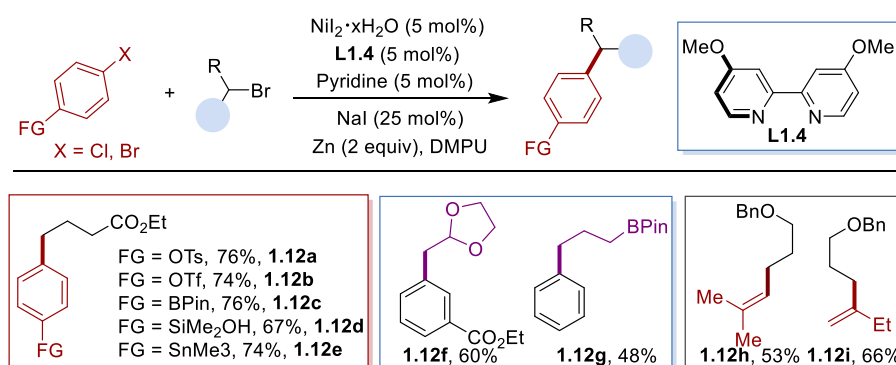
Scheme 1.10 Ni-catalyzed reductive cross-coupling of aryl iodides with alkyl iodides

Soon after, the same group reported a mechanistic study of this Ni-catalyzed reductive alkyl–aryl cross-coupling reaction (Scheme 1.11).⁵² Firstly, the authors ruled out the organomanganese reagent formation in this reaction via the result of using organic reductant TDAE instead of Mn. Further stoichiometric studies provided evidence that oxidative addition ArNi(II) complex **C1.1** reacts with alkyl halides to form the cross-coupling product **1.11b** and (L)NiI₂, without any added reductant. In addition, the author found that alkylNi(II) complexes do not react with iodobenzene to form cross-coupling product. Furthermore, radical clock experiment with cyclopropylmethyl bromide (**1.11**), only provided ring opened product **1.11c**, suggesting that alkyl radical intermediate was formed in the reaction. Taken together, the author proposed the reaction involve a radical pathway where ArNi(II) species combines with alkyl radical **III** to give a Ni(III) species **IV**, that undergoes reductive elimination to provide cross coupling product (Scheme 1.11, *right*). The resulting Ni(I) intermediate **V** engages in a SET reductive cleavage of another alkyl halide to generate a new alkyl radical and a Ni(II) complex **VI**. Finally the Ni(II) intermediate **VI** is reduced by Mn(0) to form Ni(0).

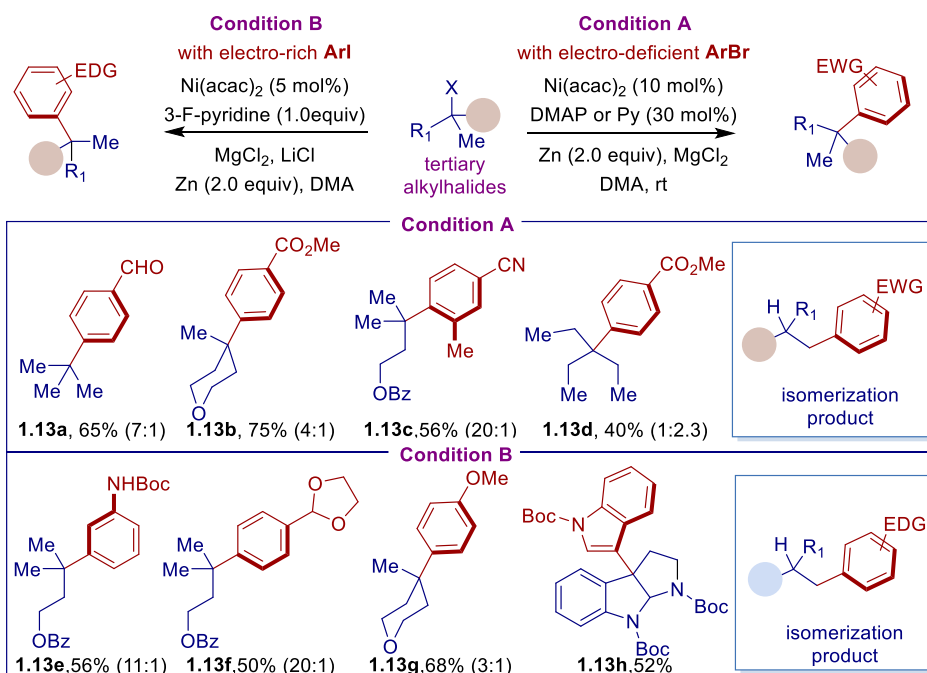


Scheme 1.11 Mechanistic study of Ni-catalyzed reductive coupling

Although the methodology and mechanistic of the C_{sp^2} – C_{sp^3} bonds formation with two organic iodides have been explored. The technique provided poor selectivity for coupling of two organic bromides. This is due to the lower reactivity of alkyl bromides than alkyl iodides, thus enabled the formation biaryl by-products from disproportionation of a supposed $ArNi(II)$ intermediate. Later work by Weix and co-workers discovered that the combination of NiI_2 , **L1.4** or phenanthroline ligand, pyridine and NaI in DMPU, and using Zn as reductant, could successfully couple two organic bromides, and could even be extended to vinyl bromides or activated aryl chlorides (Scheme 1.12).⁵³ The reaction shows broad substrate scope and excellent chemoselectivity. Particularly noteworthy, was the ability to access substrates bearing both electrophilic and nucleophilic carbon positions (C –BPin, $–SiR_3$, $–SnR_3$) which were selectively coupled at the electrophilic site (RX), while leaving the nucleophilic group available for further cross-coupling reactions.

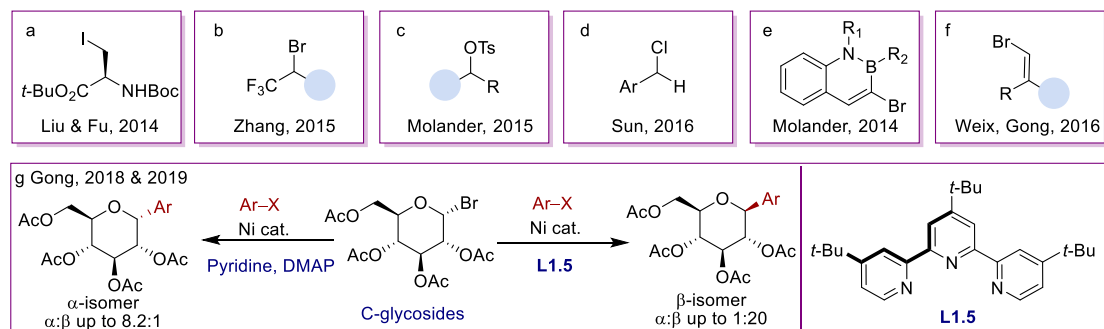


Scheme 1.12 Ni-catalyzed reductive cross-coupling of alkyl bromides with aryl bromides and chlorides



Scheme 1.13 Ni-catalyzed reductive cross-coupling of tertiary alkyl halides

A common limitation in these cross-electrophile coupling reactions is the ability to tolerate sterically encumbered electrophiles to forge all-carbon quaternary centers.⁵⁴ This is probably due to the steric bulkiness of tertiary alkyl electrophiles, which promote β -H elimination and impede oxidative addition as well as reductive elimination. Recently, Gong and co-workers have successfully realized a catalytic reductive arylation of tertiary alkyl halides with both electron-deficient and electron-rich aryl halides by the judicious choice of ligands and additives (Scheme 1.13).^{55,56} A series of electro-deficient aryl bromides could be perfectly coupled by the combination of Ni(acac)₂, DMAP, MgCl₂ and Zn system.⁵⁵ Soon after, the same group discovered that the poor coupling results for electron-rich aryl iodides were drastically improved by replacing DMAP with 3-fluoropyridine and using more reactive aryl iodides as the coupling partners and LiCl as additive.⁵⁶ Both Mg²⁺ and Cl⁻ were crucial for the reaction success. The importance of MgCl₂ and LiCl in the reaction, was not only attributed to activation of Zn in the reaction but also to enhance the solubility of the Ni(acac)₂ salt through the interaction of the Mg²⁺ cation with the acac anion. Notably, in both cases, the isomerization side products were formed through Ni-catalyzed chain-walking.⁵⁷



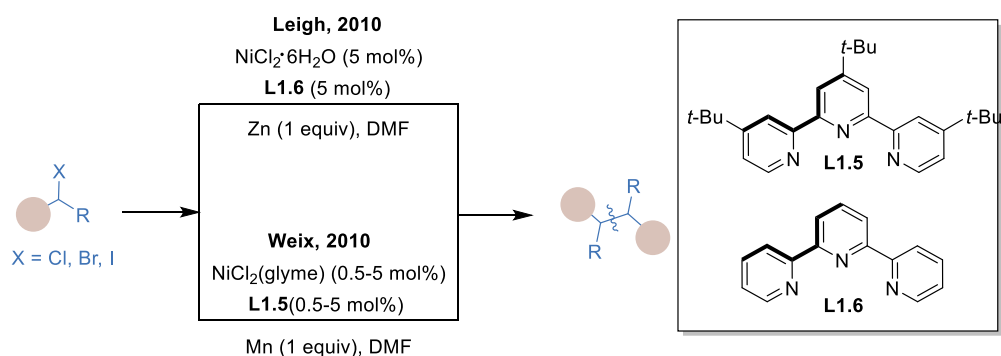
Scheme 1.14 C_{sp2} – C_{sp3} bonds formation via Ni-catalyzed reductive couplings

Additionally, the Ni-catalyzed reductive coupling strategies were extended to arylation with chiral iodoalanine,⁵⁸ α -trifluoromethylate alkyl bromides,⁵⁹ alkyl tosylates,⁶⁰ benzyl chlorides⁶¹ as well as vinylation of alkyl halides with vinyl bromides^{62,63,64} (Scheme 1.14). Specifically, the Gong group discovered that the stereoselective arylation of C1-glucosyl bromides with the corresponding aryl halides could be achieved through ligands control (Scheme 1.14, e.q. g).^{65,66} The use of pyridine/DMAP ligands afforded C-glucosides in up to 8:1 α/β selectivity,⁶⁵ while the use of the tridentate terpyridine ligand **L1.5** resulted in up to >20:1 β/α selectivity.⁶⁶

1.3.1.3 C_{sp3} – C_{sp3} Bonds Formation via Ni-Catalyzed Reductive Coupling of Alkyl Halides

The success coupling of alkyl- and aryl fragments is depending on the different reactivity profiles of the C_{sp2} -electrophiles and the C_{sp3} -electrophiles with nickel.^{29,46} However, the control of chemoselectivity becomes considerably challenging when attempting the coupling between two structurally similar alkyl electrophiles, since homocoupling of alkyl electrophiles as well as competition of β -hydride elimination of alkyl–Ni species impede the cross-coupling efficiency.^{35,36,37}

In 2010, Leigh⁶⁷ and Weix⁶⁸ reported the Ni-catalyzed homocoupling of alkyl electrophiles by using Zn and Mn as reductant, respectively (Scheme 1.15). In both cases, primary and secondary alkyl halides as well as alkyl mesylates, trifluoroacetates could successfully couple, thus providing the dimerization product in good yields. The authors proposed that the reaction could be conducted via an alkyl–Ni(III)–alkyl intermediate.



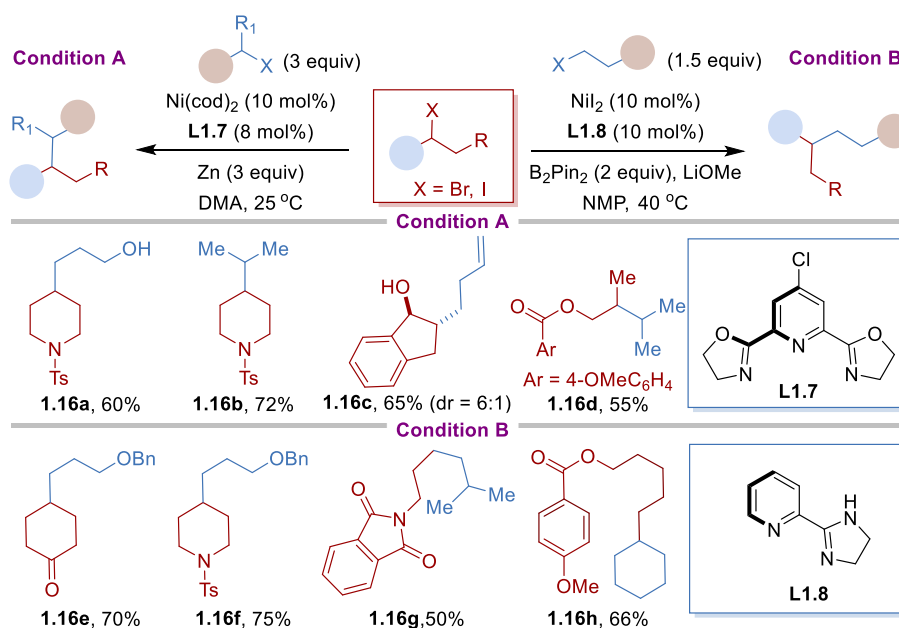
Scheme 1.15 C_{sp^3} – C_{sp^3} bonds formation via Ni-catalyzed reductive couplings

The first Ni-catalyzed cross-reductive-coupling of two different alkyl halides (commonly secondary with primary halides) was developed by Gong in 2011.⁶⁹ Notably, 3 equivalent of primary alkyl bromides were required for accessing high selectivity and yields under Ni(COD)₂/L1.7 catalysis with Zn as reductant (Scheme 1.16, *Condition A*). In addition to the formation of the cross-coupling products, the highly competitive homocoupling side reactions account for the mass balance of the excess alkyl halides. Soon after, the same group discovered that the replacement of Zn to B₂Pin₂, could improve the chemoselectivity significantly (Scheme 1.16, *Condition B*).⁷⁰ The reaction only required 1.5 equivalent of the second alkyl halides, which worked effectively for the coupling of secondary as well as hindered primary halides with another primary bromides. The preliminary mechanistic investigation ruled out the possibility of *in-situ* organoboron/Suzuki processes. The authors proposed that the formation of Ni–Bpin complexes may be the key to differentiating the coupling alkyl partners, thus providing cross-coupling product with high selectivity. Moreover, this Ni/B₂Pin₂ system was further employed in the methylation of methyl tosylates.⁷¹

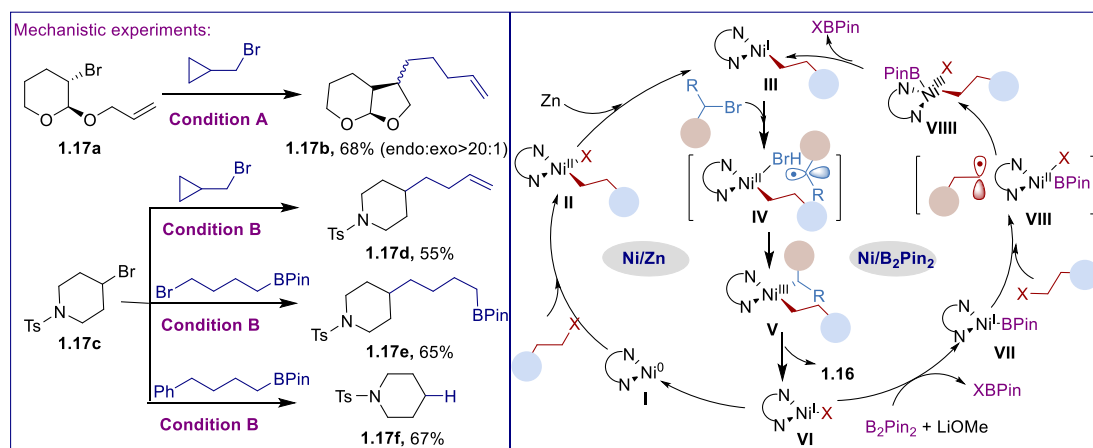
In both cases, the coupling with (bromomethyl)cyclopropane, provided ring opening products, suggesting that a radical process was involved in this reaction (Scheme 1.17, *left*). In Ni/Zn systems, the reaction is thought to go through oxidative addition of alkyl halides with low valent Ni(0) to generate Alkyl¹–Ni(II)–X complex (**II**), which is then reduced by Zn(0), resulting in a Alkyl¹–Ni(I) intermediate (**III**). This intermediate **III** is proposed to undergo a second oxidative addition with the other alkyl halides to form Alkyl¹–Ni(III)X–Alkyl² species (**V**), which subsequently release desired product upon reductive elimination. In Ni/B₂Pin₂ system, the reaction may go through a SET of Ni(I)–Bpin to alkyl halide, then rapid radical recombination to form alkyl¹–Ni(III)X–Bpin intermediate (**VIII**), followed by reductive elimination

Chapter 1.

to provide alkyl^I-Ni(I) intermediate. The following process is the same with the Ni/Zn system.

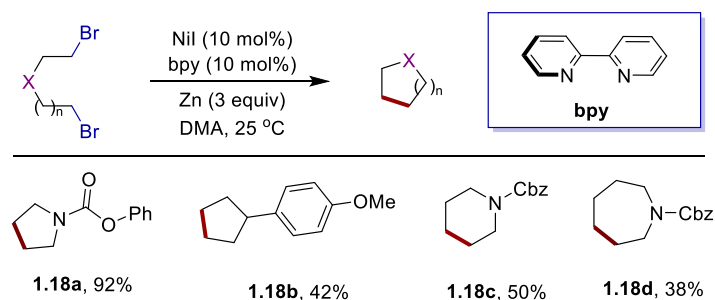


Scheme 1.16 $C_{sp^3}\text{-}C_{sp^3}$ bonds formation via Ni-catalyzed reductive couplings



Scheme 1.17 Mechanistic experiments of Ni-catalyzed cross-reductive-coupling of alkyl halides

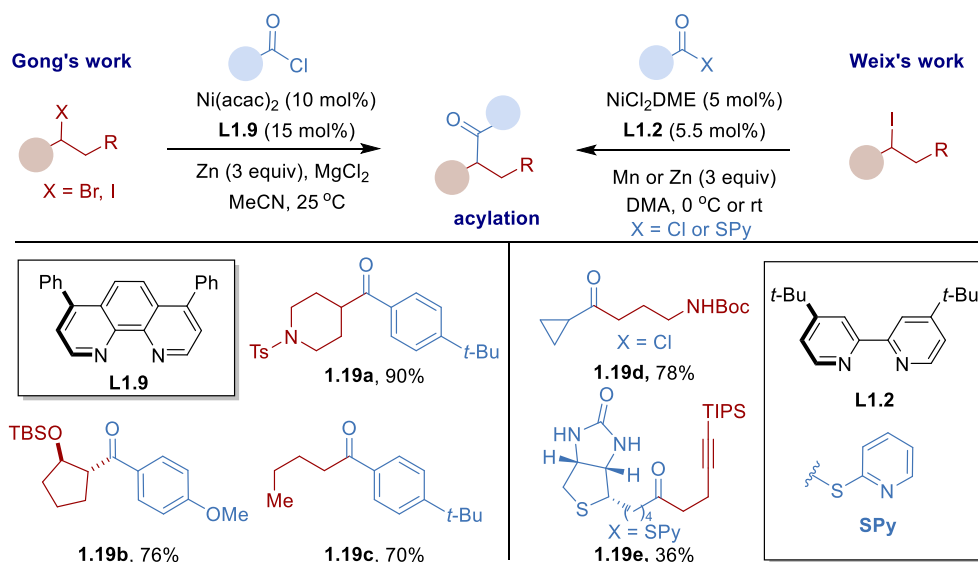
In addition to intermolecular $C_{sp^3}\text{-}C_{sp^3}$ bonds formation, the Gong group also developed an intramolecular reductive cyclization of alkyl dihalides (Scheme 1.18).⁷² Under NiI_2/bpy catalytic conditions with Zn as reductant, a series of five and six-membered rings could be facily constructed. The more challenging seven-membered ring could also be obtained in moderate yield.



Scheme 1.18 Ni-catalyzed reductive cyclization of alkyl dihalides

1.3.1.4 Ni-Catalyzed Reductive Acylation of Alkyl Halides

Alongside C_{sp^2} - C_{sp^3} bonds and C_{sp^3} - C_{sp^3} bond formation, the construction of ketones by means of Ni-catalyzed reductive acylation of alkyl (pseudo)halides have devoted much attention. The groups of Weix⁷³ and Gong⁷⁴ independently reported the Ni-catalyzed reductive coupling of acid chlorides and alkyl halides with Zn or Mn as reducing reagents. Moreover, Gong and co-workers extended this protocol to the ‘one-pot’ coupling of benzoic acids with alkyl bromides via *in-situ* activated acids in the presence of Boc_2O and MgCl_2 .⁷⁵

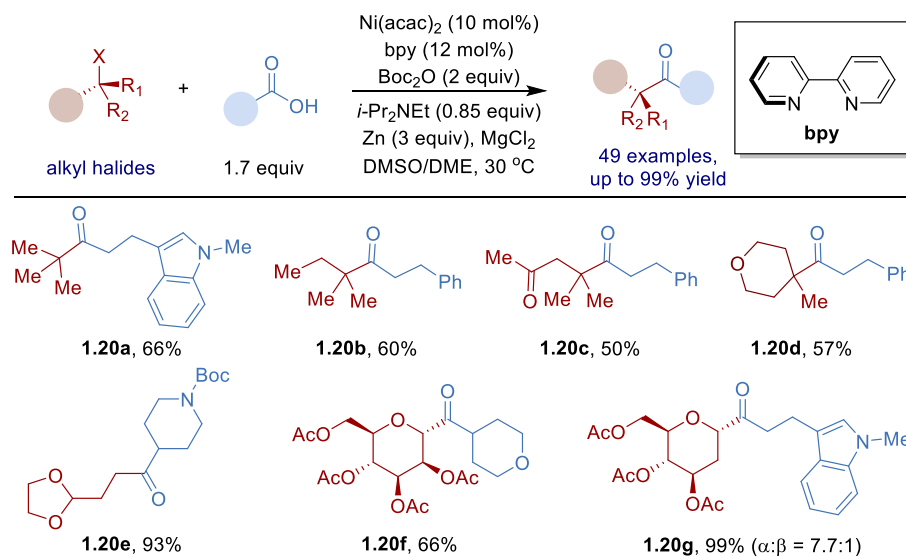


Scheme 1.19 Ni-catalyzed reductive acylation of alkyl halides with acyl chlorides

It is worth highlighting that this protocol was further refined to enable the reductive coupling of alkyl acids with alkyl halides, where sterically hindered unactivated tertiary alkyl bromides and glycosyl halides could be well tolerated, thus resulting a series of all carbon quaternary as well as sugar-type ketones (Scheme

Chapter 1.

1.20).⁷⁶ More interestingly, the α -selectivity products were obtained when coupling alkyl acids with C-acyl glycosides bromides. Preliminary mechanistic studies suggested that a radical chain process may be plausible, wherein MgCl_2 promotes the reduction of Ni(II) complexes by Zn.



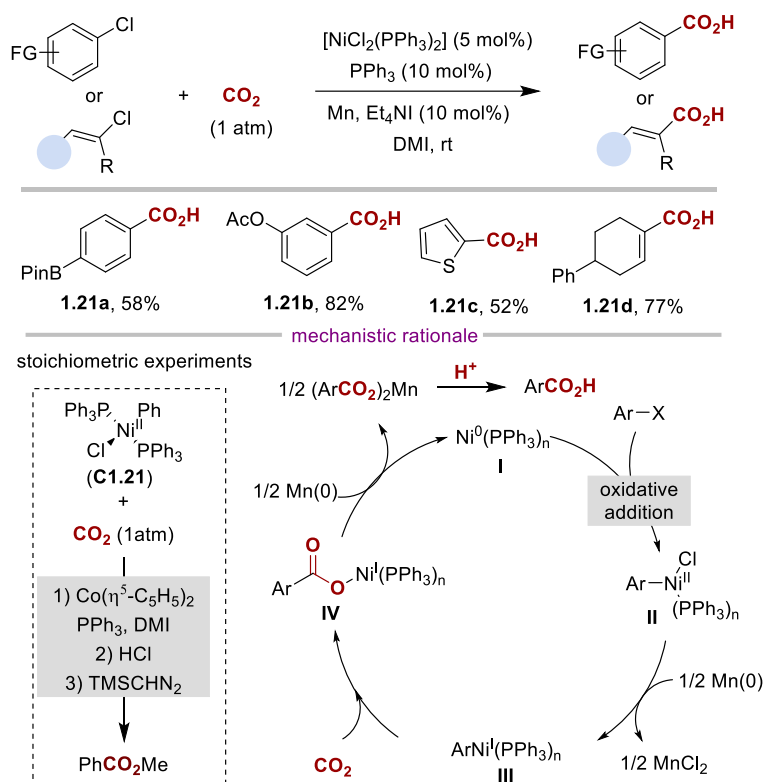
Scheme 1.20 Ni-catalyzed reductive acylation of alkyl halides with carboxylic acids

1.3.1.5 Ni-Catalyzed Reductive Carboxylation of Organic (Pseudo) Halides with CO_2

Driven by the inherent synthetic potential of carbon dioxide (CO_2) as a nontoxic, abundant, inexpensive and renewable C1 chemical feedstock, recent years have witnessed the development of process for the fixation of CO_2 into organic molecules.⁷⁷ Particularly, catalytic carboxylation reactions of organic molecules with CO_2 have received significant attention both in academia and industry, since carboxylic acid skeletons are widely present in pharmaceuticals, agrochemicals, plastics and among others.⁷⁸

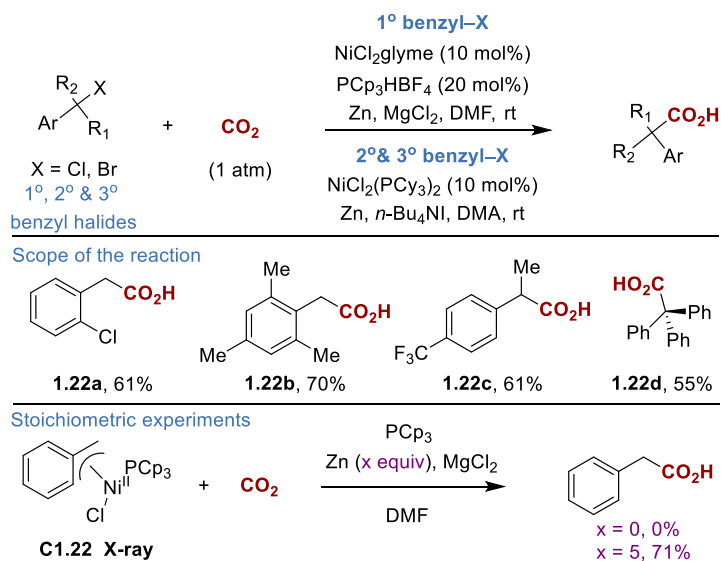
Inspiring by the pioneering work of Osakada and Yamamoto on stoichiometric reaction of Ni(II) complex with CO_2 ,⁷⁹ our group and others have successfully developed a direct reductive carboxylation protocol of organic (pseudo)halides by means of nickel catalysis.⁸⁰ Unlike traditional carboxylation protocols based on nucleophile/electrophile regimes, which often requires air and moisture-sensitive organometallic species, reductive carboxylation events offer possibility to employ simple electrophiles, thus presenting a complementary technique for the preparation

of carboxylic acids.⁸⁰



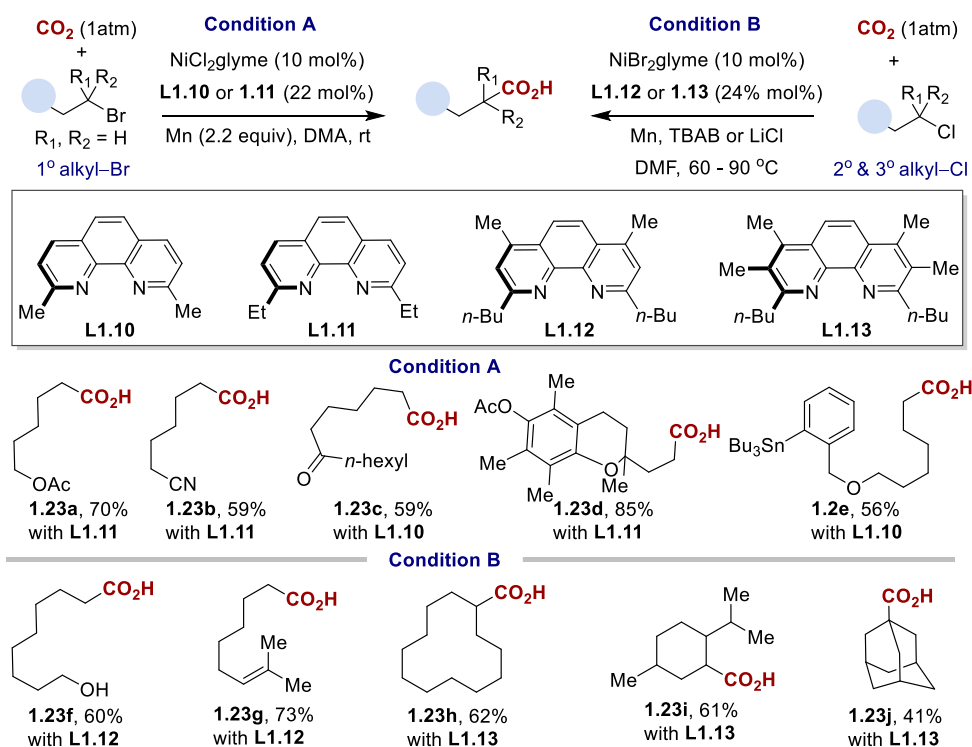
Scheme 1.21 Ni-catalyzed reductive carboxylation of aryl chlorides with CO₂

In 2009, our group reported the first Pd-catalyzed reductive carboxylation of aryl bromides with CO₂, by using Et₂Zn as reductant.⁸¹ However, high pressure CO₂ and pyrophoric reductant (Et₂Zn) were required for the reaction success. In 2012, Tsuji, Fujihara and co-workers extended the scope of catalytic carboxylation to more challenging and readily available aryl and vinyl chlorides at atmospheric pressure of CO₂ (Scheme 1.21).⁸² The combination of NiCl₂(PPh₃)₂, PPh₃ and Et₄NI in DMI, with Mn as reductant were crucial for success. It is particularly noteworthy that the oxidative addition complex PhNi(II)Cl(PPh₃)₂ (**C1.21**) did not react with CO₂ (1 bar) unless a single-electron reductant was utilized (Co(η⁵-C₅H₅)₂; E = -0.89V). With the results of stoichiometric experiments in hands, the authors proposed that the reaction occurred through oxidative addition of ArCl with Ni(0) to generate the Ar-Ni(II)-Cl intermediate (**II**), which then underwent SET reduction via Mn(0) to form the Ar-Ni(I) species (**III**). Followed by CO₂ insertion, resulting carboxylatonickel intermediate (**IV**), which was subsequently reducing by Mn, gave the corresponding manganese carboxylate (Scheme 1.21, *right bottom*).

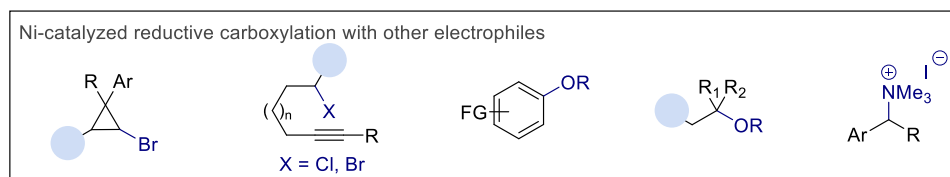


Scheme 1.22 Ni-catalyzed reductive carboxylation of benzyl halides with CO₂

Aiming to expand the catalytic reductive carboxylation portfolio beyond the utilization of aryl halides, our group described a Ni-catalyzed reductive carboxylation of primary, secondary or even tertiary benzyl halides with CO₂ (Scheme 1.22).⁸³ In this case, highly electron-rich phosphines such as PCp₃ and PCy₃ were found to be critical in the presence of Zn. Interestingly, the presence of additives was found to play a profound influence on reactivity; while the presence of MgCl₂ mediated the coupling of primary benzyl halides, and the replacement of tetrabutylammonium iodide (TBAI) for MgCl₂ was important for secondary and tertiary benzyl halides. Moreover, stoichiometric experiments with a putative η^3 -benzylNi(II) complex (**C1.22**), revealed that the reaction did not proceed in the absence of Zn. Additionally, control experiments argued against a mechanism consisting of the intermediacy of benzyl zinc reagents or styrene derivatives obtained via β -hydride elimination.



Scheme 1.23 Ni-catalyzed reductive carboxylation of unactivated alkyl halides

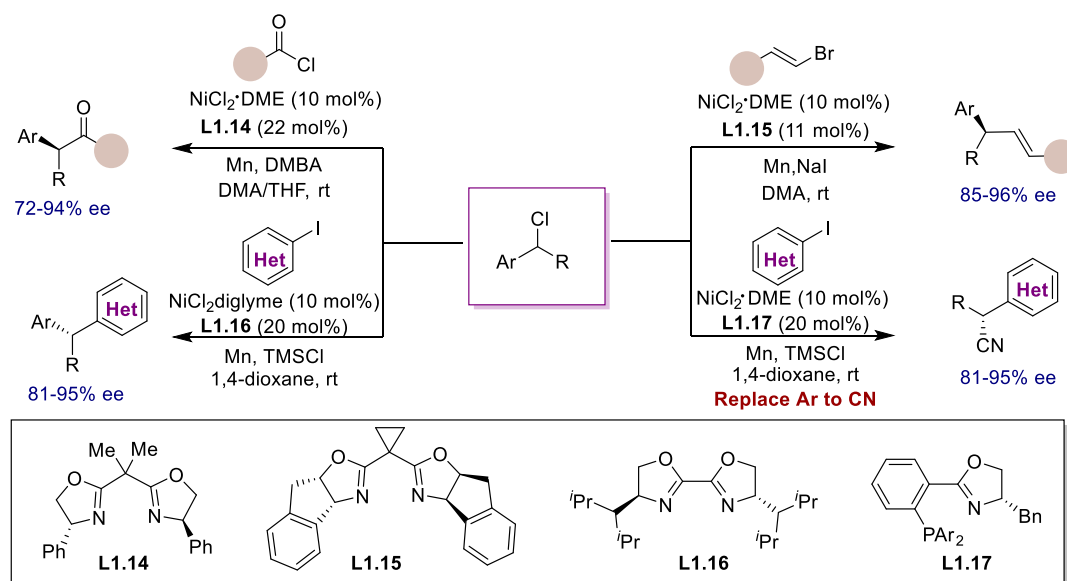
Scheme 1.24 Ni-catalyzed reductive carboxylation of other electrophiles with CO_2

In 2014, metal-catalyzed reductive carboxylations remained limited to substrates that easily undergo oxidative addition, such as aryl, vinyl, benzyl or allyl (pseudo)halides. This suggested that the extension of scope to more challenging, unactivated alkyl (pseudo)halides might be problematic. This is owing to that CO_2 is thermodynamically stable, kinetically inert and has poor solubility in commonly used solvents. Furthermore, it was anticipated that CO_2 insertion into the unstable alkyl-metal species would be very challenging. Nevertheless, our group successfully reached this challenge by utilizing 1,10-phenanthroline ligands possessing alkyl substituents adjacent to the nitrogen atom (Scheme 1.23).^{84,85} The presence of such substituents probably prevented β -hydride elimination while favoring the formation of putative alkyl-Ni(I) species prior to CO_2 insertion. Notably, the judicious choice ligands and additives, enable to couple CO_2 with unactivated alkyl bromides⁸⁴ and alkyl chlorides⁸⁵.

Additionally, our group has developed a series of Ni-catalyzed reductive carboxylations of CO₂ with different electrophiles such as bromo-cyclopropanes,⁸⁶ aryl or alkyl C–O electrophiles⁸⁷ as well as benzylic ammonium salts⁸⁸ (Scheme 1.24). Particularly interesting is that our group discovered a cyclization/carboxylation of unactivated alkyl halides possessing an alkyne on the side-chain, resulting in polycyclic carboxylic skeletons.⁸⁹

1.3.1.6 Ni-Catalyzed Enantioselective Reductive Coupling Reactions of Organic Halides

In 2013, Reisman and co-workers disclosed the first Ni-catalyzed stereoconvergent reductive cross-coupling of racemic secondary benzylic chlorides with acyl chlorides.⁹⁰ The combination of NiCl₂·DME with a chiral bis-oxazoline ligand (**L1.14**) dimethylbenzoic acid (DMBA) and with Mn as reductant, providing the acyclic α , α -disubstituted ketones with high yield and high enantioselectivity (up to 94% ee) (Scheme 1.25). The authors found that the addition of DMBA suppressed homocoupling of the benzylic chlorides. Moreover, the mixed solvent system (DMA/THF) was found to provide the optimal balance of reactivity and selectivity. Not surprising, with the judicious choice of chiral ligands and additives, Reisman group extended the scope to the coupling of racemic benzylic chlorides with vinyl bromides,⁹¹ (hetero)aryl iodides⁹² and the coupling of α -chloronitriles with (hetero)aryl iodides⁹³. Preliminary mechanistic studies suggested these catalytic enantioselective reductive coupling reactions occurred through a radical process which is consistent with former mechanism studies of racemic transformations.^{15,28,52} However, it's still unclear whether the absolute stereochemistry is set during the oxidative addition or reductive elimination steps. Noteworthy, current catalytic enantioconvergent cross-electrophile reaction remains restrict to the use of activated alkyl electrophiles such as benzylic (pseudo)halides or α -chloronitriles.⁹⁴



Scheme 1.25 Ni-Catalyzed enantioselective reductive-coupling reactions

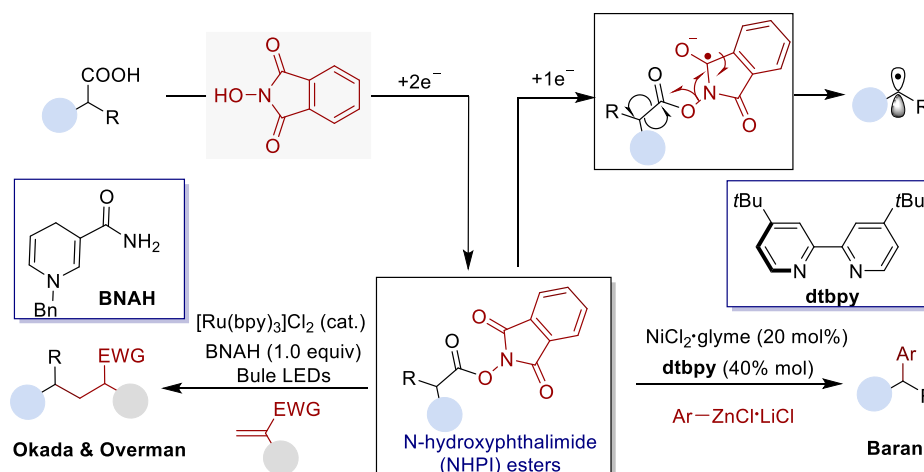
1.3.2 Nickel-Catalyzed Decarboxylative Reductive Cross-Couplings

Recently, metal-catalyzed decarboxylative cross-coupling reactions has emerged as a novel, efficient and practical strategy to form C–C and C-heteroatom bonds.⁹⁵ The advantage of this strategy is by the utilization of readily available, abundant, bench stable and non-toxic carboxylic acids as alternative to organic (pseudo) halides. In general, these strategies are thought to occur through metal-catalyzed $2e^-$ process to form nucleophilic organometallic intermediates and extrude CO_2 .⁹⁵ Additionally, a radical precursors derivatized by carboxylic acid, namely *N*-(acyloxy)phthalimides (NHPI) esters, has attracted chemists' attention.⁹⁶

In 1991, the Okada group reported a photocatalyzed radical-type Michael addition of *N*-(acyloxy)phthalimides (NHPI) esters, ($E_{1/2} = 1.56\text{--}1.66$ V) with electron-deficient olefins in the presence of $[\text{Ru}(\text{bpy})_3]\text{Cl}_2$ and a hydrogen donor (BNAH) (Scheme 1.26, *left*).⁹⁷ Overman and co-workers also employed this photoredox strategy to build up quaternary carbon centers.⁹⁸ In both cases, NHPI ester was served as a radical precursor to produce alkyl radical via photocatalyzed SET process.

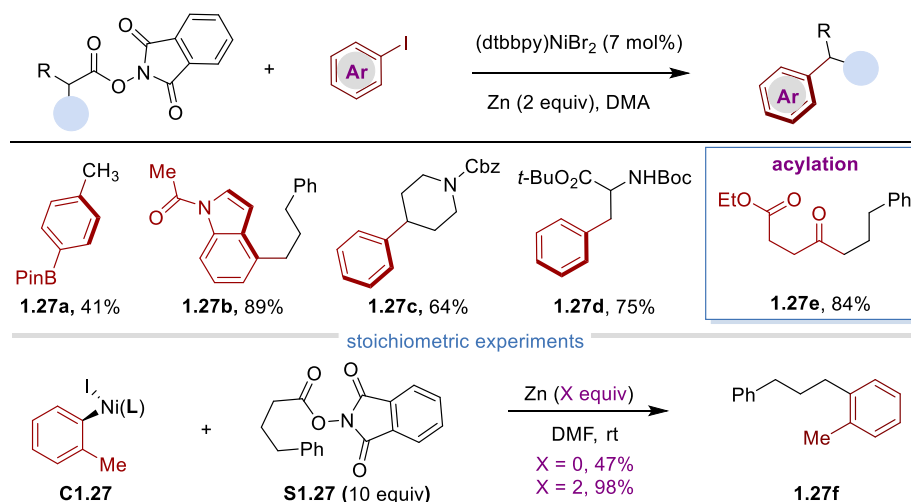
Inspired by the pioneering work from Okada and Overman, the group of Baran⁹⁹ and Weix¹⁰⁰ have independently disclosed $C_{sp^3}\text{--}C_{sp^2}$ bond forming reactions through Ni-catalyzed decarboxylative couplings. In both cases, the NHPI esters could accept

an electron from low valent nickel species, thus generating an alkyl radical. In 2016, Baran and co-workers developed a catalytic decarboxylative arylation of arylzinc reagents with NIPI esters which prepared from corresponding carboxylic acids (Scheme 1.26, right).⁹⁹



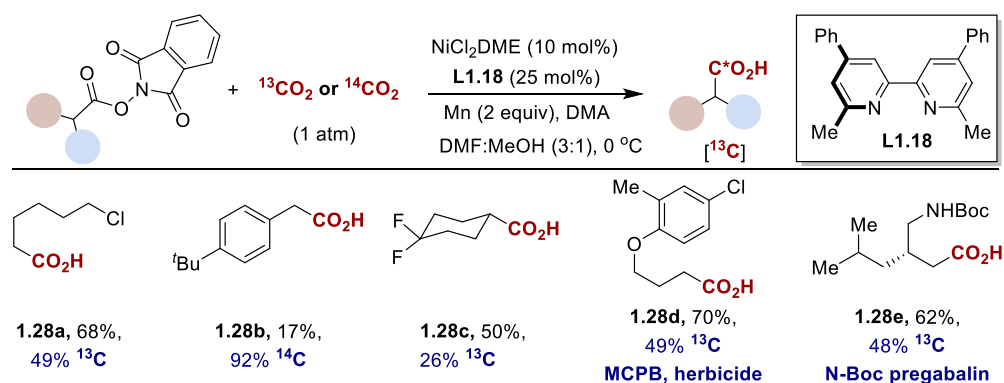
Scheme 1.26 Catalytic decarboxylative coupling of NHPI esters

Concurrent with Baran's report, Weix and co-workers reported a Ni-catalyzed reductive arylation of NHPI esters with aryl iodides, using Zn as reductant (Scheme 1.27).¹⁰⁰ Unlike Baran's protocol which was only effective with secondary NIHP esters, this reductive strategy could be expanded to methyl, primary and secondary alkyl NHPI esters, and even tolerate amino acid derivatives. More interestingly, the authors presented one decarboxylative acylation example of NHPI ester and acid chloride, suggesting the generality of NHPI esters in cross-coupling reactions. Moreover, stoichiometric experiments with oxidative addition complex **C1.27** and NHPI ester **S1.27** formed cross-coupling product **1.27f** in good yield with or without Zn, which argues against the intermediacy of arylzinc reagents in the reaction. The authors proposed that the reactions proceed via a radical chain mechanism, similar to the coupling of alkyl halides with aryl halides. Recently the scope of this catalytic decarboxylative reductive coupling strategy has been extended to alkylation¹⁰¹ and acylation¹⁰² as well as enantioselective vinylation¹⁰³.



Scheme 1.27 Ni-catalyzed reductive arylation of NHPI esters with aryl iodides

Very recently, our group reported a Ni-catalyzed carbon isotope exchange of carboxylic acids by merging decarboxylative events with carboxylation protocols with $^{13}CO_2$ or $^{14}CO_2$ (Scheme 1.28).¹⁰⁴ The novel decarboxylative/carboxylation protocol is characterized by its mild conditions, versatility, excellent chemoselectivity profile, and high isotopic incorporations (up to >99% C-labeling), thus providing an alternative technique for the preparation of labeled carboxylic acids. Particularly noteworthy was the ability to enable the targeted $^{12}C/^{13}C$ -exchange at late-stages with bioactive carboxylic acids, such as MCPB and pregabalin, among others, suggesting the potential our catalytic protocol might have in drug discovery.

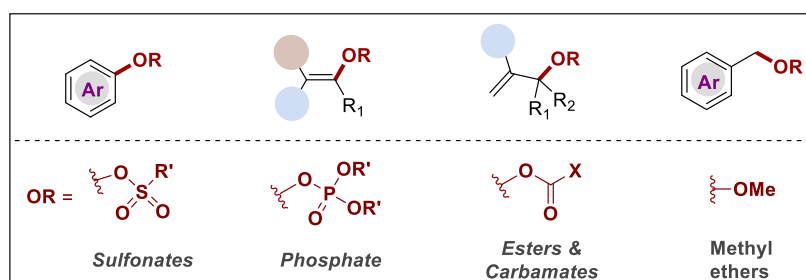


Scheme 1.28 ^{13}C - and ^{14}C -labeling carboxylation with CO_2

1.3.3 Nickel-Catalyzed Reductive Coupling of Unactivated sp^3 C–O Electrophiles

Phenols and alcohols are among the most accessible organic compounds and widely present in nature product, pharmaceutical and functional materials. In past decades, C–O electrophiles derivatized from phenols or alcohols has become ideal alternatives to organic halides in metal-catalyzed cross-coupling reactions.¹⁰⁵ This is due to the greater availability of phenol or alcohol derivatives when compared to organic halides, in addition to avoiding the generation of stoichiometric amount of halogenated waste in the reactions. **Scheme 1.29** summarizes the commonly employed C–O electrophiles such as sulfonates, phosphates, esters, carbamates and ethers.¹⁰⁵

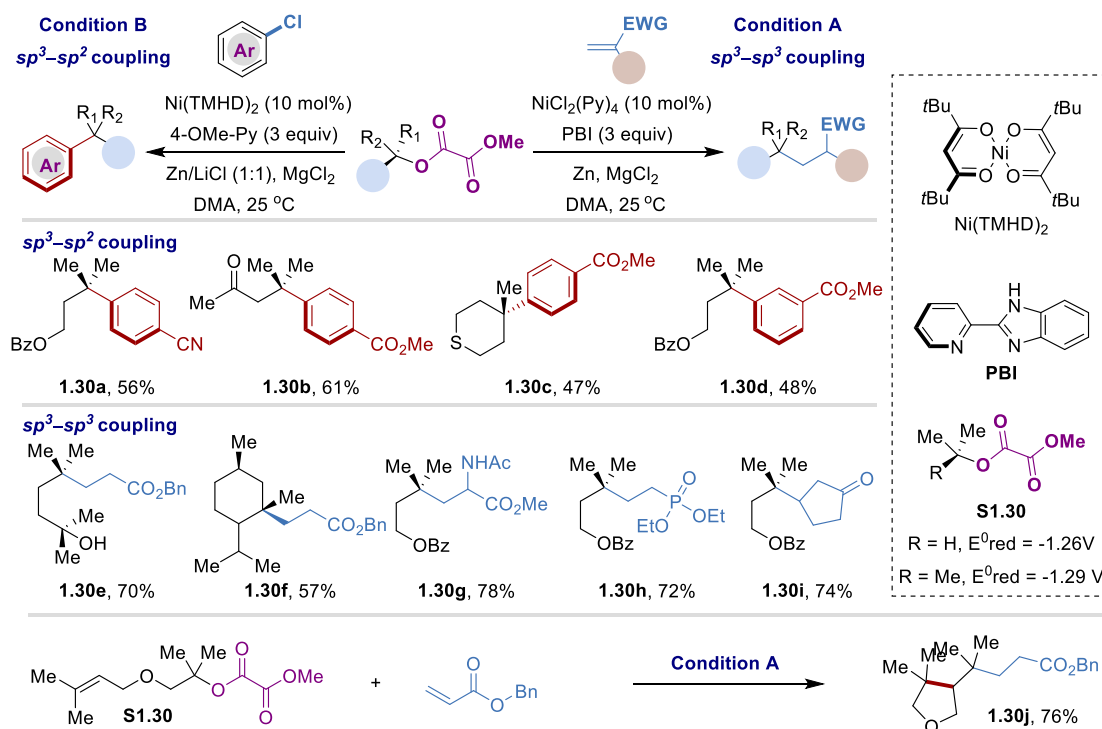
Recently, significant progress has been made by our group¹⁰⁶ as well as Chatani,¹⁰⁷ Shi¹⁰⁸ and others¹⁰⁵ in the development of catalytic C–O bond cleavage. However, most of the transformations are based on activated aryl, benzyl and allyl C–O bonds cleavage. The development of effective methodology based on cleavage of unactivated C_{sp^3} –O bonds remains a long-term challenge. In 1986, the group of Barton reported the first C_{sp^3} –O bonds fragmentation of *tert*-alkyl *N*-hydroxypyridine-2-thionyl oxalates to generate radicals.¹⁰⁹ Recently, the generation of alkyl radicals through the photoredox catalyzed C_{sp^3} –O bonds fragmentation has been reported by Overman¹¹⁰ and others¹¹¹.



Scheme 1.29 The development of C–O electrophiles in cross-couplings

Inspired by Barton's¹⁰⁹ and Overman's¹¹⁰ pioneering work on the cleavage of unactivated C_{sp^3} –O bonds to generate alkyl radicals, Gong and co-workers recently developed a dehydroxylative arylation and alkylation of tertiary alkyl oxalates through radical process (Scheme 1.30).^{112,113} The authors found that the tertiary alkyl oxalates which were prepared from corresponding alcohols undergo C_{sp^3} –O bond

fragmentation to generate tertiary alkyl radicals when treated with Zn and MgCl₂ in the presence of Ni catalyst. The tertiary radical were further trapped by Michael-accepters or ArNi(II) species to form alkylation and arylation product with quaternary carbon centers. In principle, reduction of alkyl oxalates by Zn is thermodynamically unfavorable based on the reduction potentials of *t*-Bu methyl oxalate **S1.30** ($E_{\text{red}} = -1.26$ V vs SCE) and Zn ($E_{\text{red}} = -0.76$ V vs SCE). However, the authors discovered that the addition of MgCl₂ could promote the single electron reduction, since the carbonyl-centered LUMO of the oxalate could be lowered by the coordination of Mg²⁺. Specifically, the combination of Ni(TMHD)₂, 4-OMe-pyridine, Zn, with MgCl₂ and LiCl as additive, provided the reductive arylation product in good yields with exceptionally low levels of isomerization. Preliminary mechanistic experiments suggested the radical formation via C_{sp3}-O bond cleavage.



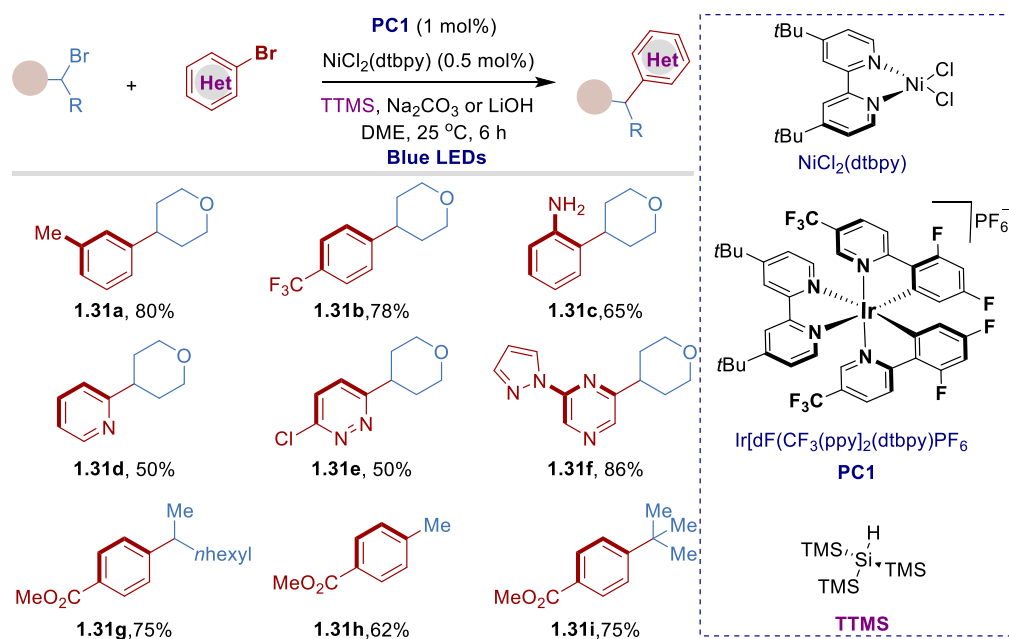
Scheme 1.30 Ni-catalyzed reductive coupling of unactivated alkyl oxalates

1.3.4 The Merger of Ni and Photoredox Dual Catalysis for Reductive Coupling Reactions

The recent interest of photoredox catalysis, especially its application to organic transformations has had a revolutionary impact on the field of homogeneous

catalysis.¹¹⁴ Particularly, the merger of nickel/photoredox dual catalysis, has emerged as a versatile platform for the development of new, highly flexible synthetic methodologies.¹¹⁵ Not surprisingly, reductive coupling reactions can also be driven with nickel/photoredox dual catalysis and allow the use of homogenous, sacrificial electron donors such as amines and silanes to be employed as reductants in place the more commonly encountered heterogeneous reductants (e.g., Zn, Mn).

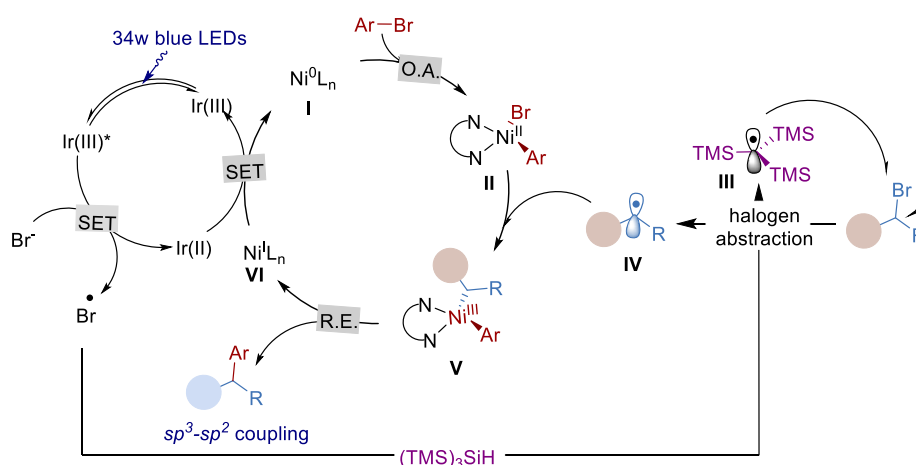
In 2016, Macmillan and co-workers developed a cross-electrophile coupling between aryl halides and alkyl halides via nickel/photoredox dual catalysis.¹¹⁶ The merger of photocatalyst **PC1** and NiCl₂(dtbpy), in the presence of tris(trimethylsilyl)silane (TTMS) under light irradiation, afforded *sp*³-*sp*² coupling products in high yield and excellent chemoselectivity. This protocol was found to be applicable to a range of structurally diverse aryl and alkyl bromides, and notably exhibited high efficiency for both sterically encumbered tertiary alkyl bromides and medicinally relevant heteroaryl bromides.



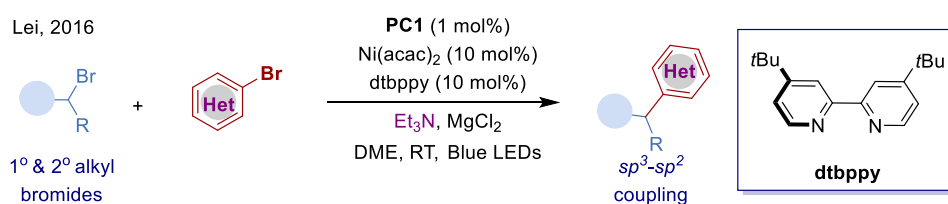
Scheme 1.31 Nickel/photoredox dual catalysis for reductive coupling of alkyl halides with aryl halides

A proposed mechanism is shown in Scheme 1.32, Ni(0) undergoes oxidative addition with aryl bromide to form Ar–Ni(II)–Br intermediate **II**. At the same time, bromide ($E_{\text{red}} = 0.80$ V vs SCE in DME) can be oxidized by the excited state of the photocatalyst $^*[\text{Ir}(\text{dF}(\text{CF}_3)\text{ppy})_2(\text{dtbbpy})]^+$ [$E_{\text{red}} (^*\text{Ir}^{\text{III}}/\text{Ir}^{\text{II}}) = 1.21$ V vs SCE in CH₃CN]

to produce bromine radical. Subsequent *hydrogen-atom-transfer* (HAT) between bromine radical and tris(trimethylsilyl)silane (TTMS) would generate a stable silyl radical **III**,¹¹⁷ which can conduct selective bromine atom abstraction from the alkyl bromide to deliver alkyl radical **IV**. The alkyl radical combine with Ar–Ni(II)–Br to generate the Ar–Ni(III)–Alkyl intermediate **V**, following reductive elimination to provide *sp*³–*sp*² coupling product and Ni(I) species. Finally, single-electron reduction by Ir^{II} species [$E_{\text{red}}(\text{Ir}^{\text{III}}/\text{Ir}^{\text{II}}) = -1.37 \text{ V vs SCE in CH}_3\text{CN}$] to form Ni(0) while simultaneously regenerating the ground-state photocatalyst **PC1**, closing both catalytic cycles.



Scheme 1.32 Mechanistic proposal for silyl-mediated cross-electrophiles coupling



Scheme 1.33 Et₃N as the terminal reductant in nickel and photoredox catalyzed reductive couplings

Concurrently, the group of Lei developed a nickel/photoredox dual catalyzed reductive cross-coupling of alkyl bromides with aryl bromides, without stoichiometric metal Mn or Zn as the reductant. In this *single-electron-transfer* (SET) process, Et₃N acts as the terminal reductant.¹¹⁸

Additionally, the scope of these strategies was extended to other organic halides¹¹⁹ and pseudohalides,¹²⁰ even for the *sp*³–*sp*³ bonds formation.¹²¹ Despite significant advances in nickel/photoredox dual catalyzed cross-electrophile coupling,

Chapter 1.

detailed mechanistic understanding remains elusive. The photocatalytic cycle is relatively well understood from previous photophysical studies, but the substrate cycle mediated by Ni remains unclear. In addition, catalytic enantioconvergent cross-electrophile coupling remains challenging.

1.4 General Aim of This Thesis

The last decade has witnessed the dramatic development of Ni-catalyzed cross-electrophile coupling reactions for the formation of C–C bonds in a highly chemo- and regio-selectivity manner. Despite the elegant advances realized, the selective construction of C_{sp3}–C_{sp3} bonds of alkyl halides remains challenging due to the similar reactivity of alkyl halides with nickel and instability of alkyl–Ni species. Moreover, the difficulty in the preparation of the corresponding alkyl halides in a chemo- and regioselective fashion and inherent toxicity of halide waste still constitute important drawbacks when designing cross-coupling reactions. Driven by the interest of our group on the development of Ni-catalyzed site-selective reductive coupling reactions, this thesis is aimed at developing new C_{sp3}–C_{sp3} bonds forming reactions in a highly chemo- and site-selectivity fashion. To such end, the following objectives will be taken into consideration:

- ★ To develop a site-selective Ni-catalyzed reductive alkylation of unactivated olefin with α -haloboronate, thus allowing incorporate the alkylboron fragments into olefin feedstocks.
- ★ To expand the scope the Ni-catalyzed reductive alkylation strategy to the utilization of alkyl amine-derivatives as alkyl electrophiles.
- ★ To unlock a multicomponent reductive coupling for the construction of two new C_{sp3}–C_{sp3} bonds in chemo- and regio-selectivity fashion via nickel/photoredox dual catalysis.

1.5 References:

1. Selected reviews on metal-catalyzed cross-coupling reactions: (a) De Meijere, A.; Bräse, S.; Oestreich, M. *Metal-Catalyzed Cross Coupling Reactions*; Wiley-VCH: Weinheim, Germany, 2004. (b) Jana, R.; Pathak, T. P.; Sigman, M. S. Advances in Transition Metal (Pd, Ni, Fe)-Catalyzed Cross-Coupling Reactions Using Alkyl-Organometallics as Reaction Partners. *Chem. Rev.* **2011**, *111*, 1417. (c) Busch, M.; Wodrich, M. D.; Corminboeuf, C. A Generalized Picture of C–C Cross-Coupling. *ACS Catal.* **2017**, *7*, 5643.
2. The Nobel Prize in Chemistry 2010 - Richard F. Heck, Ei-ichi Negishi and Akira Suzuki. https://www.nobelprize.org/nobel_prizes/chemistry/laureates/2010/press.pdf. (Accessed: 10th April 2018)
3. Selected reviews on sp^3 C–C bond formation: (a) Molander, G.; Milligan, J. A.; Phelan, J. P.; Badir, S. O. Recent Advances in Alkyl Carbon-Carbon Bond Formation by Nickel/Photoredox Cross-Coupling. *Angew. Chem. Int. Ed.* **2019**, *58*, 6152. (b) Choi, J.; Fu, G. C. Transition Metal-Catalyzed Alkyl-Alkyl Bond Formation: Another Dimension in Cross-Coupling Chemistry. *Science* **2017**, *356*, 152. (c) Hu, X. Nickel-Catalyzed Cross-Coupling of Non-Activated Alkyl Halides: A Mechanistic Perspective. *Chem. Sci.* **2011**, *2*, 1867. (d) Kambe, N.; Iwasakia, T.; Terao, J. Pd-Catalyzed Cross-Coupling Reactions of Alkyl Halides. *Chem. Soc. Rev.* **2011**, *40*, 4937. (e) Rudolph, A.; Lautens, M. Secondary Alkyl Halides in Transition-Metal-Catalyzed Cross-coupling Reactions. *Angew. Chem. Int. Ed.* **2009**, *48*, 2656. (f) Frisch, A. C.; Beller, M. Catalysts for Cross-Coupling Reactions with Non-activated Alkyl Halides. *Angew. Chem., Int. Ed.* **2005**, *44*, 674. (g) Luh, T. Y.; Leung, M. K.; Wong, K. T. Transition Metal-Catalyzed Activation of Aliphatic C–X Bonds in Carbon–Carbon Bond Formation. *Chem. Rev.* **2000**, *100*, 3187.
4. Selected reviews on reductive cross couplings: (a) Gu, J.; Wang, X.; Xue, W.; Gong, H. Nickel-Catalyzed Reductive Coupling of Alkyl Halides with Other Electrophiles: Concept and Mechanistic Considerations. *Org. Chem. Front.* **2015**, *3*, 1411. (b) Weix, J. D. Methods and Mechanisms for Cross-Electrophile Coupling of C_{sp^2} Halides with Alkyl Electrophiles. *Acc. Chem. Res.* **2015**, *48*, 1767. (c) Moragas, T.; Correa, A.; Martin, R. Metal-Catalyzed Reductive Coupling Reactions of Organic Halides with Carbonyl-Type Compounds. *Chem.* -

- Eur. J.* **2014**, *20*, 8242. (d) Knappke, C. E. I.; Grupe, S.; Gärtner, D.; Corpet, M.; Gosmini, C.; Jacobi von Wangelin, A. Reductive Cross-Coupling Reactions Between Two Electrophiles. *Chem. - Eur. J.* **2014**, *20*, 6828. (e) Liu, J.; Ye, Y.; Sessler, J. L.; Gong, H. Cross-Electrophile Couplings of Activated and Sterically Hindered Halides and Alcohol Derivatives. *Acc. Chem. Res.* **2020**, *53*, 1833. (f) Richmond, E.; Moran, J. Recent Advances in Nickel Catalysis Enabled by Stoichiometric Metallic Reducing Agents. *Synthesis* **2018**, *50*, 499.
- Wurtz, A. Ueber eine neue Klasse organischer Radicale. *Ann. Chem. Pharm.* **1855**, *96*, 364.
 - Ullmann, F.; Bielecki, J. Ueber Synthesen in der Biphenylreihe. *Chem. Ber.* **1901**, *34*, 2174.
 - Okude, Y.; Hirano, S.; Hiyama, T.; Nozaki, H. Grignard-Type Carbonyl Addition of Allyl Halides by Means of Chromous Salt. A Chemospecific Synthesis of Homoallyl Alcohols. *J. Am. Chem. Soc.* **1977**, *99*, 3179.
 - Jin, H.; Uenishi, J. I.; Christ, W. J.; Kishi, Y. Catalytic Effect of Nickel(II) Chloride and Palladium(II) Acetate on Chromium(II)-Mediated Coupling Reaction of Iodo Olefins with Aldehydes. *J. Am. Chem. Soc.* **1986**, *108*, 5644.
 - Fürstner, A.; Shi, N. A Multicomponent Redox System Accounts for the First Nozaki-Hiyama-Kishi Reactions Catalytic in Chromium. *J. Am. Chem. Soc.* **1996**, *118*, 2533.
 - Schiavon, G.; Bontempelli, G.; Corain, B. Coupling of Organic Halides Electrolyzed by the Ni(II)/Ni(I)/Ni(0)-PPh₃ System. A Mechanistic Study based on an Electroanalytical Approach. *J. Chem. Soc. Dalton Trans.* **1981**, *5*, 1074.
 - Folest, J. C.; Perichon, J.; Fauvarque, J. F.; Jutand, A. Synthèse électrochimique d'esters Arylacétique et Arylpropionique via des Complexes du Nickel. *J. Organomet. Chem.* **1988**, *342*, 259.
 - Conan, A.; Sibille, S.; d'Incan, E.; Perichon, J. Nickel-Catalysed Electroreductive Coupling of α -Halogenoesters with Aryl or Vinyl Halides. *J. Chem. Soc., Chem. Commun.* **1990**, 48.
 - Amatore, C.; Jutand, A. Activation of Carbon Dioxide by Electron Transfer and Transition Metals. Mechanism of Nickel Catalyzed Electrocarboxylation of Aromatic Halides. *J. Am. Chem. Soc.* **1991**, *113*, 2819.
 - Everson, D. A.; Weix, D. J. Cross-Electrophile Coupling: Principles of Reactivity and Selectivity. *J. Org. Chem.* **2014**, *79*, 4793.

Chapter 1.

15. Diccianni, J. B.; Diao, T. Mechanisms of Nickel-Catalyzed Cross Coupling Reactions. *Trends Chem.* **2019**, *1*, 830.
16. Selected references on Co-catalyzed reductive couplings: (a) Amatore, M.; Gosmini, C. Efficient Cobalt-Catalyzed Formation of Unsymmetrical Biaryl Compounds and Its Application in the Synthesis of a Sartan Intermediate. *Angew. Chem. Int. Ed.* **2008**, *47*, 2089. (b) Qian, X.; Auffrant, A.; Felouat, A.; Gosmini, C. Cobalt-Catalyzed Reductive Allylation of Alkyl Halides with Allylic Acetates or Carbonates. *Angew. Chem. Int. Ed.* **2011**, *50*, 10402. (c) Begouin, J.-M.; Gosmini, C. Cobalt-Catalyzed Vinylation of Aromatic Halides Using β -Halostyrene: Experimental and DFT Studies. *J. Org. Chem.* **2009**, *74*, 3221. (d) Gomes, P.; Gosmini, C.; Perichon, J. New Chemical Cross-Coupling between Aryl Halides and Allylic Acetates Using a Cobalt Catalyst. *Org. Lett.* **2003**, *5*, 1043.
17. Selected references on Pd-catalyzed reductive couplings: (a) Krasovskiy, A.; Duplais, C.; Lipshutz, B. H. Zn-Mediated, Pd-Catalyzed Cross-Couplings in Water at Room Temperature Without Prior Formation of Organozinc Reagents. *J. Am. Chem. Soc.* **2009**, *131*, 15592. (b) Krasovskiy, A.; Duplais, C.; Lipshutz, B. H. Stereoselective Negishi-like Couplings Between Alkenyl and Alkyl Halides in Water at Room Temperature. *Org. Lett.* **2010**, *12*, 4742. (c) Duplais, C.; Krasovskiy, A.; Wattenberg, A.; Lipshutz, B. H. Cross-Couplings Between Benzylic and Aryl Halides “on water”: Synthesis of Diarylmethanes. *Chem. Commun.* **2010**, *46*, 562.
18. Electrochemistry Tables.
https://chem.libretexts.org/Bookshelves/Ancillary_Materials/Reference/Reference_Table/s/Electrochemistry_Tables
19. (a) Ananikov V. P. Nickel: The "Spirited Horse" of Transition Metal Catalysis. *ACS Catal.* **2015**, *5*, 1964. (b) Tasker, S. Z.; Standley, E. A.; Jamison, T. F. Recent Advances in Homogeneous Nickel Catalysis. *Nature* **2014**, *509*, 299.
20. Wilke, G. Contributions to Organo-Nickel Chemistry. *Angew. Chem. Int. Ed.* **1988**, *27*, 185.
21. Tamaru, Y. (ed.) Modern Organonickel Chemistry (Wiley-VCH, 2005).
22. Lin, C.-Y.; Power, P. P. Complexes of Ni(I): A “Rare” Oxidation State of Growing Importance. *Chem. Soc. Rev.* **2017**, *46*, 5347.
23. Zheng, B.; Tang, F.; Luo, J.; Schultz, J. W.; Rath, N. P.; Mirica, L. M. Organometallic Nickel(III) Complexes Relevant to Cross-Coupling and Carbon–

- Heteroatom Bond Formation Reactions. *J. Am. Chem. Soc.* **2014**, *136*, 6499.
24. Camasso, N. M.; Sanford, M. S. Design, Synthesis, and Carbon–Heteroatom Coupling Reactions of Organometallic Nickel(IV) Complexes. *Science* **2015**, *347*, 1218.
25. Cornella, J.; Gomez-Bengoa, E.; Martin, R. Combined Experimental and Theoretical Study on The Reductive Cleavage of Inert C–O Bonds with Silanes: Ruling Out a Classical Ni(0)/Ni(II) Catalytic Couple and Evidence for Ni(I) Intermediates. *J. Am. Chem. Soc.* **2013**, *135*, 1997.
26. Roy, L. E.; Jakubikova, E.; Guthrie, M. G.; Batista, E. R. Calculation of One-Electron Redox Potentials Revisited. Is It Possible to Calculate Accurate Potentials with Density Functional Methods? *J. Phys. Chem. A* **2009**, *113*, 6745.
27. Poli, R.; Cacelli, I. Orbital Splitting and Pairing Energy in Open-Shell Organometallics: A Study of Two Families of 16-Electron Complexes [Cp₂M] (M = Cr, Mo, W) and [CpM(PH₃)] (M = Co, Rh, Ir). *Eur. J. Inorg. Chem.* **2005**, 2324.
28. Diccianni, J. B.; Katigbak, J.; Hu, C.; Diao, T. Mechanistic Characterization of (Xantphos)Ni(I)-Mediated Alkyl Bromide Activation: Oxidative Addition, Electron Transfer, or Halogen-Atom Abstraction. *J. Am. Chem. Soc.* **2019**, *141*, 1788.
29. Lide, D. R. (ed.) CRC Handbook of Chemistry and Physics. (ed. Lide, D. R.) (CRC Press, 2003).
30. Batsanov, S. S. Van der Waals Radii of Elements. *Inorg. Mater.* **2001**, *37*, 871.
31. Mann, J. B.; Meek, T. L.; Knight, E. T.; Capitani, J. F.; Allen, L. C. Configuration Energies of the d-Block Elements. *J. Am. Chem. Soc.* **2000**, *122*, 5132.
32. Liu, X.-W.; Echavarren, J.; Zarate, C.; Martin, R. Ni-Catalyzed Borylation of Aryl Fluorides via C–F Cleavage. *J. Am. Chem. Soc.* **2015**, *137*, 12470.
33. Rosen, B. M.; Quasdorf, K. W.; Wilson, D. A.; Zhang, N.; Resmerita, A.-M.; Garg, N. K.; Percec, V. Nickel-Catalyzed Cross-Couplings Involving Carbon-Oxygen Bonds. *Chem. Rev.* **2011**, *111*, 1346.
34. Dander, J. E.; Garg, N. K. Breaking Amides using Nickel Catalysis. *ACS Catal.* **2017**, *7*, 1413.
35. Leatherman, M. D.; Svejda, S. A.; Johnson, L. K.; Brookhart, M. Mechanistic Studies of Nickel(II) Alkyl Agostic Cations and Alkyl Ethylene Complexes: Investigations of Chain Propagation and Isomerization in (α-Diimine)Ni(II)-Catalyzed Ethylene Polymerization. *J. Am. Chem. Soc.* **2003**,

125, 3068.

36. Xu, H.W.; White, P. B.; Hu, C. T.; Diao, T. Structure and Isotope Effects of The β -H Agostic (α -Diimine)Nickel Cation as A Polymerization Intermediate. *Angew. Chem. Int. Ed.* **2017**, *56*, 1535.
37. Xu, H. W.; Hu, C. T.; Wang, X.; Diao, T. Structural Characterization of β -Agostic Bonds in Pd-Catalyzed Polymerization. *Organometallics* **2017**, *36*, 4099.
38. Ackermann, L. Modern Arylation Methods; Wiley-VCH: Weinheim, Germany, 2009.
39. McGlacken, G. P.; Bateman, L. M. Recent Advances in Aryl-Aryl Bond Formation by Direct Arylation. *Chem. Soc. Rev.* **2009**, *38*, 2447.
40. Yamaguchi, J.; Muto, K.; Itami, K. Recent Progress in Nickel-Catalyzed Biaryl Coupling. *Eur. J. Org. Chem.* **2013**, *2013*, 19.
41. Nelson, T. D.; Crouch, R. D. Cu, Ni, and Pd Mediated Homocoupling Reactions in Biaryl Syntheses: The Ullmann Reaction. *Org. React.* **2004**, *63*, 265.
42. Fillon, H.; Gosmini, C.; Perichon, J. New Chemical Synthesis of Functionalized Arylzinc Compounds from Aromatic or Thienyl Bromides under Mild Conditions Using a Simple Cobalt Catalyst and Zinc Dust. *J. Am. Chem. Soc.* **2003**, *125*, 3867.
43. Gosmini, C.; Bassene-Ernst, C.; Durandetti, M. Synthesis of Functionalized 2-Arylpyridines from 2-Halopyridines and Various Aryl Halides via A Nickel Catalysis. *Tetrahedron* **2009**, *65*, 6141.
44. Qian, Q.; Zang, Z.; Wang, S.; Chen, Y.; Lin, K.; Gong, H. Nickel-Catalyzed Reductive Cross-Coupling of Aryl Halides. *Synlett* **2013**, *24*, 619.
45. Ackerman, L. K. G.; Lovell, M. M.; Weix, D. J. Multimetallic catalysed cross-coupling of aryl bromides with aryl triflates. *Nature* **2015**, *524*, 454.
46. Bajo, S.; Laidlaw, G.; Kennedy, A. R.; Sproules, S.; Nelson, D. J. Oxidative Addition of Aryl Electrophiles to a Prototypical Nickel(0) Complex: Mechanism and Structure/Reactivity Relationships. *Organometallics* **2017**, *36*, 1662.
47. (a) Li, Z.; Zhang, S. L.; Fu, Y.; Guo, Q. X.; Liu, L. Mechanism of Ni-Catalyzed Selective C–O Bond Activation in Cross-Coupling of Aryl Esters. *J. Am. Chem. Soc.* **2009**, *131*, 8815. (b) Durr, A. B.; Yin, G. Y.; Kalvet, I.; Napoly, F.; Schoenebeck, F. Nickel-Catalyzed Trifluoromethylthiolation of C_{sp2}–O Bonds. *Chem. Sci.* **2016**, *7*, 1076. (c) Uthayopas, C.; Surawatanawong, P. Aryl C–O Oxidative Addition of Phenol Derivatives to Nickel Supported by an

- N-Heterocyclic Carbene via a Ni⁰ Five-Centered Complex. *Dalton Trans.* **2019**, *48*, 7817.
48. (a) Roy, A. H.; Hartwig, J. F. Oxidative Addition of Aryl Sulfonates to Palladium(0) Complexes of Mono- and Bidentate Phosphines. Mild Addition of Aryl Tosylates and the Effects of Anions on Rate and Mechanism. *Organometallics* **2004**, *23*, 194.
(b) Mendel, M.; Kalvet, I.; Hupperich, D.; Magnin, G.; Schoenebeck, F. Site-Selective, Modular Diversification of Polyhalogenated Aryl Fluorosulfates (ArOSO₂F) Enabled by an Air-Stable PdI Dimer. *Angew. Chem., Int. Ed.* **2020**, *59*, 2115.
49. Olivares, A. M.; Weix, D. J. Multimetallic Ni- and Pd-Catalyzed Cross-Electrophile Coupling to Form Highly Substituted 1,3-Dienes. *J. Am. Chem. Soc.* **2018**, *140*, 2446.
50. Liu, J.; Ren, Q.; Zhang, X.; Gong, H. Preparation of Vinyl Arenes by Nickel-Catalyzed Reductive Coupling of Aryl Halides with Vinyl Bromides. *Angew. Chem., Int. Ed.* **2016**, *55*, 15544.
51. Everson, D. A.; Shrestha, R.; Weix, D. J. Nickel-Catalyzed Reductive Cross-Coupling of Aryl Halides with Alkyl Halides. *J. Am. Chem. Soc.* **2010**, *132*, 920.
52. Biswas, S.; Weix, D. J. Mechanism and Selectivity in Nickel Catalyzed Cross-Electrophile Coupling of Aryl Halides with Alkyl Halides. *J. Am. Chem. Soc.* **2013**, *135*, 16192.
53. Everson, D. A.; Jones, B. A.; Weix, D. J. Replacing Conventional Carbon Nucleophiles with Electrophiles: Nickel-Catalyzed Reductive Alkylation of Aryl Bromides and Chlorides. *J. Am. Chem. Soc.* **2012**, *134*, 6146.
54. Christoffers, J.; Baro, A.; Eds. Quaternary Stereocenters-Challenges and Solutions for Organic Synthesis; Wiley-VCH: Weinheim, 2005.
55. Wang, X.; Wang, S.; Xue, W.; Gong, H. Nickel-Catalyzed Reductive Coupling of Aryl Halides with Unactivated Tertiary Alkyl Halides. *J. Am. Chem. Soc.* **2015**, *137*, 11562.
56. Wang, X.; Ma, G.; Peng, Y.; Pitsch, C. E.; Moll, B. J.; Ly, T. D.; Wang, X.; Gong, H. Ni-Catalyzed Reductive Coupling of Electron-Rich Aryl Iodides with Tertiary Alkyl Halides. *J. Am. Chem. Soc.* **2018**, *140*, 14490.

Chapter 1.

57. Janssen-Müller, D.; Sahoo, B.; Sun, S. -Z.; Martin, R. Tackling Remote sp^3 C–H Functionalization via Ni-Catalyzed “Chain-Walking” Reactions. *Isr. J. Chem.* **2020**, *60*, 195.
58. Lu, X.; Yi, J.; Zhang, Z.-Q.; Dai, J.-J.; Liu, J. H.; Xiao, B.; Fu, Y.; Liu, L. Expedient Synthesis of Chiral α -Amino Acids through Nickel-Catalyzed Reductive Cross-Coupling. *Chem. Eur. J.* **2014**, *20*, 15339.
59. Li, X.; Feng, Z.; Jiang, Z. X.; Zhang, X. Nickel-Catalyzed Reductive Cross-Coupling of (Hetero)Aryl Iodides with Fluorinated Secondary Alkyl Bromides. *Org. Lett.* **2015**, *17*, 5570.
60. Molander, G. A.; Traister, K. M.; O’Neill, B. T. Engaging Nonaromatic, Heterocyclic Tosylates in Reductive Cross-Coupling with Aryl and Heteroaryl Bromides. *J. Org. Chem.* **2015**, *80*, 2907.
61. Zhang, J.; Lu, G.; Xu, J.; Sun, H.; Shen, Q. Nickel-Catalyzed Reductive Cross-Coupling of Benzyl Chlorides with Aryl Chlorides/Fluorides: A One-Pot Synthesis of Diarylmethanes. *Org. Lett.* **2016**, *18*, 2860.
62. Molander, G. A.; Wisniewski, S. R.; Traister, K. M. Reductive Cross-Coupling of 3-Bromo-2,1-borazaronaphthalenes with Alkyl Iodides. *Org. Lett.*, **2014**, *16*, 3692.
63. Johnson, K. A.; Biswas, S.; Weix, D. J. Cross-Electrophile Coupling of Vinyl Halides with Alkyl Halides. *Chem. Eur. J.* **2016**, *22*, 7399.
64. Qiu, C.; Yao, K.; Zhang, X.; Gong, H. Ni-Catalyzed Reductive Coupling of α -Halocarbonyl Derivatives with Vinyl Bromides. *Org. Biomol. Chem.* **2016**, *14*, 11332.
65. Liu, J.; Gong, H. Stereoselective Preparation of α -C-Vinyl/Aryl Glycosides via Nickel Catalyzed Reductive Coupling of Glycosyl Halides with Vinyl and Aryl Halides. *Org. Lett.* **2018**, *20*, 7991.
66. Liu, J.; Lei, C.; Gong, H. Nickel-Catalyzed Reductive Coupling of Glucosyl Halides with Aryl/Vinyl Halides Enabling β -Selective Preparation of C-Aryl/Vinyl Glucosides. *Sci. China. Chem.* **2019**, *62*, 1492.
67. Goldup, S. M.; Leigh, D. A.; McBurney, R. T.; McGonigal, P. R.; Plant, A. Ligand-Assisted Nickel-Catalysed Sp^3 – Sp^3 Homocoupling of Unactivated Alkyl Bromides and Its Application to The Active Template Synthesis of Rotaxanes. *Chem. Sci.* **2010**, *1*, 383.

68. Prinsell, M. R.; Everson, D. A.; Weix, D. J. Nickel-Catalyzed, Sodium Iodide-Promoted Reductive Dimerization of Alkyl Halides, Alkyl Pseudohalides, and Allylic Acetates. *Chem. Commun.* **2010**, *46*, 5743.
69. Yu, X.; Yang, T.; Wang, S.; Xu, H.; Gong, H. Nickel-Catalyzed Reductive Cross-Coupling of Unactivated Alkyl Halides. *Org. Lett.* **2011**, *14*, 2138.
70. Xu, H.; Zhao, C.; Qian, Q.; Deng, W.; Gong, H. Nickel-Catalyzed Cross-Coupling of Unactivated Alkyl Halides Using Bis(pinacolato)diboron as Reductant. *Chem. Sci.* **2013**, *4*, 4022.
71. Liang, Z.; Xue, W.; Lin, K.; Gong, H. Nickel-Catalyzed Reductive Methylation of Alkyl Halides and Acid Chlorides with Methyl *p*-Tosylate. *Org. Lett.* **2014**, *16*, 5620.
72. Xue, W.; Xu, H.; Liang, Z.; Qian, Q.; Gong, H. Nickel-Catalyzed Reductive Cyclization of Alkyl Dihalides. *Org. Lett.* **2014**, *16*, 4984.
73. Wotal, A. C.; Weix, D. J. Synthesis of Functionalized Dialkyl Ketones from Carboxylic Acid Derivatives and Alkyl Halides. *Org. Lett.* **2012**, *14*, 1476.
74. Lu, W.; Liang, Z.; Zhang, Y.; Wu, F.; Qian, Q.; Gong, H. Gram-Scale Ketone Synthesis by Direct Reductive Coupling of Alkyl Iodides with Acid Chlorides. *Synthesis* **2013**, *45*, 2234.
75. Jai, X.; Zhang, X.; Qian, Q.; Gong, H. Alkyl–Aryl Ketone Synthesis via Nickel-Catalyzed Reductive Coupling of Alkyl Halides with Aryl Acids and Anhydrides. *Chem. Commun.* **2015**, *51*, 10302.
76. Zhao, C.; Jia, X.; Wang, X.; Gong, H. Ni-Catalyzed Reductive Coupling of Alkyl Acids with Unactivated Tertiary Alkyl and Glycosyl Halides. *J. Am. Chem. Soc.* **2014**, *136*, 17645.
77. Aresta, M. Carbon Dioxide as Chemical Feedstock, Wiley-VCH Verlag GmbH, 2010.
78. (a) Liu, Q.; Wu, L.; Jackstell, R.; Beller, M. Using Carbon Dioxide as A Building Block in Organic Synthesis. *Nat. Commun.* **2015**, *6*, 5933. (b) Tsuji, Y.; Fujihara, T. Carbon Dioxide as A Carbon Source in Organic Transformation: Carbon–Carbon Bond Forming Reactions by Transition-Metal Catalysts. *Chem. Commun.* **2012**, *48*, 9956.
79. Osakada, K.; Sato, R.; Yamamoto, T. Nickel-Complex-Promoted Carboxylation of Haloarenes Involving Insertion of CO₂ into NiII-C Bonds. *Organometallics*, **1994**, *13*, 4645.

80. (a) Tortajada, A.; Juliá-Hernández, F.; Börjesson, M.; Moragas, T.; Martin, R. Transition-Metal-Catalyzed Carboxylation Reactions with Carbon Dioxide. *Angew. Chem. Int. Ed.* **2018**, *57*, 15948. (b) Juliá-Hernández, F.; Gaydou, M.; Serano, E.; van Gemmeren, M.; Martin, R. Ni- and Fe-catalyzed Carboxylation of Unsaturated Hydrocarbons with CO₂. *Top. Curr. Chem.* **2016**, *374*, 45. (c) Börjesson, M.; Moragas, T.; Gallego, D.; Martin, R. Metal-Catalyzed Carboxylation of Organic (Pseudo)halides with CO₂. *ACS Catal.* **2016**, *6*, 6739.
81. Correa, A.; Martin, R. Palladium-Catalyzed Direct Carboxylation of Aryl Bromides with Carbon Dioxide. *J. Am. Chem. Soc.* **2009**, *131*, 15974.
82. Fujihara, T.; Nogi, K.; Xu, T.; Terao, J.; Tsuji, Y. Nickel-Catalyzed Carboxylation of Aryl and Vinyl Chlorides Employing Carbon Dioxide. *J. Am. Chem. Soc.* **2012**, *134*, 9106.
83. Leon, T.; Correa, A.; Martin, R. Ni-Catalyzed Direct Carboxylation of Benzyl Halides with CO₂. *J. Am. Chem. Soc.* **2013**, *135*, 1221.
84. Liu, Y.; Cornella, J.; Martin, R. Ni-Catalyzed Carboxylation of Unactivated Primary Alkyl Bromides and Sulfonates with CO₂. *J. Am. Chem. Soc.* **2014**, *136*, 11212.
85. Borjesson, M.; Moragas, T.; Martin, R. Ni-Catalyzed Carboxylation of Unactivated Alkyl Chlorides with CO₂. *J. Am. Chem. Soc.* **2016**, *138*, 7504.
86. Moragas, T.; Martin, R. Nickel-Catalyzed Reductive Carboxylation of Cyclopropyl Motifs with Carbon Dioxide. *Synthesis* **2016**, *48*, 2816.
87. (a) Correa, A.; León, T.; Martin, R. Ni-Catalyzed Carboxylation of C(sp²)- and C(sp³)-O Bonds with CO₂. *J. Am. Chem. Soc.* **2014**, *136*, 1062. (b) Moragas, T.; Cornella, J.; Martin, R. Ligand-Controlled Regiodivergent Ni-Catalyzed Reductive Carboxylation of Allyl Esters with CO₂. *J. Am. Chem. Soc.* **2014**, *136*, 17702. (c) van Gemmeren, M.; Borjesson, M.; Tortajada, A.; Sun, S.-Z.; Okura, K.; Martin, R. Switchable Site-Selective Catalytic Carboxylation of Allylic Alcohols with CO₂. *Angew. Chem. Int. Ed.* **2017**, *56*, 6558.
88. Moragas, T.; Gaydou, M.; Martin, R. Nickel-Catalyzed Carboxylation of Benzylic C-N Bonds with CO₂. *Angew. Chem. Int. Ed.* **2016**, *55*, 5053.
89. Wang, X.; Liu, Y.; Martin, R. Ni-Catalyzed Divergent Cyclization/Carboxylation of Unactivated Primary and Secondary Alkyl Halides with CO₂. *J. Am. Chem. Soc.* **2015**, *137*, 6476.

90. Cherney, A. H.; Kadunce, N. T.; Reisman, S. E. Catalytic Asymmetric Reductive Acyl Cross-Coupling: Synthesis of Enantioenriched Acyclic α , α -Disubstituted Ketones. *J. Am. Chem. Soc.* **2013**, *135*, 7442.
91. Cherney, A. H.; Reisman, S. E. Nickel-Catalyzed Asymmetric Reductive Cross-Coupling Between Vinyl and Benzyl Electrophiles. *J. Am. Chem. Soc.* **2014**, *136*, 14365.
92. Poremba, K. E.; Kadunce, N. T.; Suzuki, N.; Cherney, A. H.; Reisman, S. E. Nickel-Catalyzed Asymmetric Reductive Cross-Coupling to Access 1,1-Diarylalkanes. *J. Am. Chem. Soc.* **2017**, *139*, 5684.
93. Kadunce, N. T.; Reisman, S. E. Nickel-Catalyzed Asymmetric Reductive Cross-Coupling between Heteroaryl Iodides and α -Chloronitriles. *J. Am. Chem. Soc.* **2015**, *137*, 10480.
94. Poremba, K. E.; Dibrell, S. E.; Reisman, S. E. Nickel-Catalyzed Enantioselective Reductive Cross-Coupling Reactions. *ACS Catal.* **2020**, *10*, 8237.
95. Selected reviews on decarboxylative cross-coupling reactions: (a) Rodríguez, N.; Goossen, L. J. Decarboxylative Coupling Reactions: A Modern Strategy for C–C Bond Formation. *Chem Soc Rev.* **2011**, *40*, 5030. (b) Shang, R.; Liu, L. Transition Metal-Catalyzed Decarboxylative Cross-Coupling Reactions. *Sci. China Chem.* **2011**, *54*, 1670. (c) Guo, L.; Rueping, M. Transition-Metal-Catalyzed Decarboxylative Coupling Reactions: Concepts, Classifications, and Applications. *Chem. Eur. J.* **2018**, *24*, 7794. (d) Moon, P. J.; Lundgren, R. J. Metal-Catalyzed Ionic Decarboxylative Cross-Coupling Reactions of C(sp³) Acids: Reaction Development, Mechanisms, and Application. *ACS Catal.* **2020**, *10*, 1742.
96. Murarka, S. *N*-(Acyloxy)phthalimides as Redox-Active Esters in Cross-Coupling Reactions. *Adv. Synth. Catal.* **2018**, *36*, 1735.
97. Okada, K.; Okamoto, K.; Morita, N.; Okubo, K.; Oda, M. Photosensitized Decarboxylative Michael Addition Through *N*-(acyloxy)phthalimides via An Electron-Transfer Mechanism. *J. Am. Chem. Soc.* **1991**, *113*, 9401.
98. Pratsch, G.; Lackner, G. L.; Overman, L. E. Constructing Quaternary Carbons from *N*-(Acyloxy)phthalimide Precursors of Tertiary Radicals Using Visible-Light Photocatalysis. *J. Org. Chem.* **2015**, *80*, 6025.
99. Cornella, J.; Edwards, J.; Qin, T.; Kawamura, S.; Wang, J.; Pan, C.-M.; Gianatassio, R.; Schmidt, M.; Eastgate, M. D.; Baran, P. S. Practical Ni-Catalyzed Aryl–Alkyl

- Cross-Coupling of Secondary Redox-Active Esters. *J. Am. Chem. Soc.* **2016**, *138*, 2174.
110. Huihui, K. M. M.; Caputo, J. A.; Melchor, Z.; Olivares, A. M.; Spiewak, A. M.; Johnson, K. A.; DiBenedetto, T. A.; Kim, S.; Ackerman, L. K. G.; Weix, D. J. Decarboxylative Cross-Electrophile Coupling of *N*-Hydroxyphthalimide Esters with Aryl Iodides. *J. Am. Chem. Soc.* **2016**, *138*, 5016.
101. Huang, L.; Olivares, A. M.; Weix, D. J. Reductive Decarboxylative Alkynylation of *N*-Hydroxyphthalimide Esters with Bromoalkynes. *Angew. Chem. Int. Ed.* **2017**, *56*, 11901.
102. Wang, J.; Cary, B. P.; Beyer, P.; Gellman, S. H.; Weix, D. J. Ketones from Nickel-Catalyzed Decarboxylative, Non-Symmetric Cross-Electrophile Coupling of Carboxylic Acid Esters. *Angew. Chem. Int. Ed.* **2019**, *58*, 12081.
103. Suzuki, N.; Hofstra, J. L.; Poremba, K. E.; Reisman, S. E. Nickel-Catalyzed Enantioselective Cross-Coupling of *N*-Hydroxyphthalimide Esters with Vinyl Bromides. *Org. Lett.* **2017**, *19*, 2150.
104. Tortajada, A.; Duan, Y.; Sahoo, B.; Cong, F.; Toupalas, G.; Sallustrau, A.; Loreau, O.; Audisio, D.; Martin, R. Catalytic Decarboxylation/Carboxylation Platform for Accessing Isotopically Labeled Carboxylic Acids. *ACS Catal.* **2019**, *9*, 5897.
105. Selected reviews on C–O bond cleavage: (a) Cornella, J.; Zarate, C.; Martin, R. Metal-Catalyzed Activation of Ethers via C–O bond Cleavage: A New Strategy for Molecular Diversity. *Chem. Soc. Rev.* **2014**, *43*, 8081. (b) Zarate, C.; van Gemmeren, M.; Somerville, R. J.; Martin, R. Phenol Derivatives: Modern Electrophiles in Cross-Coupling Reactions. *Advances in Organometallic Chemistry*, Elsevier, **2016**, *66*, 143.
106. Selected references: (a) Gu, Y.; Martin, R. Ni-Catalyzed Stannylation of Aryl Esters via C–O Bond Cleavage. *Angew. Chem., Intl. Ed.* **2017**, *56*, 3187. (b) Zárate, C.; Manzano, R.; Martin, R. *Ips*o-Borylation of Aryl Ethers via Ni-Catalyzed C–OMe Cleavage. *J. Am. Chem. Soc.* **2015**, *137*, 6754. (c) Correa, A.; Martín, R. Ni-Catalyzed Direct Reductive Amidation via C–O bond Cleavage. *J. Am. Chem. Soc.* **2014**, *136*, 7253. (d) Zárate, C.; Martin, R. A Mild Ni/Cu-Catalyzed Silylation via C–O Cleavage. *J. Am. Chem. Soc.* **2014**, *136*, 2236.
107. Tobisu, M.; Chatani, N. Cross-Couplings Using Aryl Ethers via C–O Bond Activation Enabled by Nickel Catalysts. *Acc. Chem. Res.* **2015**, *48*, 1717.

108. Yu, D.-G.; Li, B.-J.; Shi, Z.-J. Exploration of New C–O Electrophiles in Cross-Coupling Reactions. *Acc. Chem. Res.* **2010**, *43*, 1486.
109. Barton, D. H. R.; Crich, D. The Invention of New Radical Chain Reactions. Part 9. Further Radical Chemistry of Thiohydroxamic Esters; Formation of Carbon–Carbon Bonds. *J. Chem. Soc., Perkin Trans. 1*, **1986**, 1603.
110. Jamison, C. R.; Overman, L. E. Fragment Coupling with Tertiary Radicals Generated by Visible-Light Photocatalysis. *Acc. Chem. Res.* **2016**, *49*, 1578.
111. Nawrat, C. C.; Jamison, C. R.; Slutskyy, Y.; MacMillan, D. W. C.; Overman, L. E. Oxalates as Activating Groups for Alcohols in Visible Light Photoredox Catalysis: Formation of Quaternary Centers by Redox-Neutral Fragment Coupling. *J. Am. Chem. Soc.* **2015**, *137*, 11270.
112. Ye, Y.; Chen, H.; Sessler, J. L.; Gong, H. Zn-Mediated Fragmentation of Tertiary Alkyl Oxalates Enabling Formation of Alkylated and Arylated Quaternary Carbon Centers. *J. Am. Chem. Soc.* **2019**, *141*, 820.
113. Gao, M.; Sun, D.; Gong, H. Ni-Catalyzed Reductive C–O Bond Arylation of Oxalates Derived from α -Hydroxy Esters with Aryl Halides. *Org. Lett.* **2019**, *21*, 1645.
114. Reviews for on photochemical events: (a) Karkas, M. D.; Porco, J. A.; Stephenson, C. R. J. Photochemical Approaches to Complex Chemotypes: Applications in Natural Product Synthesis. *Chem. Rev.* **2016**, *116*, 9683. (b) Skubi, K. L.; Blum, T. R.; Yoon, T. P. Dual Catalysis Strategies in Photochemical Synthesis. *Chem. Rev.* **2016**, *116*, 10035. (c) Romero, N. A.; Nicewicz, D. A.; Organic Photoredox Catalysis. *Chem. Rev.* **2016**, *116*, 10075. (d) Marzo, L.; Pagore, S. K.; Reiser, O.; König, B. Visible-Light Photocatalysis: Does It Make a Difference in Organic Synthesis? *Angew. Chem. Int. Ed.* **2018**, *57*, 10034.
115. (a) Milligan, J. A.; Phelan, J. P.; Badir, S. O.; Molander, G. A. Alkyl Carbon-Carbon Bond Formation by Nickel/Photoredox Cross-Coupling. *Angew. Chem. Int. Ed.* **2019**, *58*, 6152. (b) Twilton, J.; Le, C.; Zhang, P.; Shaw, M. H.; Evans, R. W.; MacMillan, D. W. C. The Merger of Transition Metal and Photocatalysis. *Nat. Rev. Chem.* **2017**, *1*, 0052. (c) Prier, C. K.; Rankic, D. A.; MacMillan, D. W. C. Visible Light Photoredox Catalysis with Transition Metal Complexes: Applications in Organic Synthesis. *Chem. Rev.* **2013**, *113*, 5322. (d) Cheng, W.-M.; Shang, R. Transition Metal-Catalyzed Organic Reactions under Visible Light: Recent Developments and Future Perspectives. *ACS Catal.* **2020**,

Chapter 1.

10, 9170.

116. Zhang, P.; Le, C. C.; MacMillan, D. W. C. Silyl Radical Activation of Alkyl Halides in Metallaphotoredox Catalysis: A Unique Pathway for Cross-Electrophile Coupling. *J. Am. Chem. Soc.* **2016**, *138*, 8084.
117. (a) Chatgililoglu, C. *Organosilanes in Radical Chemistry*; Wiley: Chichester, U. K., 2004. (b) Chatgililoglu, C.; Lalevee, J. Recent Applications of the (TMS)₃SiH Radical-Based Reagent. *Molecules* **2012**, *17*, 527.
118. Duan, Z.; Li, W.; Lei, A. Nickel-Catalyzed Reductive Cross-Coupling of Aryl Bromides with Alkyl Bromides: Et₃N as the Terminal Reductant. *Org. Lett.* **2016**, *18*, 4012.
119. Bacauanu, V.; Cardinal, S.; Yamauchi, M.; Kondo, M.; Fernández, D. F.; Remy, R.; MacMillan, D. W. C. Metallaphotoredox Difluoromethylation of Aryl Bromides. *Angew. Chem. Intl. Ed.* **2018**, *57*, 12543.
120. (a) Yi, J.; Badir, S. O.; Kammer, L. M.; Ribagorda, M.; Molander, G. A. Deaminative Reductive Arylation Enabled by Nickel/Photoredox Dual Catalysis. *Org. Lett.* **2019**, *21*, 3346. (b) Parasram, M.; Shields, B. J.; Ahmad, O.; Knauber, T.; Doyle, A. G. Regioselective Cross-Electrophile Coupling of Epoxides and (Hetero)aryl Iodides via Ni/Ti/Photoredox Catalysis. *ACS Catal.* **2020**, *10*, 5821. (c) Sahoo, B.; Bellotti, P.; Juliá-Hernández, F.; Meng, Q.-Y.; Crespi, S.; König, B.; Martin, R. Site-Selective, Remote *sp*³ C–H Carboxylation Enabled by The Merger of Photoredox and Nickel Catalysis. *Chem. Eur. J.* **2019**, *25*, 9001.
121. (a) Smith, R. T.; Zhang, X.; Rincón, J. A.; Agejas, J.; Mateos, C.; Barberis, M.; García-Cerrada, S.; de Frutos, O.; MacMillan, D. W. C. Metallaphotoredox Catalyzed Cross-Electrophile C_{sp3}–C_{sp3} Coupling of Aliphatic Bromides. *J. Am. Chem. Soc.* **2018**, *140*, 17433. (b) Sakai, H.; Liu, W.; Le, C.; MacMillan, D. W. C. Cross-Electrophile Coupling of Unactivated Alkyl Chlorides. *J. Am. Chem. Soc.* **2020**, *142*, 11691.

Chapter 2

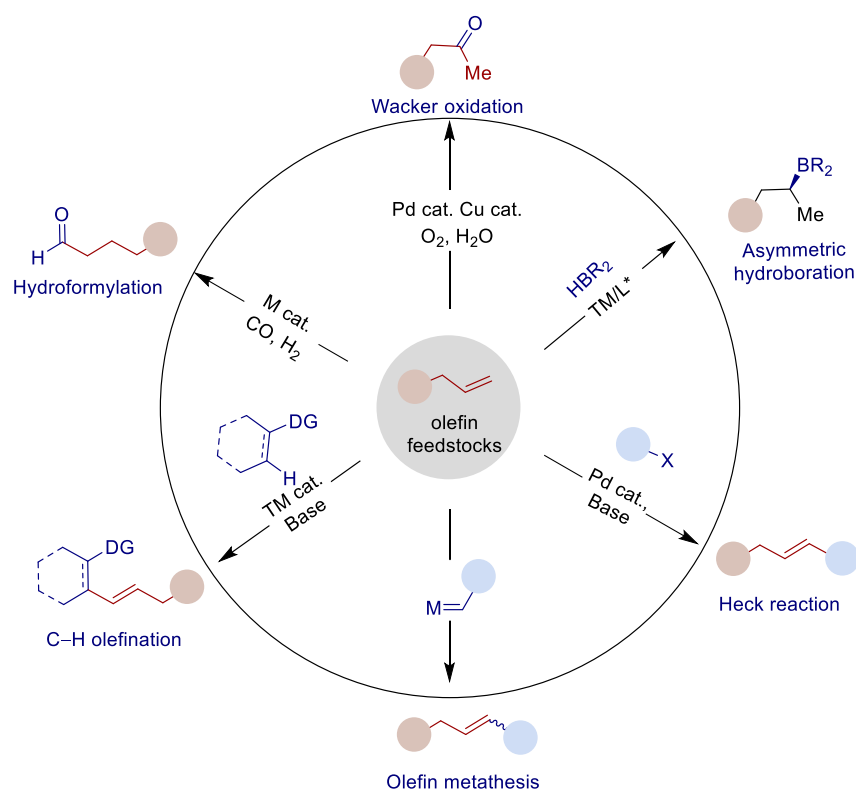
Site-Selective Ni-Catalyzed Reductive Coupling of α -Haloboranes with Unactivated Olefins

2.1 General Introduction

Transition-metal-catalyzed cross-coupling reactions of electrophiles with organometallic reagents to forge C–C bond has emerged as an important transformation strategy in organic synthetic chemistry over past decades.¹ However, the efficient protocols for the construction of C_{sp^3} centers under mild conditions remains challenging.² Despite great advances realized in recent years, the require of stoichiometric organometallic reagents has led to several limitations for their wide applications. Therefore, chemists have undertaken efforts to explore alternative stable and easily accessible coupling partners for the construction of sp^3 C–C bond.

Olefins are among the most abundant organic compounds, available in bulk quantities from petrochemical feedstocks and renewable resources.³ They are also widely present as functional groups in natural products and pharmaceuticals. Beyond their abundance, the unique chemical reactivity of olefins has attracted chemists' attention, which can be seen with the multitude of reactions that implement the olefin motif synthons to achieve a series of chemical transformations.⁴ of these reactions, transition-metals have demonstrated an exceptional ability to activate the olefin double bonds leading to highly elegant and useful reactions. Famous examples include the Wacker process,⁵ asymmetric hydroborylation,⁵ Heck reaction,⁷ olefin metathesis,^{4e, 8} olefin hydroformylation⁹ and C–H olefination^{4a,4b,10} that have been extensively used in the preparation of complex organic molecules both in academic and industrial settings (Scheme 2.1). These reactions have established olefins to present a central role in modern synthetic organic chemistry as well as the fine chemical industry.¹¹ Driven by these advantages, the development of new methodology for catalytic sp^3 C–C bond formation by using olefins feedstocks as starting materials are of great commercial interest.

*Site-Selective Ni-Catalyzed Reductive
Coupling of α -Haloboranes with Unactivated Olefins*



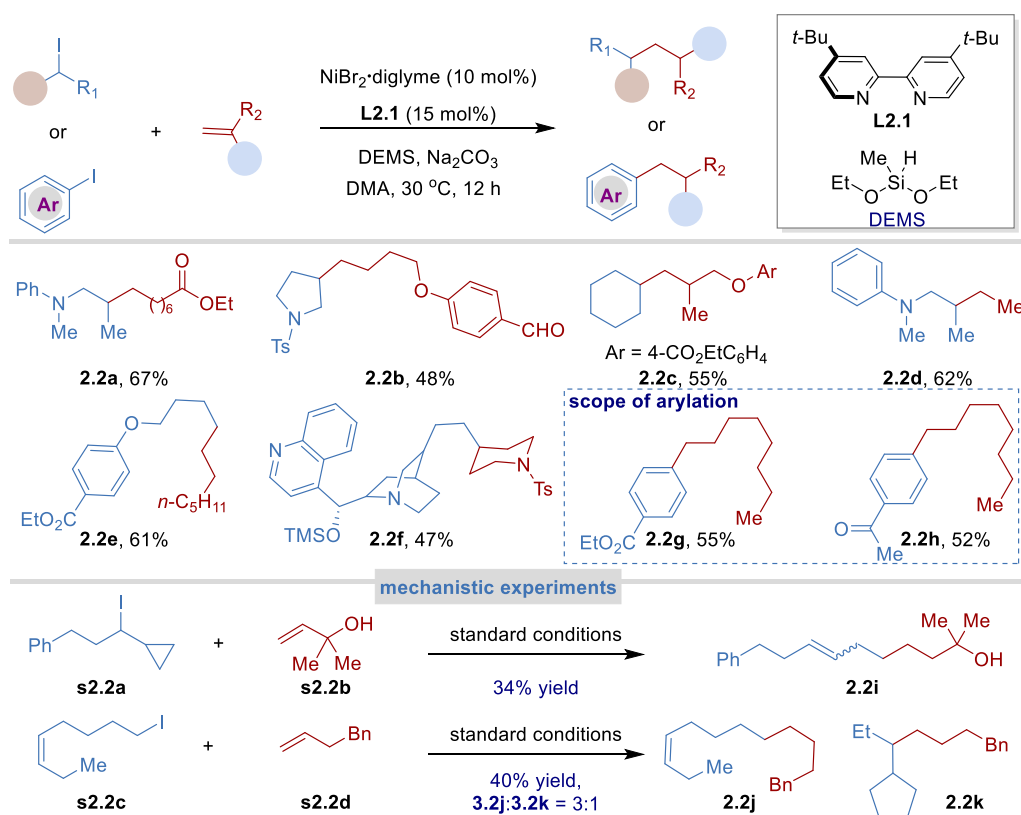
Scheme 2.1 Metal-catalyzed functionalization of olefin feedstocks

2.2 Ni-Catalyzed Reductive Coupling of Olefins

Over the past decades, transition-metal-catalyzed hydrofunctionalization of olefins has been extensively developed as an efficient and prevailing method to convert abundant alkene feedstocks to high-value chemicals.¹² The concepts behind these processes are that alkenes are reduced *in-situ* to form olefin-derived nucleophiles, which provide an alternative to the use of stoichiometric organometallic reagents in cross-coupling reactions¹³ or metal-hydride species to transfer hydrogen atoms (H•) to alkenes which form alkyl radicals¹⁴. Specifically, Fe–H,¹⁵ Co–H¹⁶ and Cu–H¹⁷ based catalysts have become powerful tools for hydrofunctionalization chemistry. In contrast, Ni-catalyzed hydrofunctionalization of olefins is rarely reported, and only very recently been realized.¹⁸

2.2.1 Ni-Catalyzed *anti*-Markovnikov Hydrofunctionalization of Olefins

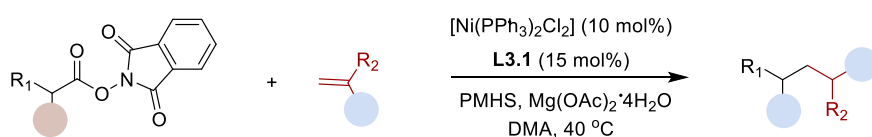
In 2016, Liu, Fu and co-workers pioneeringly reported a catalytic reductive hydrocarbonation of unactivated olefins with alkyl or aryl electrophiles in an *anti*-Markovnikov fashion (Scheme 2.2).¹⁹ The combination of NiBr₂·diglyme and bipyridine ligand (**L2.1**) catalysis, with diethoxymethylsilane (DEMS) as the hydride source, avoided the use of any organometallic reagent, and yielded *anti*-Markovnikov selectivity products in high chemo- and regio-selectivity, thus unlocking a new catalytic platform to forge C_{sp2}–C_{sp3} and C_{sp3}–C_{sp3} linkages. This protocol shown a broad substrate scope and high functional group tolerance, and were even able to demonstrate the utility of their reaction in the context of ethylene valorization or late-stage functionalization. In order to gain more insights into the reaction mechanism, the authors carried out radical clock experiments. Ring-opened product was obtained by using the substrate which contains a cyclopropyl ring (**s2.2a**). While a mixture of linear product and ring-closed product was obtained in a 3:1 ratio when using (*Z*)-8-iodooct-3-ene (**s2.2c**) as substrate. These results suggested that the reaction occurs through a radical process. Nonetheless, details for the mechanism of this reductive hydrocarbonation are not clear at present.



Scheme 2.2 Ni-catalyzed hydroalkylation/arylation of olefins with organic halides

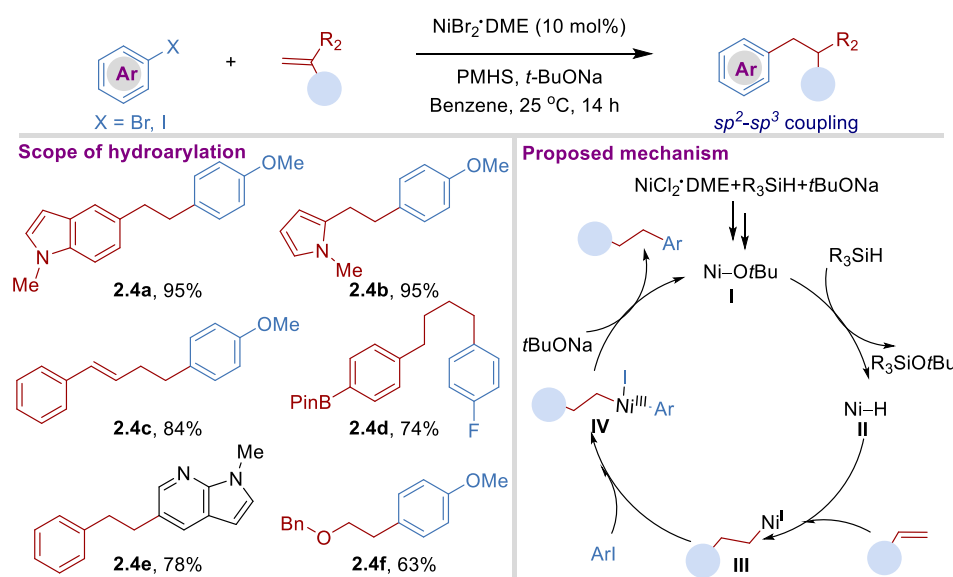
*Site-Selective Ni-Catalyzed Reductive
Coupling of α -Haloboranes with Unactivated Olefins*

Aiming to expand the catalytic reductive hydrocarbonation portfolio beyond the utilization of organic halides, the same group developed a Ni-catalyzed reductive decarboxylative hydroalkylation of olefin feedstocks with *N*-(acyloxy)phthalimides (NHPI) esters, which were derivatized from the corresponding carboxylic acids (Scheme 2.3).²⁰ In this case, polymethylhydrosiloxane (PMHS) was used as hydride source. An interesting finding was the use of $\text{Mg}(\text{OAc})_2 \cdot 4\text{H}_2\text{O}$ as a base, demonstrating that this reaction was insensitive to moisture. However, it was unclear whether the magnesium ion plays a unique role in the reaction.



Scheme 2.3 Ni-catalyzed decarboxylative hydroalkylation of olefin feedstocks

Inspired by Liu's work, the group of Lalic reported a Ni-catalyzed *anti*-Markovnikov hydroarylation of olefin feedstocks (Scheme 2.4).²¹ In this case, the utilization of $\text{NiBr}_2 \cdot \text{DME}$ as precatalyst, in the absence of ligands and using polymethylhydrosiloxane (PMHS) as hydride source, provided the linear arylation product in high regioselectivity. Linear selectivity was obtained with a wide range of olefins, including styrenes, enol ethers as well as unactivated olefins. Interestingly, 1,3-diene could be used in this protocol, providing the hydroarylation product in good yield and regio-selectivity. Preliminary mechanistic experiments suggested that this reductive *anti*-Markovnikov hydroarylation protocol involved hydrometallation of the olefin, followed by coupling of the alkyl nickel intermediate with an aryl halide.



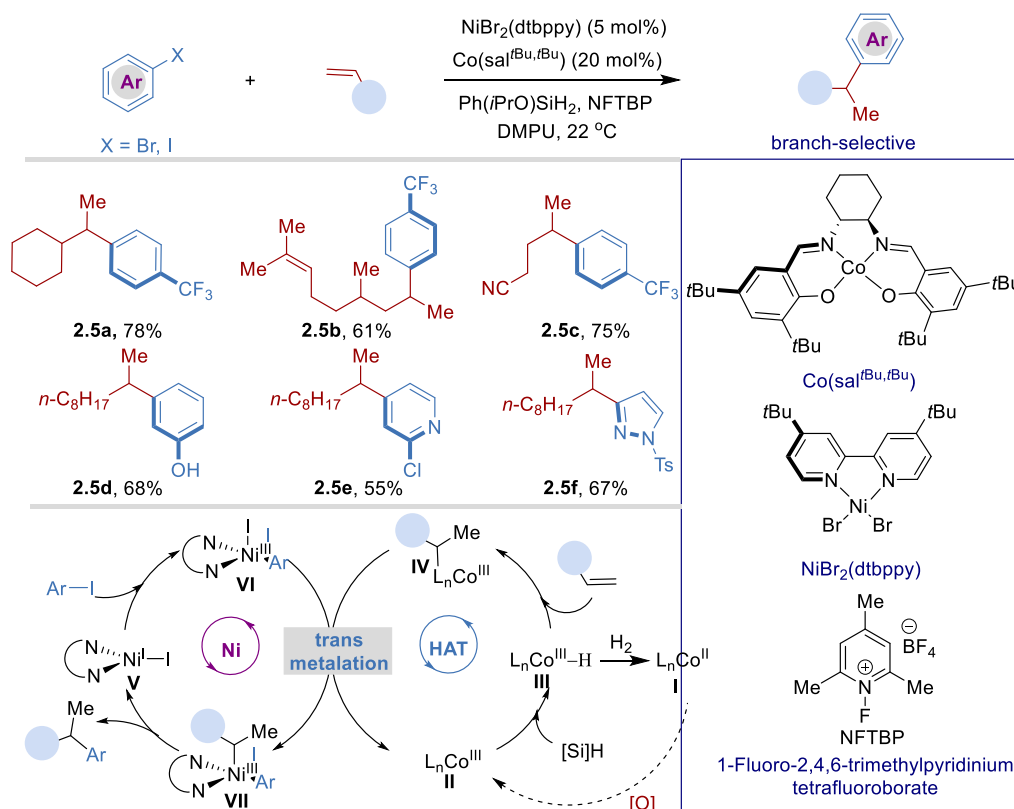
Scheme 2.4 Ni-catalyzed *anti*-Markovnikov hydroarylation of olefin feedstocks with aryl halides

2.2.2 Ni-Catalyzed Markovnikov-Selective Hydrofunctionalization of Olefins

Driven by the advances of high chemo- and regio-selectivity, metal hydride hydrogen atom transfer (MH HAT) reactions with olefins for the construction of C–C bonds have raised chemist interests.^{14,22} In 2016, the group of Shenvi reported the first Markovnikov-selective hydroarylation of unactivated terminal olefins and aryl iodides that relies on the union of Co–H HAT and nickel dual catalysis (Scheme 2.5).²³ In this case, Co(Sal^{*t*Bu}, ^{*t*Bu}) was the only effective MH HAT catalyst and required 1-fluoro-2,4,6-trimethylpyridinium tetrafluoroborate (NFTBP) as an oxidant for the Co(II)/Co(III) cycle. Moreover, Ph(*i*PrO)SiH₂ was required for hydrogen atom transfer (HAT) catalysis and reduction of Ni(II) species. This protocol presented a wide range of substrate scope with highly chemo- and regio-selectivity. Unfortunately, it is only effective with terminal olefins, however, 1,1-di-substituted olefins and internal olefins were unreactive under their reaction conditions. Mechanistic studies suggested that the reaction proceeds via direct transmetalation between Co–alkyl and Ar–Ni(III)–X.²⁴ The Co(II)(Sal^{*t*Bu}, ^{*t*Bu}) precatalyst is oxidized to Co(III) by NFTBP, and the catalytically active Co(III)–H is then generated via reaction with Ph(*i*PrO)SiH₂. HAT then occurs between the alkene and Co(III)–H leading to the formation of a caged carbon-radical/Co(II) pair. This caged radical pair collapses to form a metastable organocobalt complex IV. Then transmetalation of organocobalt

*Site-Selective Ni-Catalyzed Reductive
Coupling of α -Haloboranes with Unactivated Olefins*

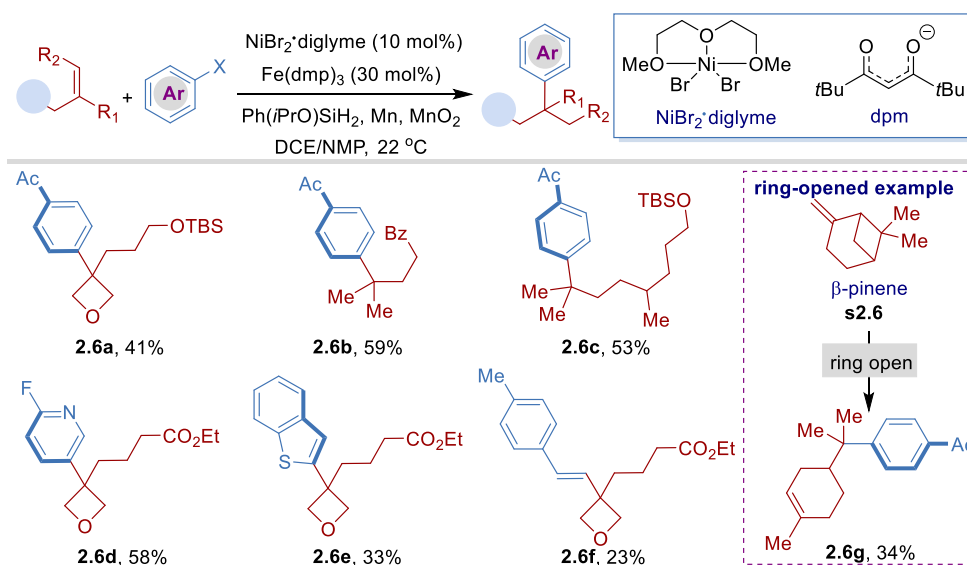
complex with Ar–Ni(III)–I species, to form Ar–Ni(III)–Alkyl intermediate **VII**. Followed by reductive elimination of Ar–Ni(III)–Alkyl complex to provide branched arylation product and Ni(I) species. Finally, the resulting Co(III) can react with the hydrosilane reagent to regenerate Co(III)–H and turn over the cobalt cycle.



Scheme 2.5 Ni/Co dual catalyzed hydroarylation of terminal olefins with aryl iodides

All-carbon quaternary centers are a key structure element that are widely present in natural products and pharmaceuticals.²⁵ However, the construction of such quaternary carbon centers remains a challenge in current cross-coupling methods due to the steric repulsion from hindered substituents.²⁶ Recently, Shenvi and co-workers have successfully overcome this challenge by combining nickel catalysis with iron mediated HAT. They reported a catalytic branch-selective hydroarylation of 1,1-di-substituted or trisubstituted olefins and aryl iodides, thus forming sp^3 – sp^2 bonds with quaternary carbon centers (Scheme 2.6).²⁷ Both cyclic and linear olefins could be coupled with equal efficiency and high regioselectivity, even in the context of late-stage functionalization. Unsaturated heterocycles could be coupled with a range of (hetero)aryl iodides and bromides. Moreover, vinyl bromides could replace haloarene to form styrene derivatives in the reaction. It is worth noting that the ring

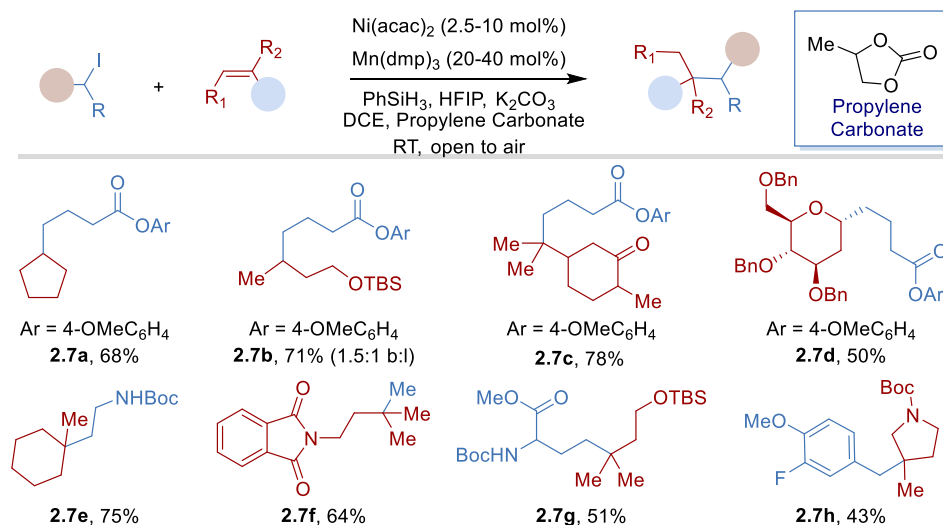
opening product was obtained when using β -pinene (**s2.6**) as substrate, suggesting a carbon-centered radical was formed via Fe–H HAT.



Scheme 2.6 Ni/Fe dual-catalyzed hydroarylation of 1,1-di-substituted or trisubstituted olefins

Very recently, the same group documented a catalytic Markovnikov-selective hydroalkylation of unactivated olefins and alkyl iodides through Ni and Mn dual catalysis, thus building up sp^3 – sp^3 bonds with quaternary carbon centers (Scheme 2.7).²⁸ In contrast with the *anti*-Markovnikov-selective hydroalkylation via Ni–H system reported by the Liu and Fu group,¹⁹ the combination of Mn–H mediated HAT catalysis and nickel catalysis were the key to achieve high regioselectivity. Not surprisingly, this protocol displayed high functional group tolerance regarding both alkyl iodides and olefins coupling partners. Notably, both branched and linear mixtures were obtained with terminal olefins. This is probably due to a background Ni-only mediated pathway,¹⁹ or a competitive hydrometalation pathway mediated by low valent Mn.²⁹ In addition, α -branched and secondary alkyl iodides were found to proceed in low yield under the reaction conditions.

*Site-Selective Ni-Catalyzed Reductive
Coupling of α -Haloboranes with Unactivated Olefins*

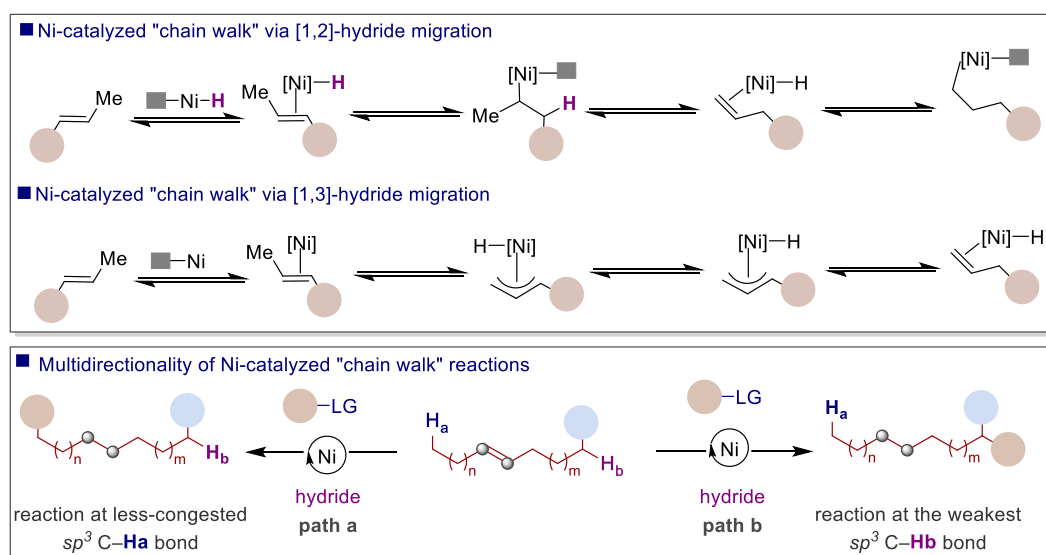


Scheme 2.7 Catalytic hydroalkylation of olefins to form quaternary carbon center

2.3 Remote sp^3 C–H Functionalization via Ni-Catalyzed Chain-Walking

During the last decades, transition metal-catalyzed C–H functionalization has gained significant momentum at the scientific community for forging C–C and C–heteroatom bonds.³⁰ While sp^2 C–H functionalization has evolved into a mature tool for advanced organic synthesis, extensions to sp^3 C–H bond linkages has shown to be not as straightforward as one might initially anticipate.³¹ This is likely due to the observation that sp^3 C–H bonds are considerably less acidic than sp^2 C–H linkages, and that these motifs lack proximal empty low-energy or filled high-energy orbitals that interact with the d orbitals of the transition metal. In addition, site-selectivity principles come into play due to the presence of multiple, yet similar, sp^3 C–H bonds in regular alkyl side-chains.³² Chemists have navigated this challenge via directing group protocols or carbene-mediated reactions.³¹ However, the introduction and detachment of directing groups might not be particularly trivial, whereas the need for carbene precursors might hamper the implementation of other C–C bond-forming events, respectively. sp^3 C–H bond-cleavage can also be triggered via open-shell species or enzyme-mediated processes.³¹ However, the former protocols are dictated by bond-dissociation energies whereas subtle changes in both the enzyme and on the

substrate might hamper reactivity and site-selectivity in the latter. Despite the advances realized, the site-selective C–C bond-formation at stronger, unactivated primary sp^3 C–H bonds is still particularly problematic. While originally designed for controlling polymer topology, the recent years have witnessed renewed interest in olefin isomerization as a vehicle for enabling bond-construction at remote, yet unfunctionalized, primary sp^3 C–H sites.³³ In a formal sense, this process – oftentimes coined as “chain-walking” – operates via dynamic displacement of the catalyst throughout the alkyl chain. Although significant progress has been made with Zr, Ru, Rh, Co or Pd complexes,³³ the versatility and flexibility in synthetic design offered by Ni catalysts have only been recognized recently in “chain-walking”.³⁴ From a mechanistic standpoint, these techniques operate via alkyl-Ni species obtained by (a) iterative migratory insertion/ β -hydride elimination events or (b) [1,3]-hydride migration (Scheme 2.8, *top*).³³



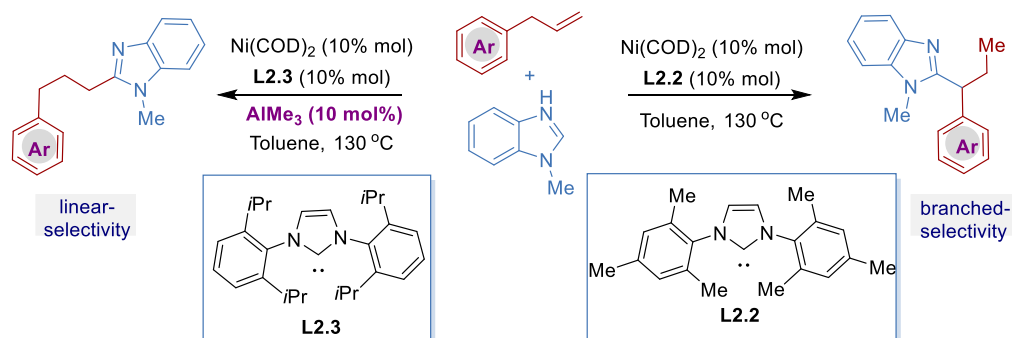
Scheme 2.8 Ni-catalyzed chain-walking reactions

In these transformations, “chain-walking” leads to the formal translocation of a double-bond (or alkyl-Ni intermediate) in a selective manner to the terminal position of the alkyl side-chain, presumably due to steric effects during the functionalization reaction (Scheme 2.8, *bottom, path a*), or to a resonance-stabilized position such as adjacent to an aromatic or a carbonyl group (Scheme 2.8, *bottom, path b*). In a formal sense, these observations stand as a testament that the “chain-walking” motion might a priori be controlled by either

subtle modification of the catalyst or the nature of the functional groups within the alkyl side-chain.^{33,34}

2.3.1 Ni-Catalyzed Remote Arylation and Alkenylation of Olefins or Alkyl Halides

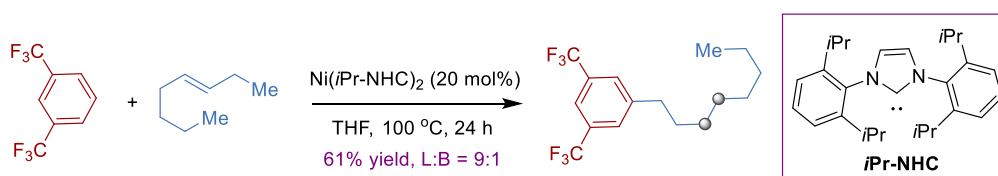
In 2013, Ong and co-workers reported a Ni-catalyzed site-selective hydroarylation of allylbenzenes (Scheme 2.9).³⁵ This platform presents that Ni(COD)₂ and *N*-heterocyclic carbene (NHC) ligand (**L2.2**, IMes) system was essential to provide remote sp^3 C–H arylation products. Although no mechanistic studies were conducted, the authors proposed a pathway consisting of [1,3]-hydride migration. In this case, a range of heteroarenes bearing acidic C–H bonds could be coupled with activated α -olefins to form 1,1-diaryllalkanes. Interestingly, replacement of **L2.2** to **L2.3**, and addition of AlMe₃ in the reaction, provided linear-selectivity product.



Scheme 2.9 Ni-catalyzed hydroarylation of allylbenzenes

In 2014, the group of Hartwig reported a related transformation with trifluoromethylarenes and internal olefins, resulting in C–C bond-formation at the terminal, primary sp^3 C–H site (Scheme 2.10).³⁶ Similar with Ong's protocol, the system was based on Ni(COD)₂ and NHC ligand, and arenes possessing low pK_a values were critical for success. The high selectivity for the primary sp^3 C–H position was attributed to the steric hindrance imposed by the bulk NHC ligand. Notably, reaction without NHC ligand led to mixture of olefins, thus suggesting that forging C–C bonds via chain-walking was due to the intermediacy of a

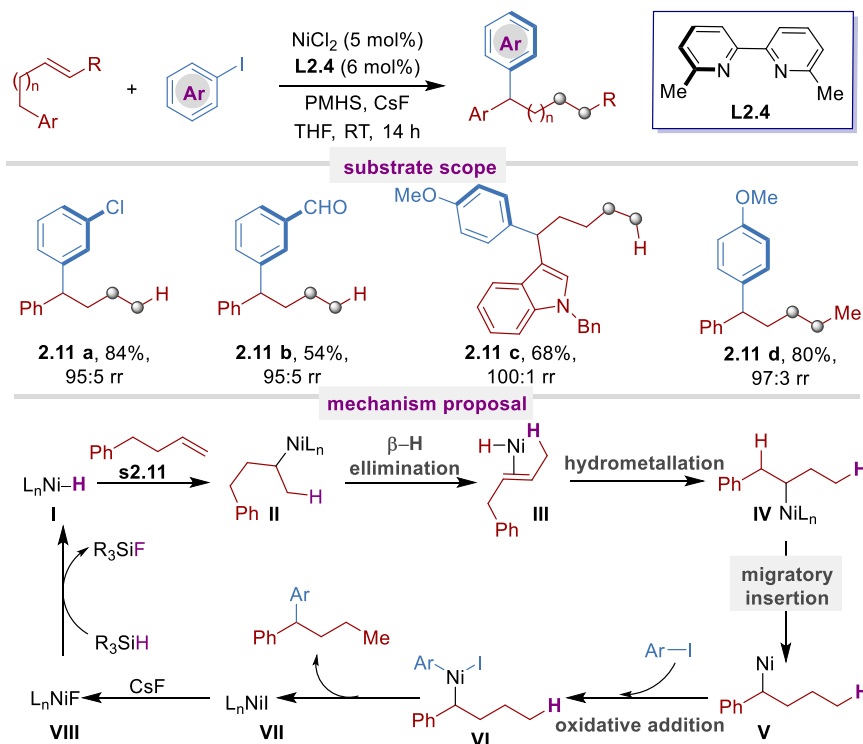
$\text{Ni}(\text{iPr-NHC})_2$ species. The authors proposed that the reaction went through a [1,2]-hydride migration pathway.



Scheme 2.10 Ni-catalyzed remote hydroarylation of unactivated olefins

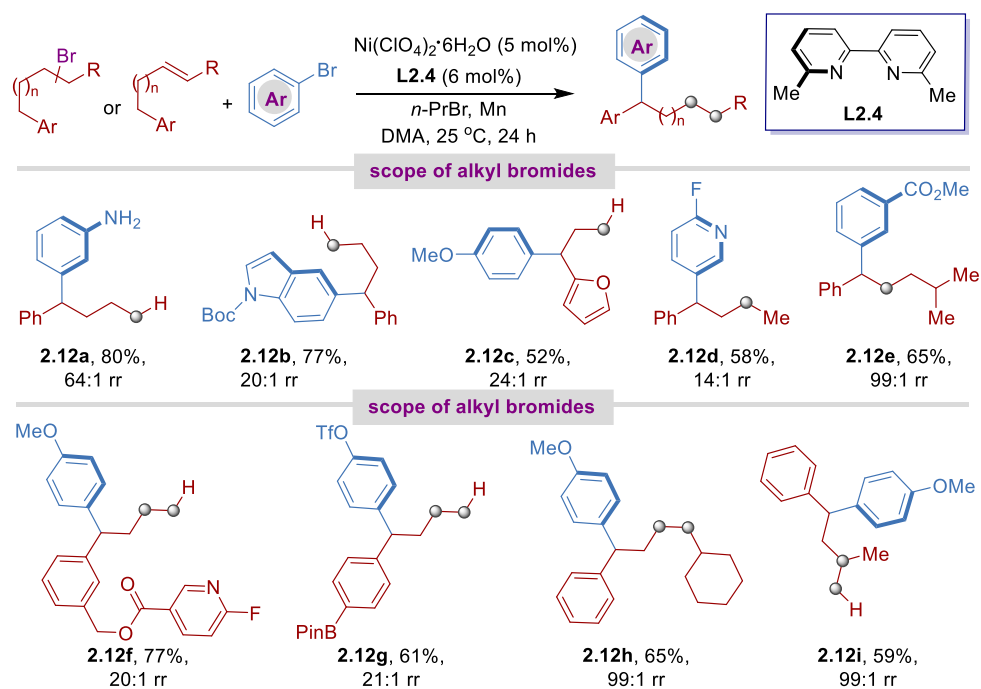
Prompted by these findings, Zhu and co-workers developed a reductive hydroarylation of olefins and (hetero)aryl iodides with C–C bond-formation occurring at remote, benzylic sp^3 C–H sites, using polymethylhydrosiloxane (PMHS) as hydride source (Scheme 2.11).³⁷ As for other Ni-catalyzed cross-coupling reactions via discrete alkyl nickel species, it was found that 2,2'-bipyridine ligands (**L2.4**) possessing substituents adjacent to the nitrogen motif were critical to achieve high selectivity and yield. The protocol presents an effective means to access 1,1-diarylalkanes in high chemo- and site-selectivity. While no mechanistic studies were performed, the authors favoured a mechanism consisting of an initial olefin migration via nickel hydrides followed by oxidative addition of (hetero)aryl iodides to *in-situ* generate a benzyl nickel species **V**. Whether “chain-walking” occurs via $\text{Ni}(\text{II})\text{L}_n$ or $\text{Ni}(\text{I})\text{L}_n$ species still remains speculative.

*Site-Selective Ni-Catalyzed Reductive
Coupling of α -Haloboranes with Unactivated Olefins*



Scheme 2.11 Ni-catalyzed benzylic C–H arylation of olefins with aryl iodides

Inspired by “chain-walking” protocols of alkyl halides developed by our group,³⁸ Zhu extended the generality of their Ni-catalyzed reductive arylation of alkyl bromides with aryl bromides at remote benzylic C–H sites by using Mn as reductant (Scheme 2.12).³⁹ In analogy with a recent reductive hydroamidation of alkynes, the authors found that 1-bromopropane (*n*-PrBr) could be used as a masked hydride source via β -hydride elimination.⁴⁰ Notably, olefins could also be employed under Ni/L2.4 and Mn system, with *n*-PrBr as hydride source, providing benzylic C–H arylation product in good yield.

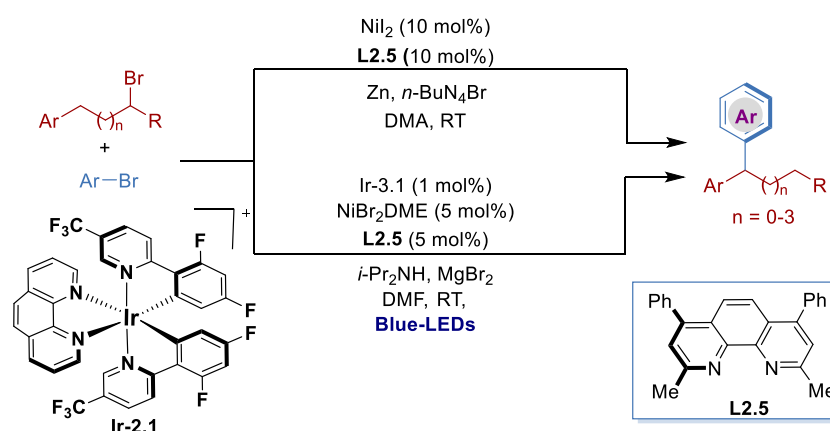


Scheme 2.12 Ni-catalyzed reductive arylation at remote benzylic sp^3 C–H site

Recently, the group of Yin reported a similar remote reductive arylation of alkyl bromides with aryl bromides by using NiI_2 /bathocuproine (**L2.5**) catalysis with Zn as reductant (Scheme 2.13).⁴¹ Surprisingly, the addition of an external hydride source was not necessary; however, in this case an ammonium halide ($n\text{-BuN}_4\text{Br}$) was required to increase product yields. In analogy with related Ni-catalyzed cross-electrophile coupling reactions,⁴² the authors suggested a pathway consisting of an initial oxidative addition of the aryl bromide to $\text{Ni}(0)(\text{L2.5})$ followed by recombination with *in-situ* generated alkyl radical species. “Chain-walking” was proposed to occur via [1,2]-hydride migrations from Aryl–Ni(III)–Alkyl species followed by final C–C bond-formation at the benzylic sp^3 site. This hypothesis tacitly suggests that β -hydride elimination should occur at a significantly faster rate than C–C bond reductive elimination, a rather provocative observation if one takes into consideration the known reported data on Ni-catalyzed cross-coupling reactions. Shortly after, the same group also described an alternative nickel/photoredox dual catalysis strategy for remote reductive arylation of alkyl bromides and aryl bromides (Scheme 2.13).⁴³ This result is particularly noteworthy, as stoichiometric amounts of Zn or Mn could be replaced by diisopropyl amine as terminal reductant;⁴⁴ although a bonus from a

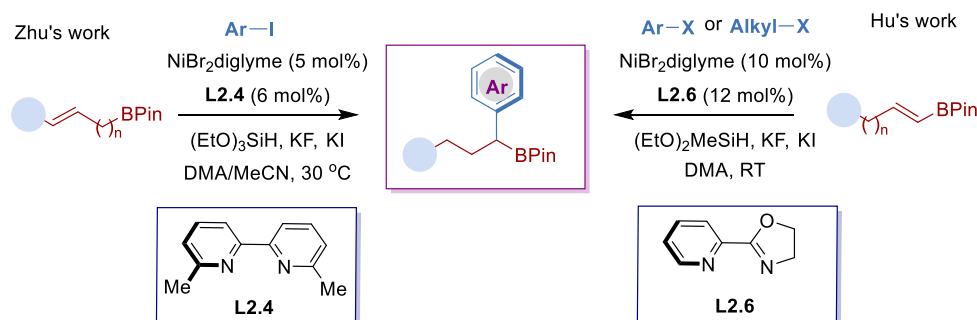
*Site-Selective Ni-Catalyzed Reductive
Coupling of α -Haloboranes with Unactivated Olefins*

synthetic standpoint, it is worth mentioning that these reactions require a photoreactor to operate.



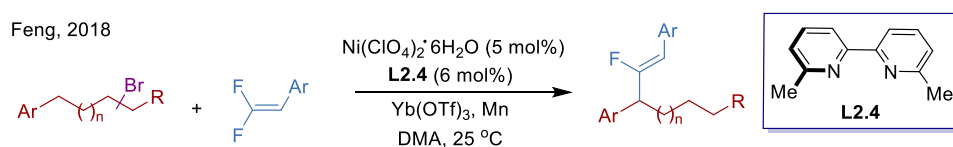
Scheme 2.13 Ni-catalyzed benzylic arylation of alkyl bromides with aryl bromides

Aiming at extending the scope of these “chain-walking” strategies to other remote sp^3 C–H site rather than benzylic position, Zhu and co-workers developed a hydroarylation of boron-containing olefins via Ni-catalyzed chain-walking, thus enabling to access arylation at the adjacent carbon atom of alkyl boronates (Scheme 2.14, *left*).⁴⁵ This platform provided an effective manner to access densely functionalized benzylic boronates in high chemo- and regio-selectivity. Particularly interesting, moderate enantioselectivity (62% ee) was obtained by replacement of ligand (**L2.4**) to chiral Cy-Biox ligand. Concurrently, the group of Hu reported a similar transformation of alkenyl boronates with aryl halides by using $\text{NiBr}_2\text{diglyme}/\text{L2.6}$ catalysis with $(\text{EtO})_2\text{MeSiH}$ (DEMS) as hydride source (Scheme 2.14, *right*).⁴⁶ Noteworthy, alkyl halides could also be equally employed in this protocol, providing a wide range of secondary alkyl boron derivatives.



Scheme 2.14 Ni-catalyzed hydroarylation of boron-containing olefins

Inspired by a series of related Ni-catalyzed remote functionalization techniques with a different set of electrophilic partners, Feng and co-workers recently extended the scope of these protocols to remote benzylic fluoro-alkenylation of alkyl bromides with *gem*-difluoroalkenes (Scheme 2.15).⁴⁷ In this case, the authors proposed a “chain-walking” based on Ni(I) intermediates followed by insertion into the difluoroolefin backbone and β -fluoride elimination to give rise to the targeted product. This assumption is certainly intriguing, particularly if one takes into account that “chain-walking” reactions have been proposed to operate via Ni(II) cationic species instead.



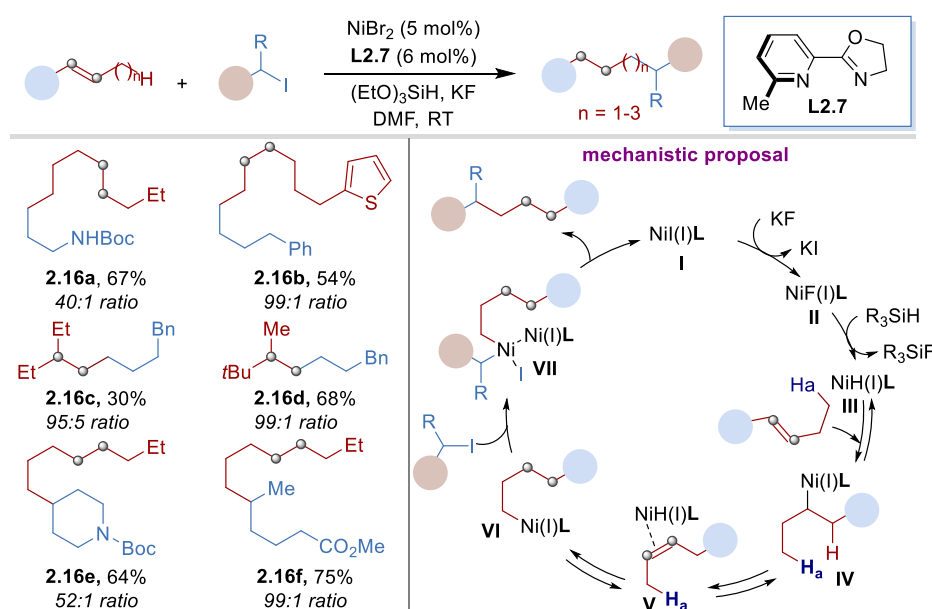
Scheme 2.15 Ni-catalyzed benzylic alkenylation with difluoroalkenes

2.3.2 C_{sp^3} – C_{sp^3} Bonds Formation via Ni-Catalyzed Remote sp^3 C–H Alkylation of Olefins

Although metal-catalyzed cross-coupling reactions of organometallics and organic (pseudo)halides has emerged as a tremendously powerful synthetic tool for the construction of sp^3 C–C bonds, the need for prefunctionalized and stoichiometric C–metal bonds might hamper the application profile of these procedures, thus reinforcing a change in strategy.^{1,2} Driven by this observation, chemists have been challenged to come up with alternate partners with improved flexibility, practicality and generality. Among these, the catalytic addition of a hydrogen atom across an unsaturated bond has received considerable attention as a powerful alternative to classical C–C bond-formations based on stoichiometric organometallic reagents or organic halides, as it generates a latent nucleophile that can further be elaborated in the presence of a suitable functional group.¹³ In line with this notion, Zhu and co-workers reported a catalytic remote sp^3 C–H alkylation of alkyl iodides with internal alkenes via Ni-catalyzed reductive “chain-walking” and sequential alkylation relay process via Ni-hydride intermediate species (Scheme 2.16).⁴⁸ Unlike the previous olefin hydroarylation

*Site-Selective Ni-Catalyzed Reductive
Coupling of α -Haloboranes with Unactivated Olefins*

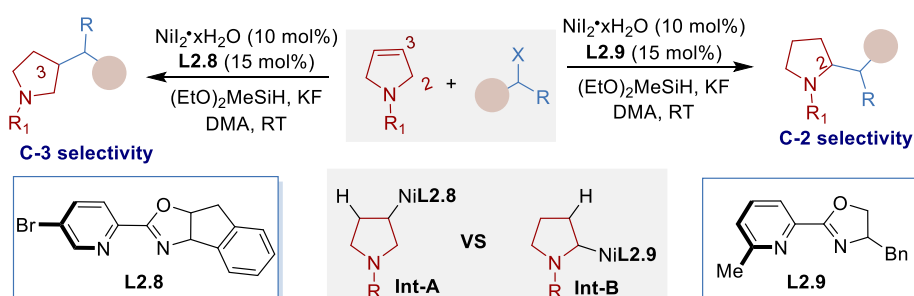
event,^{37,39} the utilization of a PyrOx-type ligand (**L2.7**) resulted in the C–C bond-formation at an unactivated primary sp^3 C–H site. These results suggested the intermediacy of alkyl-Ni complexes that undergo a rapid iterative series of β -hydride elimination/migratory insertions with a formal translocation of the nickel complex at a terminal, yet unactivated, sp^3 C–H site^{33,34} (Scheme 2.16, *right bottom*). Although the olefin isomerization tracing and deuterium incorporation experiments proved the chain-walking process, the selectivity of terminal primary sp^3 C–H sites remains unclear. In addition, there exists a reasonable ambiguity on whether “chain-walking” occurs via Ni(I) – as proposed by the authors – or Ni(II) intermediates, thus suggesting that further investigation will be needed to unravel the intricacies of this or related processes.



Scheme 2.16 Ni-catalyzed remote hydroalkylation of internal olefins

Inspired by our recent work on catalytic hydroalkylation of 3-pyrrolines,⁴⁹ Hu and co-workers reported a Ni-catalyzed site-selective hydroalkylation of pyrrolines and alkyl halides (Scheme 2.17).⁵⁰ This protocol presented a regiodivergent hydroalkylation that could be tuned via ligand control, yielding both C2 and C3 selectivity alkylated pyrrolidines. The authors proposed that the regioselectivity might be attributed to the relative stability of alkyl-Ni intermediate **Int-A** and **Int-B**, whereas **Int-B** can be stabilized by the nitrogen of pyrrolidines, so that C2 alkylation is predominant under most cases. However, a ligand such as **L2.8** might reverse the

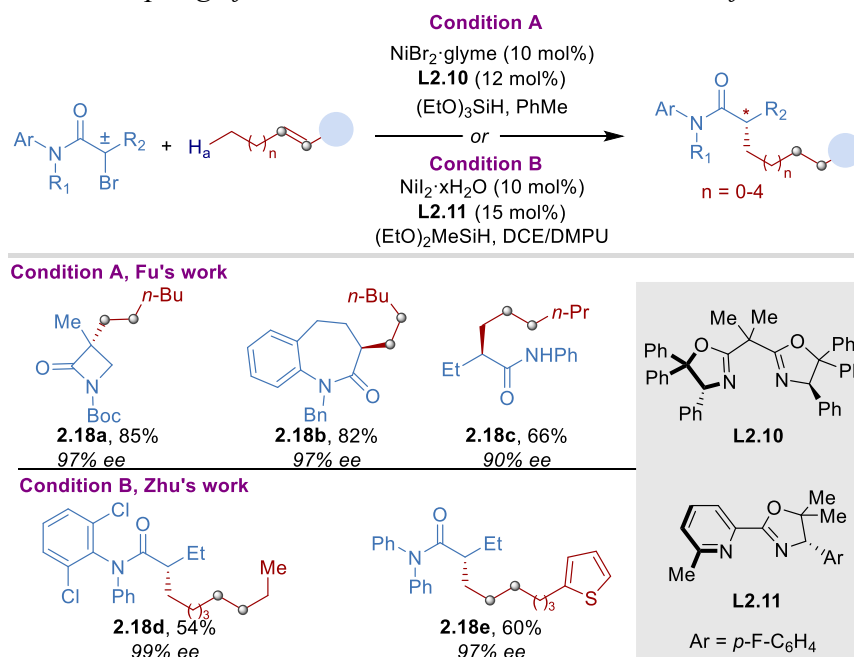
relative stability of **Int-A** and **Int-B**, adding to C3 alkylation. Furthermore, it might kinetically stabilize **Int-A** by having a high barrier for β -hydride elimination as well.



Scheme 2.17 Ni-catalyzed regiodivergent hydroalkylation of pyrrolines

The available portfolio on “chain-walking” reactions suggested that the installation of chiral sp^3 -carbon centers should by no means be an impossible. Challenged by this observation, Fu⁵¹ and Zhu⁵² independently described a Ni-catalyzed enantioconvergent coupling of racemic secondary or tertiary α -bromo amides with olefin partners in which C–C bond-formation occurred at remote sp^3 C–H sites, thus giving rise to the targeted products in good yields and high enantioselectivities by using bisoxazolines (**L2.10**) or PyrOx-type (**L2.11**) ligands (Scheme 2.18). Very recently, the scope of these Ni-catalyzed enantioconvergent hydroalkylation strategies been extended to α -phosphorus, α -sulfur alkyl bromides⁵³ and α -ester alkyl bromides⁵⁴. While undoubtedly an enormous step-forward in the field, it is worth noting that these technologies remain restricted to the utilization of activated organic halides (e.g. α -bromo amides, α -phosphorus, α -esters), leaving ample room for future asymmetric transformations, particularly when utilizing unactivated electrophilic partners.

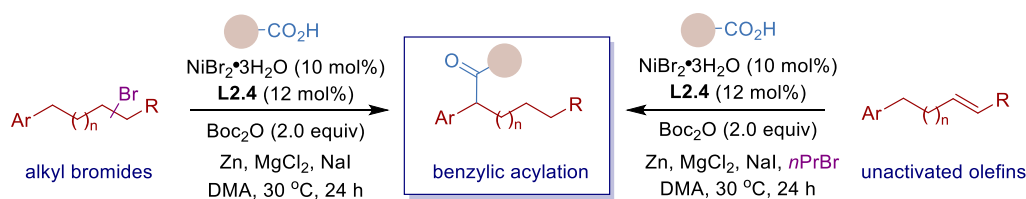
*Site-Selective Ni-Catalyzed Reductive
Coupling of α -Haloboranes with Unactivated Olefins*



Scheme 2.18 Enantioconvergent Ni-catalyzed hydroalkylation of olefins with racemic α -bromo amides

2.3.3 Ni-Catalyzed Remote sp^3 C–H Acylation of Olefins or Alkyl Halides

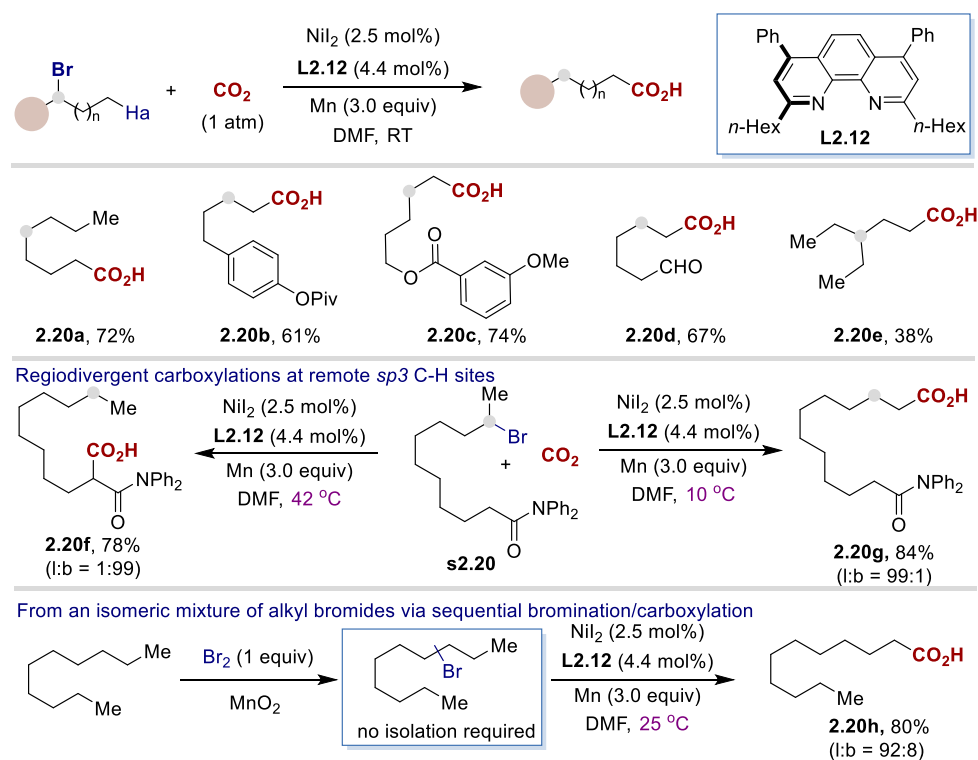
Inspired by reductive ipso-acylation of carboxylic acids with alkyl halides developed by Gong's group,⁵⁵ Zhu, Wang and co-workers recently described a remote benzylic C–H acylation by the use of the latter as electrophilic partners in the context of “chain-walking” reactions with either alkyl halides or alkene counterparts (Scheme 2.19).⁵⁶ In this case, MgCl₂ and Boc₂O were required to activate the carboxylic acid by forming an acid anhydride that precedes C–C bond-formation. The authors proposed a similar mechanistic rationale to that shown in previous “chain-walking” reactions via olefin migration triggered by nickel hydrides followed by C–C bond-formation with *in-situ* generated Boc-anhydride as the carbonyl source.



Scheme 2.19 Ni-catalyzed benzylic acylation of alkyl halides and unactivated olefins

2.3.4 Ni-Catalyzed Remote sp^3 C–H Carboxylation of Alkyl Halides and Alkenes

Ni-catalyzed reductive carboxylations have recently gained momentum as powerful alternatives to existing methods for accessing carboxylic acids,⁵⁷ privileged motifs in a wide variety of compounds that display important biological activities.⁵⁸ Despite the significant advances realized, the available carboxylation portfolio contributed to the perception that prefunctionalization was required for the reaction to occur. Challenged by this notion, our group reported a catalytic site-selective reductive carboxylation of alkyl bromides at remote sp^3 C–H sites via Ni-catalyzed “chain-walking” strategies (Scheme 2.20).³⁸

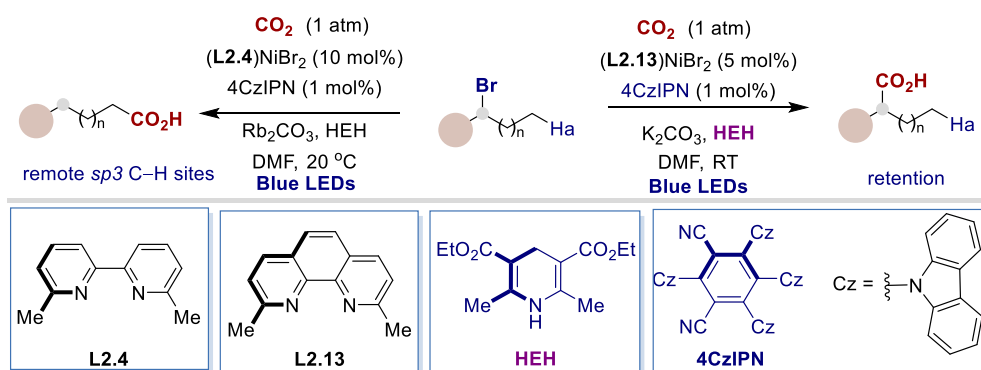


Scheme 2.20 Ni-catalyzed site-selective reductive carboxylation of alkyl bromides with CO_2

In line with our knowledge on reductive cross-couplings, bipyridine or phenanthroline ligands with substituents adjacent to the nitrogen atom were crucial for the reaction to occur, an observation that has rapidly been embraced in other C–C bond-formations. A plethora of alkyl (pseudo)halides with sensitive functional groups

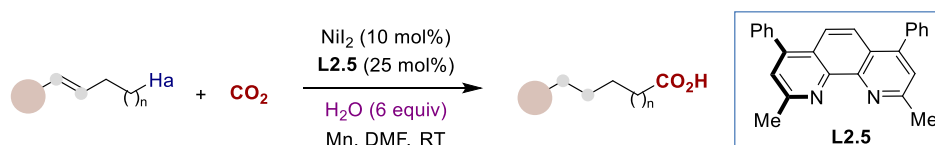
*Site-Selective Ni-Catalyzed Reductive
Coupling of α -Haloboranes with Unactivated Olefins*

were converted to carboxylic acids, constituting a bonus when compared to conventional carboxylations based on stoichiometric and highly reactive organometallics. Noteworthy, remote carboxylation occurred with the preservation of the chiral integrity of carbon centers, suggesting that the reactions proceeds via a non-dissociative mechanism in which the Ni-catalyst remains bound to the substrate to achieve the isomerization and functionalization at the same molecule. Importantly, site-selectivity could be controlled and switched by a subtle control of the temperature, enabling C–C bond-formation at different sp^3 sites (Scheme 2.20, *middle*) while challenging the perception that multidirectional “chain-walking” motions could not be implemented. As expected, regioconvergent strategies could be within reach by converting abundant alkanes or mixtures of alkenes into single carboxylic acids (Scheme 2.20, *bottom*). In addition, related protocols could be implemented by converting carboxylic acids into their corresponding isotope-labelling analogues by using either $^{13}\text{CO}_2$ or $^{14}\text{CO}_2$.



Scheme 2.21 Site-selective carboxylation of alkyl halides via nickel and photoredox dual catalysis

While the aforementioned method utilized metal reductant (Mn), which hamper this process to be implemented in industrial endeavours, in 2019, König, Martin and co-workers designed a protocol for site-selective, remote sp^3 C–H carboxylation of alkyl bromides by merging nickel and photoredox dual catalysis based on a mechanistic rationale of cooperative catalysis, where Hantzsch ester (HEH) is used as organic reductant under Blue-LED irradiation with 4-CzIPN as photocatalyst (Scheme 2.21).⁵⁹



Scheme 2.22 Site-selective Ni-catalyzed hydrocarboxylation of olefins with H_2O as hydride source

Following our interest in catalytic remote carboxylation techniques, our group developed a site-selective remote hydrocarboxylation of olefins by using water as hydride source with a protocol based on Ni/**L3.5** system (Scheme 2.22).⁶⁰ This result is particularly noteworthy, as it represents an opportunity to repurpose three abundant feedstocks (water, CO_2 and olefins). Another important advantage of this protocol is the use of water as hydride source, rather than silanes or organometallic reagents that are often used to generate the propagating Ni–H species. As expected, regioconvergence from unrefined mixtures of olefins was portrayed for site-selective carboxylation at a single, remote sp^3 C–H site. In this context, preliminary mechanistic experiments did not only confirm water as hydride source, but also revealed a non-negligible role of the substituents proximal to the nitrogen donor, an aspect worth considering for future mechanistic studies that unravel the intricacies exerted by the ligand backbone.

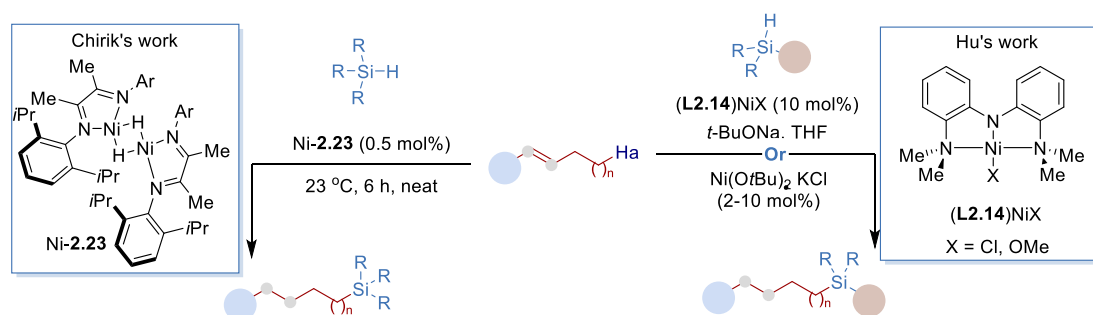
2.3.5 Ni-Catalyzed Remote C-Heteroatom Bonds Formation

Remote sp^3 C–H functionalization of olefins and alkyl halides via Ni-catalyzed “chain-walking” strategies are not only limited to the construction of C–C bonds, but access to C–heteroatom bonds has also been reported.

Catalytic hydrosilylation of olefins constitutes one of the most widely applied methods in the silicones industry for preparing monomers containing C–Si linkages and cross-linking polymers.⁶¹ In 2015, Hu and co-workers developed a chemo- and regio-selective hydrosilylation of both terminal olefins and internal olefins.⁶² In this case, pincer-type Nickamine complexes (**L2.14**)NiX (X = Cl, OMe) do not only promote the *anti*-Markovnikov hydrosilylation of terminal olefins with diarylsilanes, but also silylation of internal olefins at remote primary sp^3 C–H sites via “chain-walking” strategies (Scheme 2.23, *right*). Although the use of trialkoxysilanes might furnish industrially-relevant silicones, this process

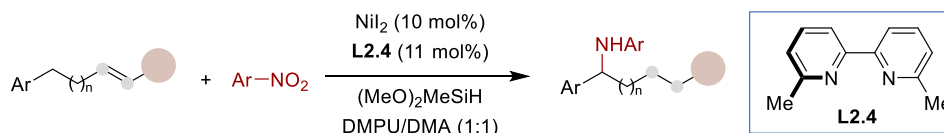
*Site-Selective Ni-Catalyzed Reductive
Coupling of α -Haloboranes with Unactivated Olefins*

remained particularly problematic. To such end, Hu developed a simple, stable and recyclable Ni-based nanocatalyst $\text{Ni}(\text{OtBu})_2 \cdot x\text{KCl}$ that turned out to outperform previous Ni-based methods and particularly applicable to the coupling of α -olefins and internal alkenes, the latter via “chain-walking” at remote sp^3 sites.⁶³ As expected, this heterogeneous protocol could be applied in regioconvergent techniques with unrefined mixture of olefins to deliver linear silicones in high site-selectivity. Later, Chirik and co-workers described the use of Ni-catalysts bearing redox-active α -diimine ligands for alkene hydrosilylation (Scheme 2.23, left).⁶⁴ Preliminary mechanistic studies suggested that this hydrosilylation protocol involved a Ni(II) intermediate with one electron reducing α -diimines.



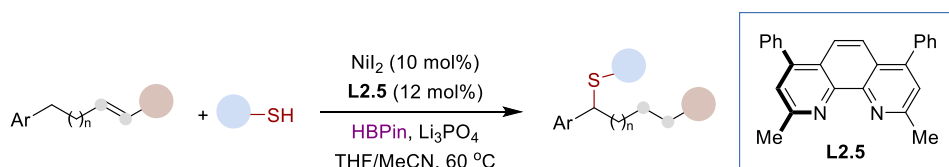
Scheme 2.23 Ni-catalyzed remote hydrosilylation of olefins

The ubiquity of (hetero)aryl amines in a myriad of pharmaceuticals or agrochemicals has prompted chemists to develop *de novo* catalytic techniques for forging sp^2 and sp^3 C–N bonds by using chemical feedstocks as precursors.⁶⁵ To such end, Zhu recently described a Ni-catalyzed reductive amination of olefins with nitroarenes at remote benzylic sp^3 C–H sites operating via alkene isomerization followed by relay hydroamination (Scheme 2.24),⁶⁶ thus complementing existing methods for preparing sp^3 C–N linkages. Interestingly, they also demonstrated that sp^3 C–N bond-formation took place at the α -position of esters, thus resulting in an intriguing route for preparing *N*-aryl amino acids. Undoubtedly, the synthetic potential of this protocol will encourage the development of alternative methods with improved atom economy or cheaper reductants to be employed in late-stage functionalization.



Scheme 2.24 Ni-catalyzed reductive hydroamination of olefins with ArNO₂

Very recently, Zhu and co-workers also described the merger of olefin isomerization via “chain-walking” with a subsequent *sp*³ C–S bond-formation at either remote benzylic sites or adjacent to ether motifs (Scheme 2.25).⁶⁷ In sharp contrast to previous reductive remote hydrofunctionalization of olefins, this reaction does not require sophisticated electrophilic reagents, but rather simple and commercially available alkyl or aryl thiols. The utilization of phenanthroline ligands possessing groups adjacent to the nitrogen motif – a common feature found in Ni-catalyzed “chain-walking” reactions and reductive couplings – and pinacolborane as hydride source were found to be critical for success. A subtle modification of the reaction conditions resulted in a site-selectivity switch, favoring the *anti*-Markovnikov hydrothiolation of terminal alkenes. Preliminary studies revealed the formation of RS–BPin species that act as the corresponding pronucleophile, whereas the nature of the solvent had a non-negligible impact on the formation of the propagating nickel hydride species.

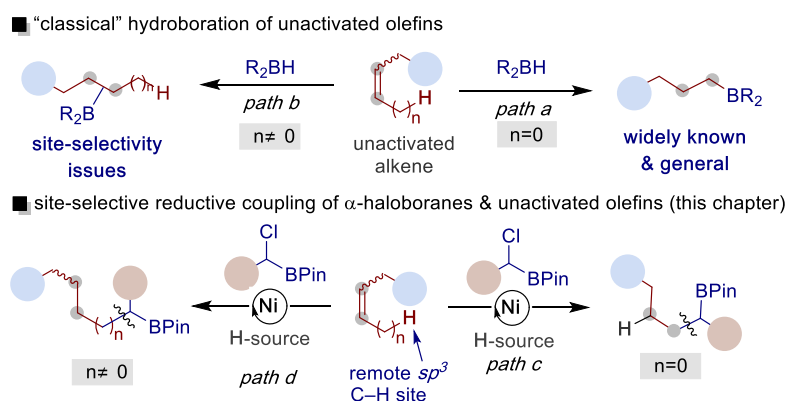


Scheme 2.25 Ni-catalyzed remote hydrothiolation of olefins

2.4 General Aim of the Project

The versatility of organoboranes as synthons in organic synthesis makes the hydroboration of alkenes one of the most fundamental reactions in organic synthesis.⁶⁸ Although the use of α -olefins has become routine, site-selectivity issues come into play with unactivated internal olefins lacking directing groups in the vicinity (Scheme 2.26, *top*).⁶⁹

At the current level of development, the catalytic regioselective incorporation of an alkylboron fragment into unactivated olefins still constitutes an uncharted territory within the hydrofunctionalization arena.⁷⁰ Aiming at extending the scope of Ni-catalyzed hydrofunctionalization of olefins, we wonder whether we could enable a site-selective catalytic reductive coupling of α -haloboranes with olefin feedstocks (Scheme 2.26, *bottom*).⁷¹ If successful, this platform would constitute an excellent alternative to existing techniques for the preparation of organoborane building blocks using simple olefins as raw materials.



Scheme 2.26 Catalytic site-selective reductive coupling of α -haloboranes with unactivated olefins

2.5 Ni-Catalyzed Reductive Alkylation of α -Haloboranes with Unactivated Olefins

2.5.1 Ni-Catalyzed Reductive Alkylation of α -Haloboranes with α -Olefins

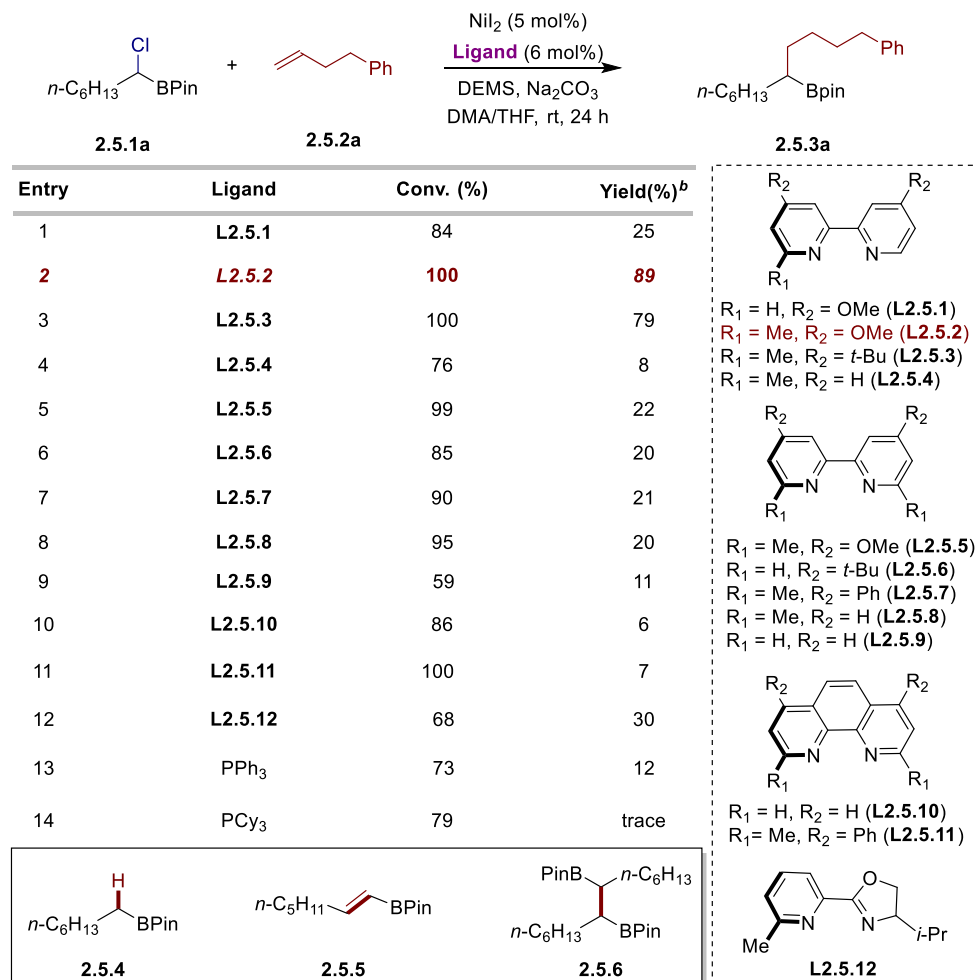
2.5.1.1 Optimization of the Reaction Conditions

Aiming to develop a site-selective hydroalkylation of olefin feedstocks, we decided to optimize the reaction conditions of terminal and internal olefins independently. The feasibility of the hydroalkylation of α -haloboranes with unactivated terminal olefins was initially investigated using 2-(1-chloroheptyl)-4,4,5,5-tetramethyl-1,3,2-dioxaborolane (**2.5.1a**) and phenyl-1-butene (**2.5.2a**) as model substrate. The choice of the model catalytic system was based on the previous studies carried out in our group on reductive coupling of unsaturated compounds as well as other relative hydrofunctionalization reports.^{33,34,72} During the screening of the optimized reaction conditions, alkyl borane (**2.5.4**), alkenyl borane (**2.5.5**), and alkyl diboranes (**2.5.6**) were observed as side products during the reaction. The formation of these compounds can be explained by competitive hydrogenolysis, β -hydride elimination and homocoupling of α -chloro borane.

Based on our group's knowledge on the reductive carboxylation,⁵⁷ amidation of alkyl bromides⁷³ and unsaturated π -compounds,⁷² special attention was paid to the use of bipyridine- and phenanthroline-type ligands (Table 2.1). As evident from the results compiled in Table 3.1, the nature of the ligand played a crucial role for the reaction success. The use of bipyridine ligands possessing a 6-methyl group and substituents at 4,4'-positions provided the best results, since more hydrolysis (**3.5.4**) and β -hydride elimination (**2.5.5**) side products were obtained when using other bipyridine- and phenanthroline-type ligands (entries 1-12). Additionally, electron-rich phosphine ligands which are commonly used on C–O bonds cleavage,⁷⁴ provided lower yields or no reaction under the reaction conditions (entries 13 and 14). Finally, 4,4'-dimethoxy-6-methyl-2,2'-bipyridine (**L2.5.2**) was identified as the optimal ligand for the studied system. A plausible explanation for the need of ortho substituted-ligands could be a

*Site-Selective Ni-Catalyzed Reductive
Coupling of α -Haloboranes with Unactivated Olefins*

gain in the stabilization of alkyl–Ni intermediates against β -hydride elimination. This stability would be achieved as steric hindrance imparted by the ligand substituents that distorts the geometry and prevents the co-planar rearrangement of the metal and the C–H $_{\beta}$ σ -bond necessary for β -hydride elimination.

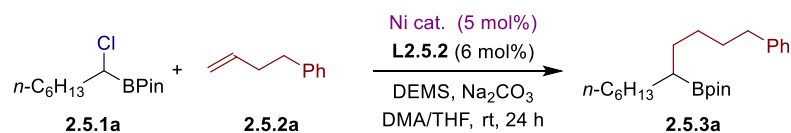


^a Conditions: **2.5.1a** (0.20 mmol, 1.0 equiv), **2.5.2a** (0.34 mmol, 1.7 equiv), NiI₂ (5 mol%), **Ligand** (6 mol%), DEMS (0.30 mmol, 1.5 equiv), Na₂CO₃ (0.15 mmol), DMA/THF (3:1, 0.4 mL), rt, 15 h. ^b Yields were determined by GC FID, using 1-decane as the internal standard. DEMS = Diethoxymethylsilane.

Table 2.1 Screening of ligands

With 4,4'-dimethoxy-6-methyl-2,2'-bipyridine (**L2.5.2**) as ligand, we then studied the effect of nickel precatalysts on the reaction outcome (Table 2.2). We found that NiI₂ provided the best results, whereas more side products were obtained when using other Ni(II) salts as precatalysts. Ni(COD)₂ also provided the product in lower yield (13%), suggesting that COD might compete with substrate binding. We next assessed whether the ratio of Ni/ligand played an influence on both reactivity and

chemoselectivity (Table 2.3). Further screening the ratio of ligand and nickel on the reaction yield, we found that a 20% ligand excess was required to make the total coordination with nickel, and 5% loading of NiI₂, hence the best results were obtained with a Ni/Ligand ratio of 1:1.2. However, lower yields were obtained when increasing the ratio to 1:2, suggesting the formation of rather stable 18-electron Ni species, thus making the whole system kinetically less-accessible. Noteworthy, 80% yield product could be obtained by reducing the catalyst loading to 2.5%.

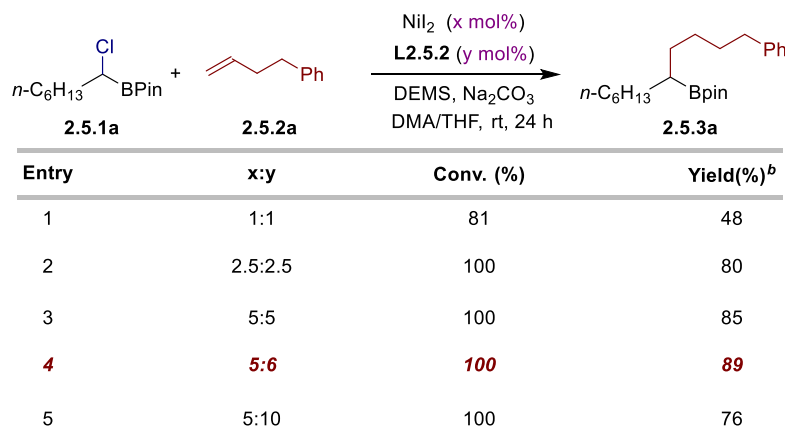


Entry	Ni cat.	Conv. (%)	Yield(%) ^b
1	NiBr ₂ ·diglyme	100	60
2	NiBr ₂ ·DME	100	61
3	NiCl ₂ ·DME	100	19
4	NiCl ₂	99	18
5	NiBr ₂	99	62
6	NiI₂	100	89
7	Ni(acac) ₂	92	trace
8	Ni(COD) ₂	100	13
9	Ni(OAc) ₂ ·4H ₂ O	94	29

^a Conditions: **2.5.1a** (0.20 mmol, 1.0 equiv), **2.5.2a** (0.34 mmol, 1.7 equiv), Ni cat. (5 mol%), **L2.5.2** (6 mol%), DEMS (0.30 mmol, 1.5 equiv), Na₂CO₃ (0.15 mmol), DMA/THF (3:1, 0.4 mL), rt, 15 h. ^b Yields were determined by GC FID, using 1-decane as the internal standard. DEMS = Diethoxymethylsilane.

Table 2.2 Screening of nickel precatalysts

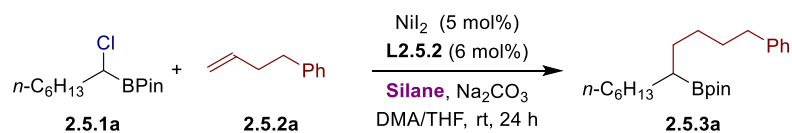
*Site-Selective Ni-Catalyzed Reductive
Coupling of α -Haloboranes with Unactivated Olefins*



^a **Conditions:** **2.5.1a** (0.20 mmol, 1.0 equiv), **2.5.2a** (0.34 mmol, 1.7 equiv), **NiI₂** (x mol%), **L2.5.2** (y mol%), DEMS (0.30 mmol, 1.5 equiv), Na₂CO₃ (0.15 mmol), DMA/THF (3:1, 0.4 mL), rt, 15 h. ^b Yields were determined by GC FID, using 1-decane as the internal standard. DEMS = Diethoxymethylsilane.

Table 2.3 Effects of the ratio of Ni/ligand

Next, we turned our attention to studying the effect of different hydride sources on the reaction outcome (Table 2.4). The evaluation of other hydride source showed that only diethoxy(methyl)silane (DEMS) and triethoxysilane were effective, DEMS providing the best results. In contrast, other silanes led to high amount of hydrolysis side product (entries 4, 5 and 8). Interestingly, the use of polymethylhydrosiloxane (PMHS) –an inexpensive, abundant and nontoxic byproduct of the silicone industry– instead of DEMS, gave moderate yields of the desired product.



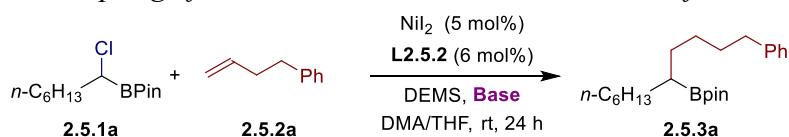
Entry	Silane	Conv. (%)	Yield(%) ^b
1	DEMS	100	89
2	(EtO) ₃ SiH	100	82
3	Et ₃ SiH	10	0
4	PhSiH ₃	100	6 (68 ^c)
5	Ph ₂ SiH ₂	100	14 (75 ^c)
6	Ph ₃ SiH	9	0
7	Ph ₂ MeSiH	52	3
8	TMS ₃ SiH	98	0 (52 ^c)
9	PMHS	100	54

^a **Conditions:** **2.5.1a** (0.20 mmol, 1.0 equiv), **2.5.2a** (0.34 mmol, 1.7 equiv), NiI₂ (5 mol%), **L2.5.2** (6 mol%), **Silane** (0.30 mmol, 1.5 equiv), Na₂CO₃ (0.15 mmol), DMA/THF (3:1, 0.4 mL), rt, 15 h. ^b Yields were determined by GC FID, using 1-decane as the internal standard. ^c Yield of **2.5.4**. DEMS = Diethoxymethylsilane. PMHS = Poly(methylhydrosiloxane).

Table 2.4 Screening of hydride source

Other parameters such as inorganic bases or solvents were investigated. As shown in Table 2.5, Na₂CO₃ provided the best yields with full conversion. In addition, the solvent also had an influence on *sp*³ C–C bond formation. Good yields were obtained with amide-containing polar aprotic solvents, such as DMF and DMA. This is probably due to the putative cationic reaction intermediate could be stabilized, in which DMA or DMF can coordinate to the metal center instead of a halide ligand. However, ethereal solvents such as THF, dioxane and diglyme were not effective for the hydroalkylation. Particularly interestingly, the combination DMA and THF (3:1) as a co-solvents system provided the best results.

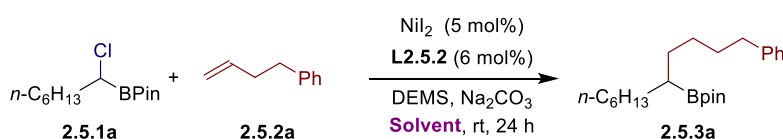
*Site-Selective Ni-Catalyzed Reductive
Coupling of α -Haloboranes with Unactivated Olefins*



Entry	Base	Conv. (%)	Yield(%) ^b
1	Li ₂ CO ₃	22	6
2	Na₂CO₃	100	89
3	K ₂ CO ₃	100	29
4	Cs ₂ CO ₃	100	1
5	NaOAc	100	1
6	KOAc	92	0
7	K ₃ PO ₄	100	19
8	NaHCO ₃	94	80
9	NaF	83	36
10	NaBr	90	0
11	NaI	96	0

^a **Conditions:** 2.5.1a (0.20 mmol, 1.0 equiv), 2.5.2a (0.34 mmol, 1.7 equiv), NiI₂ (5 mol%), L2.5.2 (6 mol%), DEMS (0.30 mmol, 1.5 equiv), Base (0.15 mmol), DMA/THF (3:1, 0.4 mL), rt, 24 h. ^b Yields were determined by GC FID, using 1-decane as the internal standard. DEMS = Diethoxymethylsilane.

Table 2.5 Screening of bases

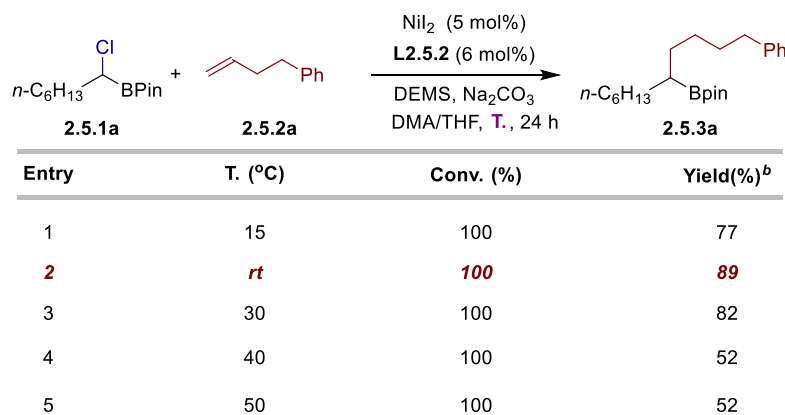


Entry	Sol.	Conv. (%)	Yield(%) ^b
1	DMA	100	70
2	DMF	100	62
3	DME	45	18
4	THF	94	9
5	NMP	100	1
6	Dioxane	33	1
7	Diglyme	89	15
8	DMA/THF(1:1)	100	68
9	DMA/THF(3:1)	100	89
10	DMA/THF(5:1)	100	78
11	DMA/NMP(3:1)	100	72
12	DMA/DME(3:1)	100	76
13	DMA/H ₂ O(3:1)	97	5

^a **Conditions:** 2.5.1a (0.20 mmol, 1.0 equiv), 2.5.2a (0.34 mmol, 1.7 equiv), NiI₂ (5 mol%), L2.5.2 (6 mol%), DEMS (0.30 mmol, 1.5 equiv), Na₂CO₃ (0.15 mmol), Sol. (0.4 mL), rt, 24 h. ^b Yields were determined by GC FID, using 1-decane as the internal standard. DEMS = Diethoxymethylsilane.

Table 2.6 Screening of solvents

With a robust Ni/**L2.5.2** catalytic system found, we next evaluated the effect of temperature on hydroalkylation reaction (Table 2.8). The best conditions were found when conducting the reaction at room temperature (around 25 °C), obtaining *sp*³ C–C formation product in 89% GC yield. When increasing the temperatures to 40 or 50 °C, significant amounts of side-products were observed (entries 4 and 5).

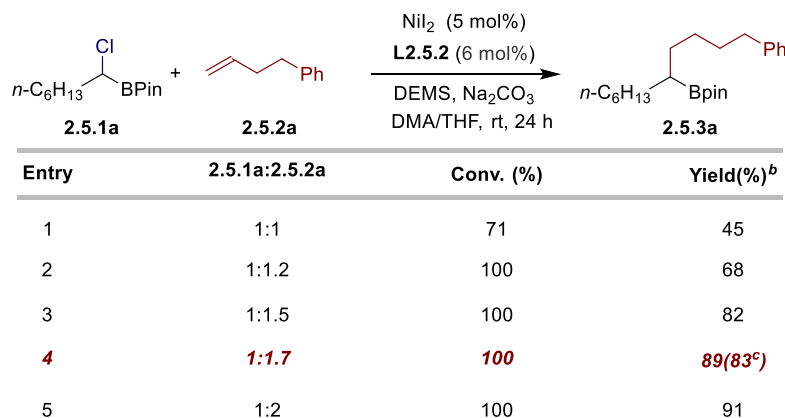


^a **Conditions:** **2.5.1a** (0.20 mmol, 1.0 equiv), **2.5.2a** (0.34 mmol, 1.7 equiv), NiI₂ (5 mol%), **L2.5.2** (6 mol%), DEMS (0.30 mmol, 1.5 equiv), Na₂CO₃ (0.15 mmol), DMA/THF (3:1, 0.4 mL), **T.**, 24 h. ^b Yields were determined by GC FID, using 1-decane as the internal standard. DEMS = Diethoxymethylsilane.

Table 2.7 Screening of temperature

Further, we thought that increasing the amount of olefin, could accelerate the rate of alkyl-Ni formation, thus promoting the coupling with α -chloroboranes and reducing the effect of side reactions. Based on this idea, we examined the effect of the ratio of starting materials. Indeed, we found that higher yields were obtained when increasing the loading of olefins (Table 2.8), with 1:2 and 1:1.7 ratio of starting materials, resulted on the formation of the product in similar yields. Considering the atom economy of the reaction, we selected 1:1.7 ratio for the reaction conditions.

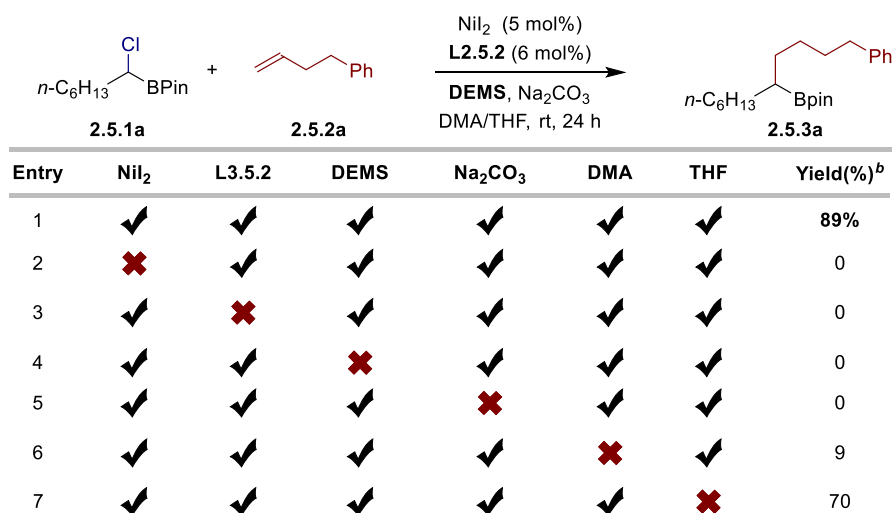
*Site-Selective Ni-Catalyzed Reductive
Coupling of α -Haloboranes with Unactivated Olefins*



^a **Conditions:** **2.5.1a** (0.20 mmol, 1.0 equiv), **2.5.2a** (x mmol, y equiv), NiI₂ (5 mol%), **L2.5.2** (6 mol%), DEMS (0.30 mmol, 1.5 equiv), Na₂CO₃ (0.15 mmol), DMA/THF (3:1, 0.4 mL), rt, 24 h. ^b Yields were determined by GC FID, using 1-decane as the internal standard. ^c isolated yield. DEMS = Diethoxymethylsilane.

Table 2.8 Effect of the substrate's ratio

Finally, control experiments were carried out in order to ensure that all the reaction parameters were essential for the hydroalkylation to take place. Indeed, Table 2.9 shows that no product was formed in the absence of nickel catalyst, ligand, silane and base (entries 2-5).



^a **Conditions:** **2.5.1a** (0.20 mmol, 1.0 equiv), **2.5.2a** (0.34 mmol, 1.7 equiv), NiI₂ (5 mol%), **L2.5.2** (6 mol%), DEMS (0.30 mmol, 1.5 equiv), Na₂CO₃ (0.15 mmol), DMA/THF (3:1, 0.4 mL), rt, 24 h. ^b Yields were determined by GC FID, using 1-decane as the internal standard. DEMS = Diethoxymethylsilane.

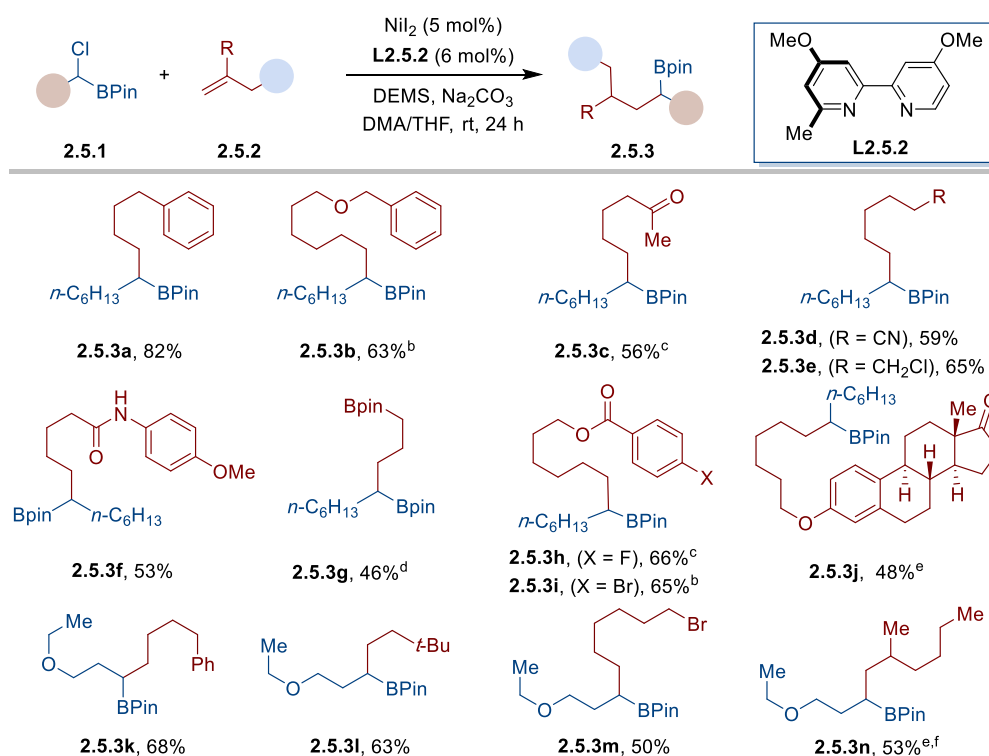
Table 2.9 Control experiments

2.5.1.2 Preparative Substrate Scope

3.5.1.2.1 Scope of Unactivated α -olefins

With the optimized reaction conditions in hand, we turned our attention on exploring the generality of our reductive hydroalkylation with unactivated α -olefins. As shown from the results compiled in Scheme 2.27, a series of α -olefins could be equally employed as substrates, providing the desired sp^3 C–C bonds formation products in good yield. Our protocol turned out to be highly chemoselective, as ketones (**2.5.3c**, **2.5.3j**), nitriles (**2.5.3d**), amides (**2.5.3f**), esters (**2.5.3h**, **2.5.3i**), or silyl ethers (**2.5.3q**), among others, could all be well accommodated. Equally interesting was the possibility to conduct this reaction in the presence of aryl halides (**2.5.3h**, **2.5.3i**), alkyl halides (**2.5.3e**, **2.5.3m**) or even boronic esters (**2.5.3g**), leaving ample room for further derivatization via classical cross-coupling technologies.¹ Notably, 1,1-disubstituted olefins (**2.5.3n**) could also be employed as substrate by slightly modify the reaction conditions.

*Site-Selective Ni-Catalyzed Reductive
Coupling of α -Haloboranes with Unactivated Olefins*



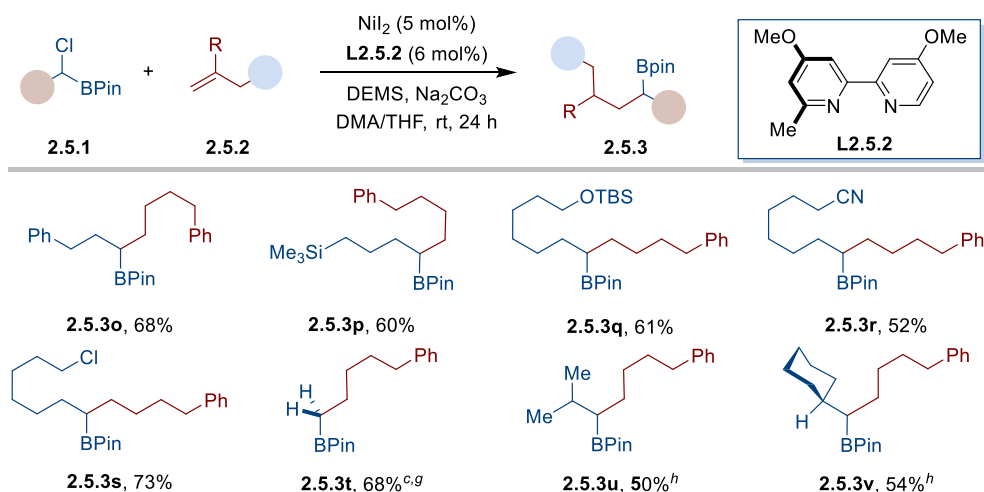
^a **Reaction Conditions:** **2.5.1** (0.20 mmol, 1.0 equiv), **2.5.2** (0.34 mmol, 1.7 equiv), NiI₂ (5 mol%), **L2.5.2** (6 mol%), DEMS (0.30 mmol, 1.5 equiv), Na₂CO₃ (0.15 mmol), DMA/THF (3:1, 0.4 mL), rt, 24 h; yield of isolated product, average of at least two independent runs. ^b NiBr₂·diglyme (10 mol%). ^c NiI₂ (10 mol%). ^d NiBr₂·diglyme (10 mol%), olefin (0.5 mmol). ^e dr = 1:1. ^f NiI₂ (10 mol%), **L2.5.12** (12 mol%). DEMS = Diethoxymethylsilane.

Scheme 2.27 Scope of unactivated α -olefins

2.5.1.2.2 Scope of α -Haloboranes

Encouraged by these initial findings, we turned our attention to explore the substitution pattern on the α -chloro alkylboronic ester backbone. As shown, a wide range of differently-substituted side-chains, including those containing, nitriles (**2.5.3r**), alkyl halides (**2.5.3s**), silyl ethers (**2.5.3q**), or silanes (**2.5.3p**), could be well-tolerated, forming the hydroalkylated products in good yields. Likewise, the reaction could be applied for unsubstituted side-chains (**2.5.3t**) or for α -substituted branched products (**2.5.3u**, **2.5.3v**). Notably, the hydroalkylation protocol could be easily scaled up without significant erosion in yield (**2.5.3t**).

Chapter 2.



^a **Reaction Conditions:** **2.5.1** (0.20 mmol, 1.0 equiv), **2.5.2** (0.34 mmol, 1.7 equiv), NiI_2 (5 mol%), **L2.5.2** (6 mol%), DEMS (0.30 mmol, 1.5 equiv), Na_2CO_3 (0.15 mmol), DMA/THF (3:1, 0.4 mL), rt, 24 h; yield of isolated product, average of at least two independent runs. ^b $\text{NiBr}_2 \cdot \text{diglyme}$ (10 mol%). ^c NiI_2 (10 mol%). ^d $\text{NiBr}_2 \cdot \text{diglyme}$ (10 mol%), olefin (0.5 mmol). ^e dr = 1:1. ^f NiI_2 (10 mol%), **L2.5.12** (12 mol%). ^g 6.0 mmol scale. ^h $\text{NiBr}_2 \cdot \text{diglyme}$ (10 mol%) at 40 °C, with α -bromoborane. DEMS = Diethoxymethylsilane.

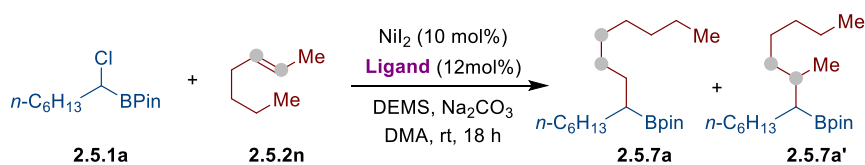
Scheme 2.28 Scope of α -haloboranes

2.5.2 Ni-Catalyzed Reductive Alkylation of α -Haloboranes with Internal Olefins

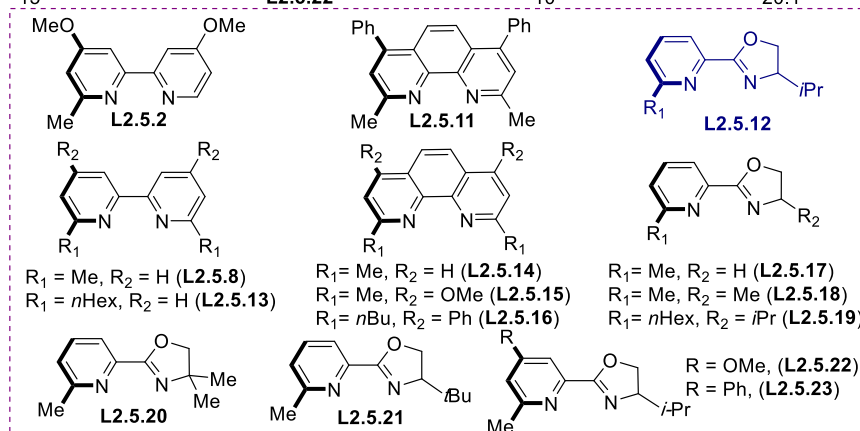
2.5.2.1 Optimization of the Reaction Conditions

The lower binding affinity of internal olefins^{33,34} and the propensity of nickel catalysts to enable C–C bond-formation at the initial reaction site⁷⁵ left a reasonable doubt as to whether the site-selectivity could be either tuned or controlled with internal alkenes.⁷⁵ Inspired by our group report on remote sp^3 C–H carboxylation via chain-walking strategies,^{38,60} we intended to forge sp^3 C–C bonds at remote sp^3 C–H site of internal olefins. Surprisingly, primary, sp^3 C–H selective alkylation product was obtained in 11% yield with 8.5:1 regioselectivity by replacing α -olefin (**2.5.2a**) with internal olefin (**2.5.2n**) under Ni/**L2.5.2** system (Table 2.10, entry 1).

*Site-Selective Ni-Catalyzed Reductive
Coupling of α -Haloboranes with Unactivated Olefins*



Entry	Ligand	Yield of 2.5.7a (%) ^b	2.5.7a:2.5.7a'
1	L2.5.2	11	8.5:1
2	L2.5.8	10	1.85:1
3	L2.5.11	4	1.6:1
4	L2.5.12	61, (70^c)	44:1
5	L2.5.13	3	2.5:1
6	L2.5.14	5	1.56:1
7	L2.5.15	9	2:1
8	L2.5.16	8	1.5:1
9	L2.5.17	9	9:1
10	L2.5.18	33	30:1
11	L2.5.19	51	51:1
12	L2.5.20	16	30:1
13	L2.5.21	43	40:1
14	L2.5.22	57	38:1
15	L2.5.22	10	20:1



^a **Reaction Conditions:** **2.5.1a** (0.20 mmol, 1.0 equiv), **2.5.2n** (0.34 mmol, 1.7 equiv), NiI₂ (10 mol%), **Ligand** (12 mol%), DEMS (0.40 mmol, 2.0 equiv), Na₂CO₃ (0.2 mmol), DMA (0.6 mL), rt, 18 h. ^b Yields and linear/branched ratio were determined by GC FID, using 1-decane as the internal standard. ^c **2.5.1a** (0.30 mmol, 1.5 equiv), **2.5.2n** (0.20 mmol, 1.0 equiv). DEMS = Diethoxymethylsilane. Ligands **L2.5.2**, **L2.5.8**, **L2.5.11** and **L2.5.12** were also used in the Ni-catalyzed reductive coupling of α -haloboranes with terminal olefins.

Table 2.10 Screening of ligand

Encouraged by this observation, we turned our attention to evaluating the effect of ligand on this remote sp^3 C–H alkylation. As evident from the results compiled in Table 2.10, the nature of the ligand played a crucial role for the reaction success. The use of ortho-disubstituted bipyridine and phenanthroline-type ligands which previously been used in chain-walking transformations led to unsatisfactory results.^{33,34} Interestingly, similar yield and regioselectivity were found by the replacement of ligand (**L2.5.2**) to 2-(6-methylpyridin-2-yl)-4,5-dihydrooxazole (**L2.5.17**). To the best of our knowledge, pyridine-oxazoline-type (PyOx)ligands are well used in Pd-catalyzed chain-walking reactions rather than nickel catalysis.⁷⁶ Promoted by the discovery, we tried to increase the reactivity and regioselectivity of the remote alkylation by modifying the backbone of PyOx ligands. If successful, this would not only provide high regioselectivity, but may also yield high enantioselectivity by using chiral PyOx ligand. As expected, increasing the steric hindrance of the ortho-substitution of oxazoline had a positive effect on both reactivity and regio-selectivity, as well as the use of isopropyl substituent (**L2.5.12**) giving the best results (entries 7-15). Moreover, the yield can be increased to 70% by slightly changing the ratio of starting materials, without have any effect on the regioselectivity.

The reaction scheme shows the nickel-catalyzed remote C-H alkylation of compound **2.5.1a** (n-C₆H₁₃-CH₂-CH(Cl)-BPin) with ligand **2.5.2n** (a 2,6-dimethyl-2,5-dihydrooxazole derivative). The reaction conditions are NiI₂ (10 mol%), **L2.5.12** (12 mol%), DEMS, Na₂CO₃, **Sol.**, rt, 18 h. The products are **2.5.7a** (linear) and **2.5.7a'** (branched).

Entry	Sol.	Yield of 2.5.7a (%) ^b	2.5.7a : 2.5.7a'
1	DMA	63(70^c)	44:1
2	DMF	59	33:1
3	NMP	33	48:1
4	DME	0	-
5	THF	trace	-
6	Dioxane	trace	-
7	DMA:THF(3:1)	50	30:1

^a **Reaction Conditions:** **2.5.1a** (0.20 mmol, 1.0 equiv), **2.5.2n** (0.34 mmol, 1.7 equiv), NiI₂ (10 mol%), **L2.5.12** (12 mol%), DEMS (0.40 mmol, 2.0 equiv), Na₂CO₃ (0.2 mmol), **Sol.** (0.6 mL), rt, 18 h. ^b Yields and linear/branched ratio were determined by GC FID, using 1-decane as the internal standard. ^c **2.5.1a** (0.30 mmol, 1.5 equiv), **2.5.2n** (0.20 mmol, 1.0 equiv). DEMS = Diethoxymethylsilane.

Table 2.11 Screening of solvents

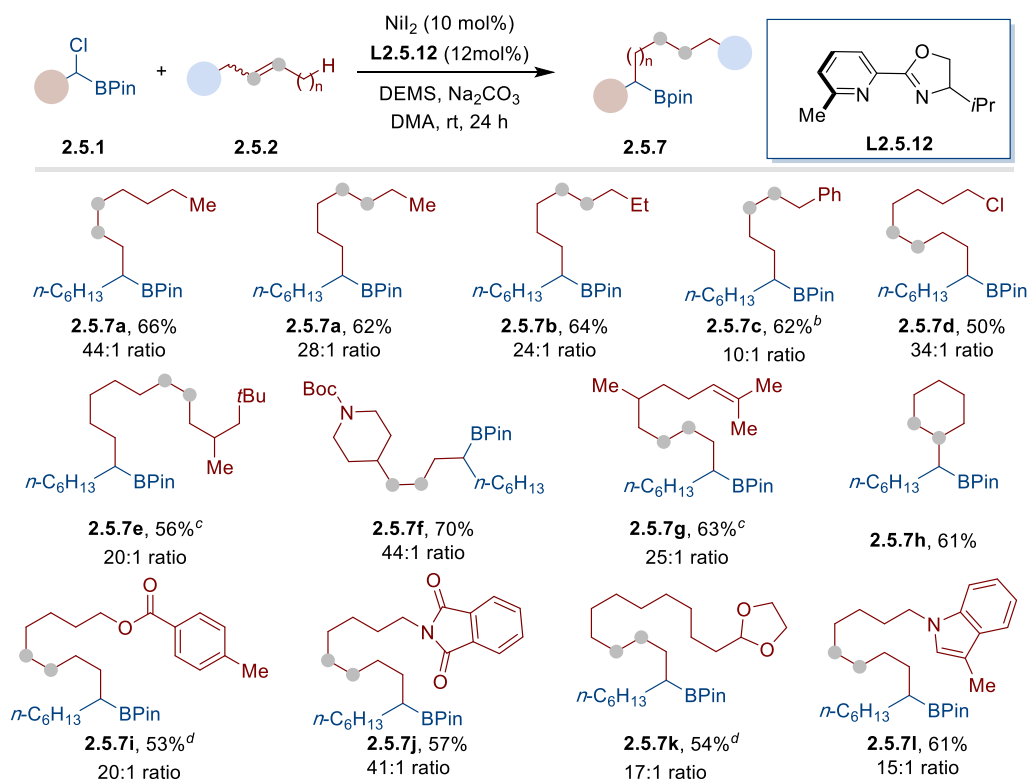
*Site-Selective Ni-Catalyzed Reductive
Coupling of α -Haloboranes with Unactivated Olefins*

With the robust Ni/L2.5.12 catalytic system in hand, we next evaluated the effect of solvents (Table 2.11). As expected, still amide-containing polar aprotic solvents, such as DMF and DMA could ensure good results.

2.5.2.2 Preparative Substrate Scope

2.5.2.2.1 Scope of Unactivated Internal Olefins

With these inspiring result in hand, we further examined the generality of the transformation by exploring a wide range of internal alkenes (Scheme 2.29). Importantly, isomeric 3-heptene or 4-octene gave rise to **2.5.7a** and **2.5.7b** in good yields and excellent site-selectivities. As shown, cyclic (**2.5.7h**) or acyclic olefins (**2.5.7a-g**, **2.5.7i-l**), regardless of the double bond geometry, posed no problems. Although one might argue that an erosion in site-selectivity might arise with side-chains containing weak, benzylic sp^3 C–H bonds, C–C bond-formation occurred preferentially at the primary sp^3 C–H site (**2.5.7c**).³⁴ Likewise, the inclusion of esters (**2.5.7i**), carbamates (**2.5.7f**), acetals (**2.5.7k**), alkyl halides (**2.5.7d**) or nitrogen-containing heterocycles (**2.5.7f**, **2.5.7j**, **2.5.7l**) did not interfere with productive chain-walking. Of particular relevance was the functionalization of polyunsaturated backbones (**2.5.7g**) or substrates containing branched methyl groups (**2.5.7e**, **2.5.7g**); while the less-sterically hindered olefin was selectively functionalized in the former, reaction took place at the most accessible primary sp^3 C–H site in the latter.



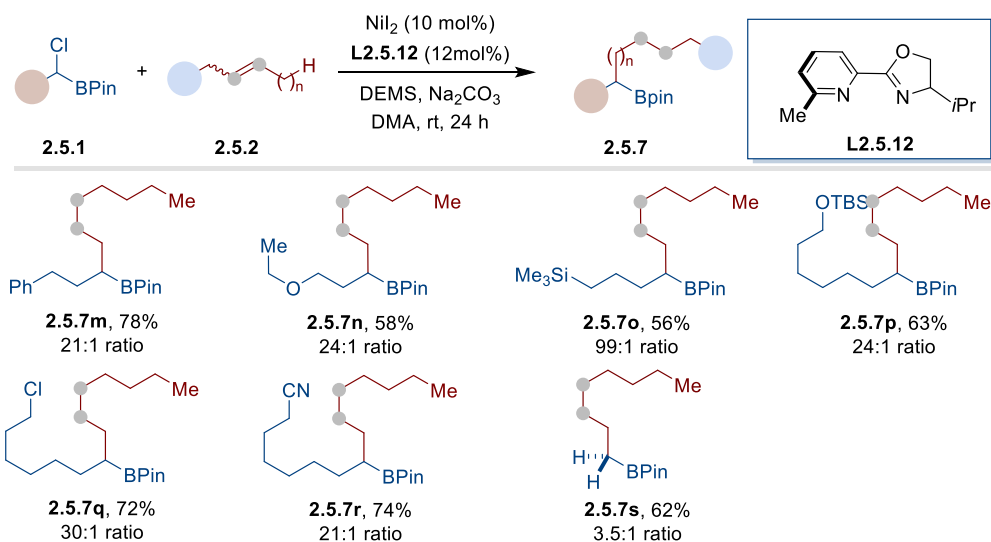
^a **Reaction Conditions:** **2.5.1** (0.20 mmol, 1.0 equiv), **2.5.2** (0.34 mmol, 1.7 equiv), NiI_2 (10 mol%), **L2.5.12** (12 mol%), Na_2CO_3 (1.0 equiv) in DMA; Isolated yields, average of two independent runs (regioisomeric ratios are indicated in parenthesis). ^b 10 °C. ^c dr = 1:1. ^d α -haloborane (2.0 equiv), $\text{NiBr}_2 \cdot \text{diglyme}$ (10 mol%).

Scheme 2.29 Scope of internal olefins

2.5.2.2.2 Scope of α -Haloboranes

To further prove the efficiency of our technology, a wide range of α -chloro alkylboronic ester were explored (Scheme 2.30). As shown, a wide range of differently-substituted side-chains, including those containing ethers (**2.5.7n**), nitriles (**2.5.7r**), alkyl halides (**2.5.7q**), silyl ethers (**2.5.7p**), or silanes (**2.5.7o**), could be well-tolerated, resulting in hydroalkylated products at remote primary sp^3 C–H site. It is worth to note that no chain-walking along the hydrocarbon side-chain of α -chloro alkylboronic ester was found under these reaction conditions.³⁴

*Site-Selective Ni-Catalyzed Reductive
Coupling of α -Haloboranes with Unactivated Olefins*



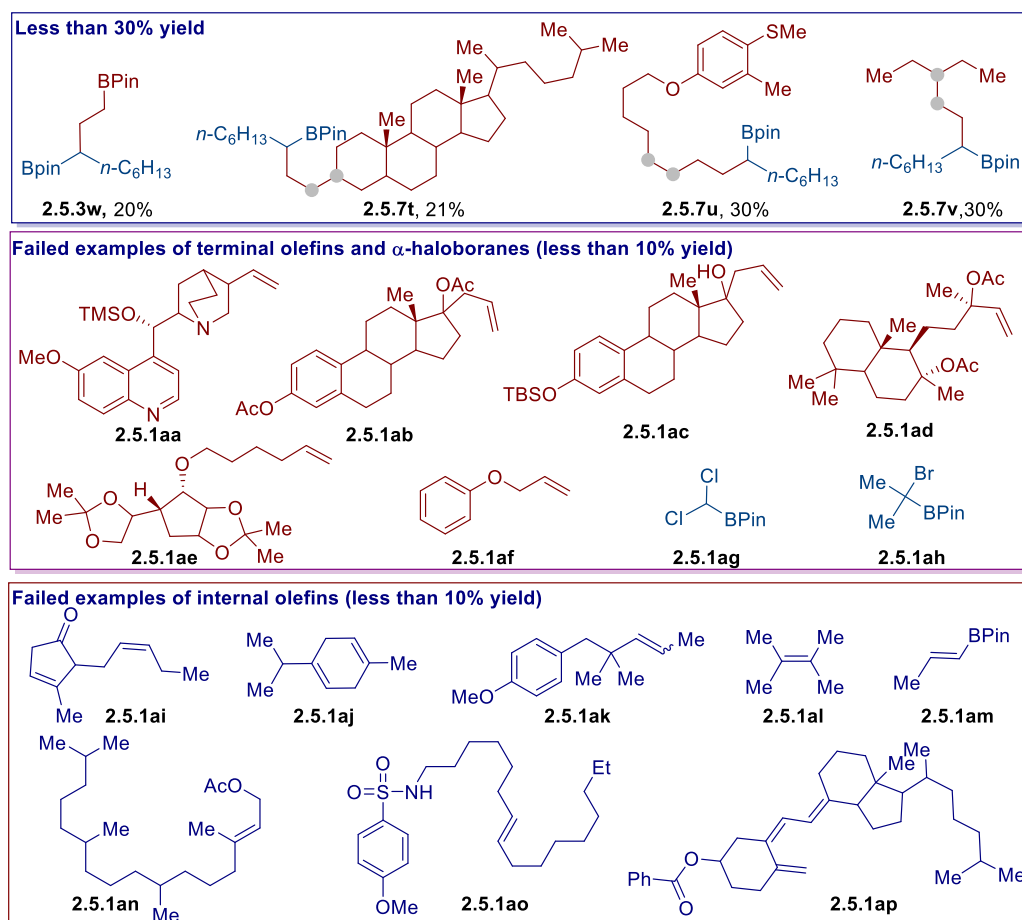
^a **Reaction Conditions:** **2.5.1** (0.20 mmol, 1.0 equiv), **2.5.2** (0.34 mmol, 1.7 equiv), NiI₂ (10 mol%), **L2.5.12** (12 mol%), Na₂CO₃ (1.0 equiv) in DMA; Isolated yields, average of two independent runs (regioisomeric ratios are indicated in parenthesis).

Scheme 2.30 Scope of α -haloboranes with internal olefins

2.5.2.3 Unsuccessful Substrates

Although we demonstrated that the reductive hydroalkylation of unactivated olefins occurred with a wide substrate scope, a number of examples failed to provide the desired product or gave lower yield (around 20-30%) (Scheme 2.31). For example, activated alkenyl boronic esters provided the product in 20% yield (**2.5.3w**) or less than 5% yield (**2.5.1am**), with some branched side products, which had been later reported by Zhu⁴⁵ and Hu⁴⁶ group, independently. The formation of branched side products is due to the formation of α -boron stabilization of alkyl-Ni species. Additionally, the substrate bearing a strong coordinating group such quinine (**2.5.1aa**), sulfonamide (**2.5.1o**) or with unprotected alcohol group (**2.5.1c**), resulted in no conversion. The presence of multiple C–O (**2.5.1aa–2.5.1ae**) or C–S (**2.5.7u**) bonds was equally incompatible, due to the strong binding to Ni centers. Moreover, sterically-crowded substrates such as (**2.5.7t**, **2.5.7v**) gave lower yield (less than 30%), whereas (**2.5.1ak**, **2.5.1al**) resulted in no conversion. In this particular case, the presence of (homo)allylic acetate (**2.5.1ab**, **2.5.1ad**, **2.5.1an**) and allylic ether (**2.5.1af**)

provided trace amounts of product, probably due to the formation of π -allylic-Ni species, forming C–O cleavage side products.⁷⁷ Unfortunately, substrates possessing dienes (**2.5.1ai**, **2.5.1aj** and **2.5.1ap**) provided the desired C–C bonds formation products in low yields with complicated mixtures, possibly owing to the strong binding with nickel and which may result in site-selectivity issues. The more activated dichloroboronic ester (**2.5.1ag**) and bulky tertiary α -bromo boronic ester (**2.5.1ah**) failed to provide even traces of the targeted products.

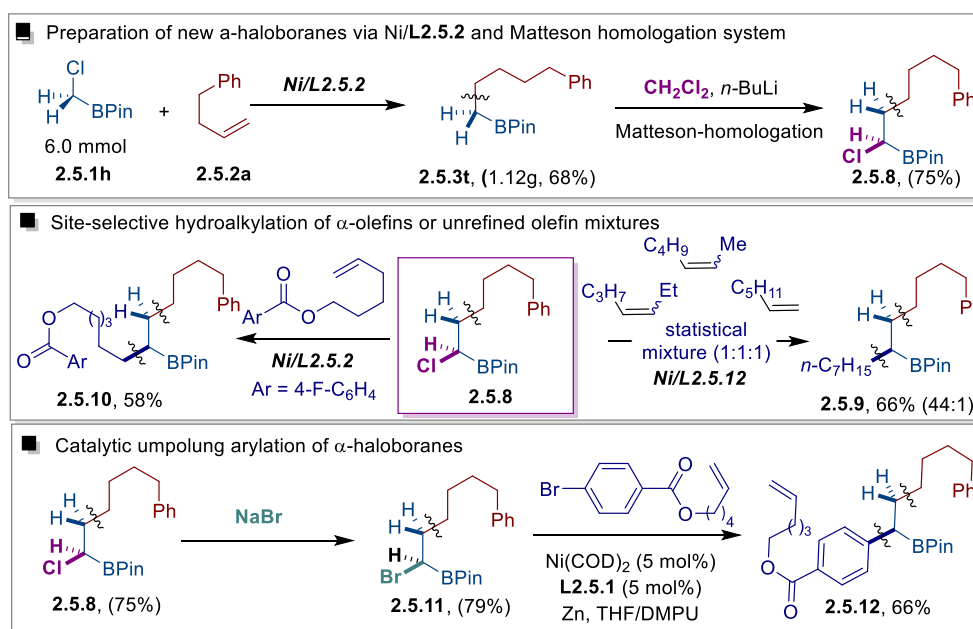


Scheme 2.31 Unsuccessful substrates

2.5.3 Iterative Platform for C–C Bond-Formations

Promoted by the results we obtained in Schemes 2.27–2.30, we thought that our protocol might serve as a platform to build up C_{sp^3} – C_{sp^3} bonds in an iterative manner by using simple olefin feedstocks as starting materials. As shown in Scheme 2.32, this turned out to be the case. Specifically, Ni/**L2.5.2**-catalyzed reductive coupling of

commercially-available α -chloro boronic ester (**2.5.1h**) with phenyl-1-butene (**2.5.2a**) followed by Matteson homologation⁷⁸ cleanly furnished a new α -chloro boronic ester **2.5.8** in 75% yield on a gram scale. As expected, exposure of **2.5.8** under a Ni/L**2.5.12** protocol in the presence of statistical mixtures (1:1:1) of isomeric heptenes gave rise to **2.5.9** (44:1 ratio). Likewise, **2.5.10** could be easily prepared by using a terminal olefin with Ni/L**2.5.2** couple. Bromination of **2.5.8** with NaBr, produced α -bromo alkylboronic ester **2.5.11** in 79% yield, whereas C_{sp^3} – C_{sp^2} bond-formation en route to **2.5.12** could be enabled by a catalytic umpolung arylation by using Ni/L**2.5.1** system with Zn as reductant.^{71b} Particularly noteworthy is the orthogonality observed with pendant alkenes in the latter, suggesting that subsequent homologations at the alkene terminus might be easily within reach.

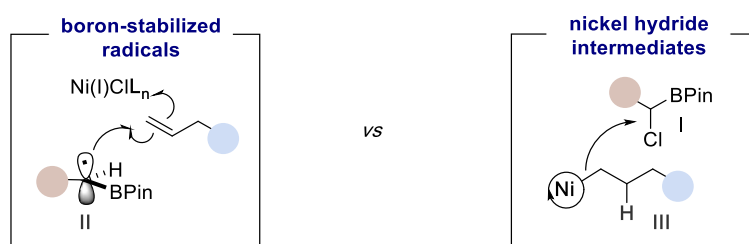


Scheme 2.32 Iterative platform for C–C bond-formations

2.5.4 Mechanism Experiments

With the preparative results of our regioselective hydroalkylation in hand, we next focused our attention to elucidating the mechanism of our protocol. In principle, two different mechanistic interpretations are conceivable for our results: (a) initial *single-electron-transfer* (SET) from Ni(0)L_n to α -haloboranes (**I**), leading to boron-stabilized alkyl radicals⁷⁹ **II** prior to addition across the olefin partner (Scheme 2.33, *top left*) or (b) hydrofunctionalization of an olefin via nickel hydride species en

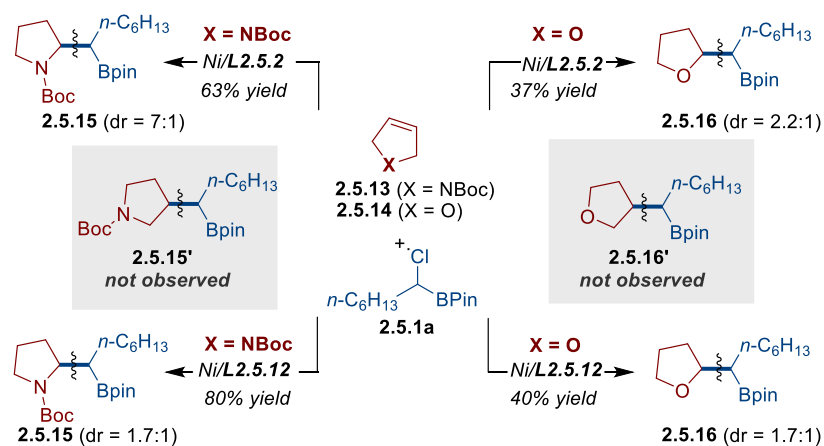
route to **III**, ultimately enabling C–C bond-formation by reaction with **I** (Scheme 2.33, *top right*).



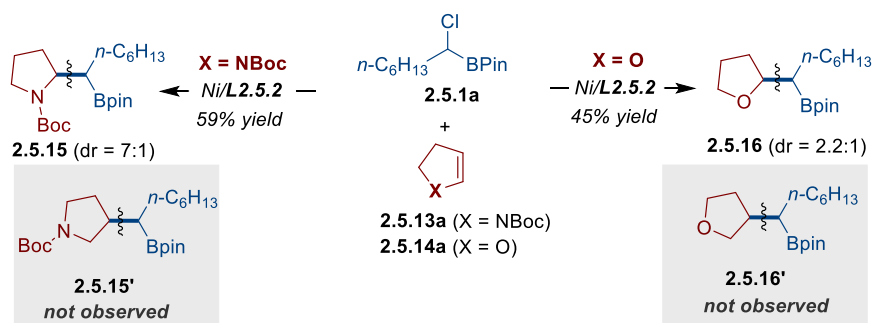
Scheme 2.33 Mechanism proposal

2.5.4.1 Studying the Regioselectivity of Dihydrofuran and Dihydropyrrole

Although our experimental data does not allow us to rigorously distinguish between these two manifolds, we decided to gather indirect evidence about the mechanism by studying the reaction of dihydroheterocycles (**2.5.13** and **2.5.14**) with **2.5.1a**. C3-selectivity was anticipated for a mechanism consisting of the intermediacy of **II**; on the contrary, C–C bond-formation at C2 would suggest the involvement of a nickel hydride that might generate **III** prior to addition to **2.5.1a**. As shown in Scheme 2.34, C2 selectivity products **2.5.15** and **2.5.16** were exclusively obtained using either a Ni/**L2.5.2** or a Ni/**L2.5.12** protocol; under the limits of detection, not even traces of **2.5.15'** or **2.5.16'** were detected in the crude mixtures, suggesting that a nickel hydride scenario seems more likely. Moreover, C3 selectivity would also be expected if olefin isomerization occurs at early stages, as stabilized α -amino or α -oxygen radicals should be generated upon addition of **II** across the olefin. As shown, only C2 selectivity products were found with 1,2-dihydroheterocycle under Ni/**L2.5.2** system (Scheme 2.35). These findings are in agreement with our previous conclusion. The olefin isomerization process was further confirmed via control experiment in the absence of **2.5.1a** (Table 2.12). Whether these outcomes suggest the involvement of Ni(I) entities or other mechanistic interpretations are currently ongoing.

Coupling of α -Haloboranes with Unactivated Olefins

Scheme 2.34 Studying the regioselectivity of 2.5.13 and 2.5.14



Scheme 2.35 Studying the regioselectivity of 2.5.13a and 2.5.14a

Entry	Time	Yield of 2.5.13a (%) <i>Ni/L2.5.2</i>	Yield of 2.5.13a (%) <i>Ni/L2.5.2</i>
1	10 min	16	13
2	20 min	24	22
3	30 min	25	29
4	1 h	31	38
5	2 h	34	49
6	24 h	31	43

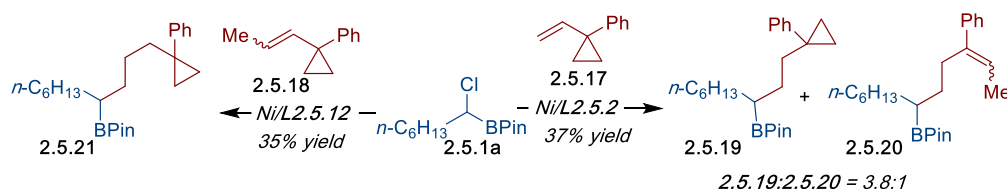
Table 2.12 Isomerization of 2.5.13 under the reaction conditions

2.5.4.2 Experiments with radical probes

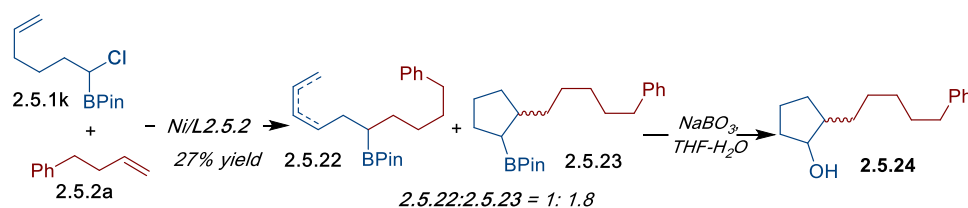
To further elucidate the mechanism, we decided to carry out radical trap experiments. We found that olefins decorated with an adjacent cyclopropyl motif as 2.5.17 or 2.5.18 do not undergo substantial ring-opening, thus ruling out a radical **II** addition into olefin process (Scheme 2.36). However, when 2-(1-chlorohex-5-en-1-yl)

Chapter 2.

-4,4,5,5-tetramethyl-1,3,2-dioxaborolane (**2.5.1k**) was submitted to the optimized reaction conditions, a mixture of direct hydroalkylation product **2.5.22** and 5-*exo-trig* cyclization product **2.5.23** were obtained as a 1:1.8 ratio, suggesting oxidative addition with **I** may go through a SET pathway (Scheme 2.37).



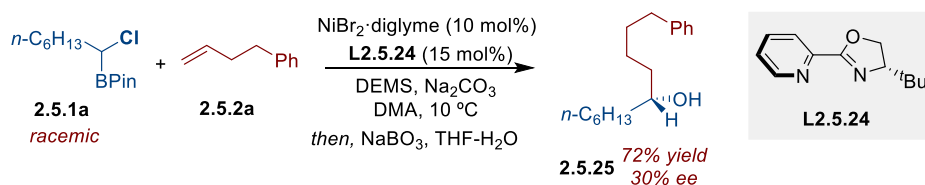
Scheme 2.36 Radical trap experiments of **2.5.17** and **2.5.18**



Scheme 2.37 Radical trap experiments of **2.5.1k**

2.5.5 Preliminary Enantioconvergent Coupling Reaction

With these preliminary mechanistic experiments in hand, we questioned that whether an enantioselective reductive hydroalkylation could be developed by using racemic precursors with and appropriate chiral ligands. As shown in Scheme 2.38, **2.5.25** could be preliminary obtained in good yields and modest enantioselectivity under Ni/L2.5.24 regime, setting the basis for designing highly enantioselective routes. Particularly noteworthy, during that stage, the development of enantioselective reductive hydroalkylation of unactivated alkenes remained poorly explored.



Scheme 2.38 Preliminary enantioconvergent coupling reaction

2.6 Conclusions

This chapter summarizes the efforts towards the development of a Ni-catalyzed site-selective reductive alkylation of α -haloboranes with unactivated olefins, thus allowing to incorporate an alkylboron fragment into simple and available olefin feedstocks. Exquisite *anti*-Markovnikov-selectivity hydroalkylation was obtained with α -olefins by using Ni/L2.5.2 system with silane as hydride source. The utilization of internal, unactivated olefins results in C–C bond-formation at remote unfunctionalized sp^3 C–H sites via Ni-catalyzed chain-walking strategies.

The mild reaction conditions utilized and the broad functional group tolerance makes this transformation a useful entry point for preparing useful building blocks from simple olefins as raw materials, while providing a complementary alternative to existing borylation techniques. Moreover, this protocol can be employed in iterative synthesis for building up molecular complexity. Preliminary mechanistic studies suggested that hydrofunctionalization of olefins occurs via nickel hydride species, followed by the coupling with the α -haloborane. However, whether the reaction occurs via Ni(I) or Ni(II) intermediates remains unclear and further mechanistic studies are required to fully elucidate the mechanism.

Preliminary enantioselective studies of this transformation provided moderate enantioselectivity. Very recently, the group of Fu and Zhu, independently developed a Ni-catalyzed enantioconvergent coupling of racemic secondary or tertiary α -bromo amides with unactivated olefins.

2.7 References

1. For selected reviews on catalytic C–C bond formation: (a) De Meijere, A.; Bräse, S.; Oestreich, M. *Metal-Catalyzed Cross Coupling Reactions*; Wiley-VCH: Weinheim, Germany, 2004. (b) Jana, R.; Pathak, T. P.; Sigman, M. S. *Advances in Transition Metal (Pd, Ni, Fe)-Catalyzed Cross-Coupling Reactions Using Alkyl-Organometallics as Reaction Partners*. *Chem. Rev.* **2011**, *111*, 1417. (c) Busch, M.; Wodrich, M. D.; Corminboeuf, C. A Generalized Picture of C–C Cross-Coupling. *ACS Catal.* **2017**, *7*, 5643.
2. (a) Molander, G.; Milligan, J. A.; Phelan, J. P.; Badir, S. O. Recent Advances in Alkyl Carbon-Carbon Bond Formation by Nickel/Photoredox Cross-Coupling. *Angew. Chem. Int. Ed.* **2019**, *58*, 6152. (b) Choi, J.; Fu, G. C. Transition Metal-Catalyzed Alkyl-Alkyl Bond Formation: Another Dimension in Cross-Coupling Chemistry. *Science* **2017**, *356*, 152. (c) Hu, X. Nickel-Catalyzed Cross-Coupling of Non-Activated Alkyl Halides: A Mechanistic Perspective. *Chem. Sci.* **2011**, *2*, 1867. (d) Kambe, N.; Iwasakia, T.; Terao, J. Pd-Catalyzed Cross-Coupling Reactions of Alkyl Halides. *Chem. Soc. Rev.* **2011**, *40*, 4937. (e) Rudolph, A.; Lautens, M. Secondary Alkyl Halides in Transition-Metal-Catalyzed Cross-coupling Reactions. *Angew. Chem. Int. Ed.* **2009**, *48*, 2656. (f) Frisch, A. C.; Beller, M. Catalysts for Cross-Coupling Reactions with Non-activated Alkyl Halides. *Angew. Chem., Int. Ed.* **2005**, *44*, 674. (g) Luh, T. Y.; Leung, M. K.; Wong, K. T. Transition Metal-Catalyzed Activation of Aliphatic C–X Bonds in Carbon–Carbon Bond Formation. *Chem. Rev.* **2000**, *100*, 3187.
3. Amghizar, I.; Vandewalle, L. A.; Van Geem, K. M.; Marin, G. B. New Trends in Olefin Production. *Engineering*, **2017**, *3*, 171.
4. For representative classes of synthetically important alkene functionalization reactions, see: (a) Dong, Z.; Ren, Z.; Thompson, S. J.; Xu, Y.; Dong, G. Transition-Metal-Catalyzed C–H alkylation Using Alkenes. *Chem. Rev.* **2017**, *117*, 9333. (b) Tang, S.; Liu, K.; Liu, C.; Lei, A. Olefinic C–H Functionalization through Radical Alkenylation. *Chem. Soc. Rev.* **2015**, *44*, 1070. (c) Saini, V.; Stokes, B. J.; Sigman, M. S. Transition-Metal-Catalyzed Laboratory-Scale Carbon–Carbon Bond-Forming Reactions of Ethylene. *Angew. Chem., Int. Ed.* **2013**, *52*, 11206. (d) McDonald, R. I.; Liu, G.; Stahl, S. S. Palladium(II)-Catalyzed Alkene Functionalization via Nucleopalladation: Stereochemical Pathways and

*Site-Selective Ni-Catalyzed Reductive
Coupling of α -Haloboranes with Unactivated Olefins*

- Enantioselective Catalytic Applications. *Chem. Rev.* **2011**, *111*, 2981. (e) Hoveyda, A. H.; Zhugralin, A. R. The Remarkable Metal-Catalysed Olefin Metathesis Reaction. *Nature* **2007**, *450*, 243.
5. Takacs, J. M.; Jiang, X. The Wacker Reaction and Related Alkene Oxidation Reactions. *Curr. Org. Chem.* **2003**, *7*, 369.
 6. (a) Obligacion, J. V.; Chirik, P. J. Earth-Abundant Transition Metal Catalysts for Alkene Hydrosilylation and Hydroboration. *Nat. Rev. Chem.* **2018**, *2*, 15. (b) Crudden, C. M.; Edwards, D. Catalytic Asymmetric Hydroboration: Recent Advances and Applications in Carbon–Carbon Bond-Forming Reactions. *Eur. J. Org. Chem.* **2003**, 4695.
 7. (a) Cartney, D. M.; Guiry, P. J. The Asymmetric Heck and Related Reactions. *Chem. Soc. Rev.* **2011**, *40*, 5122. (b) Beletskaya, I. P.; Cheprakov, A. V. The Heck Reaction as A Sharpening Stone of Palladium Catalysis. *Chem. Rev.* **2000**, *100*, 3009.
 8. (a) Ogba, O. M. Warner, N. C.; O’Leary, D. J.; Grubbs, R. H. Recent Advances in Ruthenium-Based Olefin Metathesis. *Chem. Soc. Rev.* **2018**, *47*, 4510. (b) Connon, S. J.; Blechert, S. Recent Developments in Olefin Cross-Metathesis. *Angew. Chem. Int. Ed.* **2003**, *42*, 1900.
 9. (a) Franke, R.; Selent, D.; Börner, A. "Applied Hydroformylation". *Chem. Rev.* **2012**, *112*, 5675. (b) Evans, P. A. Modern Rhodium-Catalyzed Organic Reactions 93–110 (Wiley-VCH, 2005).
 10. He, J.; Wasa, M.; Chan, K. S. L.; Shao, Q.; Yu, J.-Q. Palladium-Catalyzed Alkyl C–H Bond Activation. *Chem. Rev.* **2017**, *117*, 8754.
 11. Corey, E. J.; Chen, X.-M. The Logic of Chemical Synthesis (John Wiley & Sons, Inc., 1995).
 12. (a) Crossley, S. W. M.; Martinez, R. M.; Obradors, C.; Shenvi, R. A. Mn, Fe, and Co-Catalyzed Radical Hydrofunctionalization of Olefins. *Chem. Rev.* **2016**, *116*, 8912. (b) Chen, J.; Guo, J.; Lu, Z. Recent Advances in Hydrometallation of Alkenes and Alkynes via The First Role Transition Metal Catalysis. *Chin. J. Chem.* **2018**, *36*, 1075.
 13. Nguyen, K. D.; Park, B. Y.; Luong, T.; Sato, H.; Garza, V. J.; Krische, M. J. Metal-Catalyzed Reductive Coupling of Olefin-Derived Nucleophiles: Reinventing Carbonyl Addition. *Science* **2016**, *354*, 300.

Chapter 2.

14. (a) Hoffmann, R. W. Markovnikov Free Radical Addition Reactions, A Sleeping Beauty Kissed to Life. *Chem. Soc. Rev.* **2016**, *45*, 577. (b) Hu, Y.; Shaw, A. P.; Estes, D. P.; Norton, J. Transition-Metal Hydride Radical Cations. *Chem. Rev.* **2016**, *116*, 8427.
15. (a) Lo, J. C.; Gui, J.; Yabe, Y.; Pan, C. M.; Baran, P. S. Functionalized Olefin Cross-Coupling to Construct Carbon–Carbon Bonds. *Nature* **2014**, *516*, 343. (b) Lo, J. C.; Yabe, Y.; Baran, P. S. A Practical and Catalytic Reductive Olefin Coupling. *J. Am. Chem. Soc.* **2014**, *136*, 1304.
16. (a) Gaspar, B.; Carreira E. M. Mild Cobalt-Catalyzed Hydrocyanation of Olefins with Tosyl Cyanide. *Angew. Chem. Int. Ed.* **2007**, *46*, 4519. (b) Gaspar, B.; Carreira E. M. Catalytic Hydrochlorination of Unactivated Olefins with *para*-Toluenesulfonyl Chloride. *Angew. Chem. Int. Ed.* **2008**, *47*, 5758.
17. (a) Zhu, S.; Niljianskul, N.; Buchwald, S. L. Enantio- and Regioselective CuH-Catalyzed Hydroamination of Alkenes. *J. Am. Chem. Soc.* **2013**, *135*, 15746. (b) Yang, Y.; Shi, S. L.; Niu, D.; Liu, P.; Buchwald, S. L. Catalytic Asymmetric Hydroamination of Unactivated Internal Olefins to Aliphatic Amines. *Science* **2015**, *349*, 62.
18. Wang, X.-X.; Lu, X.; Li, Y.; Wang, J.-W.; Fu, Y. Recent Advances in Nickel-Catalyzed Reductive Hydroalkylation and Hydroarylation of Electronically Unbiased Alkenes. *Sci. Chin. Chem.* **2020**, doi.org/10.1007/s11426-020-9838-x.
19. Lu, X.; Xiao, B.; Zhang, Z.; Gong, T.; Su, W.; Yi, J.; Fu, Y.; Liu, L. Practical Carbon–Carbon Bond Formation from Olefins Through Nickel-Catalyzed Reductive Olefin Hydrocarbonation. *Nat. Commun.* **2016**, *7*, 11129.
20. Lu, X.; Xiao, B.; Liu, L.; Fu, Y. Formation of C(sp³)–C(sp³) Bonds through Nickel-Catalyzed Decarboxylative Olefin Hydroalkylation Reactions. *Chem. Eur. J.* **2016**, *22*, 11161.
21. Nguyen, J.; Chong, A.; Lalic, G. Nickel-Catalyzed Anti-Markovnikov Hydroarylation of Alkenes. *Chem. Sci.* **2019**, *10*, 3231.
22. Green, S. A.; Crossley, S. W. M.; Matos, J. L. M.; Vásquez-Céspedes, S.; Shevick, S. L.; Shenvi, R. A. The High Chemofidelity of Metal-Catalyzed Hydrogen Atom Transfer. *Acc. Chem. Res.* **2018**, *51*, 2628.
23. Green, S. A.; Matos, J. L. M.; Yagi, A.; Shenvi, R. A. Branch-Selective Hydroarylation: Iodoarene–Olefin Cross-Coupling. *J. Am. Chem. Soc.* **2016**, *138*, 12779.

*Site-Selective Ni-Catalyzed Reductive
Coupling of α -Haloboranes with Unactivated Olefins*

24. Shevick, S. L.; Obradors, C.; Shenvi, R. A. Mechanistic Interrogation of Co/Ni-Dual Catalyzed Hydroarylation. *J. Am. Chem. Soc.* **2018**, *140*, 12056.
25. Ling, T.; Rivas, F. All-Carbon Quaternary Centers in Natural Products and Medicinal Chemistry: Recent Advances. *Tetrahedron* **2016**, *72*, 6729.
26. (a) Christoffers, J.; Baro, A.; Eds. Quaternary Stereocenters-Challenges and Solutions for Organic Synthesis; Wiley-VCH: Weinheim, 2005. (b) Quasdorf, K. W.; Overman, L. E. Catalytic Enantioselective Synthesis of Quaternary Carbon Stereocentres. *Nature* **2014**, *516*, 181.
27. Green, S. A.; Vásquez-Céspedes, S.; Shenvi, R. A. Iron–Nickel Dual-Catalysis: A New Engine for Olefin Functionalization and the Formation of Quaternary Centers. *J. Am. Chem. Soc.* **2018**, *140*, 11317.
28. Green, S. A.; Huffman, T. R.; McCourt, R. O.; van der Puyl, V.; Shenvi, R. A. Hydroalkylation of Olefins to Form Quaternary Carbons. *J. Am. Chem. Soc.* **2019**, *141*, 7709.
29. Carney, J. R.; Dillon, B. R.; Campbell, L.; Thomas, S. P. Manganese-Catalyzed Hydrofunctionalization of Alkenes. *Angew. Chem., Int. Ed.* **2018**, *57*, 10620.
30. For selected reviews on C–H functionalization, see: (a) Gensch, T.; Hopkinson, M. N.; Glorius, F.; Wencel-Delord, J. Mild Metal-Catalyzed C–H Activation: Examples and Concepts. *Chem. Soc. Rev.* **2016**, *45*, 2900. (b) Crabtree, R. H.; Lei, A. Introduction: C–H Activation. *Chem. Rev.* **2017**, *117*, 8481. (c) Gandeepan, P.; Müller, T.; Zell, D.; Cera, G.; Warratz, S.; Ackermann, L. 3d Transition Metals for C–H Activation. *Chem. Rev.* **2019**, *119*, 2192. (d) Lyons, T. W.; Sanford, M. S. Palladium-Catalyzed Ligand-Directed C–H Functionalization Reactions. *Chem. Rev.* **2010**, *110*, 1147. (e) Chen, X.; Engle, K. M.; Wang, D. –H.; Yu, J. –Q. Palladium(II)-Catalyzed C–H Activation/C–C Cross-Coupling Reactions: Versatility and Practicality. *Angew. Chem. Int. Ed.* **2009**, *48*, 5094.
31. For selected reviews: (a) Li, H.; Li, B.–J.; Shi, Z.–J. Challenge and Progress: Palladium-Catalyzed sp^3 C–H Activation. *Catal. Sci. Technol.* **2011**, *1*, 191. (b) Jazzar, R.; Hitce, J.; Renaudat, A.; Sofack-Kreutzer, J.; Baudoin, O. Functionalization of Organic Molecules by Transition-Metal-Catalyzed C(sp^3)–H Activation. *Chem. – Eur. J.* **2010**, *16*, 2654. (c) Herrmann, P.; Bach, T. Diastereotopos-Differentiating C–H Activation Reactions at Methylene Groups. *Chem. Soc. Rev.* **2011**, *40*, 2022. (d) Davies, H. M. L.; Morton, D. Collective Approach to Advancing C–H Functionalization. *ACS Cent. Sci.* **2017**, *3*, 936. (e) Hartwig, J. F.; Larsen, M. A.

- Undirected, Homogeneous C–H Bond Functionalization: Challenges and Opportunities. *ACS Cent. Sci.* **2016**, *2*, 281. (f) Chu, J. C. K.; Rovis, T. Complementary Strategies for Directed C(sp³)–H Functionalization: A Comparison of Transition-Metal-Catalyzed Activation, Hydrogen Atom Transfer, and Carbene/Nitrene Transfer. *Angew. Chem. Int. Ed.* **2018**, *57*, 62.
32. Bergman, R. G. C–H Activation. *Nature* **2007**, *446*, 391.
33. (a) Sommer, H.; Juliá-Hernández, F.; Martin, R.; Marek, I. *ACS Cent. Sci.* **2018**, *4*, 153. (b) Vasseur, A.; Bruffaerts, J.; Marek, I. *Nat. Chem.* **2016**, *8*, 209. (c) Franzoni, I.; Mazet, C. *Org. Biomol. Chem.* **2014**, *12*, 233. (d) Jardine, F. H. Hydrogenation & Isomerization of Alkenes in *Encycl. Inorg. Chem.*, John Wiley & Sons, Ltd, Chichester, UK, **2006**.
34. Janssen-Müller, D.; Sahoo, B.; Sun, S.–Z.; Martin, R. Tackling Remote sp³ C–H Functionalization via Ni-Catalyzed “Chain-Walking” Reactions. *Isr. J. Chem.* **2020**, *60*, 195.
35. Lee, W. C.; Wang, C. H.; Lin, Y. H.; Shih, W. C.; Ong, T. G. Tandem Isomerization and C–H Activation: Regioselective Hydroheteroarylation of Allylarenes. *Org. Lett.* **2013**, *15*, 5358.
36. Bair, J. S.; Schramm, Y.; Sergeev, A. G.; Clot, E.; Eisenstein, O.; Hartwig, J. F. Linear-Selective Hydroarylation of Unactivated Terminal and Internal Olefins with Trifluoromethyl-Substituted Arenes. *J. Am. Chem. Soc.* **2014**, *136*, 13098.
37. He, Y.; Cai, Y.; Zhu, S. Mild and Regioselective Benzylic C–H Functionalization: Ni-Catalyzed Reductive Arylation of Remote and Proximal Olefins. *J. Am. Chem. Soc.* **2017**, *139*, 1061.
38. Julia-Hernandez, F.; Moragas, T.; Cornella, J.; Martin, R. Remote Carboxylation of Halogenated Aliphatic Hydrocarbons with Carbon Dioxide. *Nature* **2017**, *545*, 84.
39. Chen, F.; Chen, K.; Zhang, Y.; He, Y.; Wang, Y.-M.; Zhu, S. Remote Migratory Cross-Electrophile Coupling and Olefin Hydroarylation Reactions Enabled by In Situ Generation of NiH. *J. Am. Chem. Soc.* **2017**, *139*, 13929.
40. Wang, X.; Nakajima, M.; Serrano, E.; Martin, R. Alkyl Bromides as Mild Hydride Sources in Ni-Catalyzed Hydroamidation of Alkynes with Isocyanates. *J. Am. Chem. Soc.* **2016**, *138*, 15531.
41. Peng, L.; Li, Y.; Li, Y.; Wang, W.; Pang, H.; Yin, G. Ligand-Controlled Nickel-Catalyzed Reductive Relay Cross Coupling of Alkyl Bromides and Aryl Bromides. *ACS Catal.* **2018**, *8*, 310.

*Site-Selective Ni-Catalyzed Reductive
Coupling of α -Haloboranes with Unactivated Olefins*

42. For reviews on reductive cross couplings: (a) Gu, J.; Wang, X.; Xue, W.; Gong, H. Nickel-Catalyzed Reductive Coupling of Alkyl Halides with Other Electrophiles: Concept and Mechanistic Considerations. *Org. Chem. Front.* **2015**, *3*, 1411. (b) Weix, J. D. Methods and Mechanisms for Cross-Electrophile Coupling of C_{sp2} Halides with Alkyl Electrophiles. *Acc. Chem. Res.* **2015**, *48*, 1767. (c) Moragas, T.; Correa, A.; Martin, R. Metal-Catalyzed Reductive Coupling Reactions of Organic Halides with Carbonyl-Type Compounds. *Chem. - Eur. J.* **2014**, *20*, 8242. (d) Knappke, C. E. I.; Grupe, S.; Gärtner, D.; Corpet, M.; Gosmini, C.; Jacobi von Wangelin, A. Reductive Cross-Coupling Reactions Between Two Electrophiles. *Chem. - Eur. J.* **2014**, *20*, 6828.
43. Peng, L.; Li, Z.; Yin, G. Photochemical Nickel-Catalyzed Reductive Migratory Cross-Coupling of Alkyl Bromides with Aryl Bromides. *Org. Lett.* **2018**, *20*, 1880.
44. Reviews for on photochemical events: (a) Milligan, J. A.; Phelan, J. P.; Badir, S. O.; Molander, G. A. Alkyl Carbon-Carbon Bond Formation by Nickel/Photoredox Cross-Coupling. *Angew. Chem. Int. Ed.* **2019**, *58*, 6152. (b) Twilton, J.; Le, C.; Zhang, P.; Shaw, M. H.; Evans, R. W.; MacMillan, D. W. C. The Merger of Transition Metal and Photocatalysis. *Nat. Rev. Chem.* **2017**, *1*, 0052. (c) Karkas, M. D.; Porco, J. A.; Stephenson, C. R. J. Photochemical Approaches to Complex Chemotypes: Applications in Natural Product Synthesis. *Chem. Rev.* **2016**, *116*, 9683. (d) Prier, C. K.; Rankic, D. A.; MacMillan, D. W. C. Visible Light Photoredox Catalysis with Transition Metal Complexes: Applications in Organic Synthesis. *Chem. Rev.* **2013**, *113*, 5322. (e) Skubi, K. L.; Blum, T. R.; Yoon, T. P. Dual Catalysis Strategies in Photochemical Synthesis. *Chem. Rev.* **2016**, *116*, 10035. (f) Romero, N. A.; Nicewicz, D. A. Organic Photoredox Catalysis. *Chem. Rev.* **2016**, *116*, 10075. (g) Marzo, L.; Pagore, S. K.; Reiser, O.; König, B. Visible-Light Photocatalysis: Does It Make a Difference in Organic Synthesis? *Angew. Chem. Int. Ed.* **2018**, *57*, 10034.
45. Zhang, Y.; Han, B.; Zhu, S. Rapid Access to Highly Functionalized Alkylboronates via NiH-Catalyzed Remote Hydroarylation of Boron-Containing Alkenes. *Angew. Chem. Int. Ed.* **2019**, *58*, 13860.
46. Bera, S.; Hu, X. Nickel-Catalyzed Regioselective Hydroalkylation and Hydroarylation of Alkenyl Boronic Esters. *Angew. Chem. Int. Ed.* **2019**, *58*, 13854.
47. Zhou, L.; Zhu, C.; Bi, P.; Feng, C. Ni-Catalyzed Migratory Fluoro-Alkenylation of Unactivated Alkyl Bromides with *gem*-Difluoroalkenes. *Chem. Sci.* **2019**, *10*, 1144.

Chapter 2.

48. Zhou, F.; Zhu, J.; Zhang, Y.; Zhu, S. NiH-Catalyzed Reductive Relay Hydroalkylation: A Strategy for The Remote C(sp³)-H Alkylation of Alkenes. *Angew. Chem., Int. Ed.* **2018**, *57*, 4058.
49. Sun, S.-Z.; Borjesson, M.; Martin-Montero, R.; Martin, R. Site-Selective Ni-Catalyzed Reductive Coupling of α -Haloboranes with Unactivated Olefins. *J. Am. Chem. Soc.* **2018**, *140*, 12765.
50. Qian, D.; Hu, X. Ligand-Controlled Regiodivergent Hydroalkylation of Pyrrolines. *Angew. Chem., Int. Ed.* **2019**, *58*, 18519.
51. Wang, Z.; Yin, H.; Fu, G. C. Catalytic Enantioconvergent Coupling of Secondary and Tertiary Electrophiles with Olefins. *Nature* **2018**, *563*, 379.
52. Zhou, F.; Zhang, Y.; Xu, X.; Zhu, S. NiH-Catalyzed Asymmetric Remote Hydroalkylation of Alkenes with Racemic α -Bromo Amides. *Angew. Chem., Int. Ed.* **2019**, *58*, 1754.
53. He, S. J.; Wang, J. W.; Li, Y.; Xu, Z. Y.; Wang, X. X.; Lu, X.; Fu, Y. Nickel-Catalyzed Enantioconvergent Reductive Hydroalkylation of Olefins with α -Heteroatom Phosphorus or Sulfur Alkyl Electrophiles. *J. Am. Chem. Soc.* **2020**, *142*, 214.
54. Yang, Z. P.; Fu, G. C. Convergent Catalytic Asymmetric Synthesis of Esters of Chiral Dialkyl Carbinols. *J. Am. Chem. Soc.* **2020**, *142*, 5870.
55. Zhao, C.; Jia, X.; Wang, X.; Gong, H. Ni-Catalyzed Reductive Coupling of Alkyl Acids with Unactivated Tertiary Alkyl and Glycosyl Halides. *J. Am. Chem. Soc.* **2014**, *136*, 17645.
56. He, J.; Song, P.; Xu, X.; Zhu, S.; Wang, Y. Migratory Reductive Acylation Between Alkyl Halides or Alkenes and Alkyl Carboxylic Acids by Nickel Catalysis. *ACS Catal.* **2019**, *9*, 3253.
57. (a) Tortajada, A.; Juliá-Hernández, F.; Börjesson, M.; Moragas, T.; Martin, R. Transition-Metal-Catalyzed Carboxylation Reactions with Carbon Dioxide. *Angew. Chem. Int. Ed.* **2018**, *57*, 15948. (b) Juliá-Hernández, F.; Gaydou, M.; Serano, E.; van Gemmeren, M.; Martin, R. Ni- and Fe-catalyzed Carboxylation of Unsaturated Hydrocarbons with CO₂. *Top. Curr. Chem.* **2016**, *374*, 45. (c) Börjesson, M.; Moragas, T.; Gallego, D.; Martin, R. Metal-Catalyzed Carboxylation of Organic (Pseudo)halides with CO₂. *ACS Catal.* **2016**, *6*, 6739. (d) Liu, Q.; Wu, L.; Jackstell, R.; Beller, M. Using Carbon Dioxide as a Building Block in Organic Synthesis. *Nat. Commun.* **2015**, *6*, 5933. (e) Tsuji, Y.; Fujihara, T. Carbon Dioxide as A Carbon

*Site-Selective Ni-Catalyzed Reductive
Coupling of α -Haloboranes with Unactivated Olefins*

- Source in Organic Transformation: Carbon–Carbon Bond Forming Reactions by Transition-Metal Catalysts. *Chem. Commun.* **2012**, 48, 9956. (f) Zhang, L.; Hou, Z. *N*-Heterocyclic Carbene (NHC)–Copper-Catalysed Transformations of Carbon Dioxide. *Chem. Sci.* **2013**, 4, 3395.
58. Maag, H. Prodrugs of Carboxylic Acids, Springer, New York, **2007**.
59. Sahoo, B.; Bellotti, P.; Juliá-Hernández, F.; Meng, Q.-Y.; Crespi, S.; König, B.; Martin, R. Site-Selective, Remote sp^3 C–H Carboxylation Enabled by The Merger of Photoredox and Nickel Catalysis. *Chem. Eur. J.* **2019**, 25, 9001.
60. Gaydou, M.; Moragas, T.; Juliá-Hernández, F.; Martin, R. Site-Selective Catalytic Carboxylation of Unsaturated Hydrocarbons with CO₂ and Water. *J. Am. Chem. Soc.* **2017**, 139, 12161.
61. (a) Marciniak, B. Hydrosilylation: A Comprehensive Review on Recent Advances, Springer, Berlin, **2009**. (b) Risangud, N.; Li, Z.; Anastasaki, A.; Wilson, P.; Kempe, K.; Haddleton, D. M. Hydrosilylation as an Efficient Tool for Polymer Synthesis and Modification with Methacrylates. *RSC Adv.* **2015**, 5, 5879.
62. Buslov, I.; Becouse, J.; Mazza, S.; Montandon-Clerc, M.; Hu, X. Chemoselective Alkene Hydrosilylation Catalyzed by Nickel Pincer Complexes. *Angew. Chem. Int. Ed.* **2015**, 54, 14523.
63. Buslov, I.; Song, F.; Hu, X. An Easily Accessed Nickel Nanoparticle Catalyst for Alkene Hydrosilylation with Tertiary Silanes. *Angew. Chem. Int. Ed.* **2016**, 55, 12295.
64. Pappas, I.; Treacy, S.; Chirik, P. J. Alkene Hydrosilylation Using Tertiary Silanes with α -Diimine Nickel Catalysts. Redox-Active Ligands Promote a Distinct Mechanistic Pathway from Platinum Catalysts. *ACS Catal.* **2016**, 6, 4105.
65. Roughley, S. D.; Jordan, A. M. The Medicinal Chemist's Toolbox: An Analysis of Reactions Used in the Pursuit of Drug Candidates. *J. Med. Chem.* **2011**, 54, 3451.
66. Xiao, J.; He, Y.; Ye, F.; Zhu, S. Remote sp^3 C–H Amination of Alkene with Nitroarenes. *Chem.* **2018**, 4, 1645.
67. Zhang, Y.; Xu, X.; Zhu, S. Nickel-Catalyzed Selective Migratory Hydrothiolation of Alkenes and Alkynes with Thiols. *Nat. Commun.* **2019**, 10, 1752.
68. (a) D. G. Hall, Ed. Boronic Acids: Preparation and Applications in Organic Synthesis, Medicine and Materials. Wiley-VCH, Weinheim, Germany, 2011. (b) Burgess, K.; Ohlmeyer, M. J. Transition-Metal-Promoted Hydroborations of

Chapter 2.

- Alkenes, Emerging Methodology for Organic Transformations. *Chem. Rev.* **1991**, *91*, 1179.
69. For recent catalytic protocols that incorporate boron fragments into α -olefins: (a) Iwamoto, H.; Imamoto, T.; Ito, H. Computational Design of High-Performance Ligand for Enantioselective Markovnikov Hydroboration of Aliphatic Terminal Alkenes. *Nat. Commun.* **2018**, *9*, 2290. (b) Cai, Y.; Yang, X.-T.; Zhang, S.-Q.; Li, F.; Li, Y.-Q.; Ruan, L.-X.; Hong, X.; Shi, S.-L. Copper-Catalyzed Enantioselective Markovnikov Hydroboration of α -olefins Enabled by a Buttressed NHC Ligand. *Angew. Chem. Int. Ed.* **2018**, *57*, 1376. (c) Smith, J. R.; Collins, B. S. L.; Hesse, M. J.; Graham, M. A.; Myers, E. L.; Aggarwal, V. K. Enantioselective Rhodium(III)-Catalyzed Markovnikov Hydroboration of Unactivated Terminal Alkenes. *J. Am. Chem. Soc.* **2017**, *139*, 9148. (d) Kerchner, H. A.; Montgomery, J. Synthesis of Secondary and Tertiary Alkylboranes via Formal Hydroboration of Terminal and 1,1-Disubstituted Alkenes. *Org. Lett.* **2016**, *18*, 5760.
70. For recent site-selective hydrofunctionalization of internal olefins that require directing groups: (a) Wang, H.; Bai, Z.; Jiao, T.; Deng, Z.; Tong, H.; He, G.; Peng, Q.; Chen, G. Palladium-Catalyzed Amide-Directed Enantioselective Hydrocarbofunctionalization of Unactivated Alkenes Using a Chiral Monodentate Oxazoline Ligand. *J. Am. Chem. Soc.* **2018**, *140*, 3542. (b) Chakrabarty, S.; Takacs, J. M. Synthesis of Chiral Tertiary Boronic Esters: Phosphonate-Directed Catalytic Asymmetric Hydroboration of Trisubstituted Alkenes. *J. Am. Chem. Soc.* **2017**, *139*, 6066. (c) Yang, K. S.; Gurak, J. A., Jr.; Liu, Z.; Engle, K. M. Catalytic, Regioselective Hydrocarbofunctionalization of Unactivated Alkenes with Diverse C-H Nucleophiles. *J. Am. Chem. Soc.* **2016**, *138*, 14705. (d) Gurak, J. A., Jr.; Yang, K. S.; Liu, Z.; Engle, K. M. Directed, Regiocontrolled Hydroamination of Unactivated Alkenes via Protodepalladation. *J. Am. Chem. Soc.* **2016**, *138*, 5805, and references therein.
71. (a) Schmidt, J.; Choi, J.; Liu, A. T.; Slusarczyk, M.; Fu, G. C., A General, Modular Method for the Catalytic Asymmetric Synthesis of Alkylboronate Esters. *Science* **2016**, *354*, 1265. (b) Sun, S.-Z.; Martin, R. Nickel-Catalyzed Umpolung Arylation of Ambiphilic α -Bromoalkyl Boronic Esters. *Angew. Chem. Int. Ed.* **2018**, *57*, 3622.
72. (a) Tortajada, A.; Ninokata, R.; Martin, R. Ni-Catalyzed Site-Selective Dicarboxylation of 1,3-Dienes with CO₂. *J. Am. Chem. Soc.* **2018**, *140*, 2050. (b) Gaydou, M.; Moragas, T.; Julia-Hernández, F.; Martin, R. Site-Selective Catalytic

*Site-Selective Ni-Catalyzed Reductive
Coupling of α -Haloboranes with Unactivated Olefins*

- Carboxylation of Unsaturated Hydrocarbons with CO₂ and Water. *J. Am. Chem. Soc.* **2017**, *139*, 12161. (c) Wang, X.; Nakajima, M.; Martin, R. Ni-Catalyzed Regioselective Hydrocarboxylation of Alkynes with CO₂ by Using Simple Alcohols as Proton Sources. *J. Am. Chem. Soc.* **2015**, *137*, 8924.
73. Serrano, E.; Martin, R. Nickel-Catalyzed Reductive Amidation of Unactivated Alkyl Bromides. *Angew. Chem. Int. Ed.* **2016**, *55*, 11207.
74. Selected references: (a) Gu, Y.; Martin, R. Ni-Catalyzed Stannylation of Aryl Esters via C–O Bond Cleavage. *Angew. Chem., Intl. Ed.* **2017**, *56*, 3187. (b) Zárate, C.; Manzano, R.; Martin, R. *Ips*o-Borylation of Aryl Ethers via Ni-Catalyzed C–OMe Cleavage. *J. Am. Chem. Soc.* **2015**, *137*, 6754. (c) Correa, A.; Martín, R. Ni-Catalyzed Direct Reductive Amidation via C–O bond Cleavage. *J. Am. Chem. Soc.* **2014**, *136*, 7253. (d) Zárate, C.; Martin, R. A Mild Ni/Cu-Catalyzed Silylation via C–O Cleavage. *J. Am. Chem. Soc.* **2014**, *136*, 2236.
75. a) Ananikov V. P. Nickel: The "Spirited Horse" of Transition Metal Catalysis. *ACS Catal.* **2015**, *5*, 1964. (b) Tasker, S. Z.; Standley, E. A.; Jamison, T. F. Recent Advances in Homogeneous Nickel Catalysis. *Nature* **2014**, *509*, 299. (c) Koga, N.; Obara, S.; Kitaura, K.; Morokuma, K. Role of Agostic Interaction in β -Elimination of Palladium and Nickel Complexes. An ab Initio MO Study. *J. Am. Chem. Soc.* **1985**, *107*, 7109.
76. (a) Werner, E. W.; Mei, T.-S.; Burckle, A. J.; Sigman, M. S. Enantioselective Heck Arylations of Acyclic Alkenyl Alcohols Using a Redox-Relay Strategy. *Science*. **2012**, *338*, 1455. (b) Mei, T.-S.; Patel, H. H.; Sigman, M. S. Enantioselective Construction of Remote Quaternary Stereocenters. *Nature* **2014**, *508*, 340. (c) Ross, S. P.; Rahman, A. A.; Sigman, M. S. Development and Mechanistic Interrogation of Interrupted Chain-Walking in the Enantioselective Relay Heck Reaction. *J. Am. Chem. Soc.* **2020**, *142*, 10516.
77. Selected reviews on C–O bond cleavage: (a) Cornella, J.; Zarate, C.; Martin, R. Metal-Catalyzed Activation of Ethers via C–O bond Cleavage: A New Strategy for Molecular Diversity. *Chem. Soc. Rev.* **2014**, *43*, 8081. (b) Tobisu, M.; Chatani, N. Cross-Couplings Using Aryl Ethers via C–O Bond Activation Enabled by Nickel Catalysts. *Acc. Chem. Res.* **2015**, *48*, 1717. (c) Rosen, B. M.; Quasdorf, K. W.; Wilson, D. A.; Zhang, N.; Resmerita, A.-M.; Garg, N. K. Percec, V. Nickel-Catalyzed Cross-Couplings Involving Carbon–Oxygen Bonds. *Chem. Rev.*

Chapter 2.

- 2011**, *III*, 1346. (d) Yu, D.-G.; Li, B.-J.; Shi, Z.-J. Exploration of New C–O Electrophiles in Cross-Coupling Reactions. *Acc. Chem. Res.* **2010**, *43*, 1486.
78. (a) Matteson, D. S. α -Halo Boronic Esters: Intermediates for Stereodirected Synthesis. *Chem. Rev.* **1989**, *89*, 1535. (b) Matteson, D. S.; Ray, R. α -Chloro Boronic Esters from Homologation of Boronic Esters. *J. Am. Chem. Soc.* **1980**, *102*, 7590.
79. Quiclet-Sire, B.; Zard, S. Z. Radical Instability in Aid of Efficiency: A Powerful Route to Highly Functional MIDA Boronates. *J. Am. Chem. Soc.* **2015**, *137*, 6762.

2.8 Experimental Section

2.8.1 General Considerations

Reagents. Commercially available materials were used as received without further purification. NiI_2 and $\text{NiBr}_2 \cdot \text{diglyme}$ (97% purity) were purchased from Aldrich, $(\text{EtO})_2\text{MeSiH}$ (DEMS, 97% purity) was purchased from Fluorochem. Anhydrous Sodium Carbonate (Na_2CO_3) was purchased from Panreac. Anhydrous *N,N*-Dimethylacetamide (DMA, 99.5% purity) and Anhydrous THF (99.5% purity) were purchased from Acros.

Analytical methods. ^1H and ^{13}C NMR spectra were recorded on Bruker 300 MHz, Bruker 400 MHz and Bruker 500 MHz at 20 °C. All ^1H NMR spectra are reported in parts per million (ppm) downfield of TMS and were calibrated using the residual solvent peak of CHCl_3 (7.26 ppm), unless otherwise indicated. All ^{13}C NMR spectra are reported in ppm relative to TMS, were calibrated using the signal of residual CHCl_3 (77.16 ppm), ^{11}B NMR and ^{19}F NMR were obtained with ^1H decoupling unless otherwise indicated. Coupling constants, *J*, are reported in Hertz. Melting points were measured using open glass capillaries in a Büchi B540 apparatus. Gas chromatographic analyses were performed on Hewlett-Packard 6890 gas chromatography instrument with a FID detector. Flash chromatography was performed with EM Science silica gel 60 (230-400 mesh). Thin layer chromatography was used to monitor reaction progress and analyze fractions from column chromatography. To this purpose TLC Silica gel 60 F₂₅₄ aluminium sheets from Merck were used and visualization was achieved using UV irradiation and/or staining with Cerium Molybdate solution. The yields reported in Scheme 3.26-3.29 refer to isolated yields and represent an average of at least two independent runs. The procedures described in this section are representative. Thus, the yields may differ slightly from those given in the Schemes of the manuscript. In the cases the High-Resolution Mass Spectra of the molecular ion could not be obtained using ESI and APCI ionization modes the GC-MS of the compound was given.

2.8.2 Optimization of the Reaction Conditions

General procedure: An oven-dried 8 mL screw-cap test tube containing a stirring bar was charged with NiI₂ (5 mol%), the corresponding ligand (6 mol%) and Na₂CO₃ (0.75 mol, 15.9 mg). Subsequently, the tube was sealed with a Teflon-lined screw cap, then evacuated and back-filled with argon (3 times). Afterwards, 2-(1-chloroheptyl)-4,4,5,5-tetramethyl-1,3,2-dioxaborolane (**2.5.1a**, 52 mg, 0.20 mmol), 4-phenyl-1-butene (**2.5.2a**, 51 μL, 0.34 mmol, 1.7 equiv), (EtO)₂MeSiH (DEMS, 48 μL, 0.30 mmol, 1.5 equiv), DMA and THF (3:1, 0.4 mL) were added via syringe. Then, the tube was stirred at room temperature for 24 h. After the reaction was completed, the mixture was diluted with EtOAc, filtered through silica gel and concentrated under vacuum. The yields were determined by GC FID analysis using 1-decane as internal standard, and the product was purified by column chromatography on silica gel (Hexane/EtOAc = 50:1).

2.8.3 Determination of the Major and Minor Regioisomers

Employing Internal Olefins

2.8.3.1 GC-MS of **2.5.7a** and **2.5.7a'**

Following general procedure, using NiI₂ (10 mol%) and **L2.5.12** (12 mol%), The yield and ratio of **2.5.7a** and **2.5.7a'** were determined by GC-MS and GC analysis using 1-decane as internal standard. From GC-MS analysis we found two isomers and traces of others, t = 10.521 min (**2.5.7a**, major) and t = 10.271 min (**2.5.7a'**, minor). From GC analysis we calculated the ratio of **2.5.7a** and **2.5.7a'** is 44:1.

Site-Selective Ni-Catalyzed Reductive
Coupling of α -Haloboranes with Unactivated Olefins

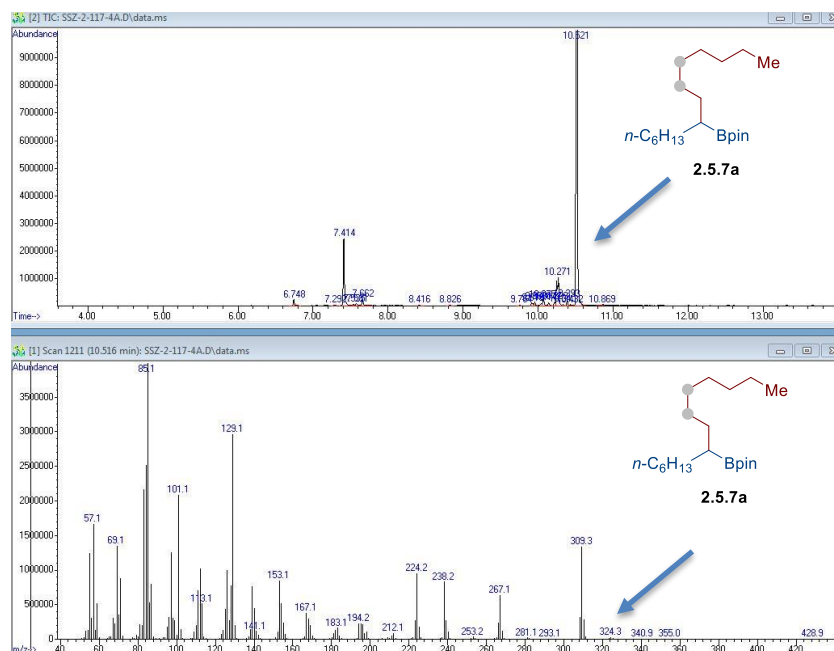


Figure 2.5.1 GC-MS of 2.5.7a

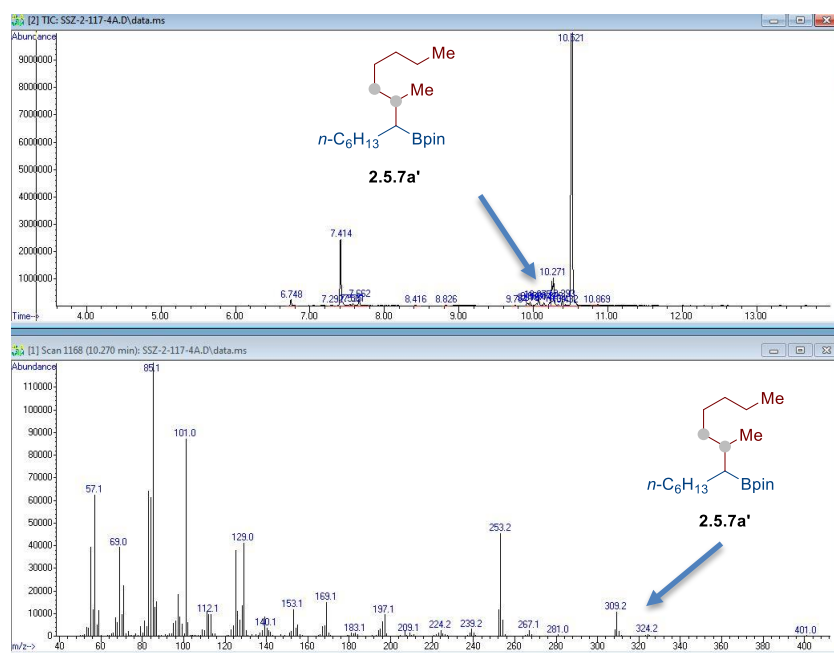
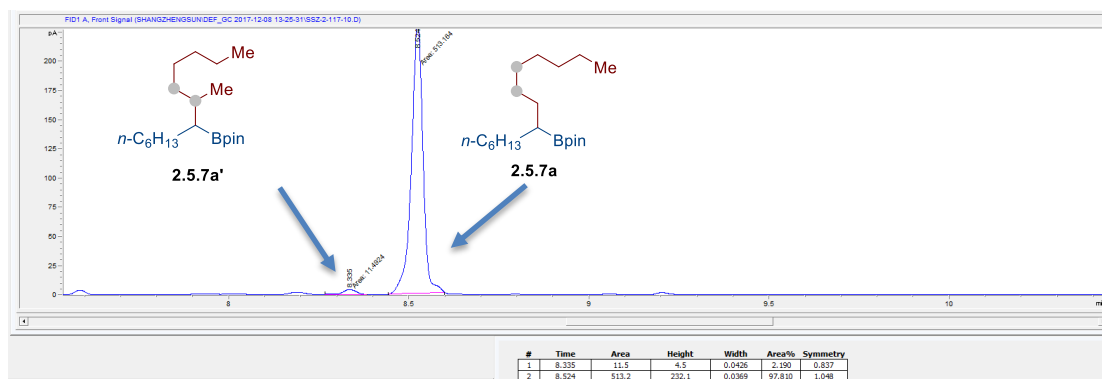
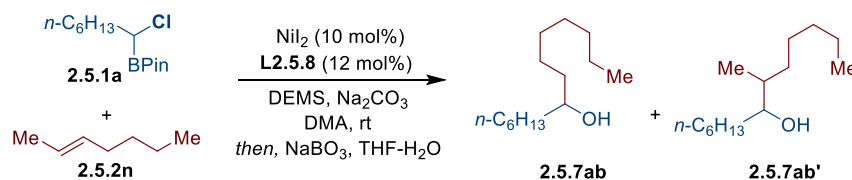


Figure 2.5.2 GC-MS of 2.5.7a'

2.8.3.2 GC-MS of 2.5.7a and 2.5.7a'

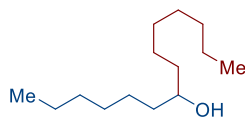
Figure 2.5.3 GC results of **2.5.7a** and **2.5.7a'**

2.8.3.3 ¹H NMR Determination of Structures **2.5.7a** and **2.5.7a'** from **2.5.7ab** and **2.5.7ab'**

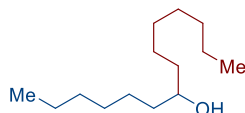


General Procedure: An oven-dried 25 mL schlenk tube containing a stirring bar was charged with NiI₂ (37.2 mg, 10 mol%), **L2.5.8** (26.5 mg, 12 mol%) and Na₂CO₃ (1.5 mmol, 95.4 mg, 0.9 mmol). Subsequently, the tube was sealed with a Teflon screw cap, then evacuated and back-filled with Ar (3 times). After then, 2-(1-chloroheptyl)-4,4,5,5-tetramethyl-1,3,2-dioxaborolane (**2.5.1a**, 312.0 mg, 1.20 mmol, 1.0 equiv), *trans*-2-heptene (**2.5.2n**, 306 μL, 2.04 mmol, 1.7 equiv), DEMS (384 μL, 2.4 mmol, 2.0 equiv) and DMA (3.6 mL) were added via syringe under Ar. Then the tube was sealed and stirred at room temperature for 15 h. After the reaction was completed, the mixture was diluted with EtOAc and filtered through silica gel and then concentrated under reduced pressure. The residue was dissolved in a mixture of THF and H₂O (1:1, 24 mL) and NaBO₃·4H₂O (2.0 g, 2.4 mmol) was added. The reaction mixture was stirred at room temperature for 4 h. After the reaction was completed, water (80 mL) was added. The aqueous phase was extracted with EtOAc (3 x 50 mL), and the combined organic phases were dried over MgSO₄ and concentrated. The residue was purified by column chromatography, affording the corresponding product **2.5.7ab** (23 mg, 9% yield, colorless oil) and **2.5.7ab'** (10 mg, 3% yield, colorless oil). Note that in this case the ratio for **2.5.7ab** and **2.5.7ab'** is 1.85:1, as **L2.5.8** is less selective to the formation of the linear regioisomer.

*Site-Selective Ni-Catalyzed Reductive
Coupling of α -Haloboranes with Unactivated Olefins*



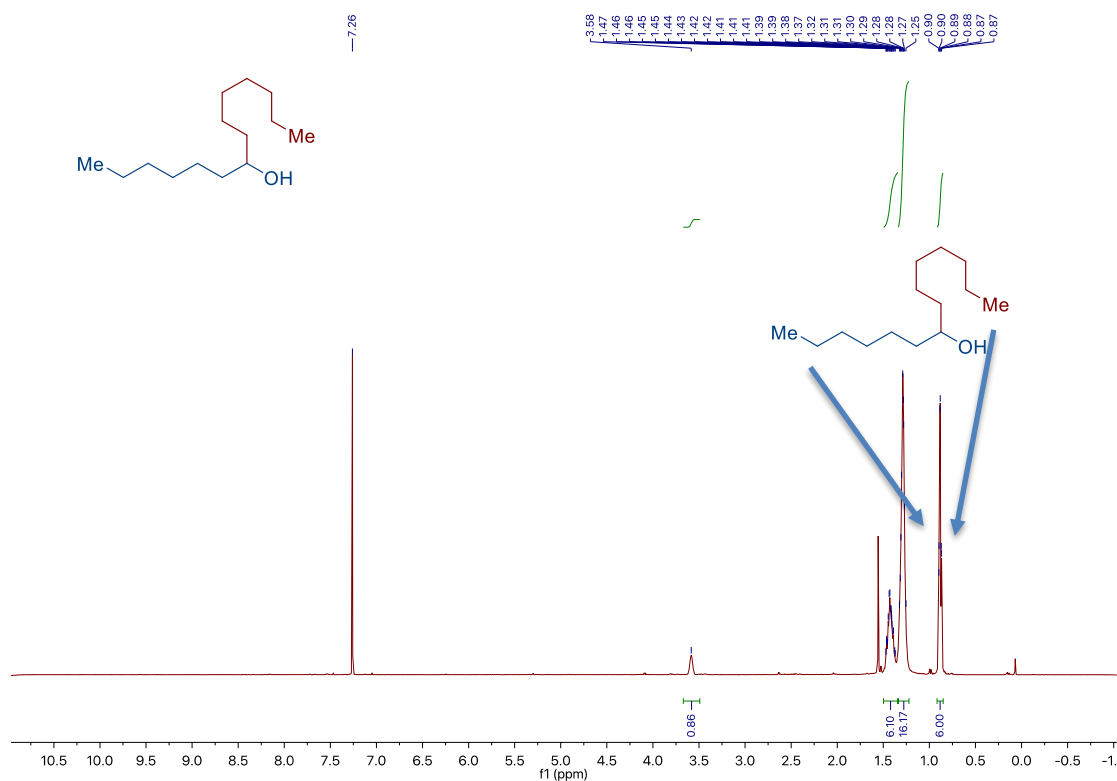
tetradecan-7-ol (2.5.7ab): $^1\text{H NMR}$ (500 MHz, CDCl_3) δ 3.58 (s, 1H), 1.47 – 1.37 (m, 6H), 1.32 – 1.25 (m, 16H), 0.90 – 0.87 (m, 6H) ppm. $^{13}\text{C NMR}$ (126 MHz, CDCl_3) δ 72.2, 37.7 (2C), 32.0 (left), 32.0 (right), 29.8, 29.5 (left), 29.5 (right), 25.8 (left), 25.8 (right), 22.8 (left), 22.8 (right), 14.2 (left), 14.2 (right) ppm.



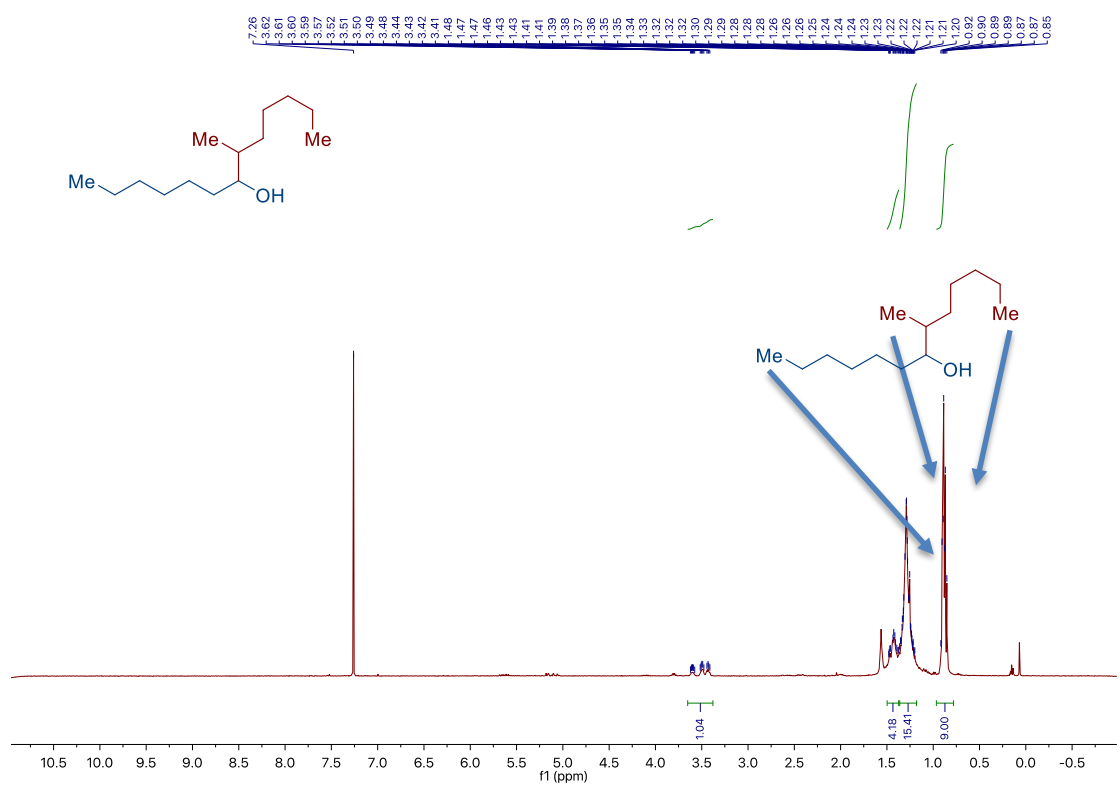
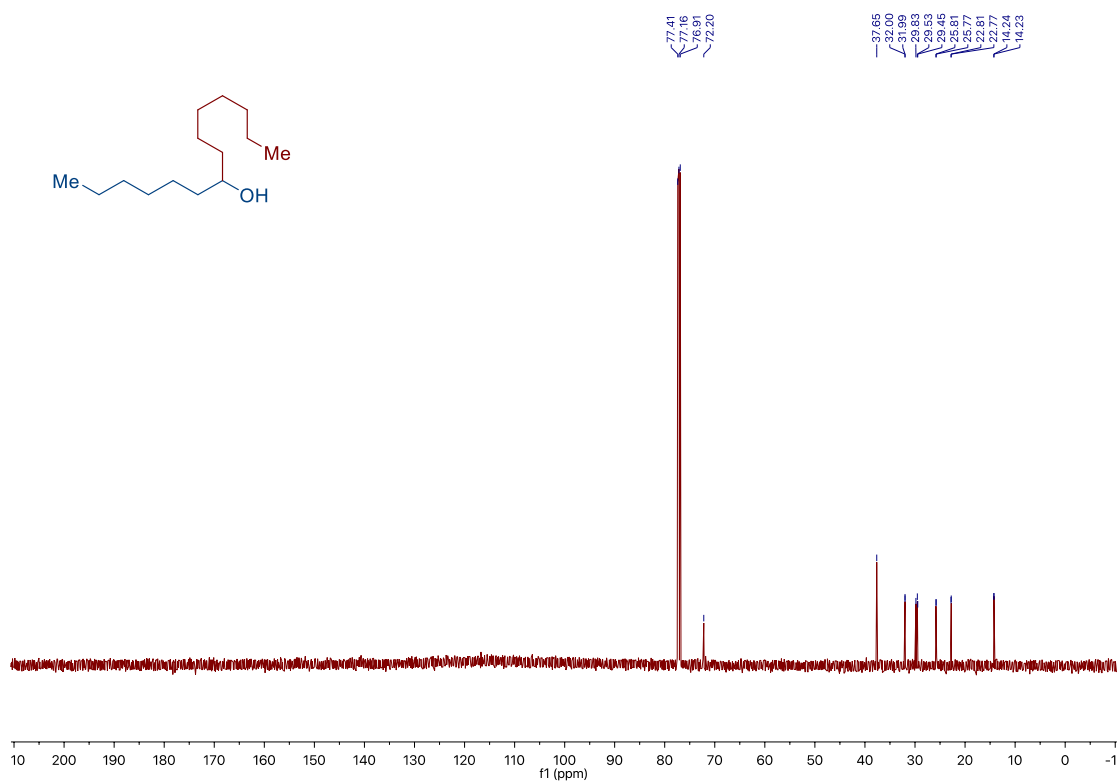
6-methyltridecan-7-ol (2.5.7ab') $^1\text{H NMR}$ (400 MHz, CDCl_3) δ 3.71 – 3.29 (m, 1H), 1.50 – 1.36 (m, 4H), 1.35 – 1.11 (m, 15H), 1.04 – 0.59 (m, 9H) ppm. $^{13}\text{C NMR}$ (101 MHz, CDCl_3) δ 76.3, 75.4, 39.0, 38.3, 34.7 (left), 34.7 (right), 33.6, 33.5, 32.4, 32.3, 32.0 (left), 32.0 (middle), 32.0 (right), 29.6 (left), 29.6 (right), 27.2 (left), 27.2 (right), 26.4, 26.3, 22.8 (left), 22.8 (2C, right), 15.5, 14.2 (4C), 13.7 ppm.

$^1\text{H-NMR}$ of 2.5.7ab and 2.5.7ab'

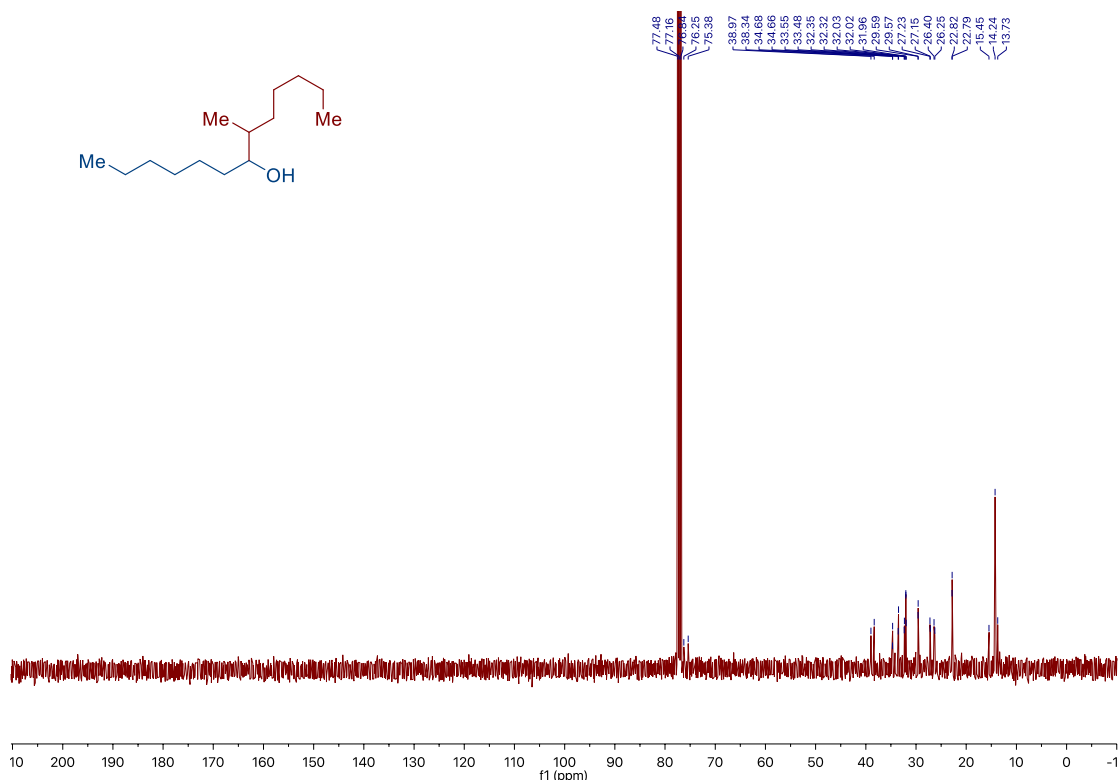
The methyl groups in each $^1\text{H NMR}$ are indicated with an arrow.



Chapter 2.



*Site-Selective Ni-Catalyzed Reductive
Coupling of α -Haloboranes with Unactivated Olefins*



To further determine which branch regioisomer is being formed, we used GC-MS to detect the fragmentation pattern. The major product detected was **2.5.7ab'** (the structure of **2.5.7ab'** and its fragmentation is shown below). The next product detected was **2.5.7ab''** (the structure of **2.5.7ab''** and its fragmentation is shown below).

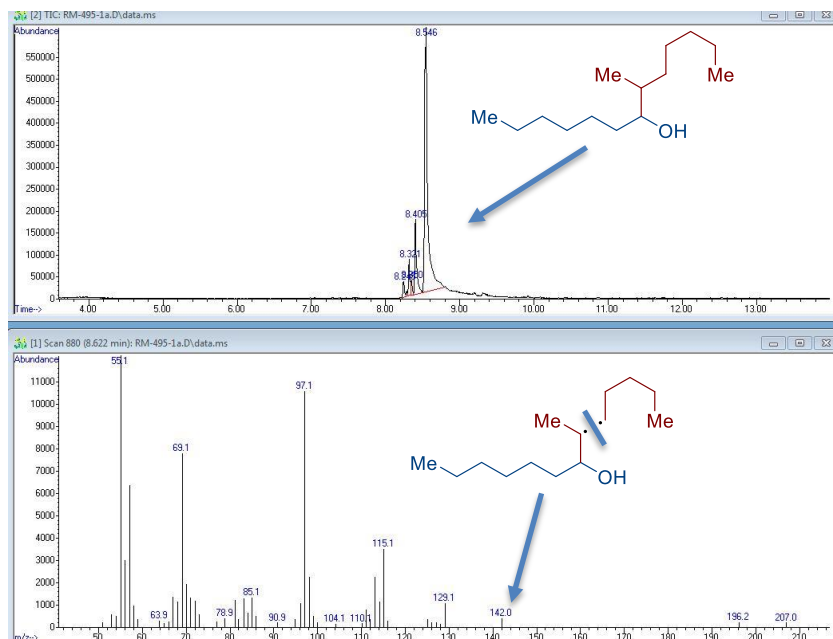


Figure 2.5.4 GC-MS results of **2.5.7ab'**

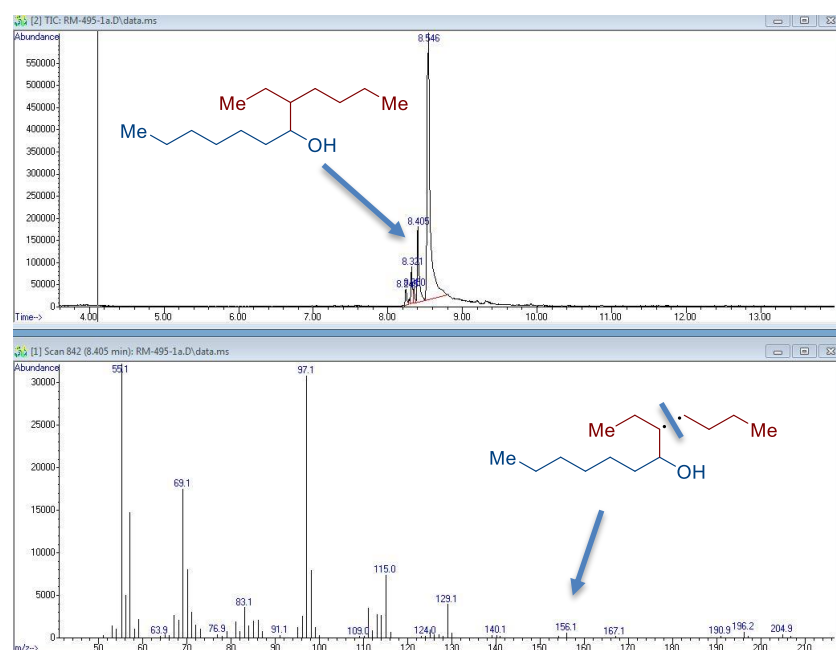


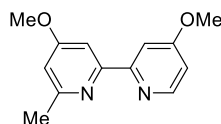
Figure 2.5.4 GC-MS results of 2.5.7ab”

2.8.4 Synthesis of Ligands and Starting Materials

Commercially available compounds were used as received without further purification. 2-(1-chloro-3-phenylpropyl)-4,4,5,5-tetramethyl-1,3,2-dioxaborolane (**2.5.1c**)¹, 2-(1-bromo-2-methylpropyl)-4,4,5,5-tetramethyl-1,3,2-dioxaborolane (**2.5.1i**)², 2-(bromo(cyclohexyl)methyl)-4,4,5,5-tetramethyl-1,3,2-dioxaborolane (**2.5.1j**)², Hex-5-en-1-yl 4-fluorobenzoate (**2.5.2h**)³, hex-5-en-1-yl 4-bromobenzoate (**2.5.2i**)⁴, *N*-(4-methoxyphenyl)pent-4-enamide (**2.5.2f**)⁴, ((hex-5-en-1-yloxy)methyl)benzene (**2.5.2b**)⁵, (8*R*,9*S*,13*S*,14*S*)-3-(hex-5-en-1-yloxy)-13-methyl-6,7,8,9,11,12,13,14,15,16-decahydro-17*H*-cyclopenta[*a*]phenanthrene-17-one (**2.5.2j**)⁶, *tert*-butyl 4-(prop-1-en-1-yl)piperidine-1-carboxylate (**2.5.2t**)⁷, pent-3-en-1-ylbenzene (**2.5.2q**)⁸, (*Z*)-8-chlorooct-3-ene (**2.5.2r**)⁹, 2-(undec-9-en-1-yl)-1,3-dioxolane (**2.5.2y**)¹⁰, 2,6-dimethyldeca-2,8-diene (**2.5.2u**)¹¹, *tert*-butyl 2,5-dihydro-1*H*-pyrrole-1-carboxylate (**2.5.13**)¹², (1-vinylcyclopropyl)benzene (**3.5.17**)⁷, (1-(prop-1-en-1-yl)cyclopropyl)benzene (**2.5.18**)¹³ were prepared by known procedures.

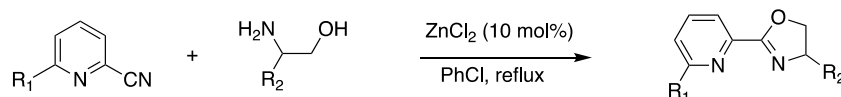
2.8.4.1 Synthesis of L2.5.2

*Site-Selective Ni-Catalyzed Reductive
Coupling of α -Haloboranes with Unactivated Olefins*



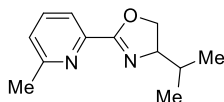
4,4'-dimethoxy-6-methyl-2,2'-bipyridine (L2.5.2): L2.5.2 was synthesized following a procedure described in the literature.¹⁰ Methyl lithium (6.3 mL of a 1.6 M solution in diethyl ether, 10 mmol, 1.0 equiv) was added slowly to a solution of 4,4'-dimethoxy-2,2'-bipyridine (2.16 g, 10 mmol, 1.0 equiv) in dry diethyl ether (50 mL, 0.2 M), under argon, at 0 °C and under vigorous agitation. The resulting red solution was heated at reflux for 4 h and after cooling to room temperature, the reaction mixture was quenched with brine (50 mL). The resulting yellow mixture was separated and the organic phase was extracted with diethyl ether (3×20 mL), dried over MgSO₄ and evaporated under reduced pressure. The obtained dark orange crude product was dissolved in acetone (20 mL) and a solution of KMnO₄ in acetone was added slowly until the color remained purple (the end point is best observed if the resulting MnO₂ is removed by filtration). The obtained crude solution was filtered through a silica-celite plug, concentrated under reduced pressure and purified through column chromatography on silica gel (Hexane/EtOAc = 2:1), affording the product as a pale yellow solid (1.24 g, 54% yield). **Mp** 104.8–106.1 °C. **¹H NMR** (500 MHz, CDCl₃) δ 8.50 (d, J = 5.2 Hz, 1H), 8.03 (d, J = 2.6 Hz, 1H), 7.81 (d, J = 2.3 Hz, 1H), 6.86 (dd, J = 5.7, 2.6 Hz, 1H), 6.74 (d, J = 2.4 Hz, 1H), 3.99 (s, 3H), 3.96 (s, 3H), 2.61 (s, 3H) ppm. **¹³C NMR** (75 MHz, CDCl₃) δ 167.1, 166.8, 159.4, 158.3, 157.3, 150.2, 110.8, 110.3, 106.7, 103.8, 55.5, 55.4, 24.8 ppm. **IR** (neat, cm⁻¹): 1579, 1560, 1438, 1398, 1343, 1294, 1241, 1201, 1029, 985, 953, 884, 840, 796. **HRMS** calcd. for (C₁₃H₁₅N₂O₂) [M+H]⁺: 231.1128, found 231.1130.

2.8.4.2 The Preparation the PyrOx Ligands

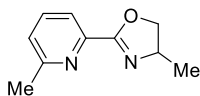


PyOx ligands were synthesized following a procedure described in the literature.¹⁴ To a dried round flask equipped with a stirring bar was added picolinonitrile (10 mmol) and ZnCl₂ (136 mg), then added chlorobenzene (20 mL) via syringe under argon. Subsequently, the corresponding amino alcohol (15 mmol) was added via syringe. The reaction mixture was stirred for 24 h under reflux. After the reaction was completed, it

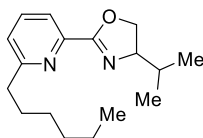
was cooled down to room temperature and then evaporated under reduced pressure to remove the remaining chlorobenzene. The residue was extracted with DCM (3×20 mL), dried over MgSO₄ and concentrated. The mixture was purified by column chromatography on silica gel.



4-isopropyl-2-(6-methylpyridin-2-yl)-4,5-dihydrooxazole (L2.5.12): Following the general procedure described above, but using 6-methylpicolinonitrile (10 mmol, 1.18 g) and 2-amino-3-methylbutan-1-ol (15 mmol, 1.65 mL), affording the product as light yellow solid (1.63 g, 80% yield). **Mp** 38.2–39.1 °C. **¹H NMR** (500 MHz, CDCl₃) δ 7.88 (d, *J* = 8.1 Hz, 1H), 7.63 (dd, *J* = 9.0, 8.0 Hz, 1H), 7.23 (d, *J* = 7.7 Hz, 1H), 4.49 (td, *J* = 9.0, 1.0 Hz, 1H), 4.20 (td, *J* = 8.5, 1.1 Hz, 1H), 4.16 – 4.09 (m, 1H), 2.62 (s, 3H), 1.94 – 1.76 (m, 1H), 1.04 (d, *J* = 6.8 Hz, 3H), 0.92 (d, *J* = 6.8 Hz, 3H) ppm. **¹³C NMR** (126 MHz, CDCl₃) δ 162.9, 158.9, 146.5, 136.8, 125.4, 121.3, 73.0, 70.8, 32.8, 24.8, 19.3, 18.2 ppm. **IR** (neat, cm⁻¹): 2960, 1634, 1589, 1572, 1461, 1357, 1111, 1081, 1040, 962, 811, 748. **HRMS** calcd. for (C₁₂H₁₇N₂O) [M+H]⁺: 205.1335, found 205.1333.



4-methyl-2-(6-methylpyridin-2-yl)-4,5-dihydrooxazole (L2.5.18): Following the general procedure described above, but using 6-methylpicolinonitrile (10 mmol, 1.18 g) and 2-aminopropan-1-ol (15 mmol, 1.12 g), affording the product as yellow oil (1.21 g, 69% yield). **¹H NMR** (400 MHz, CDCl₃) δ 7.84 (d, *J* = 7.7 Hz, 1H), 7.64 (t, *J* = 7.8 Hz, 1H), 7.24 (d, *J* = 12.7 Hz, 1H), 4.59 (dd, *J* = 9.5, 8.1 Hz, 1H), 4.47 – 4.37 (m, 1H), 4.03 (t, *J* = 8.1 Hz, 1H), 2.63 (s, 3H), 1.38 (d, *J* = 6.6 Hz, 3H) ppm. **¹³C NMR** (101 MHz, CDCl₃) δ 165.1, 157.3, 149.0, 137.5, 126.0, 119.4, 67.2, 48.1, 24.3, 17.1 ppm. **IR** (neat, cm⁻¹): 2972, 2932, 2875, 1656, 1593, 1520, 1451, 1052, 994, 730. **HRMS** calcd. for (C₁₀H₁₃N₂O) [M+H]⁺: 177.1022, found 177.1026.

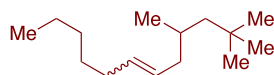


2-(6-hexylpyridin-2-yl)-4-isopropyl-4,5-dihydrooxazole (L2.5.19): Following the general procedure described above, but using 6-hexylpicolinonitrile (10 mmol, 1.88 g)

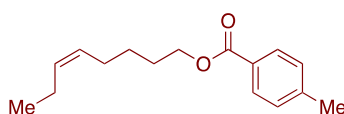
*Site-Selective Ni-Catalyzed Reductive
Coupling of α -Haloboranes with Unactivated Olefins*

and 2-amino-3-methylbutan-1-ol (15 mmol, 1.65 mL), affording the product as yellow oil (2.06 g, 75% yield). **$^1\text{H NMR}$** (400 MHz, CDCl_3) δ 7.89 (dd, $J = 7.8, 1.1$ Hz, 1H), 7.64 (t, $J = 7.8$ Hz, 1H), 7.23 (dd, $J = 7.8, 1.1$ Hz, 1H), 4.48 (dd, $J = 9.6, 8.2$ Hz, 1H), 4.20 (t, $J = 8.3$ Hz, 1H), 4.16 – 4.08 (m, 1H), 2.99 – 2.68 (m, 2H), 1.89 (dq, $J = 13.4, 6.7$ Hz, 1H), 1.76 – 1.60 (m, 2H), 1.41 – 1.23 (m, 6H), 1.03 (d, $J = 6.8$ Hz, 3H), 0.92 (d, $J = 6.8$ Hz, 3H), 0.86 (t, $J = 7.2$ Hz, 3H) ppm. **$^{13}\text{C NMR}$** (101 MHz, CDCl_3) δ 165.9, 161.3, 149.0, 137.6, 125.6, 119.6, 64.8, 58.0, 37.9, 31.8, 29.4, 29.3, 29.0, 22.7, 19.8, 18.7, 14.2 ppm. **IR** (neat, cm^{-1}): 2956, 2926, 2857, 1641, 1587, 1573, 1364, 1090, 971, 816, 729. **HRMS** calcd. for ($\text{C}_{17}\text{H}_{27}\text{N}_2\text{O}$) $[\text{M}+\text{H}]^+$: 275.2118, found 275.2111.

2.8.4.3 The Preparation of Olefins



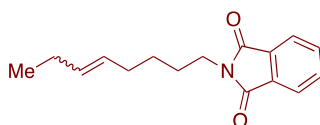
2,2,4-trimethyldec-6-ene (2.5.2s): The title compound was synthesized following a procedure described in the literature.¹⁵ To a stirred solution of the hexyltriphenylphosphonium bromide (5.15g, 12 mmol) in THF (0.35 M) under argon was added *n*-BuLi (2.5 M, 1.2 equiv) dropwise by syringe. The reaction mixture was stirred for 30 min at room temperature and 3,5,5-trimethylhexanal (1.74 mL, 10 mmol) was added slowly in a THF solution (1 M). After 12 h the reaction was quenched with a saturated solution of NH_4Cl , diluted with water and extracted with EtOAc. The solution was dried with MgSO_4 , filtered and the volatiles were removed under vacuum. The residue was then purified by silica gel flash column chromatography (hexanes), affording the title compound (1.36 g, 65%) as a colorless oil. **$^1\text{H NMR}$** (400 MHz, CDCl_3) δ 5.53 – 5.15 (m, 2H), 2.07 – 1.95 (m, 3H), 1.93 – 1.79 (m, 1H), 1.59 – 1.47 (m, 1H), 1.40 – 1.20 (m, 8H), 1.03 (dd, $J = 13.9, 6.5$ Hz, 1H), 0.94 – 0.84 (m, 14H) ppm. **$^{13}\text{C NMR}$** (101 MHz, CDCl_3) δ 130.9, 128.8, 50.8, 37.0, 31.7, 31.2, 30.2, 30.0, 29.6, 27.5, 22.7, 22.6, 14.2 ppm. **IR** (neat, cm^{-1}): 2955, 2925, 2858, 1466, 1393, 1364, 968, 725. **GC-MS**: ($\text{C}_{15}\text{H}_{30}$) $[\text{M}]^+$ found $t = 5.052$ min, m/z 210.2.



oct-5-en-1-yl 4-methylbenzoate (2.5.2w): The title compound was synthesized following a procedure described in the literature.² To a stirred solution of

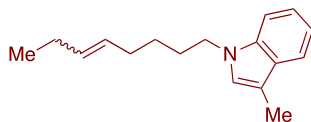
Chapter 2.

4-methylbenzoic acid (7 mmol, 1.0 equiv) in DCM (20 mL) and DMF (0.1 mL) under argon was added oxalyl chloride (9.1 mmol, 1.3 equiv) by syringe. The reaction mixture was stirred for 1 h at 0 °C and then warmed up to room temperature. After 3 h, a clear light-yellow solution was obtained and all of the volatiles were removed under vacuum. The residue was then dissolved in DCM (10 mL) and *cis*-5-octen-1-ol (5 mmol, 1.0 equiv), DMAP (0.5 mmol, 0.1 equiv) and Et₃N (10 mmol, 2.0 equiv) in DCM (10 mL) were added. The reaction was allowed to stir overnight at room temperature. Then, the mixture was quenched with NH₄Cl (aq. 10%) and extracted with DCM (3x30 mL). The organic phase was washed with brine, concentrated and purified by silica gel flash chromatography (Hexane/EtOAc = 30:1), affording the title compound (1.0 g, 81%) as a colorless oil. **¹H NMR** (300 MHz, CDCl₃) δ 7.93 (d, *J* = 8.2 Hz, 2H), 7.23 (d, *J* = 7.9 Hz, 2H), 5.49 – 5.17 (m, 2H), 4.31 (t, *J* = 6.6 Hz, 2H), 2.41 (s, 3H), 2.17 – 1.93 (m, 4H), 1.84 – 1.69 (m, 2H), 1.61 – 1.43 (m, 2H), 0.96 (t, *J* = 7.5 Hz, 3H) ppm. **¹³C NMR** (75 MHz, CDCl₃) δ 166.9, 143.6, 132.4, 129.7, 129.2, 128.7, 127.9, 64.9, 28.5, 26.8, 26.3, 21.8, 20.7, 14.5 ppm. **IR** (neat, cm⁻¹): 2960, 2933, 1715, 1612, 1269, 1177, 1106, 1021, 841, 752. **HRMS** calcd. for (C₁₆H₂₂NaO₂) [M+Na]⁺: 269.1512, found 269.1509.



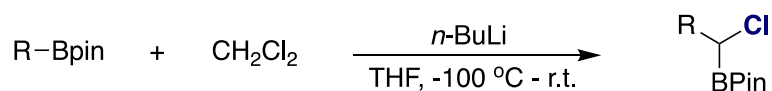
2-(oct-5-en-1-yl)isoindoline-1,3-dione (2.5.2x): The title compound was synthesized following a procedure described in the literature.¹⁶ To a solution of 8-bromooct-3-ene (869 mg, 4.69 mmol) in DMF (5 ml) was added potassium phthalimide (854 mg, 4.46 mmol). The mixture was stirred at room temperature for 20 h until completion. The mixture was saturated with brine, extracted with CHCl₃, dried over MgSO₄ and the volatiles were removed under vacuum. Flash column chromatography of the crude mixture (Hexane/EtOAc = 95:5) afforded the title compound (512 mg, 45% yield) as colorless oil. **¹H NMR** (400 MHz, CDCl₃) δ 7.83 (dd, *J* = 5.4, 3.0 Hz, 2H), 7.69 (dd, *J* = 5.5, 3.0 Hz, 2H), 5.51 – 5.22 (m, 2H), 3.67 (td, *J* = 7.3, 2.4 Hz, 2H), 2.11 – 1.90 (m, 4H), 1.75 – 1.61 (m, 2H), 1.44 – 1.34 (m, 2H), 0.93 (td, *J* = 7.5, 2.5 Hz, 3H) ppm. **¹³C NMR** (101MHz, CDCl₃) δ 168.5, 133.9, 132.7, 132.3, 128.5, 123.3, 38.1, 28.3, 27.0, 26.7, 20.6, 14.5 ppm. **IR** (neat, cm⁻¹): 2961, 2933, 2860, 1771, 1704, 1615, 1437, 1394, 1368, 1336, 1070, 1037, 967, 716, 529. **HRMS** calcd. for (C₁₆H₂₀NO₂) [M+H]⁺: 258.1489 found 258.1489.

*Site-Selective Ni-Catalyzed Reductive
Coupling of α -Haloboranes with Unactivated Olefins*



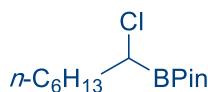
3-methyl-1-(oct-5-en-1-yl)-1H-indole (2.5.2z): The title compound was synthesized following a procedure described in the literature.¹⁷ NaH (756 mg, 31.5 mmol) and anhydrous THF (20 ml) were placed in a Schlenk flask under argon. 3-methyl-indole (1.31 g, 10 mmol) was added dropwise in THF (5 ml). The mixture was stirred for 20 min until H₂ bubbling ceased. 8-bromooct-3-ene (3.63 g, 19 mmol) was added dropwise and the reaction stirred overnight. The reaction mixture was carefully hydrolyzed with H₂O, extracted with Et₂O, dried over MgSO₄ and the volatiles were removed under vacuum. Flash column chromatography (Hexane/EtOAc = 10:1) of the crude mixture afforded the title compound (463 mg, 19% yield) as yellow oil. ¹H NMR (400 MHz, CDCl₃) δ 7.64 – 7.56 (m, 1H), 7.36 – 7.30 (m, 1H), 7.25 – 7.20 (m, 1H), 7.17 – 7.11 (m, 1H), 6.91 – 6.88 (m, 1H), 5.57 – 5.22 (m, 2H), 4.09 (td, J = 7.2, 2.9 Hz, 2H), 2.42 – 2.29 (m, 3H), 2.16 – 2.01 (m, 4H), 1.96 – 1.84 (m, 2H), 1.50 – 1.37 (m, 2H), 1.05 – 0.90 (m, 3H) ppm. ¹³C NMR (101 MHz, CDCl₃) δ 136.4, 132.3, 128.8, 128.6, 125.5, 121.4, 119.1, 118.5, 110.2, 109.3, 46.1, 30.1, 27.2, 26.8, 20.7, 14.5, 9.7 ppm. IR (neat, cm⁻¹): 3004, 2930, 2859, 1614, 1467, 1362, 1330, 1235, 1198, 1168, 1013, 967, 787, 734, 426. HRMS calcd. for (C₁₇H₂₄N) [M+H]⁺: 242.1903 found 242.1903.

2.8.4.4 The Preparation of α -Chloro Boronic Esters

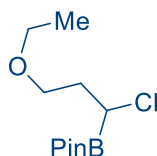


The α -chloro boronic esters were synthesized following a procedure described in the literature.¹⁸ To an oven dried round flask equipped with a stirring bar was added CH₂Cl₂ (15 mmol, 0.96 mL) and THF (20 mL) by syringe, and the solution was cooled to -100°C. Then *n*-butyllithium (2.5 M solution in hexanes, 11 mmol, 1.1 equiv) was added dropwise at -100 °C. After stirring for 45 min, a solution of corresponding alky-4,4,5,5-tetramethyl-1,3,2-dioxaborolane (10 mmol, 1.0 equiv) in diethyl ether was directly added via syringe. Then the reaction mixture was allowed to slowly warm to room temperature overnight. After the reaction was completed, 50 mL of DCM were added to precipitate the lithium chloride (optional), filtered, and

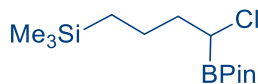
concentrated under reduced pressure. The resulting crude product was purified by silica gel flash chromatography (Hexane/EtOAc = 30:1 to 10:1).



2-(1-chloroheptyl)-4,4,5,5-tetramethyl-1,3,2-dioxaborolane (2.5.1a): Following the general procedure described above, but using 2-hexyl-4,4,5,5-tetramethyl-1,3,2-dioxaborolane, afforded **2.5.1a** (2.12 g, 81%) as a colorless oil. $^1\text{H NMR}$ (400 MHz, CDCl_3): δ 3.41 (dd, $J = 8.1, 6.7$ Hz, 1H), 1.85 – 1.78 (m, 2H), 1.50 – 1.23 (m, 8H), 1.28 (s, 12H), 0.88 (t, $J = 8.0$, 3H) ppm. $^{13}\text{C NMR}$ (101 MHz, CDCl_3) δ 84.5, 34.2, 31.8, 28.9, 27.4, 24.8, 24.7, 22.7, 14.2 ppm. $^{11}\text{B NMR}$ (128 MHz, CDCl_3) δ 31.4 ppm. **IR** (neat, cm^{-1}): 2979, 2928, 2857, 1381, 1373, 1341, 1141, 967, 847. **HRMS** calcd. for $(\text{C}_{13}\text{H}_{26}\text{BClNaO}_2)$ $[\text{M}+\text{Na}]^+$: 282.1643 found 282.1637.



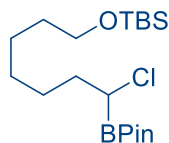
2-(1-chloro-3-ethoxypropyl)-4,4,5,5-tetramethyl-1,3,2-dioxaborolane (2.5.1b): Following the general procedure described above, but using 2-(2-ethoxyethyl)-4,4,5,5-tetramethyl-1,3,2-dioxaborolane, afforded **2.5.1b** (1.61 g, 65%) as a colorless oil. $^1\text{H NMR}$ (400 MHz, CDCl_3): δ 3.61 – 3.53 (m, 3H), 3.51 – 3.42 (m, 2H), 2.20 – 2.07 (m, 1H), 2.05 – 1.97 (m, 1H), 1.28 (s, 12H), 1.19 (t, $J = 7.1$ Hz, 3H) ppm. $^{13}\text{C NMR}$ (101 MHz, CDCl_3) δ 84.5, 67.3, 66.5, 34.3, 24.8, 24.7, 15.3 ppm. $^{11}\text{B NMR}$ (128 MHz, CDCl_3) δ 31.5 ppm. **IR** (neat, cm^{-1}): 2978, 2933, 2867, 1373, 1343, 1141, 1126, 1109, 968, 847. **HRMS** calcd. for $(\text{C}_{11}\text{H}_{22}\text{BClNaO}_3)$ $[\text{M}+\text{Na}]^+$: 271.1243 found 271.1243.



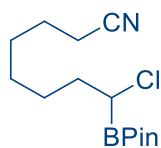
(4-chloro-4-(4,4,5,5-tetramethyl-1,3,2-dioxaborolan-2-yl)butyl)trimethylsilane (2.5.1d): Following the general procedure described above, but using trimethyl (3-(4,4,5,5-tetramethyl-1,3,2-dioxaborolan-2-yl)propyl)silane, afforded **2.5.1d** (1.80 g, 62%) as a colorless oil. $^1\text{H NMR}$ (400 MHz, CDCl_3): δ 3.44 (t, $J = 7.4$ Hz, 1H), 1.84 (q, $J = 7.5$ Hz, 2H), 1.54 – 1.34 (m, 2H), 1.28 (s, 12H), 0.60 – 0.36 (m, 2H), -0.02 (s, 9H) ppm. $^{13}\text{C NMR}$ (101 MHz, CDCl_3) δ 84.5, 37.9, 24.8, 24.7, 21.8, 16.3, -1.6 ppm. $^{11}\text{B NMR}$ (128 MHz, CDCl_3) δ 31.6 ppm. **IR** (neat, cm^{-1}): 2979, 2953, 1380, 1340,

*Site-Selective Ni-Catalyzed Reductive
Coupling of α -Haloboranes with Unactivated Olefins*

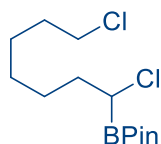
1248, 1141, 968, 835. **HRMS** calcd. for (C₁₃H₂₈SiBClNaO₂) [M+Na]⁺: 313.1569 found 313.1528.



tert-butyl((7-chloro-7-(4,4,5,5-tetramethyl-1,3,2-dioxaborolan-2-yl)heptyl)oxy)dimethylsilane (2.5.1e): Following the general procedure described above, but using *tert*-butyldimethyl((6-(4,4,5,5-tetramethyl-1,3,2-dioxaborolan-2-yl)hexyl)oxy)silane, afforded **2.5.1e** (2.31 g, 59%) as a colorless oil. **¹H NMR** (300 MHz, CDCl₃): δ 3.59 (t, J = 6.5 Hz, 2H), 3.41 (dd, J = 8.0, 6.8 Hz, 1H), 1.86 – 1.76 (m, 2H), 1.55 – 1.41 (m, 3H), 1.39 – 1.26 (m, 5H), 1.28 (s, 12H), 0.89 (s, 9H), 0.04 (s, 6H) ppm. **¹³C NMR** (101 MHz, CDCl₃) δ 84.4, 63.3, 34.1, 32.8, 29.0, 27.4, 26.1, 25.7, 24.7 (left), 24.7 (right), 18.4, -5.2 ppm. **¹¹B NMR** (128 MHz, CDCl₃) δ 31.3 ppm. **IR** (neat, cm⁻¹): 2979, 2930, 2857, 1383, 1343, 1253, 1141, 1098, 967, 834, 774; **HRMS** calcd. for (C₁₉H₄₀SiBClNaO₃) [M+Na]⁺: 413.2457 found 413.2506.



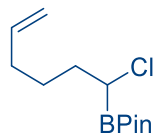
8-chloro-8-(4,4,5,5-tetramethyl-1,3,2-dioxaborolan-2-yl)octanenitrile (2.5.1f): Following the general procedure described above, but using 7-(4,4,5,5-tetramethyl-1,3,2-dioxaborolan-2-yl)-heptanenitrile as starting material, afforded **2.5.1f** (1.88 g, 66%) as a colorless oil. **¹H NMR** (400 MHz, CDCl₃): δ 3.40 (dd, J = 8.2, 6.4 Hz, 1H), 2.33 (t, J = 7.1 Hz, 2H), 1.88 – 1.76 (m, 2H), 1.69 – 1.62 (m, 2H), 1.58 – 1.32 (m, 6H), 1.28 (s, 12H) ppm. **¹³C NMR** (101MHz, CDCl₃) δ 118.8, 83.6, 32.9, 27.6, 27.4, 26.0, 24.4, 23.7, 23.6, 16.2 ppm. **¹¹B NMR** (128 MHz, CDCl₃) δ 37.0 ppm. **IR** (neat, cm⁻¹): 2979, 2934, 2860, 1382, 1342, 1140, 966, 847. **HRMS** calcd. for (C₁₄H₂₅BClNaO₂) [M+Na]⁺: 308.1595 found 308.1560.



2-(1,7-dichloroheptyl)-4,4,5,5-tetramethyl-1,3,2-dioxaborolane (2.5.1g): Following the general procedure described above, but using 2-(6-chlorohexyl)-4,4,5,5-tetramethyl-1,3,2-dioxaborolane as starting material, afforded **2.5.1g** (1.73 g, 59%) as a colorless oil. **¹H NMR** (300 MHz, CDCl₃): δ 3.51 (t, J = 6.7 Hz, 2H), 3.39 (t, J =

Chapter 2.

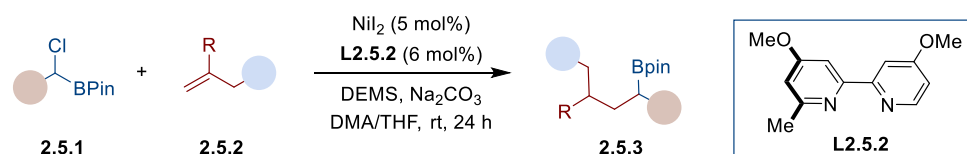
7.5 Hz, 1H), 1.88 – 1.65 (m, 4H), 1.54 – 1.30 (m, 6H), 1.27 (s, 12H) ppm. ^{13}C NMR (101 MHz, CDCl_3) δ 84.6, 45.2, 34.0, 32.6, 28.5, 27.2, 26.8, 24.8, 24.7 ppm. ^{11}B NMR (128 MHz, CDCl_3) δ 30.9 ppm. IR (neat, cm^{-1}): 2979, 2933, 2859, 1372, 1342, 1141, 967, 847. HRMS calcd. for $(\text{C}_{13}\text{H}_{25}\text{BClO}_2)$ $[\text{M}-\text{Cl}]^+$: 259.1667 found 259.1632.



2-(1-chlorohex-5-en-1-yl)-4,4,5,5-tetramethyl-1,3,2-dioxaborolane (2.5.1k):

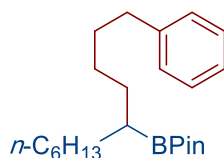
Following the general procedures, using 4,4,5,5-tetramethyl-2-(pent-4-en-1-yl)-1,3,2-dioxaborolane as starting material, afforded **2.5.1k** (1.49 g, 61%) as a colorless oil. ^1H NMR (300 MHz, CDCl_3): δ 5.80 (ddt, $J = 16.9, 10.2, 6.6$ Hz, 1H), 5.11 – 4.73 (m, 2H), 3.41 (t, $J = 9.8$ Hz, 1H), 2.16 – 2.01 (m, 2H), 1.91 – 1.75 (m, 2H), 1.65 – 1.47 (m, 2H), 1.28 (s, 12H) ppm. ^{13}C NMR (101 MHz, CDCl_3): δ 138.5, 114.9, 84.5, 33.6, 33.3, 26.7, 24.7 (left), 24.7 (right) ppm. ^{11}B NMR (128 MHz, CDCl_3) δ 31.3 ppm. IR (neat, cm^{-1}): 2979, 2933, 1381, 1372, 1340, 1140, 967, 848. GC-MS: $(\text{C}_{12}\text{H}_{22}\text{BClO}_2)$ $[\text{M}]^+$: found $t = 5.550$ min, m/z 244.1.

2.8.5 Ni-Catalyzed Reductive Coupling with Terminal Olefins



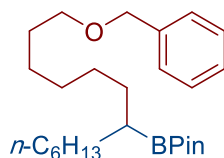
General procedure A: An oven-dried 8 mL screw-cap tube containing a stirring bar was charged with NiI_2 (3.1 mg, 5 mol%), **L2.5.2** (2.8 mg, 6 mol%) and Na_2CO_3 (15.9 mg, 0.75 mol). Subsequently, the tube was sealed with a Teflon-lined screw cap, then evacuated and backfilled with Ar (3 times). Then, the corresponding α -haloborane (0.20 mmol, 1 equiv), olefin (0.34 mmol, 1.7 equiv), DEMS (48 μL , 0.3 mmol, 1.5 equiv), DMA and THF (3:1, 0.4 mL) were added via syringe. Once added, the tube was stirred at room temperature for 24 h. After the reaction was completed, the mixture was diluted with EtOAc and filtered through silica gel and concentrated. The corresponding product was purified by column chromatography on silica gel.

*Site-Selective Ni-Catalyzed Reductive
Coupling of α -Haloboranes with Unactivated Olefins*



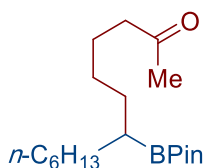
4,4,5,5-tetramethyl-2-(1-phenylundecan-5-yl)-1,3,2-dioxaborolane (2.5.3a):

Following the general procedure A, but using 4-phenyl-1-butene (44.9 mg, 0.34 mmol) afforded **2.5.3a** (59.0 mg, 83% yield) as a light-yellow oil. In an independent experiment, 58.0 mg (81%) were obtained, giving an average of 82% yield. $^1\text{H NMR}$ (400 MHz, CDCl_3): δ 7.28 – 7.24 (m, 2H), 7.20 – 7.14 (m, 3H), 2.60 (t, $J = 7.7$ Hz, 2H), 1.69 – 1.53 (m, 2H), 1.48 – 1.26 (m, 14H), 1.25 (s, 6H), 1.22 (s, 6H), 0.99 – 0.94 (m, 1H), 0.88 (t, $J = 6.8$ Hz, 3H) ppm. $^{13}\text{C NMR}$ (101 MHz, CDCl_3): δ 143.0, 128.6, 128.3, 125.6, 82.9, 36.0, 32.0, 31.9, 31.7, 31.5, 29.7, 29.4, 29.1, 24.9 (2C), 22.8, 14.2 ppm. $^{11}\text{B NMR}$ (128 MHz, CDCl_3) δ 34.6 ppm. **IR** (neat, cm^{-1}): 2977, 2956, 2924, 2854, 1456, 1378, 1370, 1314, 1143, 968, 863, 698. **HRMS** calcd. for $(\text{C}_{23}\text{H}_{39}\text{BNaO}_2)$ $[\text{M}+\text{Na}]^+$: 381.2935 found 381.2933.



2-(1-(benzyloxy)tridecan-7-yl)-4,4,5,5-tetramethyl-1,3,2-dioxaborolane (2.5.3b):

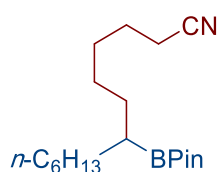
Following the general procedure A, but using ((hex-5-en-1-yloxy)methyl)benzene (64.6 mg, 0.34 mmol), $\text{NiBr}_2 \cdot \text{diglyme}$ (7.0 mg, 10 mol%) and **L2.5.2** (5.6 mg, 12 mol%), afforded **2.5.3b** (53.0 mg, 64% yield) as a light yellow oil. In an independent experiment, 42.0 mg (63% yield) were obtained, giving an average of 63% yield. $^1\text{H NMR}$ (400 MHz, CDCl_3): δ 7.34 – 7.31 (m, 4H), 7.30 – 7.22 (m, 1H), 4.50 (s, 2H), 3.46 (t, $J = 6.7$ Hz, 2H), 1.60 (dt, $J = 8.3, 6.5$ Hz, 2H), 1.44 – 1.24 (m, 18H), 1.24 (s, 12H), 0.98 – 0.92 (m, 1H), 0.88 (t, $J = 6.8$ Hz, 3H) ppm. $^{13}\text{C NMR}$ (101 MHz, CDCl_3): δ 138.9, 128.4, 127.7, 127.5, 82.9, 73.0, 70.7, 32.0, 31.6, 31.5, 29.9, 29.8, 29.7, 29.4 (2C), 26.3, 24.9 (2C), 22.8, 14.2 ppm. $^{11}\text{B NMR}$ (128 MHz, CDCl_3) δ 33.8 ppm. **IR** (neat, cm^{-1}): 2976, 2955, 2923, 2853, 1455, 1386, 1370, 1313, 1143, 1102, 966, 733. **HRMS** calcd. for $(\text{C}_{26}\text{H}_{46}\text{BO}_3)$ $[\text{M}+\text{H}]^+$: 417.3535 found 417.3534.



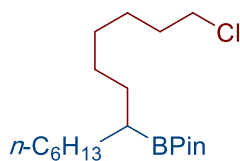
7-(4,4,5,5-tetramethyl-1,3,2-dioxaborolan-2-yl)tridecan-2-one (2.5.3c): Following

Chapter 2.

the general procedure A, but using hex-5-en-2-one (33.3 mg, 0.34 mmol), NiI₂ (6.2 mg, 10 mol%) and **L2.5.2** (5.6 mg, 12 mol%), afforded **2.5.3c** (35 mg, 54% yield) as a light yellow oil. In an independent experiment, 37.0 mg (57% yield) were obtained, giving an average of 56% yield. ¹H NMR (400 MHz, CDCl₃): δ 2.39 (t, *J* = 7.4 Hz, 2H), 2.11 (s, 3H), 1.60 – 1.49 (m, 2H), 1.43 – 1.25 (m, 14H), 1.22 (s, 12H), 0.97 – 0.89 (m, 1H), 0.85 (t, *J* = 6.7 Hz, 3H) ppm. ¹³C NMR (101 MHz, CDCl₃): δ 209.4, 82.9, 43.9, 32.0, 31.5, 31.2, 29.9, 29.7, 29.3, 28.9, 24.9 (2C), 24.3, 22.7, 14.2 ppm. ¹¹B NMR (128 MHz, CDCl₃) δ 34.5 ppm. IR (neat, cm⁻¹): 2956, 2925, 2855, 1720, 1604, 1508, 1387, 1269, 1144, 1112, 1089, 966, 853, 767. HRMS calcd. for (C₁₉H₃₇BNaO₃) [M+Na]⁺: 346.2764 found 346.2757.



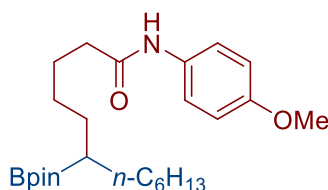
7-(4,4,5,5-tetramethyl-1,3,2-dioxaborolan-2-yl)tridecanenitrile (2.5.3d): Following the general procedure A, but using hex-5-enenitrile (32.3 mg, 0.34 mmol), afforded **2.5.3d** (36.0 mg, 56% yield) as a light yellow oil. In an independent experiment, 39.8 mg (62% yield) were obtained, giving an average of 59% yield. ¹H NMR (500 MHz, CDCl₃): δ 2.30 (t, *J* = 7.2 Hz, 2H), 1.63 (q, *J* = 7.3 Hz, 2H), 1.44 – 1.36 (m, 4H), 1.33 – 1.23 (m, 12H), 1.22 (s, 12H), 0.94 – 0.90 (m, 1H), 0.86 (t, *J* = 6.9 Hz, 3H). ppm. ¹³C NMR (126 MHz, CDCl₃): δ. 120.0, 83.0, 31.9, 31.5, 31.1, 29.7, 29.3, 29.0, 28.4, 25.4, 24.9, 24.8, 22.7, 17.1, 14.2 ppm. ¹¹B NMR (160 MHz, CDCl₃) δ 34.3 ppm. IR (neat, cm⁻¹): 2977, 2924, 2854, 1462, 1387, 1371, 1314, 1259, 1214, 1143, 733, 700. HRMS calcd. for (C₁₉H₃₆BNaNO₂) [M+Na]⁺: 344.2731 found. 344.2701.



2-(1-chlorotridecan-7-yl)-4,4,5,5-tetramethyl-1,3,2-dioxaborolane (2.5.3e): Following the general procedure A, but using 6-chlorohex-1-ene (40.1mg, 0.34 mmol), afforded **2.5.3e** (46.0 mg, 66% yield) as a light-yellow oil. In an independent experiment, 44.0 mg (64% yield) were obtained, giving an average of 65% yield. ¹H NMR (400 MHz, CDCl₃): δ 3.49 (t, *J* = 6.8 Hz, 2H), 1.77 – 1.69 (m, 2H), 1.32 – 1.35 (m, 4H), 1.32 – 1.22 (m, 14H), 1.22 (s, 12H), 0.95 – 0.90 (m, 1H), 0.85 (t, *J* = 6.8 Hz, 3H) ppm. ¹³C NMR (101 MHz, CDCl₃): δ 82.9, 45.2, 32.8, 32.0, 31.6, 31.4, 29.7,

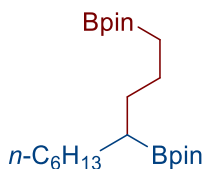
*Site-Selective Ni-Catalyzed Reductive
Coupling of α -Haloboranes with Unactivated Olefins*

29.4, 29.3, 29.2, 26.9, 24.9 (2C), 22.7, 14.2 ppm. ^{11}B NMR (128 MHz, CDCl_3) δ 34.7 ppm. IR (neat, cm^{-1}): 2977, 2956, 2923, 2854, 1386, 1379, 1313, 1143, 967, 862. HRMS calcd. for $(\text{C}_{19}\text{H}_{39}\text{BClO}_2)$ $[\text{M}+\text{H}]^+$: 345.2726 found 345.2721.



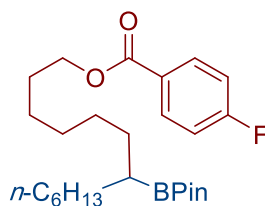
***N*-(4-methoxyphenyl)-5-(4,4,5,5-tetramethyl-1,3,2-dioxaborolan-2-yl)**

undecanamide (2.5.3f): Following the general procedure A, but using *N*-(4-methoxyphenyl)pent-4-enamide (69.7 mg, 0.34 mmol), afforded **2.5.3f** (46 mg, 55% yield) as a light yellow oil. In an independent experiment, 44.0 mg (51%) were obtained, giving an average of 53% yield. ^1H NMR (400 MHz, CDCl_3): δ 7.40 (dd, $J = 9.3, 3.0$ Hz, 2H), 7.02 (s, 1H), 6.90 – 6.81 (m, 2H), 3.78 (s, 3H), 2.32 (t, $J = 7.7$ Hz, 2H), 1.71 (dt, $J = 7.3, 3.8$ Hz, 2H), 1.48 – 1.16 (m, 25H), 0.95 (t, $J = 7.4$ Hz, 2H), 0.87 (t, $J = 6.8$ Hz, 3H) ppm. ^{13}C NMR (126 MHz, CDCl_3): δ 171.2, 156.3, 131.1, 121.7, 114.1, 82.8, 55.5, 37.7, 31.8, 31.4, 31.0, 29.6, 29.2, 28.9, 26.0, 24.8, 24.7, 22.6, 14.1 ppm. ^{11}B NMR (128 MHz, CDCl_3) δ 34.1 ppm. IR (neat, cm^{-1}): 3293, 2956, 2954, 2855, 1655, 1604, 1541, 1510, 1463, 1379, 1313, 1242, 1036. HRMS calcd. for $(\text{C}_{25}\text{H}_{42}\text{BNNaO}_4)$ $[\text{M}+\text{Na}]^+$: 454.3099 found 454.3108.



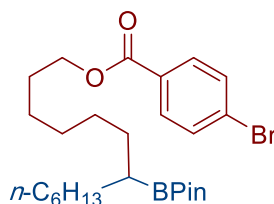
2,2'-(decane-1,4-diyl)bis(4,4,5,5-tetramethyl-1,3,2-dioxaborolane) (2.5.3g):

Following the general procedure A, but using 2-allyl-4,4,5,5-tetramethyl-1,3,2-dioxaborolane (84.0 mg, 0.5 mmol) and $\text{NiBr}_2 \cdot \text{diglyme}$ (7.0 mg, 10 mol%), afforded **2.5.3g** (47.0 mg, 47% yield) as a light yellow oil. In an independent experiment, 35.0 mg (44% yield) were obtained, giving an average of 46% yield. ^1H NMR (400 MHz, CDCl_3): δ 1.46 – 1.23 (m, 14H), 1.22 (s, 24H), 0.99 – 0.90 (m, 1H), 0.86 (t, $J = 6.6$ Hz, 3H), 0.74 (t, $J = 7.3$ Hz, 2H) ppm. ^{13}C NMR (101 MHz, CDCl_3): δ 82.9, 82.8, 34.3, 32.0, 31.4, 29.8, 29.4, 25.0 (2C), 24.9 (2C), 23.8, 22.8, 14.2 ppm. ^{11}B NMR (128 MHz, CDCl_3) δ 34.8 ppm. IR (neat, cm^{-1}): 2977, 2924, 2855, 1370, 1314, 1143, 968, 848, 688. HRMS calcd. for $(\text{C}_{22}\text{H}_{44}\text{B}_2\text{NaO}_4)$ $[\text{M}+\text{Na}]^+$: 417.3318 found 417.3300.



7-(4,4,5,5-tetramethyl-1,3,2-dioxaborolan-2-yl)tridecyl-4-fluorobenzoate (2.5.3h):

Following the general procedure A, but using hex-5-en-1-yl 4-fluorobenzoate (75.5 mg, 0.34 mmol), NiBr₂·diglyme (7.0 mg, 10 mol%) and **L2.5.2** (5.6 mg, 12 mol%), afforded **2.5.3h** (57.0 mg, 63% yield) as a light yellow oil. In an independent experiment, 61.0 mg (68% yield) were obtained, giving an average of 66% yield. ¹H NMR (400 MHz, CDCl₃): δ 8.05 (dd, *J* = 8.8, 5.2 Hz, 2H), 7.09 (t, *J* = 8.6 Hz, 2H), 4.29 (t, *J* = 6.7 Hz, 2H), 1.74 (dt, *J* = 14.8, 6.8 Hz, 2H), 1.48 – 1.17 (m, 18H), 1.23 (s, 12H), 1.02 – 0.90 (m, 1H), 0.86 (t, *J* = 6.6 Hz, 3H) ppm. ¹³C NMR (101 MHz, CDCl₃): δ 165.9, 165.8 (d, *J* = 253.6 Hz), 132.2 (d, *J* = 9.2 Hz), 126.9 (d, *J* = 3.0 Hz), 115.6 (d, *J* = 21.9 Hz), 82.9, 65.4, 32.0, 31.6, 31.5, 29.7 (left), 29.7 (right), 29.4, 29.3, 28.8, 26.1, 24.9 (2C), 22.8, 14.2 ppm. ¹¹B NMR (128 MHz, CDCl₃) δ 35.1 ppm. ¹⁹F NMR (376 MHz, CDCl₃) δ -106.2 ppm. IR (neat, cm⁻¹): 2976, 2956, 2925, 2855, 1720, 1604, 1508, 1387, 1269, 1144, 1112, 1089, 966, 767. HRMS calcd. for (C₂₆H₄₂FBNaO₄) [M+Na]⁺: 470.3089 found 470.3068.

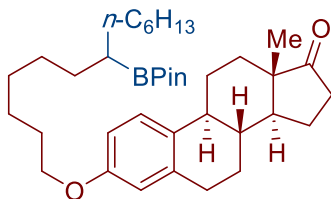


7-(4,4,5,5-tetramethyl-1,3,2-dioxaborolan-2-yl)tridecyl 4-bromobenzoate (2.5.3i):

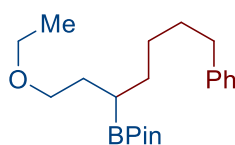
Following the general procedure A, but using hex-5-en-1-yl 4-bromobenzoate (95.9 mg, 0.34 mmol), NiBr₂·diglyme (7.0 mg, 10 mol%) and **L2.5.2** (5.6 mg, 12 mol%), afforded **2.5.3i** (66.0 mg, 65% yield) as a light yellow oil. In an independent experiment, 66.0 mg (65% yield) were obtained, giving an average of 65% yield. ¹H NMR (400 MHz, CDCl₃): δ 7.86 (d, *J* = 8.6 Hz, 2H), 7.54 (d, *J* = 8.6 Hz, 2H), 4.27 (t, *J* = 6.7 Hz, 2H), 1.76 – 1.68 (m, 2H), 1.40 – 1.23 (m, 18H), 1.21 (s, 12H), 0.96 – 0.91 (m, 1H), 0.84 (t, *J* = 6.8 Hz, 3H) ppm. ¹³C NMR (101 MHz, CDCl₃): δ 166.0, 131.7, 131.2, 129.6, 127.9, 82.9, 65.5, 31.9, 31.6, 31.4, 29.7, 29.6, 29.3, 29.2, 28.7, 26.0, 24.9 (2C), 22.7, 14.2 ppm. ¹¹B NMR (128 MHz, CDCl₃) δ 32.6 ppm. IR (neat, cm⁻¹): 2976, 2955, 2923, 2854, 1721, 1591, 1387, 1312, 1268, 1143, 1114, 1102,

*Site-Selective Ni-Catalyzed Reductive
Coupling of α -Haloboranes with Unactivated Olefins*

1012, 847, 757. **HRMS** calcd. for (C₂₆H₄₂BBrNaO₄) [M+Na]⁺: 531.2288 found 531.2247.



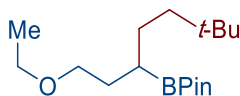
(8R,9S,13S,14S)-13-methyl-3-((7-(4,4,5,5-tetramethyl-1,3,2-dioxaborolan-2-yl)tridecyl)oxy)-6,7,8,9,11,12,13,14,15,16-decahydro-17H-cyclopenta[a]phenanthrene-17-one (2.5.3j): Following the general procedure A, but using 1-(3-bromophenyl)ethan-1-one (43.8 mg, 0.34 mmol), afforded **2.5.3j** (55.0 mg, 48% yield) as a white solid. In an independent experiment, 55.0 mg (48% yield) were obtained, giving an average of 48% yield, 1:1 dr. **Mp** 56.1–58.0 °C. **¹H NMR** (400 MHz, CDCl₃): δ 7.18 (d, J = 8.5 Hz, 1H), 6.70 (dd, J = 8.6, 2.8 Hz, 1H), 6.63 (d, J = 2.7 Hz, 1H), 3.91 (t, J = 6.6 Hz, 2H), 2.94 – 2.76 (m, 2H), 2.50 (dd, J = 18.8, 8.5 Hz, 1H), 2.43 – 2.35 (m, 1H), 2.29 – 2.21 (m, 1H), 2.19 – 1.89 (m, 5H), 1.81 – 1.70 (m, 2H), 1.69 – 1.25 (m, 23H), 1.24 (s, 12H), 0.97 – 0.92 (m, 1H), 0.91 (s, 3H), 0.87 (t, J = 7.0 Hz, 3H) ppm. **¹³C NMR** (101 MHz, CDCl₃): δ 221.1, 157.3, 137.8, 131.9, 126.4, 114.7, 112.3, 82.9, 68.1, 50.6, 48.2, 44.1, 38.5, 36.0, 32.0, 31.7, 31.6, 31.5, 29.9, 29.8, 29.7, 29.6, 29.5, 29.4, 26.7, 26.2, 26.1, 24.9 (2C), 22.8, 21.7, 14.2, 14.0 ppm. **¹¹B NMR** (128 MHz, CDCl₃) δ 35.5 ppm. **IR** (neat, cm⁻¹): 2976, 2924, 2855, 1739, 1609, 1499, 1467, 1387, 1372, 1313, 1236, 1143, 1053, 910, 732. **HRMS** calcd. for (C₃₇H₅₉BNaO₄) [M+Na]⁺: 601.4435 found 601.4410.



2-(1,7-diphenylheptan-3-yl)-4,4,5,5-tetramethyl-1,3,2-dioxaborolane (2.5.3k): Following the general procedure A, but using 2-(1-chloro-3-phenylpropyl)-4,4,5,5-tetramethyl-1,3,2-dioxaborolane (56.0 mg, 0.20 mmol), afforded **2.5.3k** (53.0 mg, 70% yield) as a light yellow oil. In an independent experiment, 50.0 mg (66% yield) were obtained, giving an average 68% yield. **¹H NMR** (400 MHz, CDCl₃): δ 7.31 (dd, J = 6.4, 1.6 Hz, 2H), 7.30 (dd, J = 6.8, 2.0 Hz, 2H), 7.24 – 7.17 (m, 6H), 2.64 (t, J = 7.4 Hz, 4H), 1.89 – 1.60 (m, 4H), 1.59 – 1.34 (m, 4H), 1.27 (s, 12H), 1.16 – 1.02 (m, 1H) ppm. **¹³C NMR** (101 MHz, CDCl₃): δ 143.2, 143.0, 128.6, 128.5, 128.4, 128.3, 125.7, 125.6, 83.0, 36.0, 35.8, 33.7, 31.8, 31.3, 28.9, 25.0, 24.9 ppm. **¹¹B NMR** (128 MHz,

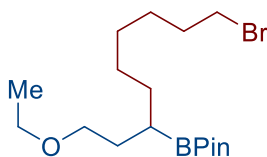
Chapter 2.

CDCl_3) δ 38.3 ppm. **IR** (neat, cm^{-1}): 2977, 2926, 2855, 1454, 1379, 1315, 1142, 966, 745, 697. **HRMS** calcd. for $(\text{C}_{25}\text{H}_{35}\text{BNaO}_2)$ $[\text{M}+\text{Na}]^+$: 369.2591 found 369.2568.



2-(1-ethoxy-6,6-dimethylheptan-3-yl)-4,4,5,5-tetramethyl-1,3,2-dioxaborolane

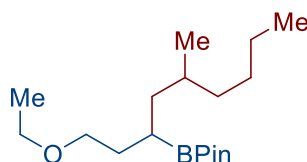
(2.5.31): Following the general procedure A, but using 2-(1-chloro-3-ethoxypropyl)-4,4,5,5-tetramethyl-1,3,2-dioxaborolane (49.6 mg, 0.20 mmol) and 3,3-dimethylbut-1-ene (28.6 mg, 0.34 mmol), afforded **2.5.31** (38.8 mg, 65% yield) as a light yellow oil. In an independent experiment, 36.0 mg (60% yield) were obtained, giving an average of 63% yield. **^1H NMR** (400 MHz, CDCl_3): δ 3.46 (q, $J = 7.0$ Hz, 2H), 3.39 (ddd, $J = 7.3, 6.5, 1.7$ Hz, 2H), 1.76 – 1.59 (m, 2H), 1.42 – 1.28 (m, 2H), 1.23 (s, 12H), 1.18 (t, $J = 7.0$ Hz, 5H), 0.96 – 0.91 (m, 1H), 0.85 (s, 9H) ppm. **^{13}C NMR** (126 MHz, CDCl_3): δ 83.0, 70.5, 66.2, 43.6, 31.6, 30.5, 29.5, 26.4, 25.0, 24.9, 15.3 ppm. **^{11}B NMR** (160 MHz, CDCl_3) δ 34.2 ppm. **IR** (neat, cm^{-1}): 3069, 3049, 2976, 2923, 2854, 1459, 1428, 1379, 1315, 1143, 1109, 967, 730, 698, 510, 488. **HRMS** calcd. for $(\text{C}_{17}\text{H}_{35}\text{BNaO}_3)$ $[\text{M}+\text{Na}]^+$: 321.2571 found 321.2564.



2-(9-bromo-1-ethoxynonan-3-yl)-4,4,5,5-tetramethyl-1,3,2-dioxaborolane

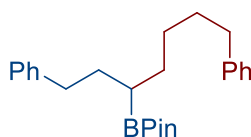
(2.5.3m): Following the general procedure A, but using 2-(1-chloro-3-ethoxypropyl)-4,4,5,5-tetramethyl-1,3,2-dioxaborolane (49.6 mg, 0.20 mmol) and 6-bromohex-1-ene (55.1 mg, 0.34 mmol), afforded **2.5.3m** (38.0 mg, 51% yield) as a light yellow oil. In an independent experiment, 37.0 mg (50% yield) were obtained, giving an average of 50% yield. **^1H NMR** (400 MHz, CDCl_3): δ 3.45 (q, $J = 7.0$ Hz, 2H), 3.42 – 3.34 (m, 4H), 1.91 – 1.79 (m, 2H), 1.78 – 1.55 (m, 3H), 1.47 – 1.27 (m, 7H), 1.23 (s, 6H), 1.22 (s, 6H), 1.18 (t, $J = 7.0$ Hz, 3H), 1.05 – 0.95 (m, 1H) ppm. **^{13}C NMR** (101 MHz, CDCl_3): δ 83.0, 70.4, 66.2, 34.1, 32.9, 31.5, 31.4, 29.1, 29.0, 28.2, 25.0, 24.9, 15.3 ppm. **^{11}B NMR** (128 MHz, CDCl_3) δ 34.3 ppm. **IR** (neat, cm^{-1}): 2976, 2928, 2856, 1378, 1372, 1314, 1143, 1109, 967, 854. **HRMS** calcd. for $(\text{C}_{17}\text{H}_{34}\text{BBrNaO}_3)$ $[\text{M}+\text{Na}]^+$: 399.1713 found 399.1691.

*Site-Selective Ni-Catalyzed Reductive
Coupling of α -Haloboranes with Unactivated Olefins*



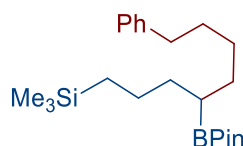
3-(1-ethoxy-5-methylnonan-3-yl)-4,4,5,5-tetramethyl-1,3,2-dioxaborolane (2.5.3n):

Following the general procedure A, but using 2-(1-chloro-3-ethoxypropyl)-4,4,5,5-tetramethyl-1,3,2-dioxaborolane (74.4 mg, 0.30 mmol), 2-methylhex-1-ene (19.6 mg, 0.20 mmol), NiI₂ (6.2 mg, 10 mol%) and 4-isopropyl-2-(6-methylpyridin-2-yl)-4,5-dihydrooxazole (**L2.5.12**, 4.9 mg, 12 mol%), afforded **2.5.3n** (32.0 mg, 52% yield, 1:1 dr) as a light yellow oil. In an independent experiment, 34.0 mg (54% yield) were obtained, giving an average of 53% yield as a 1:1 mixture of diastereoisomers. ¹H NMR (400 MHz, CDCl₃): δ 3.45 (q, $J = 7.0$ Hz, 2H), 3.39 (td, $J = 7.4, 1.9$ Hz, 2H), 1.76 – 1.54 (m, 2H), 1.53 – 1.23 (m, 8H), 1.23 (s, 12H), 1.18 (t, $J = 7.0$ Hz, 3H), 1.14 – 1.01 (m, 2H), 0.87 (t, $J = 7.0$ Hz, 3H), 0.83 (t, $J = 6.2$ Hz, 3H) ppm. ¹³C NMR (101 MHz, CDCl₃): δ 83.0, 70.5 (2C), 66.2, 39.4, 38.8, 37.5, 36.7, 32.4, 32.2, 31.9, 31.4, 29.5 (2C), 25.0 (2C), 24.9 (2C), 23.2 (2C), 19.9 (2C), 15.4, 14.3 (2C) ppm. ¹¹B NMR (128 MHz, CDCl₃) δ 34.1 ppm. IR (neat, cm⁻¹): 2976, 2957, 2926, 2858, 1459, 1378, 1314, 1141, 1109, 967, 861, 671. HRMS calcd. for (C₁₈H₃₇BNaO₃) [M+Na]⁺: 335.2731 found 335.2721.



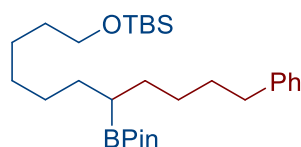
2-(1,7-diphenylheptan-3-yl)-4,4,5,5-tetramethyl-1,3,2-dioxaborolane (2.5.3o):

Following the general procedure A, but using 2-(1-chloro-3-phenylpropyl)-4,4,5,5-tetramethyl-1,3,2-dioxaborolane (56.0 mg, 0.20 mmol), afforded **2.5.3o** (53.0 mg, 70% yield) as a light yellow oil. In an independent experiment, 50.0 mg (66% yield) were obtained, giving an average 68% yield. ¹H NMR (400 MHz, CDCl₃): δ 7.30 – 7.25 (m, 4H), 7.20 – 7.15 (m, 6H), 2.61 (t, $J = 7.4$ Hz, 4H), 1.79 – 1.59 (m, 4H), 1.52 – 1.33 (m, 4H), 1.25 (s, 12H), 1.10 – 1.02 (m, 1H) ppm. ¹³C NMR (101 MHz, CDCl₃): δ 143.2, 143.0, 128.6, 128.5, 128.4, 128.3, 125.7, 125.6, 83.1, 36.0, 35.8, 33.7, 31.8, 31.3, 28.9, 25.0, 24.9 ppm. ¹¹B NMR (128 MHz, CDCl₃) δ 33.8 ppm. IR (neat, cm⁻¹): 2977, 2926, 2855, 1454, 1379, 1315, 1142, 966, 745, 697. HRMS calcd. for (C₂₅H₃₅BNaO₂) [M+Na]⁺: 401.2659 found 401.2624.



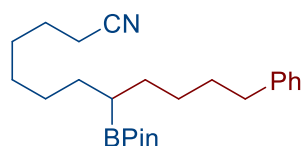
trimethyl(8-phenyl-4-(4,4,5,5-tetramethyl-1,3,2-dioxaborolan-2-yl)octyl)silane

(2.5.3p): Following the general procedure A, but using (4-chloro-4-(4,4,5,5-tetramethyl-1,3,2-dioxaborolan-2-yl)butyl)trimethylsilane (58.0 mg, 0.20 mmol), afforded **2.5.3p** (47.0 mg, 61% yield) as a light yellow oil. In an independent experiment, 46.0 mg (59% yield) were obtained, giving an average of 60% yield. $^1\text{H NMR}$ (400 MHz, CDCl_3): δ 7.26 (dd, $J = 8.4, 6.4$ Hz, 2H), 7.20 – 7.13 (m, 3H), 2.60 (t, $J = 7.6$ Hz, 2H), 1.67 – 1.55 (m, 2H), 1.49 – 1.28 (m, 8H), 1.25 (s, 6H), 1.22 (s, 6H), 1.03 – 0.96 (m, 1H), 0.58 – 0.39 (m, 2H), -0.03 (s, 9H) ppm. $^{13}\text{C NMR}$ (101 MHz, CDCl_3): δ 143.0, 128.6, 128.3, 125.6, 82.9, 36.0, 35.8, 31.8, 31.6, 29.1, 25.0, 24.9, 23.8, 17.2, -1.5 ppm. $^{11}\text{B NMR}$ (128 MHz, CDCl_3) δ 34.4 ppm. **IR** (neat, cm^{-1}): 2976, 2956, 2920, 2856, 1771, 1315, 1247, 1143, 969, 834, 744, 697. **HRMS** calcd. for ($\text{C}_{23}\text{H}_{41}\text{SiBNaO}_2$) [$\text{M}+\text{Na}$] $^+$: 411.2861 found 411.2854.



tert-butyl dimethyl((11-phenyl-7-(4,4,5,5-tetramethyl-1,3,2-dioxaborolan-2-yl)undecyl)oxy)silane

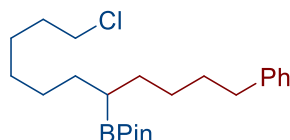
(2.5.3q): Following the general procedure A, but using *tert*-butyl((7-chloro-7-(4,4,5,5-tetramethyl-1,3,2-dioxaborolan-2-yl)heptyl)oxy)dimethylsilane (78.0 mg, 0.20 mmol), afforded **2.5.3q** (61.0 mg, 62% yield) as a light yellow oil. In an independent experiment, 60.0 mg (61% yield) were obtained, giving an average of 61% yield. $^1\text{H NMR}$ (400 MHz, CDCl_3): δ 7.26 (dd, $J = 8.2, 7.0$ Hz, 2H), 7.21 – 7.10 (m, 3H), 3.60 (t, $J = 6.7$ Hz, 2H), 2.60 (t, $J = 7.6$ Hz, 2H), 1.70 – 1.55 (m, 2H), 1.55 – 1.27 (m, 14H), 1.3 (s, 6H), 1.22 (s, 6H), 0.91 (s, 9H), 0.85 – 0.68 (m, 1H), 0.06 (s, 6H) ppm. $^{13}\text{C NMR}$ (101 MHz, CDCl_3): δ 143.0, 128.6, 128.3, 125.6, 82.9, 63.4, 36.0, 33.0, 31.8, 31.6, 31.5, 29.9, 29.4, 29.0, 26.1, 25.9, 25.0, 24.9, 18.5, -5.1 ppm. $^{11}\text{B NMR}$ (128 MHz, CDCl_3) δ 34.5 ppm. **IR** (neat, cm^{-1}): 2977, 2956, 2927, 2856, 1462, 1379, 1371, 1315, 1253, 1144, 1098, 967, 834, 774, 698. **HRMS** calcd. for ($\text{C}_{29}\text{H}_{53}\text{SiBNaO}_3$) [$\text{M}+\text{Na}$] $^+$: 511.3786 found 511.3763.



*Site-Selective Ni-Catalyzed Reductive
Coupling of α -Haloboranes with Unactivated Olefins*

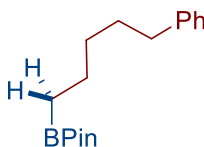
12-phenyl-8-(4,4,5,5-tetramethyl-1,3,2-dioxaborolan-2-yl)dodecanenitrile (2.3.5r):

Following the general procedure A, but using 8-chloro-8-(4,4,5,5-tetramethyl-1,3,2-dioxaborolan-2-yl)octanenitrile (57.0 mg, 0.20 mmol) afforded **2.3.5r** (40.0 mg, 52% yield) as a light yellow oil. In an independent experiment, 39.0 mg (51% yield) were obtained, giving an average of 52% yield. $^1\text{H NMR}$ (400 MHz, CDCl_3): δ 7.25 (dd, $J = 8.1, 6.6$ Hz, 2H), 7.19 – 7.12 (m, 3H), 2.59 (t, $J = 7.6$ Hz, 2H), 2.31 (t, $J = 7.1$ Hz, 2H), 1.72 – 1.55 (m, 4H), 1.49 – 1.25 (m, 12H), 1.21 (s, 12H), 0.99 – 0.90 (m, 1H) ppm. $^{13}\text{C NMR}$ (101 MHz, CDCl_3): δ 142.9, 128.5, 128.3, 125.6, 119.9, 82.9, 36.0, 31.8, 31.5, 31.4, 29.1, 29.0, 28.9, 28.7, 25.4, 24.9, 24.8, 17.2 ppm. $^{11}\text{B NMR}$ (128 MHz, CDCl_3) δ 35.1 ppm. **IR** (neat, cm^{-1}): 2977, 2926, 2855, 1455, 1380, 1371, 1315, 1143, 967, 860, 747, 699. **HRMS** calcd. for $(\text{C}_{24}\text{H}_{38}\text{BNNaO}_2)$ $[\text{M}+\text{Na}]^+$: 406.2888 found 406.2892.



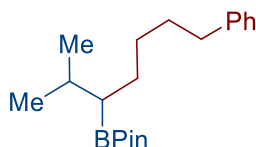
2-(11-chloro-1-phenylundecan-5-yl)-4,4,5,5-tetramethyl-1,3,2-dioxaborolane (2.5.3s):

Following the general procedure A, but using 2-(1,7-dichloroheptyl)-4,4,5,5-tetramethyl-1,3,2-dioxaborolane (58.8 mg, 0.20 mmol), afforded **2.5.3s** (60.0 mg, 76% yield) as a light yellow oil. In an independent experiment, 55.0 mg (70% yield) were obtained, giving an average of 73% yield. $^1\text{H NMR}$ (400 MHz, CDCl_3): δ 7.28 (dd, $J = 8.2, 6.7$ Hz, 2H), 7.23 – 7.09 (m, 3H), 3.54 (t, $J = 6.8$ Hz, 2H), 2.62 (t, $J = 7.6$ Hz, 2H), 1.85 – 1.71 (m, 2H), 1.69 – 1.55 (m, 2H), 1.51 – 1.29 (m, 12H), 1.27 (s, 6H), 1.23 (s, 6H), 1.02 – 0.91 (m, 1H) ppm. $^{13}\text{C NMR}$ (101 MHz, CDCl_3): δ 143.0, 128.5, 128.3, 125.6, 82.9, 45.3, 36.0, 32.7, 31.8, 31.5, 31.4, 29.2 (left), 29.2 (right), 29.0, 26.9, 24.9, 24.8 ppm. $^{11}\text{B NMR}$ (128 MHz, CDCl_3) δ 34.3 ppm. **IR** (neat, cm^{-1}): 2977, 2926, 2855, 1455, 1378, 1371, 1315, 1267, 1143, 967, 847, 729, 698. **HRMS** calcd. for $(\text{C}_{23}\text{H}_{38}\text{BClNaO}_2)$ $[\text{M}+\text{Na}]^+$: 415.2582 found 415.2533.



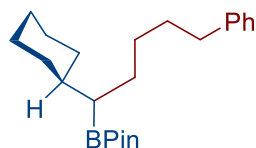
4,4,5,5-tetramethyl-2-(5-phenylpentyl)-1,3,2-dioxaborolane (2.5.3t): Following the general procedure A, but using 2-(chloromethyl)-4,4,5,5-tetramethyl-1,3,2-dioxaborolane (35.2 mg, 0.20 mmol) afforded **2.5.3t** (35.9 mg, 65% yield) as a light yellow oil. In an independent experiment, 38.6 mg (70% yield) were obtained, giving

an average of 68% yield. $^1\text{H NMR}$ (400 MHz, CDCl_3): δ 7.26 (dd, $J = 8.5, 6.3$ Hz, 2H), 7.20 – 7.11 (m, 3H), 2.70 – 2.47 (m, 2H), 1.66 – 1.58 (m, 2H), 1.50 – 1.40 (m, 2H), 1.39 – 1.30 (m, 2H), 1.23 (s, 12H), 0.78 (t, $J = 7.7$ Hz, 2H) ppm. $^{13}\text{C NMR}$ (101 MHz, CDCl_3): δ 143.1, 128.6, 128.3, 125.6, 83.0, 36.0, 32.1, 31.4, 24.9 (2C), 24.0 ppm. $^{11}\text{B NMR}$ (128 MHz, CDCl_3) δ 34.2 ppm. **IR** (neat, cm^{-1}): 2978, 2928, 2857, 1371, 1317, 1143, 968, 847, 745, 698. **HRMS** calcd. for $(\text{C}_{17}\text{H}_{27}\text{BNaO}_2)$ $[\text{M}+\text{Na}]^+$: 297.1996 found 297.1992.



4,4,5,5-tetramethyl-2-(2-methyl-7-phenylheptan-3-yl)-1,3,2-dioxaborolane

(2.5.3u): Following the general procedure A, but using 2-(1-bromo-2-methylpropyl)-4,4,5,5-tetramethyl-1,3,2-dioxaborolane and (52.6 mg, 0.20 mmol) and $\text{NiBr}_2 \cdot \text{diglyme}$ (7.0 mg, 10 mol%) afforded **2.5.3u** (32.0 mg, 51% yield) as a light yellow oil after stirring the reaction at 40 °C for 24 h. In an independent experiment, 31.0 mg (49% yield) were obtained, giving an average of 50% yield. $^1\text{H NMR}$ (400 MHz, CDCl_3): δ 7.26 (dd, $J = 8.6, 6.6$ Hz, 2H), 7.20 – 7.13 (m, 3H), 2.60 (t, $J = 7.7$ Hz, 2H), 1.73 – 1.56 (m, 3H), 1.47 – 1.36 (m, 2H), 1.22 (s, 6H), 1.21 (s, 6H), 1.12 – 1.08 (m, 1H), 0.93 (d, $J = 6.8$ Hz, 3H), 0.91 (d, $J = 6.8$ Hz, 3H), 0.86 – 0.79 (m, 2H) ppm. $^{13}\text{C NMR}$ (101 MHz, CDCl_3): δ 143.0, 128.6, 128.3, 125.6, 82.9, 36.1, 31.9, 29.8, 29.4, 29.3, 25.1, 25.0, 22.5, 22.0 ppm. $^{11}\text{B NMR}$ (128 MHz, CDCl_3) δ 34.2 ppm. **IR** (neat, cm^{-1}): 2977, 2955, 2928, 2861, 1454, 1379, 1314, 1142, 969, 849, 745, 697. **HRMS** calcd. for $(\text{C}_{20}\text{H}_{33}\text{BNaO}_2)$ $[\text{M}+\text{Na}]^+$: 339.2466 found 339.2459.



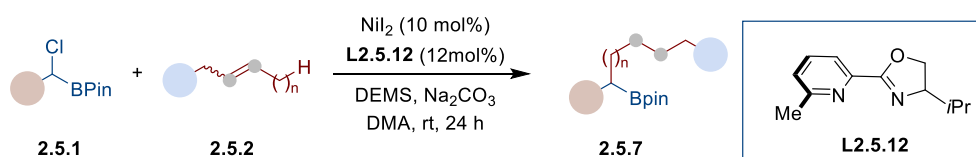
2-(1-cyclohexyl-5-phenylpentyl)-4,4,5,5-tetramethyl-1,3,2-dioxaborolane (2.5.3v):

Following the general procedure A, but using 2-(bromo(cyclohexyl)methyl)-4,4,5,5-tetramethyl-1,3,2-dioxaborolane (60.6 mg, 0.20 mmol) and $\text{NiBr}_2 \cdot \text{diglyme}$ (7.0 mg, 10 mol%), afforded **2.5.3v** (37.0 mg, 52% yield) as a light yellow oil after stirring the reaction at 40 °C for 24 h. In an independent experiment, 40.0 mg (56%) were obtained, giving an average of 54% yield. $^1\text{H NMR}$ (400 MHz, CDCl_3) δ 7.30 – 7.22 (dd, $J = 7.6, 6.0$ Hz, 2H), 7.20 – 7.11 (m, 3H), 2.60 (t, $J = 7.6$ Hz, 2H), 1.77 – 1.54 (m, 6H), 1.48 – 1.36 (m, 2H), 1.29 – 1.23 (m, 6H), 1.22 (s, 6H), 1.21 (s, 6H),

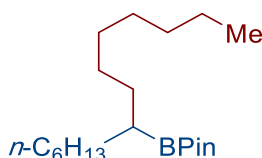
*Site-Selective Ni-Catalyzed Reductive
Coupling of α -Haloboranes with Unactivated Olefins*

1.04 – 0.82 (m, 4H) ppm. ^{13}C NMR (101 MHz, CDCl_3): δ 143.0, 128.6, 128.3, 125.6, 82.9, 39.9, 36.0, 33.0, 32.7, 31.9, 29.4, 28.8, 27.0, 26.9, 25.1, 25.0, 24.9 ppm. ^{11}B NMR (128 MHz, CDCl_3) δ 34.2 ppm. IR (neat, cm^{-1}): 2977, 2921, 2851, 1448, 1378, 1313, 1143, 970, 847, 697. GC-MS: ($\text{C}_{23}\text{H}_{37}\text{BO}_2$) $[\text{M}]^+$: found $t = 13.589$ min, m/z 356.3.

2.8.6 Ni-Catalyzed Reductive Coupling with Internal Olefins



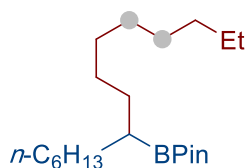
General procedure B: An oven-dried 8 mL screw-cap tube containing a stirring bar was charged with NiI_2 (6.2 mg, 10 mol%), **L2.5.12** (4.9 mg, 12 mol%) and Na_2CO_3 (21.2 mg, 0.10 mol). Subsequently, the tube was sealed with a Teflon-lined screw cap, then evacuated and back-filled with Ar (3 times). Then, the corresponding α -haloborane (0.30 mmol, 1.5 equiv), olefin (0.20 mmol, 1.0 equiv), DEMS (48 μL , 0.3 mmol, 1.50 equiv), DMA (0.6 mL) were added via syringe. Then, the tube was stirred at room temperature for 18 h. After the reaction was completed, the mixture was diluted with EtOAc and filtered through silica gel and concentrated. The corresponding product was purified by column chromatography on silica gel.



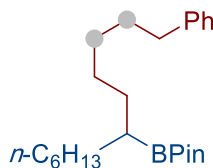
4,4,5,5-tetramethyl-2-(tetradecan-7-yl)-1,3,2-dioxaborolane (2.5.7a): Following the general procedure B, but using *trans*-2-heptene (28 μL , 0.20 mmol) afforded **2.5.7a** (43.0 mg, 66% yield) as a light-yellow oil. In an independent experiment, 42.0 mg (65% yield) were obtained, giving an average of 66% yield, 44:1 regioisomeric ratio. Following the general procedure B, but using *trans*-3-heptene (28 μL , 0.20 mmol), afforded **2.5.7a** (39.0 mg, 60% yield) as a colorless oil. In an independent experiment, 41.0 mg (63% yield) were obtained, giving an average of 62% yield, 28:1 regioisomeric ratio. ^1H NMR (400 MHz, CDCl_3): δ 1.49 – 1.24 (m, 22H), 1.23 (s, 12H), 0.94 (tt, $J = 9.3, 5.7$ Hz, 1H), 0.87 (t, $J = 6.8$ Hz, 6H) ppm. ^{13}C NMR (101 MHz, CDCl_3): δ 82.9, 32.1, 32.0, 31.7, 31.6, 30.0, 29.8, 29.5, 29.4 (2C), 24.9 (2C),

Chapter 2.

22.8, 22.7, 14.3, 14.2 ppm. ^{11}B NMR (128 MHz, CDCl_3) δ 34.2 ppm. IR (neat, cm^{-1}): 2977, 2957, 2922, 2853, 1465, 1386, 1379, 1371, 1313, 1144, 968, 864. HRMS calcd. for $(\text{C}_{20}\text{H}_{41}\text{BNaO}_2)$ $[\text{M}+\text{Na}]^+$: 347.3128 found 347.3078.

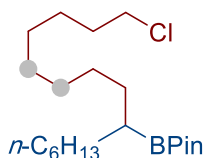


4,4,5,5-tetramethyl-2-(pentadecan-7-yl)-1,3,2-dioxaborolane (2.5.7b): Following the general procedure B, but using (*E*)-oct-4-ene (31.3 μL , 0.20 mmol), afforded **2.5.7b** (42.0 mg, 62% yield) as a light-yellow oil. In a separate experiment, 44.0 mg (65% yield) were obtained, giving an average of 64% yield, 24:1 regioisomeric ratio. ^1H NMR (500 MHz, CDCl_3): δ 1.43 – 1.35 (m, 2H), 1.34 – 1.25 (m, 22H), 1.24 (s, 12H), 0.94 (tt, $J = 9.2, 5.7$ Hz, 1H), 0.87 (t, $J = 8.0$ Hz, 3H), 0.86 (t, $J = 6.8$ Hz, 3H) ppm. ^{13}C NMR (126 MHz, CDCl_3): δ 82.9, 32.1, 32.0, 31.7 (2C), 30.1, 29.8, 29.7, 29.5, 29.4, 29.3, 24.9 (2C), 22.8, 22.7, 14.3, 14.2 ppm. ^{11}B NMR (128 MHz, CDCl_3) δ 34.0 ppm. IR (neat, cm^{-1}): 2977, 2957, 2922, 2854, 1465, 1378, 1371, 1313, 1144, 968, 864. GC-MS: $(\text{C}_{21}\text{H}_{43}\text{BO}_2)$ $[\text{M}]^+$: found $t = 10.980$ min, m/z 338.3.



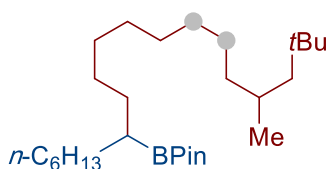
4,4,5,5-tetramethyl-2-(1-phenyldodecan-6-yl)-1,3,2-dioxaborolane (2.5.7c): Following the general procedure B, but using pent-3-en-1-ylbenzene (*E/Z* mixture) (29.2 mg, 0.20 mmol), afforded **2.5.7c** (45.0 mg, 60% yield) as a light yellow oil after stirring the reaction at 10 $^\circ\text{C}$ for 36 h. In an independent experiment, 48.0 mg (64% yield) were obtained, giving an average of 62% yield, 10:1 regioisomeric ratio. ^1H NMR (400 MHz, CDCl_3) δ 7.28 (dd, $J = 8.1, 6.8$ Hz, 2H), 7.21 – 7.10 (m, 3H), 2.61 (t, $J = 7.8$ Hz, 2H), 1.68 – 1.58 (m, 2H), 1.49 – 1.27 (m, 16H), 1.26 (s, 12H), 1.01 – 0.95 (m, 1H), 0.90 (t, $J = 6.8$ Hz, 3H) ppm. ^{13}C NMR (101 MHz, CDCl_3): δ 143.1, 128.5, 128.3, 125.6, 82.9, 36.1, 32.0, 31.6 (2C), 31.5, 29.7 (2C), 29.4, 29.3, 24.9 (2C), 22.8, 14.2 ppm. ^{11}B NMR (128 MHz, CDCl_3) δ 35.0 ppm. IR (neat, cm^{-1}): 2977, 2956, 2923, 2854, 1454, 1379, 1370, 1313, 1143, 967, 863, 698. HRMS calcd. for $(\text{C}_{24}\text{H}_{41}\text{BNaO}_2)$ $[\text{M}+\text{Na}]^+$: 395.3092 found 395.3085.

*Site-Selective Ni-Catalyzed Reductive
Coupling of α -Haloboranes with Unactivated Olefins*



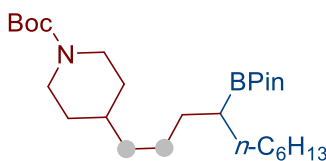
2-(15-chloropentadecan-7-yl)-4,4,5,5-tetramethyl-1,3,2-dioxaborolane (2.5.7d):

Following the general procedure B, but using (*Z*)-8-chlorooct-3-ene (34 μ l, 0.20 mmol), afforded **2.5.7d** (35.8 mg, 48% yield) as a light-yellow oil. In an independent experiment, 37.2 mg (50%) were obtained, giving an average of 49% yield 34:1 regioisomeric ratio. $^1\text{H NMR}$ (400 MHz, CDCl_3): δ 3.52 (t, $J = 6.8$ Hz, 2H), 1.81 – 1.70 (m, 2H), 1.45 – 1.35 (m, 4H), 1.33 – 1.20 (m, 30H), 0.96 – 0.91 (m, 1H), 0.91 – 0.82 (m, 3H) ppm. $^{13}\text{C NMR}$ (101 MHz, CDCl_3): δ 82.9, 45.3, 32.8, 32.0, 31.6, 31.5, 29.9, 29.8, 29.5, 29.4, 29.3, 29.0, 27.0, 24.9 (2C), 22.8, 14.2. $^{11}\text{B NMR}$ (128 MHz, CDCl_3) δ 34.4 ppm. **IR** (neat, cm^{-1}): 2979, 2925, 2854, 1465, 1381, 1313, 1143, 906, 728, 649. **HRMS** calcd. for $(\text{C}_{21}\text{H}_{42}\text{BClNaO}_2)$ $[\text{M}+\text{Na}]^+$: 395.2859 found 395.2851.



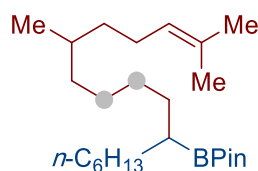
4,4,5,5-tetramethyl-2-((7*S*)-16,18,18-trimethylnonadecan-7-yl)-1,3,2-diox

aborolane (2.5.7e): Following the general procedure B, but using 2,2,4-trimethyldodec-6-ene (*E/Z* mixture) (42.0 mg, 0.20 mmol), afforded **2.5.7e** (48.0 mg, 55% yield) as a light yellow oil. In an independent experiment, 50.0 mg (57% yield) were obtained, giving an average of 56% yield as a 1:1 mixture of diastereoisomers, 20:1 regioisomeric ratio. $^1\text{H NMR}$ (400 MHz, CDCl_3): δ 1.48 – 1.16 (m, 32H), 1.25 (s, 6H), 1.24 (s, 6H), 0.98 – 0.92 (m, 1H), 0.91 – 0.82 (m, 12H) ppm. $^{13}\text{C NMR}$ (101 MHz, CDCl_3): δ 82.9, 51.5, 39.8, 32.1, 32.0, 31.7, 31.2, 30.2, 30.1, 30.0, 29.9, 29.8, 29.7, 29.6, 29.5, 29.4, 29.3, 29.2, 29.1, 27.4, 25.0 (2C), 22.8, 22.7, 14.3, 14.2 ppm. $^{11}\text{B NMR}$ (128 MHz, CDCl_3) δ 34.5 ppm. **IR** (neat, cm^{-1}): 2976, 2955, 2922, 2853, 1465, 1386, 1378, 1370, 1313, 1144, 968, 864, 688. **HRMS** calcd. for $(\text{C}_{28}\text{H}_{58}\text{BO}_2)$ $[\text{M}+\text{H}]^+$: 437.4524 found 437.4525.

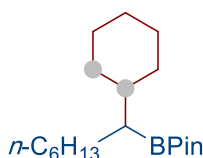


tert-butyl-4-(4-(4,4,5,5-tetramethyl-1,3,2-dioxaborolan-2-yl)decyl)piperidine-1-

carboxylate (2.5.7f): Following the general procedure B, but using tert-butyl 4-(prop-1-en-1-yl)piperidine-1-carboxylate (*E/Z* mixture) (48 μL , 0.20 mmol), afforded **2.5.7f** (65.9 mg, 73% yield) as a light yellow oil. In an independent experiment, 61.3 mg (68%) were obtained, giving an average of 70% yield, 44:1 regioisomeric ratio. $^1\text{H NMR}$ (400 MHz, CDCl_3): δ 4.03 (s, 2H), 2.64 (t, $J = 12.6$ Hz, 2H), 1.67 – 1.54 (m, 2H), 1.43 (s, 9H), 1.32 – 1.17 (m, 29H), 1.11 – 0.88 (m, 3H), 0.91 – 0.80 (m, 3H) ppm. $^{13}\text{C NMR}$ (101 MHz, CDCl_3): δ 155.0, 82.9, 79.2, 44.2, 36.9, 36.0, 32.3, 31.9, 31.7, 31.6, 29.7, 29.4, 28.6, 26.4, 24.9, 24.8, 22.7, 14.2 ppm. $^{11}\text{B NMR}$ (128 MHz, CDCl_3) δ 33.7 ppm. **IR** (neat, cm^{-1}): 2976, 2923, 2852, 1695, 1420, 1388, 1366, 1314, 1244, 1144, 967, 920, 864, 732. **HRMS** calcd. for $(\text{C}_{26}\text{H}_{50}\text{BNNaO}_4) [\text{M}+\text{Na}]^+$: 474.3731 found 474.3707.



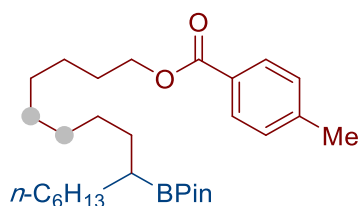
2-(12,16-dimethylheptadec-15-en-7-yl)-4,4,5,5-tetramethyl-1,3,2-dioxaborolane (2.5.7g): Following the general procedure B, but using 2,6-dimethyldeca-2,8-diene (*E/Z* mixture) (44 μL , 0.20 mmol), afforded **2.5.7g** (49.4 mg, 63% yield) as a light yellow oil. In an independent experiment, 50.3 mg (64%) were obtained, giving an average of 63% yield, as a 1:1 mixture of diastereoisomers, 25:1 regioisomeric ratio. $^1\text{H NMR}$ (400 MHz, CDCl_3): δ 5.15 – 5.04 (m, 1H), 2.04 – 1.86 (m, 2H), 1.67 (s, 3H), 1.59 (s, 3H), 1.43 – 1.19 (m, 33H), 0.96 – 0.92 (m, 1H), 0.89 – 0.80 (m, 6H) ppm. $^{13}\text{C NMR}$ (101 MHz, CDCl_3): δ 131.0, 125.3, 82.9, 37.3, 37.1, 32.5, 32.0, 31.7, 31.6, 29.8, 29.7, 29.4, 27.5, 27.4, 25.9, 25.7, 24.9, 22.8, 19.7, 17.8, 14.3 ppm. $^{11}\text{B NMR}$ (128 MHz, CDCl_3) δ 34.2 ppm. **IR** (neat, cm^{-1}): 2957, 2922, 2853, 1460, 1378, 1313, 1261, 1215, 1144, 968, 863. **HRMS** calcd. for $(\text{C}_{25}\text{H}_{50}\text{BO}_2) [\text{M}+\text{H}]^+$: 393.3898 found 393.3900.



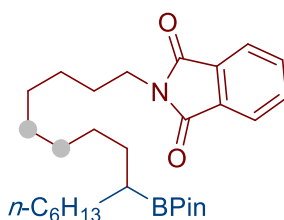
2-(1-cyclohexylheptyl)-4,4,5,5-tetramethyl-1,3,2-dioxaborolane (2.5.7h): Following the general procedure, but using cyclohexene (27.9 mg, 0.20 mmol), NiI_2 (6.2 mg, 10 mol%) and 4-isopropyl-2-(6-methylpyridin-2-yl)-4,5-dihydrooxazole (**L2.5.12**, 4.9 mg, 12 mol%), afforded **2.5.7h** (32.6 mg, 53% yield) as a light yellow

*Site-Selective Ni-Catalyzed Reductive
Coupling of α -Haloboranes with Unactivated Olefins*

oil. In an independent experiment, 30.8 mg (50% yield) were obtained, giving an average of 52% yield. $^1\text{H NMR}$ (300 MHz, CDCl_3): δ 1.78 – 1.59 (m, 5H), 1.43 – 1.10 (m, 26H), 1.06 – 0.91 (m, 2H), 0.89 – 0.77 (m, 4H). ppm. $^{13}\text{C NMR}$ (126 MHz, CDCl_3): δ 82.9, 39.9, 33.1, 32.7, 32.0, 29.8, 29.0, 27.0, 26.9, 25.1, 25.0, 22.8, 14.2 ppm. $^{11}\text{B NMR}$ (160 MHz, CDCl_3) δ 34.2 ppm. **IR** (neat, cm^{-1}): 2977, 2921, 2851, 1448, 1378, 1311, 1236, 1143, 969, 865, 846. **GC-MS**: ($\text{C}_{19}\text{H}_{37}\text{BO}_2$) $[\text{M}]^+$: found $t = 10.436$ min, m/z 308.2.

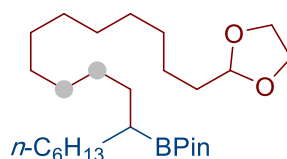


9-(4,4,5,5-tetramethyl-1,3,2-dioxaborolan-2-yl)pentadecyl 4-methylbenzoate (2.5.7i): Following general procedure B, but using 2-(1-chloroheptyl)-4,4,5,5-tetramethyl-1,3,2-dioxaborolane (104.0 mg, 0.40 mmol), (*Z*)-oct-5-en-1-yl 4-methylbenzoate (49.2 mg, 0.20 mmol) and $\text{NiBr}_2 \cdot \text{diglyme}$ (7.0 mg, 10 mol%), afforded **2.5.7i** (47.8 mg, 51% yield) as a light yellow oil after stirring the reaction at room temperature for 24 h. In an independent experiment, 51.6 mg (55% yield) were obtained, giving an average of 53% yield, 20:1 regioisomeric ratio. $^1\text{H NMR}$ (400 MHz, CDCl_3): δ 7.91 (d, $J = 8.2$ Hz, 2H), 7.21 (d, $J = 8.0$ Hz, 2H), 4.27 (t, $J = 6.7$ Hz, 2H), 2.38 (s, 3H), 1.84 – 1.66 (m, 2H), 1.47 – 1.23 (m, 22H), 1.22 (s, 12H), 0.99 – 0.90 (m, 1H), 0.86 (t, $J = 6.8$ Hz, 3H) ppm. $^{13}\text{C NMR}$ (101 MHz, CDCl_3): δ 166.8, 143.4, 129.7, 129.1, 127.9, 82.8, 65.0, 31.9, 31.6, 31.5, 29.9, 29.7, 29.6, 29.4 (3C), 28.9, 26.2, 24.9 (2C), 22.7, 21.7, 14.2 ppm. $^{11}\text{B NMR}$ (128 MHz, CDCl_3) δ 33.5 ppm. **IR** (neat, cm^{-1}): 2977, 2956, 2923, 2854, 1719, 1613, 1464, 1386, 1312, 1271, 1177, 1144, 1106, 1021, 968, 841, 753. **HRMS** calcd. for ($\text{C}_{29}\text{H}_{49}\text{BNaO}_4$) $[\text{M}+\text{Na}]^+$: 495.3652 found 495.3618.

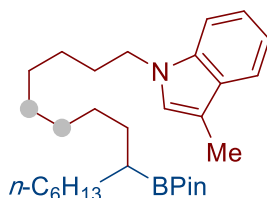


2-(9-(4,4,5,5-tetramethyl-1,3,2-dioxaborolan-2-yl)pentadecyl)isoindoline-1,3-dione (2.5.7j): Following the general procedure B, using 2-(oct-5-en-1-yl)isoindoline-1,3-dione (*E/Z* mixtures) (50 μL , 0.20 mmol), afforded

2.5.7j (58.0 mg, 60% yield) as a light yellow oil. In an independent experiment, 52.2 mg (54%) were obtained, giving an average of 57% yield 41:1 regioisomeric ratio. $^1\text{H NMR}$ (400 MHz, CDCl_3): δ 7.82 (dd, $J = 5.4, 3.1$ Hz, 2H), 7.69 (dd, $J = 5.4, 3.0$ Hz, 2H), 3.65 (t, $J = 7.3, 3.0$ Hz, 2H), 1.64 (t, $J = 6.9, 3.0$ Hz, 2H), 1.33 – 1.19 (m, 34H), 0.94 – 0.89 (m, 1H), 0.89 – 0.81 (m, 3H) ppm. $^{13}\text{C NMR}$ (101 MHz, CDCl_3): δ 168.6, 133.9, 132.3, 123.2, 82.9, 38.2, 32.0, 31.6, 31.5, 30.0, 29.7, 29.6, 29.4 (2C), 29.3, 28.8, 27.0, 24.9 (2C), 22.7, 14.2 ppm. $^{11}\text{B NMR}$ (128 MHz, CDCl_3) δ 34.7 ppm. **IR** (neat, cm^{-1}): 2976, 2923, 2853, 1774, 1712, 1466, 1437, 1393, 1369, 1313, 1264, 1143, 1057, 718. **HRMS** calcd. for $(\text{C}_{29}\text{H}_{46}\text{BNNaO}_4)$ $[\text{M}+\text{Na}]^+$: 506.3412 found 506.3420.



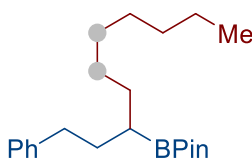
2-(18-(1,3-dioxolan-2-yl)octadecan-7-yl)-4,4,5,5-tetramethyl-1,3,2-dioxaborolane (2.5.7k): Following the general procedure B, but using 2-(1-chloroheptyl)-4,4,5,5-tetramethyl-1,3,2-dioxaborolane (104.0 mg, 0.4 mmol), 2-(undec-9-en-1-yl)-1,3-dioxolane (*E/Z* mixtures) (45.2 mg, 0.20 mmol) and $\text{NiBr}_2 \cdot \text{diglyme}$ (7.0 mg, 10 mol%) afforded **2.5.7k** (50.0 mg, 55% yield) as a light yellow oil after stirring the reaction at room temperature for 24 h. In an independent experiment, 49.0 mg (54% yield) were obtained, giving an average of 54% yield, 17:1 regioisomeric ratio. $^1\text{H NMR}$ (400 MHz, CDCl_3): δ 4.83 (t, $J = 4.8$ Hz, 1H), 3.98 – 3.92 (m, 2H), 3.86 – 3.81 (m, 2H), 1.68 – 1.60 (m, 2H), 1.45 – 1.23 (m, 30H), 1.23 (s, 12H), 0.98 – 0.90 (m, 1H), 0.86 (t, $J = 6.8$ Hz, 3H) ppm. $^{13}\text{C NMR}$ (101 MHz, CDCl_3): δ 104.9, 82.9, 65.0 (2C), 34.1, 32.0, 31.6 (2C), 30.1, 29.8, 29.7 (2C) (right), 29.6 (3C), 29.5, 29.4, 24.9 (2C), 24.2, 22.8, 14.2 ppm. $^{11}\text{B NMR}$ (128 MHz, CDCl_3) δ 34.8 ppm. **IR** (neat, cm^{-1}): 2976, 2922, 2853, 1464, 1409, 1387, 1371, 1313, 1263, 1215, 1143, 1037, 967, 863. **HRMS** calcd. for $(\text{C}_{27}\text{H}_{53}\text{BNaO}_4)$ $[\text{M}+\text{Na}]^+$: 475.3965 found 475.3923.



3-methyl-1-(9-(4,4,5,5-tetramethyl-1,3,2-dioxaborolan-2-yl)pentadecyl)-1H-indole (2.5.7l): Following the general procedure B, but using 3-methyl-1-(oct-5-en-1-yl)-1H-indole (*E/Z* mixture) (51 μL , 0.20 mmol), afforded **2.5.7l** (56.0 mg, 60% yield) as a light-yellow oil. In an independent experiment, 57.0

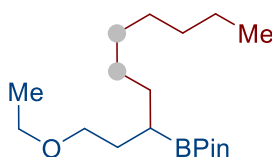
*Site-Selective Ni-Catalyzed Reductive
Coupling of α -Haloboranes with Unactivated Olefins*

mg (61%) were obtained, giving an average of 61% yield, 15:1 regioisomeric ratio. $^1\text{H NMR}$ (400 MHz, CDCl_3): δ 7.65 – 7.50 (m, 1H), 7.34 – 7.27 (m, 1H), 7.23 – 7.16 (m, 1H), 7.12 – 7.03 (m, 1H), 6.89 – 6.84 (m, 1H), 4.04 (t, $J = 7.2$ Hz, 2H), 2.34 (d, $J = 1.1$ Hz, 3H), 1.80 (t, $J = 7.2$ Hz, 2H), 1.46 – 1.16 (m, 34H), 0.96 – 0.94 (m, 1H), 0.94 – 0.84 (m, 3H) ppm. $^{13}\text{C NMR}$ (101 MHz, CDCl_3): δ 136.4, 128.8, 125.6, 121.3, 119.1, 118.5, 110.1, 109.3, 82.9, 46.2, 32.0, 31.6, 31.5, 30.5, 30.0, 29.9, 29.8, 29.6, 29.4, 29.3 (2C, right), 27.2, 24.9, 22.8, 14.3, 9.7 ppm. $^{11}\text{B NMR}$ (128 MHz, CDCl_3) δ 34.1 ppm. **IR** (neat, cm^{-1}): 2922, 2853, 1467, 1386, 1314, 1260, 1143, 735. **HRMS** calcd. for $(\text{C}_{30}\text{H}_{50}\text{BNNaO}_2)$ $[\text{M}+\text{Na}]^+$: 490.3832 found 490.3827.



4,4,5,5-tetramethyl-2-(1-phenyldecyl-3-yl)-1,3,2-dioxaborolane (2.5.7m):

Following the general procedure B, but using 2-(1-chloro-3-phenylpropyl)-4,4,5,5-tetramethyl-1,3,2-dioxaborolane (84 mg, 0.20 mmol), afforded **2.5.7m** (53.0 mg, 77% yield) as a light yellow oil. In an independent experiment, 55.0 mg (80% yield) were obtained, giving an average of 78% yield, 21:1 regioisomeric ratio. $^1\text{H NMR}$ (400 MHz, CDCl_3) δ 7.27 (dd, $J = 7.6, 6.8$ Hz, 2H), 7.23 – 7.11 (m, 3H), 2.74 – 2.44 (m, 2H), 1.87 – 1.57 (m, 2H), 1.52 – 1.34 (m, 2H), 1.32 – 1.23 (m, 10H), 1.26 (s, $J = 8.7$ Hz, 12H), 1.11 – 0.98 (m, 1H), 0.89 (t, $J = 6.8$ Hz, 3H) ppm. $^{13}\text{C NMR}$ (101 MHz, CDCl_3): δ 143.3, 128.5, 128.3, 125.7, 83.0, 35.8, 33.7, 32.0, 31.4, 30.0, 29.4, 29.3, 25.0 (left), 25.0 (right), 22.8, 14.3 ppm. $^{11}\text{B NMR}$ (128 MHz, CDCl_3) δ 34.6 ppm. **IR** (neat, cm^{-1}): 2977, 2956, 2923, 2854, 1455, 1379, 1371, 1314, 1143, 967, 851, 746, 698. **HRMS** calcd. for $(\text{C}_{22}\text{H}_{37}\text{BNaO}_2)$ $[\text{M}+\text{Na}]^+$: 367.2815 found 367.2797.

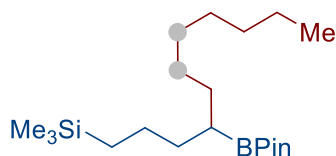


2-(1-ethoxydecyl-3-yl)-4,4,5,5-tetramethyl-1,3,2-dioxaborolane (2.5.7n):

Following the general procedure B, but using 2-(1-chloro-3-ethoxypropyl)-4,4,5,5-tetramethyl-1,3,2-dioxaborolane (74.4 mg, 0.20 mmol) afforded **2.5.7n** (37.0 mg, 59% yield) as a light yellow oil. In an independent experiment, 36.0 mg (58% yield) were obtained, giving an average of 58% yield, 24:1 regioisomeric ratio. $^1\text{H NMR}$ (500 MHz, CDCl_3) δ 3.45 (q, $J = 7.0$ Hz, 2H), 3.39 (t, $J = 7.0$ Hz, 2H), 1.75 – 1.53 (m, 2H), 1.46 – 1.24 (m, 12H), 1.23 (s, 12H), 1.17 (t, $J = 7.1$ Hz, 3H), 1.04 –

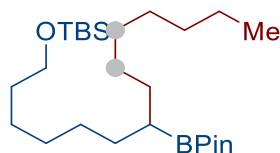
Chapter 2.

0.95 (m, 1H), 0.86 (t, $J = 6.8$ Hz, 3H) ppm. ^{13}C NMR (126 MHz, CDCl_3): δ 83.0, 70.5, 66.1, 32.0, 31.5 (left), 31.5 (right), 29.9, 29.4, 29.3, 24.9, 24.8, 22.8, 15.3, 14.2 ppm. ^{11}B NMR (128 MHz, CDCl_3) δ 35.0 ppm. IR (neat, cm^{-1}): 2976, 2924, 2854, 1460, 1378, 1313, 1144, 1110, 968, 856. HRMS calcd. for $(\text{C}_{18}\text{H}_{37}\text{BNaO}_3)$ $[\text{M}+\text{Na}]^+$: 335.2764 found 335.2701.



trimethyl(4-(4,4,5,5-tetramethyl-1,3,2-dioxaborolan-2-yl)undecyl)silane (2.5.7o):

Following the general procedure B, but using (4-chloro-4-(4,4,5,5-tetramethyl-1,3,2-dioxaborolan-2-yl)butyl)trimethylsilane (87.0 mg, 0.20 mmol), afforded **2.5.7o** (39.0 mg, 55% yield) as a light yellow oil. In an independent experiment, 41.0 mg (58% yield) were obtained, giving an average of 56% yield, 99:1 regioisomeric ratio. ^1H NMR (400 MHz, CDCl_3) δ 1.48 – 1.24 (m, 16H), 1.23 (s, 12H), 1.04 – 0.92 (m, 1H), 0.87 (t, $J = 6.8$ Hz, 3H), 0.55 – 0.38 (m, 2H), -0.05 (s, 9H) ppm. ^{13}C NMR (101 MHz, CDCl_3) δ 82.9, 35.8, 32.0, 31.7, 30.0, 29.5, 29.4, 25.0 (2C), 23.8, 22.8, 17.2, 14.3, -1.5 ppm. ^{11}B NMR (128 MHz, CDCl_3) δ 33.8 ppm. IR (neat, cm^{-1}): 2978, 2954, 2922, 2854, 1459, 1378, 1371, 1315, 1247, 1214, 1144, 969, 857, 834, 690. GC-MS: $(\text{C}_{20}\text{H}_{43}\text{SiBO}_2)$ $[\text{M}]^+$: found $t = 10.596$ min, m/z 354.2.

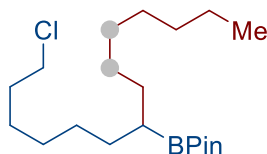


tert-butyl dimethyl((7-(4,4,5,5-tetramethyl-1,3,2-dioxaborolan-2-yl)tetradecyl)oxy)silane (2.5.7p):

Following the general procedure B, using *tert*-butyl((7-chloro-7-(4,4,5,5-tetramethyl-1,3,2-dioxaborolan-2-yl)heptyl)oxy)dimethylsilane (117.0 mg, 0.20 mmol), afforded **2.5.7p** (60.0 mg, 66% yield) as a light yellow oil. In an independent experiment, 55.0 mg (60% yield) were obtained, giving an average of 63% yield, 24:1 regioisomeric ratio. ^1H NMR (500 MHz, CDCl_3) δ 3.57 (t, $J = 6.6$ Hz, 2H), 1.53 – 1.44 (m, 2H), 1.42 – 1.23 (m, 20H), 1.22 (s, 12H), 0.97 – 0.91 (m, 1H), 0.88 (s, 9H), 0.85 (t, $J = 7.1$ Hz, 3H), 0.03 (s, 6H) ppm. ^{13}C NMR (126 MHz, CDCl_3) δ 82.9, 63.5, 33.0, 32.0, 31.6, 31.5, 30.0, 29.9, 29.5, 29.4, 29.3, 26.1, 26.0, 25.9, 24.9, 22.8, 18.5, 14.3, -5.1 ppm. ^{11}B NMR (128 MHz, CDCl_3) δ 35.3 ppm. IR (neat, cm^{-1}): 2977, 2927, 2856, 1463, 1378, 1371, 1315, 1253, 1145,

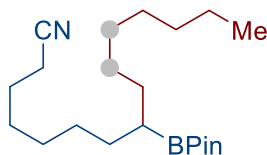
*Site-Selective Ni-Catalyzed Reductive
Coupling of α -Haloboranes with Unactivated Olefins*

1109, 968, 834, 774. **HRMS** calcd. for (C₂₆H₅₅SiBNaO₃) [M+Na]⁺: 477.3942 found 477.3900.



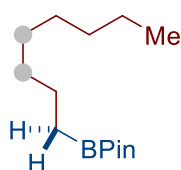
2-(1-chlorotetradecan-7-yl)-4,4,5,5-tetramethyl-1,3,2-dioxaborolane (2.5.7q):

Following the general procedure B, but using 2-(1,7-dichloroheptyl)-4,4,5,5-tetramethyl-1,3,2-dioxaborolane (88.2 mg, 0.20 mmol), afforded **2.5.7q** (53.0 mg, 74% yield) as a light yellow oil. In an independent experiment, 50.0 mg (70% yield) were obtained, giving an average of 72% yield, 30:1 regioisomeric ratio. **¹H NMR** (400 MHz, CDCl₃) δ 3.49 (t, J = 6.8 Hz, 2H), 1.86 – 1.60 (m, 2H), 1.44 – 1.34 (m, 4H), 1.34 – 1.23 (m, 16H), 1.22 (s, 12H), 0.97 – 0.90 (m, 1H), 0.85 (t, J = 6.8 Hz, 3H) ppm. **¹³C NMR** (101MHz, CDCl₃) δ 82.9, 45.2, 32.8, 32.0, 31.6, 31.4, 30.0, 29.4 (2C), 29.2, 29.1, 26.9, 24.9 (2C), 22.8, 14.2 ppm. **¹¹B NMR** (128 MHz, CDCl₃) δ 34.6 ppm. **IR** (neat, cm⁻¹): 2977, 2956, 2923, 2854, 1463, 1386, 1371, 1313, 1143, 967, 860, 726. **HRMS** calcd. for (C₂₀H₄₀BClNaO₂) [M+Na]⁺: 381.2738 found 381.2726.



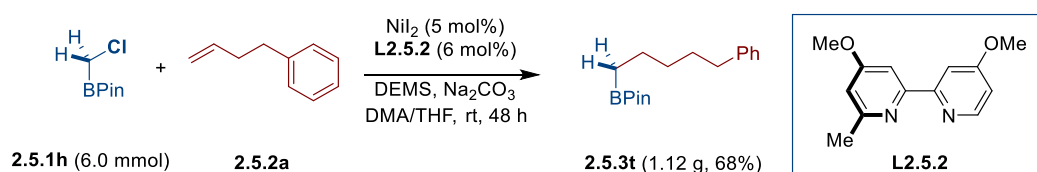
8-(4,4,5,5-tetramethyl-1,3,2-dioxaborolan-2-yl)pentadecanenitrile (2.5.7r):

Following the general procedure B, but using 8-chloro-8-(4,4,5,5-tetramethyl-1,3,2-dioxaborolan-2-yl)octanenitrile (85.5 mg, 0.20 mmol), afforded **2.5.7r** (54.0 mg, 77% yield) as a light yellow oil. In an independent experiment, 50.0 mg (71% yield) were obtained, giving an average of 74% yield, 21:1 regioisomeric ratio. **¹H NMR** (400 MHz, CDCl₃) δ 2.30 (t, J = 7.2 Hz, 2H), 1.70 – 1.57 (m, 2H), 1.46 – 1.34 (m, 4H), 1.33 – 1.24 (m, 16H), 1.22 (s, 12H), 0.97 – 0.88 (m, 1H), 0.85 (m, J = 6.8 Hz, 3H) ppm. **¹³C NMR** (101MHz, CDCl₃): δ 119.9, 82.9, 31.9, 31.5, 31.4, 30.0, 29.4 (2C), 29.1, 29.0, 28.7, 25.5, 24.9 (2C), 22.8, 17.2, 14.2 ppm. **¹¹B NMR** (128 MHz, CDCl₃) δ 35.1 ppm. **IR** (neat, cm⁻¹): 2977, 2923, 2854, 1463, 1386, 1380, 1315, 1143, 967, 860. **HRMS** calcd. for (C₂₁H₄₀BNNaO₂) [M+Na]⁺: 372.3081 found 372.3026.

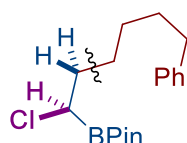


4,4,5,5-tetramethyl-2-octyl-1,3,2-dioxaborolane (2.5.7s): Following the general procedure B, but using 2-(chloromethyl)-4,4,5,5-tetramethyl-1,3,2-dioxaborolane (52.8 mg, 0.20 mmol), afforded **2.5.7s** (29.8 mg, 62% yield) as a light-yellow oil. In an independent experiment, 29.8 mg (62% yield) were obtained, giving an average of 62% yield, 3.5:1 regioisomeric ratio. $^1\text{H NMR}$ (400 MHz, CDCl_3) δ 1.38 (m, 2H), 1.32 – 1.24 (m, 10H), 1.24 (s, 12H), 0.87 (t, $J = 7.2$ Hz, 3H), 0.76 (t, $J = 7.7$ Hz, 2H) ppm. $^{13}\text{C NMR}$ (101 MHz, CDCl_3): δ 83.0, 82.9, 39.8, 32.6, 32.3, 32.0, 29.7, 29.5, 29.4, 27.1, 25.0 (left), 25.0 (right, 2C), 24.9 (2C), 24.2, 22.8, 22.6, 14.3, 14.2 ppm. $^{11}\text{B NMR}$ (128 MHz, CDCl_3) δ 34.0 ppm. **IR** (neat, cm^{-1}): 2978, 2957, 2924, 2856, 1466, 1406, 1370, 1315, 1144, 968, 847. Spectroscopic data for **2.5.7s** match those previously reported in the literature.¹⁹

2.8.7 Gram Scale Reaction and Iterative C-C Bond Formations



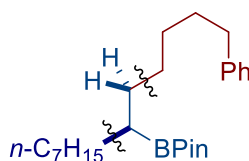
An oven-dried 50 mL schlenk tube containing a stirring bar was charged with NiI_2 (186 mg, 10 mol%), **L2.5.2** (168 mg, 12 mol%) and Na_2CO_3 (477 mg, 4.50 mmol). Subsequently, the tube was sealed with a Teflon screw cap, then evacuated and back-filled with argon (3 times). Afterwards, 2-(chloromethyl)-4,4,5,5-tetramethyl-1,3,2-dioxaborolane (**2.5.1h**, 1.06 g, 6.0 mmol, 1.0 equiv), **2.5.2a** (1.8 mL, 12.0 mmol, 2.0 equiv), DEMS (1.44 mL, 9.0 mmol, 1.5 equiv), DMA and THF (3:1, 12 mL) were added via syringe. Then, the tube was stirred at room temperature (around 25 °C) for 48 h. After the reaction was completed, the mixture was diluted with EtOAc, filtered through silica gel and then concentrated under vacuum. The residue was purified by column chromatography on silica gel (Hexane/EtOAc = 50:1), obtaining **2.5.3t** as colorless oil 1.12 g (68% yield).



2-(1-chloro-6-phenylhexyl)-4,4,5,5-tetramethyl-1,3,2-dioxaborolane (2.5.8): To an oven dried round flask equipped with a stirring bar was added CH_2Cl_2 (4.5 mmol,

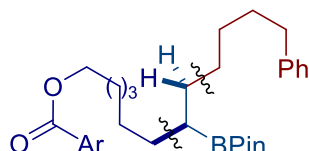
*Site-Selective Ni-Catalyzed Reductive
Coupling of α -Haloboranes with Unactivated Olefins*

0.29 mL) and THF (6 mL) by syringe, and the solution was cooled to -100°C . Then *n*-butyllithium (2.5 M solution in Hexane, 3.3 mmol, 1.10 equiv) was added dropwise under -100°C . After stirring for 45 min, a solution of 4,4,5,5-tetramethyl-2-(5-phenylpentyl)-1,3,2-dioxaborolane (0.82 g, 3.0 mmol, 1.0 equiv) in diethyl ether was directly added via syringe. Then, the reaction mixture was allowed to slowly warm to room temperature overnight. After the reaction was completed, 10 mL of DCM was added to precipitate the LiCl (optional), filtered, and concentrated under reduced pressure. The resulting crude product was purified by silica gel flash chromatography (Hexane/EtOAc = 30:1 to 10:1) obtained **2.5.8** as colorless oil 724 mg (75%). $^1\text{H NMR}$ (400 MHz, CDCl_3) δ 7.28 (dd, $J = 7.8, 7.6$ Hz, 2H), 7.22 – 7.10 (m, 3H), 3.41 (t, $J = 7.4$ Hz, 1H), 2.61 (t, $J = 7.6$ Hz, 2H), 1.93 – 1.76 (m, 2H), 1.69 – 1.60 (m, 2H), 1.48 – 1.32 (m, 4H), 1.29 (s, 12H) ppm. $^{13}\text{C NMR}$ (101 MHz, CDCl_3) δ 142.8, 128.5, 128.4, 125.8, 84.5, 35.9, 34.1, 31.4, 28.9, 27.3, 24.8, 24.7 ppm. $^{11}\text{B NMR}$ (128 MHz, CDCl_3) δ 31.7 ppm. **IR** (neat, cm^{-1}): 2979, 2931, 2857, 1726, 1454, 1382, 1373, 1342, 1141, 967, 848, 746, 699. **HRMS** calcd. for $(\text{C}_{18}\text{H}_{28}\text{ClBNaO}_2)$ $[\text{M}+\text{Na}]^+$: 345.1799 found 345.1765.

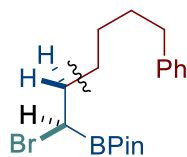


4,4,5,5-tetramethyl-2-(1-phenyltridecan-6-yl)-1,3,2-dioxaborolane (2.5.9): An oven-dried 8 mL screw-cap vial containing a stirring bar was charged with NiI_2 (9.1 mg, 10 mol%), **L2.5.12** (8.4 mg, 12 mol%) and Na_2CO_3 (31.8 mg, 0.3 mmol). Subsequently, the tube was sealed with a Teflon-lined screw cap, then evacuated and back-filled with Ar (3 times). Then, 2-(1-chloro-6-phenylhexyl)-4,4,5,5-tetramethyl-1,3,2-dioxaborolane (96.6 mg, 0.45 mmol, 1.5 equiv), the mixture of 1-heptene, *trans*-2-heptene and *trans*-3-heptene (42 μL , 1:1:1 ratio, 0.30 mmol, 1.0 equiv), DEMS (72 μL , 0.45 mmol, 1.50 equiv) and DMA (0.90 mL) were added via syringe. Then, the tube was stirred at room temperature for 18 h. After the reaction was completed, the mixture was diluted with EtOAc, filtered through silica gel and concentrated under vacuum. The corresponding product was purified by column chromatography on silica gel (Hexane/EtOAc = 100:1), obtained **2.5.9** as light-yellow oil 76 mg (66%), 44:1 regioisomeric ratio. $^1\text{H NMR}$ (400 MHz, CDCl_3) δ 7.31 – 7.24 (dd, $J = 8.2, 7.2$ Hz, 2H), 7.20 – 7.08 (m, 3H), 2.60 (t, $J = 7.8$ Hz, 2H), 1.71 – 1.54 (m, 2H), 1.48 – 1.27 (m, 18H), 1.25 (s, 12H), 1.02 – 0.92 (m, 1H), 0.89 (t, $J = 6.8$ Hz, 3H)

ppm. ^{13}C NMR (101 MHz, CDCl_3) δ 143.1, 128.5, 128.3, 125.7, 82.9, 36.1, 32.0, 31.6 (left), 31.6 (right), 31.5, 30.0, 29.8, 29.4 (left), 29.4 (right), 29.3, 24.9 (2C), 22.8, 14.3 ppm. ^{11}B NMR (128 MHz, CDCl_3) δ 34.8 ppm. IR (neat, cm^{-1}): 2977, 2923, 2853, 1455, 1386, 1370, 1313, 1143, 967, 856, 745, 697. HRMS calcd. for $(\text{C}_{25}\text{H}_{43}\text{BNaO}_2)$ $[\text{M}+\text{Na}]^+$: 409.3285 found 409.3242.



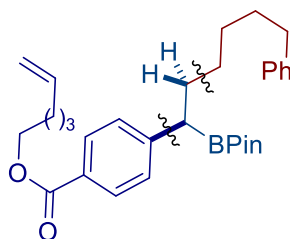
12-phenyl-7-(4,4,5,5-tetramethyl-1,3,2-dioxaborolan-2-yl)dodecyl 4-fluorobenzoate (2.5.10): An oven-dried 8 mL screw-cap vial containing a stirring bar was charged with NiI_2 (6.2 mg, 10 mol%), **L2.5.2** (5.6 mg, 12 mol%) and Na_2CO_3 (15.9 mg, 0.075 mol). Subsequently, the tube was sealed with a Teflon-lined screw cap and then evacuated and backfilled with Ar (3 times). Then, the 2-(1-chloro-6-phenylhexyl)-4,4,5,5-tetramethyl-1,3,2-dioxaborolane (64.4 mg, 0.20 mmol, 1.0 equiv), olefin (75.5 mg, 0.34 mmol, 1.70 equiv), DEMS (48 μL , 0.30 mmol, 1.50 equiv), DMA and THF (3:1, 0.40 mL) were added via syringe. Then, the tube was stirred at room temperature for 15 h. After the reaction was completed, the mixture was diluted with EtOAc, filtered through silica gel and then concentrated under vacuum. The corresponding product was purified by column chromatography on silica gel (Hexane/EtOAc = 40:1 to 20:1), obtaining **2.5.10** as light yellow oil 59 mg (58%). ^1H NMR (400 MHz, CDCl_3) δ 8.06 (dd, $J = 8.9, 5.5$ Hz, 2H), 7.31 – 7.22 (dd, $J = 8.0, 7.6$ Hz, 2H), 7.17 – 7.14 (m, 3H), 7.10 (dd, $J = 8.7, 8.4$ Hz, 2H), 4.30 (t, $J = 6.7$ Hz, 2H), 2.60 (t, $J = 7.8$ Hz, 2H), 1.82 – 1.70 (m, 2H), 1.66 – 1.57 (m, 2H), 1.49 – 1.27 (m, 14H), 1.24 (s, 12H), 1.02 – 0.93 (m, 1H) ppm. ^{13}C NMR (101 MHz, CDCl_3) δ 165.8, 165.8 (d, $J = 254.5$ Hz), 143.0, 132.2 (d, $J = 9.2$ Hz), 128.4 (d, $J = 19.2$ Hz), 126.9 (d, $J = 3.0$ Hz), 125.6, 115.6, 115.4, 82.9, 65.4, 36.0, 31.6, 31.5, 31.4, 29.7, 29.6, 29.2 (2C), 28.8, 26.1 24.9 (2C) ppm. ^{11}B NMR (128 MHz, CDCl_3) δ 35.5 ppm. ^{19}F NMR (376 MHz, CDCl_3) δ -106.16. IR (neat, cm^{-1}): 2977, 2926, 2854, 1720, 1603, 1508, 1455, 1386, 1312, 1269, 1238, 1143, 1111, 1090, 967, 854, 768, 698. HRMS calcd. for $(\text{C}_{31}\text{H}_{44}\text{FBNaO}_4)$ $[\text{M}+\text{Na}]^+$: 533.3245 found 533.3228.



*Site-Selective Ni-Catalyzed Reductive
Coupling of α -Haloboranes with Unactivated Olefins*

2-(1-bromo-6-phenylhexyl)-4,4,5,5-tetramethyl-1,3,2-dioxaborolane (2.5.11):

2-(1-chloro-6-phenylhexyl)-4,4,5,5-tetramethyl-1,3,2-dioxaborolane (322 mg, 1.0 mmol) was dissolved in 5 mL of acetone, and then added sodium bromide (5 equiv). The reaction mixture was stirred at 50 °C. Then, the mixture was extracted with EtOAc (3 x 10 mL), dried over MgSO₄, filtered and concentrated under reduced pressure. The resulting crude product was purified by column chromatography (Hexane/EtOAc = 30:1 to 10:1), obtained **2.5.11** as colourless oil 290 mg (79%). ¹H NMR (400 MHz, CDCl₃) δ 7.28 (t, *J* = 7.6 Hz, 2H), 7.20 – 7.16 (m, 3H), 3.32 (t, *J* = 7.8 Hz, 1H), 2.61 (t, *J* = 7.8 Hz, 2H), 1.93 – 1.87 (m, 2H), 1.68 – 1.60 (m, 2H), 1.57 – 1.35 (m, 4H), 1.29 (s, 12H) ppm. ¹³C NMR (101 MHz, CDCl₃) δ 142.7, 128.5, 128.4, 125.7, 84.3, 35.9, 34.1, 31.3, 28.7, 28.6, 24.6, 24.5 ppm. ¹¹B NMR (128 MHz, CDCl₃) δ 31.6 ppm. IR (neat, cm⁻¹): 2978, 2929, 2856, 1454, 1380, 1372, 1340, 1142, 967, 848, 745, 697. HRMS calcd. for (C₁₈H₂₈BrBNaO₂) [M+Na]⁺: 389.1294 found 389.1256.



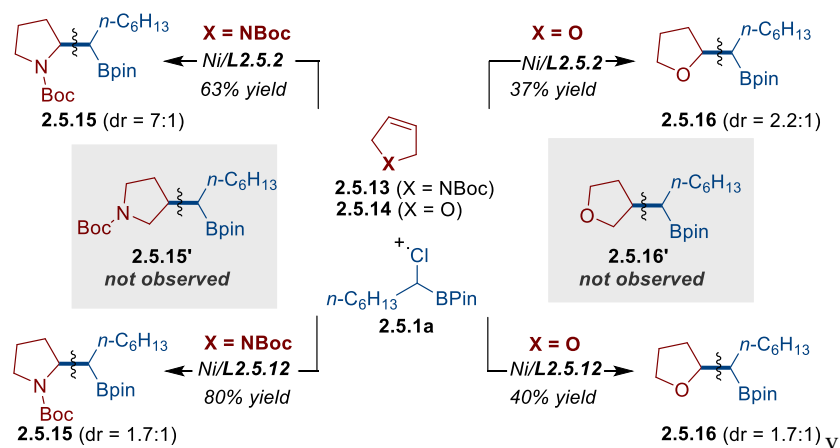
hex-5-en-1-yl-4-(6-phenyl-1-(4,4,5,5-tetramethyl-1,3,2-dioxaborolan-2-yl)hexyl)

benzoate (2.5.12): An oven-dried screw-cap vial containing a stirring bar was charged with Zn dust (0.4 mmol, 26.0 mg), and 4,4'-dimethoxy-2,2'-bipyridine (**L2.5.1**, 4.4 mg, 10 mol%). Subsequently the vial was introduced into a nitrogen-filled glove box and charged with the Ni(COD)₂ (5.60 mg, 10 mol%), THF (1 mL) and DMPU (50 μ L). The tube was sealed with a Teflon-lined screw cap and taken out from the glovebox. Then the 2-(1-bromo-6-phenylhexyl)-4,4,5,5-tetramethyl-1,3,2-dioxaborolane (**2.5.11**, 67.2 mg, 0.20 mmol, 1.0 equiv), and hex-5-en-1-yl 4-bromobenzoate (62 mg, 0.22 mmol, 1.10 equiv) were added via syringe. Then, the tube was stirred at 30 °C for 12 hours. After the reaction was completed, the mixture was diluted with EtOAc, filtered through silica gel and concentrated under vacuum. The product was purified by column chromatography on silica gel (Hexane/EtOAc = 40:1 to 20:1), obtaining **2.5.12** as light yellow oil 65 mg (66%). **Note:** the product is rather unstable, and therefore should be worked up and isolated as soon as possible, preferably storing it in the freezer at temperatures below

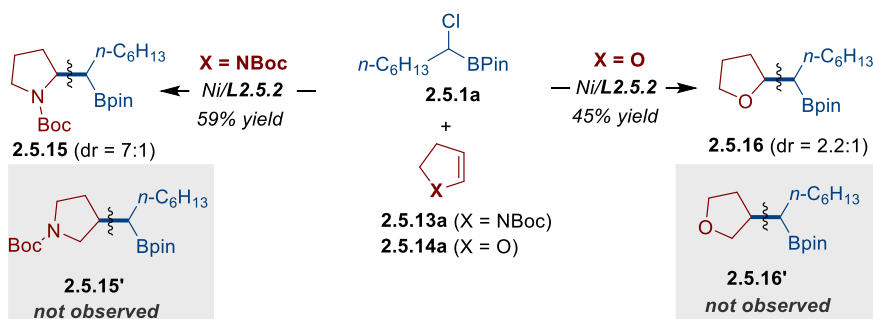
0 °C. $^1\text{H NMR}$ (400 MHz, CDCl_3) δ 7.93 (d, $J = 8.3$ Hz, 2H), 7.28 – 7.24 (m, 4H), 7.19 – 7.13 (m, 3H), 5.88 – 5.77 (m, 1H), 5.06 – 4.97 (m, 2H), 4.30 (t, $J = 6.6$ Hz, 2H), 2.56 (t, $J = 7.6$ Hz, 2H), 2.37 (t, $J = 7.9$ Hz, 1H), 2.16 – 2.11 (m, 2H), 1.90 – 1.74 (m, 3H), 1.71 – 1.52 (m, 5H), 1.37 – 1.25 (m, 4H), 1.19 (s, 6H), 1.18 (s, 6H) ppm. $^{13}\text{C NMR}$ (101 MHz, CDCl_3) δ 167.0, 149.4, 142.9, 138.5, 129.7, 128.5, 128.4, 128.3, 127.5, 125.7, 115.0, 83.6, 64.7, 36.0, 33.5, 32.2, 31.4, 29.3, 29.2, 28.4, 25.5, 24.7, 24.6 ppm. $^{11}\text{B NMR}$ (128 MHz, CDCl_3) δ 34.3 ppm. **IR** (neat, cm^{-1}): 2977, 2929, 2856, 1715, 1608, 1454, 1357, 1324, 1269, 1178, 1141, 1105, 1020, 967, 910, 857, 698. **HRMS** calcd. for $(\text{C}_{31}\text{H}_{43}\text{BNaO}_4) [\text{M}+\text{Na}]^+$: 513.3183 found 513.3137.

2.8.8 Mechanistic Experiments

2.8.8.1 Studying the Regioselectivity of 2.5.13 and 2.5.14.



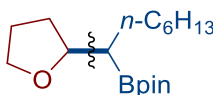
2.8.8.2 Studying the Regioselectivity of 2.5.13a and 2.5.14a.



*Site-Selective Ni-Catalyzed Reductive
Coupling of α -Haloboranes with Unactivated Olefins*



tert-butyl-2-(1-(4,4,5,5-tetramethyl-1,3,2-dioxaborolan-2-yl)heptyl)pyrrolidine-1-carboxylate (2.5.15). Following the general procedure A, but using *tert*-butyl 2,5-dihydro-1H-pyrrole-1-carboxylate (**2.5.13**, 57.5 mg), NiI₂ (3.1 mg, 5 mol%) and **L2.5.2** (2.8 mg, 6 mol%) afforded light yellow oil **2.5.15** (50.0 mg, 63% yield) as a 7:1 mixture of diastereoisomers. Following the general procedure B, using *tert*-butyl 2,5-dihydro-1H-pyrrole-1-carboxylate (**2.5.13**, 33.8 mg), NiI₂ (6.2 mg, 10 mol%) and **L2.5.12** (4.9 mg, 12 mol%) afforded light yellow oil **2.5.15** (63.2 mg, 80% yield) as a 1.7:1 mixture of diastereoisomers. Following the general procedure A, using *tert*-butyl 2,3-dihydro-1H-pyrrole-1-carboxylate (**2.5.13a**, 57.5 mg), NiI₂ (3.1 mg, 5 mol%) and **L2.5.2** (2.8 mg, 6 mol%) afforded light yellow oil **2.5.15** (46.8 mg, 63% yield) as a 7:1 mixture of diastereoisomers. ¹H NMR (400 MHz, CDCl₃): δ 3.95 – 3.77 (m, 1H), 3.60 – 3.37 (m, 1H), 3.22 – 3.10 (m, 1H), 1.93 – 1.57 (m, 5H), 1.47 – 1.40 (m, 9H), 1.34 – 1.14 (m, 22H), 0.84 (t, $J = 6.6$ Hz, 3H) ppm. ¹³C NMR (101 MHz, CDCl₃): δ . 155.1, 154.9, 83.2, 82.8, 79.0, 78.5, 58.9, 58.1, 47.4, 46.9, 46.3, 31.9, 31.8, 30.6, 30.0, 29.7, 29.6, 28.9, 28.6, 28.5, 28.5, 25.1, 25.0, 24.8, 24.1, 23.5, 22.7, 18.4, 18.3, 18.2 (left), 18.2 (right), 14.1 ppm. ¹¹B NMR (128 MHz, CDCl₃) δ 34.1 ppm. IR (neat, cm⁻¹): 2975, 2926, 2872, 2858, 1690, 1456, 1389, 1366, 1318, 1255, 1165, 1142, 1108, 863, 732. HRMS calcd. for (C₂₂H₄₂BNNaO₄) [M+Na]⁺: 418.3099 found 418.3101.

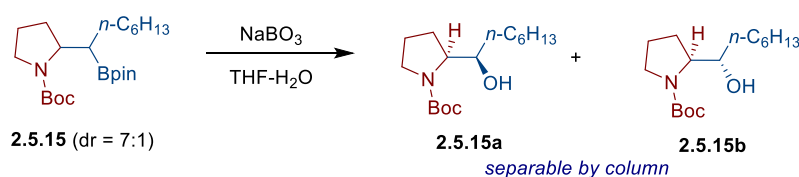


4,4,5,5-tetramethyl-2-(1-(tetrahydrofuran-2-yl)heptyl)-1,3,2-dioxaborolane (2.5.16): Following the general procedure A, but using 2,5-dihydrofuran (**2.5.14**, 23.8 mg), NiBr₂·diglyme (7.0 mg, 10 mol%) and **L2.5.2** (5.6 mg, 12 mol%), afforded light yellow oil **2.5.16** (21.9 mg, 37% yield) as a 2.2:1 mixture of diastereoisomers. Following the general procedure B, but using 2,5-dihydrofuran (**2.5.14**, 14.0 mg), NiI₂ (6.2 mg, 10 mol%) and **L3.5.12** (4.9 mg, 12 mol%) afforded light yellow oil **2.5.16** (23.7 mg, 40% yield) as a 1.7:1 mixture of diastereoisomers. Following the general procedure A, but using 2,3-dihydrofuran (**2.5.14a**, 23.8 mg), NiBr₂·diglyme (7.0 mg, 10 mol%) and **L2.5.2** (5.6 mg, 12 mol%), afforded light yellow oil **2.5.16** (26.6 mg, 45% yield) as a 2.2:1 mixture of diastereoisomers. ¹H NMR (400 MHz, CDCl₃): δ

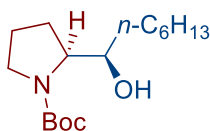
Chapter 2.

3.87 – 3.76 (m, 2H), 3.73 – 3.60 (m, 1H), 1.99 – 1.75 (m, 3H), 1.67 – 1.37 (m, 3H), 1.31 – 1.19 (m, 21H), 0.86 (t, $J = 6.9$ Hz, 3H) ppm. ^{13}C NMR (101 MHz, CDCl_3): 83.1, 83.0, 81.7, 80.9, 67.7, 67.4, 31.9, 31.8, 31.2, 31.1, 29.8, 29.7, 29.6, 29.5, 29.4, 29.2, 28.5, 26.0, 25.8, 25.1, 25.0, 24.9, 24.8, 24.7, 22.7, 14.2 ppm. ^{11}B NMR (128 MHz, CDCl_3) δ 33.6 ppm. IR (neat, cm^{-1}): 2975, 2959, 2925, 2856, 1460, 1405, 1378, 1371, 1316, 1144, 1058, 966, 867, 846. HRMS calcd. for $(\text{C}_{17}\text{H}_{33}\text{BNaO}_3)$ $[\text{M}+\text{Na}]^+$: 319.2415 found 319.2414.

2.8.8.3 Determining the Regioselectivity



The C2 regioselectivity was confirmed comparing the ^1H NMR of the corresponding purified diastereomeric alcohols with the ^1H NMR of two structurally related diastereoisomers previously reported in the literature, namely *tert*-butyl (S)-2-((R)-1-hydroxyheptyl)pyrrolidine-1-carboxylate and *tert*-butyl (S)-2-((S)-1-hydroxyheptyl)pyrrolidine-1-carboxylate.²⁰ The ^1H NMR signal integration and multiplicity of these products also confirms the C2 selectivity.

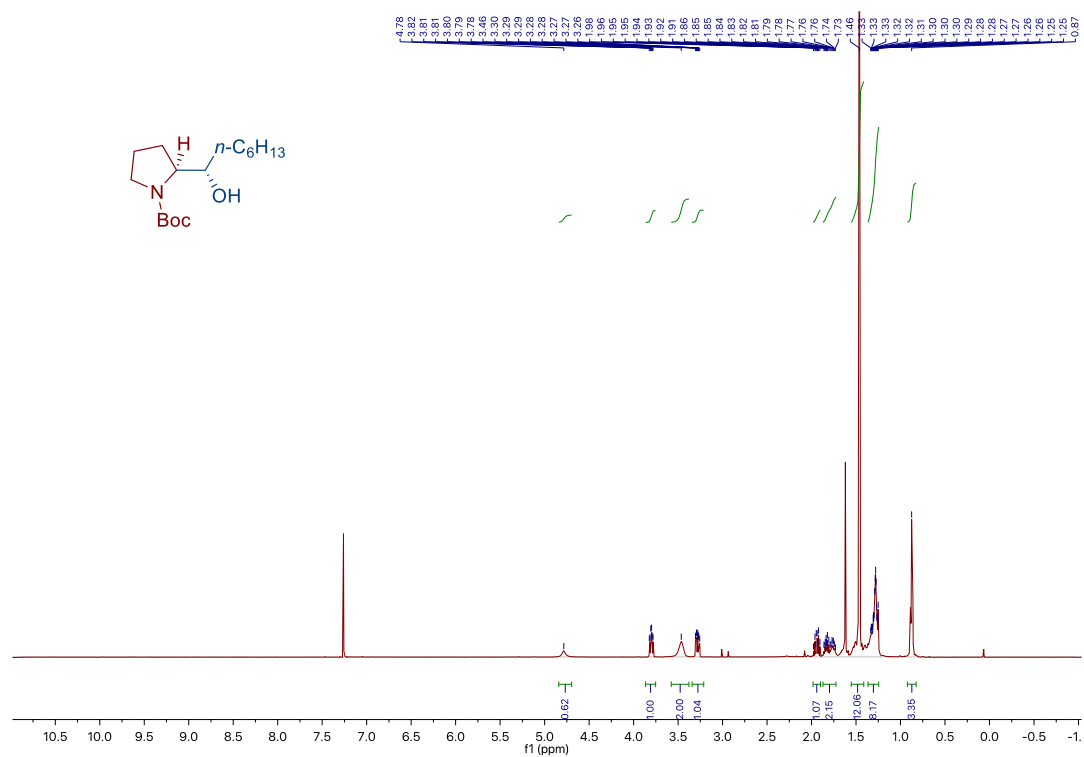
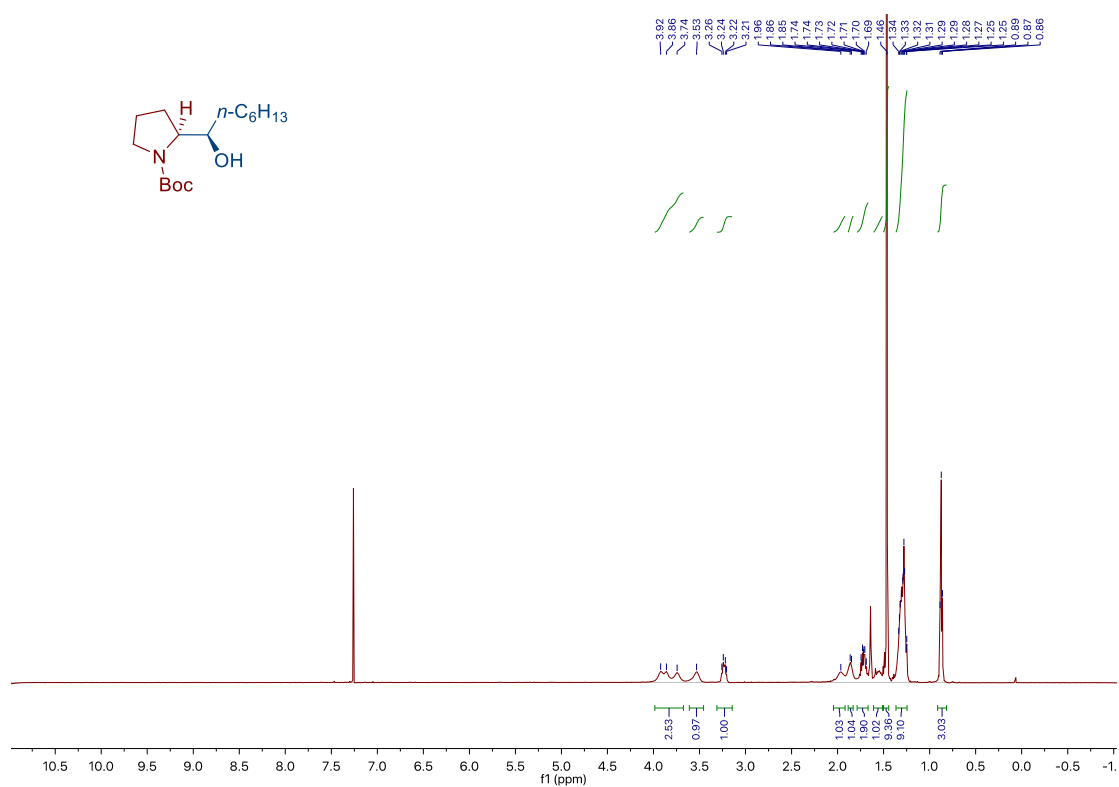


tert-butyl (S)-2-((R)-1-hydroxyheptyl)pyrrolidine-1-carboxylate (2.5.15a). ^1H NMR (500 MHz, CDCl_3) δ 3.96 – 3.67 (m, 2H), 3.53 (s, 1H), 3.32 – 3.16 (m, 1H), 1.96 (s, 1H), 1.86 (s, 1H), 1.78 – 1.67 (m, 2H), 1.59 – 1.52 (m, 1H), 1.46 (s, 9H), 1.35 – 1.23 (m, 9H), 0.87 (t, $J = 6.8$ Hz, 3H) ppm.



tert-butyl (S)-2-((S)-1-hydroxyheptyl)pyrrolidine-1-carboxylate (2.5.15b). ^1H NMR (500 MHz, CDCl_3) δ 4.78 (s, 1H), 3.80 (td, $J = 8.3, 4.1$ Hz, 1H), 3.46 (s, 2H), 3.28 (ddd, $J = 10.9, 7.3, 5.5$ Hz, 1H), 2.00 – 1.89 (m, 1H), 1.88 – 1.72 (m, 2H), 1.46 (s, 12H), 1.36 – 1.23 (m, 8H), 0.87 (t, $J = 6.8$ Hz, 3H) ppm.

*Site-Selective Ni-Catalyzed Reductive
Coupling of α -Haloboranes with Unactivated Olefins*



2.8.8.4 Control Experiments to Explore the Isomerization of 2.5.13 in the absence of 2.5.1a

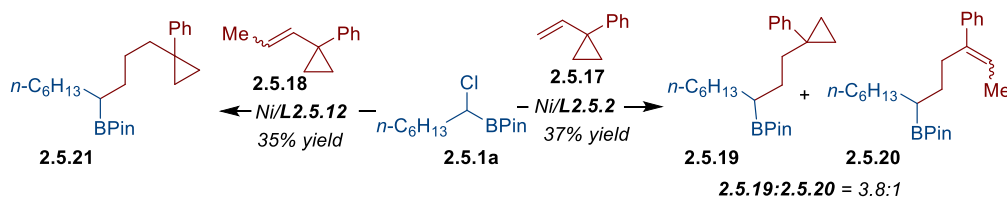
2.5.13 Boc $\xrightarrow[\text{DEMS, Na}_2\text{CO}_3]{\text{Ni/L2.5.2 or Ni/2.5.12}}$ 2.5.13a Boc

Entry	Time	Yield of 2.5.13a (%) Ni/L2.5.2	Yield of 2.5.13a (%) Ni/L2.5.2
1	10 min	16	13
2	20 min	24	22
3	30 min	25	29
4	1 h	31	38
5	2 h	34	49
6	24 h	31	43

General procedure for the isomerization of 2.5.13a with Ni/L2.5.2 system: An oven-dried 8 mL screw-cap vial containing a stirring bar was charged with NiI₂ (6.2 mg, 5 mol%), L2.5.2 (5.6 mg, 6 mol%), Na₂CO₃ (31.8 mg, 0.3 mmol) and 1-decane (78 μL, 0.4 mmol). Subsequently, the tube was sealed with a Teflon-lined screw cap, then evacuated and backfilled with Ar (3 times), Then, *tert*-butyl 2,5-dihydro-1H-pyrrole-1-carboxylate (**2.5.13**, 67.6 mg, 0.4 mmol), DEMS (96 μL, 0.6 mmol, 1.50 equiv), DMA and THF (3:1, 0.8 mL) were added by syringe. Then, the tube was stirred at room temperature for the indicated time. The yields of **2.5.13a** were determined by GC FID taking aliquots using 1-decane as internal standard.

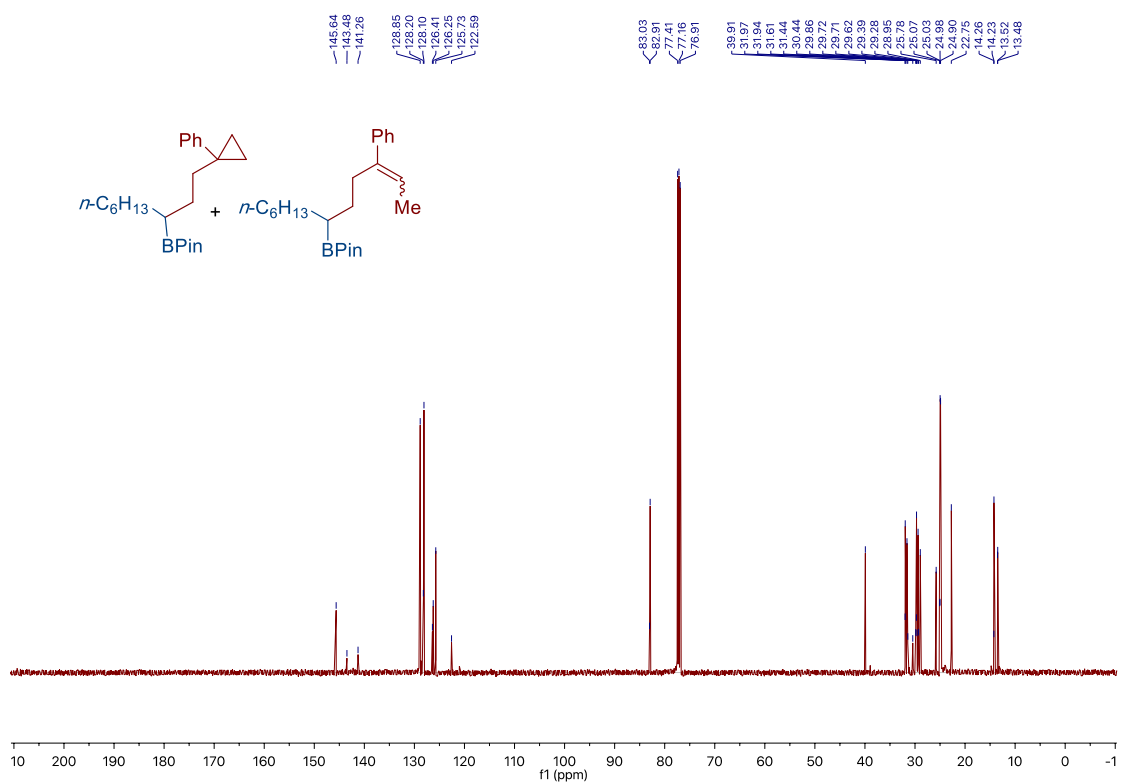
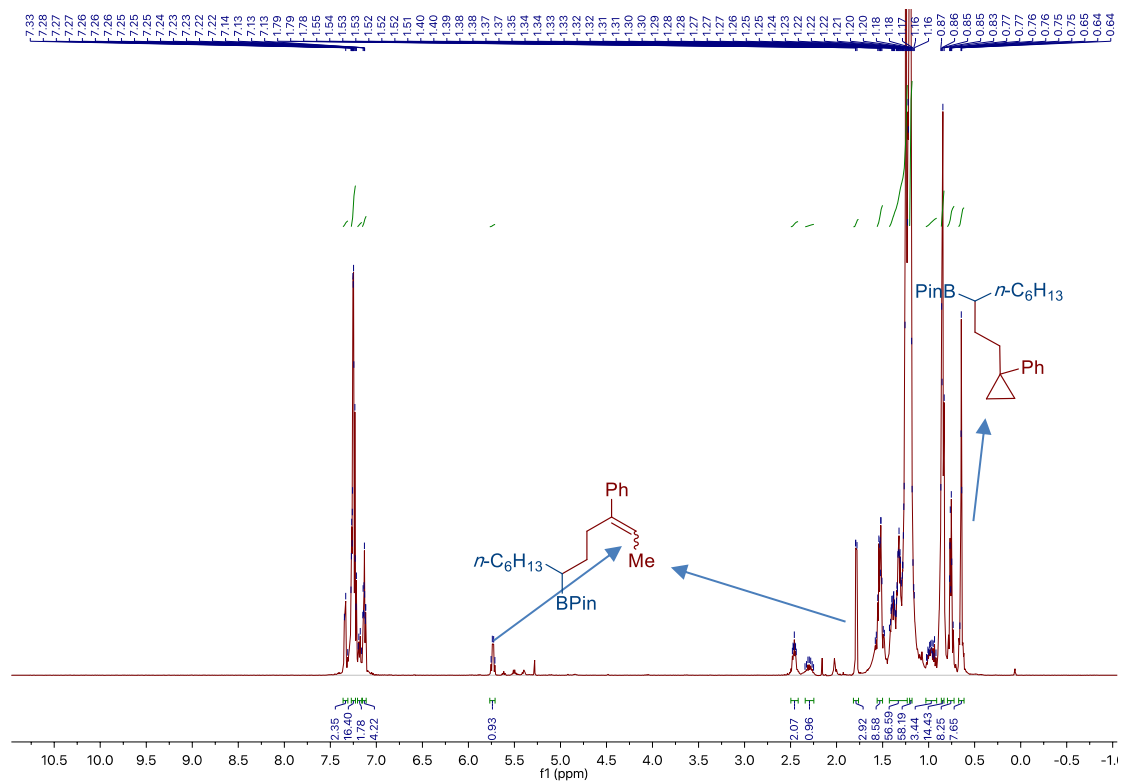
General procedure to form 2.5.13a with Ni/L2.5.12 system: An oven-dried 8 mL screw-cap vial containing a stirring bar was charged with NiI₂ (12.4 mg, 10 mol%), L2.5.12 (9.8 mg, 6 mol%), Na₂CO₃ (42.4 mg, 0.4 mmol) and 1-decane (78 μL, 0.4 mmol). Subsequently, the tube was sealed with a Teflon-lined screw cap, then evacuated and backfilled with Ar (3 times). Then, *tert*-butyl 2,5-dihydro-1H-pyrrole-1-carboxylate (**2.5.13**, 67.6 mg, 0.4 mmol), DEMS (96 μL, 0.60 mmol, 1.50 equiv) and DMA (1.2 mL) were added via syringe. Then, the tube was stirred at room temperature. The yields of **2.5.13a** were determined by GC FID taking aliquots using 1-decane as internal standard.

2.8.8.5 Experiments with Radical Probes

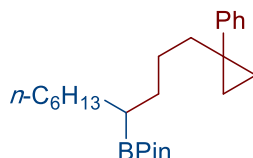


General procedure en route to 2.5.19 and 2.5.20: An oven-dried 8 mL screw-cap vial containing a stirring bar was charged with NiI_2 (3.1 mg, 5 mol%), **L2.5.2** (2.8 mg, 6 mol%) and Na_2CO_3 (15.9 mg, 0.75 mmol). Subsequently, the tube was sealed with a Teflon-lined screw cap, then evacuated and backfilled with Ar (3 times). Then, **2.5.1a** (52.0 mg, 0.20 mmol, 1.0 equiv), (1-vinylcyclopropyl)benzene (**2.5.17**, 49.0 mg, 0.34 mmol, 1.70 equiv), DEMS (48 μL , 0.3 mmol, 1.5 equiv), DMA and THF (3:1, 0.40 mL) were added via syringe. Then, the tube was stirred at room temperature for 15 h. After the reaction was completed, the mixture was diluted with EtOAc, filtered through silica gel and then concentrated under vacuum. The crude mixture was purified by silica gel chromatography, obtaining **2.5.19** and **2.5.20** (27.4 mg, 37% yield) as 3.8:1 mixture (as determined by NMR and GC analysis) (light yellow oil). $^1\text{H NMR}$ (400 MHz, CDCl_3): δ 7.35 – 7.31 (m, 2.35H), 7.31 – 7.21 (m, 16H), 7.20 – 7.16 (m, 1.8H), 7.16 – 7.09 (m, 4.2H), 5.73 (q, $J = 6.9$ Hz, 1H), 2.48 – 2.44 (m, 2H), 2.34 – 2.25 (m, 1H), 1.79 (d, $J = 6.9$ Hz, 3H), 1.58 – 1.48 (m, 8.8H), 1.42 – 1.23 (m, 56.6H), 1.22 – 1.20 (m, 58H), 1.02 – 0.92 (m, 3.4H), 0.90 – 0.83 (m, 14.4H), 0.80 – 0.71 (m, 8.2H), 0.68 – 0.60 (m, 7.6H) ppm. $^{13}\text{C NMR}$ (101 MHz, CDCl_3): δ 145.6, 143.5, 141.3, 128.9, 128.2, 128.1, 126.4, 126.3, 125.7, 122.6, 83.0, 82.9, 39.9, 32.0, 31.9, 31.6, 31.4, 30.4, 29.9, 29.7 (left), 29.7 (right), 29.6, 29.4, 29.3, 29.0, 25.8, 25.1, 25.0, 25.0, 24.9, 22.8 (2C), 14.3, 14.2, 13.5 (left), 13.5 (right) ppm. **HRMS** calcd. for $(\text{C}_{24}\text{H}_{39}\text{BNaO}_2) [\text{M}+\text{Na}]^+$: 393.2935 found 393.2933.

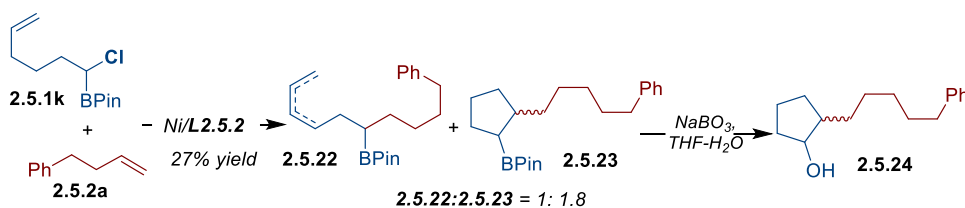
Chapter 2.



*Site-Selective Ni-Catalyzed Reductive
Coupling of α -Haloboranes with Unactivated Olefins*



General procedure en route to 2.5.21: An oven-dried 8 mL screw-cap vial containing a stirring bar was charged with NiI₂ (6.2 mg, 10 mol%), **L2.5.12** (4.9 mg, 12 mol%) and Na₂CO₃ (21.2 mg, 1.0 mmol). Subsequently, the tube was sealed with a Teflon-lined screw cap, then evacuated and backfilled with Ar (3 times). Then, **2.5.1a** (78.0 mg, 0.30 mmol, 1.5 equiv), (1-(prop-1-en-1-yl)cyclopropyl)benzene (**2.5.18**, 31.6 mg, 0.20 mmol, 1.0 equiv), DEMS (48 μ L, 0.3 mmol, 1.5 equiv) and DMA (0.60 mL) were added via syringe. Then, the tube was stirred at room temperature for 18 h. After the reaction was completed, the mixture was diluted with EtOAc, filtered through silica gel and then concentrated under vacuum. The crude mixture was purified by silica gel chromatography, obtaining **2.5.21** (26.9 mg, 35% yield) (light yellow oil). ¹H NMR (400 MHz, CDCl₃): δ 7.32 – 7.23 (m, 4H), 7.18 – 7.13 (m, 1H), 1.58 – 1.53 (m, 2H), 1.40 – 1.22 (m, 15H), 1.18 (d, J = 4.1 Hz, 12H), 0.92 – 0.87 (m, 3H), 0.80 – 0.77 (m, 2H), 0.68 – 0.65 (m, 2H) ppm. ¹³C NMR (101 MHz, CDCl₃): δ 145.6, 128.9, 127.9, 125.6, 82.7, 40.7, 31.8, 31.7, 31.6, 29.6, 29.3, 26.9, 25.7, 24.7, 24.6, 22.6, 14.1, 13.1, 12.9 ppm. ¹¹B NMR (128 MHz, CDCl₃) δ 35.09 ppm. IR (neat, cm⁻¹): 2975, 2925, 2855, 1693, 1459, 1388, 1315, 1257, 1165, 1142, 1109, 967, 863, 761, 700. HRMS calcd. for (C₂₅H₄₁BNaO₂) [M+Na]⁺: 407.3092 found 407.3088.

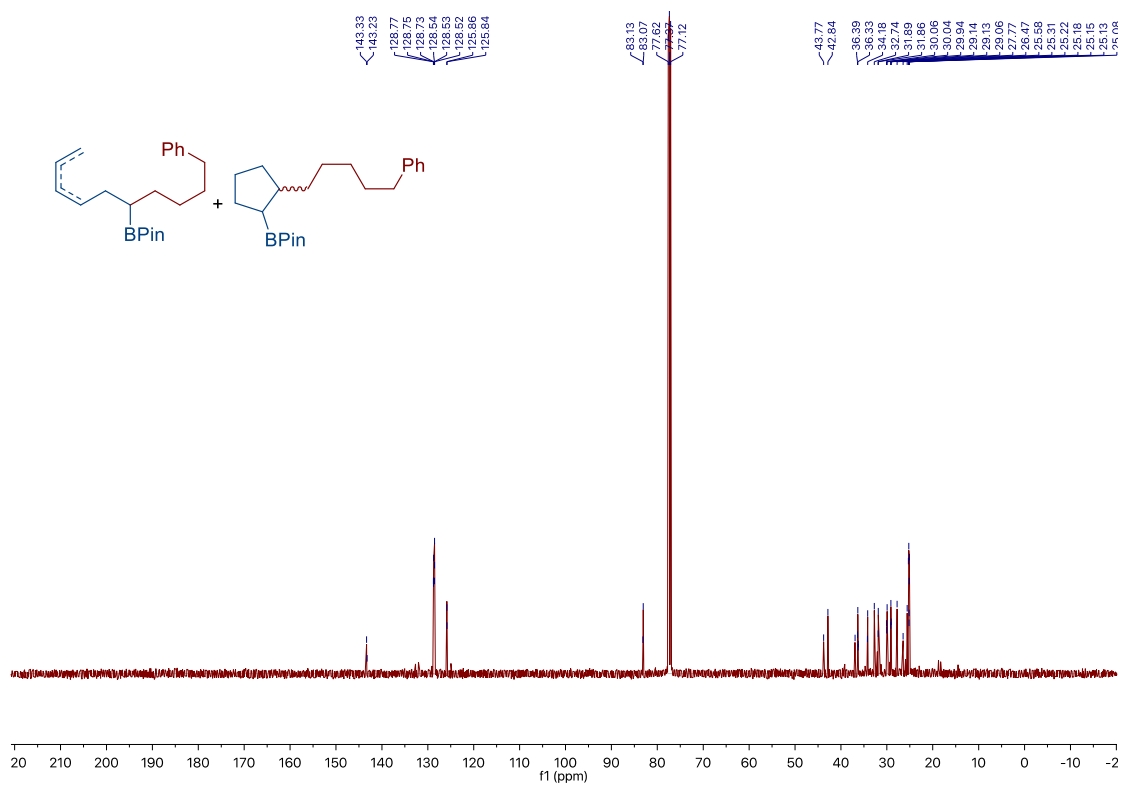
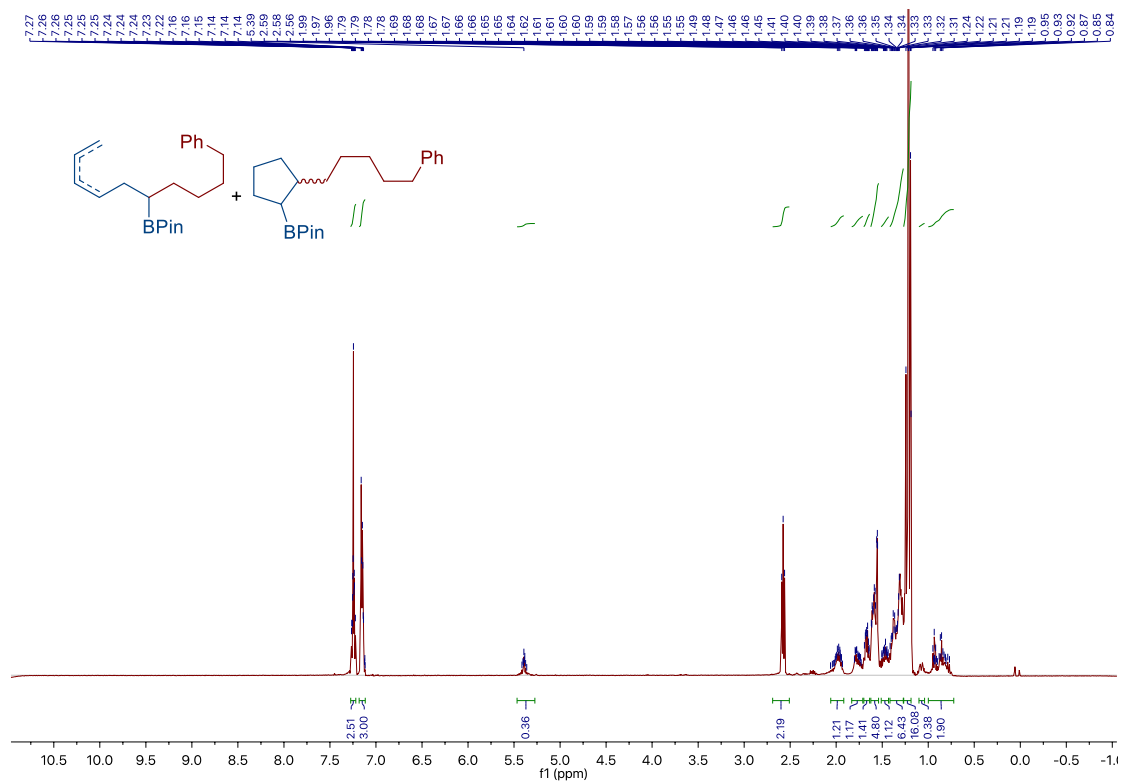


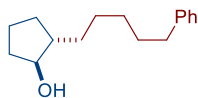
General procedure en route to 2.5.22 and 2.5.23: An oven-dried 8 mL screw-cap reaction tube containing a stirring bar was charged with NiI₂ (3.1 mg, 5 mol%), **L2.5.2** (2.8 mg, 6 mol%) and Na₂CO₃ (15.9 mg, 0.75 mol). Subsequently, the tube was sealed with a Teflon-lined screw cap, then evacuated and back-filled with Ar (3 times). Then 2-(1-chlorohex-5-en-1-yl)-4,4,5,5-tetramethyl-1,3,2-dioxaborolane (**2.5.1k**, 48.8 mg, 0.20 mmol, 1 equiv), 4-phenyl-1-butene (**2.5.2a**, 51 μ L, 0.34 mmol, 1.7 equiv) and DEMS (48 μ L, 0.3 mmol, 1.5 equiv) were added via syringe. Finally, DMA and THF (3:1, 0.4 mL) were added via syringe. Once added, the tube was stirred at room temperature (around 25 °C) for 15 h. After the reaction was complete,

Chapter 2.

the mixture was diluted with EtOAc, filtered through silica gel and concentrated. The crude product mixture was purified by silica-gel chromatography, obtaining an inseparable mixture of **2.5.22** and **2.5.23** (13 mg, 27% yield) (light yellow oil) in a 1:1.8 ratio between non-cyclized (**2.5.22**) and cyclized products (**2.5.23**) as determined by GC and GC-MS. ¹H NMR (400 MHz, CDCl₃): δ 7.27 – 7.22 (m, 2.73H), 7.16 – 7.14 (m, 3.17H), 5.46 – 5.34 (m, 0.36H), 2.58 (t, *J* = 7.8 Hz, 2.19H), 2.08 – 1.93 (m, 1.21H), 1.80 – 1.73 (m, 1.17H), 1.70 – 1.63 (m, 1.41H), 1.62 – 1.55 (m, 4.8H), 1.50 – 1.44 (m, 1.12H), 1.41 – 1.28 (m, 6.43H), 1.25 – 1.19 (m, 16.1H), 1.11 – 1.04 (m, 0.38H), 0.95 – 0.84 (m, 1.9H) ppm. ¹³C NMR (126 MHz, CDCl₃): δ 143.3, 143.2, 128.8 (left), 128.8 (right), 128.7, 128.5 (left), 128.5 (middle), 128.5 (right), 125.9, 125.8, 83.1 (left), 83.1 (right), 43.7, 42.8, 36.9, 36.4, 36.3 (left), 36.3 (right), 36.2, 34.2 (left), 34.2 (right), 32.7, 31.9 (left), 31.9 (right), 30.1, 30.0, 29.9, 29.1 (left), 29.1 (middle), 29.1 (right), 27.8, 26.5, 25.6, 25.3, 25.2 (left), 25.2 (middle), 25.2 (right), 25.1 (left), 25.1 (right) ppm. ¹¹B NMR (128 MHz, CDCl₃) δ 34.19 ppm.

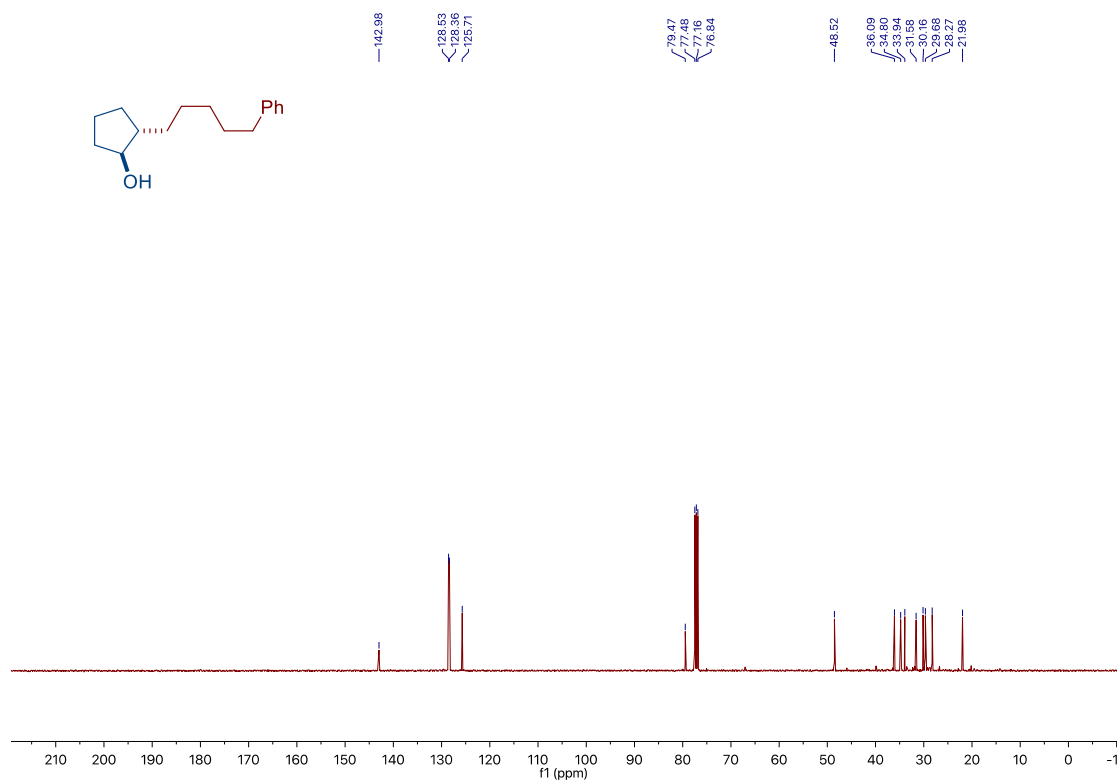
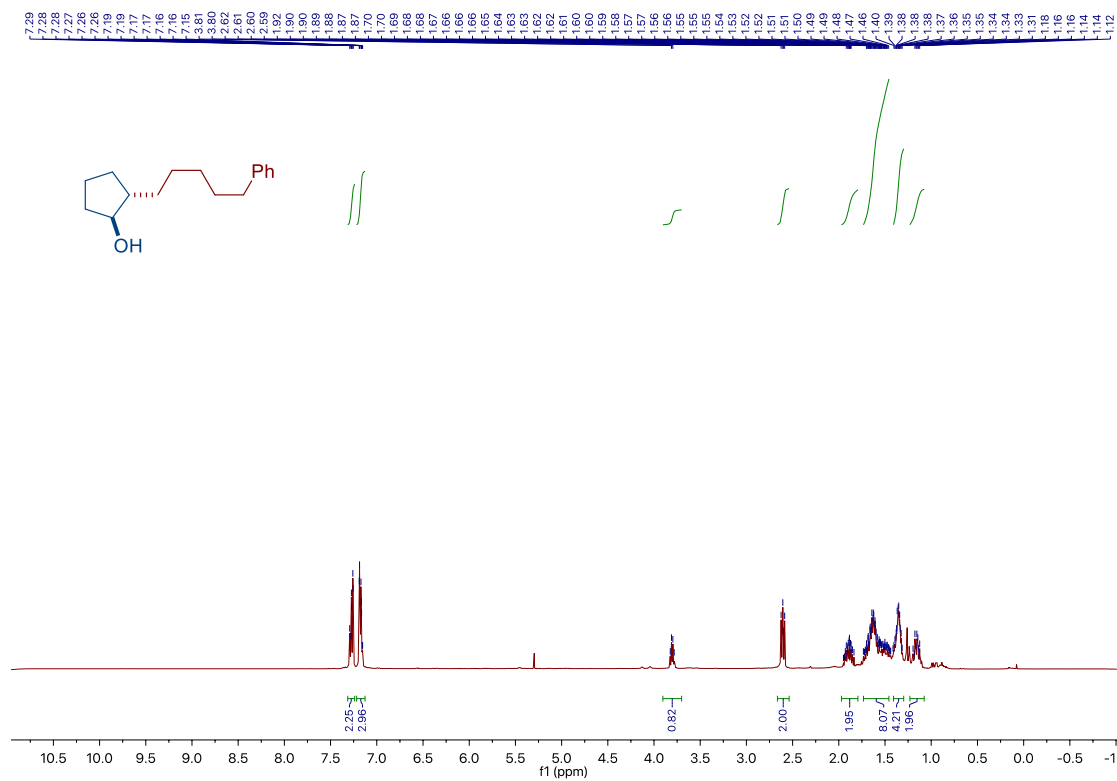
Site-Selective Ni-Catalyzed Reductive Coupling of α -Haloboranes with Unactivated Olefins





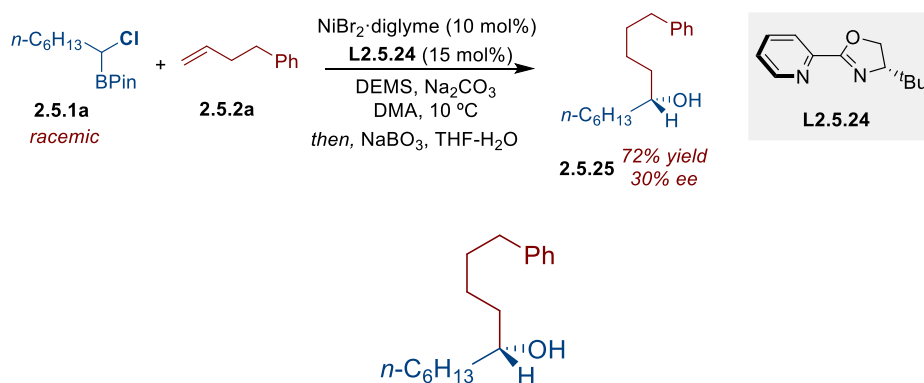
Trans-2-(5-phenylpentyl)cyclopentan-1-ol (2.5.24): The mixture of **2.5.22** and **2.5.23** (17 mg, 0.05 mmol) was dissolved in THF and H₂O (1:1, 1 mL), and NaBO₃·4H₂O (81.8 mg, 0.10 mmol) was added. The reaction mixture was stirred at room temperature for 4 h. After the reaction was completed, water (5 mL) was added. The aqueous phase was extracted with EtOAc (3 x 10 mL), and the combined organic phases were dried over MgSO₄ and concentrated. The residue was purified by column chromatography and the two diastereoisomers were separated. The *trans* diastereoisomers **2.5.24** was characterized and the configuration confirmed comparing the ¹H NMR with a related compound reported in the literature.²¹ ¹H NMR (400 MHz, CDCl₃) δ 7.40 – 7.21 (m, 2H), 7.21 – 7.02 (m, 3H), 3.80 (q, *J* = 5.6 Hz, 1H), 2.61 (t, *J* = 7.6 Hz, 2H), 1.95 – 1.84 (m, 2H), 1.76 – 1.44 (m, 8H), 1.42 – 1.31 (m, 4H), 1.20 – 1.11 (m, 2H) ppm. ¹³C NMR (101 MHz, CDCl₃): δ 143.0, 128.5, 128.4, 125.7, 79.5, 48.5, 36.1, 34.8, 33.9, 31.6, 30.2, 29.7, 28.3, 22.0 ppm. IR (neat, cm⁻¹): 3362, 2925, 2854, 1495, 1453, 1343, 1074, 745, 698. HRMS calcd. for C₁₆H₂₃O [M-H]⁺: 231.1743 found 231.1742.

*Site-Selective Ni-Catalyzed Reductive
Coupling of α -Haloboranes with Unactivated Olefins*



2.8.9 Preliminary Enantioconvergent Coupling Reaction

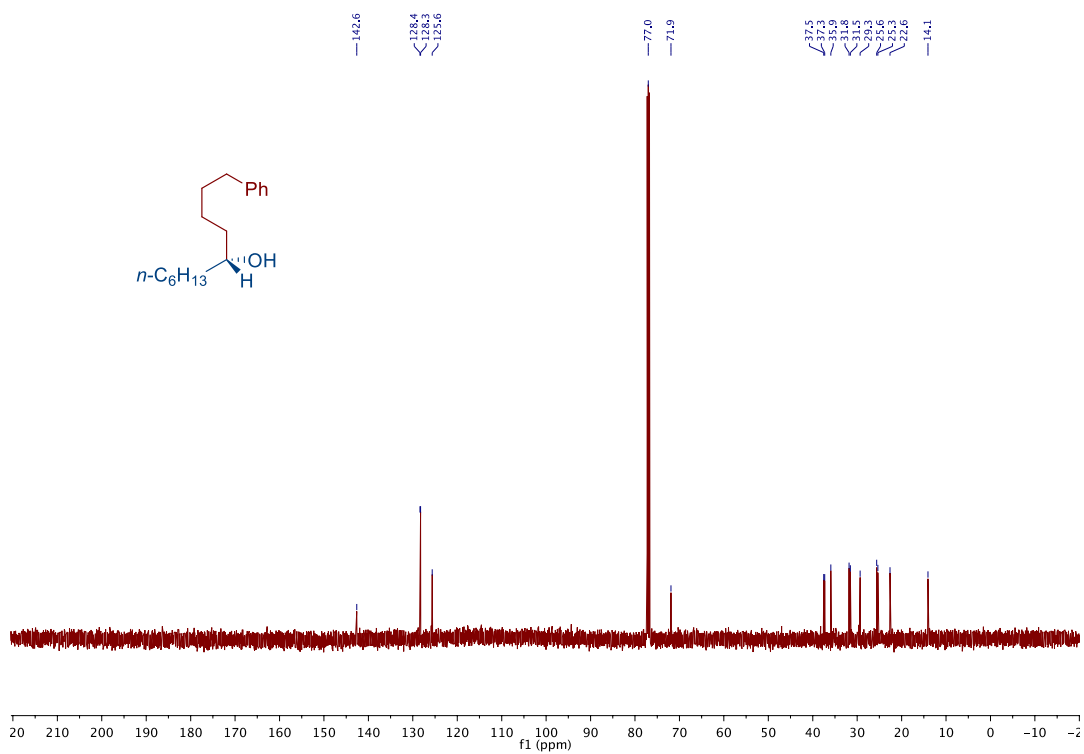
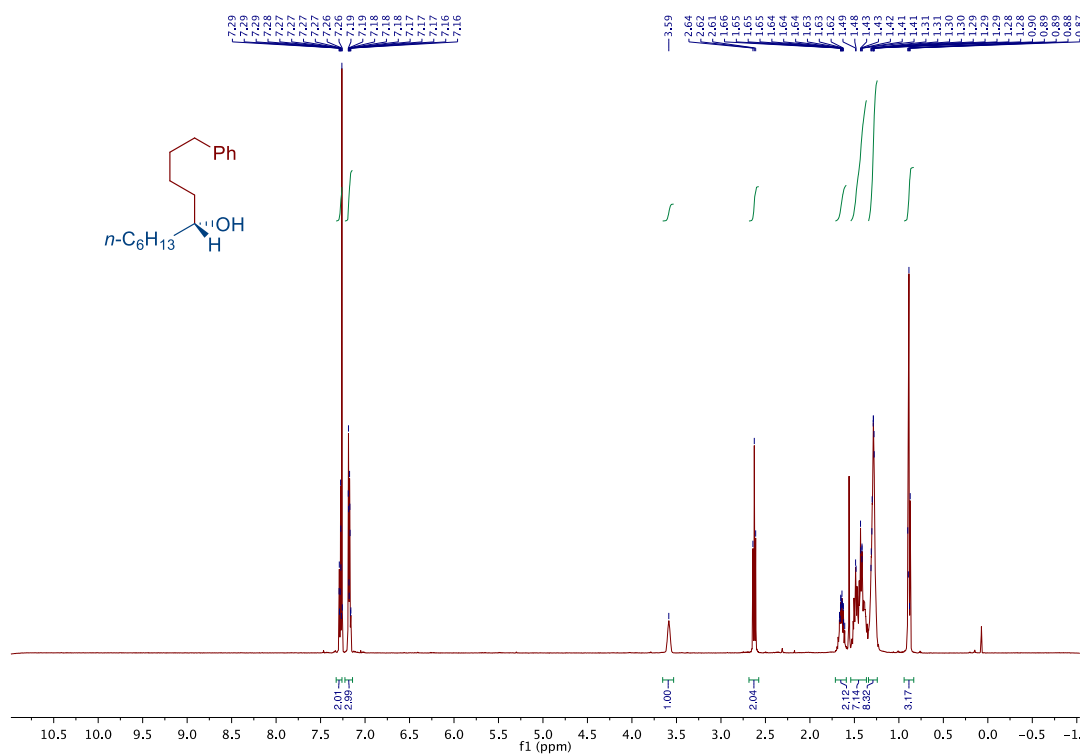
2.8.9.1 General Procedure for Enantioconvergent Coupling Reaction



(*R*)-1-phenylundecan-5-ol (2.5.25): An oven-dried 8 mL screw-cap vial containing a stirring bar was charged with $\text{NiBr}_2 \cdot \text{diglyme}$ (10 mol%), **L2.5.24** (15 mol%) and Na_2CO_3 (1.5 mmol, 15.9 mg). Subsequently, the tube was sealed with a Teflon-lined screw cap, then evacuated and backfilled with Ar (3 times). Then, DMA was added and it was stirred at room temperature 30 minutes. Subsequently, 2-(1-bromoheptyl)-4,4,5,5-tetramethyl-1,3,2-dioxaborolane (**2.5.1a**, 60.8 mg, 0.20 mmol, 1.0 equiv), 4-phenyl-1-butene (**2.5.2a**, 51 μL , 0.34 mmol, 1.70 equiv) and DEMS (64 μL , 0.4 mmol, 2.0 equiv) were added via syringe and the tube was stirred at 10 °C for 15 h. After the reaction was completed, the mixture was diluted with EtOAc, filtered through silica gel and then concentrated under reduced pressure. The residue was dissolved in a mixture of THF and H₂O (1:1, 4 mL) and $\text{NaBO}_3 \cdot 4\text{H}_2\text{O}$ (327.2 mg, 0.40 mmol) was added. The reaction mixture was stirred at room temperature for 4 h. After the reaction was completed, water (20 mL) was added. The aqueous phase was extracted with EtOAc (3 x 20 mL), and the combined organic phases were dried over MgSO_4 and concentrated. The residue was purified by column chromatography, affording the corresponding product **2.5.25** (36 mg, 72%, 30% ee) as a colorless oil. The enantiomeric excess was determined via HPLC. ¹H NMR (400 MHz, CDCl₃) δ 7.32 – 7.25 (m, 2H), 7.21 – 7.14 (m, 3H), 3.59 (s, 1H), 2.62 (t, J = 7.7 Hz, 2H), 1.71 – 1.60 (m, 2H), 1.53 – 1.37 (m, 7H), 1.34 – 1.24 (m, 8H), 0.89 (t, J = 5.7 Hz, 3H) ppm. ¹³C NMR (126 MHz, CDCl₃): δ 142.6, 128.4, 128.3, 125.6, 71.9, 37.5, 37.3, 35.9, 31.8, 31.5, 29.3, 25.6, 25.3, 22.6, 14.1 ppm. IR (neat, cm⁻¹): 3350, 3026, 2926, 2855, 1454, 1377, 1030, 697. **HPLC analysis**: The ee was determined via HPLC on a CHIRALPAK IB column (2% 2-PrOH in hexane, 1.0 mL/min) with t_R

Site-Selective Ni-Catalyzed Reductive
Coupling of α -Haloboranes with Unactivated Olefins

= 6.0 min, 6.56 min; $[\alpha]_D^{26} = -9.23$ (c = 0.1000, CH_2Cl_2).



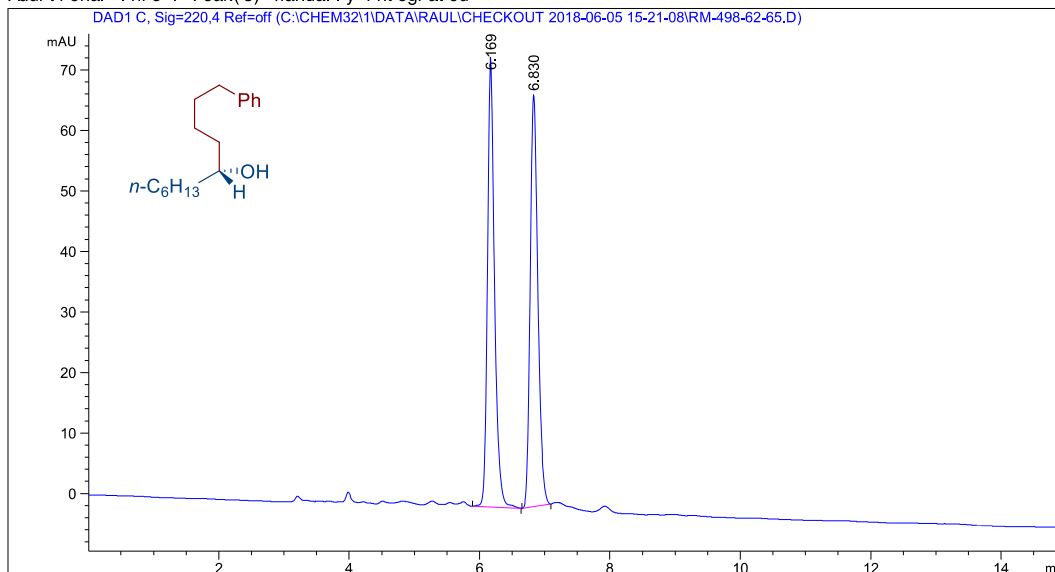
Chapter 2.

Data File C:\CHEM82\1\DATA\RAUL\CHECKOUT 2018-06-05 15-21-08\FM 498-62-65.D
 Sample Name: FM 498-62-65

```

=====
Acq. Operator   : SYSTEM                      Seq. Line :    2
Acq. Instrument : HPLC 1260                   Locat ion :   81
Injection Date  : 6/5/2018 3:37:55 PM        Inj       :    1
                                           Inj Volume: 1.000 µl

Acq. Method     : C:\Chem82\1\Dat a\Ra ul\checko ut 2018-06-05 15-21-08\Chi ral coloum IB-SZ 98-
                : 2, M
Last changed    : 6/5/2018 3:21:09 PM by SYSTEM
Analysis Method : C:\Chem82\1\Met hods\Chi ral coloum IB-SZ 98-2, M
Last changed    : 7/3/2018 1:03:47 PM by SYSTEM
                : (modified after loading)
Additional Info : Peak(s) manually integrated
  
```



Area Percent Report

```

=====
Sorted By      :      Signal
Multiplier     :      1.0000
Dilution       :      1.0000
Use Multiplier & Dilution Factor with ISTDs
  
```

Signal 1: DAD1 C, Sig=220,4 Ref=off

Peak #	Ret Time [min]	Type	Width [min]	Area [mAU*s]	Height [mAU]	Area %
1	6.169	BB	0.1158	572.73779	74.37438	51.1559
2	6.830	BB	0.1238	546.85583	68.02451	48.8441

Totals : 1119.59363 142.39889

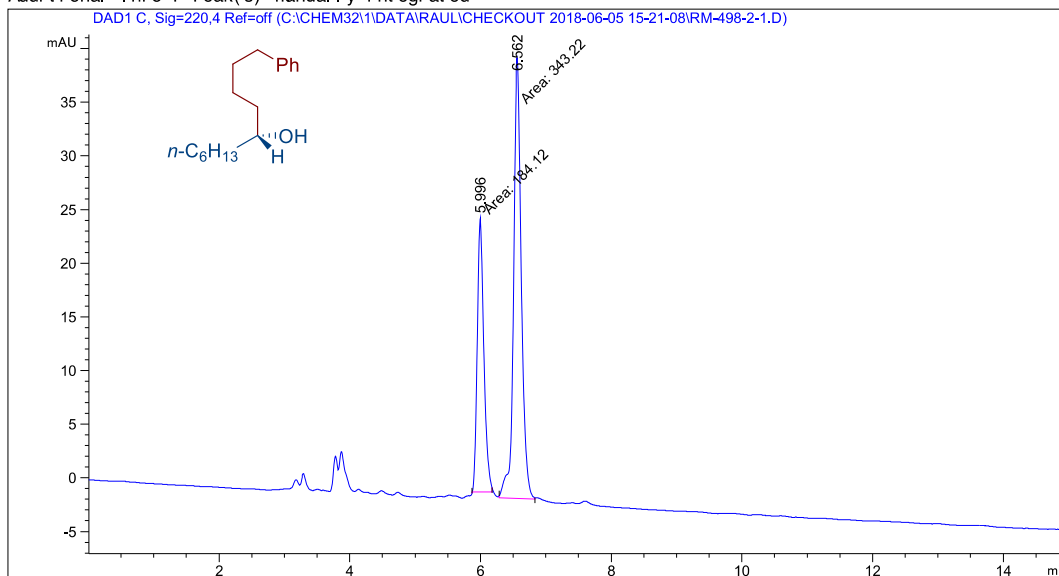
*Site-Selective Ni-Catalyzed Reductive
Coupling of α -Haloboranes with Unactivated Olefins*

Data File C:\CHEM82\1\DATA\RAUL\CHECKOUT 2018-06-05 15-21-08\RM 498-2-1.D
Sample Name: RM 498-2-1

```

=====
Acq. Operator   : SYSTEM                      Seq. Line :    3
Acq. Instrument : HPLC 1260                   Location  :   82
Injection Date  : 6/5/2018 3:53:47 PM         Inj       :    1
                                           Inj Volume: 1.000  $\mu$ l

Acq. Method     : C:\Chem82\1\Dat a\ Faul \checkout 2018-06-05 15-21-08\Chiral column IB-SZ 98-
                  2, M
Last changed    : 6/5/2018 3:21:09 PM by SYSTEM
Analysis Method : C:\Chem82\1\Methods\Chiral column IB-SZ 98-2, M
Last changed    : 7/3/2018 1:03:47 PM by SYSTEM
                  (modified after loading)
Additional Info : Peak(s) manually integrated
=====
    
```



=====
Area Percent Report
=====

```

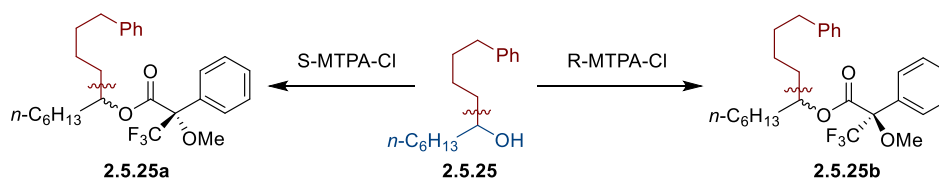
Sorted By      :      Signal
Multiplier     :      1.0000
Dilution       :      1.0000
Use Multiplier & Dilution Factor with ISTDs
    
```

Signal 1: DAD1 C, Sig=220,4 Ref=off

Peak #	Ret Time [min]	Type	Width [min]	Area [nAU*s]	Height [nAU]	Area %
1	5.996	MM	0.1199	184.11971	25.58409	34.9148
2	6.562	MM	0.1392	343.22040	41.10274	65.0852

Totals : 527.34010 66.68683

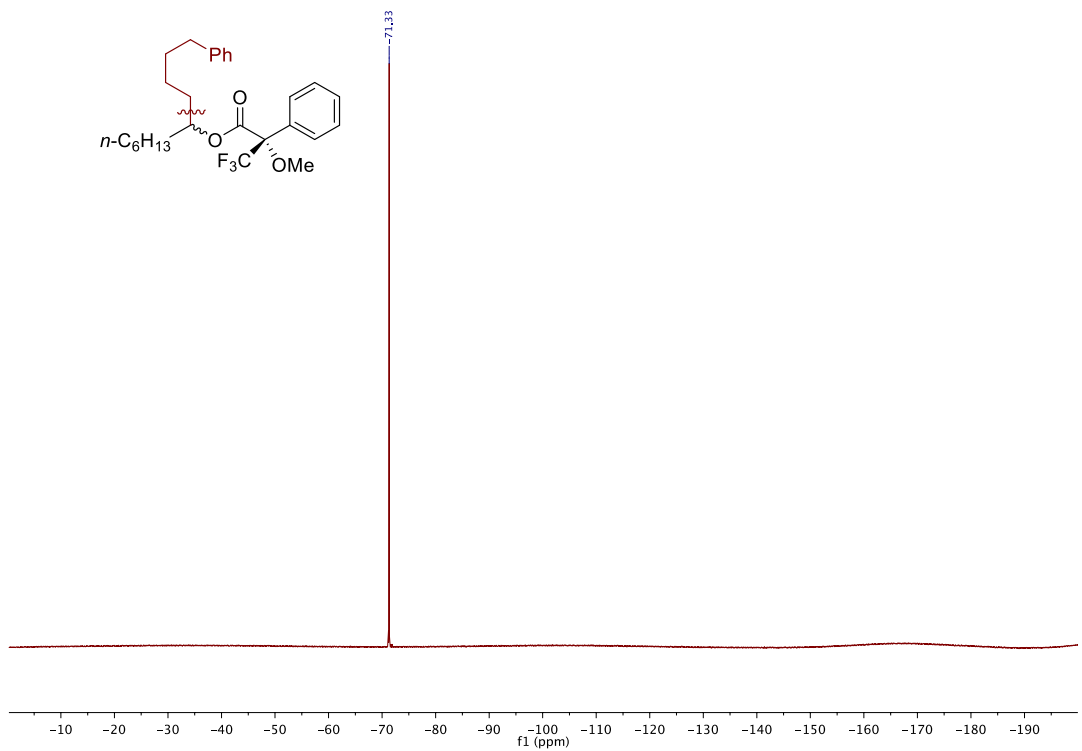
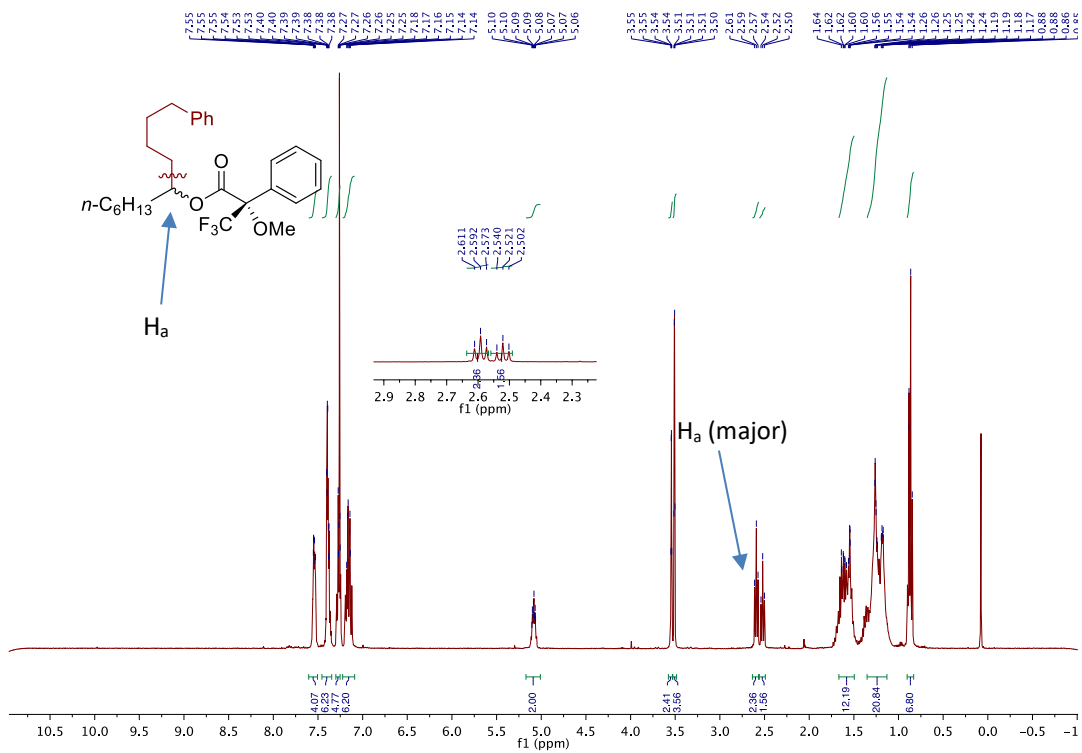
2.8.9.2 Preparation of the R- and S-MTPA-esters



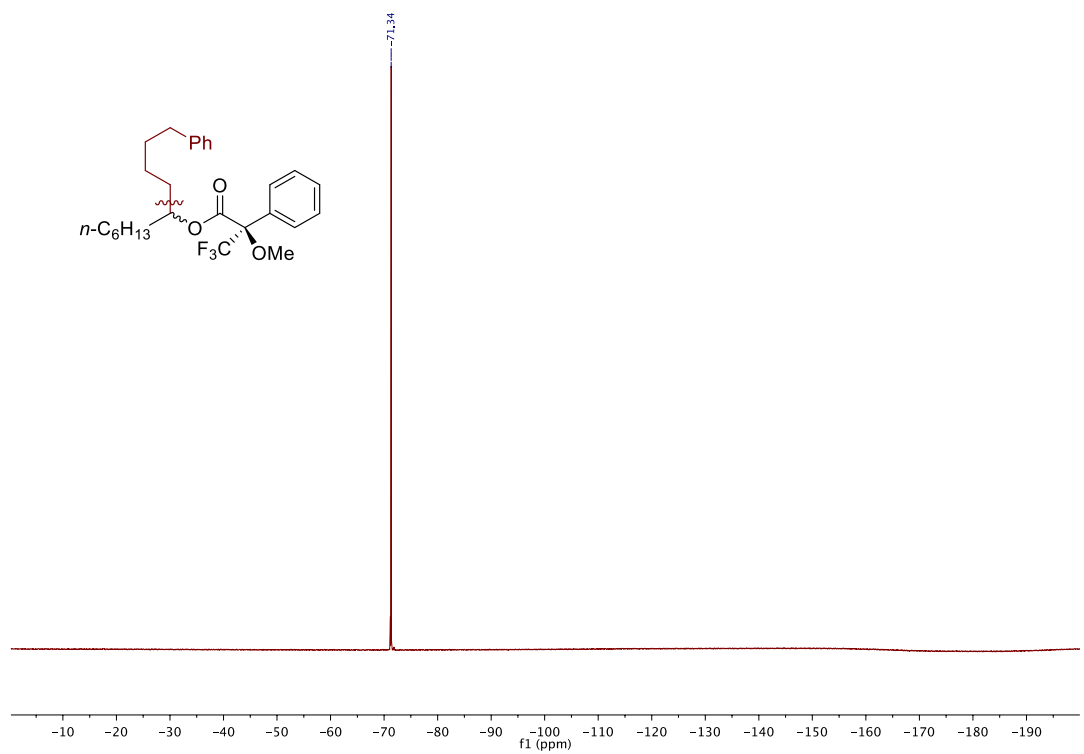
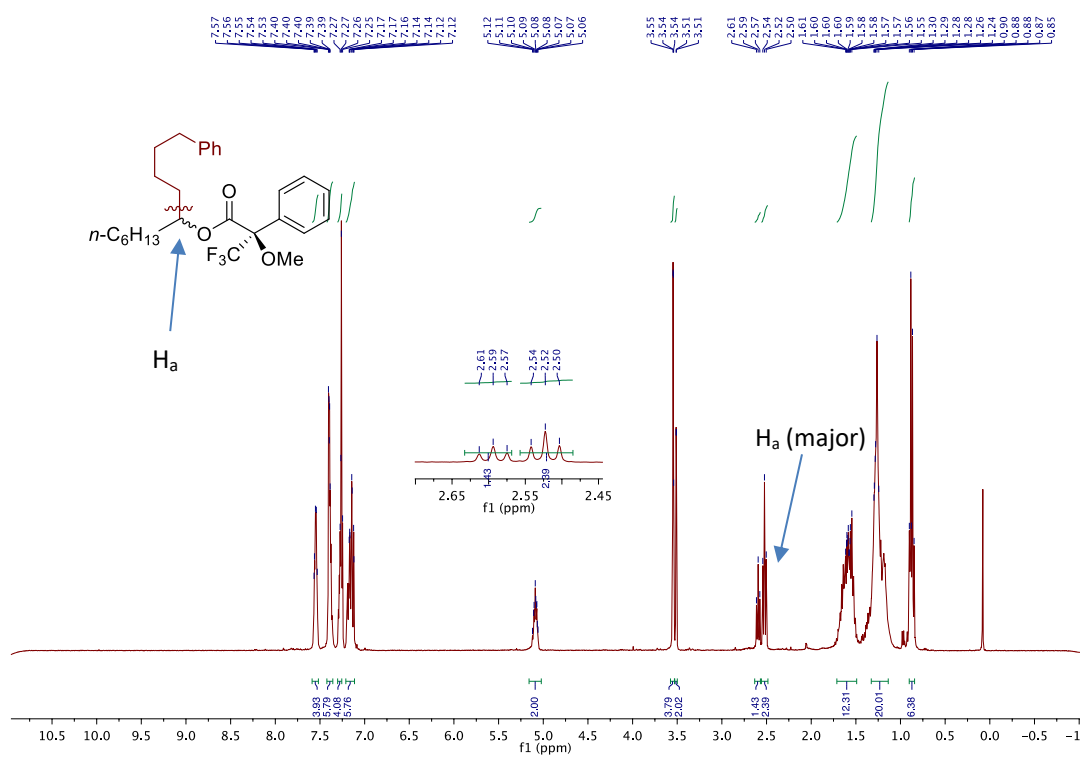
2.5.25a and **2.5.25b** were synthesized following a procedure described in the literature.²² An oven-dried screw-cap vial containing a stirring bar was charged with **2.5.25** (25.0 mg, 0.1 mmol), (*S*)-(-)- α -Methoxy- α -(trifluoromethyl)phenylacetyl chloride (38 μ L, 0.2 mmol, 2.0 equiv), and dry pyridine (24.8 μ L, 0.31 mmol, 3.1 equiv) in 2 ml dry DCM at room temperature were added. The resulting solution was stirred at room temperature, and the reaction progress was monitored by TLC (Hexane/EtOAc = 5:1). After complete consumption of **2.5.25**, the reaction mixture was quenched by the addition of water and EtOAc. The aqueous phase was extracted with EtOAc (3 x 20 mL), and the combined organic phases were dried over MgSO₄ and concentrated. The crude product mixture was purified by silica gel chromatography (Hexane/EtOAc = 20:1) to give the R-MTPA-ester **2.5.25a** (43 mg, 94%) as a colorless oil. ¹H NMR (400 MHz, CDCl₃) δ 7.60 – 7.50 (m, 4H), 7.43 – 7.35 (m, 6H), 7.30 – 7.23 (m, 4H), 7.22 – 7.10 (m, 6H), 5.08 (ddd, *J* = 7.2, 4.7, 2.0 Hz, 2H), 3.54 (d, *J* = 1.3 Hz, 3H, minor), 3.51 (d, *J* = 1.3 Hz, 3H, major), 2.59 (t, *J* = 7.6 Hz, 2H_a, major), 2.52 (t, *J* = 7.7 Hz, 2H, minor), 1.68 – 1.50 (m, 12H), 1.35 – 1.13 (m, 20H), 0.86 (t, *J* = 7.4 Hz, 6H) ppm. ¹⁹F NMR (376 MHz, CDCl₃) δ -71.3 ppm.

In an analogous fashion, the S-MTPA-ester **2.5.25b** (45 mg, 96%) was prepared using (*R*)-(-)- α -Methoxy- α -(trifluoromethyl)phenylacetyl chloride (38 μ L, 0.2 mmol, 2.0 equiv). ¹H NMR (400 MHz, CDCl₃) δ 7.55 (m, 4H), 7.42 – 7.36 (m, 6H), 7.26 (m, 4H), 7.22 – 7.11 (m, 6H), 5.09 (td, *J* = 6.0, 5.0, 2.0 Hz, 2H), 3.55 (d, *J* = 1.4 Hz, 3H, major), 3.51 (d, *J* = 1.4 Hz, 3H, minor), 2.59 (t, *J* = 7.6 Hz, 2H, minor), 2.52 (t, *J* = 7.7 Hz, 2H_a, major), 1.69 – 1.53 (m, 12H), 1.28 (d, *J* = 13.7 Hz, 20H), 0.87 (m, 6H) ppm. ¹⁹F NMR (376 MHz, CDCl₃) δ -71.3 ppm. Through the ¹H NMR $\Delta\delta^{\text{SR}}(^1\text{H}_a) < 0$, ¹⁹F NMR $\Delta\delta^{\text{SR}}(^{19}\text{F}) \text{CF}_3 < 0$ analysis, we determined that the major enantiomer found in our catalytic umpolung alkylation had **R** configuration.²³

Site-Selective Ni-Catalyzed Reductive Coupling of α -Haloboranes with Unactivated Olefins



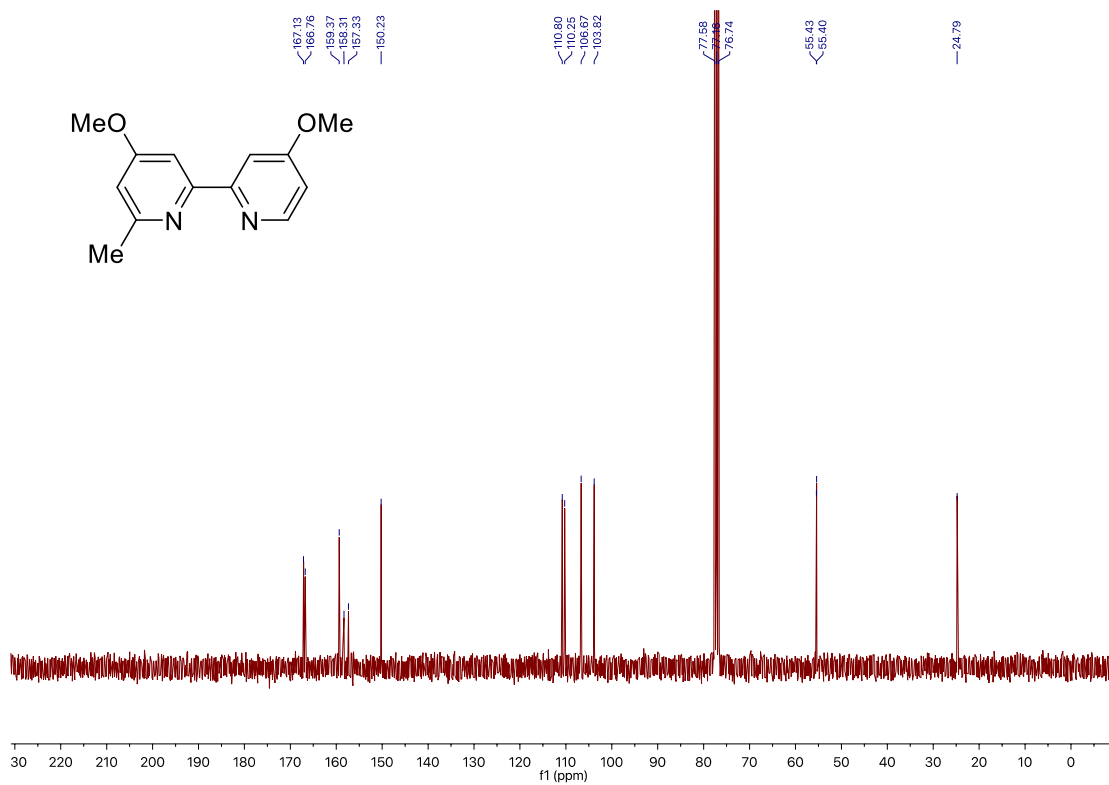
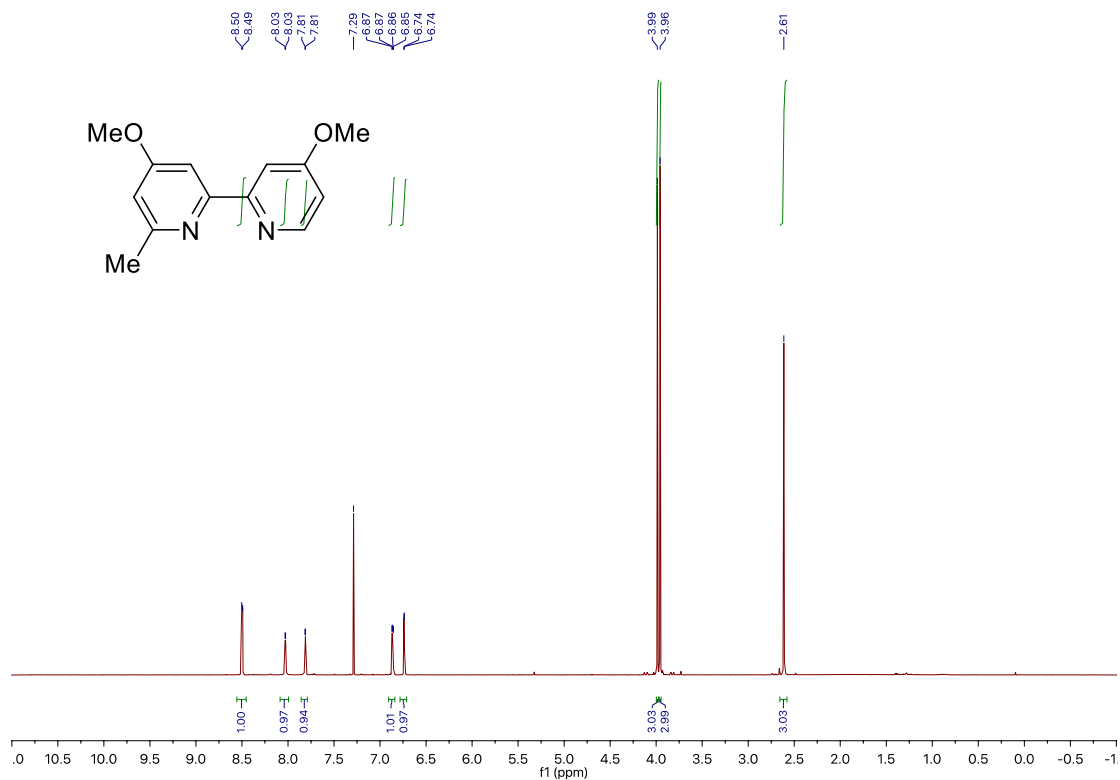
Chapter 2.



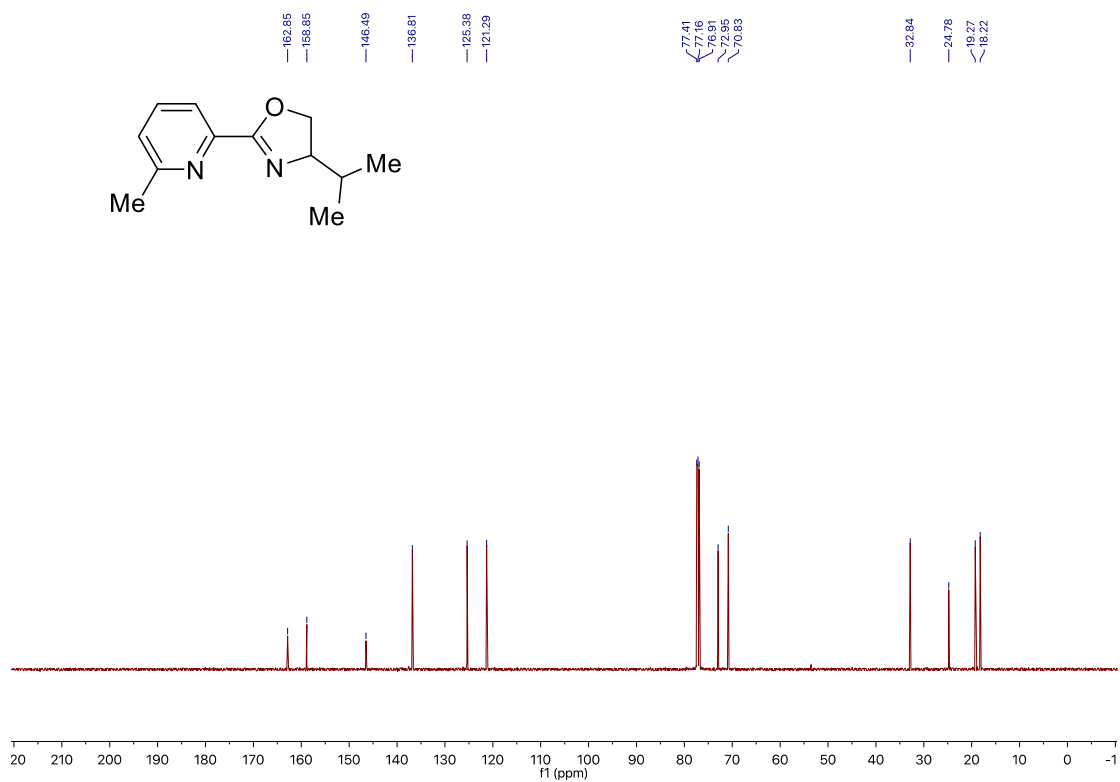
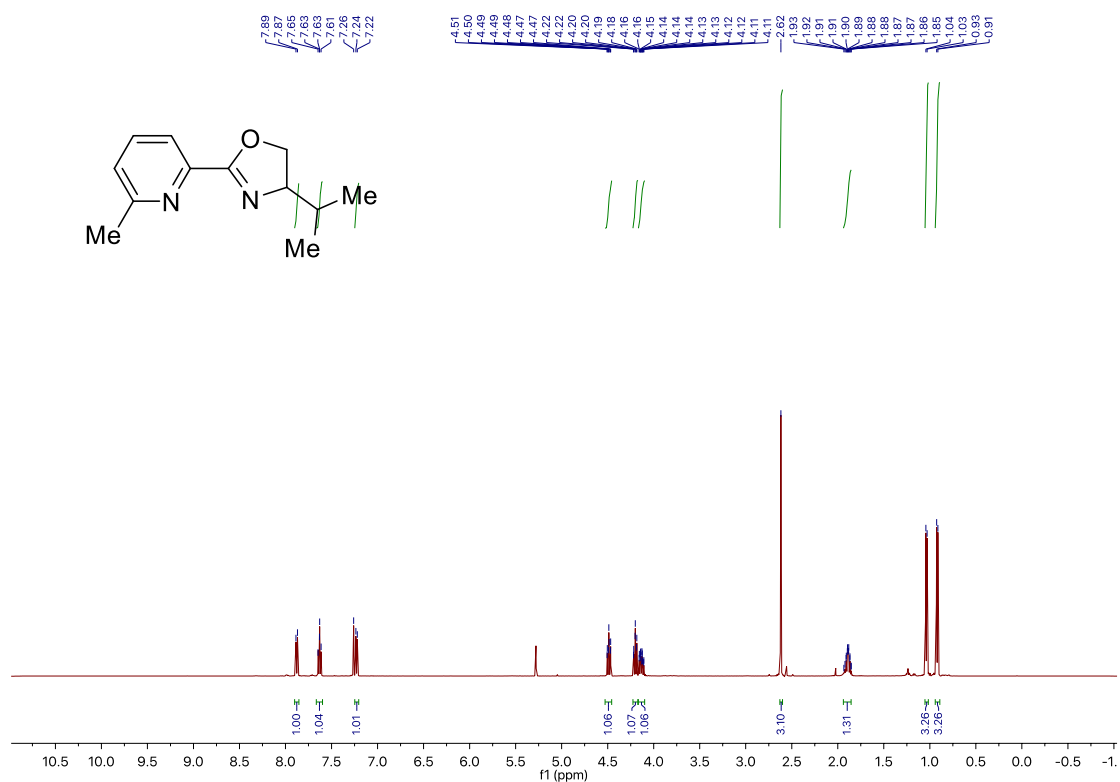
2.8.10 Bibliography of Known Compounds

1. Schmidt, J.; Choi, J.; Liu, A. T.; Slusarczyk, M.; Fu, G. C. *Science* **2016**, *354*, 1265.
2. Sun, S.-Z.; Martin, R. *Angew. Chem. Int. Ed.* **2018**, *57*, 3622.
3. Yang, T.; Lu, L.; Shen, Q. *Chem. Commun.* **2015**, *51*, 5479.
4. Dolman, S. J.; Schrock, R. R.; Hoveyda, A. H. *Org. Lett.* **2003**, *5*, 4899.
5. Itoh, T.; Matsueda, T.; Shimizu, Y.; Kanai, M. *Chem. - Eur. J.* **2015**, *21*, 15955.
6. Wang, Y.-X.; Wang, J.-H.; Li, G.-X.; He, G.; Chen, G. *Org. Lett.* **2017**, *19*, 1442.
7. L. Gonnard, A. Guerinot, J. Cossy, *Chem. Eur. J.* **2015**, *21*, 12797.
8. Okazoe, T.; Takai, K.; Utimoto, K. *J. Am. Chem. Soc.* **1987**, *109*, 951.
9. Pluempunapat, W.; Chavasiri, W. *Tetrahedron Lett* **2006**, *47*, 6821.
10. Gaydou, M.; Moragas, T.; Julia-Hernandez, F.; Martin, R. *J. Am. Chem. Soc.* **2017**, *139*, 12161.
11. Kawasaki, T.; Tanaka, H.; Tsutsumi, T.; Kasahara, T.; Sato, I.; Soai, K. *J. Am. Chem. Soc.* **2006**, *128*, 6032.
12. Kuhn, K. M.; Champagne, T. M.; Hong, S. H.; Wei, W.-H.; Nickel, A.; Lee, C. W.; Virgil, S. C.; Grubbs, R. H.; Pederson, R. L. *Org. Lett.*, **2010**, *12*, 984.
- 13 Blunt, J. W.; Hartshorn, M. P.; Soong, L. T.; Munro, M. H. G.; Vannoort, R. W.; Vaughan, J. *Aust. J. Chem.* **1983**, *36*, 1387.
14. Jnaneshwara, G. K.; Deshpande, V. H.; Lalithambika, M.; Ravindranathan, T.; Bedekar, A. V. *Tetrahedron Lett* **1998**, *39*, 459.
15. Nadres, E. T.; Lazareva, A.; Daugulis, O. *J. Org. Chem.*, **2011**, *76*, 471.
16. Kadi, N.; Arbache, S.; Song, L.; Oves-Costales, D.; Challis, G. L. *J. Am. Chem. Soc.* **2008**, *130*, 10458.
17. Sasano, K.; Takaya, J.; Iwasawa, N. *J. Am. Chem. Soc.* **2013**, *135*, 10954.
18. Matteson, D. S.; Majumdar, D. *Organometallics*, **1983**, *2*, 1529.
19. Pan, M.; Wu, C.; Zhuang, X.; Zhang, F.; Su, M.; Tong, Q.; Tung, C. H.; Wang, W. *Organometallics*, **2018**, *37*, 1462.
20. Funabiki, K.; Shibata, A.; Iwata, H.; Hatano, K.; Kubota, Y.; Komura, K.; Ebihara, M.; Matsui, M. *J. Org. Chem.* **2008**, *73*, 4694.
21. Ito, M.; Matsuomi, M.; Murugesu, M. G.; Kobayashi, Y. *J. Org. Chem.* **2001**, *66*, 5881.
22. Hoye, T. R.; Jeffrey, C. S.; Shao, F. *Nat. Protoc.* **2007**, *2*, 2451.
23. Dale, J. A.; Mosher, H. S. *J. Am. Chem. Soc.* **1968**, *90*, 3732.

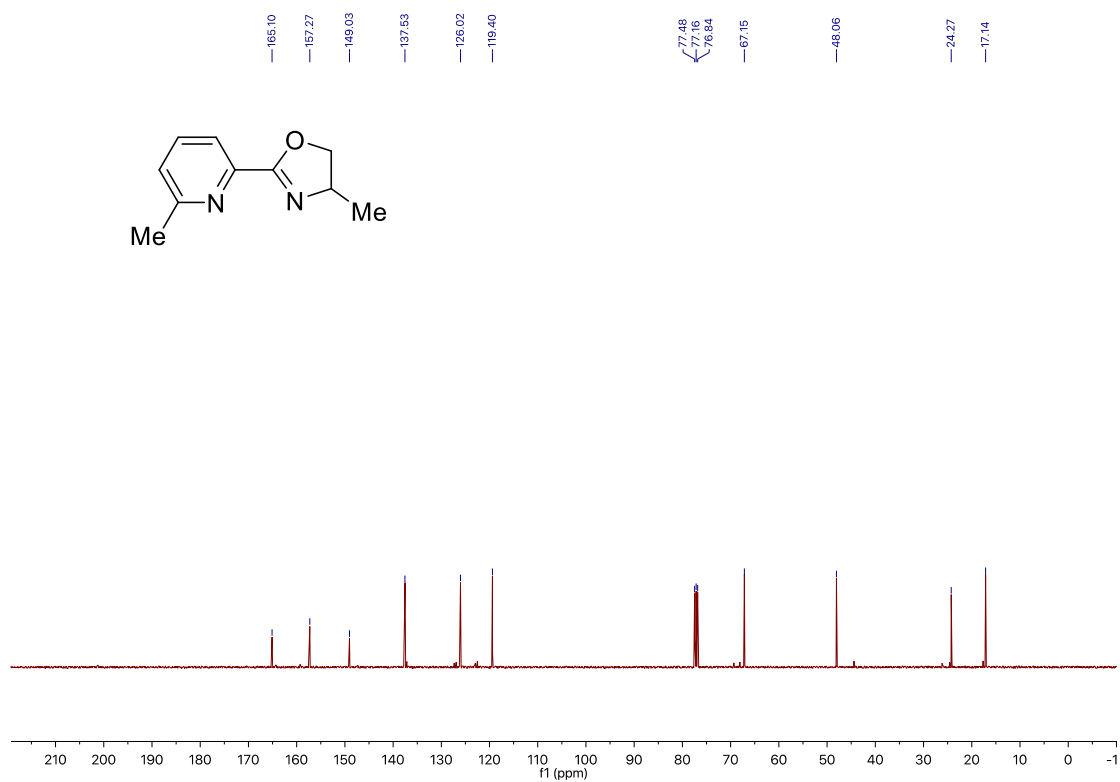
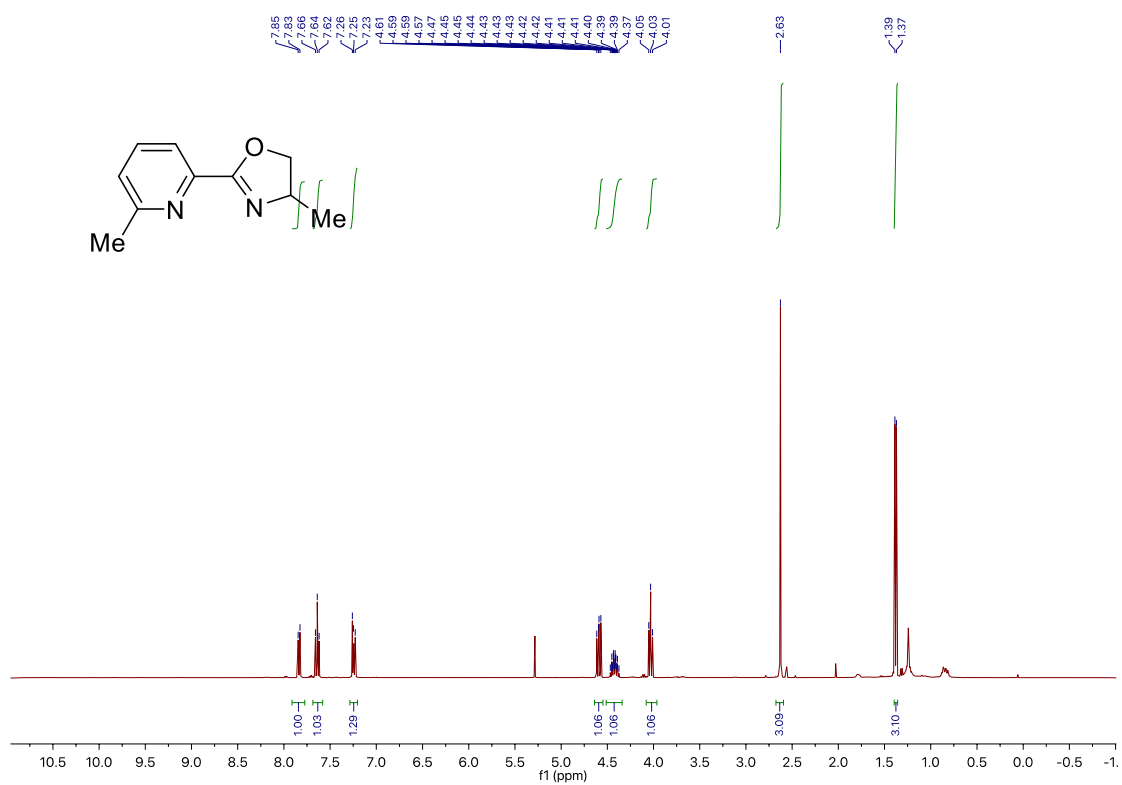
2.8.11 NMR Spectra



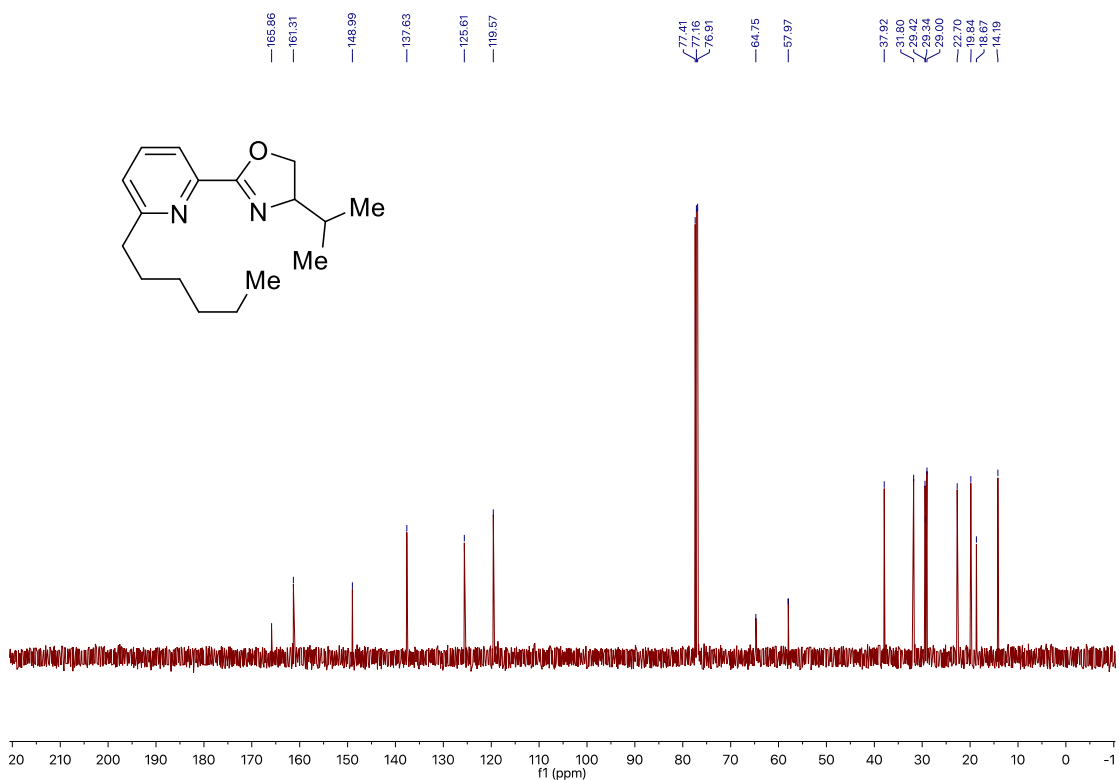
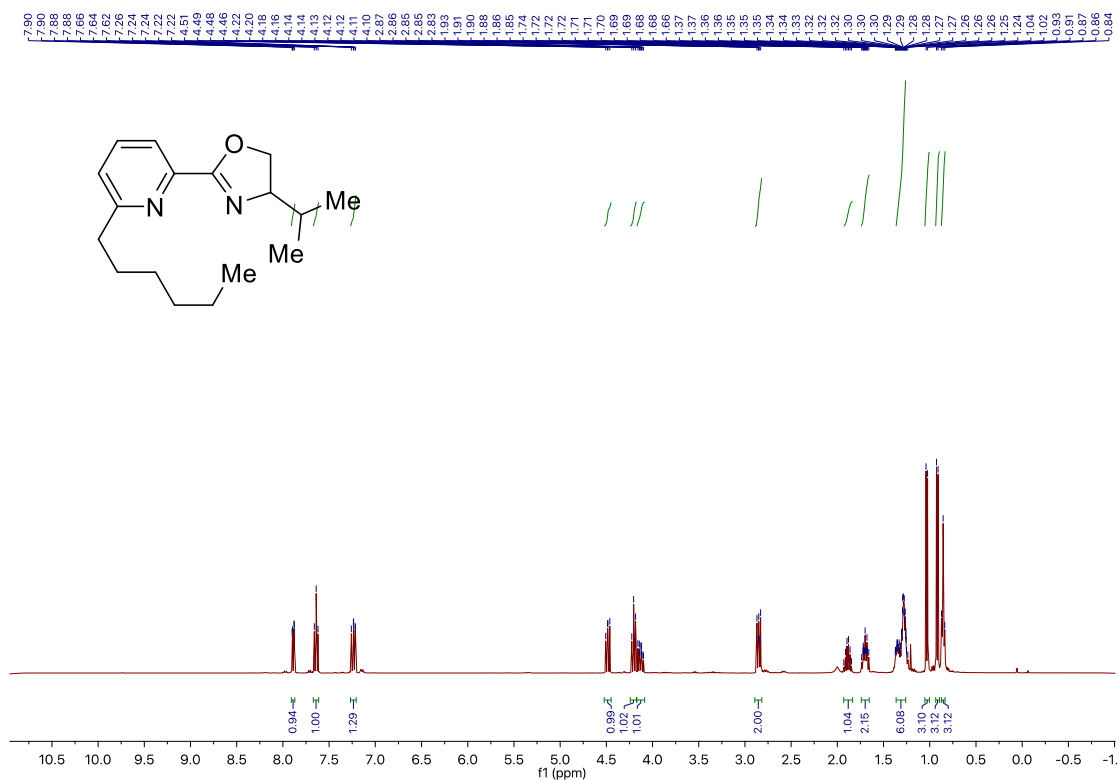
*Site-Selective Ni-Catalyzed Reductive
Coupling of α -Haloboranes with Unactivated Olefins*



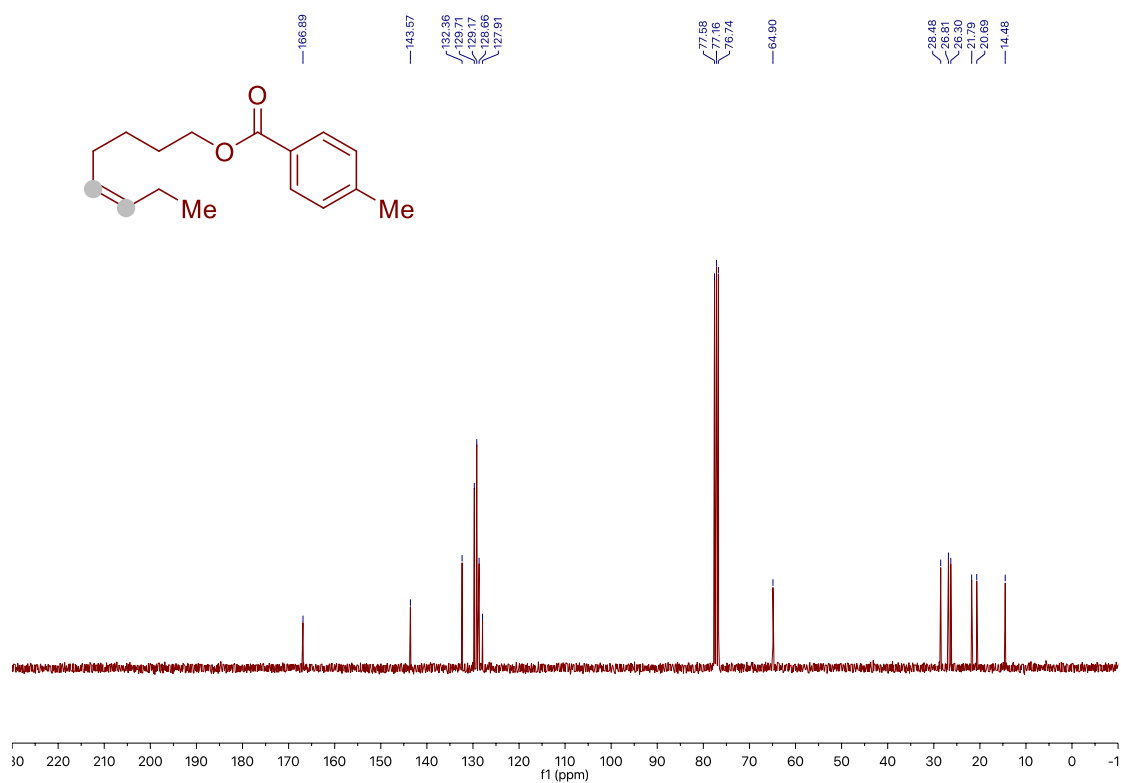
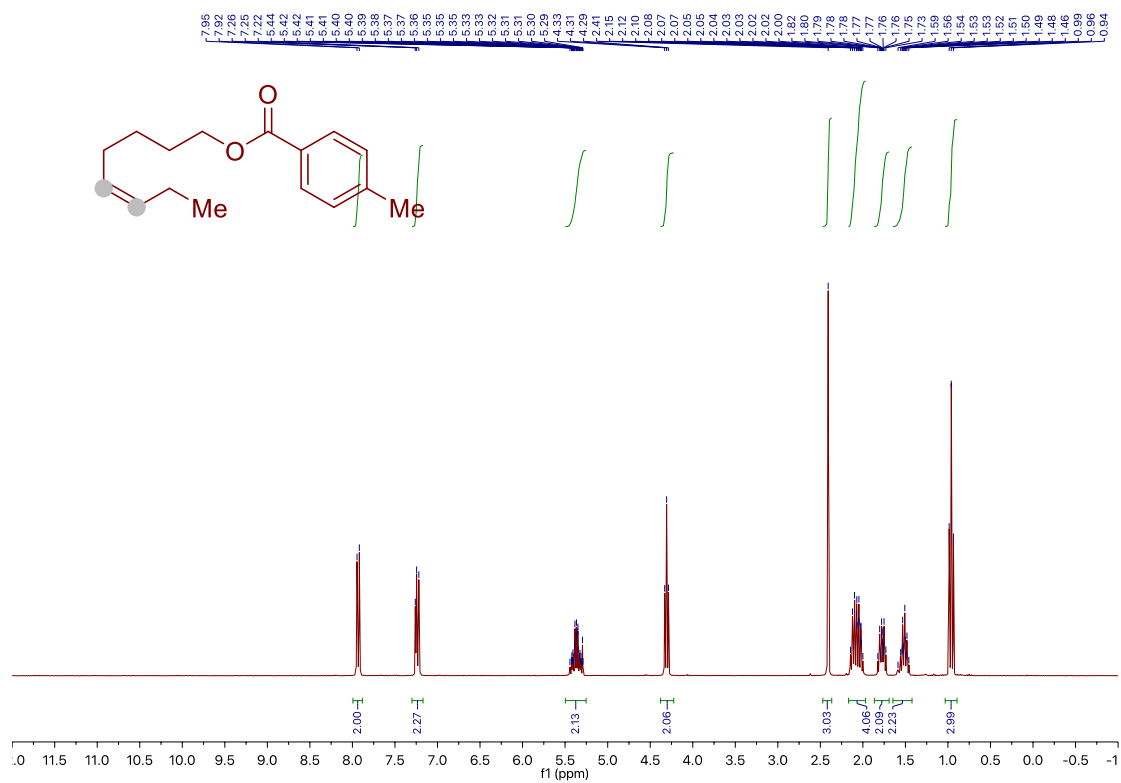
Chapter 2.



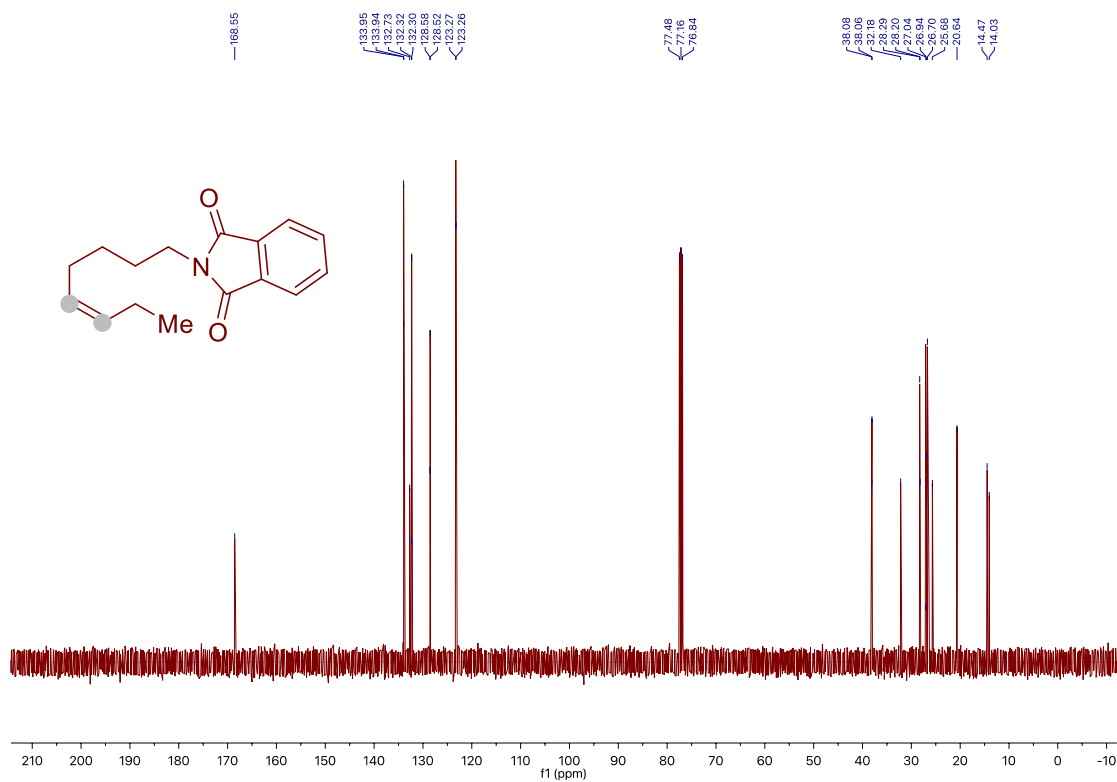
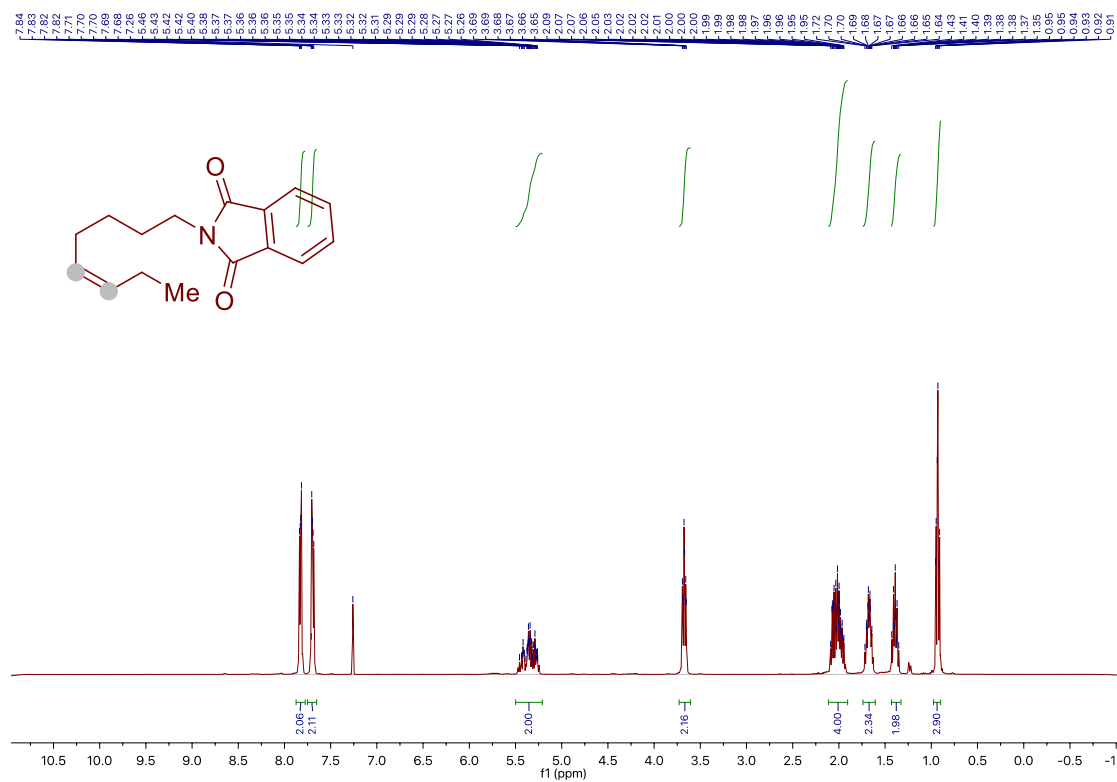
*Site-Selective Ni-Catalyzed Reductive
Coupling of α -Haloboranes with Unactivated Olefins*



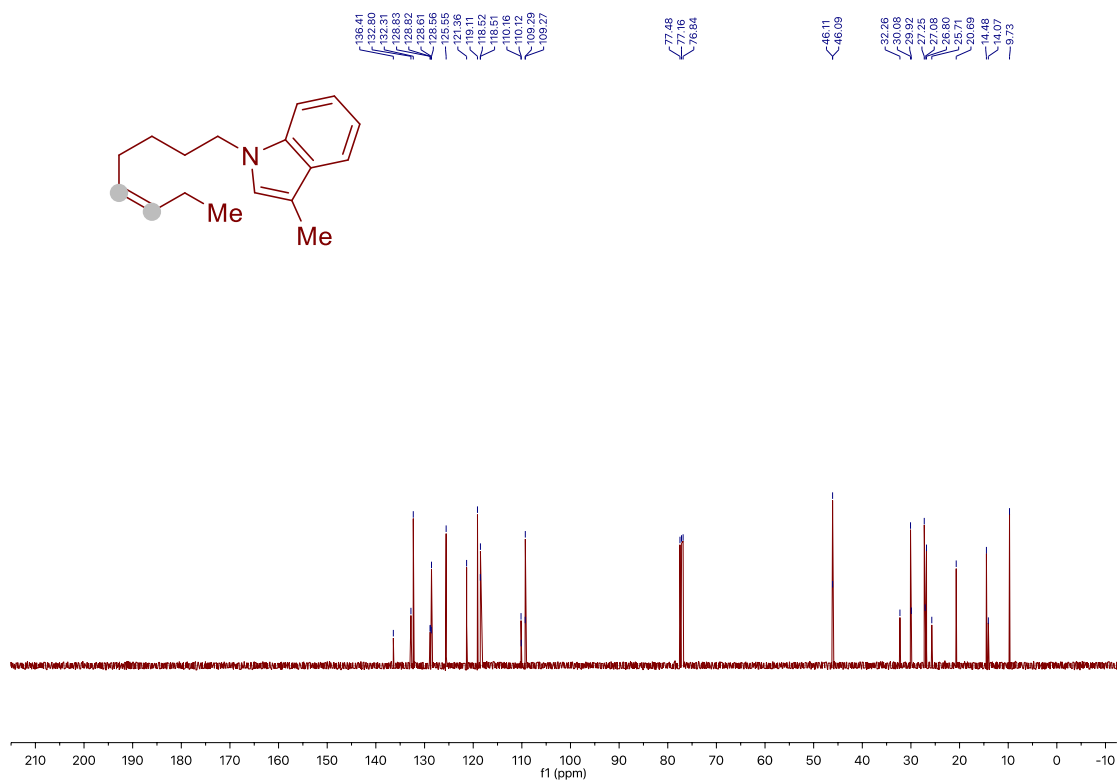
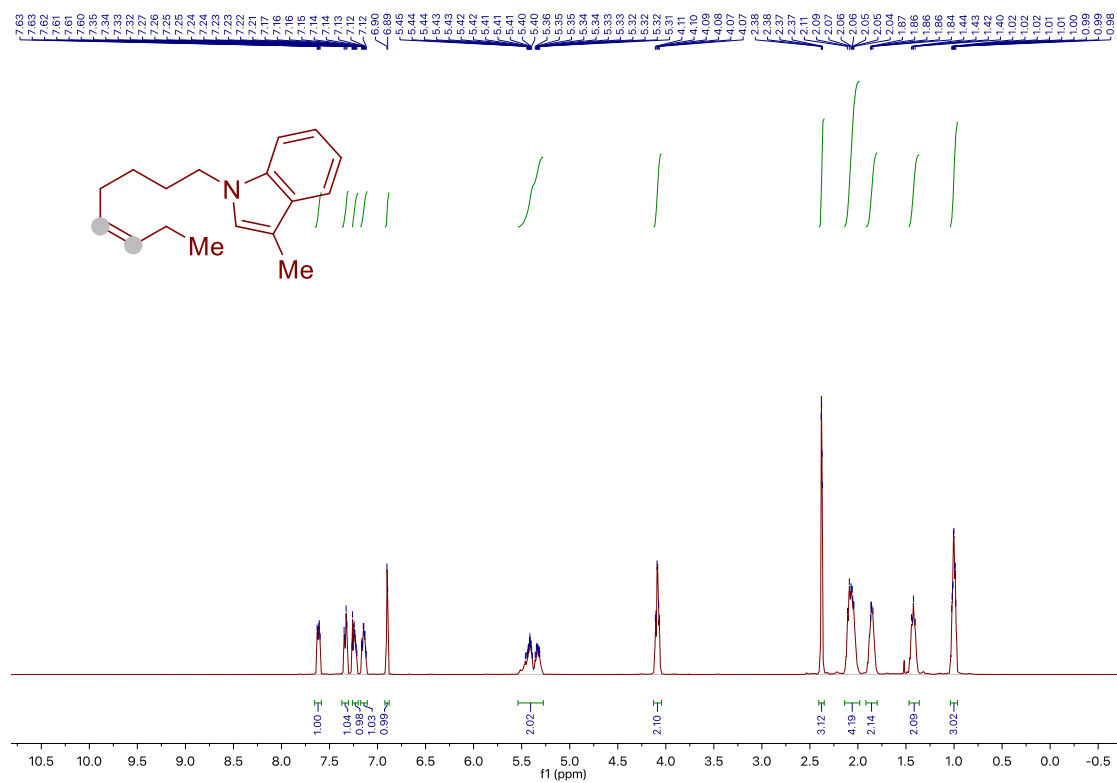
Site-Selective Ni-Catalyzed Reductive Coupling of α -Haloboranes with Unactivated Olefins



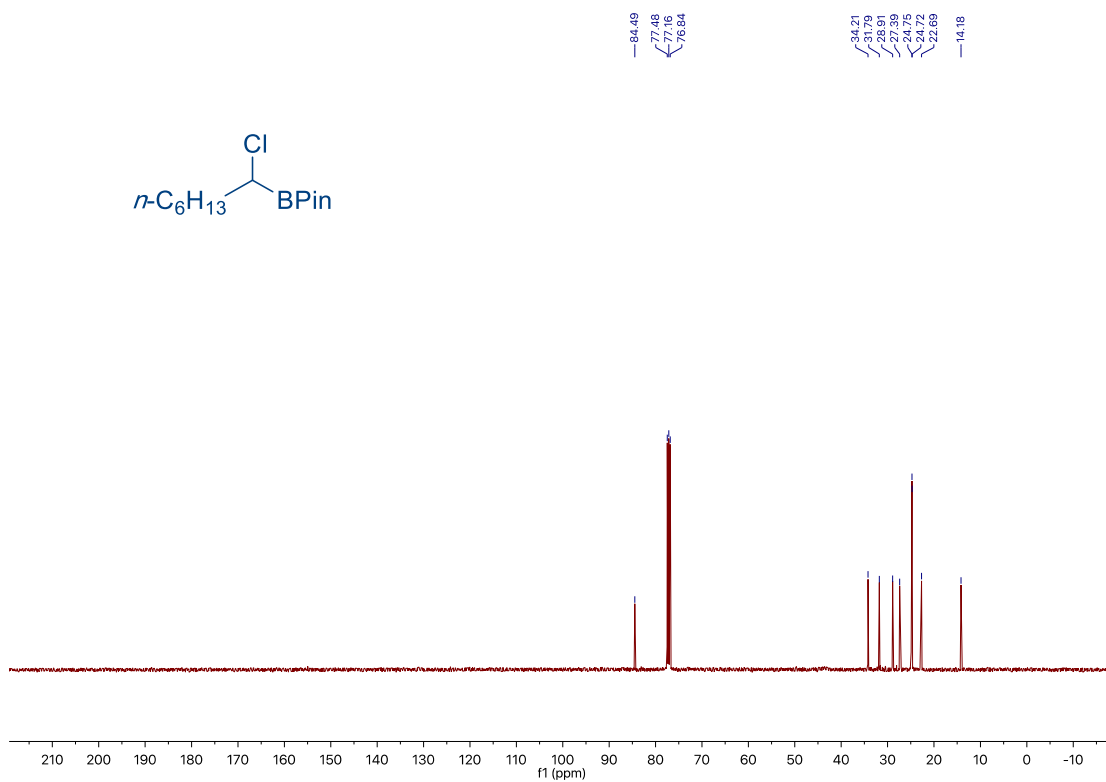
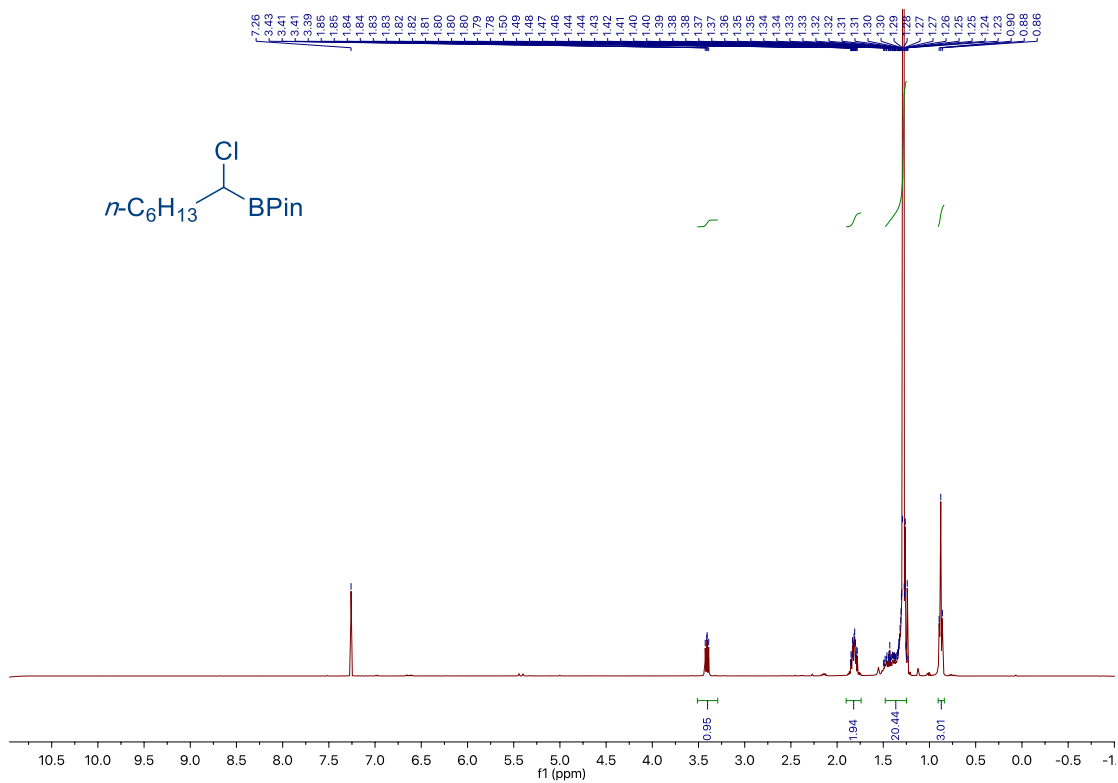
Chapter 2.



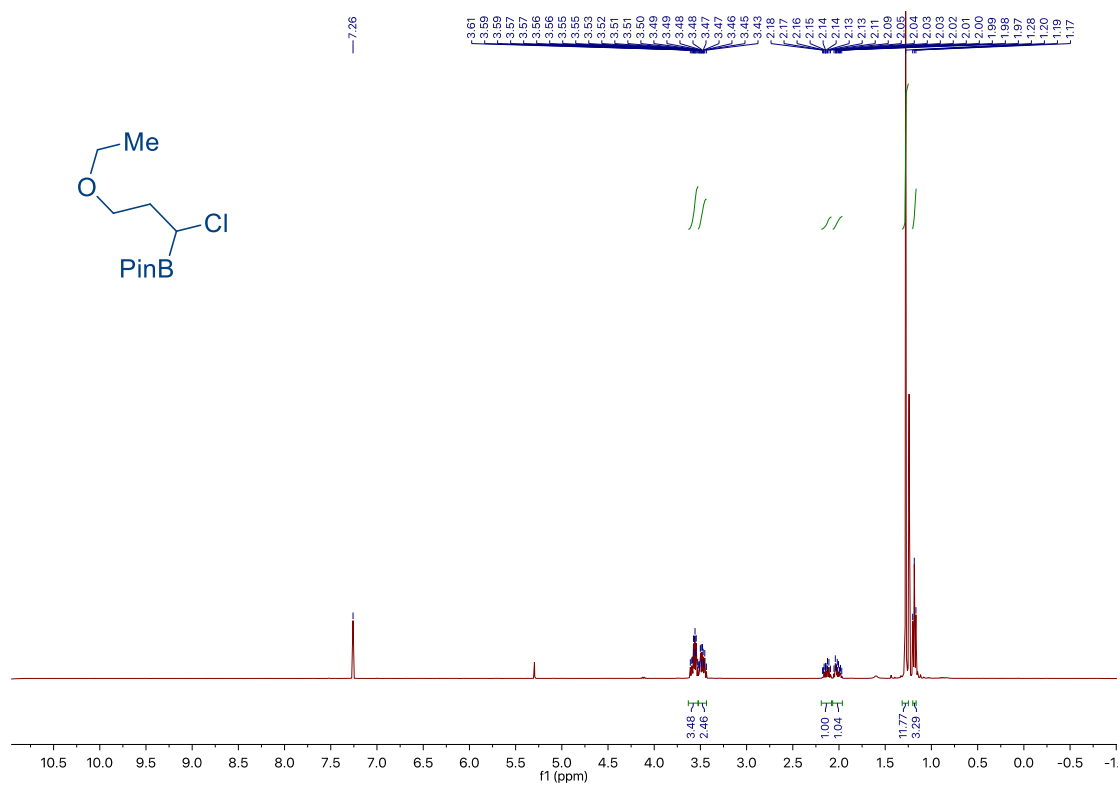
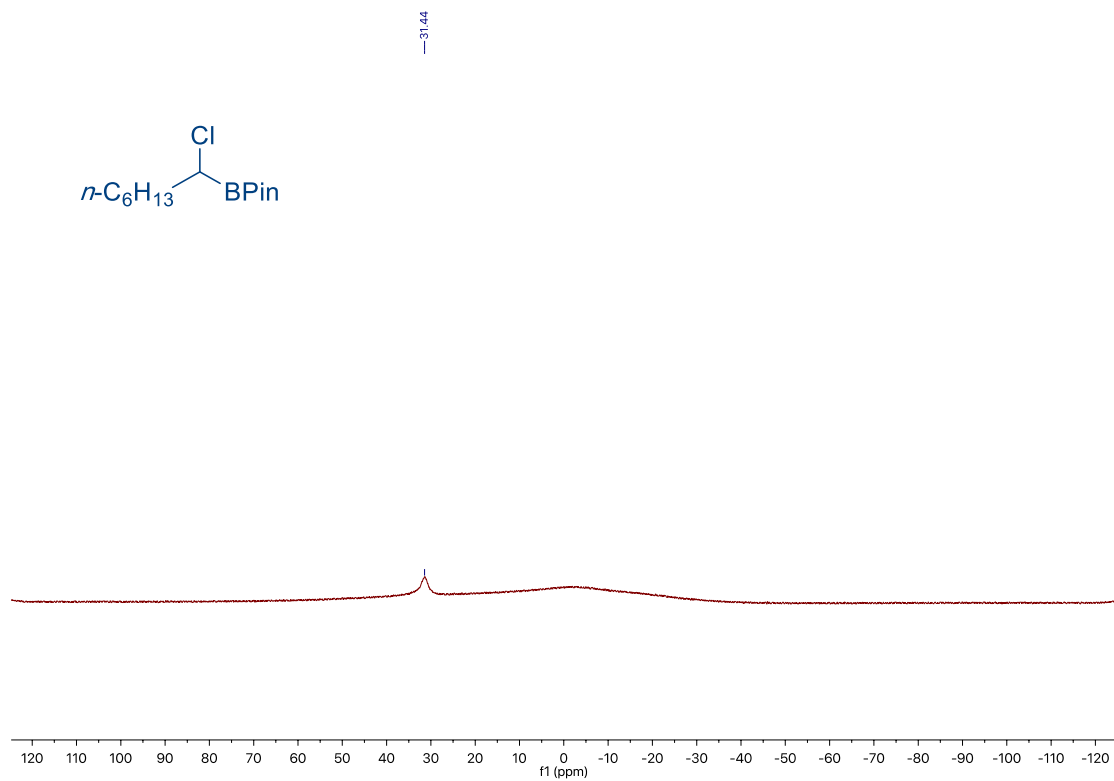
Site-Selective Ni-Catalyzed Reductive Coupling of α -Haloboranes with Unactivated Olefins



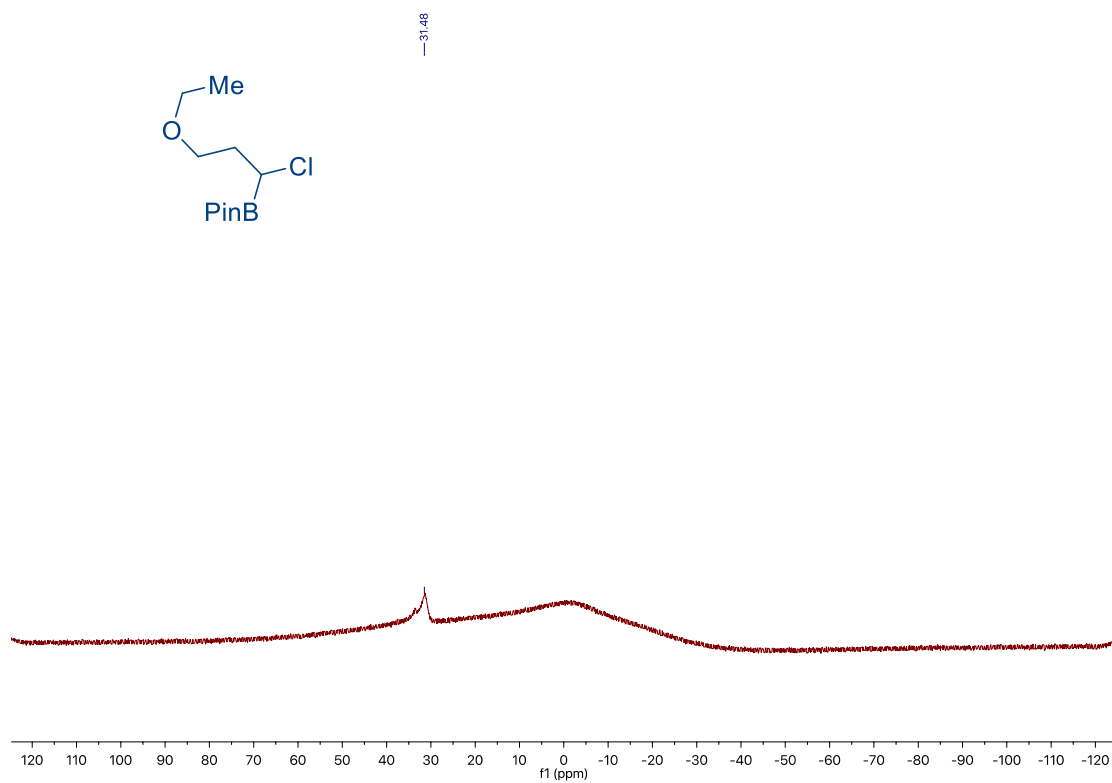
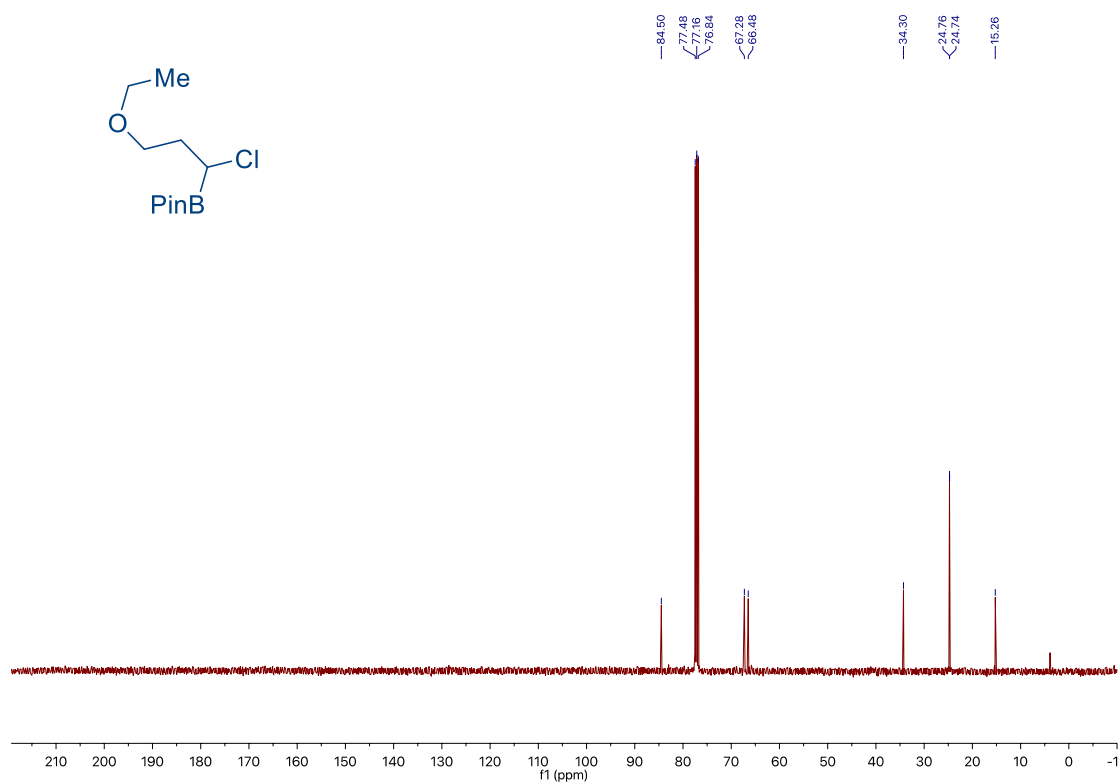
Chapter 2.



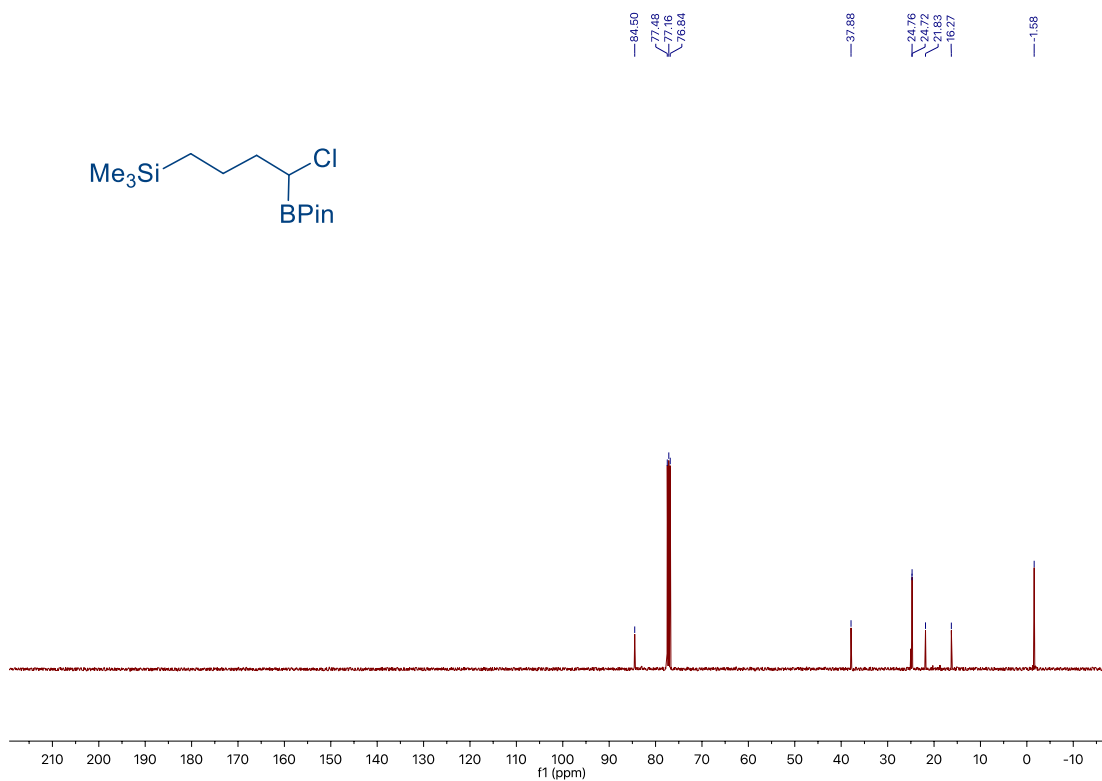
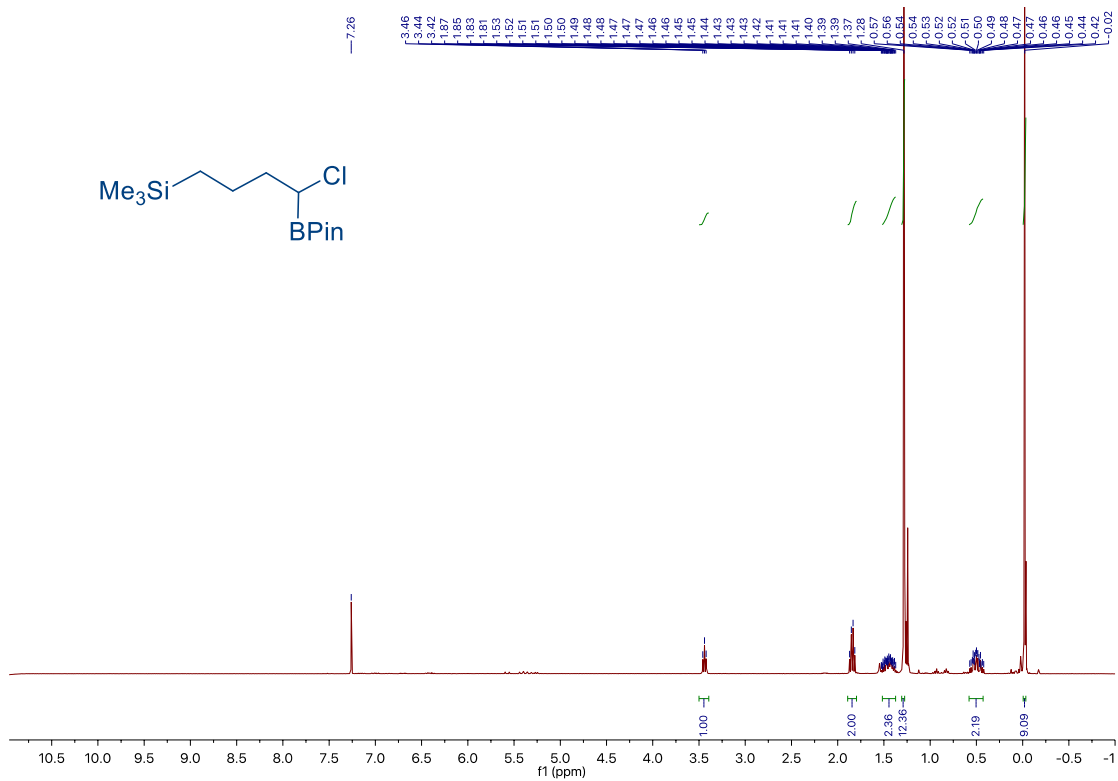
Site-Selective Ni-Catalyzed Reductive
Coupling of α -Haloboranes with Unactivated Olefins



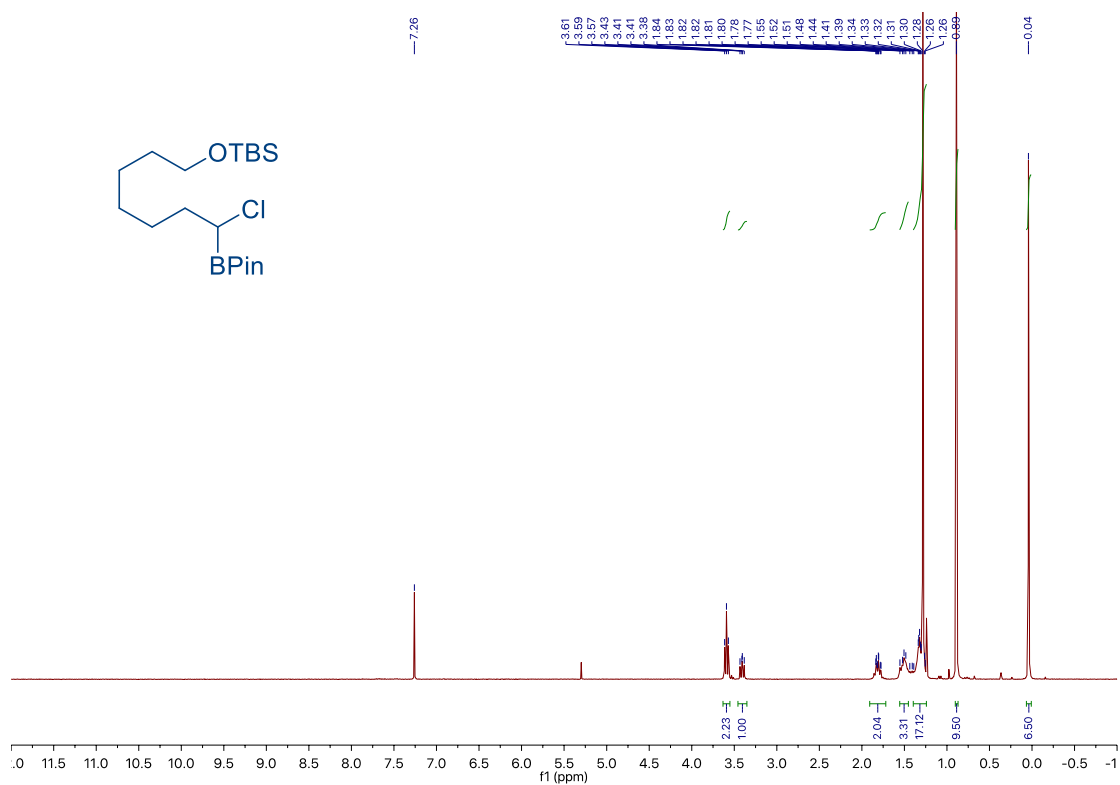
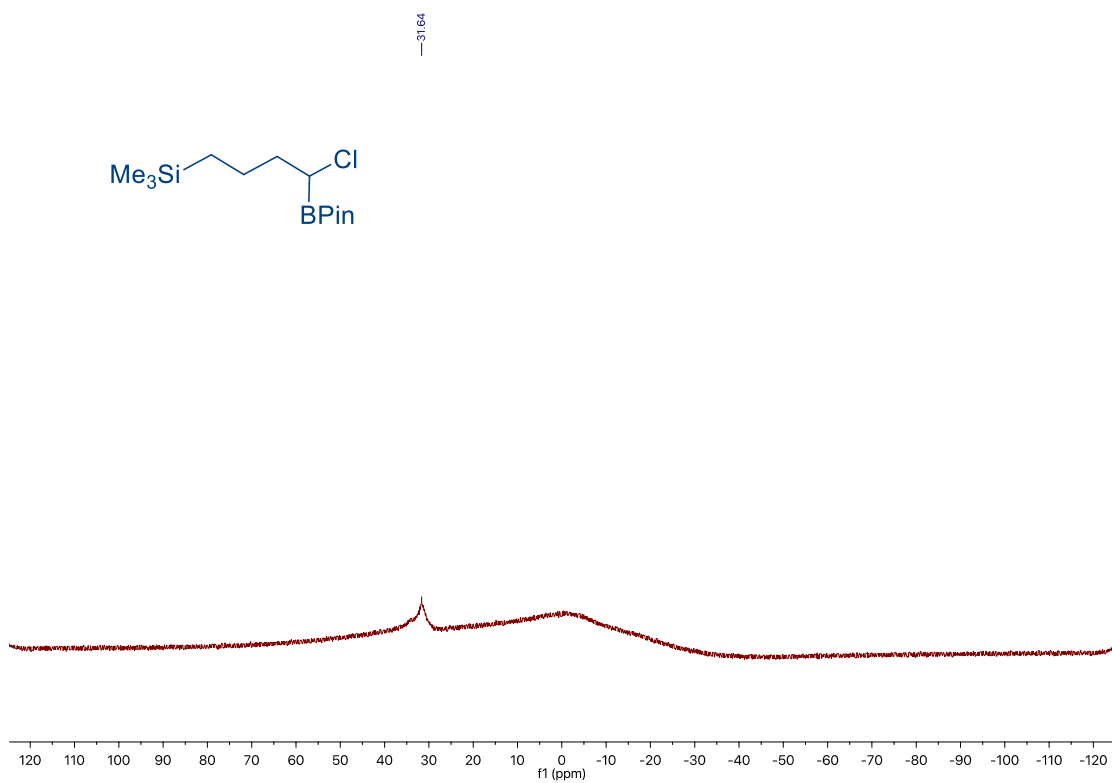
Chapter 2.



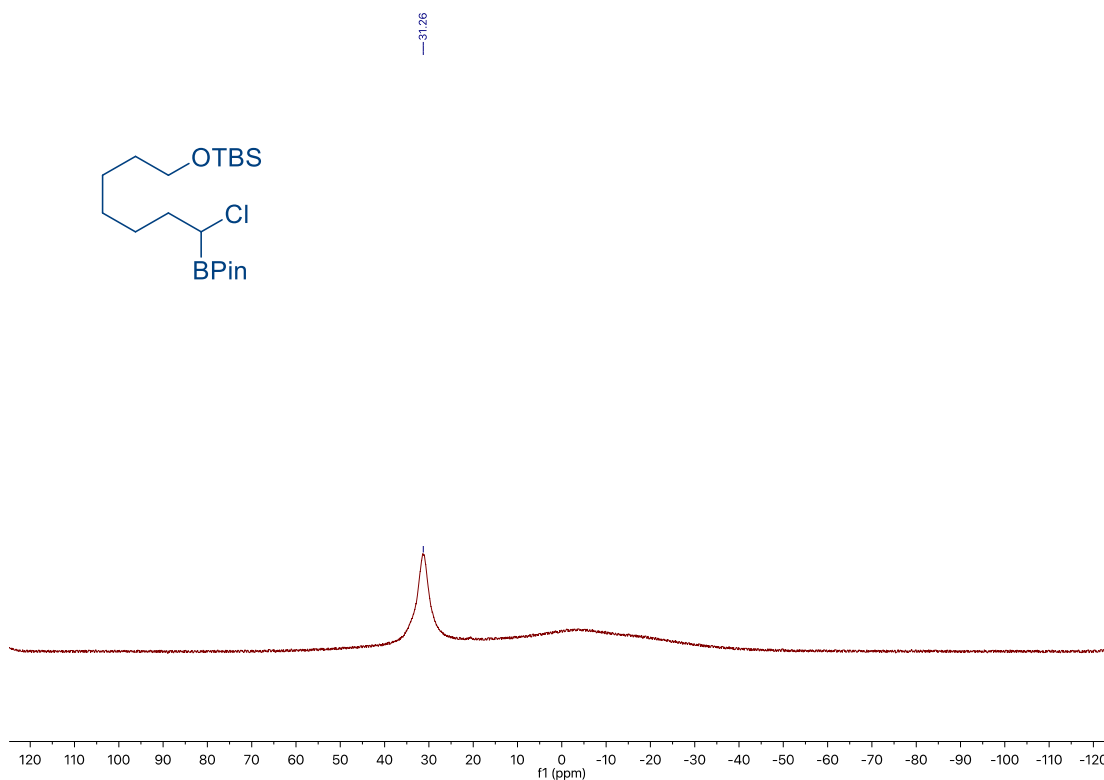
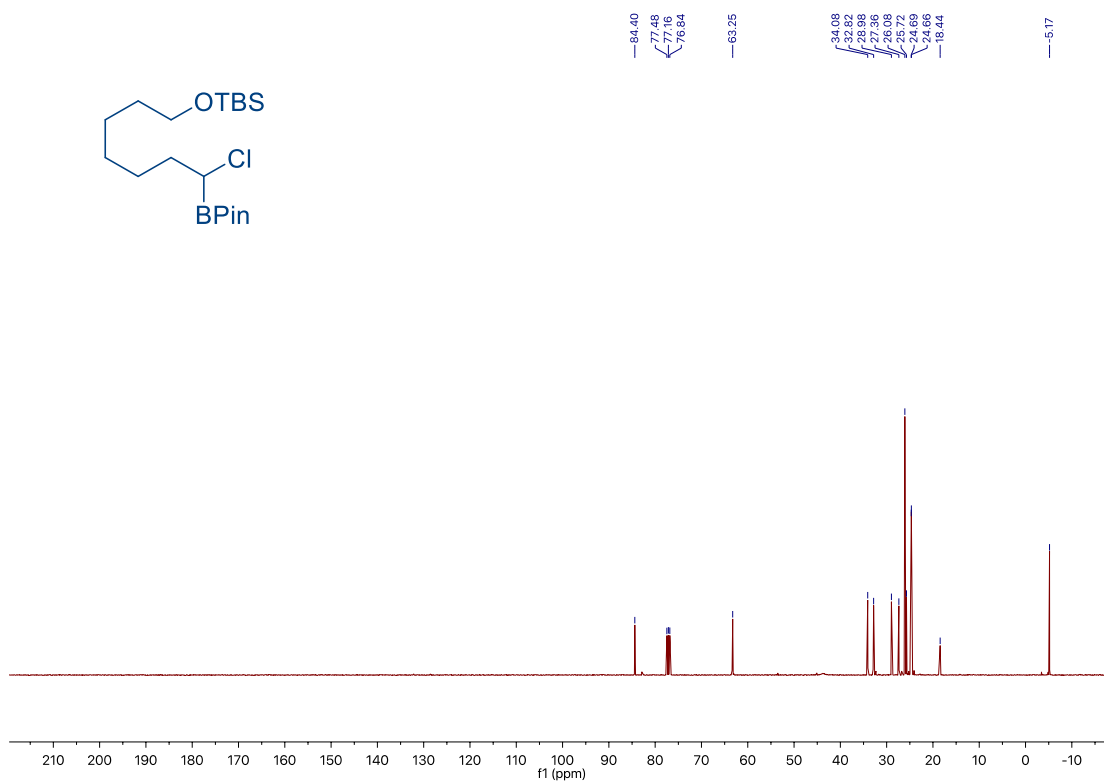
Site-Selective Ni-Catalyzed Reductive
Coupling of α -Haloboranes with Unactivated Olefins



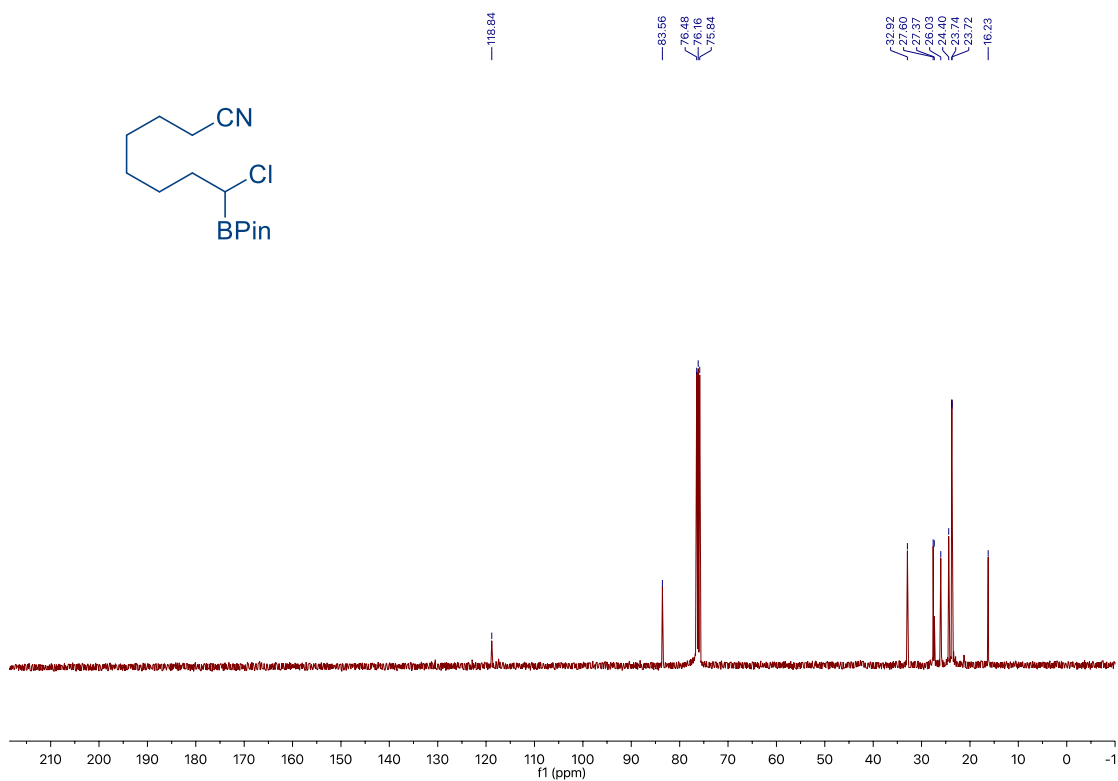
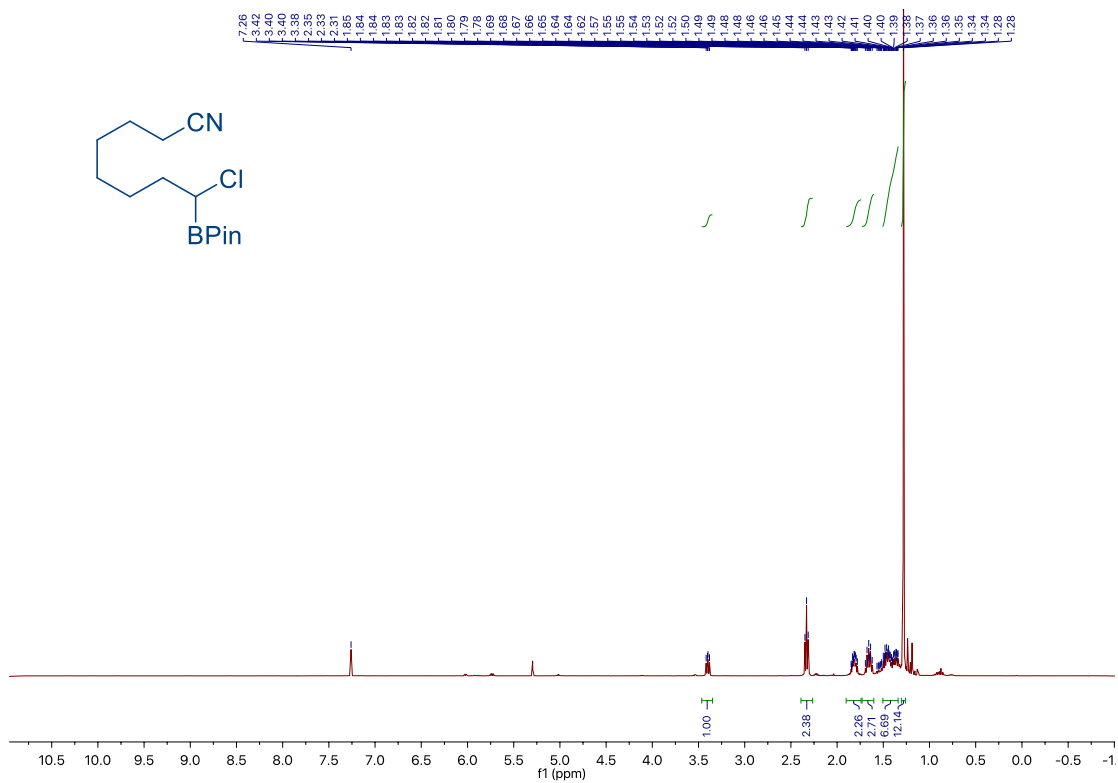
Chapter 2.



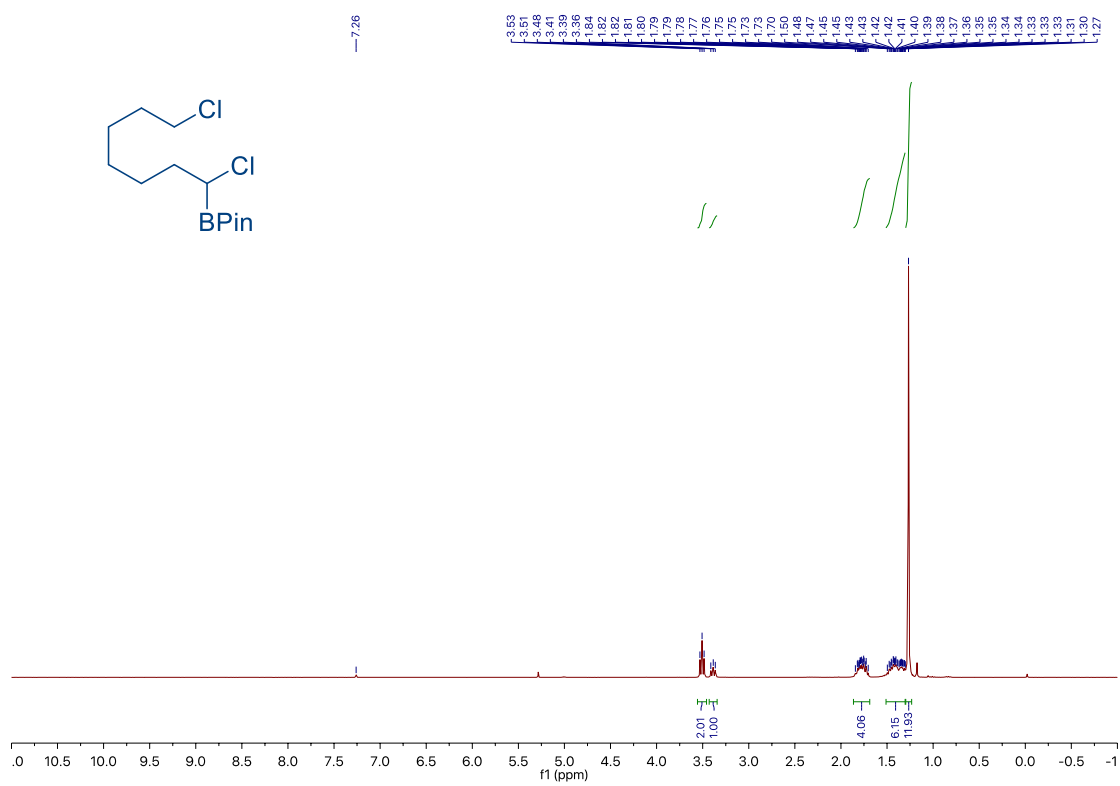
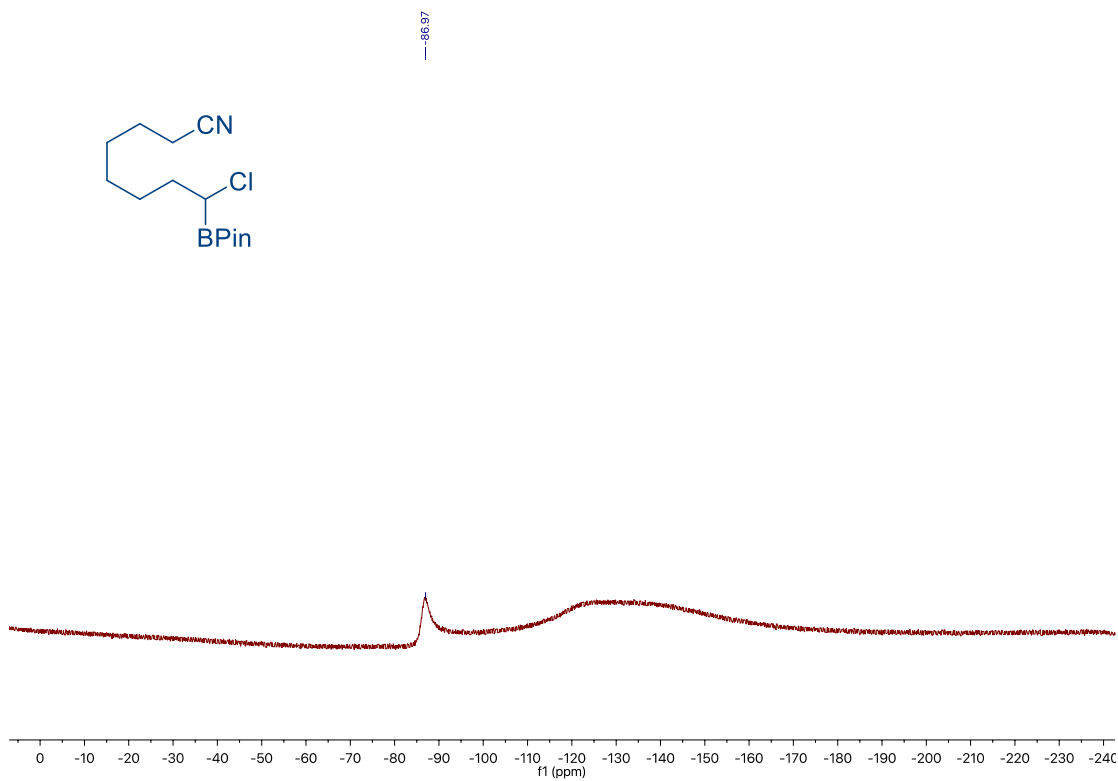
Site-Selective Ni-Catalyzed Reductive
Coupling of α -Haloboranes with Unactivated Olefins



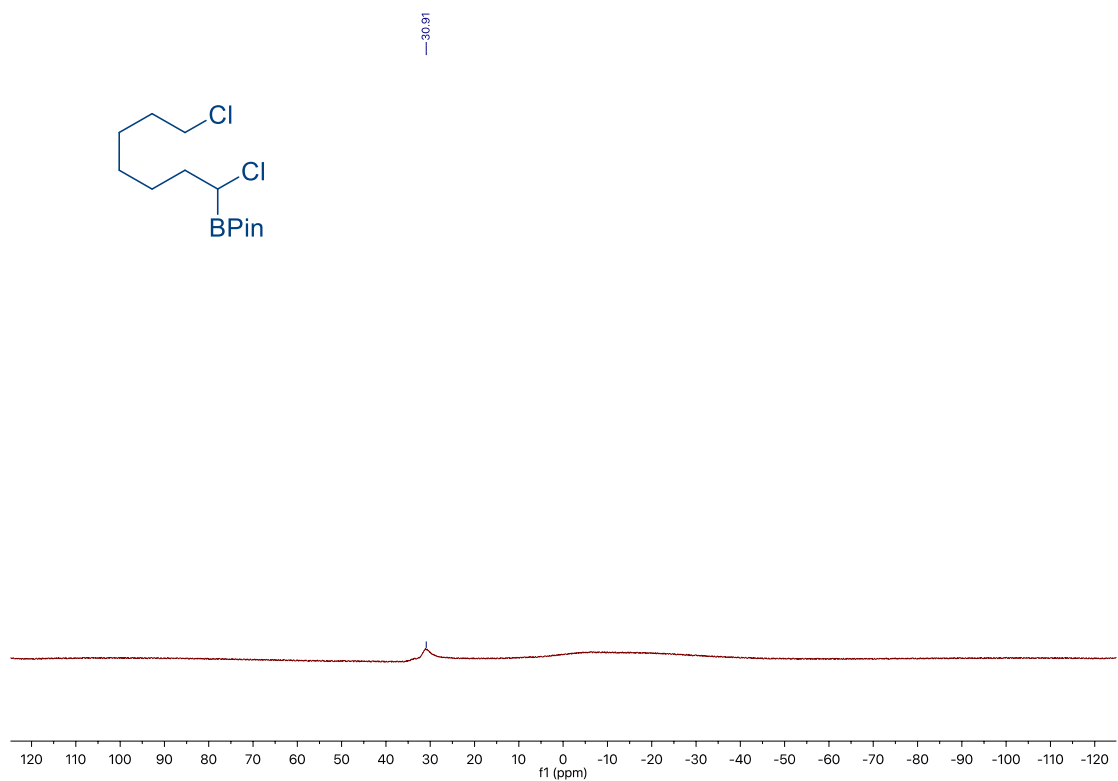
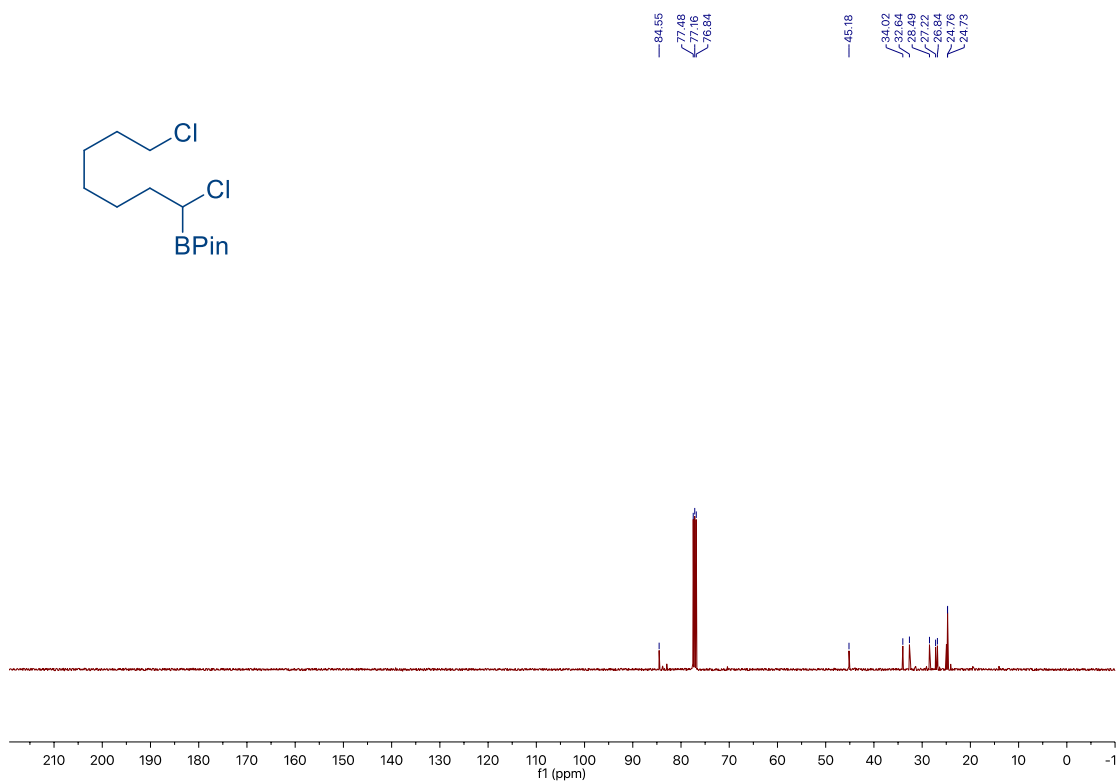
Chapter 2.



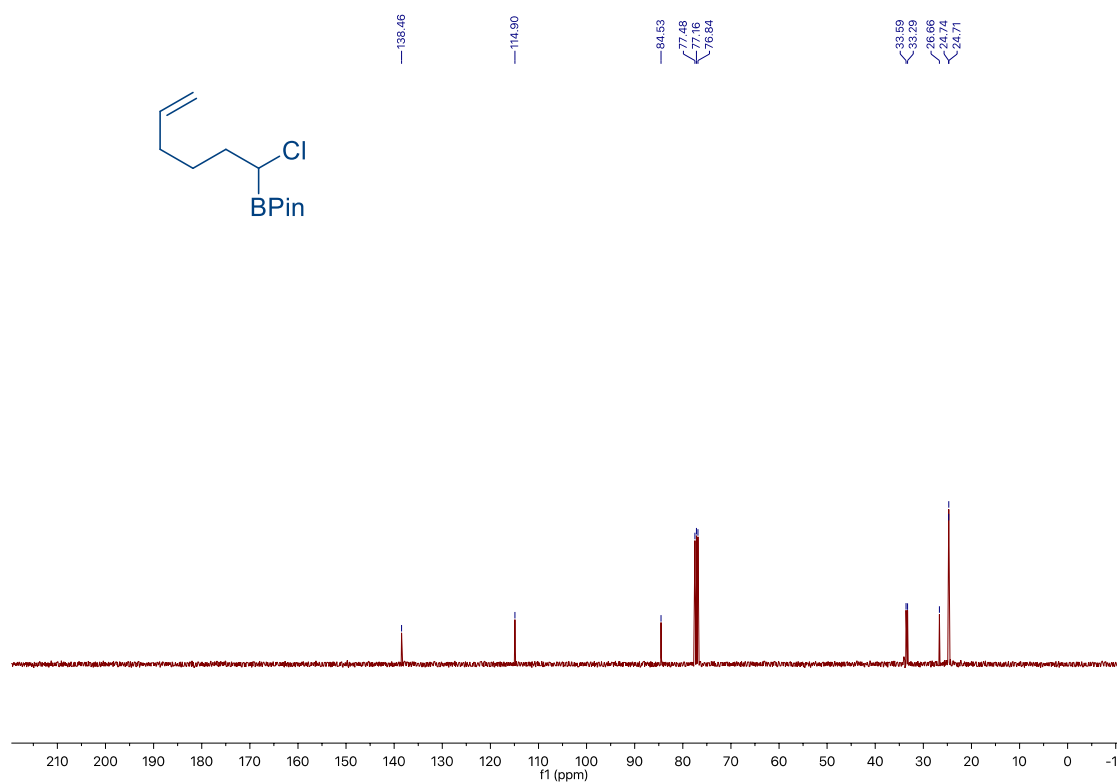
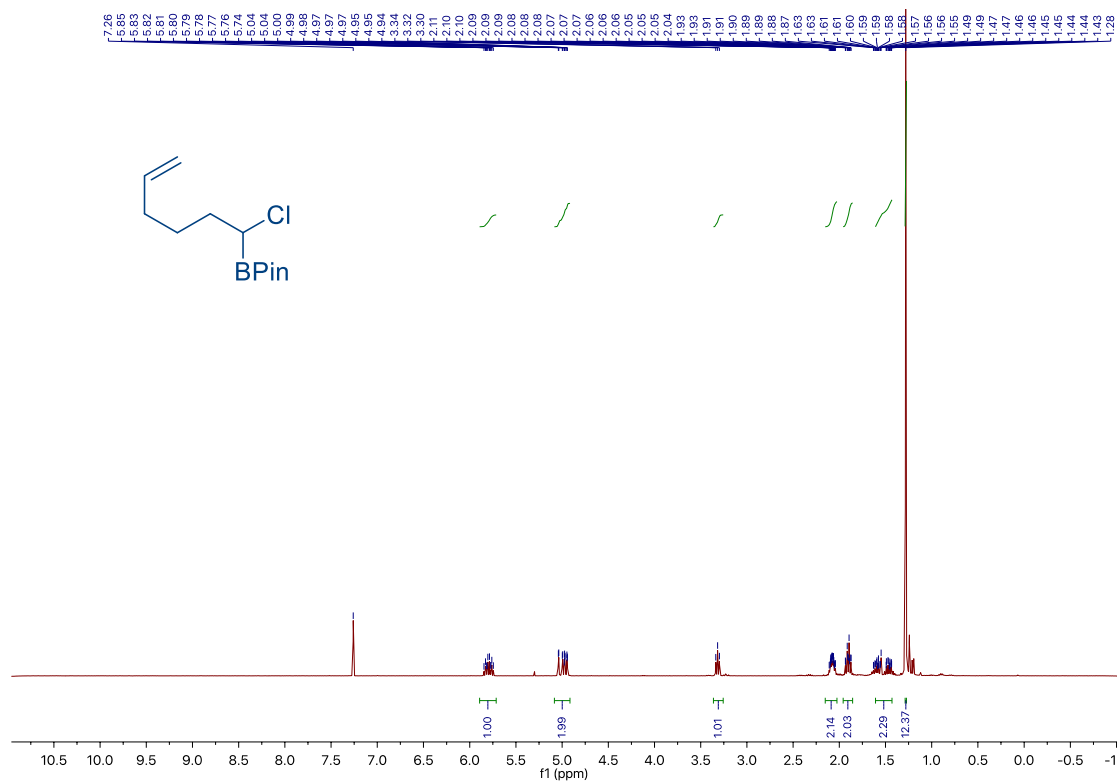
Site-Selective Ni-Catalyzed Reductive
Coupling of α -Haloboranes with Unactivated Olefins



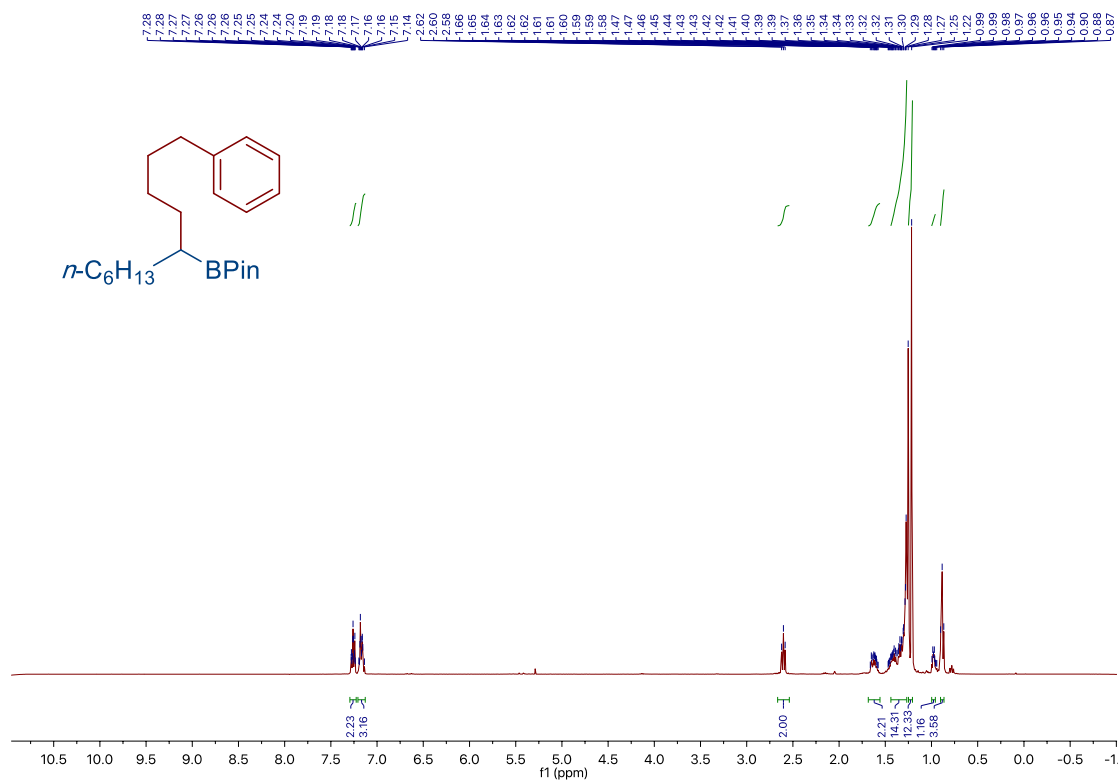
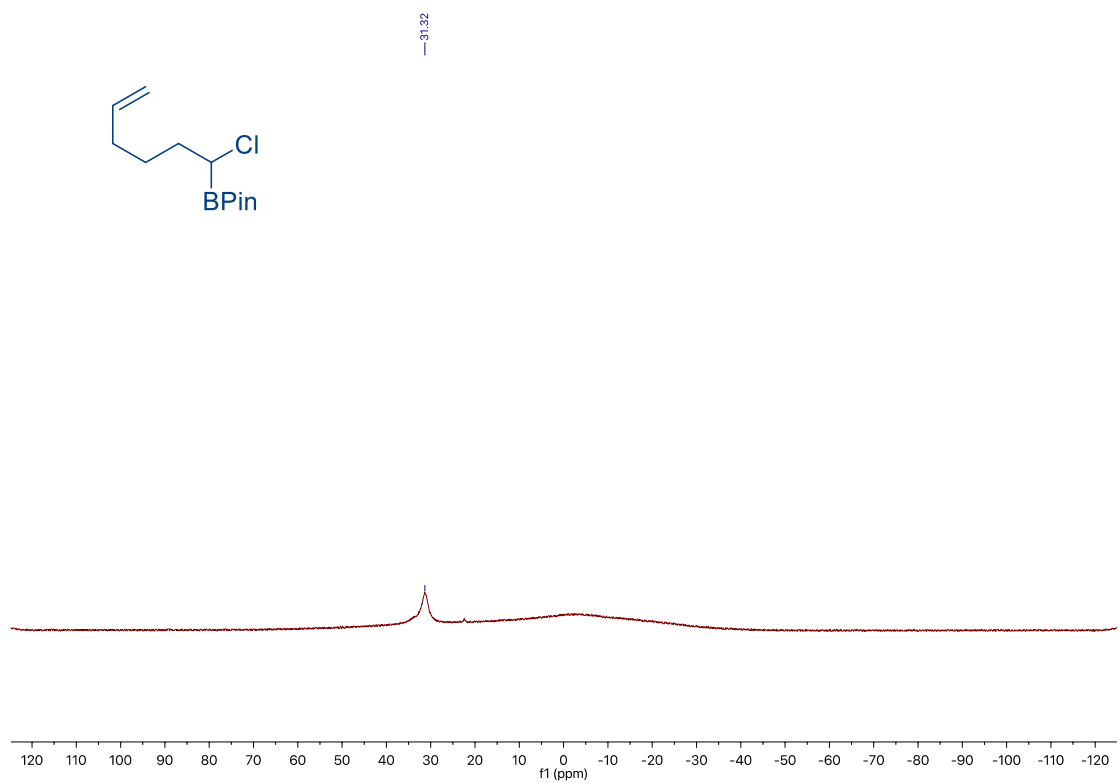
Chapter 2.



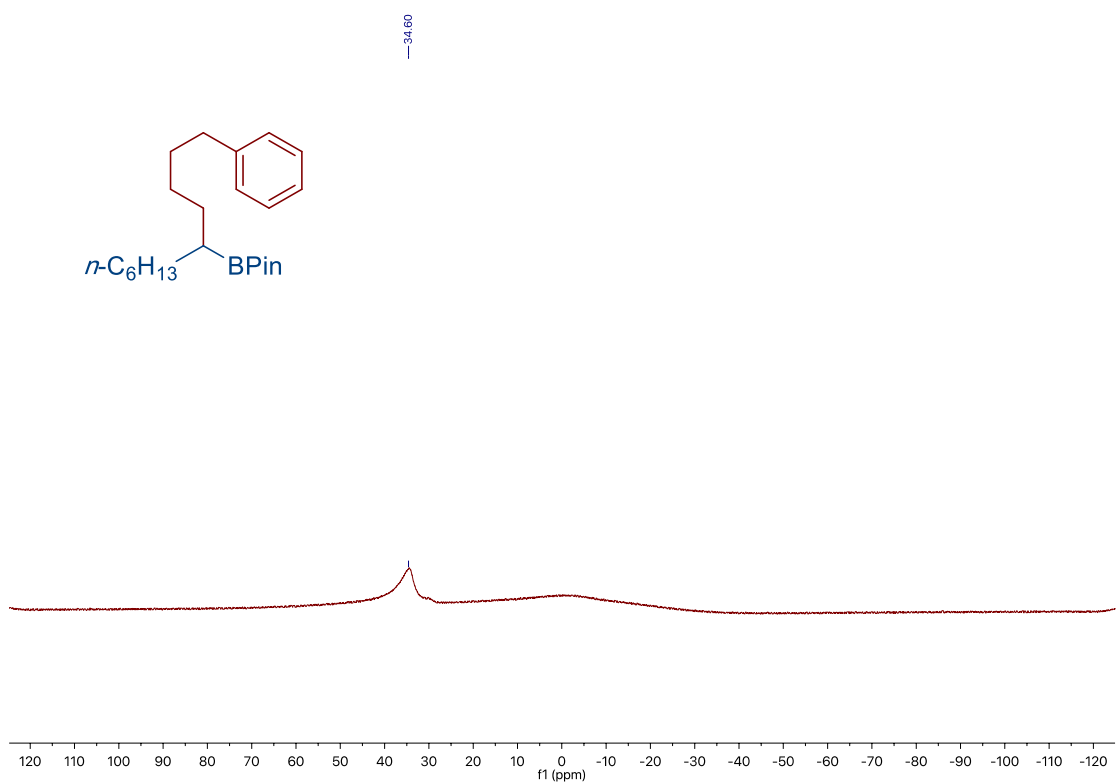
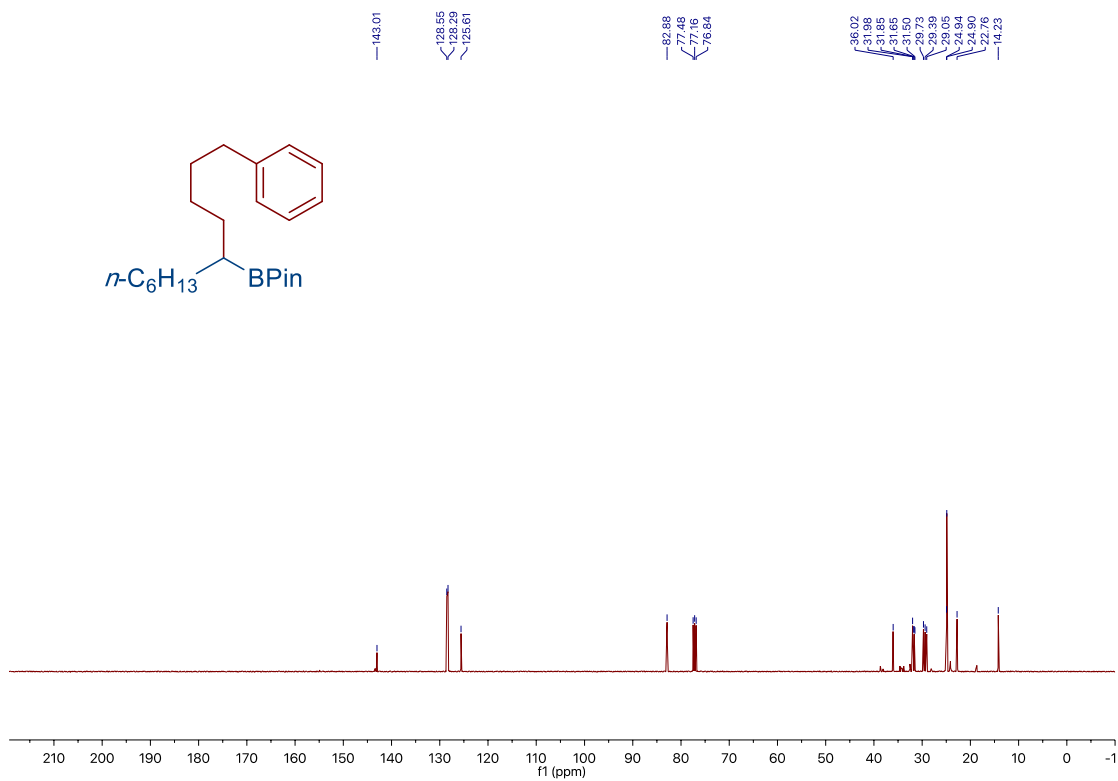
Site-Selective Ni-Catalyzed Reductive Coupling of α -Haloboranes with Unactivated Olefins



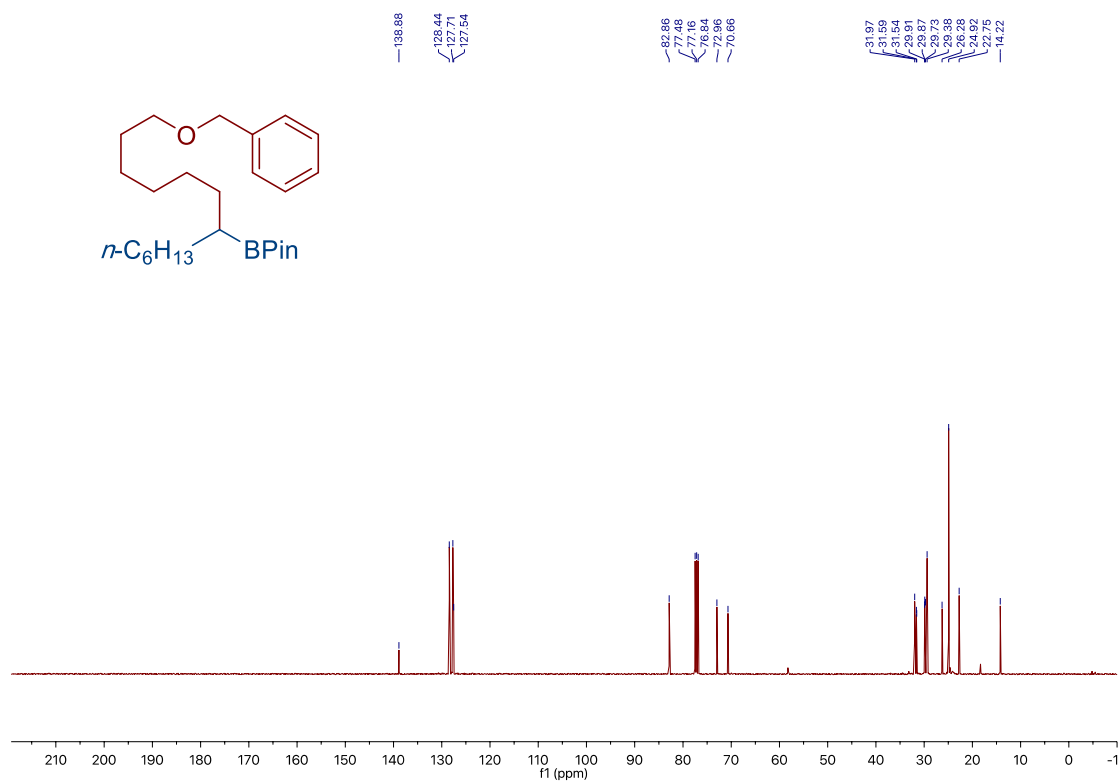
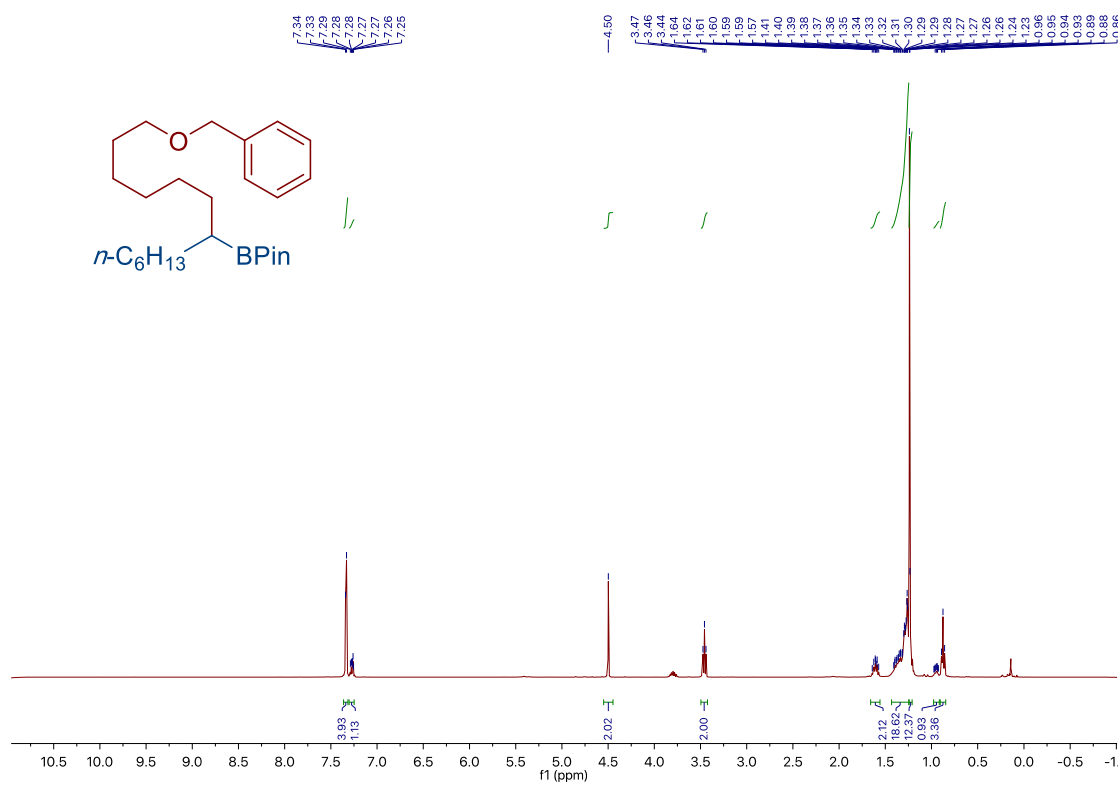
Chapter 2.



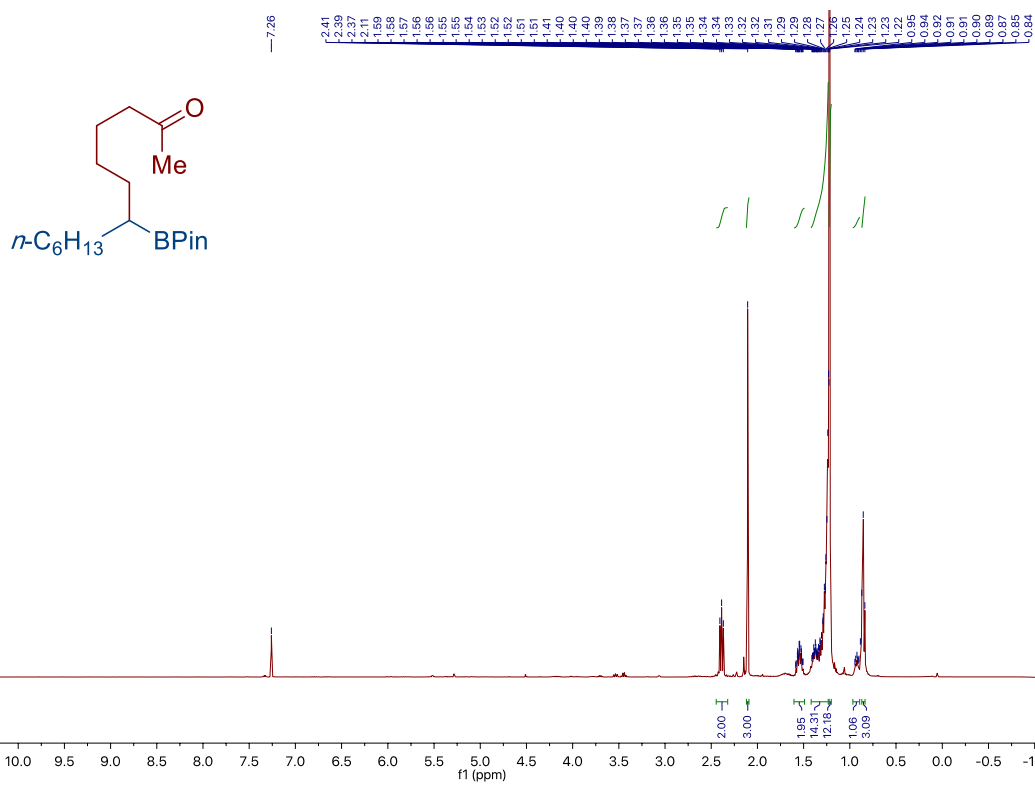
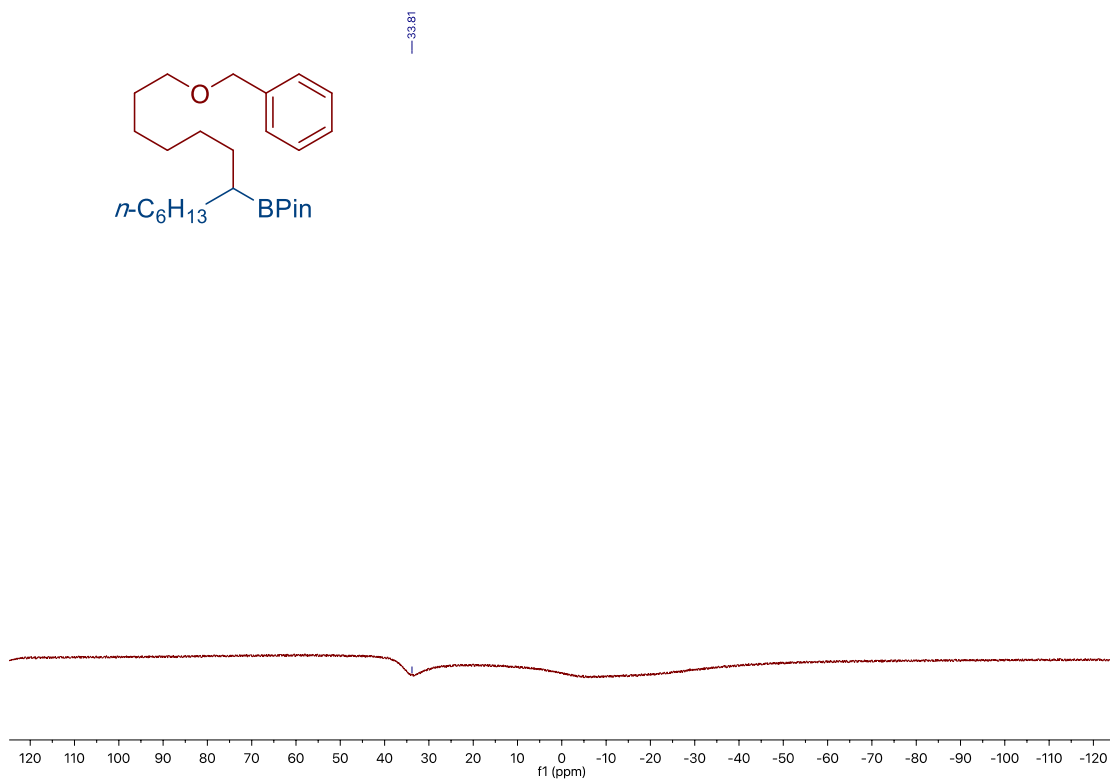
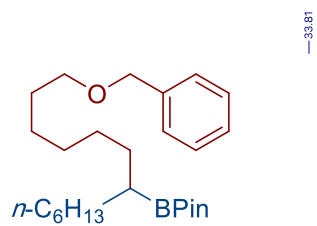
Site-Selective Ni-Catalyzed Reductive
Coupling of α -Haloboranes with Unactivated Olefins



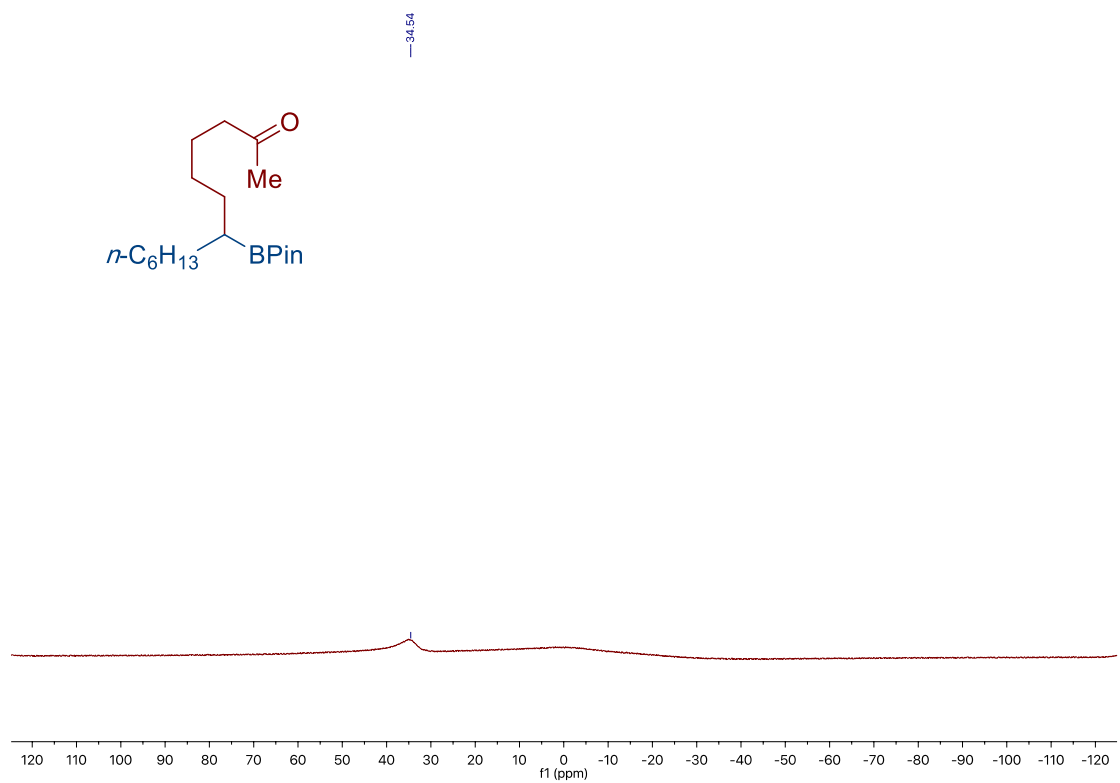
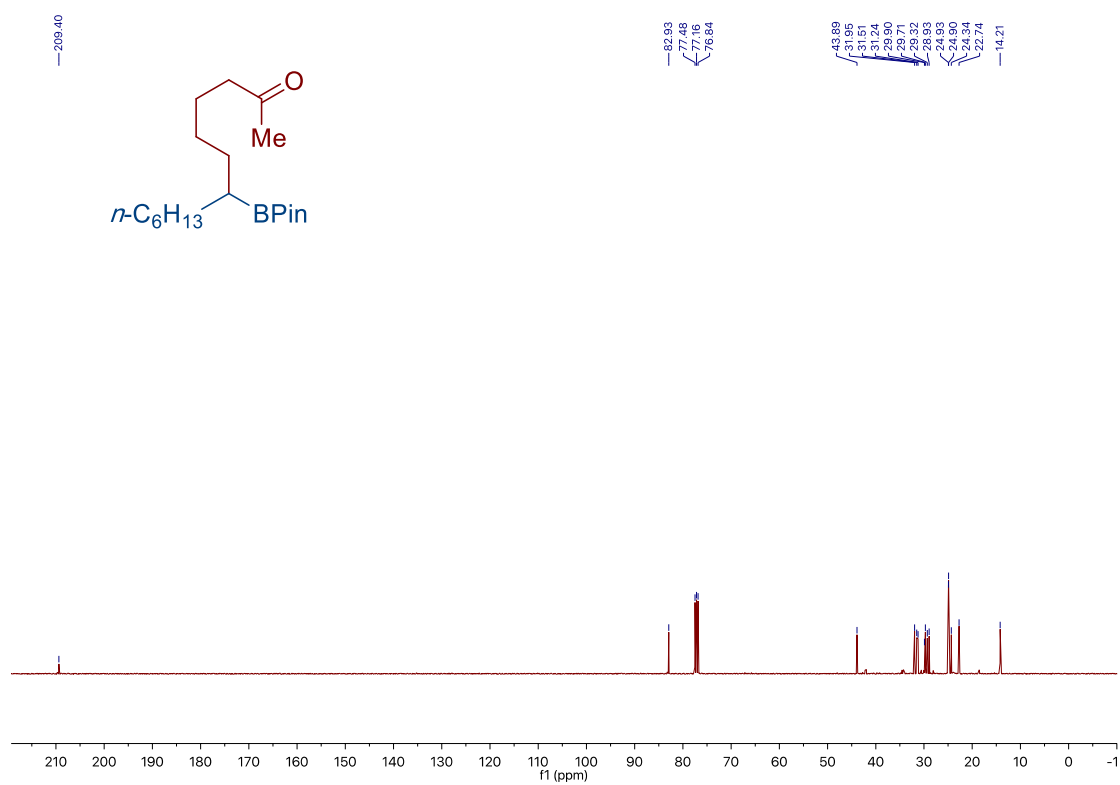
Chapter 2.



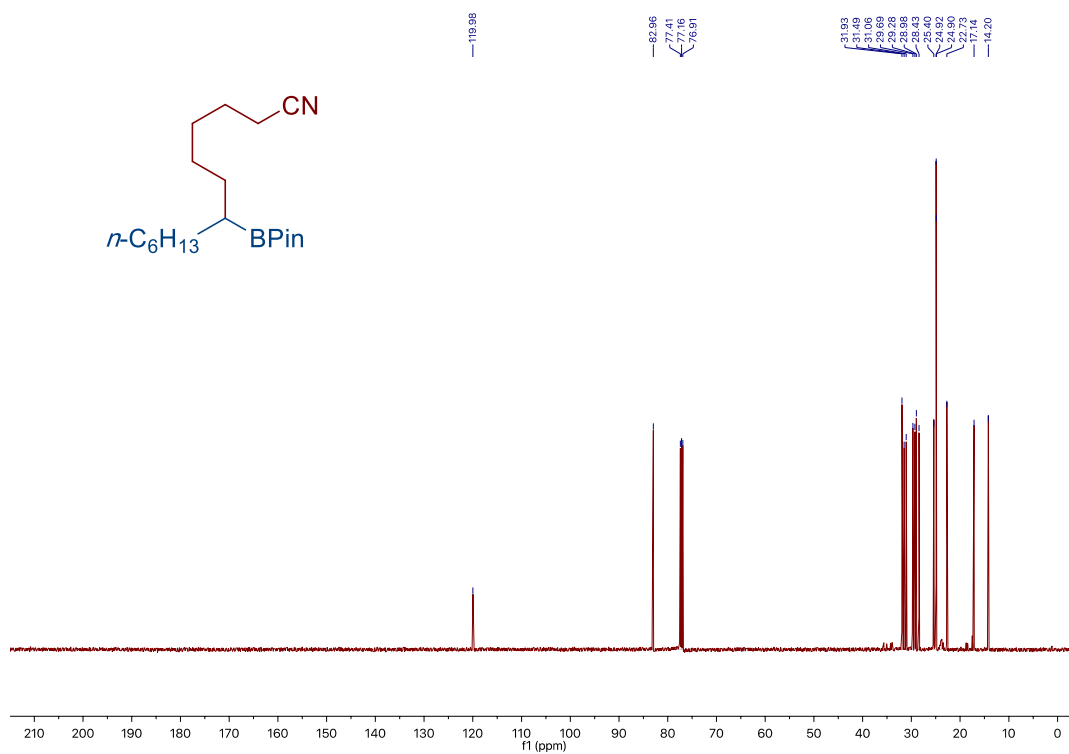
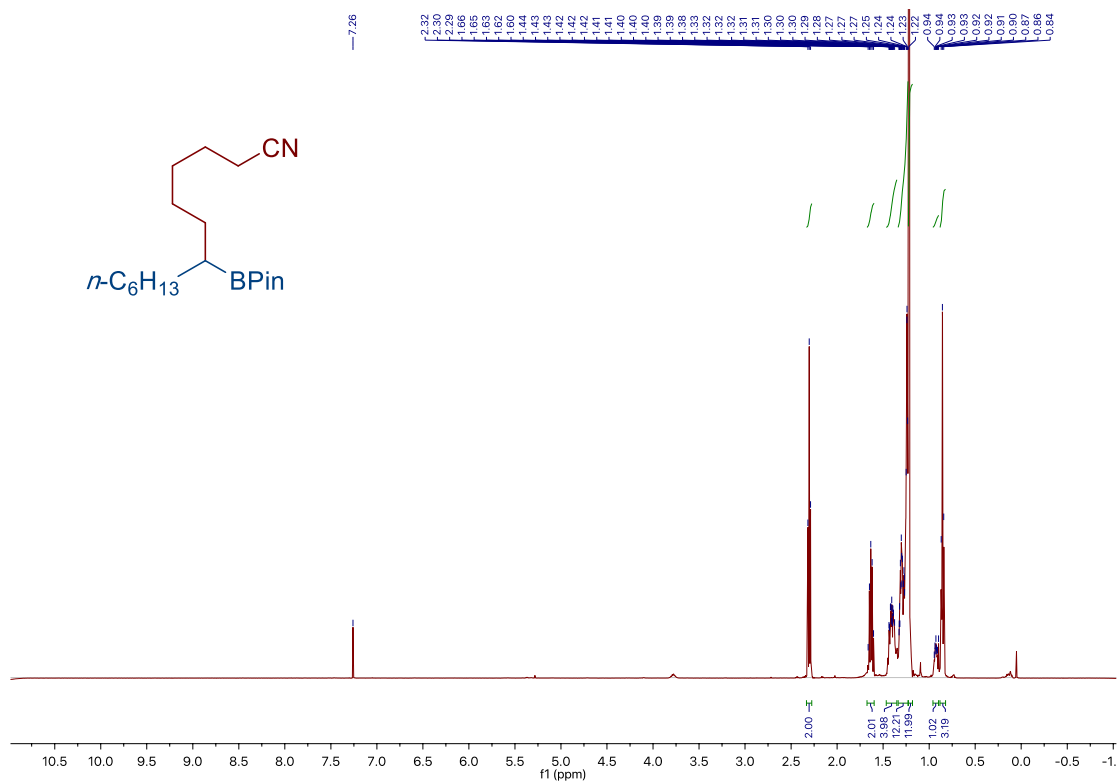
*Site-Selective Ni-Catalyzed Reductive
Coupling of α -Haloboranes with Unactivated Olefins*



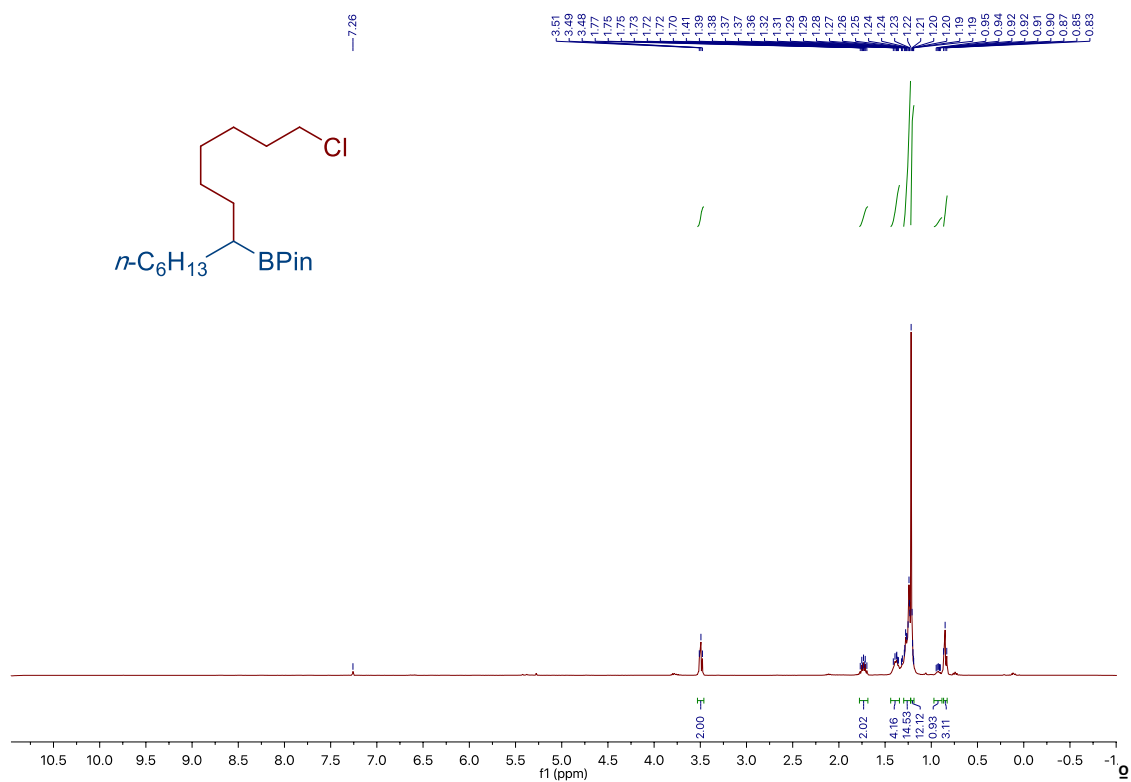
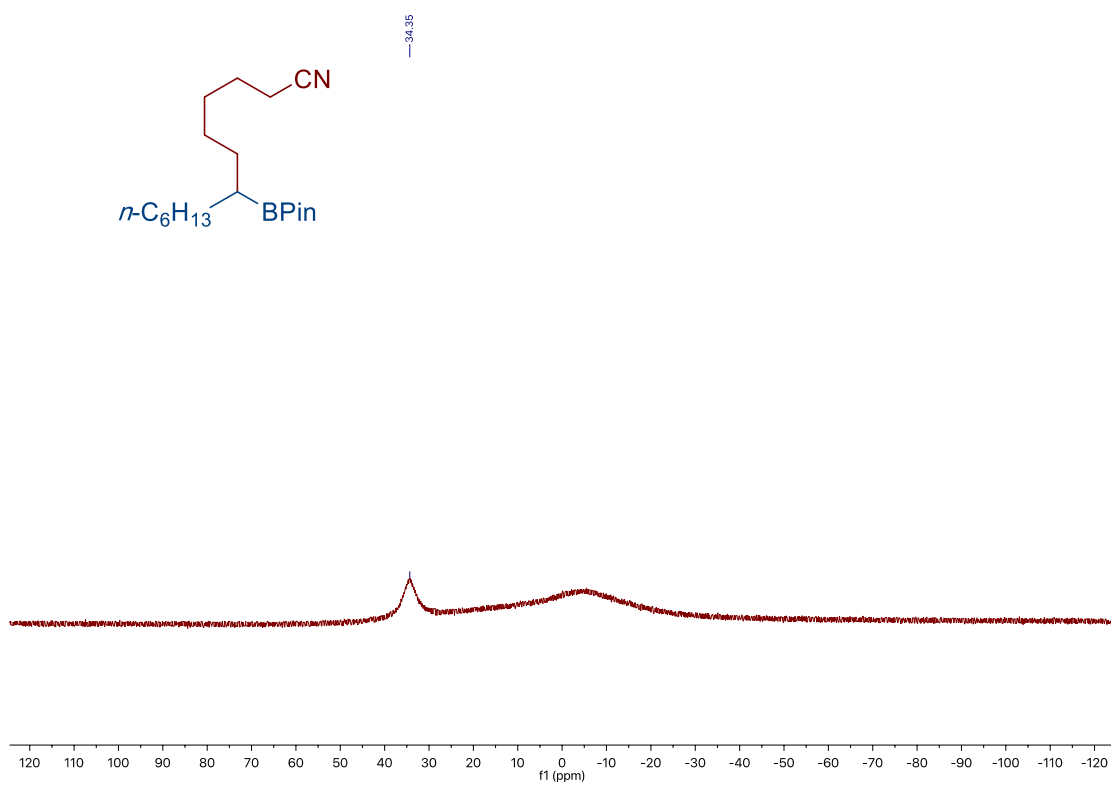
Chapter 2.



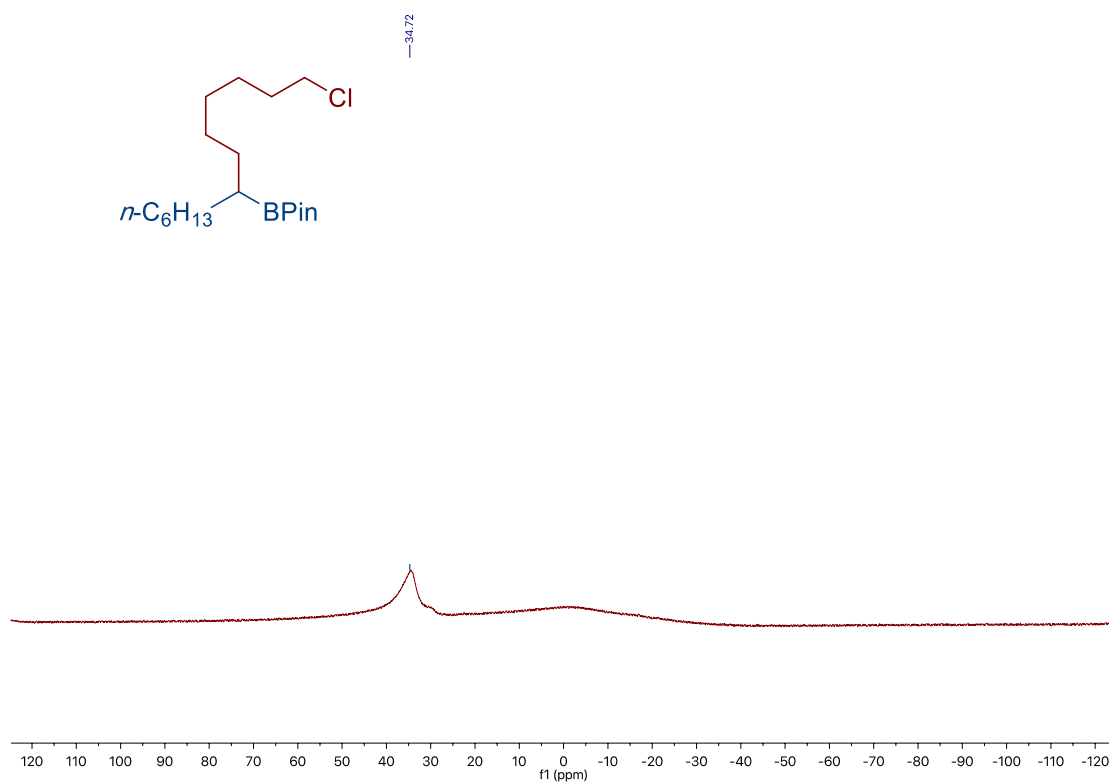
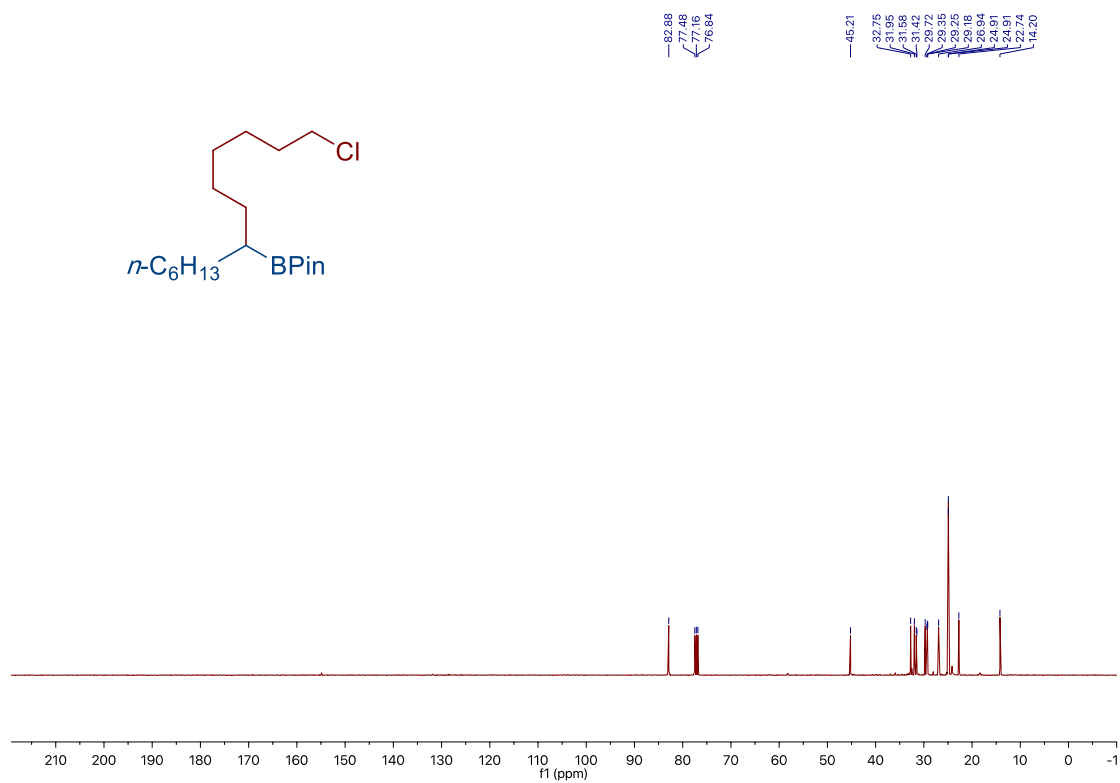
Site-Selective Ni-Catalyzed Reductive
Coupling of α -Haloboranes with Unactivated Olefins



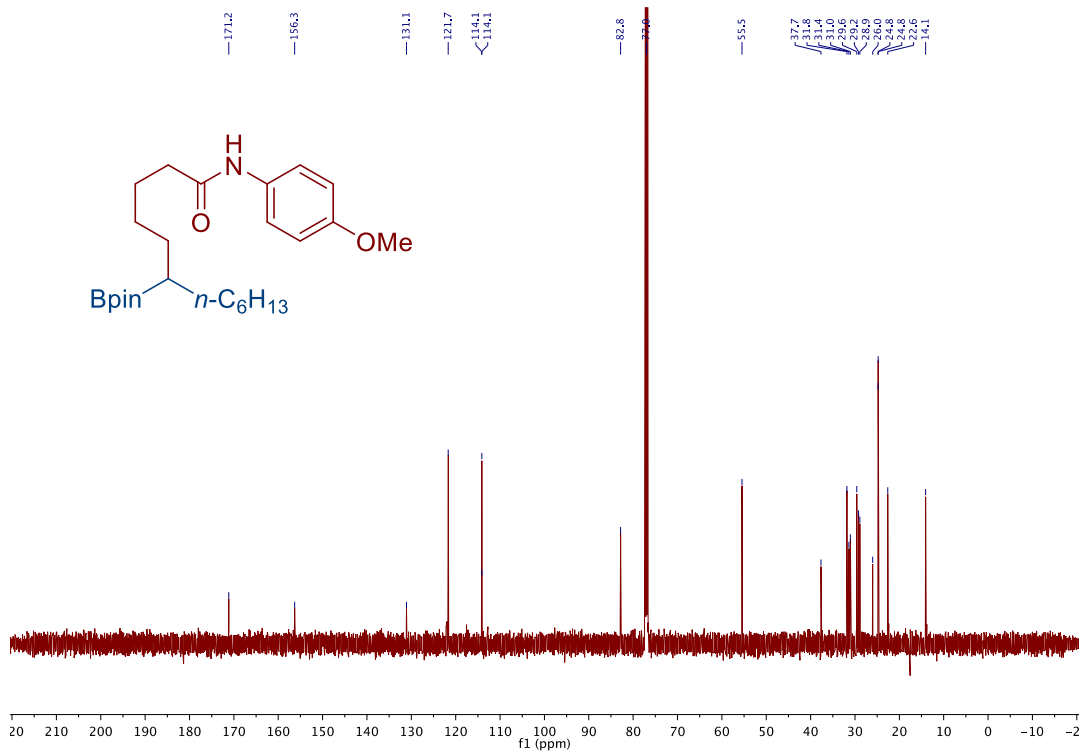
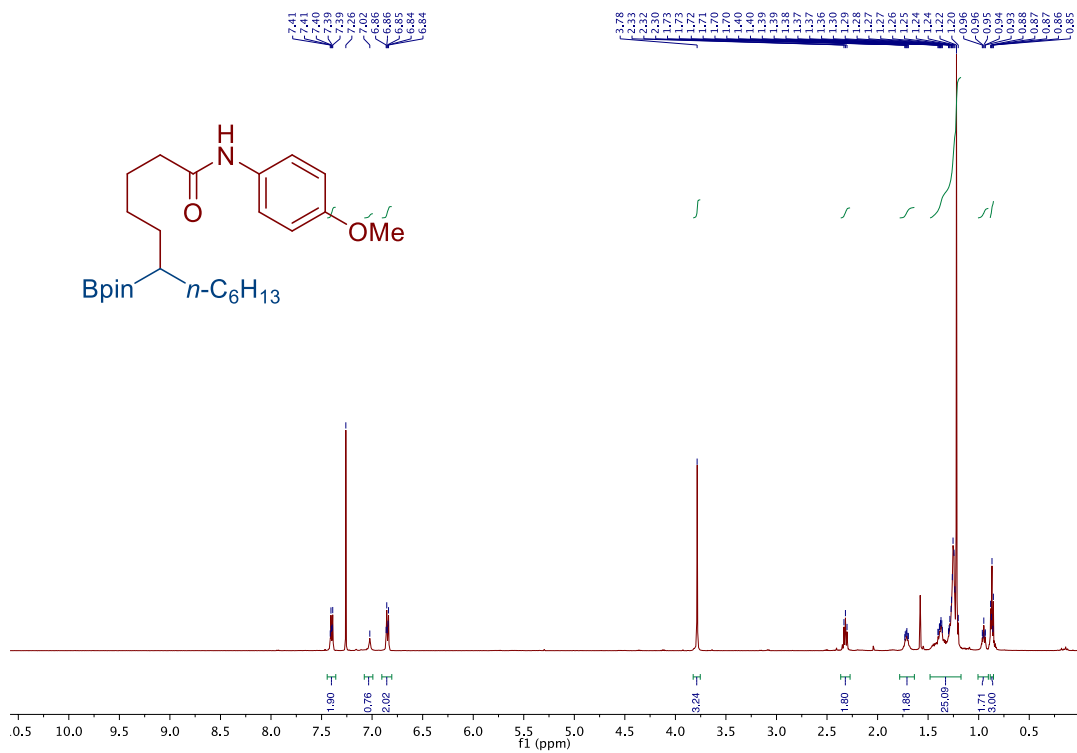
Chapter 2.



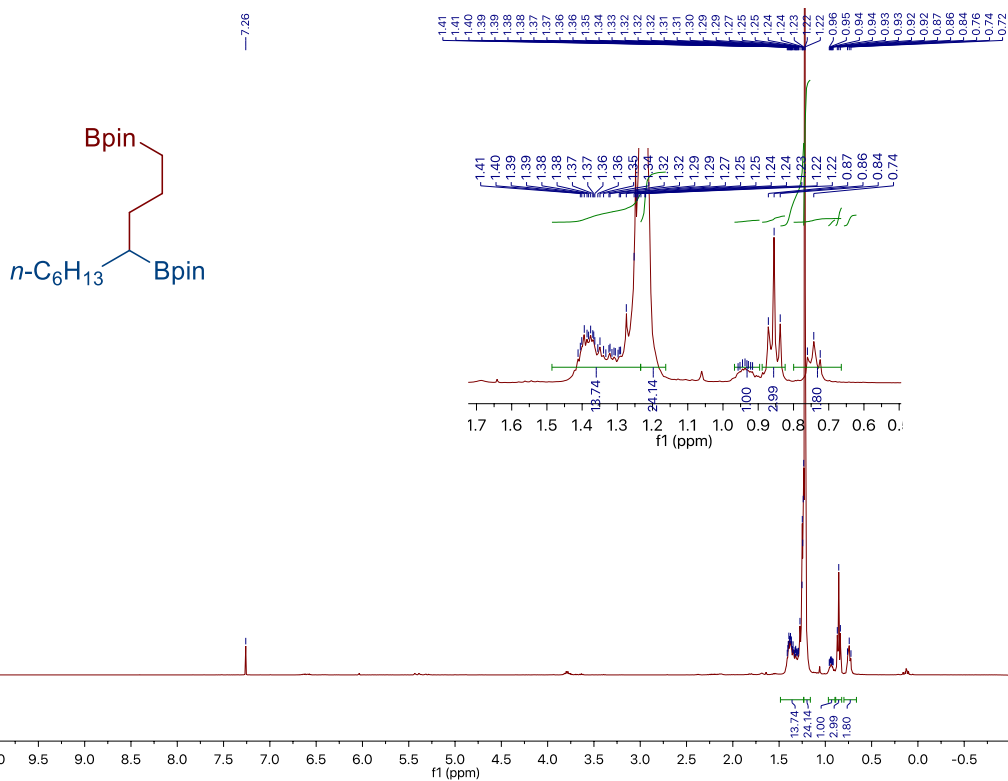
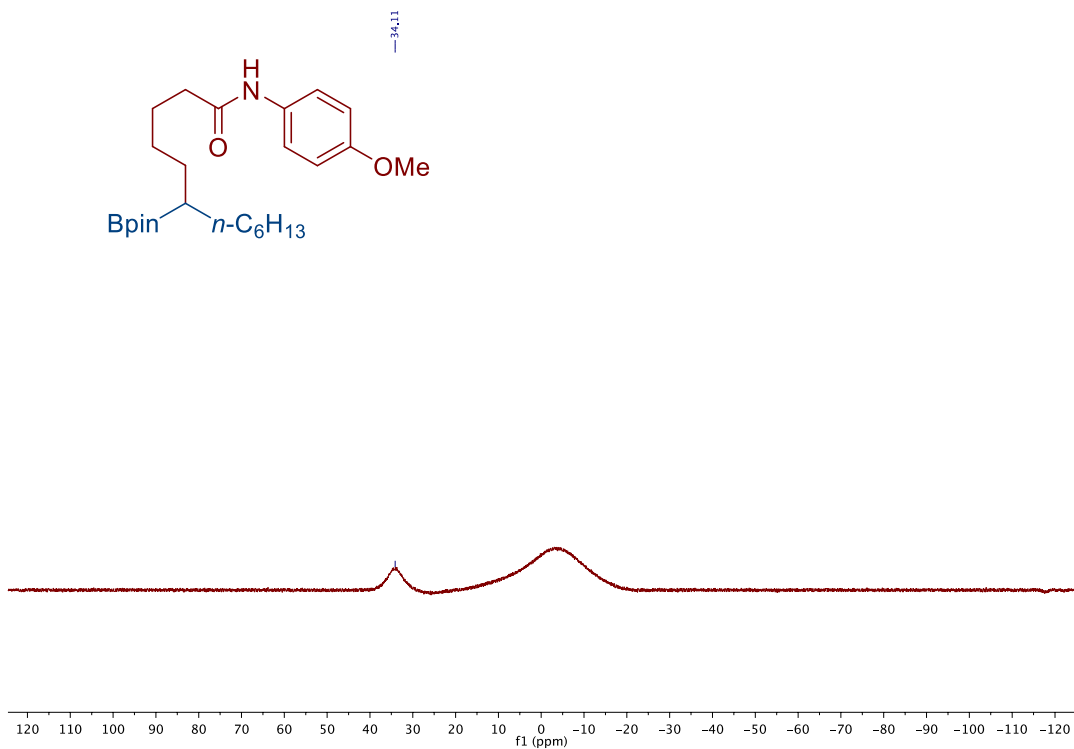
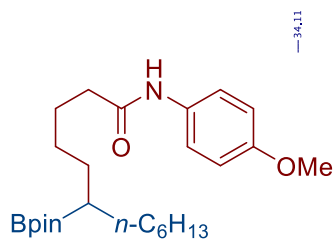
Site-Selective Ni-Catalyzed Reductive
Coupling of α -Haloboranes with Unactivated Olefins



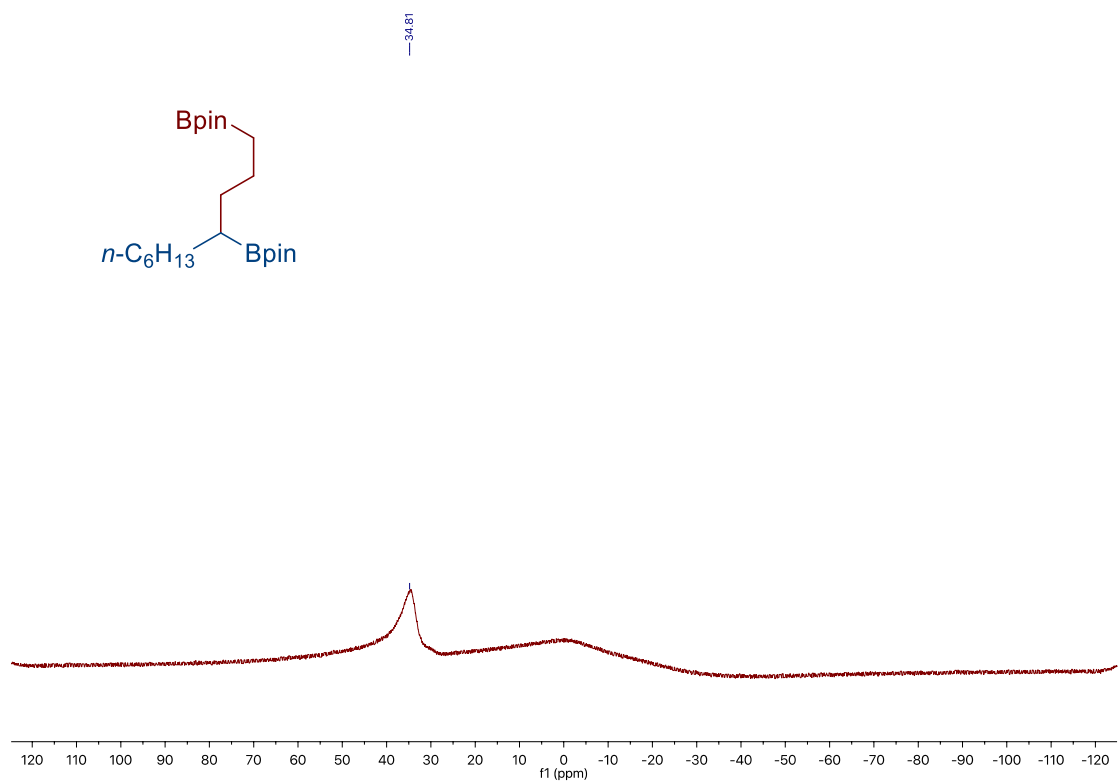
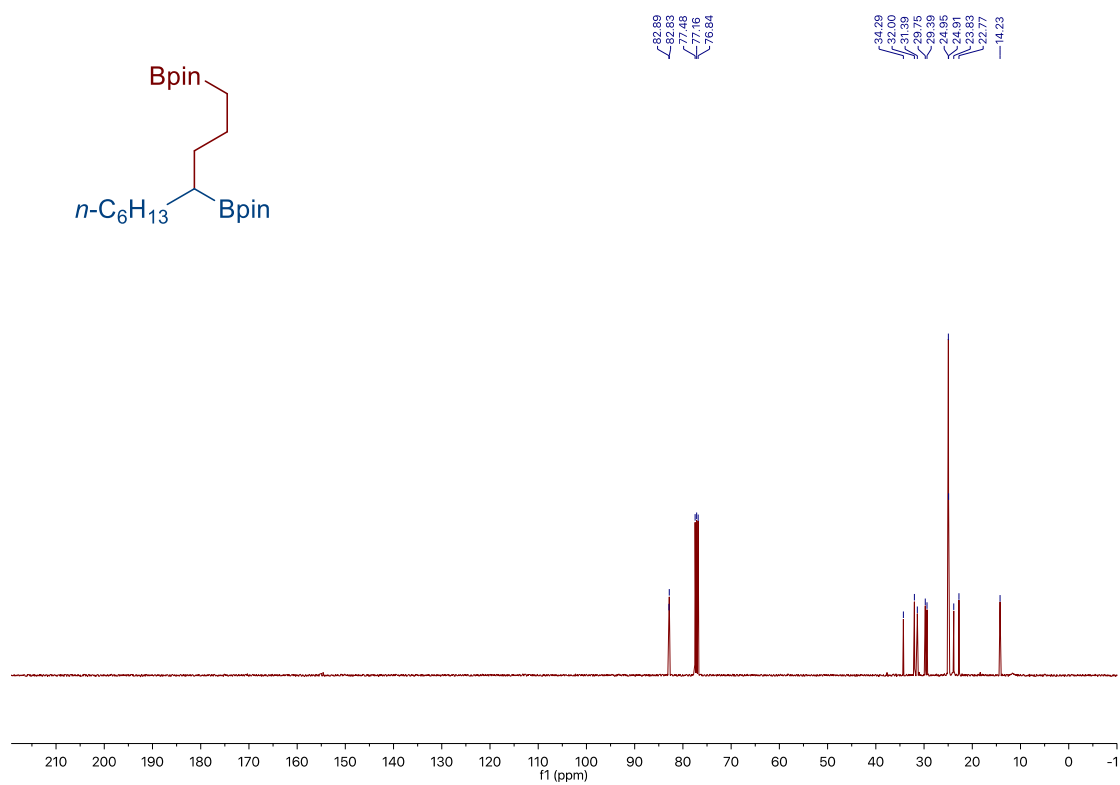
Chapter 2.



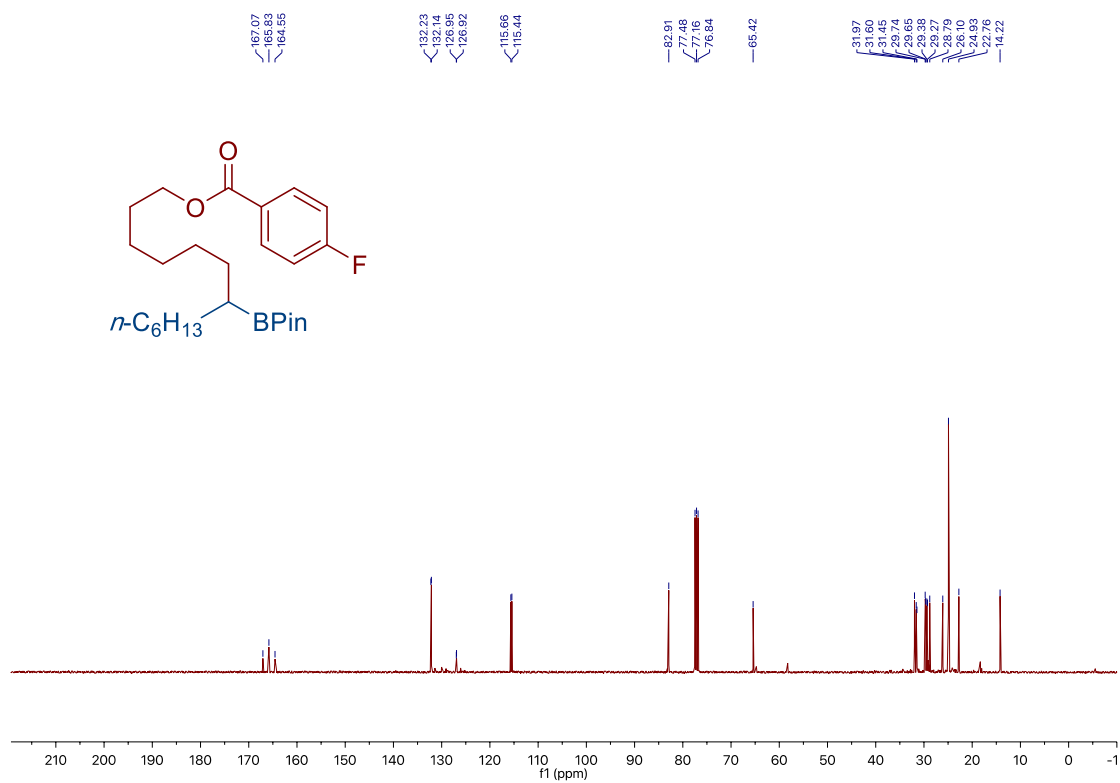
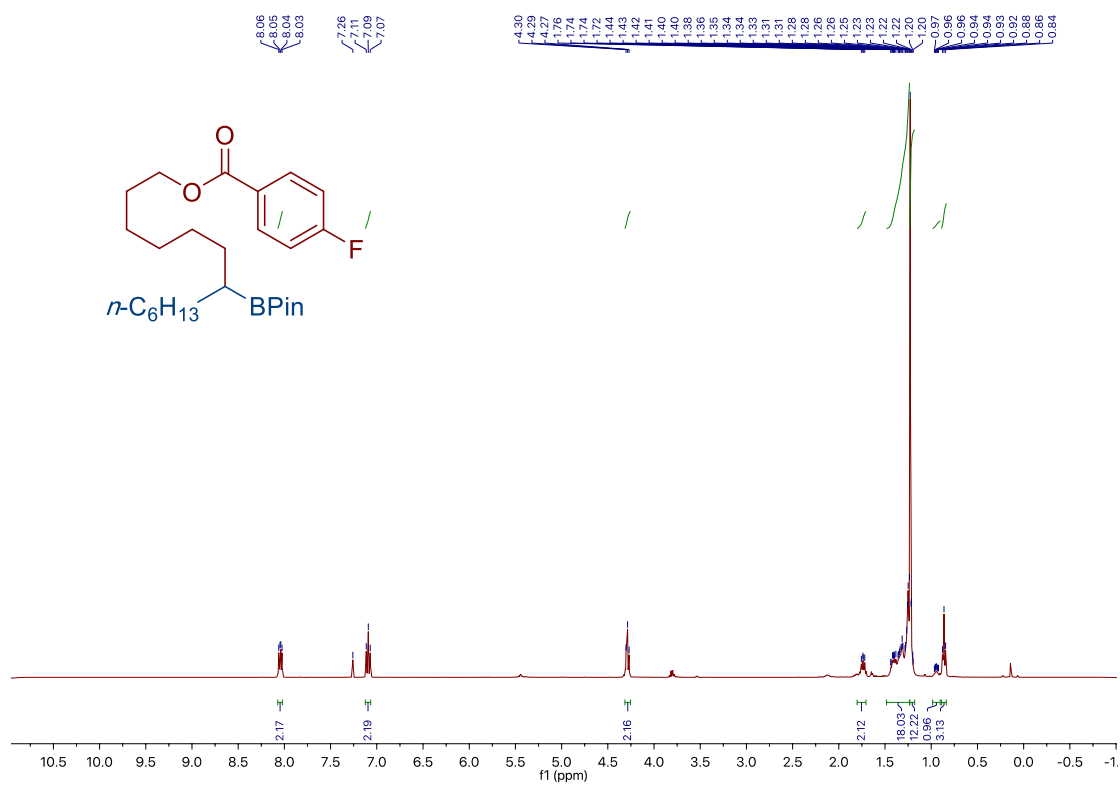
*Site-Selective Ni-Catalyzed Reductive
Coupling of α -Haloboranes with Unactivated Olefins*



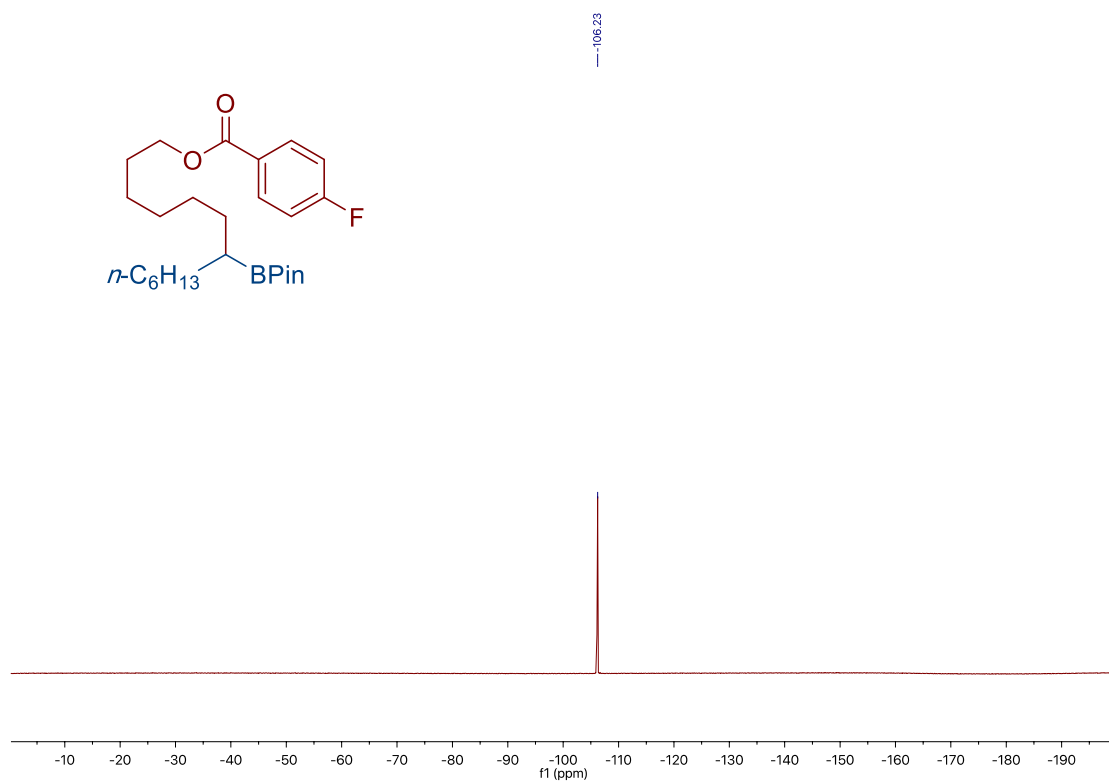
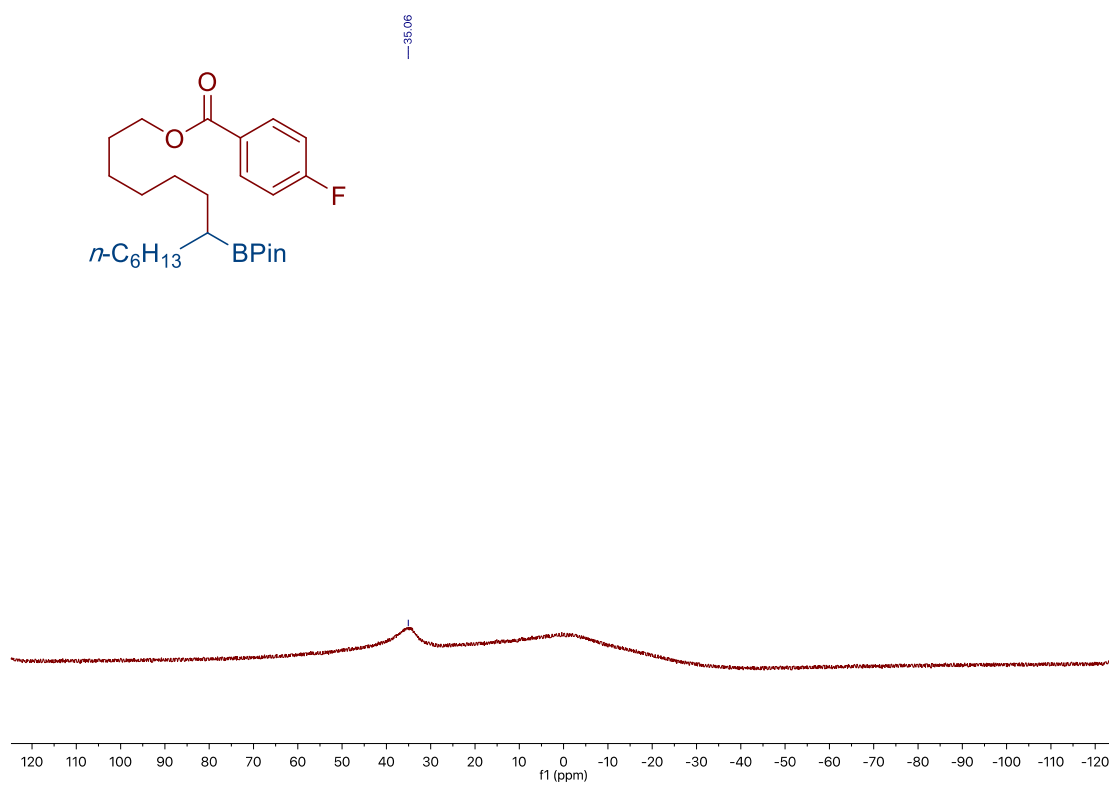
Chapter 2.



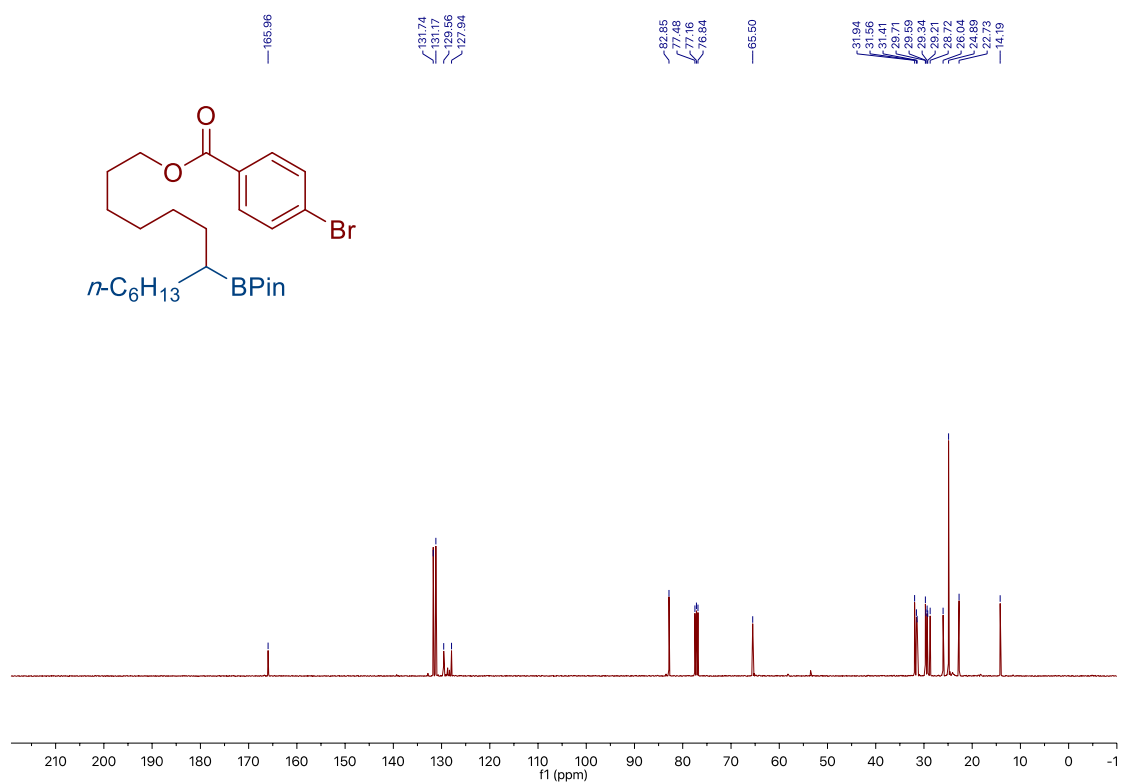
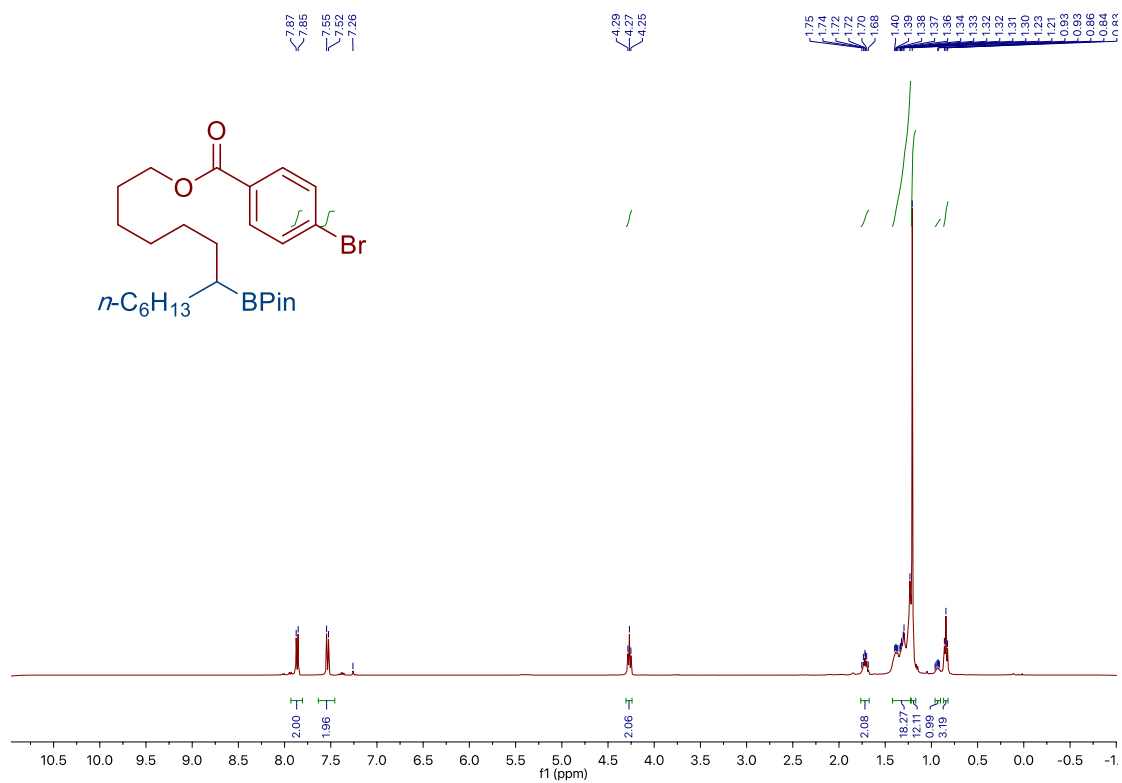
Site-Selective Ni-Catalyzed Reductive
Coupling of α -Haloboranes with Unactivated Olefins



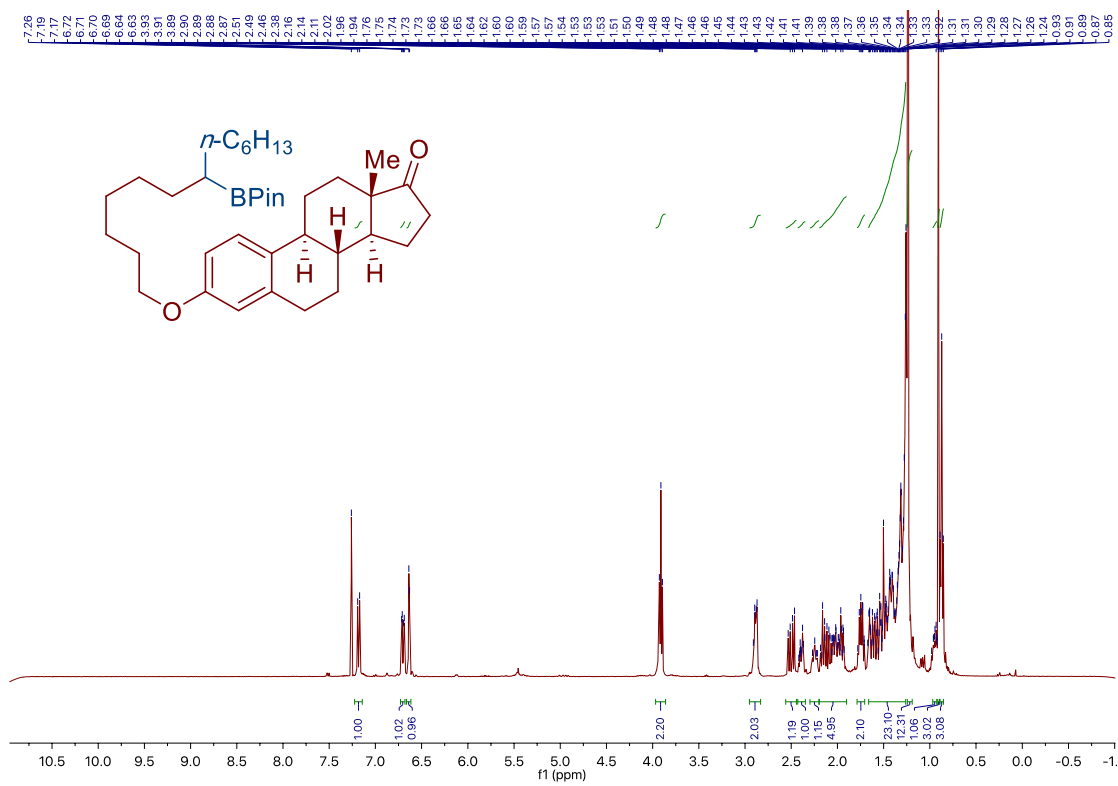
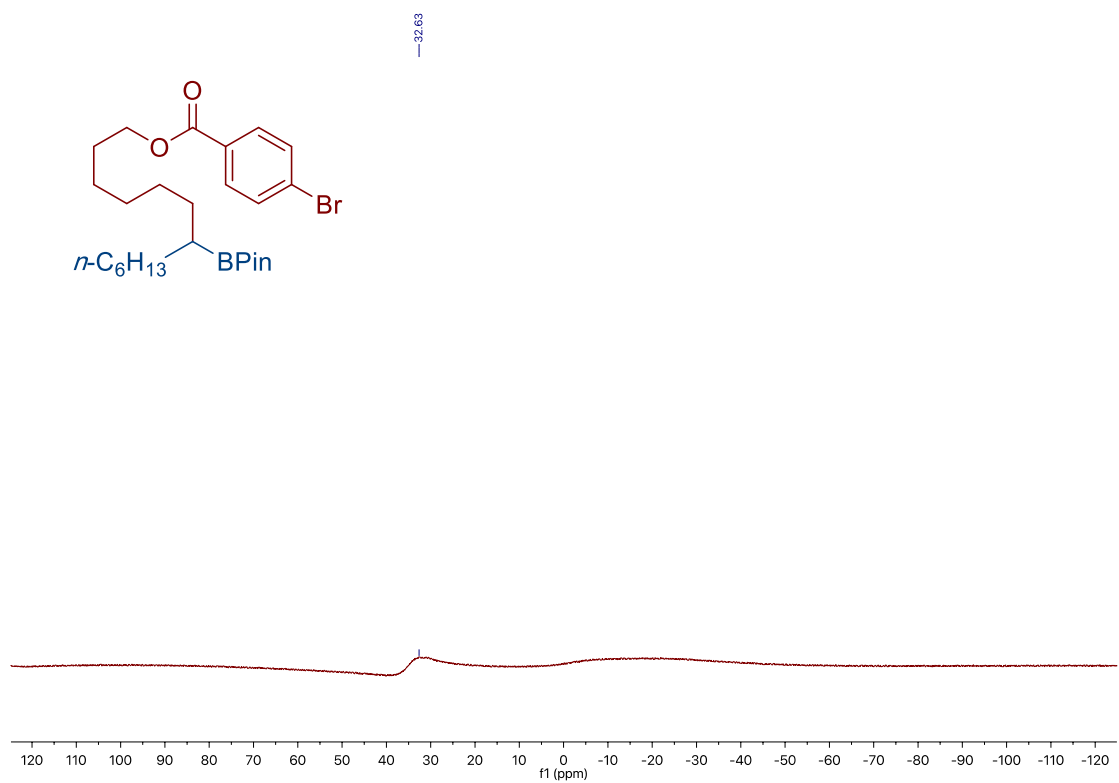
Chapter 2.



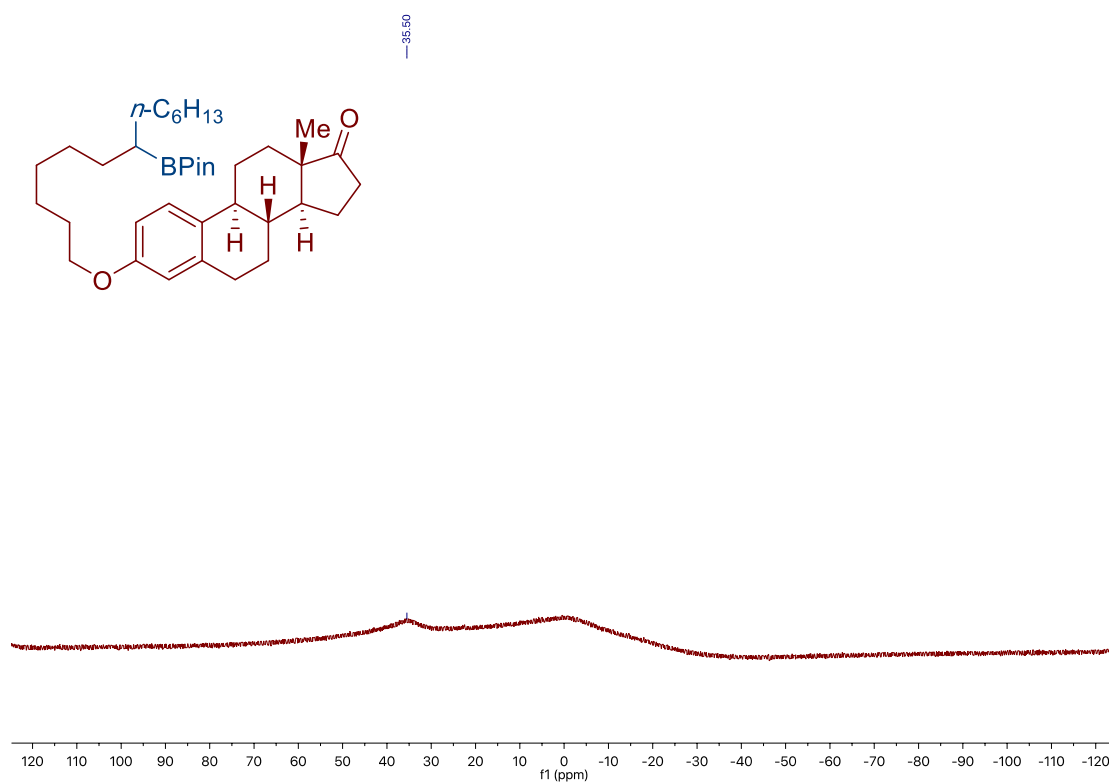
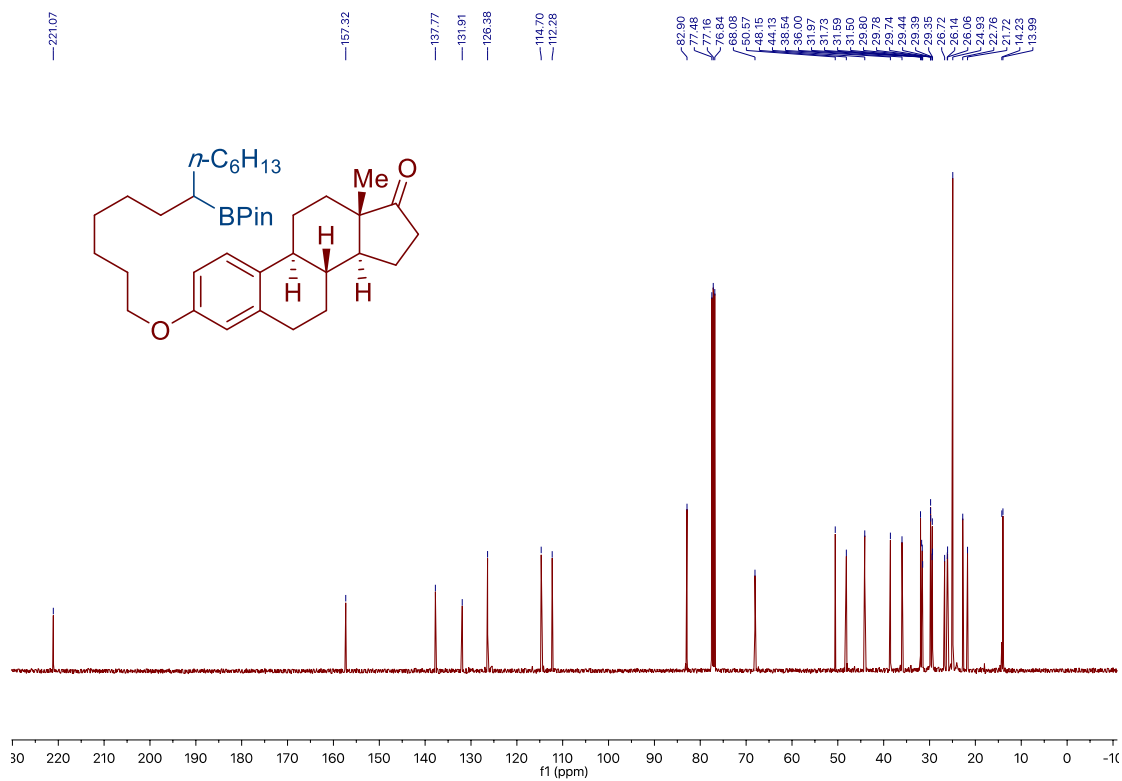
Site-Selective Ni-Catalyzed Reductive
Coupling of α -Haloboranes with Unactivated Olefins



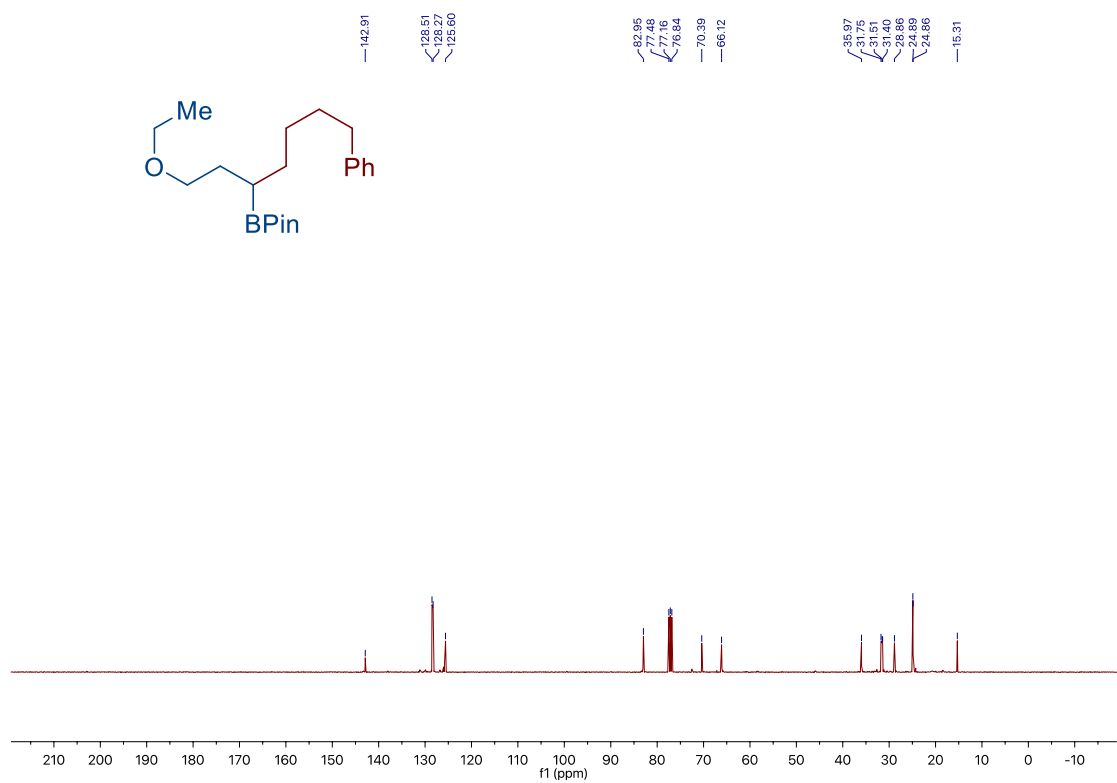
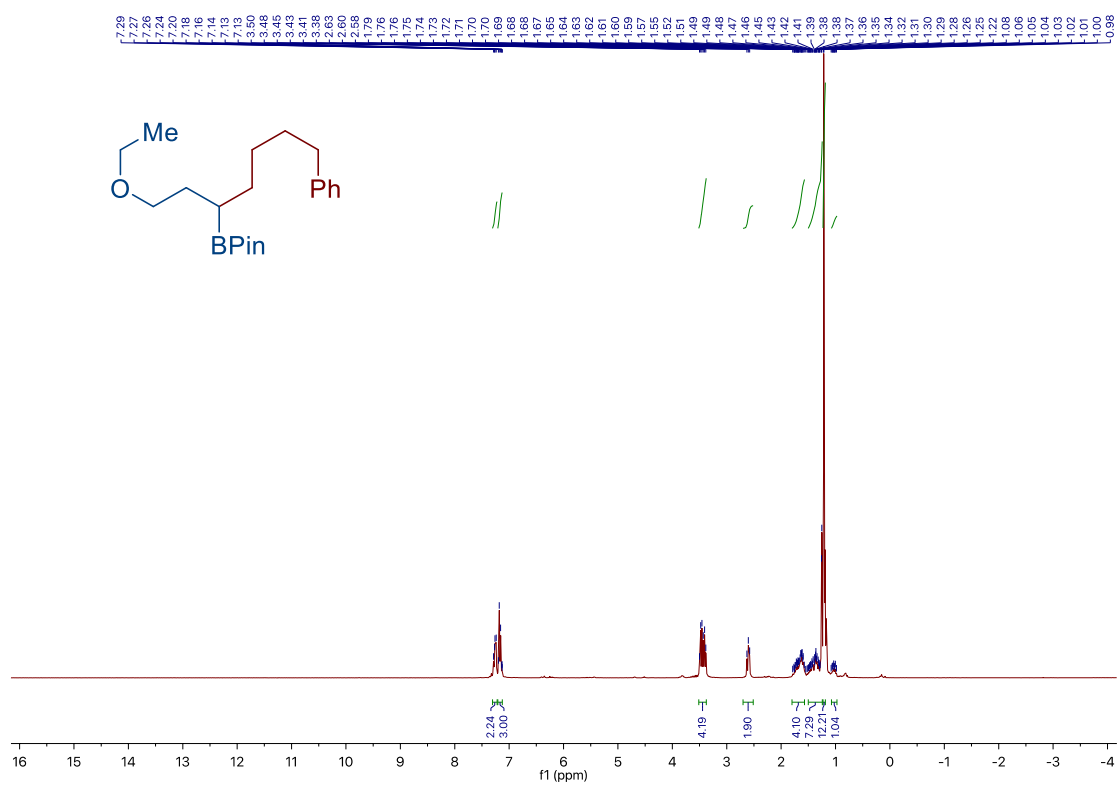
Chapter 2.



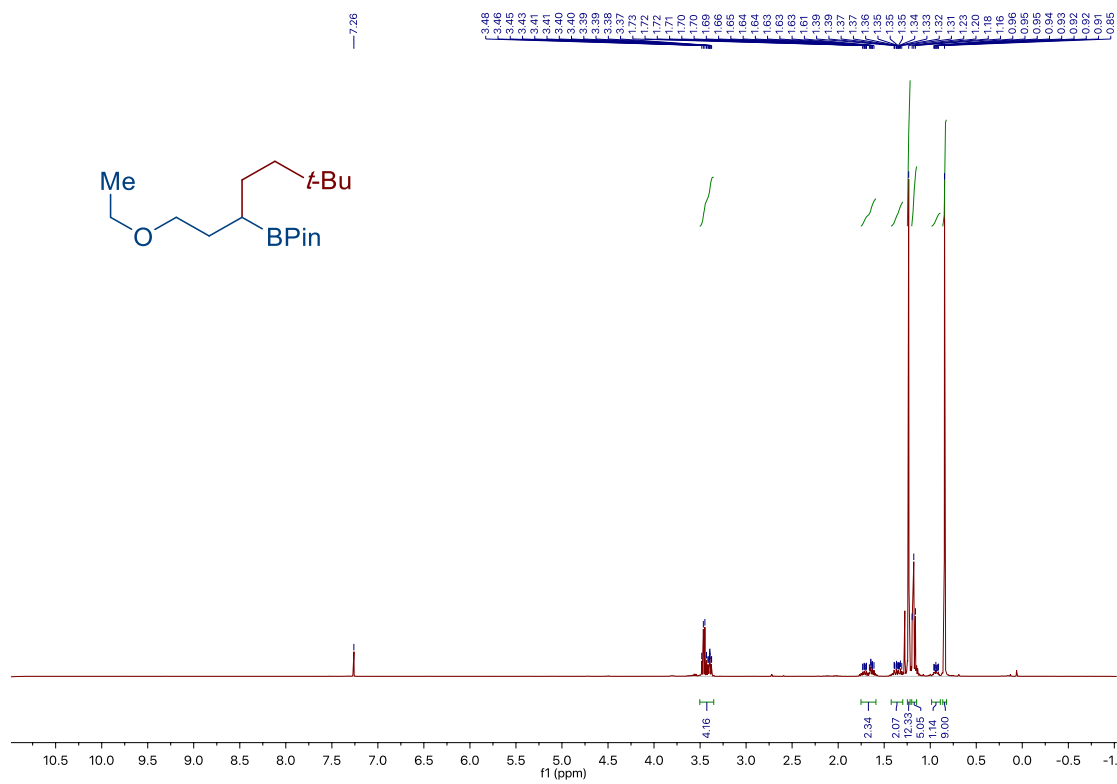
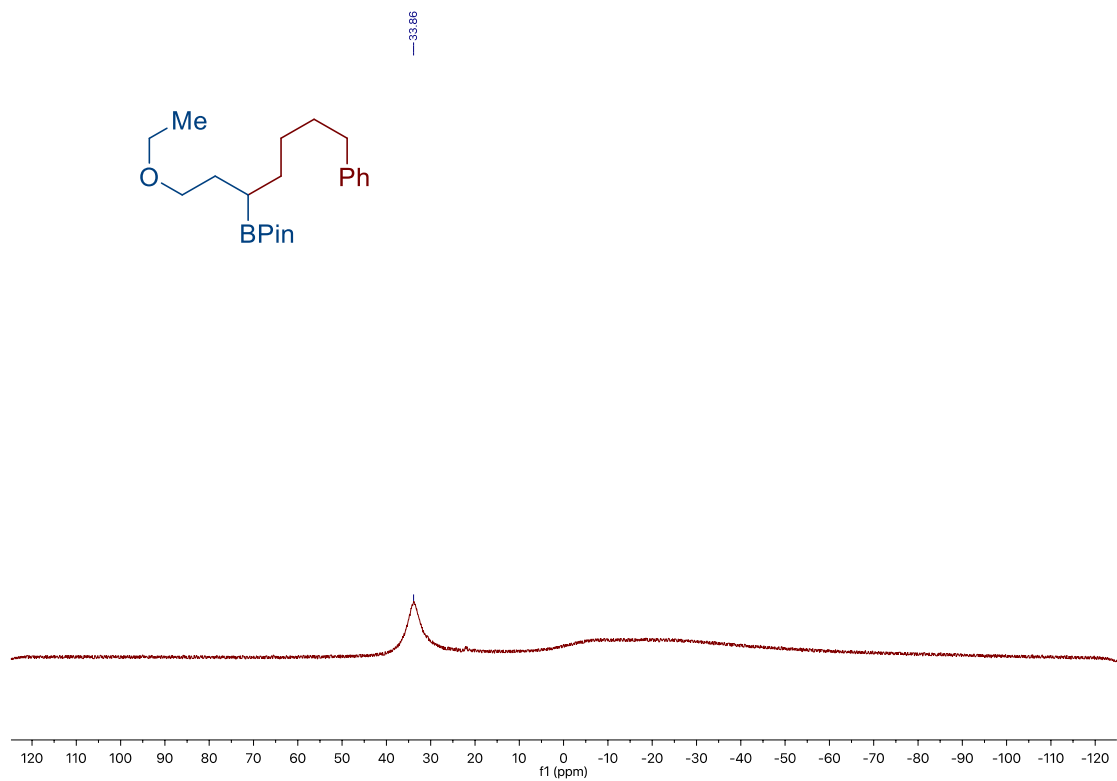
*Site-Selective Ni-Catalyzed Reductive
Coupling of α -Haloboranes with Unactivated Olefins*



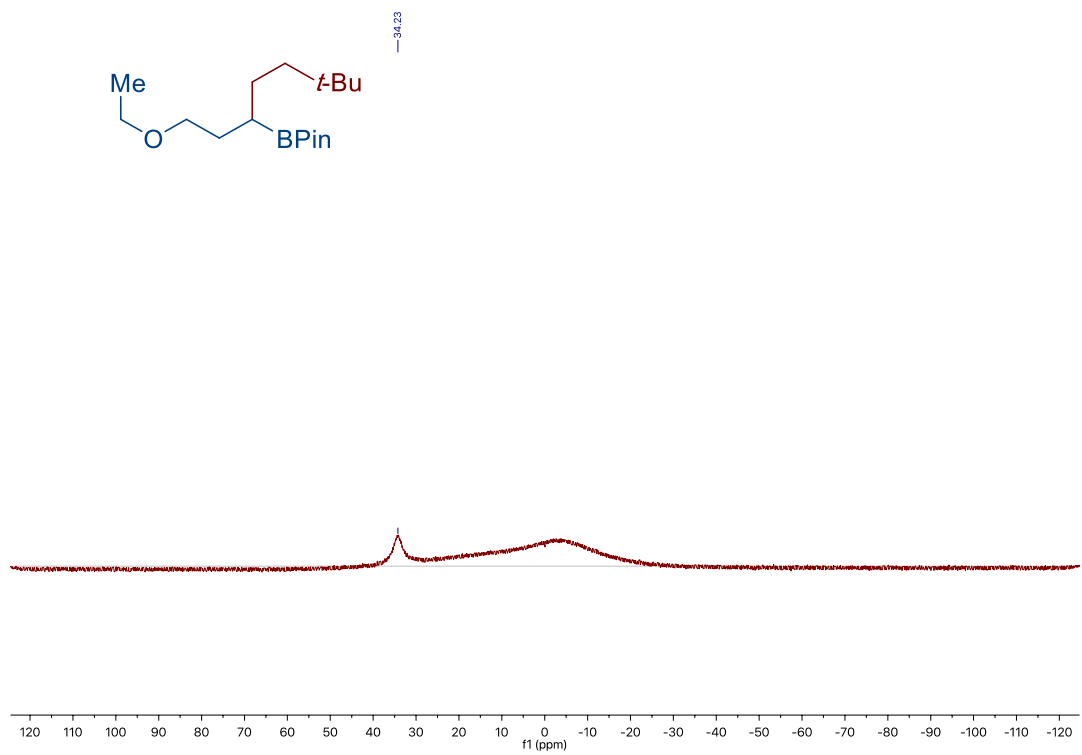
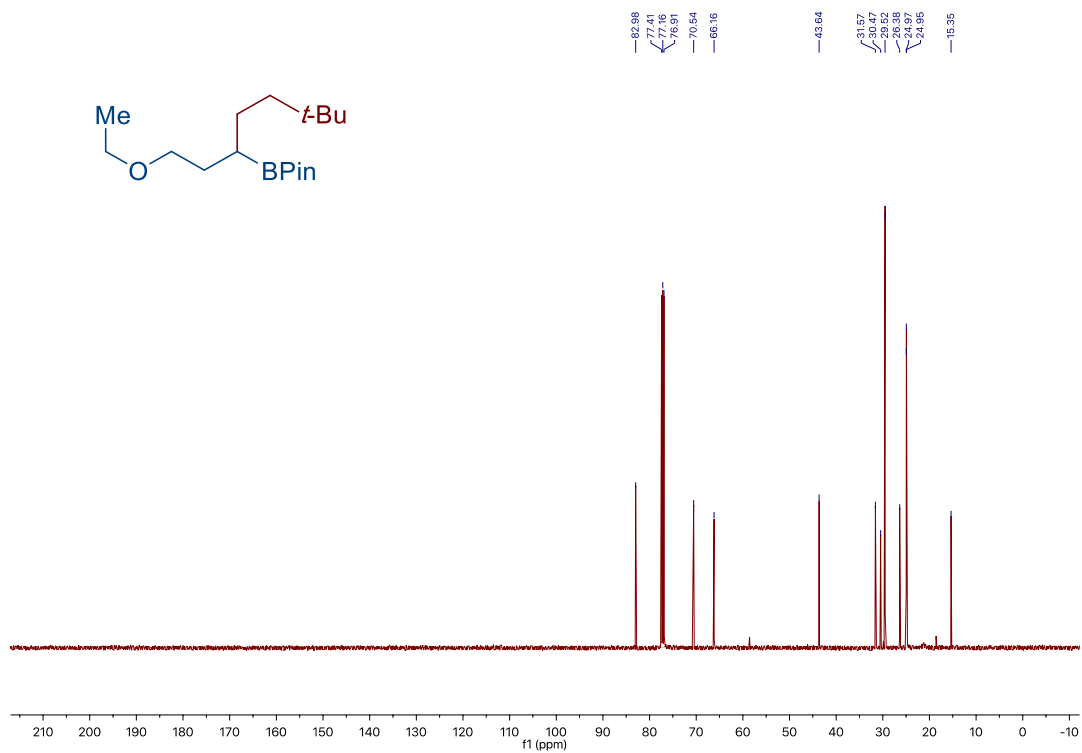
Chapter 2.



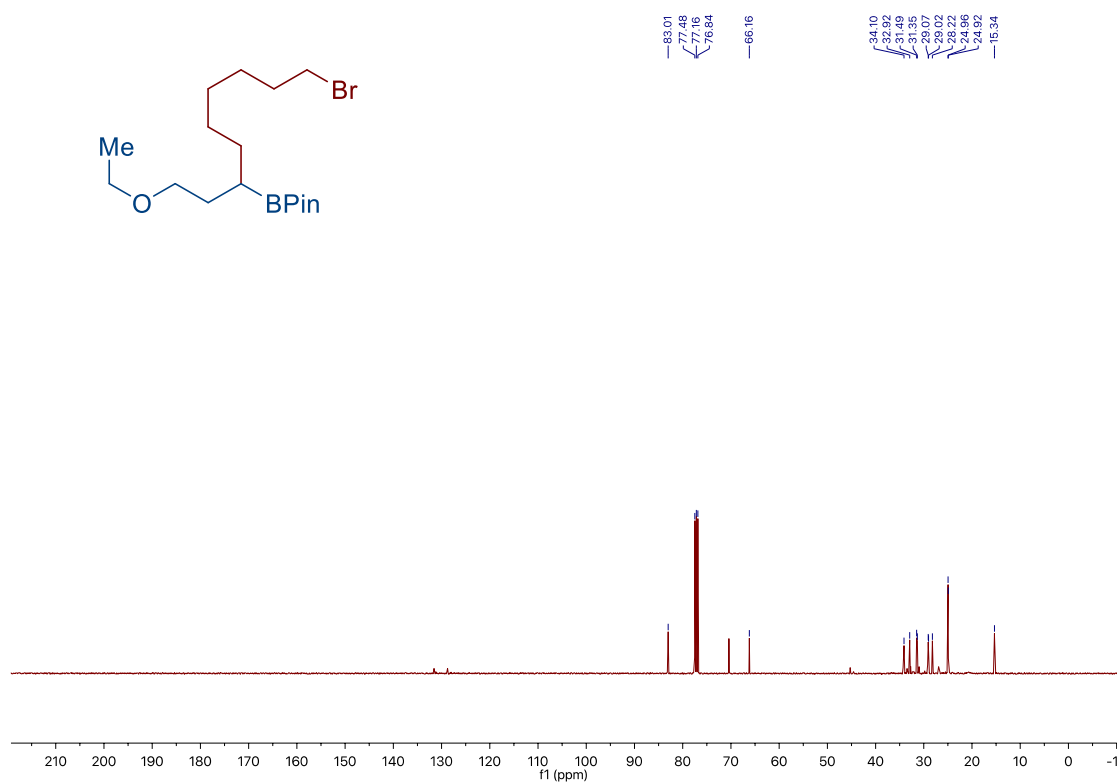
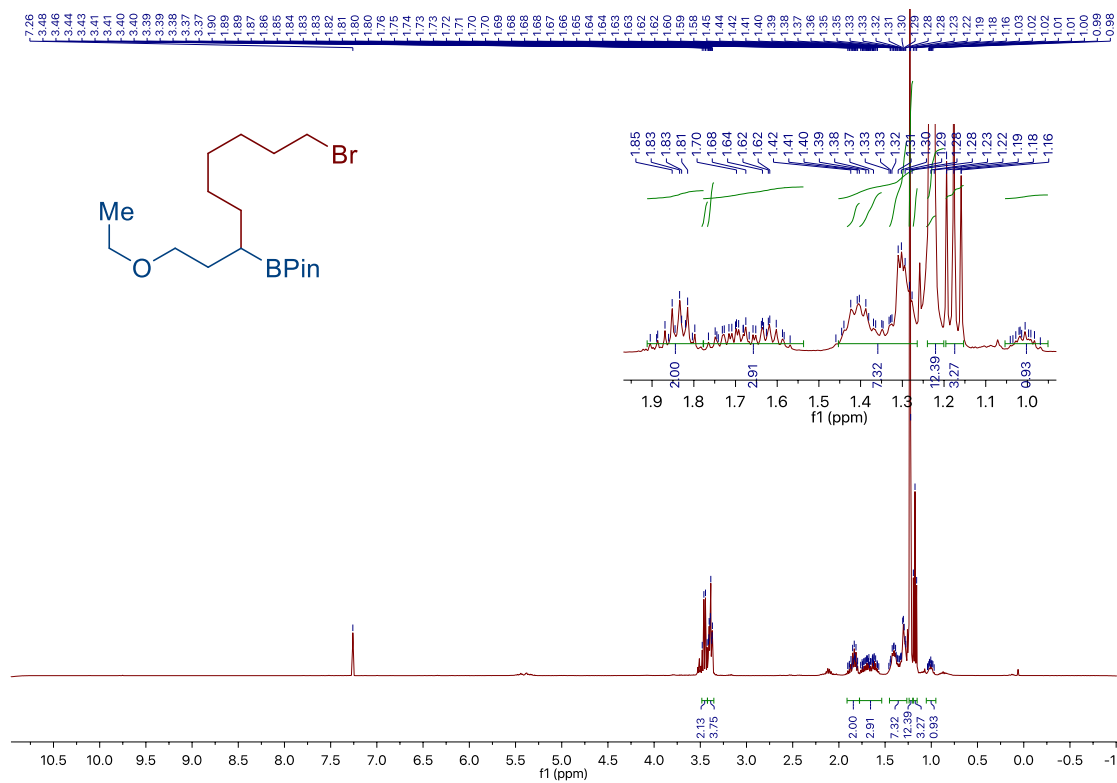
Site-Selective Ni-Catalyzed Reductive
Coupling of α -Haloboranes with Unactivated Olefins



Chapter 2.

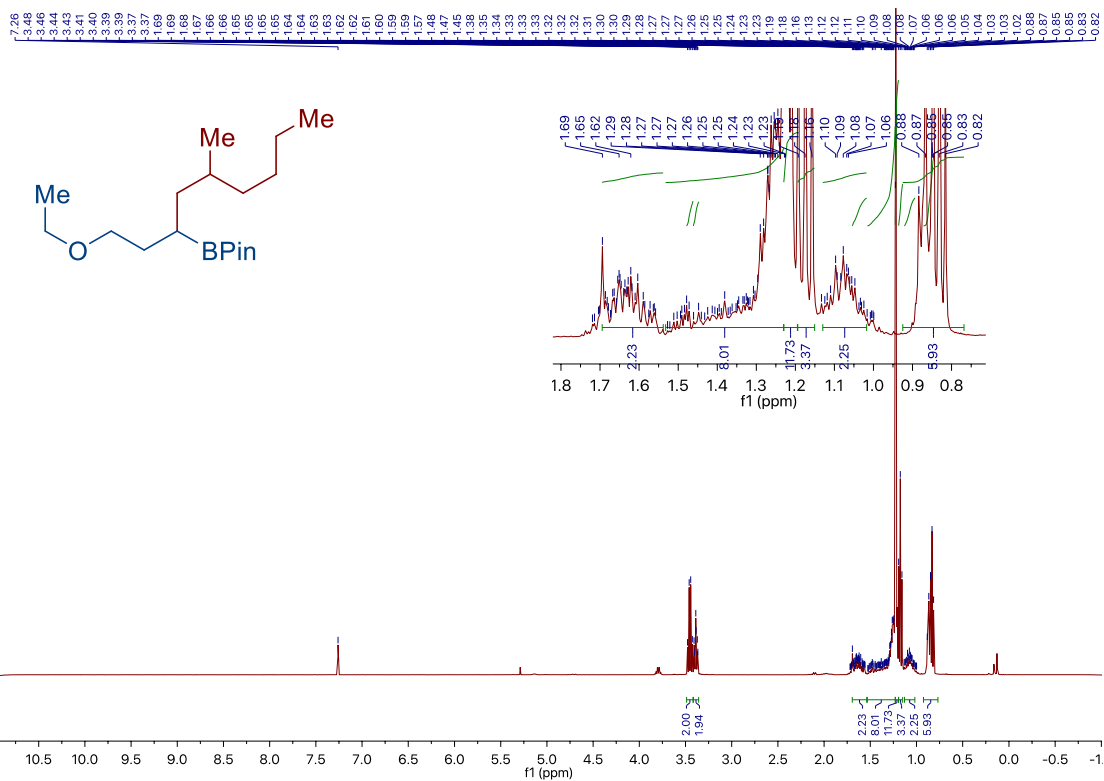
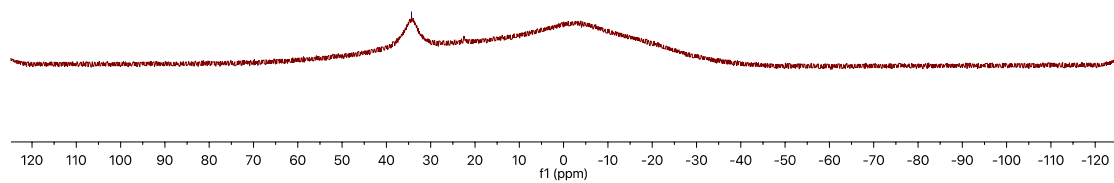
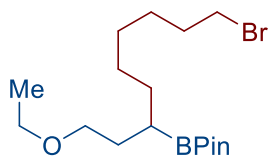


*Site-Selective Ni-Catalyzed Reductive
Coupling of α -Haloboranes with Unactivated Olefins*

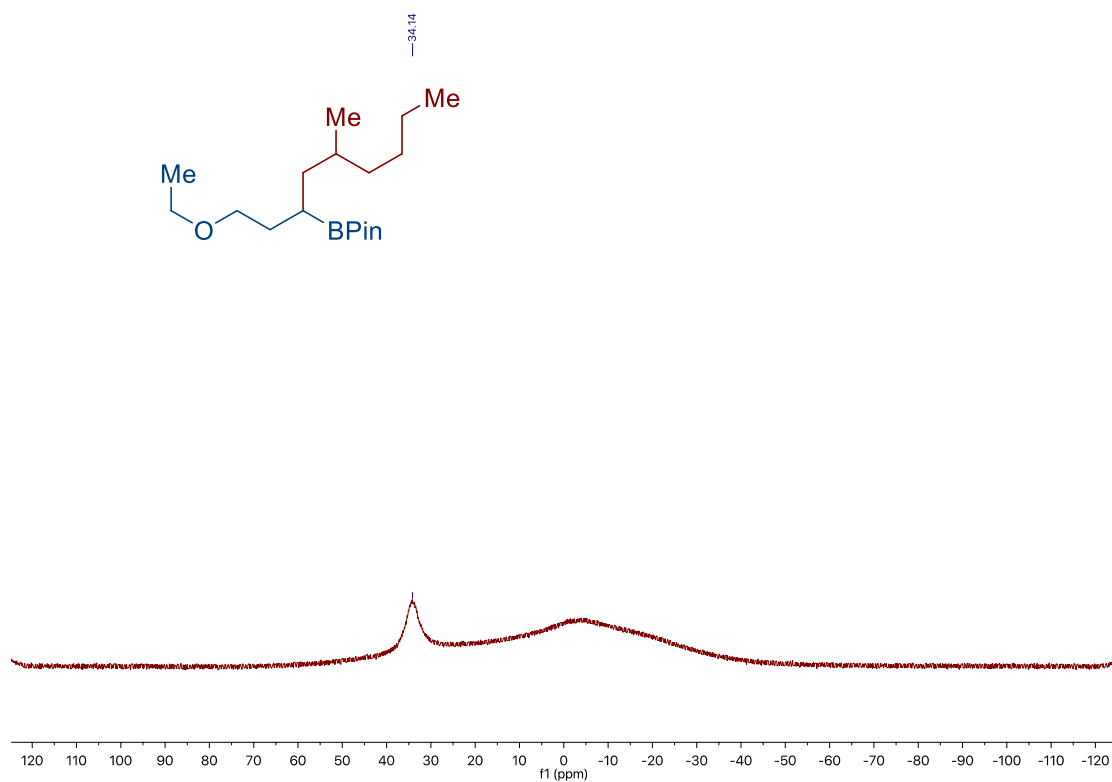
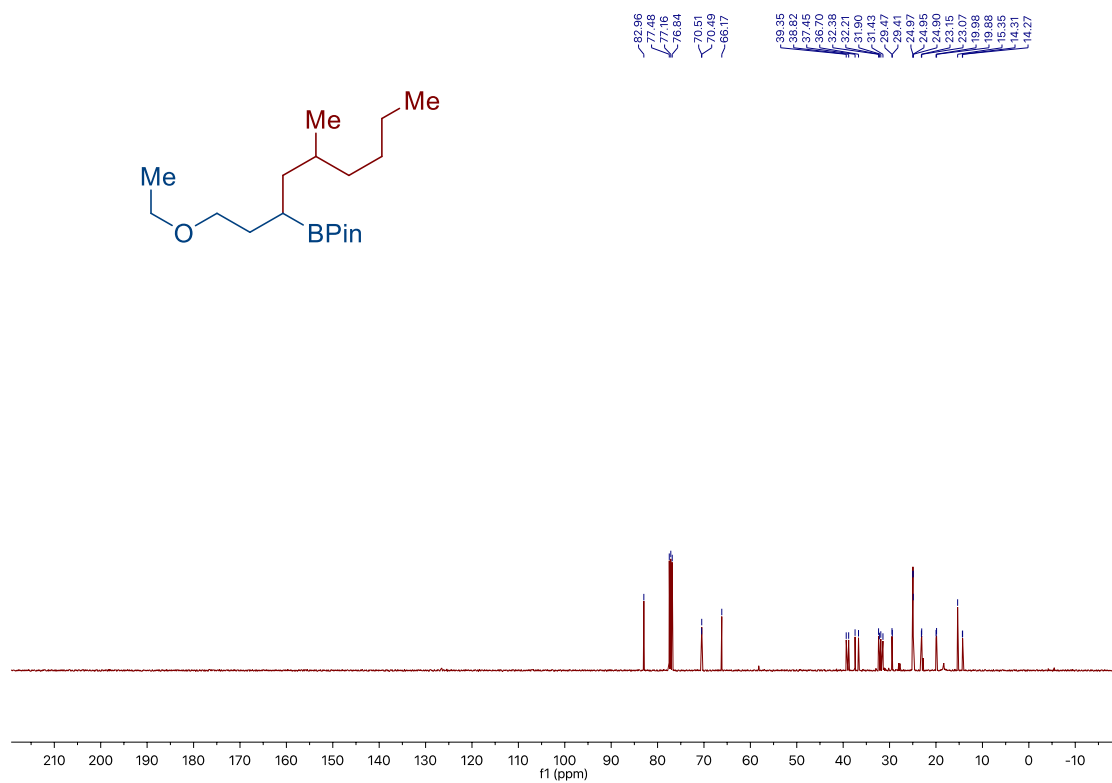


Chapter 2.

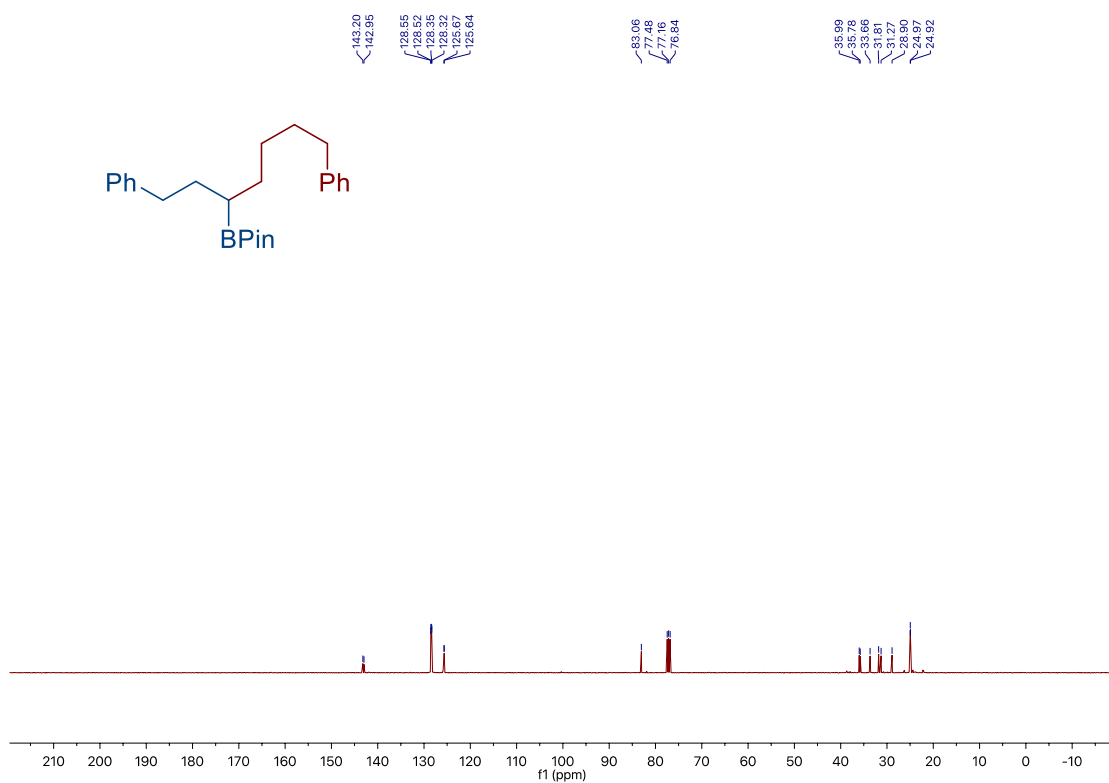
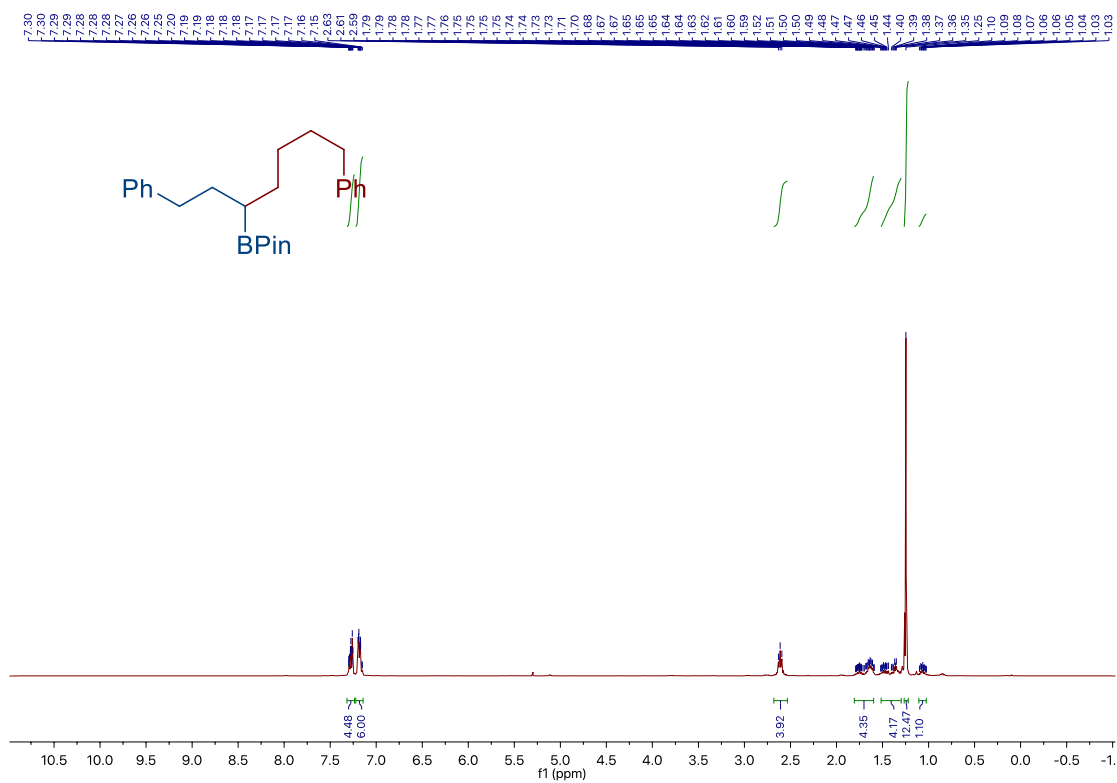
—34.33



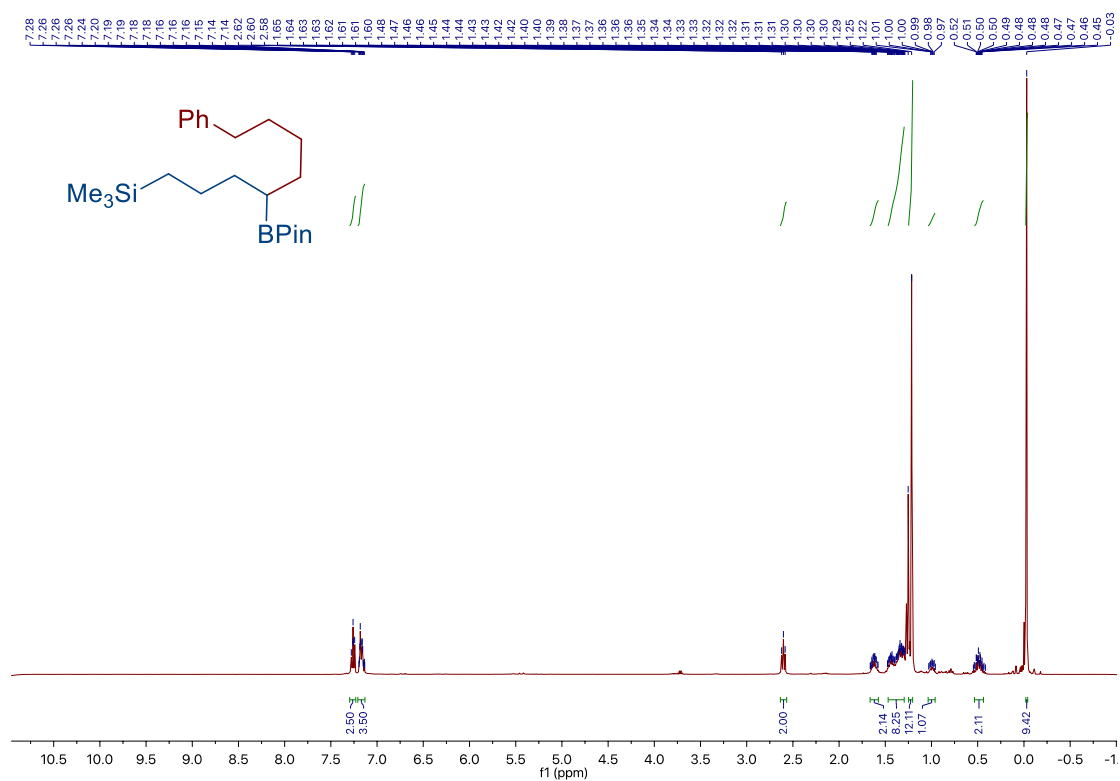
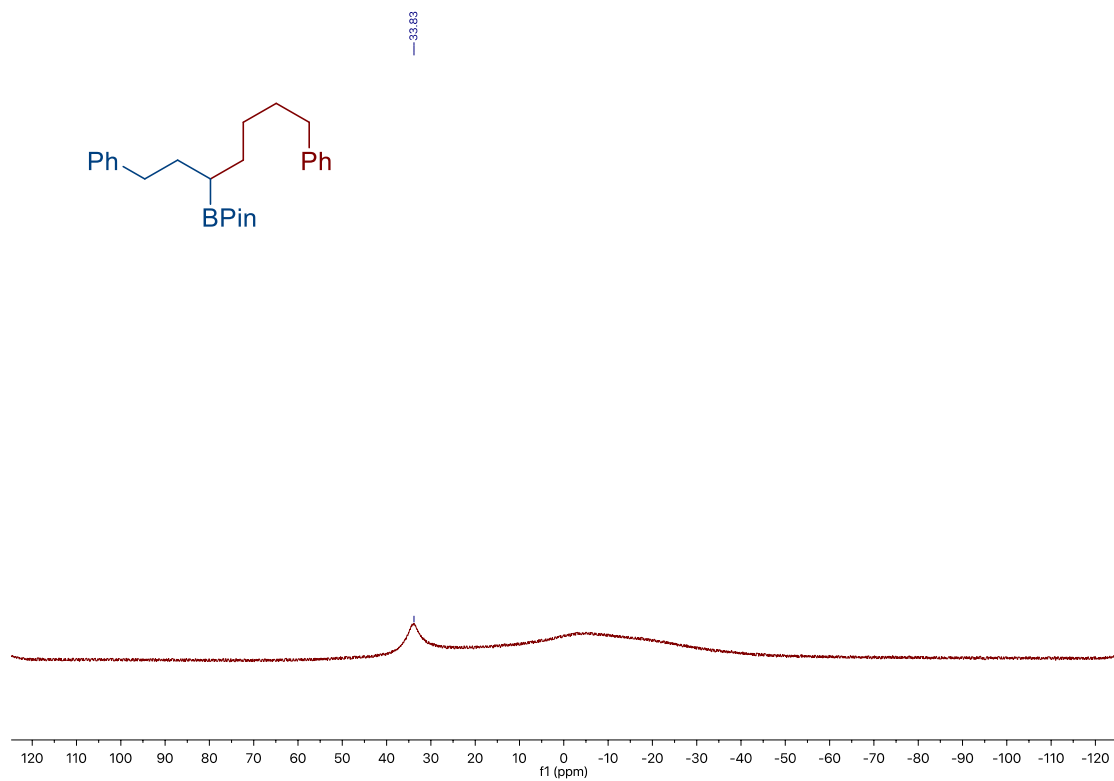
Site-Selective Ni-Catalyzed Reductive
Coupling of α -Haloboranes with Unactivated Olefins



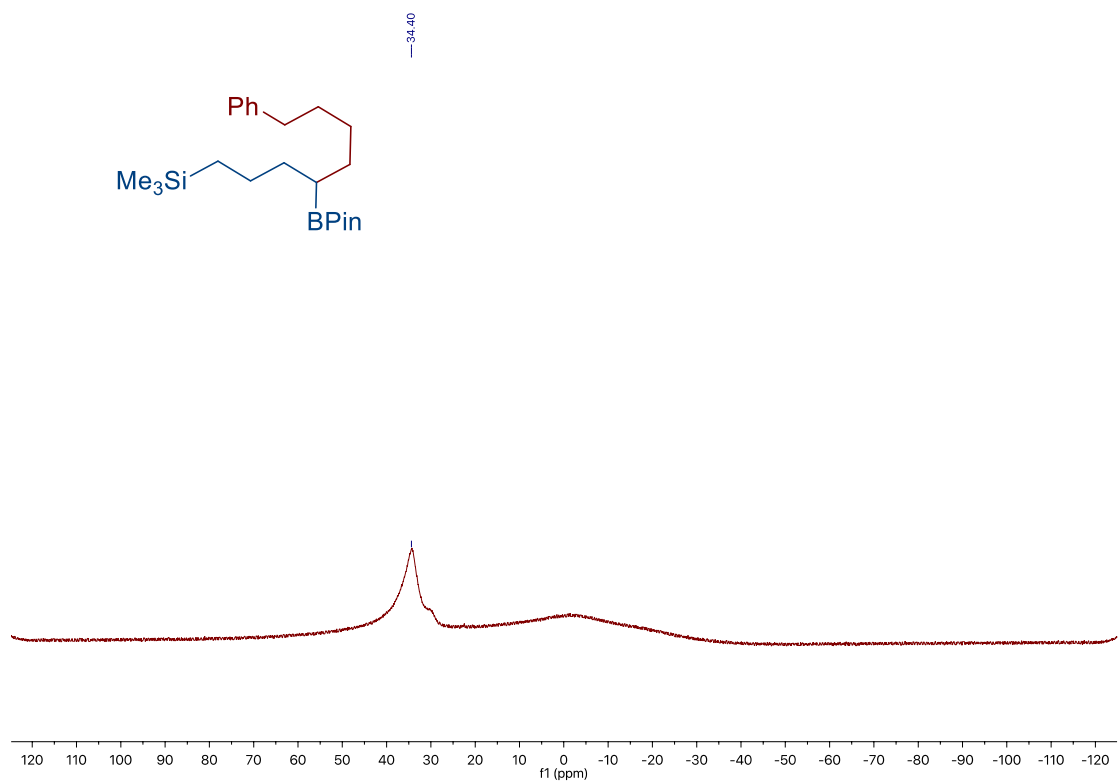
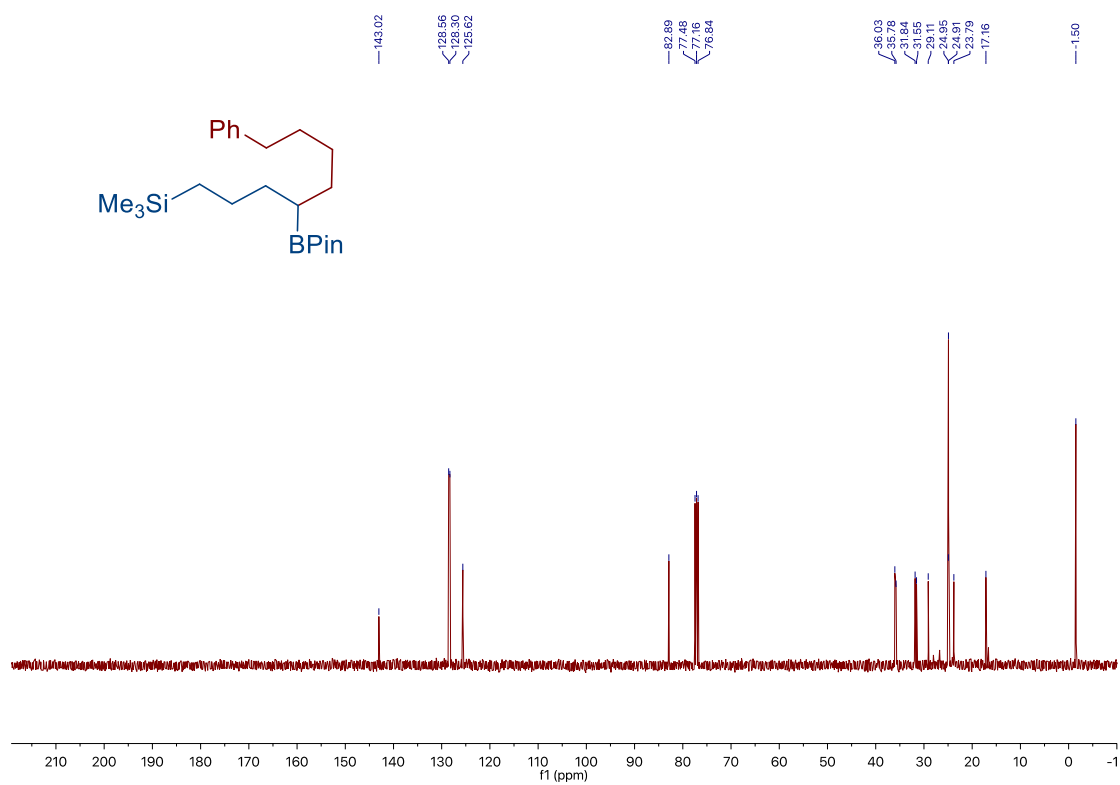
Chapter 2.



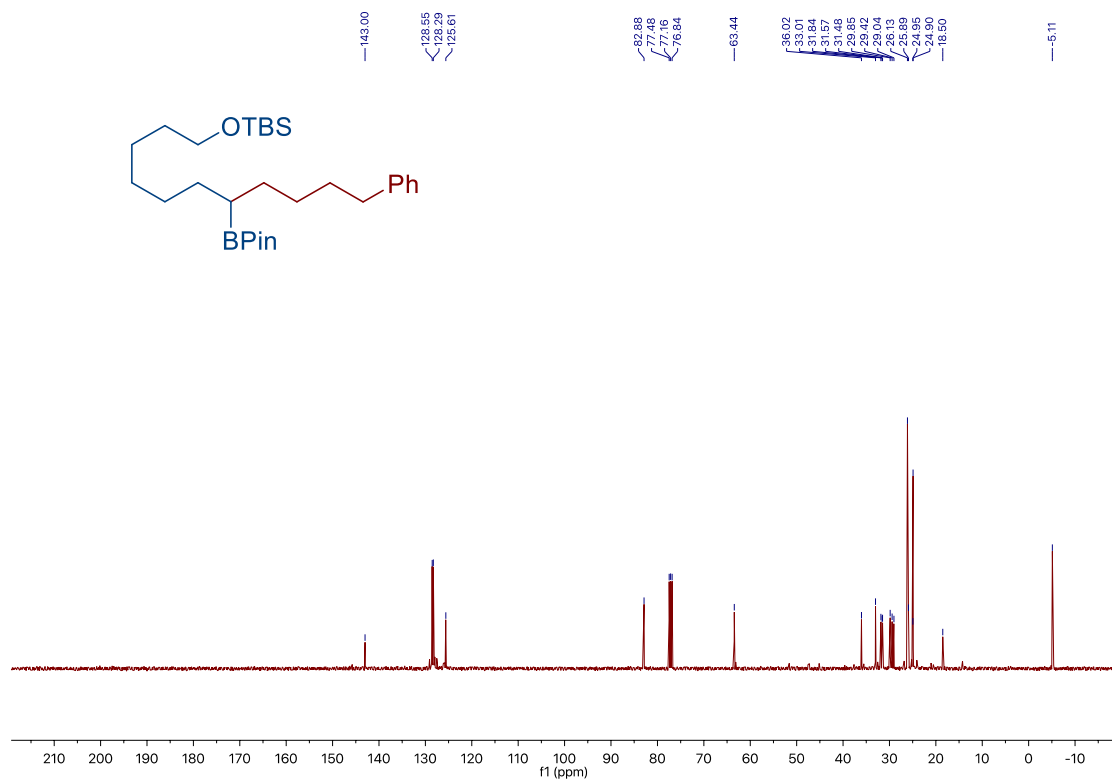
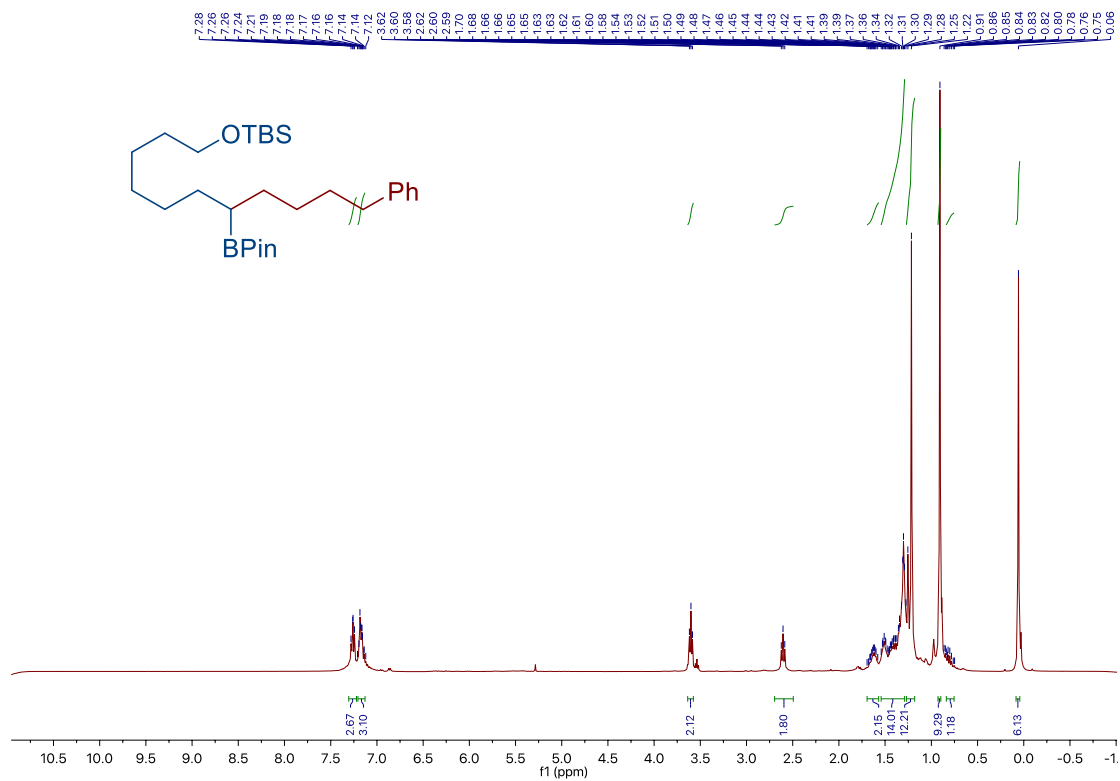
*Site-Selective Ni-Catalyzed Reductive
Coupling of α -Haloboranes with Unactivated Olefins*



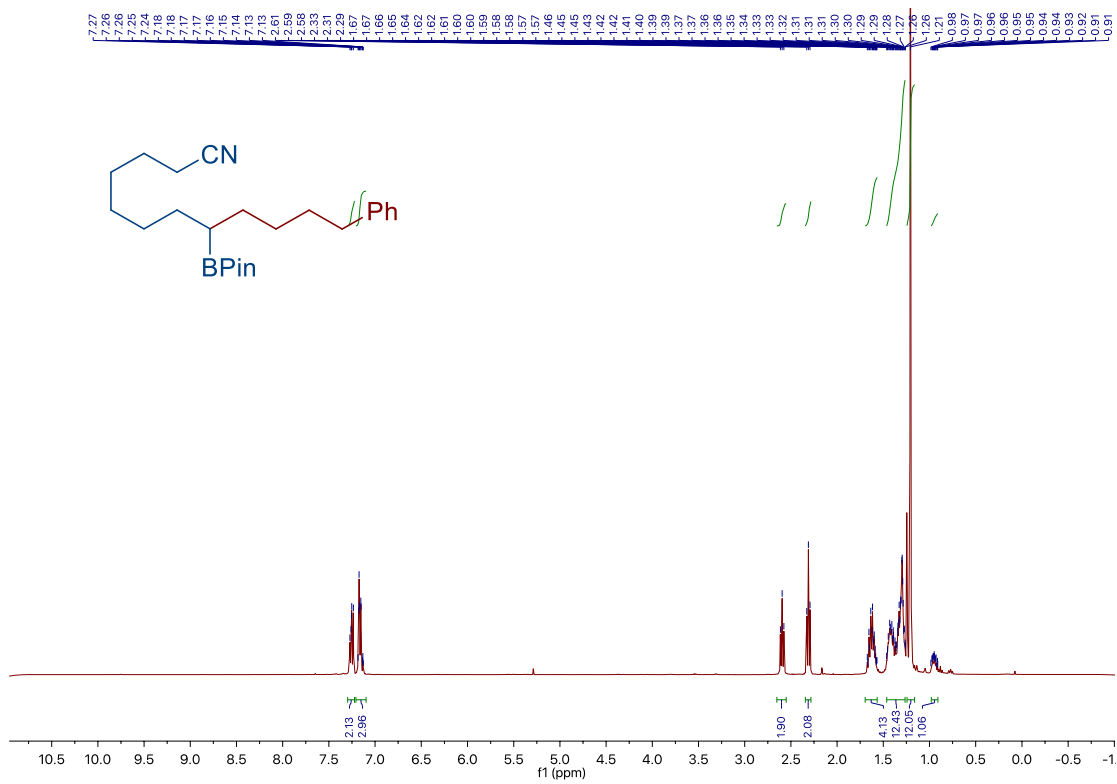
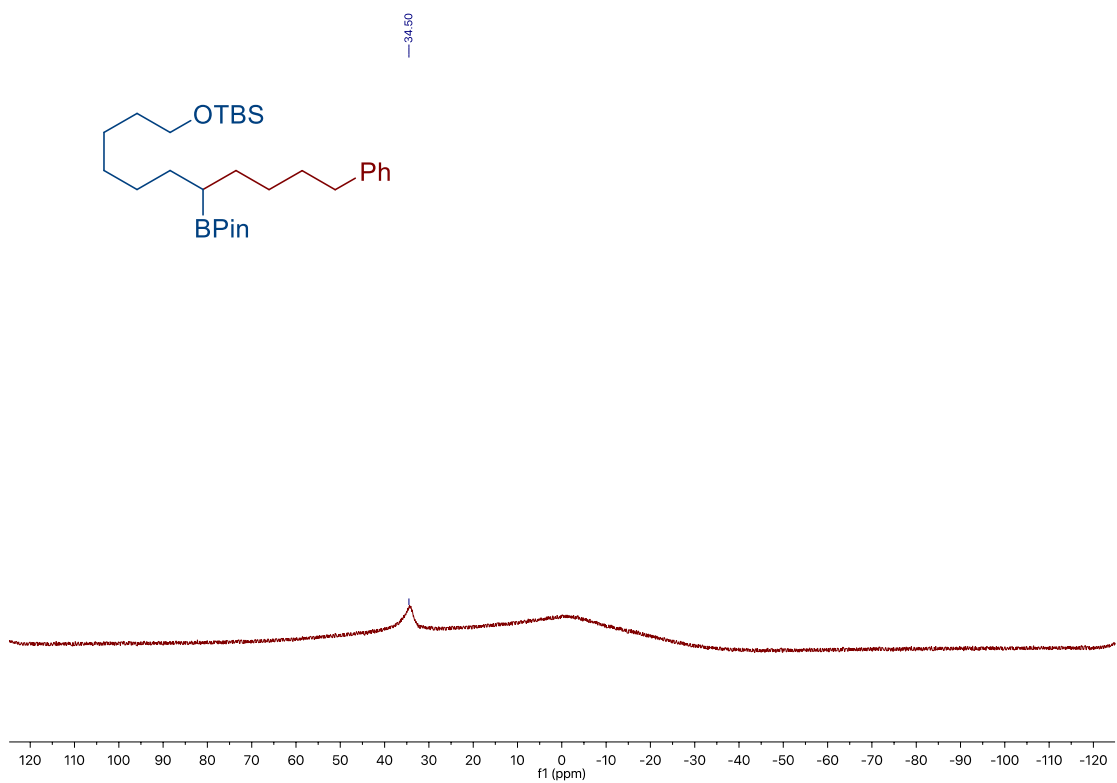
Chapter 2.



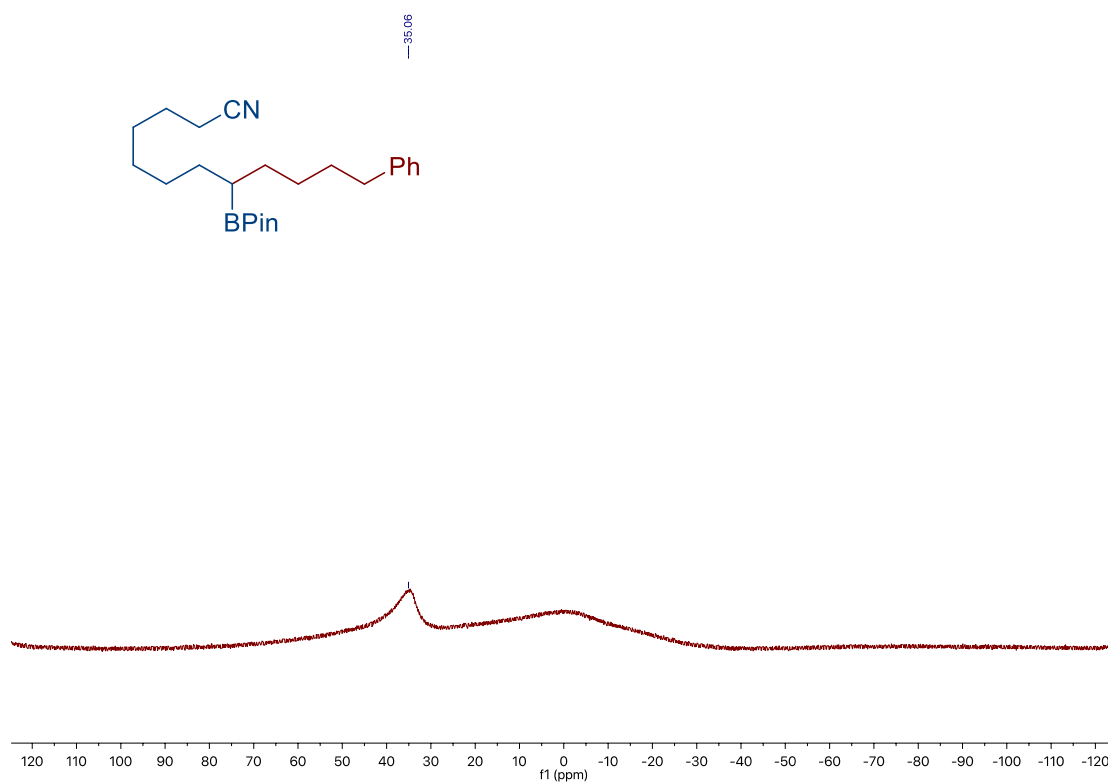
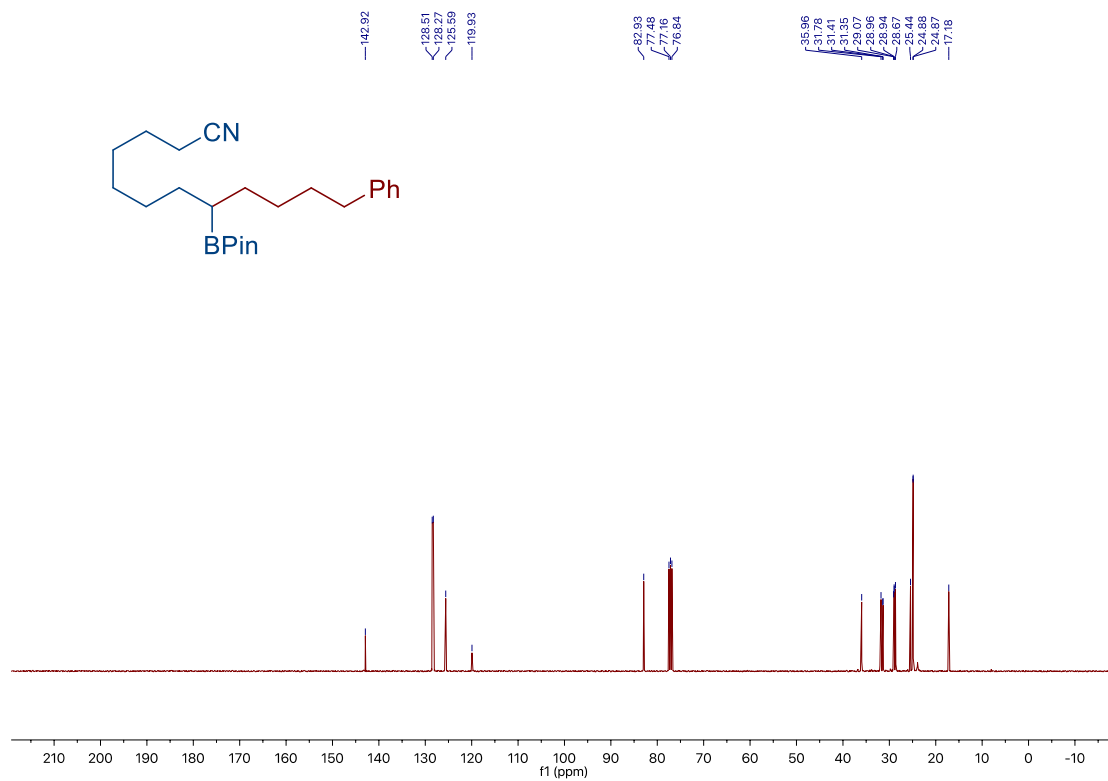
*Site-Selective Ni-Catalyzed Reductive
Coupling of α -Haloboranes with Unactivated Olefins*



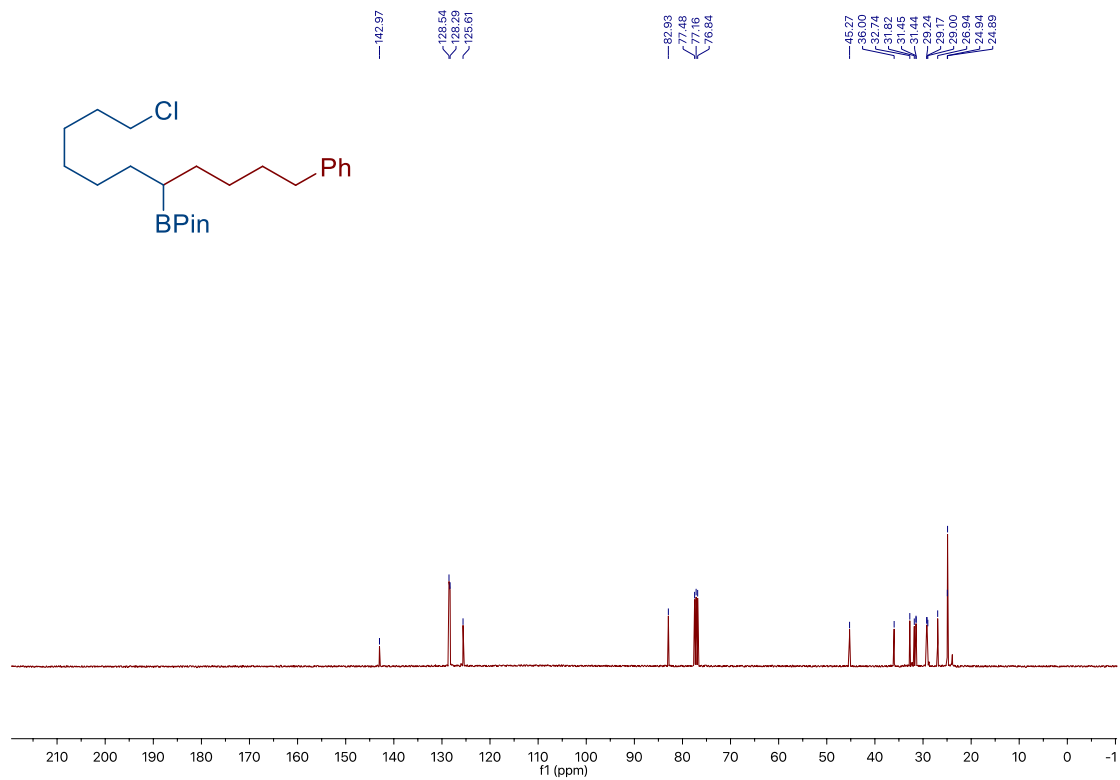
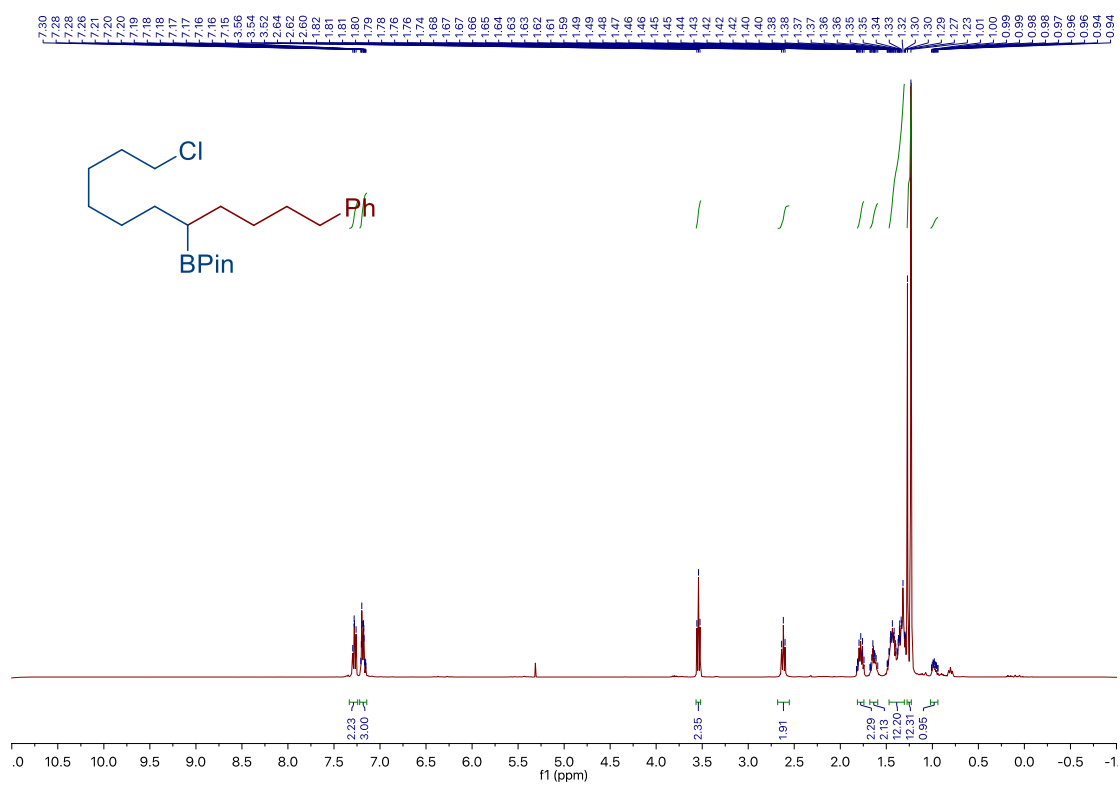
Chapter 2.



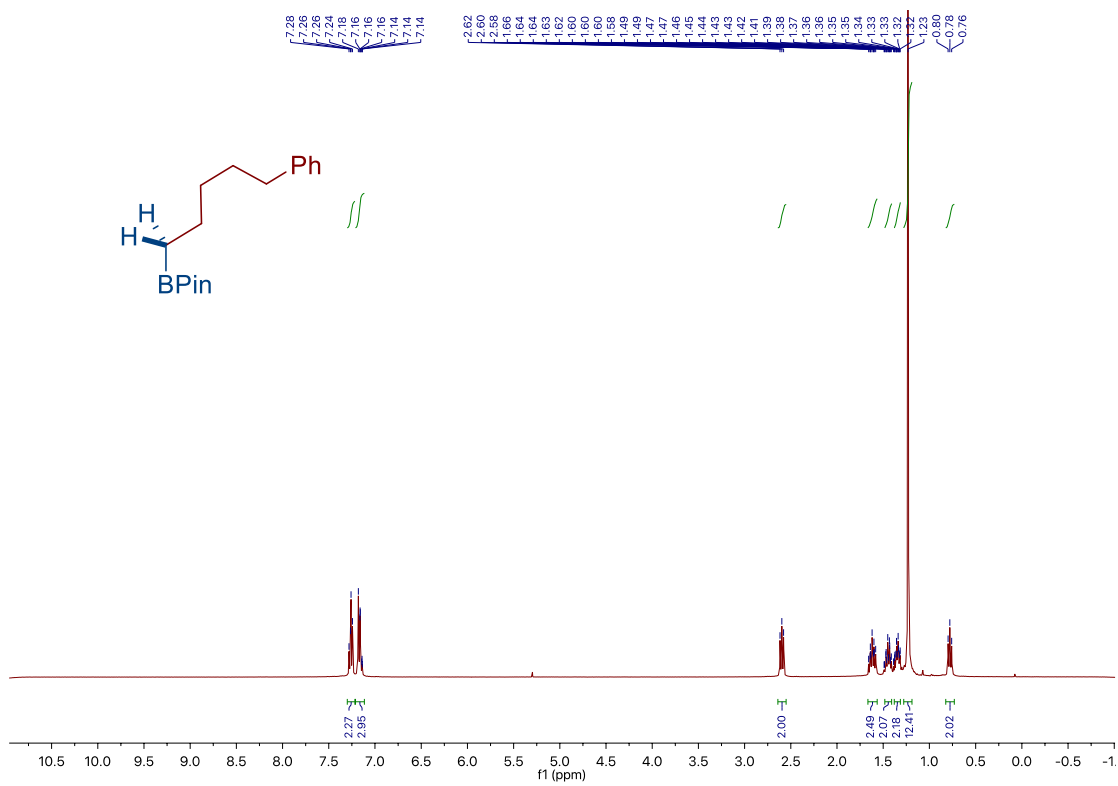
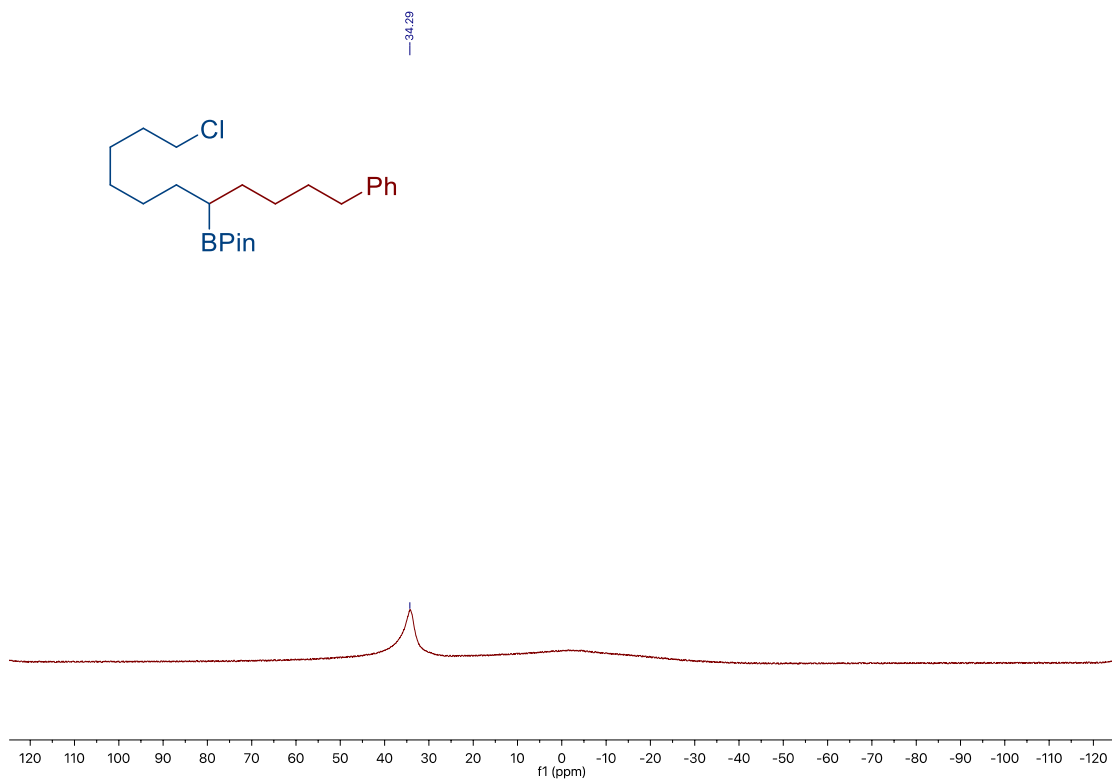
Site-Selective Ni-Catalyzed Reductive
Coupling of α -Haloboranes with Unactivated Olefins



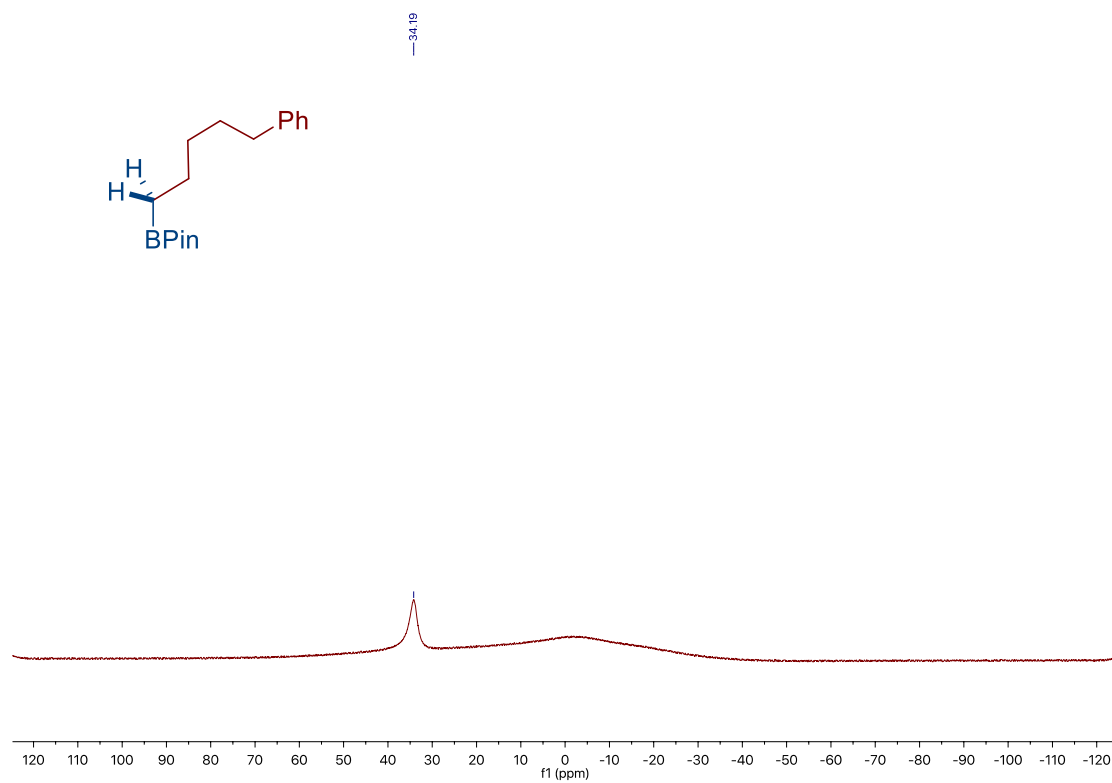
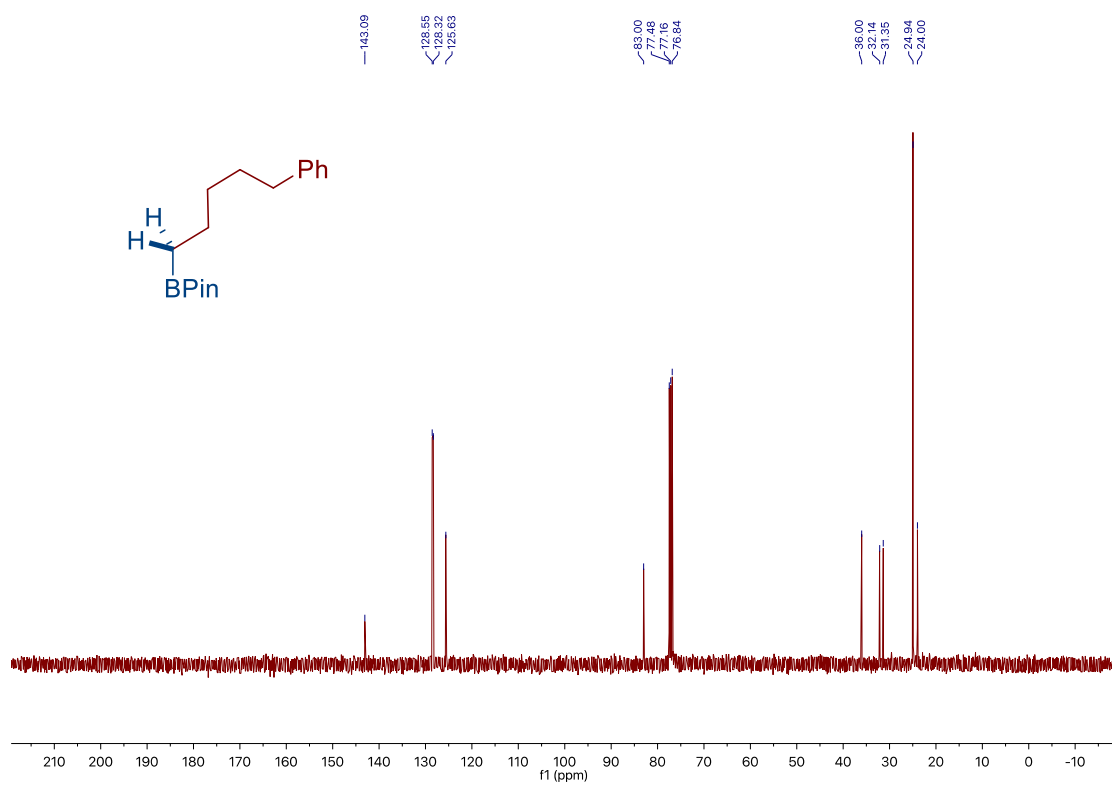
Chapter 2.



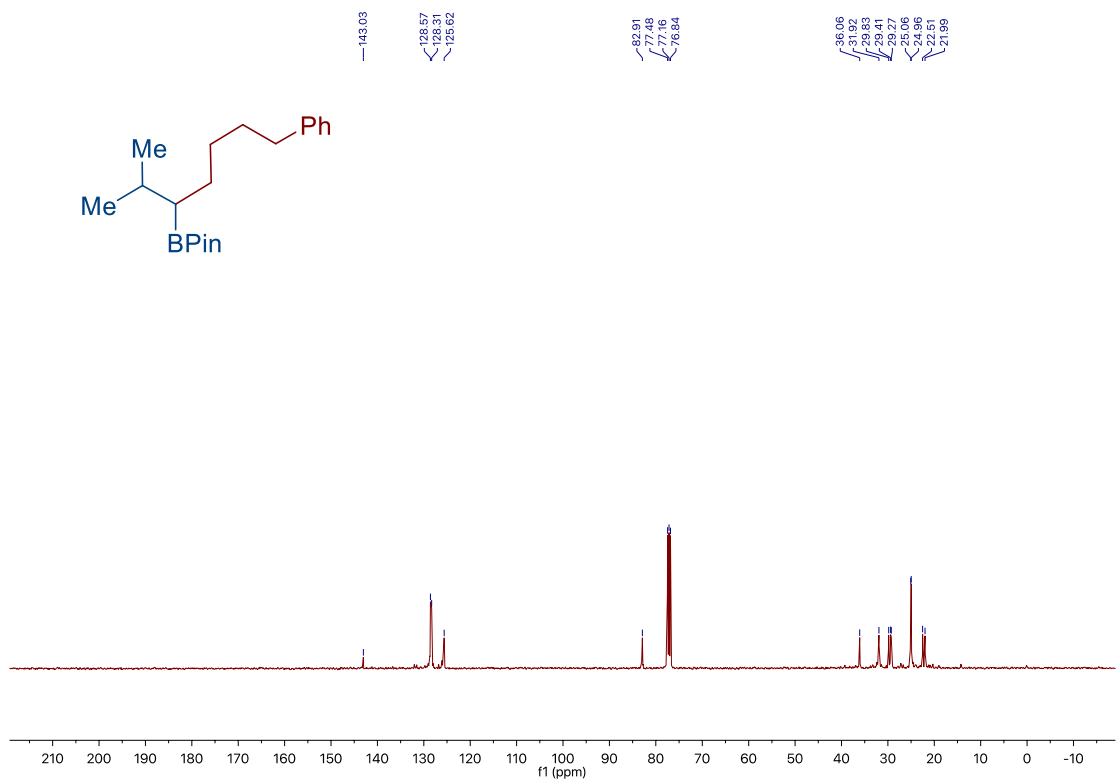
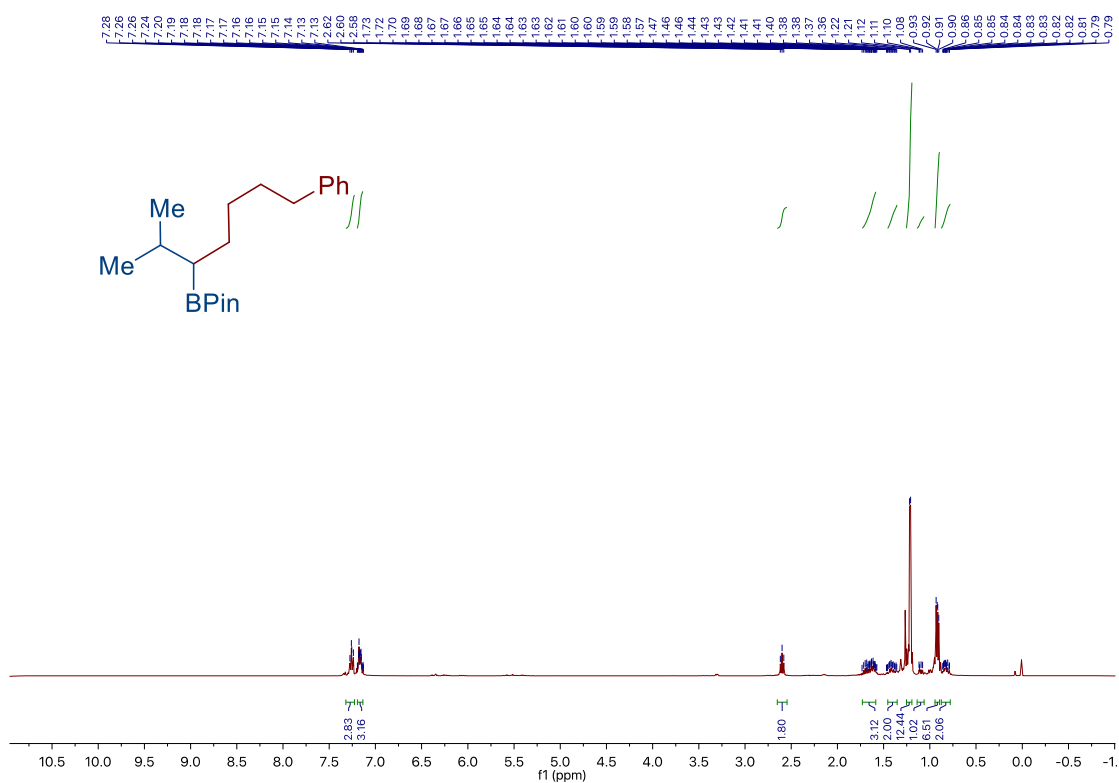
*Site-Selective Ni-Catalyzed Reductive
Coupling of α -Haloboranes with Unactivated Olefins*



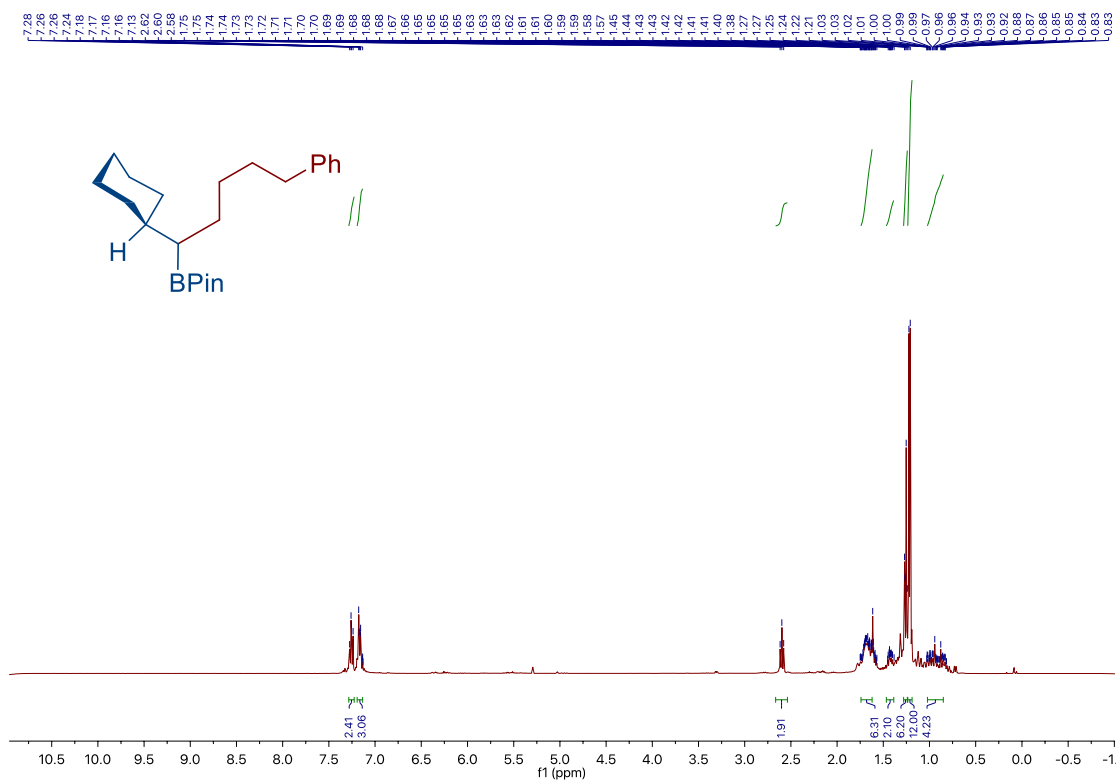
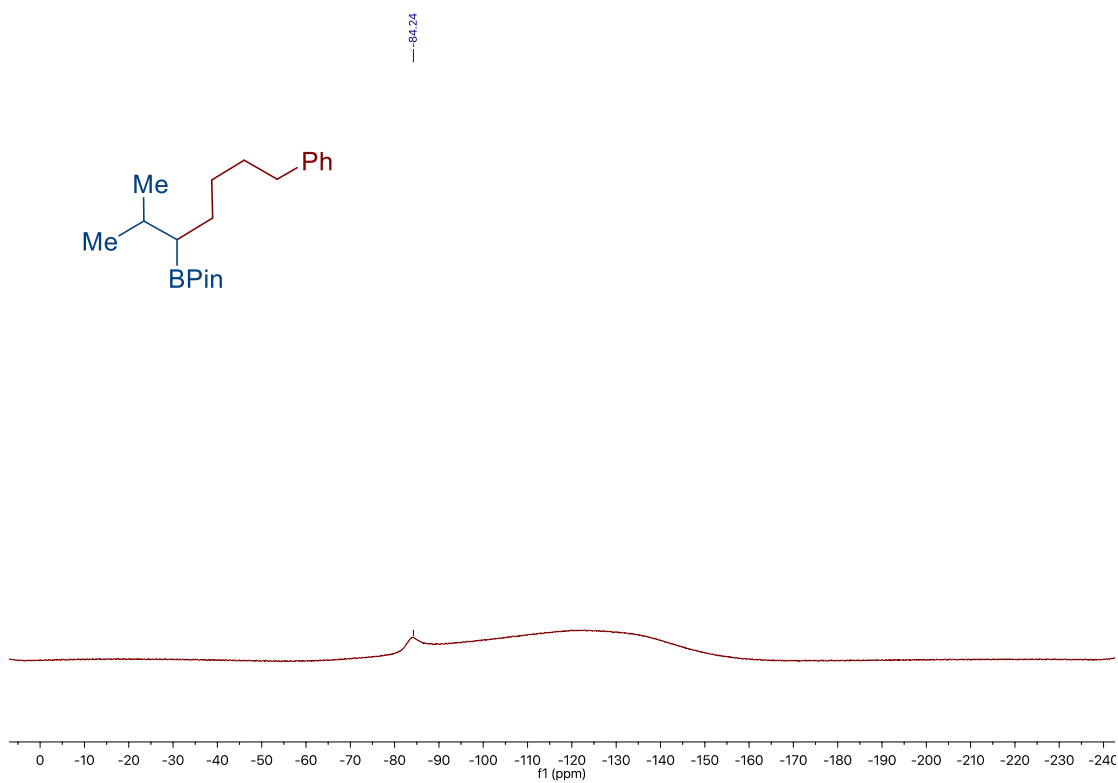
Chapter 2.



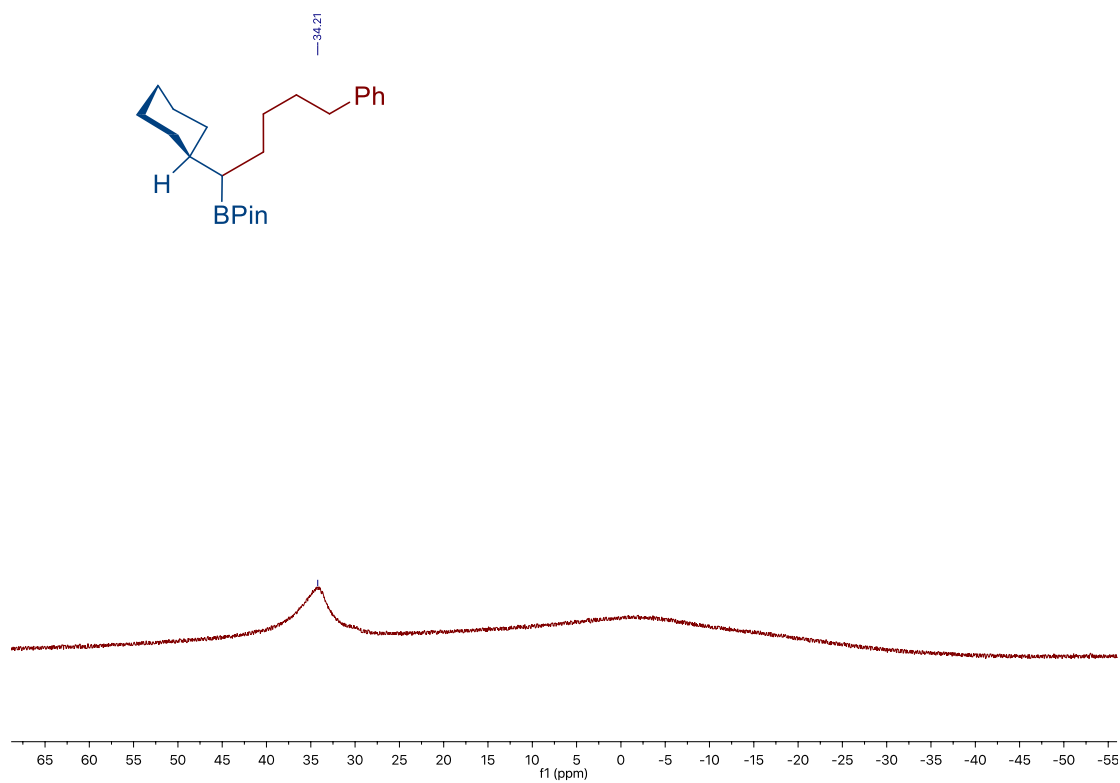
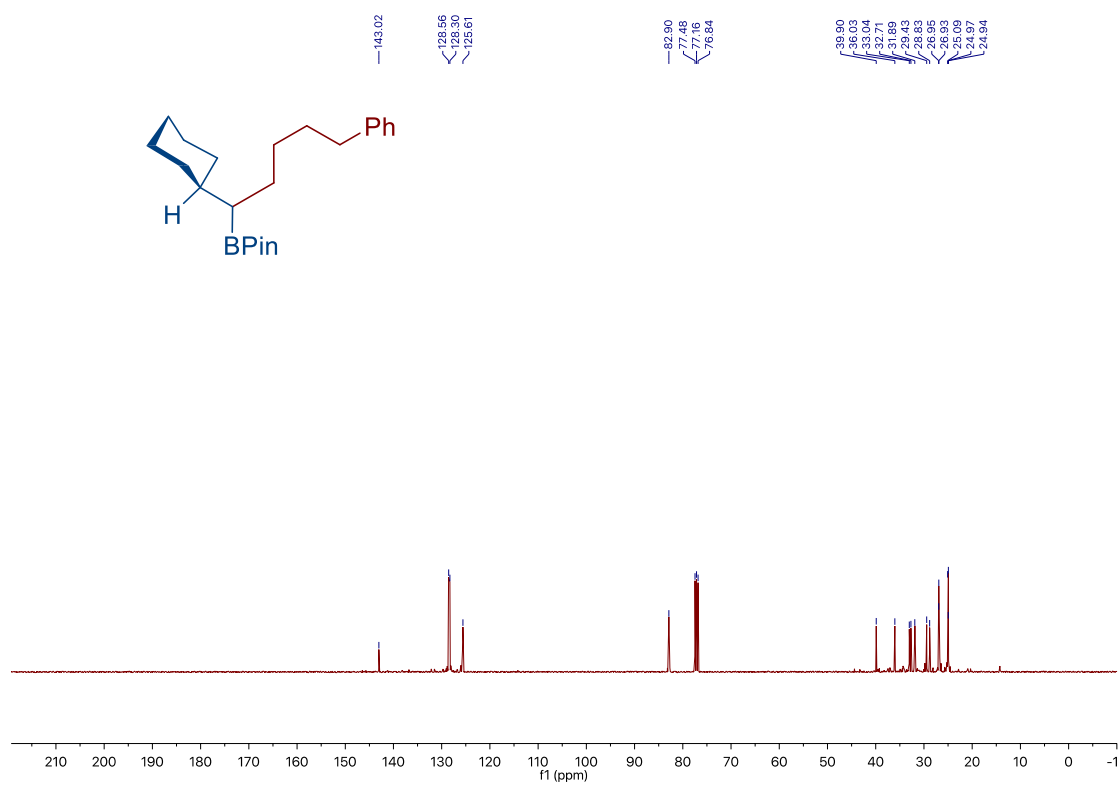
Site-Selective Ni-Catalyzed Reductive Coupling of α -Haloboranes with Unactivated Olefins



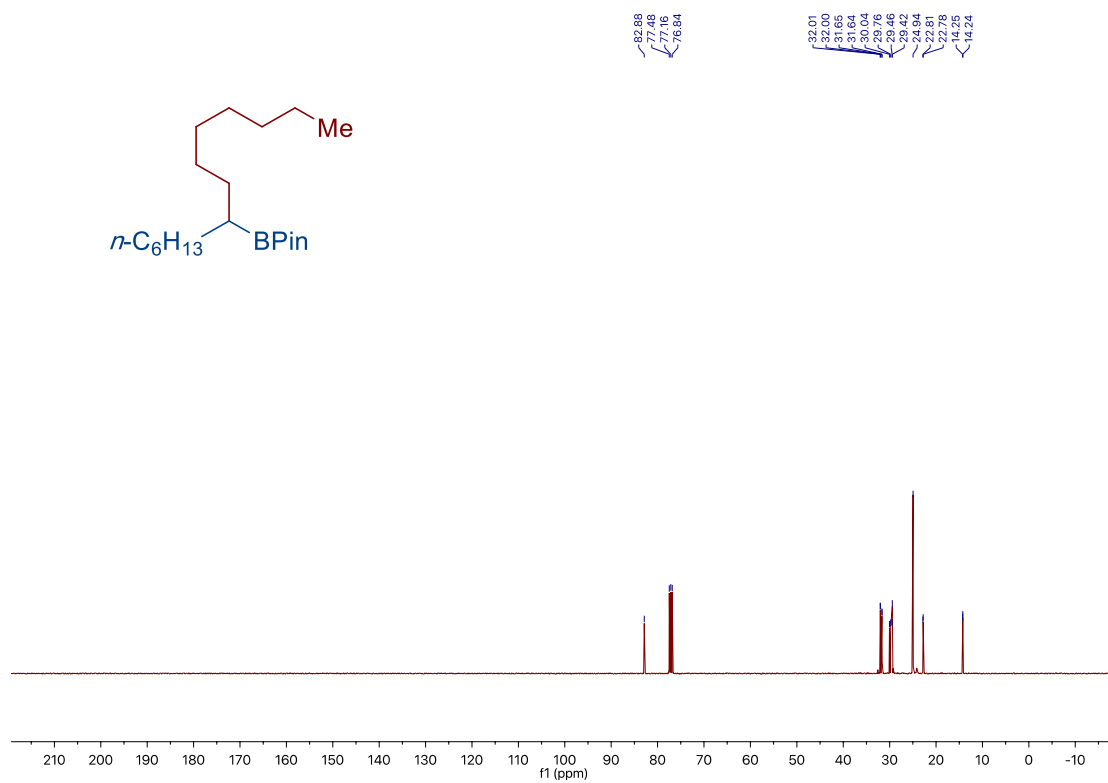
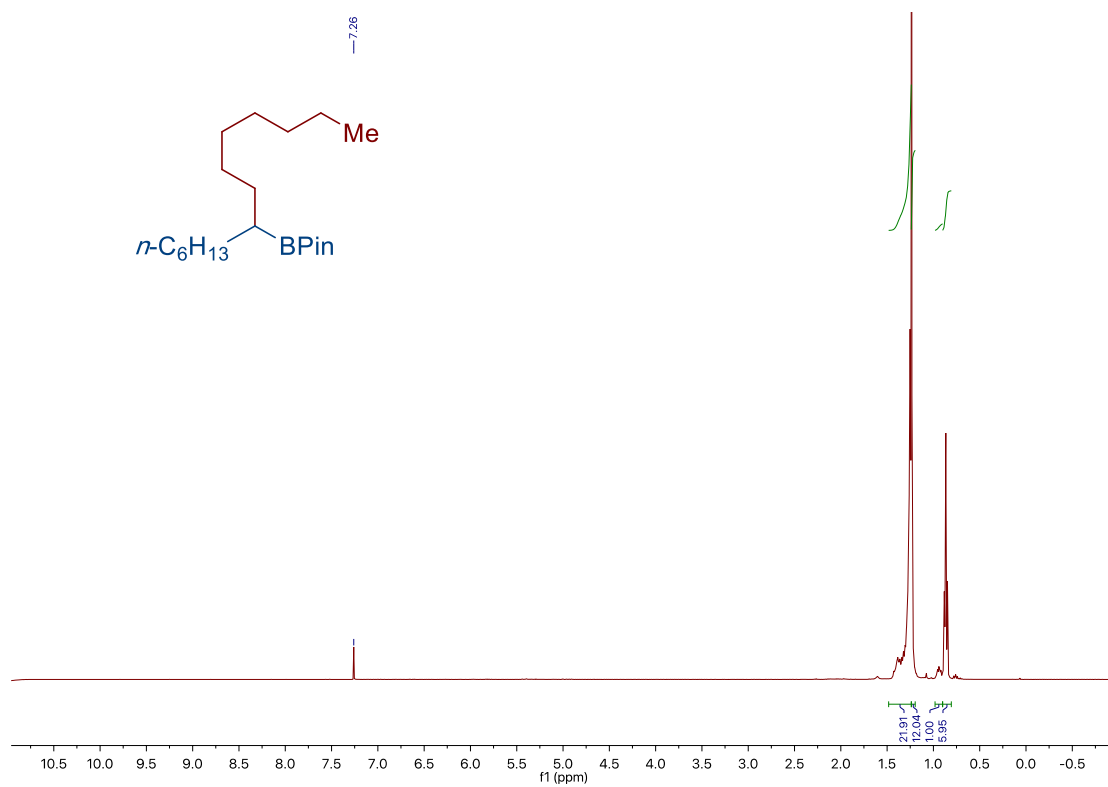
Chapter 2.



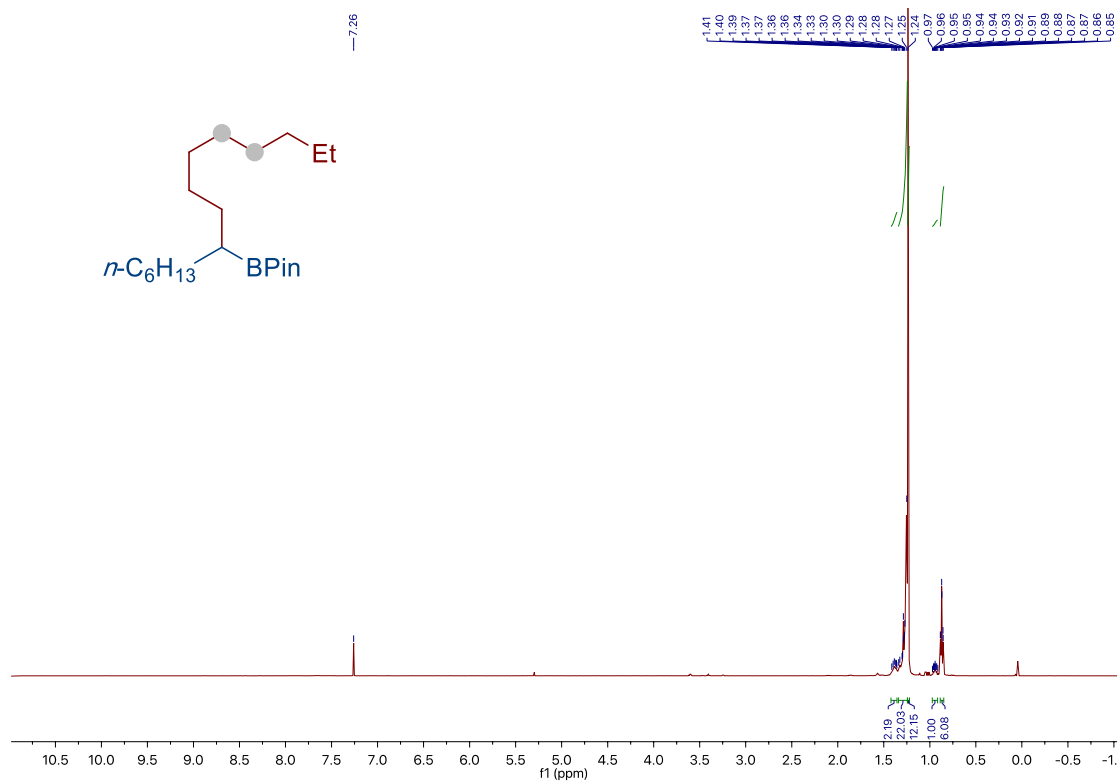
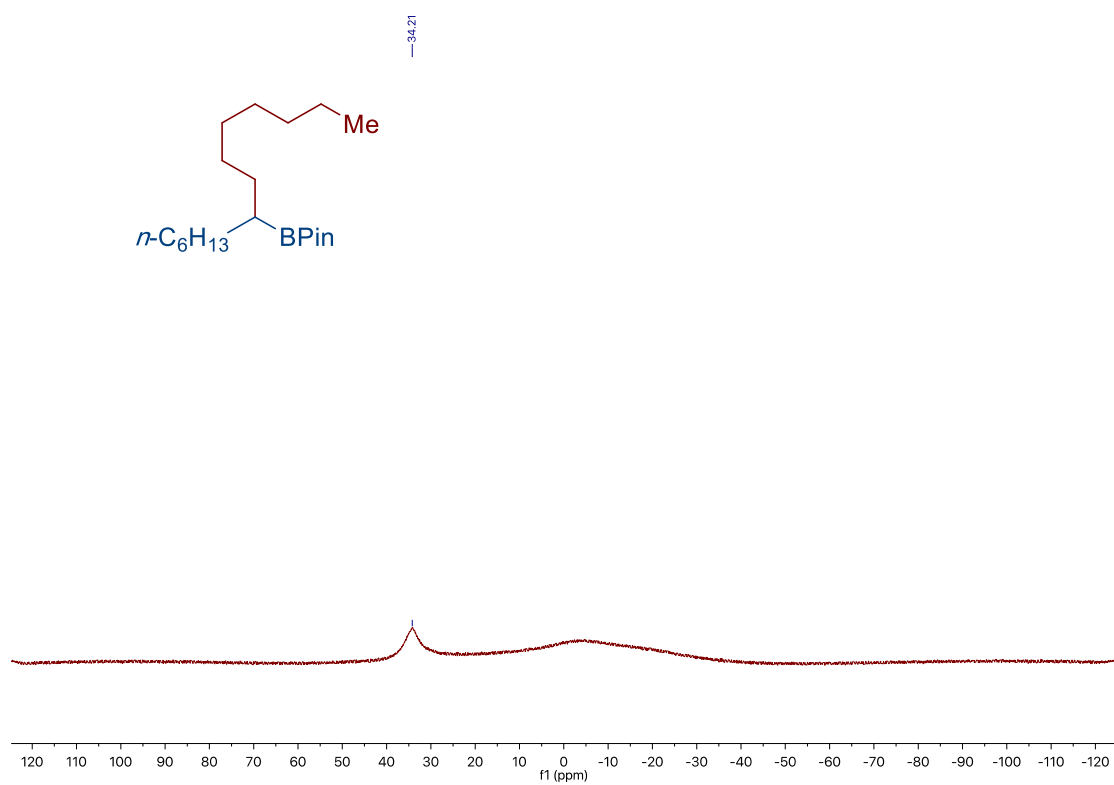
Site-Selective Ni-Catalyzed Reductive
Coupling of α -Haloboranes with Unactivated Olefins



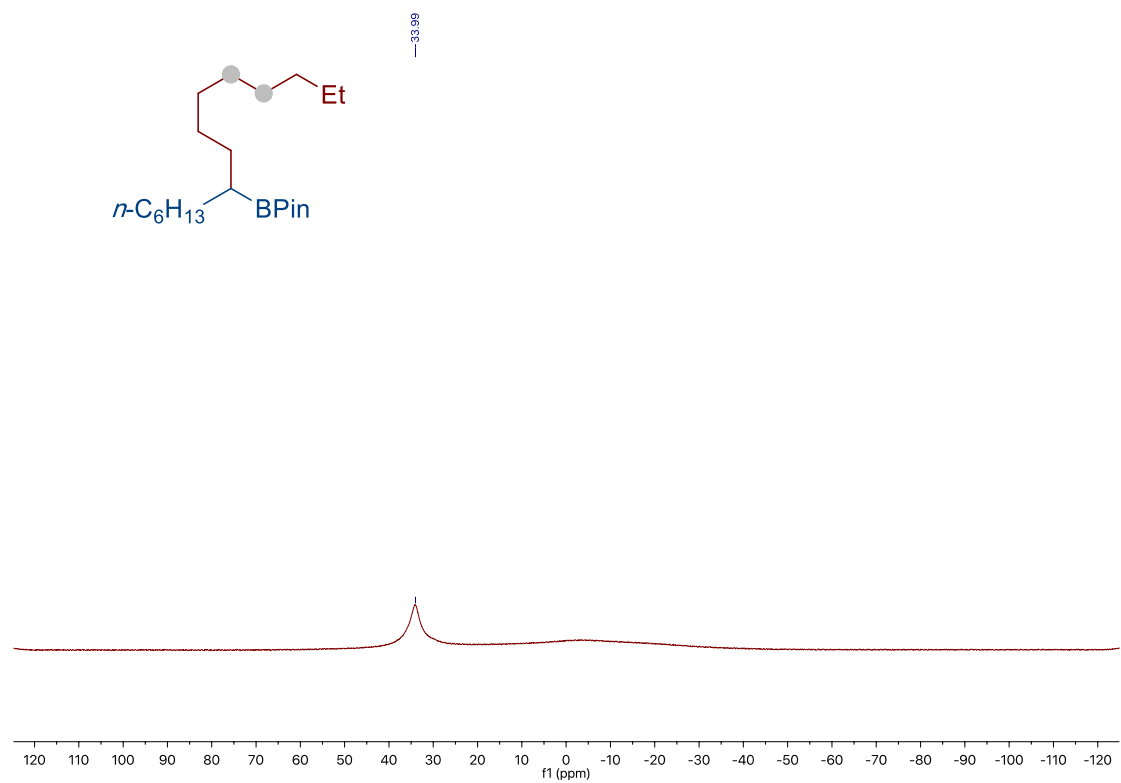
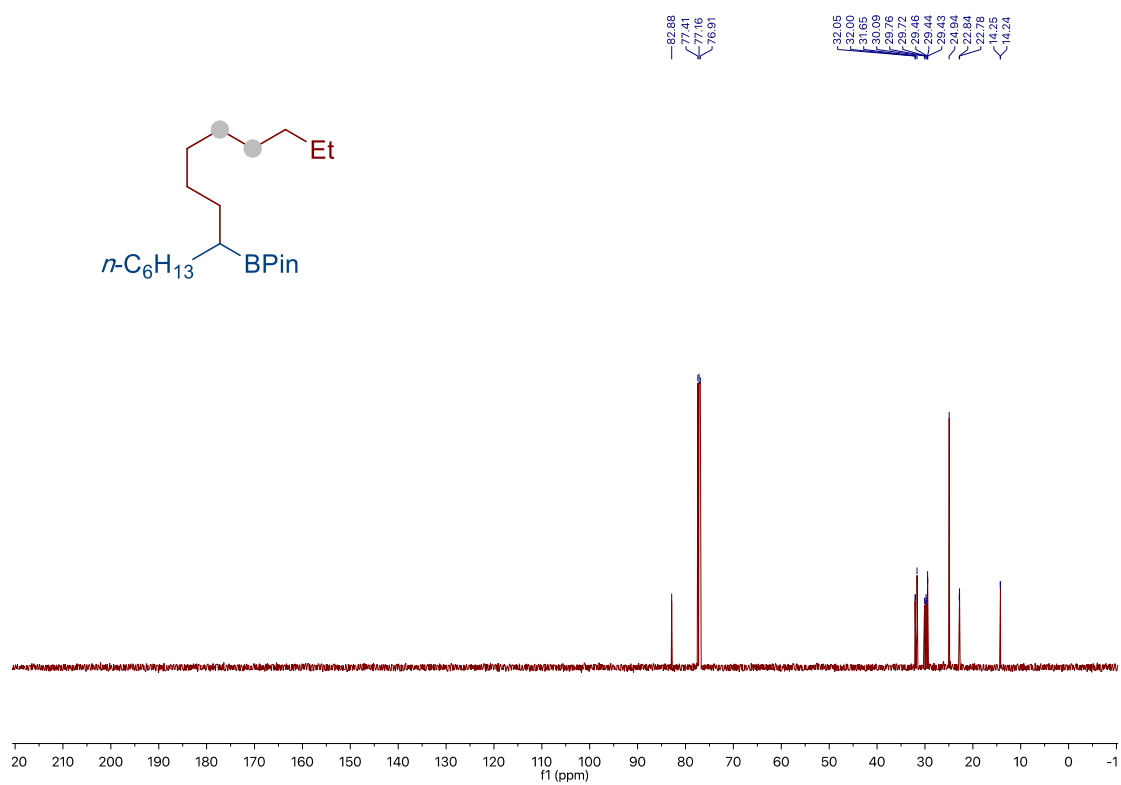
Chapter 2.



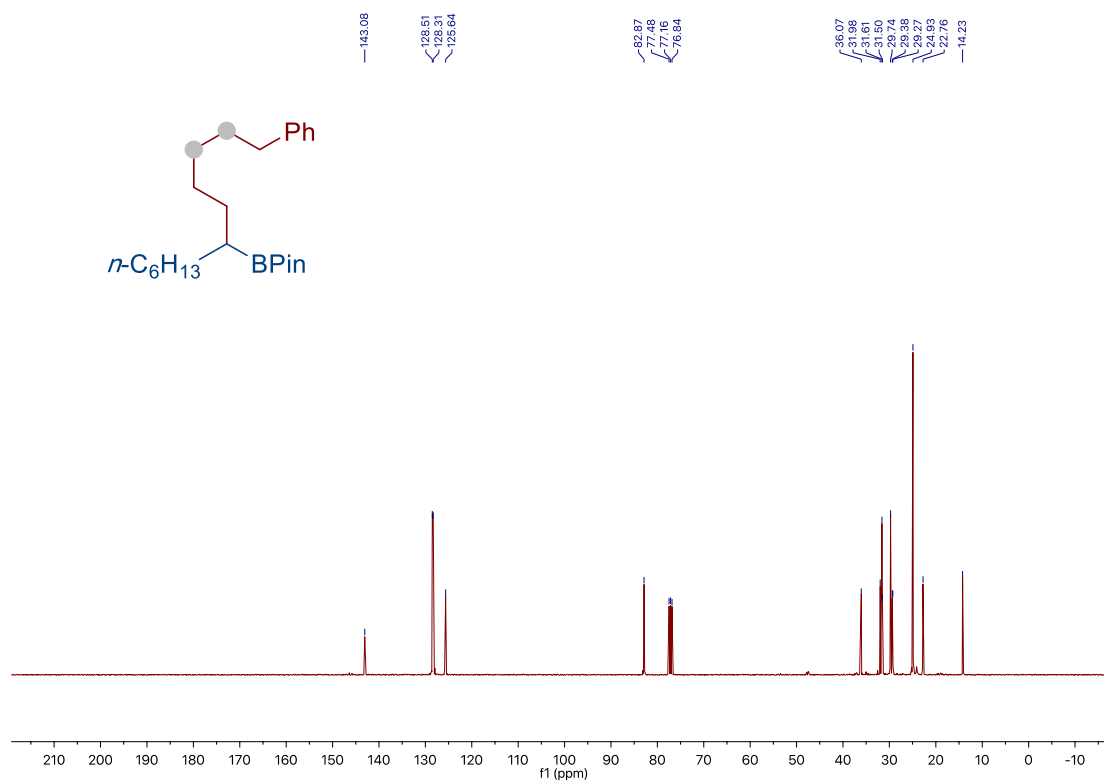
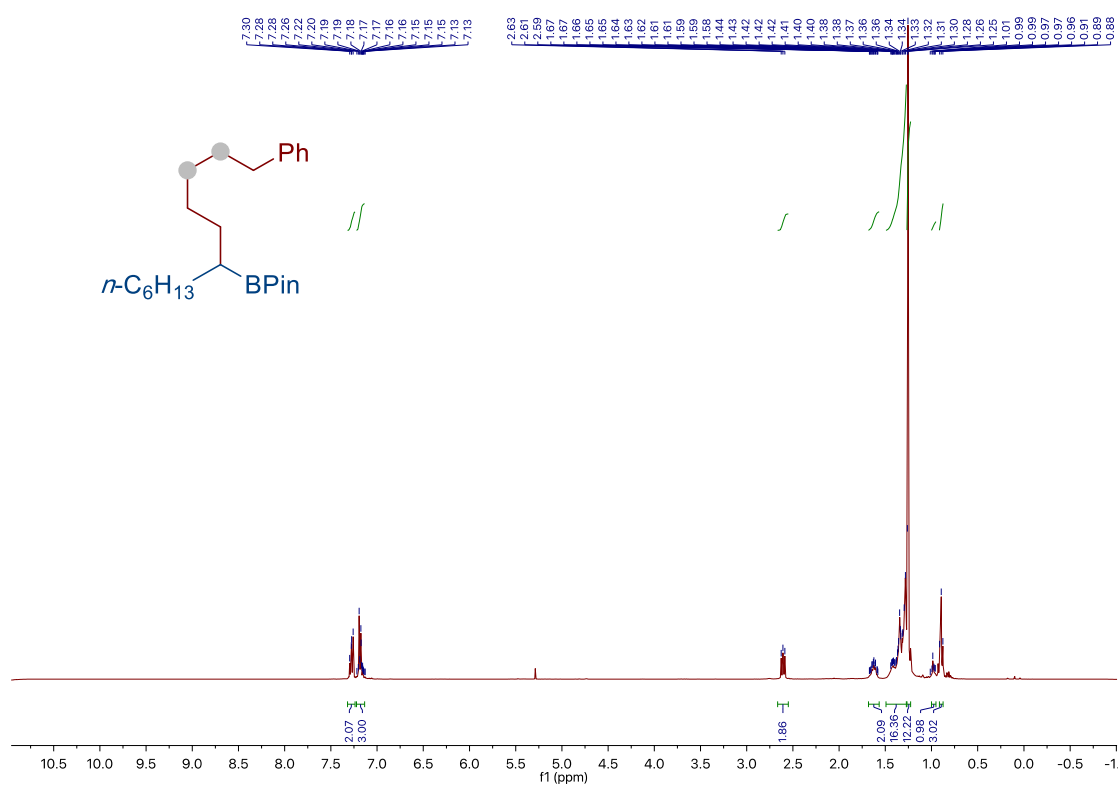
Site-Selective Ni-Catalyzed Reductive
Coupling of α -Haloboranes with Unactivated Olefins



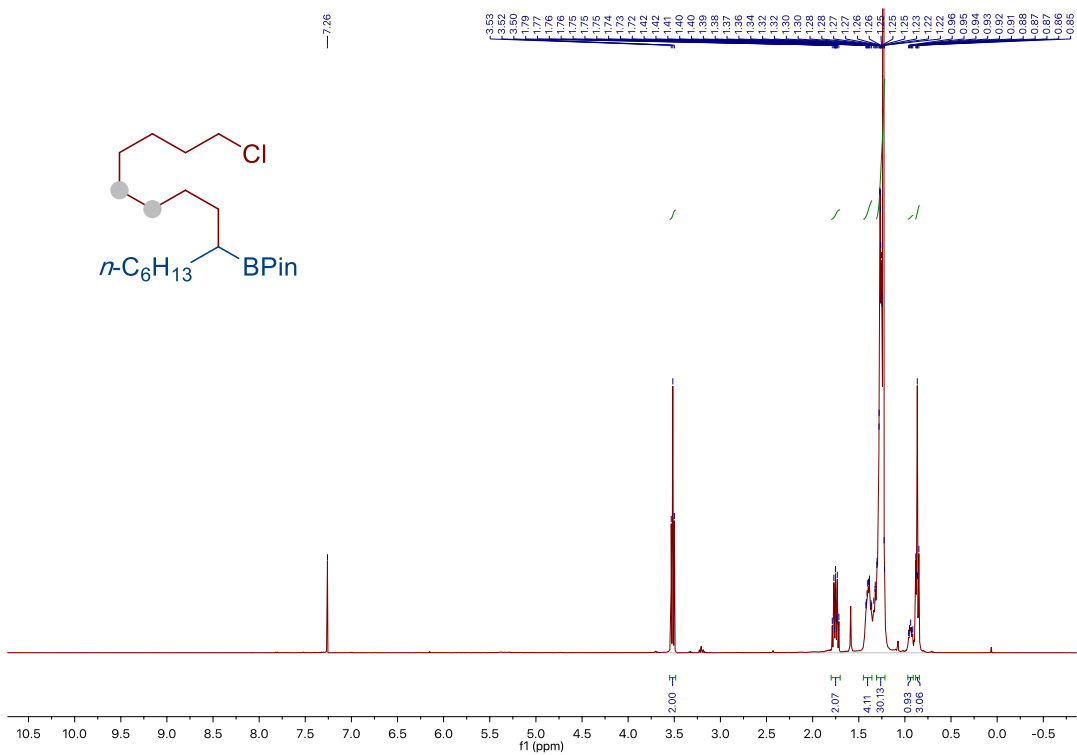
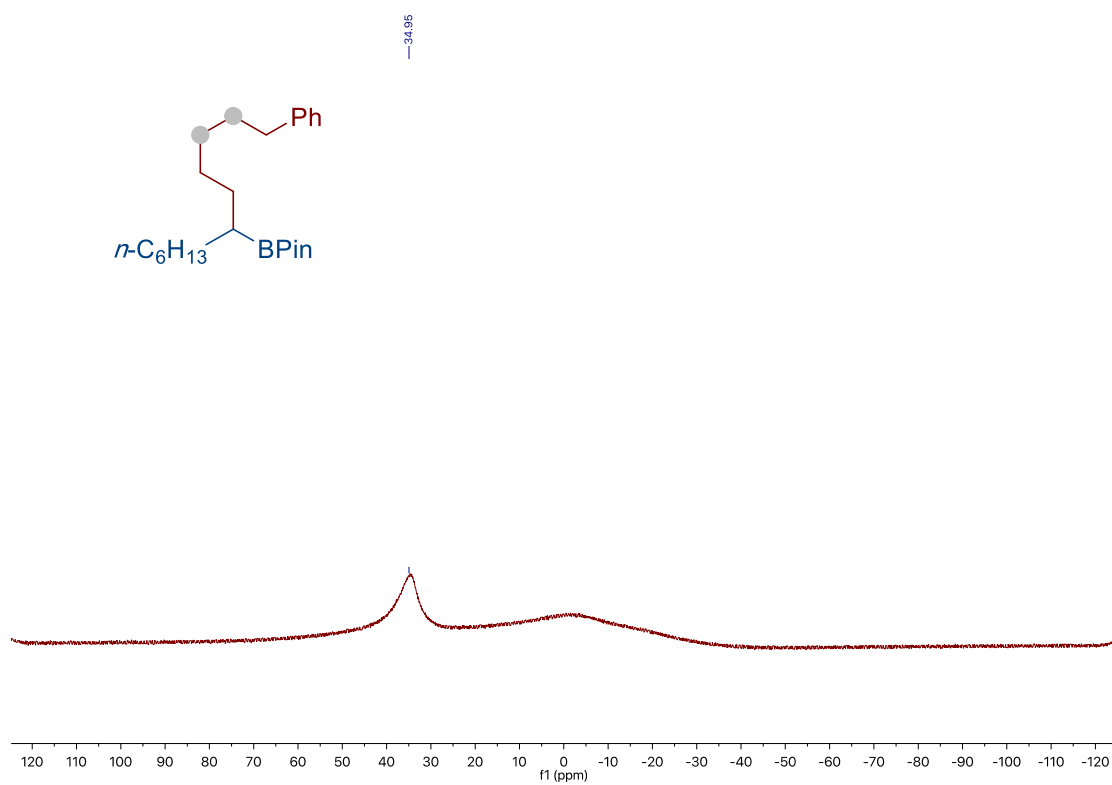
Chapter 2.



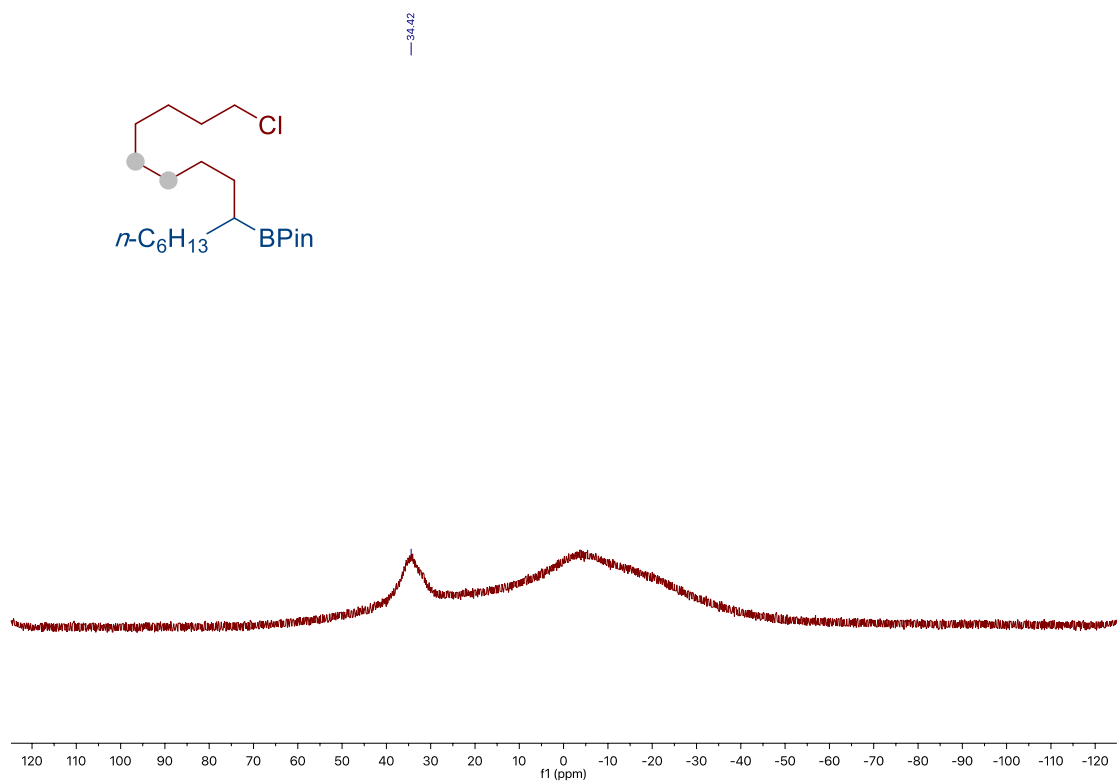
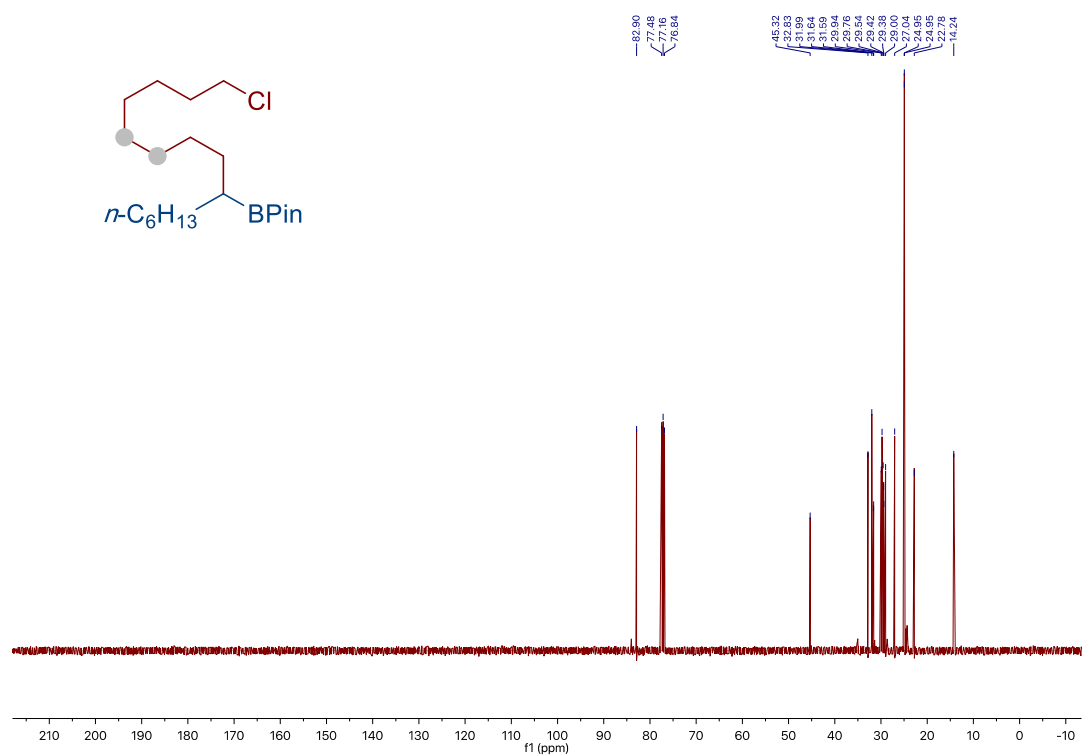
*Site-Selective Ni-Catalyzed Reductive
Coupling of α -Haloboranes with Unactivated Olefins*



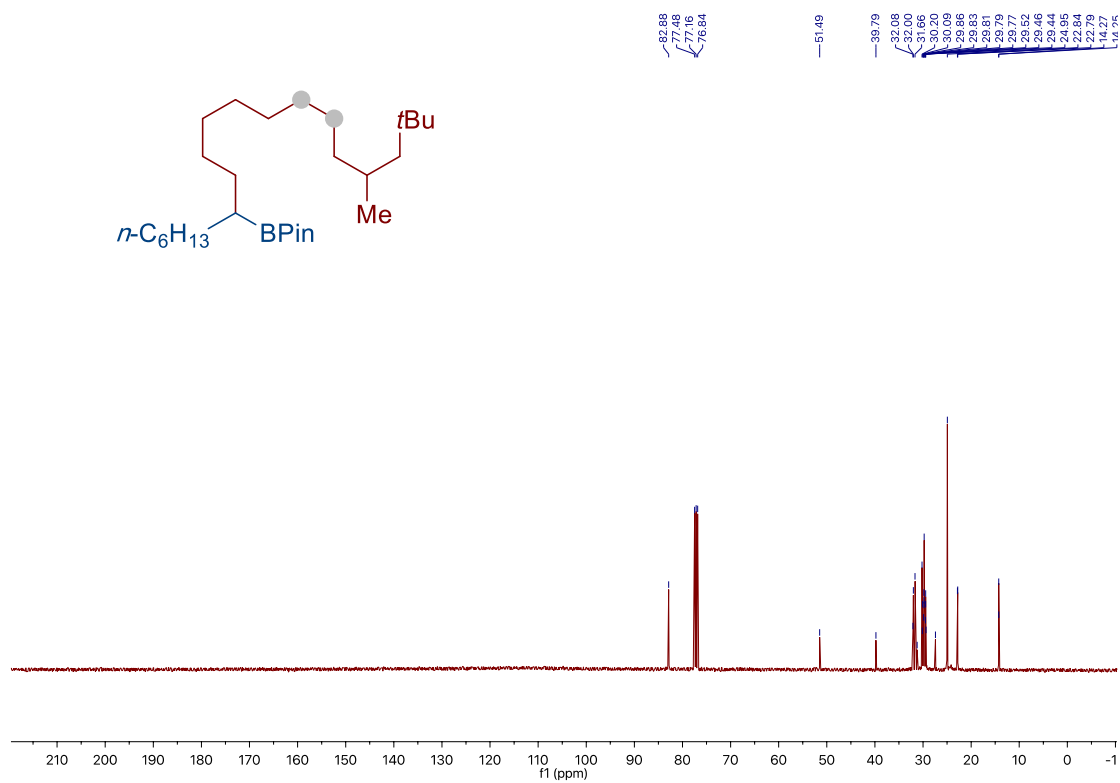
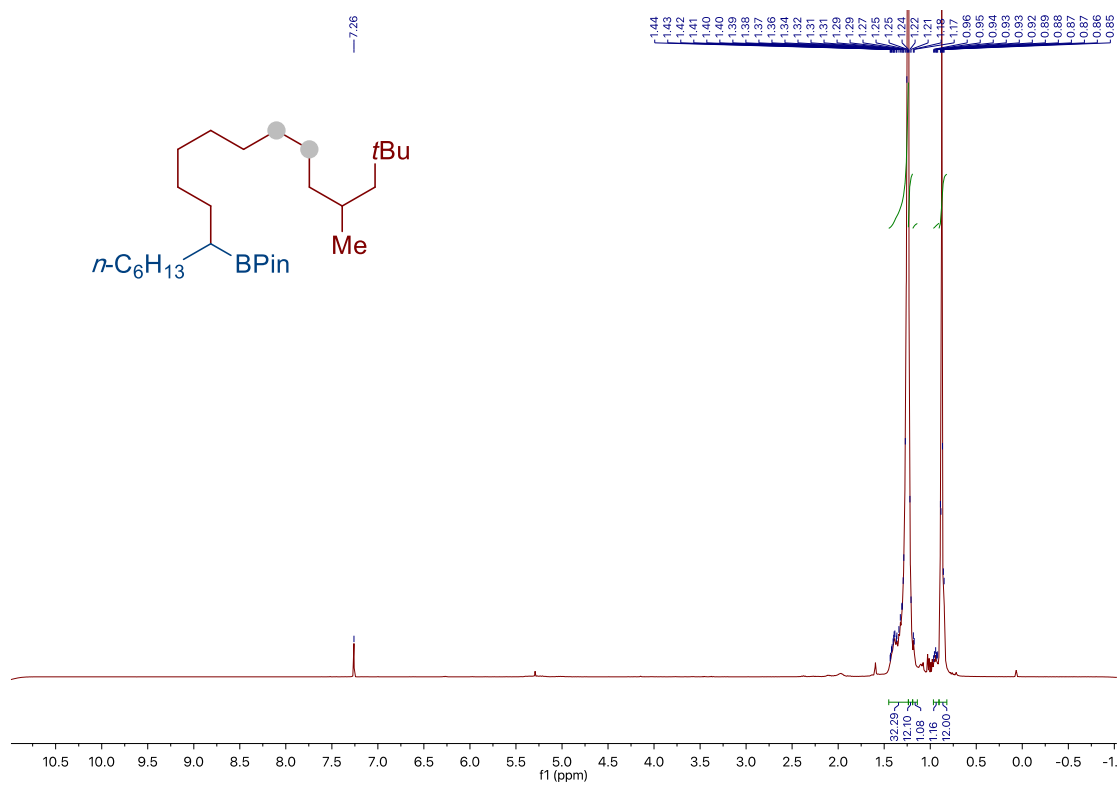
Chapter 2.



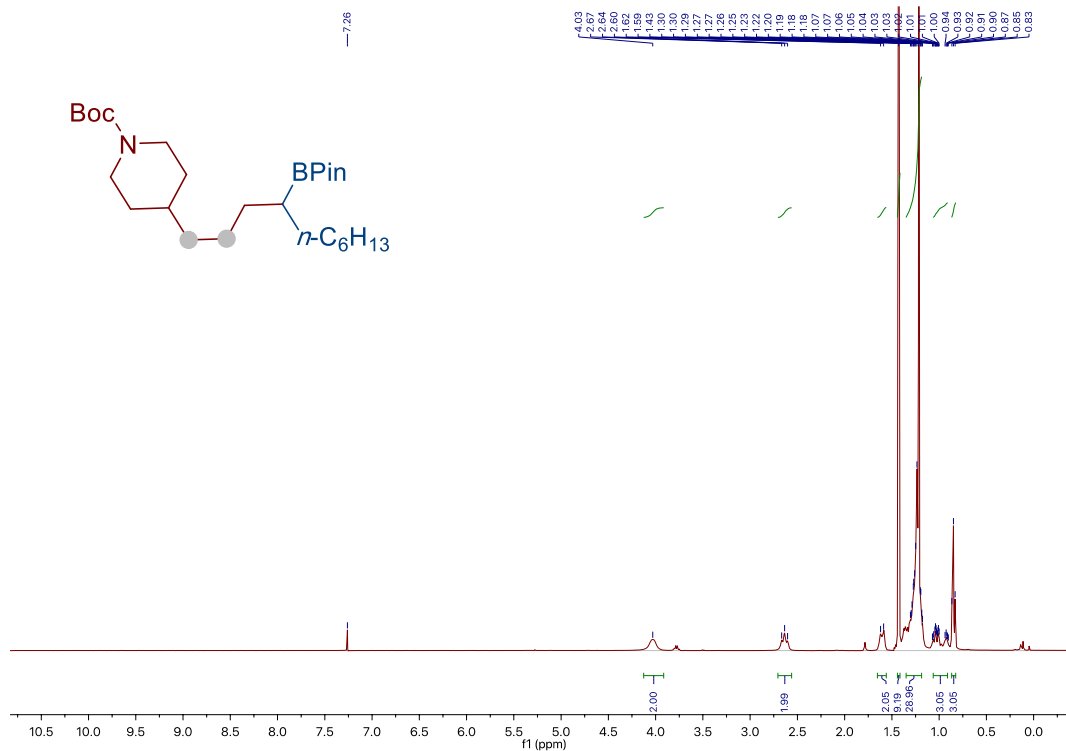
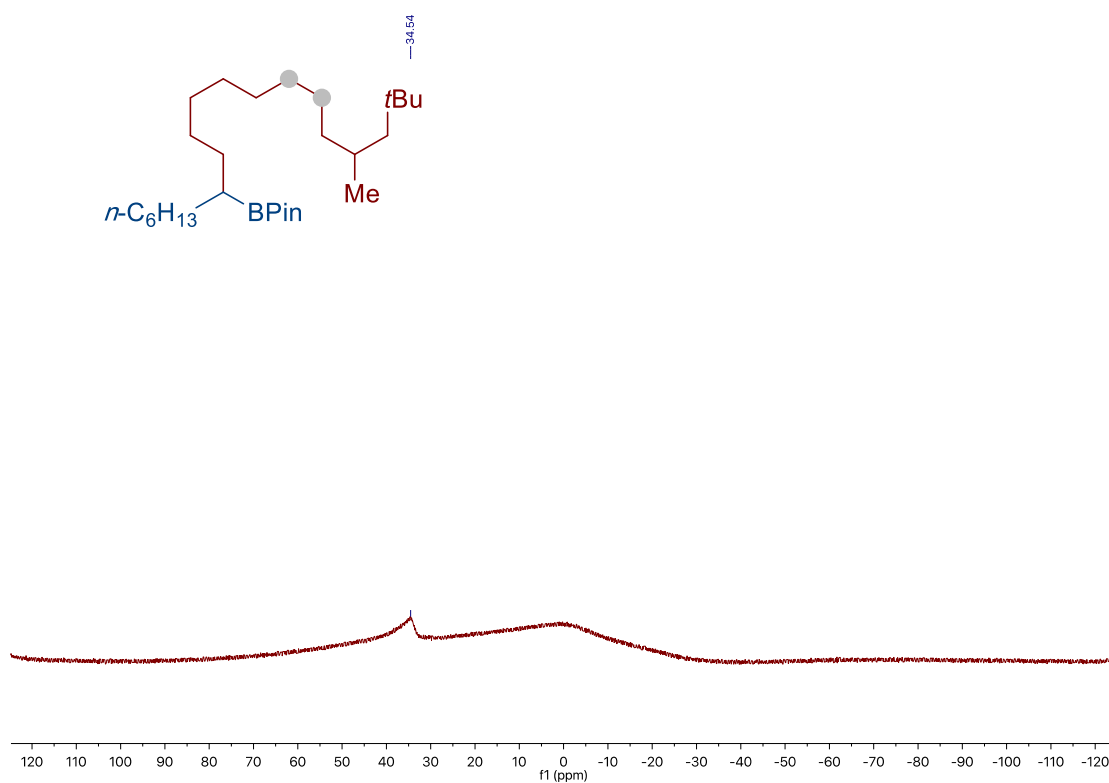
Site-Selective Ni-Catalyzed Reductive
Coupling of α -Haloboranes with Unactivated Olefins



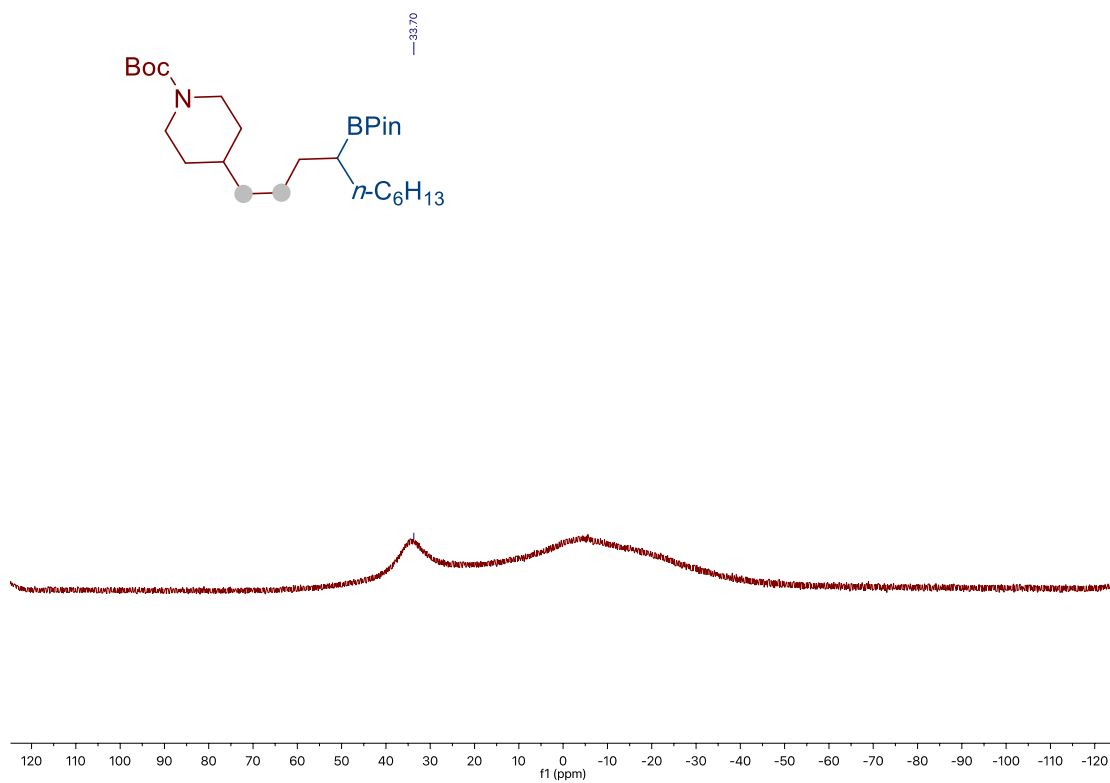
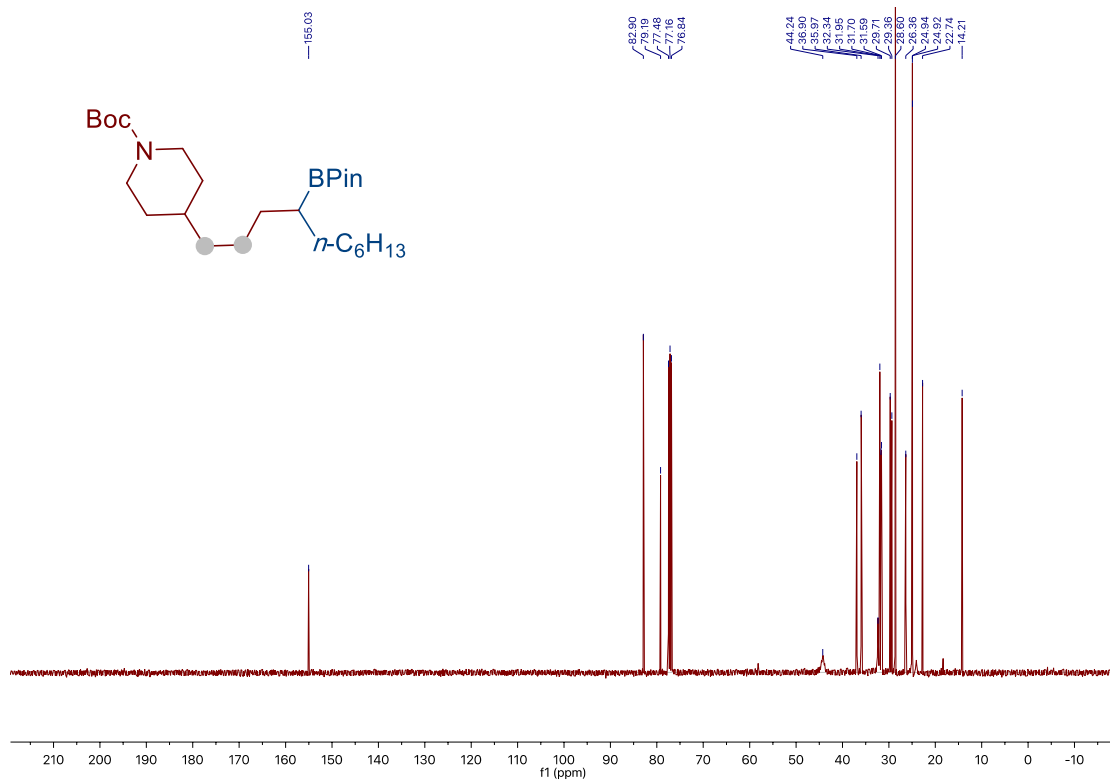
Chapter 2.



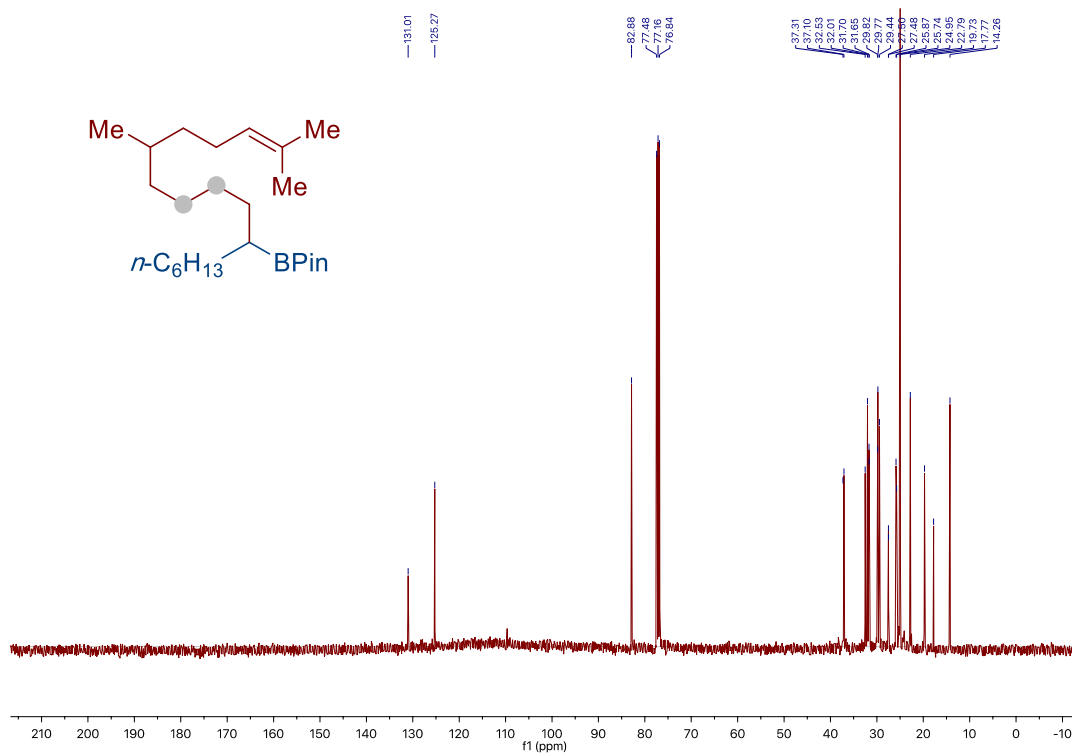
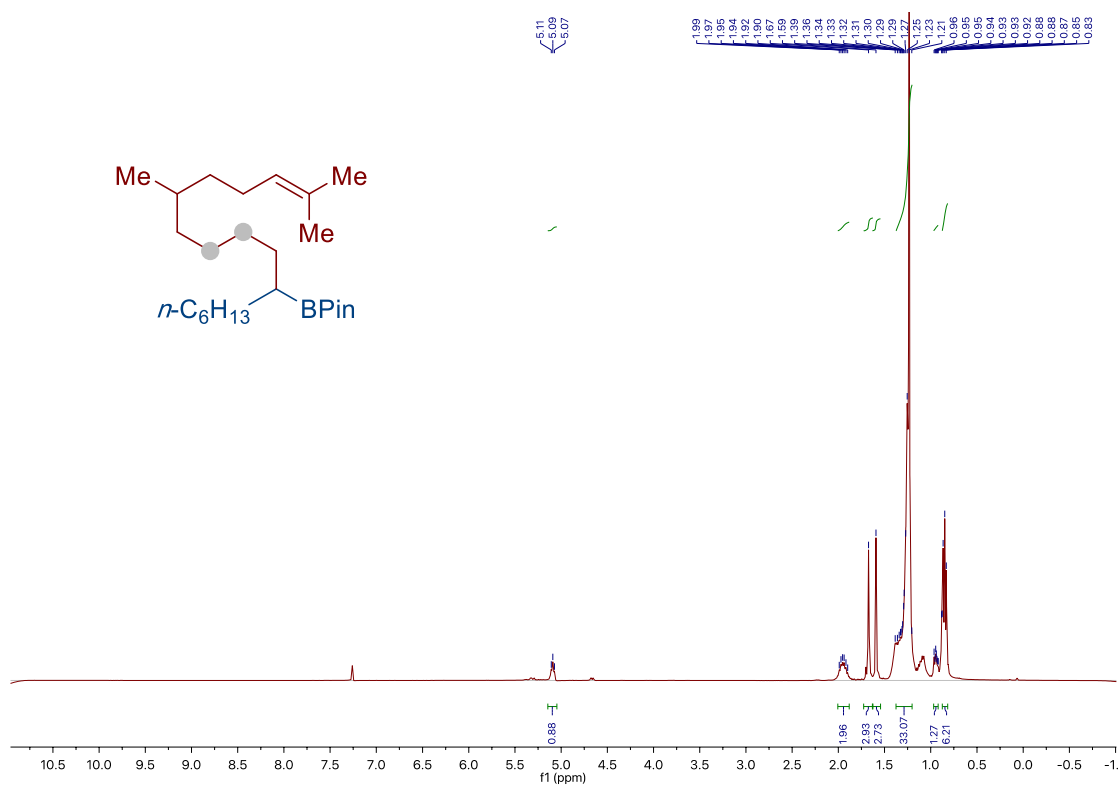
*Site-Selective Ni-Catalyzed Reductive
Coupling of α -Haloboranes with Unactivated Olefins*



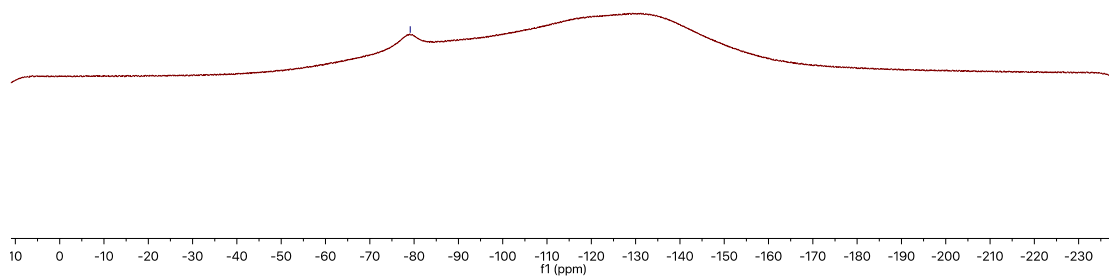
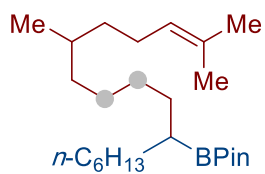
Chapter 2.



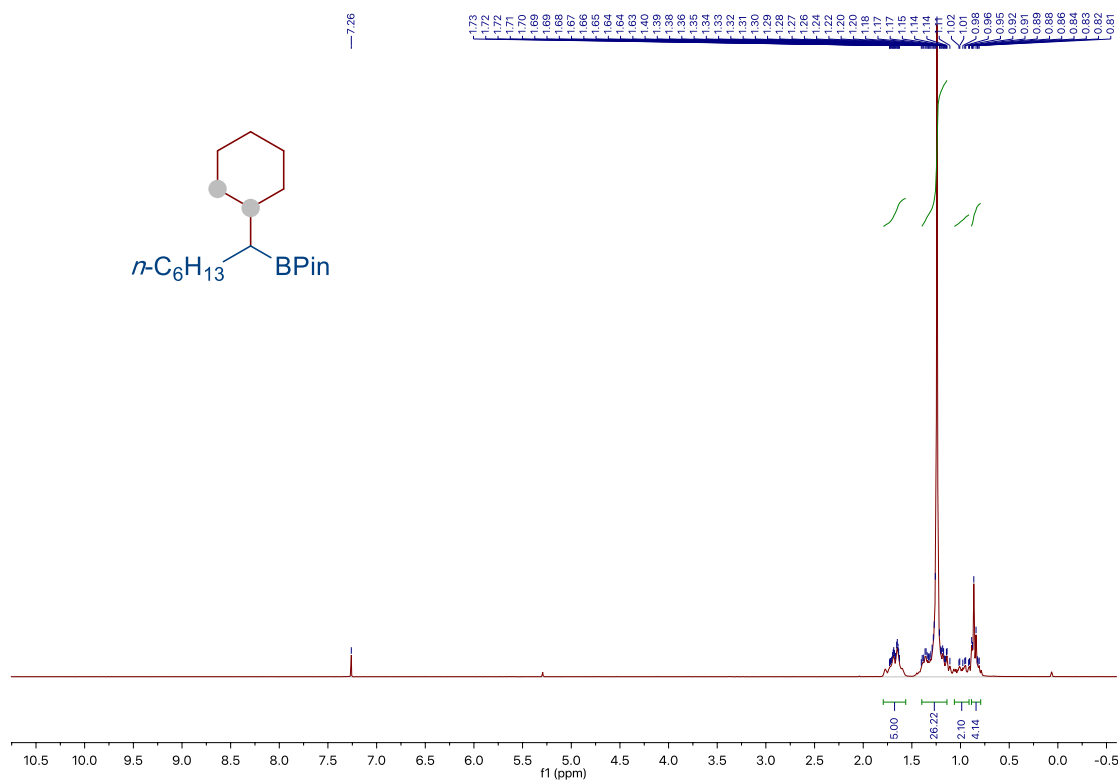
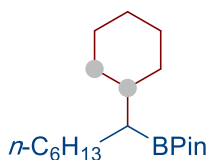
*Site-Selective Ni-Catalyzed Reductive
Coupling of α -Haloboranes with Unactivated Olefins*



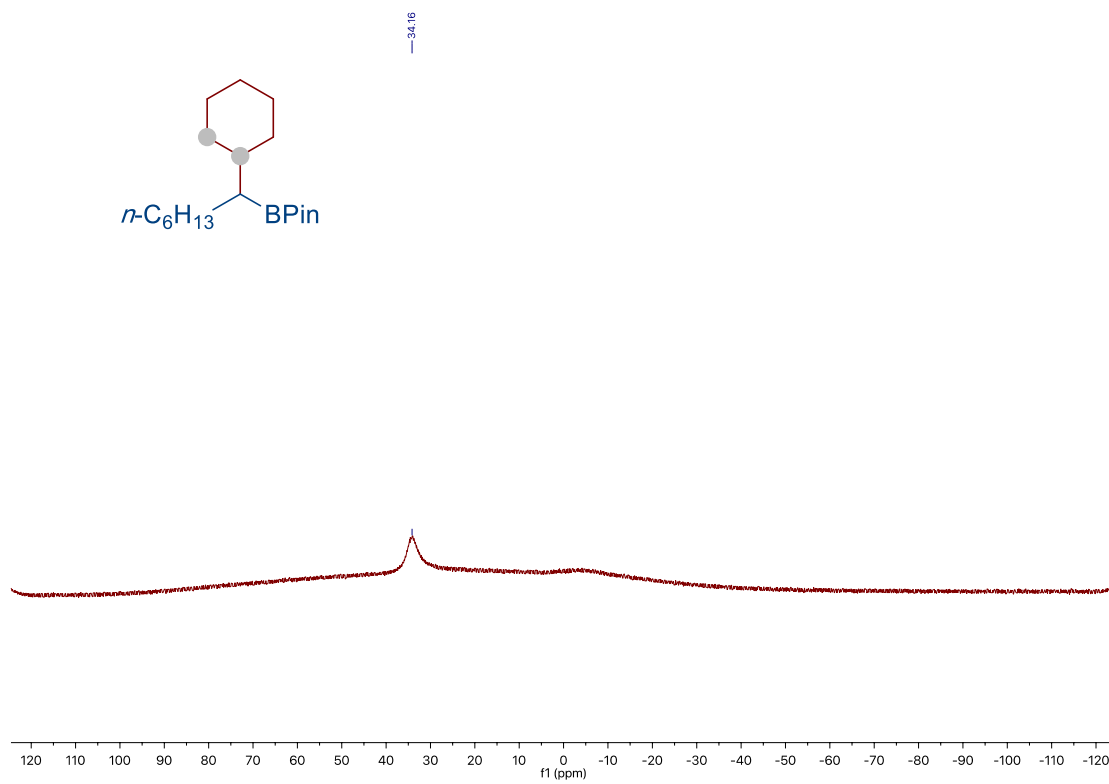
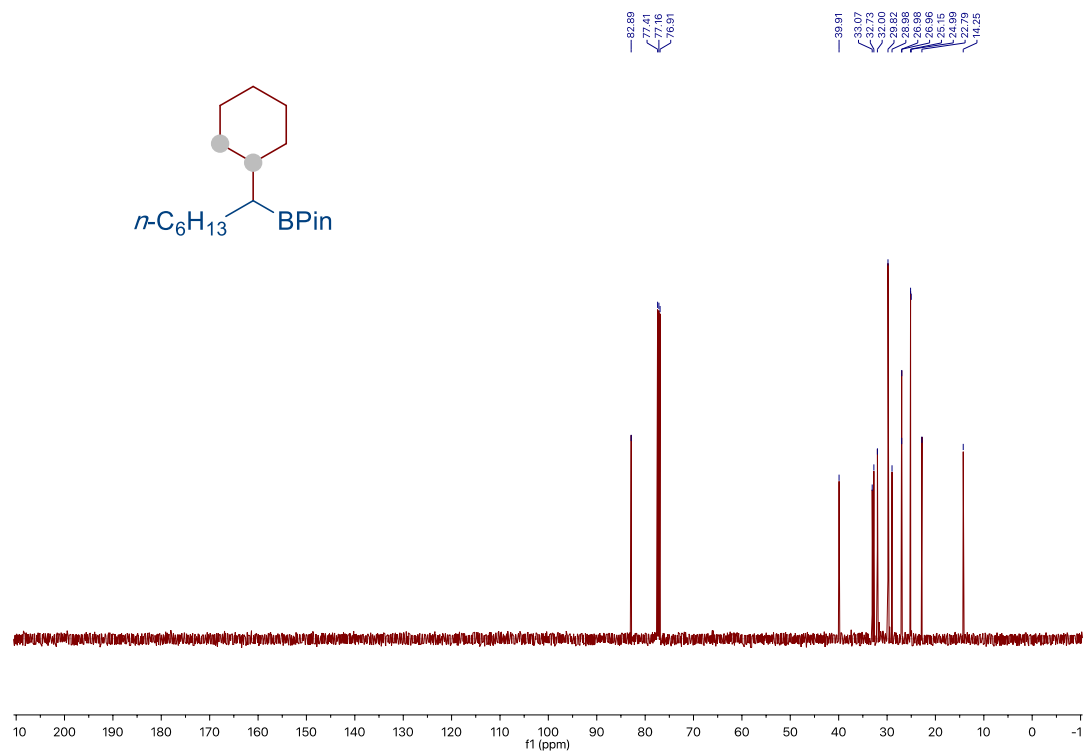
-79.12



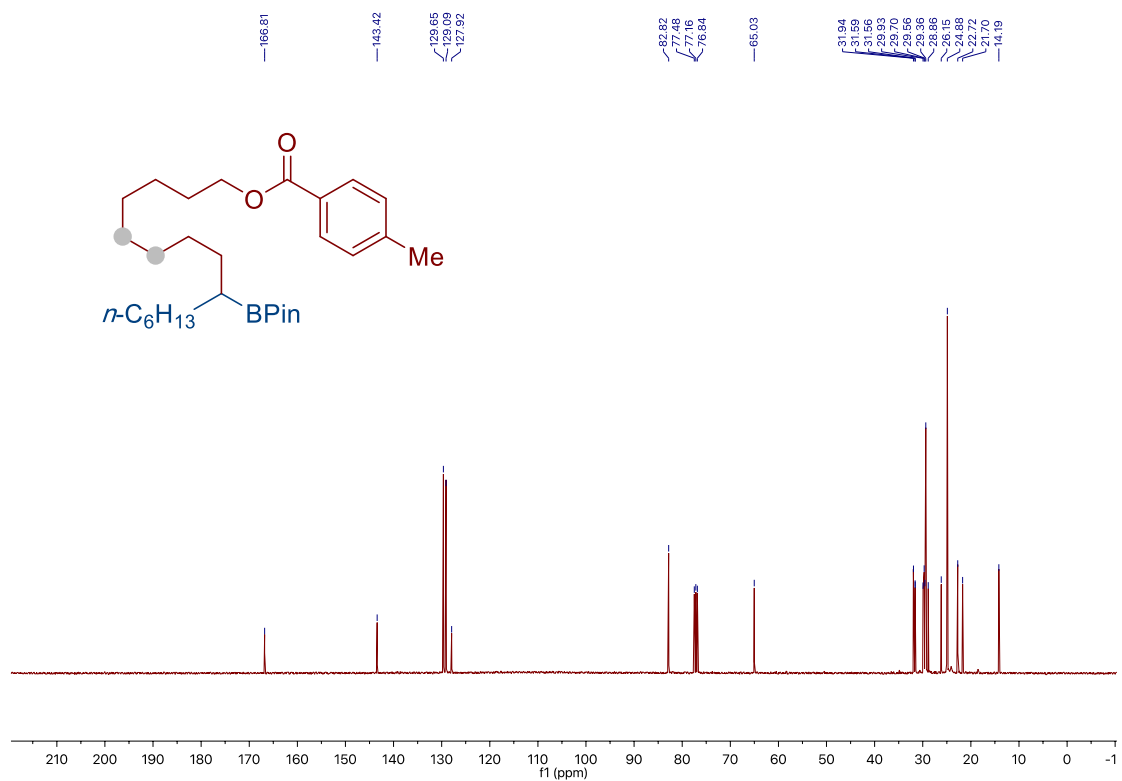
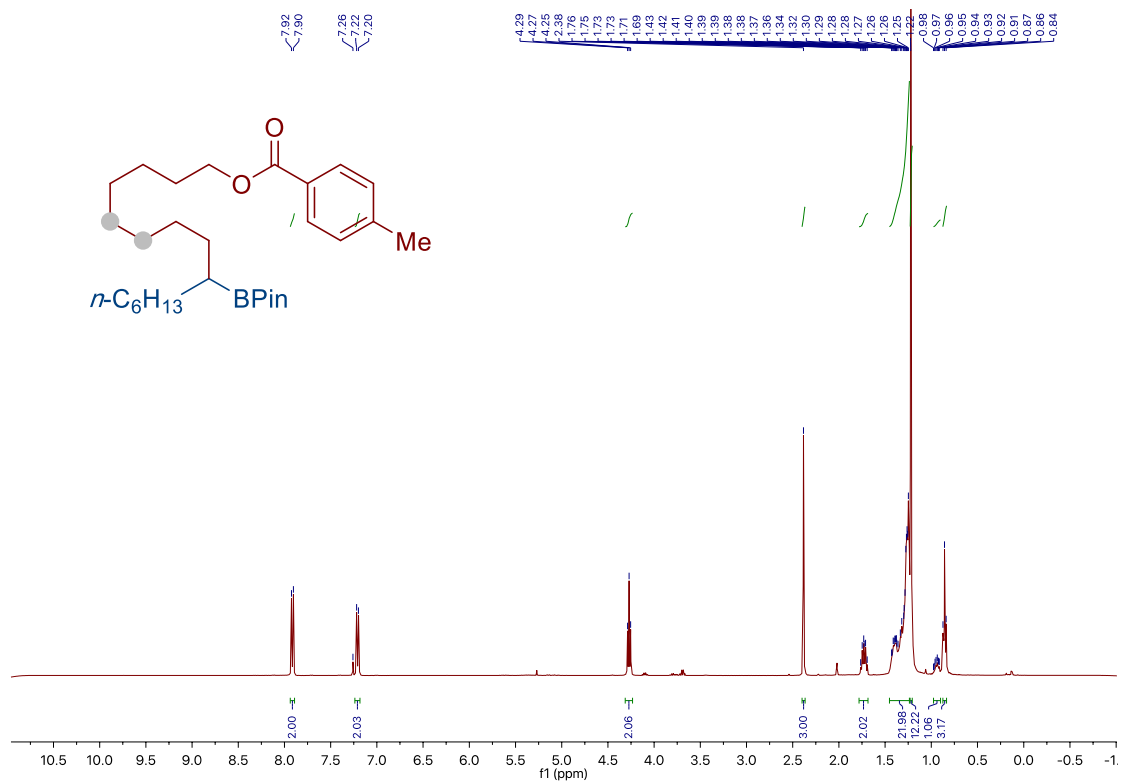
-7.26



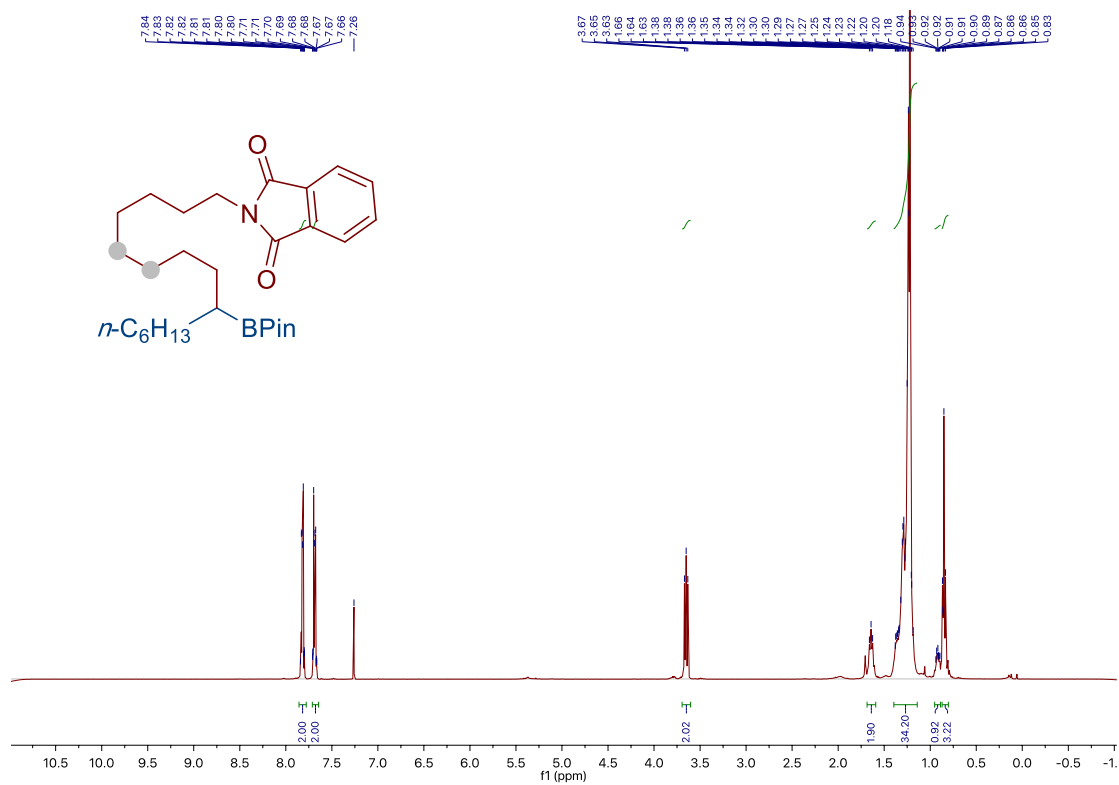
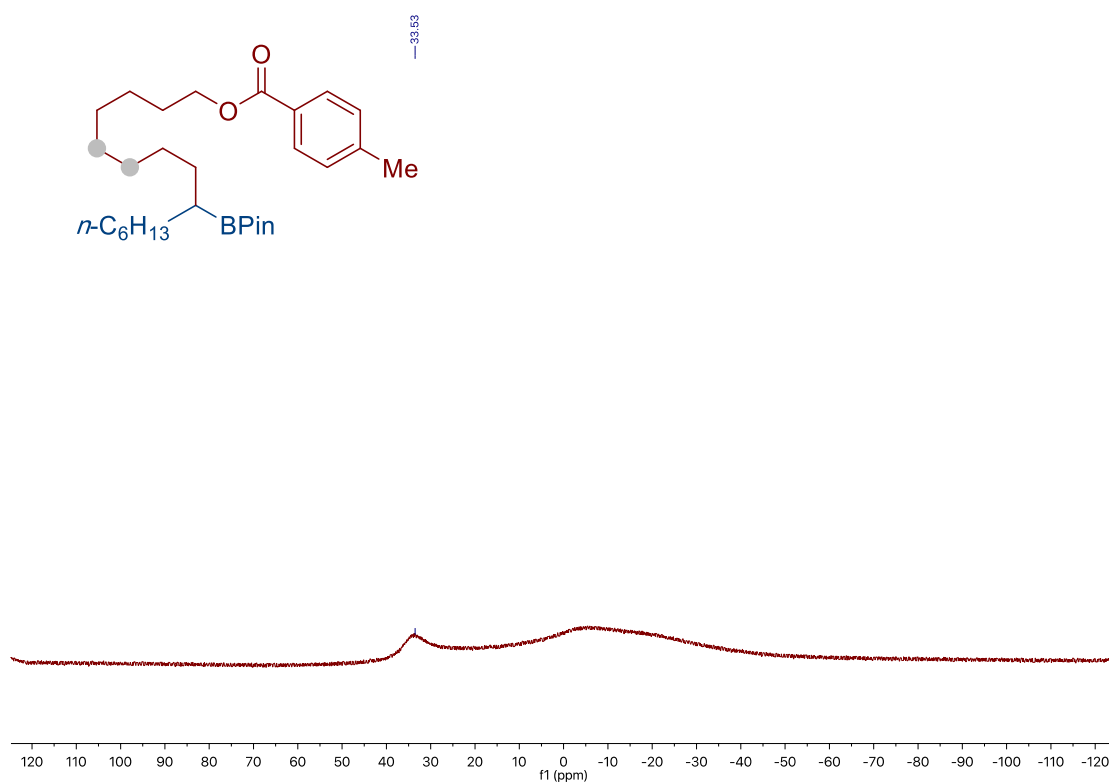
Site-Selective Ni-Catalyzed Reductive
Coupling of α -Haloboranes with Unactivated Olefins



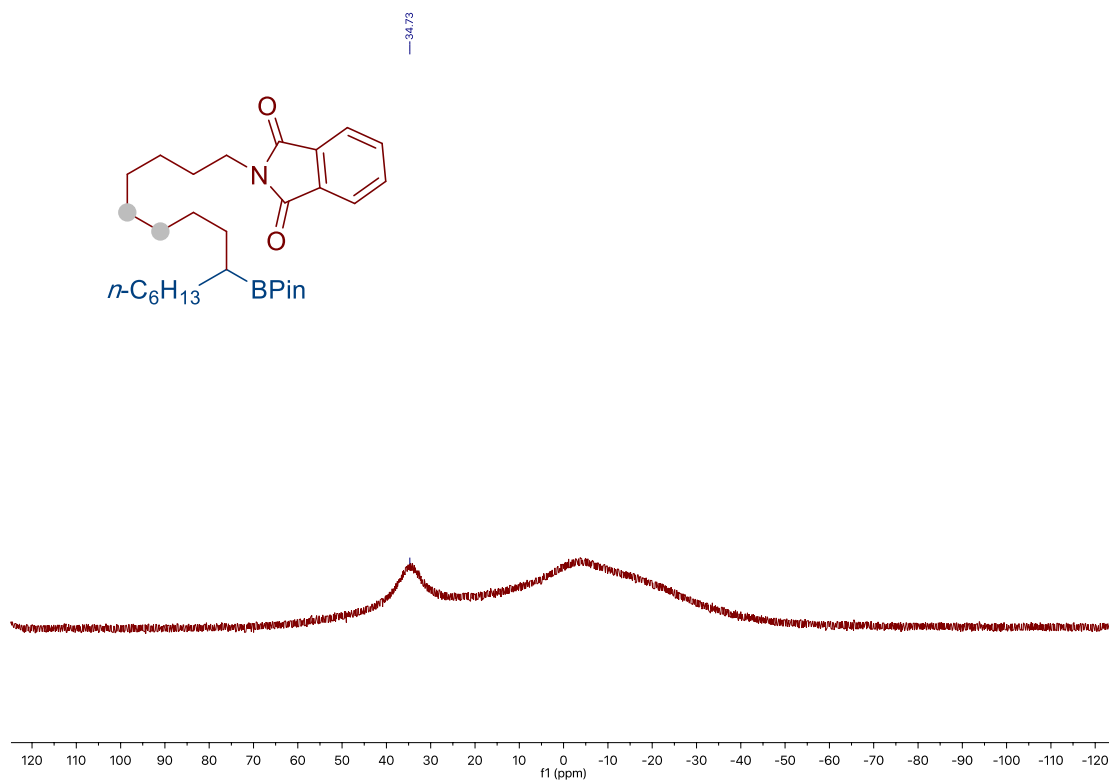
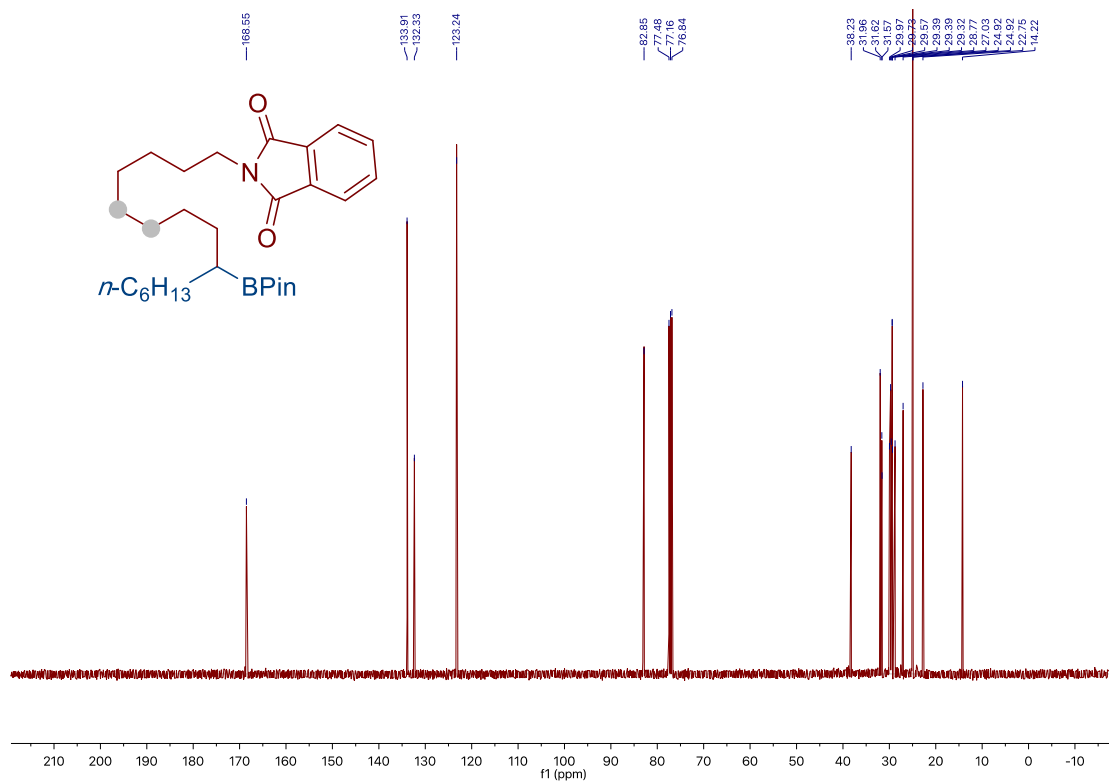
Chapter 2.



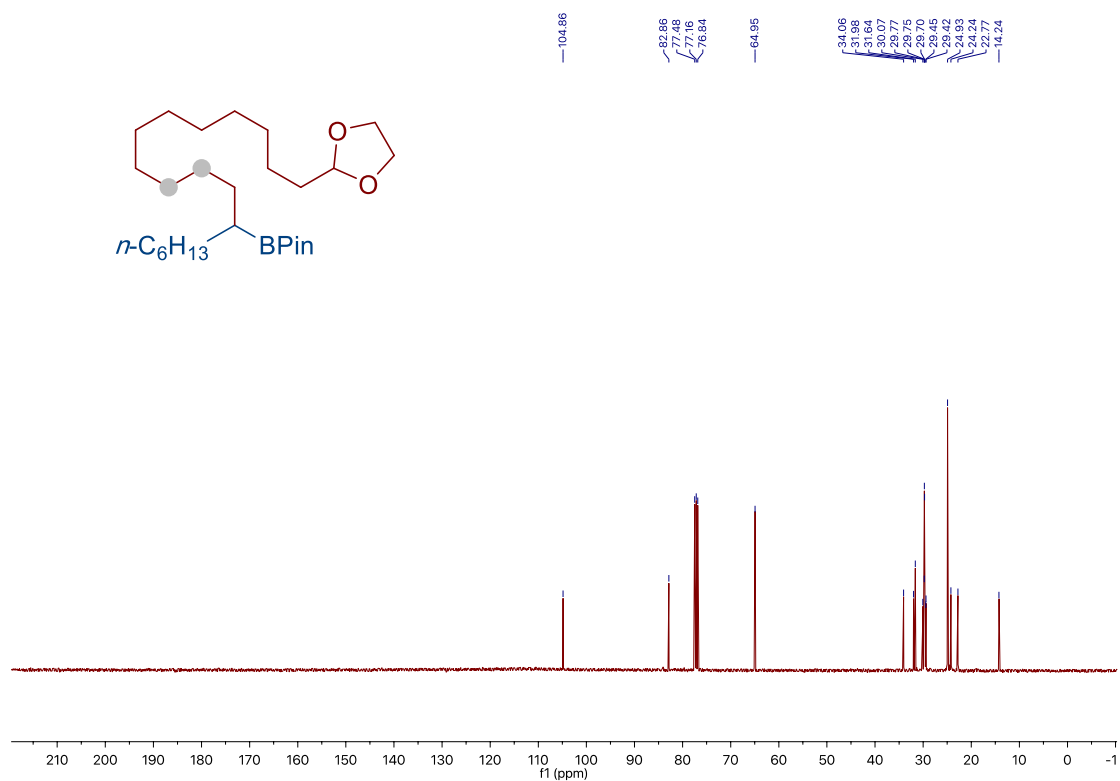
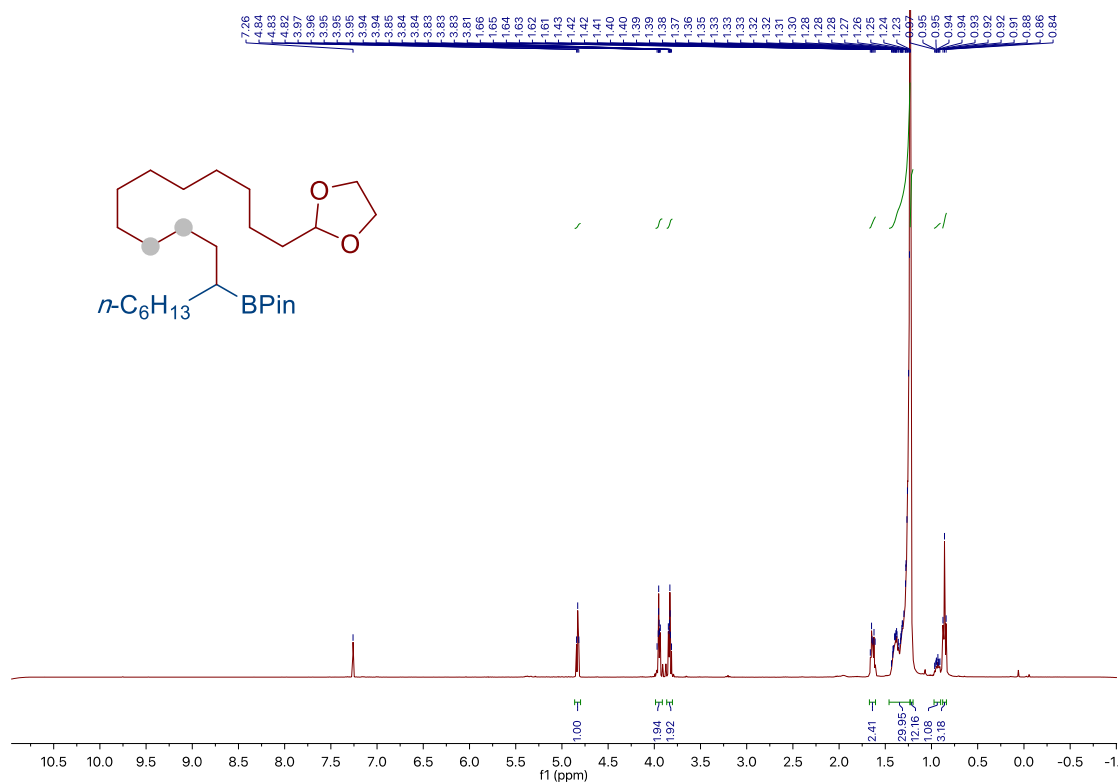
*Site-Selective Ni-Catalyzed Reductive
Coupling of α -Haloboranes with Unactivated Olefins*



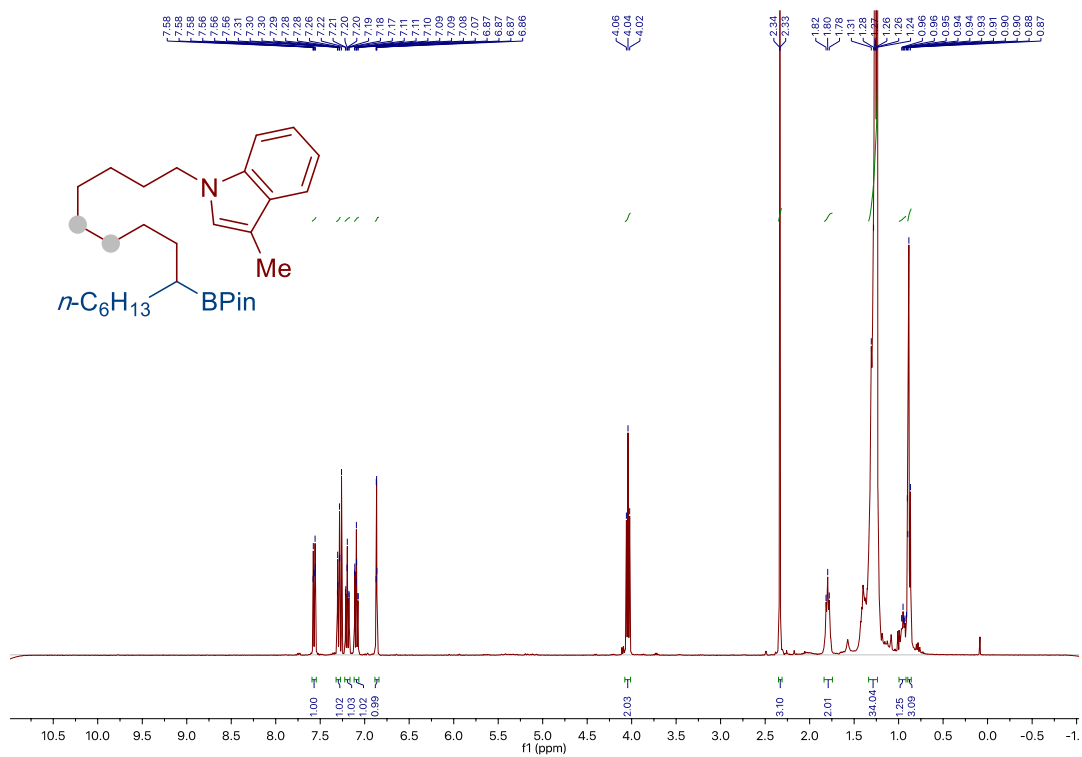
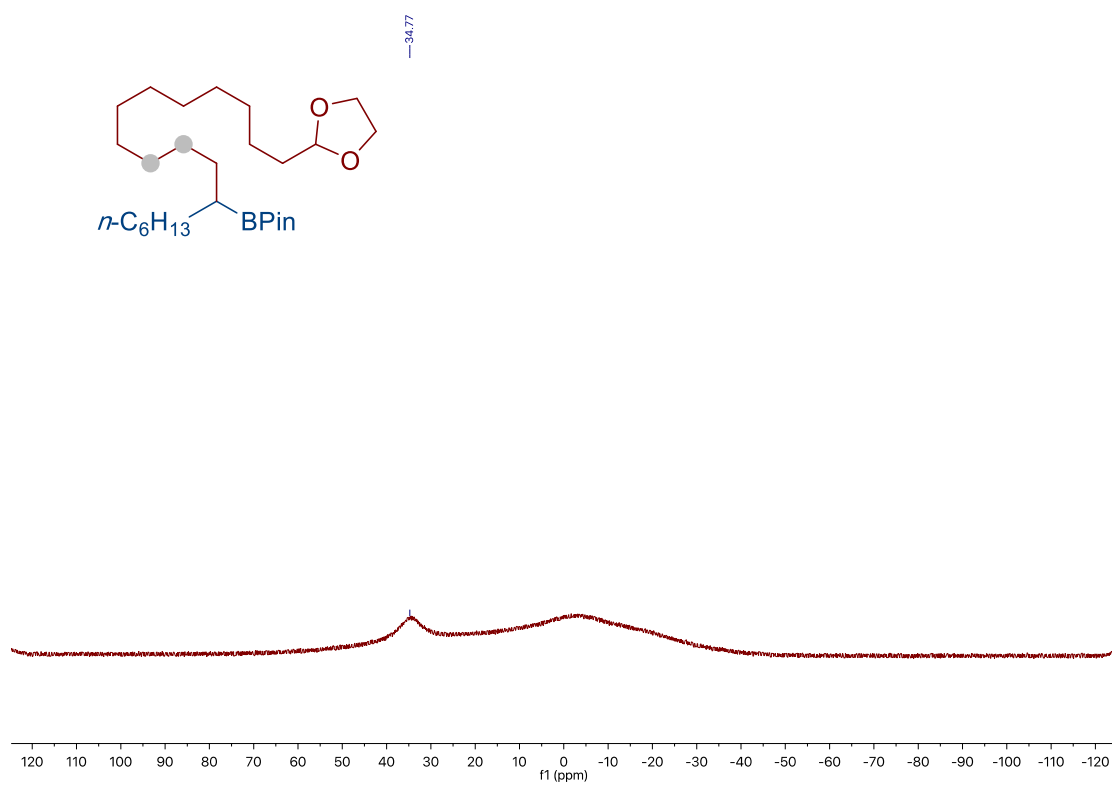
Chapter 2.



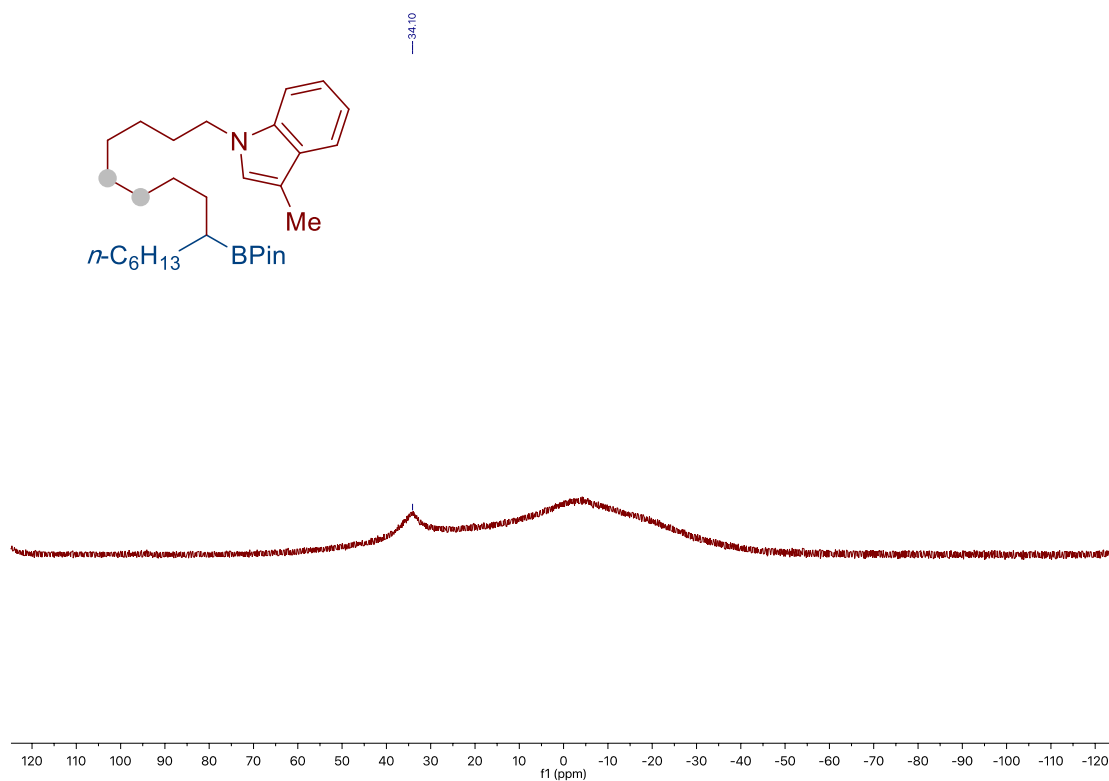
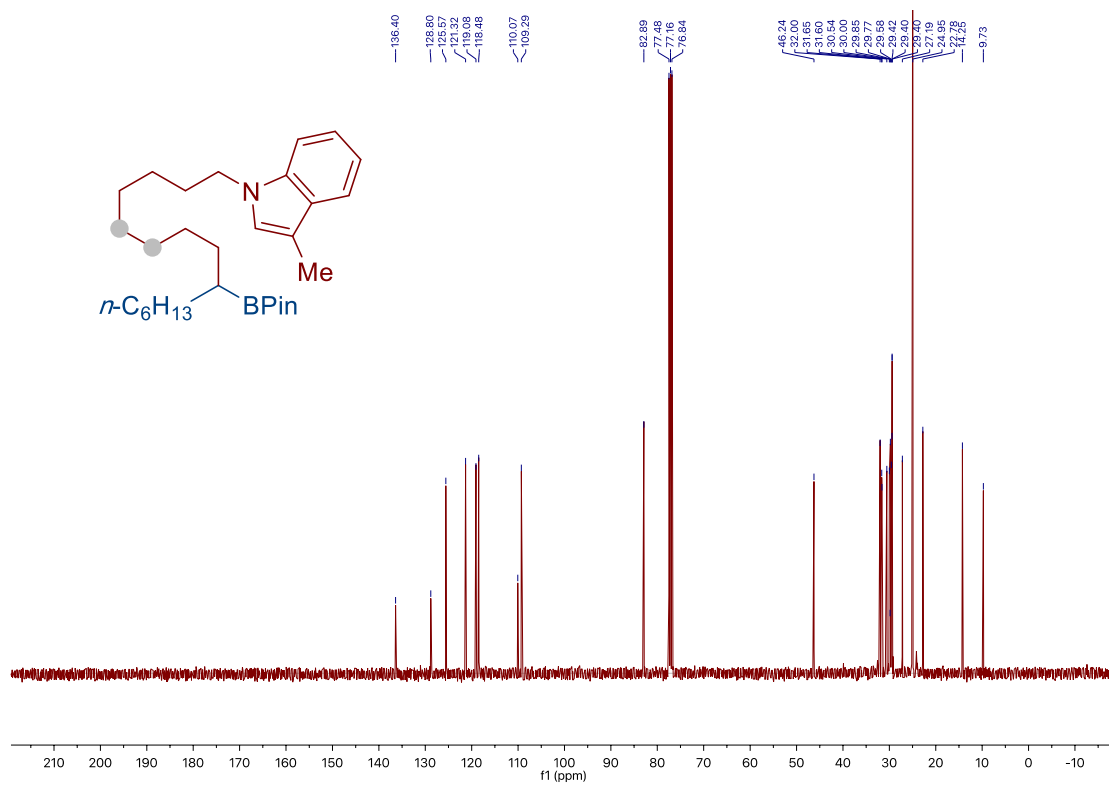
*Site-Selective Ni-Catalyzed Reductive
Coupling of α -Haloboranes with Unactivated Olefins*



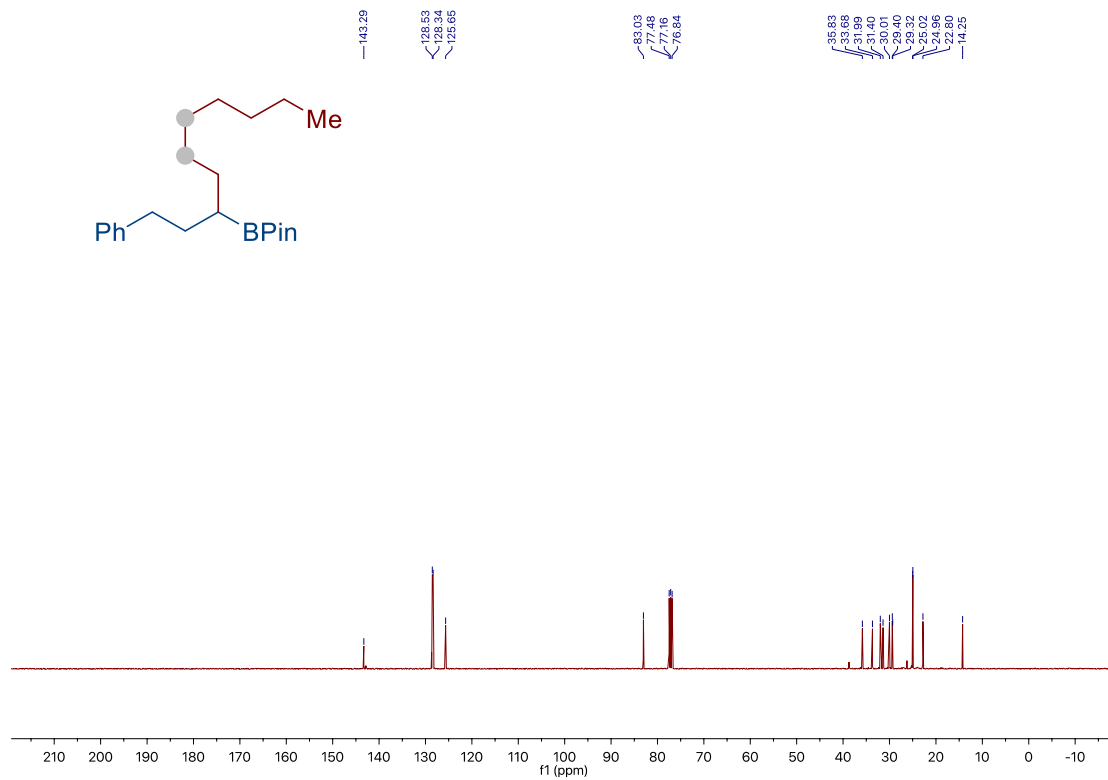
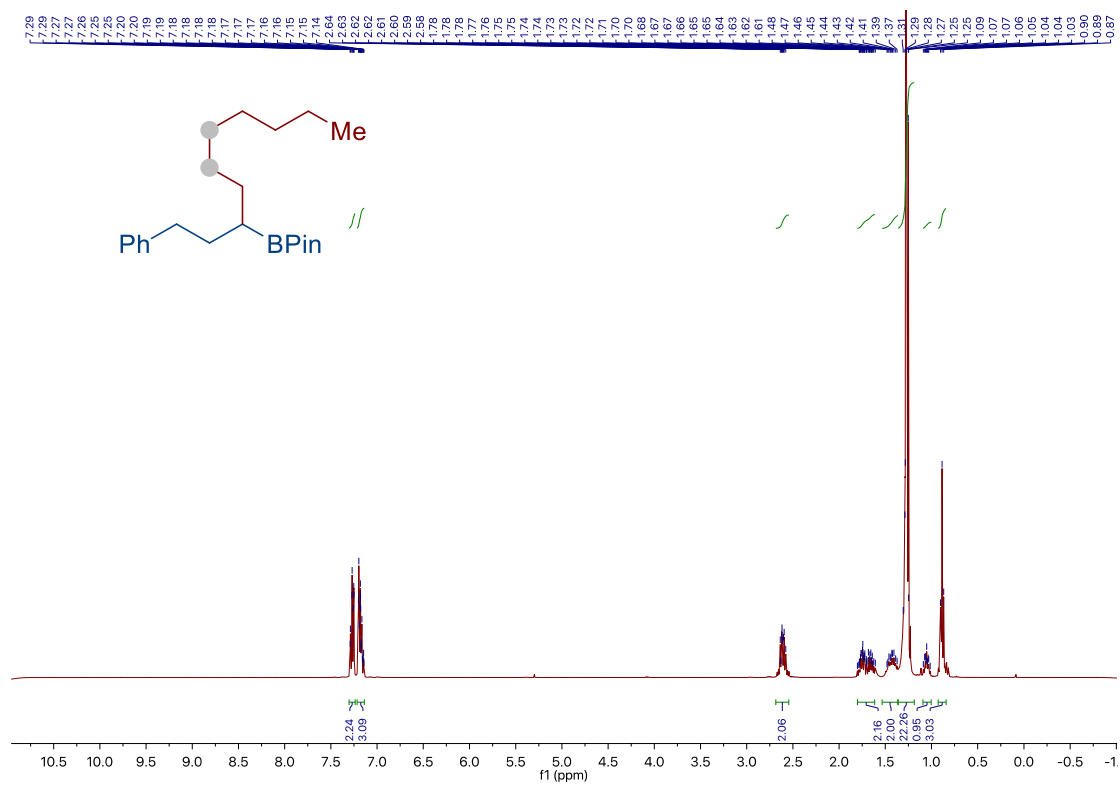
Chapter 2.



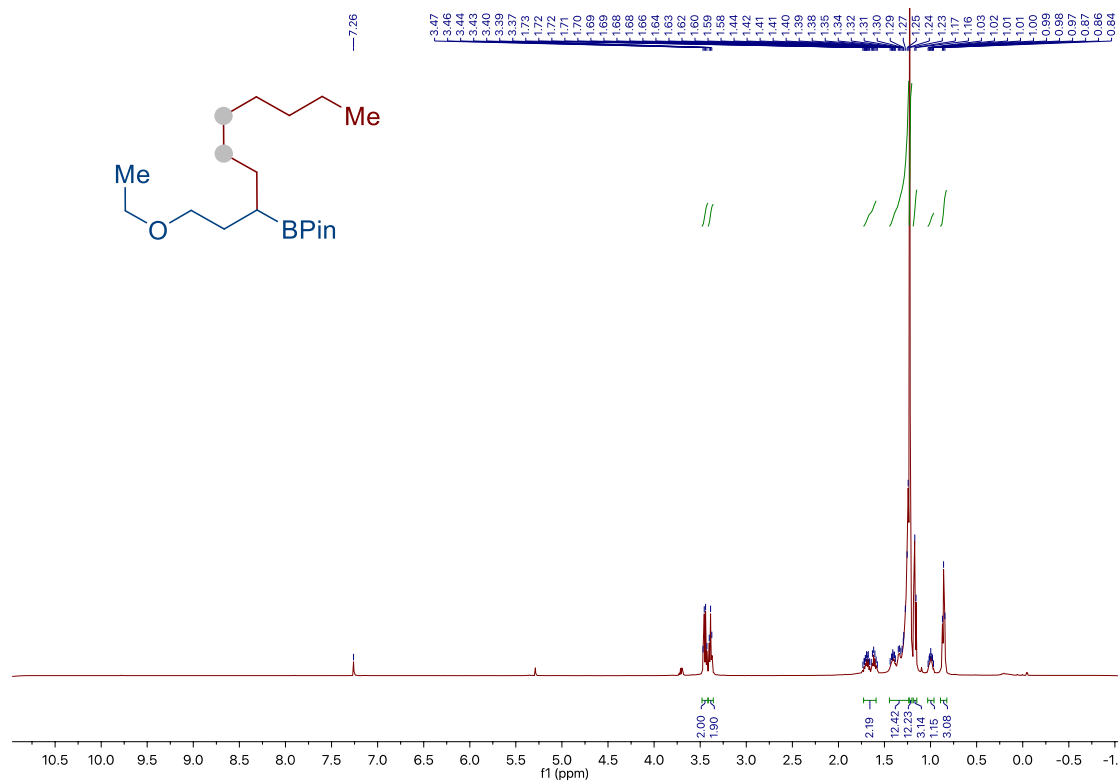
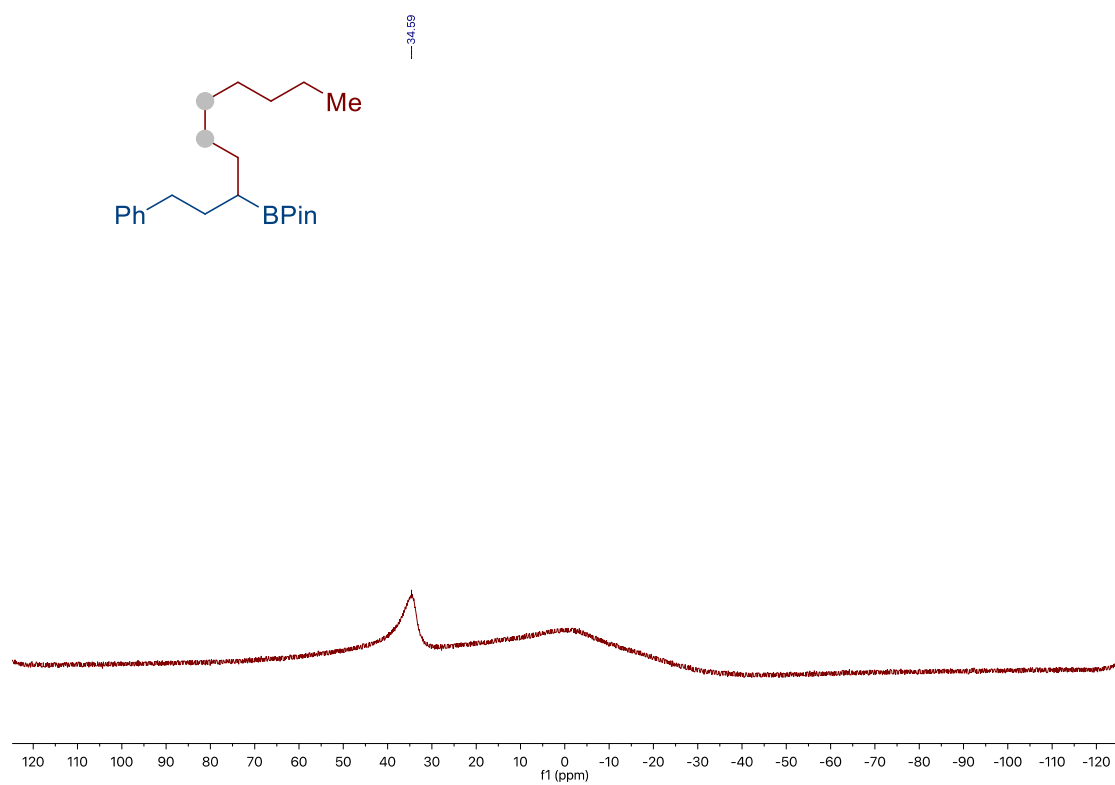
Site-Selective Ni-Catalyzed Reductive
Coupling of α -Haloboranes with Unactivated Olefins



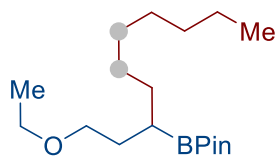
Chapter 2.



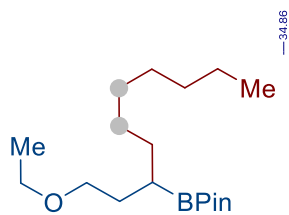
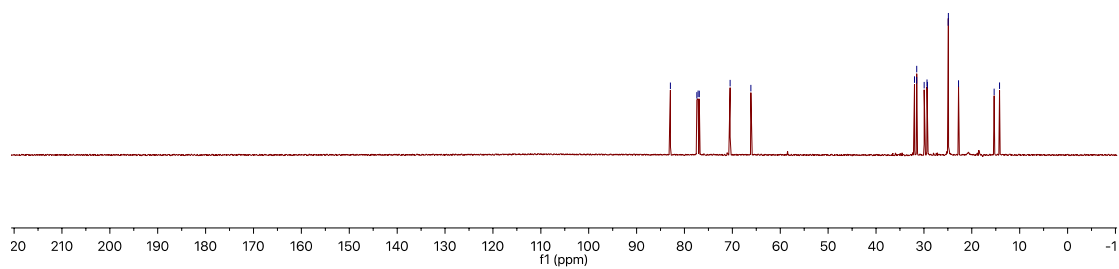
Site-Selective Ni-Catalyzed Reductive
Coupling of α -Haloboranes with Unactivated Olefins



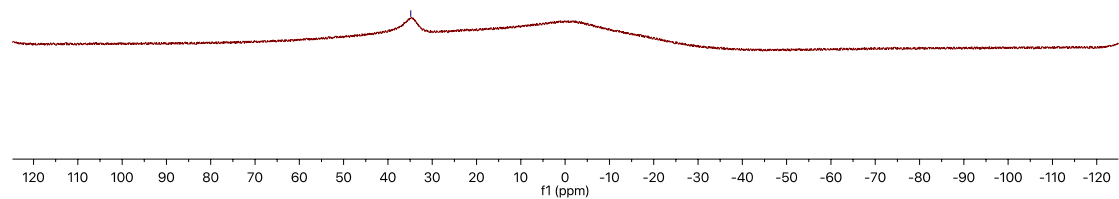
Chapter 2.



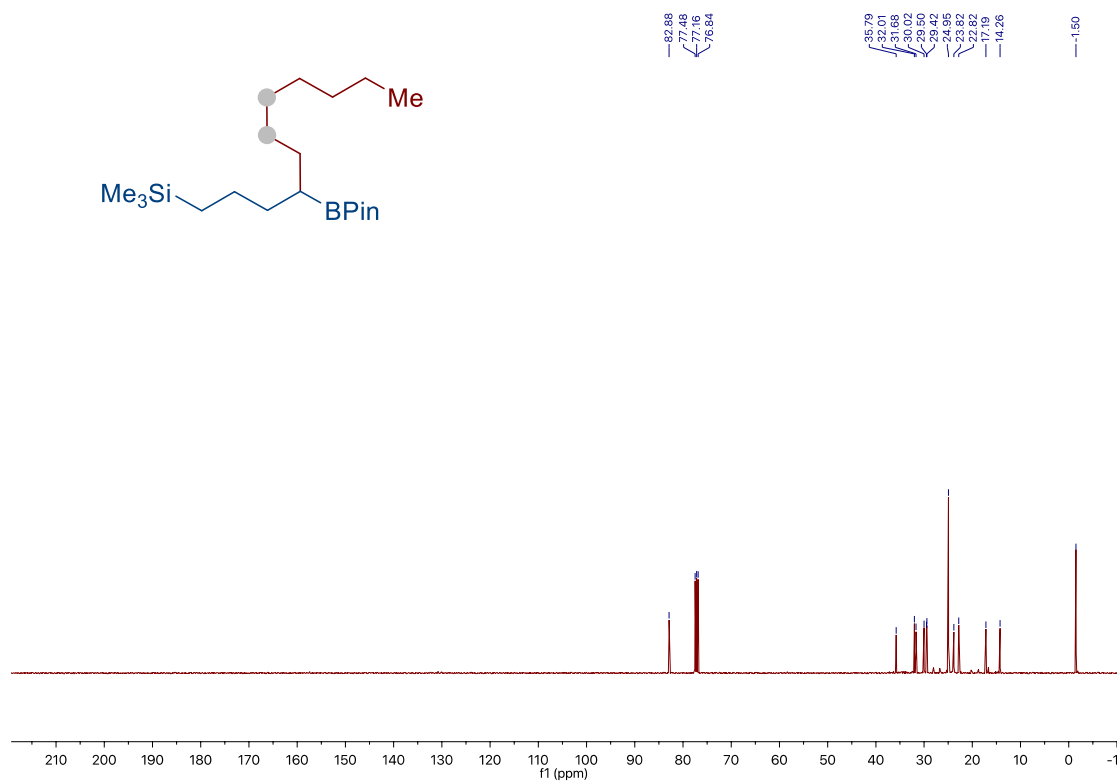
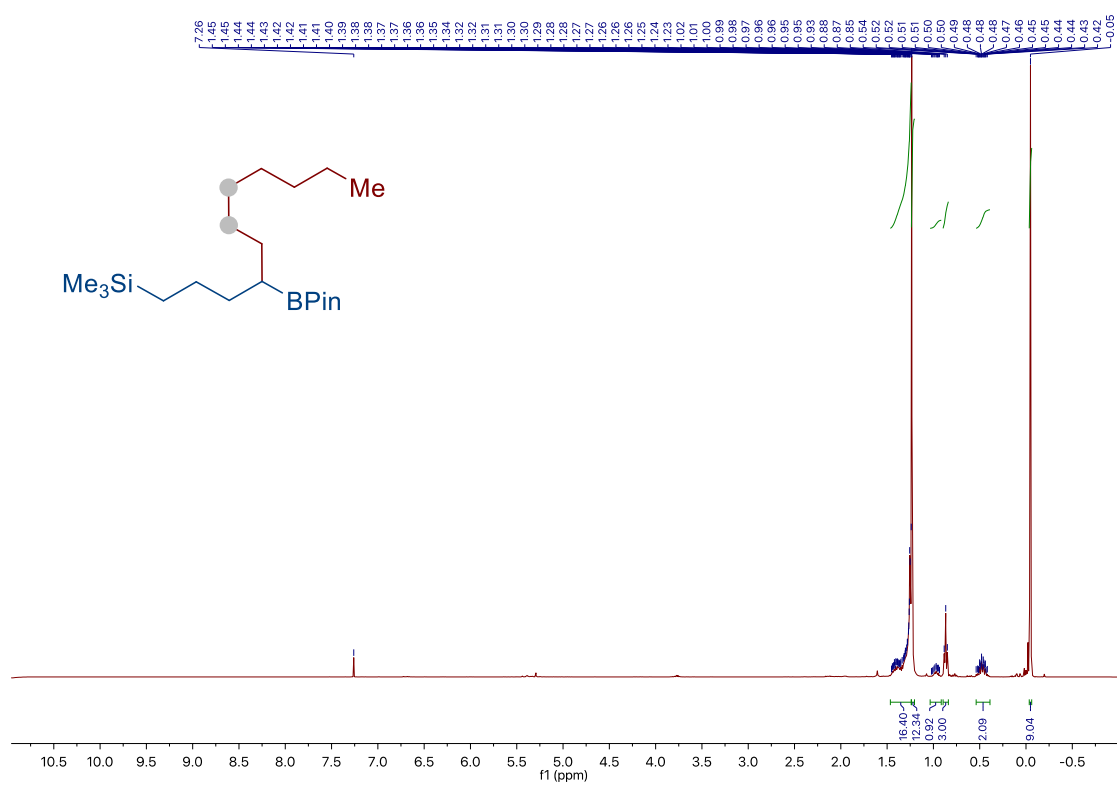
82.95
77.41
77.16
76.90
70.47
66.13
31.96
31.52
31.50
28.94
30.16
29.26
24.94
24.90
22.77
16.32
-4.22



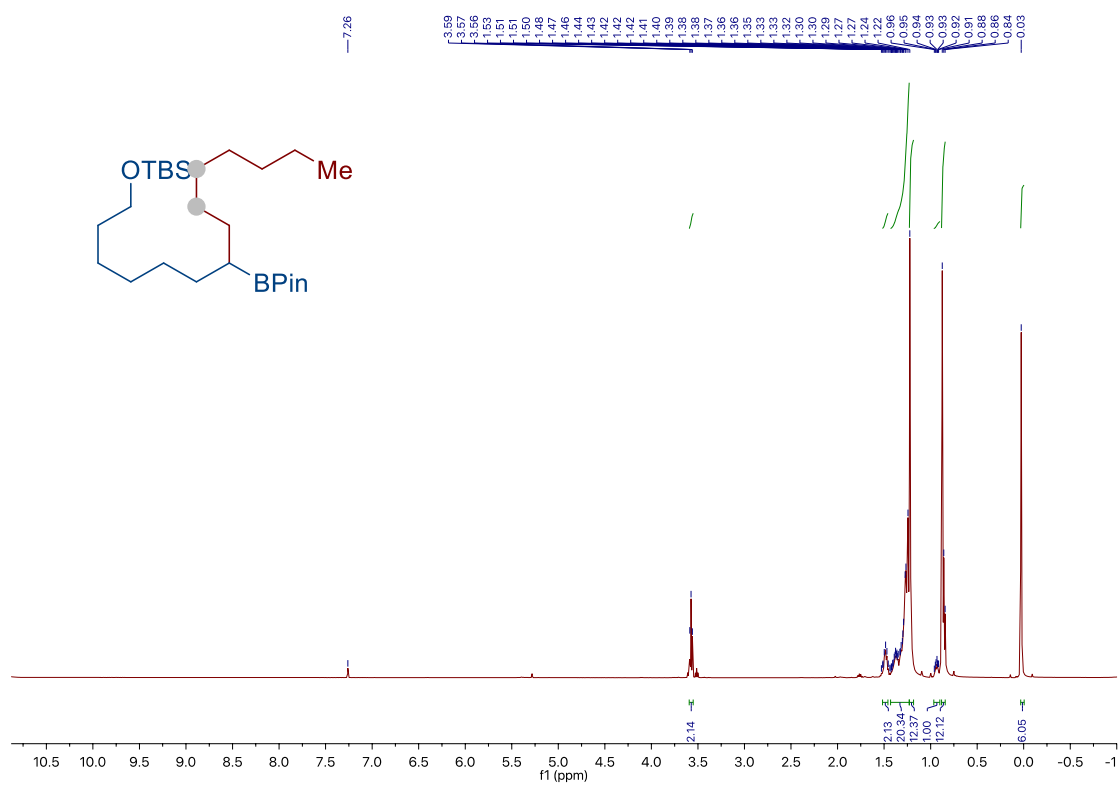
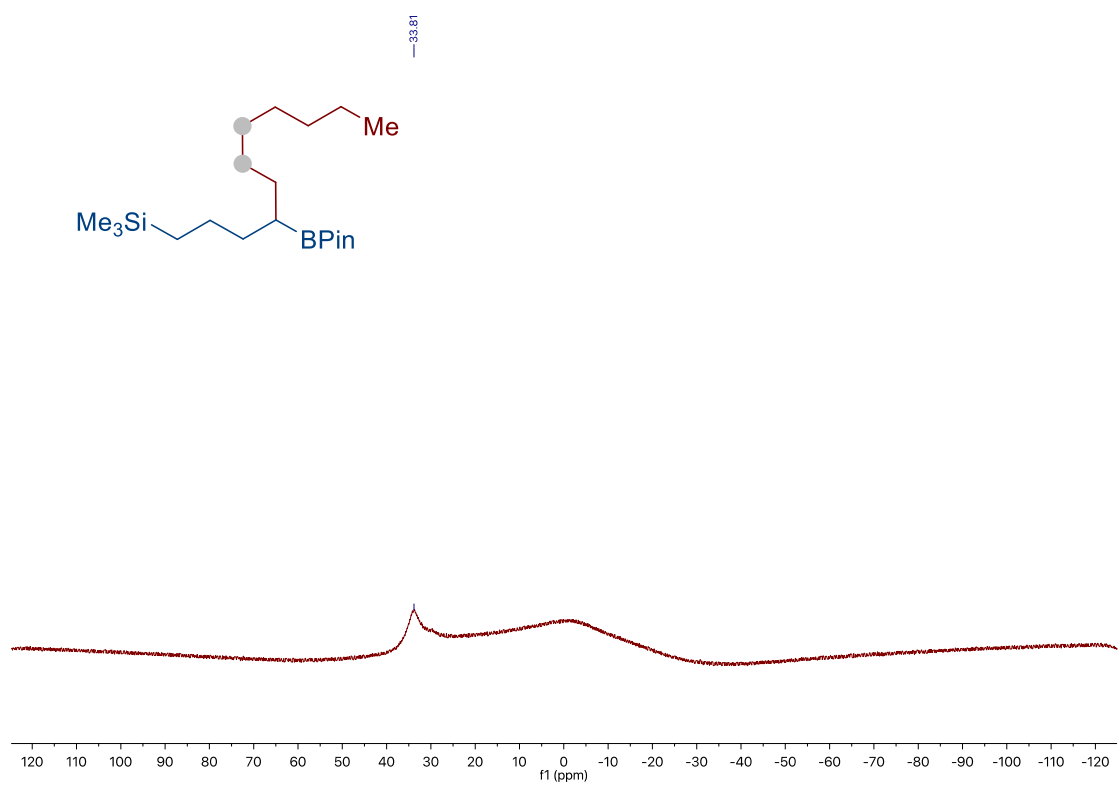
34.86



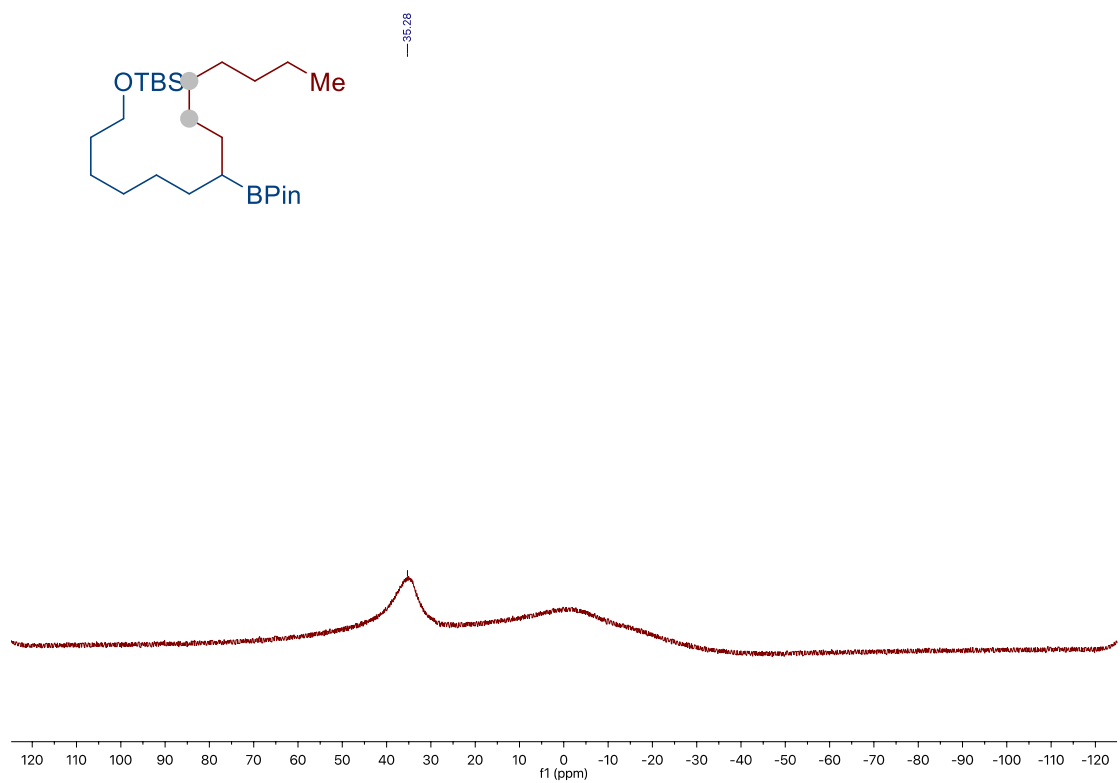
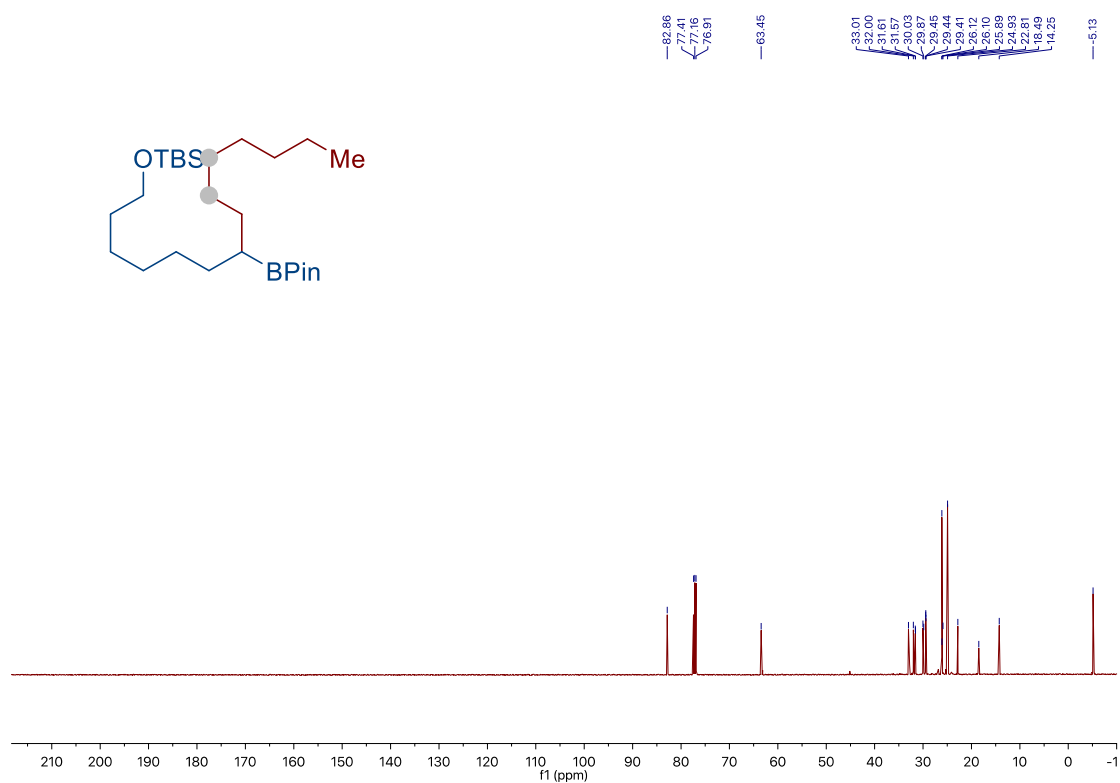
Site-Selective Ni-Catalyzed Reductive
Coupling of α -Haloboranes with Unactivated Olefins



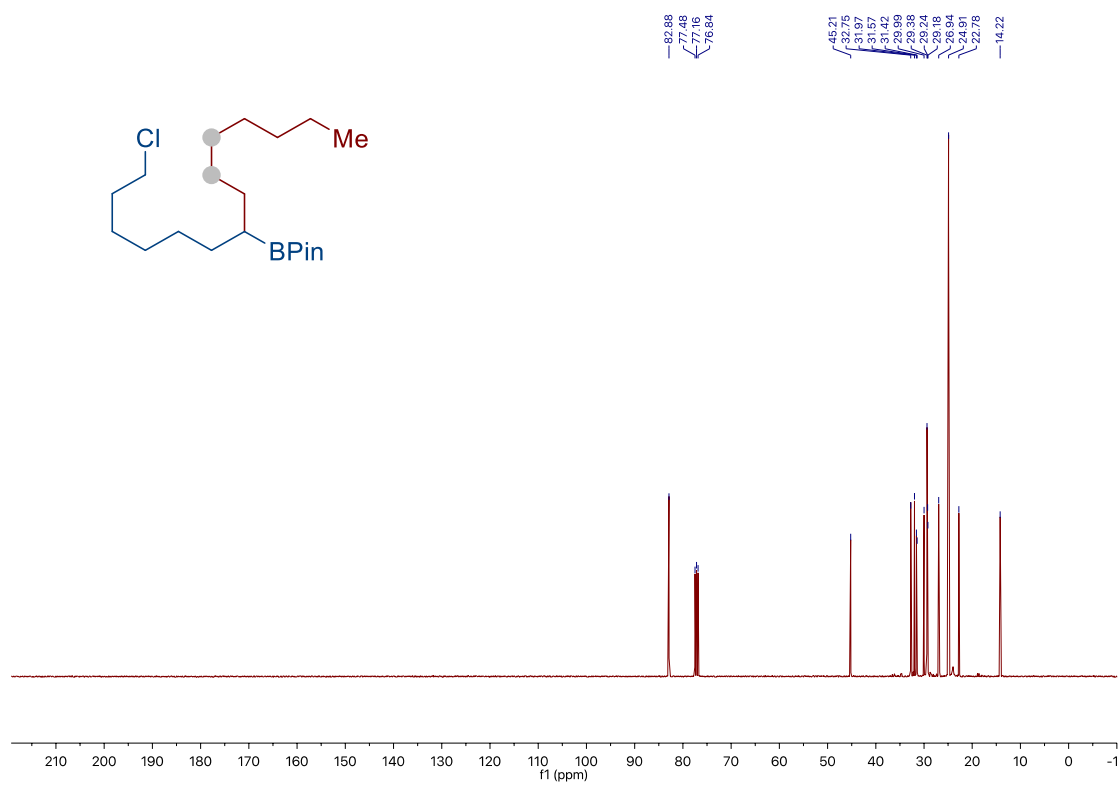
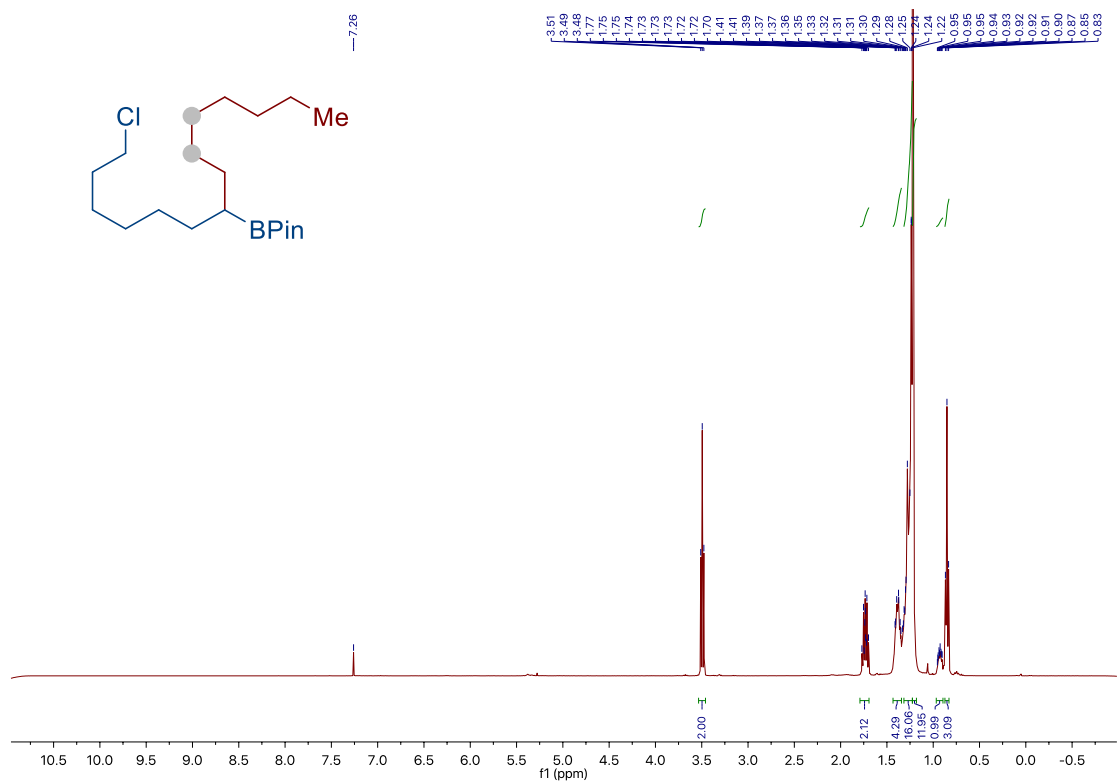
Chapter 2.



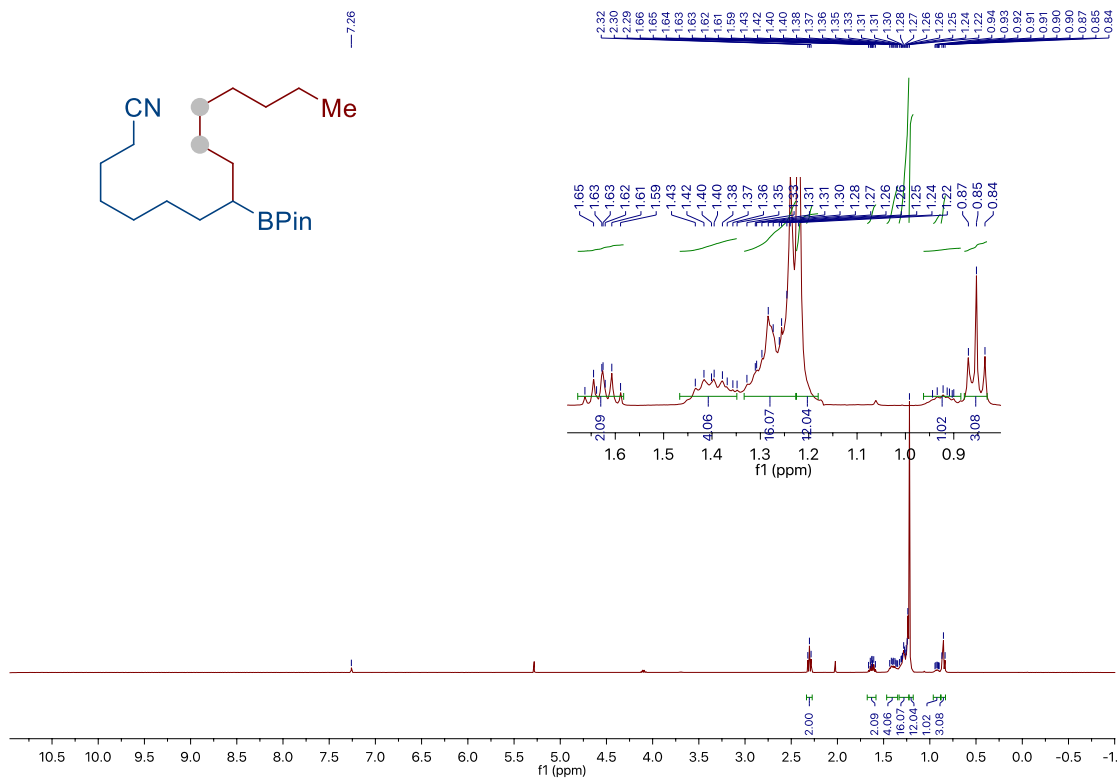
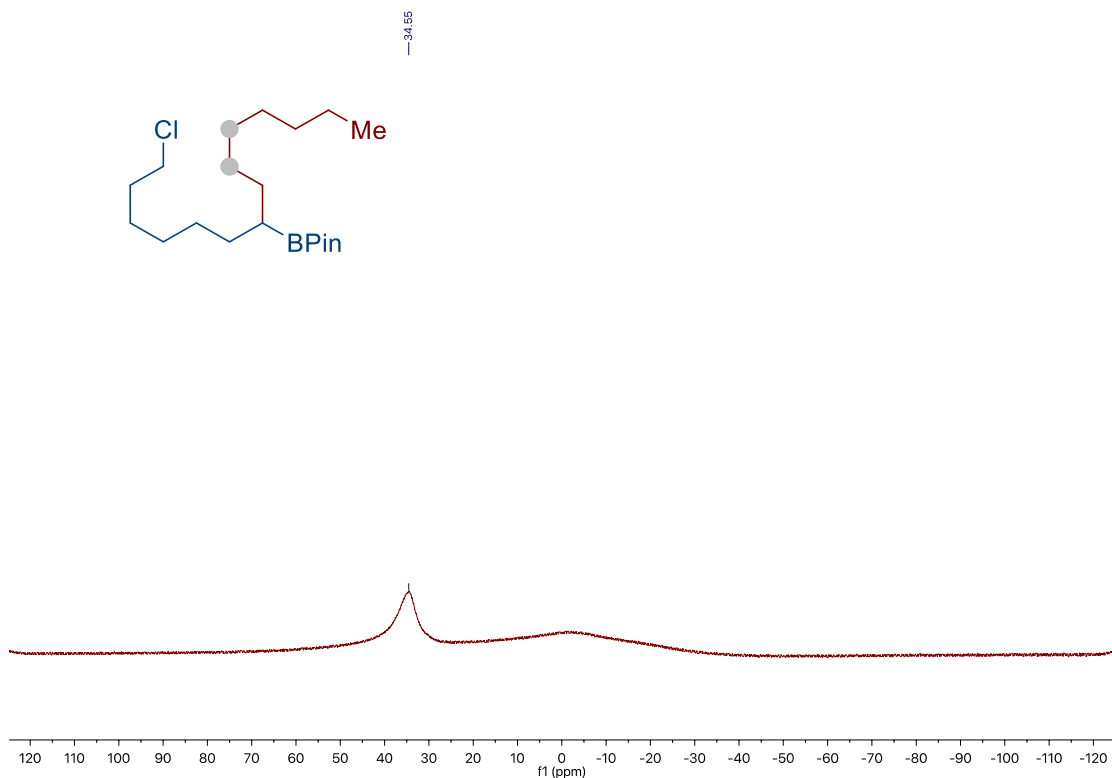
Site-Selective Ni-Catalyzed Reductive Coupling of α -Haloboranes with Unactivated Olefins



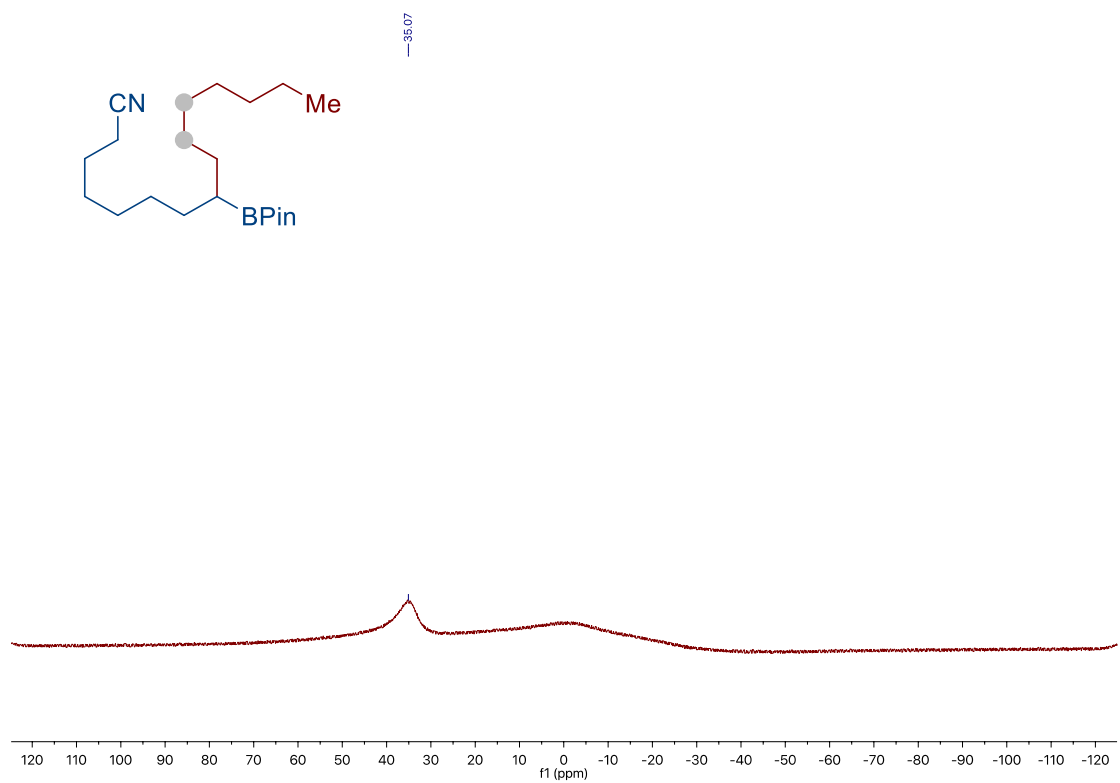
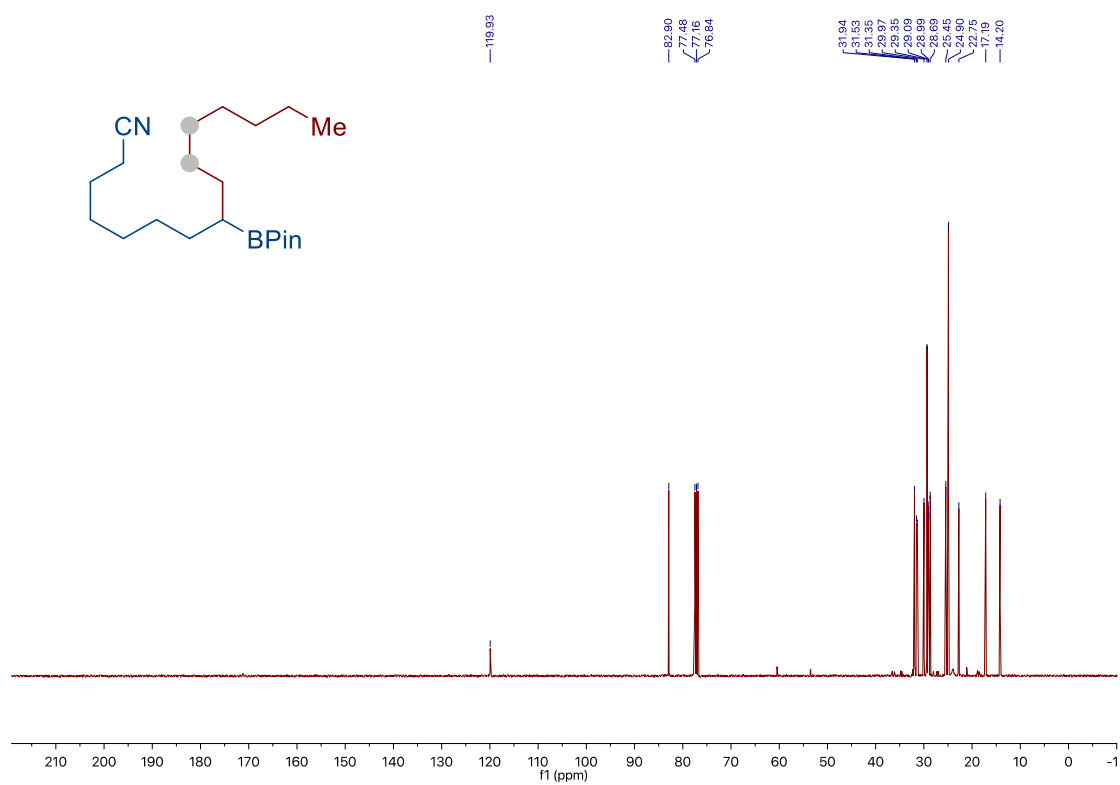
Chapter 2.



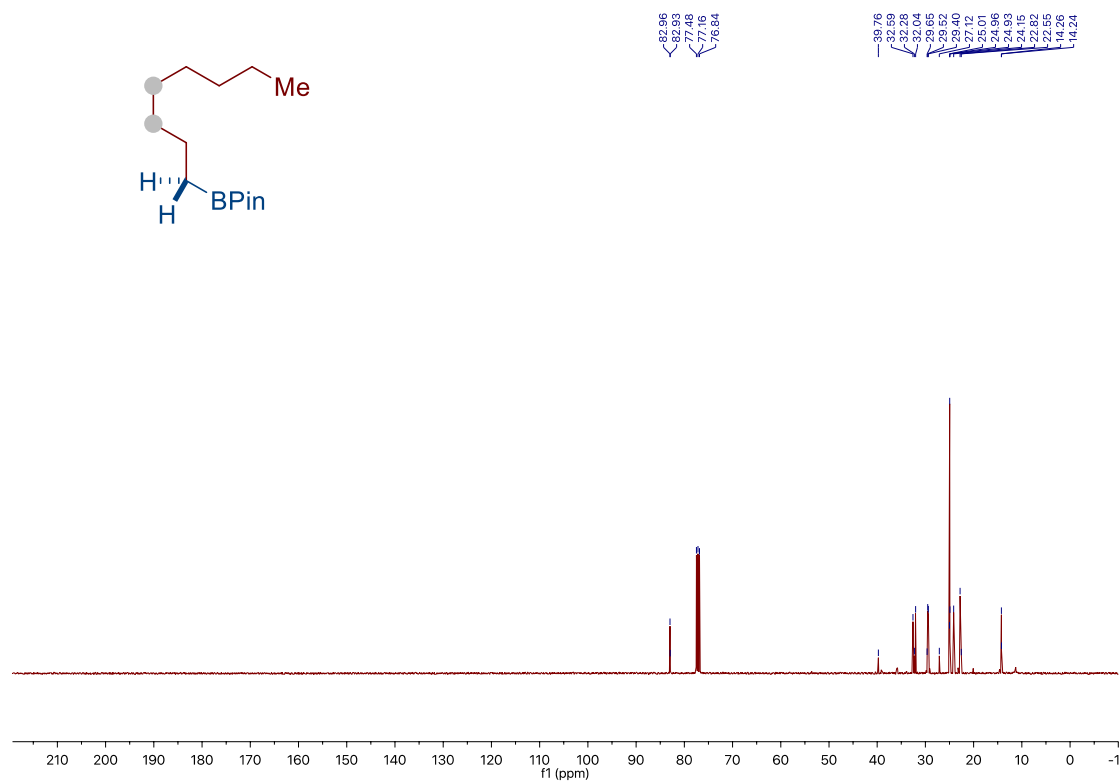
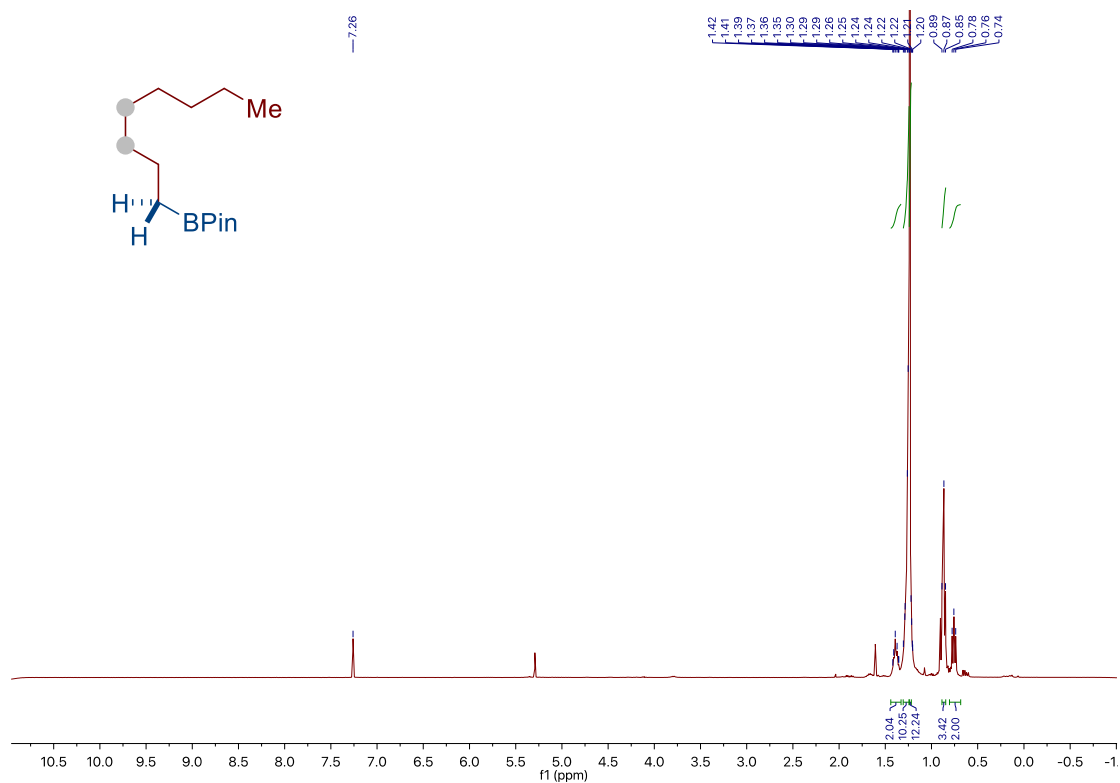
*Site-Selective Ni-Catalyzed Reductive
Coupling of α -Haloboranes with Unactivated Olefins*



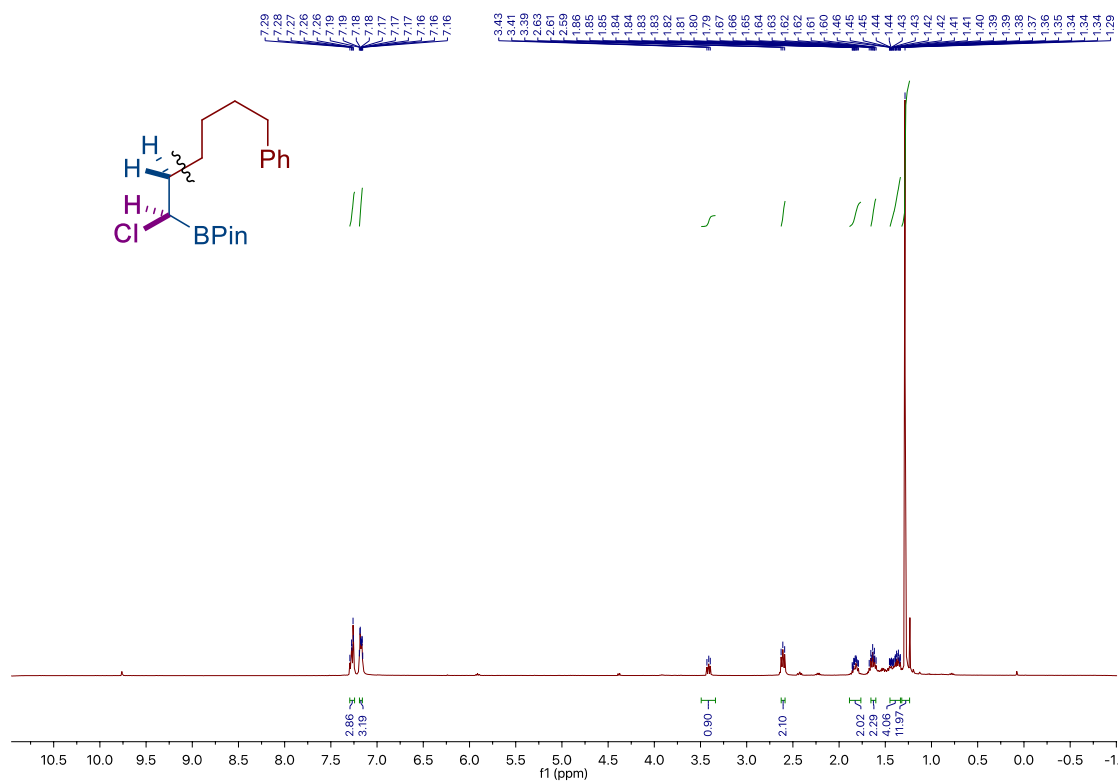
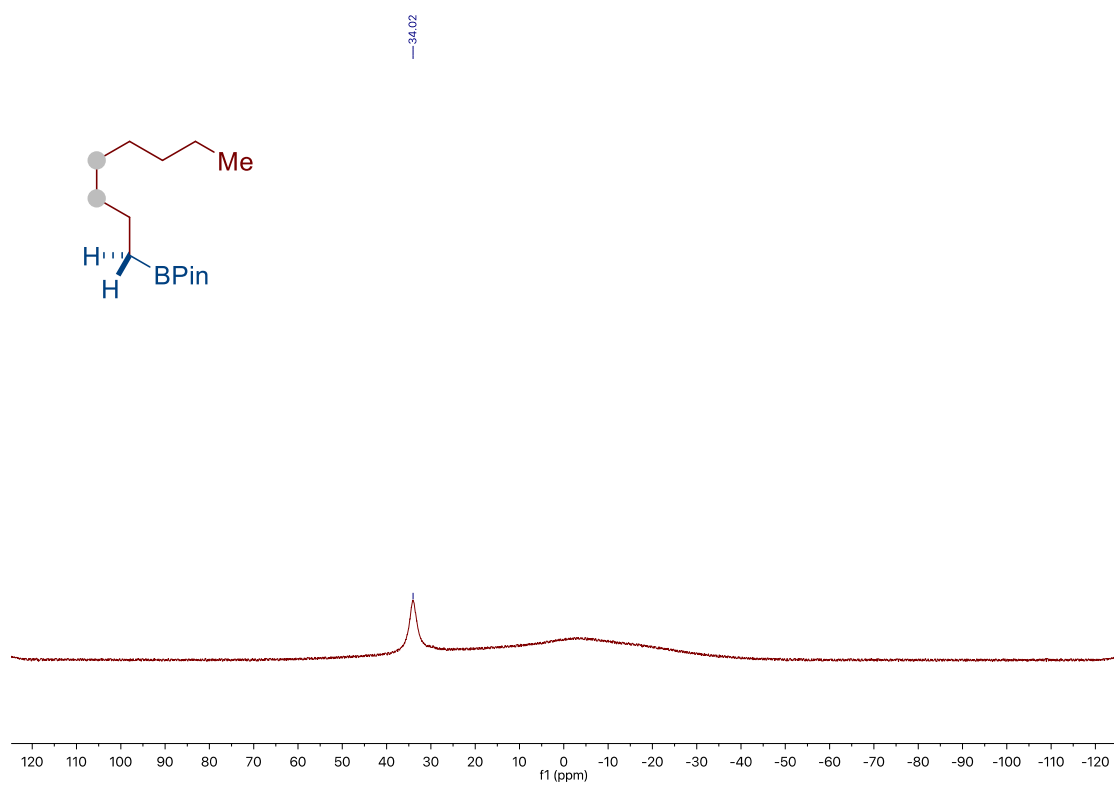
Chapter 2.



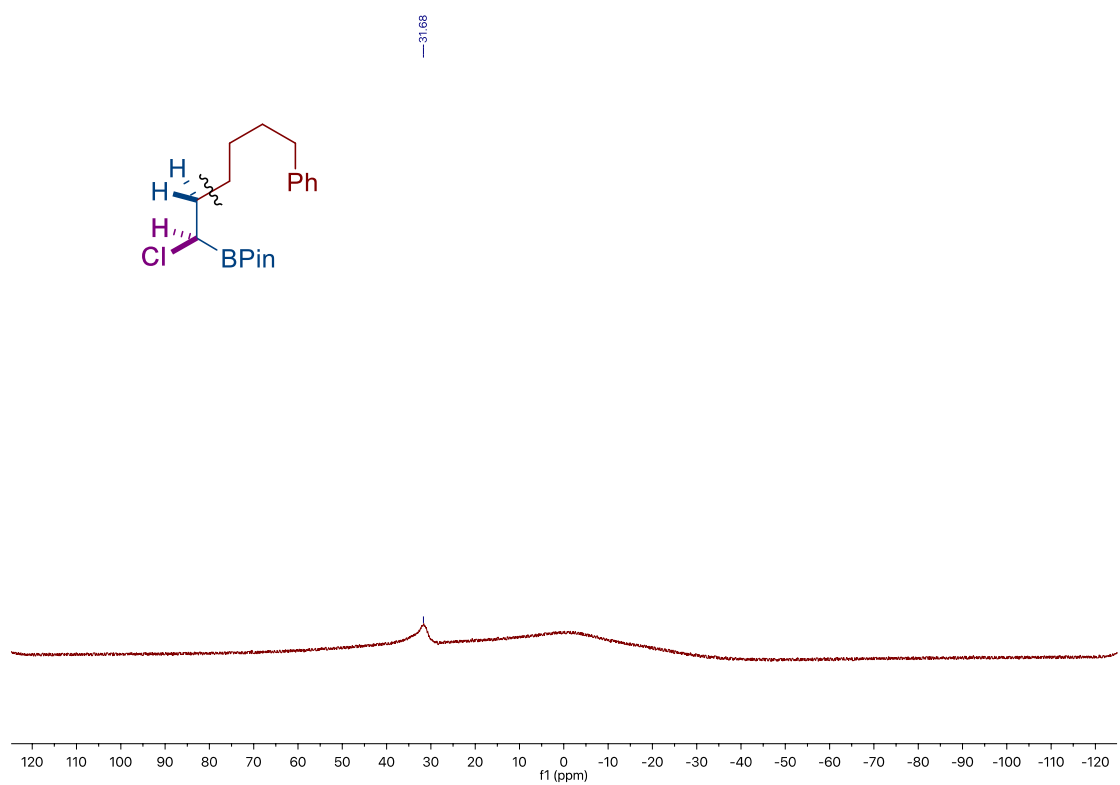
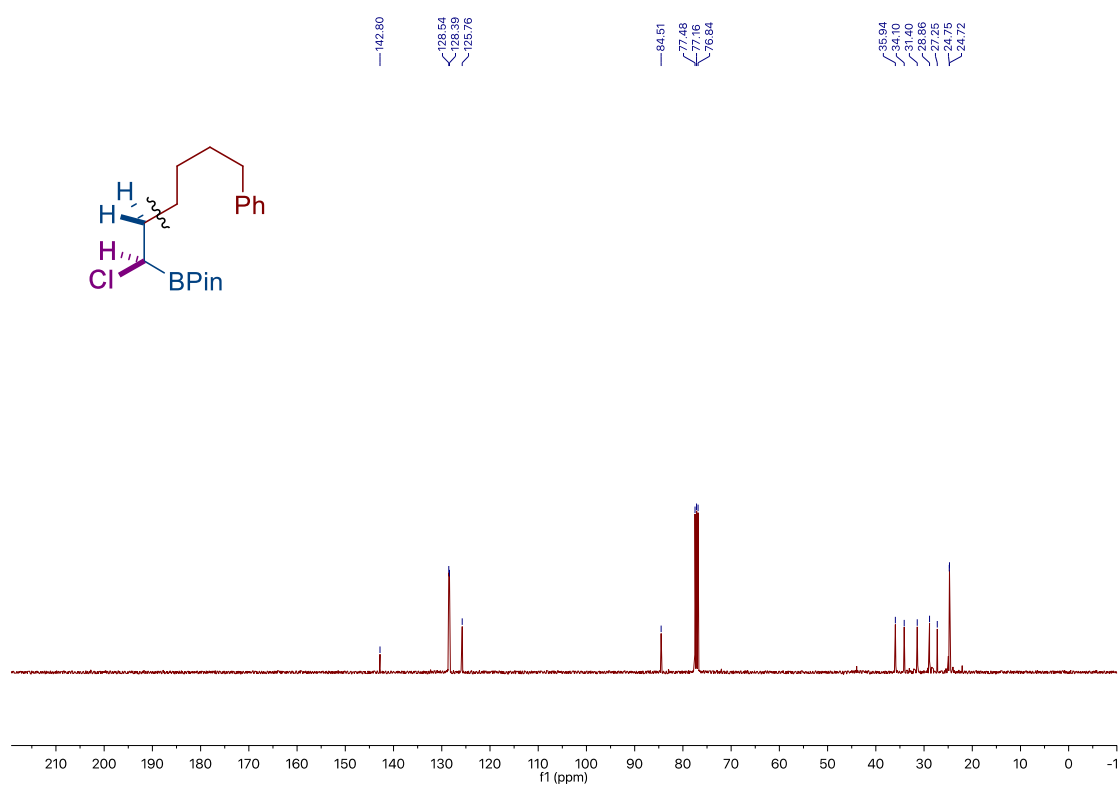
*Site-Selective Ni-Catalyzed Reductive
Coupling of α -Haloboranes with Unactivated Olefins*



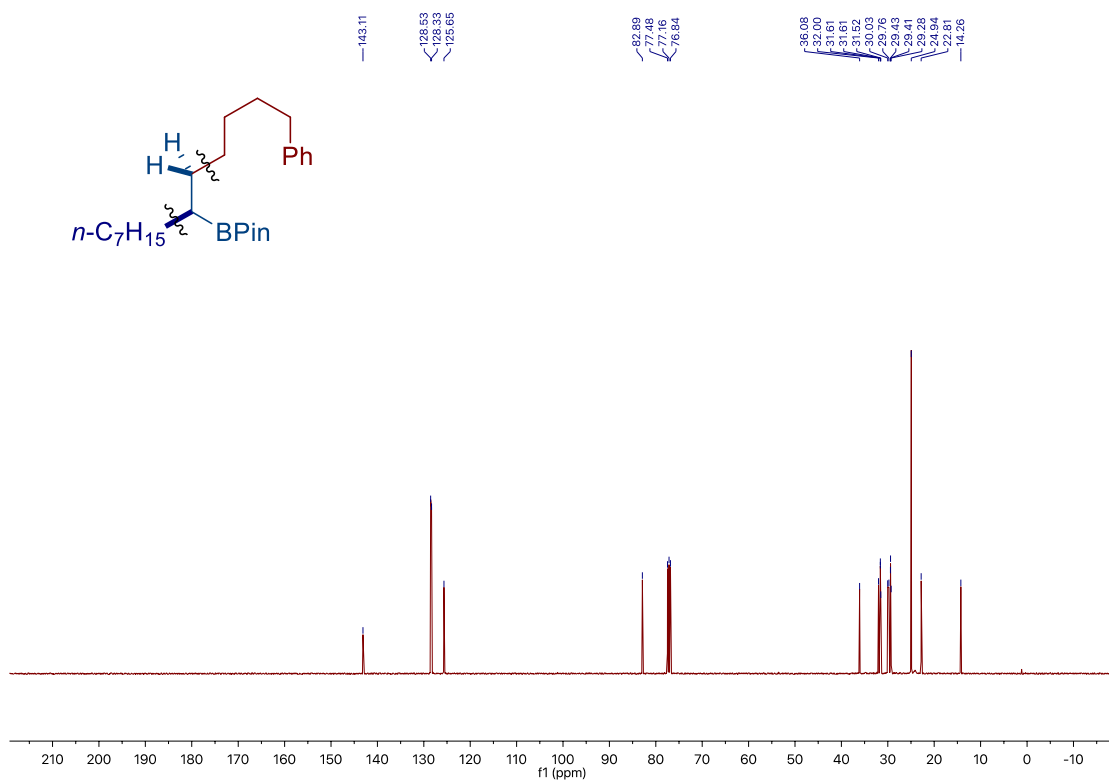
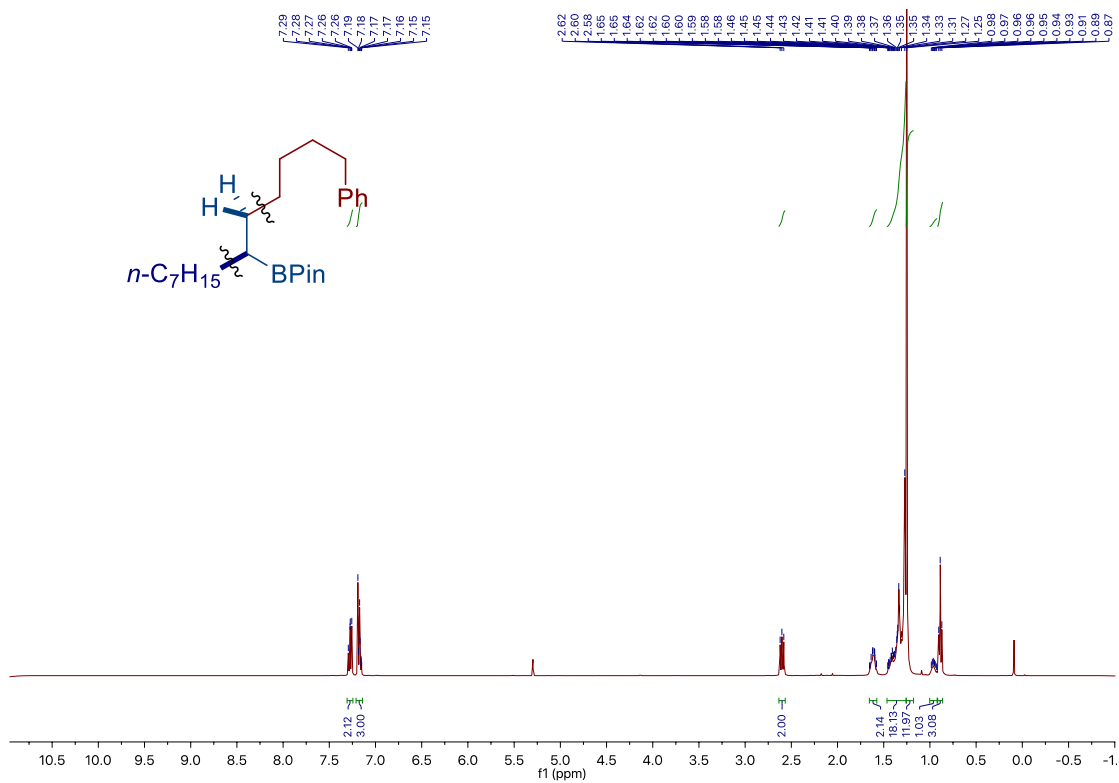
Chapter 2.



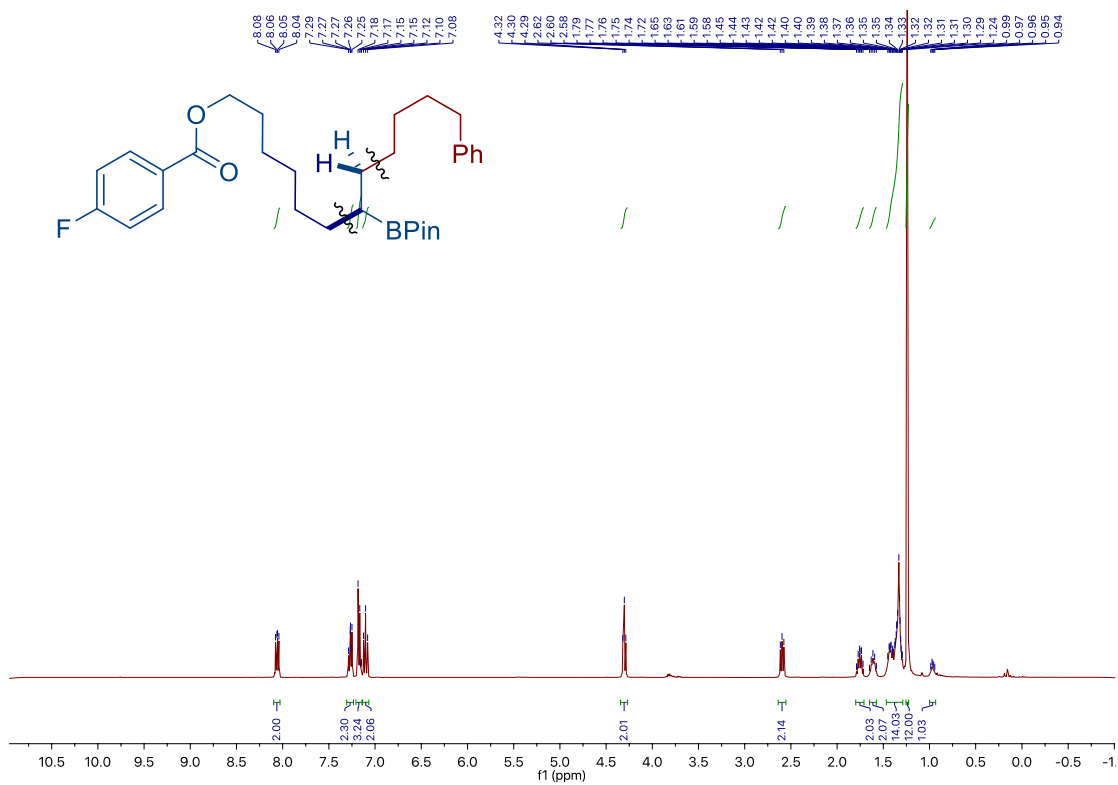
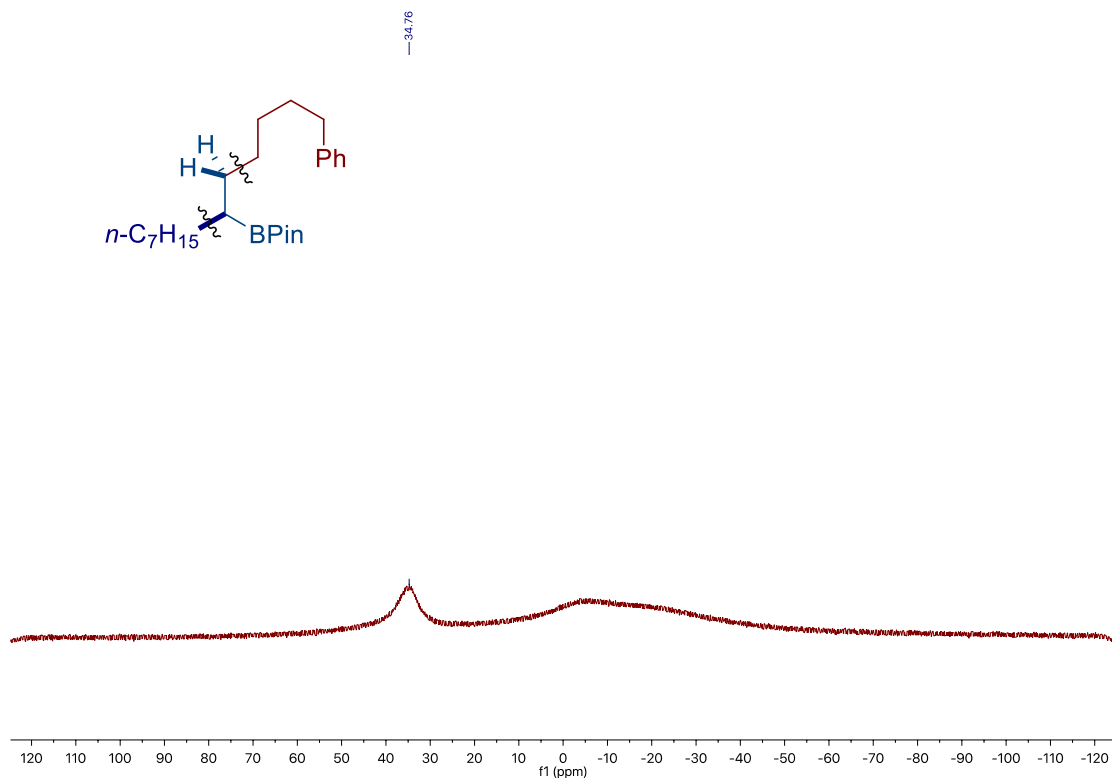
Site-Selective Ni-Catalyzed Reductive
Coupling of α -Haloboranes with Unactivated Olefins



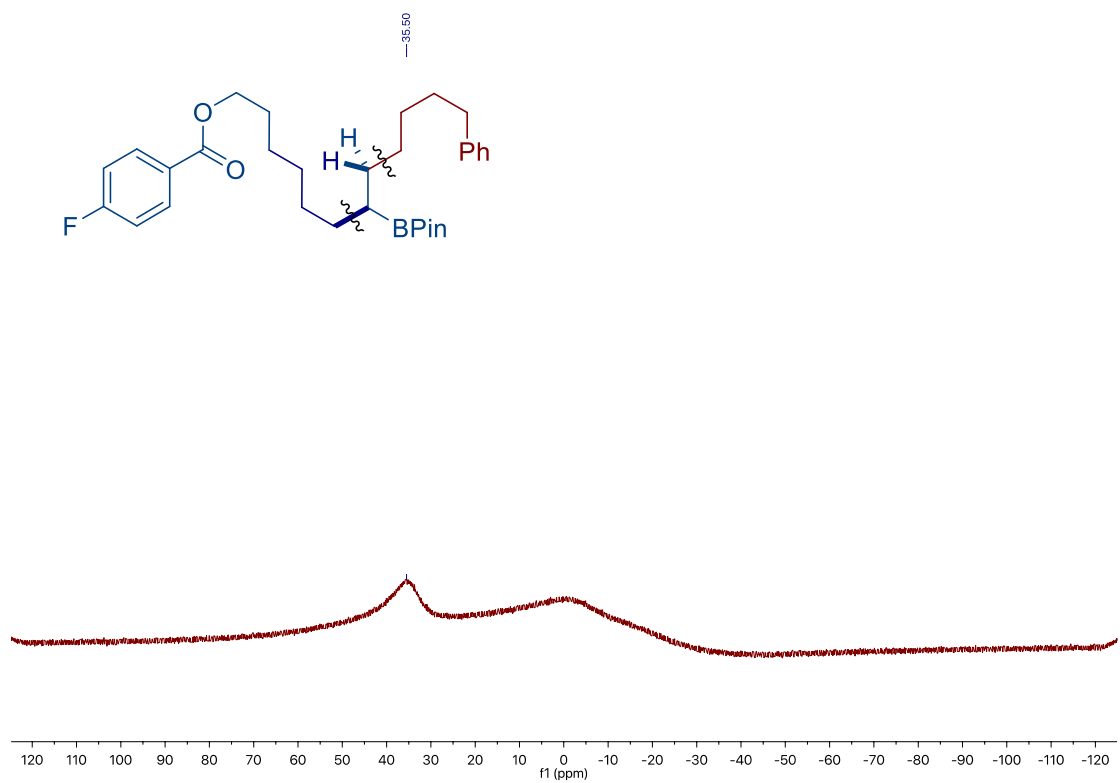
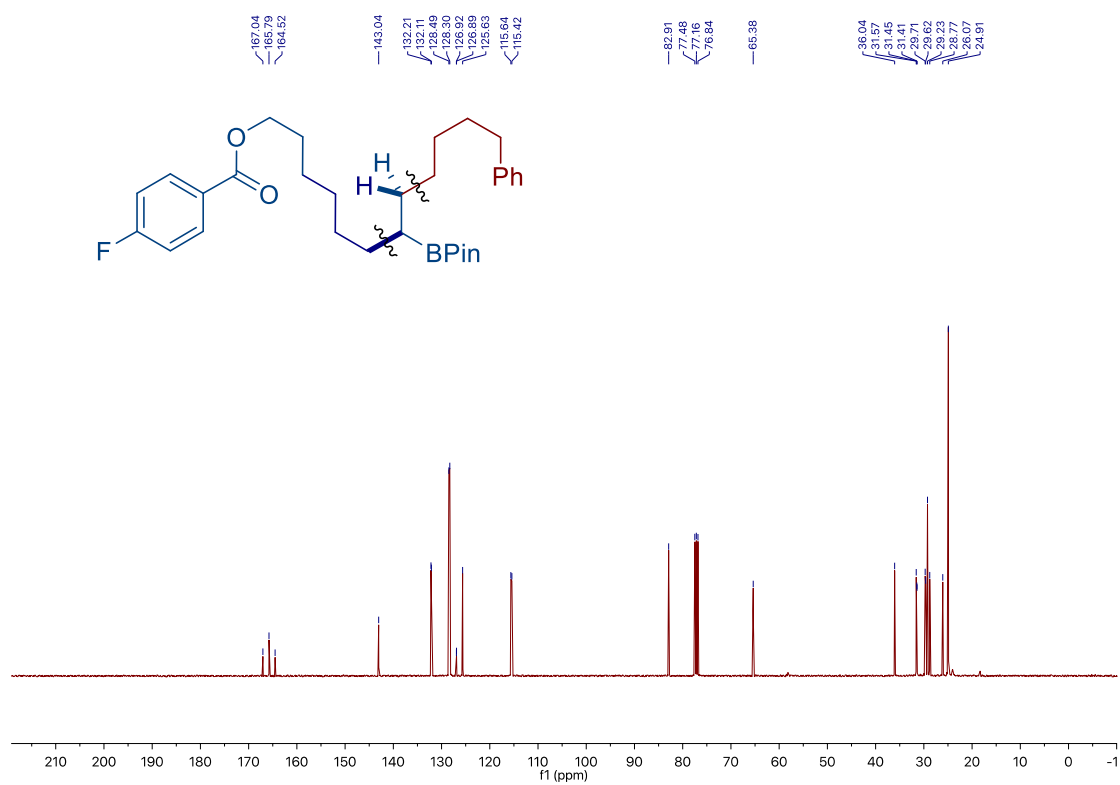
Chapter 2.



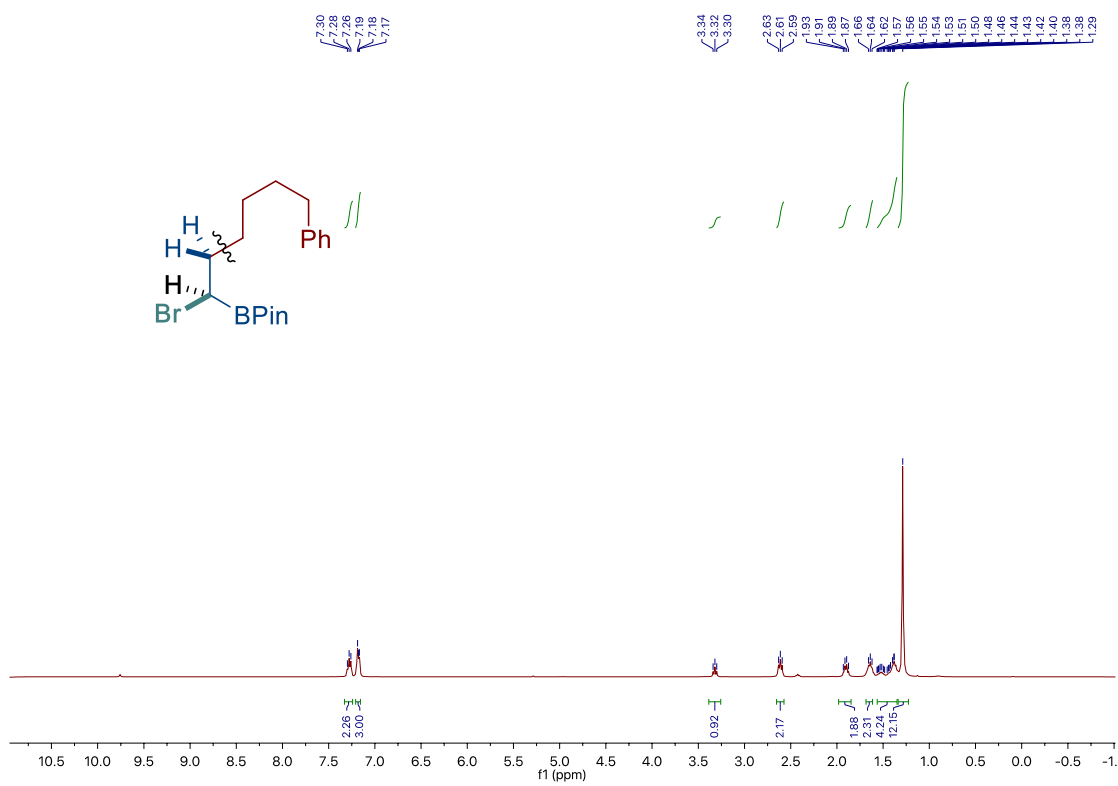
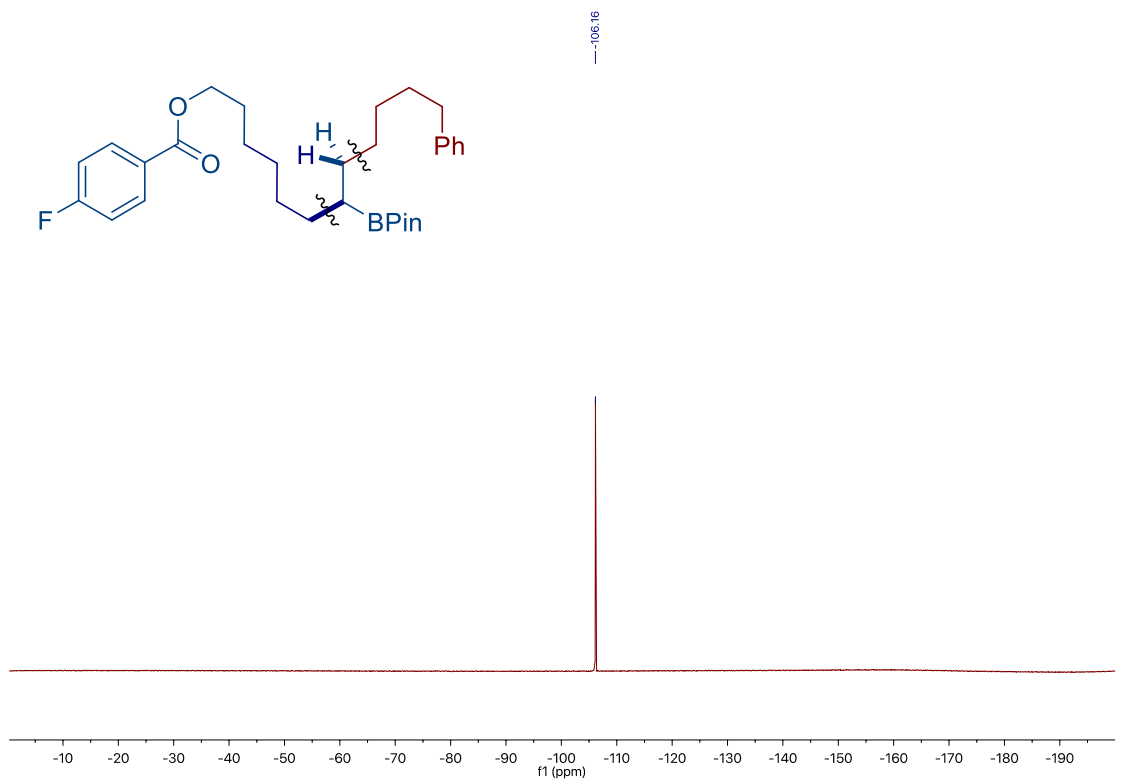
Site-Selective Ni-Catalyzed Reductive
Coupling of α -Haloboranes with Unactivated Olefins



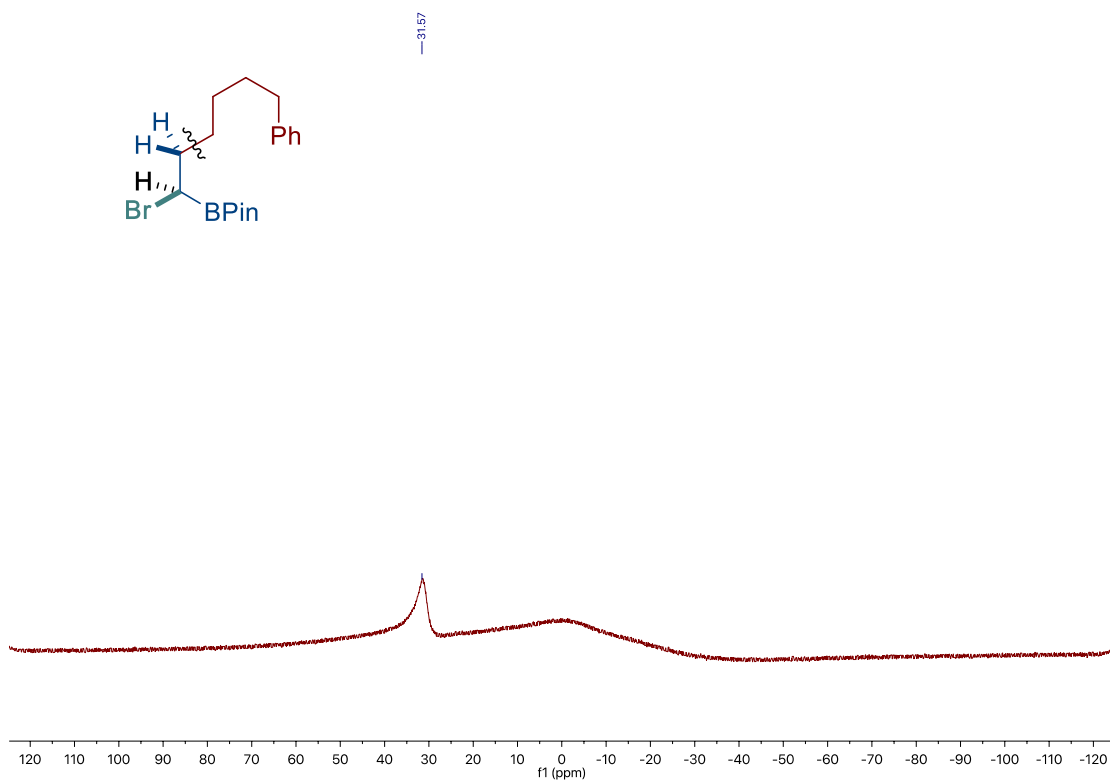
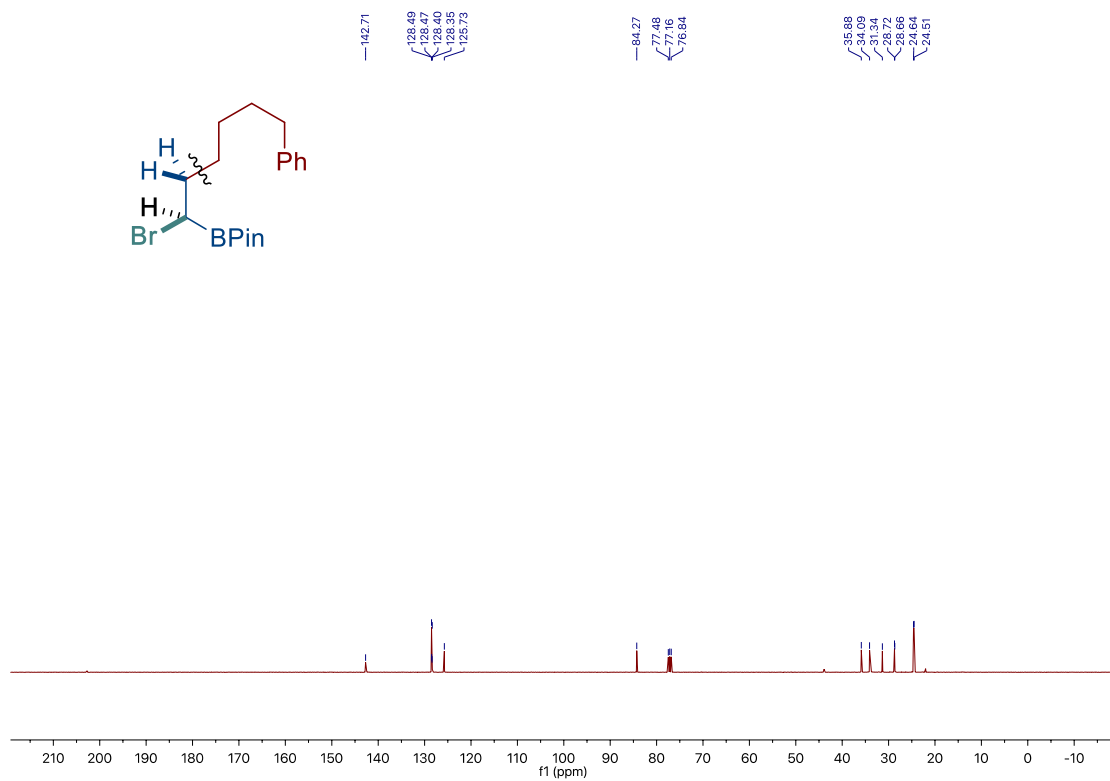
Chapter 2.



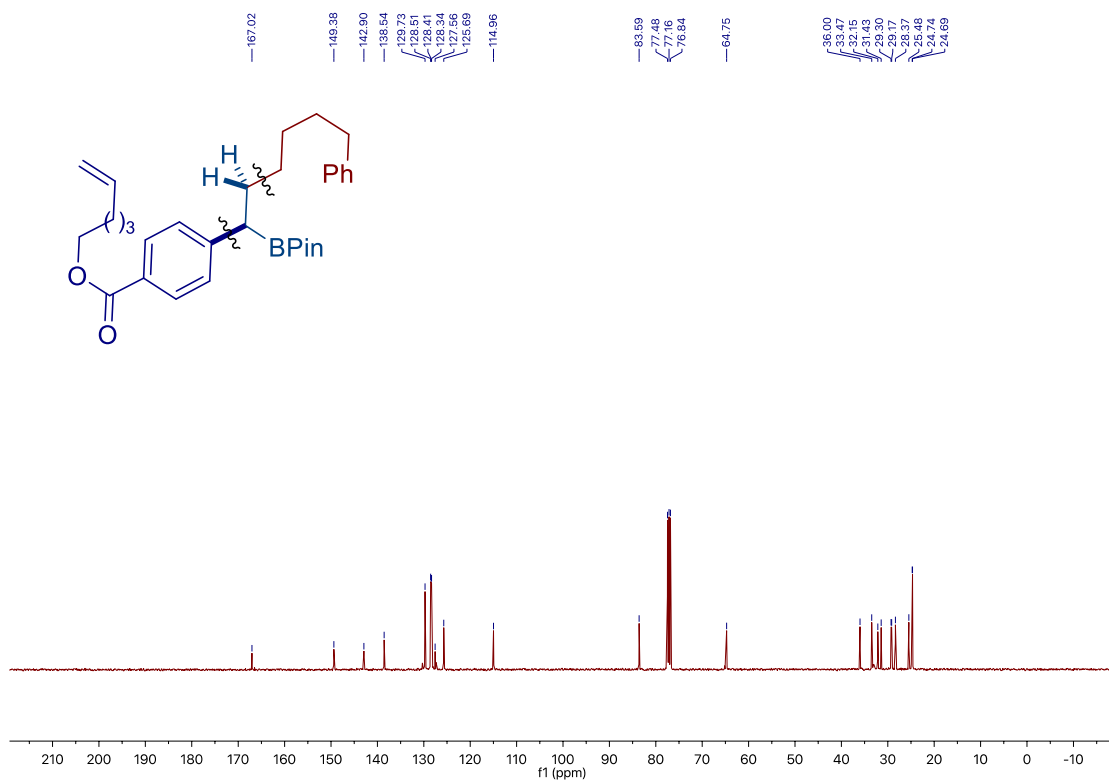
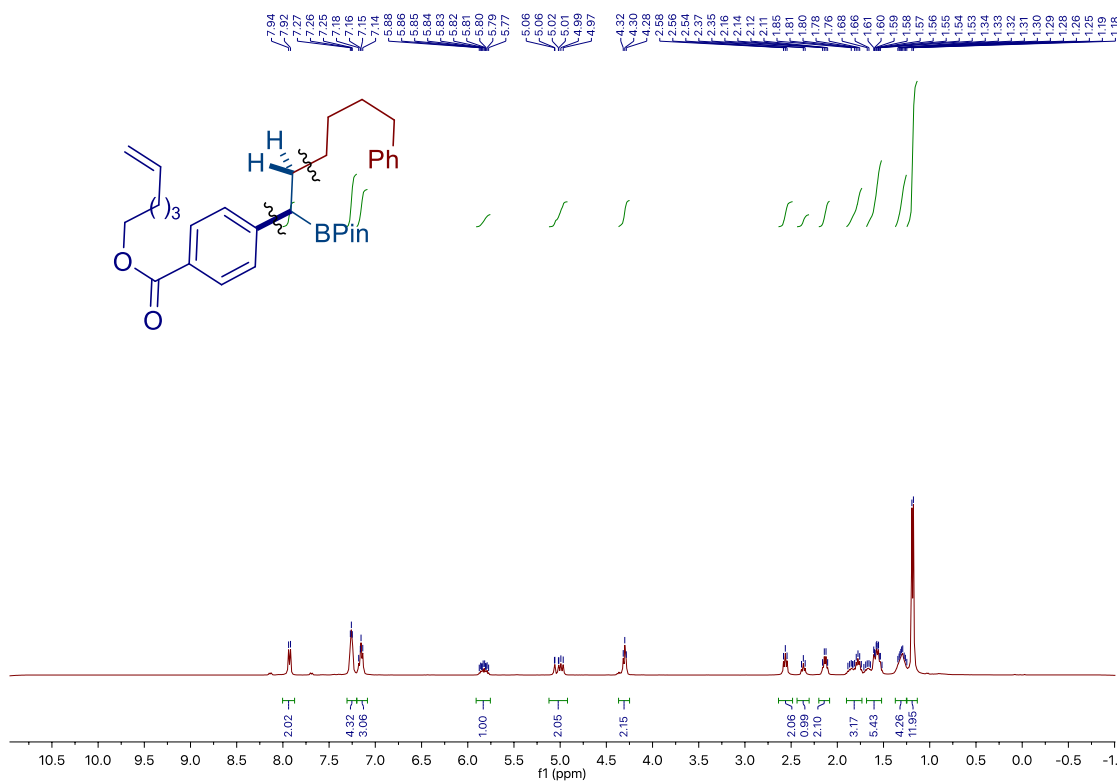
*Site-Selective Ni-Catalyzed Reductive
Coupling of α -Haloboranes with Unactivated Olefins*



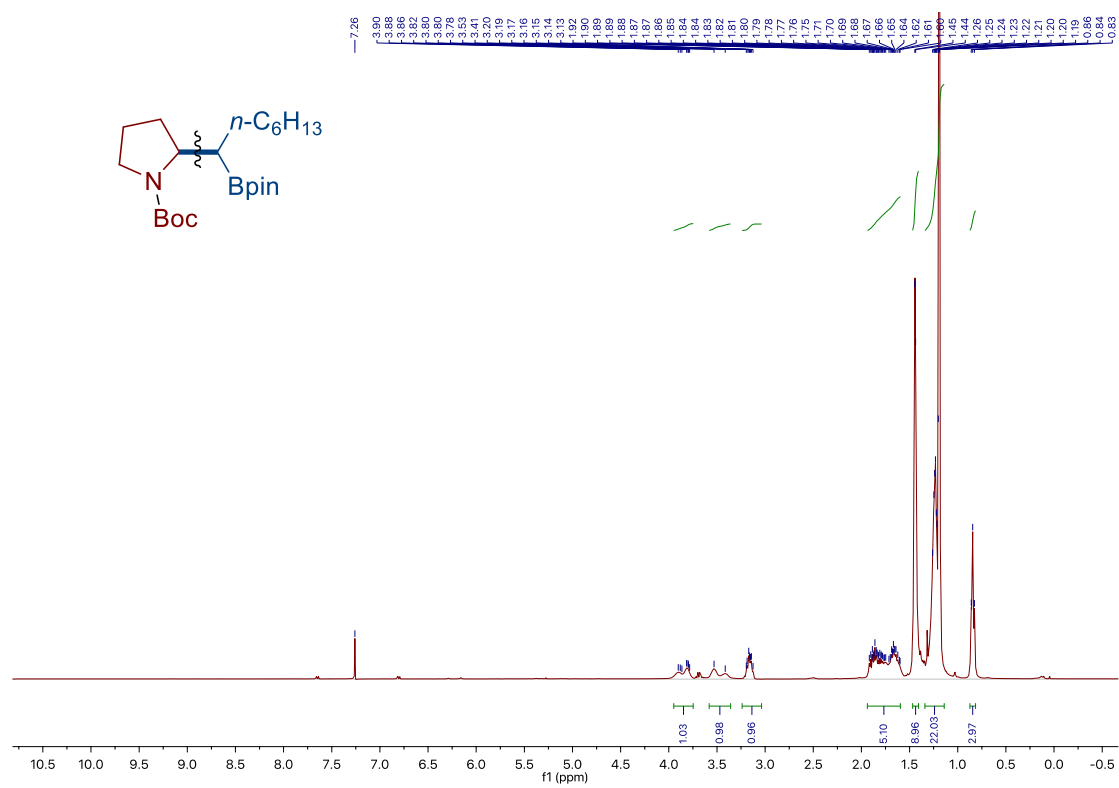
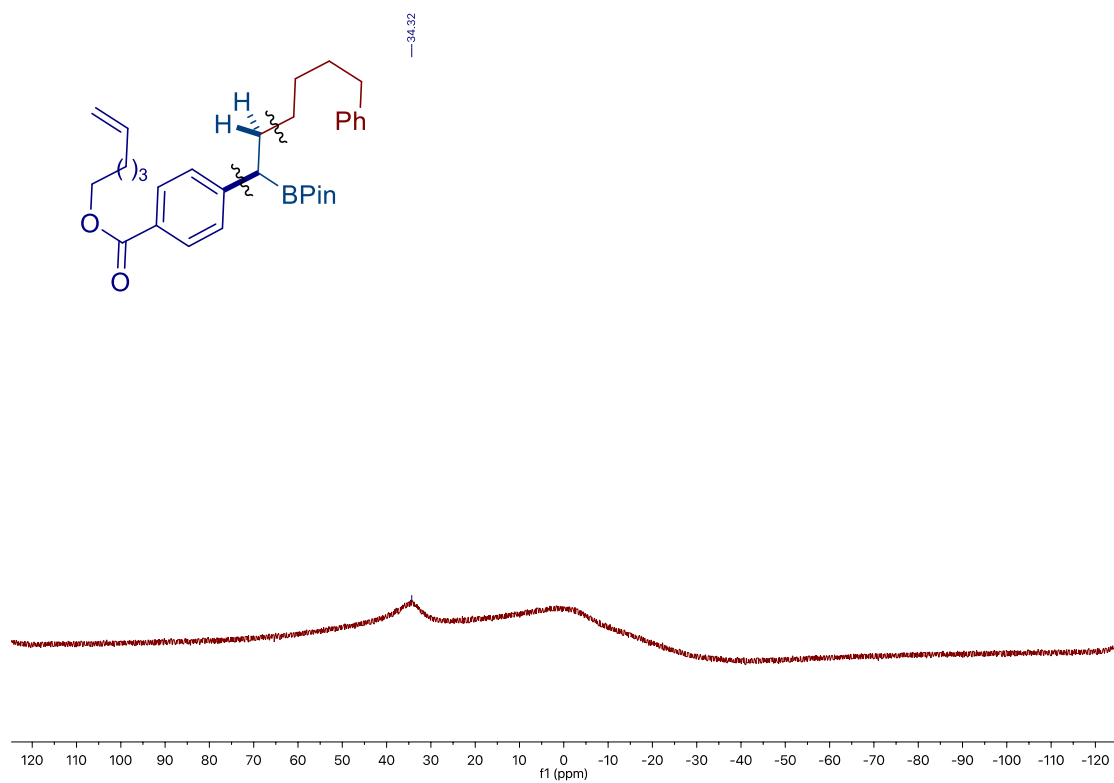
Chapter 2.



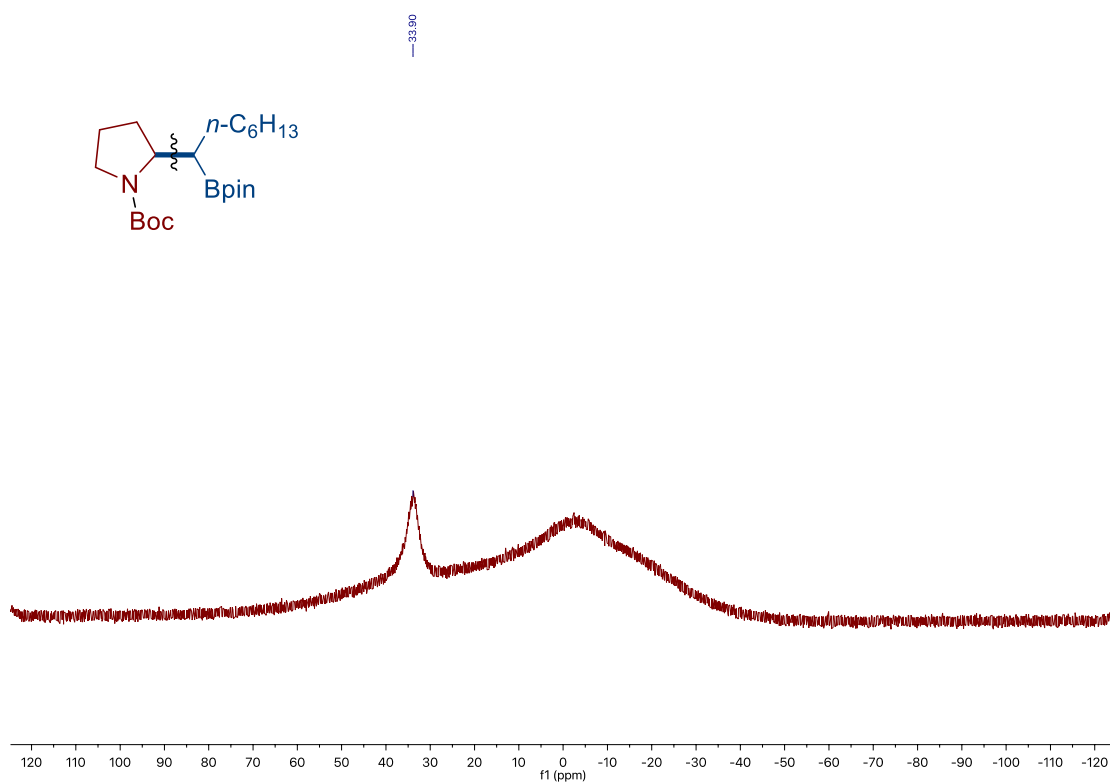
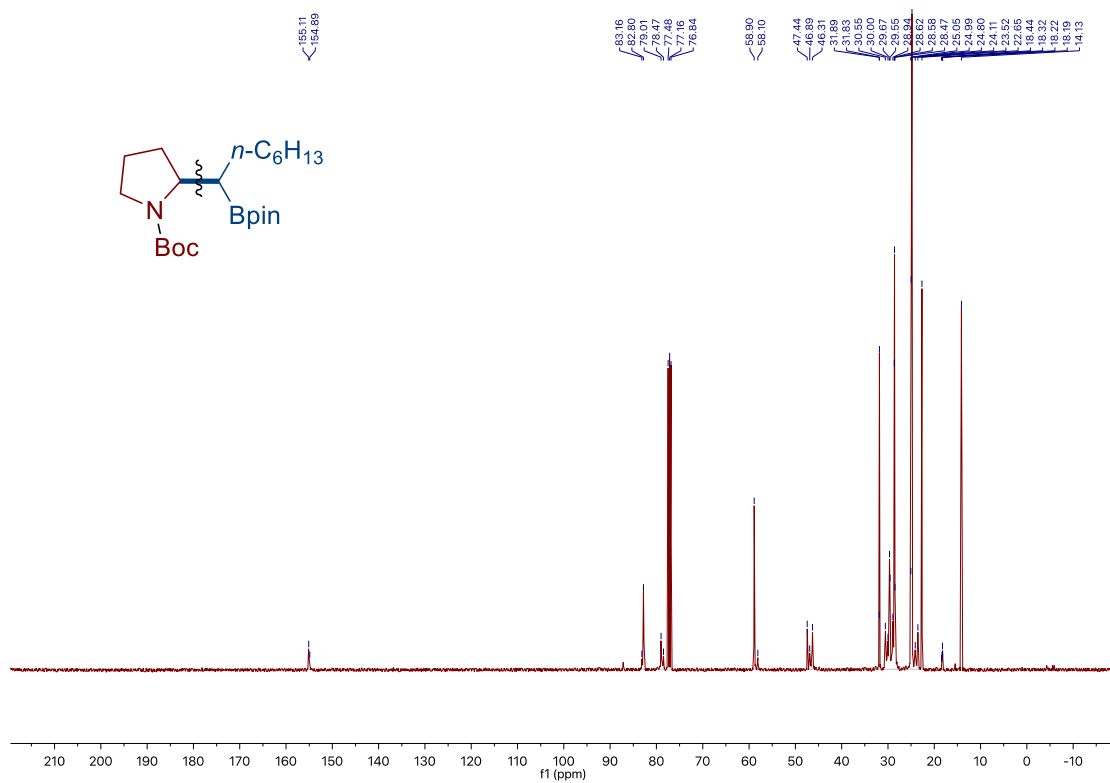
Site-Selective Ni-Catalyzed Reductive Coupling of α -Haloboranes with Unactivated Olefins



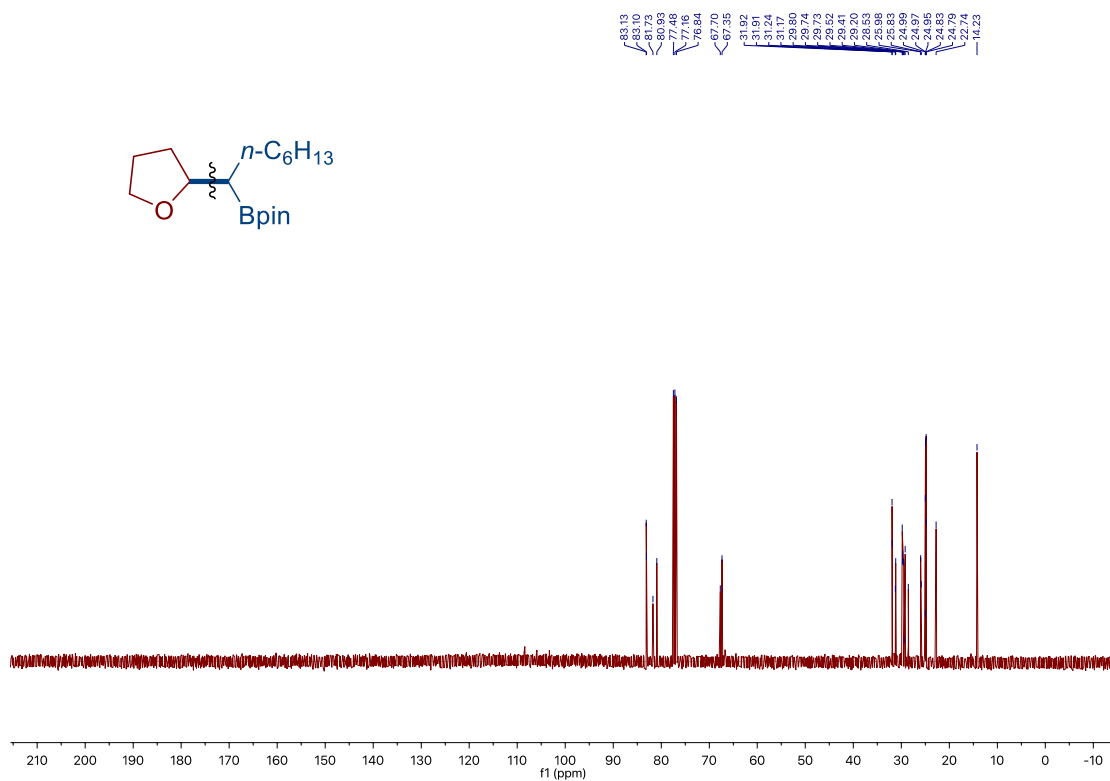
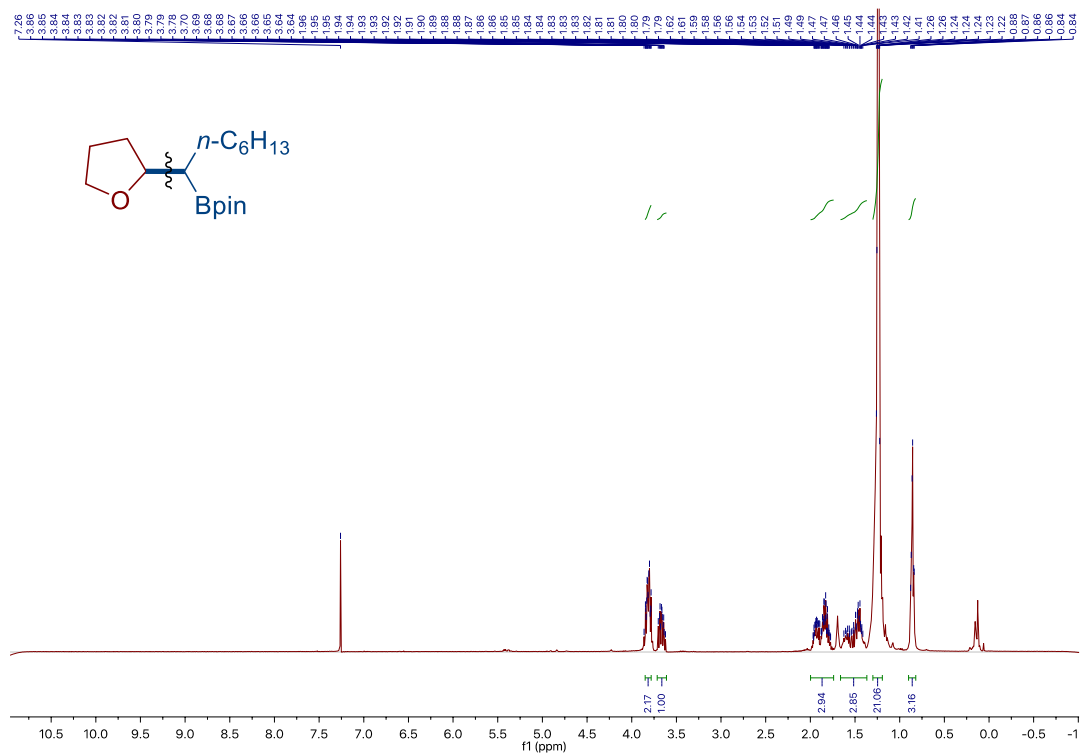
Chapter 2.



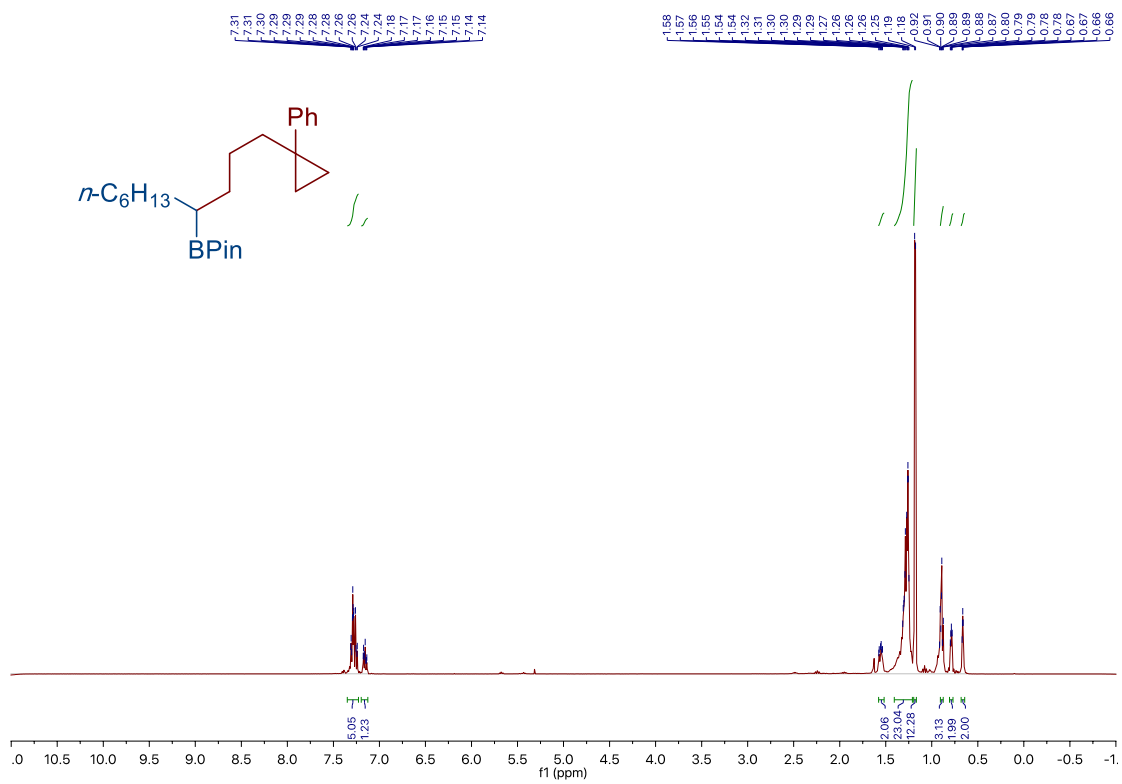
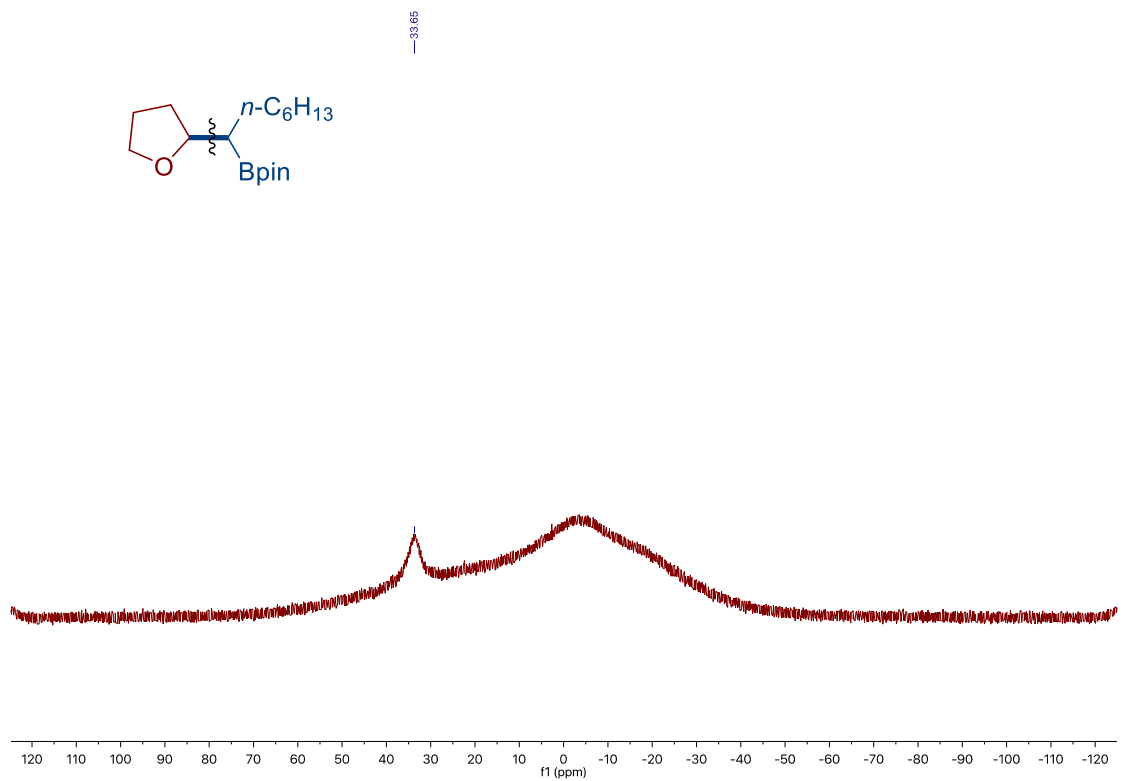
Site-Selective Ni-Catalyzed Reductive
Coupling of α -Haloboranes with Unactivated Olefins



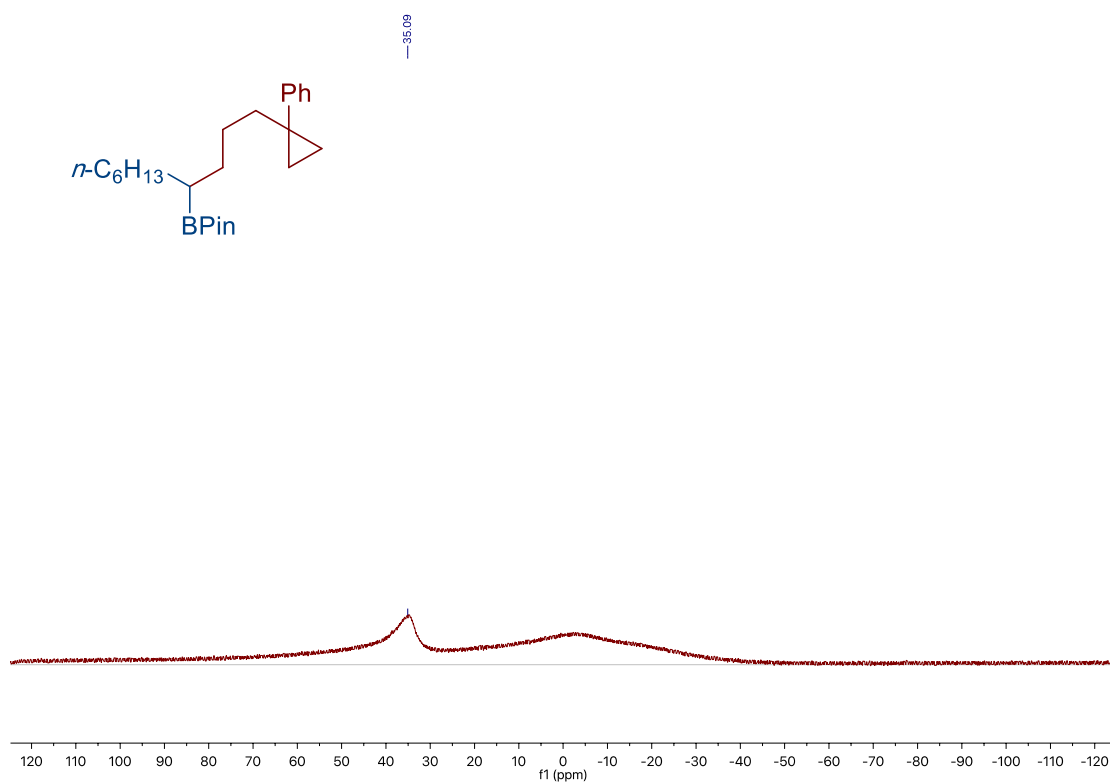
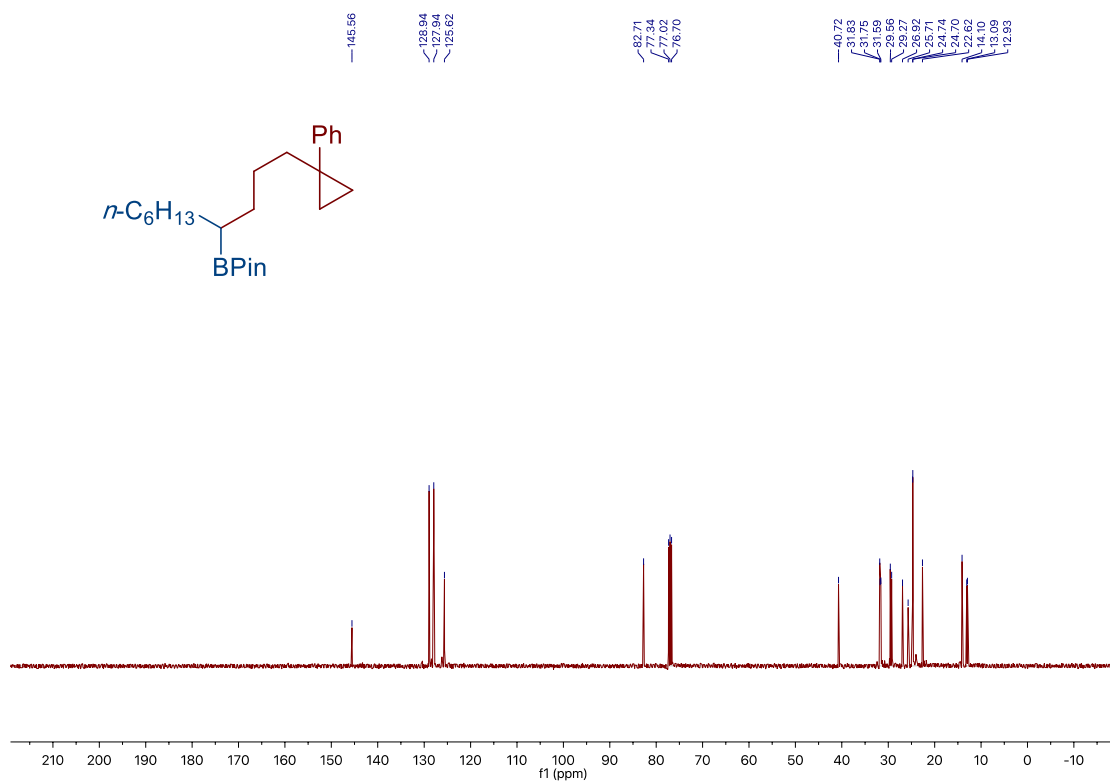
Chapter 2.



*Site-Selective Ni-Catalyzed Reductive
Coupling of α -Haloboranes with Unactivated Olefins*



Chapter 2.

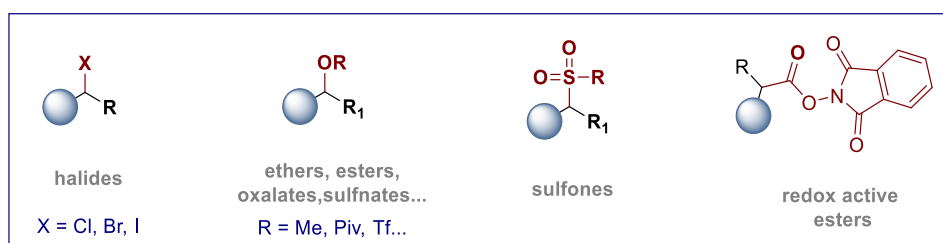


Chapter 3

Site-Selective Ni-Catalyzed Deaminative Alkylation of Unactivated Olefins

3.1 General Introduction

In modern synthetic chemistry, transition metal catalyzed cross-coupling reactions became one of the most powerful synthetic tool for the construction of C–C and C-heteroatom bonds.¹ At present, traditional cross-coupling reactions rely on the use of organic halides as electrophilic coupling partners.^{1,2} Despite the elegant advances realized, the difficulty in the preparation of the corresponding alkyl halides in a chemo- and regioselective fashion and the inherent toxicity of halide waste still constitute important drawbacks when designing cross-coupling reactions. Aiming to overcome these shortcomings, chemists made efforts to explore alternative alkyl electrophiles featured by easy and reliable synthesis, and by general application practicality for the construction of new C–C bonds. Recently, a diversity of C–O electrophiles (such as triflates, carboxylates, methyl ethers),³ redox-active esters⁴ and others⁵ were developed as alternatives to alkyl halides in C–C bond forming reactions, particularly in nickel⁶ and metallaphotoredox⁷ catalysis (Scheme 3.1). In contrast, the utilization of unactivated, primary alkyl amine derivatives as electrophiles in cross-coupling reactions remains an unmet challenge in organic synthesis and catalysis.^{8,9} On one hand, the high bond–dissociation-energy (BDE)– around 85 kcal/mol –makes the sp^3 C–N bond cleavage more difficult compared to the C-halide bond cleavage (BDE of C–Br around 69 kcal/mol) (Scheme 3.2).¹⁰ Moreover, the high affinity of the nitrogen’s lone pair for transition-metals inhibits the start and/or propagation of a catalytic cycle. In contrast the higher electronegativity of oxygen compared to nitrogen makes oxygen’s lone pairs less prone to coordinate to metals and the use of electron-withdrawing group on oxygen can easily modify the electrophilicity and reduce their affinity for transition metals further.³



Scheme 3.1. The development of electrophiles in cross-coupling reactions

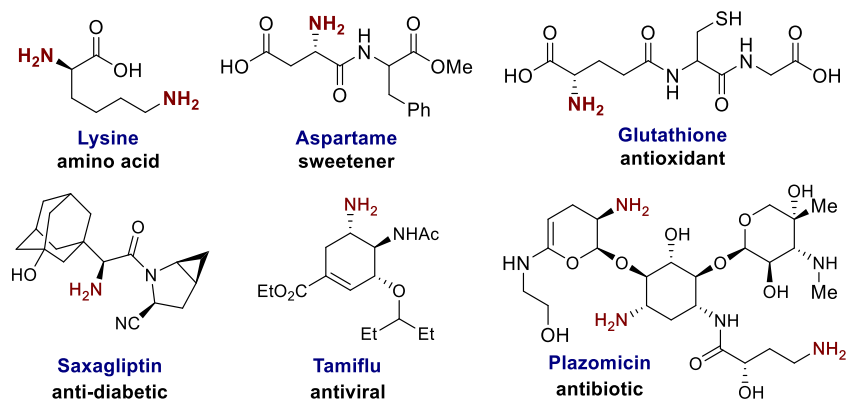


Scheme 3.2. Challenges for the sp^3 C–N bond activation

Nonetheless, some recent advances have been made in this area exploiting a diversity of approaches, all devoted to weaken the C–N bond and make it susceptible of selective cleavage.^{9,11} However, the aim of this chapter is not to furnish an extensive summary of all the existing methods for C–N cleavage but it will focus on the use of amine-derived redox-active functional groups employed in transition-metal-catalyzed cross-coupling reactions.

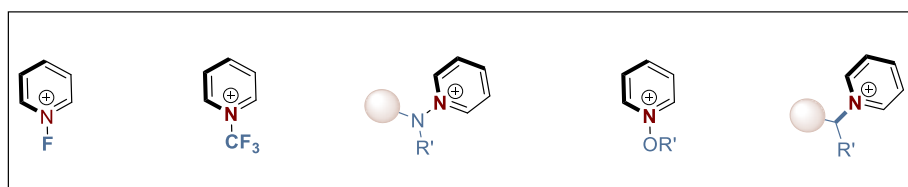
3.2 Pyridinium Salts as Electrophiles in Cross-Coupling Reactions

Driven by the wide prevalence of alkyl amines in natural products, pharmaceuticals, and life science molecules,¹¹ the development of deaminative functionalization strategies will be ideal in organic synthesis, particularly in the late-stage functionalization of drug candidates.¹² Early efforts were focused on the utilization of benzylic, allylic and ring-strained amines as activated electrophiles in cross-coupling reactions due to higher proclivity of the C–N bond.⁹ In contrast, using abundant unactivated alkyl amines as electrophiles has not been well investigated. In the late 1970s, the Katritzky group found primary alkyl amines could be used as alkylation reagents when converted to bench-stable *N*-substituted pyridinium salts.¹³ Encouraged by these pioneering discoveries, the deaminative functionalization of a particular class of pyridinium salts (the so called Katritzky salts) via sp^3 C–N bond activation has drawn considerable attention.¹⁴



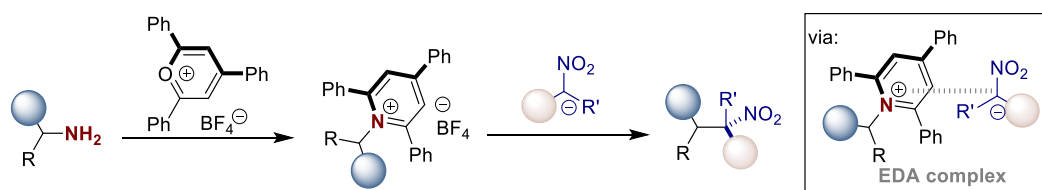
Scheme 3.3. Amine containing drug molecules

Among the amine-derivatives used in cross-coupling reactions, pyridinium salts stand as the most used electrophiles. These organic salts are widely found in many nature products, bioactive molecules and organic materials,¹⁵ and *N*-substituted derivatives have been employed as valuable synthetic intermediates in organic synthesis due to their air- and moisture- stability as well as easy availability.¹⁶ In the past decades, a variety of *N*-functionalized pyridinium salts have been employed in synthetic methodology, such as the F-, CF₃-, N- or O- substituted pyridinium salts (Scheme 3.4).^{14a,14b}



Scheme 3.4. Examples of pyridinium salt derivatives employed in organic synthesis

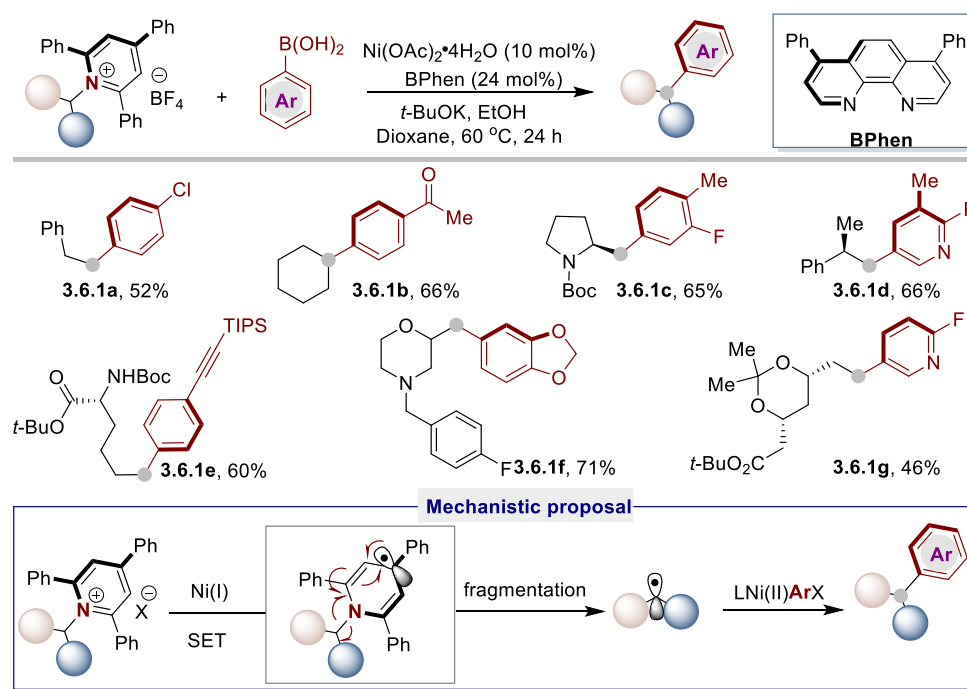
In 1981, Katritzky reported the alkylation of nitronate anions using *N*-alkyl pyridinium salts as electrophiles (Scheme 3.5).^{13a} This class of *N*-alkyl pyridinium salts (then called Katritzky salts) were prepared from primary alkyl amines with 2,4,6-triphenylpyrylium tetrafluoroborate under very mild conditions. Noteworthy, mechanistic studies suggested that the nucleophilic substitution by the nitronate proceeds through a nonchain radicaloid pathway with the intermediacy of an *electron donor-acceptor* (EDA) complex between the pyridinium salt and the nitronate anion.¹⁷



Scheme 3.5. Alkylation of nitronate anions with pyridinium salts

3.2.1 Catalytic Deaminative Alkylation of (Hetero)Arenes with Pyridinium Salts

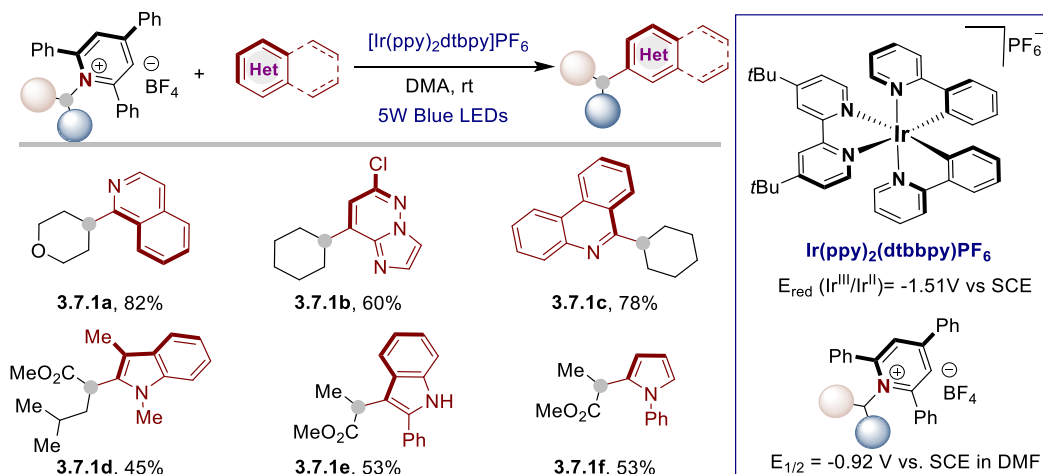
Inspired by Katritzky's work, the utilization of alkyl pyridinium salts as alkyl electrophiles in organic synthesis has blossomed in recent years. In 2017, the Watson group pioneered a Ni-catalyzed deaminative Suzuki-Miyaura coupling of aryl boronic acids with bench-stable pyridinium salts as alkyl electrophiles (Scheme 3.6).¹⁸ The combination of Ni(OAc)₂·4H₂O and bidentate bathophenanthroline ligand (BPhen), provided the deaminative arylation products in good yields. In this case, amines bearing either primary or secondary alkyl substituents were successfully employed, even in the context of late-stage functionalization. Interestingly, the addition of 5 equivalents of EtOH dramatically increased the yield probably due to its hydrotropic effect. Preliminary mechanistic studies suggested the involvement of a radical pathway within a Ni(I)/Ni(III) catalytic cycle: *single-electron-transfer* (SET) from a Ni(I) intermediate to the pyridinium moiety triggered the fragmentation of the alkyl pyridinium salt, generating an alkyl radical. The alkyl radical subsequently recombined with the Ar–Ni(II)–X species delivering an alkyl–Ni(III)–Ar intermediate, which afforded the Suzuki-Miyaura coupling product and Ni(I) species upon reductive elimination. However, the reaction initiation process and the oxidative addition mechanism were still unclear. Upon a slight modification of reaction conditions, the same group subsequently disclosed the deaminative Suzuki-Miyaura coupling of more active benzylic pyridinium salts^{19,20} and amino acid-derived pyridinium salts.²¹ Both of the methodologies displayed broad substrate scope and good functional group tolerance.



Scheme 3.6. Ni-catalyzed deaminative Suzuki-Miyaura coupling reported by Watson and co-workers

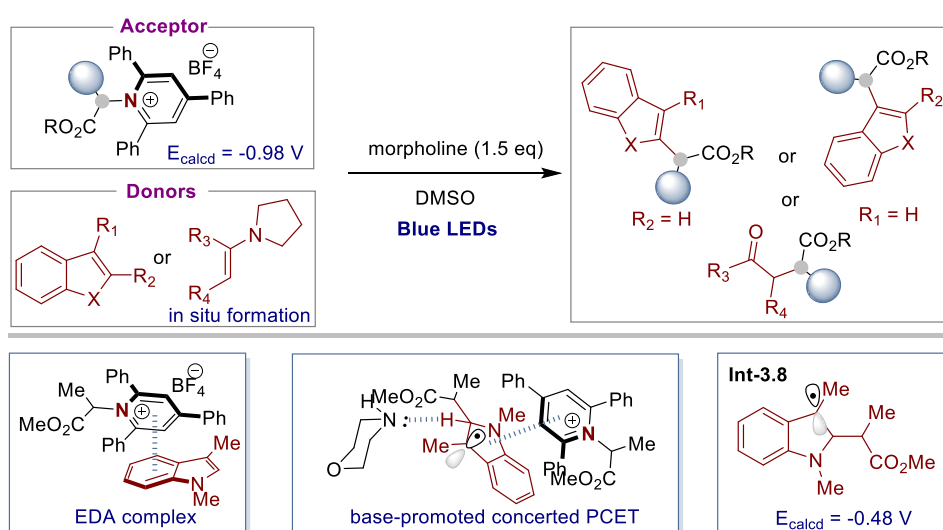
Considering that alkyl radicals could also be generated via oxidative quenching of an excited photocatalyst, in 2017, Glorius and co-workers developed a photocatalyzed deaminative Minisci-type reaction of alkyl pyridinium salts with heteroarenes (Scheme 3.7).²² In this case, the alkyl radical species were formed from the redox-active Katritzky salts under mild, visible-light-mediated conditions. A range of alkyl pyridinium salts were prepared from amines bearing secondary alkyl groups and were successfully applied in this reaction. Noteworthy, pyridinium salts derivatized from a series of natural and unnatural amino acids were efficiently coupled with electron-rich heteroarenes such as indoles and pyrrole, taking advantage of the polarity match between electrophilic radicals and electron-rich heteroarenes.

Site-Selective Ni-Catalyzed Deaminative Alkylation of Unactivated Olefins



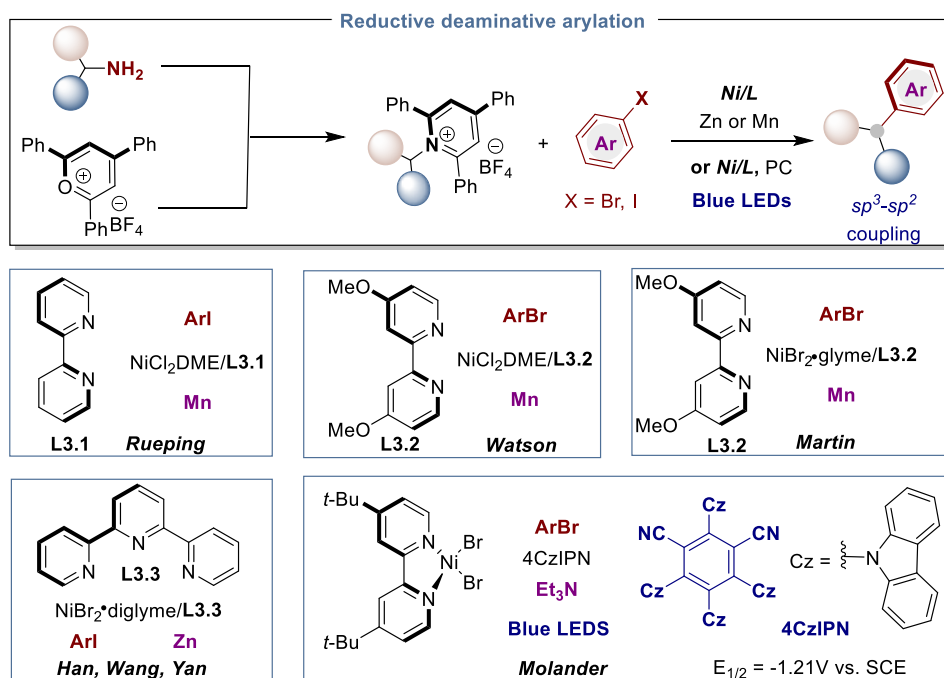
Scheme 3.7. Visible-light-mediated deaminative alkylation of heteroarenes

Very recently, the same group extended the scope of this deaminative C_{sp^3} – C_{sp^2} bond forming strategy using amino acid derived pyridinium salts with electron-rich heteroarenes or enamines. The latter could be formed *in-situ* by premixing the corresponding carbonyl compounds with pyrrolidine (Scheme 3.8).²³ This protocol was enabled by the *photoinduced-electron-transfer* (PET) of an *electron-donor-acceptor* (EDA) complex formed between electron-deficient pyridinium salts and electron-rich heteroarenes or enamines. A subsequent concerted base-promoted *proton-coupled-electron transfer* (PCET) from the benzylic radical intermediate (**Int 3.8**) to a second molecule of the Katritzky salt propagates the process.



Scheme 3.8. Photo-induced deaminative alkylation of heteroarenes and enamines via *electron-donor-acceptor* (EDA) complex

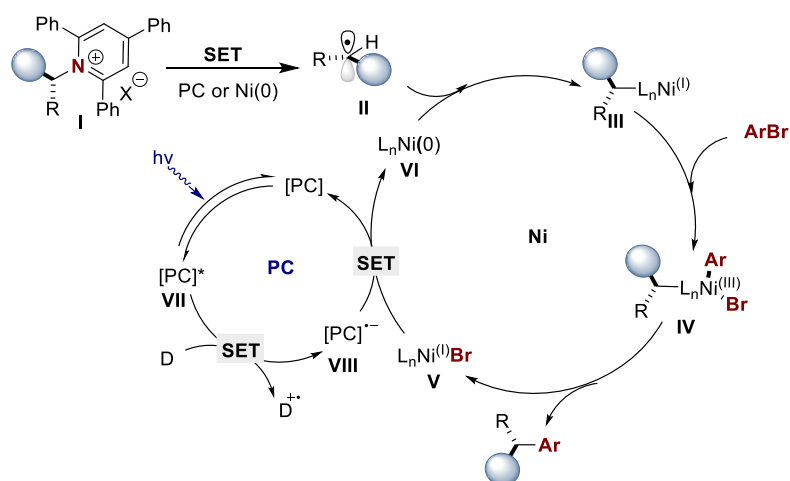
Forseeing the advantage of employing Ni-catalyzed cross-electrophiles coupling, Watson,²⁴ Rueping²⁵ and our group²⁶ independently developed a Ni-catalyzed reductive deaminative alkylation of aryl halides using *N*-alkyl pyridinium salts as alkyl electrophiles (Scheme 3.9, *middle*). Additionally, our group realized that Hantzsch ester could be employed as an organic reductant instead of Mn under photoredox/nickel dual catalysis. Such an achievement represented a remarkable improvement in the field due to the toxicity and the difficult removal of metal waste. Conversely, Han, Wang, Yan and co-worker described the reductive deaminative coupling reaction with Zn as reductant (Scheme 3.9, *bottom left*).²⁷ The employment of a tridentate ligand (**L3.3**) was crucial for the reaction success, and the substrate scope could be extended to alkyl and alkynyl bromides. Preliminary mechanistic studies and control experiments conducted in all these reports suggested the existence of a transient alkyl radical intermediate resulting from reductive fragmentation of the corresponding pyridinium salt. Noteworthy, our group found that in the presence of stoichiometric amounts of Mn, TEMPO and pyridinium salt, the corresponding TEMPO-adduct could be afforded in good yield, providing compelling evidence for Mn-mediated rather than low valent Ni-mediated SET process.



Scheme 3.9 Ni-catalyzed deaminative reductive cross-coupling with aryl halides

Another important contribution to the field was reported by the group of Molander, which developed a reductive alkylation of aryl bromides using pyridinium

salts as alkyl radical precursors through photoredox/nickel dual catalysis, employing Et_3N as the terminal organic reductant (Scheme 3.9, *bottom right*).²⁸ The proposed mechanism started with the quenching of the photo-excited $[\text{4CzIPN}]^*$ ($E_{1/2} = 1.35$ V vs SCE) by Et_3N ($E_{1/2} = 1.0$ V vs SCE) to form the reduced state $[\text{4CzIPN}]^{\cdot-}$ (Scheme 3.10). The alkyl radical **II**, generated from the pyridinium salt **I** via SET, was intercepted by a Ni(0) complex to afford an alkyl–Ni(I) intermediate **III**. Subsequent oxidative addition of aryl bromide, followed by reductive elimination, afforded the desired product and Ni(I)–Br species **V**. Eventually, **V** was reduced to Ni(0) by $[\text{4CzIPN}]^{\cdot-}$ ($E_{1/2} = -1.21$ V vs SCE) closing the catalytic cycle. However, it still remained to be understood if the alkyl radical was generated by SET from 4CzIPN ($E_{1/2} = -1.21$ V vs SCE) or from low valent nickel species.

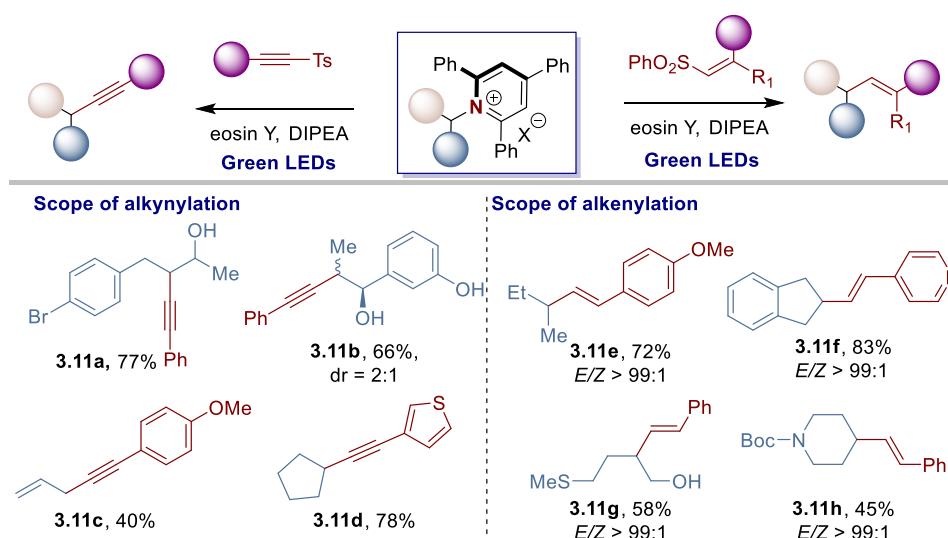


Scheme 3.10. Mechanistic proposal for the dual catalytic reductive alkylation of aryl bromides

3.2.2 Catalytic Deaminative Alkylation Strategies for the Synthesis of Alkenes and Alkynes

As previously discussed, efforts have been taken on the development of new strategies for the deaminative alkylation of (hetero)arenes starting from aryl halides or heteroarenes. However, there is still a lack of general approaches for the preparation of alkenes and alkynes by catalytic deaminative alkylation processes. In 2018, Gryko and co-workers reported a metal-free photoredox strategy for the construction of new $C_{sp^3}\text{--}C_{sp}$ and $C_{sp^3}\text{--}C_{sp^2}$ bonds starting from redox-active Katritzky salts and vinyl

sulfones or alkynyl *p*-tolylsulfones, respectively (Scheme 3.11).²⁹ The method employed an organic dye (eosin Y) as a photocatalyst, where their method was successfully applied to a series of secondary alkyl-, benzyl-, and allyl-pyridinium salts. Conversely, unactivated primary alkyl and electron-rich benzyl Katritzky salts only delivered traces of the desired product, even after prolonged reaction time. This is probably due to the low stability of primary radicals and slow reaction rates for their formation. Interestingly, the deaminative alkylation of vinyl sulfones uniformly provided the thermodynamic more stable (*E*)-alkenes.



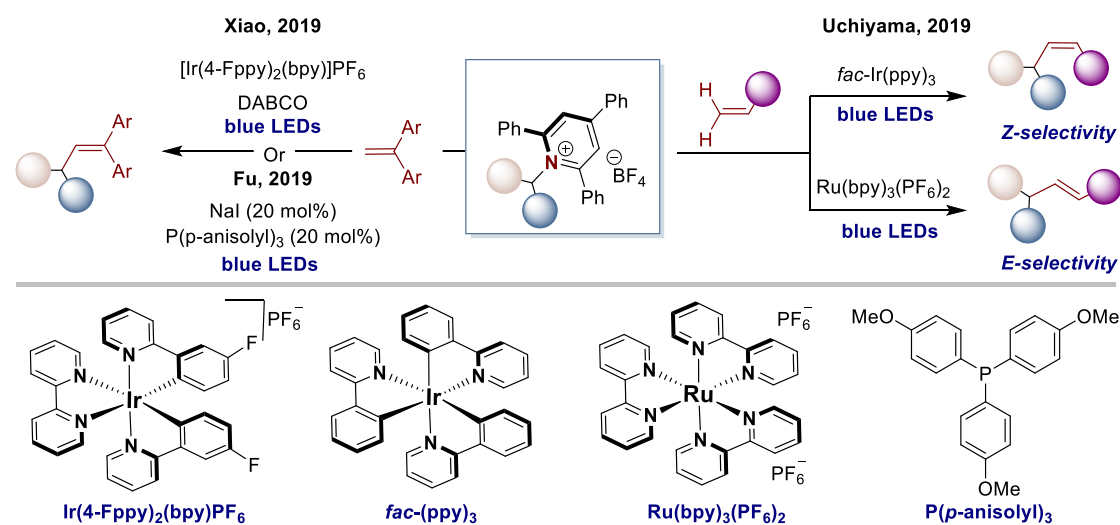
Scheme 3.11. Photo-catalyzed deaminative alkylation of vinyl- and alkynylsulfones

In the past decades, the transition-metal-catalyzed Heck reaction of aryl halides with olefins has been recognized as one of the most powerful methods for the preparation of an array of unsaturated products.³⁰ However the “alkyl-Heck” reaction, namely the coupling between an olefin and alkyl halides, is still challenging due to the instability of alkyl-metal intermediates towards β -hydride elimination. Recently, intensive efforts have been made in this field by replacing traditional two-electron processes with radical pathways through using redox-active reagents.³¹ In 2018, Xiao and co-workers reported a photoinduced deaminative alkyl Heck-type reaction of pyridinium salts with 1,1-diarylethylenes (Scheme 3.12, *top left*).³² This platform provided a complementary method to Pd-catalyzed Heck reaction for the construction of aryl-substituted alkenes.³⁰ The authors proposed that the transformation occurred via an oxidative quenching of the photocatalyst, followed by the fragmentation of the pyridinium salt and Giese-type addition of the newly formed alkyl radical to the olefin. The redox cycle was closed by converting the benzyl-radical to the corresponding

carbocation, which underwent deprotonation by the base, delivering the final olefinic product.

Recently, Uchiyama and co-workers described a similar transformation for the preparation of 1,2-disubstituted alkenes by using alkyl pyridinium salts as radical precursors (Scheme 3.12, *top right*).³³ It is worth noting that the *E/Z*-selectivity of the reaction could be switched by the appropriate choice of photocatalyst. For example, *trans* isomers were obtained by using $[\text{Ru}(\text{bpy})_3](\text{PF}_6)_2$, whereas the *cis* isomers could be accessed with *fac*- $\text{Ir}(\text{ppy})_3$, due to *E/Z* isomerization promoted by the Ir-based photocatalyst.

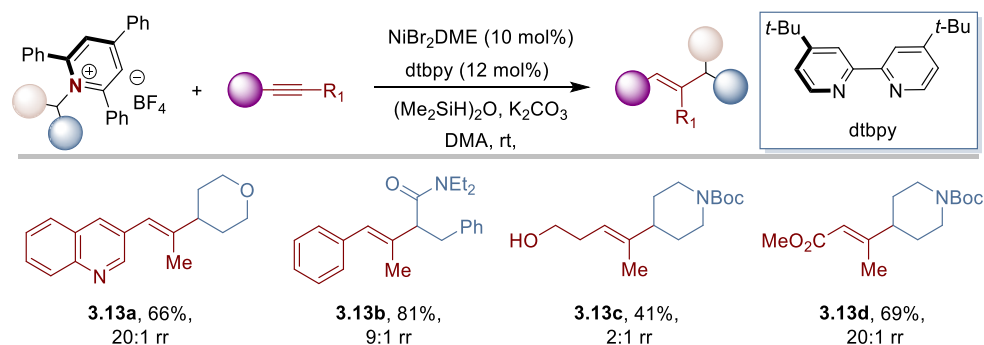
Additionally, Fu and co-workers demonstrated that the combination of NaI/PAR_3 represented an efficient photoredox catalytic system, promoting the deaminative alkyl Heck-type reactions of alkyl pyridinium salts with 1,1-diarylethylene (Scheme 3.12, *top left*).³⁴ The authors proposed that the alkyl radical was produced by photofragmentation of a *charge-transfer-complex* (CTC), generated between the alkyl pyridinium salt, NaI and PAR_3 .



Scheme 3.12. Visible-light-mediated deaminative alkyl-Heck-type reactions

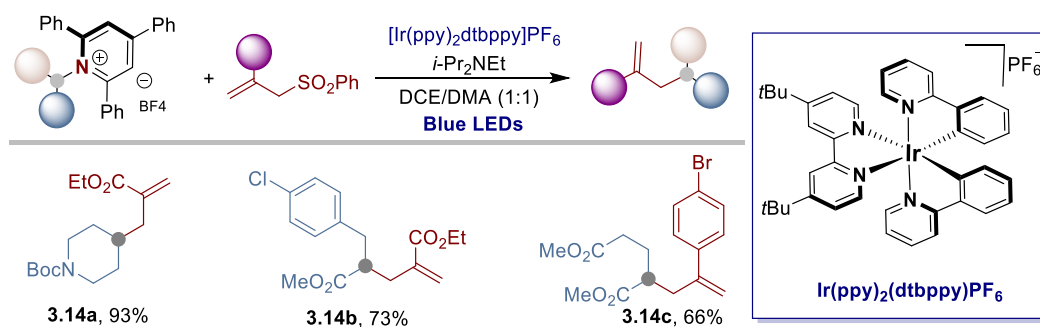
Another contribution to the field has been described by the Liu group, which disclosed a mild and efficient Ni-catalyzed regio- and stereo-selective hydroalkylation of internal alkynes with alkyl pyridinium salts (Scheme 3.13).³⁵ This method provided a unique strategy for the synthesis of a wide of tri-substituted alkenes starting from alkyl amine-derivatives. High regio-selectivities were obtained with a series of aryl alkynes and symmetrical internal alkynes, however, small electronic and/or steric difference of the alkyl substituents in unsymmetrical internal alkynes resulted in

lower yields. Preliminary mechanistic studies suggested that the reaction combined a SET-initiated radical process and a Ni-catalyzed alkylation. However, whether the reaction occurred through Ni-hydride insertion to alkyne or Ni-alkyl species insertion to alkyne remains unclear.

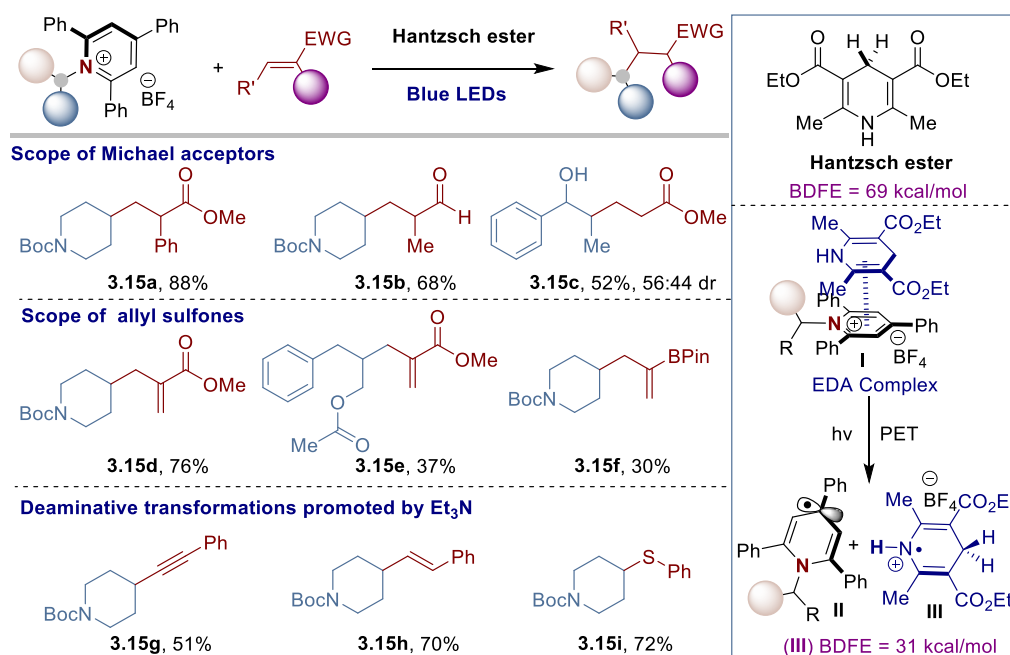


3.2.3 Catalytic Deaminative Alkylation Strategies for the Formation of New C_{sp^3} - C_{sp^3} Bonds

The prevalence of C_{sp^3} - C_{sp^3} bonds in bioactive molecules has led to intense efforts in developing methods to couple saturated reaction partners.³⁶ Recently, the Liu group developed a visible-light-mediated allylation reaction of alkyl pyridinium salts with allyl sulfones via a sp^3 C-N bond cleavage strategy (Scheme 3.14).³⁷ Using $\text{Ir}[(\text{ppy})_2(\text{dtbbpy})]\text{PF}_6$ as the photocatalyst and $i\text{-Pr}_2\text{NEt}$ as the terminal reductant, this mild approach provided facile access to new C_{sp^3} - C_{sp^3} bonds by using abundant primary amines, where even α -amino acids could be used as alkyl radical precursors. The generality of this protocol was demonstrated and a series of functional groups proved to be well tolerated.



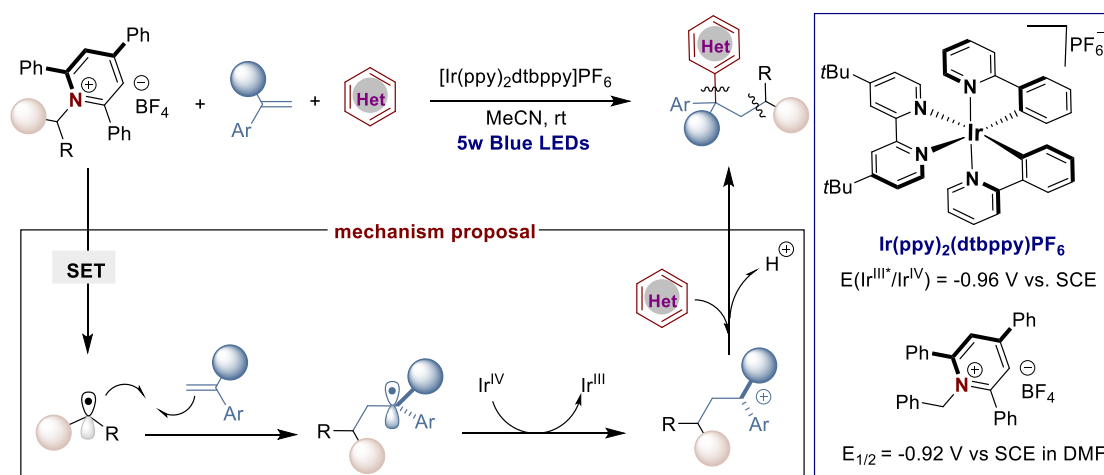
The photofragmentation of the Katritzky salt has not been achieved exclusively by the employment of a photocatalyst, as shown by Aggarwal and co-workers who developed a catalyst-free deaminative Giese-type reaction of alkyl pyridinium salts with a range of Michael acceptors (Scheme 3.15).³⁸ The authors found that the alkyl pyridinium salt and Hantzsch ester (or Et₃N) could form an *electron-donor-acceptor* (EDA) complex, and an alkyl radical could be released by an internal *photoinduced-electron-transfer* (PET).³⁹ They proposed the addition of the alkyl radical to the Michael acceptor to form an electrophilic radical intermediate. The latter underwent *hydrogen-atom-transfer* (HAT) with dihydropyridine radical cation **III** (BDFE = 31 kcal/mol)⁴⁰ generated upon PET or with another molecule of the Hantzsch ester (BDFE = 69 kcal/mol)⁴⁰ to deliver the product (BDFE ≈ 96 kcal/mol)⁴¹ (Scheme 4.15, *right*). Noteworthy, this mild and catalyst-free deaminative alkylation protocol was also expanded to a wide range of transformations, such as the desulfonylative allylation, alkynylation and alkenylation of sulfone reagents as well as the thioetherification of disulfides.



Scheme 3.15. Catalyst-free deaminative alkylation of Michael acceptors and allyl sulfones reported by Aggarwal and co-workers

Another approach for the construction of new C_{sp3}-C_{sp3} bonds is the catalytic regioselective difunctionalization of olefins.⁴² In this context, Glorius, Lautens and co-workers described a visible-light mediated three-component

dicarbofunctionalization of styrenes with benzylic pyridinium salts and electron-rich heteroarenes (Scheme 3.16).⁴³ Key to the success of this strategy was the use of rationally designed benzylic pyridinium salts ($E_{1/2} = -0.92$ V vs SCE in DMF) as radical precursors, which could be reduced by SET from $[\text{Ir}(\text{ppy})_2(\text{dtbppy})](\text{PF}_6)$, $[\text{E}(\text{Ir}^{\text{III}*}/\text{Ir}^{\text{IV}}) = -0.96$ V vs SCE in MeCN]. According to the mechanistic investigations undertaken in the paper, the authors proposed that the benzylic radical added to the double bond, thus generating a stabilized benzylic radical. This intermediate then underwent single-electron oxidation by the oxidized form of the photocatalyst to form a benzylic cation. The benzylic carbocation subsequently reacted with the electron-rich heteroarene via an electrophilic aromatic substitution to provide the desired product. Interestingly, amino acids-derived pyridinium salts could also be successfully applied as radical precursors in this reaction.

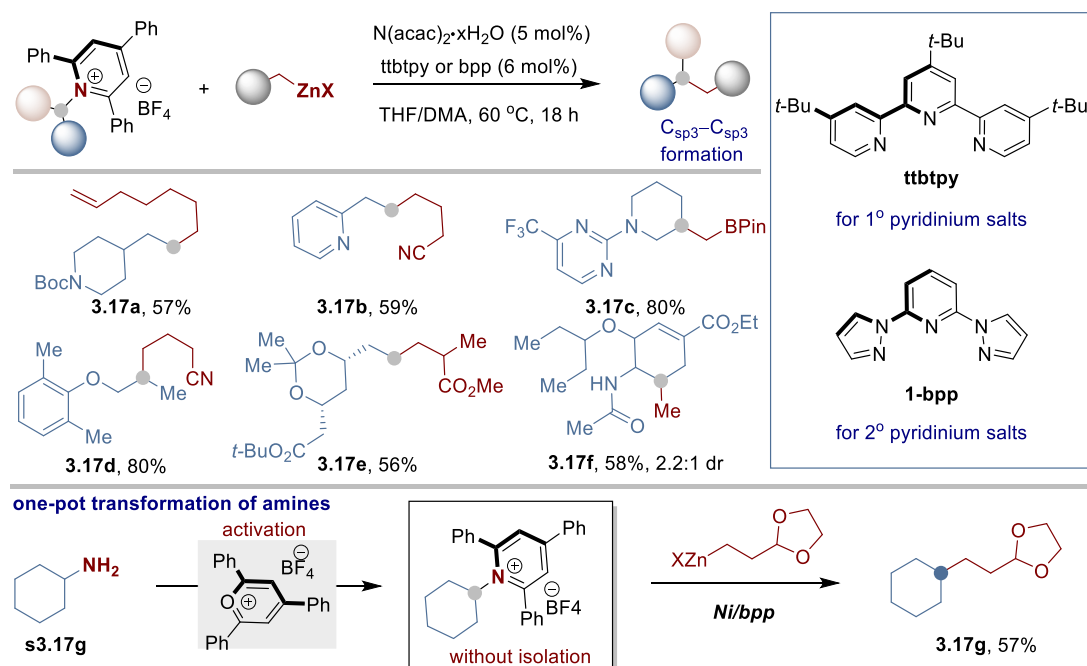


Scheme 3.16. Photocatalytic dicarbofunctionalization of styrenes with alkyl pyridinium salts and heteroarenes

Aiming to expand the scope of these deaminative coupling strategies, Watson and co-workers described a Ni-catalyzed deaminative Negishi coupling of alkyl pyridinium salts with alkylzinc reagents for the construction of $C_{sp^3}-C_{sp^3}$ bonds (Scheme 3.17).⁴⁴ In this case, the ligand effect played a crucial role for the reaction success, indeed the combination of $\text{Ni}(\text{acac})_2 \cdot x\text{H}_2\text{O}$ with 4,4',4''-tri-*tert*-butyl-terpyridine (ttbtpy) allowed the using of primary alkyl pyridinium salts as substrates, while the less sterically hindered 2,6-bis(1H-pyrazol-1-yl)pyridine (1-bpp) ligand was efficient for the reaction of secondary alkyl pyridinium salts. Notably, this protocol allowed for the formal displacement of an amino group by a sterically isosteric methyl group if methylzinc

Site-Selective Ni-Catalyzed Deaminative Alkylation of Unactivated Olefins

iodide was used as coupling partner, thus offering opportunities for *structure-activity-relationship* (SAR) studies. Similarly, the amino group could also be converted into the synthetically versatile α -methylpinacolboronate ($-\text{CH}_2\text{BPin}$) handle by the employment of the appropriate alkylzinc reagent. Noteworthy, the authors proved the feasibility of telescoping the reaction as demonstrated by the synthesis of **3.17g**, which was prepared from the corresponding free amine without the need for isolating the pyridinium salt intermediate.



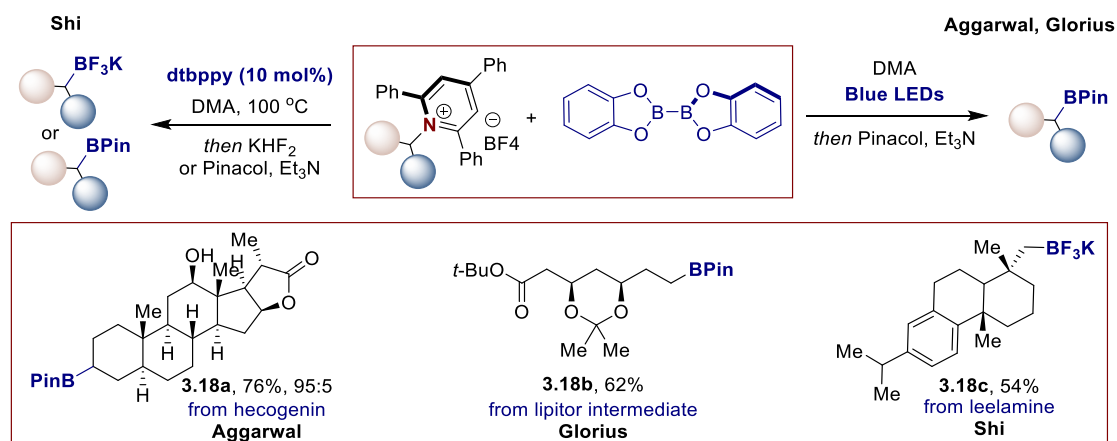
Scheme 3.17. Ni-catalyzed Negishi coupling of alkyl pyridinium salts with alkylzinc reagents

3.2.4 Catalytic Deaminative Borylation of Alkyl Pyridinium Salts

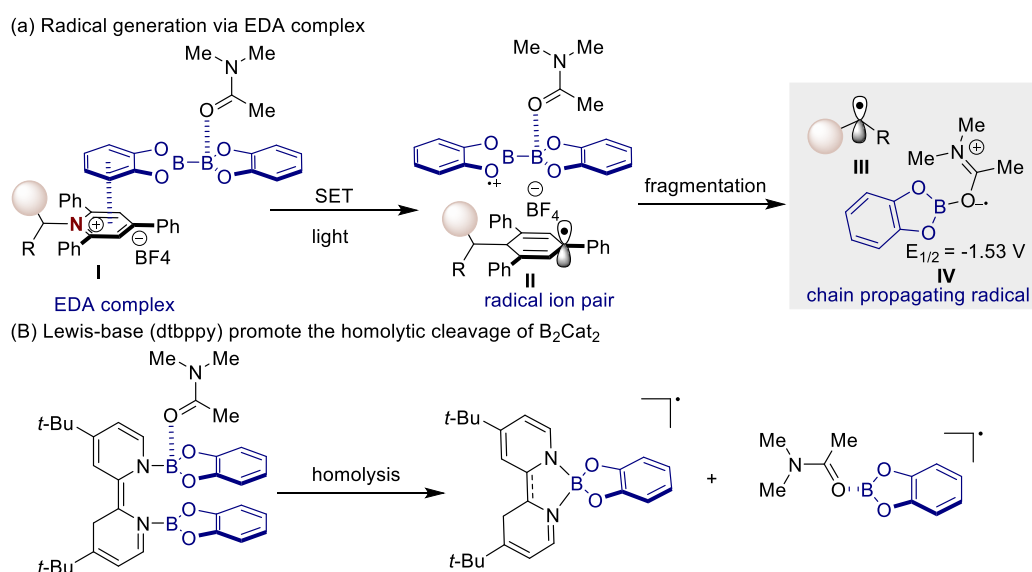
Prompted by the versatility and synthetic applicability of organoboron reagents, chemists have been challenged to design new synthetic routes for their preparation.⁴⁵ The renaissance of radical chemistry and the blossom of photochemical methods for their generation has stimulated the development of new strategies to forge $\text{C}_{\text{sp}3}\text{-B}$ bonds by the exploitation of SET pathways starting from a variety of alkyl radical precursors.⁴⁶ In 2017, Aggarwal and co-workers described a decarboxylative borylation of carboxylic acid derivatives via a visible light mediated SET process.⁴⁷ Recently, they extended this strategy to the synthesis of alkylboronates by a

photoinduced deaminative borylation approach in the absence of any catalyst and additive (Scheme 3.18).⁴⁸ Concurrently, the Glorius group reported a similar transformation,⁴⁹ independently. In both cases, the authors proposed the formation of an EDA complex **I** between the alkyl pyridinium salt and B_2Cat_2 . This was proposed to undergo photoinduced SET, forming alkyl radical **III** and DMA-stabilized boron-centered radical **IV** upon fragmentation (Scheme 3.19, *top*).

In 2018, Shi and co-workers reported a Lewis base promoted deaminative borylation of pyridinium salts with B_2Cat_2 .⁵⁰ The reaction occurred in DMA at 100 °C in presence of catalytic amount of dtbppy. Mechanistic studies and DFT calculations suggested that the Lewis-base (dtbppy) promoted the homolytic cleavage of B_2Cat_2 while coordination of a molecule of DMA stabilized the resulting boron-centered radical (Scheme 3.19, *bottom*).



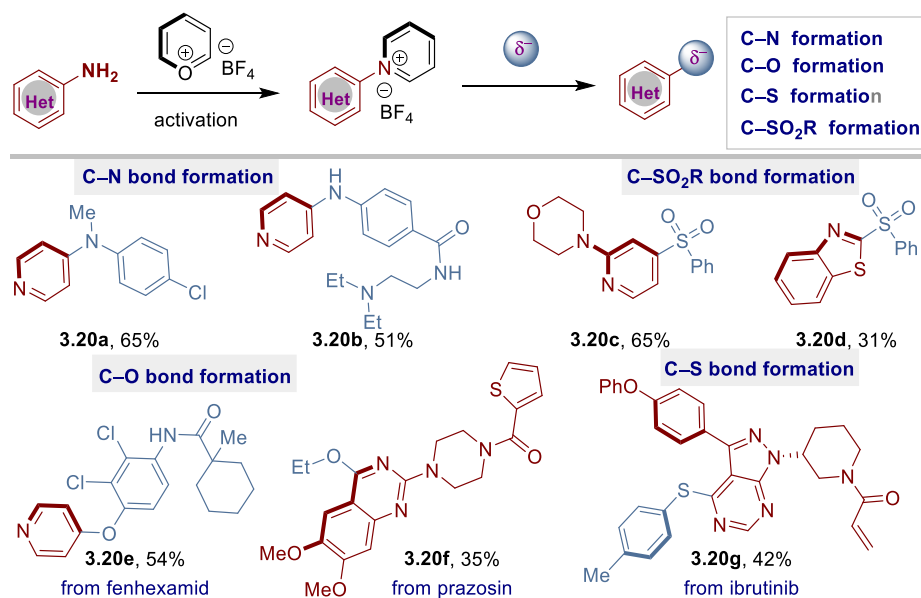
Scheme 3.18. Catalytic deaminative borylation of pyridinium salts



Scheme 3.19. Radical generation via EDA complex or Lewis base promoted homolysis

3.2.5 Catalytic Deaminative Cross-Coupling of *N*-Aryl Pyridinium Salts

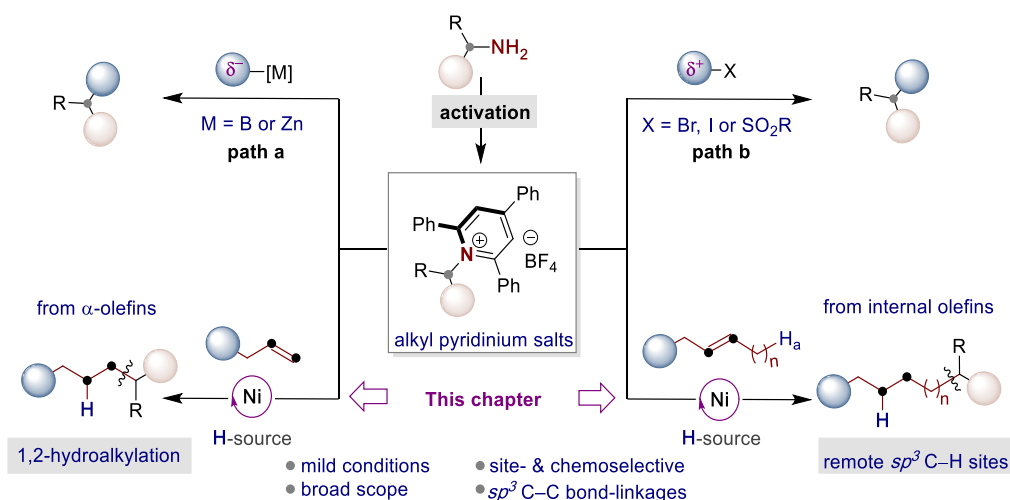
Alkyl pyridinium salts have successfully been employed in cross-coupling reactions for the conversion C_{sp^3} -NH₂ bonds to C-C or C-heteroatom bonds.¹⁴ However, the extension of this concept to the derivatization of C_{sp^2} -NH₂ still remains an enormous challenge in organic synthesis. Inspired by the work from the Katritzky group in rendering the amine functionality a more suitable leaving group for S_N2 reactions, recently, Cornella and co-workers developed a selective S_NAr functionalization of *N*-heteroaryl pyridinium salts which were prepared from corresponding heterocyclic amines (Scheme 3.20).⁵¹ This protocol proved to be very general and allowed for the synthesis of a variety of C-O, C-N, C-S, and C-SO₂R bonds starting from an array of heterocyclic amines. Very recently, they extended the applicability of this strategy to the synthesis of aryl boronic esters from aromatic amines.⁵²



Scheme 3.20 Deaminative heteroarylation strategies for the synthesis of C-X bond reported by Cornella and co-workers

3.3 General Aim of the Project

Alkyl amines are ubiquitous compounds found in natural products, pharmaceuticals and preclinical drug candidates; therefore, chemists have recently tackled the challenge to design new catalytic methods for the sp^3 C–N cleavage. Such techniques would open avenues for the straightforward construction of fully saturated compounds and would represent a new tactic for lead generation in drug discovery.^{11,12} Significant breakthroughs have been made in sp^3 C–N bond cleavage of primary amines since Watson reported the first Ni-catalyzed deaminative Suzuki-Miyaura coupling by using redox active Katritzky salts as alkyl electrophiles.¹⁸ Despite the elegant advances realized, C–C bond-forming processes still rely on the use of well-defined organometallic reagents, organic halide counterparts, or biased electron-deficient olefins (Scheme 3.21, *path a and b*).¹⁴ Based on previous achievement reported by our group on Ni-catalyzed site-selective functionalization of unactivated olefins,^{53,54} we questioned whether a site-selective catalytic deaminative alkylation could be implemented with unactivated α -olefins or even internal olefins, chemical feedstocks derived from the petroleum processes (Scheme 3.21, *bottom*). If successful, such uncharted territory might not only provide an unrecognized opportunity to explore currently inaccessible chemical space in both olefin functionalization and deamination events, but would also offer a new strategic approach for rapidly and reliably generating structural diversity via unconventional C_{sp^3} – C_{sp^3} bond disconnections.



Scheme 3.21 Catalytic site-selective deaminative alkylation of unactivated olefins

3.4 Site-Selective Ni-Catalyzed Deaminative Alkylation of Unactivated Olefins

3.4.1 Catalytic Deaminative Alkylation of α -Olefins

3.4.1.1 Optimization of the Reaction Conditions

The feasibility of the deaminative alkylation of unactivated olefins with alkyl pyridinium salts was initially studied using **3.4.1a** and phenyl-1-butene (**3.4.2a**) as model substrates. The choice of the model system was based on the previous project carried out on the site-selective alkylation of unactivated olefins with *a*-haloboranes, which presents some similarities with the one aimed to develop.⁵³ We began our investigation by using **L3.4.1** as bidentate ligand and diethoxymethylsilane (DEMS) as the hydride source, however, only trace amount of hydroalkylation product was detected by GC-MS, but this discovery augured well for the feasibility of the process. Based on our knowledge on nickel catalysis, we thought that the nature of ligand probably plays the crucial role for reaction success,⁵⁵ therefore, we decided to initially study the effect of ligands on our reaction (Table 3.1). As anticipated, bipyridine ligands without any substituent at the *ortho* position with respect to the nitrogen atom (entries 3-7) provided **3.4.3a** in good yields, specifically, 4,4'-di-*tert*-butyl-2,2'-bipyridine (dtbppy, **L3.4.6**) resulted in the best yield, along with some hydrolysis side product (**3.4.4a**). Interestingly, the use of bipyridine ligands possessing a methyl group at the *ortho* position (entries 1-2 and 8-9) or PyOx ligands (entries 10-11) significantly suppressed the reaction, whereas large amount of hydrolysis **3.4.4a** and trace amount of homocoupling side product **3.4.4b** were detected. The formation of side product **3.4.4b** was probably due to the olefin migration via nickel hydrides species, followed by the homocoupling of benzyl-Ni intermediates.⁵⁶ However, in all cases, we could not detect any deaminative alkylation product at the remote, benzylic position, which would be produced via chain-walking processes.⁵⁷

Entry	Ligand	3.4.3a (%) ^b
1	L3.4.1	trace
2	L3.4.2	trace
3	L3.4.3	54
4	L3.4.4	58
5	L3.4.5	60
6	L3.4.6	72
7	L3.4.7	46
8	L3.4.8	trace
9	L3.4.9	trace
10	L3.4.10	11
11	L3.4.11	2
12	L3.4.12	52
13	L3.4.13	trace
14	PPh ₃	0
15	PCy ₃	0

R₁ = H; R₂ = H (L3.4.3)
 R₁ = H; R₂ = Me (L3.4.4)
 R₁ = H; R₂ = OMe (L3.4.5)
R₁ = H; R₂ = *t*-Bu (L3.4.6)
 R₁ = H; R₂ = CF₃ (L3.4.7)
 R₁ = Me; R₂ = H (L3.4.8)
 R₁ = Me; R₂ = *t*-Bu (L3.4.9)

R = H (L3.4.10)
 R = *i*-Pr (L3.4.11)

R₁ = H; R₂ = H (L3.4.12)
 R₁ = Me; R₂ = Ph (L3.4.13)

^a **Reaction Conditions:** 3.4.1a (0.20 mmol, 1.0 equiv), 3.4.2a (0.60 mmol, 3.0 equiv), NiBr₂·DME (10 mol%), Ligand (15 mol%), DEMS (0.60 mmol, 3.0 equiv), Na₂HPO₄ (0.40 mmol, 2.0 equiv), NMP (1.0 mL), 40 °C, 24 h. ^b Yields were determined by GC FID, using 1-decane as the internal standard. DEMS = Diethoxymethylsilane ((EtO)₂MeSiH).

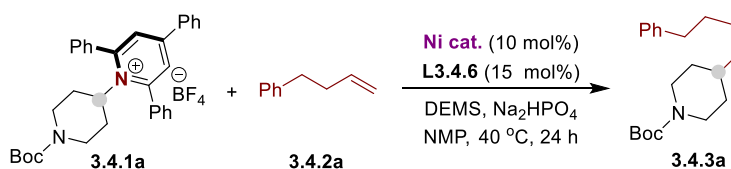
Table 3.1 Screening of ligands

With dtbppy (L3.4.6) as the optimal ligand, we next studied the effect of nickel precatalyst on the reaction outcome (Table 3.2). We found that NiBr₂·DME provided the best results whereas increasing amounts of side products were obtained when using other Ni(II) precatalysts. The use of Ni(COD)₂ resulted the desired product in lower yields, probably due to the competition between COD and substrate for metal binding.

Next, the effect of solvents on the reaction outcome was studied (Table 3.3). Amide containing solvents such as DMA, NMP performed better than ethereal solvents (THF and dioxane). Unfortunately, after the screening of a number of solvents, we found no improvement of the reaction yield with a single solvent system.

Site-Selective Ni-Catalyzed Deaminative Alkylation of Unactivated Olefins

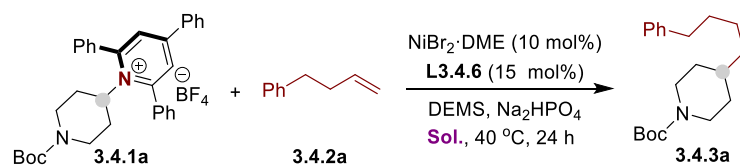
Based on our experience on the hydrofunctionalization of unsaturated compounds, we anticipated that the use of co-solvent system might lead to better results. Indeed, the use of NMP and 1,4-dioxane in a 4:1 ratio, provided the product **3.4.3a** in 81% yield. The role of the co-solvent system is still unclear, but it might be possible that the solvent coordinates to nickel center, thus stabilizing the alkyl–Ni species.



Entry	Ni cat.	3.4.3a (%) ^b
1	NiBr ₂	trace
2	NiI ₂	trace
3	NiBr ₂ diglyme	69
4	NiBr₂DME	72
5	NiCl ₂ DME	42
6	NiBr ₂ (bpy)	40
7	Ni(COD) ₂	33
8	Ni(acac) ₂	0

^a **Reaction Conditions:** **3.4.1a** (0.20 mmol, 1.0 equiv), **3.4.2a** (0.60 mmol, 3.0 equiv), Ni cat. (10 mol%), L3.4.6 (15 mol%), DEMS (0.60 mmol, 3.0 equiv), Na₂HPO₄ (0.40 mmol, 2.0 equiv), NMP (1.0 mL), 40 °C, 24 h. ^b Yields were determined by GC FID, using 1-decane as the internal standard. DEMS = Diethoxymethylsilane ((EtO)₂MeSiH).

Table 3.2 Screening of nickel precatalysts



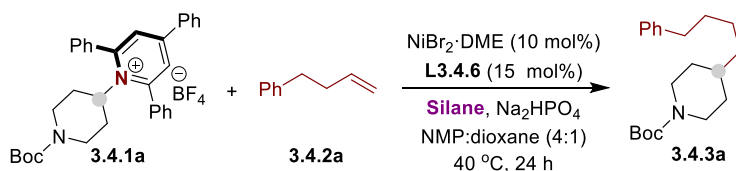
Entry	Solvents	3.4.3a (%) ^b
1	DMA	42
2	NMP	72
3	THF	20
4	DME	41
5	1,4-dioxane	6
6	DMSO	41
7	NMP:THF (4:1)	58
8	NMP:dioxane (4:1)	81
9	NMP:DMA (4:1)	55

^a **Reaction Conditions:** **3.4.1a** (0.20 mmol, 1.0 equiv), **3.4.2a** (0.60 mmol, 3.0 equiv), NiBr₂·DME (10 mol%), **L3.4.6** (15 mol%), DEMS (0.60 mmol, 3.0 equiv), Na₂HPO₄ (0.40 mmol, 2.0 equiv), **Sol.** (1.0 mL), 40 °C, 24 h. ^b Yields were determined by GC FID, using 1-decane as the internal standard. DEMS = Diethoxymethylsilane ((EtO)₂MeSiH).

Table 3.3 Screening of solvents

We then undertook the evaluation of other parameters, such as the hydride source and the inorganic base. As shown in Table 3.4, other alkoxy silanes showed some reactivity, whereas Ph₃SiH and Et₃SiH completely suppressed the reaction. The investigation of inorganic bases revealed Na₂HPO₄ as the optimal choice since all the other tested produced higher amount of side products (Table 3.5).

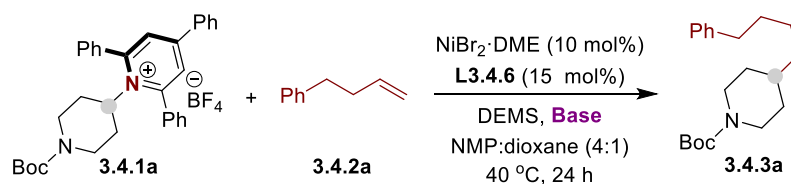
Site-Selective Ni-Catalyzed Deaminative Alkylation of Unactivated Olefins



Entry	Silane	3.4.3a (%) ^b
1	DMES	81
2	(MeO) ₂ MeSiH	63
3	(EtO) ₃ SiH	32
4	PMHS	38
5	Ph ₃ SiH	0
6	Et ₃ SiH	0

^a Reaction Conditions: **3.4.1a** (0.20 mmol, 1.0 equiv), **3.4.2a** (0.60 mmol, 3.0 equiv), NiBr₂·DME (10 mol%), **L3.4.6** (15 mol%), **Silane** (0.60 mmol, 3.0 equiv), Na₂HPO₄ (0.40 mmol, 2.0 equiv), NMP: 1,4-Dioxane (4:1, 1.0 mL), 40 °C, 24 h. ^b Yields were determined by GC FID, using 1-decane as the internal standard. DEMS = Diethoxymethylsilane. PMHS = Poly(methylhydrosiloxane).

Table 3.4 Screening of hydride source



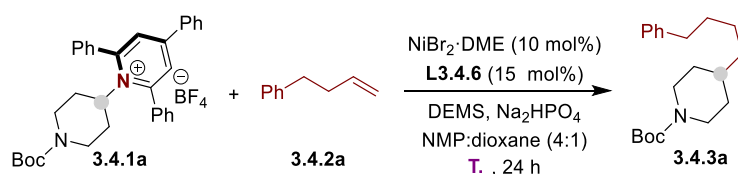
Entry	Base	3.4.3a (%) ^b
1	Na ₂ CO ₃	51
2	K ₂ CO ₃	48
3	Cs ₂ CO ₃	33
4	NaHCO ₃	46
5	NaOAc	trace
6	Na₂HPO₄	81
7	Na ₃ PO ₄	36
8	KF	35
9	CsF	33

^a Reaction Conditions: **3.4.1a** (0.20 mmol, 1.0 equiv), **3.4.2a** (0.60 mmol, 3.0 equiv), NiBr₂·DME (10 mol%), **L3.4.6** (15 mol%), DEMS (0.60 mmol, 3.0 equiv), **Base** (0.40 mmol, 2.0 equiv), NMP: 1,4-Dioxane (4:1, 1.0 mL), 40 °C, 24 h. ^b Yields were determined by GC FID, using 1-decane as the internal standard.

Table 3.5 Screening of bases

Chapter 3.

With the robust Ni/**L3.4.6** catalytic system found we next evaluated the effect of temperature on this transformation (Table 3.6). The best outcome was found when conducting the reaction at 40 °C, obtaining C_{sp^3} - C_{sp^3} coupling product in 81% GC yield, while lowering the temperatures to 30 °C or to room temperature resulted in significant amounts of side-products (entries 1 and 2). Finally, control experiments were carried out in order to ensure that all the reaction parameters were essential for the deaminative alkylation to take place. Indeed, as shown in Table 3.7, no product was formed in the absence of nickel catalyst, ligand, silane and base (entries 2-5). After this intense screening campaign, the optimal reaction conditions were determined to be the combination of NiBr₂·DME/**L3.4.6** system, with DEMS as hydride source and Na₂HPO₄ as base in a 4:1 NMP/1,4-dioxane mixture.

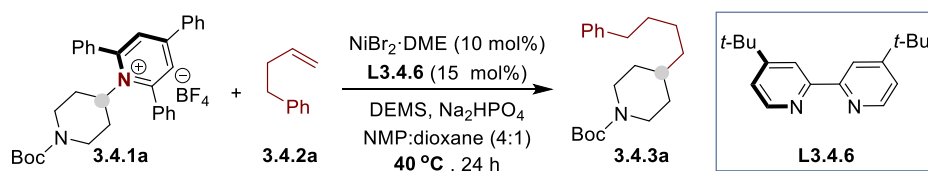


Entry	T. (°C)	3.4.3a (%) ^b
1	RT	41
2	30	54
3	35	70
4	40	81
5	50	75

^a **Reaction Conditions:** **3.4.1a** (0.20 mmol, 1.0 equiv), **3.4.2a** (0.60 mmol, 3.0 equiv), NiBr₂·DME (10 mol%), **L3.4.6** (15 mol%), DEMS (0.60 mmol, 3.0 equiv), Na₂HPO₄ (0.40 mmol, 2.0 equiv), NMP:1,4-Dioxane (4:1, 1.0 mL), T °C, 24 h. ^b Yields were determined by GC FID, using 1-decane as the internal standard. DEMS = Diethoxymethylsilane ((EtO)₂MeSiH).

Table 3.6 Screening of reaction temperature

Site-Selective Ni-Catalyzed Deaminative Alkylation of Unactivated Olefins



Entry	$\text{NiBr}_2\cdot\text{DME}$	L3.4.6	DEMS	Na_2HPO_4	NMP	dioxane	Yield(%) ^b
1	✓	✓	✓	✓	✓	✓	81(80 ^c)
2	✗	✓	✓	✓	✓	✓	0
3	✓	✗	✓	✓	✓	✓	0
4	✓	✓	✗	✓	✓	✓	0
5	✓	✓	✓	✗	✓	✓	0
6	✓	✓	✓	✓	✗	✓	6
7	✓	✓	✓	✓	✓	✗	72

^a Reaction Conditions: **3.4.1a** (0.20 mmol, 1.0 equiv), **3.4.2a** (0.60 mmol, 3.0 equiv), $\text{NiBr}_2\cdot\text{DME}$ (10 mol%), **L3.4.6** (15 mol%), DEMS (0.60 mmol, 3.0 equiv), Na_2HPO_4 (0.40 mmol, 2.0 equiv), NMP:1,4-Dioxane (4:1, 1.0 mL), 40 °C, 24 h. ^b Yields were determined by GC FID, using 1-decane as the internal standard. ^c Isolated yield. DEMS = Diethoxymethylsilane ((EtO)₂MeSiH).

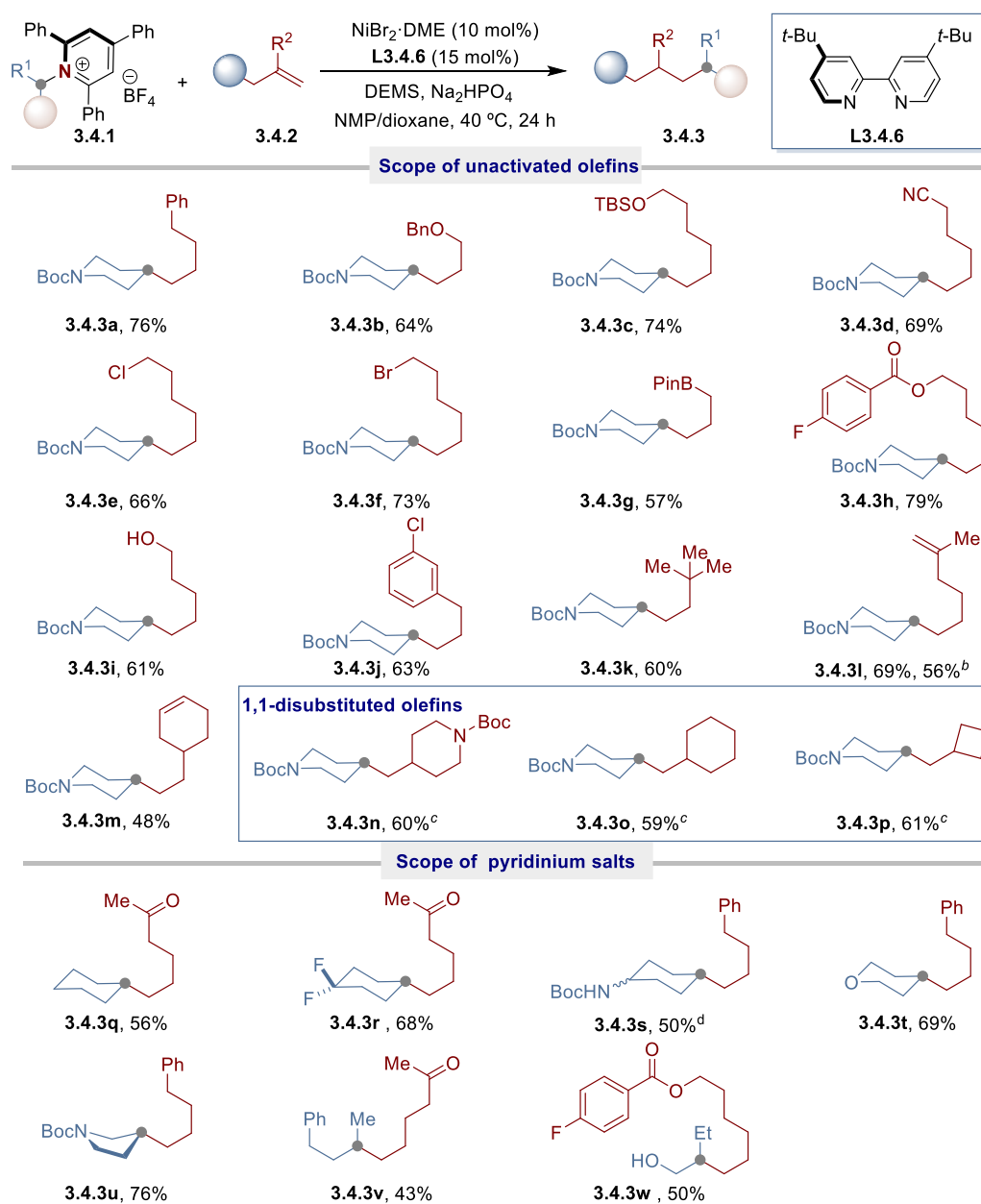
Table 3.7 Control experiments

3.4.1.2 Scope of the Deaminative Alkylation of α -Olefins

With a robust set of reaction conditions in hand, we turned our attention to study the generality of the deaminative alkylation of pyridinium salts with unactivated α -olefins. As evident from the results compiled in Scheme 3.22, a wide range of functionalized α -olefins and pyridinium salts could be applied as substrates, providing the target product in good yields with excellent chemo- and regioselectivity. For example, nitriles (**3.4.3d**), esters (**3.4.3h**, **3.4.3w**), carbamates (**3.4.3n**, **3.4.3s**), silyl ethers (**3.4.3c**) or ketones (**3.4.3q**, **3.4.3r**, **3.4.3v**) were perfectly accommodated, thus illustrating the chemoselectivity profile of our method. Notably, alkylboronates (**3.4.3g**), alkyl halides (**3.4.3e**, **3.4.3f**, **3.4.3r**) and aryl halides (**3.4.3h**, **3.4.3j**, **3.4.3w**) were well-tolerated, thus providing ample opportunities for further derivatization via conventional cross-coupling reactions.¹ The presence of free alcohol moieties, which might potentially interfere with the catalytic cycle, posed no problems as shown by the formation of products **3.4.3i** and **3.4.3w**. Noteworthy, the deaminative alkylation of substrates possessing multiple unsaturation motifs occurred exclusively at the

Chapter 3.

less-substituted olefin (**3.4.3l**, **3.4.3m**). Importantly, 1,1-disubstituted alkenes as substrates demonstrated no problems (**3.4.3n-3.4.3p**).



^a **Reaction Conditions:** **3.4.1** (0.20 mmol, 1.0 equiv), **3.4.2** (0.60 mmol, 3.0 equiv), NiBr₂·DME (10 mol%), **L3.4.6** (15 mol%), DEMS (0.60 mmol, 3.0 equiv), Na₂HPO₄ (0.40 mmol, 2.0 equiv), NMP:1,4-Dioxane (4:1, 1.0 mL), 40 °C, 24 h; yield of isolated product, average of at least two independent runs. ^b 2.0 mmol scale. ^c NiI₂ (10 mol%), **L3.4.10** (20 mol%), in DMSO/1,4-Dioxane (3:1, 1.2 mL) at 35 °C. ^d dr = 1.5:1. DEMS = Diethoxymethylsilane ((EtO)₂MeSiH).

Scheme 3.22 Scope of the deaminative alkylation with α-olefins

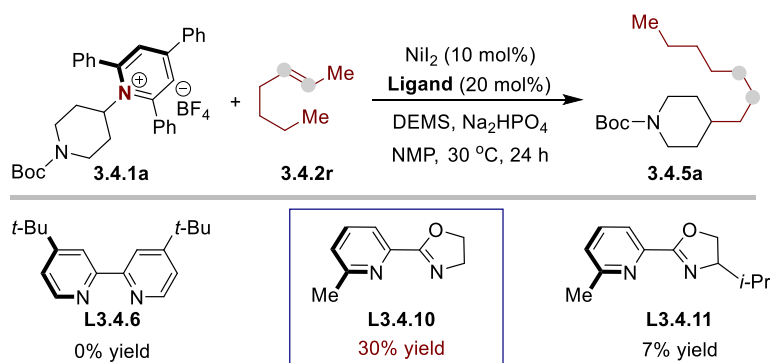
Encouraged by these initial findings, we turned our attention to exploring the

substitution pattern on the alkyl amine counterpart. Much to our satisfaction, the targeted C_{sp^3} - C_{sp^3} bond-formation could be obtained with both cyclic analogues (**3.4.3q**-**3.4.3u**) and acyclic *N*-alkyl pyridinium derivatives (**3.4.3v**, **3.4.3w**). It is worth noting that **3.4.3s** was obtained with identical diastereomeric ratios with respect to the parent pyridinium salts, this result suggested that the diastereoselectivity was not dictated by the conformational preference of the substituents on the cyclohexyl ring during the product-forming step. Notably, the reaction delivering **3.4.3l** could be carried out on a 2 mmol scale without significant erosion in yield (56% vs 69% yield).

3.4.2 Catalytic Deaminative Alkylation with Internal Olefins

3.4.2.1 Optimization of the Reaction Conditions

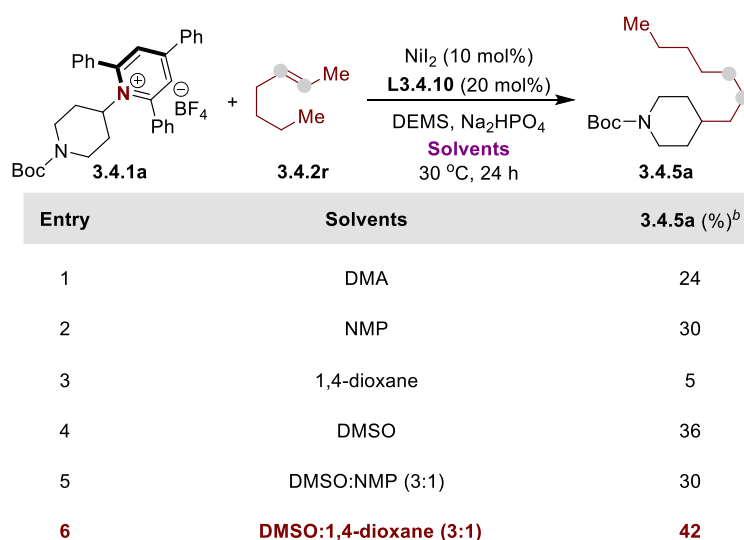
Having established a reliable method for the deaminative alkylation of α -olefins, we wondered if we could exploit the group knowledge on the Ni-catalyzed to achieve the remote alkylation of internal olefins. Such a method would allow the use of more challenging yet more available internal olefins as precursor to attain functionalization at a distal position onto a hydrocarbon chain. At the very beginning, we decided to study the remote, benzylic sp^3 C-H alkylation of phenyl-1-butene (**3.4.2a**).⁵⁷ Unfortunately, we could not detect any benzylic alkylation product by the screening of all the reaction parameters. We then envisioned that the remote alkylation might occur at the less sterically-hindered, primary sp^3 C-H site. To our delight, the remote, primary sp^3 C-H alkylation product was obtained in 30% yield with excellent regioselectivity by using *trans*-2-heptene (**3.4.2r**) as substrate under Ni/**L3.4.10** catalysis (Table 3.8). No desired product was observed when **L3.4.6** was used as ligand, while **3.4.11** yielded only 7% of **3.4.5a**, although it represented the optimal ligand in a related remote functionalization method recently reported by our group.



^a **Reaction Conditions:** **3.4.1a** (0.20 mmol, 1.0 equiv), **3.4.2r** (0.60 mmol, 3.0 equiv), NiI₂ (10 mol%), **Ligand** (20 mol%), DEMS (0.40 mmol, 2.0 equiv), Na₂HPO₄ (0.80 mmol, 4.0 equiv), NMP (1.2 mL), 30 °C, 24 h; ^b Yields were determined by GC FID, using 1-decane as the internal standard.

Table 3.8 Preliminary screening for the remote deaminative alkylation of internal olefins

Encouraged by these preliminary results, we turned our attention to evaluate the effect of solvents on this remote *sp*³ C–H alkylation strategy (Table 3.9). We quickly found that DMSO provided better results than other amide-containing solvents such as DMA and NMP. Based on the experience gained during the development of the deaminative alkylation of α -olefins, we investigated the use of co-solvent system and found that the combination of DMSO and 1,4-dioxane in a 3:1 ratio, provided the best results.

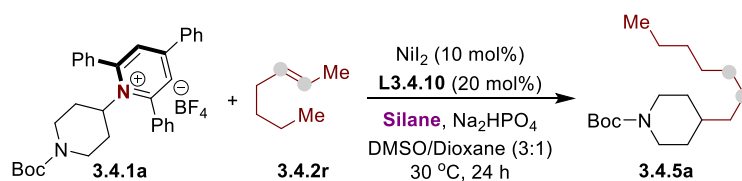


^a **Reaction Conditions:** **3.4.1a** (0.20 mmol, 1.0 equiv), **3.4.2r** (0.60 mmol, 3.0 equiv), NiI₂ (10 mol%), **L3.4.10** (20 mol%), DEMS (0.40 mmol, 2.0 equiv), Na₂HPO₄ (0.80 mmol, 4.0 equiv), **Solvents** (1.2 mL), 30 °C, 24 h; ^b Yields were determined by GC FID, using 1-decane as the internal standard.

Table 3.9 Screening of the solvents

Site-Selective Ni-Catalyzed Deaminative Alkylation of Unactivated Olefins

Next, we decided to study the effect of the hydride source on this remote sp^3 C–H alkylation (Table 3.10). As anticipated, alkoxy silanes provided better results, and $(\text{EtO})_3\text{SiH}$ was the best hydride source for the reaction success.

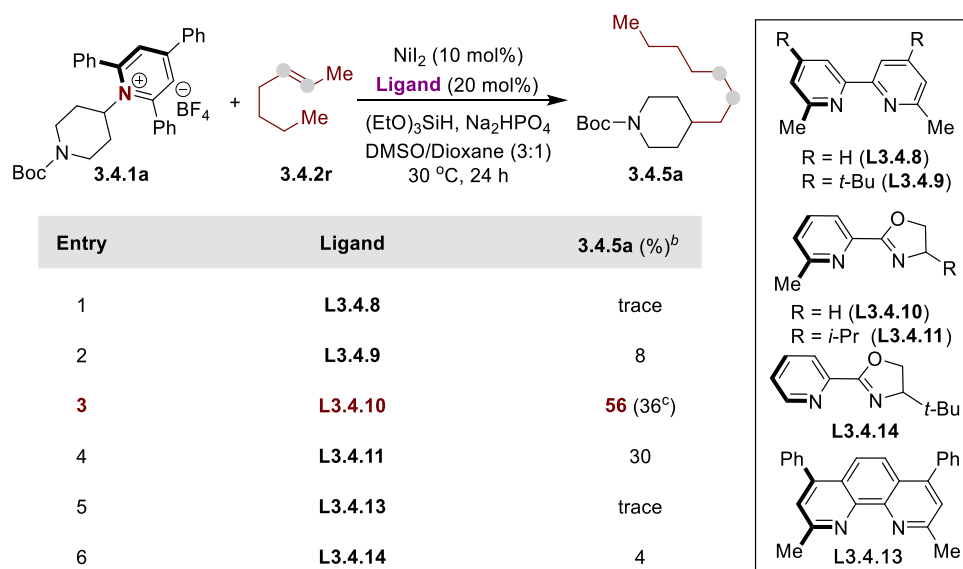


Entry	Silane	3.4.5a (%) ^b
1	$(\text{EtO})_2\text{MeSiH}$ (DEMS)	42
2	$(\text{MeO})_2\text{MeSiH}$	43
3	$(\text{EtO})_3\text{SiH}$	56
4	PMHS	48
5	Ph_3SiH	0
6	Et_3SiH	0

^a **Reaction Conditions:** **3.4.1a** (0.20 mmol, 1.0 equiv), **3.4.2r** (0.60 mmol, 3.0 equiv), NiI_2 (10 mol%), **L3.4.10** (20 mol%), Silane (0.40 mmol, 2.0 equiv), Na_2HPO_4 (0.80 mmol, 4.0 equiv), DMSO/1,4-Dioxane (3:1, 1.2 mL), 30 °C, 24 h; ^b Yields were determined by GC FID, using 1-decane as the internal standard. ^c **L3.4.10** (15 mol%). PMHS = Poly(methylhydrosiloxane).

Table 3.10 Screening of the hydride source

With these results in hand, we then focused on studying the effect of ligands. As shown in Table 3.11, the nature of the ligand played a crucial role for the reaction success. 6-methyl substituted PyOx ligand **L3.4.10** provided the best results. The *ortho*-disubstituted bipyridine and phenanthroline-type ligands which have previously been used in chain-walking transformations were not effective in this transformation.⁵⁶ Notably, a 1:2 ratio of nickel precatalyst and ligand was also critical for the reaction outcome and only 36% product was obtained by changing the ratio to 1:1.5.

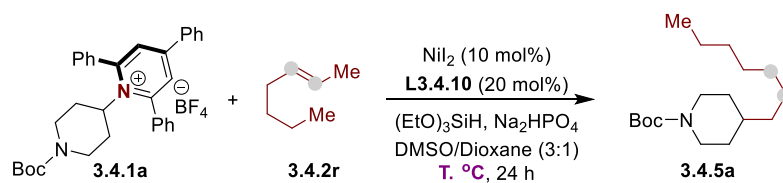


^a **Reaction Conditions:** **3.4.1a** (0.20 mmol, 1.0 equiv), **3.4.2r** (0.60 mmol, 3.0 equiv), NiI₂ (10 mol%), **Ligand** (20 mol%), (EtO)₃SiH (0.40 mmol, 2.0 equiv), Na₂HPO₄ (0.80 mmol, 4.0 equiv), DMSO/1,4-Dioxane (3:1, 1.2 mL), 30 °C, 24 h; ^b Yields were determined by GC FID, using 1-decane as the internal standard. ^c L3.4.10 (15 mol%).

Table 3.10 Screening of the ligands

With the robust NiI₂/L3.4.10 catalytic system in hand, we next evaluated the effect of temperature of this transformation (Table 3.11). The yield was slightly improved when increasing the temperature to 35 °C. After judicious evaluation of the reaction parameters, we found that the combination of NiI₂ (10 mol%), L3.4.10 (20 mol%), (EtO)₃SiH (0.40 mmol), Na₂HPO₄ (0.80 mmol) in DMSO/1,4-Dioxane at 35 °C, providing the remote *sp*³ C–H alkylation product in 60% GC-yield with 36:1 regioselectivity.

Site-Selective Ni-Catalyzed Deaminative Alkylation of Unactivated Olefins



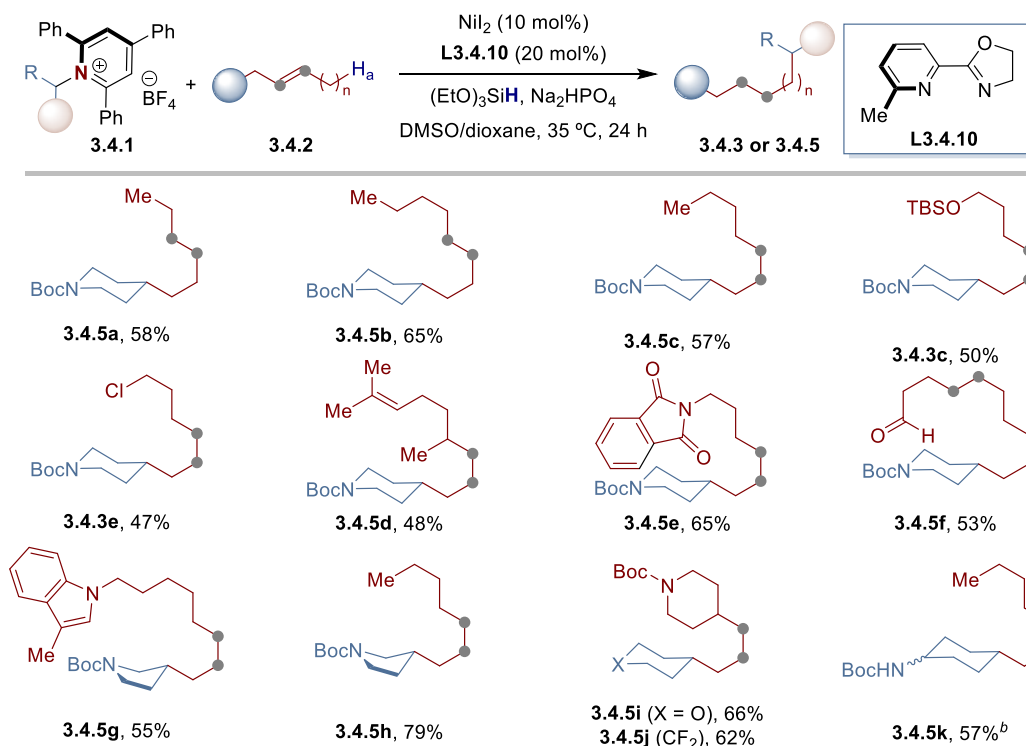
Entry	T. (°C)	3.4.5a (%) ^b
1	RT	34
2	30	56
3	35	60
4	40	59
5	60	36

^a **Reaction Conditions:** **3.4.1a** (0.20 mmol, 1.0 equiv), **3.4.2r** (0.60 mmol, 3.0 equiv), NiI₂ (10 mol%), **L3.4.10** (20 mol%), (EtO)₃SiH (0.40 mmol, 2.0 equiv), Na₂HPO₄ (0.80 mmol, 4.0 equiv), DMSO/1,4-Dioxane (3:1, 1.2 mL), **T**, °C, 24 h; ^b Yields were determined by GC FID, using 1-decane as the internal standard.

Table 3.11 Screening of the reaction temperature

3.4.2.2 Scope of remote Deaminative Alkylation with Internal Olefins

Having optimized the reaction conditions, the scope of the remote *sp*³ C–H alkylation was studied by evaluating a range of unactivated internal olefins in combination with pyridinium salts (Scheme 3.23). Overall, the mild reaction conditions, characteristic of chain-walking processes, allowed to forge C_{*sp*3}–C_{*sp*3} bonds with high chemo- and regio-selectivity, and in satisfactory yields. As shown, the reaction could also accommodate silyl ethers (**3.4.3c**), phthalimides (**3.4.5e**), aldehydes (**3.4.5f**), alkyl halides (**3.4.3e**), carbamates (**3.4.5i**, **3.4.5j**) or nitrogen-containing heterocycles (**3.4.5g**). Importantly, excellent site-selectivity for C_{*sp*3}–C_{*sp*3} bond-formation at distal primary *sp*³ C–H sites was found regardless of the position of the double bond, even at long-range (**3.4.5f**). Even branched substituents or trisubstituted olefins (**3.4.5d**) do not compete with the efficacy of the reaction, with deaminative alkylation invariably occurring at the less-sterically hindered primary *sp*³ C–H site.



^a **Reaction Conditions:** **3.4.1** (0.20 mmol, 1.0 equiv), **3.4.2** (0.60 mmol, 3.0 equiv), NiI_2 (10 mol%), **L3.4.10** (20 mol%), $(\text{EtO})_3\text{SiH}$ (0.40 mmol, 2.0 equiv), Na_2HPO_4 (0.80 mmol, 4.0 equiv), DMSO/1,4-Dioxane (3:1, 1.2 mL), 35 °C, 24 h; yield of isolated product, average of at least two independent runs. ^b dr = 1.5:1.

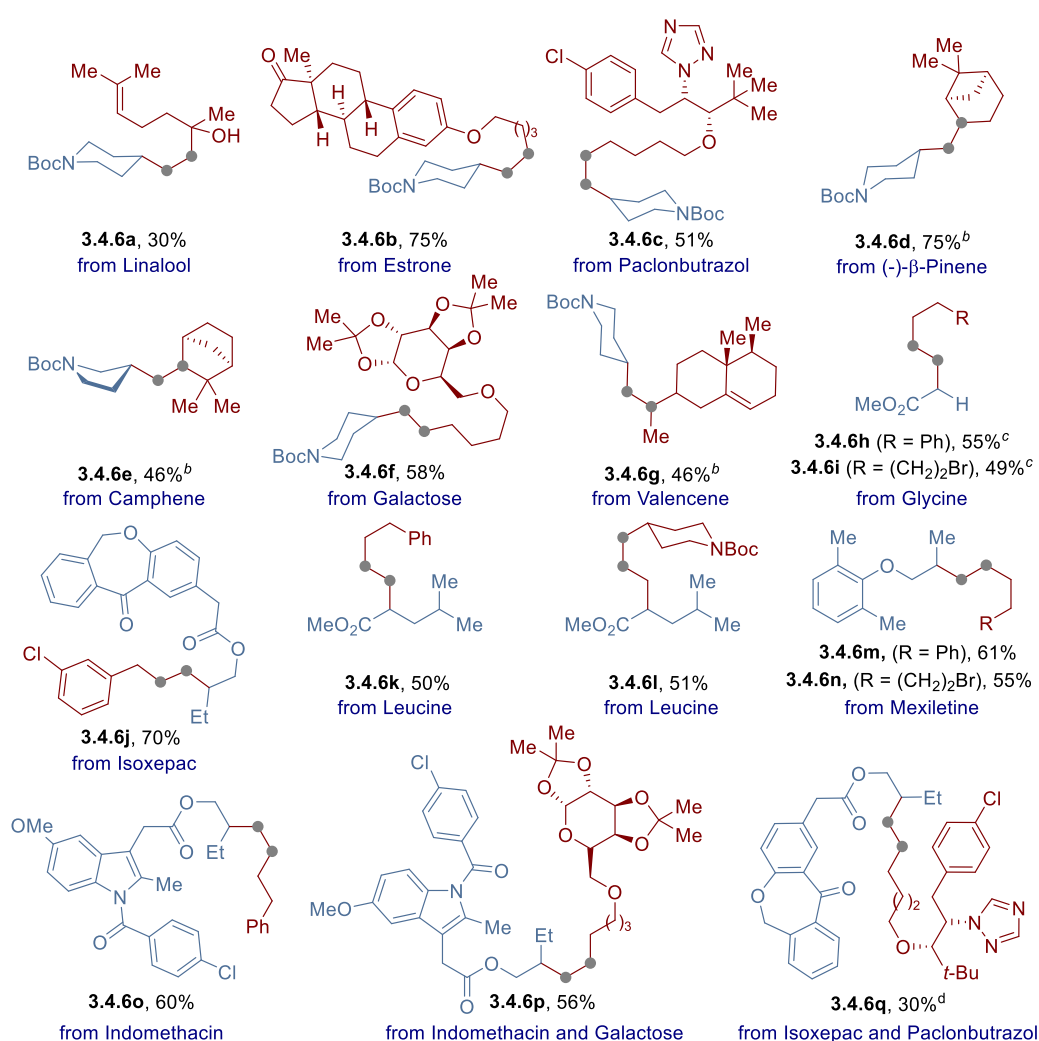
Scheme 3.23 Scope of remote deaminative alkylation with internal olefins

3.4.3 Late-stage Functionalization

Promoted by the generality of the site-selective deaminative alkylation, we anticipated that our protocol might be applied within the context of late-stage functionalization.⁵⁸ To this end, we found that a wide variety of pharmaceuticals possessing either olefins or alkyl amines underwent late-stage alkylation with excellent chemo- and regio-selectivity (Scheme 4.24). Although modest yields were obtained in certain cases, these results should be interpreted against the challenge that is addressed, particularly with substrates possessing multiple functional groups such as linalool (**3.4.6a**), paclonbutrazol (**3.4.6c**), galactose (**3.4.6f**) or valencene (**3.4.6g**), with C–C bond-formation taking place exclusively at the least substituted olefin site. Similarly, β -pinene (**3.4.6d**), camphene (**3.4.6e**) or estrone derivatives (**3.4.6b**) posed

Site-Selective Ni-Catalyzed Deaminative Alkylation of Unactivated Olefins

no problems. Interestingly, the reaction could also be extended to amino acid derivatives (**3.4.6h**, **3.4.6i**, **3.4.6k**, **3.4.6l**), either using glycine-derivative (**3.4.6h**, **3.4.6i**) or the α -substituted ones (**3.4.6k**, **3.4.6l**). Particularly noteworthy, a single regioisomer was obtained by using an internal olefin as substrate (**3.4.6l**), thus indicating that late-stage deaminative alkylation is not limited to α -olefins. As shown for compounds **3.4.6m-3.4.6q**, this technique could be employed to derivatized mexiletine, isoxepac or indomethacin via sp^3 C–N bond-cleavage with simple olefin counterparts. It is worth noting that the protocol allowed the coupling of two different drug-derivatives (**3.4.6p**, **3.4.6q**), thus showing high potential in late-stage functionalization of drug candidates.



^a **Reaction Conditions:** α -olefins: as **Scheme 3.22**; internal olefins: as **Scheme 3.23**; yield of isolated product, average of at least two independent runs. ^b **3.4.6d** (dr = 97:3), **3.4.6e** (dr = 46:40:7:7), **3.4.6g** (dr = 9:1). ^c 80 °C. ^d NiBr₂·DME (15 mol%).

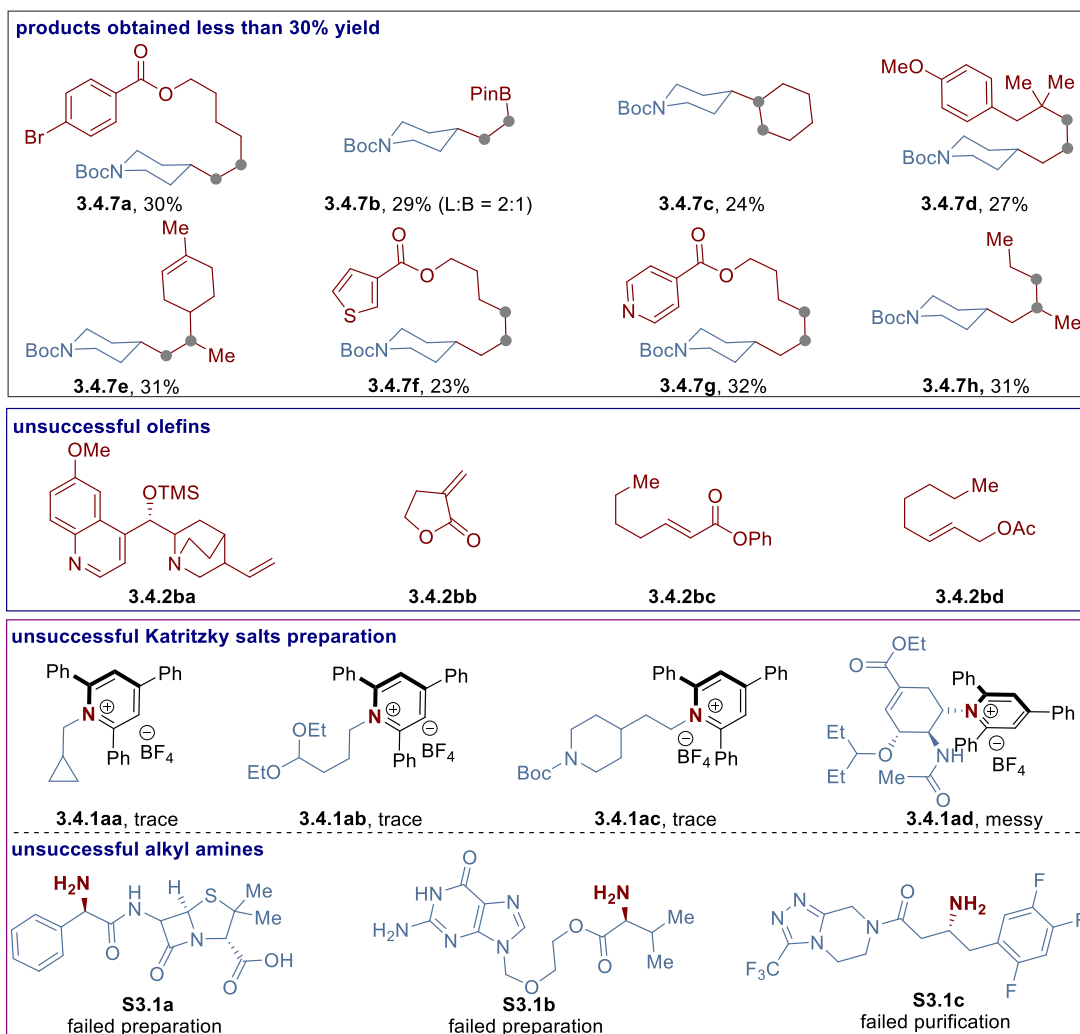
Scheme 3.23 Late-stage functionalization by catalytic deaminative alkylation

3.4.4 Unsuccessful Substrates

Unfortunately, the deaminative alkylation technique displayed some limitations in a series of substrates, probably due to the presence of functional groups that either shut down or hamper the desired reactivity (Scheme 3.25). For example, the substrate bearing aryl bromide (**3.4.7a**), provided the desired sp^3 - sp^3 bond formation in only 30% yield, probably due to the competitive oxidative addition and proton-dehalogenation with nickel species. Moreover, substrates possessing strong coordinating groups, resulted in lower yields (**3.4.7f**, **3.4.7g**) or were completely unreactive (**3.4.2ba**). On the other hand, an activated vinyl boronic ester provided the sp^3 - sp^3 bond formation with a mixture of linear and branched regioisomers in 2:1 ratio.⁵⁹ The formation of both regioisomers is a strong indication that the reaction does not proceed through a radical addition pathway. The linear and branched mixtures were obtained by using activated vinyl boronic ester, suggesting that the reaction did not undergo through a radical addition pathway. Additionally, sterically-crowded substrates such as (**3.4.7d**, **3.4.7e** and **3.4.7h**) resulted desired product in lower yields.

Notably, a mixture of regioisomers were obtained when the substrate possessing multiple, similar reactivity primary sp^3 C-H bonds (**3.4.7h**). Unfortunately, α,β -unsaturated esters (**3.4.2bb**, **3.4.2bc**) completely suppressed the reaction, probably due to the strong binding of the conjugated system to the nickel center. Not surprisingly, the allylic acetate (**3.4.2bd**) delivered only trace amount of product, probably due to the formation of π -allyl-Ni species, resulting from the oxidative addition to the allylic system.⁶⁰

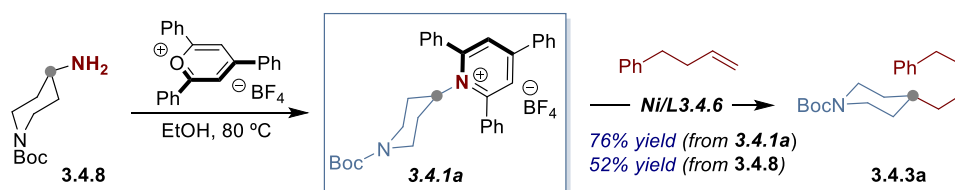
In addition to some functionalized olefins, our deaminative alkylation also failed with unactivated, primary pyridinium salts (**3.4.1aa-3.4.1ac**). On the other hand, an untraceable crude mixture was obtained when the standard reaction conditions were applied to the Tamiflu-derived substrate **3.4.1ad**. Moreover, it was not possible to test the reactivity of Katritzky salts carrying a free carboxylic acid (**s3.1a**) or both an aromatic and aliphatic amine (**s3.1b**) because their synthesis was not met with success.



Scheme 3.25 Unsuccessful substrates

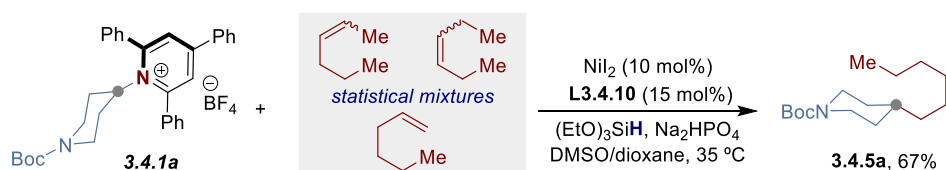
3.4.5 Synthetic Applications

In order to further illustrate the synthetic value of the catalytic deaminative alkylation technique, we decided to telescope the preparation of the Katritzky salt, by directly submitting **3.4.8** to the catalytic conditions without intermediate purification. As shown in Scheme 3.26, **3.4.3a** was within reach from *N*-Boc 4-aminopiperidine (**3.4.8**) without the need for isolating pyridinium **3.4.1a**, thus showing the feasibility of this approach.

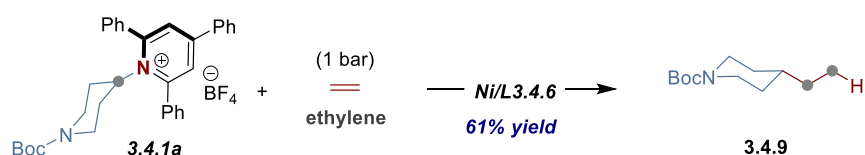


Scheme 3.26 One-pot deaminative alkylation without isolation of pyridinium salts

The opportunity to apply the present methodology to a mixture of positional isomers of the olefin would unlock the possibility to use inexpensive and largely available industrial raw materials derived directly from petrochemical sources. Therefore, unveiling a regioconvergent process to produce value-added chemicals would be of considerable interest. As a proof of concept, subjecting statistical mixtures of olefins under the standard conditions, invariably led to **3.4.5a** as a single regioisomer in 67% yield (Scheme 3.27). Importantly, even ethylene – the largest-volume chemical produced in industry – could be employed as substrate under atmospheric pressure en route to **3.4.9** (Scheme 3.28).⁶¹



Scheme 3.27 Regioconvergent deaminative alkylation of statistical mixture of olefins



Scheme 3.28 Catalytic deaminative alkylation using ethylene as coupling partner

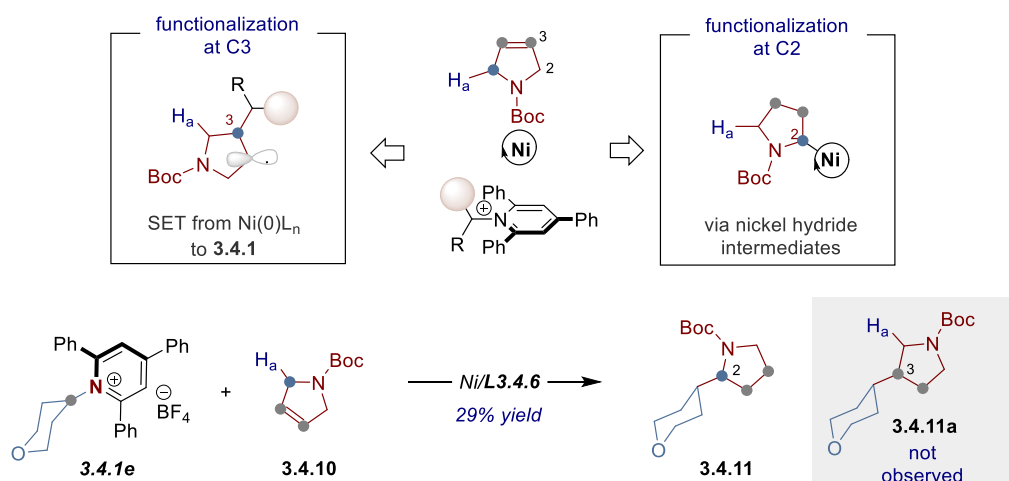
3.4.6 Mechanistic Investigation

In order to shed light on the mechanism of the catalytic deaminative alkylation reaction, some experiments were conducted. As shown in Scheme 3.29, two conceivable pathways might be viable for the catalytic deaminative alkylation of unactivated olefins, similarly to the Ni-catalyzed hydroalkylation of unactivated olefins previously reported by our group⁵³: (a) *single-electron-transfer* (SET) from

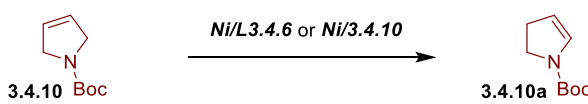
low-valent Ni(0)L_n complexes to pyridinium salt **3.4.1**, followed by the addition of the resulting alkyl radical to the olefin; (b) initial hydrometallation of the olefin by a nickel hydride species and subsequent oxidative addition of the pyridinium salt **3.4.1**. At present, we believe that the former manifold makes a minor contribution, if any, to productive *sp*³–*sp*³ bond-formation due to an unfavorable polarity-mismatch addition of a nucleophilic radical intermediates to an electron-rich olefin.

3.4.6.1 Regioselectivity Studies

Additional support to the abovementioned statement was gained by the outcome observed for the reaction of *tert*-butyl 2,5-dihydro-1H-pyrrole-1-carboxylate (**3.4.10**) as olefinic partner (Scheme 3.29, *bottom*). If an initial SET to pyridinium salt **3.4.1** is operative, radical addition to the olefin would ultimately lead to C3-functionalized product **4.4.11a**. As shown, C2-functionalization en route to **3.4.11** was solely observed, thus supporting a catalytic scenario consisting of an olefin isomerization triggered by the intermediacy of nickel hydrides prior to the C–C bond-forming step (*top right*). The olefin isomerization process was further confirmed via a control experiment run in the absence of **3.4.1** (Table 3.12). As expected, the isomerization of *tert*-butyl 2,5-dihydro-1H-pyrrole-1-carboxylate (**3.4.10**) was obtained under both Ni/L**3.4.6** and Ni/L**3.4.10** catalytic system.



Scheme 3.29 Regioselectivity studies of **3.4.10**

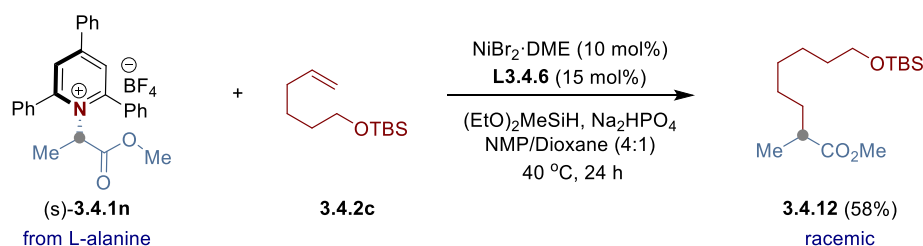


Entry	Time	Yield of 3.4.10a (%) Ni/L3.4.6	Yield of 3.4.10a (%) Ni/L3.4.10
1	30 min	18	18
2	1 h	17	23
3	2 h	19	23
4	6 h	22	27
5	12 h	25	33
6	24 h	25	40

Table 3.12 To explore the isomerization of **3.4.10** in absence of **3.4.1**

3.4.6.2 Reaction Stereospecificity

The intermediacy of an alkyl radical was supported by the outcome of the reaction run in presence of an enantioenriched Katritzky salt. Racemic product **3.4.12** was obtained, reinforcing the hypothesis of a SET process from the Ni-center to the pyridinium salt (Scheme 3.30).

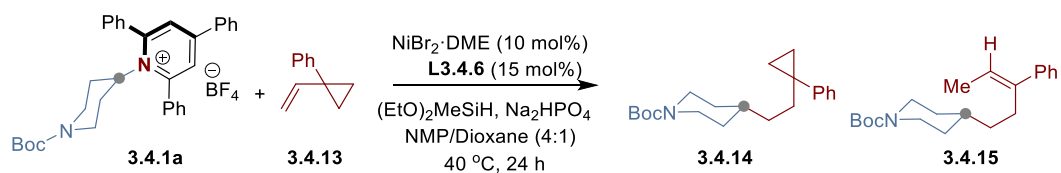


Scheme 3.30 Stereospecificity of the reaction with pyridinium salts derived from L-alanine

3.4.6.3 Radical Clock Experiments with Radical Probe **3.4.13**

A radical clock experiment was designed in order to gain additional information about the mechanism. The Katritzky salt **3.4.1** was reacted with the radical probe (1-vinylcyclopropyl)benzene (**3.4.13**) (Scheme 3.31). As expected, a mixture of the cyclopropyl-derived (**3.4.14**) and ring-opened (**3.4.15**) products was obtained, supporting the notion of a cyclopropylmethyl radical generated upon SET. More interestingly, the ratio between these two products remained constant (2.6:1) at different Ni/L ratios, even at particularly low loadings, thus arguing against a radical escape-rebound mechanism.⁶²

Site-Selective Ni-Catalyzed Deaminative Alkylation of Unactivated Olefins



Entry	Concentration	Yield (%)	3.4.14 : 3.4.15
1	0.4 M	70	2.7 : 1
2	0.2 M	77	2.7 : 1
3	0.1 M	65	2.6 : 1

Scheme 3.31 Radical clock experiments with the radical probe **3.4.13**

3.5 Conclusions

This chapter summarizes the efforts towards the development of a site-selective Ni-catalyzed reductive alkylation of unactivated olefins by using redox-active Katritzky salts as alkyl electrophiles. This protocol could be applied to either unactivated α -olefins or internal olefins, with the latter undergoing alkylation at remote, primary sp^3 C–H site via a chain-walking mechanism. This technique operated under mild reaction conditions and showcased broad substrate scope and excellent chemo- and regio-selectivity. The use of statistical isomeric mixtures of olefins has been showed to produce a single product in a regioconvergent process and even the highly valuable ethylene gas could be successfully employed. Importantly, a wide range of drug derivatives could be modified in a late-stage functionalization setting, thus witnessing the potential of the deaminative alkylation technique for lead generation in drug discovery.

Presently, this methodology is restricted to the use of secondary and activated primary alkyl pyridinium salts, therefore further optimization of the reaction conditions will be required to improve the reactivity of these substrates.

Preliminary mechanistic experiments were carried out, indicating that the hydrofunctionalization of olefin occurred initially via nickel hydride species, which then coupled with alkyl pyridinium salt. However, further experimental evidences are required in order to confirm origin of such Ni-hydride intermediate and to elucidate the subtleties of the chain-walking process.

3.6 References

1. Selected reviews: (a) De Meijere, A.; Bräse, S.; Oestreich, M. Metal-Catalyzed Cross Coupling Reactions; Wiley-VCH: Weinheim, Germany, 2004. (b) Jana, R.; Pathak, T. P.; Sigman, M. S. Advances in Transition Metal (Pd, Ni, Fe)-Catalyzed Cross-Coupling Reactions Using Alkyl-Organometallics as Reaction Partners. *Chem. Rev.* **2011**, *111*, 1417. (c) Busch, M.; Wodrich, M. D.; Corminboeuf, C. A Generalized Picture of C–C Cross-Coupling. *ACS Catal.* **2017**, *7*, 5643. (d) Kaga, K.; Chiba, S. Engaging Radicals in Transition Metal-Catalyzed Cross-Coupling with Alkyl Electrophiles: Recent Advances. *ACS Catal.* **2017**, *7*, 4697. (e) Choi, J.; Fu, G. C. Transition Metal-Catalyzed Alkyl-Alkyl Bond Formation: Another Dimension in Cross-Coupling Chemistry. *Science* **2017**, *356*, 152.
2. (a) Kambe, N.; Iwasakia, T.; Terao, J. Pd-Catalyzed Cross-Coupling Reactions of Alkyl Halides. *Chem. Soc. Rev.* **2011**, *40*, 4937. (b) Hu, X. Ni-Catalyzed Cross Coupling of Non-Activated Alkyl Halides: A Mechanistic Perspective. *Chem. Sci.* **2011**, *2*, 1867. (c) Luh, T. Y.; Leung, M. K.; Wong, K. T. Transition Metal-Catalyzed Activation of Aliphatic C–X Bonds in Carbon–Carbon Bond Formation. *Chem. Rev.* **2000**, *100*, 3187. (d) Frisch, A. C.; Beller, M. Catalysts for Cross-Coupling Reactions with Non-activated Alkyl Halides. *Angew. Chem., Int. Ed.* **2005**, *44*, 674.
3. Selected reviews for C–O bond cleavage: (a) Cornella, J.; Zarate, C.; Martin, R. Metal-Catalyzed Activation of Ethers via C–O Bond Cleavage: A New Strategy for Molecular Diversity. *Chem. Soc. Rev.* **2014**, *43*, 8081. (b) Tobisu, M.; Chatani, N. Cross-Couplings Using Aryl Ethers via C–O Bond Activation Enabled by Nickel Catalysts. *Acc. Chem. Res.* **2015**, *48*, 1717. (c) Rosen, B. M.; Quasdorf, K. W.; Wilson, D. A.; Zhang, N.; Resmerita, A.-M.; Garg, N. K.; Percec, V. Nickel-Catalyzed Cross-Couplings Involving Carbon–Oxygen Bonds. *Chem. Rev.* **2011**, *111*, 1346. (d) Yu, D.-G.; Li, B.-J.; Shi, Z.-J. Exploration of New C–O Electrophiles in Cross-Coupling Reactions. *Acc. Chem. Res.* **2010**, *43*, 1486.
4. Selected references: (a) Cornella, J.; Edwards, J. T.; Qin, T.; Kawamura, S.; Wang, J. Pan, C.-M.; Gianatassio, R.; Schmidt, M. A.; Eastgate, M. D.; Baran, P. S. Practical Ni-Catalyzed Aryl-Alkyl Cross-Coupling of Secondary Redox-Active Esters, *J. Am. Chem. Soc.* **2016**, *138*, 2174. (b) Qin, T.; Cornella, J.; Li, C.; Malins, L. R.; Edwards, J. T.; Kawamura, S.; Maxwell, B. D.; Eastgate, M. D.; Baran, P. S.

Chapter 3.

- A General Alkyl-Alkyl Cross-Coupling Enabled by Redox-Active Esters and Alkylzinc Reagents, *Science* **2016**, 352, 801. (c) Toriyama, F.; Cornella, J.; Wimmer, L.; Chen, T.-G.; Dixon, D. D.; Creech, G.; Baran, P. S. Redox-Active Esters in Fe-catalyzed C–C Coupling. *J. Am. Chem. Soc.* **2016**, 138, 11132.
5. (a) Merchant, R. R.; Edwards, J. T.; Qin, T.; Kruszyk, M. M.; Bi, C.; Che, G.; Bao D-H.; Qiao, W.; Sun, L.; Collins, M. R.; Gallego, G. M.; Mousseau, J. J.; Nuhant, P.; Baran, P. S. Modular Radical Cross-Coupling with Sulfones Enables Access to sp^3 -Rich (Fluoro)Alkylated Scaffolds. *Science* **2018**, 360, 75. (b) Nambo, M.; Keske, E. C.; Rygus, J. P. G.; Yim, J. C.-H.; Crudden, C. M. Development of Versatile Sulfone Electrophiles for Suzuki–Miyaura Cross-Coupling Reactions. *ACS Catal.* **2017**, 7, 1108.
6. (a) Tasker, S. Z.; Standley, E. A.; Jamison, T. F. Recent Advances in Homogeneous Nickel Catalysis. *Nature* **2014**, 509, 299. (b) Ananikov, V. P. Nickel: The “Spirited Horse” of Transition Metal Catalysis. *ACS Catal.* **2015**, 5, 1964. (c) Diccianini, J. B.; Diao, T. Mechanisms of Nickel-Catalyzed Cross Coupling Reactions. *Trends Chem.* **2019**, 1, 830.
7. (a) Twilton, J.; Le, C.; Zhang, P.; Shaw, M. H.; Evans, R. W.; MacMillan, D. W. C. The Merger of Transition Metal and Photocatalysis. *Nat. Rev. Chem.* **2017**, 1, 0052. (b) Milligan, J. A.; Phelan, J. P.; Badir, S. O; Molander, G. A. Alkyl Carbon–Carbon Bond Formation by Nickel/Photoredox Cross-Coupling. *Angew. Chem. Int. Ed.* **2019**, 58, 6152. (c) Cheng, W.-M.; Shang, R. Transition Metal-Catalyzed Organic Reactions under Visible Light: Recent Developments and Future Perspectives. *ACS Catal.* **2020**, 10, 9170.
8. Selected references for sp^2 C–N bond cleavage, see: (a) Blakey, S.; MacMillan, D. The First Suzuki Cross-Couplings of Aryltrimethylammonium Salts. *J. Am. Chem. Soc.* **2003**, 125, 6046. (b) Buszek, K. R.; Brown, N. *N*-Vinylpyridinium and -ammonium Tetrafluoroborate Salts: New Electrophilic Coupling Partners for Pd(0)-Catalyzed Suzuki Cross-Coupling Reactions. *Org. Lett.* **2007**, 9, 707. (c) Tobisu, M.; Nakamura, K.; Chatani, N. Nickel-Catalyzed Reductive and Borylative Cleavage of Aromatic Carbon–Nitrogen Bonds in *N*-Aryl Amides and Carbamates. *J. Am. Chem. Soc.* **2014**, 136, 5587. (d) Hie, L.; Baker, E. L.; Anthony, S. M.; Desrosiers, J.-N.; Senanayake, C.; Garg, N. K. Nickel-Catalyzed Esterification of Aliphatic Amides. *Angew. Chem., Int. Ed.* **2016**, 55, 15129. (e) Shi, S.; Meng, G.; Szostak, M. Synthesis of Biaryls through Nickel-Catalyzed

Suzuki-Miyaura Coupling of Amides by Carbon-Nitrogen Bond Cleavage. *Angew. Chem., Int. Ed.* **2016**, *55*, 6959.

9. Selected references for benzylic, allylic and strain-activated C–N bonds cleavage, see: (a) Huang, C.-Y.; Doyle, A. G. Nickel-Catalyzed Negishi Alkylations of Styrenyl Aziridines. *J. Am. Chem. Soc.* **2012**, *134*, 9541. (b) Li, M.-B.; Wang, Y.; Tian, S.-K. Regioselective and Stereospecific Cross-Coupling of Primary Allylic Amines with Boronic Acids and Boronates through Palladium-Catalyzed C–N Bond Cleavage. *Angew. Chem., Int. Ed.* **2012**, *51*, 2968. (c) Maity, P.; Shacklady-McAtee, D. M.; Yap, G. P. A.; Sirianni, E. R.; Watson, M. P. Nickel-Catalyzed Cross Couplings of Benzylic Ammonium Salts and Boronic Acids: Stereospecific Formation of Diarylethanes via C–N Bond Activation. *J. Am. Chem. Soc.* **2013**, *135*, 280. (d) Jensen, K. L.; Standley, E. A.; Jamison, T. F. Highly Regioselective Nickel-Catalyzed Cross-Coupling of *N*-Tosylaziridines and Alkylzinc Reagents. *J. Am. Chem. Soc.* **2014**, *136*, 11145. (e) Zhang, H.; Hagihara, S.; Itami, K. Making Dimethylamino a Transformable Directing Group by Nickel-Catalyzed C–N Borylation. *Chem. - Eur. J.* **2015**, *21*, 16796. (f) Moragas, T.; Gaydou, M.; Martin, R. Nickel-Catalyzed Carboxylation of Benzylic C–N Bonds with CO₂. *Angew. Chem., Int. Ed.* **2016**, *55*, 5053. (g) Basch, C. H.; Cobb, K. M.; Watson, M. P. *Org. Lett.* **2016**, *18*, 136. (d) Hu, J.; Sun, H.; Cai, W.; Pu, X.; Zhang, Y.; Shi, Z. Nickel-Catalyzed Borylation of Aryl- and Benzyltrimethylammonium Salts via C–N Bond Cleavage. *J. Org. Chem.* **2016**, *81*, 14.
10. Blanksby, S. J.; Ellison, G. B. Bond Dissociation Energies of Organic Molecules. *Acc. Chem. Res.* **2003**, *36*, 255.
11. Ouyang, K.; Hao, W.; Zhang, W.-X.; Xi, Z. Transition-Metal-Catalyzed Cleavage of C–N Single Bonds. *Chem. Rev.* **2015**, *115*, 12045.
12. For selected references: (a) Blakemore, D. C.; Castro, L.; Churcher, I.; Rees, D. C.; Thomas, A. W.; Wilson, D. M.; Wood, A. Organic Synthesis Provides Opportunities to Transform Drug Discovery. *Nat. Chem.* **2018**, *10*, 383. (b) Mayol-Llinas, J.; Nelson, A.; Farnaby, W.; Ayscough, A. Assessing Molecular Scaffolds for CNS Drug Discovery. *Drug Discovery Today* **2017**, *22*, 965. (c) Ruiz-Castillo, P.; Buchwald, S. L. Applications of Palladium-Catalyzed C–N Cross-Coupling Reactions. *Chem. Rev.* **2016**, *116*, 12564. (d) Marciano, D. P.; Chang, M. R.; Corzo, C. A.; Lam, V. Q.; Pascal, B. D.; Griffin, P. R. The Therapeutic Potential of Nuclear Receptor Modulators for the Treatment of

Chapter 3.

- Metabolic Disorders: PPAR γ , RORs and Rev-erbs. *Cell Metab.* **2014**, *19*, 193. (e) Lawrence, S. A. Amines: Synthesis, Properties and Applications; Lawrence, S. A., Ed.; Cambridge University Press: Cambridge, New York, NY, 2004. (f) Amino Group Chemistry: From Synthesis to the Life Sciences; Ricci, A., Ed.; Wiley-VCH: Weinheim, 2008
13. (a) Katritzky, A. R. Conversions of Primary Amino Groups into Other Functionality Mediated by Pyrylium Cations. *Tetrahedron* **1980**, *36*, 679. (b) Katritzky, A. R.; Langthorne, R. T.; Patel, R. C.; Lhommet, G. Transformations of Pyridiniums Derived from Amino-Alcohols and from Diamines: Novel Ring Closures. *Tetrahedron* **1981**, *37*, 2383. (c) Katritzky, A. R.; Marson, C. M. Pyrylium Mediated Transformations of Primary Amino Groups into Other Functional Groups. New Synthetic Methods. *Angew. Chem. Int. Ed.* **1984**, *23*, 420.
14. Selected reviews, (a) Rosser, S. L.; Jelier, B. J.; Magnier, E.; Dagousset, G.; Carreira, E.; Togni, A. Pyridinium Salts as Redox-Active Functional Group Transfer Reagents. *Angew. Chem. Int. Ed.* **2020**, *59*, 9264. (b) He, F.-S.; Ye, S.; Wu, J. Recent Advances in Pyridinium Salts as Radical Reservoirs in Organic Synthesis. *ACS Catal.* **2019**, *9*, 8943. (c) Pang, Y.; Moser, D.; Cornella, J. Pyrylium Salts: Selective Reagents for the Activation of Primary Amino Groups in Organic Synthesis. *Synthesis* **2020**, *52*, 489. (d) Correia, J. T. M.; Fernandes, V. A.; Matsuo, B. T.; Delgado, J. A. C.; de Souza, W. C.; Paixao, M. W. Photoinduced Deaminative Strategies: Katritzky salts as Alkyl Radical Precursors. *Chem. Commun.* **2020**, *56*, 503. (e) Kong, D.; Moon, P. J.; Lundgren, R. J. Radical Coupling from Alkyl Amines. *Nat. Catal.* **2019**, *2*, 473.
15. Sowmiah, S.; Esperanca, J. M. S. S.; Rebelo, L. P. N.; Afonso, C. A. M. Pyridinium Salts: from Synthesis to Reactivity and Applications. *Org. Chem. Front.* **2018**, *5*, 453.
16. (a) Nolsøe, J. M. J.; Aursnes, M.; Tungen, J. E.; Hansen, T. V. Dienals Derived from Pyridinium Salts and Their Subsequent Application in Natural Product Synthesis. *J. Org. Chem.* **2015**, *80*, 5377. (b) Kiselyov, A. S. Chemistry of *N*-Fluoropyridinium Salts. *Chem. Soc. Rev.* **2005**, *34*, 1031.
17. Katritzky, A. R.; Kashmiri, M. A.; de Viile, G. Z.; Patel, R. C. Kinetics and Mechanism of the C-Alkylation of Nitroalkane Anions by 1-Alkyl-2,4,6-triphenylpyridiniums: A Nonchain Reaction with Radicaloid Characteristics. *J. Am. Chem. Soc.* **1983**, *105*, 90.

18. Basch, C. H.; Liao, J.; Xu, J.; Piane, J. J.; Watson, M. P. Harnessing Alkyl Amines as Electrophiles for Nickel-Catalyzed Cross-Couplings via C–N Bond Activation. *J. Am. Chem. Soc.* **2017**, *139*, 5313.
19. Liao, J.; Guan, W.; Boscoe, B. P.; Tucker, J. W.; Tomlin, J. W.; Garnsey, M. R.; Watson, M. P. Transforming Benzylic Amines into Diarylmethanes: Cross-Couplings of Benzylic Pyridinium Salts via C–N Bond Activation. *Org. Lett.* **2018**, *20*, 3030.
20. Guan, W.; Liao, J.; Watson, M. P. Vinylation of Benzylic Amines via C–N Bond Functionalization of Benzylic Pyridinium Salts. *Synthesis* **2018**, *50*, 3231.
21. Hoerrner, M. E.; Baker, K. M.; Basch, C. H.; Bampo, E. M.; Watson, M. P. Deaminative Arylation of Amino Acid-derived Pyridinium Salts. *Org. Lett.* **2019**, *21*, 7356.
22. Klauck, F. J. R.; James, M. J.; Glorius, F. Deaminative Strategy for the Visible-Light-Mediated Generation of Alkyl Radicals. *Angew. Chem., Int. Ed.* **2017**, *56*, 12336.
23. James, M. J.; Strieth-Kalthoff, F.; Sandfort, F.; Klauck, F. J. R.; Wagener, F.; Glorius, F. Visible-Light-Mediated Charge Transfer Enables C–C Bond Formation with Traceless Acceptor Groups. *Chem. - Eur. J.* **2019**, *25*, 8240.
24. Liao, J.; Basch, C. H.; Hoerrner, M. E.; Talley, M. R.; Boscoe, B. P.; Tucker, J. W.; Garnsey, M. R.; Watson, M. P. Deaminative Reductive Cross-Electrophile Couplings of Alkylpyridinium Salts and Aryl Bromides. *Org. Lett.* **2019**, *21*, 2941.
25. Yue, H.; Zhu, C.; Shen, L.; Geng, Q.; Hock, K. J.; Yuan, T.; Cavallo, L.; Rueping, M. Nickel-Catalyzed C–N Bond Activation: Activated Primary Amines as Alkylating Reagents in Reductive Cross Coupling. *Chem. Sci.* **2019**, *10*, 4430.
26. Martin-Montero, R.; Yatham, V. R.; Yin, H.; Davies, J.; Martin, R. Ni-Catalyzed Reductive Deaminative Arylation at sp^3 Carbon Centers. *Org. Lett.* **2019**, *21*, 2947.
27. Ni, S.; Li, C.; Han, J.; Mao, Y.; Pan, Y. Ni-Catalyzed Deamination Cross-Electrophile Coupling of Katritzky Salts with Halides via C–N Bond Activation. *Sci. Adv.* **2019**, *5*, 9516.
28. Yi, J.; Badir, S. O.; Kammer, L. M.; Ribagorda, M.; Molander, G. A. Deaminative Reductive Arylation Enabled by Nickel/Photoredox Dual Catalysis. *Org. Lett.* **2019**, *21*, 3346.

Chapter 3.

29. Ociepa, M.; Turkowska, J.; Gryko, D. Redox-Activated Amines in C(sp³)–C(sp) and C(sp³)–C(sp³) Bond Formation Enabled by Metal-Free Photoredox Catalysis. *ACS Catal.* **2018**, *8*, 11362.
30. Cartney, D. M.; Guiry, P. J. The Asymmetric Heck and Related Reactions. *Chem. Soc. Rev.* **2011**, *40*, 5122. (d) Beletskaya, I. P.; Cheprakov, A. V. The Heck Reaction as A Sharpening Stone of Palladium Catalysis. *Chem. Rev.* **2000**, *100*, 3009.
31. (a) Wang, G.-Z.; Shang, R.; Cheng, W.-M.; Fu, Y. Irradiation-Induced Heck Reaction of Unactivated Alkyl Halides at Room Temperature. *J. Am. Chem. Soc.* **2017**, *139*, 18307. (b) Cao, H.; Jiang, H.; Feng, H.; Kwan, J. M. C.; Liu, X.; Wu, J. Photo-induced Decarboxylative Heck-Type Coupling of Unactivated Aliphatic Acids and Terminal Alkenes in The Absence of Sacrificial Hydrogen Acceptors. *J. Am. Chem. Soc.* **2018**, *140*, 16360.
32. Jiang, X.; Zhang, M. M.; Xiong, W.; Lu, L. Q.; Xiao, W. J. Deaminative (Carboxylative) Alkyl-Heck-Type Reactions Enabled by Photocatalytic C–N Bond Activation. *Angew. Chem., Int. Ed.* **2019**, *58*, 2402.
33. Yang, Z.-K.; Xu, N.-X.; Wang, C.; Uchiyama, M. Photoinduced C(sp³)–N Bond Cleavage Leading to the Stereoselective Syntheses of Alkenes. *Chem. - Eur. J.* **2019**, *25*, 5433.
34. Fu, M.-C.; Shang, R.; Zhao, B.; Wang, B.; Fu, Y. Photocatalytic Decarboxylative Alkylations Mediated by Triphenylphosphine and Sodium Iodide. *Science* **2019**, *363*, 1429.
35. Zhu, Z.-F.; Tu, J.-L.; Liu, F. Ni-Catalyzed Deaminative Hydroalkylation of Internal Alkynes. *Chem. Commun.* **2019**, *55*, 11478.
36. (a) Lovering, F.; Bikker, J.; Humblet, C. Escape from Flatland: Increasing Saturation as an Approach to Improving Clinical Success. *J. Med. Chem.* **2009**, *52*, 6752. (b) Choi, J.; Fu, G. C. Transition Metal-Catalyzed Alkyl-Alkyl Bond Formation: Another Dimension in Cross-Coupling Chemistry. *Science* **2017**, *356*, 7230. (c) Geist, E.; Kirschning, A.; Schmidt, T. *Sp³-Sp³* Coupling Reactions in the Synthesis of Natural Products and Biologically Active Molecules. *Nat. Prod. Rep.* **2014**, *31*, 441.
37. Zhang, M.-M.; Liu, F. Visible-Light-Mediated Allylation of Alkyl Radicals with Allylic Sulfones Via a Deaminative Strategy. *Org. Chem. Front.* **2018**, *5*, 3443.

38. Wu, J.; Grant, P. S.; Li, X.; Noble, A.; Aggarwal, V. K. Catalyst-Free Deaminative Functionalizations of Primary Amines by Photoinduced Single-Electron Transfer. *Angew. Chem. Int. Ed.*, **2019**, *58*, 5697.
39. (a) Rosokha, S. V.; Kochi, J. K. Fresh Look at Electron-Transfer Mechanisms via the Donor/Acceptor Bindings in the Critical Encounter Complex. *Acc. Chem. Res.* **2008**, *41*, 641. (b) Lima, C. G. S.; de M. Lima, T.; Duarte, M.; Jurberg, I. D.; Paixão, M. W. Organic Synthesis Enabled by Light-Irradiation of EDA Complexes: Theoretical Background and Synthetic Applications. *ACS Catal.* **2016**, *6*, 1389. (c) Postigo, A. Electron Donor-Acceptor Complexes in Perfluoroalkylation Reactions. *Eur J. Org. Chem.* **2018**, *2018*, 6391.
40. Zhu, X.-Q.; Li, H.-R.; Li, Q.; Ai, T.; Lu, J.-Y.; Yang, Y.; Cheng, J.-P. Determination of the C4–H Bond Dissociation Energies of NADH Models and Their Radical Cations in Acetonitrile. *Chem. Eur. J.* **2003**, *9*, 871.
41. Brocks, J. J.; Beckhaus, H.-D.; Beckwith, A. L. J.; Rüchardt, C. Estimation of Bond Dissociation Energies and Radical Stabilization Energies by ESR Spectroscopy. *J. Org. Chem.* **1998**, *63*, 1935.
42. (a) Yin, G.; Mu, X.; Liu, G. Palladium(II)-Catalyzed Oxidative Difunctionalization of Alkenes: Bond Forming at a High-Valent Palladium Center. *Acc. Chem. Res.* **2016**, *49*, 2413. (b) Lan, X.-W.; Wang, N.-X.; Xing, Y. Recent Advances in Radical Difunctionalization of Simple Alkenes. *Eur. J. Org. Chem.* **2017**, 5821. (c) Zhang, J.-S.; Liu, L.; Chen, T.; Han, L.-B. Transition-Metal-Catalyzed Three-Component Difunctionalizations of Alkenes. *Chem. Asian J.* **2018**, *13*, 2277. (d) Dhungana, R. K.; Kc, S.; Basnet, P.; Giri, R. Transition Metal-Catalyzed Dicarbofunctionalization of Unactivated Olefins. *Chem. Rec.* **2018**, *18*, 1314. (e) Derosa, J.; Kang, T.; Apolinar, O.; Tran, V. T.; Engle, K. M. Recent Developments in Nickel-Catalyzed Intermolecular Dicarbofunctionalization of Alkenes. *Chem. Sci.* **2020**, *11*, 4287. (f) Luo, Y.-C.; Xu, C.; Zhang, X. Nickel-Catalyzed Dicarbofunctionalization of Alkenes. *Chin. J. Chem.* **2020**, *38*, 1371.
43. Klauck, F. J. R.; Yoon, H.; James, M. J.; Lautens, M.; Glorius, F. Visible-Light-Mediated Deaminative Three-Component Dicarbofunctionalization of Styrenes with Benzylic Radicals. *ACS Catal.* **2019**, *9*, 236.
44. Plunkett, S.; Basch, C. H.; Santana, S. O.; Watson, M. P. Harnessing Alkylpyridinium Salts as Electrophiles in Deaminative Alkylalkyl Cross

Chapter 3.

- Couplings. *J. Am. Chem. Soc.* **2019**, *141*, 2257.
45. Boronic Acids: Preparation and Applications in Organic Synthesis Medicine and Materials (Ed.: D. G. Hall), Wiley-VCH, Weinheim, 2011.
46. (a) Friese, F. W.; Studer, A. New Avenues for C–B Bond Formation via Radical Intermediates. *Chem. Sci.* **2019**, *10*, 8503. (b) Duret, G.; Quinlan, R.; Bisseret, P.; Blanchard, N. Boron Chemistry in a New Light. *Chem. Sci.* **2015**, *6*, 5366.
47. Fawcett, A.; Pradeilles, J.; Wang, Y.; Mutsuga, T.; Myers, E. L.; Aggarwal, V. K. Photoinduced Decarboxylative Borylation of Carboxylic Acids. *Science* **2017**, *357*, 283.
48. Wu, J.; He, L.; Noble, A.; Aggarwal, V. K. Photoinduced Deaminative Borylation of Alkylamines. *J. Am. Chem. Soc.* **2018**, *140*, 10700.
49. Sandfort, F.; Strieth-Kalthoff, F.; Klauck, F. J. R.; James, M. J.; Glorius, F. Deaminative Borylation of Aliphatic Amines Enabled by Visible Light Excitation of an Electron Donor–Acceptor Complex. *Chem. - Eur. J.* **2018**, *24*, 17210.
50. Hu, J.; Wang, G.; Li, S.; Shi, Z. Selective C–N Borylation of Alkylamines Promoted by Lewis Base. *Angew. Chem., Int. Ed.* **2018**, *57*, 15227.
51. Moser, D.; Duan, Y.; Wang, F.; Ma, Y.; O’Neill, M. J.; Cornella, J. Selective Functionalization of Aminoheterocycles by a Pyrylium Salt. *Angew. Chem. Int. Ed.* **2018**, *57*, 11035.
52. Ma, Y.; Pang, Y.; Chhabra, S.; Reijerse, E. J.; Schnegg, A.; Niski, J.; Leutzsch, M.; Cornella, J. Radical C–N Borylation of Aromatic Amines Enabled by a Pyrylium Reagent. *Chem. -Eur. J.* **2020**, *26*, 3738.
53. Sun, S.-Z.; Borjesson, M.; Martin-Montero, R.; Martin, R. Site-Selective Ni-Catalyzed Reductive Coupling of α -Haloboranes with Unactivated Olefins. *J. Am. Chem. Soc.* **2018**, *140*, 12765.
54. Gaydou, M.; Moragas, T.; Juliá-Hernández, F.; Martin, R. Site-Selective Catalytic Carboxylation of Unsaturated Hydrocarbons with CO₂ and Water. *J. Am. Chem. Soc.* **2017**, *139*, 12161.
55. For selected Ni-catalyzed reductive coupling reactions enabled by nitrogen-containing ligands possessing substituents adjacent to the nitrogen atom, see (a) Julia-Hernandez, F.; Moragas, T.; Cornella, J.; Martin, R. Remote Carboxylation of Halogenated Aliphatic Hydrocarbons with Carbon Dioxide. *Nature* **2017**, *545*, 84. (b) Serrano, E.; Martin, R. Nickel-Catalyzed Reductive Amidation of Unactivated Alkyl Bromides. *Angew. Chem. Int. Ed.* **2016**, *55*,

11207. (c) Wang, X.; Nakajima, M.; Martin, R. Ni-catalyzed Regioselective Hydrocarboxylation of Alkynes with CO₂ by Using Simple Alcohols as Proton Sources. *J. Am. Chem. Soc.* **2015**, *137*, 8924. (d) Moragas, T.; Cornella, J.; Martin, R. Ligand-Controlled Regiodivergent Ni-Catalyzed Reductive Carboxylation of Allyl Esters with CO₂. *J. Am. Chem. Soc.* **2014**, *136*, 17702.
56. Selected reviews for Ni-catalyzed chain-walking reactions: (a) Vasseur, A.; Bruffaerts, J.; Marek, I. Remote Functionalization Through Alkene Isomerization. *Nat. Chem.* **2016**, *8*, 209. (b) Larionov, E.; Li, H.; Mazet, C. Well-Defined Transition Metal Hydrides in Catalytic Isomerizations. *Chem. Commun.* **2014**, *50*, 9816. (c) Sommer, H.; Julia-Hernandez, F.; Martin, R.; Marek, I. Walking Metals for Remote Functionalization. *ACS Cent. Sci.* **2018**, *4*, 153. (d) Janssen-Müller, D.; Sahoo, B.; Sun, S.-Z.; Martin, R. Tackling Remote *sp*³ C–H Functionalization via Ni-Catalyzed “chain-walking” Reactions. *Isr. J. Chem.* **2020**, *60*, 195.
57. Selected references for Ni-catalyzed remote benzylic C–H functionalization of unactivated olefins: (a) He, Y.; Cai, Y.; Zhu, S. Mild and Regioselective Benzylic C–H Functionalization: Ni-Catalyzed Reductive Arylation of Remote and Proximal Olefins. *J. Am. Chem. Soc.* **2017**, *139*, 1061. (b) Xiao, J.; He, Y.; Ye, F.; Zhu, S. Remote *sp*³ C–H Amination of Alkene with Nitroarenes. *Chem.* **2018**, *4*, 1645. (c) Remote Migratory Cross-Electrophile Coupling and Olefin Hydroarylation Reactions Enabled by in Situ Generation of NiH. *J. Am. Chem. Soc.* **2017**, *139*, 13929. (d) Zhang, Y.; Xu, X.; Zhu, S. Nickel-Catalyzed Selective Migratory Hydrothiolation of Alkenes and Alkynes with Thiols. *Nat. Commun.* **2019**, *10*, 1752. (e) He, J.; Song, P.; Xu, X.; Zhu, S.; Wang, Y. Migratory Reductive Acylation Between Alkyl Halides or Alkenes and Alkyl Carboxylic Acids by Nickel Catalysis. *ACS Catal.* **2019**, *9*, 3253.
58. Cernak, T.; Dykstra, K. D.; Tyagarajan, S.; Vachal, P.; Krska, S. W. The Medicinal Chemist’s Toolbox for Late Stage Functionalization of Drug-like Molecules. *Chem. Soc. Rev.* **2016**, *45*, 546. (b) Krska, S. W.; Vachal, P.; Welch, C. J.; Smith, G. F. Compound Diversification Using Late Stage Functionalization. WO 2014052174A1, 2014
59. Examples for the formation of α -boron-stabilized alkyl-Ni species: (a) Zhang, Y.; Han, B.; Zhu, S. Rapid Access to Highly Functionalized Alkylboronates via NiH-Catalyzed Remote Hydroarylation of Boron-Containing Alkenes. *Angew. Chem. Int. Ed.* **2019**, *58*, 13860. (b) Bera, S.; Hu, X. Nickel-Catalyzed

Chapter 3.

Regioselective Hydroalkylation and Hydroarylation of Alkenyl Boronic Esters. *Angew. Chem. Int. Ed.* **2019**, *58*, 13854.

60. Moragas, T.; Cornella, J.; Martin, R. Ligand-Controlled Regiodivergent Ni-Catalyzed Reductive Carboxylation of Allyl Esters with CO₂. *J. Am. Chem. Soc.* **2014**, *136*, 17702.
61. (a) Research and Markets. “The Ethylene Technology Technology Report 2016 - Research and Martets.” (b) “Ethylene (ET): 2019 World Market Outlook and Forecast up to 2023.” www.researchandmarkets.com
62. Diccianni, J.; Lin, Q.; Diao, T. Mechanisms of Nickel-Catalyzed Coupling Reactions and Applications in Alkene Functionalization. *Acc. Chem. Res.* **2020**, *53*, 906.

3.7 Experimental Section

3.7.1 General Considerations

Reagents. Commercially available materials were used as received without further purification. NiI₂ and NiBr₂·DME (97% purity) were purchased from Aldrich, (EtO)₂MeSiH (DEMS, 97% purity) and (EtO)₃SiH were purchased from Fluorochem and Alfa Aesar. Sodium phosphate dibasic (Na₂HPO₄) was purchased from Scharlau. Anhydrous *N, N*-Dimethylacetamide (NMP, 99.5% purity), Anhydrous 1,4-dioxane (99.5% purity) and Dimethyl sulfoxide (DMSO, 99.5% purity) were purchased from Acros.

Analytical methods. ¹H and ¹³C NMR spectra were recorded on Bruker 300 MHz, Bruker 400 MHz and Bruker 500 MHz at 20 °C. All ¹H NMR spectra are reported in parts per million (ppm) downfield of TMS and were calibrated using the residual solvent peak of CHCl₃ (7.26 ppm), unless otherwise indicated. All ¹³C NMR spectra are reported in ppm relative to TMS, were calibrated using the signal of residual CHCl₃ (77.16 ppm), ¹¹B NMR and ¹⁹F NMR were obtained with ¹H decoupling unless otherwise indicated. Coupling constants, *J*, are reported in Hertz. Melting points were measured using open glass capillaries in a Büchi B540 apparatus. Gas chromatographic analyses were performed on Hewlett-Packard 6890 gas chromatography instrument with FID detector. Flash chromatography was performed with EM Science silica gel 60 (230-400 mesh). Thin layer chromatography was used to monitor reaction progress and analyze fractions from column chromatography. To this purpose TLC Silica gel 60 F₂₅₄ aluminium sheets from Merck were used and visualization was achieved using UV irradiation and/or staining with KMnO₄. The yields reported in scheme 3.22-3.24 refer to isolated yields and represent an average of at least two independent runs. The procedures described in this section are representative. Thus, the yields may differ slightly from those given in the Schemes of the manuscript. In the cases the High-Resolution Mass Spectra of the molecular ion could not be obtained using ESI and APCI ionization modes the GC-MS of the compound was given.

3.7.2 Optimization of the Reaction Conditions

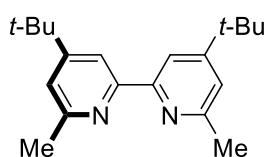
General procedure: An oven-dried 8 mL screw-cap test tube containing a stirring bar was charged with NiBr₂·DME (6.2 mg, 10 mol%), the corresponding ligand (15 mol%), Na₂HPO₄ (0.4 mmol, 56.8 mg) and 1-(1-(*tert*-butoxycarbonyl) piperidin-4-yl)-2,4,6-triphenylpyridin-1-ium tetrafluoroborate (**3.4.1a**, 113.6 mg, 0.2 mmol). Subsequently, the tube was sealed with a Teflon-lined screw cap, then evacuated and back-filled with Ar (3 times). Afterwards, 4-phenyl-1-butene (**3.4.2a**, 90 μL, 0.6 mmol, 3.0 equiv), (EtO)₂MeSiH (DEMS, 96 μL, 0.60 mmol, 3.0 equiv), NMP and 1,4-dioxane (4:1, 1.0 mL) were added via syringe. Then, the tube was stirred at 40 °C for 24 h. After the reaction was completed, the mixture was diluted with EtOAc, filtered through silica gel and concentrated under vacuum. The yields were determined by GC FID analysis using 1-decane as internal standard, and the product was purified by column chromatography on silica gel (Hexane/EtOAc = 120:1 to 60:1).

3.7.3 Synthesis of Ligands and Starting Materials

Commercially available compounds were used as received without further purification. 2-(6-methylpyridin-2-yl)-4,5-dihydrooxazole (**L3.4.10**),¹ 4-isopropyl-2-(6-methylpyridin-2-yl)-4,5-dihydrooxazole (**L3.4.11**),¹ 1-(1-(*tert*-butoxycarbonyl)piperidin-4-yl)-2,4,6-triphenylpyridin-1-ium tetrafluoroborate (**3.4.1a**),² 1-cyclohexyl-2,4,6-triphenylpyridin-1-ium tetrafluoroborate (**3.4.1b**),² 1-(4,4-difluorocyclohexyl)-2,4,6-triphenylpyridin-1-ium tetrafluoroborate (**3.4.1c**),² 2,4,6-triphenyl-1-(tetrahydro-2*H*-pyran-4-yl)pyridin-1-ium tetrafluoroborate (**3.4.1e**),² 1-(1-(*tert*-butoxycarbonyl)pyrrolidin-3-yl)-2,4,6-triphenylpyridin-1-ium tetrafluoroborate (**3.4.1f**),³ 2,4,6-triphenyl-1-(4-phenylbutan-2-yl)pyridin-1-ium tetrafluoroborate (**3.4.1g**),² 1-(1-methoxy-4-methyl-1-oxopentan-2-yl)-2,4,6-triphenylpyridin-1-ium tetrafluoroborate (**3.4.1j**),⁴ 1-(1-(2,6-dimethylphenoxy)propan-2-yl)-2,4,6-triphenylpyridin-1-ium tetrafluoroborate (**3.4.1i**),² (S)-1-(1-methoxy-1-oxopropan-2-yl)-2,4,6-triphenylpyridin-1-ium tetrafluoroborate (**3.4.1n**),⁵ ((allyloxy)methyl)benzene (**3.4.2b**),⁶ *tert*-butyl(hex-5-en-1-yloxy) dimethylsilane (**3.4.2c**),⁷ Hex-5-en-1-yl 4-fluorobenzoate (**3.4.2h**),⁸ (*E*)-*tert*-butyl(hex-4-en-1-yloxy) dimethylsilane (**3.4.2u**),⁹

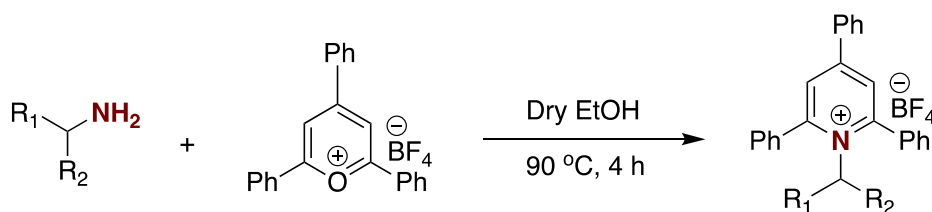
2-(oct-5-en-1-yl)isoindoline-1,3-dione (**3.4.2x**),¹⁰ 3-methyl-1-(oct-5-en-1-yl)-1H-indole (**3.4.2z**),¹ *tert*-butyl 4-(prop-1-en-1-yl)piperidine-1-carboxylate (**3.4.2aa**),¹¹ (8*R*,9*S*,13*S*,14*S*)-3-(hex-5-en-1-yloxy)-13-methyl-6,7,8,9,11,12,13,14,15,16-decahydro-17*H*-cyclopenta [*a*] phenanthrene-17-one (**3.4.2ac**),¹² *tert*-butyl 2,5-dihydro-1*H*-pyrrole-1-carboxylate (**3.4.11a**),¹³ (1-vinylcyclopropyl)benzene (**3.4.13**)¹⁴ were prepared by known procedures, the NMR data matched those reported previously.

3.7.3.1 General Procedure for the Preparation of L3.4.9

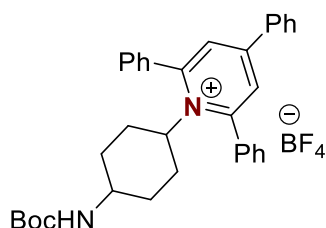


4,4'-di-*tert*-butyl-6,6'-dimethyl-2,2'-bipyridine (L3.4.9). To a solution of 4,4'-di-*tert*-butyl-2,2'-bipyridine (4.02g, 15.0 mmol, 1 equiv.) in THF (75 mL) at 0 °C under argon atmospheres was added a 1.6 M solution of MeLi in Et₂O (47 mL, 75 mmol, 5.0 equiv.) and the mixture was stirred for 14 h. The solution was then quenched water and extracted with Et₂O, dried over MgSO₄, and concentrated under reduced pressure. The latter was then dissolved in DCM (50 mL) and MnO₂ (13 g, 150 mmol, 10 equiv.) was added and the mixture stirred at 60 °C for 4 h. At this point the solution was filtered through a short pad of silica and concentrated under vacuum. The product was purified by flash chromatography (Hexane/EtOAc), obtained pale yellow solid 2.58g (58%). **Mp** 190–192 °C. **¹H NMR** (400 MHz, CDCl₃): δ 8.13 (d, *J* = 1.8 Hz, 2H), 7.14 (d, *J* = 1.8 Hz, 2H), 2.63 (s, 6H), 1.37 (s, 18H) ppm. **¹³C NMR** (101 MHz, CDCl₃): δ 161.0, 157.8, 156.7, 120.2, 115.8, 35.0, 30.8, 25.0 ppm. **IR** (neat, cm⁻¹): 2959, 2903, 2867, 1591, 1557, 1460, 1390, 1290, 917, 863. **HRMS** calcd. for (C₂₀H₂₉N₂) [M+H]⁺: 297.2325 found 297.2316.

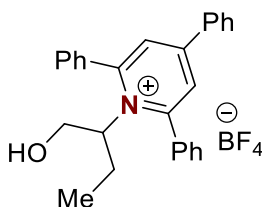
3.7.3.2 General Procedure for the Preparation of Katritzky Pyridinium Salts



General Procedure: 2,4,6-triphenylpyrylium tetrafluoroborate (1.0 equiv) and an amine (1.2 equiv) were added to a Schlenk containing a stirring bar. This was followed by addition of dry EtOH (1.0 M), resulting in a color change from yellow to black orange. The mixture was then stirred and heated at reflux in an oil bath at 90 °C for 5h. At that time, the mixture was allowed to cool to room temperature. Et₂O was then added (15 mL) and shaken vigorously, forming a solid precipitate that was filtered, washed with Et₂O (2x15 mL) and dried under high vacuum. If the pyridinium salt failed to precipitate, it was subjected to flash column chromatography, eluting with DCM/Acetone mixtures.

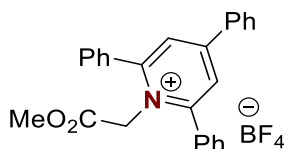


1-(4-((*tert*-butoxycarbonyl)amino)cyclohexyl)-2,4,6-triphenylpyridin-1-ium tetra-fluoroborate (3.4.1d): Following the general procedure, but using *tert*-butyl (4-aminocyclohexyl)carbamate (*trans/cis* = 1.5:1 ratio) (1.28 g, 6.0 mmol), afforded **3.4.1d** (1.78 g, 60% yield) as a white solid. **Mp** 192 – 193 °C. **¹H NMR** (400 MHz, CDCl₃): δ 7.76 – 7.64 (m, 8H), 7.59 – 7.46 (m, 7H), 7.39 (td, *J* = 8.2, 7.3, 2.4 Hz, 2H), 4.56 (t, *J* = 12.2 Hz, 1H), 4.28 – 4.05 (m, 1H), 2.88 (brs, 1H), 2.14 (d, *J* = 12.2 Hz, 2H), 1.80 (d, *J* = 12.8 Hz, 2H), 1.64 – 1.51 (m, 2H), 1.38 – 1.27 (s, 9H), 0.60 (q, *J* = 12.5 Hz, 2H) ppm. **¹³C NMR** (101 MHz, CDCl₃): δ 157.1, 155.2, 155.0, 134.1, 134.0, 132.0, 131.1, 129.6, 129.4, 129.0, 128.4, 128.2, 79.5, 70.6, 48.0, 33.0, 31.7, 28.4 ppm. **¹⁹F NMR** (376 MHz, CDCl₃) δ -152.6 (s), -152.7 (s) ppm. **¹¹B NMR** (128 MHz, CDCl₃) δ -119.2 ppm. **IR** (neat, cm⁻¹): 3368, 3244, 2944, 1682, 1529, 1181, 1030, 1026, 853. **HRMS** calcd. for (C₃₄H₃₇N₂O₂) [M-BF₄]⁺: 505.2850 found 505.2866.



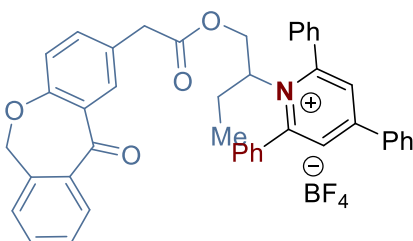
1-(1-hydroxybutan-2-yl)-2,4,6-triphenylpyridin-1-ium tetrafluoroborate (3.4.1h): Following the general procedure, but using 2-aminobutan-1-ol (0.54 mL, 6.0 mmol), afforded **3.4.1h** (1.5 g, 65% yield) as a white solid. **Mp** 97 – 98 °C. **¹H NMR** (400 MHz, CDCl₃): δ 8.11 – 7.67 (m, 6H), 7.66 – 7.29 (m, 11H), 5.17 – 5.00 (m, 1H), 3.81

– 3.64 (m, 2H), 3.62 – 3.51 (m, 1H), 1.72 (dt, $J = 14.6, 7.3$ Hz, 1H), 1.64 (s, 1H), 1.46 – 1.38 (m, 1H), 0.68 (t, $J = 7.4$ Hz, 3H) ppm. ^{13}C NMR (101 MHz, CDCl_3): δ 155.3, 133.7, 132.5, 129.9, 128.4, 74.0, 63.1, 25.7, 11.2 ppm. ^{19}F NMR (376 MHz, CDCl_3) δ -153.1 (s), -153.2 (s) ppm. ^{11}B NMR (128 MHz, CDCl_3) δ -1.2 ppm. IR (neat, cm^{-1}): 3524, 3063, 2971, 2881, 1617, 1599, 1561, 1410, 1053, 1049, 890. HRMS calcd. for $(\text{C}_{27}\text{H}_{26}\text{NO}) [\text{M-BF}_4]^+$: 380.2009 found 380.2000.



1-(2-methoxy-2-oxoethyl)-2,4,6-triphenylpyridin-1-ium tetrafluoroborate (3.4.1i):

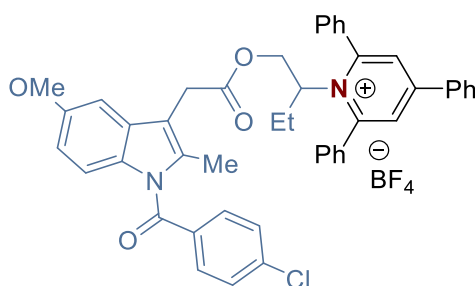
Following the general procedure, but using glycine methyl ester hydrochloride (753 mg, 6.0 mmol) and Et_3N (0.83 mL, 6 mmol), afforded **3.4.1i** (1.68 g, 72% yield) as a white solid. **Mp** 183 – 184 °C. ^1H NMR (400 MHz, CDCl_3): δ 7.96 (s, 2H), 7.84 – 7.79 (m, 2H), 7.71 (brs, 3H), 7.63 – 7.50 (m, 10H), 5.11 (s, 2H), 3.54 (s, 3H) ppm. ^{13}C NMR (101 MHz, CDCl_3): δ 167.5, 157.4, 157.1, 134.0, 132.6, 132.2, 131.5, 129.9, 129.0, 128.4, 126.3, 56.4, 53.4 ppm. ^{19}F NMR (376 MHz, CDCl_3) δ -153.0 (s), -153.1(s) ppm. ^{11}B NMR (128 MHz, CDCl_3) δ -119.1 ppm. IR (neat, cm^{-1}): 3041, 3010, 1752, 1619, 1594, 1561, 1414, 1369, 1220, 1184, 1039, 997, 904. HRMS calcd. for $(\text{C}_{26}\text{H}_{22}\text{NO}_2) [\text{M-BF}_4]^+$: 380.1645 found 380.1642.



1-(1-(2-(11-oxo-6,11-dihydrodibenzo[b,e]oxepin-2-yl)acetoxy)butan-2-yl)-2,4,6-triphenylpyridin-1-ium tetrafluoroborate (3.4.1j):

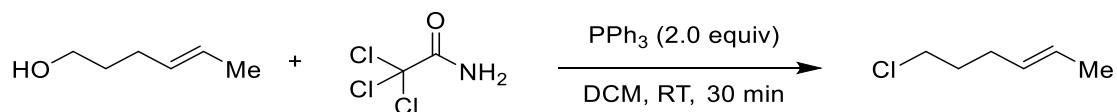
To a solution of 6,11-Dihydro-11-oxodibenz[b,e]oxepin-2-acetic acid (1.0 mmol, 268 mg) and 1-(1-hydroxybutan-2-yl)-2,4,6-triphenylpyridin-1-ium tetrafluoroborate (**3.4.1h**, 1.0 mmol, 437 mg) in dry DCM (10 mL) was added DCC (1.0 mmol, 206 mg) and DMAP (0.05 mmol, 6 mg). The reaction mixture was stirring at rt for 24 h, then remove the solid by filter. The residue was purified by flash column chromatography (DCM/Acetone = 10:1) to provide **3.4.1j** (516 mg, 72%) as a white solid. **Mp** 115 – 116 °C. ^1H NMR (400 MHz, CDCl_3): δ 8.00 (d, $J = 2.3$ Hz, 1H), 7.94 – 7.65 (m, 7H), 7.64 – 7.35 (m, 12H), 7.34 – 7.25 (m, 3H), 6.92 (d, $J = 8.4$ Hz, 1H), 4.98 (d, $J = 1.6$

Hz, 2H), 4.95 – 4.86 (m, 1H), 4.03 – 3.92 (m, 2H), 3.59 (s, 2H), 2.38 – 2.30 (m, 1H), 1.60 – 1.48 (m, 1H), 0.64 (t, $J = 7.3$ Hz, 3H) ppm. ^{13}C NMR (101 MHz, CDCl_3): δ 190.5, 170.1, 160.7, 155.7, 140.1, 136.2, 135.6, 133.6, 133.2, 132.4, 132.3, 131.3, 129.7, 129.5, 128.6, 128.1, 127.0, 125.3, 121.5, 73.7, 69.9, 64.1, 40.2, 26.9, 11.5 ppm (2 carbons missing due to signal broadening). ^{19}F NMR (376 MHz, CDCl_3) δ -153.08 (s), -153.09 (s) ppm. ^{11}B NMR (128 MHz, CDCl_3) δ -1.4 ppm. IR (neat, cm^{-1}): 3061, 2940, 2928, 2852, 1738, 1644, 1617, 1598, 1562, 1490, 1412, 1300, 1242, 1139, 1050. HRMS calcd. for $(\text{C}_{43}\text{H}_{36}\text{NO}_4) [\text{M-BF}_4]^+$: 630.2639 found 630.2630.

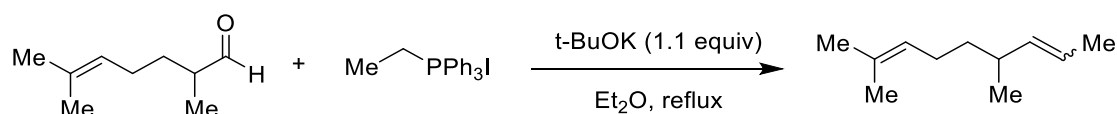


1-(1-(2-(1-(4-chlorobenzoyl)-5-methoxy-2-methyl-1H-indol-3-yl)acetoxy)butan-2-yl)-2,4,6-triphenylpyridin-1-ium tetrafluoroborate (3.4.1m): To a solution of 1-(4-Chlorobenzoyl)-5-methoxy-2-methyl-3-indoleacetic Acid (2.0 mmol, 717.6 mg) and 1-(1-hydroxybutan-2-yl)-2,4,6-triphenylpyridin-1-ium tetrafluoroborate (**3.4.1h**, 2mmol, 934 mg) in dry DCM (20 mL) was added DCC (2.0 mmol, 412 mg) and DMAP (0.1 mmol, 12 mg). The reaction mixture was stirring at rt for 24 h, then remove the solid by filter. The residue was purified by flash column chromatography (DCM/Acetone = 10:1) to provide **3.4.1m** (1.2 mg, 74%) as a yellow solid. **Mp** 149 – 150 °C. ^1H NMR (400 MHz, CDCl_3): δ 7.89 – 7.30 (m, 20H), 7.03 (s, 1H), 6.83 (d, $J = 2.5$ Hz, 1H), 6.69 (d, $J = 9.0$ Hz, 1H), 6.52 (dd, $J = 9.0, 2.5$ Hz, 1H), 4.91 – 4.84 (m, $J = 9.7, 5.2$ Hz, 1H), 4.03 (dd, $J = 12.6, 5.5$ Hz, 1H), 3.86 – 3.79 (m, 1H), 3.71 – 3.63 (s, 5H), 2.29 – 2.23 (m, 4H), 1.61 – 1.48 (m, 1H), 0.60 (t, $J = 7.4$ Hz, 3H) ppm. ^{13}C NMR (101 MHz, CDCl_3): δ 169.7, 168.2, 156.1, 155.5, 139.9, 136.1, 133.6, 133.3, 132.4, 131.3, 130.7, 130.4, 129.7, 129.3, 128.8, 128.7, 128.6, 114.9, 111.8, 111.5, 101.8, 69.6, 64.0, 55.9, 30.2, 26.9, 13.2, 11.4 ppm. ^{19}F NMR (376 MHz, CDCl_3) δ -152.8 (s), -152.9(s) ppm. ^{11}B NMR (128 MHz, CDCl_3) δ -1.38 ppm. IR (neat, cm^{-1}): 3064, 2931, 2852, 1739, 1679, 1617, 1598, 1561, 1477, 1457, 1355, 1315, 1256, 1223, 1143, 1051, 1030. HRMS calcd. for $(\text{C}_{46}\text{H}_{40}\text{ClN}_2\text{O}_4) [\text{M-BF}_4]^+$: 719.2671 found 719.2690.

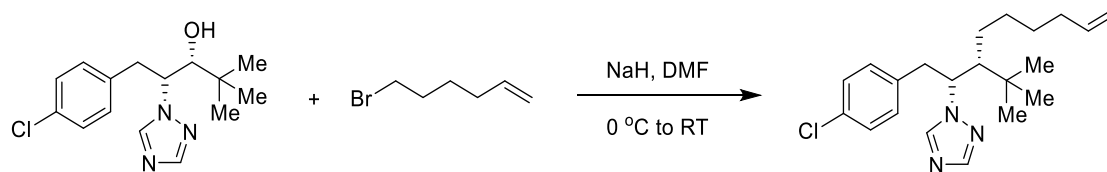
3.7.3.3 Procedure for the Preparation of Olefins



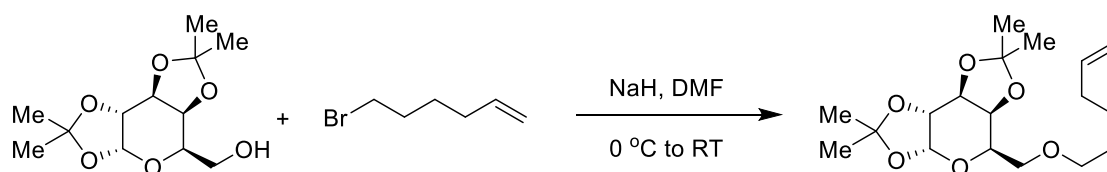
6-chloro-2-hexene (3.4.2v): To a stirred solution of the (*E*)-hex-4-en-1-ol (0.59 mL, 5.0 mmol) and PPh₃ (2.62 g, 10.0 mmol) in dry DCM (10 mL) was added 2,2,2-trichloroacetamide (1.62 g, 10.0 mmol) under Ar. The reaction mixture was stirring at rt for 30 min, then quenched with cold water. The aqueous phase was extracted with DCM (3 x 10 mL), and the combined organic phases were dried over MgSO₄ then concentrated. The residue was purified by flash column chromatography (Hexane/EtOAc = 100:1) to provide **3.4.2v** (390 mg, 66%) as a colorless oil. ¹H NMR (400 MHz, CDCl₃): δ 5.56 – 5.43 (m, 1H), 5.43 – 5.31 (m, 1H), 3.53 (t, *J* = 6.7 Hz, 2H), 2.16 – 2.10 (m, 2H), 1.85 – 1.78 (m, 2H), 1.65 (dq, *J* = 6.3, 1.3 Hz, 3H) ppm. ¹³C NMR (101 MHz, CDCl₃): δ 129.5, 126.5, 44.6, 32.5, 29.8, 18.0 ppm. IR (neat, cm⁻¹): 2959, 2936, 2919, 2855, 1441, 1561, 1414, 1283, 965, 734, 653. GC-MS: (C₆H₁₁Cl) [M]⁺: found *t* = 4.663 min, *m/z* 118.1.



2,6-dimethylnona-2,7-diene (3.4.2w): To a stirred solution of the ethyltriphenylphosphonium iodide (4.6 g, 11.0 mmol) and *t*-BuOK (1.23 g, 11.0 mmol) in Et₂O (30 mL) was added 2,6-dimethylhept-5-enal (1.59 mL, 10.0 mmol) by syringe. The reaction mixture was refluxed for 12 h. The crude reaction mixture was purified by flash column chromatography (Hexane/EtOAc = 300:1) to provide **3.4.2w** (1.08 g, 71%) as a colorless oil. ¹H NMR (400 MHz, CDCl₃): δ 5.43 – 5.35 (m, 1H), 5.20 – 5.06 (m, 2H), 2.53 – 2.41 (m, 1H), 2.00 – 1.88 (m, 2H), 1.69 (d, *J* = 1.4 Hz, 3H), 1.60 (dd, *J* = 6.8, 1.8 Hz, 6H), 1.38 – 1.17 (m, 2H), 0.94 (d, *J* = 6.7 Hz, 3H) ppm. ¹³C NMR (101 MHz, CDCl₃): δ 137.3, 131.3, 125.0, 122.5, 37.8, 31.1, 26.2, 25.9, 21.2, 17.8, 13.1 ppm. IR (neat, cm⁻¹): 2963, 2916, 2855, 1452, 1375, 967, 949, 720. HRMS calcd. for (C₁₁H₁₉) [M-H]⁺: 151.1481 found 151.1477.



1-((2R,3R)-1-(4-chlorophenyl)-3-(hex-5-en-1-yloxy)-4,4-dimethylpentan-2-yl)-1H-1,2,4-triazole (3.4.2ad): An oven-dried 50 mL flask containing a stirring bar was charged with Paclobutrazol (2.93 g, 10 mmol) and dry DMF (10 mL), cooling down to 0 °C, the 60% NaH (720 mg, 30 mmol) was added slowly. The reaction mixture was stirring at rt for 15 min until H₂ bubbling ceased. 6-bromo-1-hexene (1.55 mL, 11 mmol) was added dropwise and the reaction stirred overnight. The reaction mixture was quenched by saturated NH₄Cl under 0 °C, extracted with DCM, dried over MgSO₄ and the volatiles were removed under vacuum. Flash column chromatography (Hexane/EtOAc = 5:1) of the crude mixture afforded the title compound 2.36 g (63%) as white solid. **Mp** 54.5 – 55.6 °C. **¹H NMR** (400 MHz, CDCl₃): δ 8.38 (s, 1H), 7.75 (d, *J* = 2.2 Hz, 1H), 7.18 (dd, *J* = 8.5, 2.1 Hz, 2H), 6.92 (dd, *J* = 8.4, 1.8 Hz, 2H), 5.87 – 5.77 (m, 1H), 5.08 – 4.95 (m, 2H), 4.82 – 4.77 (m, 1H), 3.69 (td, *J* = 6.4, 1.5 Hz, 2H), 3.27 – 3.05 (m, 3H), 2.14 – 2.08 (m, 2H), 1.75 – 1.62 (m, 2H), 1.60 – 1.48 (m, 2H), 0.74 (d, *J* = 1.5 Hz, 9H) ppm. **¹³C NMR** (101 MHz, CDCl₃): δ 150.0, 143.7, 138.5, 135.4, 133.0, 130.0, 129.0, 115.0, 87.3, 75.5, 63.6, 40.9, 36.4, 33.7, 30.1, 26.6, 25.8 ppm. **IR** (neat, cm⁻¹): 2973, 2938, 2897, 2874, 1504, 1491, 1370, 1267, 1139, 1088, 1014, 906, 754. **HRMS** calcd. for (C₂₁H₃₁ClN₃O) [M+H]⁺: 376.2150 found 376.2149.

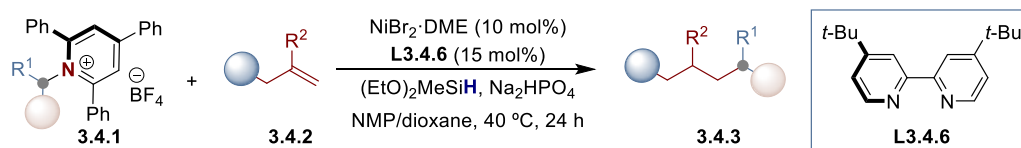


(3aR,5R,5aS,8aS,8bR)-5-((hex-5-en-1-yloxy)methyl)-2,2,7,7-tetramethyl tetrahydro-5H-bis([1,3]dioxolo)[4,5-*b*:4',5'-*d*]pyran (3.4.2ag): An oven-dried 50 mL flask containing a stirring bar was charged with 1,2:3,4-Di-*O*-isopropylidene- α -D-galactopyranose (2.6 g, 10 mmol) and dry DMF (10 mL), cooling down to 0 °C, the 60% NaH (720 mg, 30 mmol) was added slowly. The reaction mixture was stirring at rt for 15 min until H₂ bubbling ceased. 6-bromo-1-hexene (1.55 mL, 11 mmol) was added dropwise and the reaction stirred overnight. The reaction mixture was quenched by saturated NH₄Cl under 0 °C, extracted with DCM, dried over

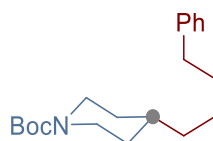
Site-Selective Ni-Catalyzed Deaminative Alkylation of Unactivated Olefins

MgSO₄ and the volatiles were removed under vacuum. Flash column chromatography (Hexane/EtOAc = 5:1) of the crude mixture afforded the title compound 2.4 g (70%) as colorless. **¹H NMR** (400 MHz, CDCl₃): δ 4.82 – 5.72 (m, 1H), 5.50 (d, *J* = 5.0 Hz, 1H), 5.02 – 4.87 (m, 2H), 4.57 (dd, *J* = 7.9, 2.4 Hz, 1H), 4.33 – 4.20 (m, 2H), 3.93 (td, *J* = 6.3, 1.9 Hz, 1H), 3.63 – 3.40 (m, 4H), 2.07 – 2.01 (m, 2H), 1.61 – 1.54 (m, 2H), 1.51 (s, 3H), 1.46 – 1.38 (m, 5H), 1.34 – 1.27 (m, 6H) ppm. **¹³C NMR** (101 MHz, CDCl₃): δ 139.0, 114.6, 109.3, 108.7, 96.5, 71.5, 71.4, 70.81, 70.80, 69.5, 66.9, 33.7, 29.2, 26.2, 26.14, 25.5, 25.1, 24.6 ppm. **IR** (neat, cm⁻¹): 2982, 2934, 2865, 1640, 1380, 1254, 1210, 1111, 1068, 999, 916. **HRMS** calcd. for (C₁₈H₃₀NaO₆) [M+Na]⁺: 365.1935 found 365.1937.

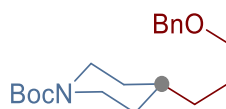
3.7.4 Ni-Catalyzed Deaminative Alkylation with Terminal Olefins



General procedure: An oven-dried 8 mL screw-cap test tube containing a stirring bar was charged with $\text{NiBr}_2 \cdot \text{DME}$ (6.2 mg, 10 mol%), 4,4'-di-*tert*-butyl-2,2'-dipyridyl (**L3.4.6**, 8.0 mg, 15 mol%), Na_2HPO_4 (56.8 mg, 0.40 mmol) and pyridinium salt (**3.4.1**, 0.20 mmol). Subsequently, the tube was sealed with a Teflon-lined screw cap, then evacuated and back-filled with Ar (3 times). Afterwards, α -olefin (**3.4.2**, 0.6 mmol), $(\text{EtO})_2\text{MeSiH}$ (DEMS, 96 μL , 0.60 mmol), NMP and 1,4-dioxane (4:1, 1.0 mL) were added via syringe. Then, the tube was stirred at 40 °C for 24 h. After the reaction was completed, the mixture was diluted with EtOAc, filtered through silica gel and concentrated under vacuum. The corresponding product was purified by column chromatography on silica gel. **Note:** if the corresponding product possesses a similar R_f to that of 2,4,6-triphenylpyridine, then toluene should be used as eluent followed by Hexane/EtOAc mixtures.

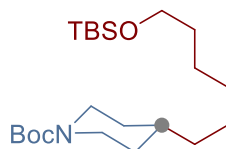


tert-butyl 4-(4-phenylbutyl)piperidine-1-carboxylate (3.4.3a): Following the general procedure, but using 4-phenyl-1-butene (90 μL , 0.60 mmol), afforded **3.4.3a** (51 mg, 80% yield) as a colorless oil. In an independent experiment, 46 mg (73% yield) were obtained, giving an average of 76% yield. $^1\text{H NMR}$ (400 MHz, CDCl_3): δ 7.31 – 7.25 (m, 2H), 7.21 – 7.14 (m, 3H), 4.08 (br, 2H), 2.66 (t, $J = 12.8$ Hz, 2H), 2.62 (t, $J = 3.6$ Hz, 2H), 1.72 – 1.56 (m, 4H), 1.47 (s, 9H), 1.40 – 1.30 (m, 3H), 1.30 – 1.23 (m, 2H), 1.12 – 1.02 (m, 2H) ppm. $^{13}\text{C NMR}$ (101 MHz, CDCl_3): δ 154.9, 142.7, 128.4, 128.3, 125.7, 79.1, 44.1, 36.4, 36.0, 35.9, 32.3, 31.7, 28.5, 26.3 ppm. **IR** (neat, cm^{-1}): 2975, 2927, 2853, 1689, 1419, 1364, 1277, 1239, 1154, 866. **HRMS** calcd. for $(\text{C}_{20}\text{H}_{31}\text{NNaO}_2)$ $[\text{M}+\text{Na}]^+$: 340.2247 found 340.2244.



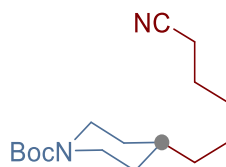
tert-butyl 4-(3-(benzyloxy)propyl)piperidine-1-carboxylate (3.4.3b): Following the general procedure, but using ((allyloxy)methyl)benzene (88.8 mg, 0.60 mmol), afforded **3.4.3b** (44 mg, 66% yield) as a colorless oil. In an independent experiment, 42 mg (63% yield) were obtained, giving an average of 64% yield. $^1\text{H NMR}$ (400

MHz, CDCl₃) δ 7.38 – 7.27 (m, 5H), 4.50 (s, 2H), 4.06 (d, *J* = 13.1 Hz, 2H), 3.46 (t, *J* = 6.6 Hz, 2H), 2.65 (t, *J* = 11.9 Hz, 2H), 1.72 – 1.59 (m, 4H), 1.45 (s, 9H), 1.39 – 1.26 (m, 3H), 1.11 – 1.05 (m, 2H) ppm. ¹³C NMR (101 MHz, CDCl₃): δ 155.0, 138.7, 128.5, 127.7, 127.6, 79.3, 73.0, 70.6, 44.2, 36.0, 33.1, 32.3, 28.6, 27.0 ppm. IR (neat, cm⁻¹): 2974, 2929, 2851, 1688, 1420, 1364, 1277, 1242, 1167, 1145, 1097, 938, 864. HRMS calcd. for (C₂₀H₃₁NNaO₃) [M+Na]⁺: 356.2196 found 356.2199.



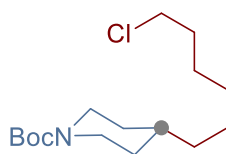
tert-butyl 4-(6-((tert-butyldimethylsilyloxy)hexyl)piperidine-1-carboxylate (3.4.3c): **Method A:** Following the general procedure, but using *tert*-butyl(hex-5-en-1-yloxy)dimethylsilane (128.4 mg, 0.60 mmol), afforded **3.4.3c** (58 mg, 73% yield) as a colorless oil. In an independent experiment, 60 mg (75% yield) were obtained, giving an average of 74% yield.

Method B: Following the general procedure, but using NiI₂ (6.2 mg, 10 mol%), 2-(6-methylpyridin-2-yl)-4,5-dihydrooxazole (**L3.4.10**, 6.4 mg, 20 mol%), Na₂HPO₄ (113.6 mg, 0.80 mmol), (EtO)₃SiH (74 μL, 0.40 mmol) in DMSO/1,4-dioxane and (*E*)-*tert*-butyl(hex-4-en-1-yloxy)dimethylsilane (**3.4.2u**, 128.4 mg, 0.60 mmol), afforded **3.4.3c** (38 mg, 48% yield) as a colorless oil. In an independent experiment, 41 mg (52% yield) were obtained, giving an average of 50% yield, 48:1 ratio. ¹H NMR (400 MHz, CDCl₃) δ 4.05 (d, *J* = 13.1 Hz, 2H), 3.59 (t, *J* = 6.6 Hz, 2H), 2.65 (t, *J* = 12.3 Hz, 2H), 1.63 (d, *J* = 12.9 Hz, 2H), 1.49 (t, *J* = 6.5 Hz, 2H), 1.44 (s, 9H), 1.37 – 1.14 (m, 9H), 1.11 – 0.96 (m, 2H), 0.88 (s, 9H), 0.04 (s, 6H) ppm. ¹³C NMR (101 MHz, CDCl₃): δ 155.1, 79.2, 63.4, 44.2, 36.6, 36.1, 33.0, 32.4, 29.7, 28.6, 26.7, 26.1, 25.9, 18.5, -5.1 ppm. IR (neat, cm⁻¹): 2975, 2927, 2855, 1695, 1420, 1364, 1247, 1160, 1097, 834. HRMS calcd. for (C₂₂H₄₅NNaO₃Si) [M+Na]⁺: 422.3061 found 422.3069.



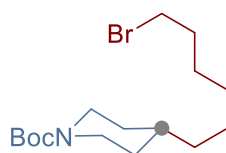
tert-butyl 4-(5-cyanopentyl)piperidine-1-carboxylate (3.4.3d): Following the general procedure, but using hex-5-enenitrile (68.1 μL, 0.60 mmol), afforded **3.4.3d** (39 mg, 70% yield) as a light yellow oil. In an independent experiment, 38 mg (68% yield) were obtained, giving an average of 69% yield. ¹H NMR (400 MHz, CDCl₃) δ 4.05 (d, *J* = 13.4 Hz, 2H), 2.64 (t, *J* = 12.8 Hz, 2H), 2.32 (t, *J* = 7.1 Hz, 2H), 1.75 – 1.55 (m, 4H), 1.43 (s, 9H), 1.43 – 1.38 (m, 2H), 1.38 – 1.28 (m, 3H), 1.27 – 1.19 (m, 2H), 1.10 – 0.99 (m, 2H) ppm. ¹³C NMR (101 MHz, CDCl₃) δ 155.0, 119.8, 79.3,

44.1, 36.3, 36.0, 32.2, 28.9, 28.6, 25.9, 25.4, 17.2 ppm. **IR** (neat, cm^{-1}): 2974, 2927, 2854, 1687, 1421, 1365, 1276, 1245, 1155, 1088, 865. **HRMS** calcd. for $(\text{C}_{16}\text{H}_{28}\text{N}_2\text{NaO}_2)$ $[\text{M}+\text{Na}]^+$: 303.2043 found 303.2044.

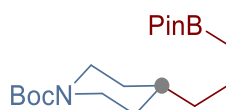


tert-butyl 4-(6-chlorohexyl)piperidine-1-carboxylate (3.4.3e): Method A: Following the general procedure, but using 6-chloro-1-hexene (79 μL , 0.60 mmol), afforded **3.4.3e** (40 mg, 66% yield) as a colorless oil. In an independent experiment, 40 mg (66% yield) were obtained, giving an average of 66% yield.

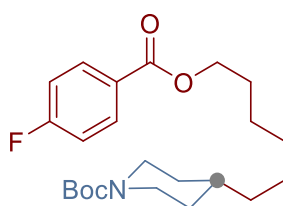
Method B: Following the general procedure, but using NiI_2 (6.2 mg, 10 mol%), 2-(6-methylpyridin-2-yl)-4,5-dihydrooxazole (**L3.4.10**, 6.4 mg, 20 mol%), Na_2HPO_4 (113.6 mg, 0.80 mmol), $(\text{EtO})_3\text{SiH}$ (74 μL , 0.40 mmol) in DMSO/1,4-dioxane and (*Z*)-6-chloro-2-hexene (**3.4.2v**, 70.8 mg, 0.60 mmol), afforded **3.4.3e** (30 mg, 50% yield) as a colorless oil. In an independent experiment, 27 mg (45% yield) were obtained, giving an average of 47% yield, 28:1 ratio. **^1H NMR** (400 MHz, CDCl_3) δ 4.05 (d, $J = 13.2$ Hz, 2H), 3.51 (t, $J = 6.7$ Hz, 2H), 2.65 (t, $J = 12.7$ Hz, 2H), 1.79 – 1.72 (m, 2H), 1.66 – 1.58 (m, 2H), 1.44 (s, 9H), 1.42 – 1.37 (m, 2H), 1.35 – 1.25 (m, 5H), 1.23 – 1.19 (m, 2H), 1.10 – 0.99 (m, 2H) ppm. **^{13}C NMR** (101 MHz, CDCl_3) δ 155.0, 79.2, 45.2, 44.2, 36.5, 36.1, 32.7, 32.3, 29.2, 28.6, 27.0, 26.6 ppm. **IR** (neat, cm^{-1}): 2975, 2926, 2853, 1688, 1419, 1364, 1277, 1242, 1153, 965, 868. **HRMS** calcd. for $(\text{C}_{16}\text{H}_{30}\text{ClNNaO}_2)$ $[\text{M}+\text{Na}]^+$: 326.1857 found 326.1859.



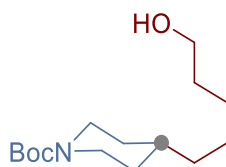
tert-butyl 4-(6-bromohexyl)piperidine-1-carboxylate (3.4.3f): Following the general procedure, but using 6-bromo-1-hexene (80 μL , 0.60 mmol), afforded **3.4.3f** (49 mg, 71% yield) as a colorless oil. In an independent experiment, 52 mg (75% yield) were obtained, giving an average of 73% yield. **^1H NMR** (400 MHz, CDCl_3) δ 4.05 (d, $J = 13.3$ Hz, 2H), 3.39 (t, $J = 6.8$ Hz, 2H), 2.65 (td, $J = 12.7, 2.7$ Hz, 2H), 1.93 – 1.77 (m, 2H), 1.62 (dt, $J = 13.3, 3.1$ Hz, 2H), 1.44 (s, 9H), 1.43 – 1.37 (m, 2H), 1.36 – 1.27 (m, 5H), 1.25 – 1.16 (m, 2H), 1.10 – 1.00 (m, 2H) ppm. **^{13}C NMR** (101 MHz, CDCl_3) δ 155.0, 79.3, 44.2, 36.5, 36.1, 34.1, 32.9, 32.3, 29.1, 28.6, 28.3, 26.5 ppm. **IR** (neat, cm^{-1}): 2974, 2926, 2853, 1689, 1420, 1364, 1276, 1242, 1154, 964, 868. **HRMS** calcd. for $(\text{C}_{16}\text{H}_{30}\text{BrNNaO}_2)$ $[\text{M}+\text{Na}]^+$: 370.1352 found 370.1356.



tert-butyl 4-(3-(4,4,5,5-tetramethyl-1,3,2-dioxaborolan-2-yl)propyl)piperidine-1-carboxylate (3.4.3g): Following the general procedure, but using 2-allyl-4,4,5,5-tetramethyl-1,3,2-dioxaborolane (112.6 μL , 0.60 mmol), afforded **3.4.3g** (40 mg, 56% yield) as a colorless oil. In an independent experiment, 41 mg (58% yield) were obtained, giving an average of 57% yield. $^1\text{H NMR}$ (400 MHz, CDCl_3) δ 4.03 (d, $J = 13.2$ Hz, 2H), 2.64 (td, $J = 14, 2.8$ Hz, 2H), 1.72 – 1.56 (m, 2H), 1.43 (s, 9H), 1.42 – 1.29 (m, 3H), 1.22 (s, 12H), 1.19 (t, $J = 3.3$ Hz, 2H), 1.09 – 0.98 (m, 2H), 0.73 (t, $J = 7.8$ Hz, 2H) ppm. $^{13}\text{C NMR}$ (101 MHz, CDCl_3) δ 155.1, 83.0, 79.2, 44.2, 39.4, 36.8, 35.9, 32.3, 28.6, 24.9, 21.2 ppm. $^{11}\text{B NMR}$ (128 MHz, CDCl_3) δ 34.2 ppm. **IR** (neat, cm^{-1}): 2976, 2927, 2859, 1693, 1420, 1365, 1319, 1276, 1246, 1144, 966, 847. **HRMS** calcd. for $(\text{C}_{19}\text{H}_{36}\text{NNaBO}_4)$ $[\text{M}+\text{Na}]^+$: 375.2666 found 375.2666.

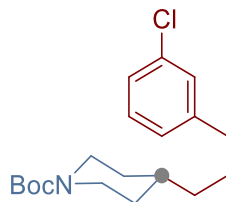


tert-butyl 4-(6-((4-fluorobenzoyl)oxy)hexyl)piperidine-1-carboxylate (3.4.3h): Following the general procedure, but using hex-5-en-1-yl 4-fluorobenzoate (133.2 mg, 0.60 mmol), afforded **3.4.3h** (62 mg, 77% yield) as a light yellow oil. In an independent experiment, 62 mg (77% yield) were obtained, giving an average of 77% yield. $^1\text{H NMR}$ (400 MHz, CDCl_3) δ 8.02 (dd, $J = 8.9, 5.4$ Hz, 2H), 7.07 (t, $J = 8.7$ Hz, 2H), 4.27 (t, $J = 6.7$ Hz, 2H), 4.03 (d, $J = 13.2$ Hz, 2H), 2.73 – 2.56 (m, 2H), 1.77 – 1.68 (m, 2H), 1.65 – 1.55 (m, 2H), 1.42 (s, 9H), 1.41 – 1.36 (m, 2H), 1.35 – 1.26 (m, 5H), 1.23 – 1.16 (m, 2H), 1.08 – 0.98 (m, 2H) ppm. $^{13}\text{C NMR}$ (101 MHz, CDCl_3) δ 165.7 (d, $J = 252.2$ Hz), 165.8, 155.0, 132.2 (d, $J = 9.3$ Hz), 126.9 (d, $J = 3.1$ Hz), 115.6 (d, $J = 22.1$ Hz), 79.2, 65.3, 44.2, 36.5, 36.0, 32.3, 29.5, 28.8, 28.5, 26.6, 26.1 ppm. $^{19}\text{F NMR}$ (376 MHz, CDCl_3) δ -106.1 ppm. **IR** (neat, cm^{-1}): 2974, 2929, 2856, 1716, 1693, 1603, 1508, 1412, 1366, 1270, 1239, 1153, 1112, 1090, 854. **HRMS** calcd. for $(\text{C}_{23}\text{H}_{34}\text{FNNaO}_4)$ $[\text{M}+\text{Na}]^+$: 430.2364 found 430.2358.



tert-butyl 4-(6-hydroxyhexyl)piperidine-1-carboxylate (3.4.3i): Following the general procedure, but using 5-hexene-1-ol (70.6 μL , 0.60 mmol), afforded **3.4.3i** (35 mg, 61% yield) as a light yellow solid. **Mp.** 47 – 48 $^{\circ}\text{C}$. In an independent experiment, 34 mg (61% yield) were obtained, giving an average of 61% yield. $^1\text{H NMR}$ (400 MHz, CDCl_3) δ 4.05 (d, $J = 13.2$ Hz, 2H), 3.62 (t, $J = 6.6$ Hz, 2H), 2.65 (td, $J = 12.8, 2.7$ Hz, 2H), 1.68 – 1.58 (m, 2H), 1.58 – 1.52 (m, 2H), 1.44 (s, 9H), 1.39 – 1.26 (m,

8H), 1.25 – 1.18 (m, 2H), 1.10 – 0.99 (m, 2H) ppm. ^{13}C NMR (101 MHz, CDCl_3) δ 155.1, 79.3, 63.1, 44.2, 36.6, 36.1, 32.9, 32.4, 29.7, 28.6, 26.7, 25.9 ppm. IR (neat, cm^{-1}): 2971, 2931, 2854, 1686, 1468, 1408, 1365, 1277, 1245, 1171, 1150, 1124, 1095, 865. The observed spectral data are in agreement with the ones reported in literature.¹⁵

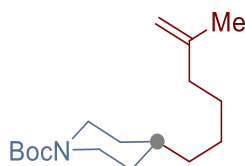


tert-butyl 4-(3-(3-chlorophenyl)propyl)piperidine-1-carboxylate (3.4.3j):

Following the general procedure, but using 1-allyl-3-chlorobenzene (87.2 μL , 0.60 mmol), afforded **3.4.3j** (42 mg, 62% yield) as a colorless oil. In an independent experiment, 44 mg (65% yield) were obtained, giving an average of 63% yield. ^1H NMR (400 MHz, CDCl_3) δ 7.23 – 7.12 (m, 3H), 7.05 – 7.02 (m, 1H), 4.06 (d, J = 12.2 Hz, 2H), 2.65 (t, J = 12.7 Hz, 2H), 2.56 (t, J = 7.7 Hz, 2H), 1.79 – 1.54 (m, 4H), 1.45 (s, 9H), 1.40 – 1.33 (m, 1H), 1.33 – 1.21 (m, 2H), 1.13 – 0.99 (m, 2H) ppm. ^{13}C NMR (101 MHz, CDCl_3) δ 155.0, 144.7, 134.1, 129.6, 128.6, 126.7, 126.0, 79.3, 44.1, 36.2, 36.0, 35.9, 32.3, 28.6, 28.4 ppm. IR (neat, cm^{-1}): 2975, 2928, 2854, 1687, 1476, 1420, 1364, 1276, 1243, 1155, 1120, 1079, 967, 867. HRMS calcd. for $(\text{C}_{19}\text{H}_{28}\text{ClNNaO}_2)$ $[\text{M}+\text{Na}]^+$: 360.1701 found 360.1705.

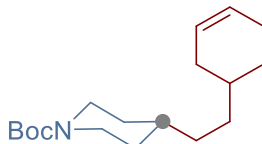


tert-butyl 4-(3,3-dimethylbutyl)piperidine-1-carboxylate (3.4.3k): Following the general procedure, but using 3,3-dimethylbut-1-ene (77 μL , 0.60 mmol), afforded **3.4.3k** (32 mg, 59% yield) as a colorless oil. In an independent experiment, 33 mg (61% yield) were obtained, giving an average of 60% yield. ^1H NMR (400 MHz, CDCl_3) δ 4.05 (d, J = 13.1 Hz, 2H), 2.65 (td, J = 12.8, 2.7 Hz, 2H), 1.67 – 1.62 (m, 2H), 1.44 (s, 9H), 1.30 – 1.22 (m, 1H), 1.17 (d, J = 3.2 Hz, 4H), 1.11 – 1.00 (m, 2H), 0.85 (s, 9H) ppm. ^{13}C NMR (101 MHz, CDCl_3) δ 155.1, 79.2, 44.3, 41.2, 37.0, 32.5, 31.4, 30.3, 29.5, 28.6 ppm. IR (neat, cm^{-1}): 2975, 2924, 2855, 1693, 1468, 1420, 1364, 1277, 1248, 1231, 1156, 965, 868. HRMS calcd. for $(\text{C}_{16}\text{H}_{31}\text{NNaO}_2)$ $[\text{M}+\text{Na}]^+$: 292.2247 found 292.2240.



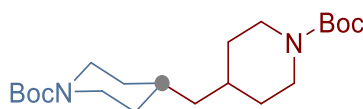
tert-butyl 4-(5-methylhex-5-en-1-yl)piperidine-1-carboxylate (3.4.3l): Following the general procedure, but using 2-methylhexa-1,5-diene (80.9 μL , 0.60 mmol),

afforded **3.4.3l** (38 mg, 68% yield) as a colorless oil. In an independent experiment, 40 mg (70% yield) were obtained, giving an average of 69% yield. $^1\text{H NMR}$ (400 MHz, CDCl_3) δ 4.79 – 4.53 (m, 2H), 4.05 (s, 2H), 2.65 (t, $J = 12.8$ Hz, 2H), 2.07 – 1.88 (m, 2H), 1.70 (s, 3H), 1.66 – 1.57 (m, 2H), 1.44 (s, 9H), 1.42 – 1.35 (m, 2H), 1.34 – 1.16 (m, 5H), 1.10 – 1.00 (m, 2H) ppm. $^{13}\text{C NMR}$ (101 MHz, CDCl_3) δ 155.1, 146.2, 109.8, 79.2, 44.2, 37.9, 36.6, 36.1, 32.4, 28.6, 27.9, 26.4, 22.5 ppm. **IR** (neat, cm^{-1}): 2974, 2927, 2853, 1692, 1419, 1364, 1277, 1240, 1155, 970, 884. **HRMS** calcd. for $(\text{C}_{17}\text{H}_{31}\text{NNaO}_2)$ $[\text{M}+\text{Na}]^+$: 304.2247 found 304.2248.

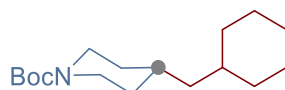


tert-butyl 4-(2-(cyclohex-3-en-1-yl)ethyl)piperidine-1-carboxylate (3.4.3m):

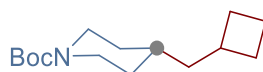
Following the general procedure, but using 4-vinylcyclohex-1-ene (78 μL , 0.60 mmol), afforded **3.4.3m** (27 mg, 46% yield) as a colorless oil. In an independent experiment, 29 mg (50% yield) were obtained, giving an average of 48% yield. $^1\text{H NMR}$ (400 MHz, CDCl_3) δ 5.77 – 5.40 (m, 2H), 4.06 (d, $J = 13.2$ Hz, 2H), 2.66 (td, $J = 13.2$ Hz, 2.4 Hz, 2H), 2.22 – 1.91 (m, 3H), 1.81 – 1.53 (m, 4H), 1.45 (s, 9H), 1.52 – 1.42 (m, 1H), 1.40 – 1.14 (m, 6H), 1.12 – 1.01 (m, 2H) ppm. $^{13}\text{C NMR}$ (101 MHz, CDCl_3) δ 155.1, 127.2, 126.7, 79.3, 44.2, 36.4, 33.9, 33.8, 33.7, 32.4, 32.1, 29.1, 28.6, 25.4 ppm. **IR** (neat, cm^{-1}): 2974, 2915, 2849, 1691, 1420, 1364, 1276, 1239, 1157, 1127, 967, 868. **HRMS** calcd. for $(\text{C}_{18}\text{H}_{31}\text{NNaO}_2)$ $[\text{M}+\text{Na}]^+$: 316.2247 found 316.2258.



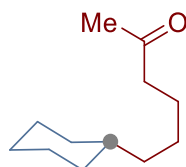
di-tert-butyl 4,4'-methylenebis(piperidine-1-carboxylate) (3.4.3n): Following the general procedure, but using NiI_2 (6.2 mg, 10 mol%), 2-(6-methylpyridin-2-yl)-4,5-dihydrooxazole (**L3.4.10**, 6.4 mg, 20 mol%), Na_2HPO_4 (113.6 mg, 0.80 mmol), $(\text{EtO})_3\text{SiH}$ (74 μL , 0.40 mmol) and *tert*-butyl 4-methylenepiperidine-1-carboxylate (**3.4.2n**, 122 μL , 0.60 mmol), in DMSO and 1,4-dioxane (3:1, 1.2 mL) at 35 $^\circ\text{C}$ stirring 24 h, afforded **3.4.3n** (46 mg, 60% yield) as a light yellow solid. **Mp** 90 – 91 $^\circ\text{C}$. In an independent experiment, 46 mg (60% yield) were obtained, giving an average of 60% yield. $^1\text{H NMR}$ (400 MHz, CDCl_3) δ 4.05 (brs, 4H), 2.65 (t, $J = 12.8$ Hz, 4H), 1.68 – 1.56 (m, 4H), 1.52 – 1.47 (m, 2H), 1.44 (s, 18H), 1.14 (t, $J = 7.0$ Hz, 2H), 1.11 – 0.92 (m, 4H) ppm. $^{13}\text{C NMR}$ (101 MHz, CDCl_3) δ 155.0, 79.3, 44.1, 43.6, 32.7, 32.5, 28.6 ppm. **IR** (neat, cm^{-1}): 2972, 2910, 2845, 1684, 1142, 1364, 1279, 1229, 1165, 1137, 1091, 976, 863. **HRMS** calcd. for $(\text{C}_{21}\text{H}_{38}\text{N}_2\text{NaO}_4)$ $[\text{M}+\text{Na}]^+$: 405.2724 found 405.2712.



tert-butyl 4-(cyclohexylmethyl)piperidine-1-carboxylate (3.4.3o): Following the general procedure B, but using NiI_2 (6.2 mg, 10 mol%), 2-(6-methylpyridin-2-yl)-4,5-dihydrooxazole (**L3.4.10**, 6.4 mg, 20 mol%), Na_2HPO_4 (113.6 mg, 0.80 mmol), $(\text{EtO})_3\text{SiH}$ (74 μL , 0.40 mmol, 3.0 equiv) and methylenecyclohexane (72.1 μL , 0.60 mmol), in DMSO and 1,4-dioxane (3:1, 1.2 mL) at 35 °C stirring 24 h, afforded **3.4.3o** (33 mg, 59% yield) as a white solid. **Mp** 47 – 48 °C. In an independent experiment, 33 mg (59% yield) were obtained, giving an average of 59% yield. $^1\text{H NMR}$ (400 MHz, CDCl_3) δ 4.05 (d, $J = 13.2$ Hz, 2H), 2.66 (td, $J = 12.9, 2.7$ Hz, 2H), 1.75 – 1.55 (m, 7H), 1.44 (s, 9H), 1.37 – 1.12 (m, 5H), 1.12 – 0.96 (m, 4H), 0.89 – 0.79 (m, 2H) ppm. $^{13}\text{C NMR}$ (101 MHz, CDCl_3) δ 155.1, 79.2, 44.6, 44.2, 34.3, 33.8, 32.9, 32.7, 28.6, 26.8, 26.5 ppm. **IR** (neat, cm^{-1}): 2980, 2917, 2848, 1448, 1679, 1447, 1413, 1366, 1281, 1233, 1161, 1118, 1009, 974, 866. **HRMS** calcd. for $(\text{C}_{17}\text{H}_{31}\text{NNaO}_2)$ $[\text{M}+\text{Na}]^+$: 304.2247 found 304.2246.

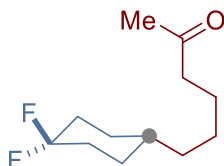


tert-butyl 4-(cyclobutylmethyl)piperidine-1-carboxylate (3.4.3p): Following the general procedure B, but using NiI_2 (6.2 mg, 10 mol%), 2-(6-methylpyridin-2-yl)-4,5-dihydrooxazole (**L3.4.10**, 6.4 mg, 20 mol%), Na_2HPO_4 (113.6 mg, 0.80 mmol), $(\text{EtO})_3\text{SiH}$ (74 μL , 0.40 mmol, 3.0 equiv) and methylenecyclobutane (55.5 μL , 0.60 mmol), in DMSO and 1,4-dioxane (3:1, 1.2 mL) at 35 °C stirring 24 h, afforded **3.4.3p** (32 mg, 62% yield) as a colorless oil. In an independent experiment, 30 mg (60% yield) were obtained, giving an average of 61% yield. $^1\text{H NMR}$ (400 MHz, CDCl_3) δ 4.03 (d, $J = 13.0$ Hz, 2H), 2.64 (td, $J = 12.9, 2.8$ Hz, 2H), 2.35 (m, 1H), 2.05 – 1.98 (m, 2H), 1.87 – 1.73 (m, 2H), 1.66 – 1.51 (m, 4H), 1.44 (s, 9H), 1.38 – 1.20 (m, 3H), 1.16 – 0.93 (m, 2H) ppm. $^{13}\text{C NMR}$ (101 MHz, CDCl_3) δ 142.7, 128.4, 128.3, 125.6, 68.2, 36.8, 36.0, 35.0, 33.3, 31.6, 26.0 ppm. **IR** (neat, cm^{-1}): 2974, 2927, 2850, 1691, 1419, 1364, 1277, 1245, 1164, 1145, 972, 867. **HRMS** calcd. for $(\text{C}_{15}\text{H}_{27}\text{NNaO}_2)$ $[\text{M}+\text{Na}]^+$: 276.1934 found 276.1945.



6-cyclohexylhexan-2-one (3.4.3q): Following the general procedure, but using 1-cyclohexyl-2,4,6-triphenylpyridin-1-ium tetrafluoroborate (**3.4.1b**, 95.8 mg, 0.20 mmol) and 5-hexene-2-one (69.3 μL , 0.60 mmol), afforded **3.4.3q** (19 mg, 52% yield) as a light-yellow oil. In an independent experiment, 22 mg (60% yield) were obtained,

giving an average of 56% yield. $^1\text{H NMR}$ (400 MHz, CDCl_3) δ 2.41 (t, $J = 7.5$ Hz, 2H), 2.13 (s, 3H), 1.76 – 1.59 (m, 5H), 1.54 (dt, $J = 14.8, 7.6$ Hz, 2H), 1.32 – 1.23 (m, 3H), 1.23 – 1.10 (m, 5H), 0.95 – 0.72 (m, 2H) ppm. $^{13}\text{C NMR}$ (101 MHz, CDCl_3) δ 209.5, 44.0, 37.6, 37.4, 33.5, 30.0, 26.9, 26.57, 26.6, 24.3 ppm. **IR** (neat, cm^{-1}): 2920, 2850, 1715, 1448, 1357, 1163, 962, 890. **HRMS** calcd. for $(\text{C}_{12}\text{H}_{22}\text{NaO})$ $[\text{M}+\text{Na}]^+$: 205.1563 found 205.1558.

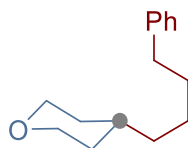


6-(4,4-difluorocyclohexyl)hexan-2-one (3.4.3r): Following the general procedure, but using 1-(4,4-difluorocyclohexyl)-2,4,6-triphenylpyridin-1-ium tetrafluoroborate (**3.4.1c**, 102.6 mg, 0.20 mmol) and 5-hexene-2-one (69.3 μL , 0.60 mmol), afforded **3.4.3r** (30 mg, 69% yield) as a light yellow oil. In an independent experiment, 29 mg (67% yield) were obtained, giving an average of 68% yield. $^1\text{H NMR}$ (400 MHz, CDCl_3) δ 2.42 (t, $J = 7.4$ Hz, 2H), 2.13 (s, 3H), 2.10 – 1.99 (m, 2H), 1.84 – 1.67 (m, 3H), 1.64 – 1.49 (m, 3H), 1.42 – 1.17 (m, 7H). ppm. $^{13}\text{C NMR}$ (101 MHz, CDCl_3) δ 209.2, 124.0 (dd, $J = 241.8, 239.4$ Hz), 43.8, 35.65 (dd, $J = 5.9, 2.1$ Hz), 33.6 (dd, $J = 25.4, 22.3$ Hz), 30.0, 29.1, 29.0, 26.8, 24.0 ppm. $^{19}\text{F NMR}$ (376 MHz, CDCl_3) δ -91.55 (d, $J = 234.3$ Hz), -102.04 (d, $J = 234.2$ Hz) ppm. **IR** (neat, cm^{-1}): 2935, 2863, 1715, 1449, 1358, 1272, 1164, 1115, 1081, 960. **GC-MS**: $(\text{C}_{12}\text{H}_{20}\text{F}_2\text{O})$ $[\text{M}]^+$: found $t = 5.492$ min, m/z 218.2.

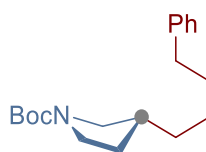


tert-butyl (4-(4-phenylbutyl)cyclohexyl)carbamate (3.4.3s): Following the general procedure, but using 1-((tert-butoxycarbonyl)amino)cyclohexyl)-2,4,6-triphenylpyridin-1-ium tetrafluoroborate (**3.4.1d**, 118.4 mg, 0.20 mmol) and 4-phenyl-1-butene (90 μL , 0.60 mmol), afforded **3.4.3s** (34 mg, 51% yield) as a white solid. In an independent experiment, 33 mg (50% yield) were obtained, giving an average of 50% yield, as a 1.5:1 ratio of diastereoisomers. **Mp** 69 – 70 $^{\circ}\text{C}$. $^1\text{H NMR}$ (400 MHz, CDCl_3) δ 7.32 – 7.23 (m, 2H), 7.19 – 7.15 (m, 3H), 4.70 – 4.35 (m, 1H), 3.75 – 3.35 (m, 1H), 2.60 (td, $J = 7.7, 3.8$ Hz, 2H), 1.97 (d, $J = 14.0$ Hz, 1H), 1.74 (d, $J = 12.2$ Hz, 1H), 1.68 – 1.49 (m, 5H), 1.45 (s, 9H), 1.39 – 1.16 (m, 4H), 1.17 – 1.08 (m, 2H), 1.08 – 0.87 (m, 2H) ppm. $^{13}\text{C NMR}$ (101 MHz, CDCl_3) δ 155.4, 142.94, 142.91, 128.5, 128.37, 128.36, 125.73, 125.71, 79.1, 50.2, 46.8, 37.0, 36.8, 36.1, 35.8, 35.6, 33.7, 32.0, 31.9, 31.8, 29.9, 28.60, 28.58, 28.1, 26.9, 26.8 ppm. **IR** (neat, cm^{-1}):

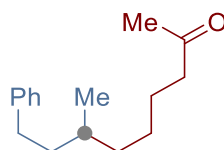
3354, 2980, 2923, 2848, 1680, 1517, 1497, 1389, 1364, 1322, 1240, 1168, 1030, 978, 880. **HRMS** calcd. for (C₂₁H₃₃NNaO₂) [M+Na]⁺: 354.2404 found 354.2407.



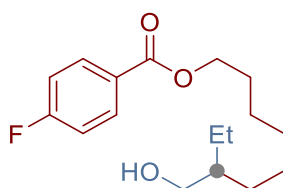
6-(tetrahydro-2H-pyran-4-yl)hexan-2-one (3.4.3t): Following the general procedure, but using 2,4,6-triphenyl-1-(tetrahydro-2H-pyran-4-yl)pyridin-1-ium tetrafluoroborate (**3.4.1e**, 95.8 mg, 0.20 mmol) and 4-phenyl-1-butene (90 μ L, 0.60 mmol), afforded **3.4.3t** (30 mg, 69% yield) as a colorless oil. In an independent experiment, 30 mg (69% yield) were obtained, giving an average of 69% yield. **¹H NMR** (400 MHz, CDCl₃) δ 7.32 – 7.24 (m, 2H), 7.21 – 7.17 (m, 3H), 4.05 – 3.82 (m, 2H), 3.36 (td, J = 11.8, 2.1 Hz, 2H), 2.68 – 2.51 (m, 2H), 1.70 – 1.54 (m, 4H), 1.52 – 1.41 (m, 1H), 1.39 – 1.32 (m, 2H), 1.31 – 1.21 (m, 4H) ppm. **¹³C NMR** (101 MHz, CDCl₃) δ 142.8, 128.5, 128.4, 125.8, 68.3, 36.9, 36.1, 35.1, 33.4, 31.8, 26.1 ppm. **IR** (neat, cm⁻¹): 2925, 2841, 1496, 1454, 1386, 1236, 1137, 1094, 1014, 981, 856. **HRMS** calcd. for (C₁₅H₂₃O) [M+H]⁺: 219.1743 found 219.1746.



tert-butyl-3-(4-phenylbutyl)pyrrolidine-1-carboxylate (3.4.3u): Following the general procedure, but using 1-(1-(*tert*-butoxycarbonyl)pyrrolidin-3-yl)-2,4,6-triphenylpyridin-1-ium tetrafluoroborate (**3.4.1f**, 112.8 mg, 0.20 mmol) and 4-phenyl-1-butene (90 μ L, 0.60 mmol), afforded **3.4.3u** (46 mg, 76% yield) as a colorless oil. In an independent experiment, 46 mg (76% yield) were obtained, giving an average of 76% yield. **¹H NMR** (400 MHz, CDCl₃) δ 7.32 – 7.23 (m, 2H), 7.18 (t, J = 6.4 Hz, 3H), 3.57 – 7.23 (m, 2H), 3.28 – 3.17 (m, 1H), 2.84 (dt, J = 19.9, 9.7 Hz, 1H), 2.61 (dt, J = 7.9, 2.8 Hz, 2H), 2.13 – 2.04 (m, 1H), 1.98 – 1.91 (m, 1H), 1.63 (dt, J = 11.2, 3.6 Hz, 2H), 1.46 (s, 9H), 1.44 – 1.31 (m, 5H) ppm. **¹³C NMR** (101 MHz, CDCl₃) δ 154.7, 142.6, 128.5, 128.4, 125.8, 79.0, 51.8, 51.4, 45.9, 45.6, 39.2, 38.4, 35.9, 33.2, 32.0, 31.6, 31.3, 28.7, 27.9 ppm. **IR** (neat, cm⁻¹): 2974, 2929, 2857, 1692, 1454, 1400, 1365, 1168, 1121, 910, 881. **HRMS** calcd. for (C₁₉H₂₉NNaO₂) [M+Na]⁺: 326.2090 found 326.2088.

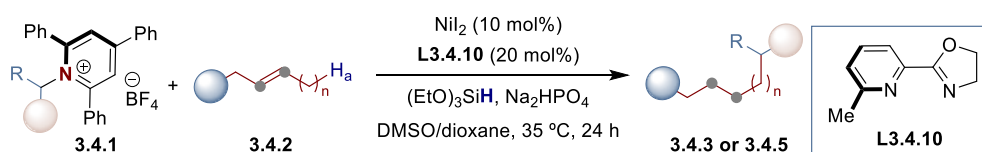


7-methyl-9-phenylnonan-2-one (3.4.3v): Following the general procedure, but using 2,4,6-triphenyl-1-(4-phenylbutan-2-yl)pyridin-1-ium tetrafluoroborate (**3.4.1g**, 210.8 mg, 0.40 mmol) and 5-hexene-2-one (23.1 μ L, 0.20 mmol), afforded **3.4.3v** (19 mg, 41% yield) as a light yellow oil. In an independent experiment, 21 mg (45% yield) were obtained, giving an average of 43% yield. $^1\text{H NMR}$ (300 MHz, CDCl_3) δ 7.32 – 7.24 (m, 2H), 7.21 – 7.12 (m, 3H), 2.75 – 2.50 (m, 2H), 2.42 (t, $J = 7.4$ Hz, 2H), 2.13 (s, 3H), 1.79 – 1.04 (m, 9H), 0.92 (d, $J = 6.2$ Hz, 3H) ppm. $^{13}\text{C NMR}$ (75 MHz, CDCl_3) δ 209.4, 143.2, 128.5, 128.4, 125.7, 43.9, 39.0, 36.8, 33.6, 32.5, 30.0, 26.7, 24.3, 19.7 ppm. **IR** (neat, cm^{-1}): 2977, 2928, 2858, 1715, 1454, 1357, 1164, 1030, 957. **HRMS** calcd. for ($\text{C}_{16}\text{H}_{24}\text{NaO}$) $[\text{M}+\text{Na}]^+$: 255.1719 found 255.1724.

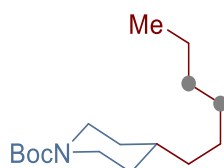


7-(hydroxymethyl)nonyl 4-fluorobenzoate (3.4.3w): Following the general procedure, but using 1-(1-hydroxybutan-2-yl)-2,4,6-triphenylpyridin-1-ium tetrafluoroborate (**3.4.1h**, 93.4 mg, 0.20 mmol) and hex-5-en-1-yl 4-fluorobenzoate (133.2 mg, 0.60 mmol), afforded **3.4.3w** (30 mg, 51% yield) as a colorless oil. In an independent experiment, 29 mg (49% yield) were obtained, giving an average of 50% yield. $^1\text{H NMR}$ (400 MHz, CDCl_3) δ 8.05 (dd, $J = 8.9, 5.5$ Hz, 2H), 7.10 (t, $J = 8.7$ Hz, 2H), 4.30 (t, $J = 6.7$ Hz, 2H), 3.54 (d, $J = 5.1$ Hz, 2H), 1.83 – 1.66 (m, 2H), 1.54 – 1.06 (m, 12H), 0.89 (t, $J = 7.3$ Hz, 3H) ppm. $^{13}\text{C NMR}$ (101 MHz, CDCl_3) δ 165.9, 165.8 (d, $J = 254.4$ Hz), 132.2 (d, $J = 9.3$ Hz), 126.9 (d, $J = 2.8$ Hz), 115.6 (d, $J = 22.0$ Hz), 65.38, 65.37, 42.1, 30.5, 29.8, 28.8, 26.9, 26.1, 23.5, 11.3 ppm. $^{19}\text{F NMR}$ (376 MHz, CDCl_3) δ -106.12 (tt, $J = 8.5, 5.4$ Hz) ppm. **IR** (neat, cm^{-1}): 3436, 2975, 2928, 2858, 1718, 1603, 1508, 1462, 1270, 1238, 1153, 1112, 1090, 1037, 854. **HRMS** calcd. for ($\text{C}_{17}\text{H}_{25}\text{FNaO}_3$) $[\text{M}+\text{Na}]^+$: 319.1680 found 319.1682.

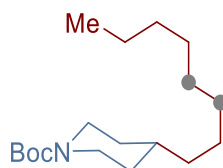
3.7.5 Ni-Catalyzed Deaminative Alkylation with Internal Olefins



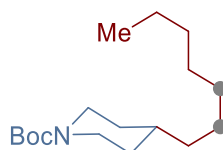
General procedure B: An oven-dried 8 mL screw-cap test tube containing a stirring bar was charged with NiI_2 (6.2 mg, 10 mol%), 2-(6-methylpyridin-2-yl)-4,5-dihydrooxazole (**L3.4.10**, 6.4 mg, 20 mol%), Na_2HPO_4 (113.6 mg, 0.80 mmol) and pyridinium salt (**3.4.1**, 0.20 mmol). Subsequently, the tube was sealed with a Teflon-lined screw cap, then evacuated and back-filled with Ar (3 times). Afterwards, olefin (**3.4.2**, 0.60 mmol), $(\text{EtO})_3\text{SiH}$ (74 μL , 0.40 mmol, 2.0 equiv), DMSO and 1,4-dioxane (3:1, 1.2 mL) were added via syringe. Then, the tube was stirred at 35 °C for 24 h. After the reaction was completed, the mixture was diluted with EtOAc, filtered through silica gel and concentrated under vacuum. The corresponding product was purified by column chromatography on silica gel. **Note:** if the corresponding product possesses a similar R_f to that of 2,4,6-triphenylpyridine, then toluene should be used as eluent followed by Hexane/EtOAc mixtures.



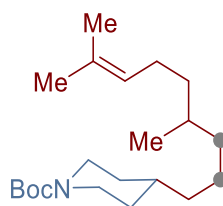
tert-butyl 4-hexylpiperidine-1-carboxylate (3.4.5a): Following the general procedure B, but using *trans*-3-hexene (**3.4.2r**, 74.5 μL , 0.60 mmol), afforded **3.4.5a** (32 mg, 59% yield) as a colorless oil. In an independent experiment, 31 mg (57% yield) were obtained, giving an average of 58% yield, 99:1 ratio. $^1\text{H NMR}$ (400 MHz, CDCl_3) δ 4.05 (brs, 2H), 2.65 (t, $J = 12.7$ Hz, 2H), 1.62 (d, $J = 12.5$ Hz, 2H), 1.44 (s, 9H), 1.42 – 1.16 (m, 11H), 1.10 – 0.99 (m, 2H), 0.87 (t, $J = 6.8$ Hz, 3H) ppm. $^{13}\text{C NMR}$ (101 MHz, CDCl_3) δ 155.1, 79.2, 44.2, 36.7, 36.1, 32.4, 32.0, 29.6, 28.6, 26.7, 22.8, 14.2 ppm. **IR** (neat, cm^{-1}): 2957, 2923, 2853, 1693, 1449, 1419, 1365, 1277, 1238, 1169, 1149, 1097, 968, 867. **HRMS** calcd. for $(\text{C}_{16}\text{H}_{31}\text{NNaO}_2)$ $[\text{M}+\text{Na}]^+$: 292.2247 found 292.2240.



tert-butyl 4-octylpiperidine-1-carboxylate (3.4.5b): Following the general procedure B, but using *trans*-4-octene (**3.4.2s**, 94.1 μ L, 0.60 mmol), afforded **3.4.5b** (40 mg, 67% yield) as a colorless oil. In an independent experiment, 37 mg (63% yield) were obtained, giving an average of 65% yield, 39:1 ratio. $^1\text{H NMR}$ (400 MHz, CDCl_3) δ 4.05 (brs, 2H), 2.65 (t, $J = 12.9$ Hz, 2H), 1.66 – 1.54 (m, 2H), 1.44 (s, 9H), 1.38 – 1.16 (m, 15H), 1.12 – 0.97 (m, 2H), 0.87 (t, $J = 6.8$ Hz, 3H) ppm. $^{13}\text{C NMR}$ (101 MHz, CDCl_3) δ 155.1, 79.2, 44.3, 36.7, 36.1, 32.4, 32.0, 30.0, 29.7, 29.5, 28.6, 26.8, 22.8, 14.2 ppm. **IR** (neat, cm^{-1}): 2971, 2922, 2852, 1694, 1449, 1419, 1364, 1277, 1242, 1164, 1101, 964, 869. **HRMS** calcd. for $(\text{C}_{18}\text{H}_{35}\text{NNaO}_2)$ $[\text{M}+\text{Na}]^+$: 320.2560 found 320.2562.

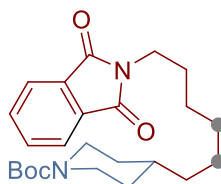


tert-butyl 4-heptylpiperidine-1-carboxylate (3.4.5c): Following the general procedure B, but using *trans*-4-heptene (**3.4.2t**, 84 μ L, 0.60 mmol), afforded **3.4.5c** (33 mg, 58% yield) as a colorless oil. In an independent experiment, 32 mg (56% yield) were obtained, giving an average of 57% yield, 36:1 ratio. $^1\text{H NMR}$ (400 MHz, CDCl_3) δ 4.05 (brs, 2H), 2.66 (t, $J = 12.5$ Hz, 2H), 1.68 – 1.60 (m, 2H), 1.44 (s, 9H), 1.38 – 1.13 (m, 13H), 1.10 – 0.99 (m, 2H), 0.87 (t, $J = 6.8$ Hz, 3H) ppm. $^{13}\text{C NMR}$ (101 MHz, CDCl_3) δ 155.1, 79.2, 44.3, 36.7, 36.1, 32.4, 32.0, 29.9, 29.5, 28.6, 26.8, 22.8, 14.2 ppm. **IR** (neat, cm^{-1}): 2975, 2923, 2852, 1694, 1449, 1419, 1365, 1277, 1245, 1168, 1099, 970, 868. **HRMS** calcd. for $(\text{C}_{17}\text{H}_{33}\text{NNaO}_2)$ $[\text{M}+\text{Na}]^+$: 306.2404 found 306.2404.



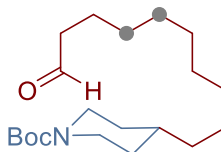
tert-butyl 4-(4,8-dimethylnon-7-en-1-yl)piperidine-1-carboxylate (3.4.5d): Following the general procedure B, but using 2,6-dimethylnona-2,7-diene (**3.4.2w**, 99.6 mg, 0.60 mmol), afforded **3.4.5d** (34 mg, 50% yield) as a colorless oil. In an independent experiment, 31 mg (46% yield) were obtained, giving an average of 48% yield, 54:1 ratio. $^1\text{H NMR}$ (400 MHz, CDCl_3) δ 5.23 – 4.97 (m, 1H), 4.05 (brs, 2H), 2.66 (t, $J = 12.7$ Hz, 2H), 2.06 – 1.87 (m, 2H), 1.74 – 1.56 (m, 7H), 1.45 (s, 9H), 1.41 – 1.16 (m, 9H), 1.15 – 1.01 (m, 4H), 0.85 (d, $J = 6.5$ Hz, 3H) ppm. $^{13}\text{C NMR}$ (101 MHz, CDCl_3) δ 155.1, 131.1, 125.2, 79.2, 44.3, 37.3, 37.0, 36.2, 32.5, 32.42, 32.37, 28.6, 25.9, 25.7, 24.1, 19.7, 17.8 ppm. **IR** (neat, cm^{-1}): 3356, 2977, 2924, 2851, 1694,

1421, 1365, 1277, 1244, 1161, 968, 867. **HRMS** calcd. for (C₂₁H₃₉NNaO₂) [M+Na]⁺: 360.2873 found 360.2873.



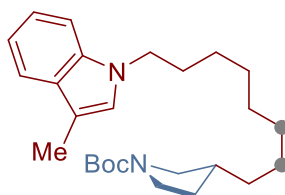
tert-butyl 4-(6-(1,3-dioxoisindolin-2-yl)hexyl)piperidine-1-carboxylate (3.4.5e):

Following the general procedure B, but using 2-(hex-4-en-1-yl)isoindoline-1,3-dione (**3.4.2x**, 137.4 mg, 0.60 mmol), afforded **3.4.5e** (42 mg, 51% yield) as a colorless oil. In an independent experiment, 41 mg (50% yield) were obtained, giving an average of 50% yield, 40:1 ratio. ¹H NMR (400 MHz, CDCl₃) δ 7.82 (dd, *J* = 5.4, 3.0 Hz, 2H), 7.69 (dd, *J* = 5.5, 3.0 Hz, 2H), 4.03 (brs, 2H), 3.65 (t, *J* = 7.8 Hz, 2H), 2.63 (t, *J* = 12.7 Hz, 2H), 1.71 – 1.54 (m, 4H), 1.43 (s, 9H), 1.35 – 1.23 (m, 7H), 1.22 – 1.15 (m, 2H), 1.07 – 0.97 (m, 2H) ppm. ¹³C NMR (101 MHz, CDCl₃) δ 168.5, 155.0, 134.0, 132.3, 123.2, 79.2, 44.2, 38.1, 36.5, 36.0, 32.3, 29.4, 28.6 (left), 28.6 (right), 26.9, 26.5 ppm. **IR** (neat, cm⁻¹): 2974, 2926, 2854, 1772, 1710, 1687, 1421, 1394, 1364, 1238, 1161, 1087, 964, 867. **HRMS** calcd. for (C₂₄H₃₄N₂NaO₄) [M+Na]⁺: 437.2411 found 437.2415.



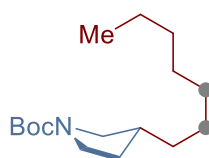
tert-butyl 4-(4,8-dimethylnon-7-en-1-yl)piperidine-1-carboxylate (3.4.5f):

Following the general procedure B, but using 4-decenal (**3.4.2y**, 108 μL, 0.60 mmol), afforded **3.4.5f** (35 mg, 52% yield) as a light yellow oil. In an independent experiment, 37 mg (54% yield) were obtained, giving an average of 53% yield, 29:1 ratio. ¹H NMR (400 MHz, CDCl₃) δ 4.10 (t, *J* = 7.1 Hz, 2H), 2.75 (t, *J* = 12.7 Hz, 2H), 2.51 – 2.28 (m, 3H), 1.76 (t, *J* = 13.5 Hz, 2H), 1.59 – 1.50 (m, 3H), 1.50 – 1.47 (m, 1H), 1.44 (s, 9H), 1.31 – 1.20 (m, 12H), 0.86 (t, *J* = 6.8 Hz, 3H) ppm. ¹³C NMR (101 MHz, CDCl₃) δ 212.6, 154.8, 79.7, 48.7, 43.4, 40.7, 32.0, 29.5, 29.4, 29.37, 28.6, 27.7, 23.8, 22.8, 14.2 ppm. **IR** (neat, cm⁻¹): 2974, 2924, 2854, 1692, 1448, 1420, 1365, 1277, 1234, 1166, 1132, 1013, 976, 866. **HRMS** calcd. for (C₂₀H₃₇NNaO₃) [M+Na]⁺: 362.2666 found 362.2661.

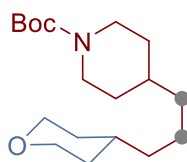


tert-butyl-3-(8-(3-methyl-1*H*-indol-1-yl)octyl)pyrrolidine-1-carboxylate (3.4.5g):

Following the general procedure B, but using 1-(1-(*tert*-butoxycarbonyl)pyrrolidin-3-yl)-2,4,6-triphenylpyridin-1-ium tetrafluoroborate (**3.4.1f**, 112.8 mg, 0.20 mmol) and 3-methyl-1-(oct-5-en-1-yl)-1*H*-indole (**3.4.2z**, 144.6 mg, 0.60 mmol), afforded **3.4.5g** (45 mg, 55% yield) as a colorless oil. In an independent experiment, 45 mg (55% yield) were obtained, giving an average of 55% yield, 99:1 ratio. ¹H NMR (400 MHz, CDCl₃) δ 7.57 (dt, *J* = 7.9, 1.0 Hz, 1H), 7.29 (dt, *J* = 8.2, 0.9 Hz, 1H), 7.19 (ddd, *J* = 8.2, 6.9, 1.2 Hz, 1H), 7.09 (ddd, *J* = 7.9, 6.9, 1.0 Hz, 1H), 6.87 (q, *J* = 1.1 Hz, 1H), 4.05 (t, *J* = 7.1 Hz, 2H), 3.53 – 3.40 (m, 2H), 3.27 – 3.20 (m, 1H), 2.83 (t, *J* = 9.6 Hz, 1H), 2.33 (d, *J* = 1.1 Hz, 3H), 2.11 – 2.03 (m, 1H), 1.99 – 1.92 (m, 1H), 1.84 – 1.77 (m, 2H), 1.487 (s, 9H), 1.33 – 1.25 (m, 13H) ppm. ¹³C NMR (101 MHz, CDCl₃) δ 154.8, 136.4, 128.8, 125.5, 121.3, 119.1, 118.5, 110.1, 109.3, 79.0, 51.6, 46.2, 45.8, 38.9, 33.3, 31.7, 30.5, 29.8, 29.5, 29.4, 28.7, 28.3, 27.1, 9.7 ppm. IR (neat, cm⁻¹): 2975, 2925, 2854, 1693, 1467, 1401, 1364, 1169, 1126, 1110, 882. HRMS calcd. for (C₂₆H₄₀N₂NaO₂) [M+Na]⁺: 435.2982 found 435.2990.

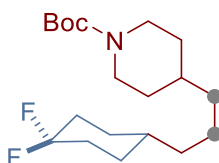


tert-butyl-3-heptylpyrrolidine-1-carboxylate (3.4.5h): Following the general procedure B, but using 1-(1-(*tert*-butoxycarbonyl)pyrrolidin-3-yl)-2,4,6-triphenylpyridin-1-ium tetrafluoroborate (**3.4.1f**, 112.8 mg, 0.20 mmol) and *trans*-2-heptene (**3.4.2t**, 84 μL, 0.60 mmol), afforded **3.4.5h** (43 mg, 80% yield) as a light yellow oil. In an independent experiment, 42 mg (78% yield) were obtained, giving an average of 79% yield, 99:1 ratio. ¹H NMR (400 MHz, CDCl₃) δ 3.68 – 3.32 (m, 2H), 3.30 – 3.11 (m, 1H), 2.82 (dt, *J* = 19.6, 9.7 Hz, 1H), 2.12 – 2.01 (m, 1H), 1.98 – 1.91 (m, 1H), 1.44 (s, 9H), 1.40 – 1.11 (m, 13H), 0.87 (t, *J* = 6.8 Hz, 3H) ppm. ¹³C NMR (126 MHz, CDCl₃) δ 154.8, 79.0, 51.9, 51.4, 45.9, 45.5, 39.3, 38.4, 33.4, 32.1, 32.0, 31.3, 29.84, 29.8, 29.4, 28.7, 28.4, 22.8, 14.2 ppm. IR (neat, cm⁻¹): 2977, 2959, 2924, 2855, 1696, 1455, 1399, 1364, 1254, 1168, 1135, 1111, 883. HRMS calcd. for (C₁₆H₃₁NNaO₂) [M+Na]⁺: 292.2247 found 292.2235.

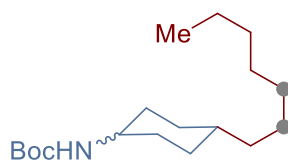


tert-butyl 4-(3-(tetrahydro-2*H*-pyran-4-yl)propyl)piperidine-1-carboxylate (3.4.5i): Following the general procedure B, but using 2,4,6-triphenyl-1-(tetrahydro-2*H*-pyran-4-yl)pyridin-1-ium tetrafluoroborate (**3.4.1e**, 95.8 mg, 0.20 mmol) and *tert*-butyl-4-(prop-1-en-1-yl)piperidine-1-carboxylate (135.7 mg, 0.60 mmol),

afforded **3.4.5i** (42 mg, 68% yield) as a colorless oil. In an independent experiment, 40 mg (64% yield) were obtained, giving an average of 66% yield, 99:1 ratio. $^1\text{H NMR}$ (400 MHz, CDCl_3) δ 4.04 (brs, 2H), 3.92 (ddt, $J = 11.5, 4.5, 1.1$ Hz, 2H), 3.34 (td, $J = 11.8, 2.1$ Hz, 2H), 2.64 (t, $J = 12.7$ Hz, 2H), 1.70 – 1.51 (m, 4H), 1.46 – 1.38 (m, 1H), 1.43 (s, 9H), 1.35 – 1.26 (m, 3H), 1.25 – 1.15 (m, 6H), 1.09 – 0.99 (m, 2H) ppm. $^{13}\text{C NMR}$ (101 MHz, CDCl_3) δ 155.0, 79.2, 68.3, 44.1, 37.2, 36.8, 36.1, 35.0, 33.3, 32.3, 28.6, 23.4 ppm. **IR** (neat, cm^{-1}): 2974, 2925, 2856, 2840, 1693, 1401, 1409, 1363, 1274, 1234, 1163, 1145, 1095, 975, 865. **HRMS** calcd. for $(\text{C}_{18}\text{H}_{33}\text{NNaO}_3)$ $[\text{M}+\text{Na}]^+$: 334.2353 found 334.2345.



tert-butyl 4-(3-(4,4-difluorocyclohexyl)propyl)piperidine-1-carboxylate (3.4.5j): Following the general procedure B, but using 1-(4,4-difluorocyclohexyl)-2,4,6-triphenylpyridin-1-ium tetrafluoroborate (**3.4.1c**, 102.6 mg, 0.20 mmol) and *tert*-butyl-4-(prop-1-en-1-yl)piperidine-1-carboxylate (135.7 mg, 0.60 mmol), afforded **3.4.5j** (42 mg, 61% yield) as a light yellow oil. In an independent experiment, 44 mg (64% yield) were obtained, giving an average of 62% yield, 22:1 regioisomeric ratio. $^1\text{H NMR}$ (400 MHz, CDCl_3) δ 4.04 (brs, 2H), 2.65 (t, $J = 12.8$ Hz, 2H), 2.23 – 1.95 (m, 2H), 1.77 – 1.70 (m, 3H), 1.67 – 1.58 (m, 3H), 1.44 (s, 9H), 1.39 – 1.16 (m, 10H), 1.10 – 1.00 (m, 2H) ppm. $^{13}\text{C NMR}$ (101 MHz, CDCl_3) δ 155.0, 124.0 (dd, $J = 241.8, 239.4$ Hz), 79.3, 44.2, 36.8, 36.1, 35.9 (dd, $J = 17.1, 2.0$ Hz), 33.7 (dd, $J = 25.4, 22.2$ Hz), 32.3, 29.1, 29.0, 28.6, 24.2 ppm. $^{19}\text{F NMR}$ (376 MHz, CDCl_3) δ -91.51 (d, $J = 234.3$ Hz), -102.01 (d, $J = 234.0$ Hz) ppm. **IR** (neat, cm^{-1}): 2975, 2927, 2851, 1689, 1448, 1420, 1364, 1274, 1243, 1166, 1149, 1117, 1081, 961, 869. **HRMS** calcd. for $(\text{C}_{19}\text{H}_{33}\text{F}_2\text{NNaO}_2)$ $[\text{M}+\text{Na}]^+$: 368.2372 found 368.2373.

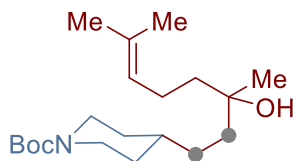


tert-butyl (4-heptylcyclohexyl)carbamate (3.4.5k): Following the general procedure B, but using 1-(4-((*tert*-butoxycarbonyl)amino)cyclohexyl)-2,4,6-triphenylpyridin-1-ium tetrafluoroborate (**3.4.1d**, 118.4 mg, 0.20 mmol) and *trans*-2-heptene (**3.4.2t**, 84 μL , 0.60 mmol), afforded **3.4.5k** (33 mg, 56% yield) as a white solid. In an independent experiment, 35 mg (59% yield) were obtained, giving an average of 57% yield, as a 1.5:1 mixture of diastereoisomers. **Mp** 69 – 70 $^\circ\text{C}$. $^1\text{H NMR}$ (400 MHz, CDCl_3) δ 4.64 – 4.3 (m, 1H), 3.72 – 3.33 (m, 1H), 2.00 – 1.93 (m, 1H), 1.76 – 1.71 (m, 1H), 1.65 – 1.53 (m, 2H), 1.43 (d, $J = 3.0$ Hz, 9H), 1.35 – 0.91 (m, 17H), 0.87 (td, $J =$

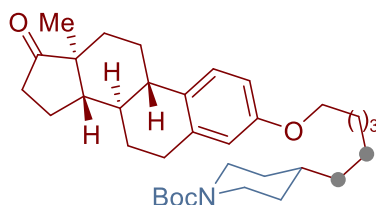
Site-Selective Ni-Catalyzed Deaminative Alkylation of Unactivated Olefins

6.9, 1.9 Hz, 3H) ppm. ^{13}C NMR (101 MHz, CDCl_3) δ 155.4, 79.1, 50.2, 46.8, 37.02 (left), 37.02 (right), 35.8, 35.7, 33.7, 32.1, 32.0, 30.02, 30.0, 29.95, 29.5, 28.59, 28.57, 28.1, 27.22, 27.17, 22.8, 14.2 ppm. **IR** (neat, cm^{-1}): 3370, 3726, 2920, 2849, 1683, 1515, 1453, 1388, 1363, 1174, 1043, 783. **HRMS** calcd. for $(\text{C}_{18}\text{H}_{35}\text{NNaO}_2)$ $[\text{M}+\text{Na}]^+$: 320.2560 found 320.2558.

3.7.6 Deaminative Alkylation in Late-Stage Functionalization

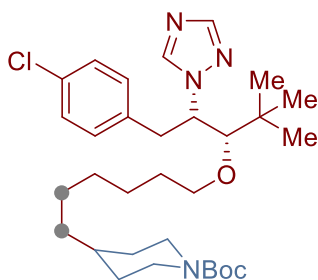


tert-butyl 4-(3-hydroxy-3,7-dimethyloct-6-en-1-yl)piperidine-1-carboxylate (3.4.6a): Following the general procedure, but using linalool (106 μL , 0.60 mmol), afforded **3.4.6a** (27 mg, 40% yield) as a colorless oil. In an independent experiment, 28 mg (41% yield) were obtained, giving an average of 40% yield. $^1\text{H NMR}$ (400 MHz, CDCl_3) δ 5.17 – 5.09 (m, 1H), 4.12 – 4.01 (m, 2H), 2.72 – 2.59 (m, 2H), 2.08 – 1.96 (m, 2H), 1.70 – 1.60 (m, 8H), 1.50 – 1.45 (m, 3H), 1.44 (s, 9H), 1.34 – 1.22 (m, 5H), 1.15 (s, 3H), 1.13 – 1.03 (m, 2H) ppm. $^{13}\text{C NMR}$ (101 MHz, CDCl_3) δ 155.0, 131.9, 124.5, 79.3, 72.8, 44.2, 41.6, 39.0, 36.7, 32.4, 30.8, 28.6, 27.0, 25.8, 22.8, 17.8 ppm. **IR** (neat, cm^{-1}): 3451, 2969, 2927, 2855, 1672, 1424, 1365, 1277, 1244, 1157, 965, 866. **HRMS** calcd. for $(\text{C}_{20}\text{H}_{37}\text{NNaO}_3)$ $[\text{M}+\text{Na}]^+$: 362.2666 found 362.2654.

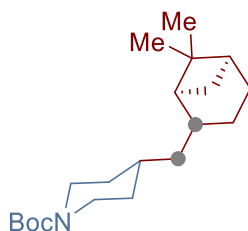


tert-butyl 4-(6-(((8R,9S,13S,14S)-13-methyl-17-oxo-7,8,9,11,12,13,14,15,16,17-decahydro-6H-cyclopenta[a]phenanthren-3-yl)oxy)hexyl)piperidine-1-carboxylate (3.4.6b): Following the general procedure, but using (8R,9S,13S,14S)-3-(hex-5-en-1-yloxy)-13-methyl-6,7,8,9,11,12,13,14,15,16-decahydro-17H-cyclopenta[a]phenanthrene-17-one (202.9 mg, 0.60 mmol), afforded **3.4.6b** (81 mg, 75% yield) as a white solid. In an independent experiment, 81 mg (75% yield) were obtained, giving an average of 75% yield. **Mp** 119–119 $^{\circ}\text{C}$. $[\alpha]_{\text{D}}^{20} = +84.6^{\circ}$ ($c = 0.1$, CH_2Cl_2). $^1\text{H NMR}$ (400 MHz, CDCl_3) δ 7.18 (dd, $J = 8.7, 1.1$ Hz, 1H), 6.70 (dd, $J = 8.6, 2.8$ Hz, 1H), 6.63 (d, $J = 2.7$ Hz, 1H), 4.06 (d, $J = 13.2$ Hz, 2H), 3.92 (t, $J = 6.5$ Hz, 2H), 2.93 – 2.83 (m, 2H), 2.66 (td, $J = 12.8, 2.7$ Hz, 2H), 2.54 – 2.44 (m, 1H), 2.41 – 2.35 (m, 1H), 2.29 – 2.19 (m, 1H), 2.18 – 1.90 (m, 4H), 1.79 – 1.69 (m, 2H), 1.67 – 1.52 (m, 5H), 1.48 – 1.40 (m, 5H), 1.45 (s, 9H), 1.36 – 1.30 (m, 5H), 1.25 – 1.21 (m, 2H), 1.11 – 1.01 (m, 2H), 0.90 (s, 3H) ppm. $^{13}\text{C NMR}$ (101 MHz, CDCl_3) δ 220.9, 157.2, 154.9, 137.7, 126.3, 114.6, 112.1, 79.1, 67.9, 50.4, 48.0, 44.1, 44.0, 38.4, 36.5, 36.0, 35.9, 32.2, 31.6, 29.7, 29.6, 29.3, 28.5, 26.6, 26.55, 26.1, 25.9, 21.6, 13.9 ppm. **IR** (neat, cm^{-1}): 2926, 2851, 2837, 1735, 1694, 1473, 1407, 1366, 1276, 1239, 1165, 1148, 1096, 1056, 1007, 869. **HRMS** calcd. for $(\text{C}_{34}\text{H}_{51}\text{NNaO}_4)$ $[\text{M}+\text{Na}]^+$:

560.3710 found 560.3720.

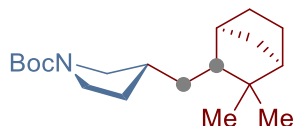


tert-butyl 4-(6-(((2*S*,3*S*)-1-(4-chlorophenyl)-4,4-dimethyl-2-(1*H*-1,2,4-triazol-1-yl)pentan-3-yl)oxy)hexyl)piperidine-1-carboxylate (3.4.6c): Following the general procedure, but using 1-(1-(*tert*-butoxycarbonyl)piperidin-4-yl)-2,4,6-triphenylpyridin-1-ium tetrafluoroborate (**3.4.1a**, 231.2 mg, 0.40 mmol), 1-((2*R*,3*R*)-1-(4-chlorophenyl)-3-(hex-5-en-1-yloxy)-4,4-dimethylpentan-2-yl)-1*H*-1,2,4-triazole (**3.4.2 ad**, 75 mg, 0.20 mmol), NiBr₂·DME (15 mol%, 9.3 mg) and **L3.4.10** (22.5 mol%, 12 mg) afforded **3.4.6c** (57 mg, 51% yield) as a light yellow oil. In an independent experiment, 57 mg (51% yield) were obtained, giving an average of 51% yield. ¹H NMR (400 MHz, CDCl₃) δ 8.39 (s, 1H), 7.74 (s, 1H), 7.21 – 7.13 (m, 2H), 6.95 – 6.87 (m, 2H), 4.81 – 4.77 (m, 1H), 4.05 (s, 2H), 3.66 (t, *J* = 6.5 Hz, 2H), 3.23 – 3.05 (m, 3H), 2.65 (t, *J* = 12.7 Hz, 2H), 1.70 – 1.58 (m, 4H), 1.43 (s, 9H), 1.42 – 1.39 (m, 1H), 1.36 – 1.28 (m, 5H), 1.22 (d, *J* = 6.9 Hz, 3H), 1.10 – 1.00 (m, 2H), 0.72 (s, 9H) ppm. ¹³C NMR (101 MHz, CDCl₃) δ 155.0, 149.8, 143.6, 135.4, 132.9, 130.0, 128.9, 87.2, 79.2, 75.6, 63.6, 44.2, 40.8, 36.6, 36.3, 36.1, 32.3, 30.7, 29.9, 28.6, 26.7, 26.54, 26.50 ppm. IR (neat, cm⁻¹): 3076, 2982, 2934, 2865, 1457, 1380, 1254, 1210, 1168, 1111, 1068, 999, 916. HRMS calcd. for (C₃₁H₅₀ClN₄O₃) [M+H]⁺: 561.3566 found 561.3578.

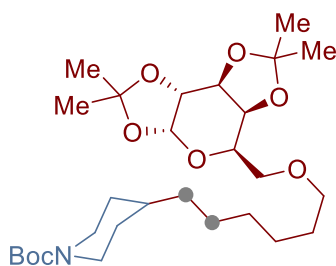


tert-butyl 4-(((1*S*,5*S*)-6,6-dimethylbicyclo[3.1.1]heptan-2-yl)methyl)piperidine-1-carboxylate (3.4.6d): Following the general procedure B, but using (–)-β-pinene (**3.4.2ae**, 93.6 μL, 0.60 mmol), afforded **3.4.6d** (48 mg, 75% yield) as a colorless oil. In an independent experiment, 49 mg (76% yield) were obtained, giving an average of 75% yield, as a 97:3 mixture of diastereoisomers. [α]_D²⁰ = +4.0° (c = 0.1, CH₂Cl₂) ¹H NMR (400 MHz, CDCl₃) δ 5.06 (dt, *J* = 2.5, 1.3 Hz, 1H), 4.05 (brs, 2H), 2.67 (q, *J* = 14.2 Hz, 2H), 1.96 – 1.77 (m, 2H), 1.75 – 1.50 (m, 6H), 1.44 (s, 9H), 1.42 – 1.35 (m, 1H), 1.34 – 1.08 (m, 4H), 0.97 (td, *J* = 10.2, 5.1 Hz, 2H), 0.90 (s, 3H), 0.75 (s, 3H) ppm. ¹³C NMR (101 MHz, CDCl₃) δ 155.0, 133.6, 131.1, 79.2, 44.2, 40.2, 37.0, 34.7,

34.0, 33.97, 31.6, 30.5, 29.2, 28.6, 24.9, 23.6, 23.2 ppm. **IR** (neat, cm^{-1}): 2959, 2923, 2862, 1692, 1421, 1364, 1278, 1245, 1220, 1165, 1150, 1125, 1069, 967. **HRMS** calcd. for $(\text{C}_{20}\text{H}_{35}\text{NNaO}_2)$ $[\text{M}+\text{Na}]^+$: 344.2560 found 344.2558.

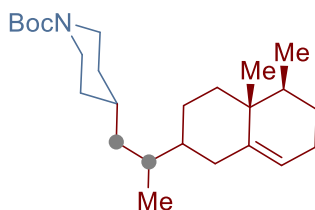


tert-butyl-3-((1S,4R)-3,3-dimethylbicyclo[2.2.1]heptan-2-yl)methylpyrrolidine-1-carboxylate (3.4.6e): Following the general procedure B, but using 1-(1-(*tert*-butoxycarbonyl)pyrrolidin-3-yl)-2,4,6-triphenylpyridin-1-iumtetrafluoroborate (**3.4.1f**, 112.8 mg, 0.20 mmol) and camphene (**3.4.2af**, 96.9 μL , 0.60 mmol), afforded **3.4.6e** (31 mg, 50% yield) as a colorless oil. In an independent experiment, 25 mg (41% yield) were obtained, giving an average of 46% yield, as a 46:40:7:7 mixture of diastereoisomers. **^1H NMR** (400 MHz, CDCl_3) δ 3.61 – 3.35 (m, 2H), 3.26 – 3.15 (m, 1H), 2.94 – 2.71 (m, 1H), 2.18 – 1.86 (m, 3H), 1.74 – 1.53 (m, 3H), 1.45 (s, 9H), 1.44 – 1.10 (m, 7H), 1.07 – 0.74 (m, 7H) ppm. **^{13}C NMR** (101 MHz, CDCl_3) δ 154.8, 79.0, 52.9, 52.5, 52.1, 51.6, 51.3, 49.5, 49.4, 49.2, 49.1, 48.9, 48.8, 48.6, 46.0, 45.9, 45.7, 45.6, 44.5, 44.48, 44.4, 41.3, 41.2, 41.1, 41.0, 40.6, 38.42, 38.4, 38.2, 38.11, 38.1, 37.8, 37.77, 37.6, 37.5, 37.46, 37.14, 37.1, 36.6, 35.9, 33.0, 32.5, 32.4, 32.3, 32.0, 31.9, 31.6, 31.0, 30.3, 30.2, 29.9, 29.8, 29.5, 28.7, 28.1, 25.9, 24.9, 24.8, 24.2, 23.02, 23.0, 21.9, 21.6, 21.5, 21.0, 20.2, 20.1 ppm. **IR** (neat, cm^{-1}): 2933, 2874, 1695, 1478, 1455, 1399, 1364, 1255, 1169, 1118, 883. **HRMS** calcd. for $(\text{C}_{19}\text{H}_{33}\text{NNaO}_2)$ $[\text{M}+\text{Na}]^+$: 330.2404 found 330.2404.

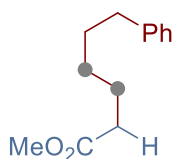


tert-butyl-4-(6-(((3aR,5R,5aS,8aS,8bR)-2,2,7,7-tetramethyltetrahydro-5H-bis([1,3]dioxolo)[4,5-b:4',5'-d]pyran-5-yl)methoxy)hexyl)piperidine-1-carboxylate (3.4.6f): Following the general procedure, but using (3aR,5R,5aS,8aS,8bR)-5-((hex-5-en-1-yloxy)methyl)-2,2,7,7-tetramethyltetrahydro-5H-bis([1,3]dioxolo)[4,5-b:4',5'-d]pyran (**3.4.2ag**, 195 mg, 0.60 mmol), afforded **3.4.6f** (61 mg, 58% yield) as a colorless oil. In an independent experiment, 61 mg (58% yield) were obtained, giving an average of 58% yield. **^1H NMR** (400 MHz, CDCl_3) δ 5.51 (d, $J = 5.0$ Hz, 1H), 4.57 (dd, $J = 7.9, 2.4$ Hz, 1H), 4.28 (dd, $J = 5.0, 2.4$ Hz, 1H), 4.23 (dd, $J = 7.9, 1.9$ Hz, 1H), 4.03 (d, $J = 13.3$ Hz, 2H), 3.93 (td, $J = 6.2, 1.9$ Hz, 1H), 3.64 – 3.52 (m, 2H), 3.50 – 3.39 (m, 2H), 2.63 (td, $J = 12.9, 2.7$ Hz, 2H), 1.64 – 1.52 (m, 5H), 1.51 (s,

3H), 1.43 (s, 9H), 1.42 (s, 3H), 1.31 (s, 3H), 1.30 (s, 3H), 1.28 – 1.16 (m, 8H), 1.08 – 0.97 (m, 2H) ppm. ^{13}C NMR (101 MHz, CDCl_3) δ 155.0, 109.3, 108.6, 96.5, 79.2, 71.6, 71.3, 70.8, 70.7, 69.4, 66.8, 44.2, 36.6, 36.1, 32.3, 29.7, 29.67, 28.6, 26.7, 26.2, 26.13, 26.1, 25.1, 24.6 ppm. IR (neat, cm^{-1}): 2980, 2928, 2855, 1740, 1691, 1422, 1367, 1244, 1211, 1166, 1111, 1069, 1001, 892. HRMS calcd. for $(\text{C}_{28}\text{H}_{49}\text{NNaO}_8)$ $[\text{M}+\text{Na}]^+$: 550.3350 found 550.3334.

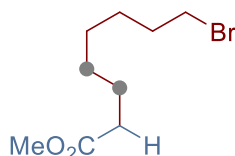


tert-butyl 4-(2-((8*S*,8*aR*)-8,8*a*-dimethyl-1,2,3,4,6,7,8,8*a*-octahydronaphthalen-2-yl)propyl)piperidine-1-carboxylate (3.4.6g): Following the general procedure B, but using valencene (3.4.2ah, 133 μL , 0.60 mmol), afforded 3.4.6g (37 mg, 48% yield) as a colorless oil. In an independent experiment, 34 mg (44% yield) were obtained, giving an average of 46% yield, as a 9:1 mixture of diastereoisomers. ^1H NMR (400 MHz, CDCl_3) δ 5.28 (dt, $J = 4.3, 2.0$ Hz, 1H), 4.05 (brs, 2H), 2.91 – 2.57 (m, 2H), 2.34 – 2.15 (m, 1H), 2.12 – 1.80 (m, 2H), 1.77 – 1.54 (m, 5H), 1.44 (s, 9H), 1.49 – 1.33 (m, 5H), 1.29 – 1.17 (m, 2H), 1.13 – 0.93 (m, 4H), 0.94 – 0.74 (m, 10H) ppm. ^{13}C NMR (101 MHz, CDCl_3) δ 155.0, 144.8 (left), 144.8 (right), 143.97 (left), 143.97 (right), 119.84, 119.8, 119.3, 119.2, 79.2, 44.4, 44.35, 44.2, 43.9, 42.5, 41.9, 41.44, 41.4, 41.28, 41.27, 41.0, 40.8, 40.5, 38.8, 38.7, 38.2, 38.1, 38.0, 37.8, 35.1, 34.8, 34.3, 34.2, 34.0, 33.7, 33.69, 33.6, 33.5, 33.4, 33.1, 32.9, 32.7, 32.68, 31.9, 31.7, 31.28, 31.26, 30.0, 29.8, 28.6, 28.1, 28.0, 27.33, 27.3, 26.0, 18.68, 18.67, 18.2, 18.18, 16.5, 16.45, 16.2, 16.1, 15.9, 15.8 ppm. IR (neat, cm^{-1}): 2965, 2918, 2853, 1693, 1422, 1365, 1277, 1246, 1170, 1149, 973, 910, 865. HRMS calcd. for $(\text{C}_{25}\text{H}_{43}\text{NNaO}_2)$ $[\text{M}+\text{Na}]^+$: 412.3186 found 412.3195.

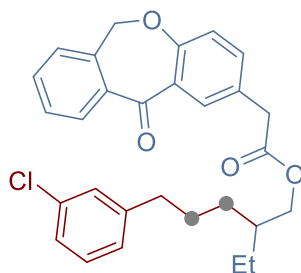


methyl 6-phenylhexanoate (4.4.6h): Following the general procedure, but using 1-(2-methoxy-2-oxoethyl)-2,4,6-triphenylpyridin-1-ium tetrafluoroborate (3.4.1i, 93.6 mg, 0.2 mmol) and 4-phenyl-1-butene (90 μL , 0.60 mmol) at 80 $^\circ\text{C}$, afforded 3.4.6h (24 mg, 58% yield) as a light yellow oil. In an independent experiment, 20 mg (52% yield) were obtained, giving an average of 55% yield. ^1H NMR (400 MHz, CDCl_3) δ 7.31 – 7.25 (m, 2H), 7.21 – 7.14 (m, 3H), 3.67 (s, 3H), 2.62 (t, $J = 7.6$ Hz, 2H), 2.31 (t, $J = 7.5$ Hz, 2H), 1.72 – 1.59 (m, 4H), 1.43 – 1.32 (m, 2H) ppm. ^{13}C NMR (101 MHz, CDCl_3) δ 174.3, 142.6, 128.5, 128.4, 125.8, 51.6, 35.8, 34.1, 31.2, 28.9, 24.9 ppm. IR

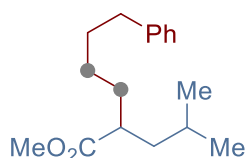
(neat, cm^{-1}): 3027, 2933, 2858, 1734, 1496, 1453, 1368, 1263, 1193, 1158, 1030, 822. The observed spectral data are in agreement with the ones reported in literature.¹⁶



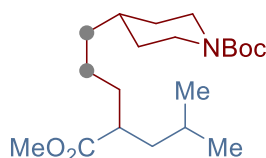
methyl 8-bromooctanoate (3.4.6i): Following the general procedure, but using 1-(2-methoxy-2-oxoethyl)-2,4,6-triphenylpyridin-1-ium tetrafluoroborate (**3.4.1i**, 93.6 mg, 0.2 mmol) and 6-bromo-1-hexene (**3.4.2f**, 80 μL , 0.60 mmol) at 80 $^{\circ}\text{C}$, afforded **3.4.6i** (23 mg, 49% yield) as a light yellow oil. In an independent experiment, 23 mg (49% yield) were obtained, giving an average of 49% yield. $^1\text{H NMR}$ (400 MHz, CDCl_3) δ 3.66 (s, 3H), 3.39 (t, $J = 6.8$ Hz, 2H), 2.30 (t, $J = 7.5$ Hz, 2H), 1.89 – 1.80 (m, 2H), 1.66 – 1.58 (m, 2H), 1.45 – 1.39 (m, 2H), 1.34 – 1.24 (m, 4H) ppm. $^{13}\text{C NMR}$ (101 MHz, CDCl_3) δ 174.3, 51.6, 34.2, 34.0, 32.8, 29.1, 28.5, 28.1, 25.0 ppm. **IR** (neat, cm^{-1}): 2931, 2856, 1736, 1435, 1361, 1237, 1194, 1170, 1122, 1016, 881. The observed spectral data are in agreement with the ones reported in literature.¹⁷



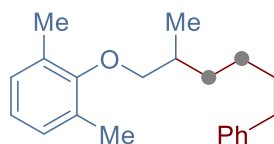
5-(3-chlorophenyl)-2-ethylpentyl 2-(11-oxo-6,11-dihydrodibenzo[*b,e*]oxepin-2-yl)acetate (3.4.6j): Following the general procedure, but using 1-(1-(2-(11-oxo-6,11-dihydrodibenzo[*b,e*]oxepin-2-yl)acetoxymethyl)butan-2-yl)-2,4,6-triphenylpyridin-1-ium tetrafluoroborate (**3.4.1j**, 143 mg, 0.20 mmol) and 1-allyl-3-chlorobenzene (87.2 μL , 0.60 mmol), afforded **3.4.6j** (68 mg, 71% yield) as a colorless oil. In an independent experiment, 67 mg (70% yield) were obtained, giving an average of 70% yield. $^1\text{H NMR}$ (400 MHz, CDCl_3) δ 8.13 (d, $J = 2.4$ Hz, 1H), 7.88 (dd, $J = 7.7, 1.4$ Hz, 1H), 7.55 (td, $J = 7.5, 1.4$ Hz, 1H), 7.46 (td, $J = 7.6, 1.3$ Hz, 1H), 7.41 (dd, $J = 8.4, 2.4$ Hz, 1H), 7.36 (dd, $J = 7.4, 1.3$ Hz, 1H), 7.23 – 7.08 (m, 3H), 7.04 – 7.00 (m, 2H), 5.17 (s, 2H), 4.02 (dd, $J = 5.8, 1.4$ Hz, 2H), 3.63 (s, 2H), 2.53 (t, $J = 7.7$ Hz, 2H), 1.65 – 1.52 (m, 3H), 1.37 – 1.25 (m, 4H), 0.85 (t, $J = 7.5$ Hz, 3H) ppm. $^{13}\text{C NMR}$ (101 MHz, CDCl_3) δ 190.9, 171.6, 160.6, 144.6, 140.6, 136.5, 135.7, 134.1, 132.9, 132.6, 129.6, 129.58, 129.4, 128.6, 128.1, 127.9, 126.7, 126.0, 125.3, 121.1, 73.7, 67.2, 40.5, 38.8, 35.9, 30.4, 28.3, 23.8, 11.1 ppm. **IR** (neat, cm^{-1}): 3061, 2960, 2933, 2861, 1731, 1647, 1611, 1598, 1571, 1489, 1456, 1413, 1379, 1299, 1211, 1284, 1255, 1241, 1220, 1203, 1160, 1138, 1120, 1014. **HRMS** calcd. for ($\text{C}_{29}\text{H}_{29}\text{ClNaO}_4$) $[\text{M}+\text{Na}]^+$: 499.1647 found 499.1644.



methyl-2-isobutyl-6-phenylhexanoate (3.4.6k): Following the general procedure, but using 1-(1-methoxy-4-methyl-1-oxopentan-2-yl)-2,4,6-triphenylpyridin-1-ium tetra-fluoroborate (**3.4.1k**, 104.6 mg, 0.20 mmol) and 4-phenyl-1-butene (90 μ L, 0.60 mmol), afforded **3.4.6k** (26 mg, 50% yield) as a light yellow oil. In an independent experiment, 26 mg (50% yield) were obtained, giving an average of 50% yield. $^1\text{H NMR}$ (400 MHz, CDCl_3) δ 7.30 – 7.24 (m, 2H), 7.20 – 7.13 (m, 3H), 3.65 (s, 3H), 2.63 – 2.56 (m, 2H), 2.43 (tt, $J = 9.3, 5.3$ Hz, 1H), 1.65 – 1.42 (m, 6H), 1.35 – 1.20 (m, 3H), 0.88 (t, $J = 6.7$ Hz, 6H) ppm. $^{13}\text{C NMR}$ (101 MHz, CDCl_3) δ 177.3, 142.7, 128.5, 128.4, 125.8, 51.5, 43.8, 42.0, 35.9, 33.0, 31.5, 27.3, 26.4, 23.2, 22.3 ppm. **IR** (neat, cm^{-1}): 3027, 2933, 2858, 1734, 1496, 1453, 1368, 1263, 1193, 1155, 1030, 822. **HRMS** calcd. for $(\text{C}_{17}\text{H}_{26}\text{NaO}_2)$ $[\text{M}+\text{Na}]^+$: 285.1825 found 285.1822.

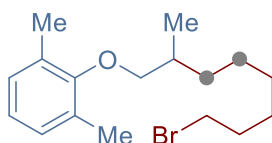


tert-butyl-4-(4-(methoxycarbonyl)-6-methylheptyl)piperidine-1-carboxylate (4.4.6l): Following the general procedure B, but using 1-(1-methoxy-4-methyl-1-oxopentan-2-yl)-2,4,6-triphenylpyridin-1-ium tetrafluoroborate (**3.4.1k**, 104.6 mg, 0.20 mmol) and *tert*-butyl-4-(prop-1-en-1-yl) piperidine-1-carboxylate (**3.4.2aa**, 135.7 mg, 0.60 mmol), afforded **3.4.6l** (35 mg, 49% yield) as a light yellow oil. In an independent experiment, 38 mg (53% yield) were obtained, giving an average of 51% yield, 26:1 ratio. $^1\text{H NMR}$ (400 MHz, CDCl_3) δ 4.04 (brs, 2H), 3.64 (s, 3H), 2.63 (t, $J = 12.4$ Hz, 2H), 2.41 (tt, $J = 9.3, 5.2$ Hz, 1H), 1.66 – 1.48 (m, 5H), 1.43 (s, 9H), 1.39 – 1.14 (m, 7H), 1.10 – 0.95 (m, 2H), 0.86 (dd, $J = 7.8, 6.5$ Hz, 6H) ppm. $^{13}\text{C NMR}$ (101 MHz, CDCl_3) δ 177.2, 155.0, 79.3, 51.4, 44.3, 43.8, 41.9, 36.5, 35.9, 33.2, 32.3, 32.2, 28.6, 26.3, 24.6, 23.1, 22.2 ppm. **IR** (neat, cm^{-1}): 2975, 2929, 2851, 1735, 1691, 1421, 1365, 1276, 1244, 1158, 972, 868. **HRMS** calcd. for $(\text{C}_{20}\text{H}_{37}\text{NNaO}_4)$ $[\text{M}+\text{Na}]^+$: 378.2615 found 378.2612.

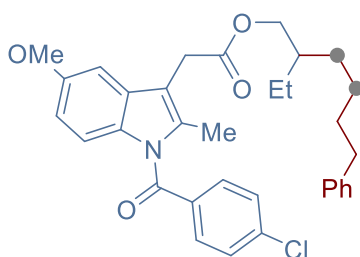


1,3-dimethyl-2-((2-methyl-6-phenylhexyl)oxy)benzene (3.4.6m): Following the general procedure, but using 1-(1-(2,6-dimethylphenoxy)propan-2-yl)-2,4,6-triphenylpyridin-1-ium tetrafluoroborate (**3.4.1l**, 111.6 mg, 0.2 mmol) and 4-phenyl-1-butene (90 μ L, 0.60 mmol), afforded **3.4.6m** (38 mg, 64% yield) as a light

yellow oil. In an independent experiment, 35 mg (59% yield) were obtained, giving an average of 61% yield. $^1\text{H NMR}$ (400 MHz, CDCl_3) δ 7.34 – 7.26 (m, 2H), 7.23 – 7.17 (m, 3H), 7.02 (dq, $J = 7.2, 0.7$ Hz, 2H), 6.92 (dd, $J = 8.2, 6.7$ Hz, 1H), 3.66 – 3.48 (m, 2H), 2.66 (t, $J = 7.7$ Hz, 2H), 2.01 – 1.93 (s, 6H), 1.97 (m, 1H), 1.75 – 1.59 (m, 3H), 1.52 – 1.37 (m, 2H), 1.34 – 1.28 (m, 1H), 1.10 (d, $J = 6.7$ Hz, 3H) ppm. $^{13}\text{C NMR}$ (101 MHz, CDCl_3) δ 156.0, 142.8, 131.0, 128.8, 128.4, 128.3, 125.6, 123.6, 77.1, 36.0, 34.3, 33.4, 31.8, 26.8, 17.2, 16.3 ppm. **IR** (neat, cm^{-1}): 3025, 2974, 2926, 2856, 1475, 1463, 1383, 1263, 1202, 1091, 1007, 980, 827. **HRMS** calcd. for $(\text{C}_{21}\text{H}_{29}\text{O})$ $[\text{M}+\text{H}]^+$: 297.2213 found 297.2214.

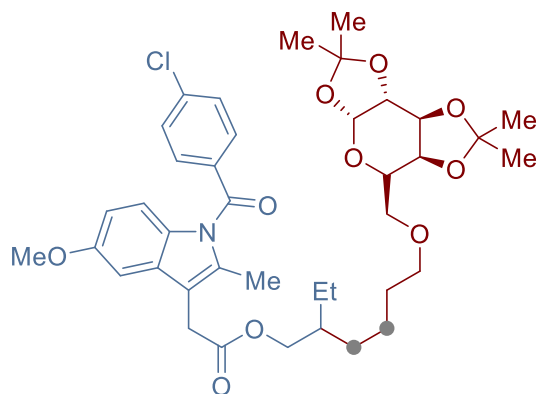


2-((8-bromo-2-methyloctyl)oxy)-1,3-dimethylbenzene (3.4.6n): Following the general procedure, but using 1-(1-(2,6-dimethylphenoxy)propan-2-yl)-2,4,6-triphenylpyridin-1-ium tetrafluoroborate (**3.4.11**, 111.6 mg, 0.2 mmol) and 6-bromo-1-hexene (**3.4.2f**, 80 μL , 0.60 mmol), afforded **3.4.6n** (37 mg, 57% yield) as a light yellow oil. In an independent experiment, 35 mg (54% yield) were obtained, giving an average of 55% yield. $^1\text{H NMR}$ (400 MHz, CDCl_3) δ 7.01 (d, $J = 7.2$ Hz, 2H), 6.91 (dd, $J = 8.2, 6.7$ Hz, 1H), 3.66 – 3.50 (m, 2H), 3.42 (t, $J = 6.9$ Hz, 2H), 2.28 (s, 6H), 2.01 – 1.83 (m, 3H), 1.64 – 1.56 (m, 1H), 1.49 – 1.43 (m, 2H), 1.41 – 1.33 (m, 3H), 1.31 – 1.22 (m, 2H), 1.10 (d, $J = 6.7$ Hz, 3H) ppm. $^{13}\text{C NMR}$ (101 MHz, CDCl_3) δ 156.0, 131.1, 128.9, 123.7, 77.3, 34.4, 34.1, 33.5, 32.9, 29.2, 28.3, 27.1, 17.2, 16.4 ppm. **IR** (neat, cm^{-1}): 2975, 2925, 2855, 1463, 1383, 1262, 1202, 1091, 1013, 981, 840. **HRMS** calcd. for $(\text{C}_{17}\text{H}_{28}\text{BrO}_2)$ $[\text{M}+\text{H}]^+$: 327.1318 found 327.1320.

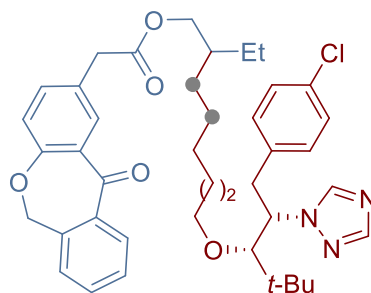


2-ethyl-6-phenylhexyl 2-(1-(4-chlorobenzoyl)-5-methoxy-2-methyl-1H-indol-3-yl)acetate (3.4.6o): Following the general procedure, but using 1-(1-(2-(1-(4-chlorobenzoyl)-5-methoxy-2-methyl-1H-indol-3-yl)acetoxyl)butan-2-yl)-2,4,6-triphenylpyridin-1-ium tetrafluoroborate (**3.4.1m**, 155 mg, 0.20 mmol) and 4-phenyl-1-butene (90 μL , 0.60 mmol), afforded **3.4.6o** (65 mg, 60% yield) as a light yellow oil. In an independent experiment, 67 mg (61% yield) were obtained, giving an average of 60% yield. $^1\text{H NMR}$ (400 MHz, CDCl_3) δ 6.42 – 6.34 (m, 2H), 6.23 – 6.15 (m, 2H), 6.05 – 5.96 (m, 2H), 5.94 – 5.85 (m, 3H), 5.71 (d, $J = 2.5$ Hz, 1H), 5.59

(d, $J = 8.9$ Hz, 1H), 5.40 (dd, $J = 9.0, 2.5$ Hz, 1H), 2.75 (d, $J = 5.7$ Hz, 2H), 2.56 (s, 3H), 2.40 (s, 2H), 1.32 – 1.23 (m, 2H), 1.14 (s, 3H), 0.33 – 0.21 (m, 3H), 0.04 – -0.04 (m, 6H), -0.42 (t, $J = 7.5$ Hz, 3H) ppm. ^{13}C NMR (101 MHz, CDCl_3) δ 171.1, 168.4, 156.2, 142.7, 139.4, 136.0, 134.1, 131.3, 130.9, 130.8, 129.2, 128.5, 128.4, 125.8, 115.1, 112.9, 111.8, 101.5, 67.4, 55.8, 38.9, 35.9, 31.8, 30.7, 30.6, 26.5, 23.9, 13.4, 11.1 ppm. IR (neat, cm^{-1}): 2958, 2929, 2857, 1731, 1682, 1603, 1477, 1455, 1355, 1313, 1260, 1222, 1164, 1141, 1066, 1036, 1015. HRMS calcd. for $(\text{C}_{33}\text{H}_{36}\text{ClNNaO}_4)$ $[\text{M}+\text{Na}]^+$: 568.2225 found 568.2227.



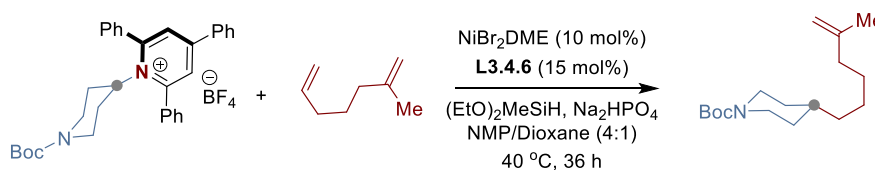
2-ethyl-8-(((3aR,5S,5aS,8aS,8bR)-2,2,7,7-tetramethyltetrahydro-5H-bis([1,3]dioxolo)[4,5-b:4',5'-d]pyran-5-yl)methoxy)octyl 2-(1-(4-chlorobenzoyl)-5-methoxy-2-methyl-1H-indol-3-yl)acetate (3.4.6p): Following the general procedure, but using 1-(1-(2-(1-(4-chlorobenzoyl)-5-methoxy-2-methyl-1H-indol-3-yl)acetoxyl)butan-2-yl)-2,4,6-triphenylpyridin-1-ium tetrafluoroborate (**3.4.1m**, 155 mg, 0.20 mmol) and (3aR,5R,5aS,8aS,8bR)-5-((hex-5-en-1-yloxy)methyl)-2,2,7,7-tetramethyl tetrahydro-5H-bis([1,3]dioxolo)[4,5-b:4',5'-d]pyran (**3.4.2ag**, 195 mg, 0.60 mmol), afforded **3.4.6p** (87 mg, 57% yield) as a light yellow oil. In an independent experiment, 83 mg (55% yield) were obtained, giving an average of 56% yield. ^1H NMR (400 MHz, CDCl_3) δ 7.70 – 7.62 (m, 2H), 7.51 – 7.44 (m, 2H), 6.96 (d, $J = 2.5$ Hz, 1H), 6.86 (d, $J = 9.0$ Hz, 1H), 6.66 (dd, $J = 9.0, 2.5$ Hz, 1H), 5.53 (d, $J = 5.0$ Hz, 1H), 4.59 (dd, $J = 7.9, 2.4$ Hz, 1H), 4.30 (dd, $J = 5.0, 2.4$ Hz, 1H), 4.25 (dd, $J = 7.9, 1.9$ Hz, 1H), 4.00 (dd, $J = 5.8, 2.6$ Hz, 2H), 3.98 – 3.93 (m, 1H), 3.83 (s, 3H), 3.65 (s, 2H), 3.63 – 3.53 (m, 2H), 3.50 – 3.40 (m, 2H), 2.38 (s, 3H), 1.57 – 1.50 (m, 6H), 1.44 (s, 3H), 1.33 (s, 3H), 1.32 (s, 3H), 1.30 – 1.24 (m, 5H), 1.23 – 1.18 (m, 5H), 0.82 (t, $J = 7.5$ Hz, 3H) ppm. ^{13}C NMR (101 MHz, CDCl_3) δ 171.1, 168.4, 156.2, 139.4, 135.9, 134.1, 131.3, 130.9, 130.8, 129.2, 115.1, 112.9, 111.8, 109.3, 108.6, 101.4, 96.5, 71.7, 71.4, 70.8, 70.8, 69.5, 67.4, 66.9, 55.8, 38.9, 30.8, 30.6, 29.9, 29.8, 29.7, 26.8, 26.2, 26.1, 25.1, 24.6, 23.9, 13.4, 11.1 ppm. IR (neat, cm^{-1}): 2978, 2930, 2856, 1732, 1684, 1593, 1478, 1457, 1371, 1357, 1314, 1255, 1212, 1167, 1110, 1067, 1000. HRMS calcd. for $(\text{C}_{41}\text{H}_{54}\text{ClNNaO}_{10})$ $[\text{M}+\text{Na}]^+$: 778.3328 found 778.3358.



8-(((2*S*,3*R*)-1-(4-chlorophenyl)-4,4-dimethyl-2-(1*H*-1,2,4-triazol-1-yl)pentan-3-yl)oxy)-2-ethyloctyl 2-(11-oxo-6,11-dihydrodibenzo[*b,e*]oxepin-2-yl)acetate (3.4.6q**):** Following the general procedure, but using 1-(1-(2-(11-oxo-6,11-dihydrodibenzo[*b,e*]oxepin-2-yl)acetoxy)butan-2-yl)-2,4,6-triphenylpyridin-1-ium tetrafluoroborate (**3.4.1j**, 286 mg, 0.40 mmol), 1-((2*R*,3*R*)-1-(4-chlorophenyl)-3-(hex-5-en-1-yloxy)-4,4-dimethylpentan-2-yl)-1*H*-1,2,4-triazole (**3.4.2ad**, 75 mg, 0.20 mmol), NiBr₂·DME (15 mol%, 9.3 mg) and **L3.4.6** (22.5 mol%, 12 mg), afforded **3.4.6q** (42 mg, 30% yield) as a colorless oil. In an independent experiment, 43 mg (30% yield) were obtained, giving an average of 30% yield. ¹H NMR (400 MHz, CDCl₃) δ 8.44 (s, 1H), 8.12 (d, *J* = 2.4 Hz, 1H), 7.88 (dd, *J* = 7.7, 1.4 Hz, 1H), 7.78 (s, 1H), 7.55 (td, *J* = 7.4, 1.4 Hz, 1H), 7.49 – 7.40 (m, 2H), 7.35 (dd, *J* = 7.4, 1.3 Hz, 1H), 7.21 – 7.15 (m, 2H), 7.02 (d, *J* = 8.4 Hz, 1H), 6.92 (d, *J* = 8.4 Hz, 2H), 5.18 (s, 2H), 4.83 – 4.78 (m, 1H), 4.02 (dd, *J* = 5.8, 1.5 Hz, 2H), 3.72 – 3.60 (m, 4H), 3.24 – 3.07 (m, 3H), 1.68 – 1.55 (m, 3H), 1.41 – 1.25 (m, 10H), 0.86 (t, *J* = 7.5 Hz, 3H), 0.74 (s, 9H) ppm. ¹³C NMR (101 MHz, CDCl₃) δ 190.9, 171.7, 160.6, 149.5, 143.5, 140.6, 136.5, 135.7, 135.4, 133.0, 132.9, 132.6, 130.0, 129.6, 129.4, 129.0, 128.2, 127.9, 125.3, 121.1, 87.3, 75.7, 73.8, 67.4, 63.8, 40.9, 40.5, 38.9, 36.4, 30.8, 30.7, 30.0, 26.8, 26.6, 26.5, 23.9, 11.2 ppm. IR (neat, cm⁻¹): 2956, 2928, 2858, 1731, 1648, 1612, 1599, 1490, 1456, 1412, 1377, 1299, 1275, 1220, 1201, 1161, 1136, 1120, 1094, 1014. HRMS calcd. for (C₄₁H₅₀ClN₃NaO₅) [M+Na]⁺: 722.3331 found 722.3354.

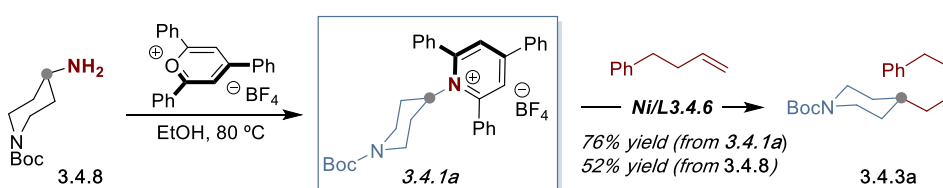
3.7.7 Large Scale Reaction and Synthetic Applications

3.7.7.1 Large Scale Reaction



An oven-dried 25 mL schlenk tube containing a stirring bar was charged with NiBr₂·DME (62 mg, 10 mol%), 4,4'-di-*tert*-butyl-2,2'-dipyridyl (**L3.4.6**, 80 mg, 15 mol%), Na₂HPO₄ (568 mg, 4.0 mmol) and 1-(1-(*tert*-butoxycarbonyl)piperidin-4-yl)-2,4,6-triphenylpyridin-1-ium tetrafluoroborate (**3.4.1a**, 1.156 g, 2.0 mmol). Subsequently, the tube was sealed with a Teflon screw cap, then evacuated and back-filled with Ar (3 times). Afterwards, 2-methylhexa-1,5-diene (**3.4.2I**, 674 μ L, 5.0 mmol), (EtO)₂MeSiH (960 μ L, 6 mmol, 3.0 equiv), NMP and 1,4-dioxane (4:1, 10 mL) were added via syringe. Then, the tube was stirred at 40 °C for 36 h. After the reaction was completed, and cool down to room temperature. The mixture was diluted with EtOAc, and washed with water. The aqueous phase was extracted with EtOAc (3 x 10 mL), and the combined organic phases were dried over MgSO₄ then concentrated. The residue was purified by column chromatography on silica gel (step gradient, Toluene to Hexane/EtOAc = 30:1), obtaining **3.4.3I** as colorless oil 315 mg (56% yield).

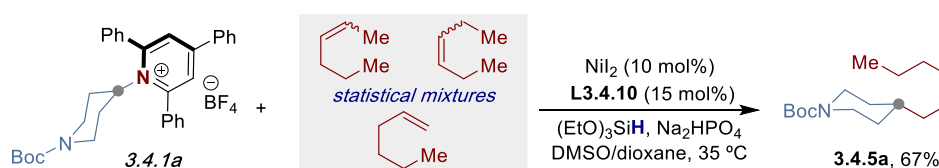
3.7.7.2 One-Pot Deaminative Alkylation without Isolation of Pyridinium Salts



An oven-dried 50 mL round-bottomed flask containing a stirring bar was charged with *tert*-butyl 4-aminopiperidine-1-carboxylate (**3.4.8**, 200 mg, 1.0 mmol) and 2,4,6-triphenylpyridinium tetrafluoroborate (400 mg, 1.0 mmol). After then EtOH (1.0 mL) was added via syringe. The mixture was stirred and heated at reflux in an oil bath at 80–85 °C for 4 h. After the reaction was completed, cool down to room temperature and concentrated. To the flask was added NiBr₂·DME (31 mg, 10 mol%), 4,4'-di-*tert*-butyl-2,2'-dipyridyl (**L3.4.6**, 40 mg, 15 mol%), Na₂HPO₄ (284 mg, 2.0 mmol). Subsequently, the flask was sealed with a cap, then evacuated and back-filled with Ar (3 times). Afterwards, 4-phenyl-1-butene (450 μ L, 3.0 mmol, 3.0 equiv),

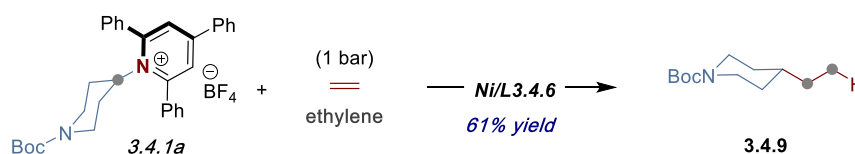
(EtO)₂MeSiH (480 μ L, 3.0 mmol, 3.0 equiv), NMP and 1,4-dioxane (4:1, 5.0 mL) were added via syringe. Then, the flask was stirred at 40 °C for 24 h. After the reaction was completed, and cool down to room temperature. The mixture was diluted with EtOAc, and washed with water. The aqueous phase was extracted with EtOAc (3 x 10 mL), and the combined organic phases were dried over MgSO₄ then concentrated. The residue was purified by column chromatography on silica gel (step gradient, Toluene to Hexane/EtOAc = 30:1), obtaining **3.4.3a** as light-yellow oil 166 mg (52% yield).

3.7.7.3 Regioconvergent Alkylation of Unrefined Mixtures of Olefins



An oven-dried 8 mL screw-cap test tube containing a stirring bar was charged with NiI₂ (6.2 mg, 10 mol%), 2-(6-methylpyridin-2-yl)-4,5-dihydrooxazole (**L3.4.10**, 6.4 mg, 20 mol%), Na₂HPO₄ (113.6 mg, 0.80 mmol) and 1-(1-(*tert*-butoxycarbonyl)piperidin-4-yl)-2,4,6-triphenylpyridin-1-ium tetrafluoroborate (**3.4.1a**, 115.6 mg, 0.20 mmol). Subsequently, the tube was sealed with a Teflon-lined screw cap, then evacuated and back-filled with Ar (3 times). Afterwards, the mixture of hexene (1:1:1, 74.6 μ L, 0.60 mmol, 3.0 equiv), (EtO)₃SiH (74 μ L, 0.40 mmol, 2.0 equiv), DMSO and 1,4-dioxane (3:1, 1.2 mL) were added via syringe. Then, the tube was stirred at 35 °C for 24 h. After the reaction was completed, the mixture was diluted with EtOAc, filtered through silica gel and concentrated under vacuum. The corresponding product was purified by column chromatography on silica gel (step gradient, Toluene to Hexane/EtOAc = 30:1), obtaining **3.4.5a** as colorless oil 36 mg (67% yield), 99:1 ratio.

3.7.7.4 Utilization of Ethylene as Coupling Partner

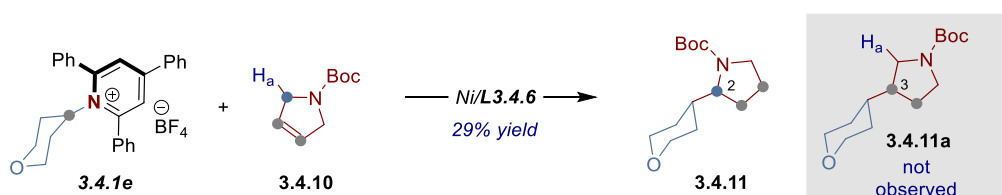


An oven-dried 8 mL screw-cap test tube containing a stirring bar was charged with NiBr₂·DME (6.2 mg, 10 mol%), 4,4'-di-*tert*-butyl-2,2'-dipyridyl (**L3.4.6**, 8.0 mg, 15 mol%), Na₂HPO₄ (56.8 mg, 0.40 mmol) and 1-(1-(*tert*-butoxycarbonyl)piperidin-4-yl)-2,4,6-triphenylpyridin-1-ium tetrafluoroborate (**3.4.1a**, 115.6 mg, 0.20 mmol).

Subsequently, the tube was sealed with a Teflon-lined screw cap, then evacuated and back-filled with ethylene (3 times). Afterwards, (EtO)₂MeSiH (96 μ L, 0.60 mmol), NMP and 1,4-dioxane (4:1, 1.0 mL) were added via syringe. Then, the tube was stirred at 40 $^{\circ}$ C for 24 h. The reaction under ethylene atmosphere with an ethylene balloon. After the reaction was completed, the mixture was diluted with EtOAc, filtered through silica gel and concentrated under vacuum. The corresponding product was purified by column chromatography on silica gel (step gradient, Hexane/EtOAc = 100:1 to 50:1 to 30:1), obtaining **3.4.9** as colorless oil 26 mg (61% yield). **¹H NMR** (400 MHz, CDCl₃) δ 4.06 (brs, 2H), 2.65 (t, J = 12.7 Hz, 2H), 1.64 (d, J = 13.0 Hz, 2H), 1.44 (s, 9H), 1.30 – 1.22 (m, 3H), 1.05 (qd, J = 11.9, 11.0, 6.3 Hz, 2H), 0.88 (t, J = 7.2 Hz, 3H) ppm. **¹³C NMR** (75MHz, CDCl₃) δ 154.9, 79.1, 44.1, 37.7, 31.8, 29.2, 28.5, 11.1 ppm. **IR** (neat, cm⁻¹): 2965, 2926, 2852, 1692, 1418, 1365, 1229, 1174, 1149, 1079. The observed spectral data are in agreement with the ones reported in literature.¹⁸

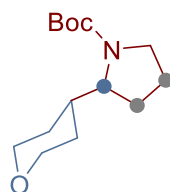
3.7.8 Mechanistic Experiments

3.7.8.1 Regioselectivity Studies



Ni/L3.4.6 system: An oven-dried 8 mL screw-cap test tube containing a stirring bar was charged with NiBr₂·DME (6.2 mg, 10 mol%), 4,4'-di-*tert*-butyl-2,2'-dipyridyl (L3.4.6, 8.0 mg, 15 mol%), Na₂HPO₄ (56.8 mg, 0.40 mmol) and 2,4,6-triphenyl-1-(tetrahydro-2H-pyran-4-yl)pyridin-1-ium tetrafluoroborate (3.4.1e, 95.8 mg, 0.20 mmol). Subsequently, the tube was sealed with a Teflon-lined screw cap, then evacuated and back-filled with Ar (3 times). Afterwards, *tert*-butyl 2,5-dihydro-1H-pyrrole-1-carboxylate (3.4.10, 101.4 mg, 0.6 mmol), (EtO)₂MeSiH (96 μL, 0.60 mmol), NMP and 1,4-dioxane (4:1, 1.0 mL) were added via syringe. Then, the tube was stirred at 40 °C for 24 h. After the reaction was completed, the mixture was diluted with EtOAc, filtered through silica gel and concentrated under vacuum. The corresponding product 3.4.11 were purified by column chromatography on silica gel (Hexane/EtOAc = 10 :1 to 5:1), affording light yellow oil 15 mg (29% yield).

Ni/L3.4.10 system: An oven-dried 8 mL screw-cap test tube containing a stirring bar was charged with NiI₂ (6.2 mg, 10 mol%), 2-(6-methylpyridin-2-yl)-4,5-dihydrooxazole (L3.4.10, 6.4 mg, 20 mol%), Na₂HPO₄ (113.6 mg, 0.80 mmol) and 2,4,6-triphenyl-1-(tetrahydro-2H-pyran-4-yl)pyridin-1-ium tetrafluoroborate (3.4.1e, 95.8 mg, 0.20 mmol). Subsequently, the tube was sealed with a Teflon-lined screw cap, then evacuated and back-filled with Ar (3 times). Afterwards, *tert*-butyl 2,5-dihydro-1H-pyrrole-1-carboxylate (3.4.10, 101.4 mg, 0.6 mmol, 3.0 equiv), (EtO)₃SiH (74 μL, 0.60 mmol), DMSO and 1,4-dioxane (3:1, 1.2 mL) were added via syringe. Then, the tube was stirred at 35 °C for 24 h. After the reaction was completed, the mixture was diluted with EtOAc, filtered through silica gel and concentrated under vacuum. The corresponding product 3.4.11 were purified by column chromatography on silica gel (Hexane/EtOAc = 10 :1 to 5:1), affording light yellow oil 31 mg (61% yield).



***tert*-buty-2-(tetrahydro-2*H*-pyran-4-yl)pyrrolidine-1-carboxylate (3.4.11)** ¹H NMR (400 MHz, CDCl₃) δ 3.92 (d, *J* = 11.0 Hz, 2H), 3.75 – 3.57 (m, 1H), 3.52 – 3.31 (m, 1H), 3.35 – 3.21 (m, 2H), 3.19 – 3.04 (m, 1H), 2.08 – 1.63 (m, 5H), 1.39 (s, 9H), 1.45 – 1.14 (m, 4H) ppm. ¹³C NMR (101 MHz, CDCl₃) δ 155.1, 79.2, 79.0, 68.2, 68.0, 61.2, 47.1, 46.3, 39.1, 38.2, 28.5, 27.9, 26.4, 24.3, 23.4 ppm. The observed spectral data are in agreement with the ones reported in literature.¹⁹

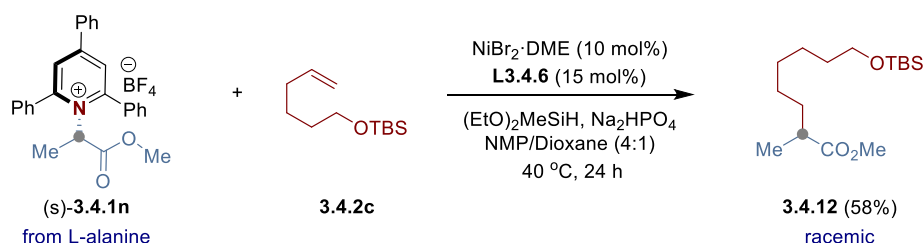
3.7.8.2 Control Experiments to Explore the Isomerization of 3.4.10 in the Absence of 3.4.1

Entry	Time	Yield of 3.4.10a (%) Ni/L3.4.6	Yield of 3.4.10a (%) Ni/L3.4.10
1	30 min	18	18
2	1 h	17	23
3	2 h	19	23
4	6 h	22	27
5	12 h	25	33
6	24 h	25	40

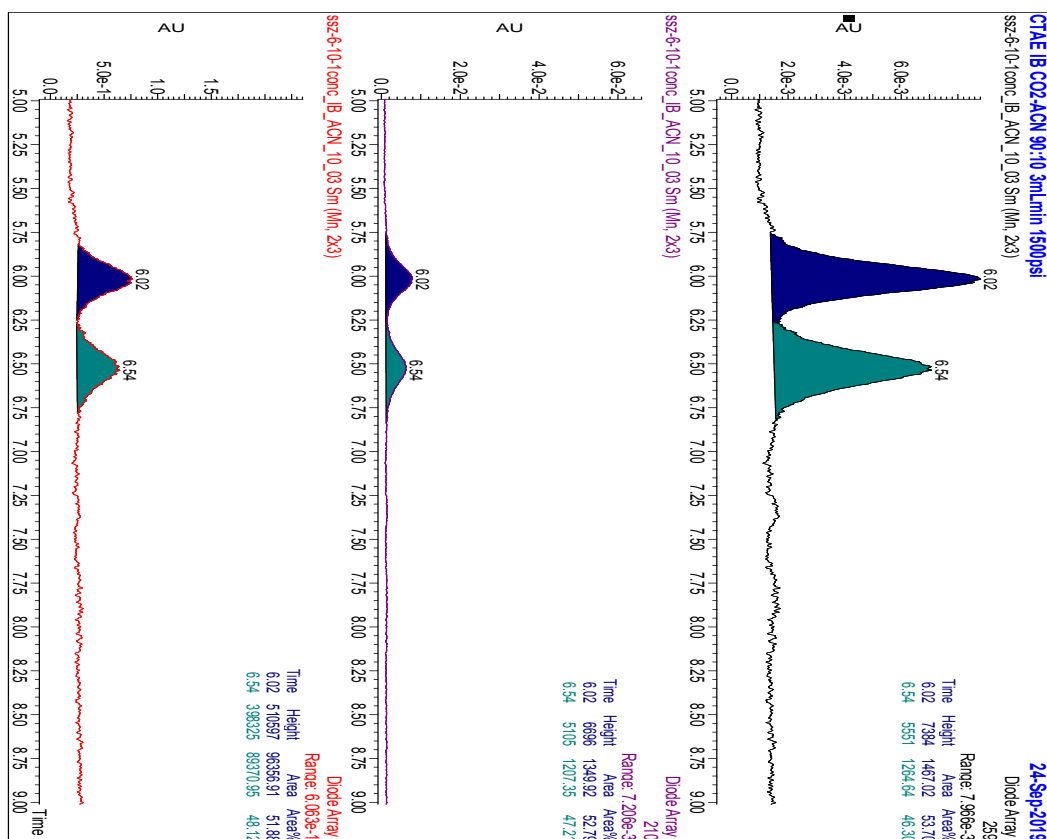
General procedure for the isomerization of 3.4.10a with Ni/L3.4.6 system: An oven-dried 8 mL screw-cap vial containing a stirring bar was charged with NiBr₂·DME (6.2 mg, 5 mol%), **L3.4.6** (8.0 mg, 7.5 mol%), Na₂HPO₄ (56.8 mg, 0.4 mmol). Subsequently, the tube was sealed with a Teflon-lined screw cap, then evacuated and backfilled with Ar (3 times), Then, *tert*-butyl 2,5-dihydro-1*H*-pyrrole-1-carboxylate (**3.4.10**, 67.6 mg, 0.4 mmol), DEMS (96 μL, 0.60 mmol, 1.50 equiv), NMP and THF (4:1, 1.0 mL) were added by syringe. Then, the tube was stirred at 40 °C for the indicated time. The yields of **3.4.10a** were determined by GC FID taking aliquots using 1-decane as internal standard.

General procedure to form 3.4.10a with Ni/L3.4.10 system: An oven-dried 8 mL screw-cap vial containing a stirring bar was charged with NiI₂ (6.2 mg, 5 mol%), **L3.4.10** (6.4 mg, 10 mol%), Na₂HPO₄ (113.6 mg, 0.8 mmol). Subsequently, the tube was sealed with a Teflon-lined screw cap, then evacuated and backfilled with Ar (3 times). Then, *tert*-butyl 2,5-dihydro-1*H*-pyrrole-1-carboxylate (**3.4.10**, 67.6 mg, 0.4 mmol), (EtO)₃SiH (74 μL, 0.40 mmol, 1.0 equiv), DMSO and 1,4-dioxane (3:1, 1.2 mL) were added via syringe. Then, the tube was stirred at 35 °C. The yields of **3.4.10a** were determined by GC FID taking aliquots using 1-decane as internal standard.

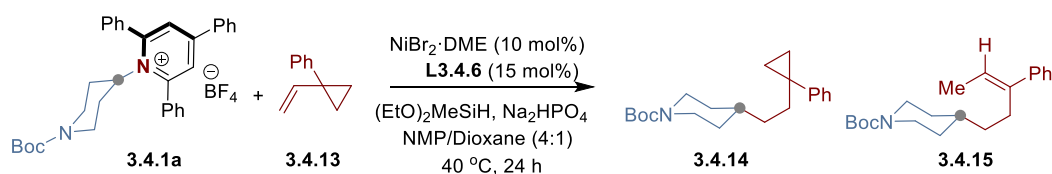
3.7.8.3 Test for Stereospecificity from L-alanine



An oven-dried 8 mL screw-cap test tube containing a stirring bar was charged with $\text{NiBr}_2 \cdot \text{DME}$ (6.2 mg, 10 mol%), 4,4'-di-*tert*-butyl-2,2'-dipyridyl (**L3.4.6**, 8.0 mg, 15 mol%), Na_2HPO_4 (56.8 mg, 0.40 mmol) and (S)-1-(1-methoxy-1-oxopropan-2-yl)-2,4,6-triphenylpyridin-1-ium tetrafluoroborate ((S)-**3.4.1n**, 96.2 mg, 0.20 mmol). Subsequently, the tube was sealed with a Teflon-lined screw cap, then evacuated and back-filled with Ar (3 times). Afterwards, *tert*-butyl(hex-5-en-1-yloxy)dimethylsilane (**3.4.2c**, 128.4 mg, 0.6 mmol), $(\text{EtO})_2\text{MeSiH}$ (96 μL , 0.60 mmol), NMP and 1,4-dioxane (4:1, 1.0 mL) were added via syringe. Then, the tube was stirred at 40 °C for 24 h. After the reaction was completed, the mixture was diluted with EtOAc, filtered through silica gel and concentrated under vacuum. The corresponding product were purified by column chromatography on silica gel (Toluene to Hexane/EtOAc = 20:1), affording colorless oil **3.4.12** (35 mg, 58% yield). The enantiomeric excess was determined to be 9% by chiral HPLC analysis (CHIRALPAK IB (100 x 4.6 mm, 3 μ), 3.0 mL/min, CO_2/MeCN = 90:10, $\lambda=210$ nm); tR (enantiomer A) = 6.02 min, tR (enantiomer B) = 6.54 min. $^1\text{H NMR}$ (400 MHz, CDCl_3) δ 3.66 (s, 3H), 3.58 (t, J = 6.6 Hz, 2H), 2.53 – 2.32 (m, 1H), 1.70 – 1.58 (m, 1H), 1.53 – 1.45 (m, 2H), 1.44 – 1.35 (m, 1H), 1.31 – 1.21 (m, 6H), 1.13 (d, J = 7.0 Hz, 3H), 0.88 (s, 9H), 0.03 (s, 6H) ppm. $^{13}\text{C NMR}$ (101 MHz, CDCl_3) δ 177.5, 63.4, 51.6, 39.6, 33.9, 32.9, 29.4, 27.4, 26.1, 25.8, 18.5, 17.2, -5.1 ppm. IR (neat, cm^{-1}): 2930, 2857, 1739, 1433, 1253, 1195, 1162, 1095, 834, 714. HRMS calcd. for $(\text{C}_{16}\text{H}_{35}\text{O}_3\text{Si})$ $[\text{M}+\text{H}]^+$: 303.2350 found 303.2352.



3.7.8.4 Experiments with radical probe 3.4.13.

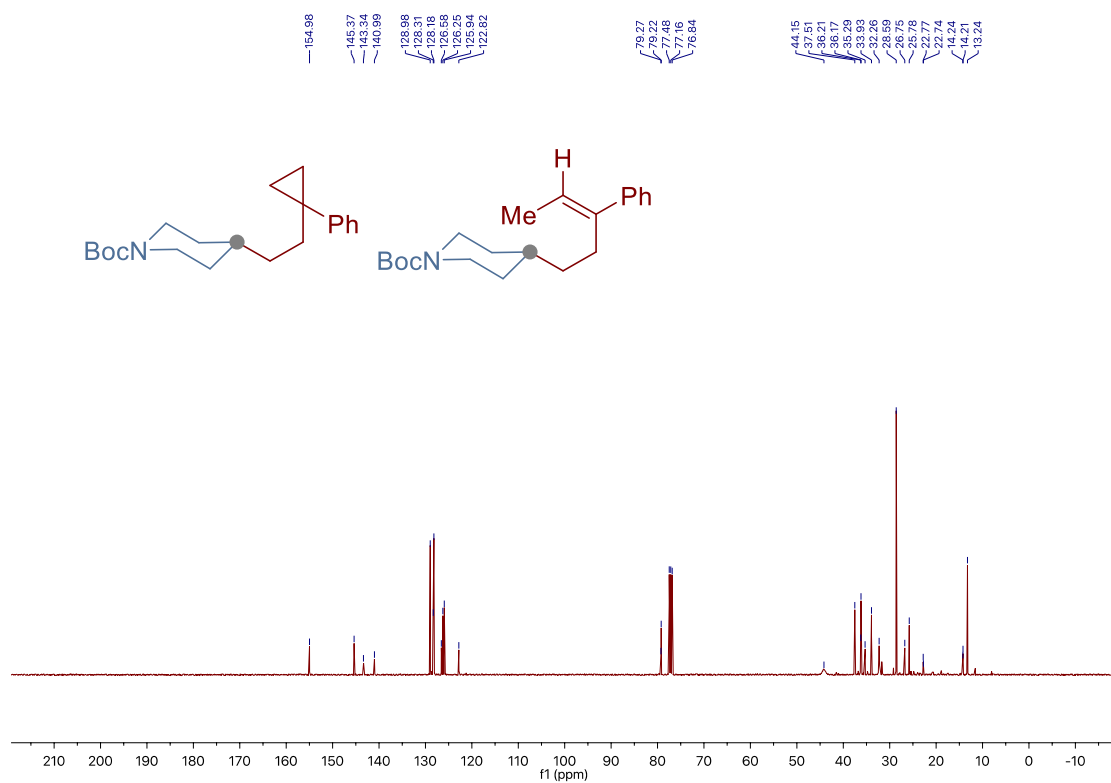
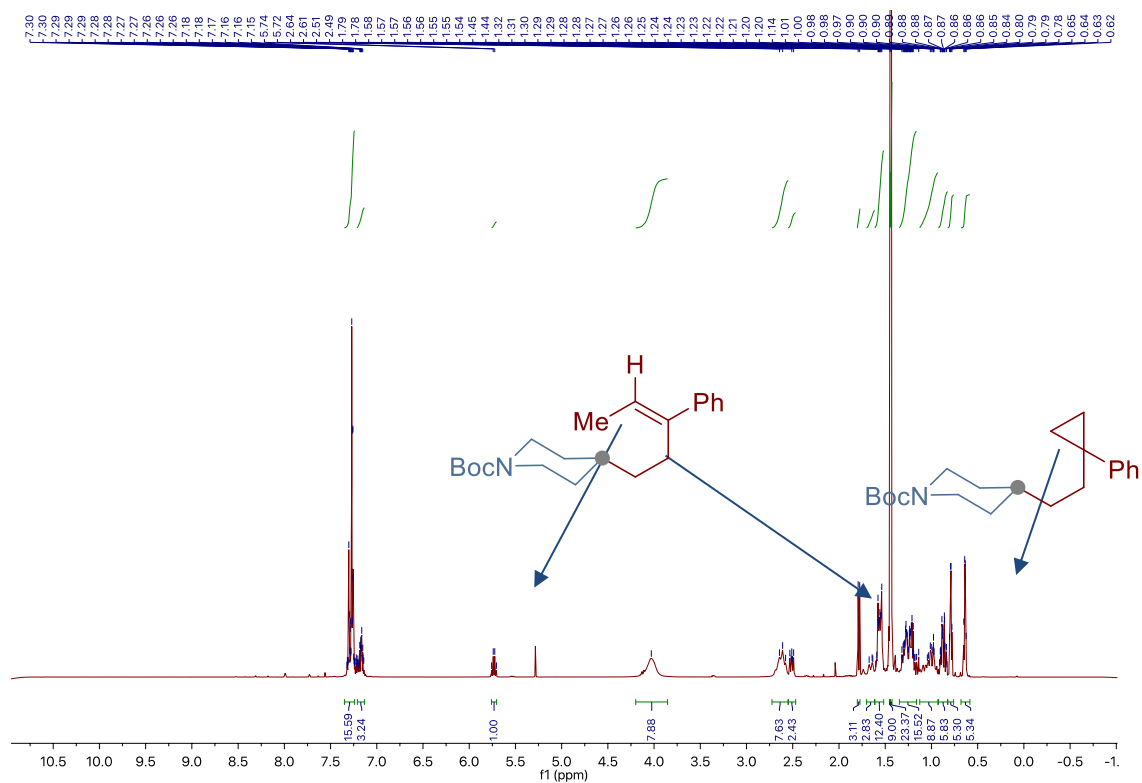


Entry	Concentration	Yield (%)	3.4.14 : 3.4.15
1	0.4 M	70	2.7 : 1
2	0.2 M	77	2.7 : 1
3	0.1 M	65	2.6 : 1

The reaction of **3.4.1** with alkenes bearing a proximal cyclopropyl ring (**3.4.13**) is rather illustrative. While a cyclopropylmethyl radical generated upon SET to **3.4.1** followed by addition to the olefin should undergo a rapid ring-opening rearrangement, we observed a constant ratio of no ring-opening vs ring-opening C–C bond-formation (2.6:1) at different Ni/L ratios, even at particularly low loadings, although tentative these experiments argue against a radical escape rebound mechanism.

General procedure en route to 3.4.14 and 3.4.15: An oven-dried 8 mL screw-cap test tube containing a stirring bar was charged with NiBr₂·DME (6.2 mg, 10 mol%), 4,4'-di-*tert*-butyl-2,2'-dipyridyl (**L3.4.6**, 8.0 mg, 15 mol%), Na₂HPO₄ (56.8 mg, 0.40 mmol) and 1-(1-(*tert*-butoxycarbonyl)piperidin-4-yl)-2,4,6-triphenylpyridin-1-ium tetrafluoroborate (**3.4.1a**, 115.6 mg, 0.20 mmol). Subsequently, the tube was sealed with a Teflon-lined screw cap, then evacuated and back-filled with Ar (3 times). Afterwards, (1-vinylcyclopropyl) benzene (**3.4.13**, 86.4 mg, 0.6 mmol), (EtO)₂MeSiH (96 μL, 0.60 mmol), NMP and 1,4-dioxane (4:1, 1.0 mL) were added via syringe. Then, the tube was stirred at 40 °C for 24 h. After the reaction was completed, the mixture was diluted with EtOAc, filtered through silica gel and concentrated under vacuum. The corresponding product were purified by column chromatography on silica gel (Hexane/EtOAc = 100 :1 to 40:1), affording colorless oil **3.4.14** and **3.4.15** (51 mg, 77% yield) as 2.7:1 mixture (determined by NMR and GC analysis) (colorless oil). ¹H NMR (400 MHz, CDCl₃) δ 7.34 – 7.24 (m, 15.59H), 7.23 – 7.13 (m, 3.24H), 5.73 (q, *J* = 6.9 Hz, 1H), 4.03 (brs, 7.88H), 2.63 (m, 7.63H), 2.55 – 2.45 (m, 2.43H), 1.78 (d, *J* = 6.9 Hz, 3.11H), 1.70 – 1.62 (m, 2.83H), 1.60 – 1.51 (m, 12.40H), 1.45 (s, 9. H), 1.44 (s, *J* = 4.9 Hz, 23.37H), 1.33 – 1.17 (m, 15.52H), 1.14 – 0.93 (m, 8.87H), 0.92 – 0.82 (m, 5.83H), 0.81 – 0.77 (m, 5.30H), 0.67 – 0.53 (m, 5.34H) ppm. ¹³C NMR (101 MHz, CDCl₃) δ 155.0, 145.4, 143.3, 145.0, 129.0, 128.3, 128.2, 126.6, 126.3, 125.9, 122.8, 79.3, 79.2, 44.2, 37.5, 36.2, 36.2, 35.3, 33.93, 28.6, 26.8, 25.8, 22.8, 22.7, 14.2, 14.2, 13.2 ppm. IR (neat, cm⁻¹): 2975, 2925, 2850, 1689, 1421, 1365, 1276, 1238, 1160, 1129, 1076, 968, 866. HRMS calcd. for (C₂₁H₃₁NNaO₂) [M+H]⁺: 352.2247 found 352.2248.

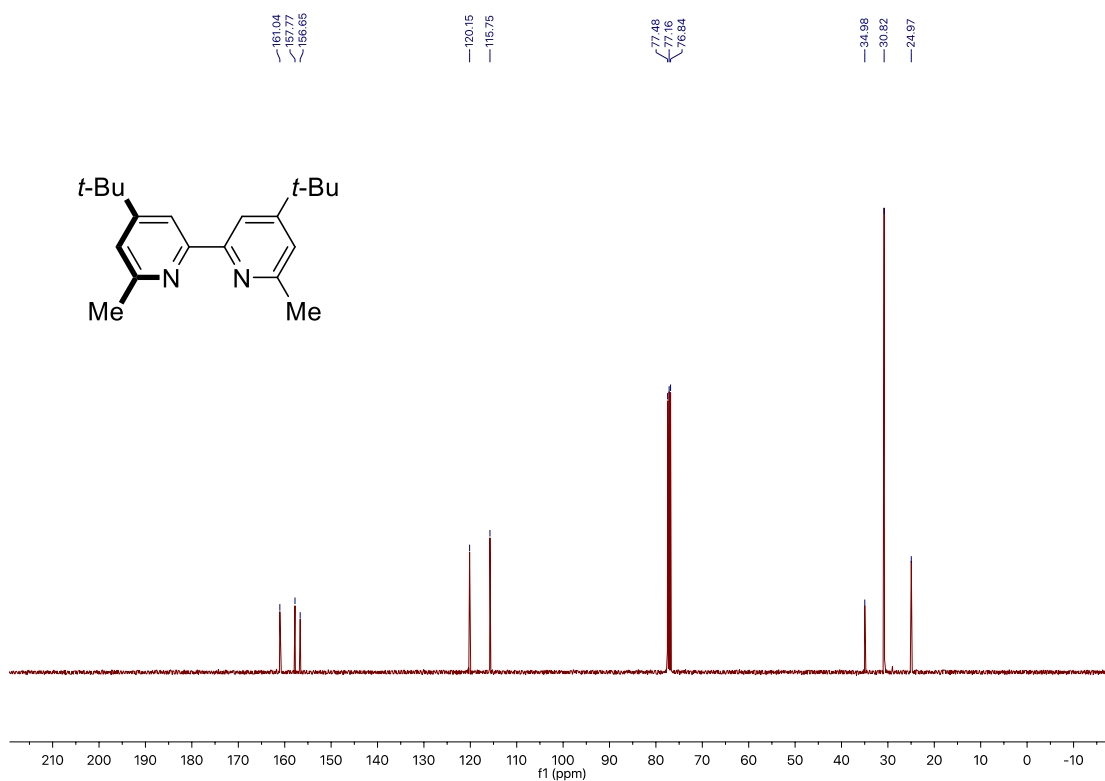
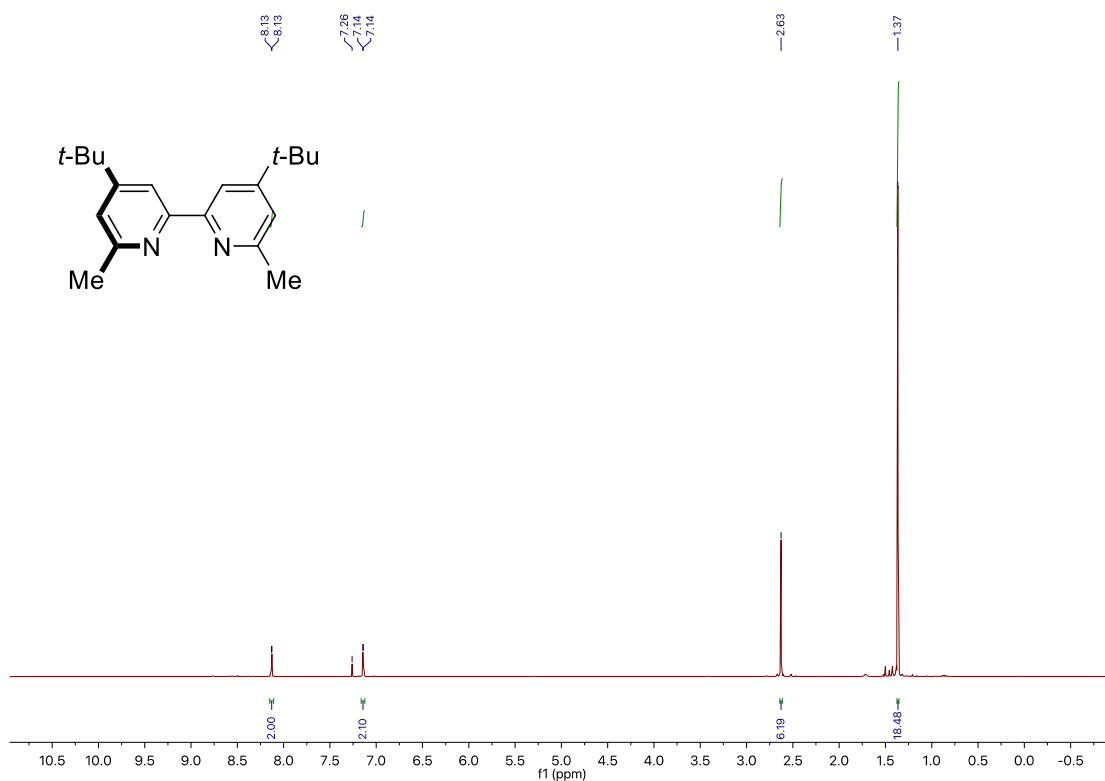
Site-Selective Ni-Catalyzed Deaminative Alkylation of Unactivated Olefins



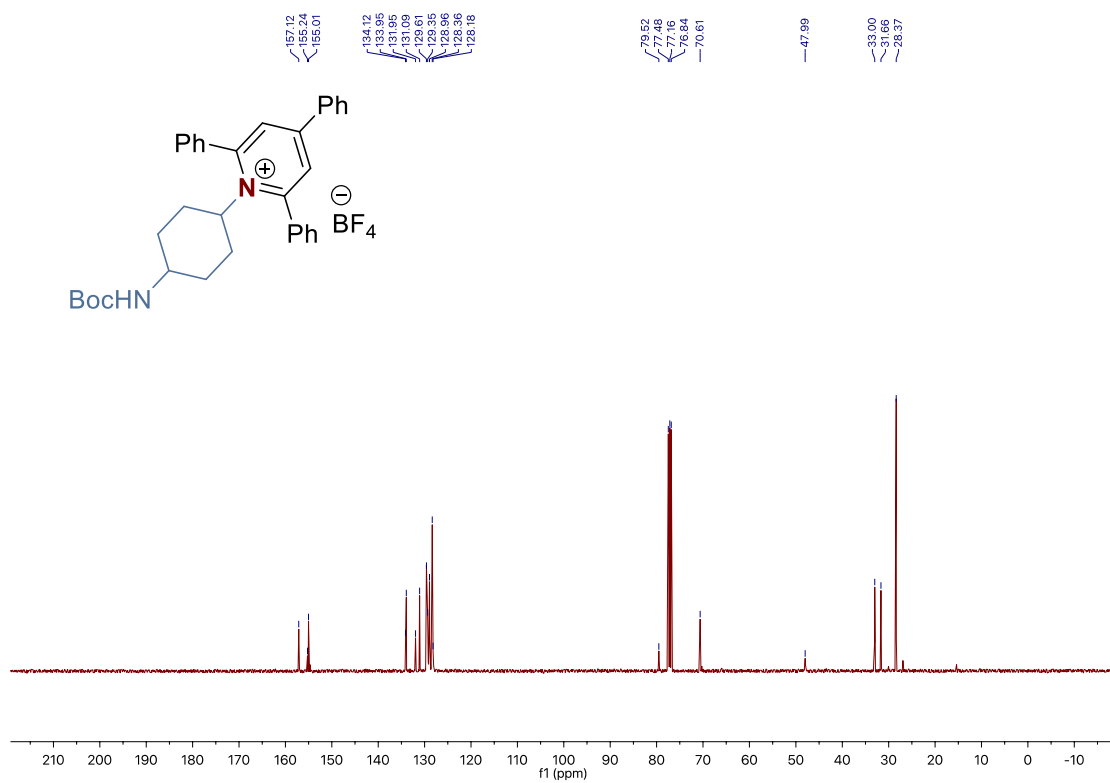
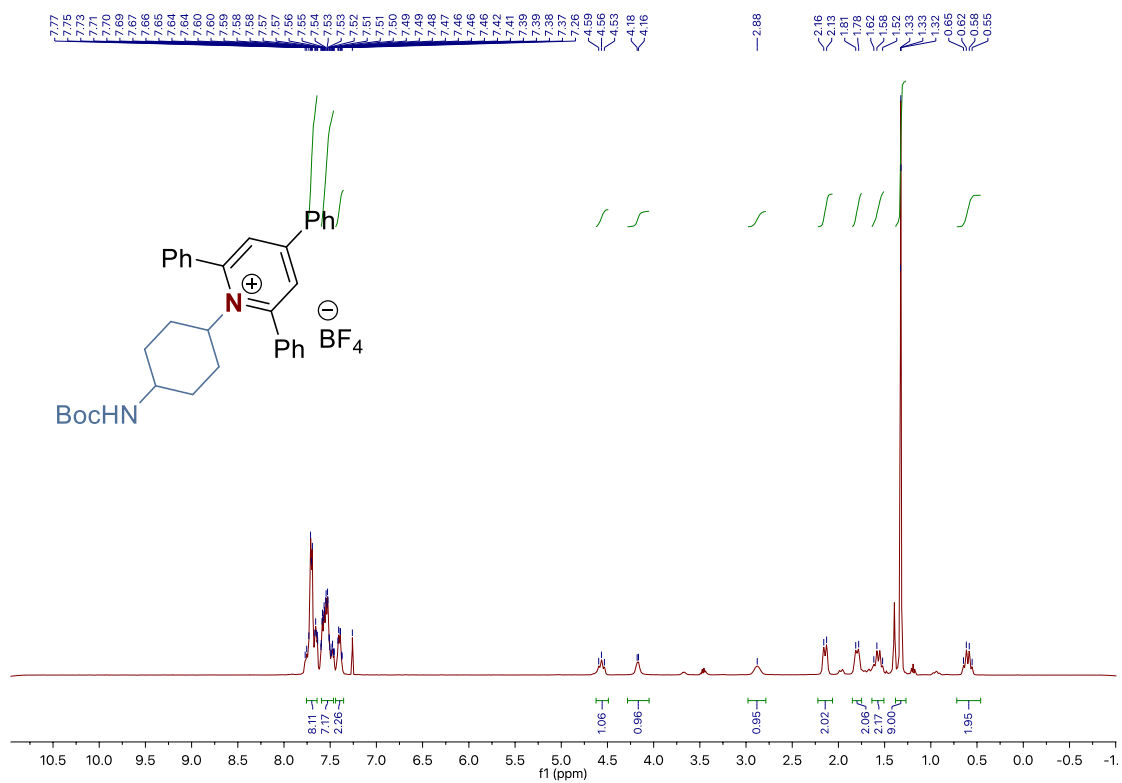
3.7.9 Bibliography

1. Sun, S.-Z.; Borjesson, M.; Martin-Montero, R.; Martin, R. *J. Am. Chem. Soc.* **2018**, *140*, 12765.
2. Martin-Montero, R.; Yatham, V. R.; Yin, H.; Davies, J.; Martin, R. *Org. Lett.* **2019**, *21*, 2947.
3. Plunkett, S.; Basch, C. H.; Santana, S. O.; Watson, M. P. *J. Am. Chem. Soc.* **2019**, *141*, 2257.
4. Klauck, F. J. R.; James, M. J.; Glorius, F. *Angew. Chem. Int. Ed.* **2017**, *56*, 12336.
5. Hoerrner, M. E.; Baker, K. M.; Basch, C. H.; Bampo, E. M.; Watson, M. P. *Org. Lett.* **2019**, *21*, 7356.
6. Bag, S.; Jayarajan, R.; Mondal, R.; Maiti, D. *Angew. Chem. Int. Ed.* **2017**, *56*, 3182.
7. Ho, G.-M.; Judkele, L.; Bruffaerts, J.; Marek, I. *Angew. Chem. Int. Ed.* **2018**, *57*, 8012.
8. Yang, T.; Lu, L.; Shen, Q. *Chem. Commun.* **2015**, *51*, 5479.
9. Yoshida, M.; Saito, K.; Kato, Hikaru.; Tsukamoto, S.; Doi, T. *Angew. Chem. Int. Ed.* **2018**, *57*, 5147.
10. Gao, D.-W.; Vinogradova, E. V.; Nimmagadda, S. K.; Medina, J. M.; Xiao, Y.; Suci, R. M.; Cravatt, B. F.; Engle, K. M. *J. Am. Chem. Soc.* **2018**, *140*, 8069.
11. L. Gonnard, A. Guerinot, J. Cossy, *Chem. Eur. J.* **2015**, *21*, 12797.
12. Wang, Y.-X.; Wang, J.-H.; Li, G.-X.; He, G.; Chen, G. *Org. Lett.* **2017**, *19*, 1442.
13. Kuhn, K. M.; Champagne, T. M.; Hong, S. H.; Wei, W.-H.; Nickel, A.; Lee, C. W.; Virgil, S. C.; Grubbs, R. H.; Pederson, R. L. *Org. Lett.* **2010**, *12*, 984.
14. Gandon, V.; Bertus, P.; Szymoniak, J. *Eur. J. Org. Chem.* **2000**, *22*, 3713.
15. Bazin, H. G.; Li, Y.; Khalaf, J. K.; Mwakawari, S.; Livesay, M. T.; Evans, J. T.; Johnson, D. A. *Bioorg. Med. Chem. Lett.* **2015**, *25*, 1318.
16. Hanessian, S.; Moitessier, N.; Cantin, L.-D. *Tetrahedron* **2001**, *57*, 6885.
17. Perlikowska, W.; Mikołajczyk, M. *Synthesis* **2009**, *16*, 2715.
18. Dai, X.-J.; Li, C.-J. *J. Am. Chem. Soc.* **2016**, *138*, 5433.
19. Johnson, C. P.; Smith, R. T.; Allmendinger, S.; MacMillan, D. W. C. *Nature* **2016**, *535*, 32

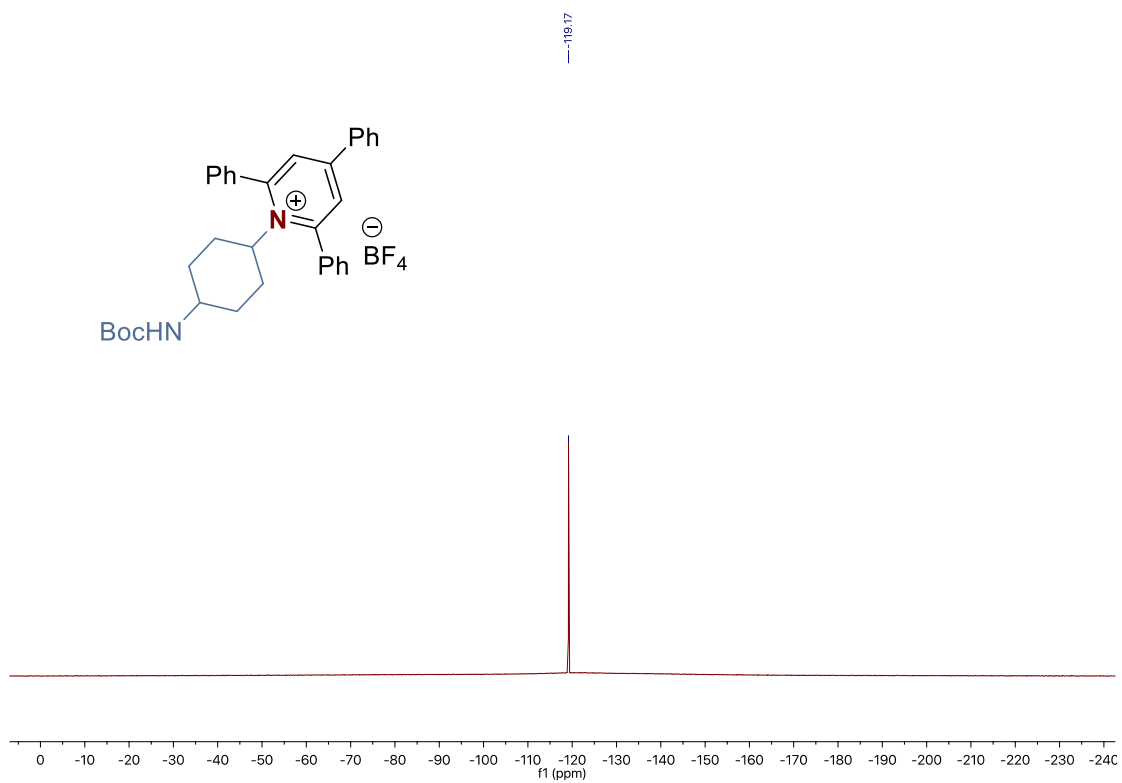
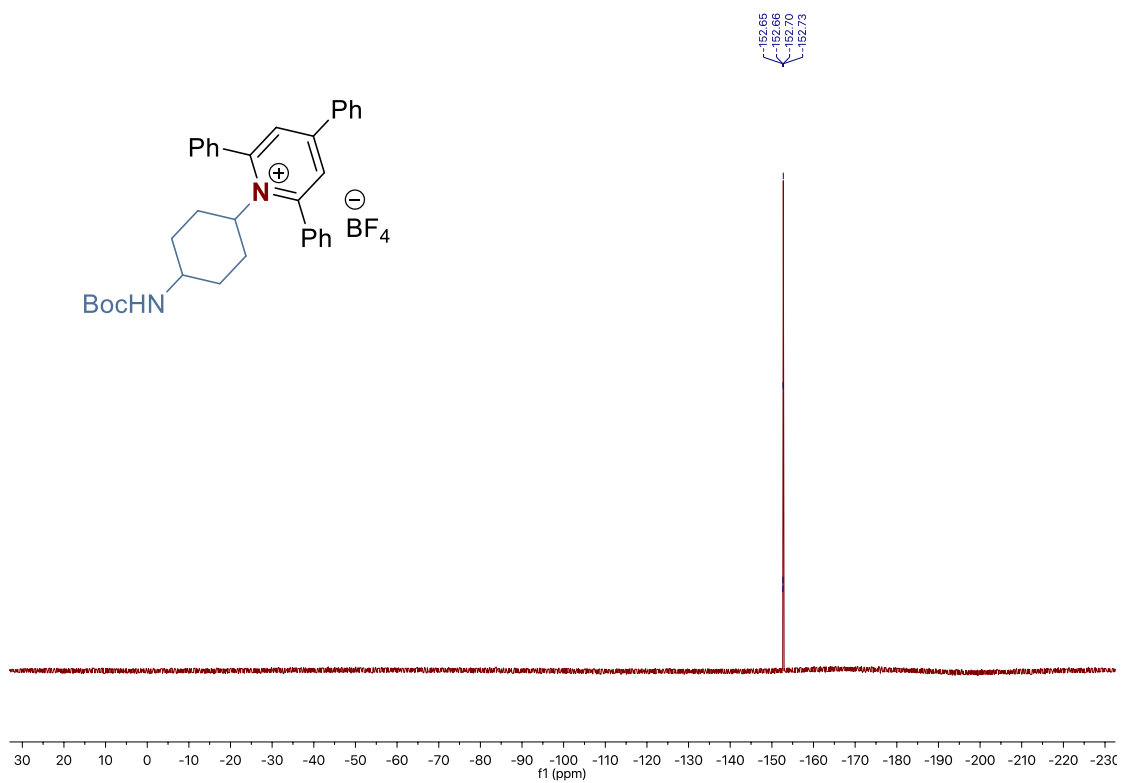
3.7.10 NMR Spectra



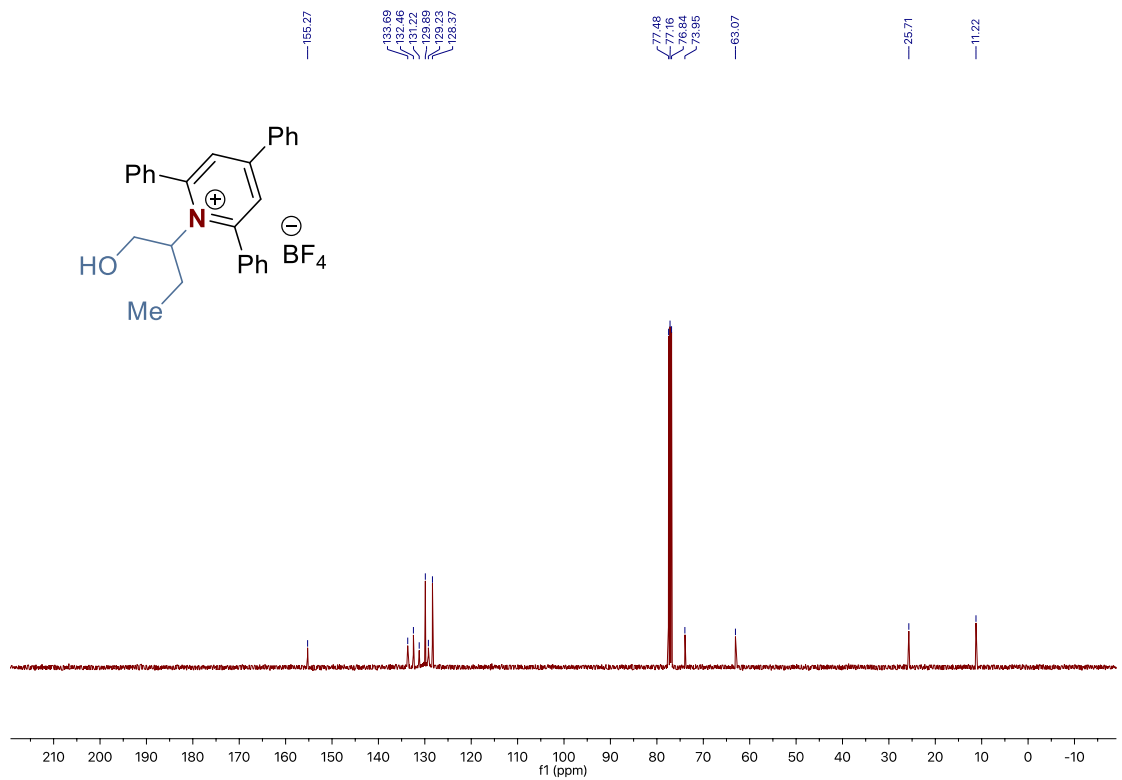
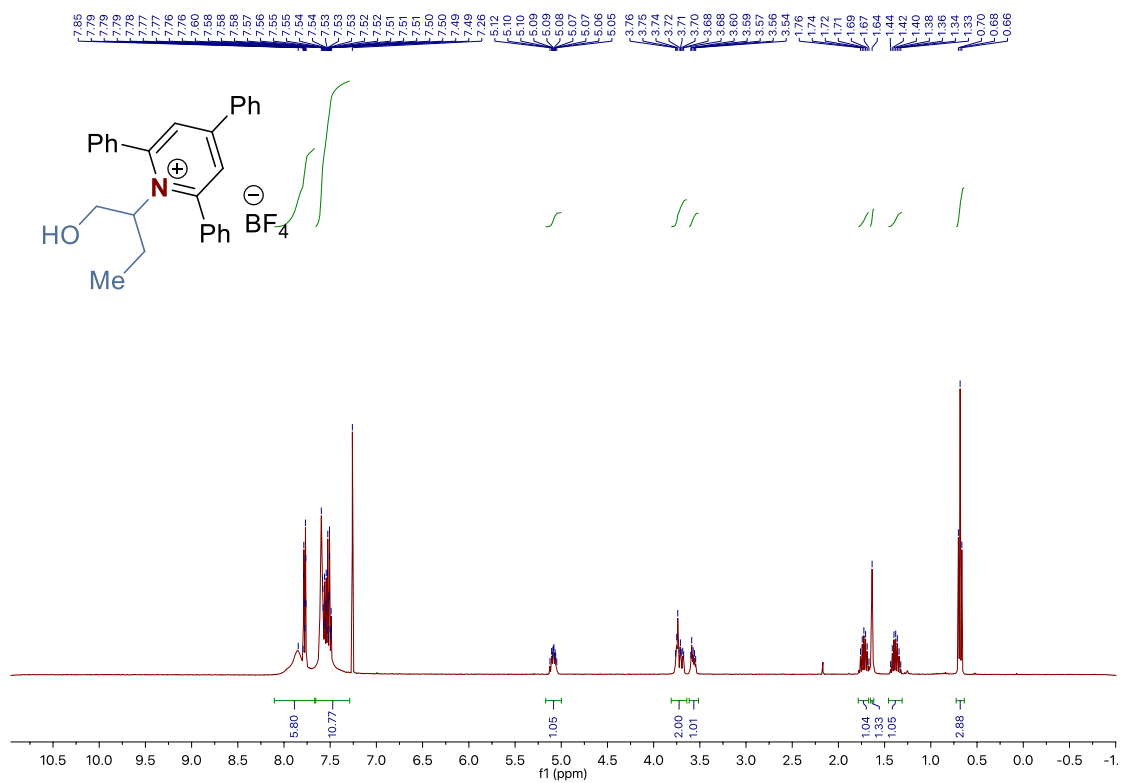
Chapter 3.



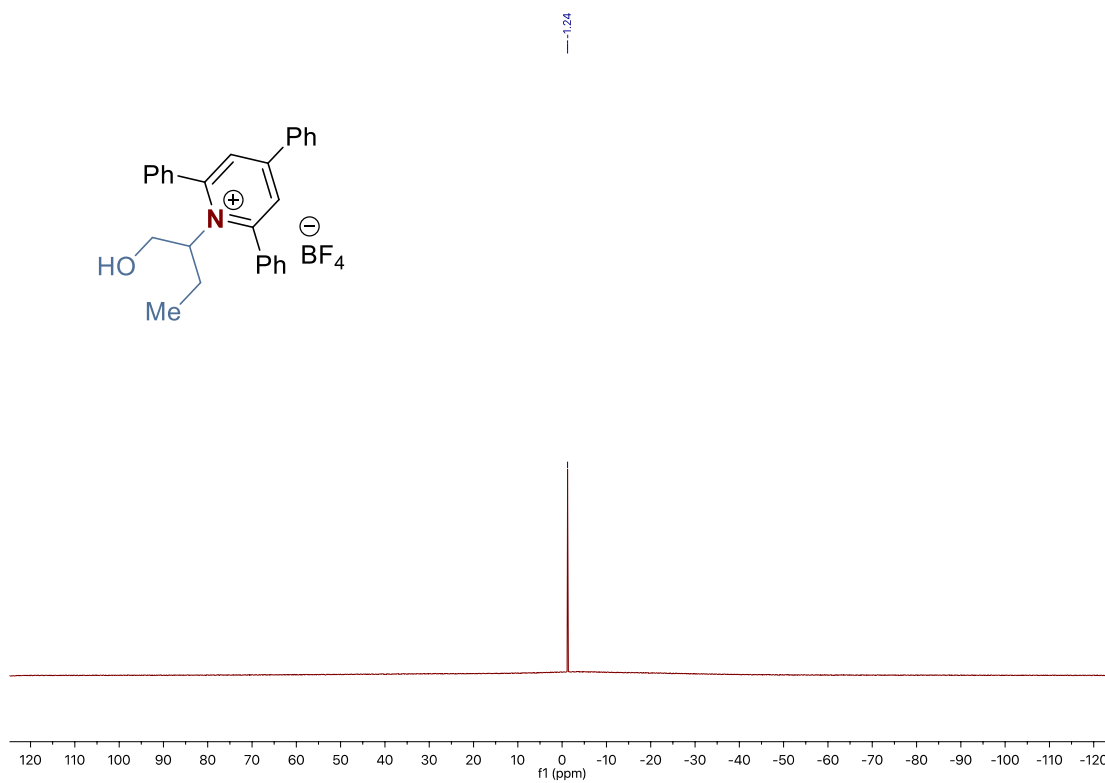
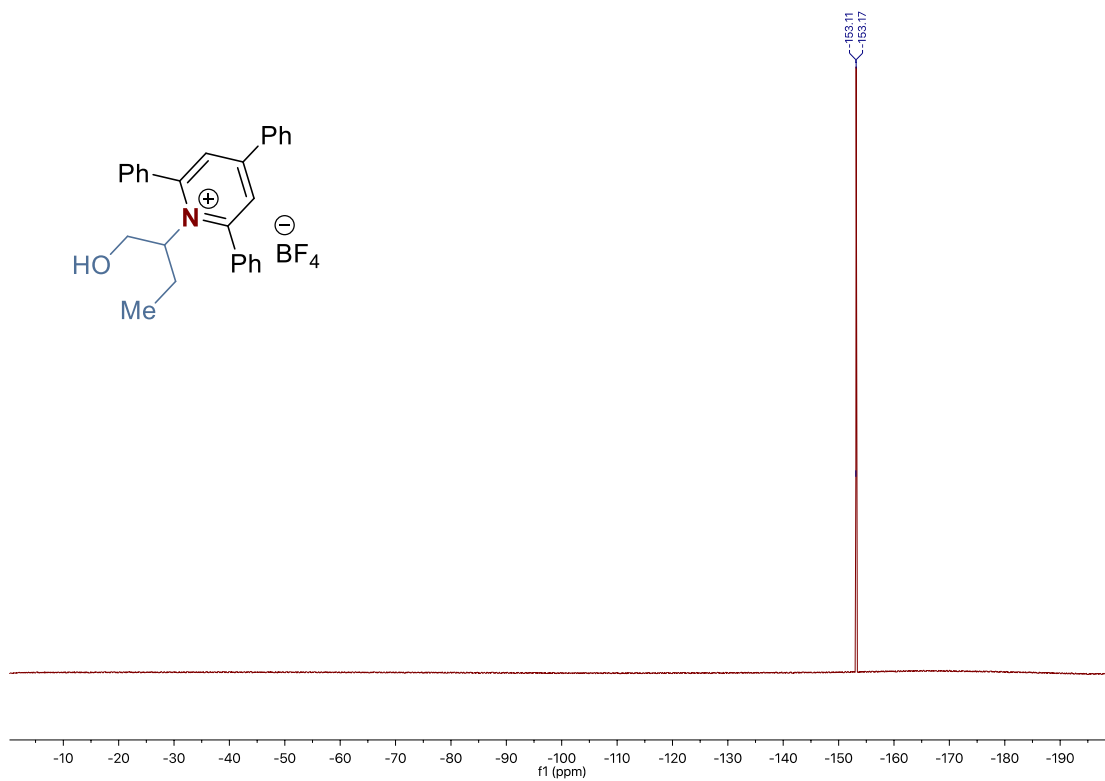
Site-Selective Ni-Catalyzed Deaminative Alkylation of Unactivated Olefins



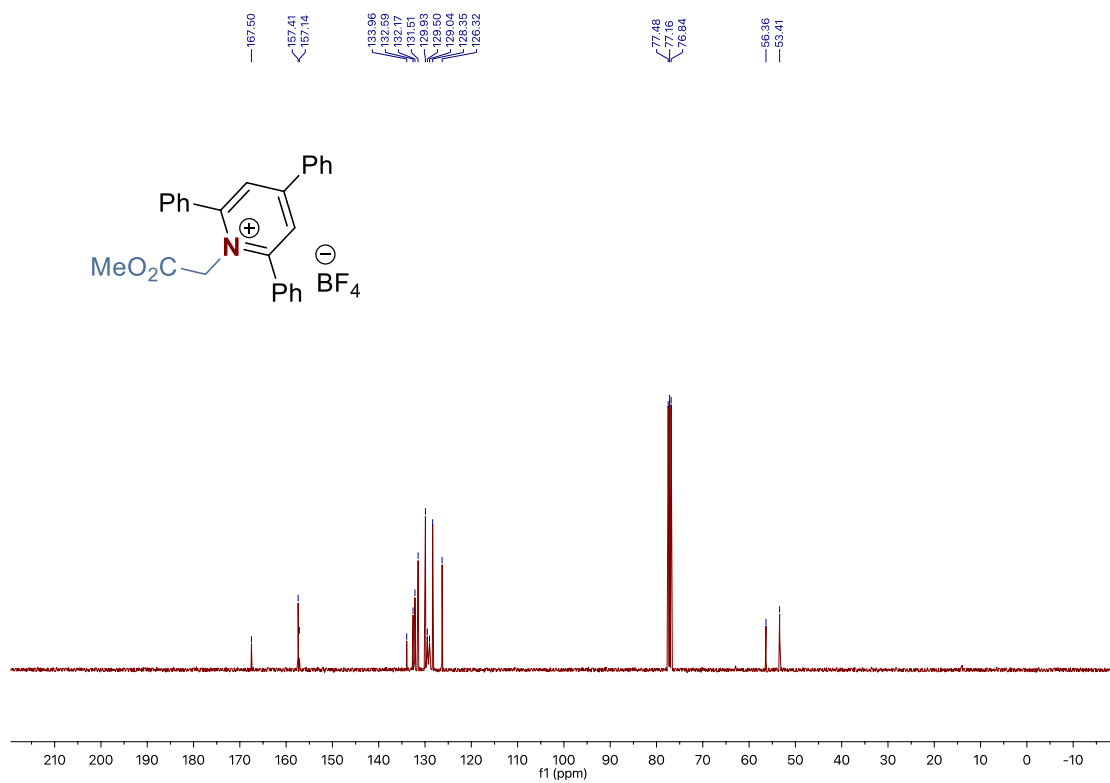
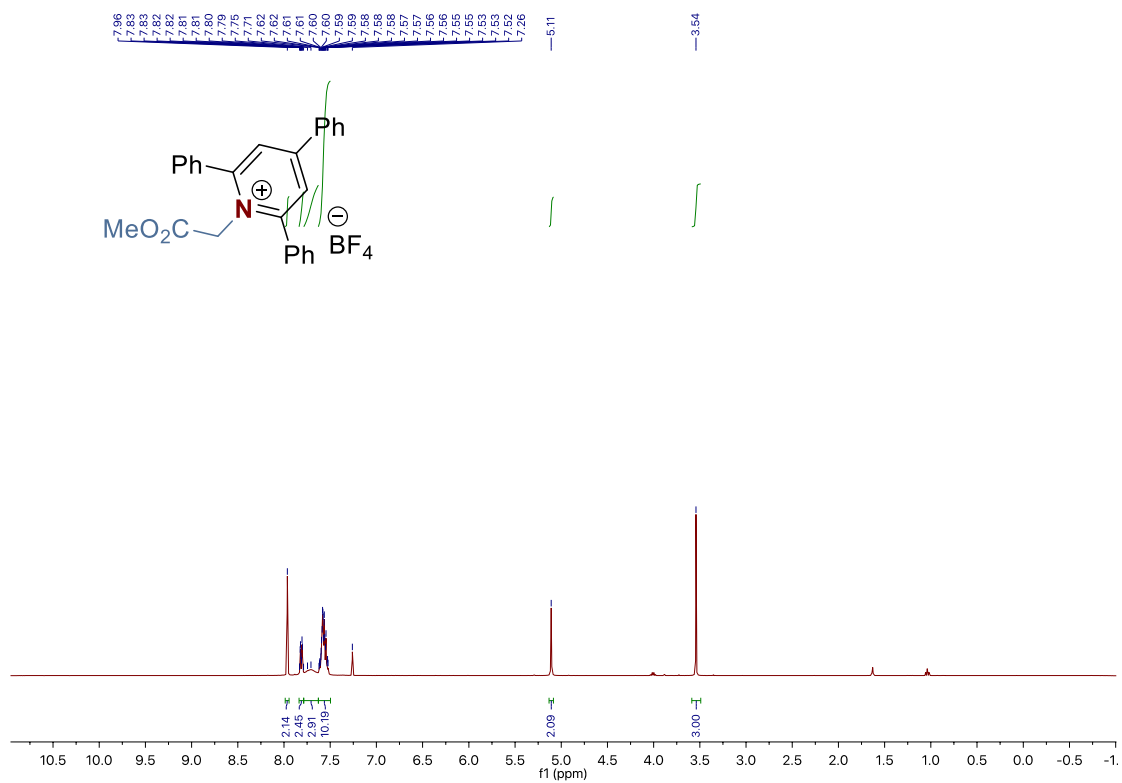
Chapter 3.



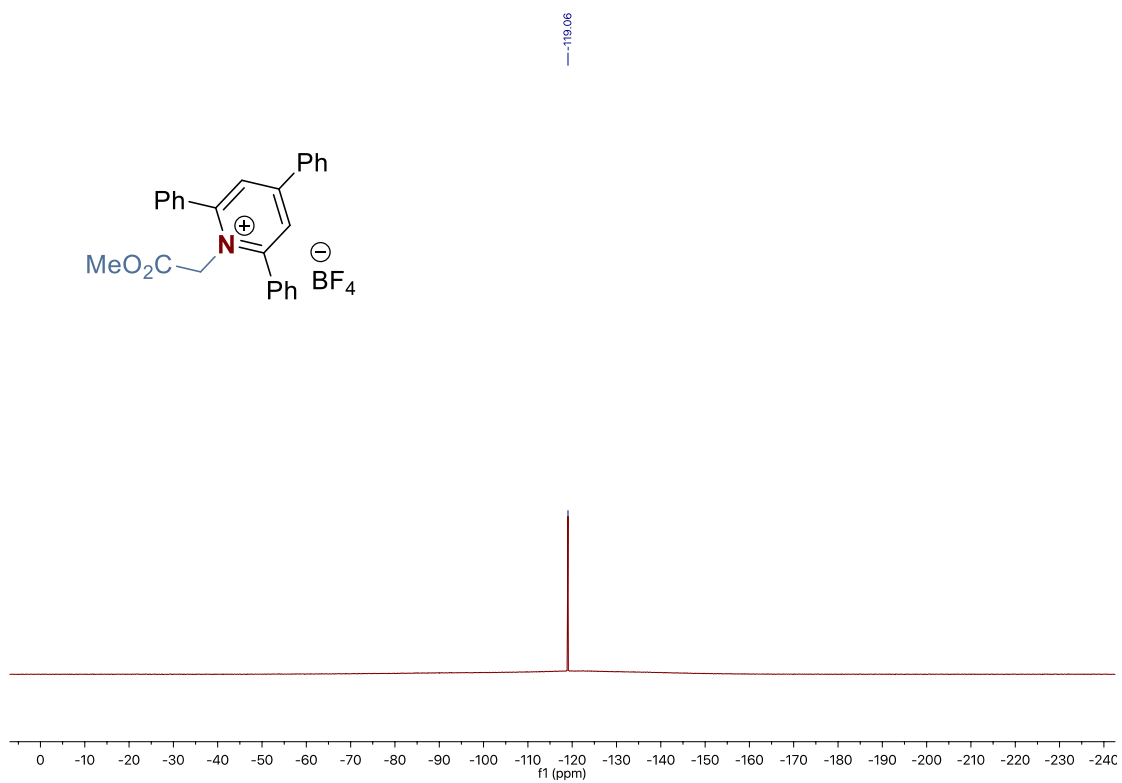
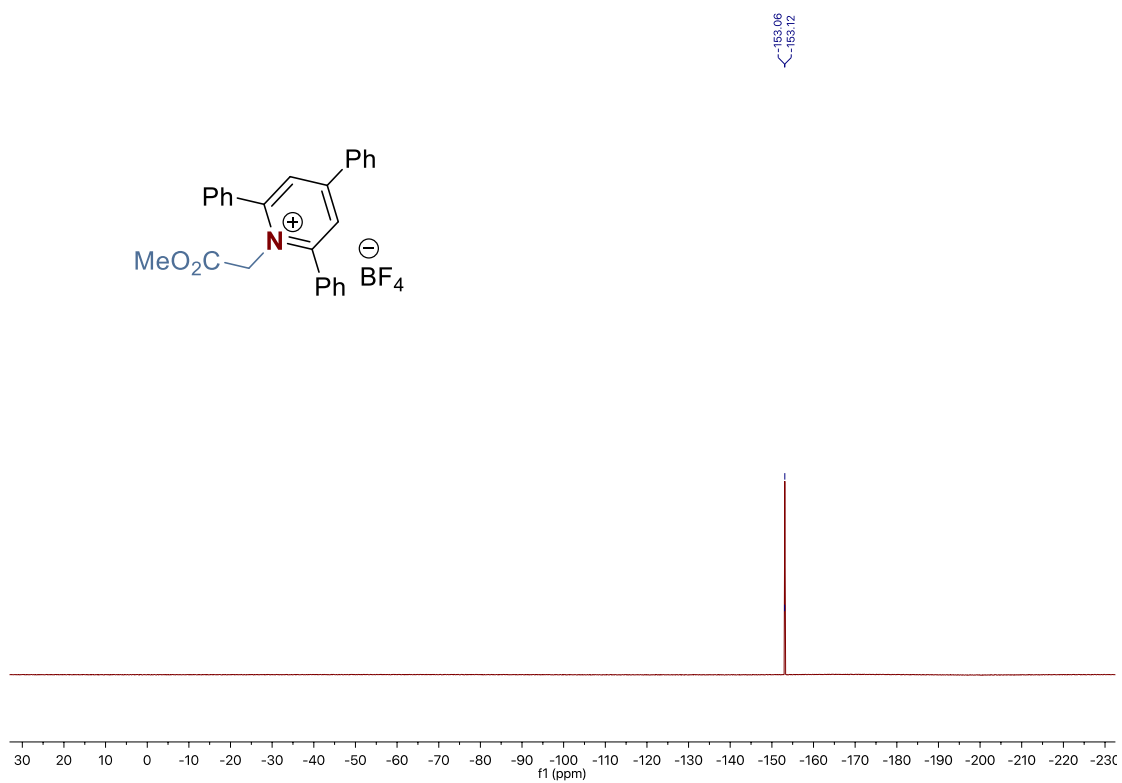
Site-Selective Ni-Catalyzed Deaminative Alkylation of Unactivated Olefins



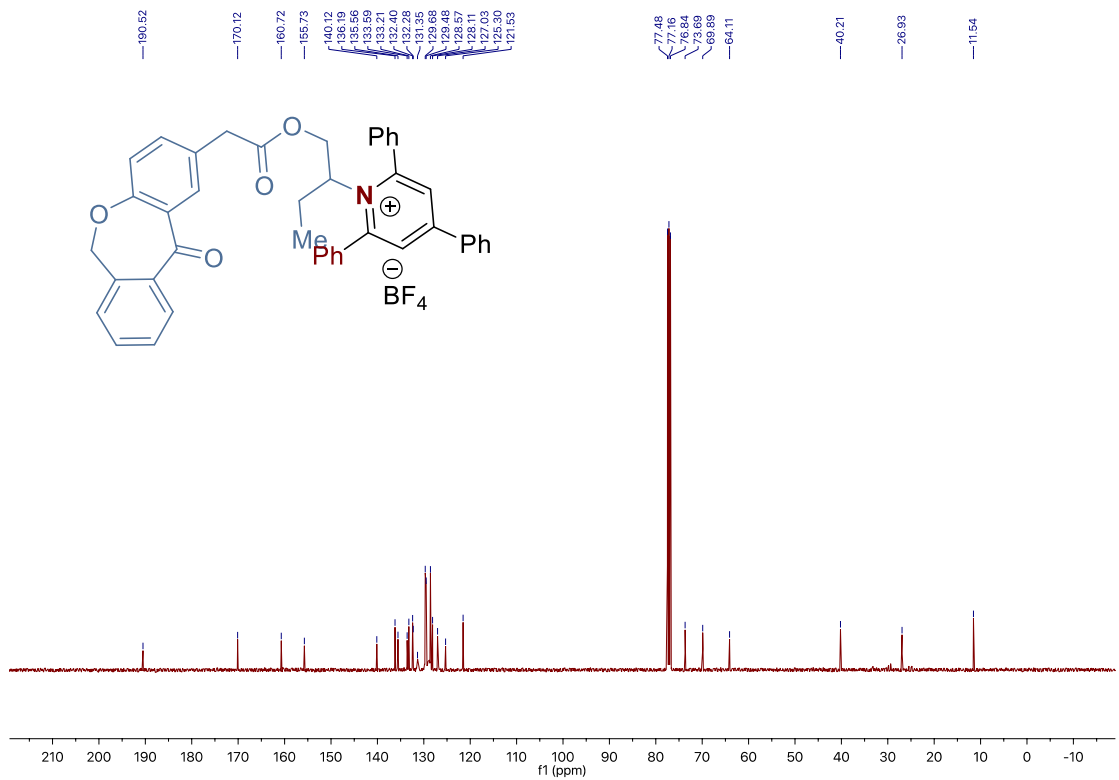
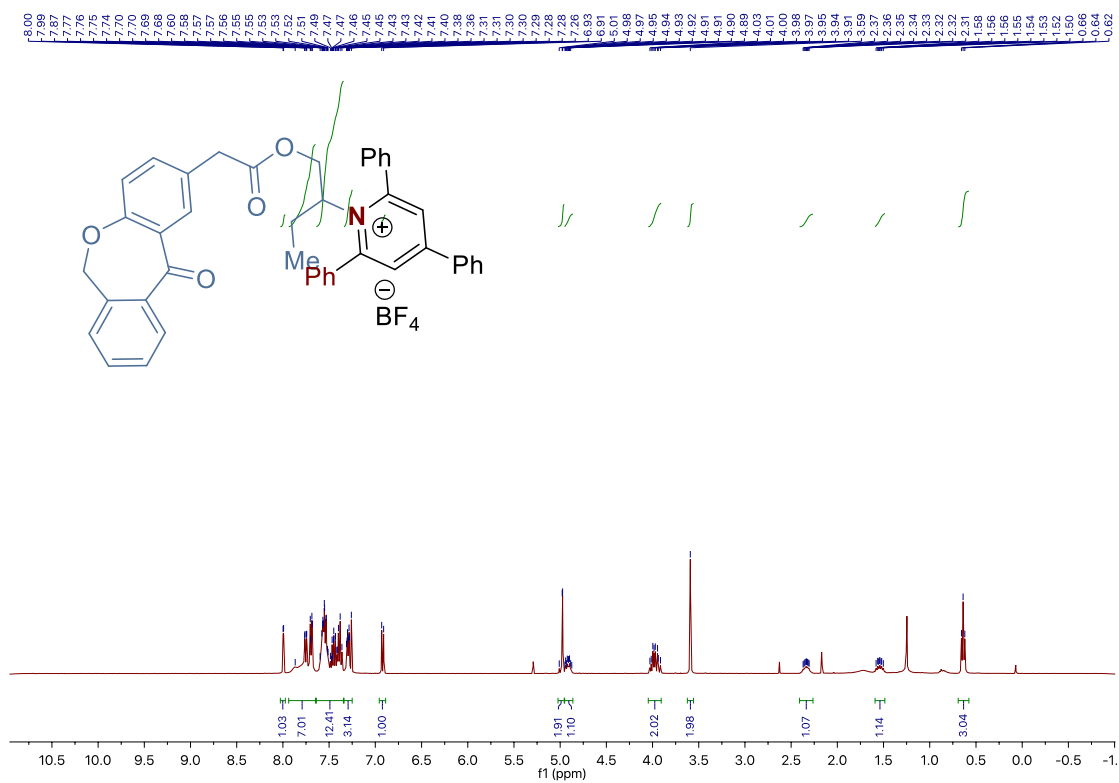
Chapter 3.



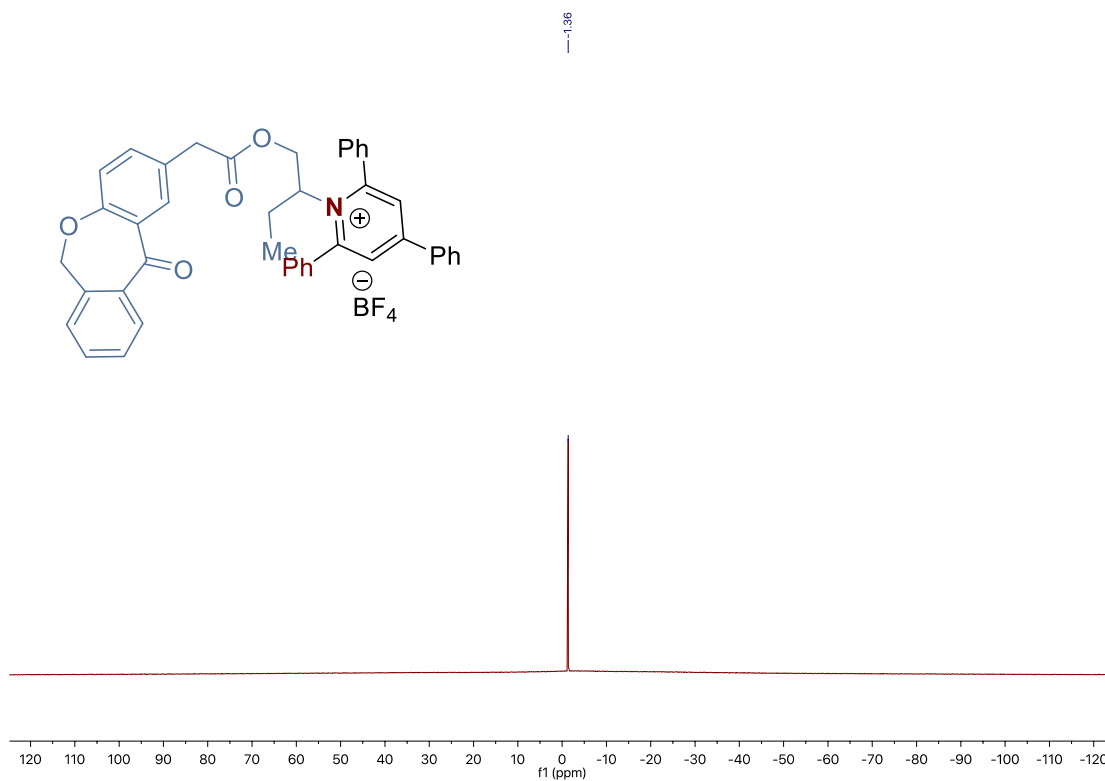
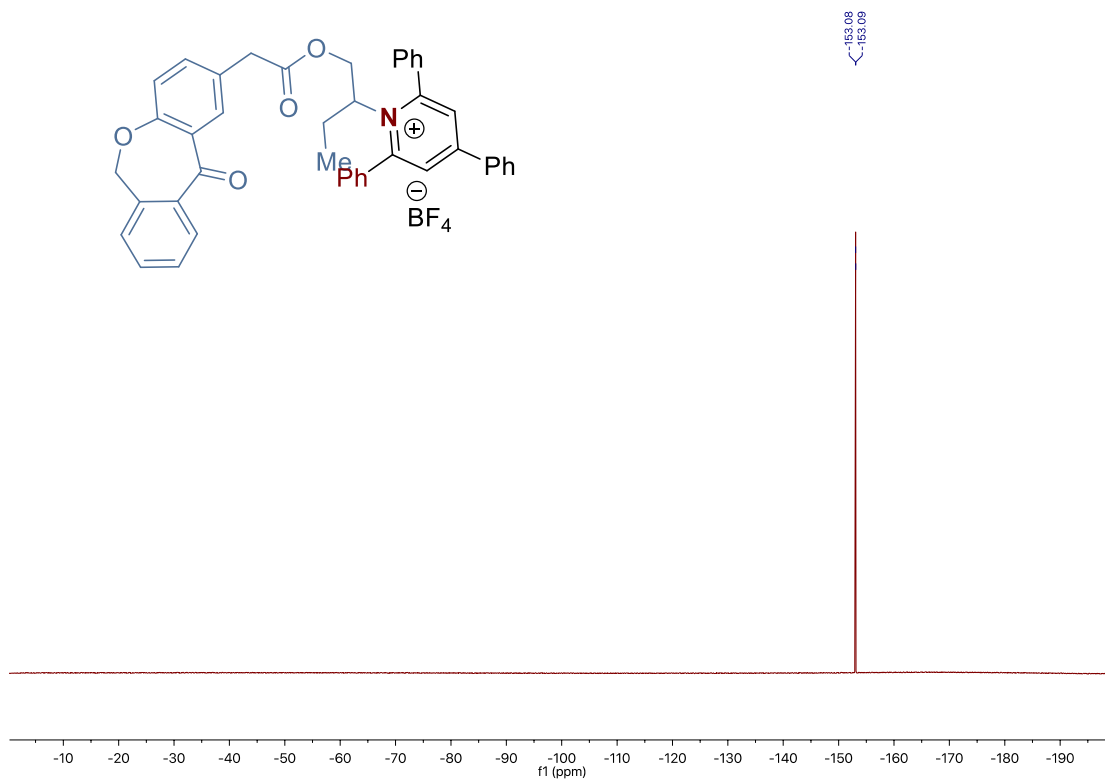
Site-Selective Ni-Catalyzed Deaminative Alkylation of Unactivated Olefins



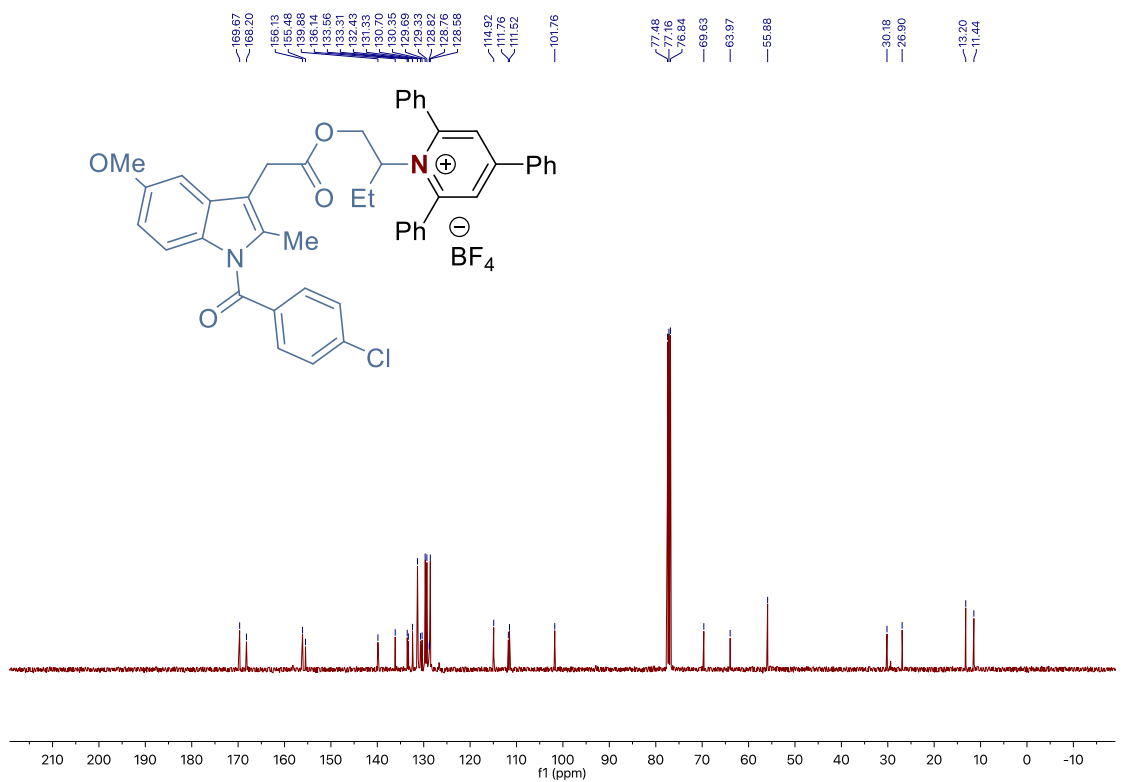
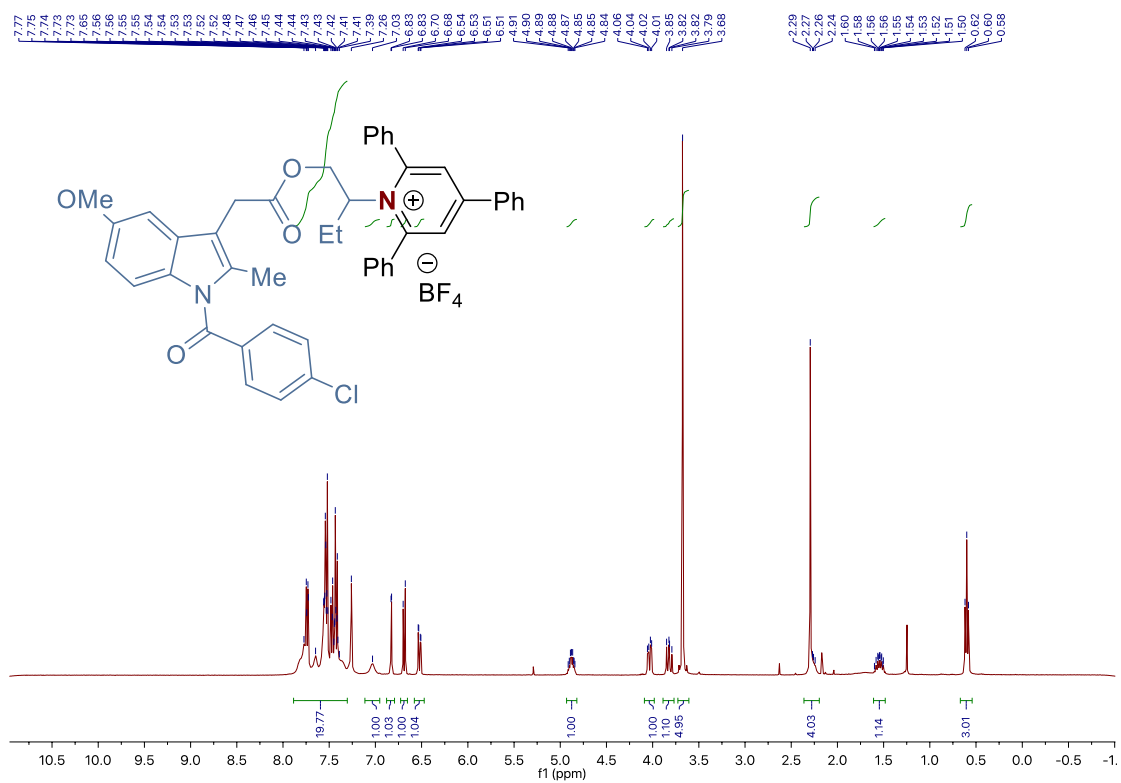
Chapter 3.



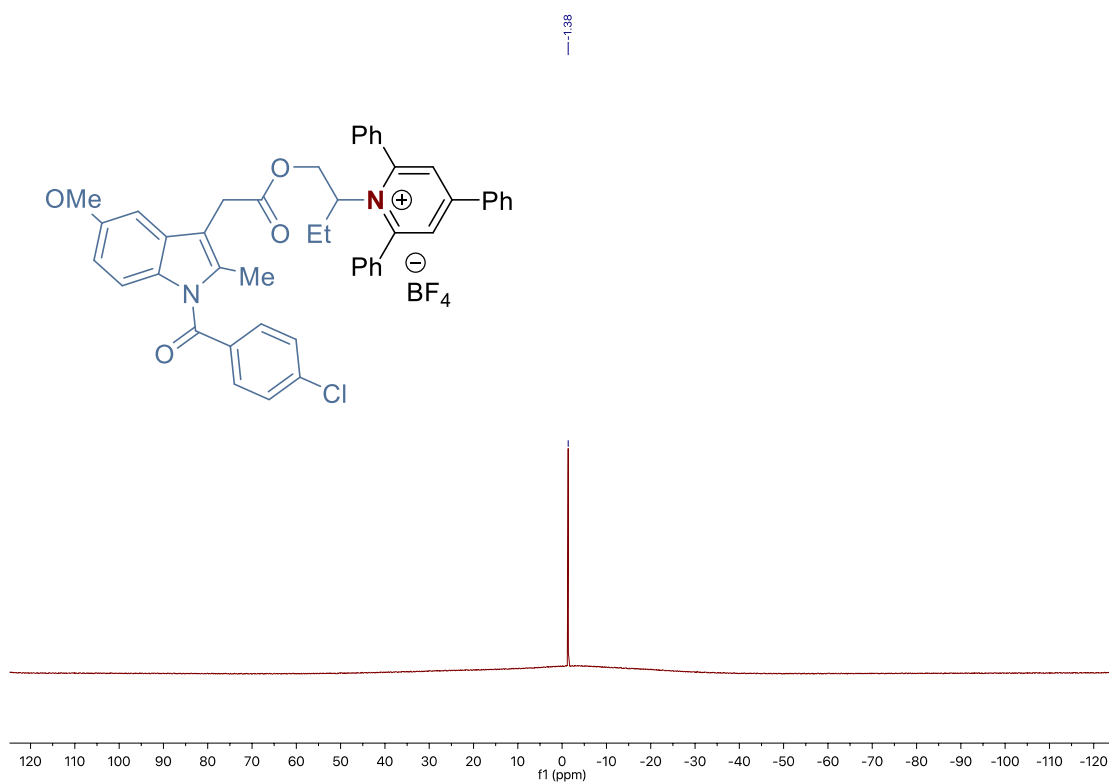
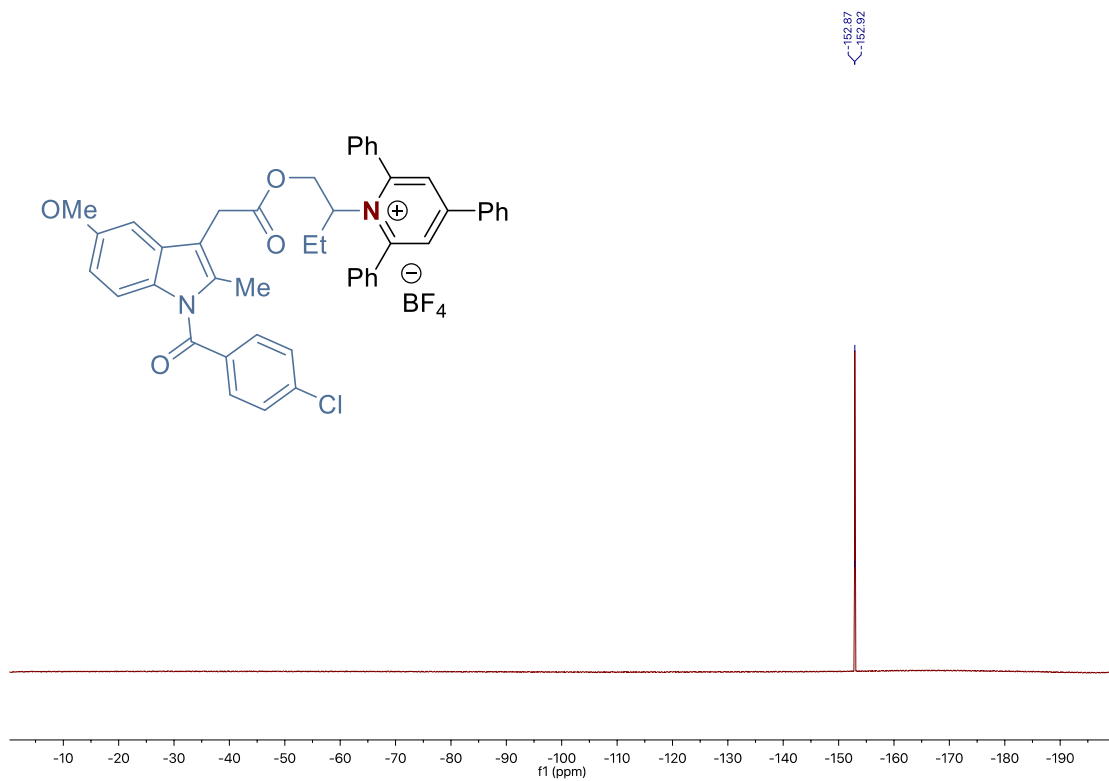
Site-Selective Ni-Catalyzed Deaminative Alkylation of Unactivated Olefins



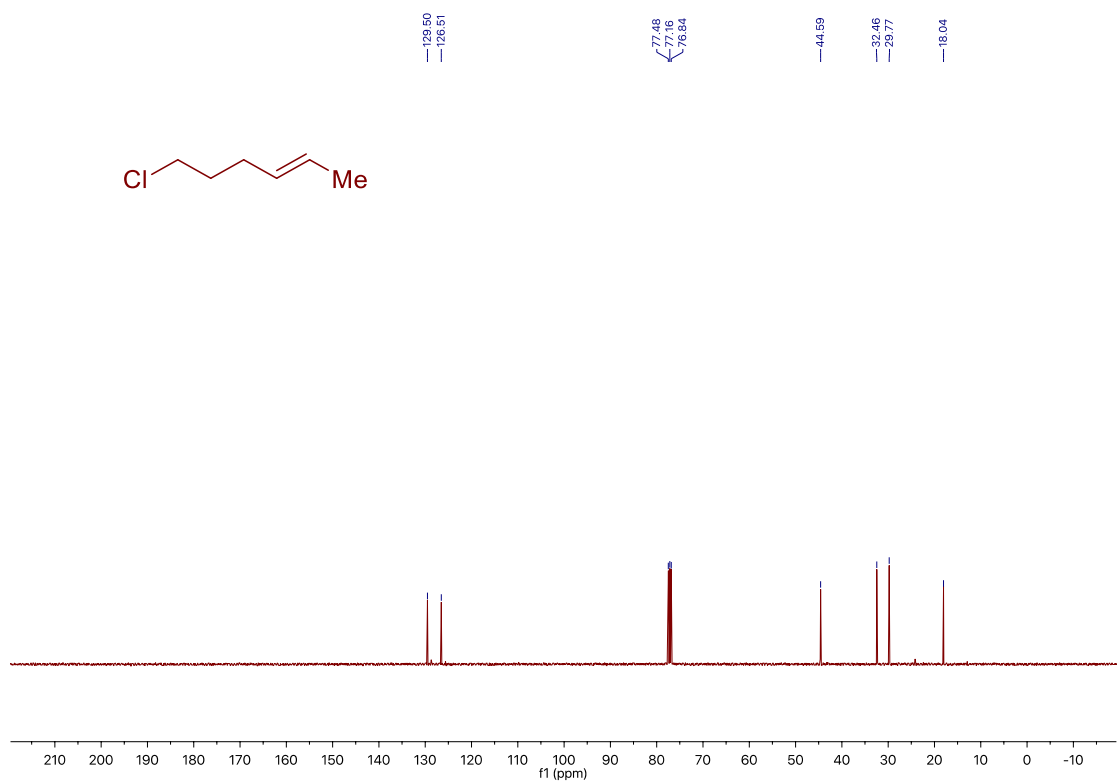
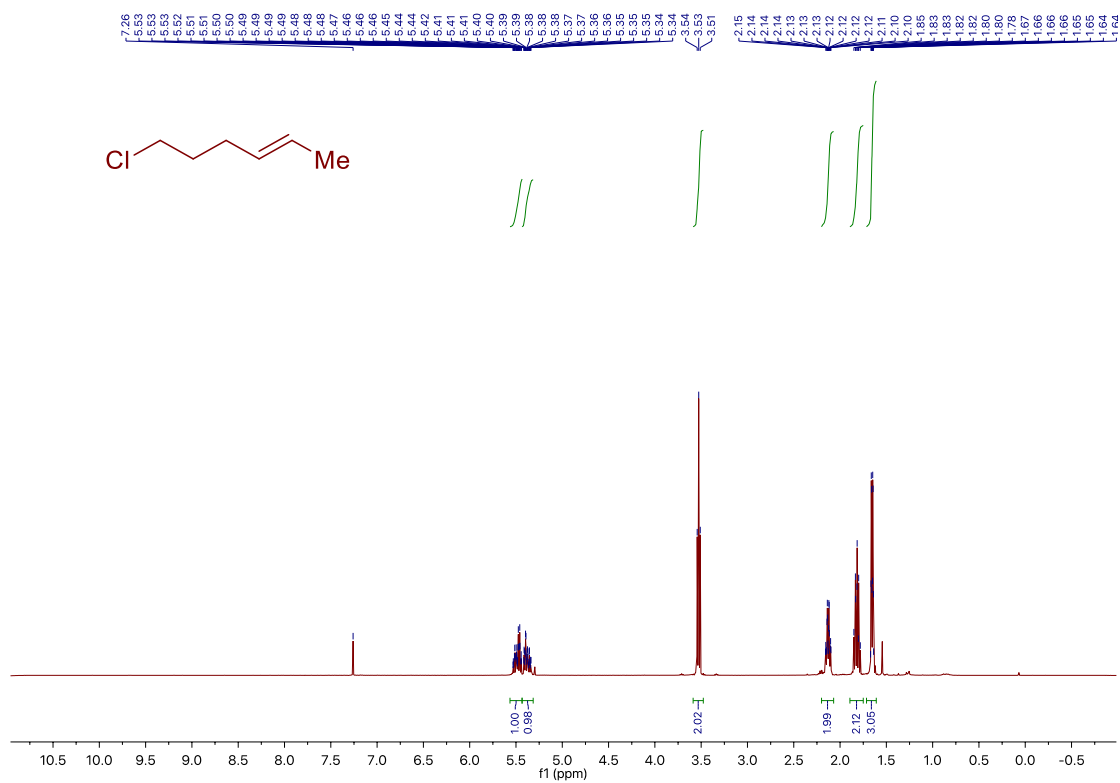
Chapter 3.



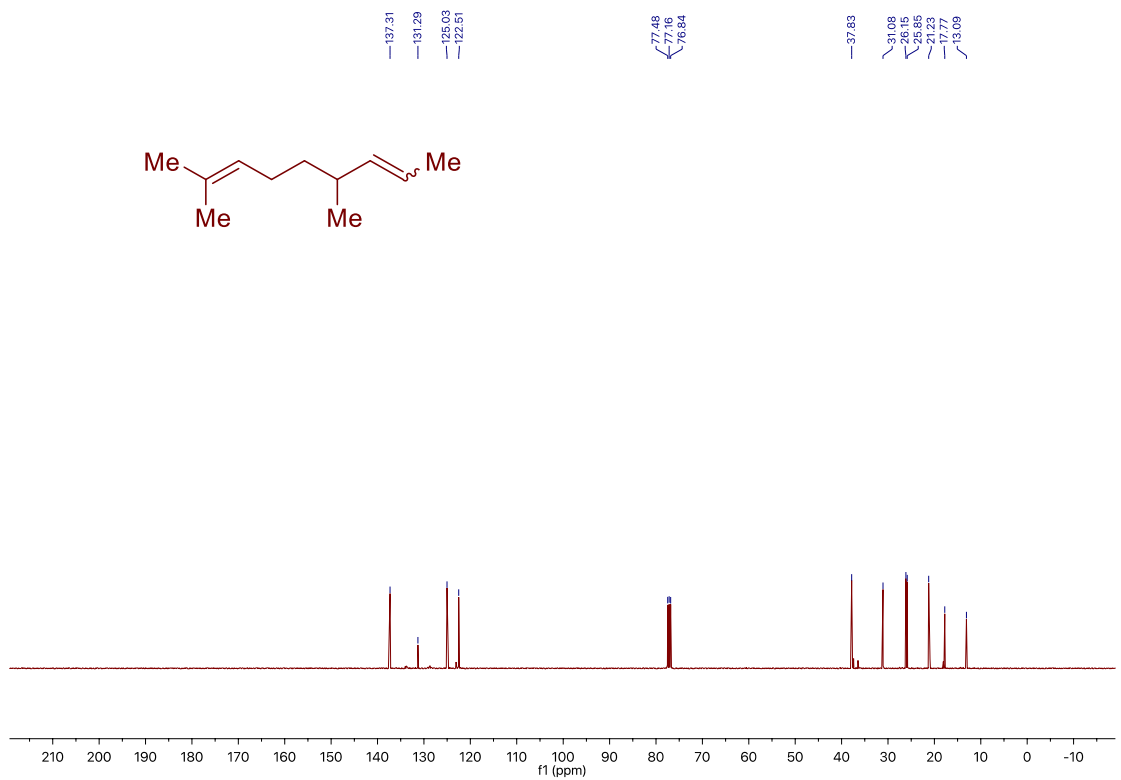
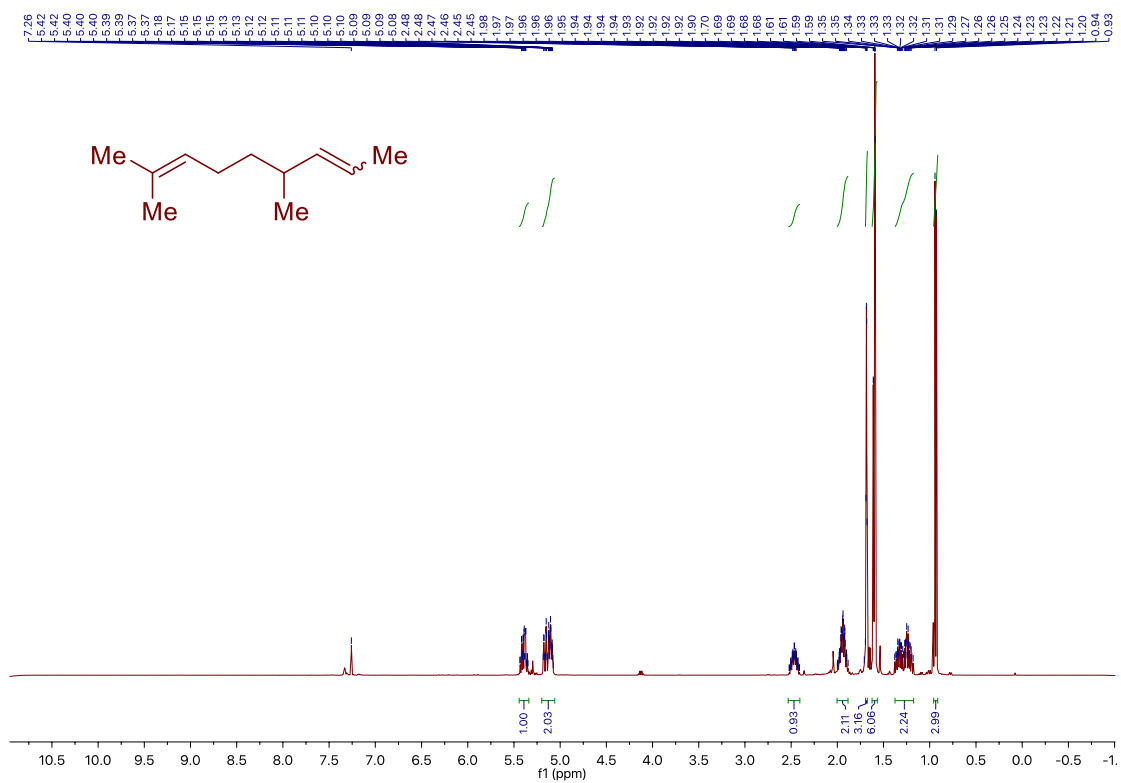
Site-Selective Ni-Catalyzed Deaminative Alkylation of Unactivated Olefins



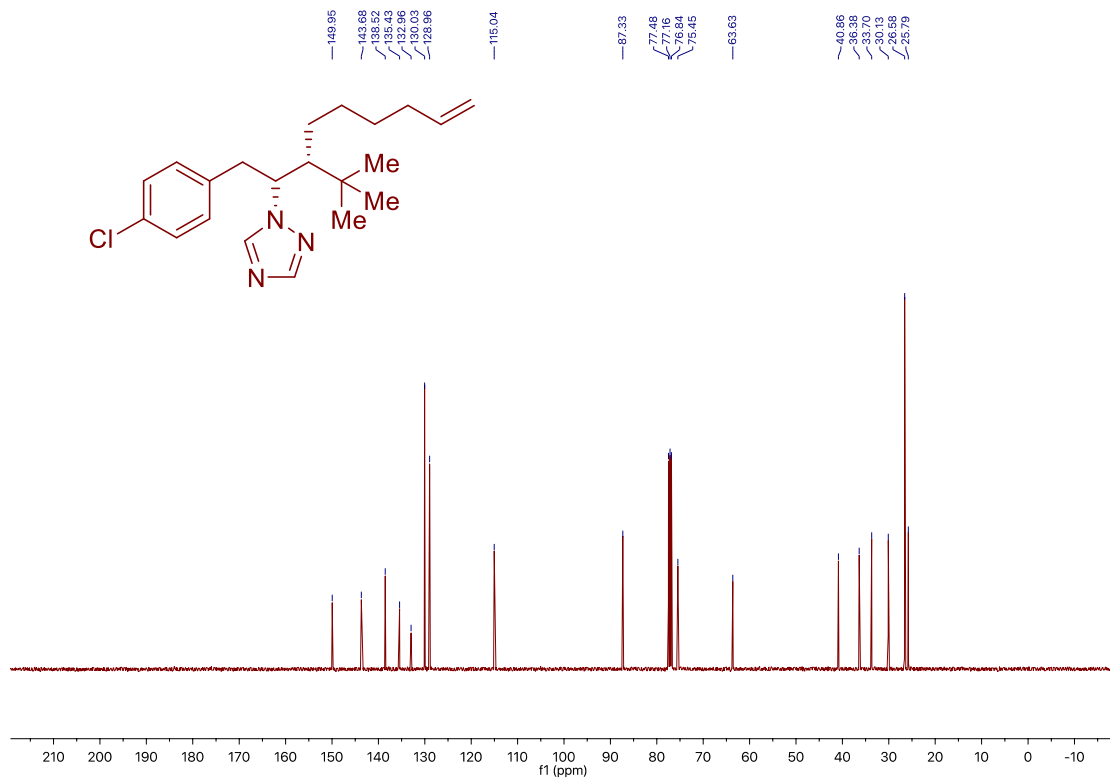
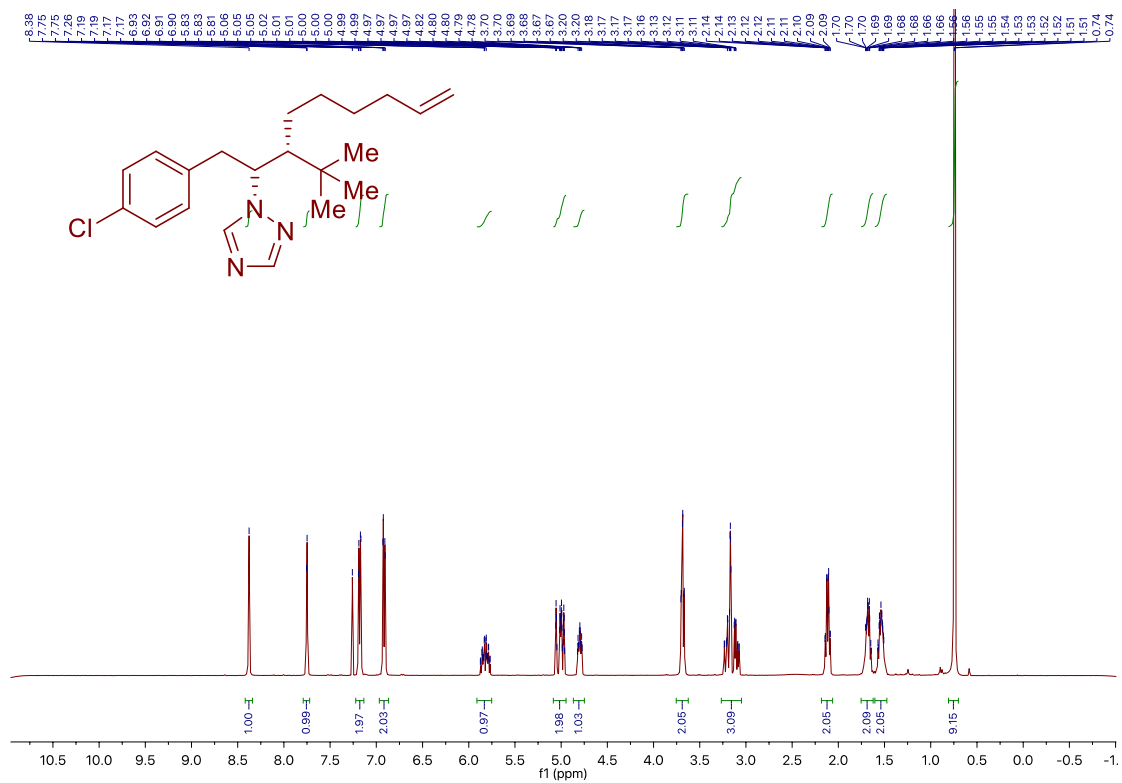
Chapter 3.



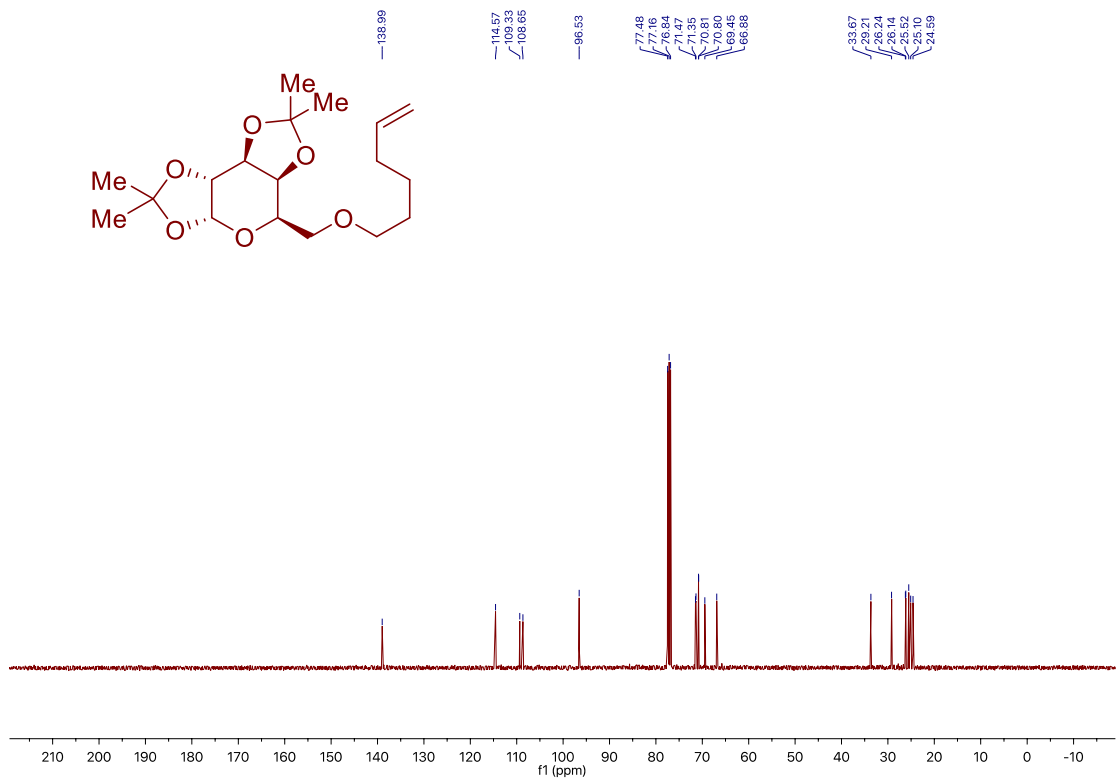
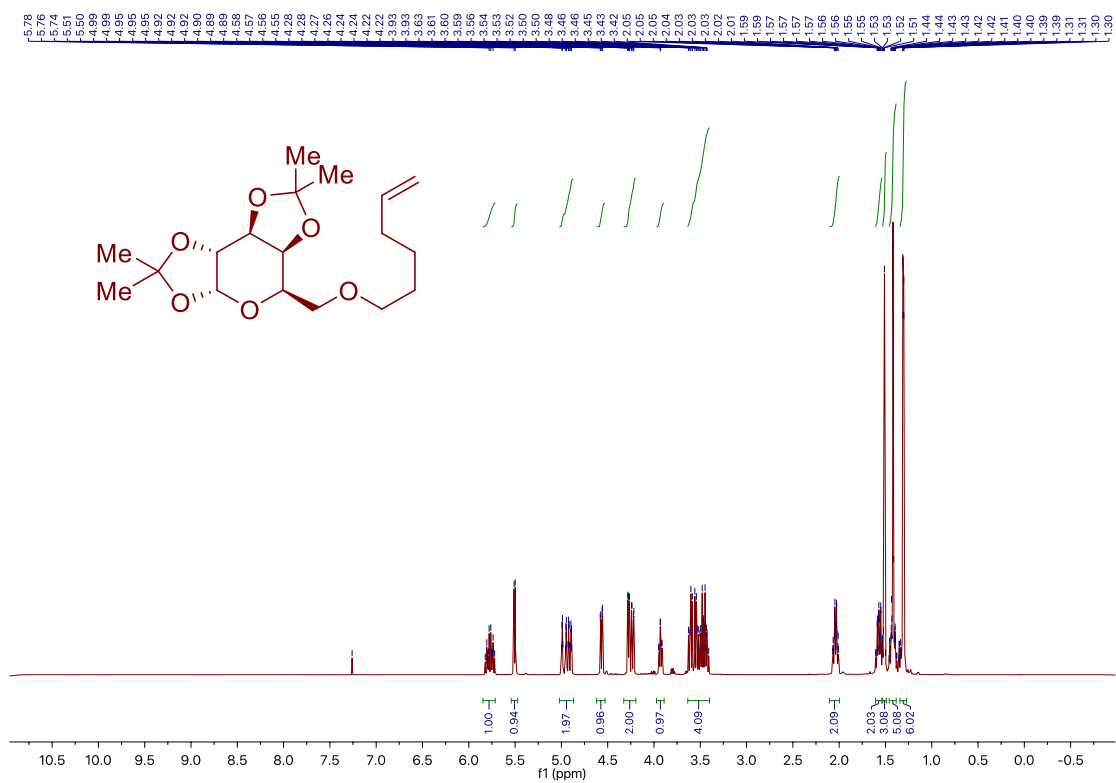
Site-Selective Ni-Catalyzed Deaminative Alkylation of Unactivated Olefins



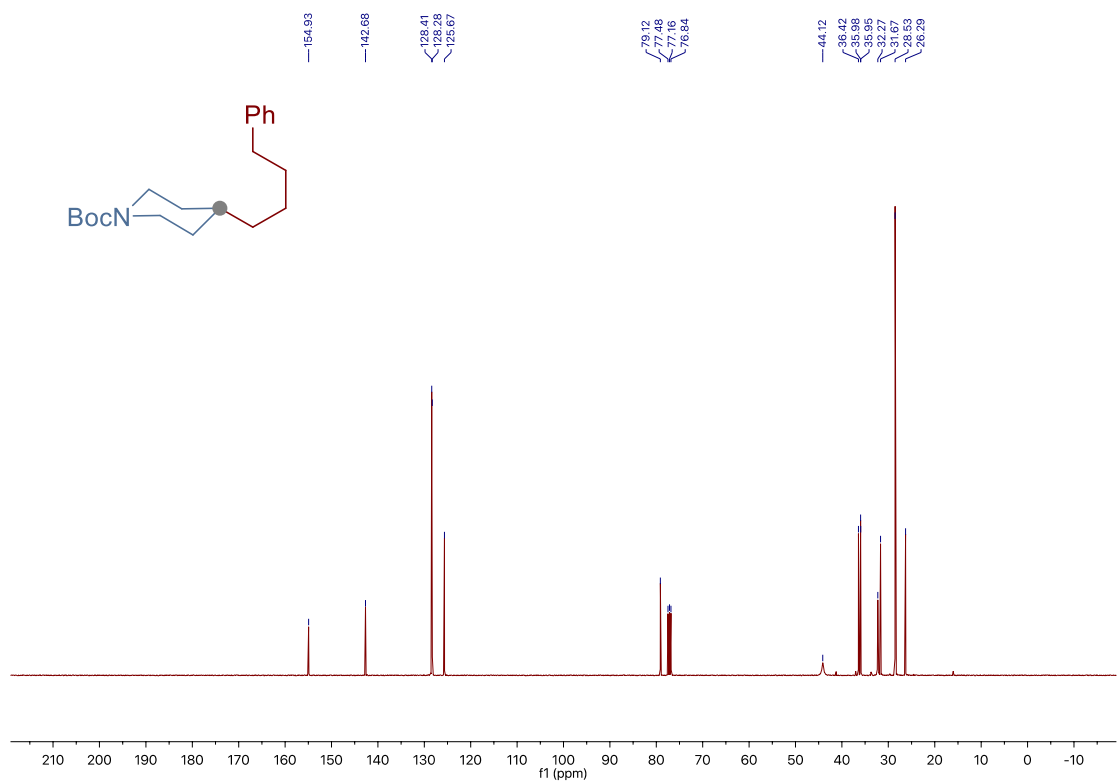
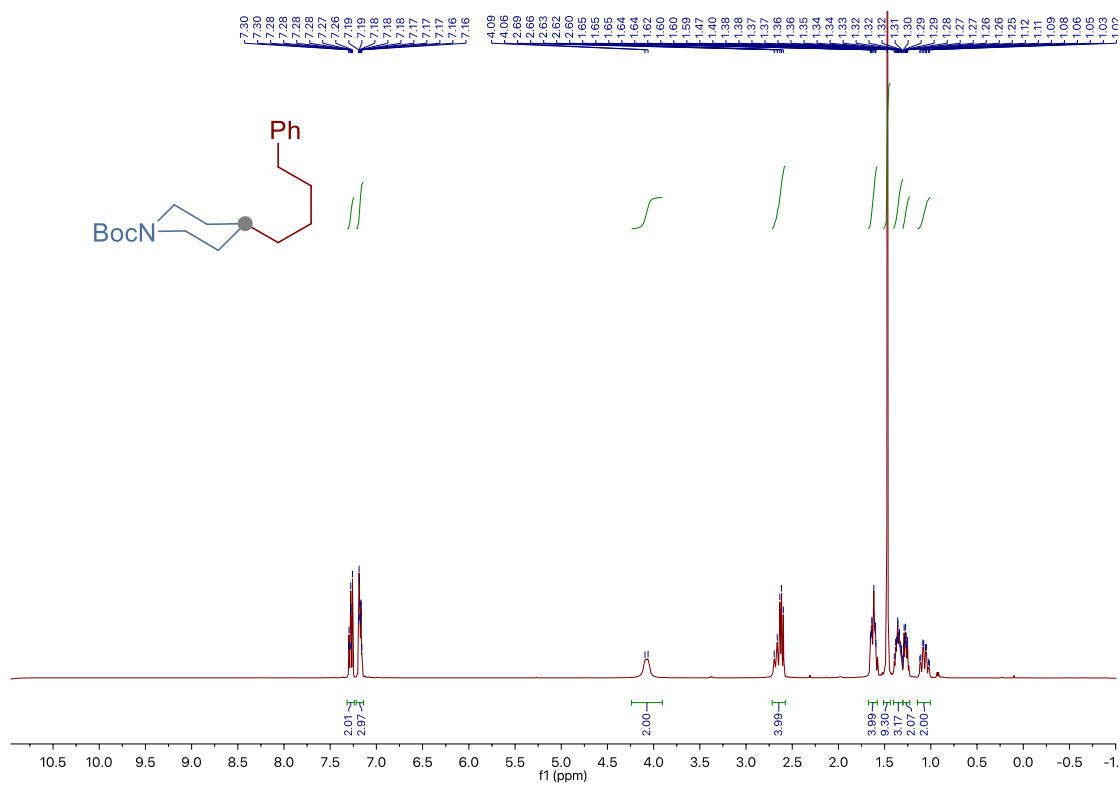
Chapter 3.



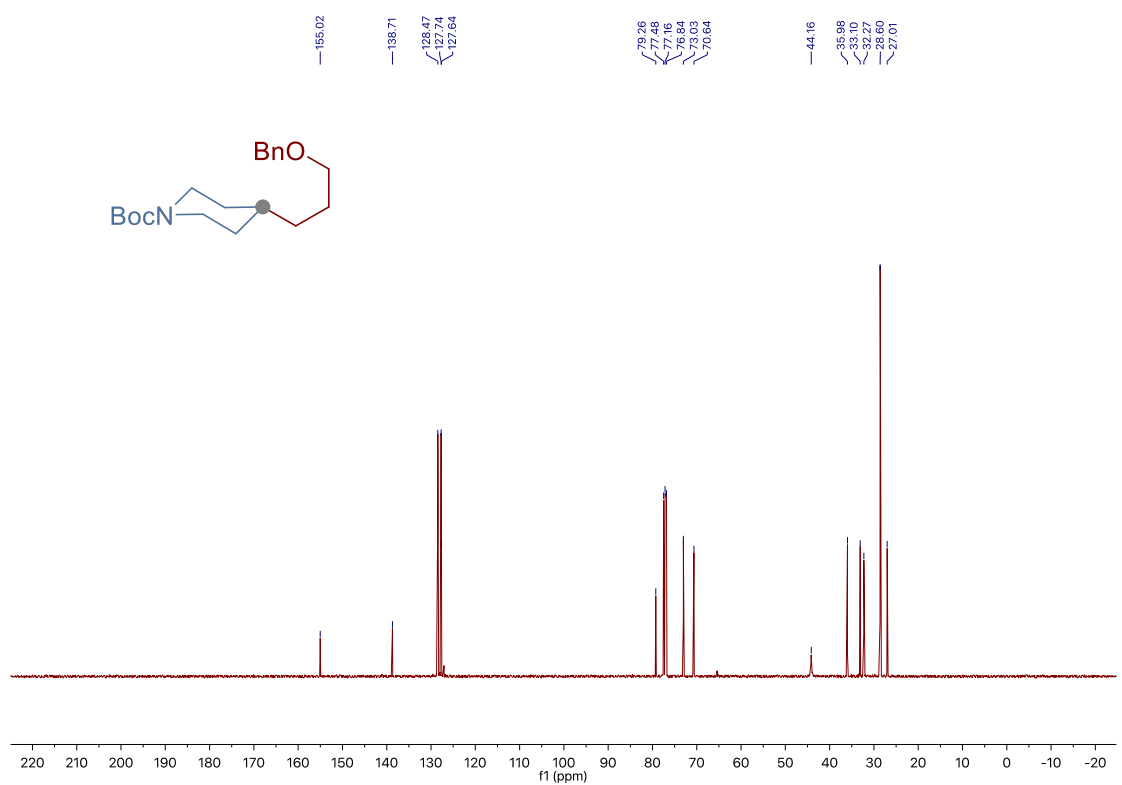
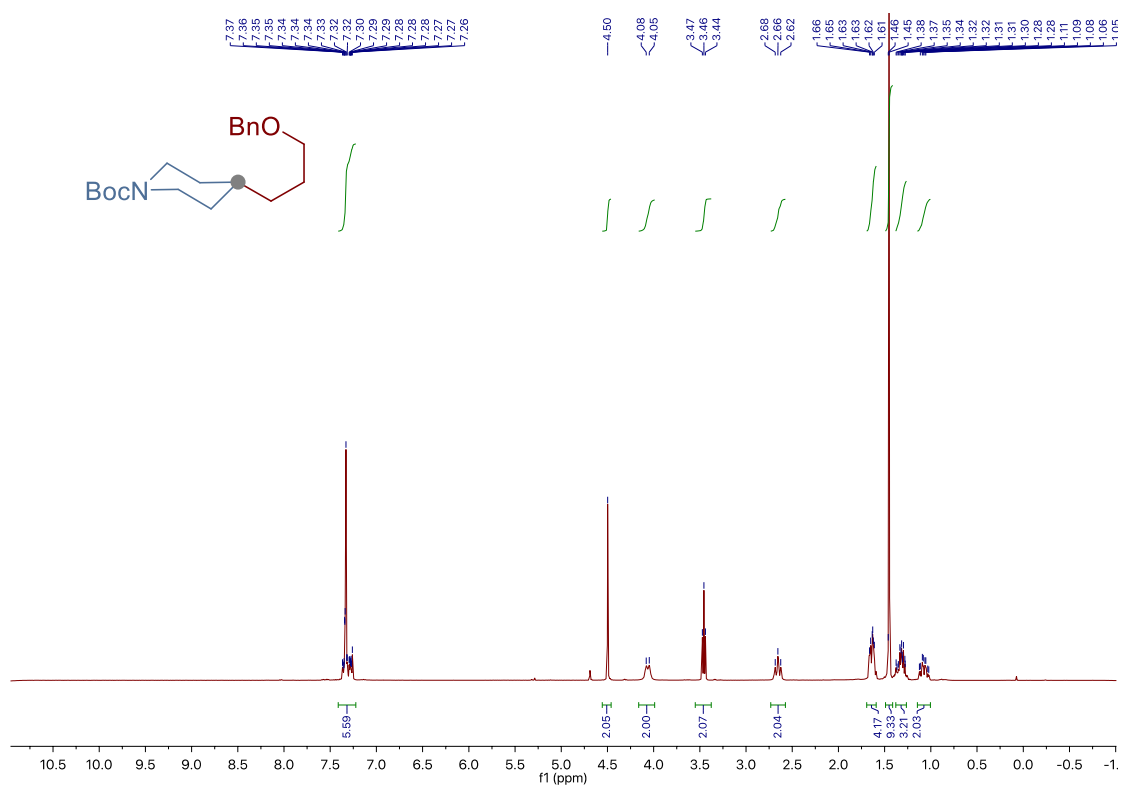
Site-Selective Ni-Catalyzed Deaminative Alkylation of Unactivated Olefins



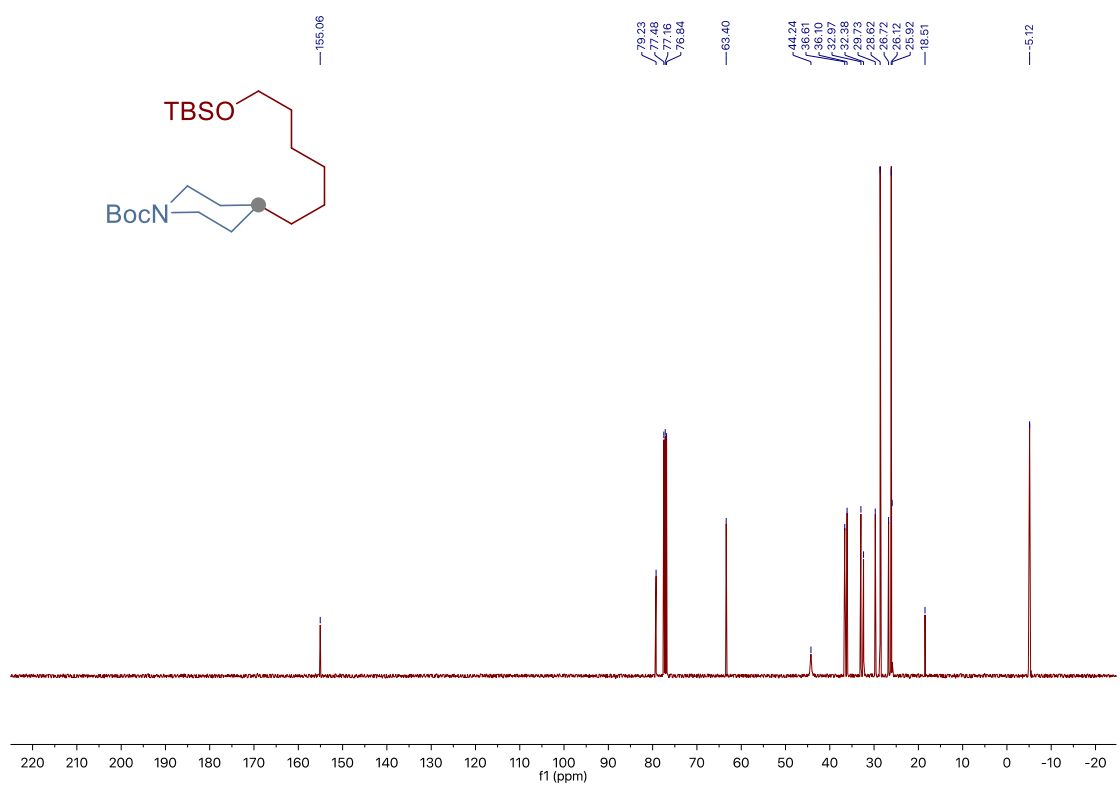
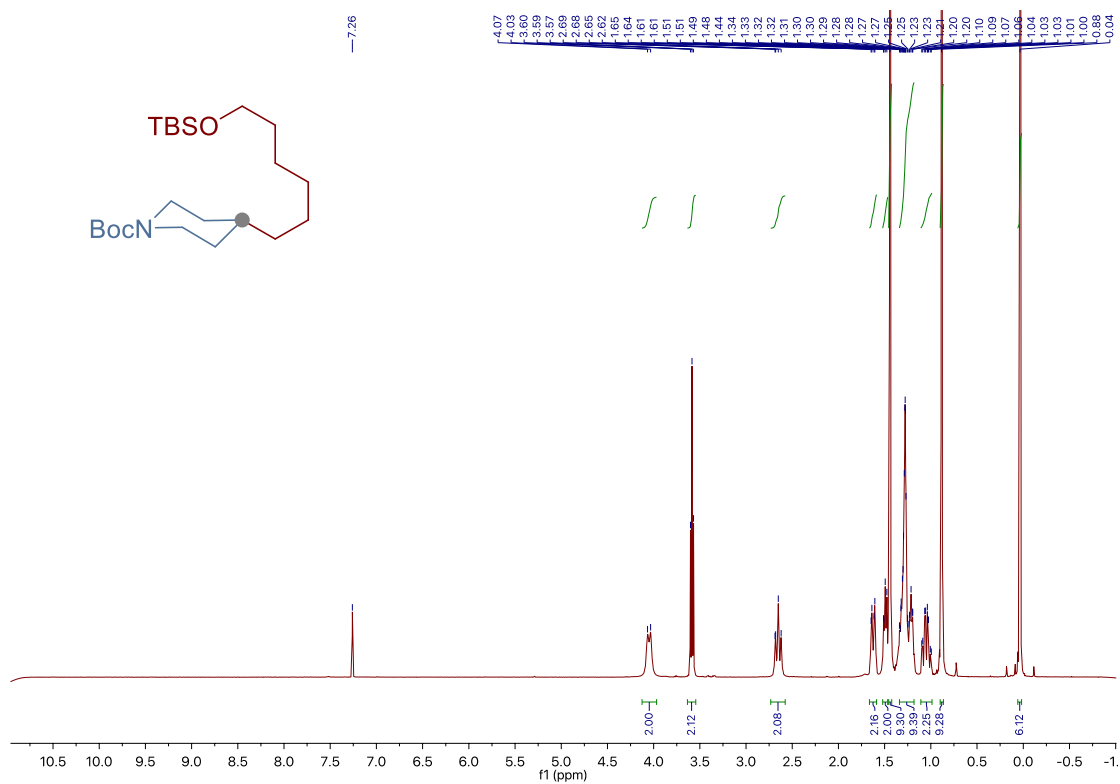
Chapter 3.



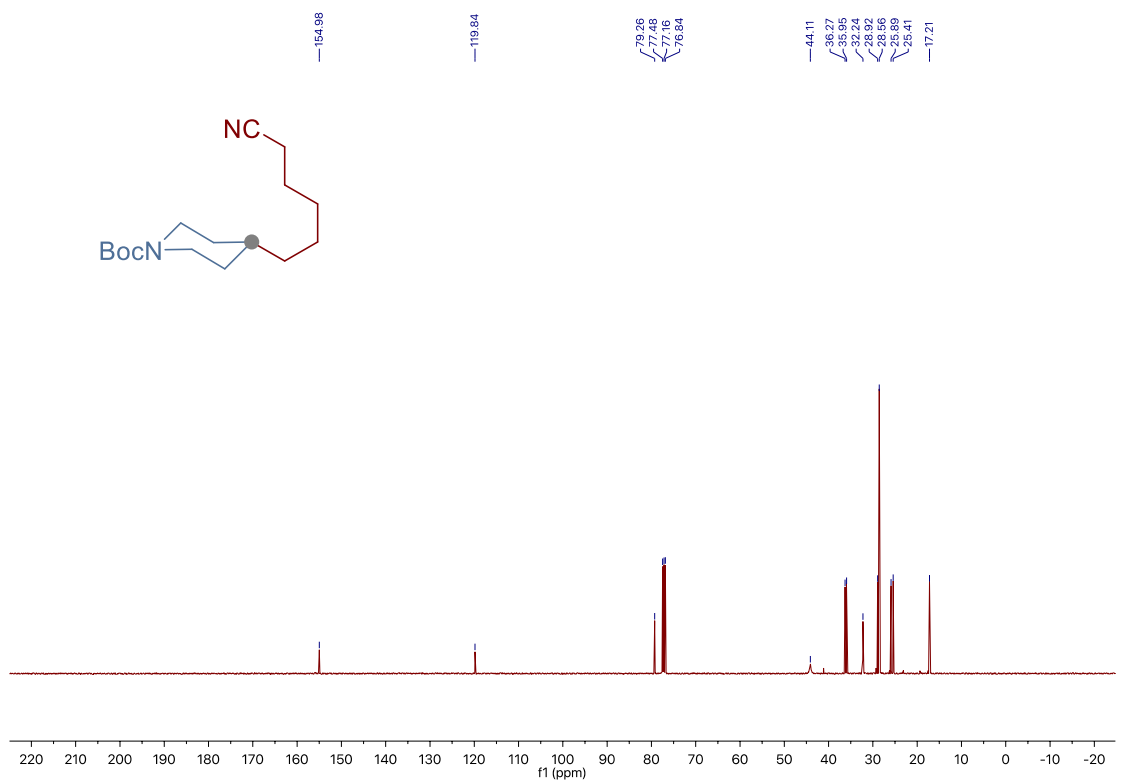
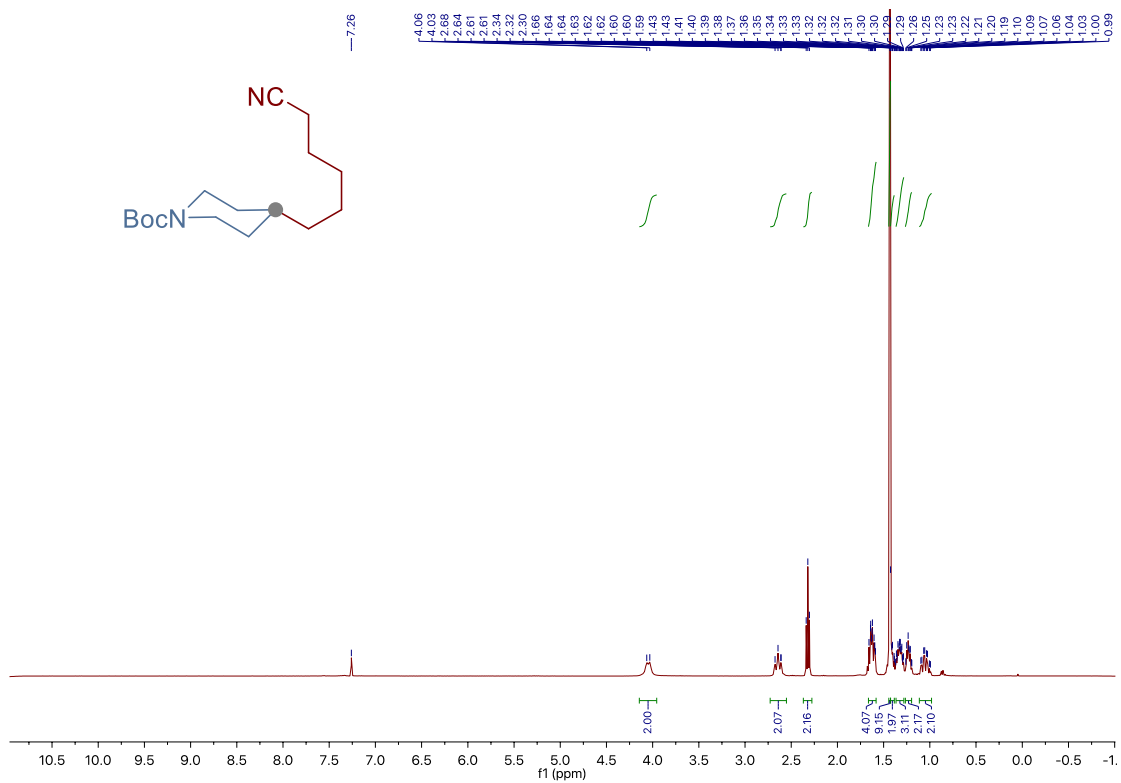
Site-Selective Ni-Catalyzed Deaminative Alkylation of Unactivated Olefins



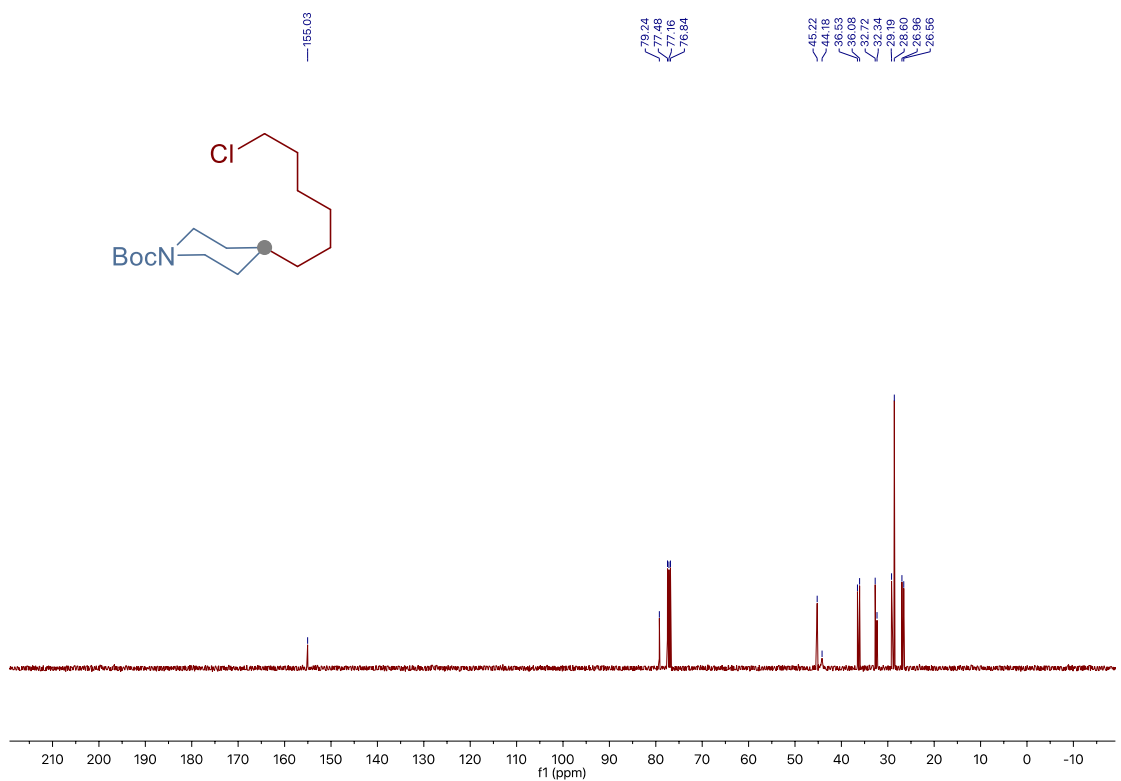
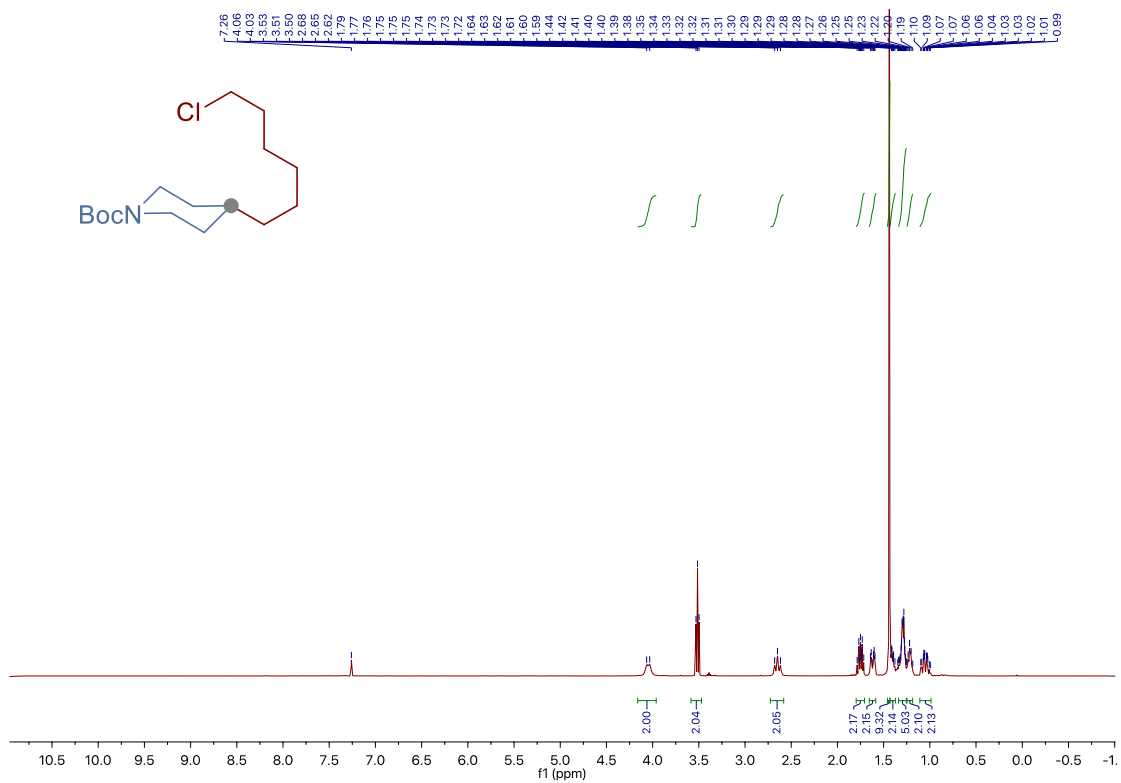
Chapter 3.



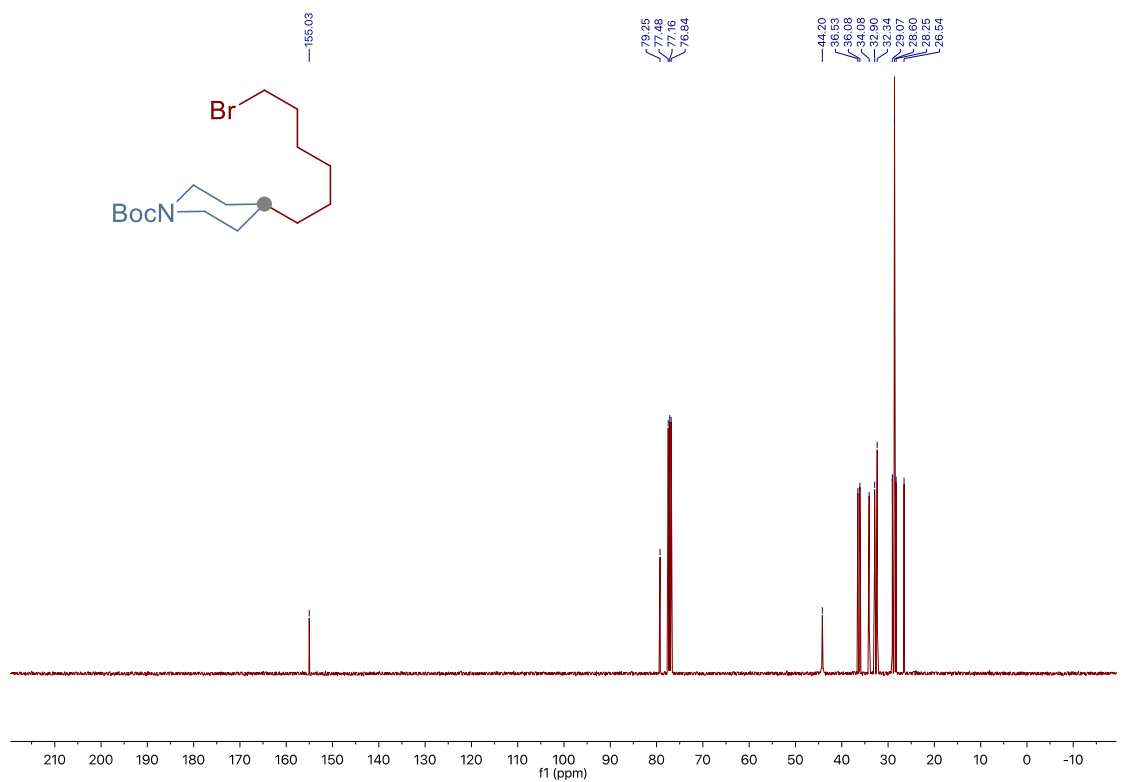
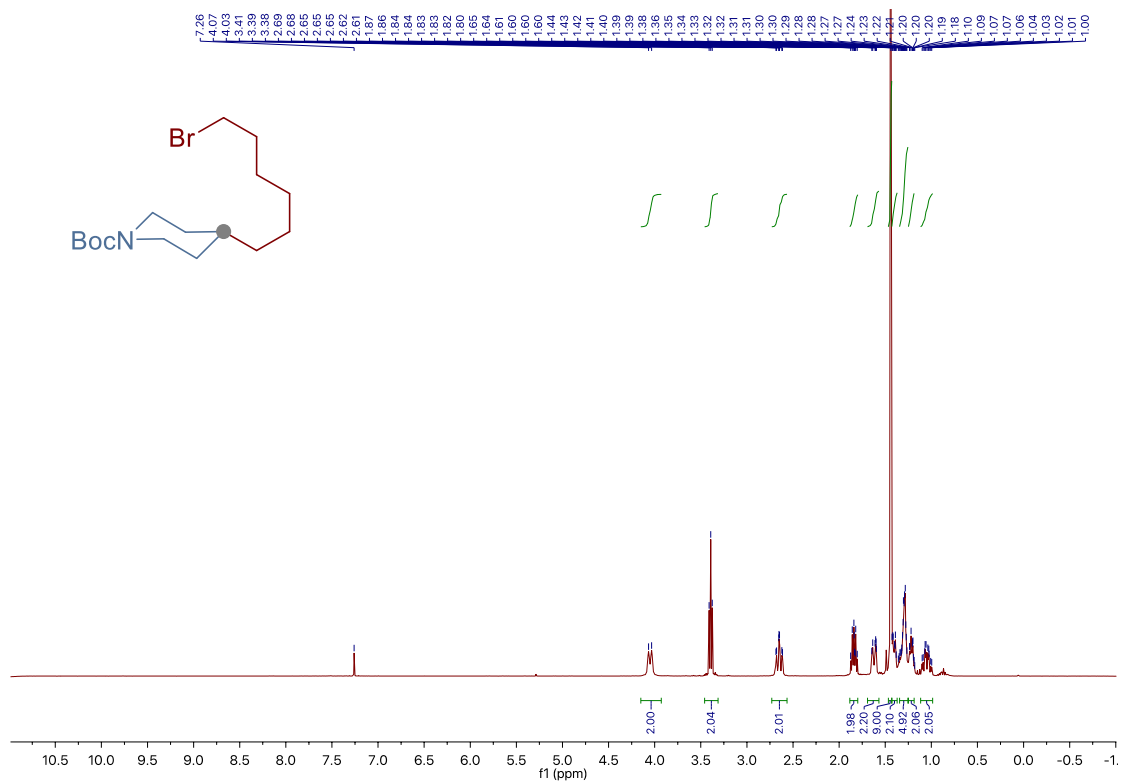
Site-Selective Ni-Catalyzed Deaminative Alkylation of Unactivated Olefins



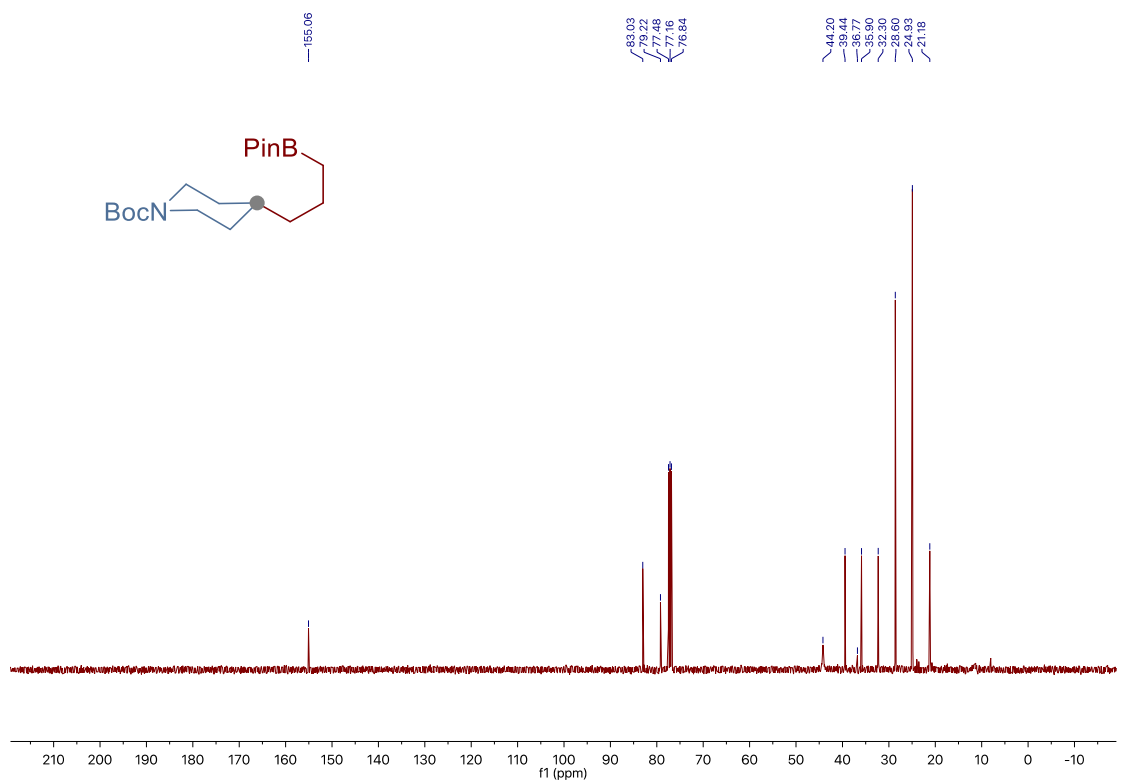
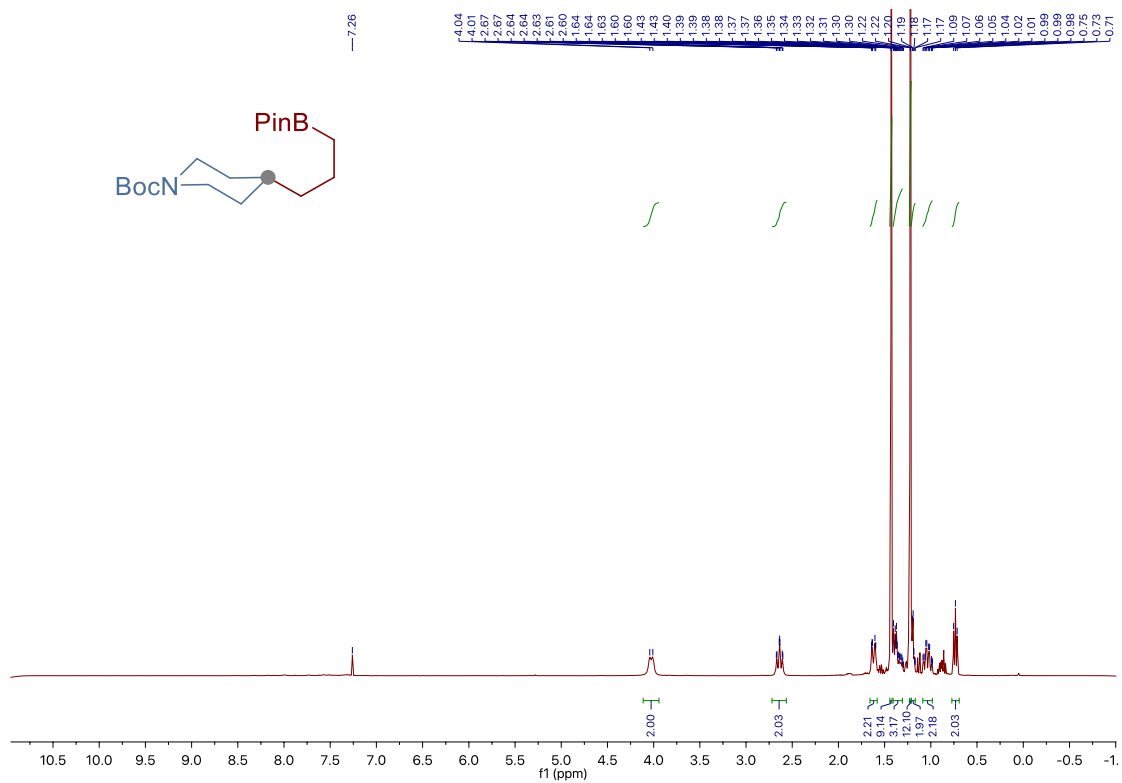
Chapter 3.



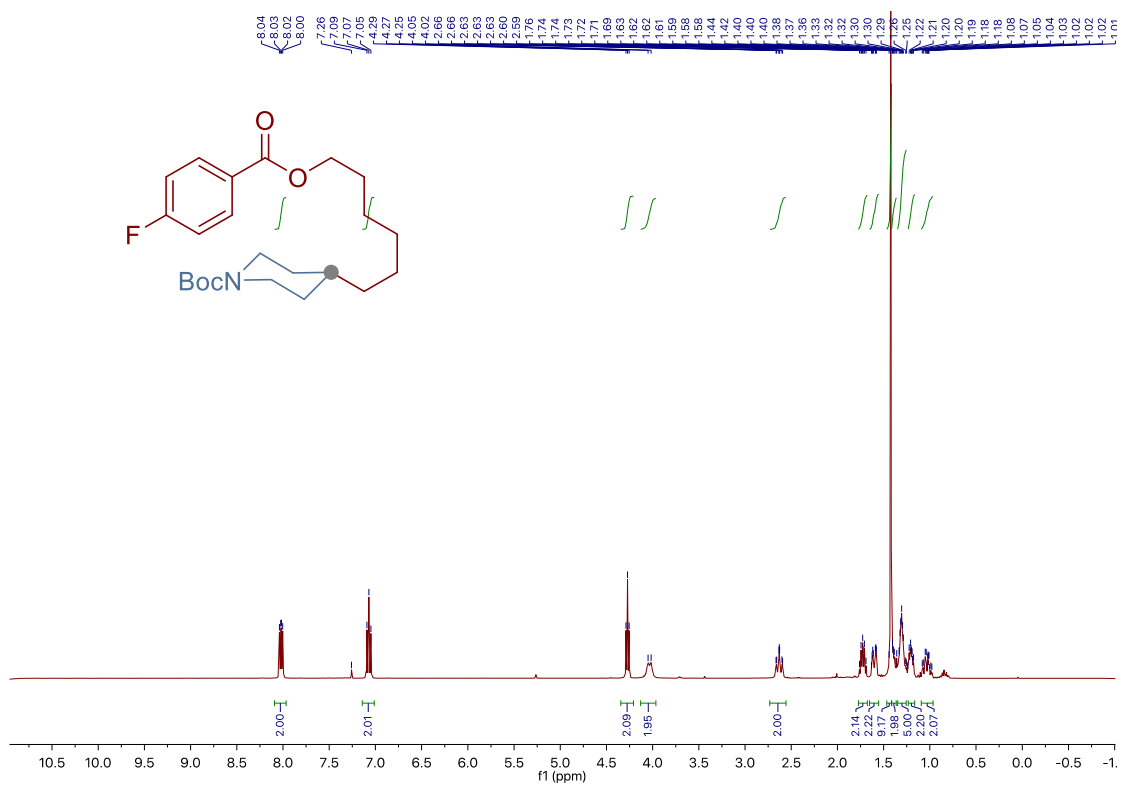
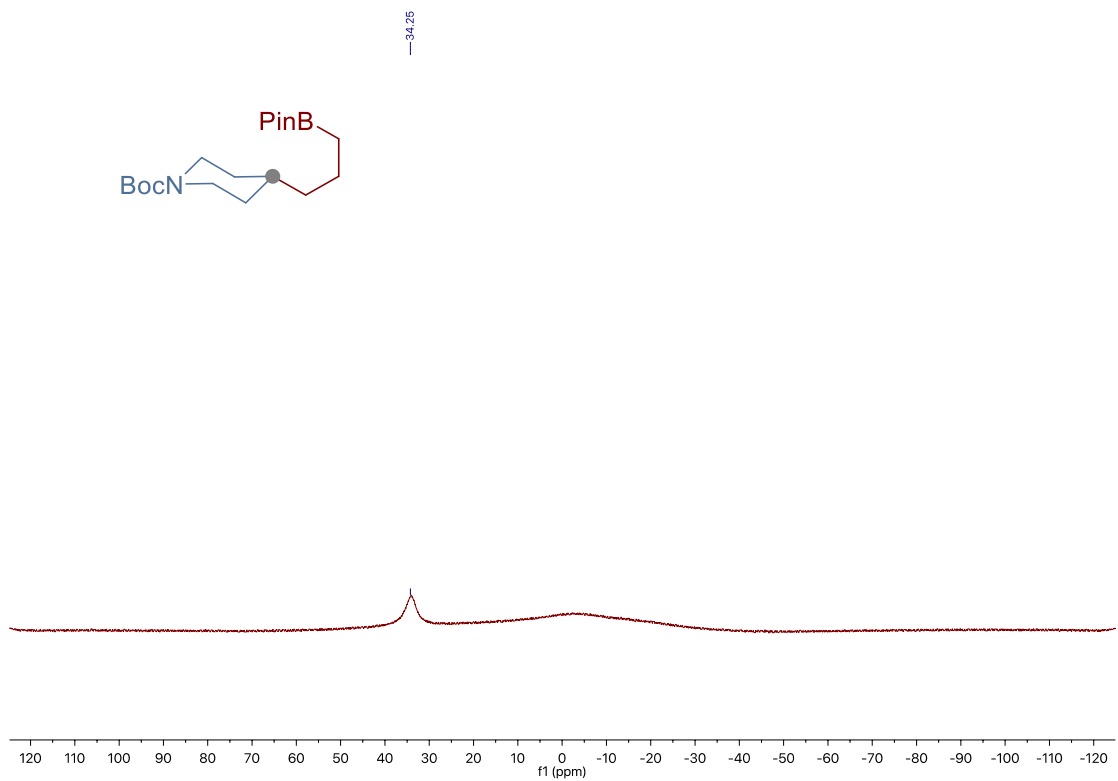
Site-Selective Ni-Catalyzed Deaminative Alkylation of Unactivated Olefins



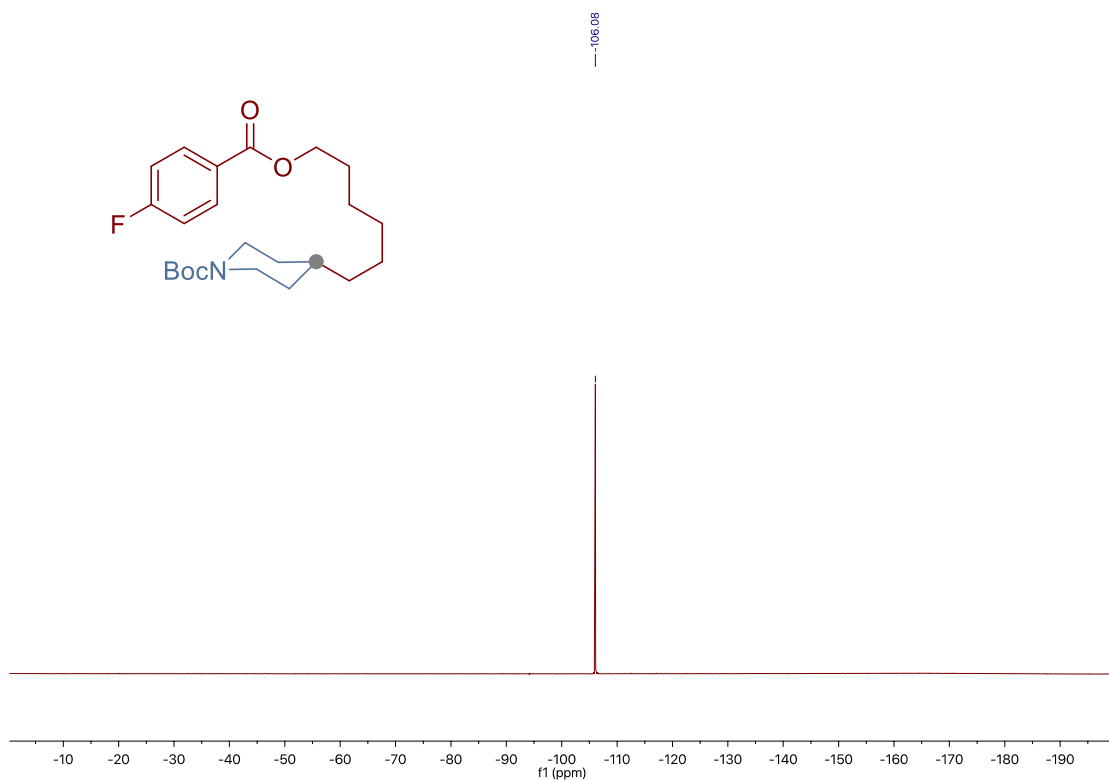
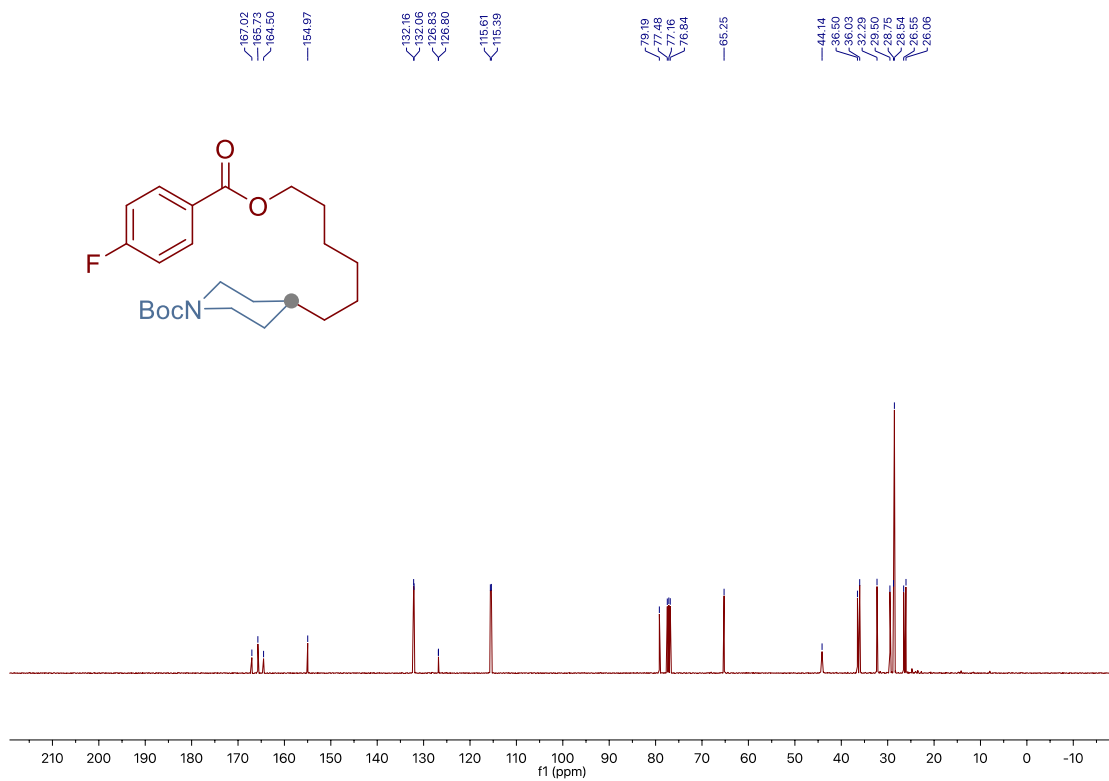
Chapter 3.



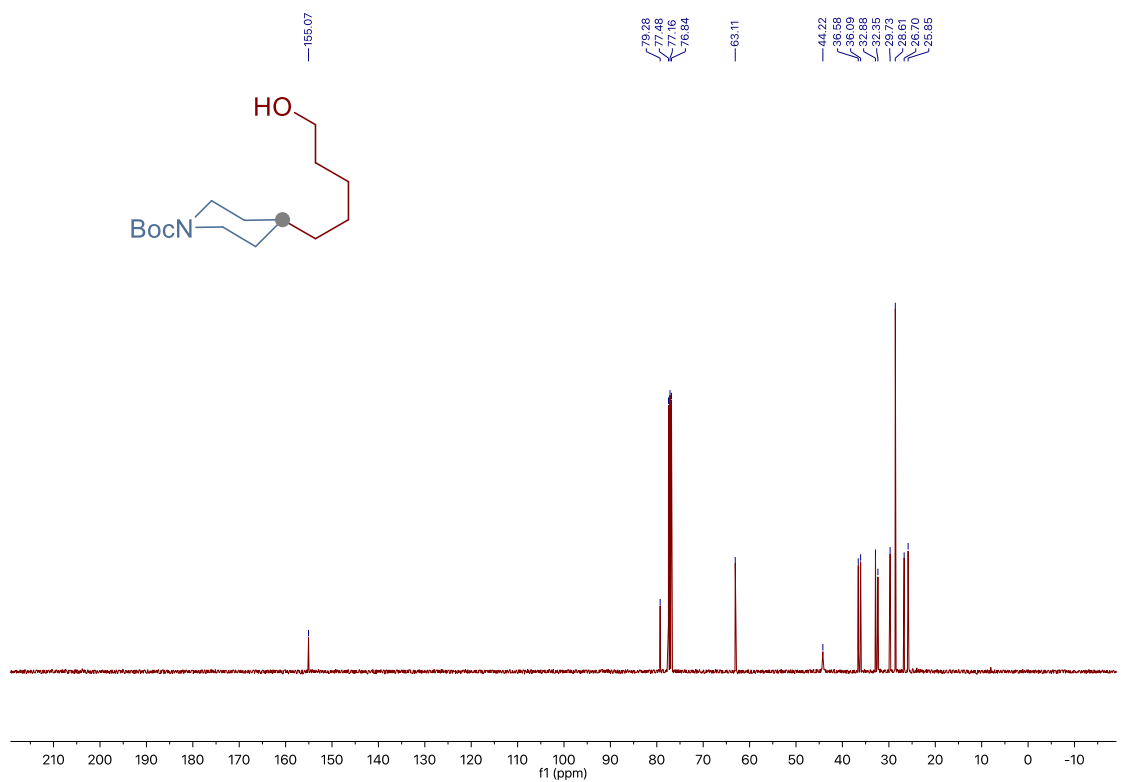
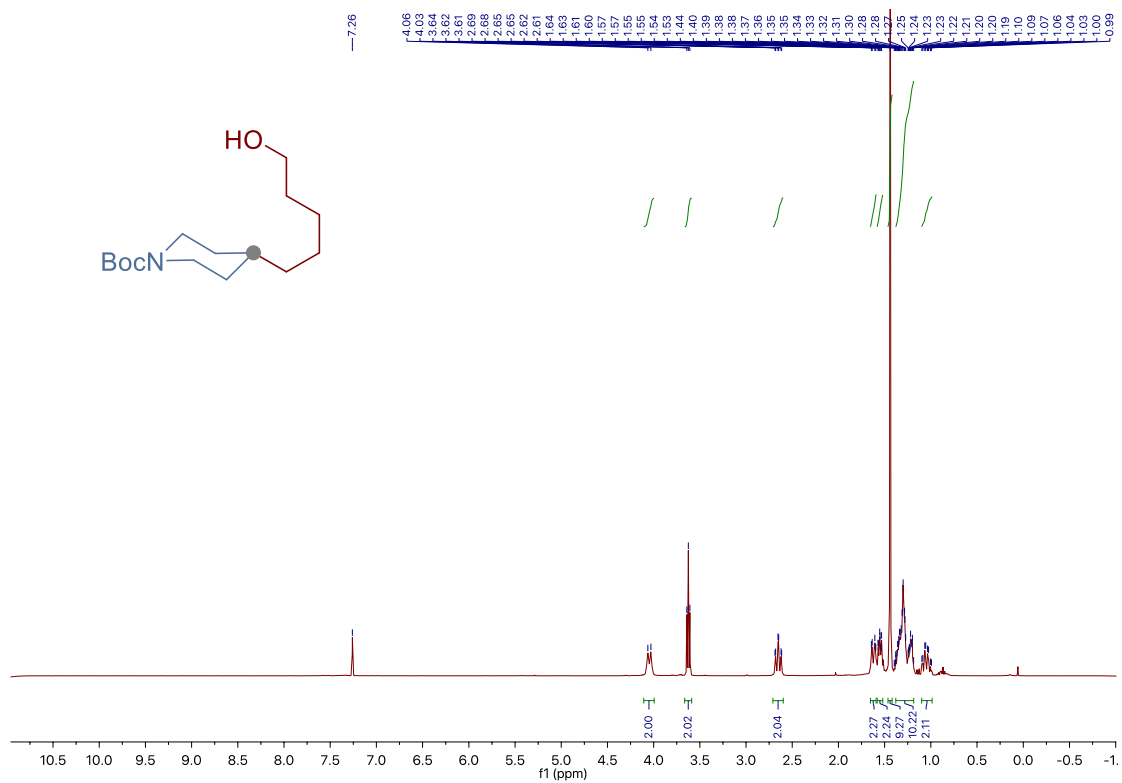
Site-Selective Ni-Catalyzed Deaminative Alkylation of Unactivated Olefins



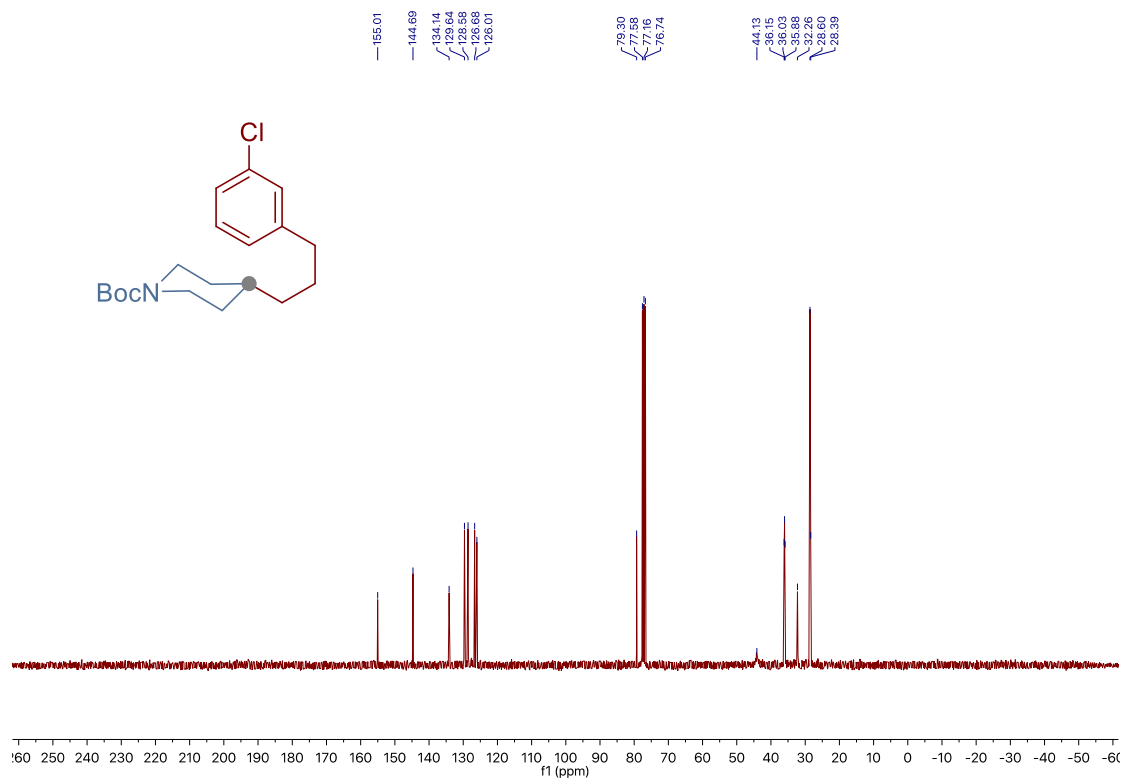
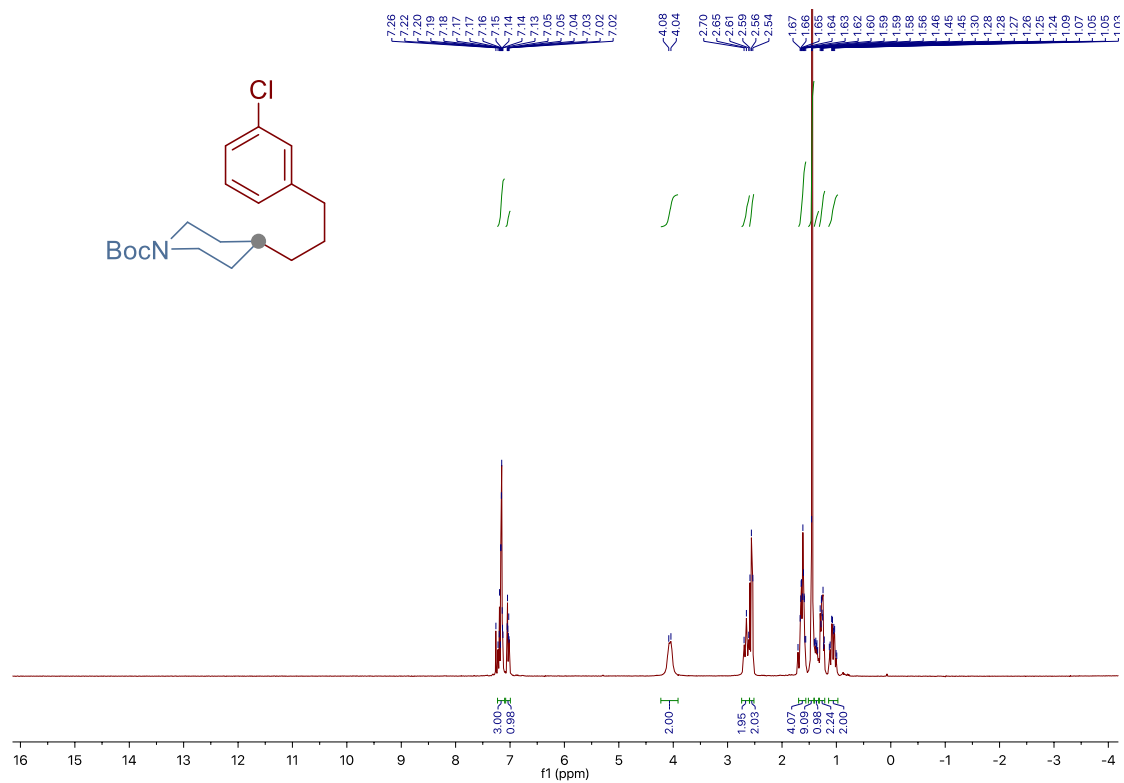
Chapter 3.



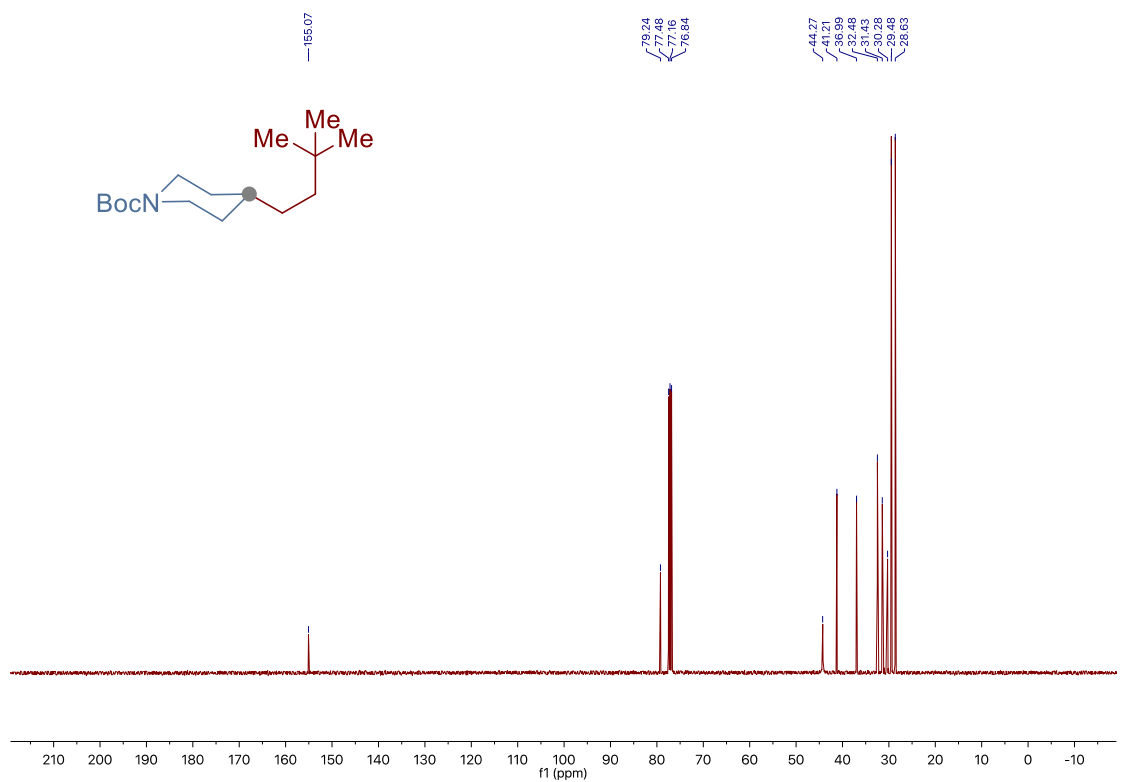
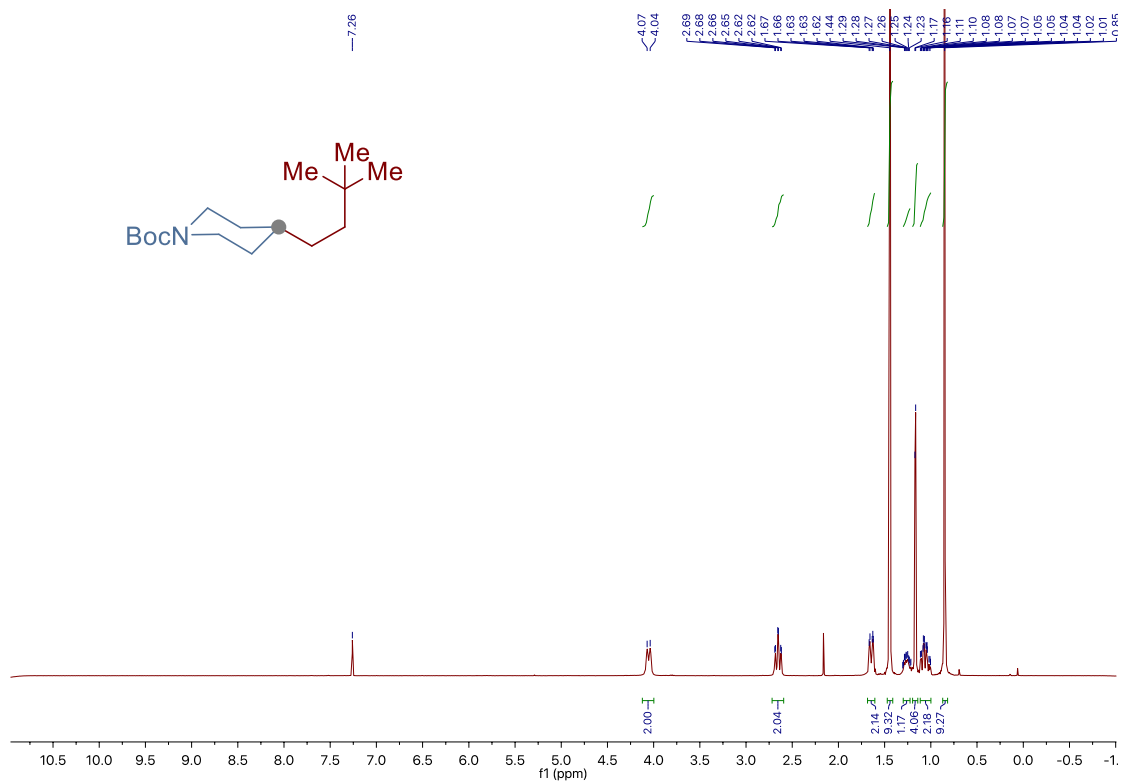
Site-Selective Ni-Catalyzed Deaminative Alkylation of Unactivated Olefins



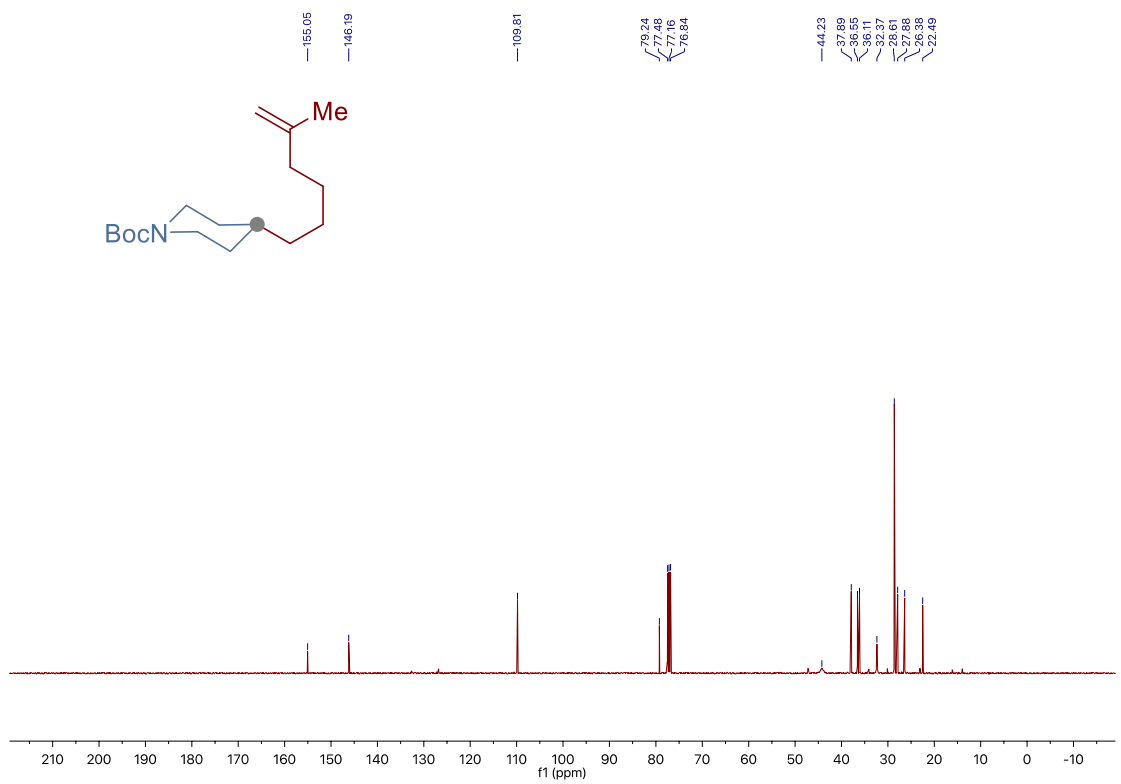
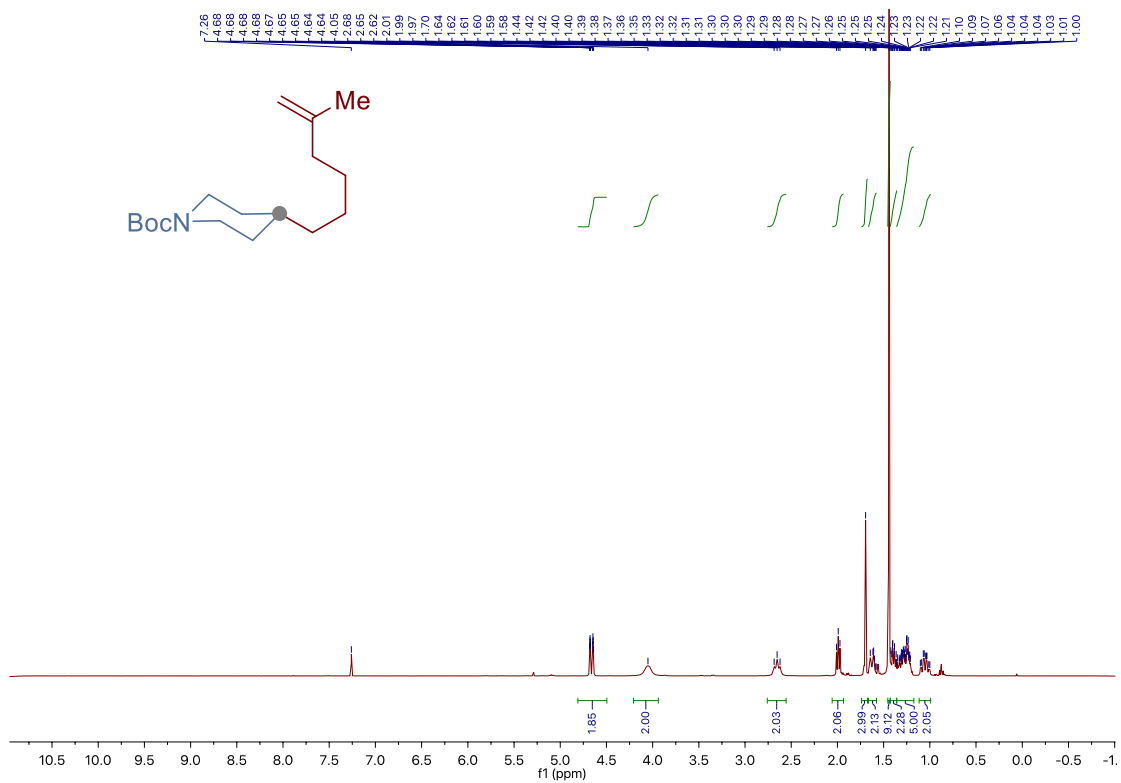
Chapter 3.



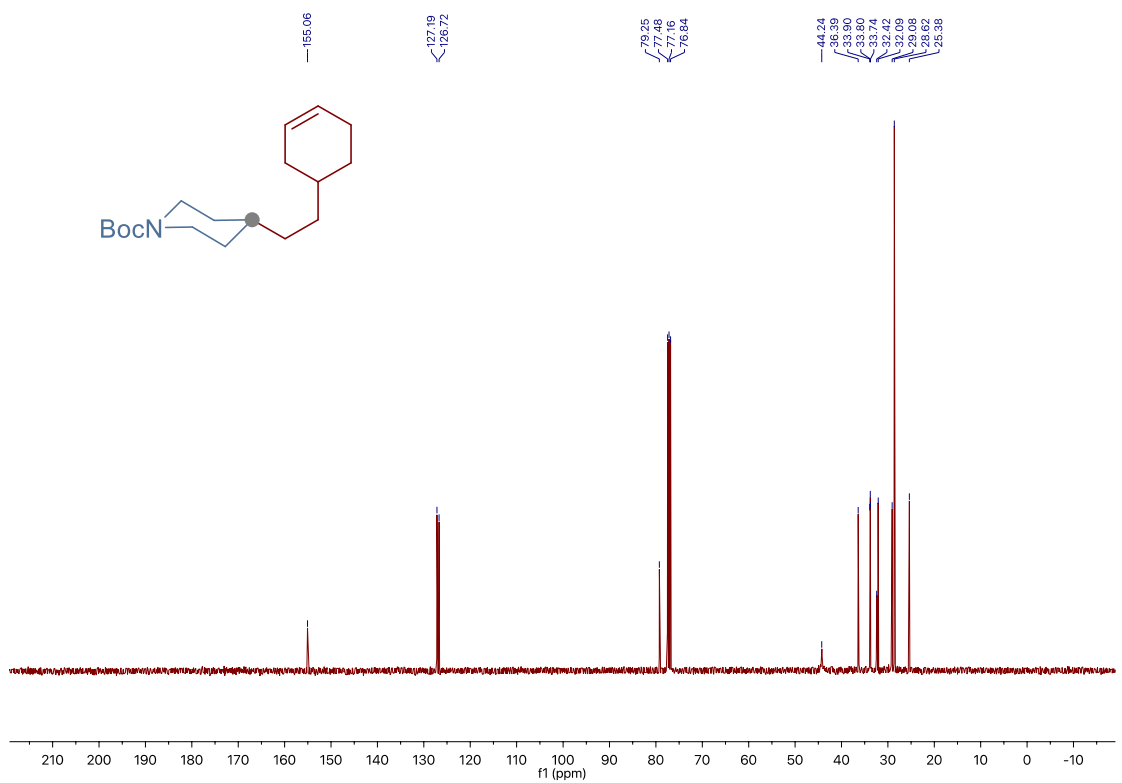
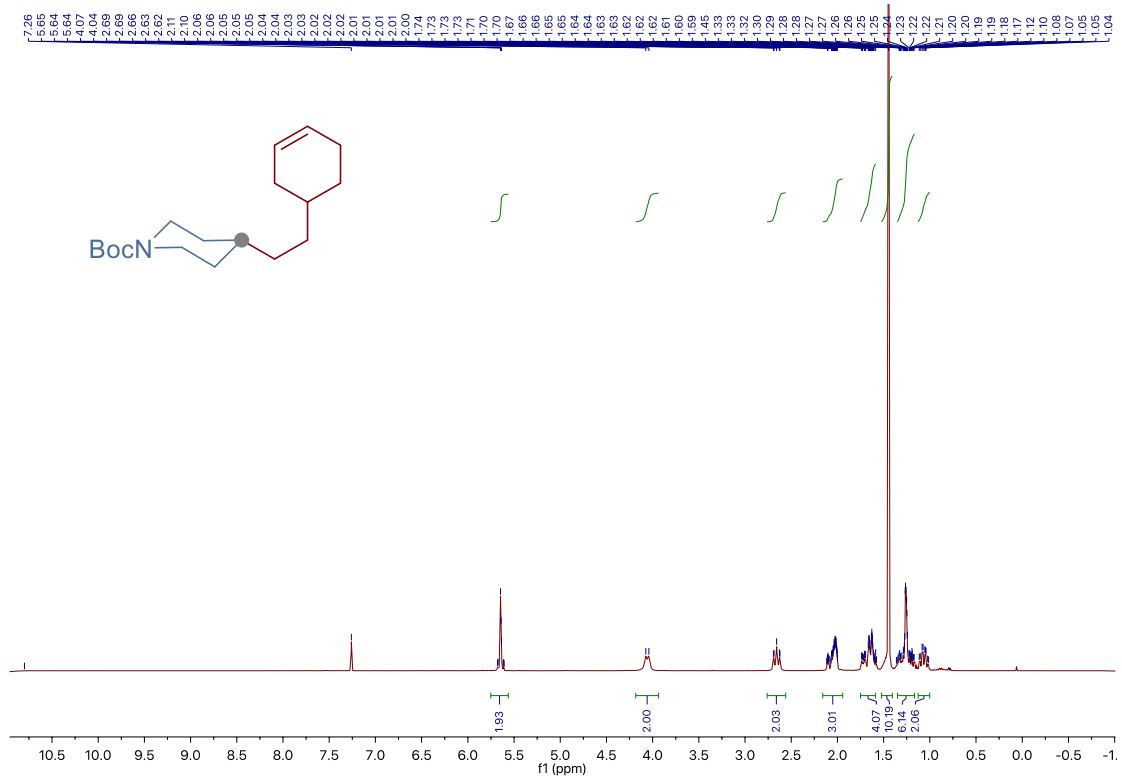
Site-Selective Ni-Catalyzed Deaminative Alkylation of Unactivated Olefins



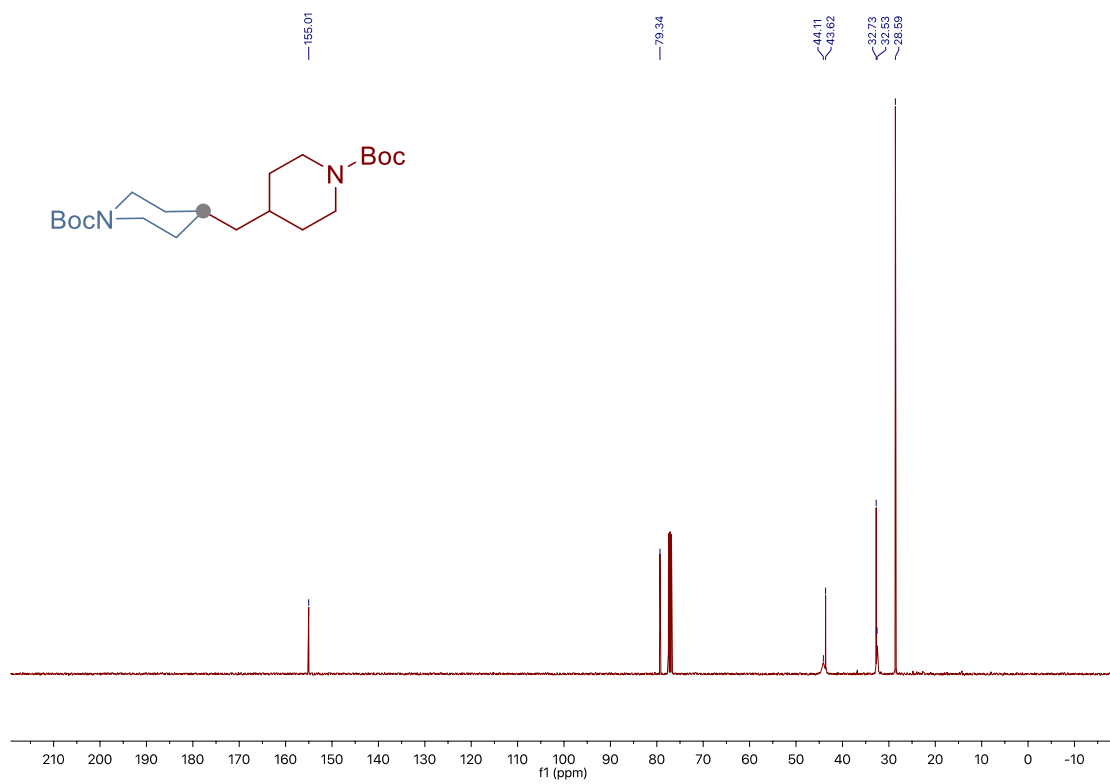
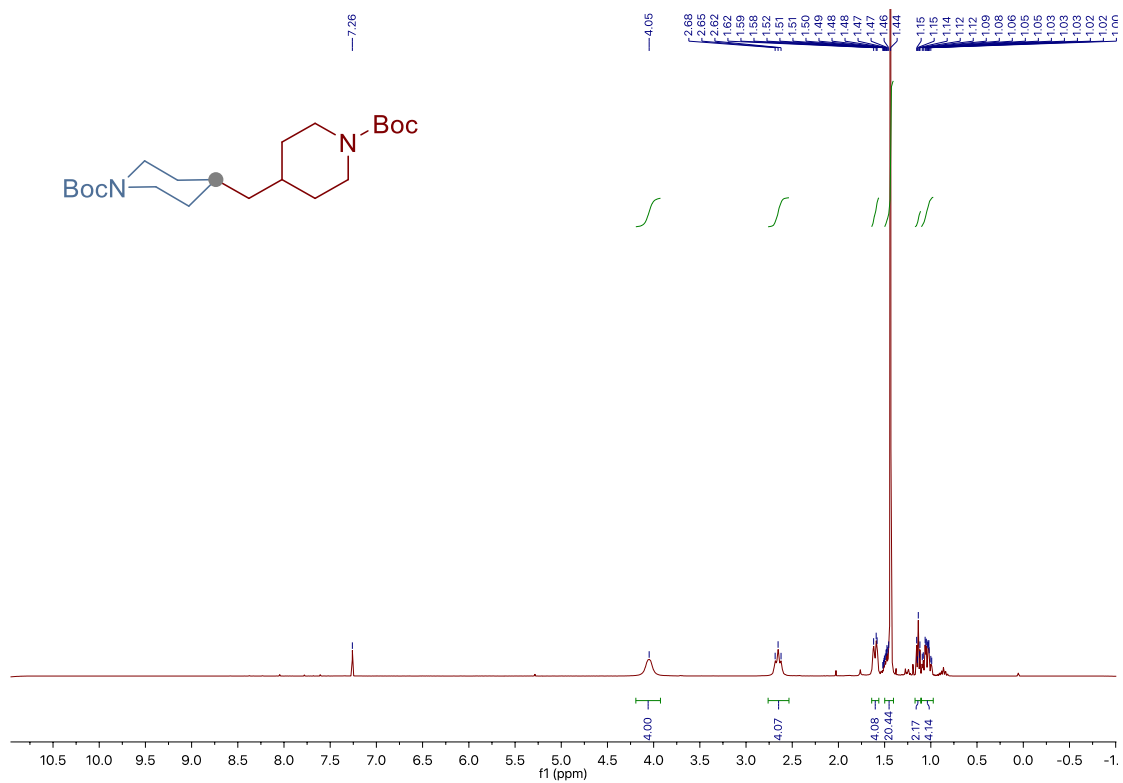
Chapter 3.



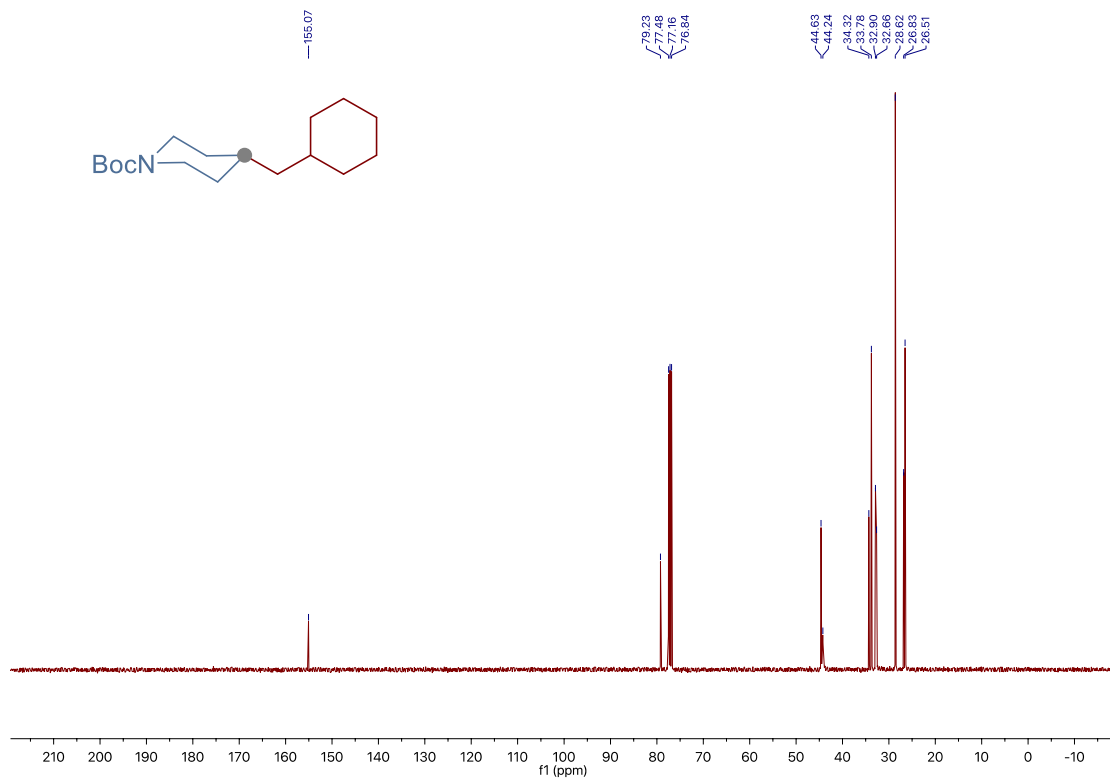
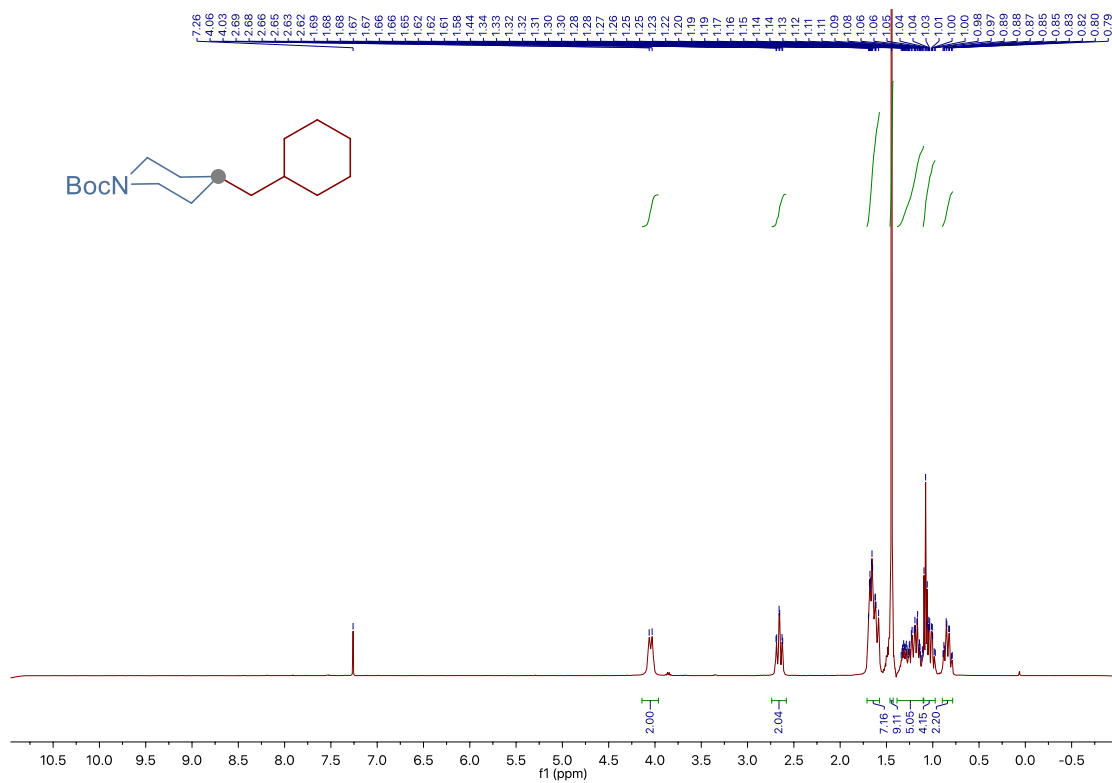
Site-Selective Ni-Catalyzed Deaminative Alkylation of Unactivated Olefins



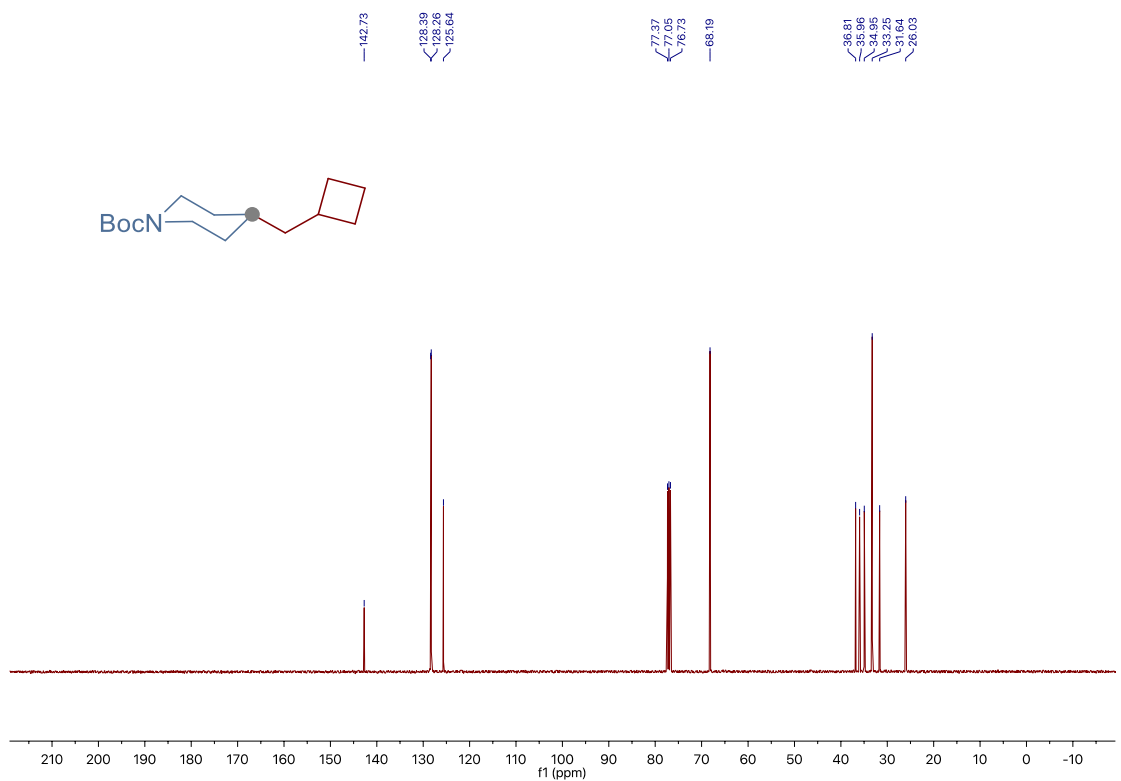
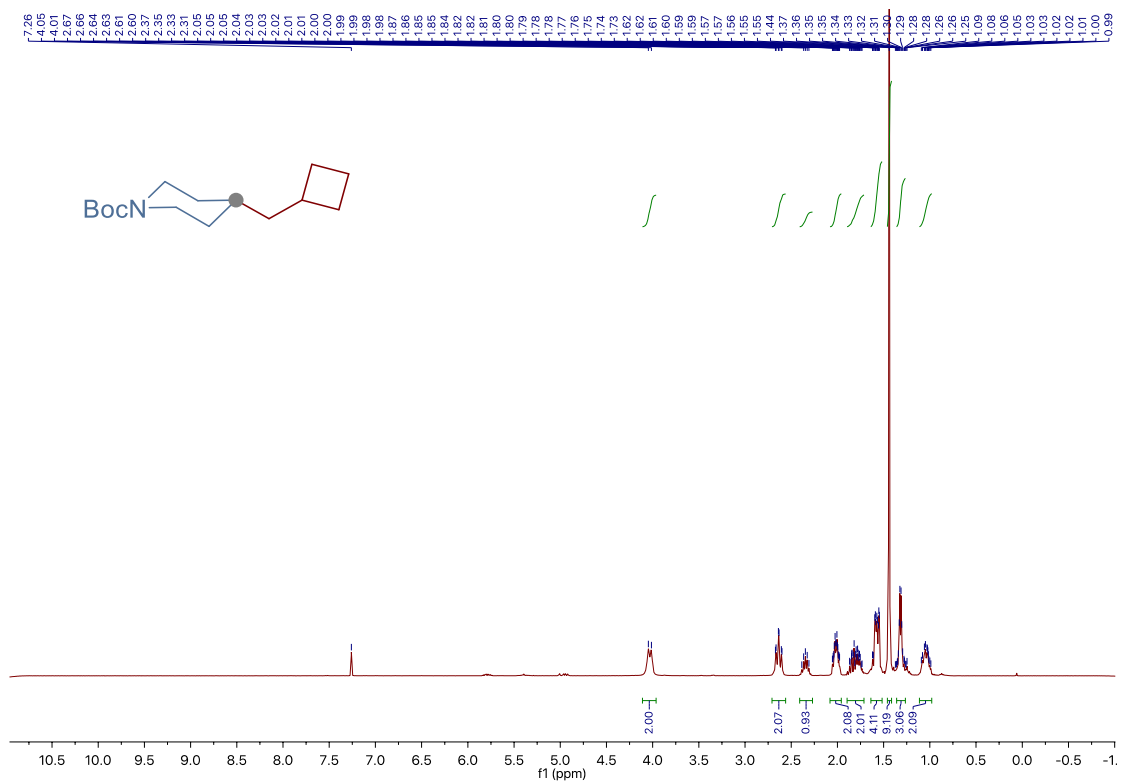
Chapter 3.



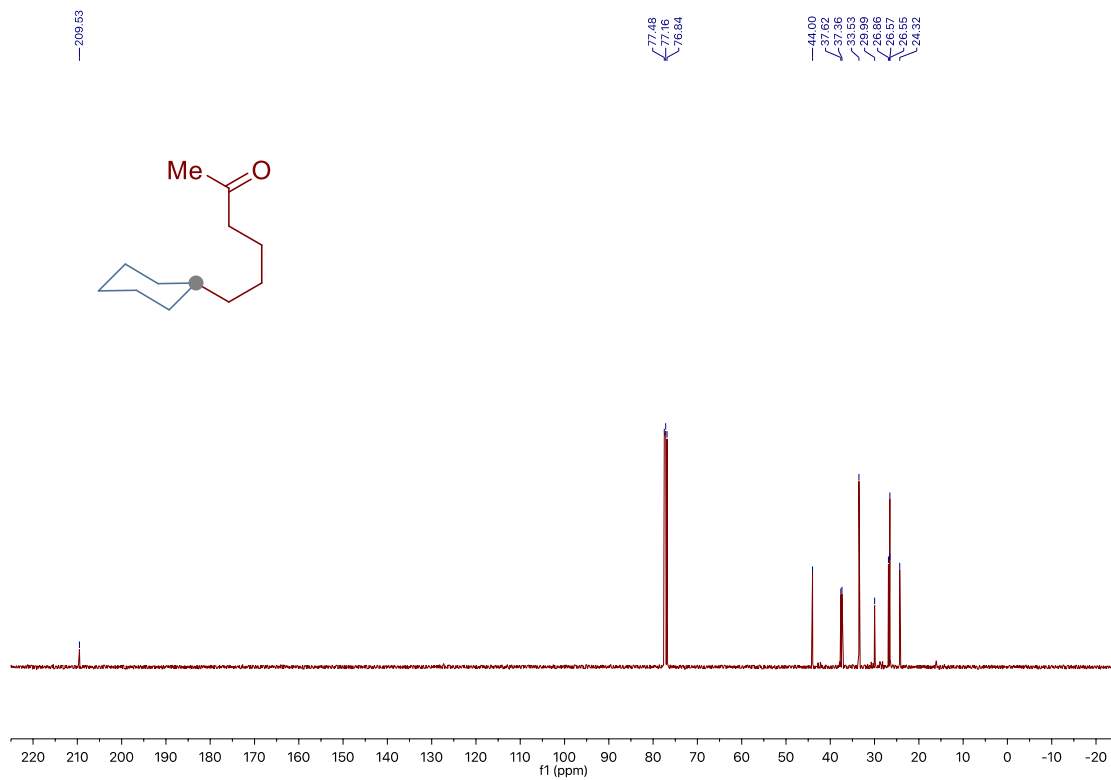
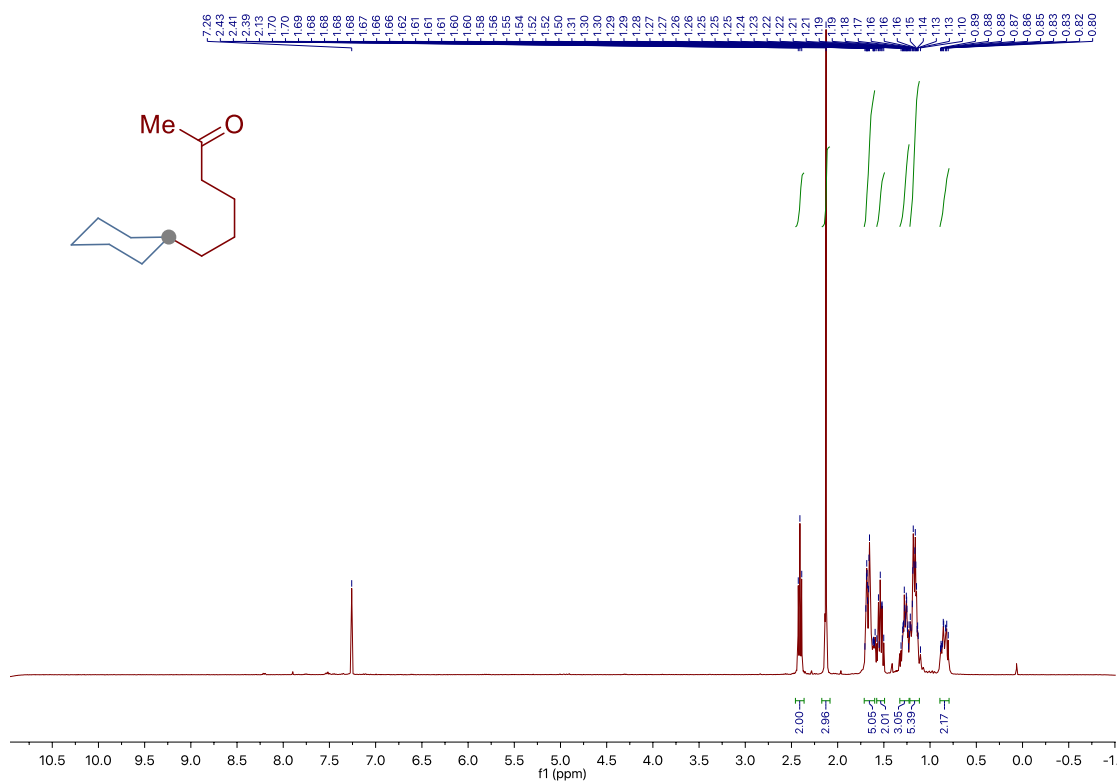
Site-Selective Ni-Catalyzed Deaminative Alkylation of Unactivated Olefins



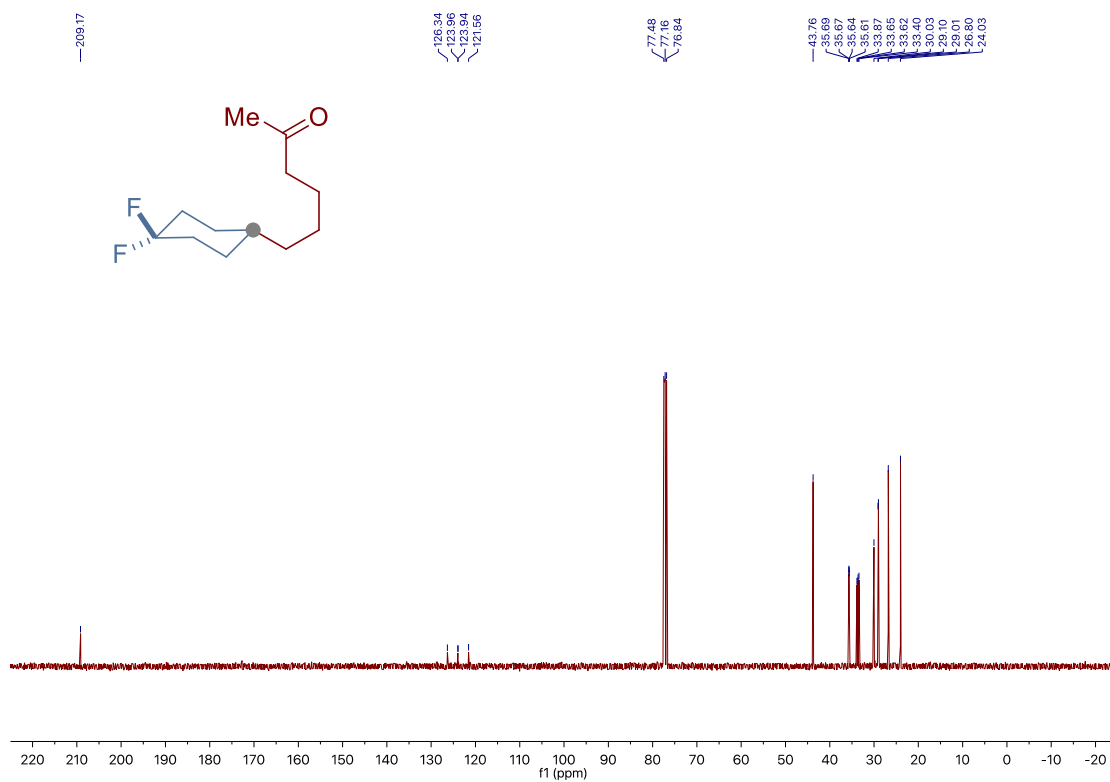
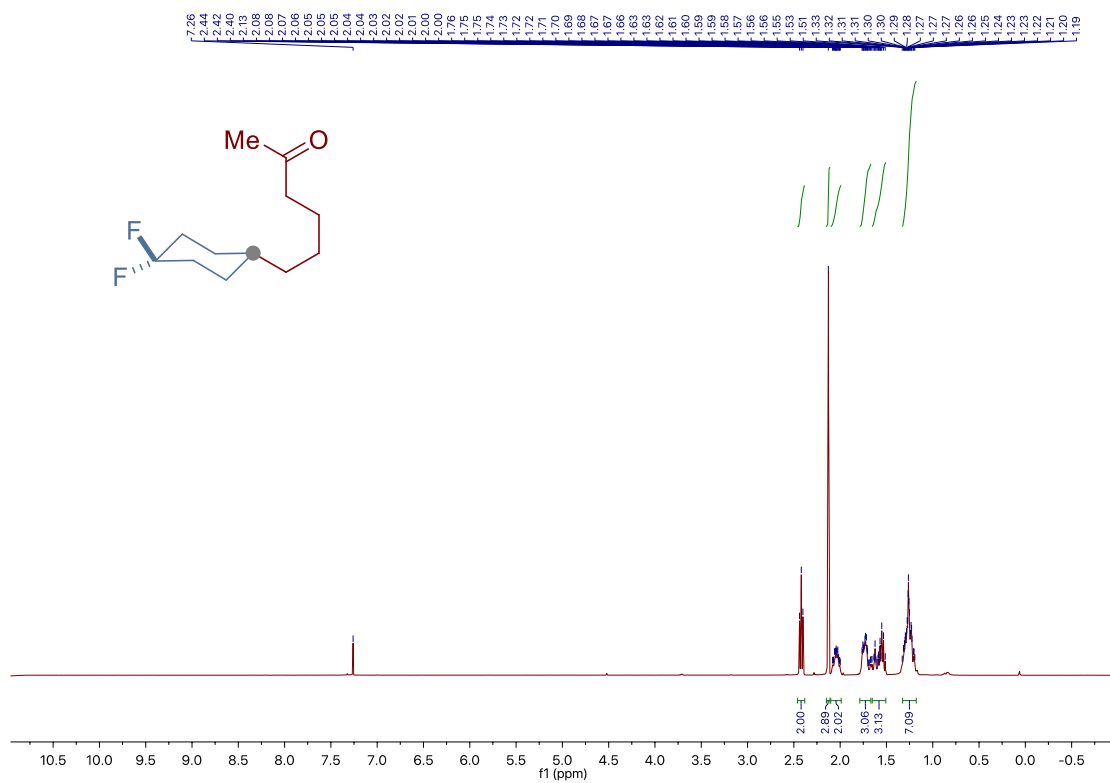
Chapter 3.



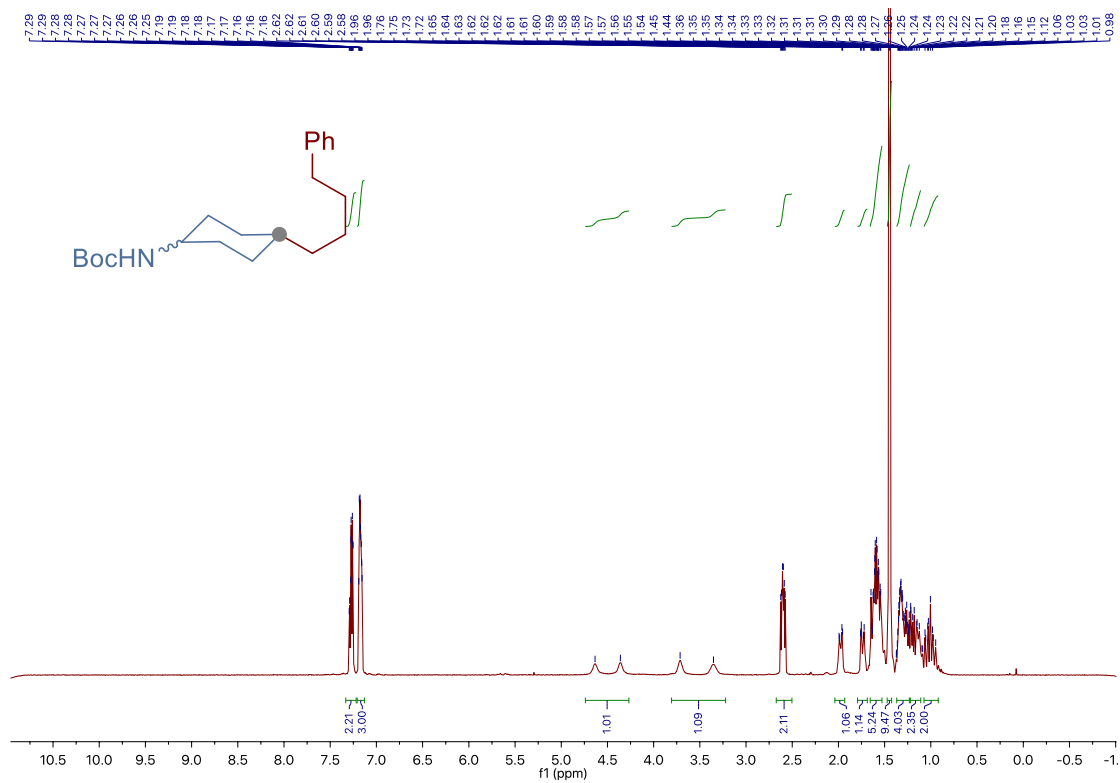
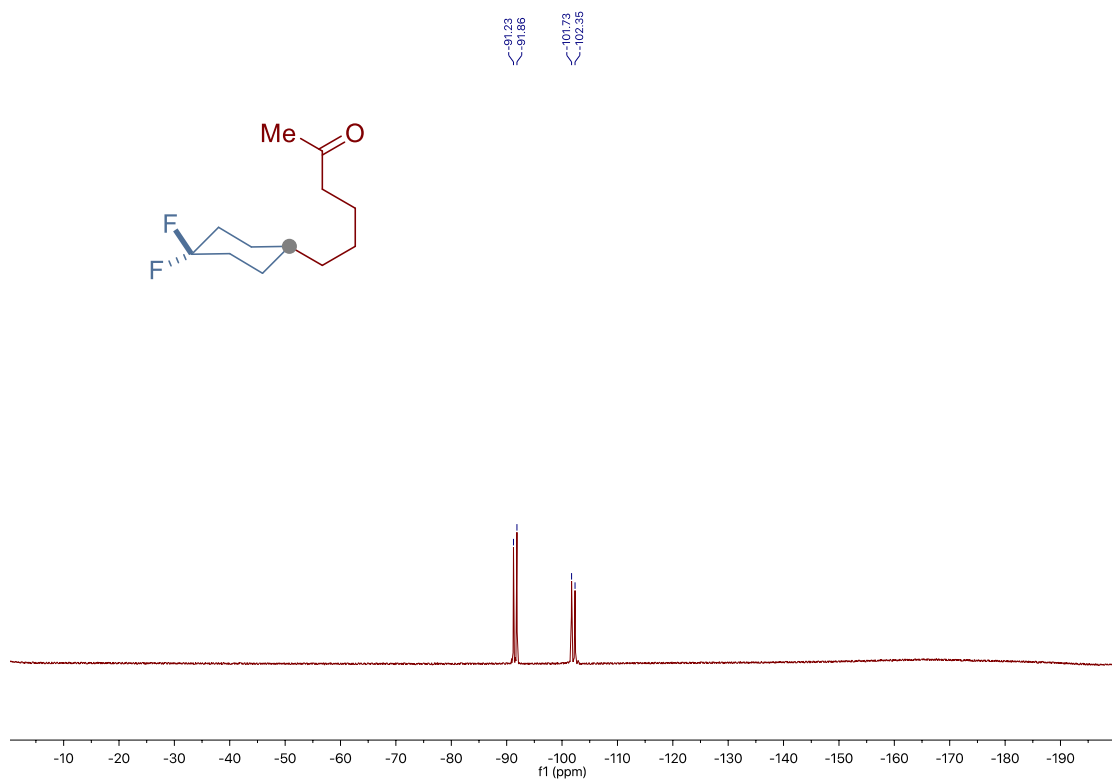
Site-Selective Ni-Catalyzed Deaminative Alkylation of Unactivated Olefins



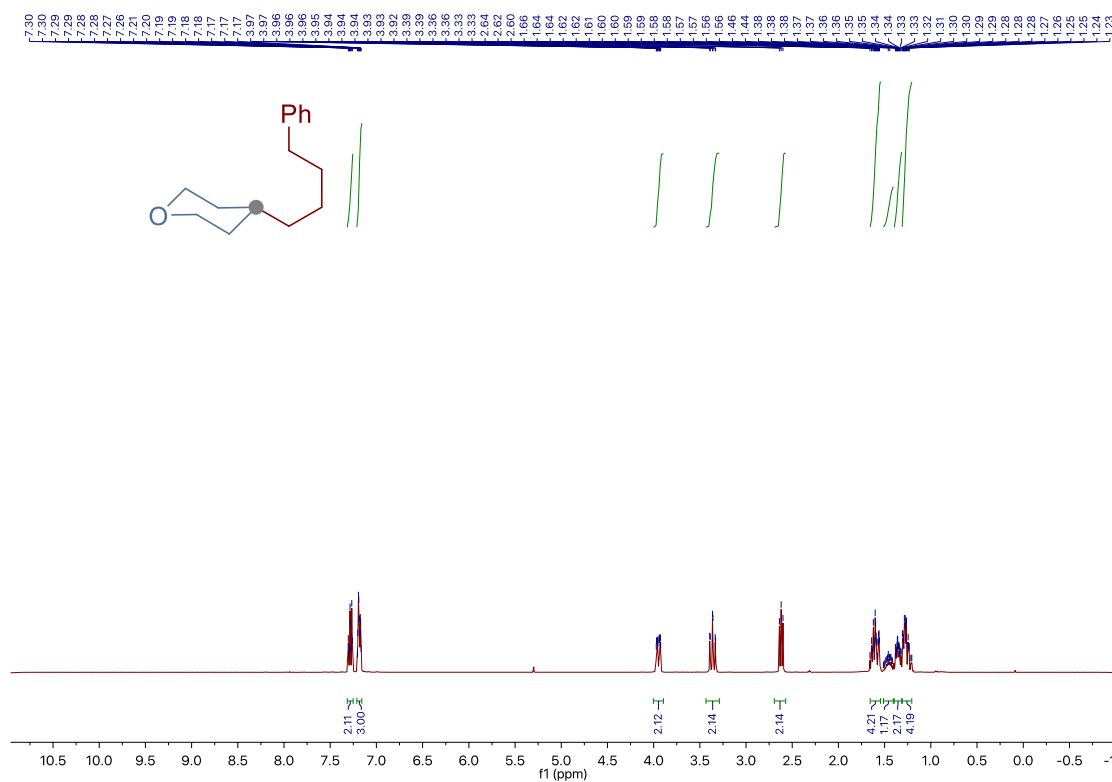
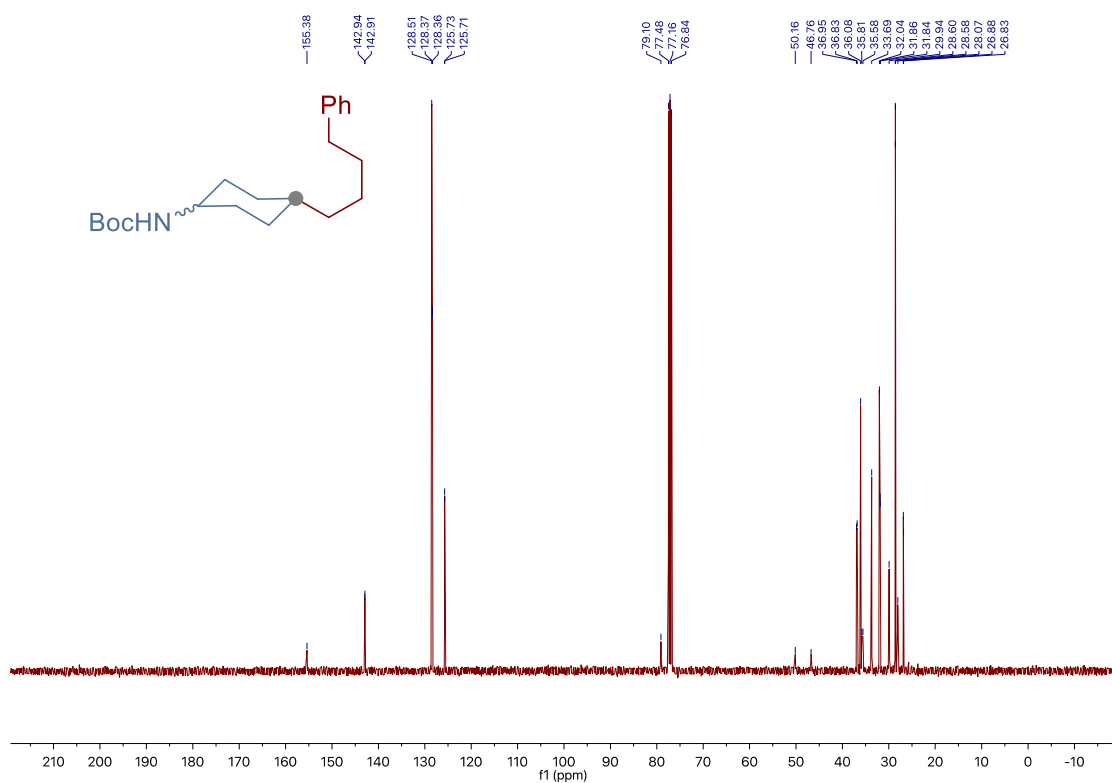
Chapter 3.



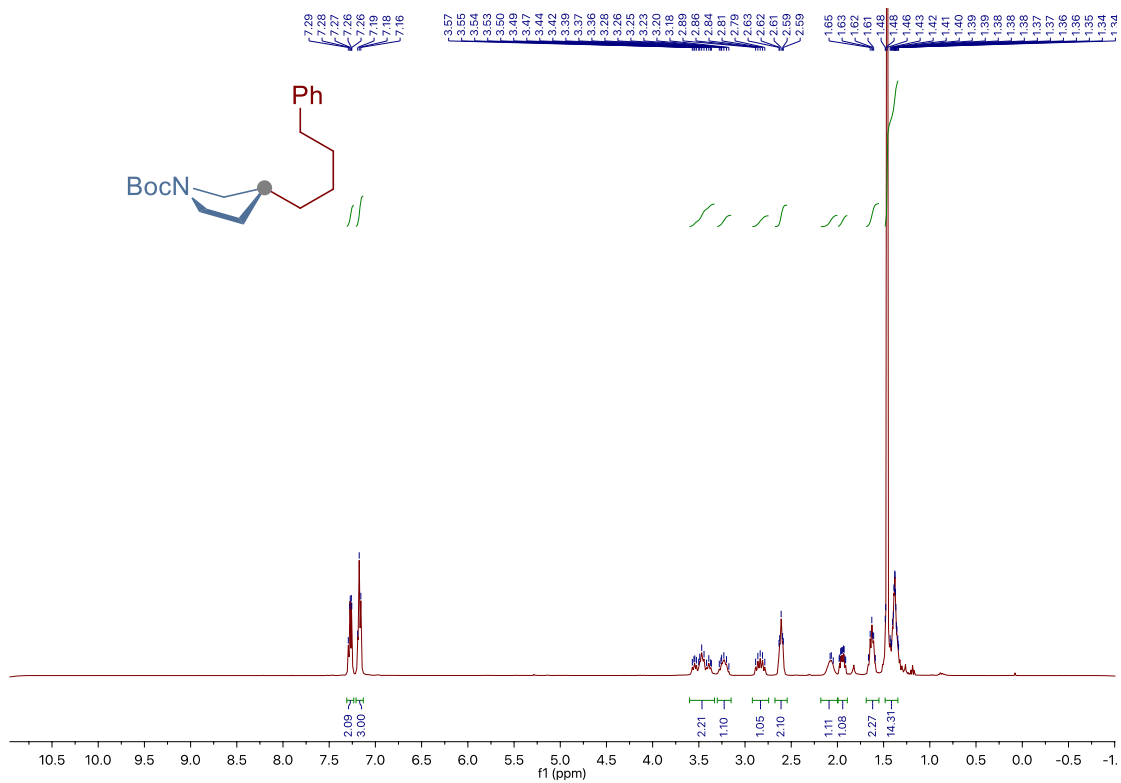
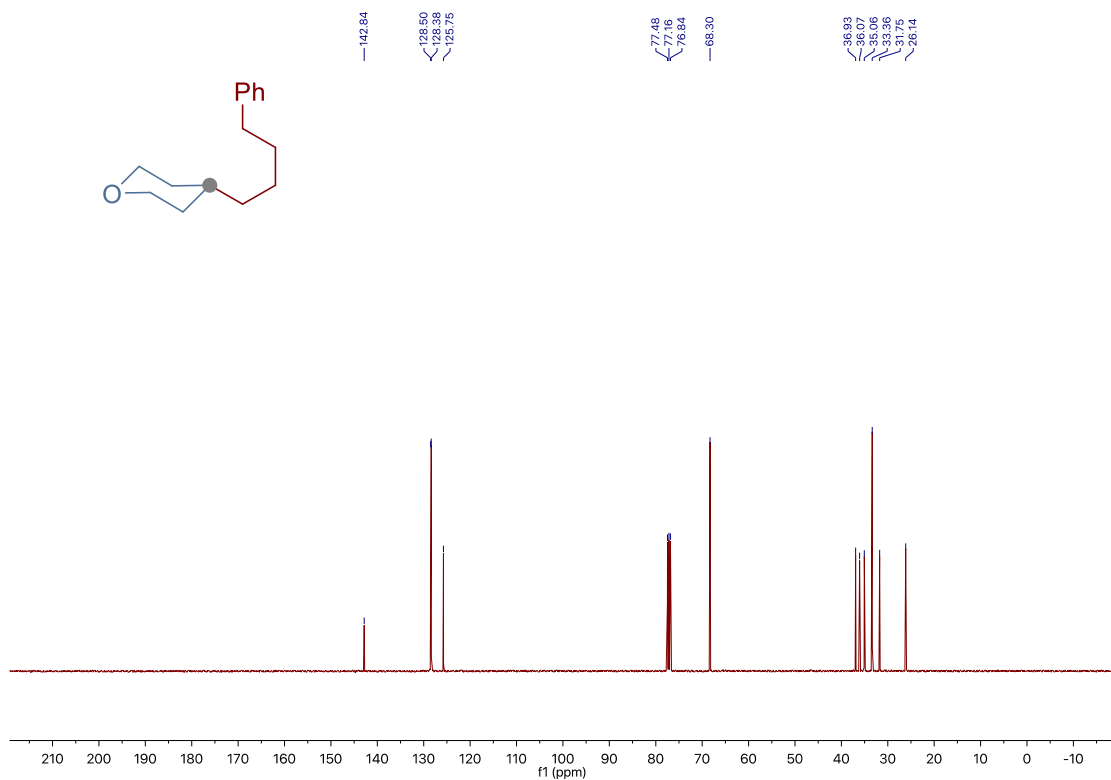
Site-Selective Ni-Catalyzed Deaminative Alkylation of Unactivated Olefins



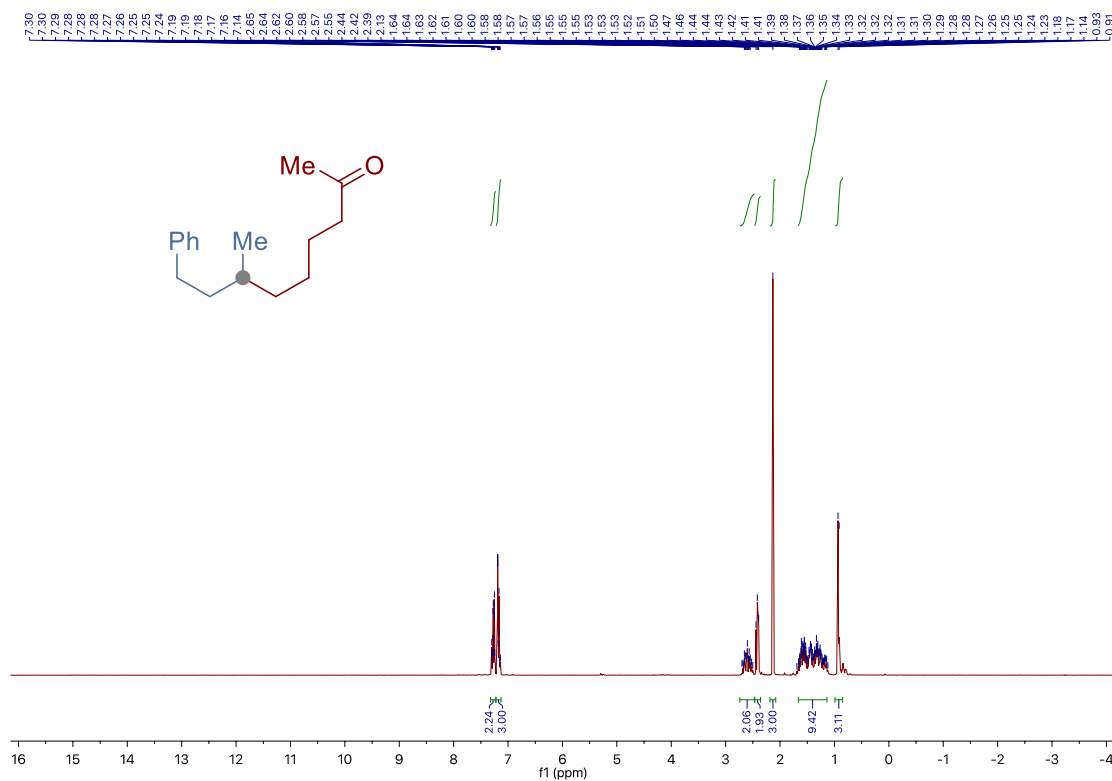
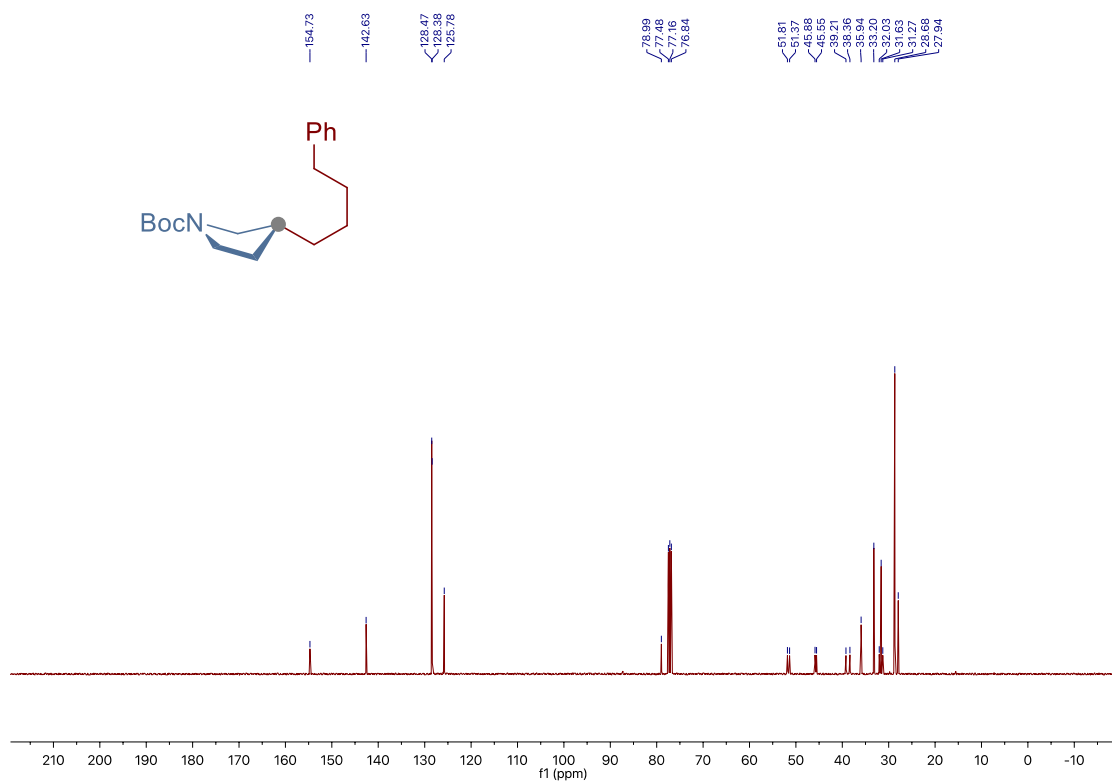
Chapter 3.



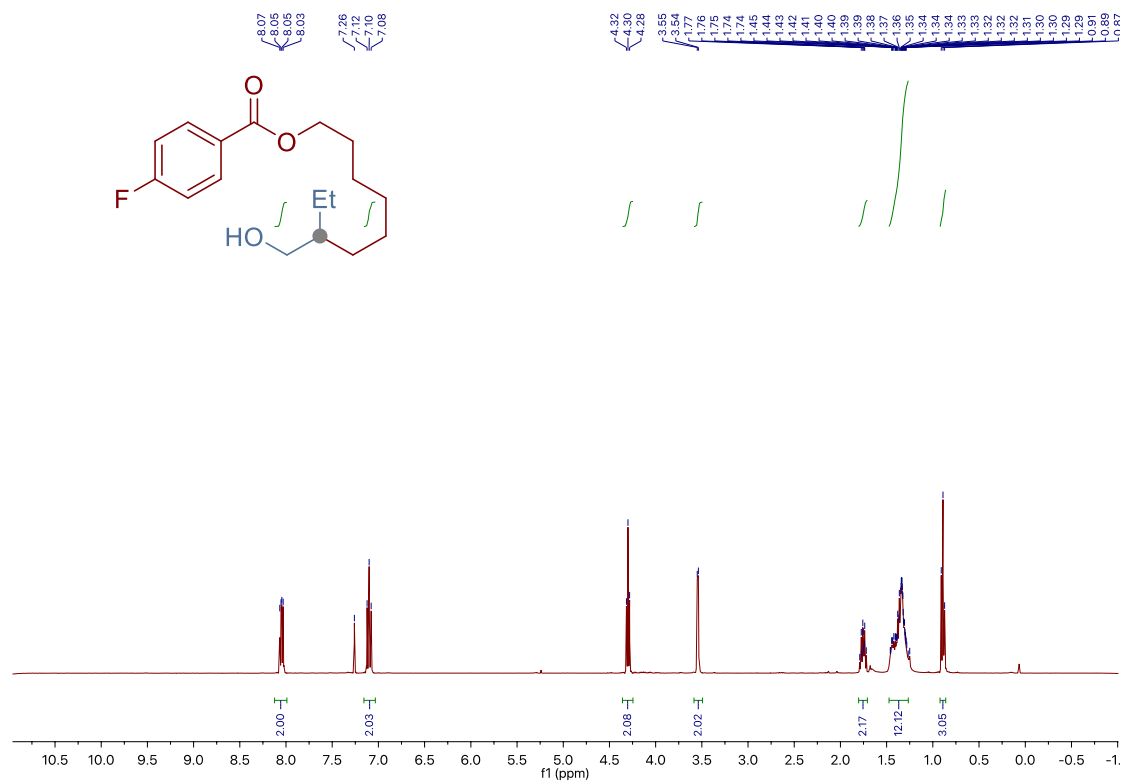
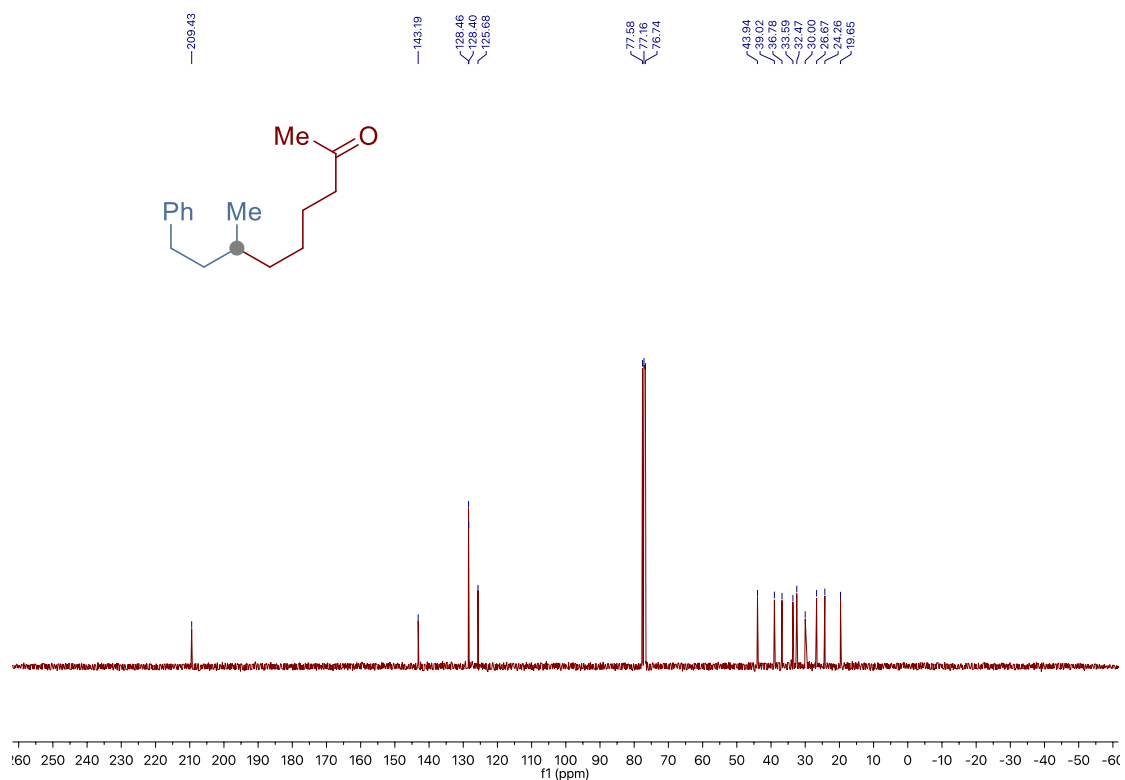
Site-Selective Ni-Catalyzed Deaminative Alkylation of Unactivated Olefins



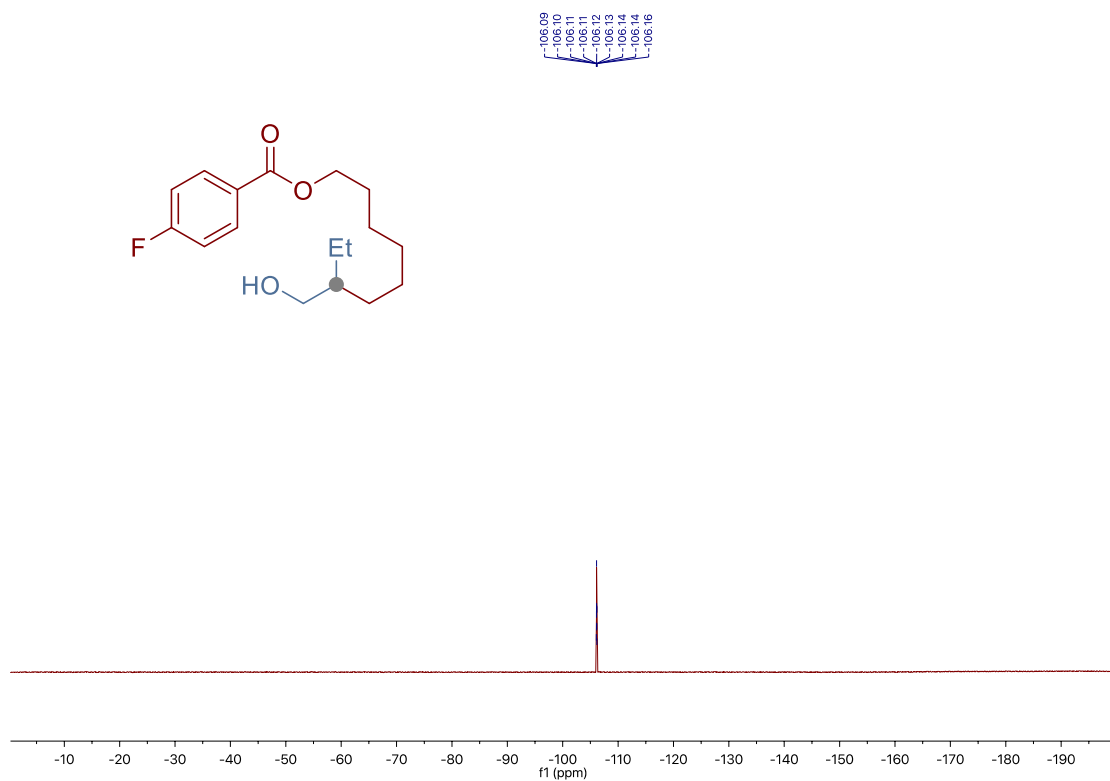
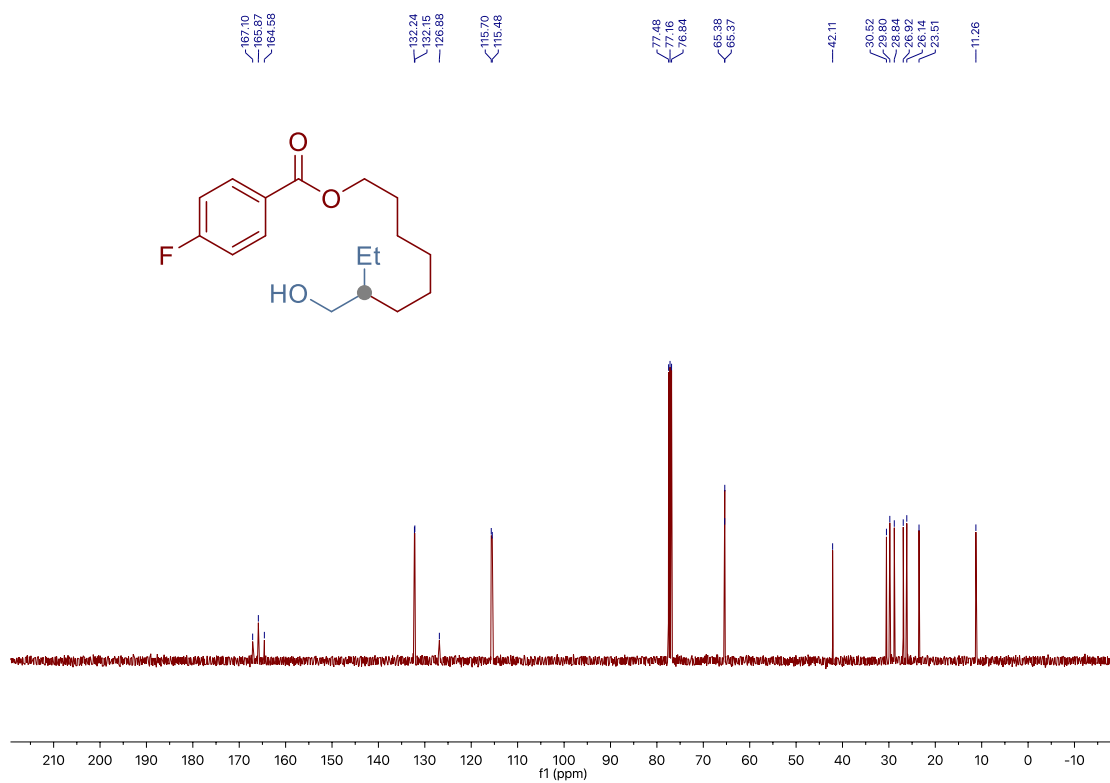
Chapter 3.



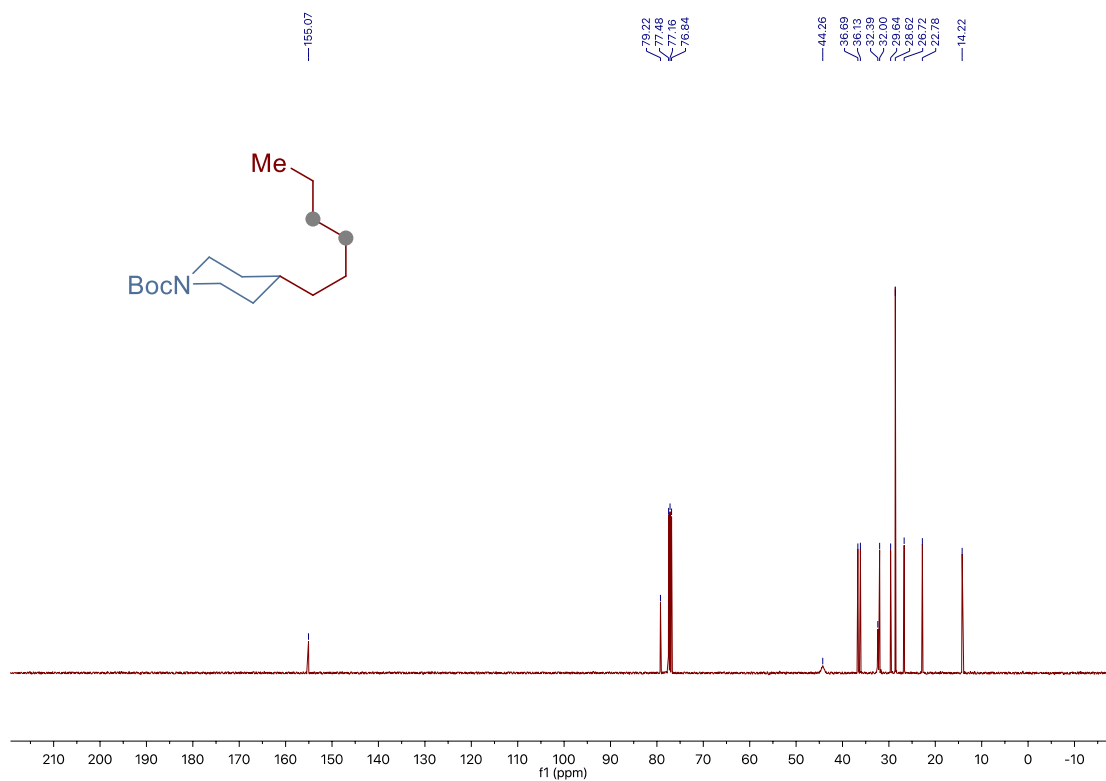
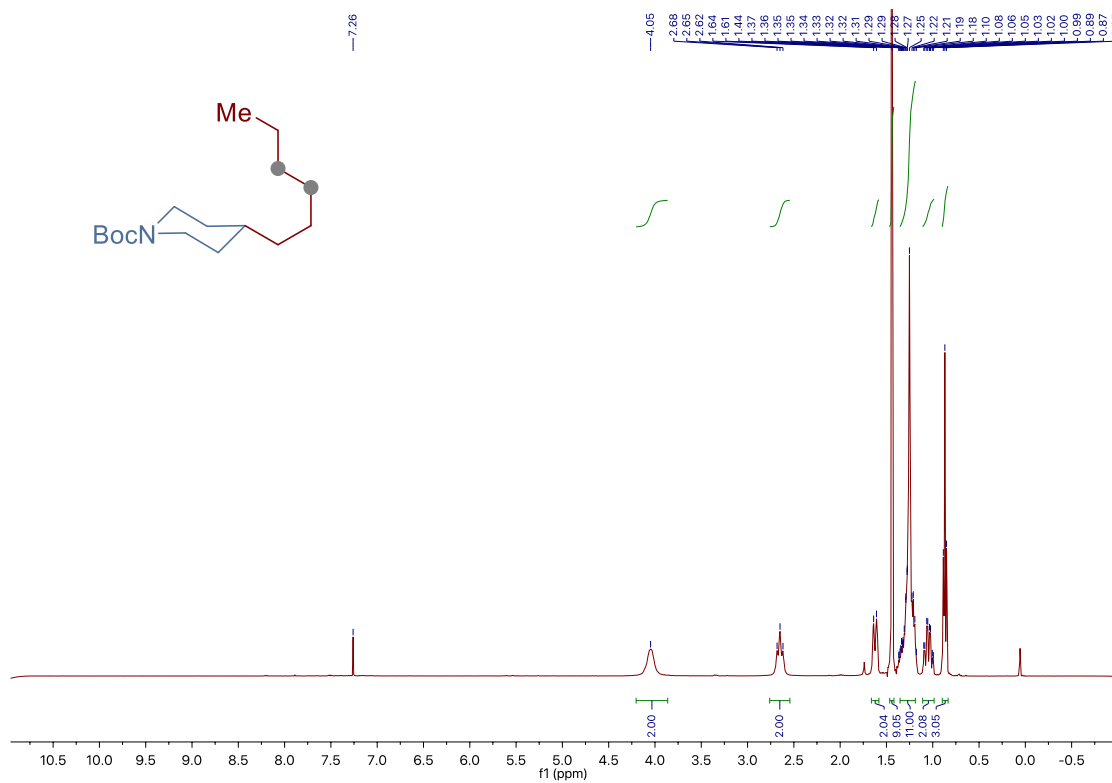
Site-Selective Ni-Catalyzed Deaminative Alkylation of Unactivated Olefins



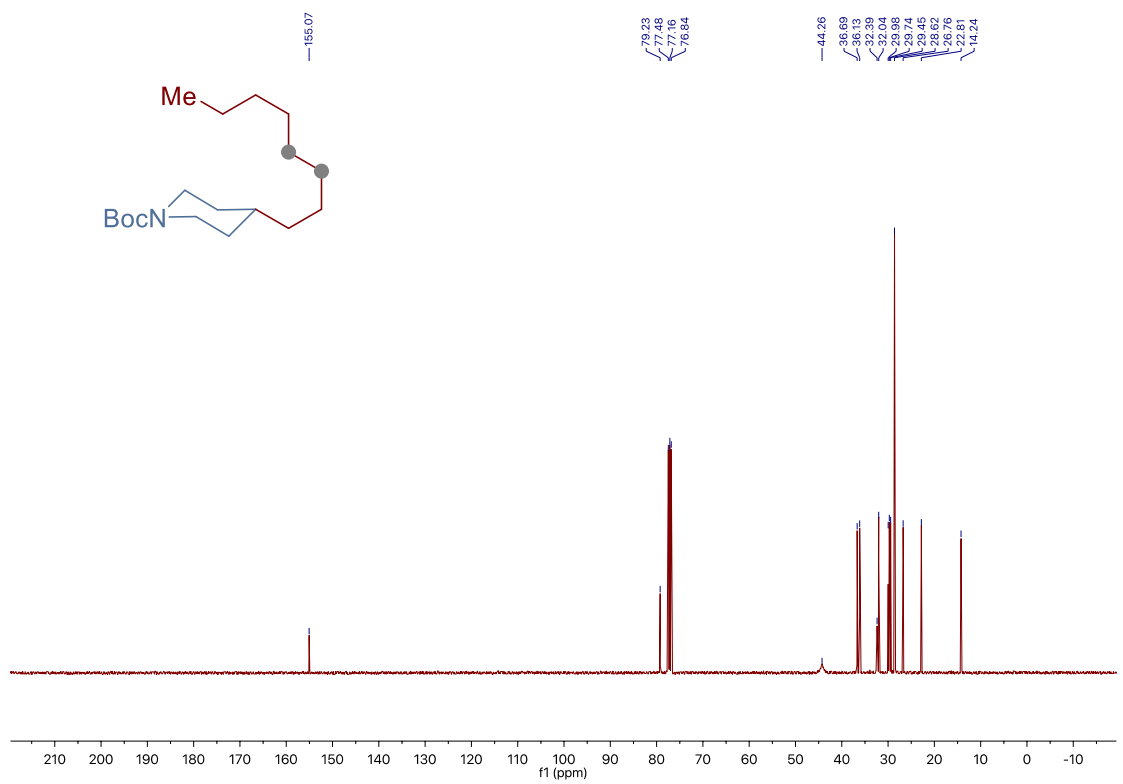
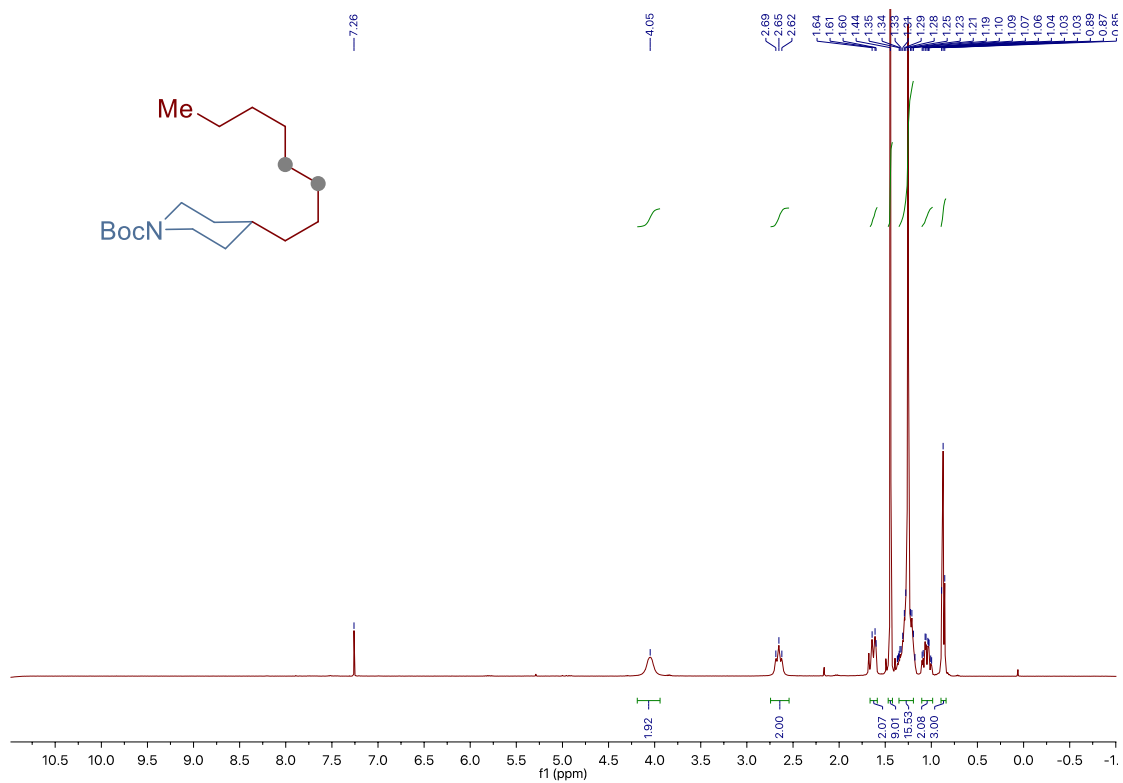
Chapter 3.



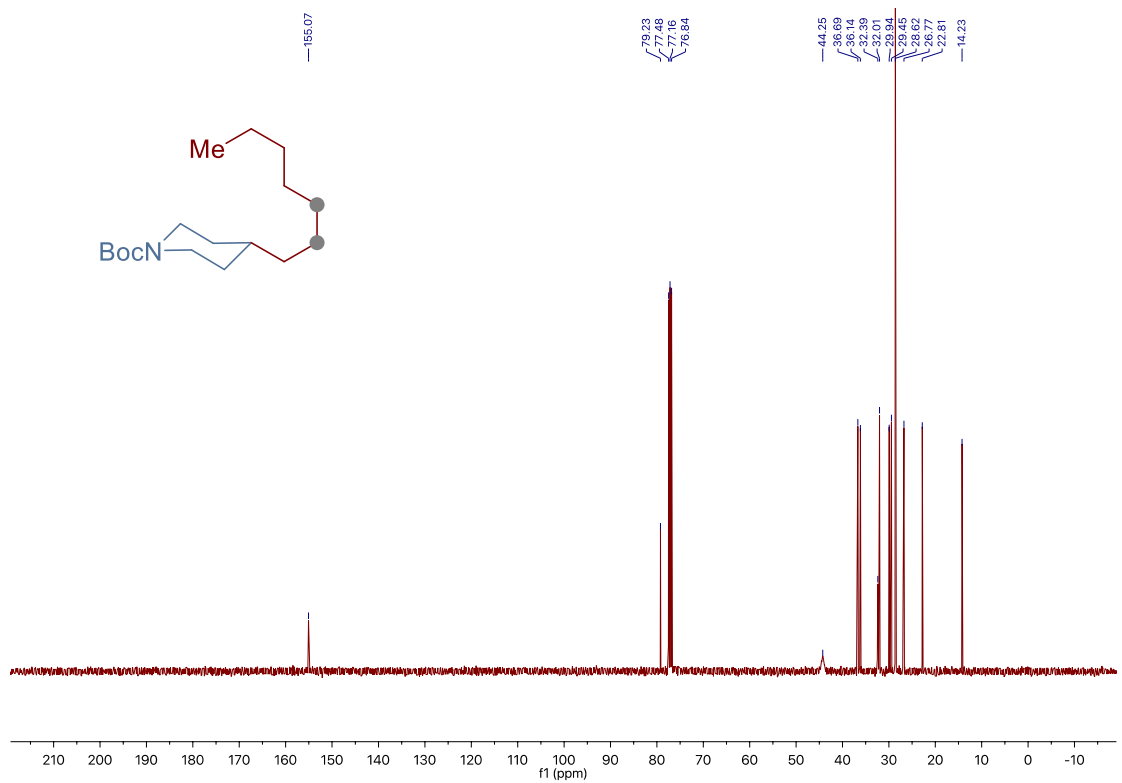
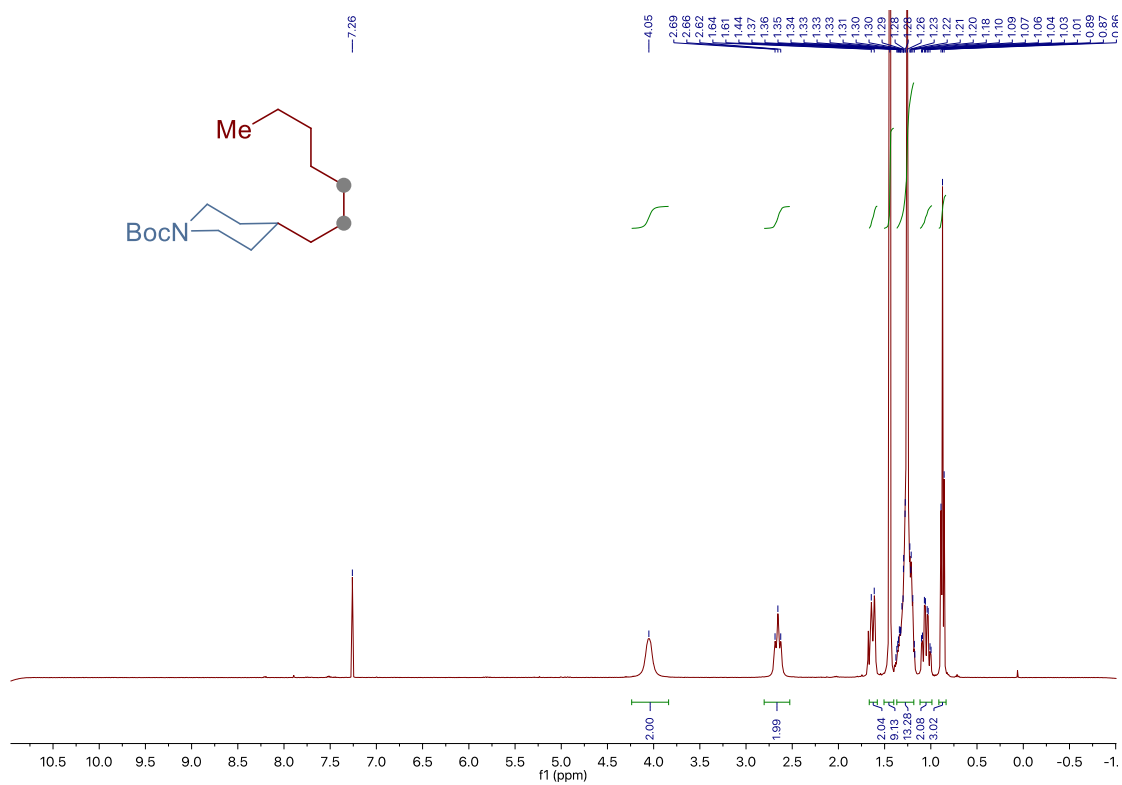
Site-Selective Ni-Catalyzed Deaminative Alkylation of Unactivated Olefins



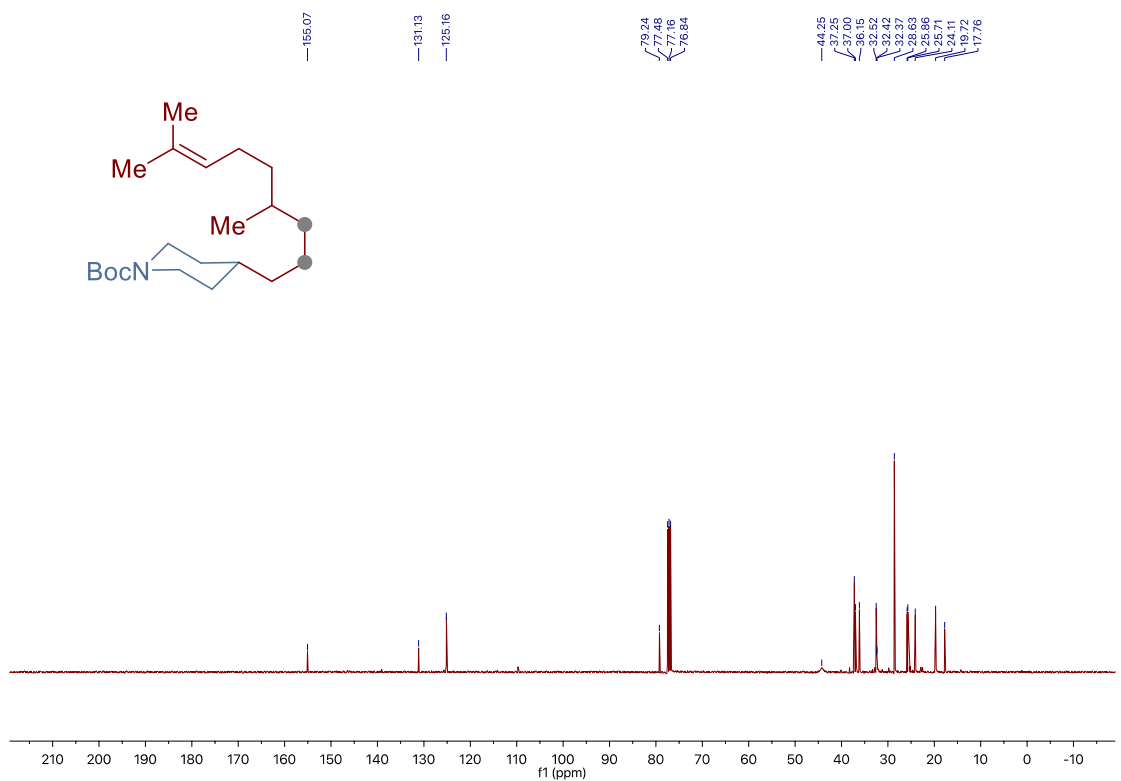
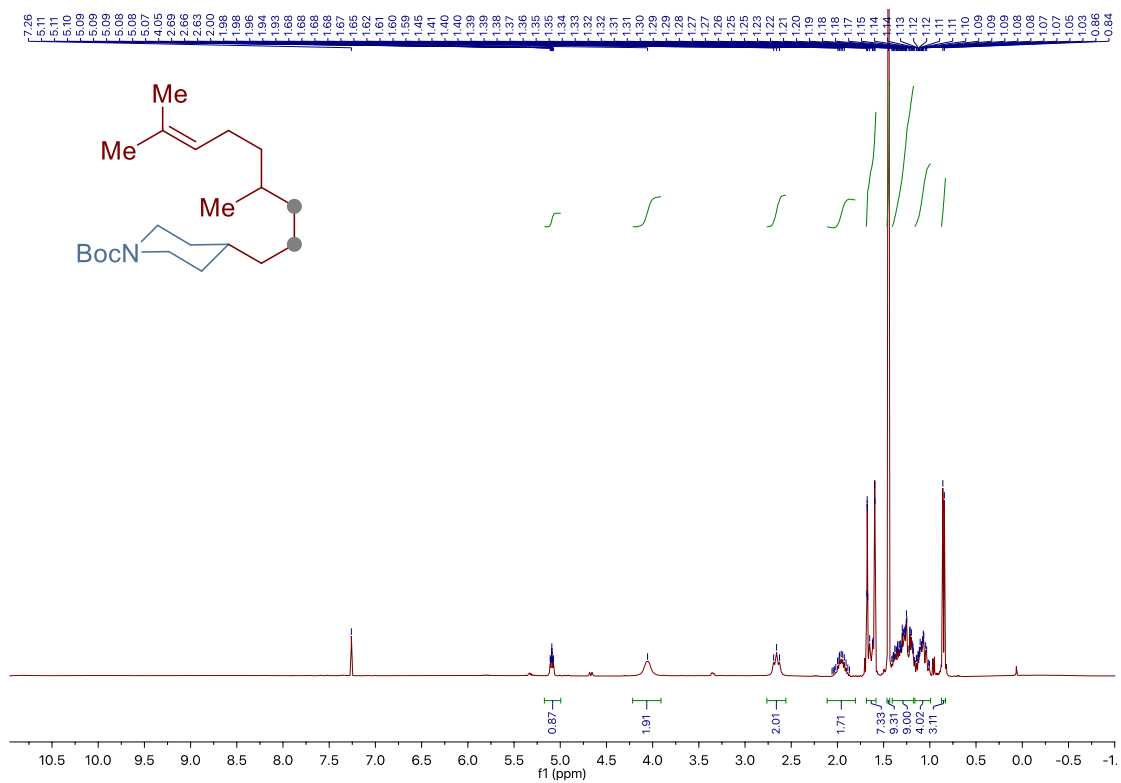
Chapter 3.



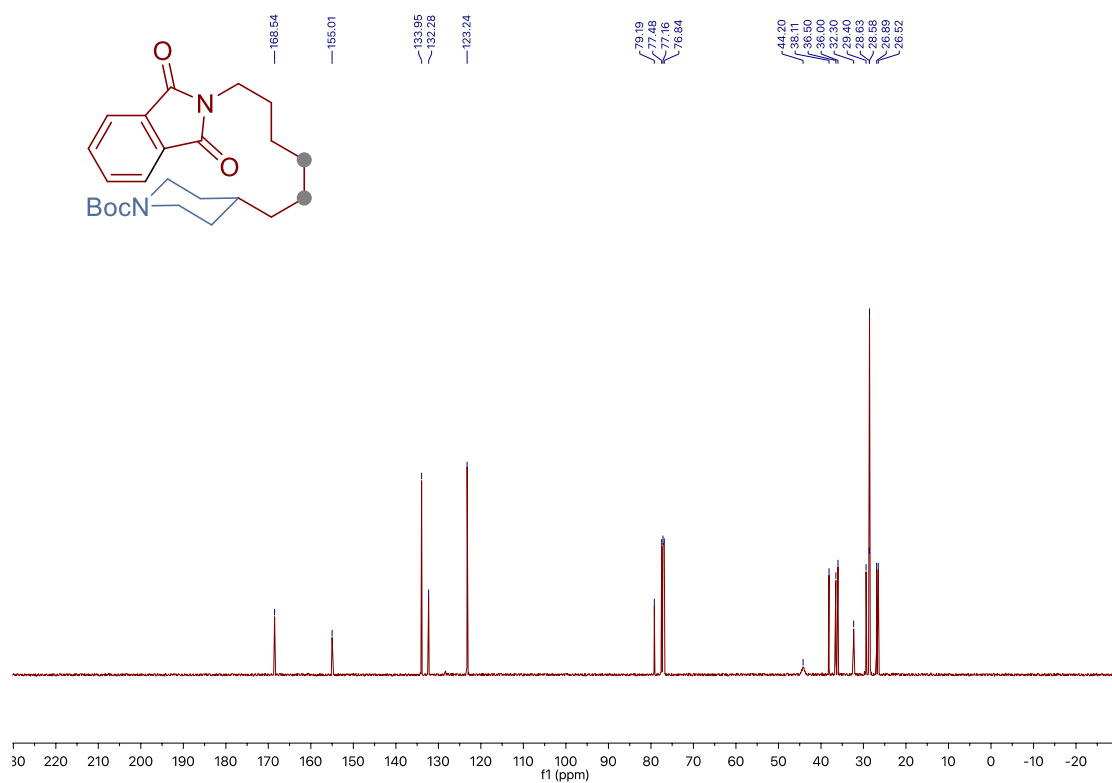
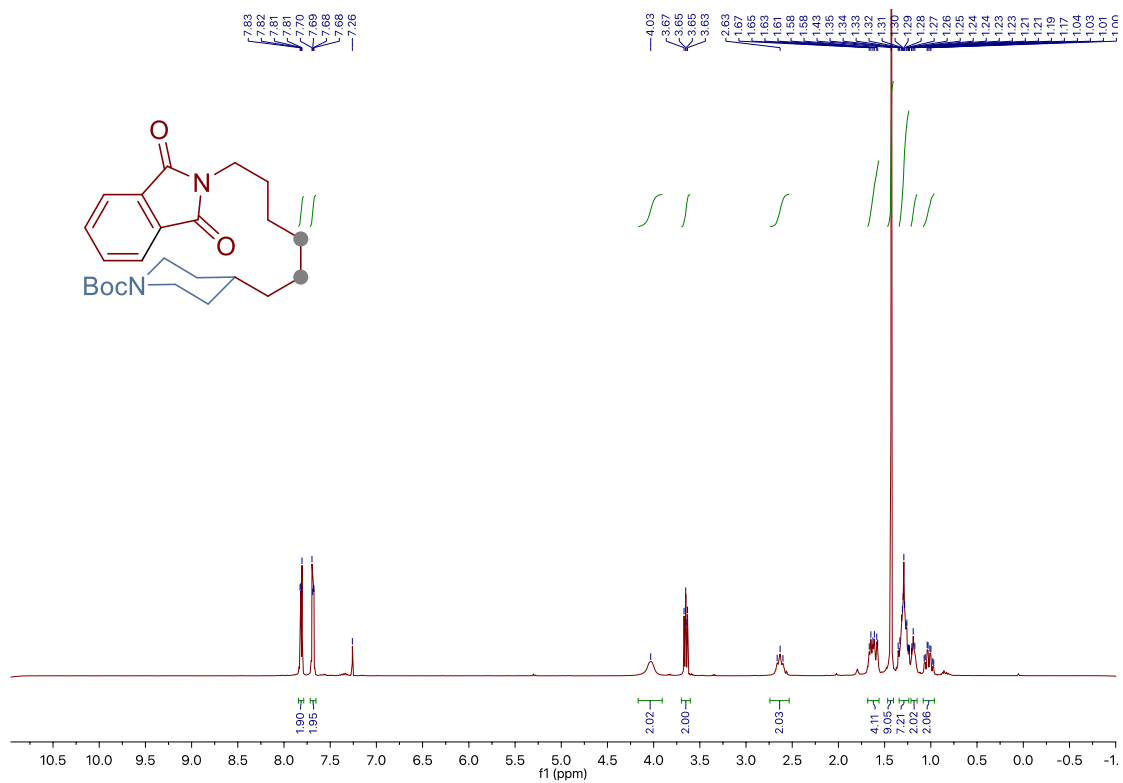
Site-Selective Ni-Catalyzed Deaminative Alkylation of Unactivated Olefins



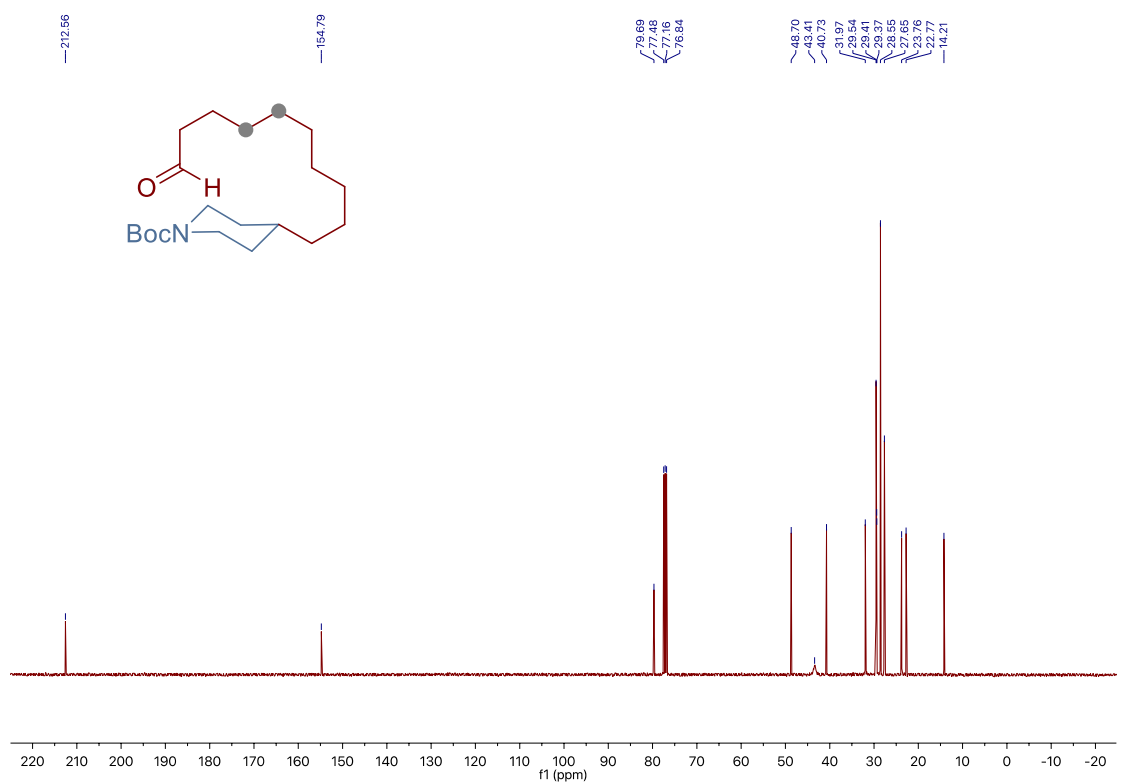
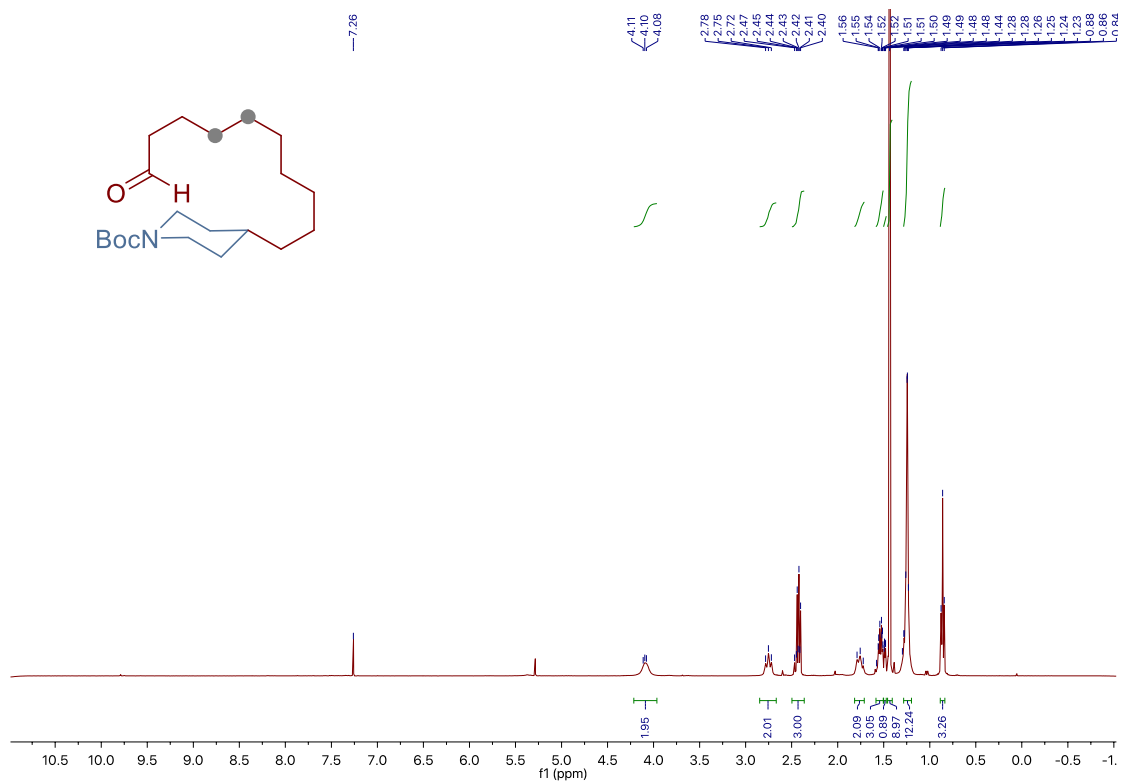
Chapter 3.



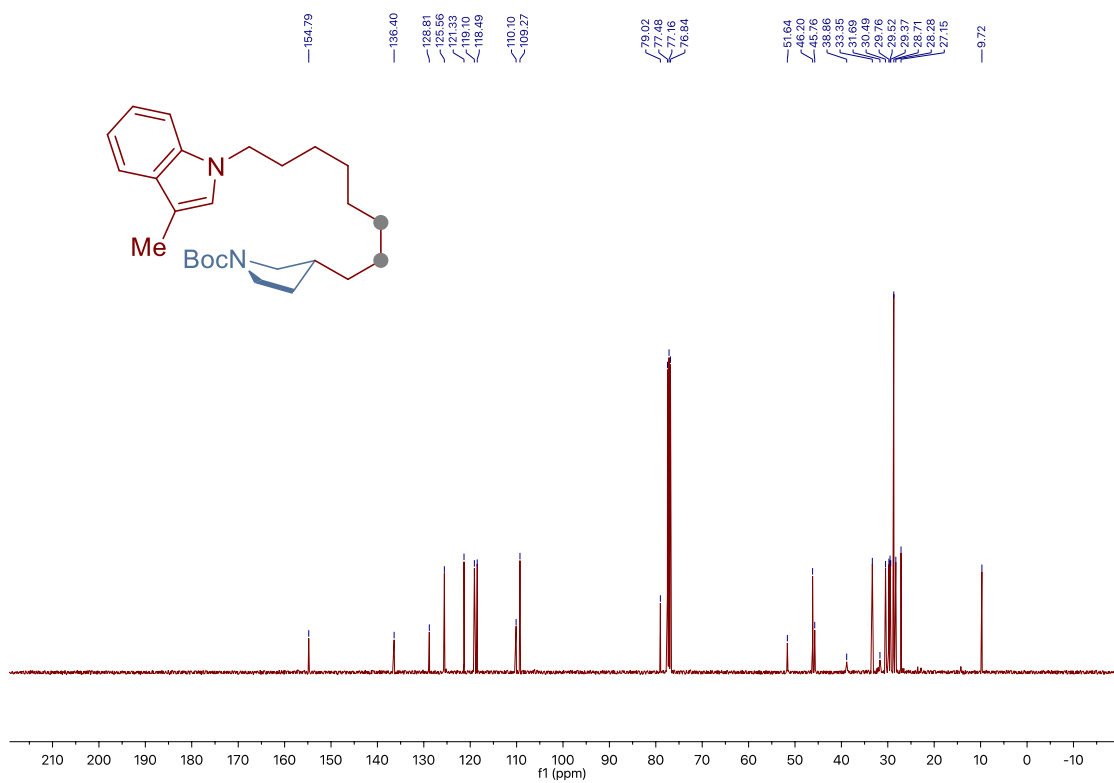
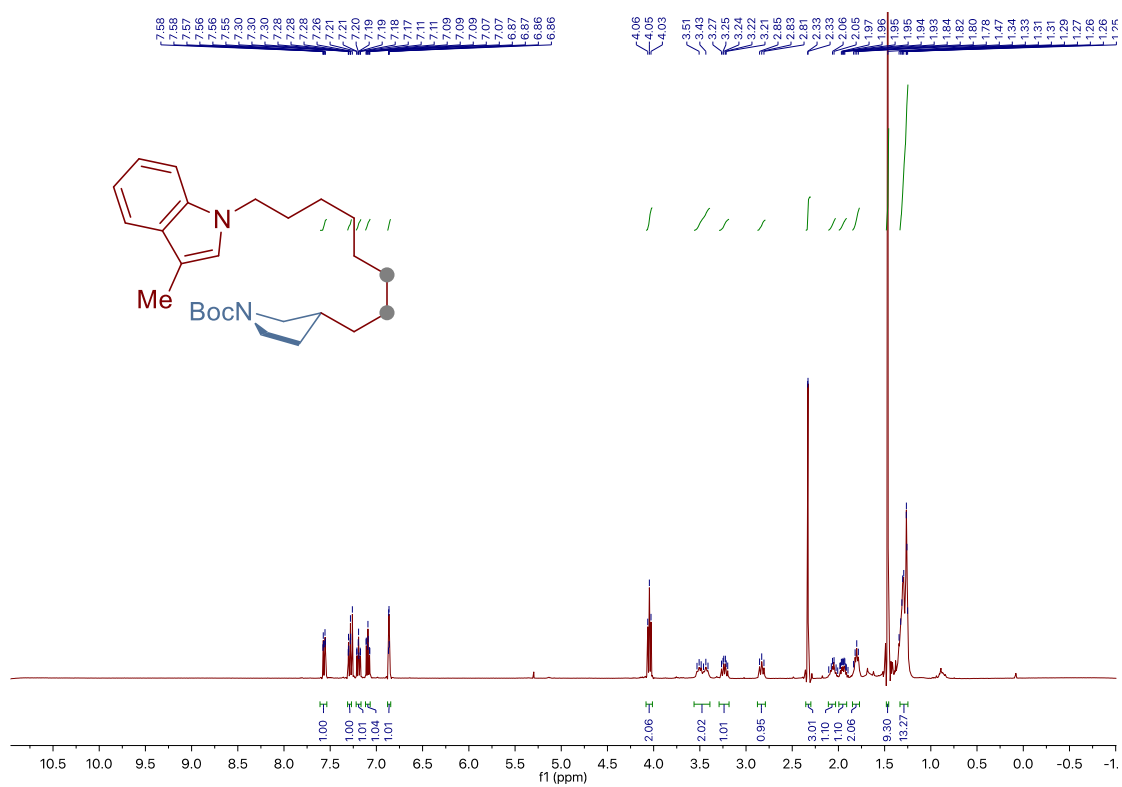
Site-Selective Ni-Catalyzed Deaminative Alkylation of Unactivated Olefins



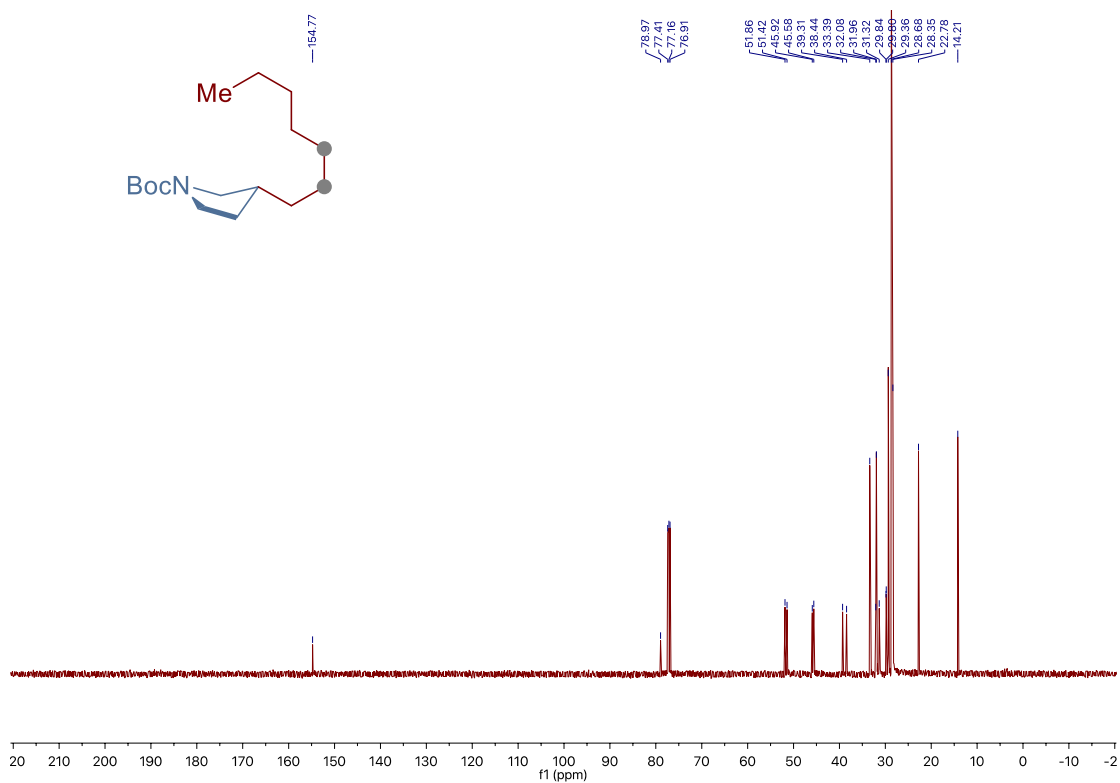
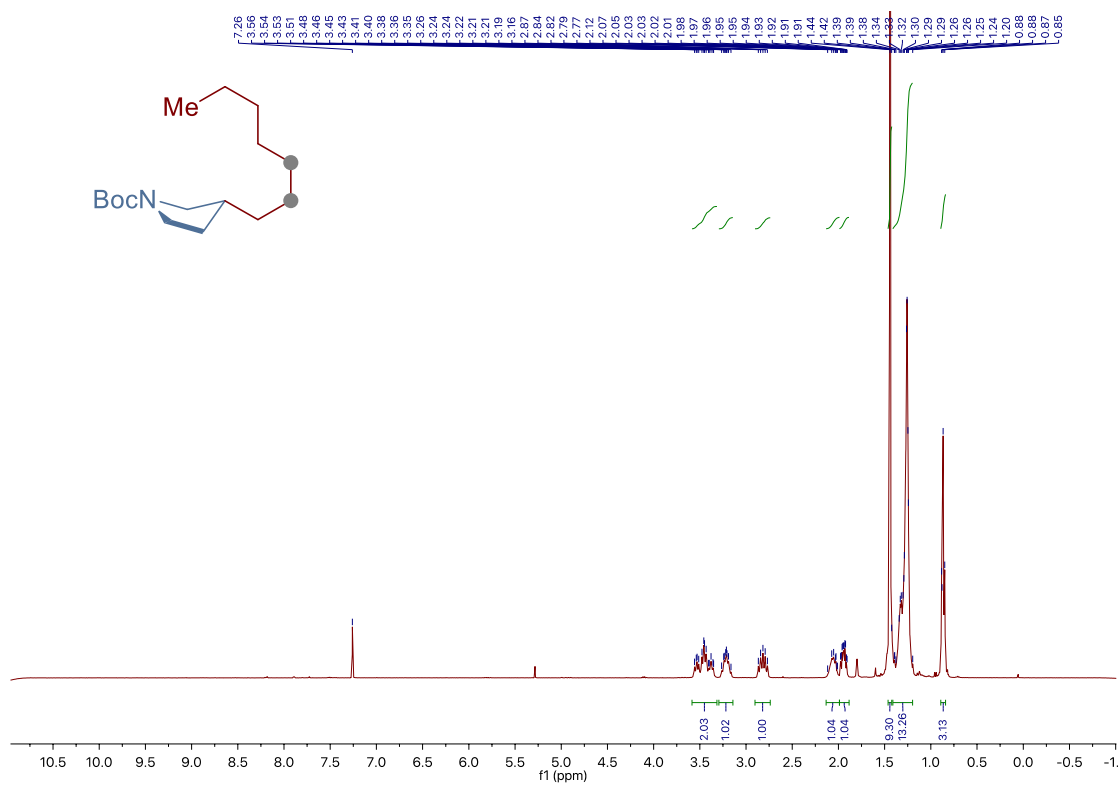
Chapter 3.



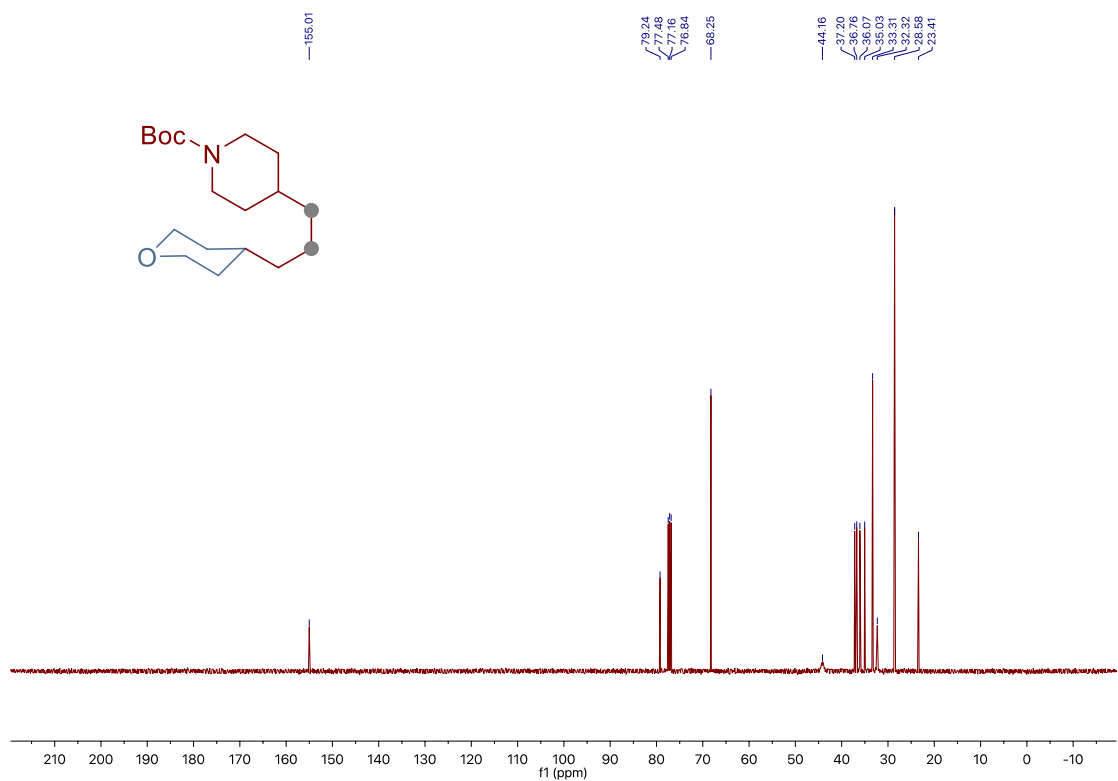
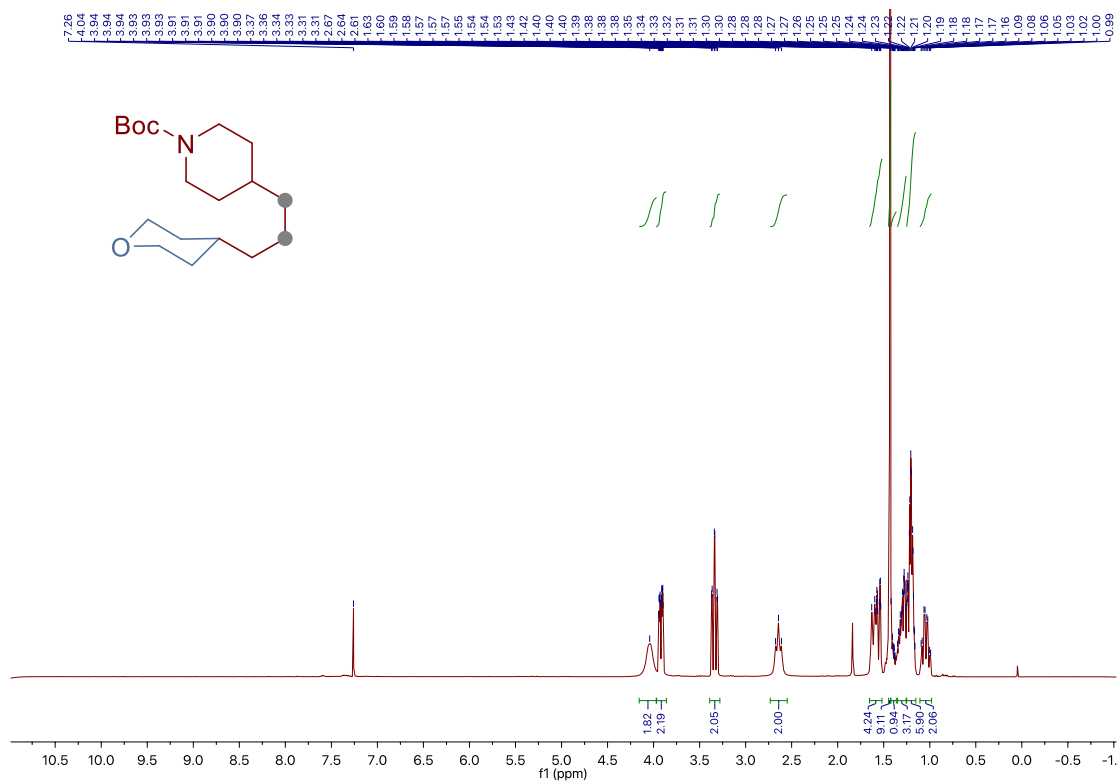
Site-Selective Ni-Catalyzed Deaminative Alkylation of Unactivated Olefins



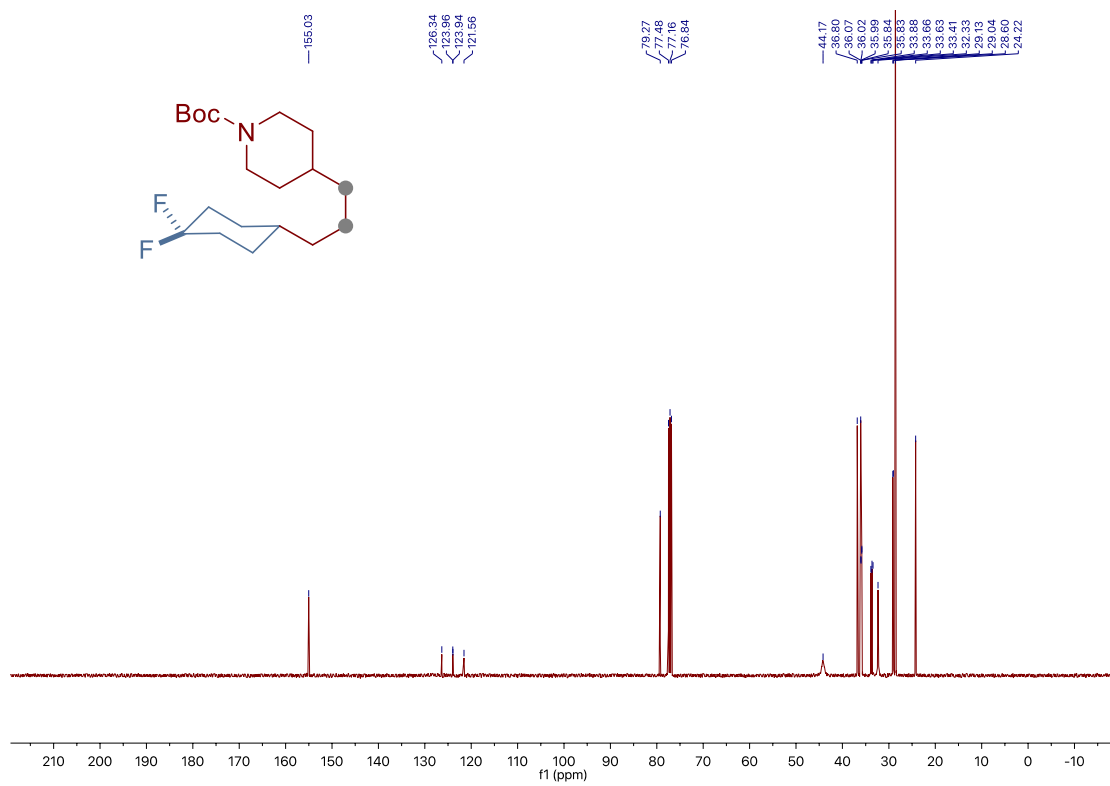
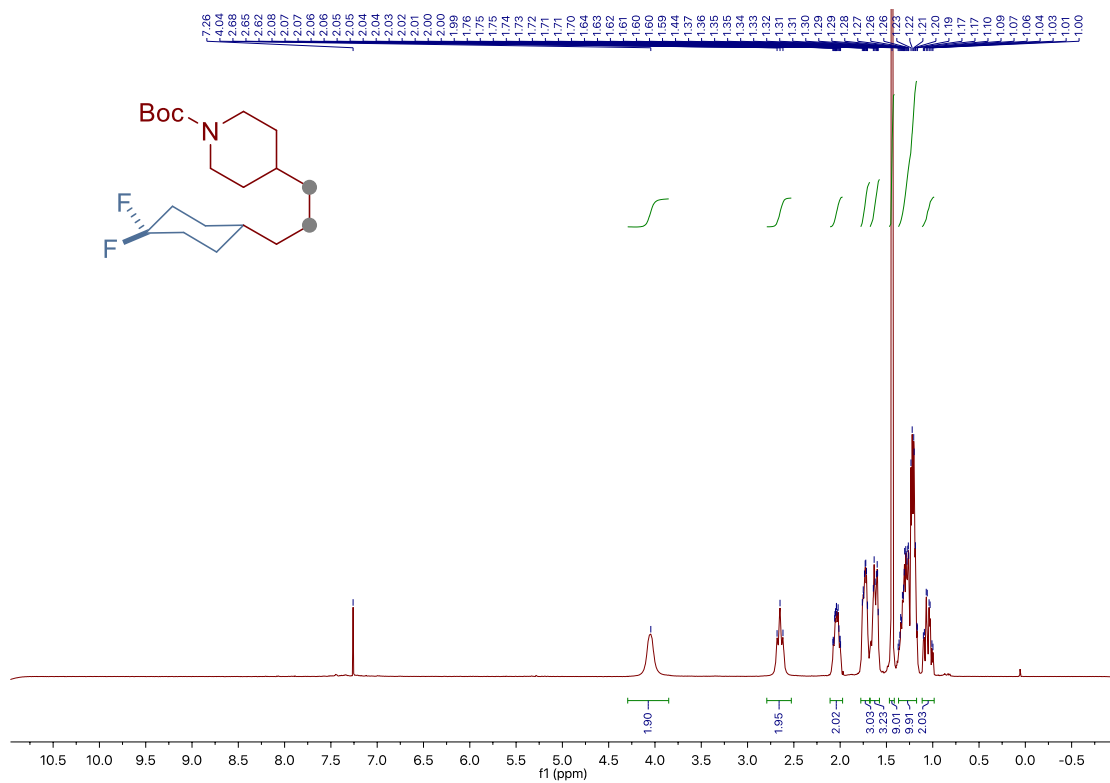
Chapter 3.



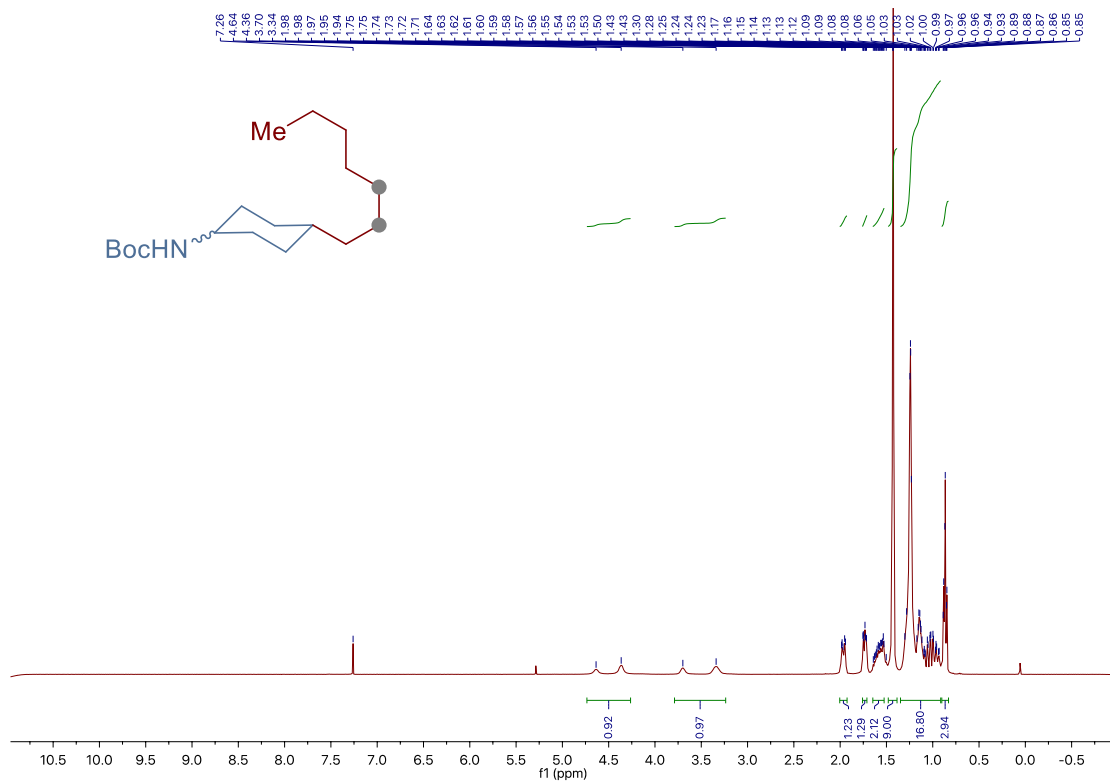
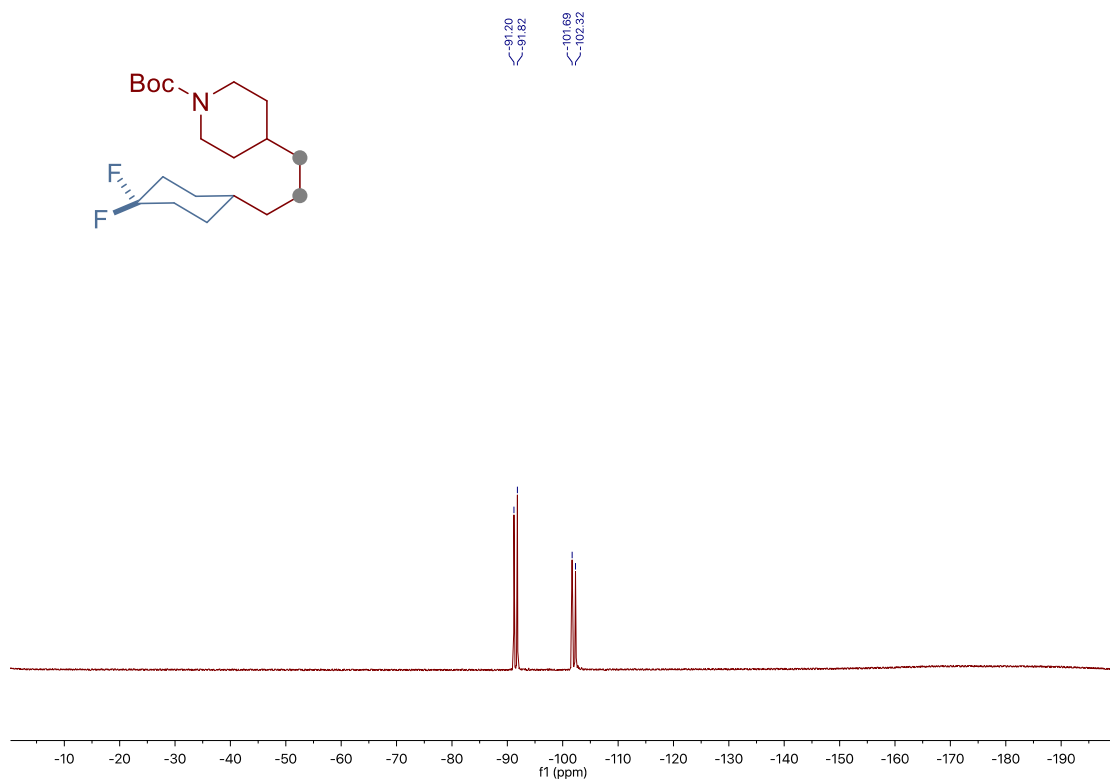
Site-Selective Ni-Catalyzed Deaminative Alkylation of Unactivated Olefins



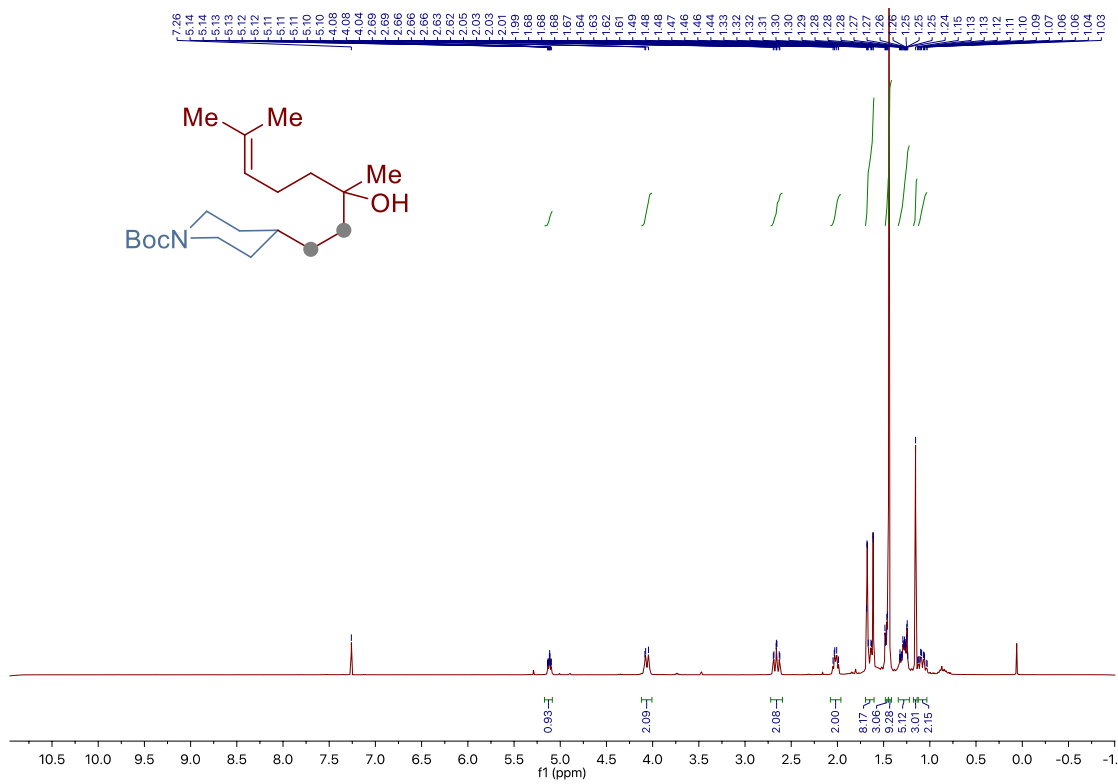
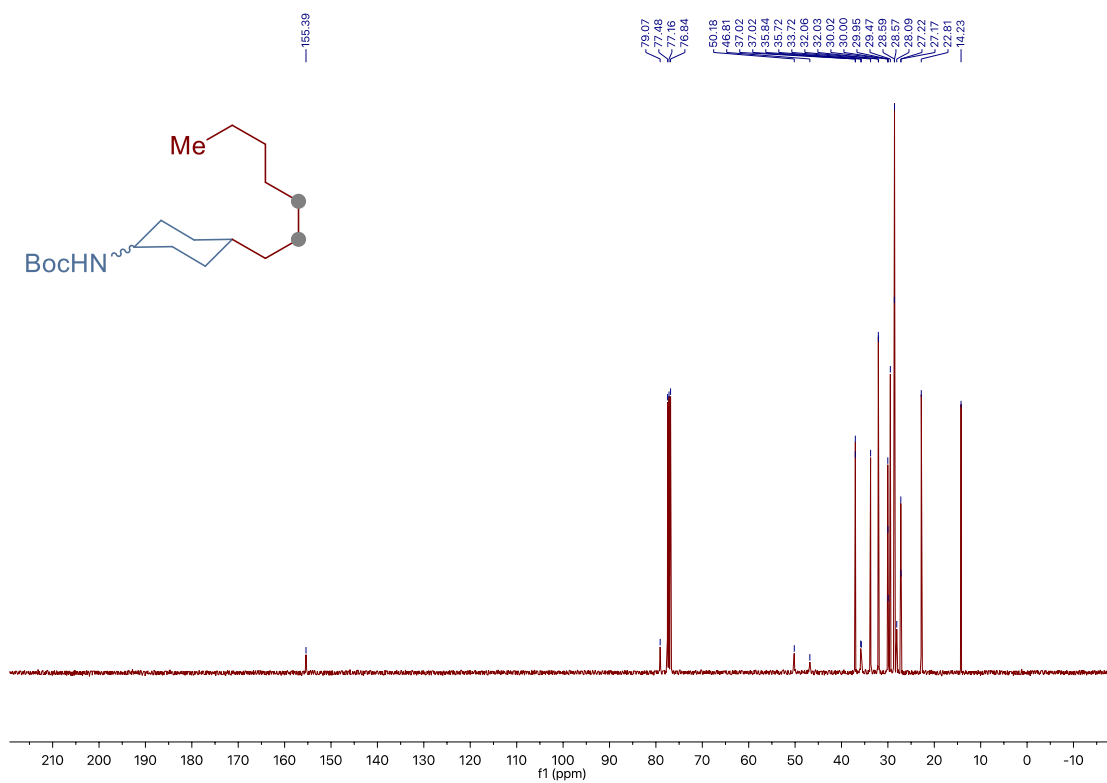
Chapter 3.



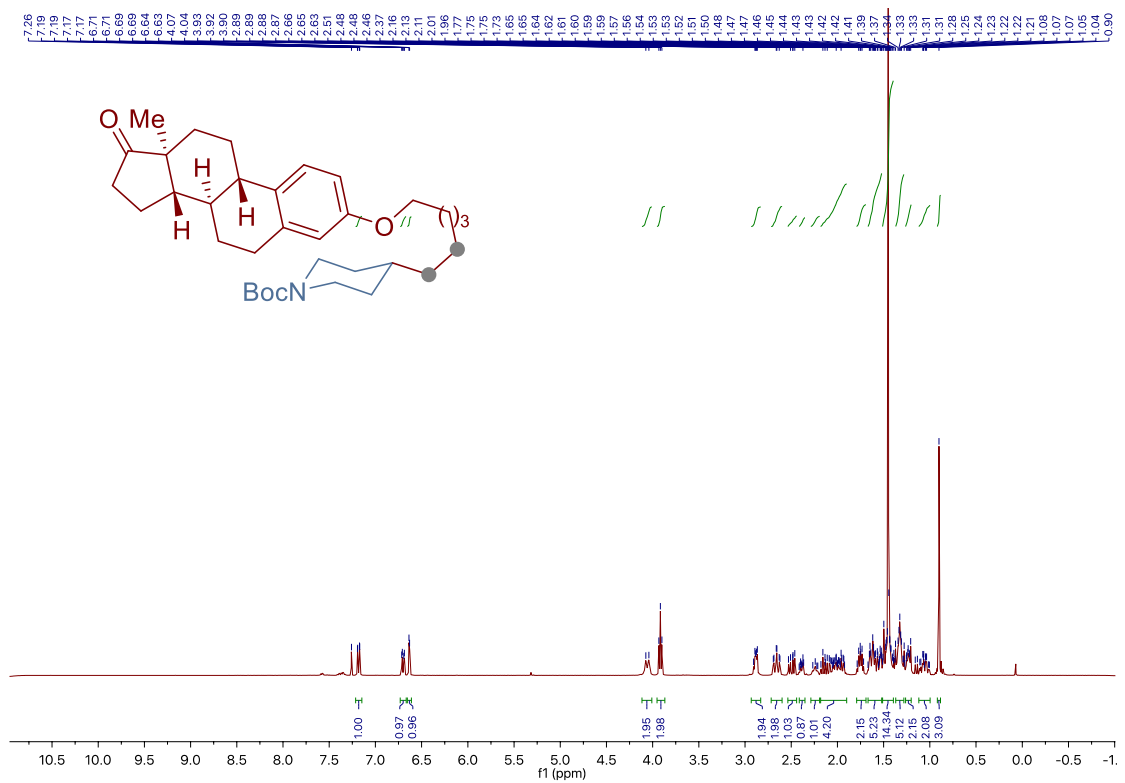
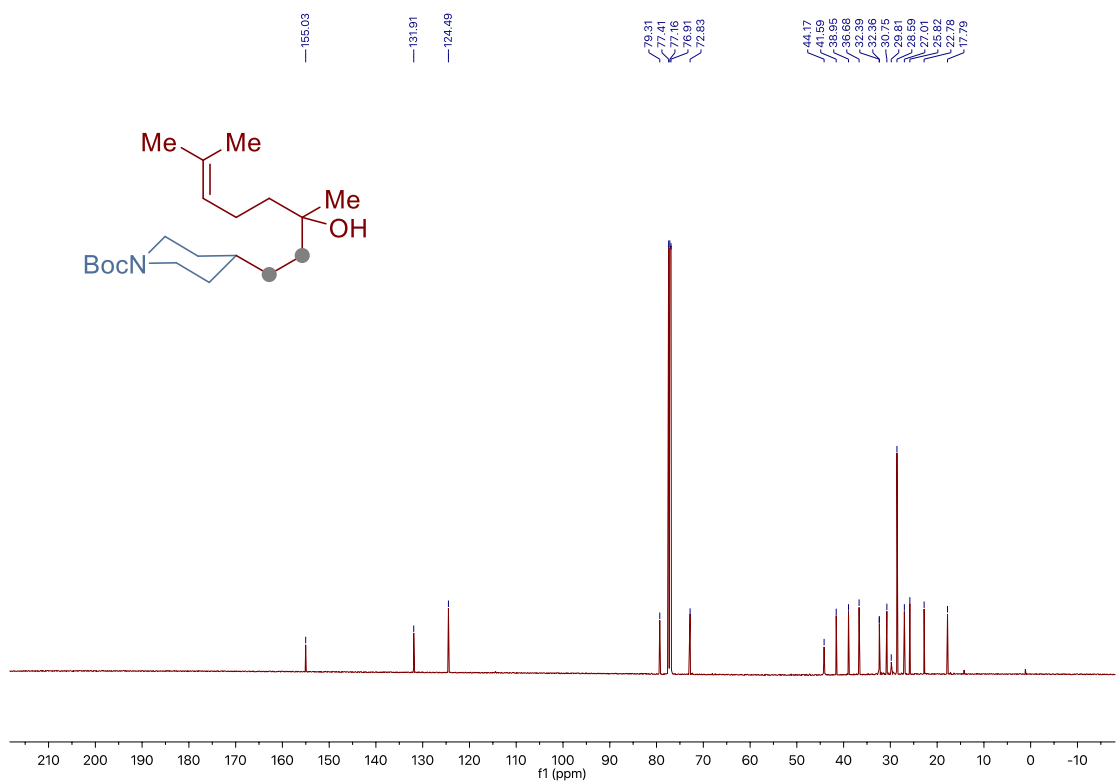
Site-Selective Ni-Catalyzed Deaminative Alkylation of Unactivated Olefins



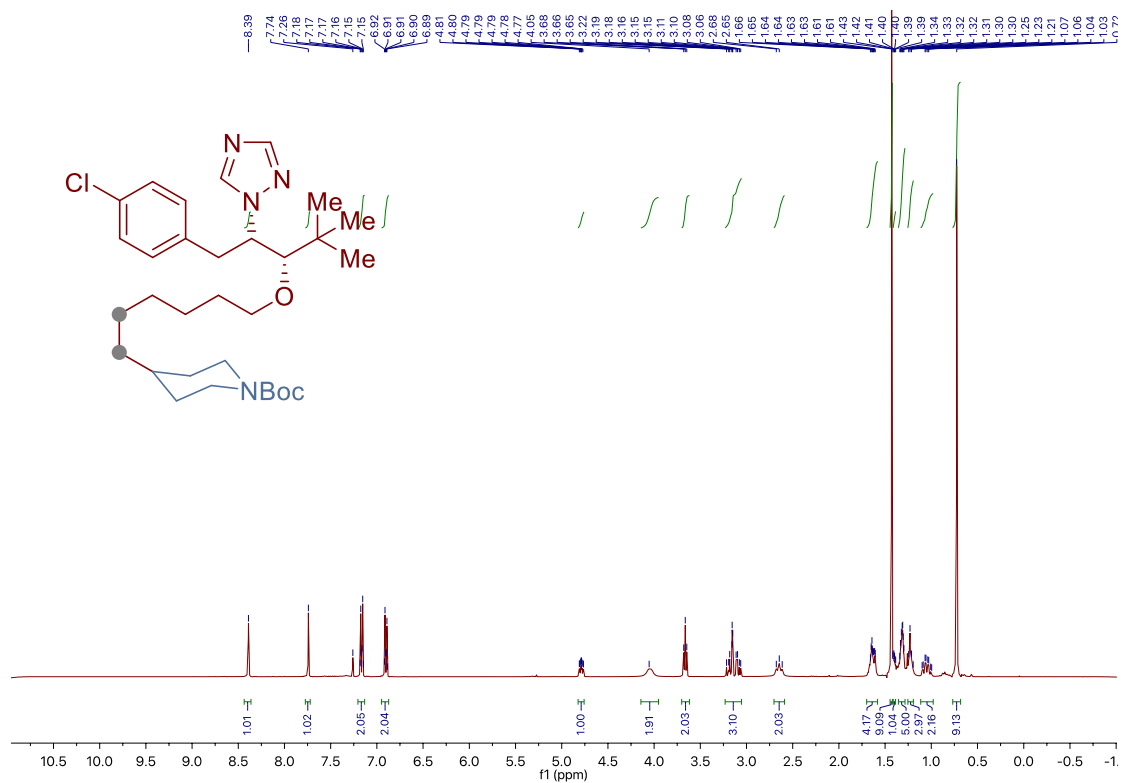
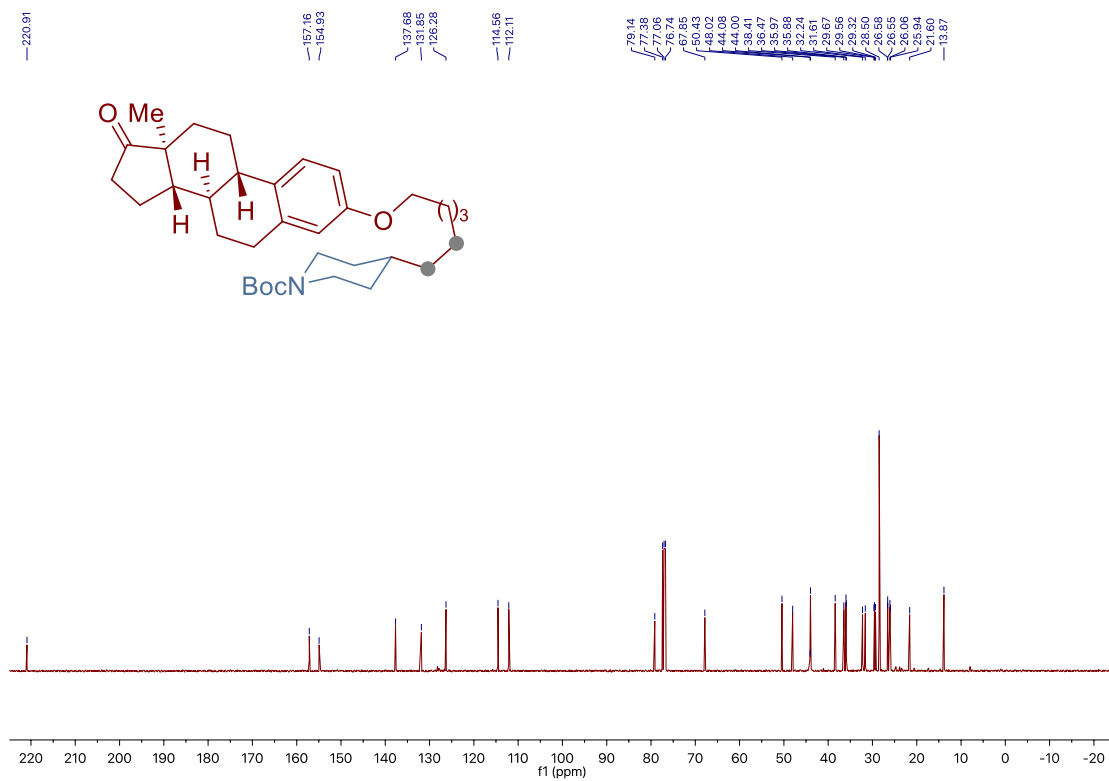
Chapter 3.



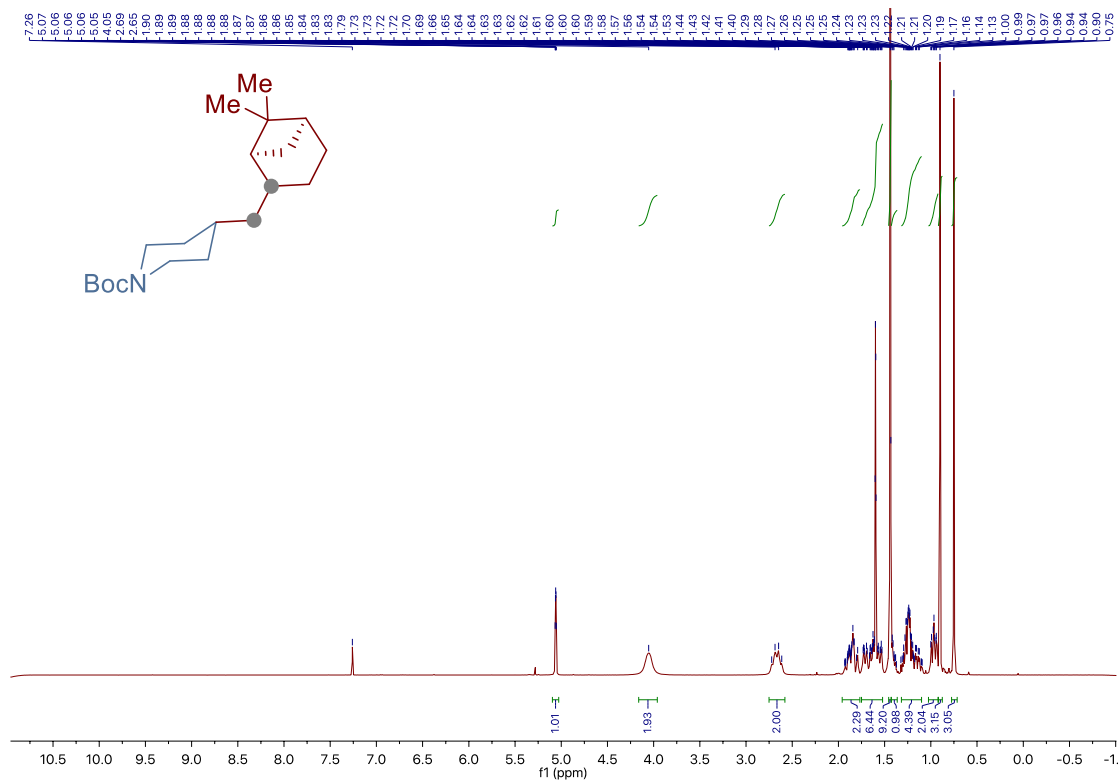
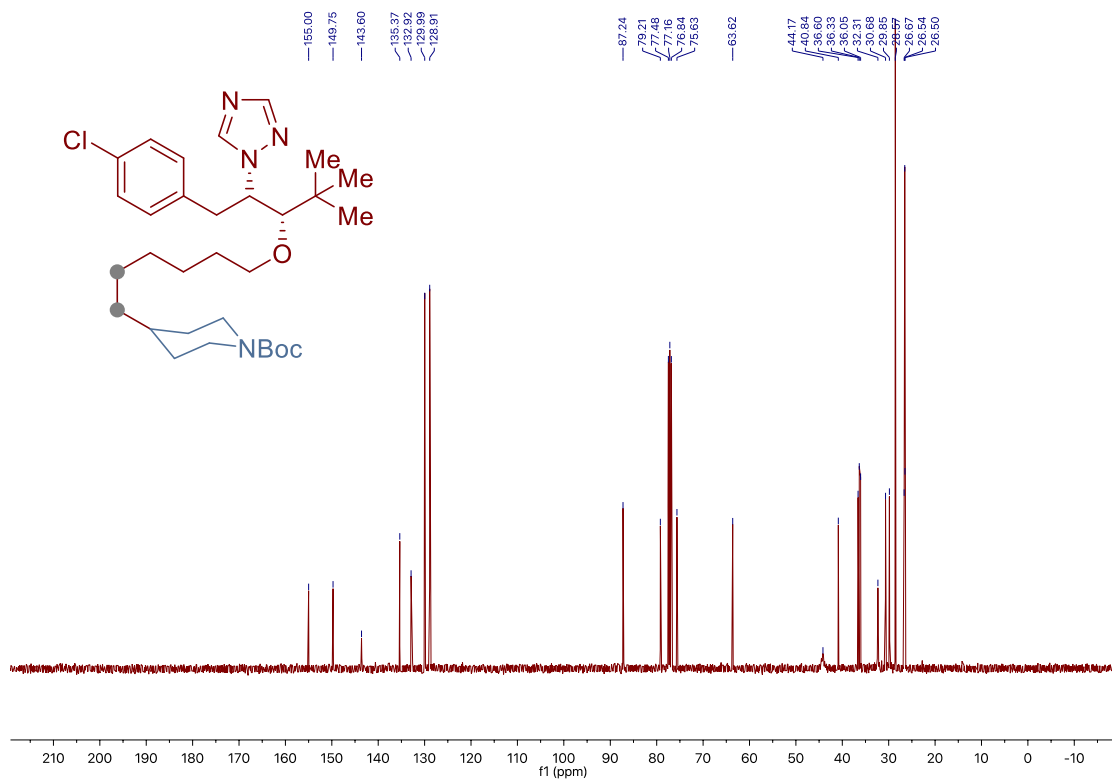
Site-Selective Ni-Catalyzed Deaminative Alkylation of Unactivated Olefins



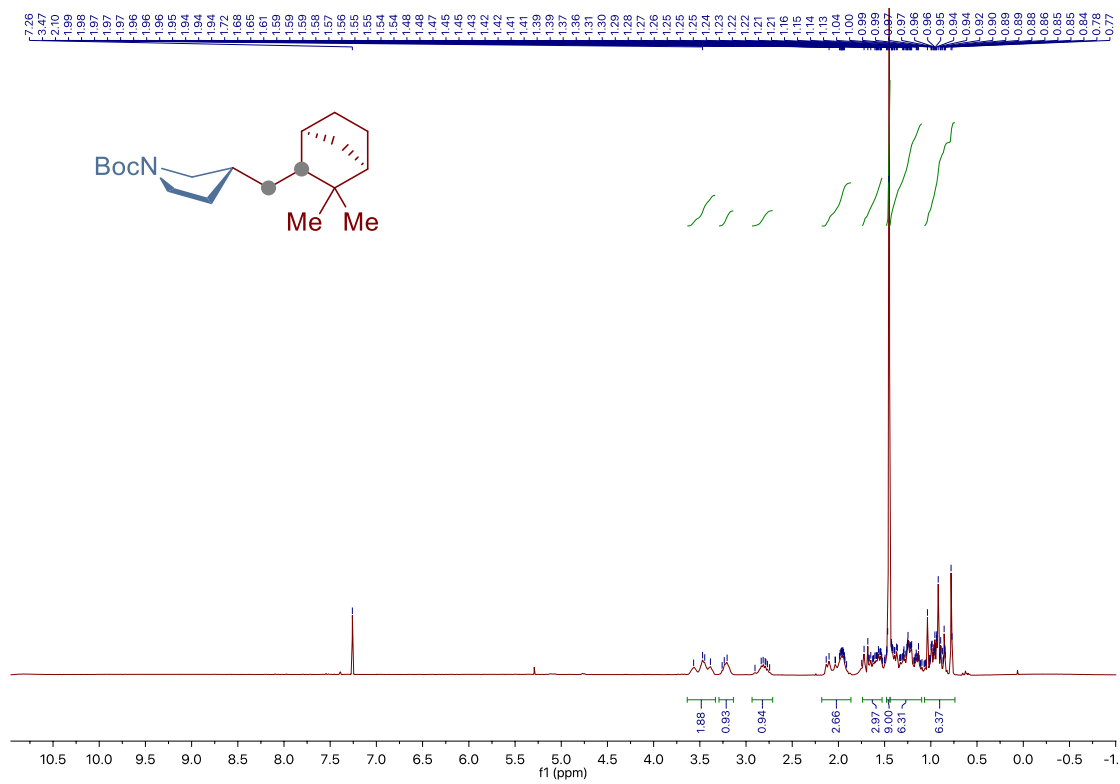
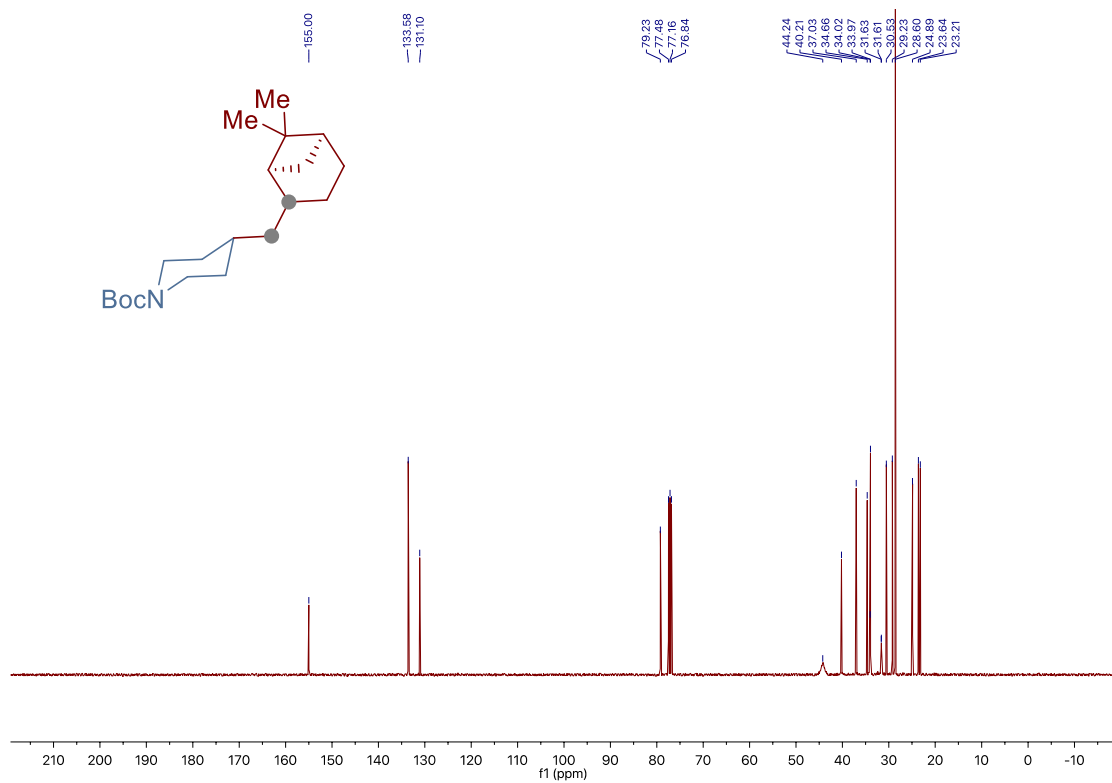
Chapter 3.



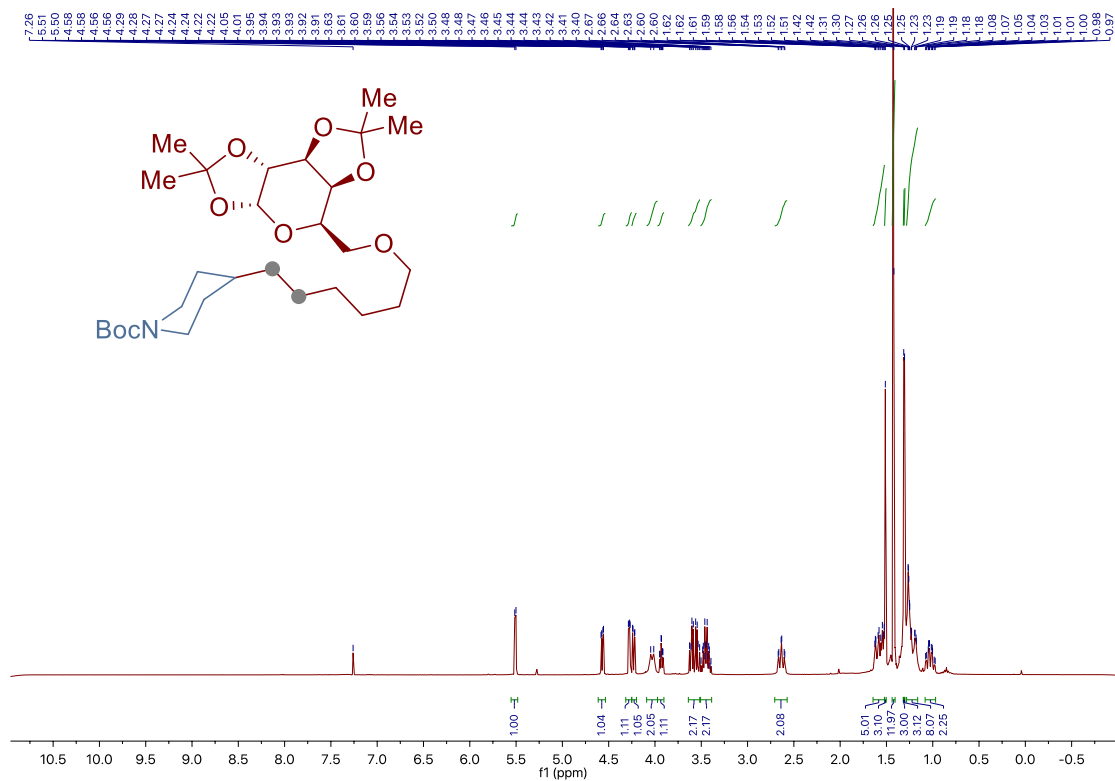
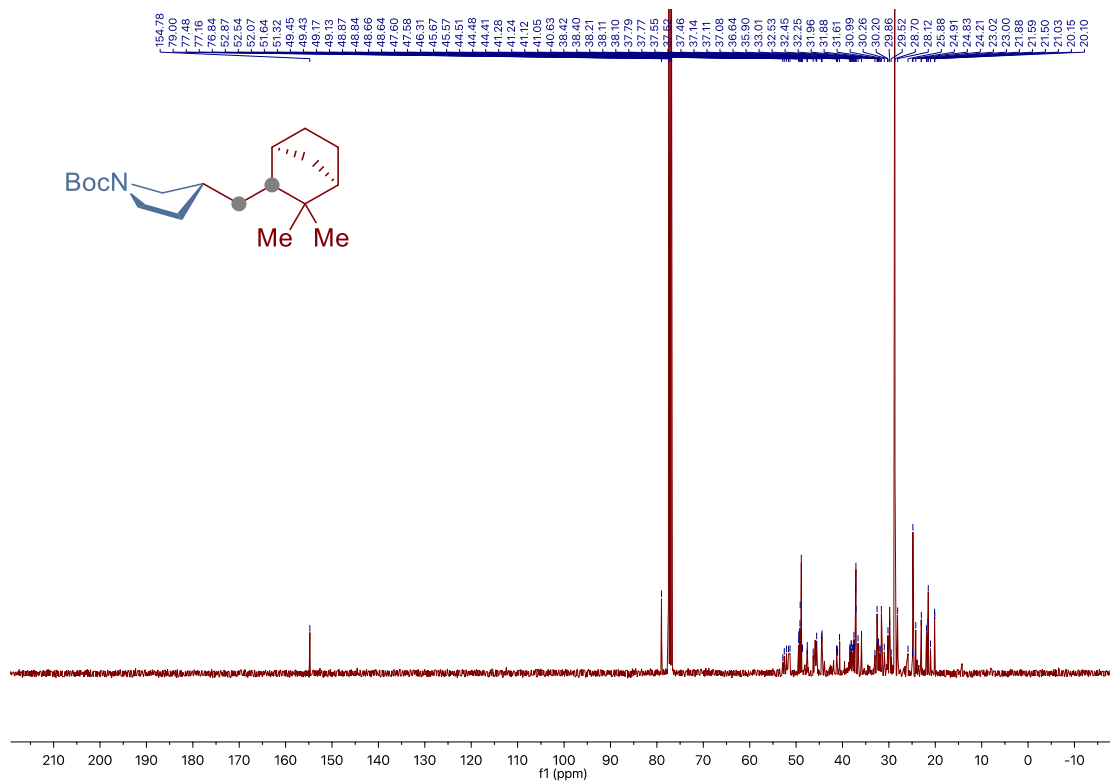
Site-Selective Ni-Catalyzed Deaminative Alkylation of Unactivated Olefins



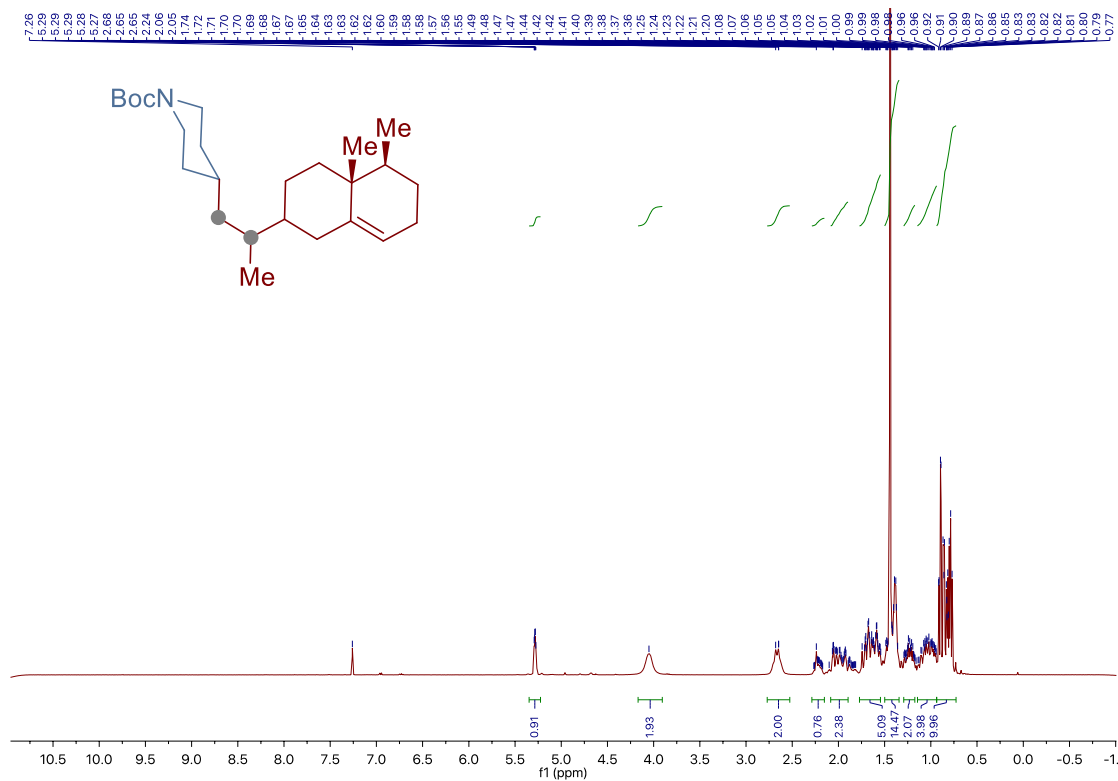
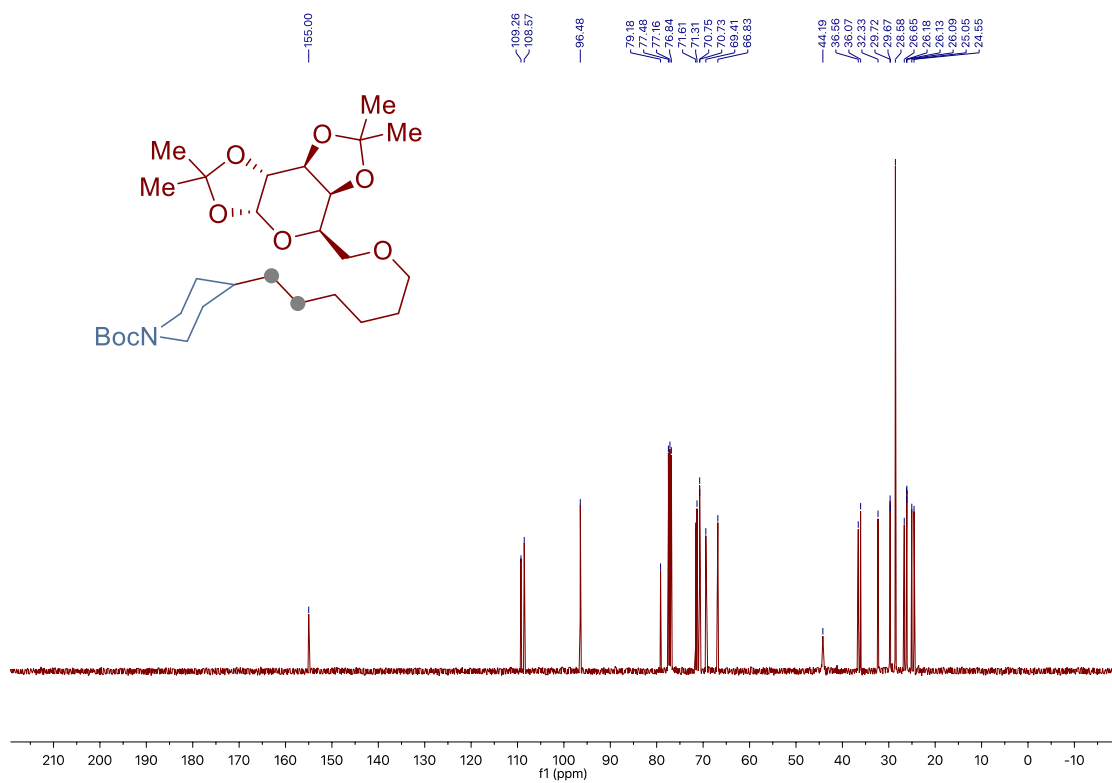
Chapter 3.



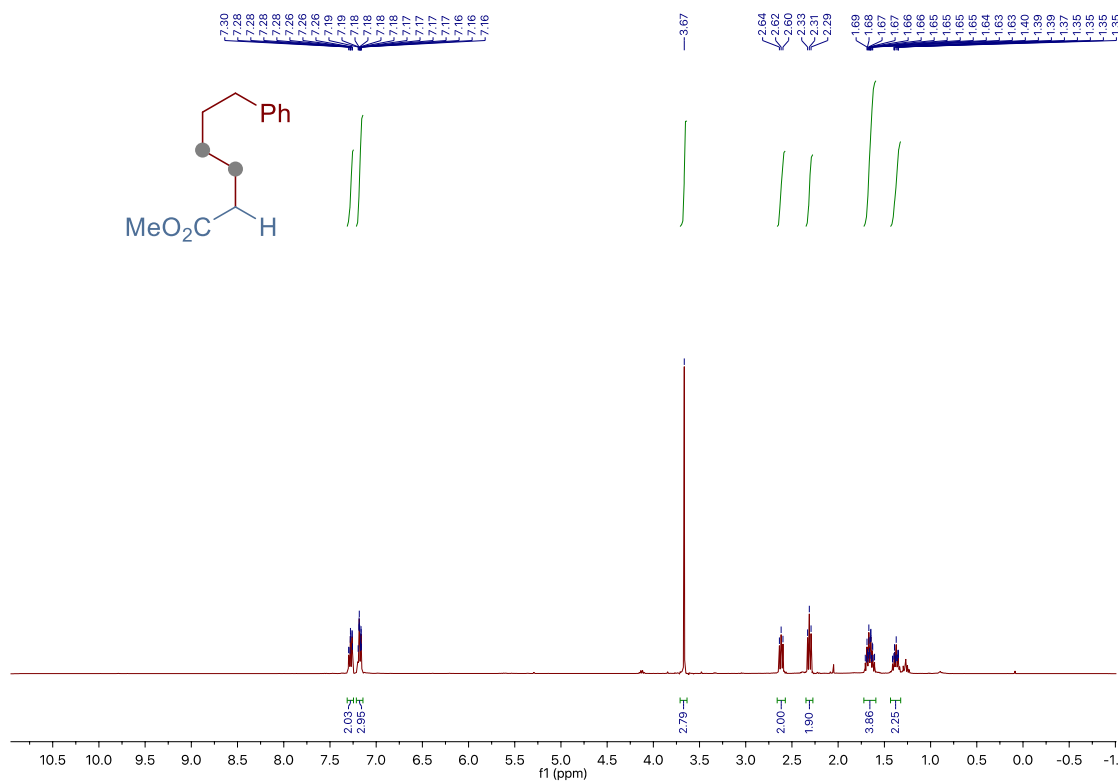
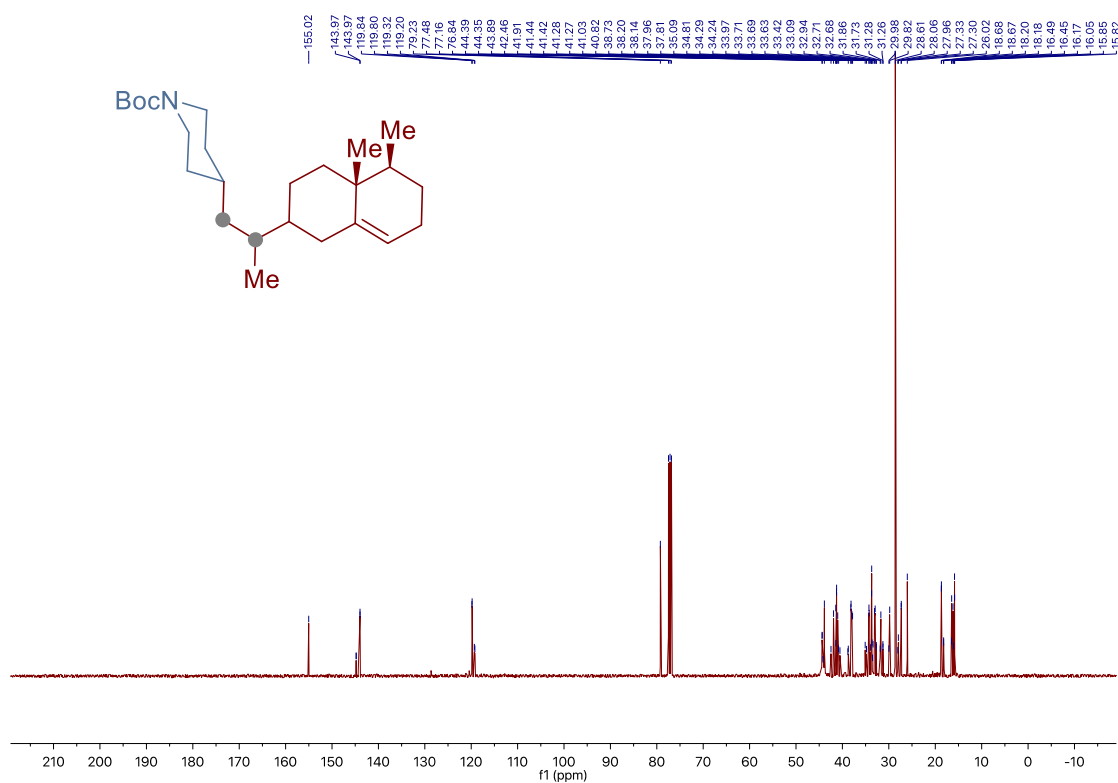
Site-Selective Ni-Catalyzed Deaminative Alkylation of Unactivated Olefins



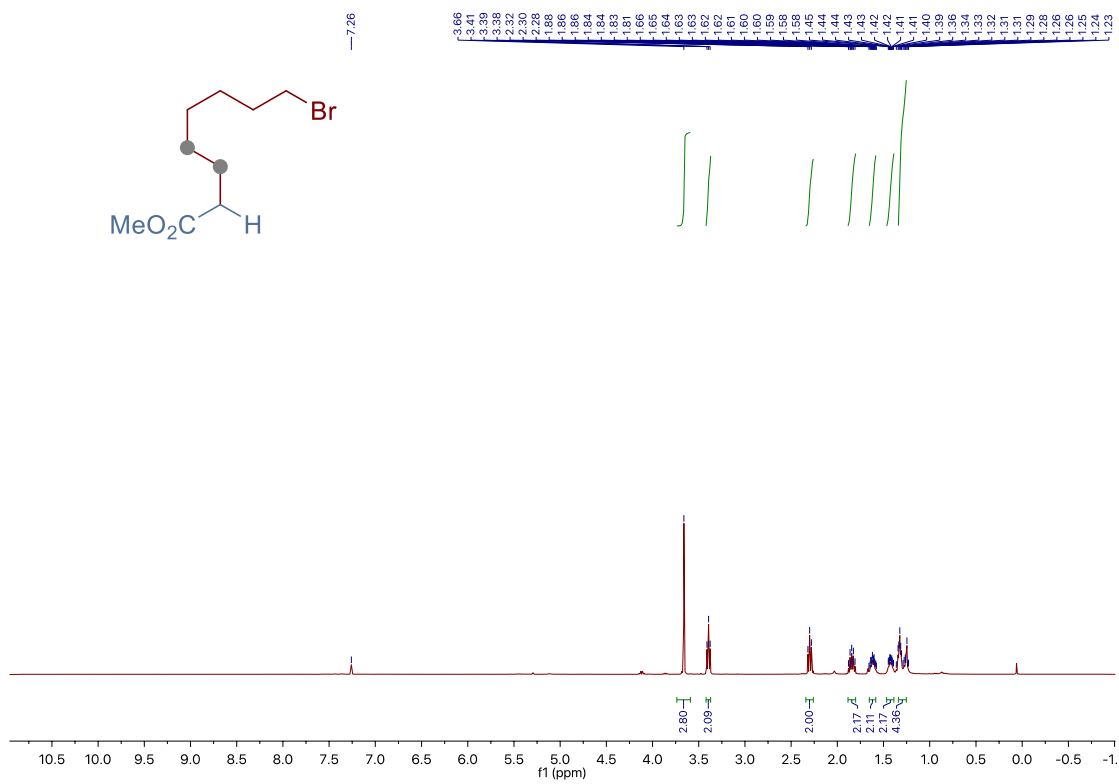
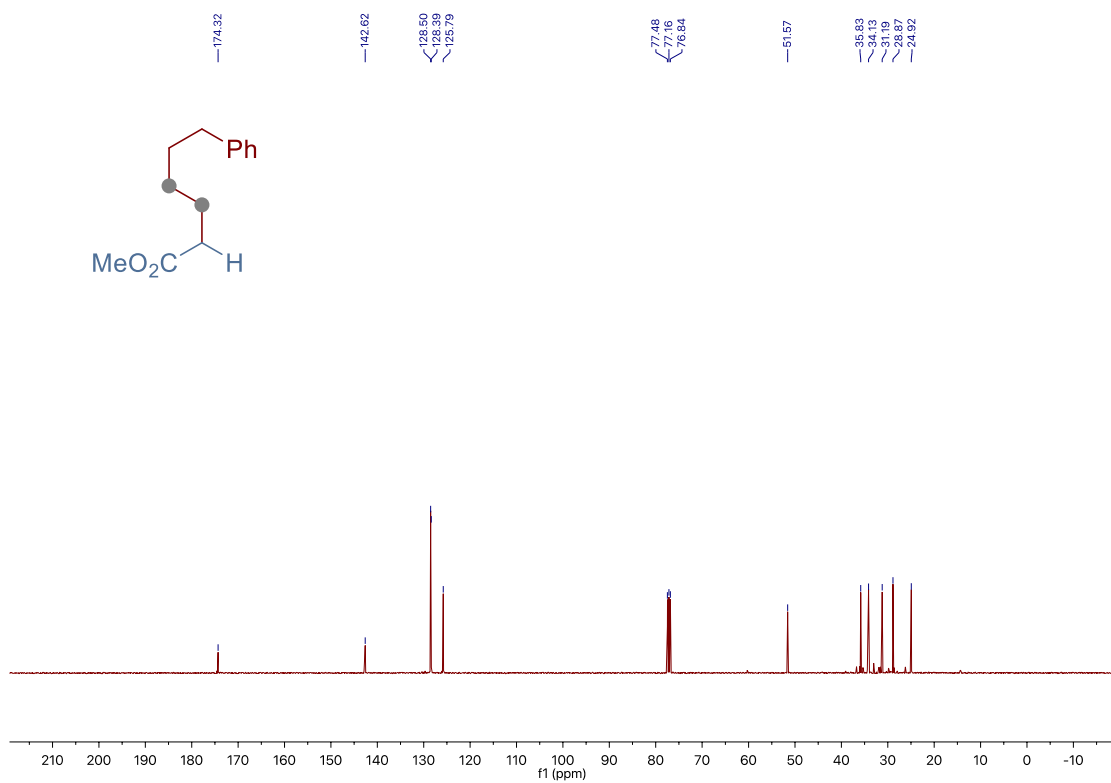
Chapter 3.



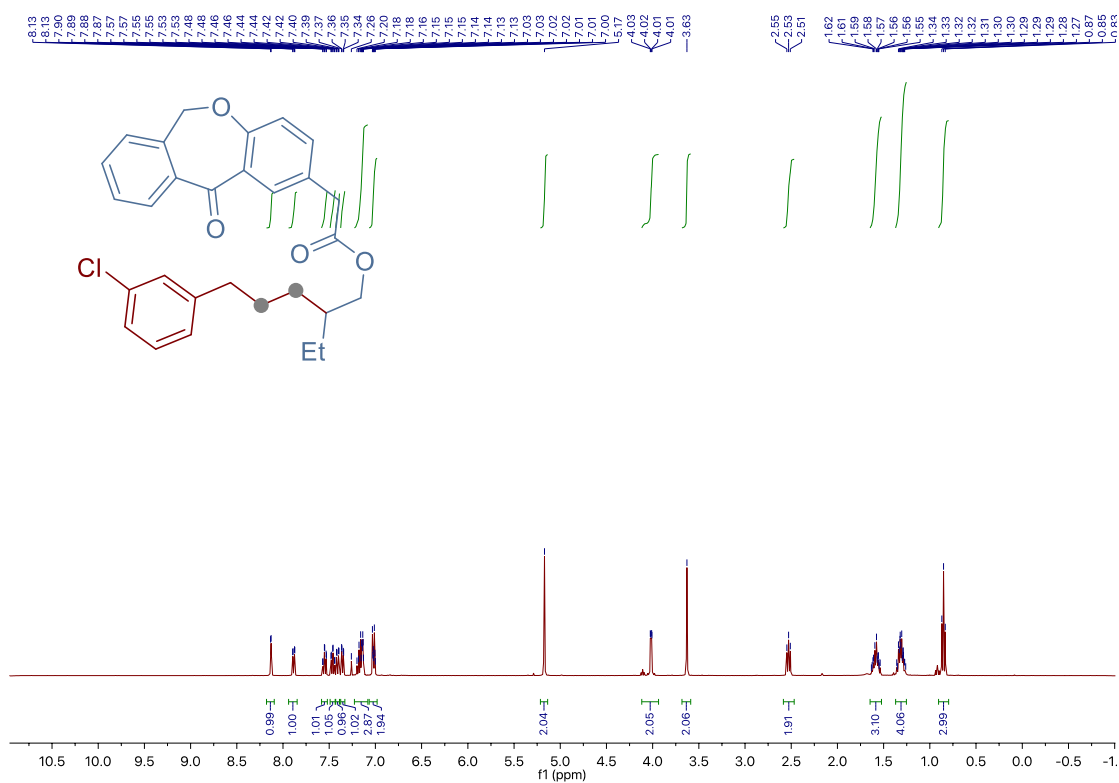
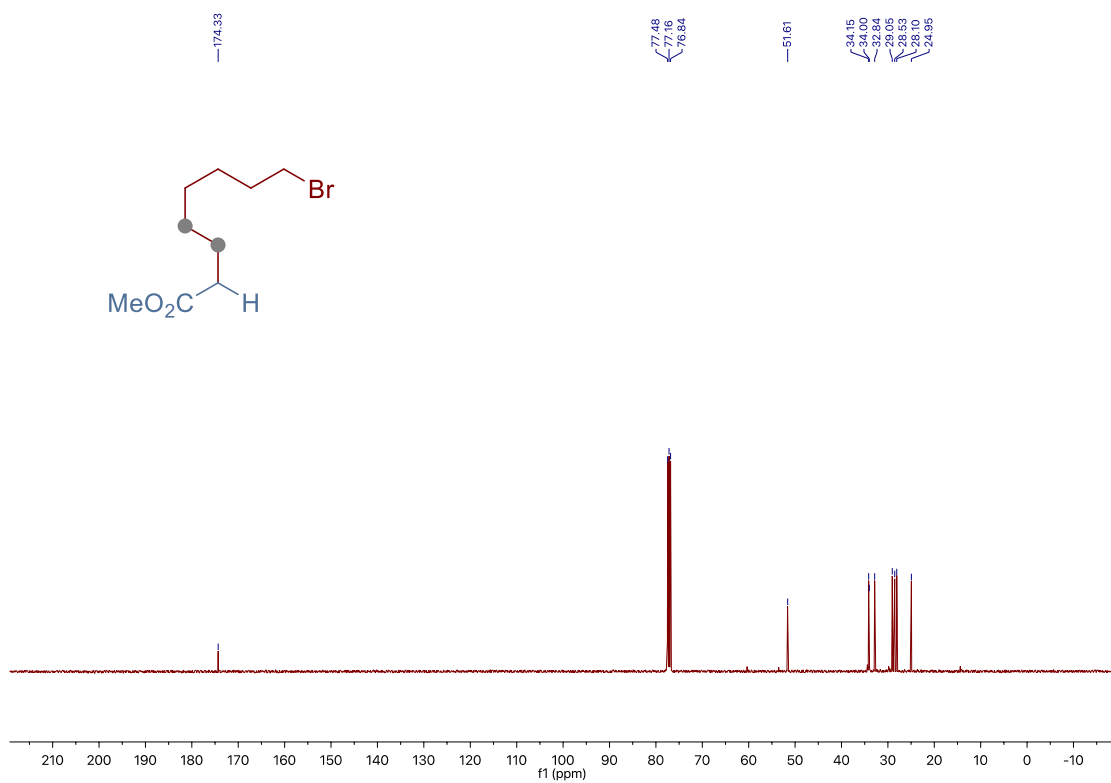
Site-Selective Ni-Catalyzed Deaminative Alkylation of Unactivated Olefins



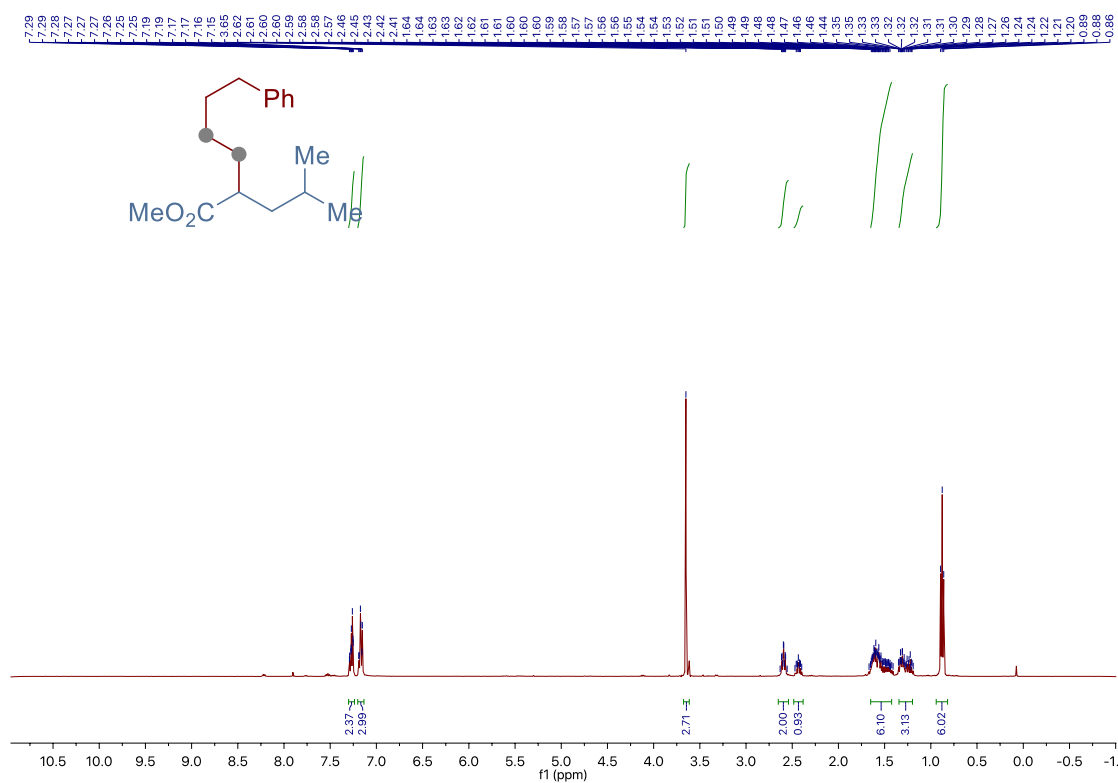
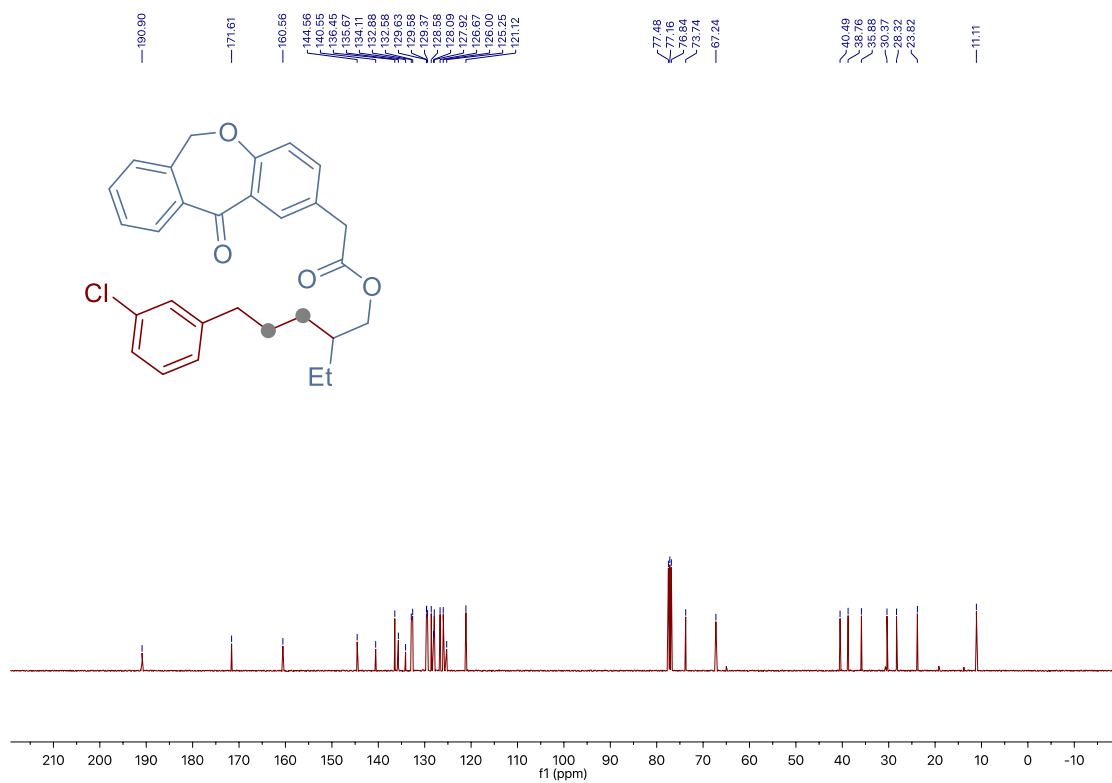
Chapter 3.



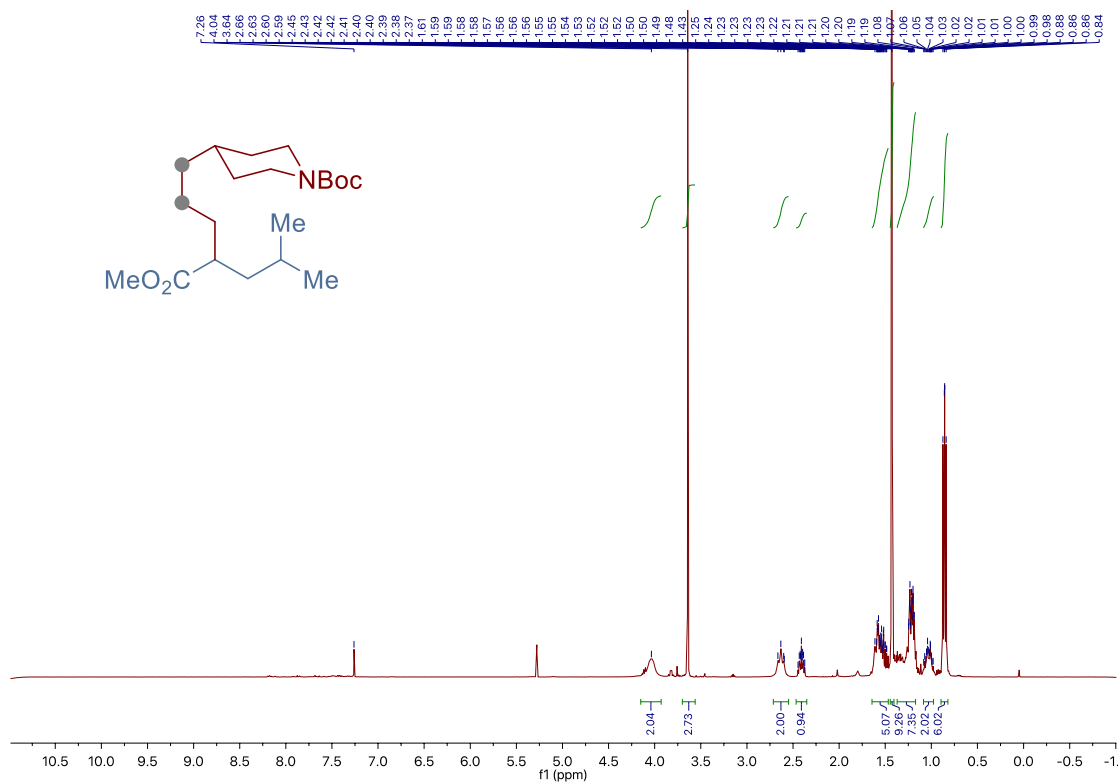
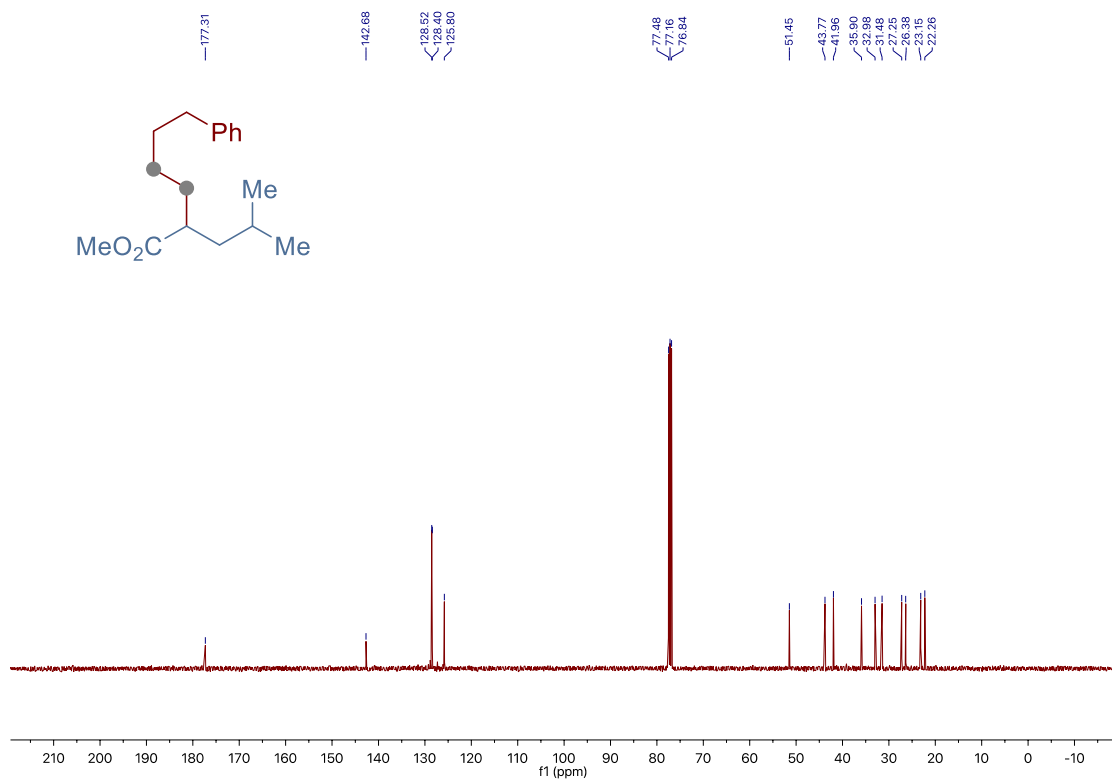
Site-Selective Ni-Catalyzed Deaminative Alkylation of Unactivated Olefins



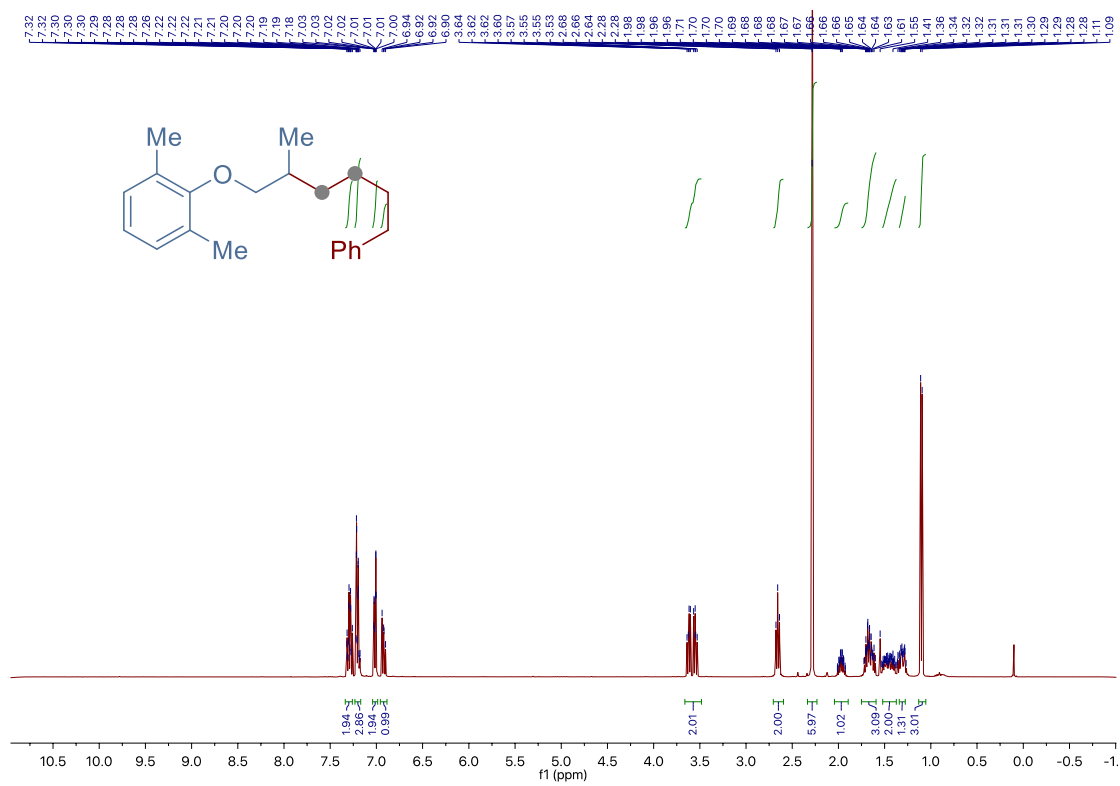
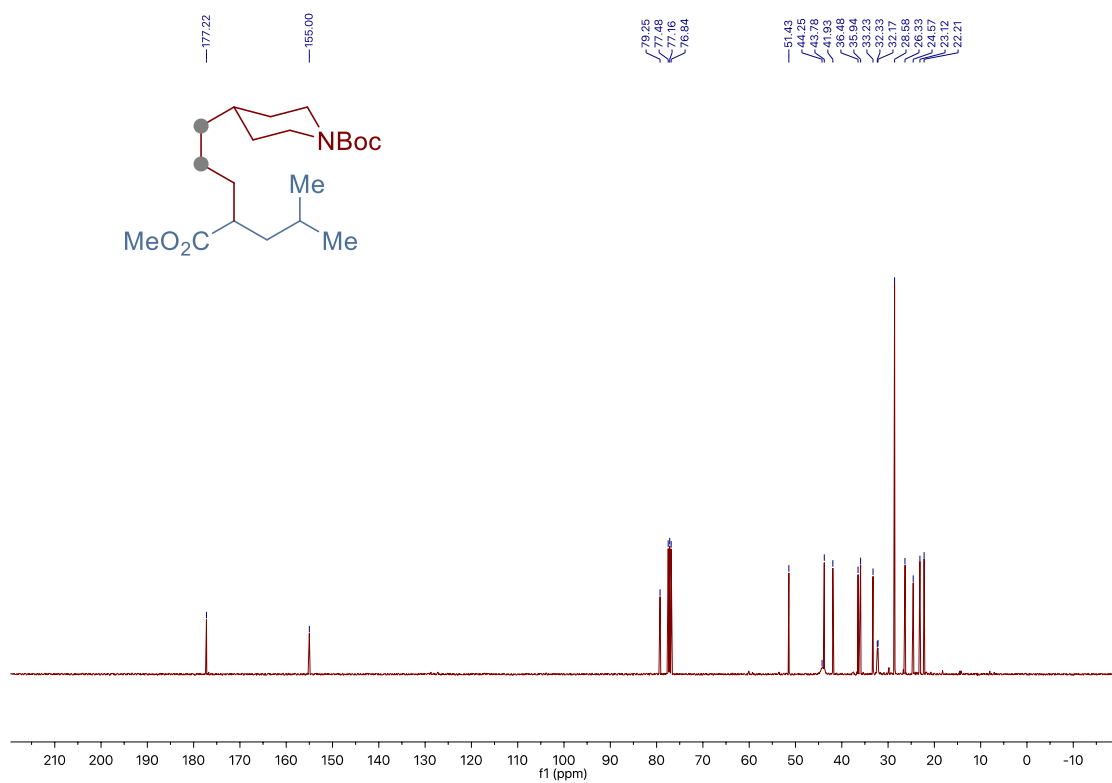
Chapter 3.



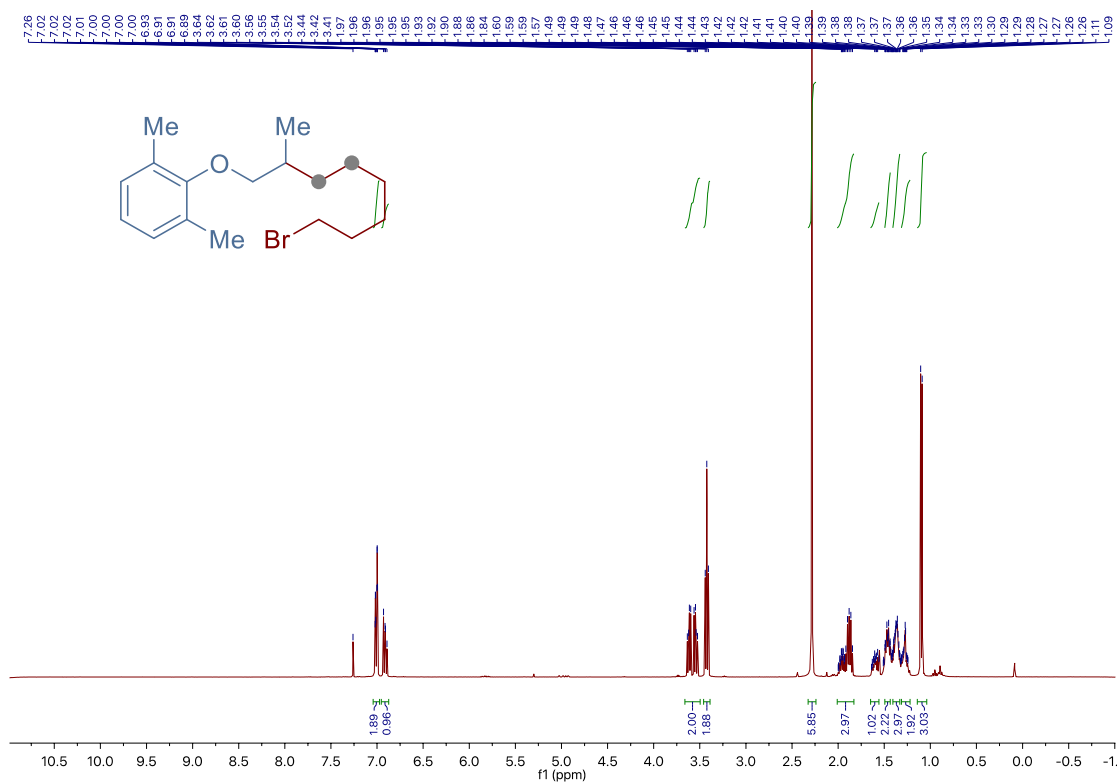
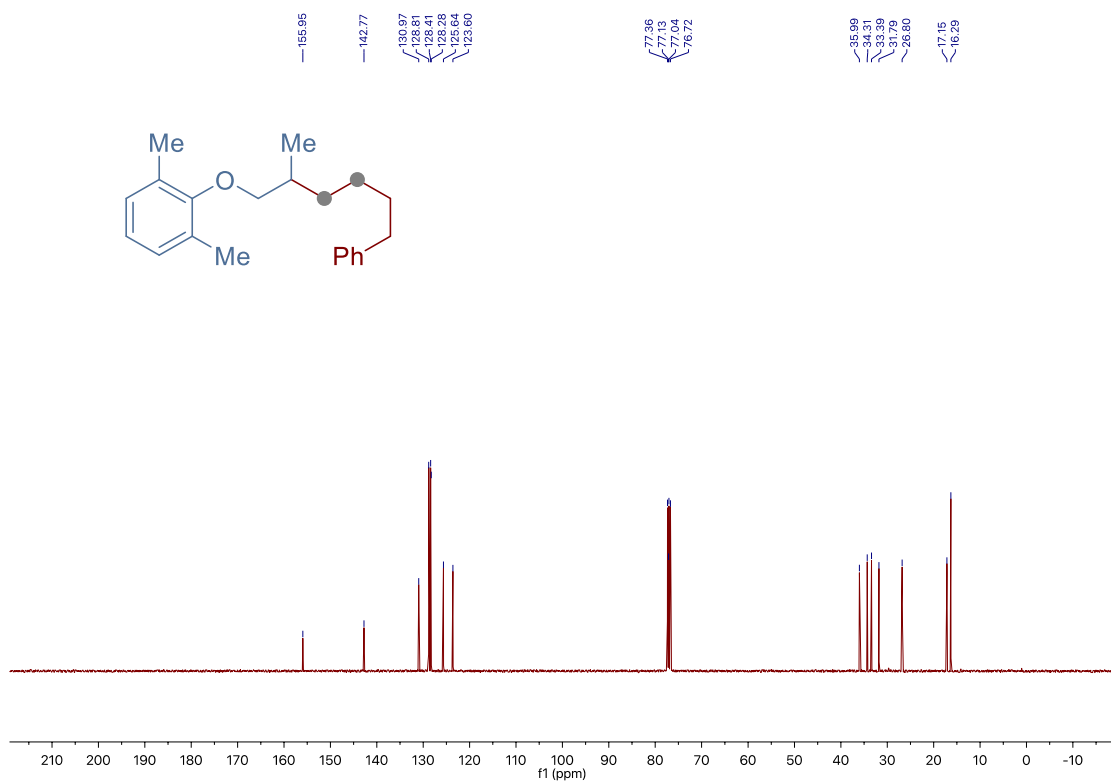
Site-Selective Ni-Catalyzed Deaminative Alkylation of Unactivated Olefins



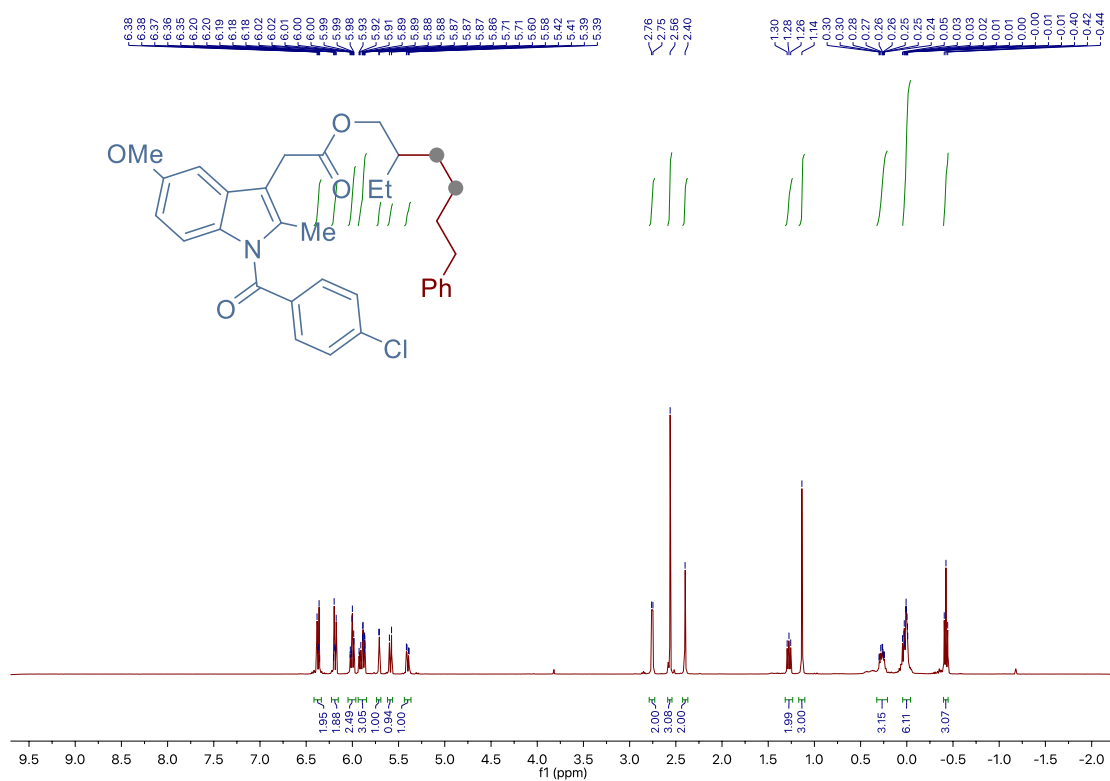
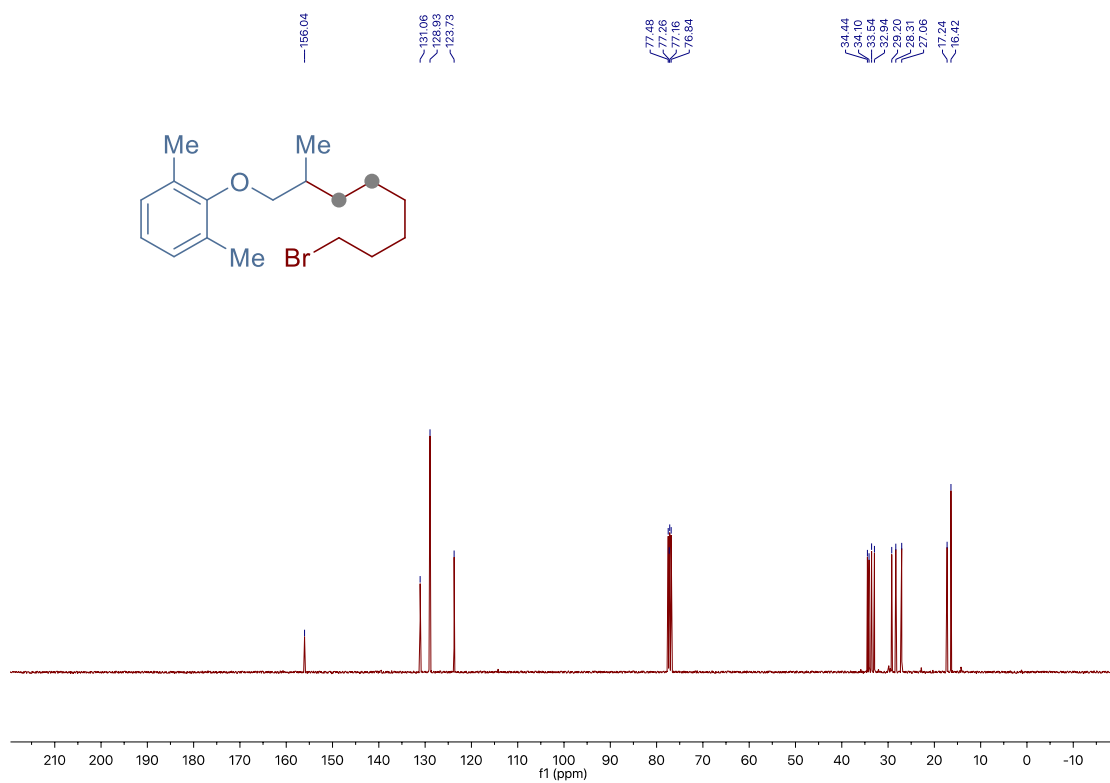
Chapter 3.



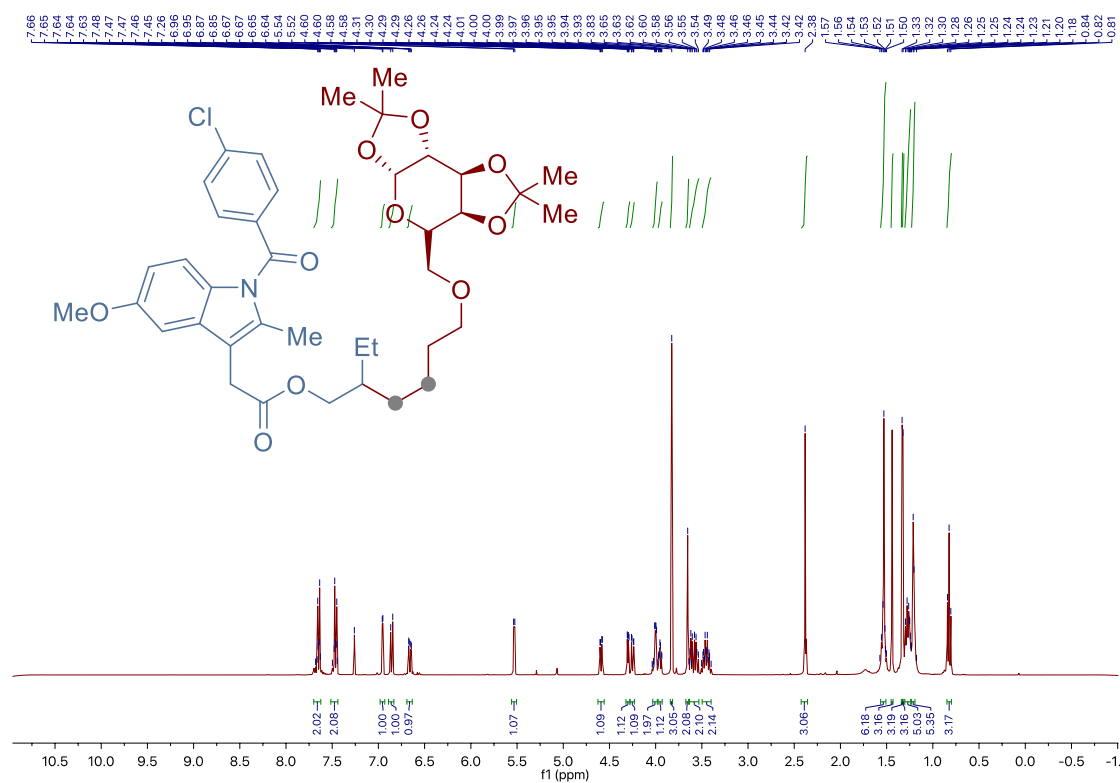
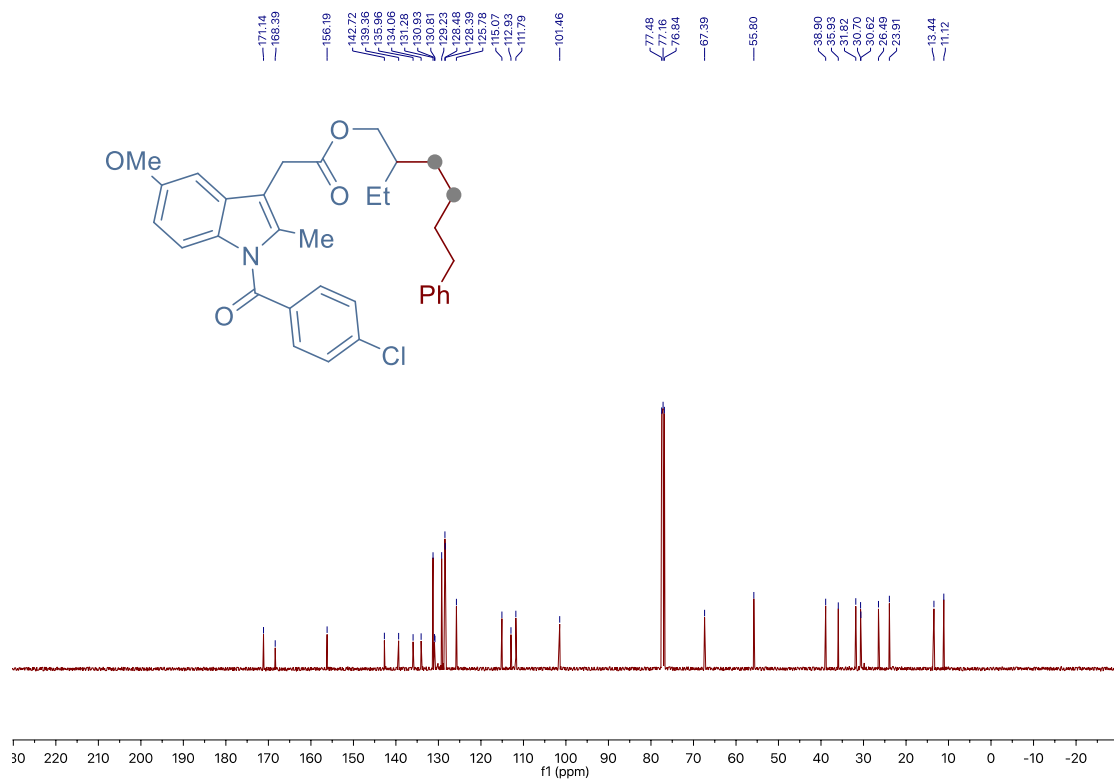
Site-Selective Ni-Catalyzed Deaminative Alkylation of Unactivated Olefins



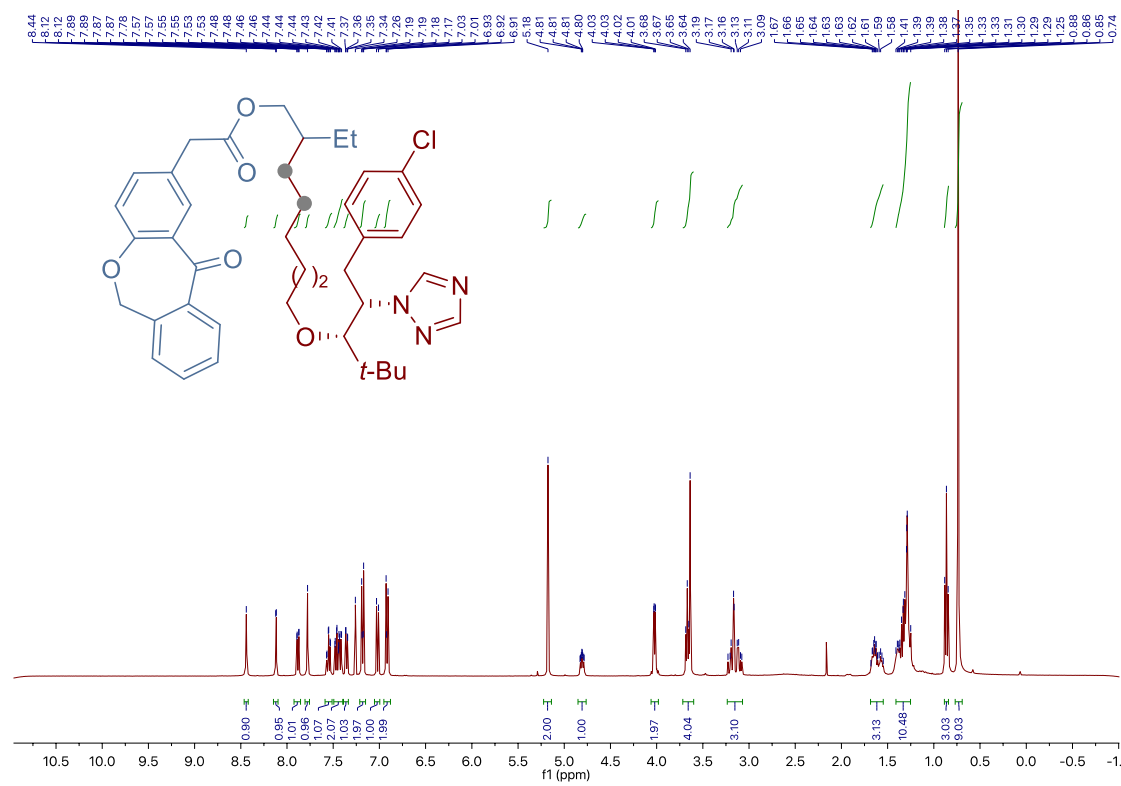
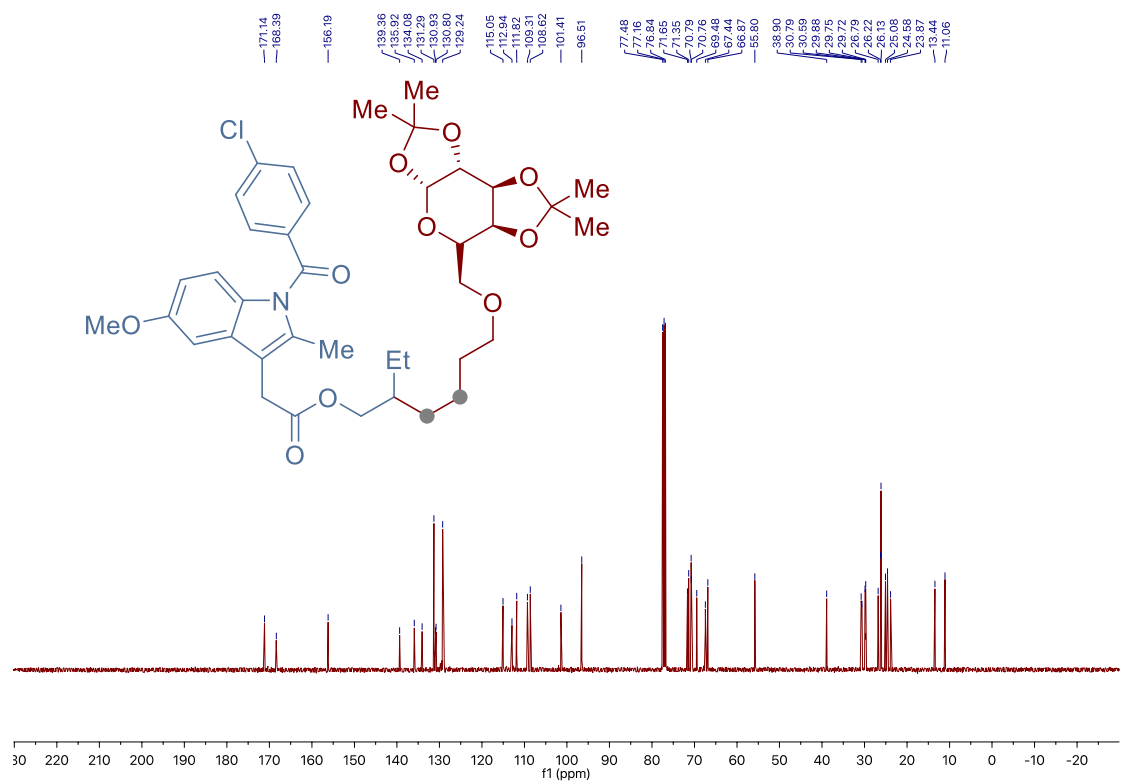
Chapter 3.



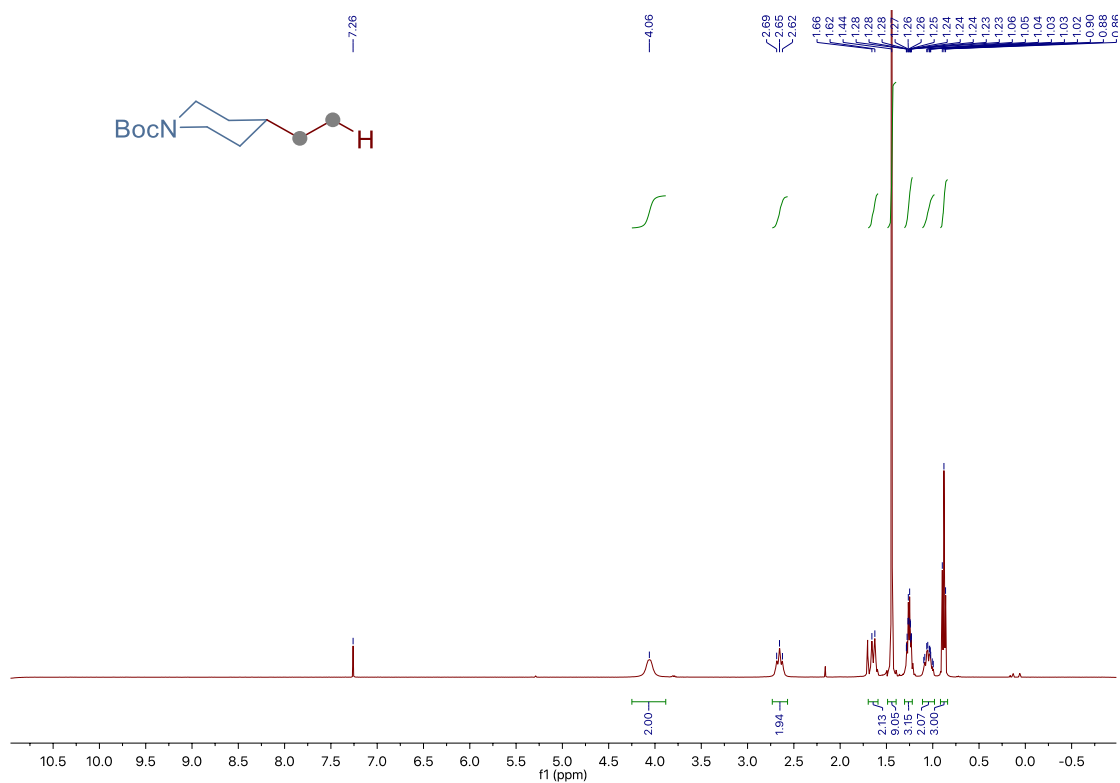
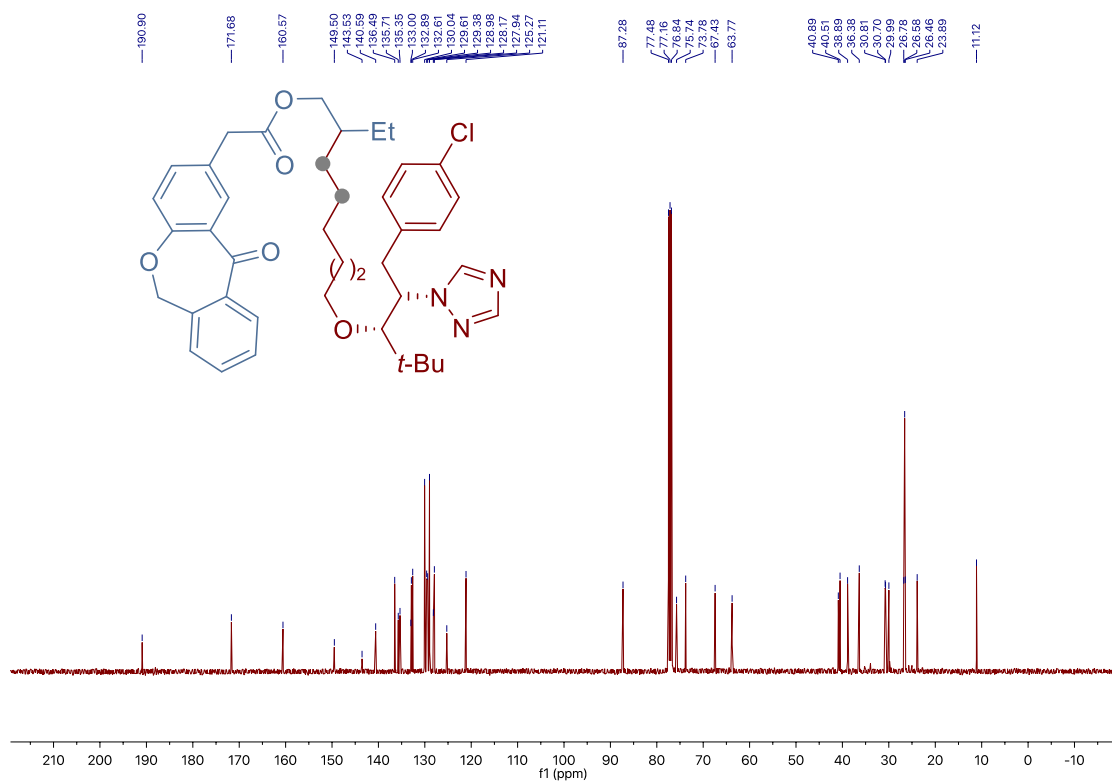
Site-Selective Ni-Catalyzed Deaminative Alkylation of Unactivated Olefins



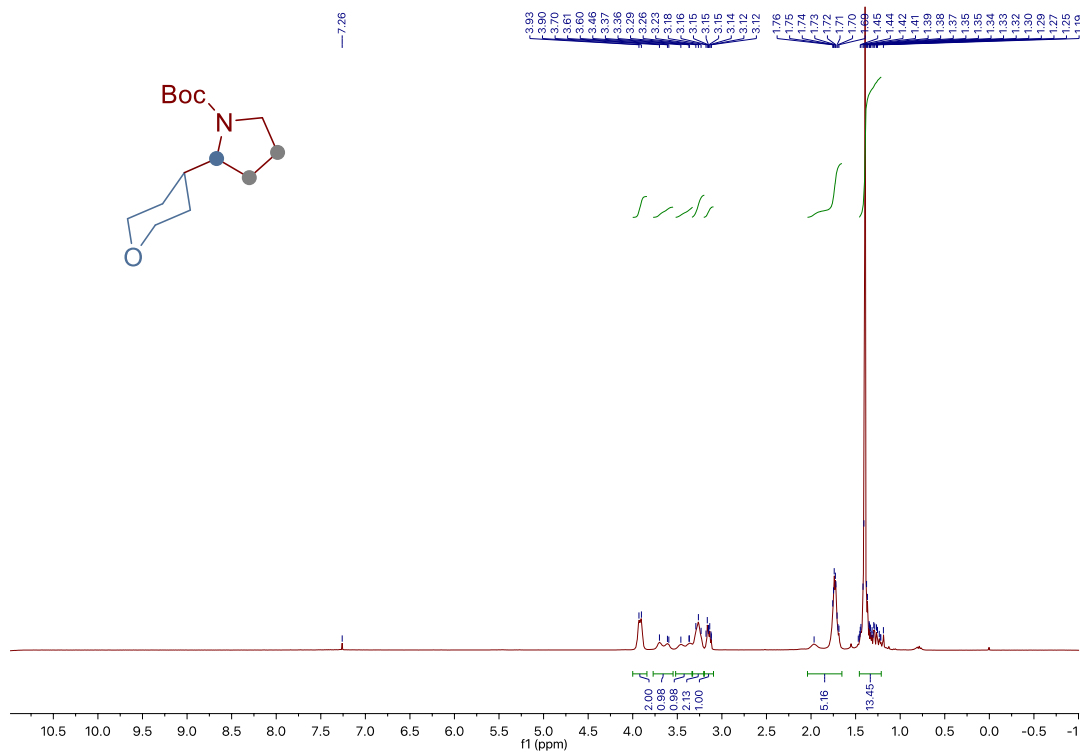
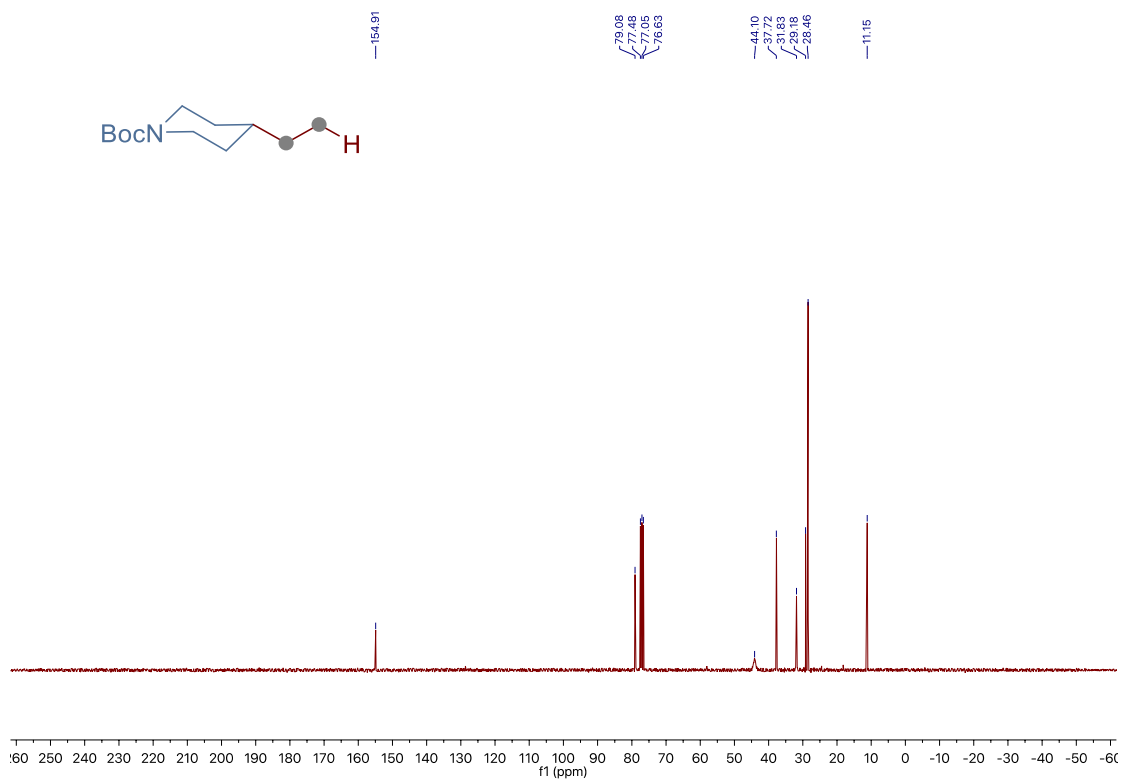
Chapter 3.



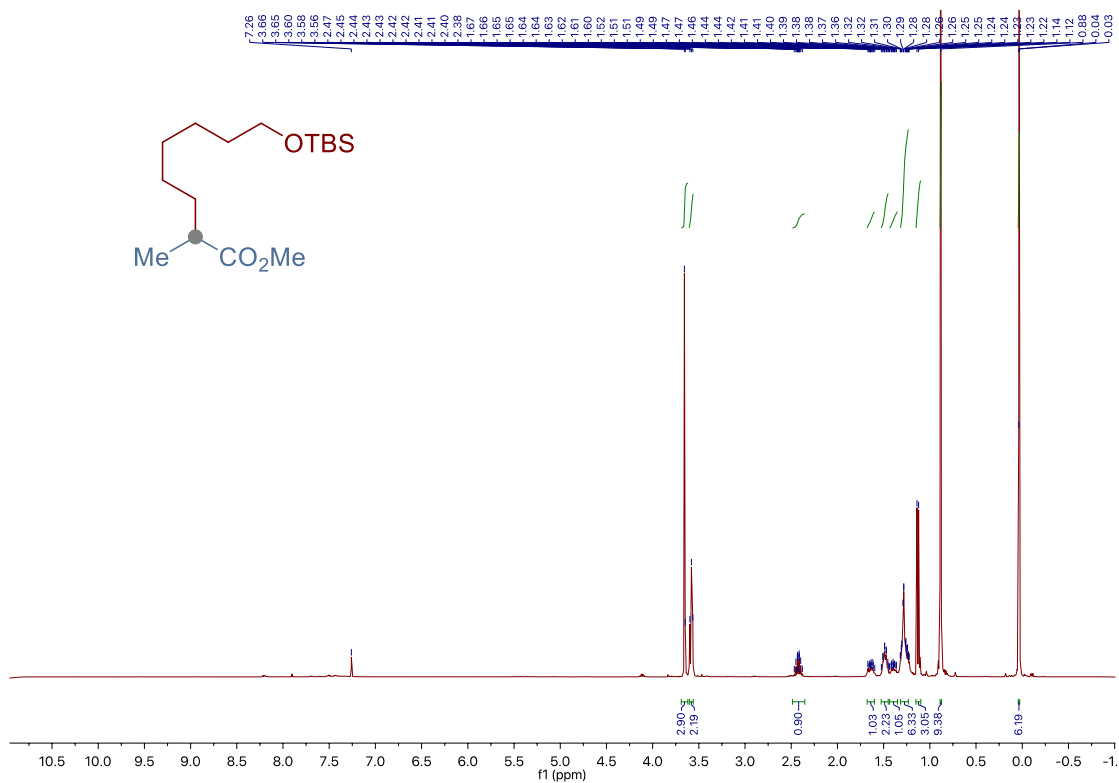
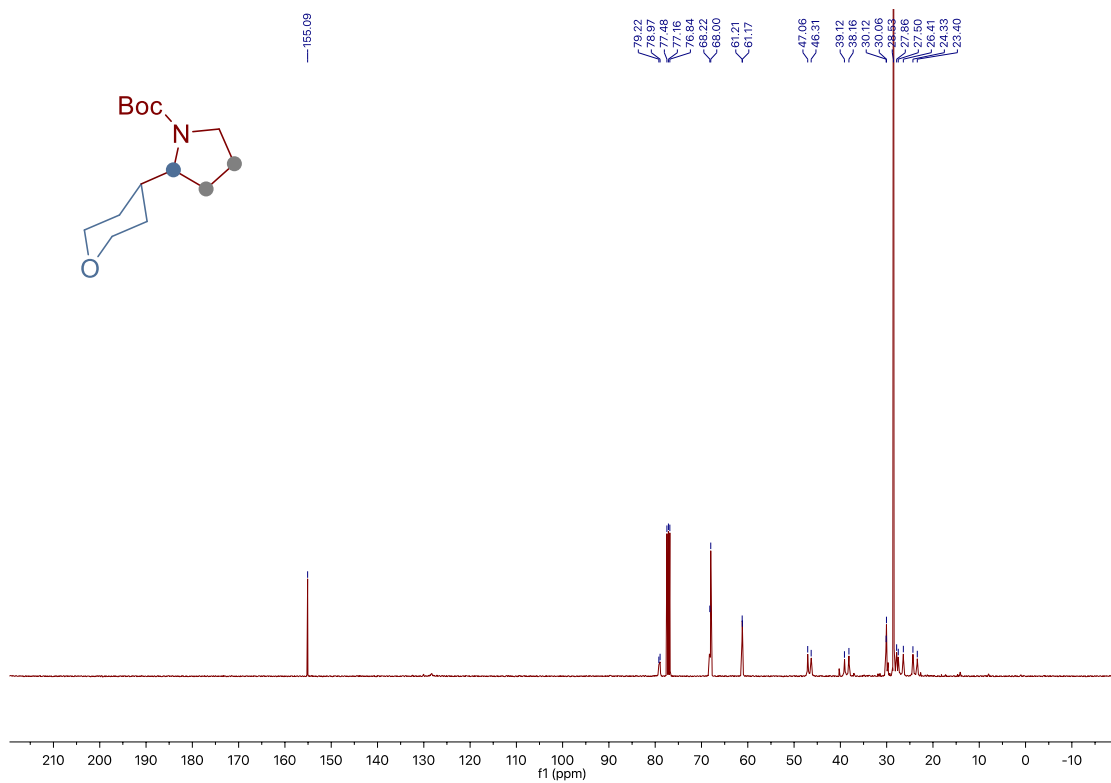
Site-Selective Ni-Catalyzed Deaminative Alkylation of Unactivated Olefins



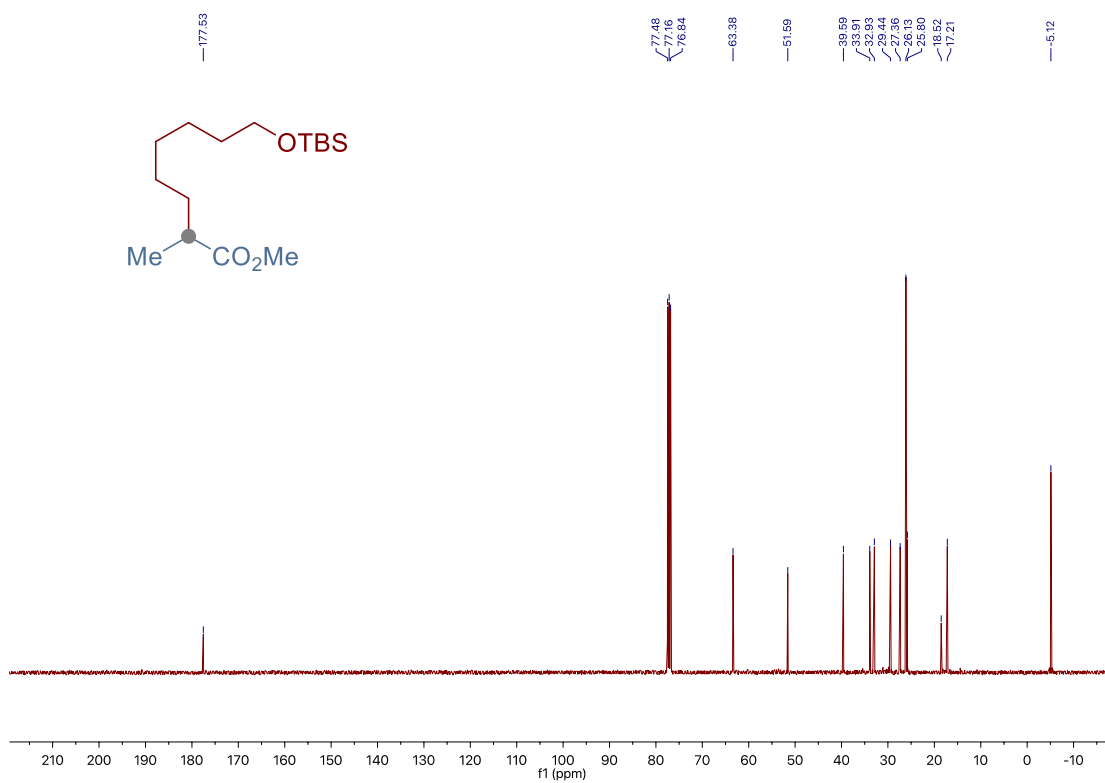
Chapter 3.



Site-Selective Ni-Catalyzed Deaminative Alkylation of Unactivated Olefins



Chapter 3.

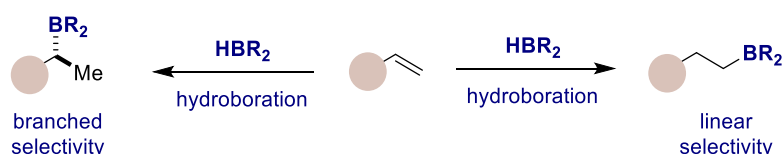


Chapter 4

Site-Selective 1,2-Dicarbofunctionalization of Vinyl Boronates through Dual Catalysis

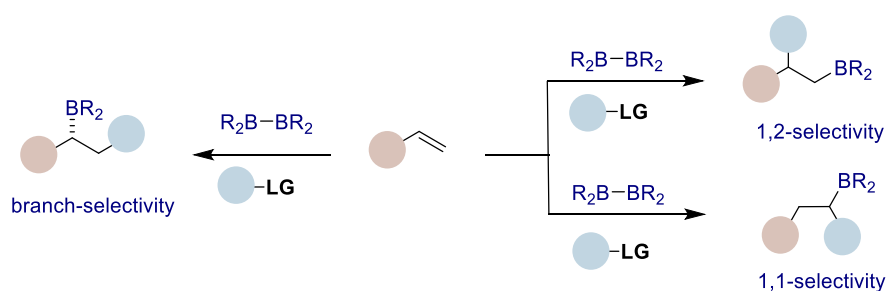
4.1 General Introduction

Organoboron compounds are versatile synthetic intermediates with the ability to transform C–B bonds into a broad range of functional groups.¹ Catalytic hydroboration of unsaturated bonds has become a routine technique for the preparation of organoboron compounds since the pioneering report by H. C. Brown in 1956.² Particularly, significant achievements have been made through hydroboration of olefin feedstocks in both site- and stereo-selective manner (Scheme 4.1).^{2,3}



Scheme 4.1 Catalytic hydroboration of olefins

Moreover, the difunctionalization of olefins represents one of the most widely used strategies to build synthetic complexity with control of chemo-, regio-, and stereoselectivity.⁴ Driven by these advances, chemists have started to investigate carboboration of olefins, which could install a carbon and a boron moiety across a C=C bond, thus allowing the construction of densely functionalized organoboron compounds (Scheme 4.2).⁵ Despite significant breakthroughs has been made in carboboration of olefins by transition metals (Cu, Ni, Pd), several outstanding problems still remain to be addressed.⁵



Scheme 4.2 Catalytic carboboration of olefins

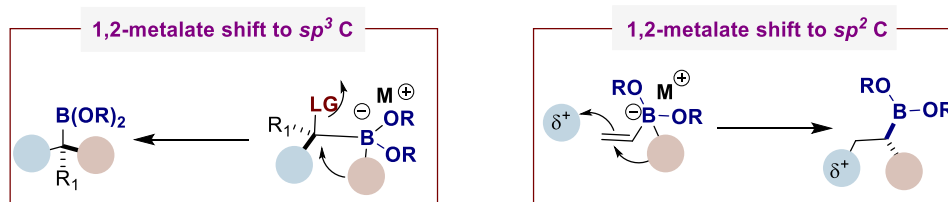
Vinyl borons are highly important building blocks in organic synthesis.⁶ Such boron substituted alkenes can be employed in catalytic difunctionalization events, providing an alternative process for the preparation of organoboron compounds from simple and easily accessible materials.⁷ In this chapter, recent advances of the dicarbofunctionalization of vinyl borons for the preparation of densely functionalized

organoboron compounds are presented.

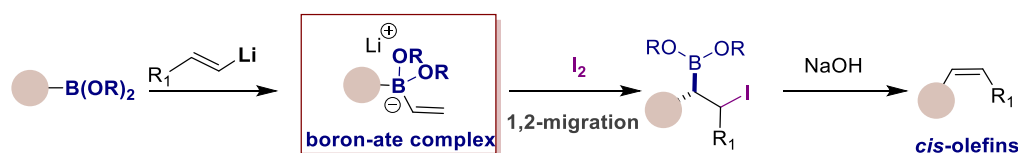
4.2 Catalytic Dicarbofunctionalization of Vinyl Borons

4.2.1 Catalytic Difunctionalization of Vinyl Boron “Ate” Complex

The 1,2-migration of a boron-ate complex to an acceptor is the most useful application of organoboron compounds in synthetic methodology.⁷ The homologation of organoboron compounds through 1,2-metalate shift to an attached sp^3 carbon center has been well developed by Matteson⁸ and Aggarwal⁹ (Scheme 4.3, *left*). Not surprisingly, the 1,2-metalate shift of vinyl boron “ate” complex to the adjacent unsaturated carbon has also attracted much attention in recent years (Scheme 4.3, *right*). For example, Zweifel and co-workers found the first electrophile induced 1,2-migration of vinyl boron-ate complexes to prepare β -iodoboranes¹⁰ (Scheme 4.4). Noteworthy, in this process only *cis*-olefins were obtained after the deboroniodination of β -iodo boranes. Subsequently, Matteson^{8,11} and Evans¹² extended this olefination to vinyl boronates. In all cases, *cis*-olefins were generated through iodine promoted 1,2-metalate shift of vinyl boron “ate” complexes and base mediated β -elimination.



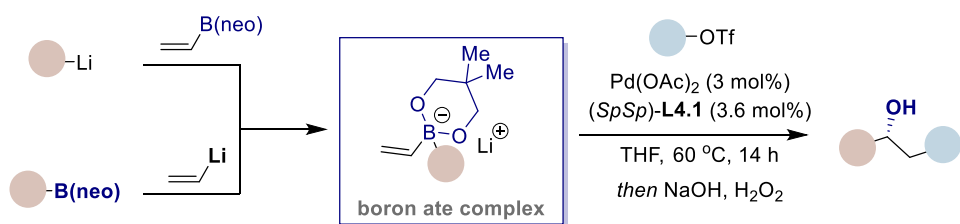
Scheme 4.3. 1,2-Metalate shift of boron “ate” complexes



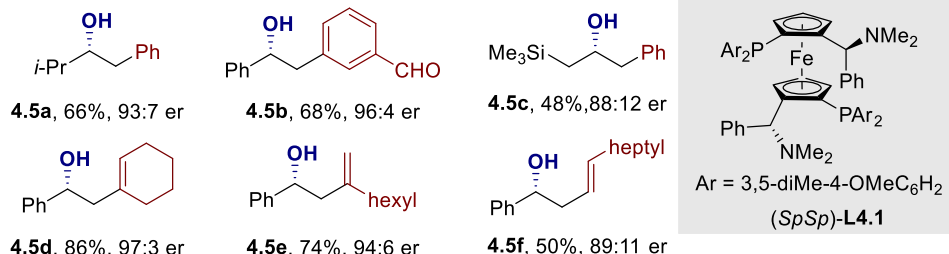
Scheme 4.4. Iodination of vinyl boron “ate” complex and olefination (Zweifel, Matteson and Evans)

4.2.2 Pd-Catalyzed Conjunctive Coupling of Vinyl Boron “Ate” Complex

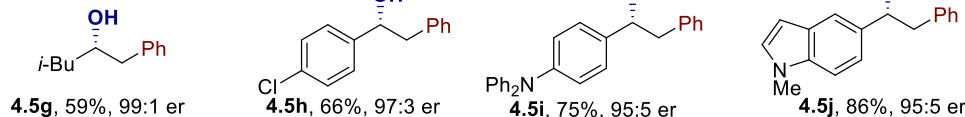
The first transition metal oxidative addition complex induced 1,2-metalate shift of vinyl boron “ate” complex to construct two new sp^3 C–C bonds in one pot was been developed by Morken and co-workers.¹³ In 2015, they reported a Pd-catalyzed enantioselective three-component coupling of organolithium reagents, organoboronates and organotriflates which was named as conjunctive cross coupling (Scheme 4.6).¹³ Unlike the classical Suzuki-Miyaura coupling reactions, the vinyl boron “ate” complex (**II**) that was prepared *in-situ* from an organoboronate and organolithium, while the oxidative addition Pd(II) complex could activate the alkenyl boron “ate” complex and induced a 1,2-metalate shift to form the Pd(II) intermediate **IV** (Scheme 4.6). The bidentate ligand MandyPhos (SpSp)-**L1** was critical for the reaction success, as its large bite angle promoted reductive elimination and prevented β -H elimination from Pd(II) intermediate **IV**. A wide range of aryl- or alkenyl-triflates were employed as electrophiles in the reaction, since the triflate anion can rapidly dissociate and promote olefin coordination at Pd. This new protocol tolerated a variety of functionalized organotriflates and vinyl boron-ate complexes, and accessed to secondary organoboronates in good yields and excellent enantioselectivities. In this case, both aryl and alkyl groups could successfully migrate from boron to the adjunct sp^2 carbon. Noteworthy, the vinyl boron “ate” complex was easily prepared from organolithium and vinylB(neo) or organoboronates and vinyl lithium. Demonstrating the synthetic potential of this conjunctive cross-coupling, the natural product (–)-combretastatin could also be prepared in good yield.



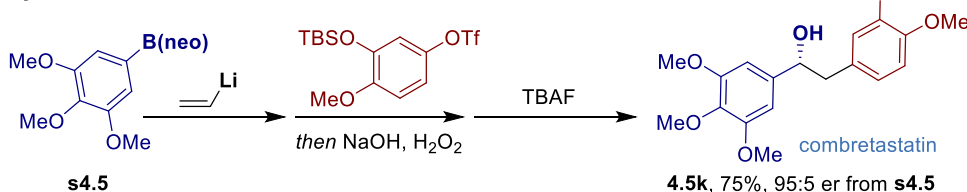
Scope of vinyl boronic esters



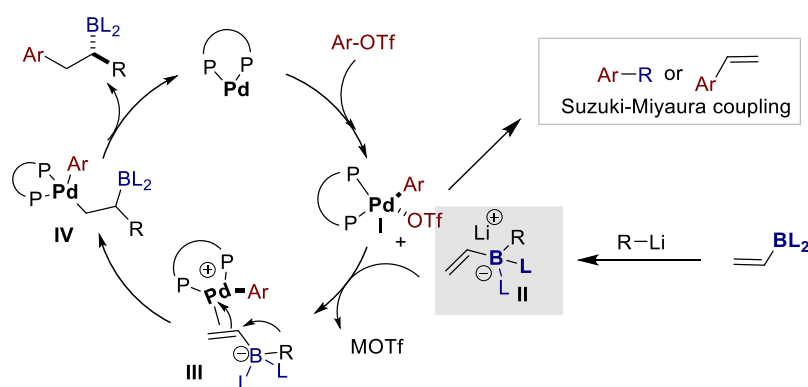
Scope of vinyl lithium



Synthesis of combretastatin



Scheme 4.5. Pd-catalyzed enantioenriched conjunctive coupling

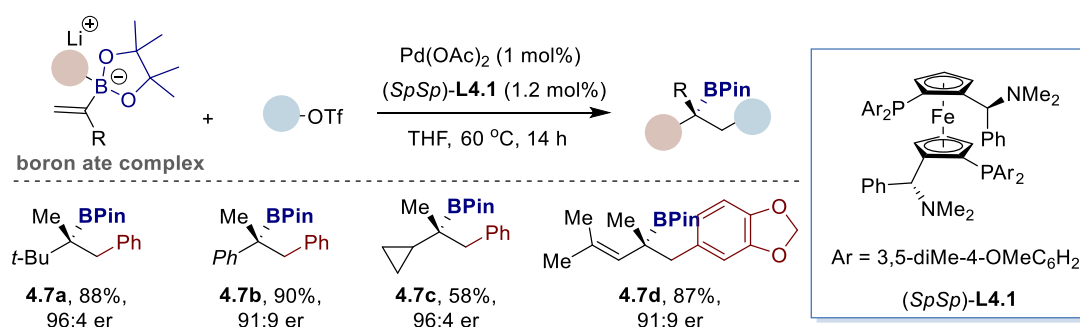


Scheme 4.6. Mechanism proposal of Pd-catalyzed conjunctive coupling

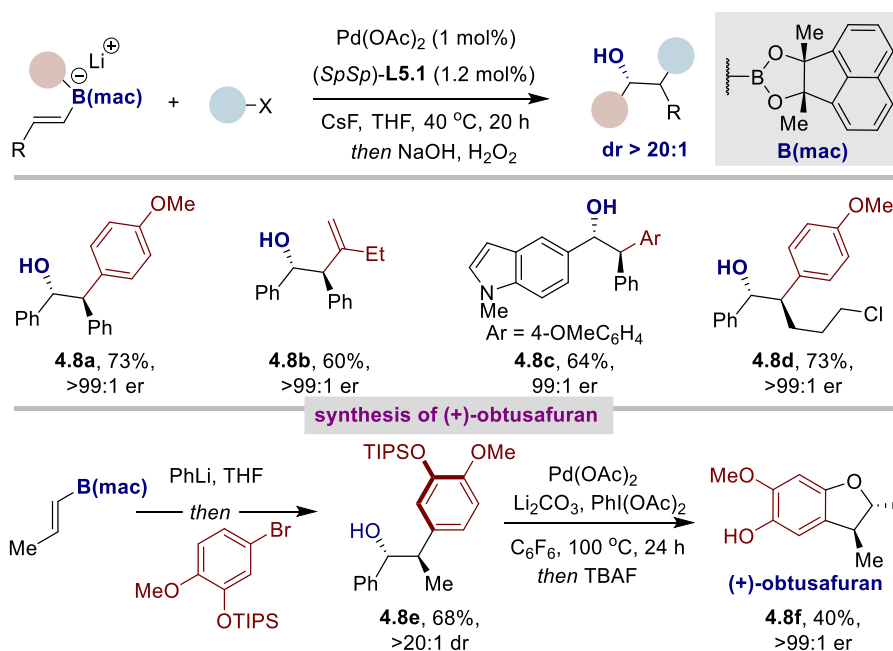
Later on, the Morcken group extended the scope of the Pd-catalyzed conjunctive coupling strategy to α -substituted vinyl boron “ate” complexes (Scheme 4.7).¹⁴ In this case, a range of densely functionalized highly hindered tertiary boronic esters could be formed in good yield and high enantioselectivity. Not only α -substituted vinyl boronates can be employed in the Pd-catalyzed conjunctive coupling, the utilization of

Chapter 4.

β -substituted vinyl boronates as substrates have been developed by the same group. In 2018, they reported a Pd-catalyzed diastereo- and enantioselective conjunctive coupling with β -substituted vinyl boronates (Scheme 4.8).¹⁵ The reaction showed broad substrate scope and high functional group tolerance, providing the desired product in high diastereoselectivity (>20:1 dr) and enantioselectivity (generally above 98:2). Notably, the synthetic utility was illustrated by the synthesis of (+)-obtusafuran which has *anti*-carcinogenic activity. This process employs an encumbered diolato ligand (termed “mac”) to control the reaction of vinyl boron “ate” complexes, thus avoiding the competing Suzuki-Miyaura reaction and favoring a 1,2-metalate shift-based pathway.



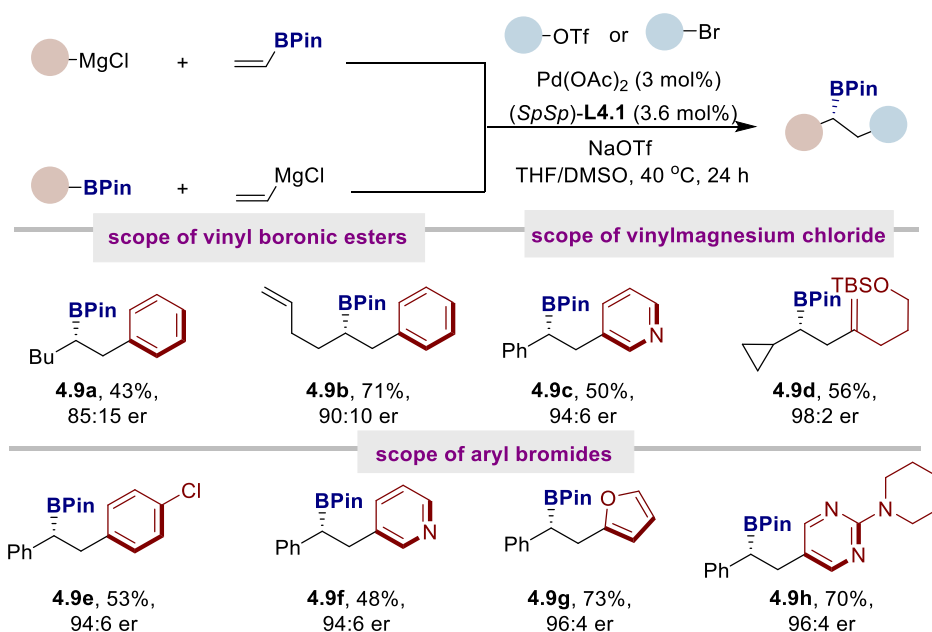
Scheme 4.7. Enantioselective construction of tertiary boronates



Scheme 4.8. Catalytic conjunctive coupling with β -substituted vinyl boronates

While these reports indicate that the Pd-catalyzed conjunctive coupling is

efficient and highly selective, halide inhibition can be a significant limitation in these reactions due to the halide ion outcompeting the vinyl boron “ate” complex for binding to Pd(II). Therefore, before preparation of boron “ate” complexes, the organolithium reagents need to be recrystallized to remove the halide impurities. In 2017, Morken and co-worker addressed this problem by using Grignard reagents to replace organolithium reagents (Scheme 4.9).¹⁶ The key points to the reaction success were using NaOTf as an additive and a THF/DMSO co-solvent system. The authors proposed that NaOTf could promote boron “ate” complex formation between Grignard reagents and organoboronates, and DMSO could aid in stabilizing the boron-ate complex in the reaction.

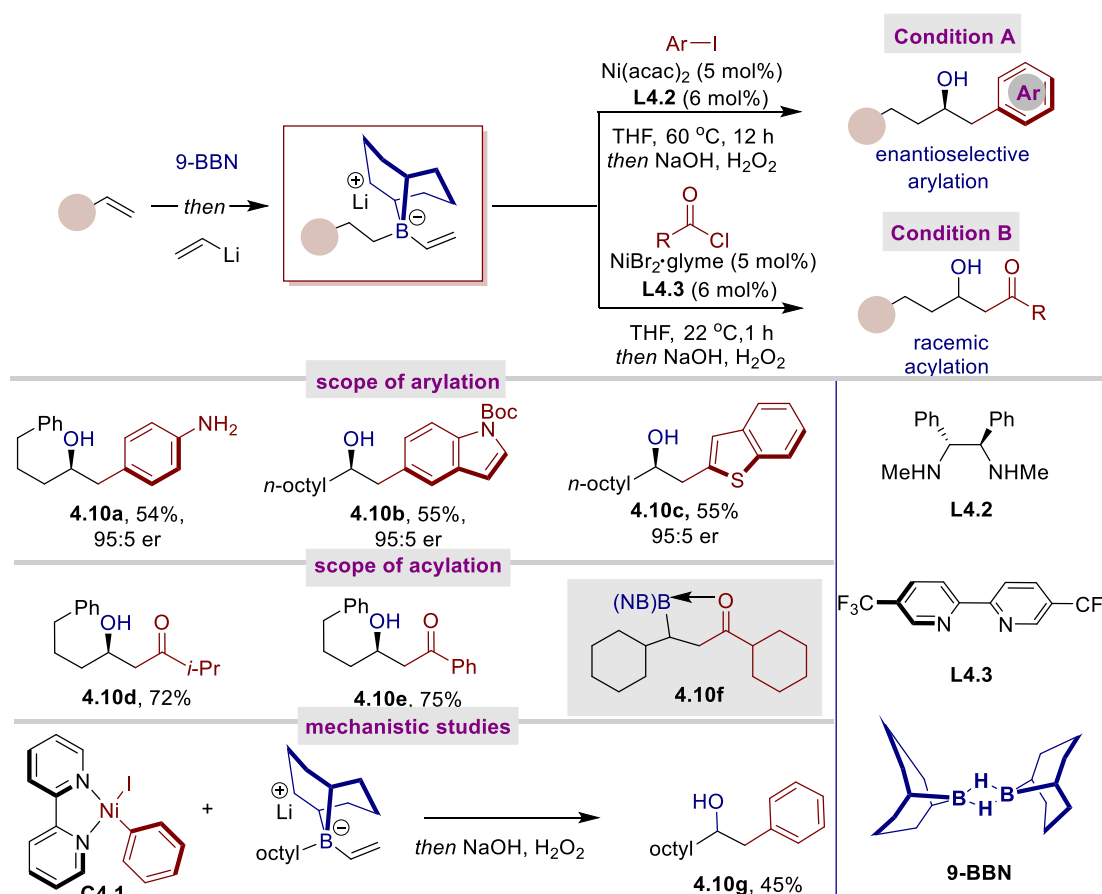


Scheme 4.9. Catalytic conjunctive coupling with Grignard reagents

4.2.3 Ni-Catalyzed Conjunctive Coupling of Vinyl Boron “Ate” Complex

Despite the advances achieved with Pd-catalyzed conjunctive coupling of vinyl boron “ate” complex; the majority of these transformations are restricted to the use of aryl or alkenyl electrophiles. Therefore, it would be particularly attractive to develop a Ni-catalyzed conjunctive coupling with a broad array of electrophilic coupling partners. In 2017, Morken and co-workers reported an enantioselective arylation of

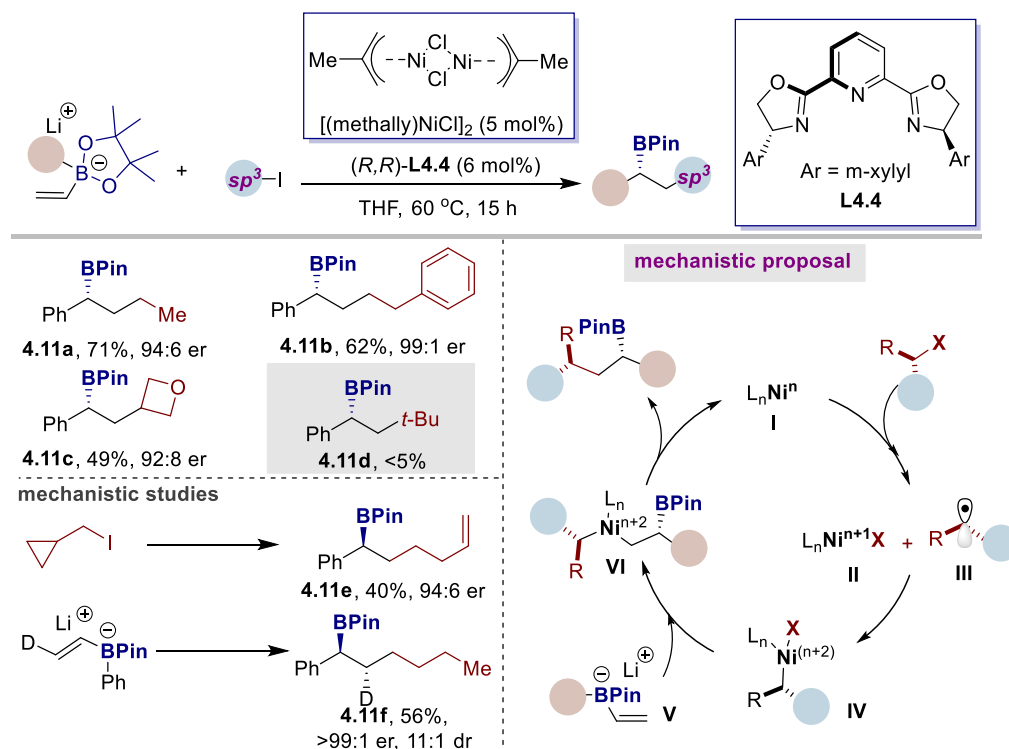
9-BBN derived “ate” complexes with a Ni(acac)₂ and chiral diamine (**L4.2**) ligand system (Scheme 4.10, *condition A*).¹⁷ Unlike previous reports with organoboronic esters, they developed the first conjunctive coupling with more electrophilic trialkyl boranes which were in situ generated by hydroborylation between 9-BBN and alkenes. It should be noted that the Pd/Mandyphos system provided the desired product as racemates, suggesting nickel catalysis was crucial for the reaction success. Stoichiometric experiment with oxidative addition complex between (bpy)Ni(0) and PhI were carried out and obtained the desired product in 45% yield, suggesting that oxidative addition takes place before the 1,2-metallate shift. Preliminary mechanistic experiments also suggested that this process operates by a net Ni(0)/Ni(II) redox cycle, similar to the Pd-based catalyst.



Scheme 4.10. Ni-catalyzed conjunctive coupling with 9-BBN derived “ate” complex

Very recently, the same group extended this strategy to acylation of 9-BBN derived ate complexes with acyl chlorides or anhydrides (Scheme 4.10, *condition B*).¹⁸ In this case, a broad range of β -boryl carbonyl compounds were prepared under the combination of NiBr₂·glyme and **L4.3** system. Interestingly, the ¹¹B NMR and

XRD studies show that the tight coordination between boron and carbonyl oxygen atom of β -trialkyl-(boryl) ketones which could enhance the acidity of carbonyl α -protons.



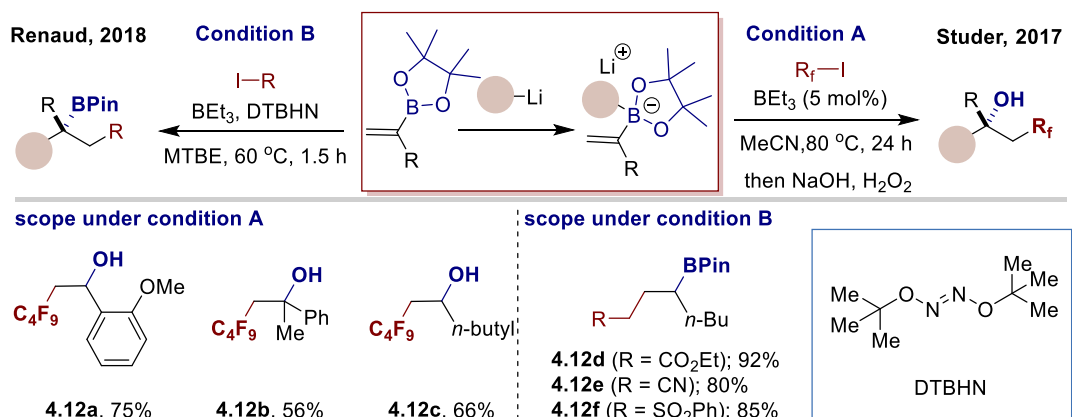
Scheme 4.11. Ni-catalyzed conjunctive coupling with alkyl electrophiles

Previous reports indicated that the Pd- or Ni-catalyzed enantioenriched conjunctive coupling of vinyl boron ate complex could perfectly react with a range of sp^2 carbon electrophiles. However, the utilization of sp^3 carbon electrophile as substrates in conjunctive coupling is still challenging due to the slow oxidative addition and facile β -H elimination. Encouraged by the development of Ni-catalyzed cross couplings, it was considered that the use of Ni catalysis might help avoid parasitic β -H elimination and favour the desired cross-coupling. Indeed, this turned out to be the case, Morcken and co-workers described an enantioenriched Ni-catalyzed conjunctive coupling with a range of unactivated primary and secondary organohalides (Scheme 4.11).¹⁹ This process operates under mild conditions and provides densely functionalized alkyl boronates in good yield and high enantioselectivity. Unfortunately, steric crowded tertiary alkyl iodides were not tolerated under standard conditions. Radical clock and radical capture experiments indicated that an alkyl radical was formed in this process. Based on the outcomes

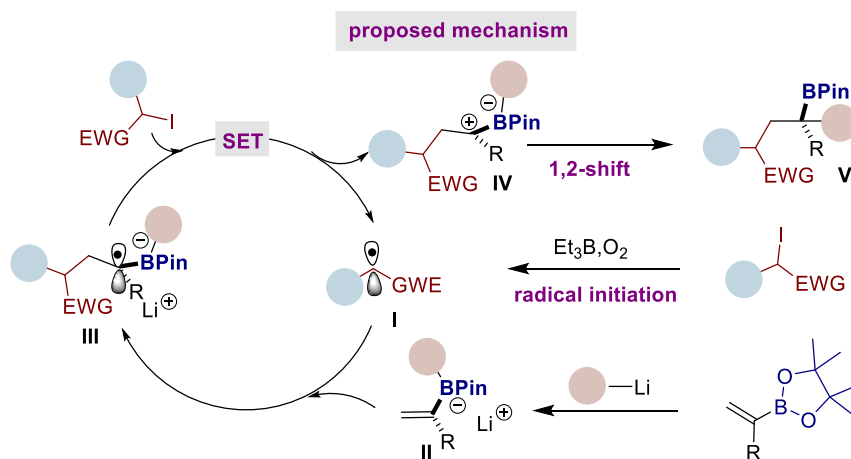
from mechanistic experiments, the authors proposed that alkyl radical **III** was generated via SET by low valent nickel species (**I**), which subsequent recombination of alkyl radical **III** and nickel species **II** to form Ni intermediate **IV**. Finally, intermediate **VI** was formed by the coordination and metal migration, followed by reductive elimination to provide desired product.

4.2.4 Radical Induced Conjunctive Coupling of Vinyl Boron “Ate” Complex

The transition metal catalyzed conjunctive coupling of vinyl boron-ate complexes via a two electron process represents a powerful method to establish new C–C bonds while retaining the boron moiety in the product. Generally speaking, the vinyl boron “ate” complex is activated by an oxidative addition metal complex to induce a 1,2-shift from boron to an adjacent sp^3 or sp^2 carbon atom. In 2017, a complementary technique was developed by Studer and co-workers (Scheme 4.12, *condition A*).²⁰ In this case, a radical generated from activated fluoroalkyl iodides by Et_3B and O_2 , could affect a 1,2-metalate shift of vinyl boron “ate” complexes. This radical-polar crossover process occurred without using a transition metal catalyst, and could couple both α - and β -substituted vinyl boron “ate” complexes with a range of radical precursors such as perfluoroalkyl iodides, α -iodoesters, α -iodonitriles, thus forging C–C bonds to organoboron compounds. A short time later, a similar radical triggered three-component coupling of vinyl boronates, α -halocarbonyl compounds and organolithium reagents was developed by Renaud group (Scheme 4.12, *condition B*).²¹ They found that using 30% di-*tert*-butyl hyponitrite (DTBHN) as an additive at 60 °C increased the yield and reproducibility. In both cases, the electrophilic radical **I** was generated by Et_3B and trace O_2 which initiated the catalytic cycle, and subsequent addition of **I** to electron-rich vinyl boron-ate complex **II** formed the new radical intermediate **III** (Scheme 4.13). Radical intermediate **III** was proposed to react with alkyl iodides via SET oxidation to deliver radical **I** and a short-lived carbocation **IV**, which underwent 1,2-shift to produce product **V**.

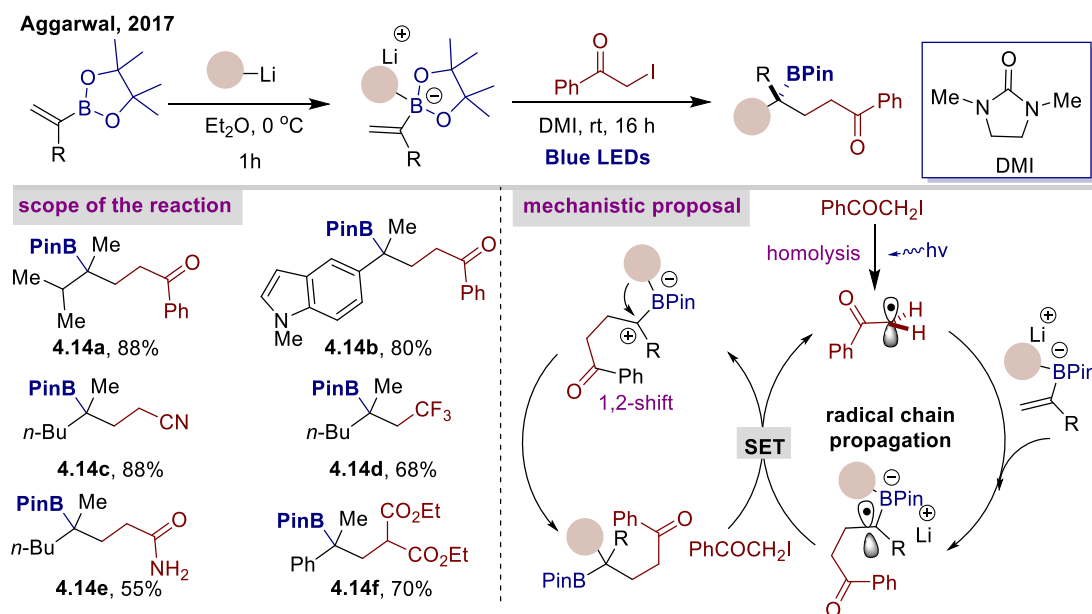


Scheme 4.12. Radical induced three-component coupling using Et_3B initiator



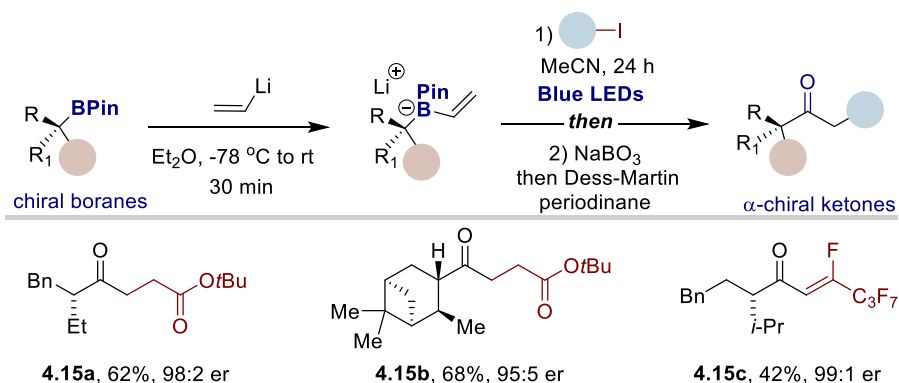
Scheme 4.13. General mechanism for radical induced conjunctive coupling

Concurrently, Aggarwal and co-workers described a photocatalyzed three-component conjunctive coupling of vinyl boronates, organohalides and organolithium reagents (Scheme 4.14).²² Unlike Studer's $\text{Et}_3\text{B}/\text{O}_2$ system, the reaction initiation proceeds under visible light irradiation without a photocatalyst. This protocol was found to tolerate a wide range of electron-deficient alkyl iodides and vinyl boron "ate" complexes. Moreover, less reactive but easily accessible alkyl bromides could be successfully employed in the presence of NaI (20 mol%) or a Ru photosensitizer (1 mol%). A similar radical chain mechanism was proposed by the group, where the reaction was proposed to occur by addition of an electrophilic radical addition to vinyl boronate, followed by SET with another electron-deficient alkyl halide and then triggered a 1,2-metalate shift to deliver the product.



Scheme 4.14. Photocatalyzed conjunctive coupling of vinyl boron “ate” complexes

Recently, the radical induced stereospecific 1,2-metalate shift of chiral boron-ate complexes with alkyl iodides was developed by Studer and co-workers (Scheme 4.15).²³ In this case, various chiral alkyl boronates were employed as substrates for the formation of chiral boron-ate complex with vinyl lithium.

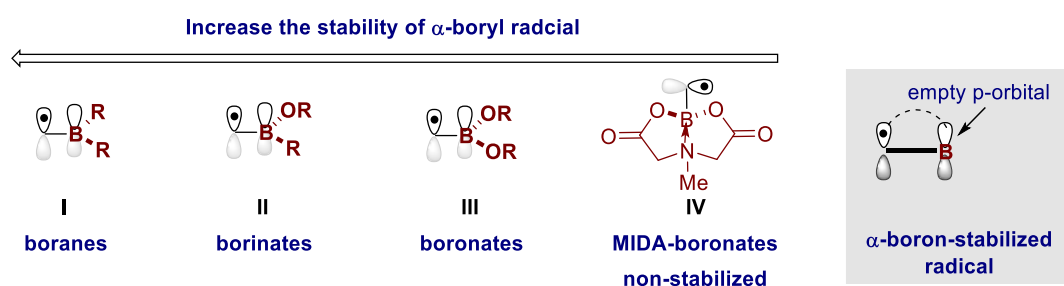


Scheme 4.15. Stereospecific radical induced conjunctive coupling of enantioenriched boron “ate” complex

4.2.5 Catalytic 1,2-Dicarbonylation of Vinyl Boronates

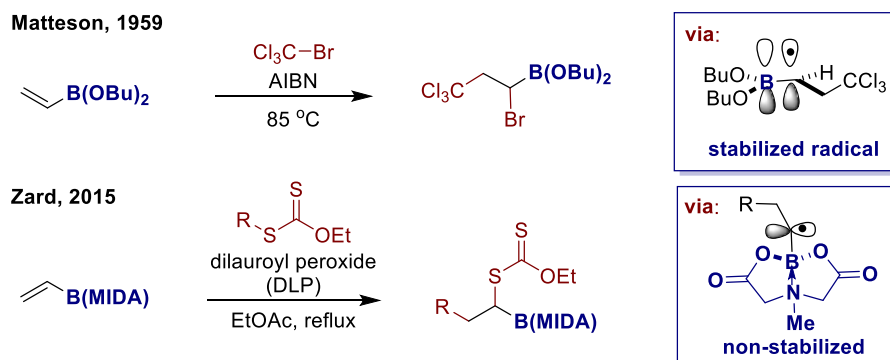
The α -boryl radicals which are generated through radical addition with vinyl boronates are more stabilized than a secondary radical due to the unpaired electron can be delocalized to the empty p-orbital of the adjacent boron atom.²⁴ The stability of

α -boryl radicals are presented in Scheme 4.16.²⁵ For example, the *radical-stabilization-energy* (RSE) of α -boryl radical obtained from Et₃B is 14.5 kcal/mol, a value similar to a benzylic radical (RSE = 14–15 kcal/mol).²⁶ Increasing the number of oxygen substituents on the boron decreases the radical stabilization energy because of the oxygen lone pair donation into the boron p-orbital, resulting in decreased availability of the empty p-orbital of boron for radical stabilization.²⁷ Nevertheless, this is a rather strong stabilization, such as the radical stabilization energy of α -boronate radical is around 6–7 kcal/mol. However, the radical of MIDA-boronate (MIDA: N-methyliminodiacetic acid) is non-stabilized because the p-orbital is filled by the lone electron pair from nitrogen and the boron hybridization changes from sp^2 to sp^3 .²⁴



Scheme 4.16. Stabilization of α -boryl radical

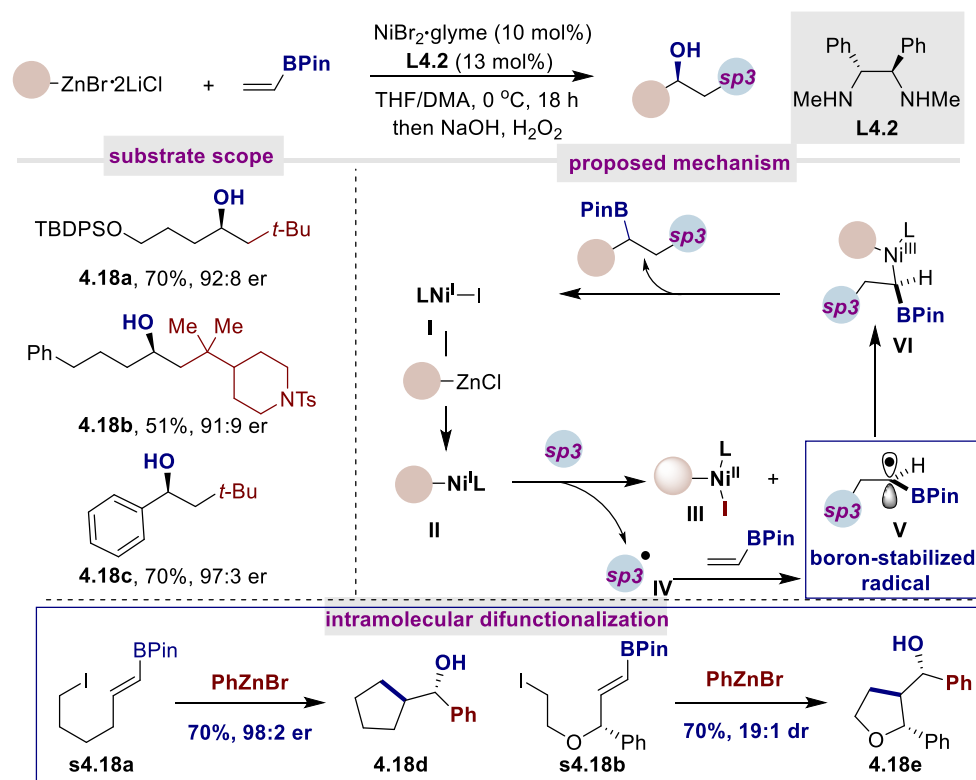
Pioneering studies by Matteson and co-workers provided the first evidence that vinyl boron compounds could undergo radical chemistry through their report of *atom-transfer-radical-addition* (ATRA) of dibutyl ethyleneboronate with BrCCl₃, using azobisisobutyronitrile (AIBN) as radical initiator.²⁸ Notable, this discovery demonstrated that radical intermediates can be stabilized by the C–B π -bonding (Scheme 4.17, *top*). In 2015, the Zard group extended this ATRA type reaction to xanthate transfer addition to vinyl MIDA-boronates by using dilauroyl peroxide (DLP) as a radical initiator (Scheme 4.17, *bottom*).²⁴ The use of vinyl MIDA-boronates in place of vinyl boronates makes the xanthate transfer addition reaction successful. The authors proposed that the use of four coordinated vinyl B(MIDA) instead of vinyl boronate could accelerate the xanthate transfer and radical chain propagation since the α -boryl radical is no longer stabilized.



Scheme 4.17. Atom-transfer-radical-addition (ATRA) reaction with vinyl borons

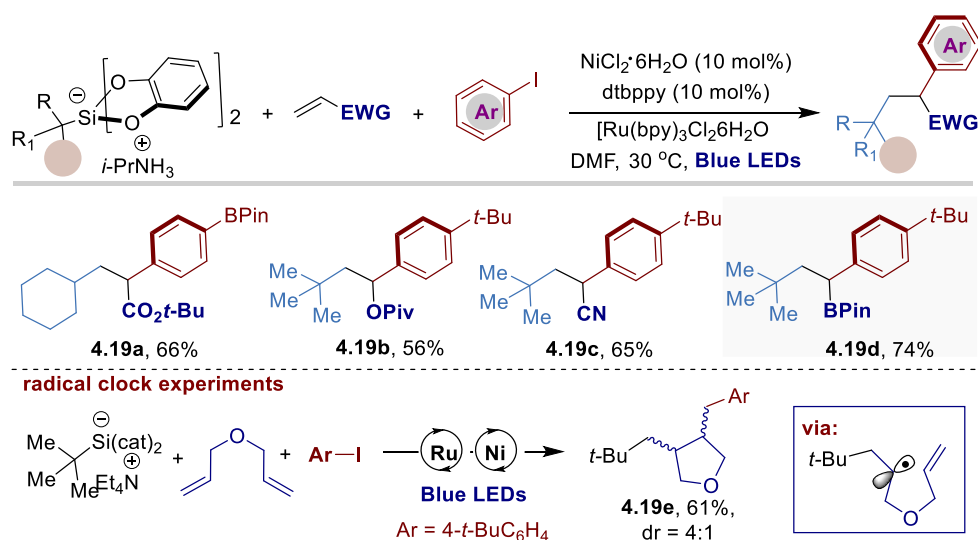
In recent years, remarkable breakthroughs have been made in the construction of organoboron skeletons via 1,2-metalate shift—either through two electron or one electron processes— of a four coordinated boron “ate” complexes.⁷ Despite the great advances realized in the field, several challenges remain to be addressed, especially avoiding the preparation of boron “ate” pre-complexes with air and moisture sensitive organometallic reagents.

In 2019, the Morcken group addressed this shortcoming through an alternate process that involves a catalytic radical addition/cross-coupling cascade pathway (Scheme 4.18).²⁹ They described an enantioselective three-component coupling of vinyl boronates with alkyl iodides and organozinc reagents via a nickel and chiral diamine ligand system, thus allowing to rapidly build up molecular complexity. Unlike previous reports based on the formation of boron “ate” complexes, the success of this three-component coupling depends on the generation of a transient α -boron stabilized radical via nucleophilic alkyl radical addition to vinyl boronate. Noteworthy, a variety of 5- or 6-member ring containing boronates can be obtained via intramolecular radical cyclization/cross-coupling with substrates bearing a tether between the alkyl iodide and vinyl boronate. Mechanistic studies and intramolecular cyclization experiments suggested that the low valent nickel intermediate **II** derived from the organozinc reagent abstracts a halide from the sp^3 electrophile to form nickel species **III** and alkyl radical **IV**, followed by radical addition and recombination with **III** furnished intermediate **VI**, then reductive elimination released dicarbofunctionalized organoboron compounds.



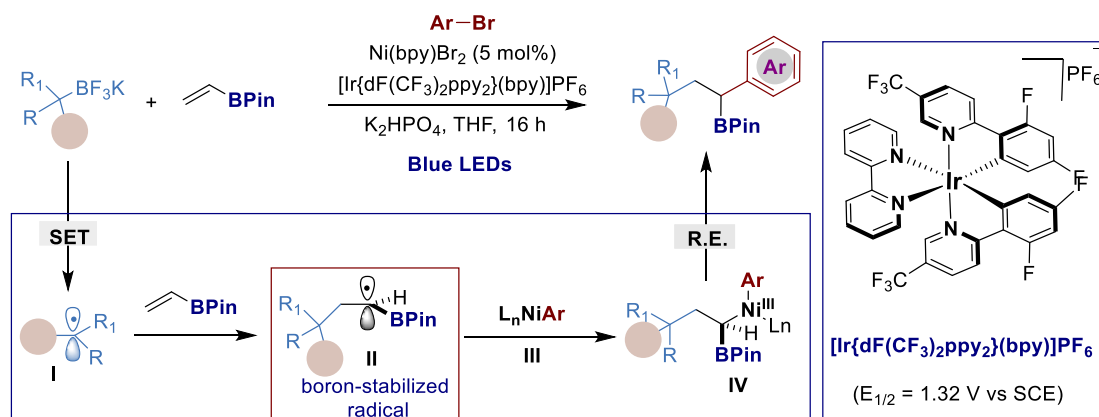
Scheme 4.18. Ni-catalyzed enantioselective coupling of vinyl boronates with alkyl iodides and organozinc reagents

Very recently, Nevado and co-workers described a dicarbonylation of alkenes via photoredox and nickel dual catalysis (Scheme 5.19).³⁰ In this case, the secondary and tertiary alkyl silicates ($E_{\text{ox}} = 0.3\text{--}0.9$ V vs. SCE in DMF) were successfully employed as alkyl radical precursors, which could undergo a SET oxidation with an excited Ru photocatalyst to produce alkyl radicals [$\text{Ru}(\text{bpy})_3\text{Cl}_2 \cdot 6\text{H}_2\text{O}$, $E_{\text{red}} = 0.77$ V vs. SCE in MeCN]. A range of aryl iodides could be employed in the process, with excellent chemo- and regio-selectivity. Notably, the Hiyama-type coupling products between alkyl silicates and aryl iodides could be avoided by using tertiary alkyl silicates, thus allowing produce the dicarbonylation product with activated olefins. It is worthy to point out that vinyl boronates could be selectively coupled with aryl iodides and tertiary alkyl silicates, providing secondary boronates in good yields. Radical clock experiments with diallyl ether provided 5-exo-cyclized product in 61% yield as a 4:1 diastereoisomers, indicating that the alkyl radical addition to olefin was involved in this process.



Scheme 4.19. Catalytic dicarbofunctionalization of alkenes with alkylsilicates and aryl iodides

Soon after, the preparation of alkyl boronates of vinyl boronates with alkyltrifluoroborates and aryl bromides by merging photoredox and nickel catalysis was reported by Molander and co-workers (Scheme 4.20).³¹ This modular and regioselective protocol enables rapid construction of densely functionalized alkyl boron reagents from simple materials, but also allows access to quaternary and tertiary centers. A wide range of alkyl trifluoroborates, vinyl boronic esters as well as aryl bromides containing either electron-withdrawing or electron-donating functional groups were all well tolerated, delivering densely functionalized alkyl boronates in good yield and high selectivity. Interestingly, the bis-borylated product was obtained when employed verbenone derived trifluoroborates as substrates, indicating a radical cascade reaction. Notably, competition experiments between tertiary alkyl boronates and secondary alkyl boronates showed that the dicarbofunctionalization of vinyl boronates is 16 times faster than direct coupling of tertiary alkyl boronates with aryl bromides and 2.5 times faster than secondary alkyl boronates coupling with aryl bromides. Preliminary mechanistic experiments suggest that the alkyl radical **I** was generated from alkyl boronates ($E_{1/2} = 1.26$ V vs SCE) via a SET oxidation by the excited $[\text{Ir}(\text{dF-CF}_3\text{ppy})_2(\text{bpy})]\text{PF}_6$ ($E_{1/2} = 1.32$ V vs SCE), followed by subsequent addition to a vinyl boronate to form a α -boron stabilized radical intermediate **II**. The boron stabilized radical then recombines with Ar–Ni species, followed by reductive elimination to deliver the dicarbofunctionalized product.

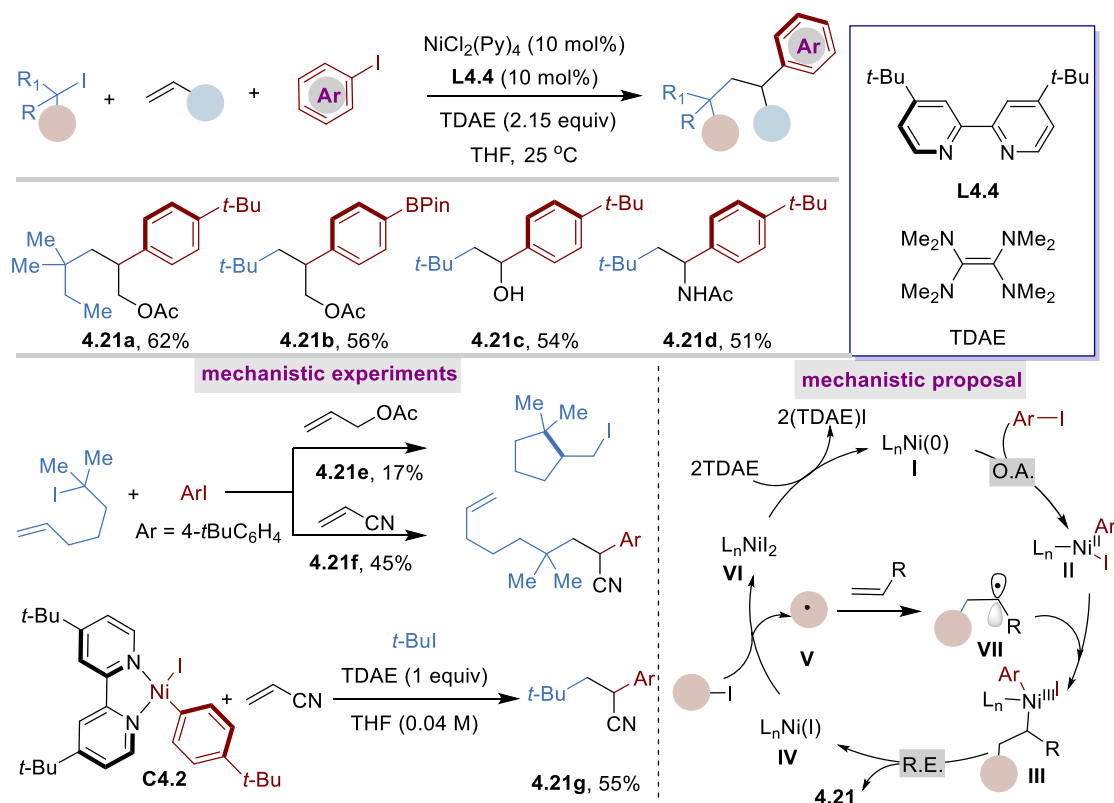


Scheme 4.20. Catalytic dicarbofunctionalization of vinyl boronates with alkyltrifluoroborates and aryl bromides

4.3 Ni-Catalyzed Intermolecular Reductive Difunctionalization of Olefins

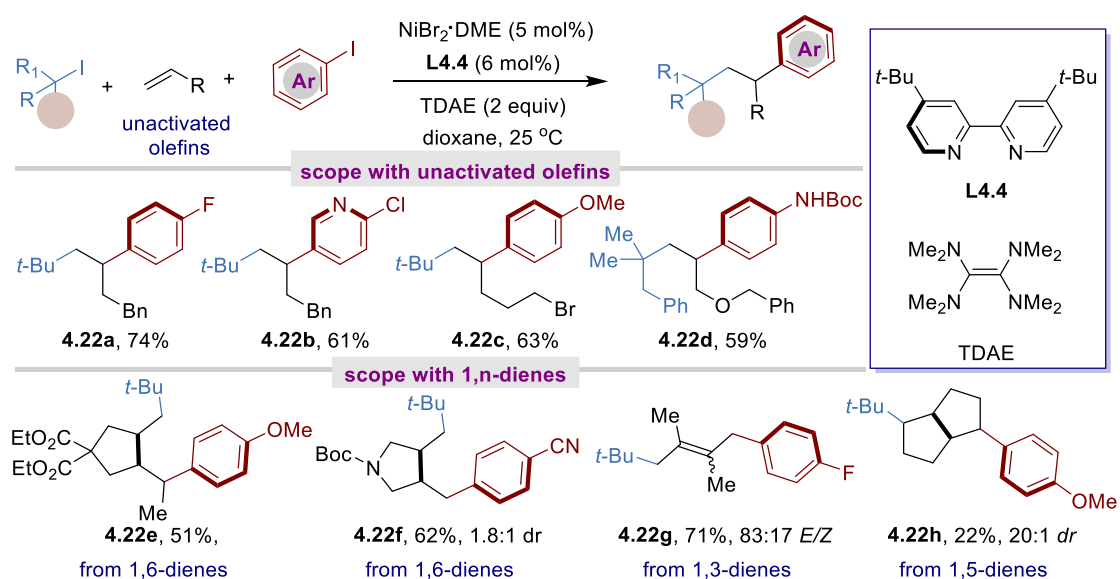
Metal catalyzed dicarbofunctionalization of olefins has attracted substantial interest in organic synthesis, medicinal chemistry and materials science, due to the ability to construct carbon skeletons by assembling two carbon moieties across the C=C bond and forming two new C–C bonds in a one-pot reaction, thus enabling the rapid construction of molecular complexity.⁴ Over the past decade, considerable efforts has been devoted to this area and impressive progress has been achieved. Particularly, the dicarbofunctionalization of olefins with an electrophile and a nucleophile are well defined, which can provide good regioselectivity due to the inherently different reactivities of the electrophile and the nucleophile.³² However, the development of a catalytic intermolecular, reductive dicarbofunctionalization of olefins with two electrophiles remains challenging due to the difficulty in controlling chemo- and regio-selectivity for two electrophiles with similar reactivity. In 2017, Nevado and co-workers reported the first Ni-catalyzed intermolecular, reductive dicarbofunctionalization of olefins with alkyl and aryl iodides (Scheme 4.21).³³ Importantly, the use of TDAE as reductant and the olefin with a coordinating group were crucial for reaction success. Notably, stoichiometric experiment using oxidative addition complex **C4.2** reacted with olefin and *t*-BuI, providing the desired coupling product in 55% yield, thus indicating the competence of ArNi(II) species as potential reaction intermediates in the reaction. Based on the outcomes of mechanistic

experiments, the authors proposed that the reaction was initiated by the reaction of Ni(I) species with alkyl iodide to generate an alkyl radical **V**, which subsequently underwent radical addition to the alkenes to produce the new alkyl radical **VII** (Scheme 4.21, *right bottom*). The ArNi(II) species **II** resulting from oxidative addition of ArI to Ni(0), recombined with **VII** to produce the key intermediate Ni(III) complex **III**. **III** then underwent reductive elimination to deliver the final product and regenerated Ni(I), which was reduced by TDAE to give Ni(0).



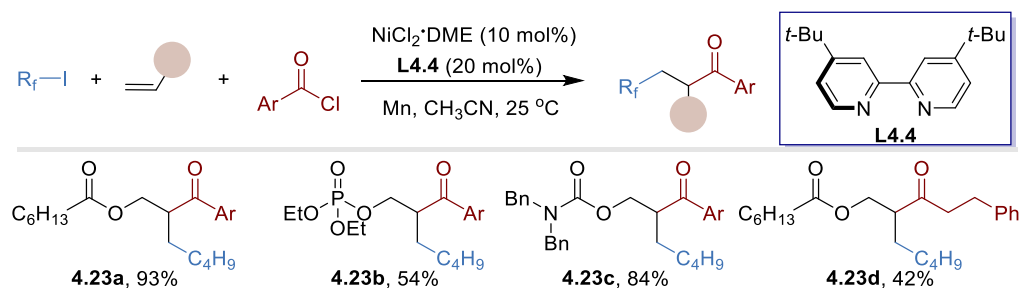
Scheme 4.21. Nickel-catalyzed reductive dicarbofunctionalization of alkenes by using TDAE as reductant

Aiming to extend the scope of this reductive difunctionalization strategy, in 2019, the group of Nevado developed an intermolecular dicarbofunctionalization of unactivated olefins as well as 1,*n*-dienes (Scheme 4.22).³⁴ A variety of unactivated olefins without directing groups were successfully applied in this protocol. Particularly interesting, 5-*exo* cyclization products were obtained when using 1,5- or 1,6-dienes as substrates, and 1,4-difunctionalization product were obtained in high regioselectivity when using 1,3-dienes as substrates. The role of TDAE was also investigated in depth, suggesting that a single electron reduction of Ni(II) species to Ni(I) is thermodynamically favored.



Scheme 4.22. Nickel-catalyzed reductive dicarbofunctionalization of unactivated olefins or 1,n-dienes

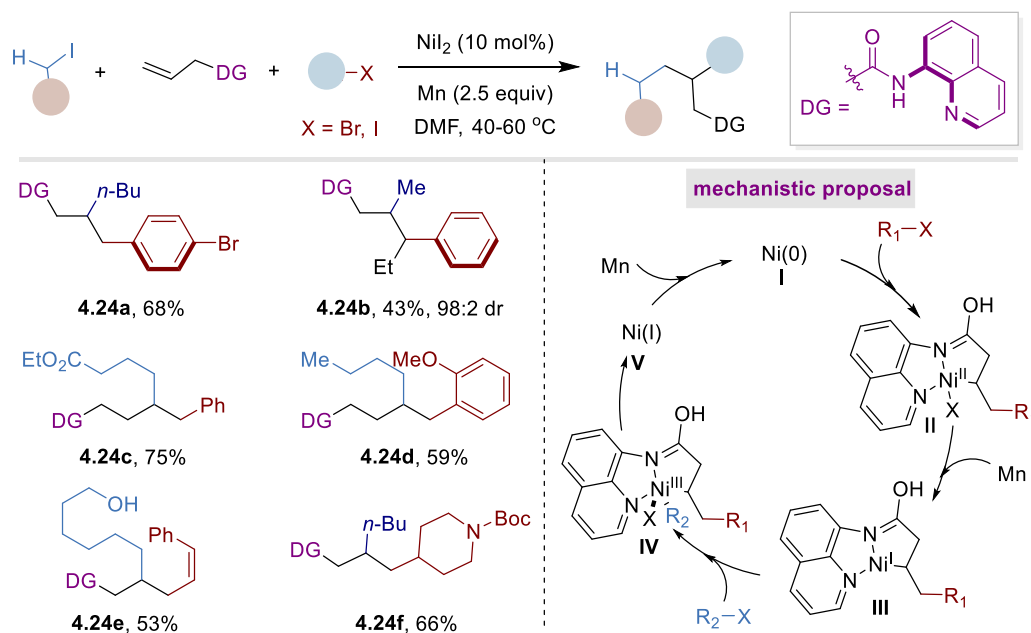
Inspired by the directing group strategies, Chu and co-workers recently developed a Ni-catalyzed intermolecular, three-component reductive carboacylation of alkenes with acyl chlorides and fluoroalkyl iodides using Mn as the reductant (Scheme 4.23).³⁵ The reaction is effective for olefins possessing chelating groups such as esters, carbonates, sulfonates, and phosphates. This protocol enables facile access to β -fluoroalkyl ketones through a regioselective, sequential formation of two C–C bonds in one step under mild conditions. Notably, stoichiometric reaction of oxidative addition complex between acyl chloride and Ni(0) with alkene and $\text{C}_4\text{F}_9\text{I}$ in the presence of Mn, provided the desired coupling product in 42% yield, suggesting that the catalytic pathway via oxidative addition of Ni(0) species with acyl chloride could be operative.



Scheme 4.23. Nickel-catalyzed reductive carboacylation of olefins

Very recently, Koh and co-workers described a nickel-catalyzed reductive dicarbofunctionalization of 8-aminoquinoline-tethered alkenes with a series of

carbon-electrophiles (aryl/alkenyl/alkyl halides) and primary alkyl iodides (Scheme 4.24).³⁶ In contrast to Nevado's work, a reversed regioselectivity was observed in this reaction due to the use of 8-aminoquinoline as the chelating group. The stereospecific carbo-alkylation of internal alkenes suggested that a carbometallation process instead of radical addition pathway may be involved in this reaction.



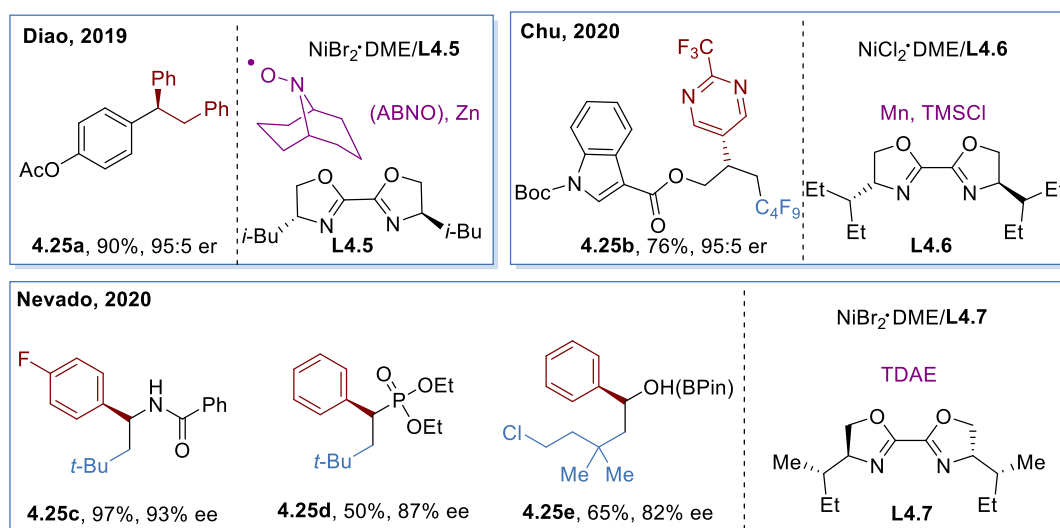
Scheme 4.24. Nickel-catalyzed reductive dicarbofunctionalization of olefins with 8-aminoquinoline-tethered olefins

Despite the significant progress that has been made in catalytic reductive difunctionalization of olefins with electrophiles, the development of enantioselective dicarbofunctionalization remains challenging. In 2019, Diao and co-workers described an asymmetric diarylation reaction of styrenes with aryl bromides using Ni/L4.5 catalyst with Zn as reductants (Scheme 4.25, *top left*).³⁷ The protocol provided a broad range of chiral α, α, β -triarylated ethane scaffolds. Importantly, the presence of a *N*-oxyl radical (ABNO) significantly improved the enantioselectivity. The required 1:1 ratio of Ni/ABNO implied that ABNO may serve as a ligand to nickel, but its exact role remains elusive. Additionally, the reaction is restricted to installing two identical aryl groups across the double bond, and to use vinylarenes as coupling partners.

Very recently, the group of Chu developed an enantioselective 1,2-fluoroalkylation of allyl esters with heteroaryl halides and perfluoroalkyl iodides

(Scheme 4.25, *top right*).³⁸ The use of NiCl₂·DME, a chiral BiOx ligands (**L4.6**) and indole 3-carboxylate ester derived allyl esters were crucial for achieving high yields and enantioselectivity. Preliminary mechanistic studies suggested that the reaction is likely initiated by the addition of the perfluoroalkyl radical to the allyl ester, followed by cross-coupling with the aryl halide.

Concurrently, Nevado and co-workers described an enantioselective reductive 1,2-alkylarylation of olefins with alkyl iodides and aryl halides via a Ni-catalyzed radical relay strategy (Scheme 4.25, *bottom*).³⁹ The reaction proceeds at room temperature in the presence of an organic reductant (TDAE). An alkyl Ni(III) intermediate ligated with (L)-isoleucine derived BiOx (**L4.7**) is proposed based on DFT calculations. This intermediate is stabilized by the coordination of amides or other coordinating groups on the alkene, which contribute to defining the stereochemical outcome.

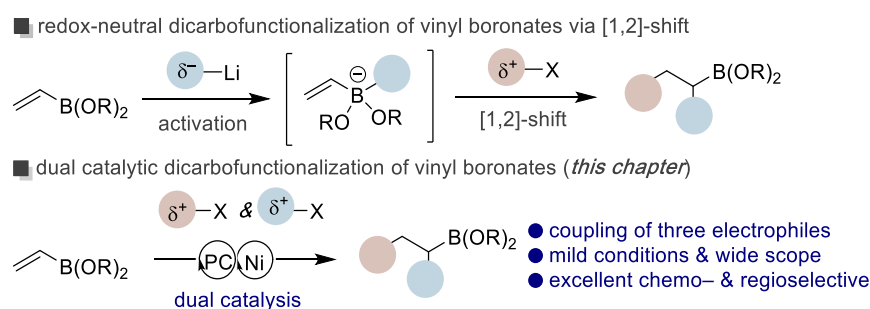


Scheme 4.25. Nickel-catalyzed asymmetric reductive dicarbofunctionalization of olefins

4.4 General Aim of the Project

Recent elegant disclosures have shown the viability of accessing organoboranes via boron “ate” complexes – generated from stoichiometric organolithium reagents –, inducing a 1,2-shift that forges two C–C bonds via one- or two-electron events (Scheme 4.26, *top*).^{7,9} Despite the advances realized, several challenges remain to be addressed. Among these, a complementary method for triggering a catalytic 1,2-dicarbonylation with simple electrophilic partners that obviates the need for stoichiometric organometallics while enabling a rapid, reliable and modular access to organoboron skeletons would constitute a worthwhile endeavour for chemical invention.

Motivated by our group achievements in cross-electrophile-coupling reactions⁴⁰ and site-selective functionalization of olefins,⁴¹ we wondered whether we could design a catalytic blueprint that would allow the incorporation of two different electrophilic partners into readily accessible vinyl boronates in a 1,2-fashion with total control of the regioselectivity pattern (4.26, *bottom*). If successful, we anticipated that this multicomponent reaction with an exquisite control of the site-selectivity would not only expand the range of technologies to access alkyl organoboron reagents, but also open up new strategic approaches in the realm of cross-electrophile coupling events.



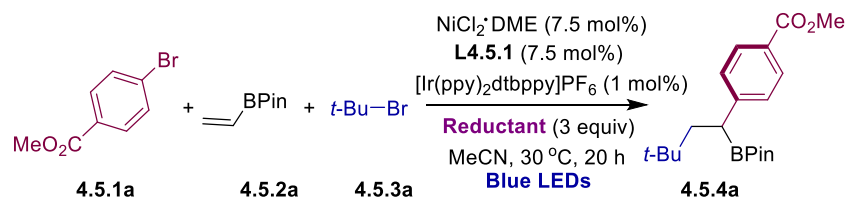
Scheme 4.26. Site-selective 1,2-dicarbonylation of vinyl boronates through dual catalysis

4.5 Site-Selective 1,2-Dicarbofunctionalization of Vinyl Boronates through Dual Catalysis

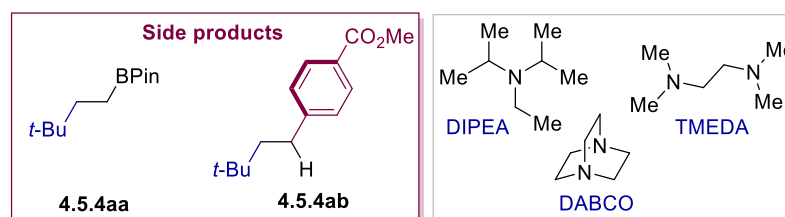
4.5.1 Optimization of Reaction Conditions

We began our investigation using methyl 4-bromobenzoate (**4.5.1a**) and 2-bromo-2-methylpropane (**4.5.2a**) as model substrates, reacting with vinyl boronate (**4.5.2a**). We first applied a Ni/bipy system, with [Ir(ppy)₂dtbpy]PF₆ as photocatalyst and triethylamine (TEA) as electron donor in MeCN under blue light-emitting diodes (LEDs) irradiation.⁴² Under these conditions, 1,2-alkylarylation product (**4.5.4a**) was obtained in 19% yield, together with Giese-type (**4.5.4aa**) and deborylative (**4.5.4ab**) side products (Table 4.1, entry 1).⁴³ We anticipated that electron donors may play a crucial role in our 1,2-dicarbofunctionalization reaction due to the nucleophilic alkyl radical might be generated upon a SET reduction from an electron donor.⁴⁴

As anticipated, 1,2-dicarbofunctionalization products were found when using trialkyl amine as the electron donor under irradiation (Table 4.1, entries 1-6). *N,N,N',N'*-tetramethylethylenediamine (TMEDA) provided the best results, however, the cyclic alkyl amine such as DABCO, completely shut down the reaction. Additionally, we found that the loading of electron donor also affected the reaction, and 3 equivalents of TMEDA provided desired product in 62% yield. More side products were obtained when increasing and reducing the loading of electron donor. Importantly, in all the cases, we only obtained the product in a single regioisomer, with arylation at the α -boron position.



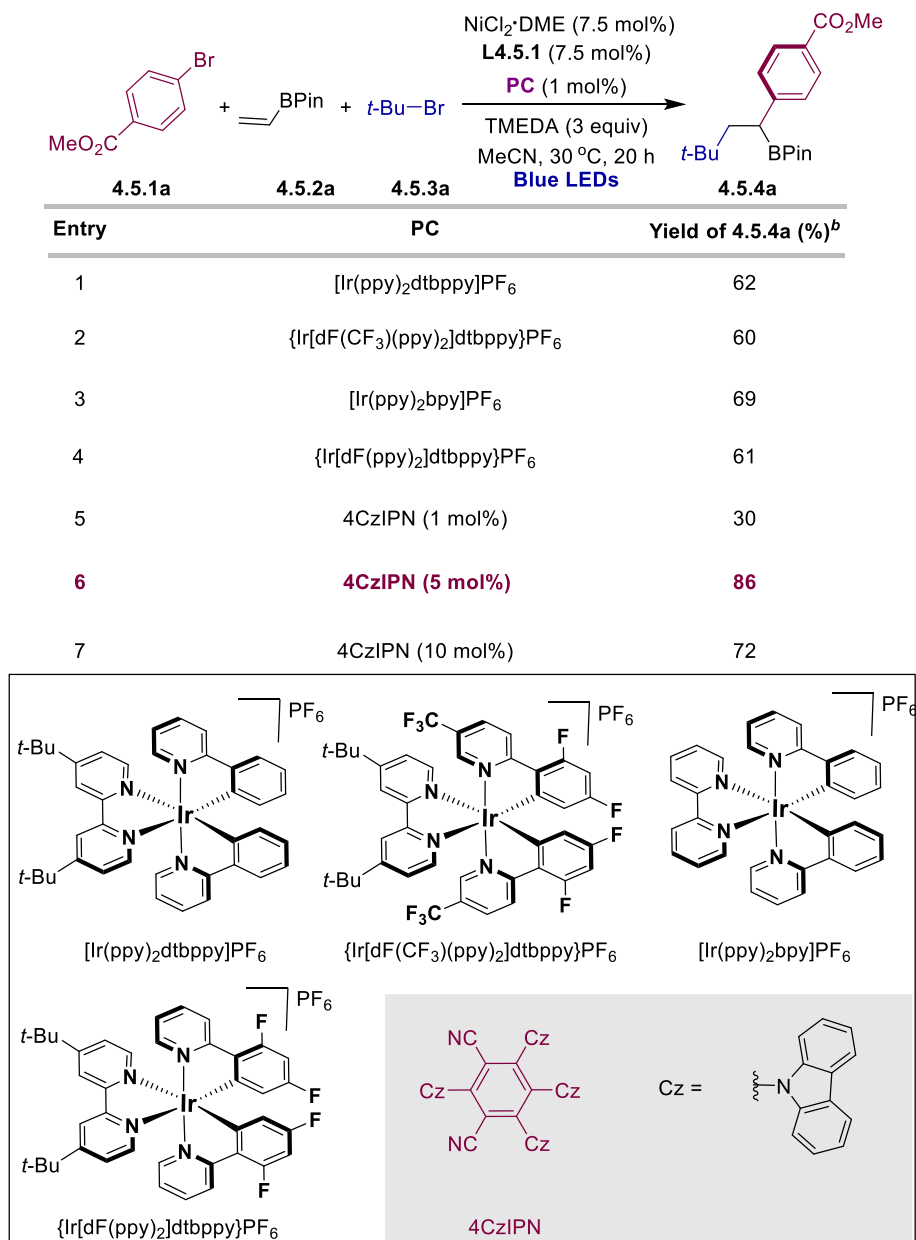
Entry	Reductant	Yield of 4.5.4a (%) ^b
1	Et ₃ N	19
2	DIPEA	7
3	TMEDA	62(46^c)
4	Cy ₂ NMe	27
5	<i>i</i> Pr ₂ NMe	20
6	<i>i</i> PrNMe ₂	10
7	DABCO	0
8		0



^a **Reaction Conditions:** 4.5.1a (0.4 mmol, 2.0 equiv), 4.5.2a (0.20 mmol, 1.0 equiv), 4.5.3a (0.50 mmol, 2.5 equiv), NiCl₂·DME (3.3 mg, 7.5 mol%), L4.5.1 (2.3 mg, 7.5 mol%), [Ir(ppy)₂bpy]PF₆ (1 mol%), Reductant (0.60 mmol, 3.0 equiv), MeCN (3.0 mL) at 30 °C under irradiation of blue LEDs with a fan for 20 hours. ^b ¹H NMR yields were determined by using CH₂Br₂ as internal standard. ^c TMEDA (0.3 mmol). TMEDA = *N,N,N',N'*-tetramethylethylenediamine. BPin = bis(pinacolato)diboron.

Table 4.1 Screening of reductant

Next, we evaluated the effect of photocatalyst in our 1,2-difunctionalization, with Ir-catalysts, providing around 60% yields (Table 4.2, entries 1-5). 30% yield was obtained when using inexpensive organic photocatalyst (4CzIPN, 1 mol%) instead of Ir-catalyst.⁴⁵ To our delight, 86% yield was obtained when increasing the loading to 5 mol%. Under these conditions, only trace amount of the Giese-type and deborylative side products were detected in the crude reaction mixtures. More side products were observed when further increasing the loading to 10 mol%.

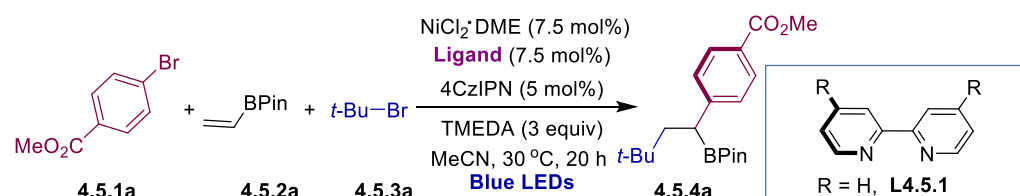


^a **Reaction Conditions:** 4.5.1a (0.4 mmol, 2.0 equiv), 4.5.2a (0.20 mmol, 1.0 equiv), 4.5.3a (0.50 mmol, 2.5 equiv), NiCl₂·DME (3.3 mg, 7.5 mol%), L4.5.1 (2.3 mg, 7.5 mol%), PC (1 mol%), TMEDA (90 μ L, 0.60 mmol, 3.0 equiv), MeCN (3.0 mL) at 30 °C under irradiation of blue LEDs with a fan for 20 hours. ^b ¹H NMR yields were determined by using CH₂Br₂ as internal standard. TMEDA = *N,N,N',N'*-tetramethylethylenediamine. BPin = bis(pinacolato)diboron.

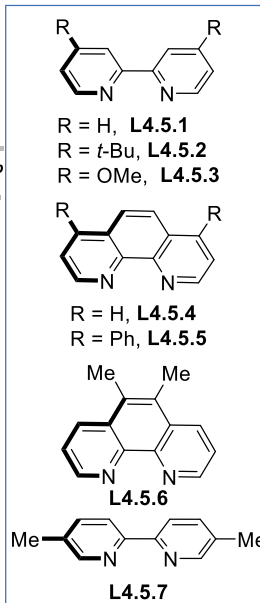
Table 4.2 Screening of photocatalysts

With these results in hand, we then studied the effect of ligands on the reaction outcome (Table 4.3). In contrast to the known literature data on cross-electrophile coupling reactions,⁴⁰ the substitution pattern at the ligand backbone did not play a

significant role on reactivity or regioselectivity. Bipyridine ligand **L4.5.1** provided the best results (entry 1). Moreover, the phenanthroline-type ligands gave slightly lower yields compared to the bipyridine-type ligands (entries 4-6).



Entry	Solvents	Yield of 4.5.4a (%) ^b
1	L4.5.1	86
2	L4.5.2	76
3	L4.5.3	40
4	L4.5.4	71
5	L4.5.5	70
6	L4.5.6	65
7	L4.5.7	56

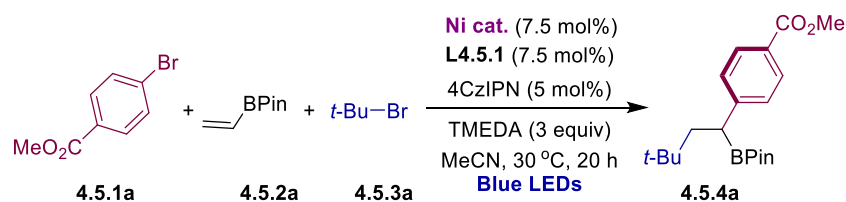


R = H, **L4.5.1**
R = *t*-Bu, **L4.5.2**
R = OMe, **L4.5.3**
R = H, **L4.5.4**
R = Ph, **L4.5.5**
L4.5.6
L4.5.7

^a **Reaction Conditions:** **4.5.1a** (0.4 mmol, 2.0 equiv), **4.5.2a** (0.20 mmol, 1.0 equiv), **4.5.3a** (0.50 mmol, 2.5 equiv), NiCl₂·DME (3.3 mg, 7.5 mol%), **Ligand** (7.5 mol%), 4CzIPN (7.9 mg, 5 mol%), TMEDA (90 μ L, 0.60 mmol, 3.0 equiv), MeCN (3.0 mL) at 30 °C under irradiation of blue LEDs with a fan for 20 hours. ^b ¹H NMR yields were determined by using CH₂Br₂ as internal standard. TMEDA = *N,N,N',N'*-tetramethylethylenediamine. BPin = bis(pinacolato)diboron.

Table 4.3 Screening of ligands

Next, we focused our attention on studying the effect of nickel precatalysts (Table 4.4). A significant erosion in yield was observed when using NiCl₂ or NiBr₂ as the nickel source, while comparable yields were observed with Ni(COD)₂. Other Ni(II) sources also gave slightly lower yields, with more side products. With this robust Ni/**L4.5.1** system in hand, we next examined the effect of the loading of nickel and ligand (entry 3). The screening showed that 7.5 mol% loading for both nickel and ligand were the best; although increasing the loading to 10 mol% also gave good yield.



Entry	Ni cat.	Yield of 4.5.4a (%) ^b
1	NiCl ₂	35
2	NiBr ₂	28
3	NiCl₂·DME	86(32^c, 80^d, 74^e)
4	NiBr ₂ ·DME	70
5	NiBr ₂ ·diglyme	70
6	NiCl ₂ ·6H ₂ O	55
7	Ni(COD) ₂	81

^a **Reaction Conditions:** **4.5.1a** (0.4 mmol, 2.0 equiv), **4.5.2a** (0.20 mmol, 1.0 equiv), **4.5.3a** (0.50 mmol, 2.5 equiv), Ni cat. (7.5 mol%), **L5.5.1** (2.3 mg, 7.5 mol%), 4CzIPN (7.9 mg, 5 mol%), TMEDA (90 μ L, 0.60 mmol, 3.0 equiv), MeCN (3.0 mL) at 30 °C under irradiation of blue LEDs with a fan for 20 hours. ^b ¹H NMR yields were determined by using CH₂Br₂ as internal standard. ^c NiCl₂·DME (5 mol%). ^d NiCl₂·DME (10 mol%). ^e NiCl₂·DME (7.5 mol%), **L4.5.1** (10 mol%). TMEDA = *N,N,N',N'*-tetramethylethylenediamine. BPin = bis(pinacolato)diboron.

Table 4.4 Screening of nickel precatalysts

The effect of solvents was also studied (Table 4.5). Acetonitrile (MeCN) provided the best result; other nitriles had a deleterious effect on reactivity (entries 1-3). Etheral and amide-containing solvents markedly influenced the reactivity profile. Moreover, the concentration of the reaction was also studied (entry 3). The results show that the current concentration of 0.07 M was still optimal, slightly lower yield was obtained when decreasing the concentration to 0.05 M, and a significant drop in yield was observed when the concentration was increased to 0.10 M.

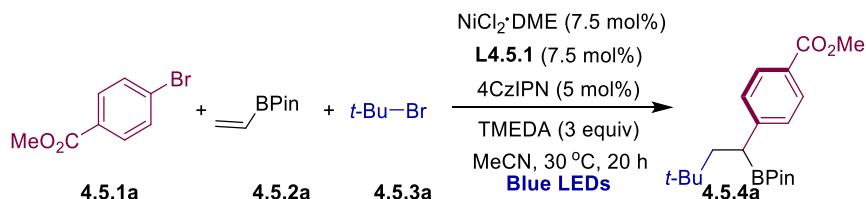
Entry	Solvents	Yield of 4.5.4a (%) ^b
1	MeCN	86(66) ^c (76) ^d
2		45
3		30
4	DME	56
5	Anisole	21
6	Dioxane	7
7	THF	0
8	DMA	0
9	NMP	0

^a **Reaction Conditions:** 4.5.1a (0.4 mmol, 2.0 equiv), 4.5.2a (0.20 mmol, 1.0 equiv), 4.5.3a (0.50 mmol, 2.5 equiv), NiCl₂·DME (3.3 mg, 7.5 mol%), L4.5.1 (2.3 mg, 7.5 mol%), 4CzIPN (7.9 mg, 5 mol%), TMEDA (90 μ L, 0.60 mmol, 3.0 equiv), Solvents (3.0 mL) at 30 °C under irradiation of blue LEDs with a fan for 20 hours. ^b ¹H NMR yields were determined by using CH₂Br₂ as internal standard. ^c MeCN (2.0 mL). ^d MeCN (4.0 mL). TMEDA = *N,N,N',N'*-tetramethylethylenediamine. BPin = bis(pinacolato)diboron.

Table 4.5 Screening of solvents

With the optimal results in hand, the effect of light sources was then evaluated (Table 4.6). Three different light sources were studied, the standard blue LED strips, Kessil lamps and homemade LED plates (from ICIQ workshop). As shown more powerful 2x Kessil Lamps (with fans) gave a slightly lower yield of the desired product. Notably, temperature played an important role for the reaction success, hence a cooling fan was required to keep the temperature around 30 °C.

Finally, we carried out the corresponding control experiments in order to show that all reaction parameters were critical for reaction success (Table 4.7). As shown, no reactivity was observed when the reaction was carried out in the absence of nickel, ligand, photocatalyst, electron donor or light irradiation.



Entry	light source	Yield of 4.5.4a (%) ^b
1	LED strips with fan cooling	86
2	LED strips without fan cooling	35
3	2xkessil lamps with fan cooling	61
4	homemade LED plate with fan or chiller	30

^a **Reaction Conditions:** **4.5.1a** (0.4 mmol, 2.0 equiv), **4.5.2a** (0.20 mmol, 1.0 equiv), **4.5.3a** (0.50 mmol, 2.5 equiv), $\text{NiCl}_2 \cdot \text{DME}$ (3.3 mg, 7.5 mol%), **L4.5.1** (2.3 mg, 7.5 mol%), 4CzIPN (7.9 mg, 5 mol%), TMEDA (90 μL , 0.60 mmol, 3.0 equiv), MeCN (3.0 mL) at 30 °C under irradiation of blue LEDs with a fan for 20 hours. ^b ¹H NMR yields were determined by using CH_2Br_2 as internal standard. TMEDA = *N,N,N',N'*-tetramethylethylenediamine. BPin = bis(pinacolato)diboron.

Table 4.6 Screening of light source

Reaction scheme for Table 4.6 showing the site-selective 1,2-dicarbofunctionalization of vinyl boronate **4.5.1a** with **4.5.2a** and **4.5.3a** to form product **4.5.4a**. Conditions: $\text{NiCl}_2 \cdot \text{DME}$ (7.5 mol%), **L4.5.1** (7.5 mol%), 4CzIPN (5 mol%), TMEDA (3 equiv), MeCN, 30 °C, 20h, Blue LEDs.

Entry	$\text{NiCl}_2 \cdot \text{DME}$	L4.5.1	4CzIPN	TMEDA	light	Yield(%) ^b
1	✓	✓	✓	✓	✓	86(73 ^c)
2	✗	✓	✓	✓	✓	0
3	✓	✗	✓	✓	✓	0
4	✓	✓	✗	✓	✓	0
5	✓	✓	✓	✗	✓	0
6	✓	✓	✓	✓	✗	0

^a **Reaction Conditions:** **4.5.1a** (0.4 mmol, 2.0 equiv), **4.5.2a** (0.20 mmol, 1.0 equiv), **4.5.3a** (0.50 mmol, 2.5 equiv), $\text{NiCl}_2 \cdot \text{DME}$ (3.3 mg, 7.5 mol%), **L4.5.1** (2.3 mg, 7.5 mol%), 4CzIPN (7.9 mg, 5 mol%), TMEDA (90 μL , 0.60 mmol, 3.0 equiv), MeCN (3.0 mL) at 30 °C under irradiation of blue LEDs with a fan for 20 hours. ^b ¹H NMR yields were determined by using CH_2Br_2 as internal standard.

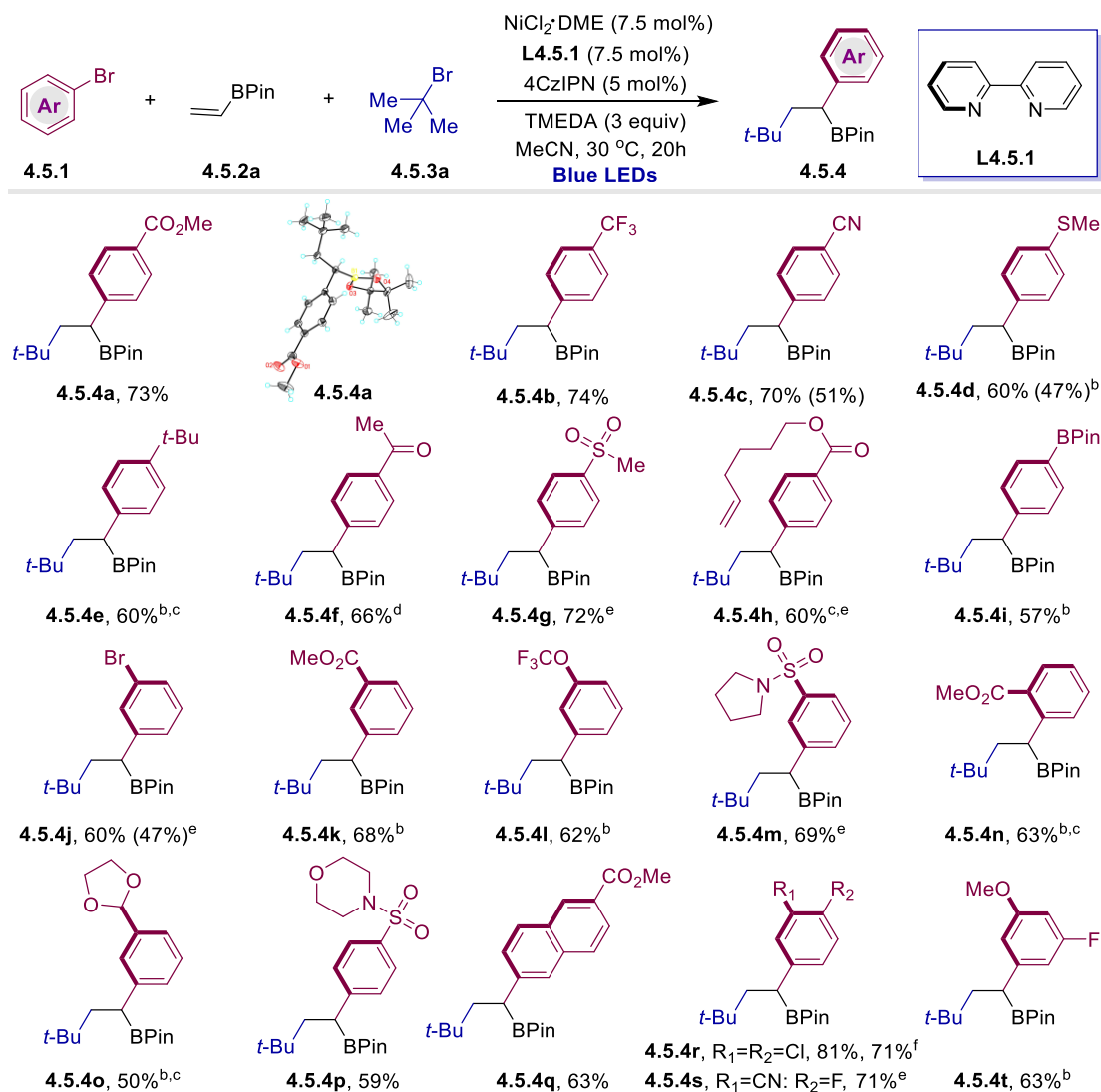
^c Isolated yield. TMEDA = *N,N,N',N'*-tetramethylethylenediamine. BPin = bis(pinacolato)diboron.

Table 4.6 Control experiments

4.5.2 Preparative Substrate Scope

4.5.2.1 Scope of Aryl Bromides

With a set of aryl bromides in hand, we tested their performance under the optimized reaction conditions. As shown in Scheme 4.27, the scope of aryl halides turned out to be rather wide regardless of the electronic and steric parameters of the substituents on the arene partner. Note, however, that the addition of LiCl was required in some cases to reach high conversion to products.⁴⁶ A series of functional groups such as esters (**4.5.4a**, **4.5.4h**, **4.5.4k**, **4.5.4n**, **4.5.4q**), nitriles (**4.5.4c**, **4.5.4s**), sulfonamides (**4.5.4m**, **4.5.4p**), sulfones (**4.5.4g**), acetals (**4.5.4o**) and ketones (**4.5.4f**) were all well tolerated, thus illustrating the chemoselectivity profile of our reaction. It is worth mentioning that no reaction occurred at unactivated olefin site when the substrate possessing an external unactivated olefin (**4.5.4h**).³⁴ More interestingly, aryl boronic esters (**4.5.4i**) and aryl halides (**4.5.4j**, **4.5.4r**, **4.5.4s**, **4.5.4t**) were well tolerated, thus leaving ample room for further derivatization via classical redox-neutral cross-coupling reactions.⁴⁷ Notably, this reaction can be executed on a gram scale, affording **4.5.4r** without significant erosion in yield. Related to this work, a 1,2-dicarbofunctionalizations of vinyl boronates using dual catalysis was also reported concurrently by Aggarwal and co-workers.⁴⁸ Inspired by our work, very recently, Fu and co-workers developed a Ni-catalyzed 1,2-dialkylation of vinyl boronates with two alkyl halides using Mn as reductant.⁴⁹

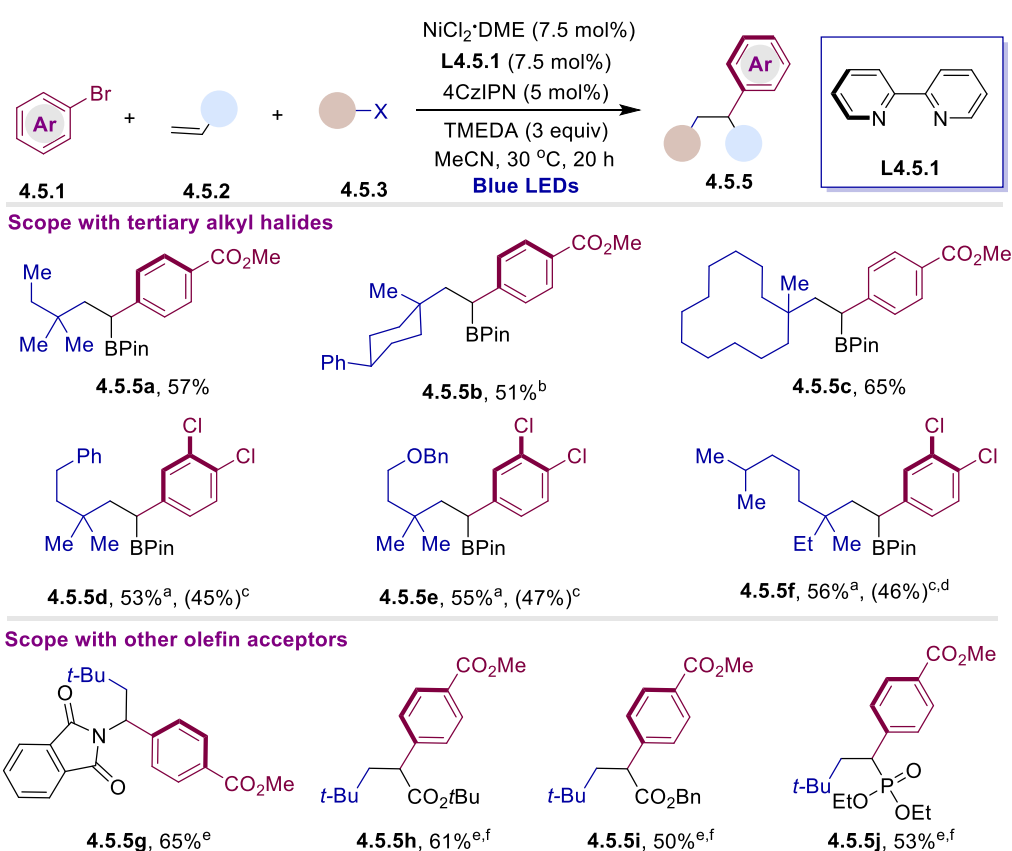


^a **Reaction Conditions:** 4.5.1 (0.4 mmol, 2.0 equiv), 4.5.2 (0.20 mmol, 1.0 equiv), 4.5.3 (0.50 mmol, 2.5 equiv), $\text{NiCl}_2 \cdot \text{DME}$ (3.3 mg, 7.5 mol%), **L4.5.1** (2.3 mg, 7.5 mol%), 4CzIPN (7.9 mg, 5 mol%), TMEDA (90 μL , 0.60 mmol, 3.0 equiv), MeCN (3.0 mL) at 30 °C under irradiation of blue LEDs with a fan for 20 hours, yields of isolated products given, average of at least two independent runs. ^b $\text{Ir}(\text{ppy})_2\text{bpyPF}_6$ (2 mol%), $\text{Ni}(\text{COD})_2$ (7.5 mol%), **L4.5.2** (7.5 mol%), LiCl (0.5–0.6 mmol). ^c Yield of isolated product upon oxidation with NaBO_3 . ^d Isolated yield of the corresponding BF_3K salts upon exposure to KHF_2 . ^e $\text{Ni}(\text{COD})_2$ (7.5 mol%), **L4.5.2** (7.5 mol%). ^f 4.5.4r (5.0 mmol) was used. TMEDA = *N,N,N',N'*-tetramethylethylenediamine. BPin = bis(pinacolato)diboron.

Scheme 4.27. Scope with aryl bromides

4.5.2.2 Scope of Alkyl Bromides and Olefin Acceptors

Encouraged by these results, we wondered whether our 1,2-difunctionalization protocol could be extended to alkyl halides and alkenes other than **4.5.2a** and **4.5.3a**, respectively. As shown in Scheme 4.28, this turned out to be the case and a variety of tertiary alkyl bromides bearing different groups on the side-chain could be used as coupling partners (**4.5.5a-4.5.5f**). Notably, olefins end-capped with phthalimides (**4.5.5g**), esters (**4.5.5h**, **4.5.5i**) and phosphonates (**4.5.5j**) could be utilized as counterparts in lieu of **4.5.2a**, albeit in slightly lower yields.



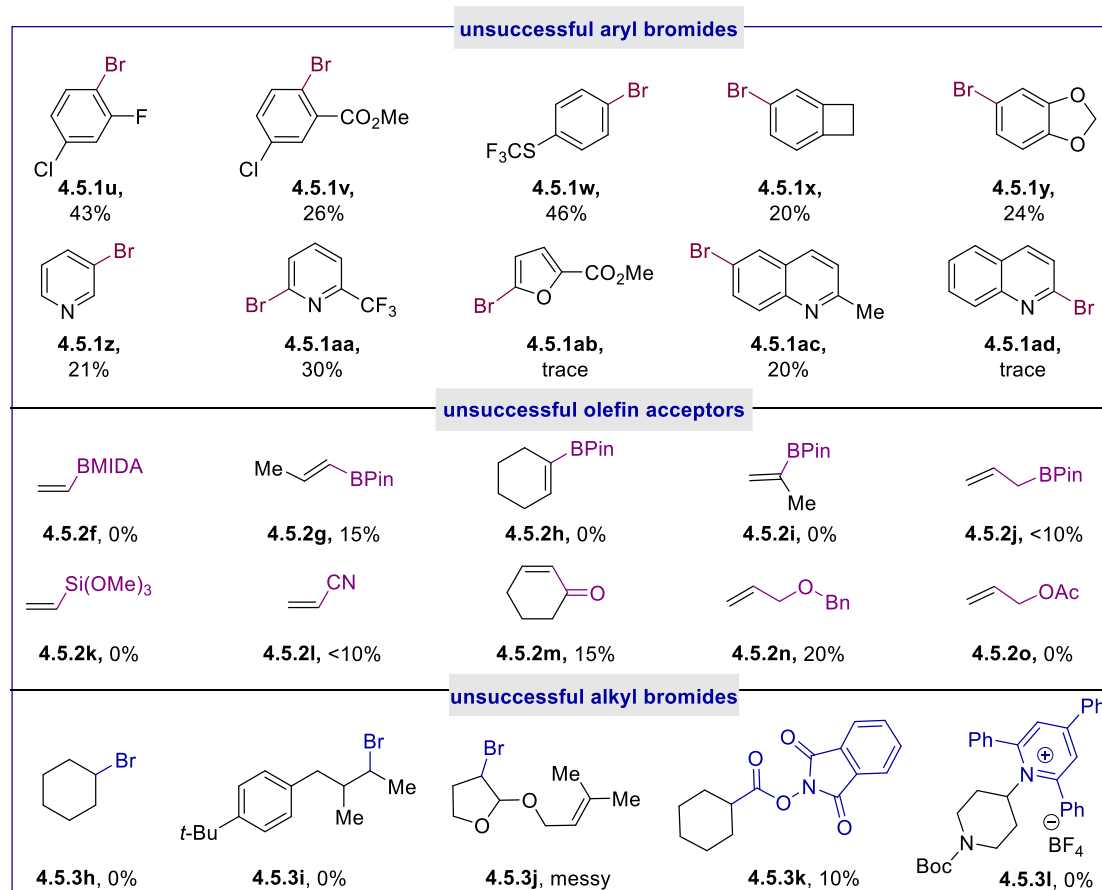
^a **Reaction Conditions**: **4.5.1** (0.4 mmol, 2.0 equiv), **4.5.2** (0.20 mmol, 1.0 equiv), **4.5.3** (0.50 mmol, 2.5 equiv), $\text{NiCl}_2 \cdot \text{DME}$ (3.3 mg, 7.5 mol%), **L4.5.1** (2.3 mg, 7.5 mol%), 4CzIPN (7.9 mg, 5 mol%), TMEDA (90 μL , 0.60 mmol, 3.0 equiv), MeCN (3.0 mL) at 30 °C under irradiation of blue LEDs with a fan for 20 hours, yields of isolated products given, average of at least two independent runs. ^b dr = 2.8:1. ^c $\text{Ni}(\text{COD})_2$ (7.5 mol%), **L4.5.2** (7.5 mol%). ^d dr = 1:1. ^e **4.5.3a** (0.6 mmol), **L4.5.2** (7.5 mol%) was used instead of **L4.5.1** for 36 hours. ^f Isolated yield.

Scheme 4.28. Scope with tertiary alkyl bromides and olefin acceptors

4.5.2.3 Unsuccessful Substrates

During the study of the generality of our 1,2-dicarbofunctionalization reaction, we found that a variety of substrates either failed to provide the desired product or resulted in lower yield (around 20-30% yield) (Scheme 4.29). Generally, electron-rich aryl bromide (**4.5.1x**, **4.5.1y**) provided lower yields than electron-deficient aryl bromides, probably due to slower oxidative addition with nickel. Additionally, we also found that ortho-substituted aryl bromides led to more deborylative side products (**4.5.1u**, **4.5.1v**). Not surprisingly, heterocycles with strong coordinating groups presented lower reactivity, thus indicating that such motifs likely compete for metal binding (**4.5.1z-4.5.1ad**).

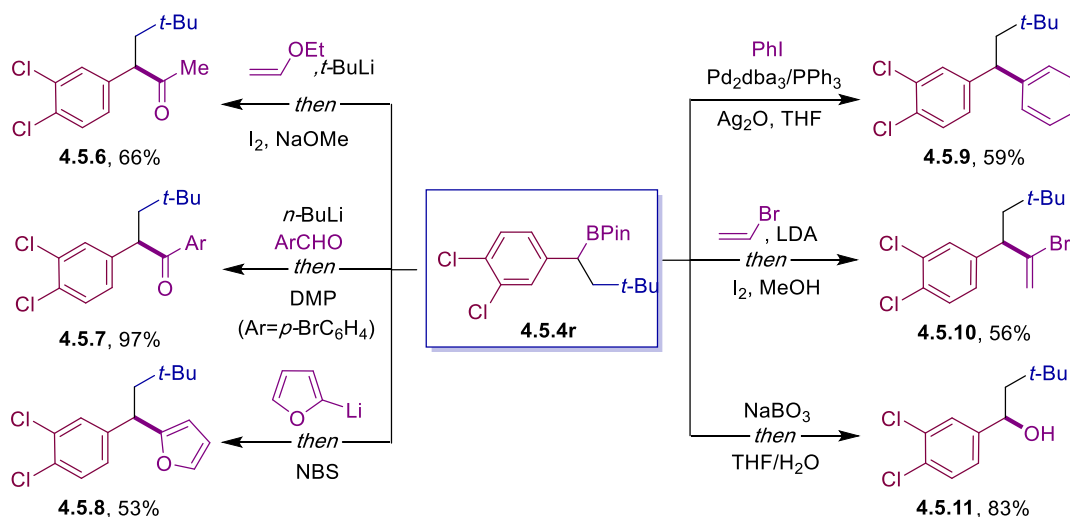
Unfortunately, α - or β -substituted vinyl boronates failed to participate in the targeted difunctionalization event, which suggested that steric effects of the acceptor alkene have a profound influence on reactivity (**4.5.2g-4.5.2i**). Electron-rich olefins were also not tolerated under reaction conditions, due to the mismatched polarity (**4.5.2f**, **4.5.2k**, **4.5.2n** and **4.5.2o**). In addition, the utilization of secondary alkyl bromides resulted in unavoidable competitive cross-electrophile coupling between the two distinct organic halides (**4.5.3h-4.5.3j**).⁵⁰ Importantly, we also examined other alkyl electrophiles apart from alkyl bromide, such as redox activated esters⁵¹ (**4.5.3k**) and pyridinium salts⁵² (**4.5.3l**), but only 10% yield was obtained under optimized conditions.



Scheme 4.29. Unsuccessful substrates

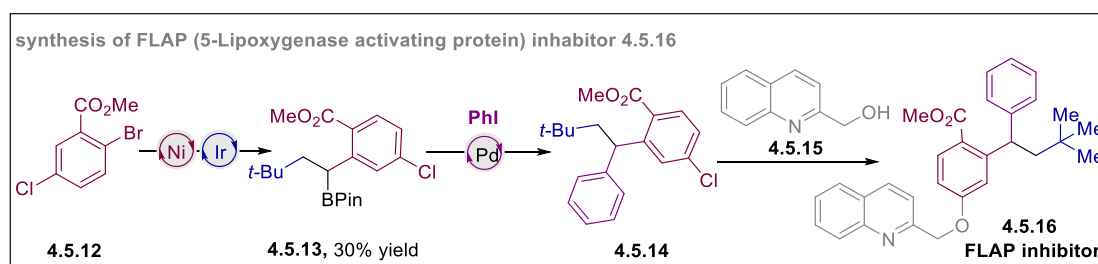
4.5.3 Synthetic Applicability

The utility of our methodology is further illustrated via derivatization of **4.5.4r** (Scheme 4.30). As initially anticipated, a canonical oxidation with NaBO_3 cleanly delivered **4.5.11** in good yields.⁵³ The introduction of (hetero)aryl motifs were within reach by treatment with organolithium reagents (**4.5.8**)⁵⁴ or Suzuki-Miyaura protocols (**4.5.9**)⁵⁵. Likewise, the incorporation of a vinyl halides (**4.5.10**)⁵⁶ or ketone backbones (**4.5.6**, **4.5.7**)^{57,58} at the C–B terminus could also be carried out.



Scheme 4.30. Synthetic application of **4.5.4r**

With these results in hand, we next wondered whether our 1,2-difunctionalization strategy could be applied in the synthesis of more complicated molecules. For example, compound **4.5.16** has been reported to show strong bioactivity against membrane protein FLAP.⁵⁹ As the FLAP inhibitor **4.5.16** has been synthesized by Merck in 12 steps,⁵⁹ we anticipated that through employing our method its preparation could be reduced to 3 steps. The targeted synthesis would include the 1,2-difunctionalization of vinyl boronate, then followed by Pd-catalyzed Suzuki-Miyaura coupling and base promoted etheration. As expected, we could obtain the key intermediate **4.5.13** in 30% yield using easily available **4.5.12**, vinyl boronate (**4.5.2a**) and *t*-BuBr (**4.5.3a**) as starting material. Unfortunately, since we could not improve the yield of **4.5.13**, we didn't pursue the synthesis of **4.5.16** further.



Scheme 4.31. Preliminary experiments for the synthesis of **4.5.16**

4.5.4 Mechanistic Experiments

4.5.4.1 Stern-Volmer Quenching Experiments

With the preparative results of our dicarbofunctionalization in hand, we next focused our attention to elucidate the mechanism of our protocol. In order to do so, we started by studying the Stern-Volmer luminescence (Figures 4.1-4.3). As shown in Figure 4.1, 4CzIPN was irradiated and the emission intensity at 435 nm was observed. The UV-Vis spectra of 4CzIPN was measured at 0.01 mM and 0.05 mM concentration, no significant change could be observed when adding *t*-BuBr or ArBr or TMEDA. Additionally, no quenching effect was observed when adding different amounts of *t*-BuBr (Figure 4.2). However, a significant decrease of 4CzIPN luminescence was observed when increasing the loading of TMEDA, thus suggesting the excited state of 4CzIPN was quenched by TMEDA. These experiments supported the notion that a reductive quenching photocatalytic cycle is occurring, whereby a transient carbon-centered radical is generated via *single-electron-transfer* (SET) from the reduced photocatalyst to a tertiary alkyl halide, with TMEDA serving as sacrificial electron donor.

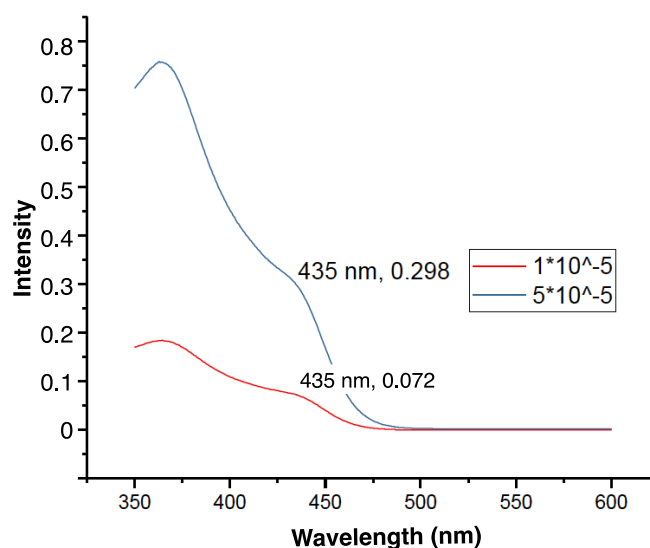


Figure 4.1. UV-Vis spectra of the photocatalyst

***t*-BuBr:** No quenching effect was observed when *t*-BuBr was added (Figure 4.2).

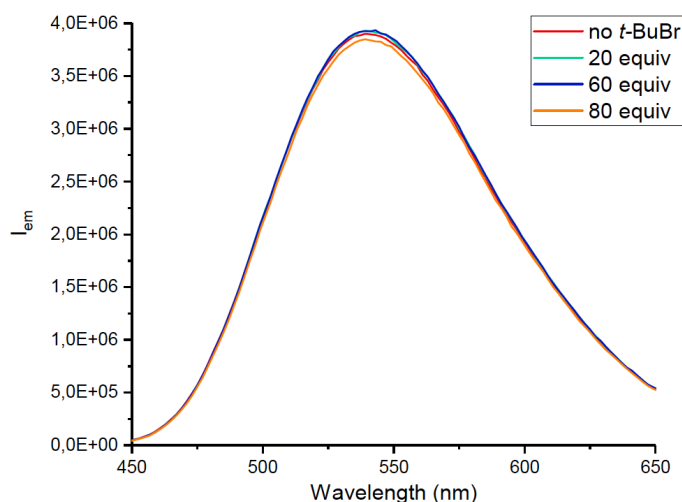


Figure 4.2. The Stern-Volmer of *t*-BuBr

TMEDA: A stock solution of TMEDA (6 μ L, 0.04 mmol) in 4 ml of MeCN was prepared ($C_0 = 10$ mM). Then, different amounts (5 μ L, 5 μ L, 10 μ L, 10 μ L, 10 μ L, 10 μ L, 30 μ L, 20 μ L) of this stock solution were added to a solution of the photocatalyst 4CzIPN in MeCN (0.01 M). As shown, a significant decrease of 4CzIPN luminescence was observed, suggesting that the mechanism might operate via a canonical photocatalytic cycle consisting of a reductive quenching with TMEDA.

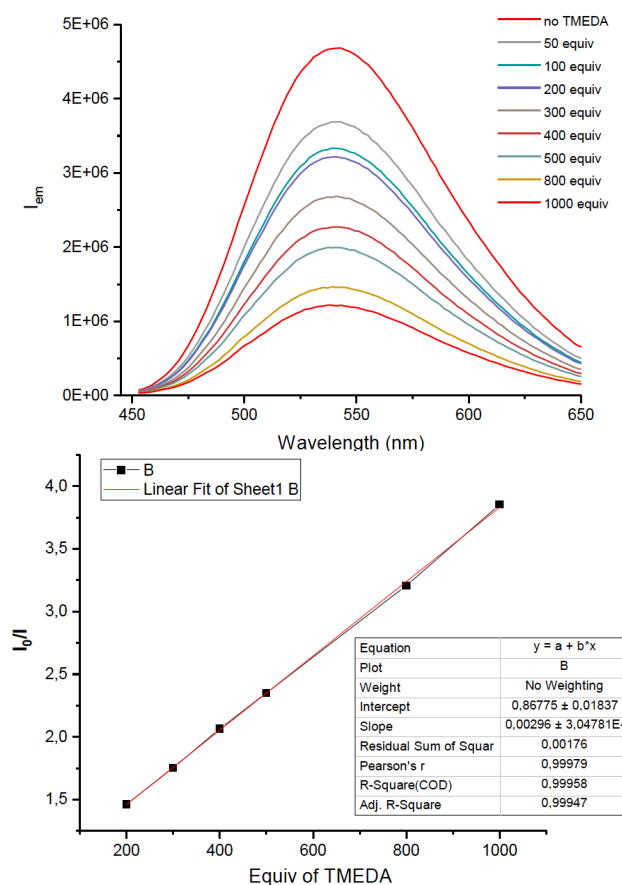


Figure 4.3. The Stern-Volmer of TMEDA

4.5.4.2 Radical Trapping Experiments

As expected, the formation of **4.5.4a** was significantly inhibited when adding 1,4-cyclohexadiene, TEMPO or 5,5-dimethyl-1-pyrroline *N*-oxide (DMPO) as spin-trapping reagents in the reaction (Figure 4.4). Moreover, the generation of an open-shell radical intermediate was further corroborated by exclusively forming five-membered **4.5.19** and **4.5.20** from the corresponding dienes under our optimized reaction conditions (Scheme 4.32).⁶⁰ Notably, EPR experiment was also measured at 77K (liquid nitrogen), presenting the **g-value** is 2.0006 (Figure 4.5). This experiment confirm the intermediacy of alkyl radical under our reaction conditions.

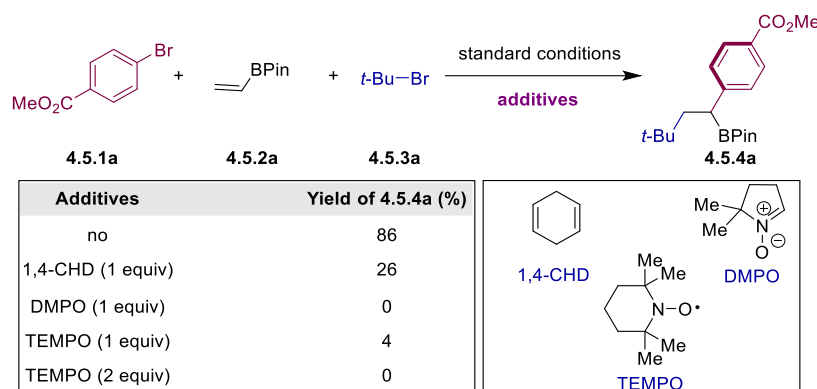
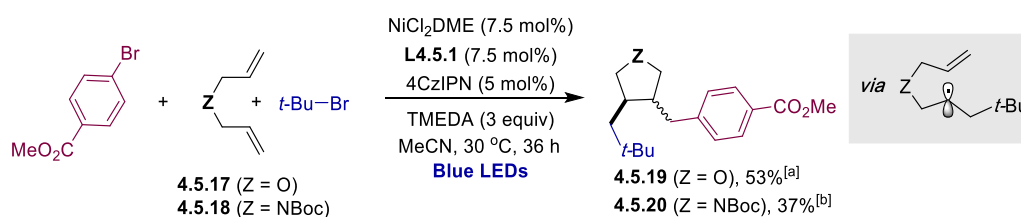


Figure 4.4. Radical trapping experiments



Scheme 4.32. Radical trapping experiments with radical probes

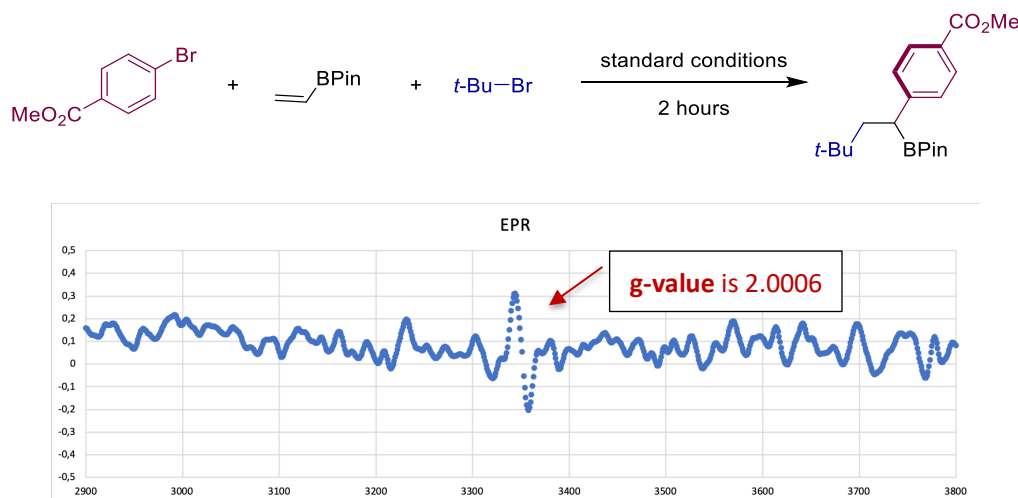
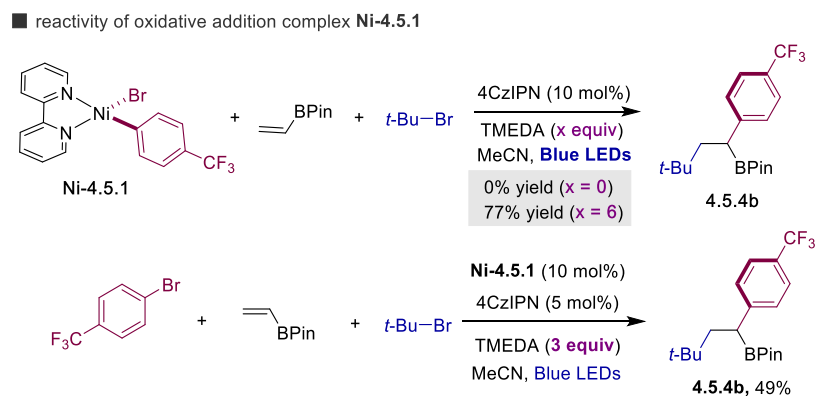


Figure 4.5. EPR experiment of reaction system under irradiation

4.5.4.3 Stoichiometric Experiments of Oxidative Addition Complex Ni-4.5.1

To further elucidate the mechanism, we decided to isolate the putative oxidative addition complex. In order to do so, we prepared Ni-4.5.1 by exposing 4-trifluoromethyl bromobenzene **4.5.1b** to Ni(COD)bpy in THF at room temperature. Under these conditions, we could isolate Ni-4.5.1 in pure form and in high yield. As

expected, **Ni-4.5.1** was shown to be catalytically competent in the reaction, leading to **4.5.4b** in a comparable yield as shown in Scheme 4.27 (Scheme 4.33, *bottom*). More importantly, stoichiometric experiments with **Ni-4.5.1** revealed that **4.5.4b** could only be obtained in the presence of TMEDA (Scheme 4.33, *top*), suggesting that TMEDA played an important role for the reaction success.



Scheme 4.33. Stoichiometric experiments of **Ni-4.5.1**

4.5.4.4 Recovery of the Photocatalyst (4CzIPN)

Finally, we found that the photocatalyst could be recovered in quantitative yield, indicating that the photocatalyst was not decomposed after the reaction completion.

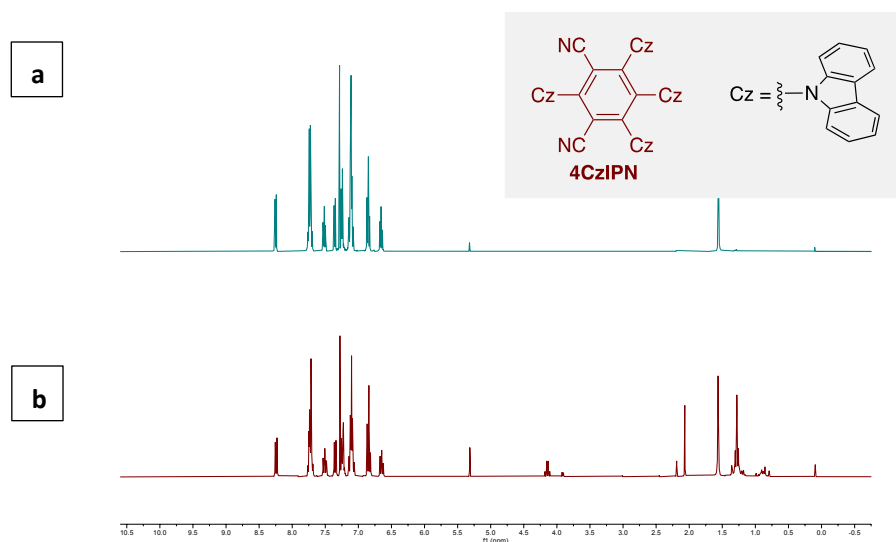
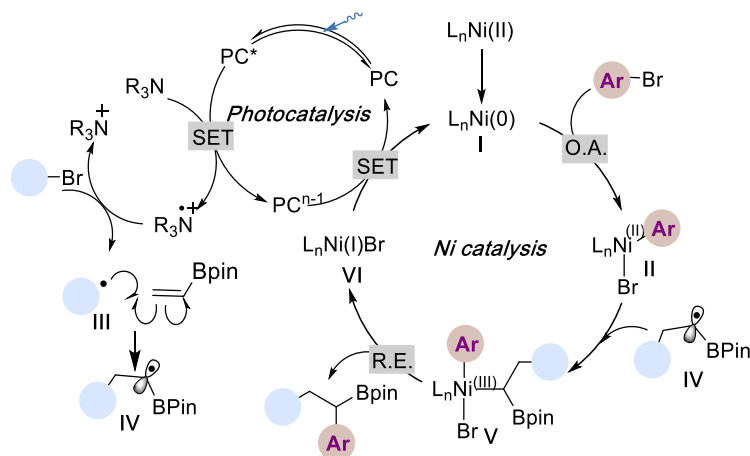


Figure 4.6. (a) ^1H NMR of 4CzIPN before the reaction. (b) ^1H NMR of 4CzIPN after the reaction.

4.5.4.5 Mechanism Proposal

Based on the preliminary results presented above, at present we propose a mechanistic rationale. As shown in scheme 4.34, the nucleophilic radical **III** would be generated by *single-electron-transfer* (SET) from the corresponding alkyl bromide and would preferentially add to electron-deficient vinyl boronate in a regioselective manner to yield an α -boron-stabilized radical **IV**. Concurrently, the ArNi(II)Br species **II** resulting from the oxidative addition of aryl bromide to Ni(0) recombined with α -boron-stabilized radical **IV** to produce the key intermediate Ni(III) complex **V**. Finally, the desired product would be released through reductive elimination and regeneration of Ni(0) (**I**) to close the catalytic cycle via another SET reduction of the Ni(I)-X (**VI**).



Scheme 4.34 Mechanism proposal

4.6 Conclusion

In summary, we have developed a modular chemo- and regioselective 1,2-difunctionalization of simple vinyl boronates with readily available organic halides by nickel and photoredox dual catalytic platform. This protocol not only provides a new technique for preparing densely functionalized alkyl boron fragments from simple and accessible precursors but also serves as a testament to the viability of conducting a reductive cross-coupling of three different electrophiles in a synergistic manner. Moreover, the scope of our 1,2-dicarbofunctionalization can be extended to other electron-deficient olefins beyond vinyl boronates. Unfortunately, our 1,2-difunctionalization strategy is mainly restricted to tertiary alkyl bromides, but efforts to incorporate primary and secondary alkyl halides are currently ongoing in our lab. Preliminary mechanistic studies were carried out, which indicated that the reaction proceeds with an *in-situ* generated tertiary alkyl radical adding across a vinyl boronate in a regioselective manner prior to recombination with an oxidative addition species.

4.7 References

1. (a) Boronic Acids: Preparation and Applications in Organic Synthesis Medicine and Materials (Ed.: D. G. Hall), Wiley-VCH, Weinheim, 2011. (b) Miyaura, N.; Suzuki, A. Palladium-Catalyzed Cross-Coupling Reactions of Organoboron Compounds. *Chem. Rev.* **1995**, *95*, 2457.
2. (a) Brown, H. C.; Zweifel, G. A Stereospecific Cis Hydration of the Double Bond in Cyclic Derivatives. *J. Am. Chem. Soc.* **1959**, *81*, 247. (b) Burgess, K.; Ohlmeyer, M. J. Transition-Metal-Promoted Hydroborations of Alkenes, Emerging Mechanistic Experiments Methodology for Organic Transformations. *Chem. Rev.* **1991**, *91*, 1179.
3. For recent catalytic protocols that incorporate boron fragments into α -olefins, see: (a) Iwamoto, H.; Imamoto, T.; Ito, H. Computational Design of High-Performance Ligand for Enantioselective Markovnikov Hydroboration of Aliphatic Terminal Alkenes. *Nat. Commun.* **2018**, *9*, 2290. (b) Cai, Y.; Yang, X.-T.; Zhang, S.-Q.; Li, F.; Li, Y.-Q.; Ruan, L.-X.; Hong, X.; Shi, S.-L. Copper-Catalyzed Enantioselective Markovnikov Protoboration of α -olefins Enabled by a Buttressed NHC Ligand. *Angew. Chem., Int. Ed.* **2018**, *57*, 1376. (c) Smith, J. R.; Collins, B. S. L.; Hesse, M. J.; Graham, M. A.; Myers, E. L.; Aggarwal, V. K. Enantioselective Rhodium(III)-Catalyzed Markovnikov Hydroboration of Unactivated Terminal Alkenes. *J. Am. Chem. Soc.* **2017**, *139*, 9148. (d) Kerchner, H. A.; Montgomery, J. Synthesis of Secondary and Tertiary Alkylboranes via Formal Hydroboration of Terminal and 1,1-Disubstituted Alkenes. *Org. Lett.* **2016**, *18*, 5760.
4. (a) Yin, G.; Mu, X.; Liu, G. Palladium(II)-Catalyzed Oxidative Difunctionalization of Alkenes: Bond Forming at a High-Valent Palladium Center. *Acc. Chem. Res.* **2016**, *49*, 2413. (b) Lan, X.-W.; Wang, N.-X.; Xing, Y. Recent Advances in Radical Difunctionalization of Simple Alkenes. *Eur. J. Org. Chem.* **2017**, 5821. (c) Zhang, J.-S.; Liu, L.; Chen, T.; Han, L.-B. Transition-Metal-Catalyzed Three-Component Difunctionalizations of Alkenes. *Chem. Asian J.* **2018**, *13*, 2277. (d) Dhungana, R. K.; Kc, S.; Basnet, P.; Giri, R. Transition Metal-Catalyzed Dicarbofunctionalization of Unactivated Olefins. *Chem. Rec.* **2018**, *18*, 1314. (e) Derosa, J.; Kang, T.; Apolinar, O.; Tran, V. T.; Engle, K. M. Recent Developments in Nickel-Catalyzed Intermolecular Dicarbofunctionalization of Alkenes. *Chem. Sci.* **2020**, *11*, 4287. (f) Luo, Y.-C.; Xu, C.; Zhang, X.

Chapter 4.

- Nickel-Catalyzed Dicarbofunctionalization of Alkenes. *Chin. J. Chem.* **2020**, *38*, 1371. (g) Qi, X.; Diao, T. Nickel-Catalyzed Dicarbofunctionalization of Alkenes. *ACS Catal.* **2020**, *10*, 8542.
- (a) Suginome, M. Catalytic Carboborations. *Chem. Rec.* **2010**, *10*, 348. (b) Liu, Z.; Gao, Y.; Zeng, T.; Engle, K. M. Transition-Metal-Catalyzed 1,2-Carboboration of Alkenes: Strategies, Mechanisms, and Stereocontrol. *Isr. J. Chem.* **2020**, *60*, 219.
 - Carreras, J.; Caballero, A.; Perez, P. J. Alkenyl Boronates: Synthesis and Applications. *Chem. Asian. J.* **2019**, *14*, 329.
 - (a) Lovinger, G. J.; Morken, J. P. Recent Advances in Radical Addition to Alkenylboron Compounds. *Eur. J. Org. Chem.* **2020**, 2362. (b) Kischkewitz, M.; Friese, F. W.; Studer, A. Radical-Induced 1,2-Migrations of Boron Ate Complexes. *Adv. Synth. Catal.* **2020**, *362*, 2077. (c) Tappin, N.D. C.; Renaud, P. Radical Reactions of Boron-Ate Complexes Promoting a 1,2-Metallate Rearrangement. *Chimia* **2020**, *74*, 33. (d) Namirembe, S.; Morken, J. P. Reactions of organoboron compounds enabled by catalyst-promoted metalate shifts. *Chem. Soc. Rev.* **2019**, *48*, 3464.
 - Matteson, D. S. α -Halo Boronic Esters: Intermediates for Stereodirected Synthesis. *Chem. Rev.* **1989**, *89*, 1535.
 - Leonori, D.; Aggarwal, V. K. Lithiation–Borylation Methodology and Its Application in Synthesis. *Acc. Chem. Res.* **2014**, *47*, 3174.
 - Zweifel, G.; Arzoumanian, H.; Whitney, C. C. A Convenient Stereoselective Synthesis of Substituted Alkenes via Hydroboration-Iodination of Alkynes. *J. Am. Chem. Soc.* **1967**, *89*, 3652.
 - Matteson, D. S.; Jesthi, P. K. Lithium Bis(ethylenedioxyboryl)methide and Its Reactions with Carbonyl Compounds and with the Chlorotriphenyl Derivatives of Germanium, Tin and Lead. *J. Organomet. Chem.* **1976**, *110*, 25.
 - Evans, D. A.; Crawford, T. C.; Thomas, R. C.; Walker, J. A. Studies Directed toward the Synthesis of Prostaglandins. Useful Boron-Mediated Olefin Syntheses. *J. Org. Chem.* **1976**, *41*, 3947.
 - Zhang, L.; Lovinger, G. J.; Edelstein, E. K.; Szymaniak, A. A.; Chierchia, M. P.; Morken, J. P. Catalytic Conjunctive Cross-Coupling Enabled by Metal-Induced Metallate Rearrangement. *Science* **2016**, *351*, 70.

14. Edelstein, E. K.; Namirembe, S.; Morken, J. P. Enantioselective Conjunctive Cross-Coupling of Bis(alkenyl) Borates: A General Synthesis of Chiral Allylboron Reagents. *J. Am. Chem. Soc.* **2017**, *139*, 5027.
15. Myhill, J. A.; Wilhelmsen, C. A.; Zhang, L.; Morken, J. P. Diastereoselective and Enantioselective Conjunctive Cross-Coupling Enabled by Boron Ligand Design. *J. Am. Chem. Soc.* **2018**, *140*, 15181.
16. Lovinger, G. J.; Aparece, M. D.; Morken, J. P. Pd-Catalyzed Conjunctive Cross-Coupling Between Grignard-Derived Boron "Ate" Complexes and C(sp²) Halides or Triflates: NaOTf as a Grignard Activator and Halide Scavenger. *J. Am. Chem. Soc.* **2017**, *139*, 3153.
17. Chierchia, M.; Law, C.; Morken, J. P. Ni-Catalyzed Enantioselective Conjunctive Cross-Coupling of 9-BBN Borates. *Angew. Chem. Int. Ed.* **2017**, *56*, 11870.
18. Law, C.; Meng, Y.; Koo, S. M.; Morken, J. P. Catalytic Conjunctive Coupling of Carboxylic Acid Derivatives with 9-BBN-Derived Ate Complexes. *Angew. Chem. Int. Ed.* **2019**, *58*, 6654.
19. Lovinger, G. J.; Morken, J. P. Ni-Catalyzed Enantioselective Conjunctive Coupling with C(sp³) Electrophiles: A Radical-Ionic Mechanistic Dichotomy. *J. Am. Chem. Soc.* **2017**, *139*, 17293.
20. Kischkewitz, M.; Okamoto, K.; Muck-Lichtenfeld, C.; Studer, A. Radical-Polar Crossover Reactions of Vinylboron Ate Complexes. *Science* **2017**, *355*, 936.
21. Tappin, N. D. C.; Gnagi-Lux, M.; Renaud, P. Radical-Triggered Three-Component Coupling Reaction of Alkenylboronates, α -Halocarbonyl Compounds, and Organolithium Reagents: The Inverse Ylid Mechanism. *Chem. Eur. J.* **2018**, *24*, 11498.
22. Silvi, M.; Sandford, C.; Aggarwal, V. K. Merging Photoredox with 1,2-Metallate Rearrangements: The Photochemical Alkylation of Vinyl Boronate Complexes. *J. Am. Chem. Soc.* **2017**, *139*, 5736.
23. Gerleve, C.; Kischkewitz, M.; Studer, A. Synthesis of α -Chiral Ketones and Chiral Alkanes Using Radical Polar Crossover Reactions of Vinyl Boron Ate Complexes. *Angew. Chem., Int. Ed.* **2018**, *57*, 2441.
24. Quiclet-Sire, B.; Zard, S. Z. Radical Instability in Aid of Efficiency: A Powerful Route to Highly Functional MIDA Boronates. *J. Am. Chem. Soc.* **2015**, *137*, 6762.
25. (a) Kumar, N.; Reddy, R. R.; Eghbarieh, N.; Masarwa, A. α -Borylalkyl radicals: their distinctive reactivity in modern organic synthesis. *Chem. Commun.* **2020**, *56*,

Chapter 4.

13. (b) Ollivier, C.; Renaud, P. Organoboranes as a Source of Radicals. *Chem. Rev.* **2001**, *101*, 3415.
26. Grotewold, J.; Lissi, E. A.; Scaiano, J. C. On the Gas Phase Reactions of Bromine Atoms with Triethylborane. *J. Organomet. Chem.* **1969**, *19*, 431.
27. Walton, J. C.; McCarroll, A. J.; Chen, Q.; Carboni, B.; Nziengui, R. The Influence of Boryl Substituents on the Formation and Reactivity of Adjacent and Vicinal Free Radical Centers. *J. Am. Chem. Soc.* **2000**, *122*, 5455.
28. Matteson, D. S. Radical Catalyzed Additions to Dibutyl Ethyleneboronate. *J. Am. Chem. Soc.* **1959**, *81*, 5004.
29. Chierchia, M. P.; Xu, P.; Lovinger, G. J.; Morken, J. P. Enantioselective Radical Addition/Cross-Coupling of Organozinc Reagents, Alkyl Iodides, and Alkenylboron Reagents. *Angew. Chem., Int. Ed.* **2019**, *58*, 14245.
30. García-Domínguez, A.; Mondal, R.; Nevado, C. Dual Photoredox/Nickel-Catalyzed Three-Component Carbonylation of Alkenes. *Angew. Chem. Int. Ed.* **2019**, *58*, 12286.
31. Campbell, M. W.; Compton, J. S.; Kelly, C. B.; Molander, G. A. Three-Component Olefin Dicarboxylation Enabled by Nickel/Photoredox Dual Catalysis. *J. Am. Chem. Soc.* **2019**, *141*, 20069.
32. Selected examples for Ni-catalyzed intermolecular 1,2-dicarboxylation of olefins with an electrophile and a nucleophile, (a) Qin, T.; Cornella, J.; Li, C.; Malins, L. R.; Edwards, J. T.; Kawamura, S.; Maxwell, B. D.; Eastgate, M. D.; Baran, P. S. A General Alkyl-Alkyl Cross-Coupling Enabled by Redox-Active Esters and Alkylzinc Reagents. *Science* **2016**, *352*, 801. (b) Gu, J.-W.; Min, Q.-Q.; Yu, L.-C.; Zhang, X. Tandem Difluoroalkylation-Arylation of Enamides Catalyzed by Nickel. *Angew. Chem., Int. Ed.* **2016**, *55*, 12270. (c) Shrestha, B.; Basnet, P.; Dhungana, R. K.; KC, S.; Thapa, S.; Sears, J. M. Giri, R. Ni-Catalyzed Regioselective 1,2-Dicarboxylation of Olefins by Intercepting Heck Intermediates as Imine-Stabilized Transient Metallacycles. *J. Am. Chem. Soc.* **2017**, *139*, 10653. (d) Gao, P.; Chen, L.-A.; Brown, M. K. Nickel-Catalyzed Stereoselective Diarylation of Alkenylarenes. *J. Am. Chem. Soc.* **2018**, *140*, 10653. (e) Derosa, J.; Tran, V. T.; Boulous, M. N.; Chen, J. S.; Engle, K. M. Nickel-Catalyzed β,γ -Dicarboxylation of Alkenyl Carbonyl Compounds via Conjunctive Cross-Coupling. *J. Am. Chem. Soc.* **2017**, *139*, 10657.

33. García-Domínguez, A.; Li, Z.; Nevado, C. Nickel-Catalyzed Reductive Dicarbofunctionalization of Alkenes. *J. Am. Chem. Soc.* **2017**, *139*, 6835.
34. Shu, W.; García-Domínguez, A.; Quiroz, M. T.; Mondal, R.; Cardenas, D. J.; Nevado, C. Ni-Catalyzed Reductive Dicarbofunctionalization of Nonactivated Alkenes: Scope and Mechanistic Insights. *J. Am. Chem. Soc.* **2019**, *141*, 13812.
35. Zhao, X.; Tu, H.-Y.; Guo, L.; Zhu, S.; Qing, F.-L.; Chu, L. Intermolecular Selective Carboacylation of Alkenes via Nickel-Catalyzed Reductive Radical Relay. *Nat. Commun.* **2018**, *9*, 3488.
36. Yang, T.; Chen, X.; Rao, W.; Koh, M. J. Broadly Applicable Directed Catalytic Reductive Difunctionalization of Alkenyl Carbonyl Compounds. *Chem* **2020**, *6*, 738.
37. Anthony, D.; Lin, Q.; Baudet, J.; Diao, T. Nickel-Catalyzed Asymmetric Reductive Diarylation of Vinylarenes. *Angew. Chem. Int. Ed.* **2019**, *58*, 3198.
38. Tu, H.-Y.; Wang, F.; Huo, L.; Li, Y.; Zhu, S.; Zhao, X.; Li, H.; Qing, F.-L.; Chu, L. Enantioselective Three-Component Fluoroalkylation of Unactivated Olefins through Nickel-Catalyzed Cross-Electrophile Coupling. *J. Am. Chem. Soc.* **2020**, *142*, 9604.
39. Wei, X.; Shu, W.; García-Domínguez, A.; Merino, E.; Nevado, C. Asymmetric Ni-Catalyzed Radical Relayed Reductive Coupling. *J. Am. Chem. Soc.* **2020**, *142*, 13515.
40. Selected reviews for cross-electrophile-couplings, see: (a) Gu, J.; Wang, X.; Xue, W.; Gong, H. Nickel-Catalyzed Reductive Coupling of Alkyl Halides with Other Electrophiles: Concept and Mechanistic Considerations. *Org. Chem. Front.* **2015**, *2*, 1411. (b) Weix, J. D. Methods and Mechanisms for Cross-Electrophile Coupling of Csp² Halides with Alkyl Electrophiles. *Acc. Chem. Res.* **2015**, *48*, 1767. (c) Moragas, T.; Correa, A.; Martin, R. Metal-Catalyzed Reductive Coupling Reactions of Organic Halides with Carbonyl-Type Compounds. *Chem. Eur. J.* **2014**, *20*, 8242. (d) Knappke, C. E. I.; Grupe, S.; Gartner, D.; Corpet, M.; Gosmini, C.; von Wangelin, A. J. Reductive Cross-Coupling Reactions between Two Electrophiles. *Chem. Eur. J.* **2014**, *20*, 6828.
41. Selected references: (a) Sun, S.-Z.; Romano, C.; Martin, R. Site-Selective Catalytic Deaminative Alkylation of Unactivated Olefins. *J. Am. Chem. Soc.* **2019**, *141*, 16197. (b) Martin-Montero, R.; Yatham, V. R.; Yin, H.; Davies, J.; Martin, R. Ni-Catalyzed Reductive Deaminative Arylation at sp³ Carbon Centers. *Org. Lett.*

- 2019**, *21*, 2947. (c) Sun, S.-Z.; Borjesson, M.; Martin-Montero, R.; Martin, R. Site-Selective Ni-Catalyzed Reductive Coupling of α -Haloboranes with Unactivated Olefins. *J. Am. Chem. Soc.* **2018**, *140*, 12765. (d) Tortajada, A.; Ninokata, R.; Martin, R. Ni-Catalyzed Site-Selective Dicarboxylation of 1,3-Dienes with CO₂. *J. Am. Chem. Soc.* **2018**, *140*, 2050. (e) Sun, S.-Z.; Martin, R. Nickel-Catalyzed Umpolung Arylation of Ambiphilic α -Bromoalkyl Boronic esters. *Angew. Chem., Int. Ed.* **2018**, *57*, 3622. (f) Julia-Hernandez, F.; Moragas, T.; Cornella, J.; Martin, R. Remote Carboxylation of Halogenated Aliphatic Hydrocarbons with Carbon Dioxide. *Nature* **2017**, *545*, 84.
42. Reviews for on dual photochemical events: (a) Milligan, J. A.; Phelan, J. P.; Badir, S. O.; Molander, G. A. Alkyl Carbon-Carbon Bond Formation by Nickel/Photoredox Cross-Coupling. *Angew. Chem. Int. Ed.* **2019**, *58*, 6152. (b) Twilton, J.; Le, C.; Zhang, P.; Shaw, M. H.; Evans, R. W.; MacMillan, D. W. C. The Merger of Transition Metal and Photocatalysis. *Nat. Rev. Chem.* **2017**, *1*, 0052. (c) Karkas, M. D.; Porco, J. A.; Stephenson, C. R. J. Photochemical Approaches to Complex Chemotypes: Applications in Natural Product Synthesis. *Chem. Rev.* **2016**, *116*, 9683. (d) Prier, C. K.; Rankic, D. A.; MacMillan, D. W. C. Visible Light Photoredox Catalysis with Transition Metal Complexes: Applications in Organic Synthesis. *Chem. Rev.* **2013**, *113*, 5322. (e) Skubi, K. L.; Blum, T. R.; Yoon, T. P. Dual Catalysis Strategies in Photochemical Synthesis. *Chem. Rev.* **2016**, *116*, 10035.
43. Recently, Aggarwal and co-workers reported a photoinduced decarboxylative Giese-type reaction of vinyl boronates: Noble, A.; Mega, R. S.; Pflästerer, D.; Myers, E. L.; Aggarwal, V. K. Visible-Light-Mediated Decarboxylative Radical Additions to Vinyl Boronic Esters: Rapid Access to γ -Amino Boronic Esters. *Angew. Chem. Int. Ed.* **2018**, *57*, 2155.
44. Dual Ni/photoredox-catalyzed reductive cross-couplings using organo amines as electron donor: (a) Duan, Z. Li, W. Lei, A. Nickel-Catalyzed Reductive Cross-Coupling of Aryl Bromides with Alkyl Bromides: Et₃N as the Terminal Reductant. *Org. Lett.* **2016**, *18*, 4012. (b) Paul, A.; Smith, M. D.; Vannucci, A. K. Photoredox-Assisted Reductive Cross-Coupling: Mechanistic Insight into Catalytic Aryl-Alkyl Cross-Couplings. *J. Org. Chem.* **2017**, *82*, 1996. (c) Yu, W.; Chen, L.; Tao, J.; Wang, T.; Fu, J. Dual Nickel- and Photoredox-Catalyzed Reductive

- Cross-Coupling of Aryl Vinyl Halides and Unactivated Tertiary Alkyl Bromides. *Chem. Commun.* **2019**, 55, 5918.
45. Selected references for using 4CzIPN as photocatalysts, (a) Shang, T.-Y.; Lu, L.-H.; Cao, Z.; Liu, Y.; He, W.-M.; Yu, B. Recent Advances of 1,2,3,5-Tetrakis(carbazol-9-yl)-4,6-dicyanobenzene (4CzIPN) in Photocatalytic Transformations. *Chem. Commun.* **2019**, 55, 5408. (b) Uoyama, H.; Goushi, K.; Shizu, K.; Nomura, H.; Adachi, C. Highly Efficient Organic Light-Emitting Diodes from Delayed Fluorescence. *Nature* **2012**, 492, 234.
46. The effect of LiCl on reduction of organic halides has been studied in some detail. See: Huang, L.; Ackerman, L. K. G.; Kang, K.; Parsons, A. M.; Weix, D. J. LiCl-Accelerated Multimetallic Cross-Coupling of Aryl Chlorides with Aryl Triflates. *J. Am. Chem. Soc.* **2019**, 141, 10978.
47. De Meijere, A.; Bräse, S.; Oestreich, M. *Metal-Catalyzed Cross Coupling Reactions*; Wiley-VCH: Weinheim, Germany, 2004.
48. Mega, R. S.; Duong, V. K.; Noble, A.; Aggarwal, V. K. Decarboxylative Conjunctive Cross-coupling of Vinyl Boronic Esters Using Metallaphotoredox Catalysis. *Angew. Chem. Int. Ed.* **2020**, 59, 4375.
49. Wang, X.-X.; Lu, X.; He, S.-J.; Fu, Y. Nickel-Catalyzed Three-Component Olefin Reductive Dicarbonylation to Access Alkylborates. *Chem. Sci.* **2020**, 11, 7950.
50. Selected examples for Ni/Photoredox dual-catalyzed cross-electrophile coupling: (a) Zhang, P.; Le, C. C.; MacMillan, D. W. C. Silyl Radical Activation of Alkyl Halides in Metallaphotoredox Catalysis: A Unique Pathway for Cross-Electrophile Coupling. *J. Am. Chem. Soc.* **2016**, 138, 8084. (b) ref. 44
51. Murarka, S. N-(Acyloxy)phthalimides as Redox-Active Esters in Cross-Coupling Reactions. *Adv. Synth. Catal.* **2018**, 360, 1735.
52. Selected reviews, (a) Rosser, S. L.; Jelier, B. J.; Magnier, E.; Dagousset, G.; Carreira, E.; Togni, A. Pyridinium Salts as Redox-Active Functional Group Transfer Reagents. *Angew. Chem. Int. Ed.* **2020**, 59, 9264. (b) He, F.-S.; Ye, S.; Wu, J. Recent Advances in Pyridinium Salts as Radical Reservoirs in Organic Synthesis. *ACS Catal.* **2019**, 9, 8943. (c) Pang, Y.; Moser, D.; Cornella, J. Pyrylium Salts: Selective Reagents for the Activation of Primary Amino Groups in Organic Synthesis. *Synthesis* **2020**, 52, 489.

Chapter 4.

53. J. Cossy in *Comprehensive Organic Functional Group Transformations II* (Eds.: A. Katritzky, R. J. K. Taylor), Elsevier, Oxford, 2004.
54. Bonet, A.; Odachowski, M.; Leonori, D.; Essafi, S.; Aggarwal, V. K. Enantiospecific sp^2 - sp^3 Coupling of Secondary and Tertiary Boronic Esters. *Nat. Chem.* **2014**, *6*, 584.
55. Imao, D.; Glasspole, B. W.; Laberge, V. S.; Crudden, C. M. Cross Coupling Reactions of Chiral Secondary Organoboronic Esters with Retention of Configuration. *J. Am. Chem. Soc.* **2009**, *131*, 5024.
56. Wang, Y.; Noble, A.; Myers, E. L. Aggarwal, V. K. Enantiospecific Alkynylation of Alkylboronic Esters. *Angew. Chem. Int. Ed.* **2016**, *55*, 4270.
57. Sonawane, R. P.; Jheengut, V.; Rabalakos, C.; Larouche-Gauthier, R.; Scott, H. K.; Aggarwal, V. K. Enantioselective Construction of Quaternary Stereogenic Centers from Tertiary Boronic Esters: Methodology and Applications. *Angew. Chem. Int. Ed.* **2011**, *50*, 3760.
58. Hollerbach, M. R.; Barker, T. J. Chemoselective Benzoylation of Aldehydes Using Lewis Base Activated Boronate Nucleophiles. *Organometallics* **2018**, *37*, 1425.
59. Chu, L.; Armstrong, H. M.; Chang, L. L.; Cheng, A. F.; Colwell, L.; Cui, J.; Evans, J.; Galka, A.; Goulet, M. T.; Hayes, N.; Lo, J.; Menke, J.; Ok, H. O.; Ondeyka, D. L.; Patel, M.; Quaker, G. M.; Sings, H.; Witkin, S. L.; Zhao, A.; Ujjainwalla, F. Evaluation of Endo and Exo-Aryl-Substitutions and Central Scaffold Modifications on Diphenyl Substituted Alkanes as 5-Lipoxygenase Activating Protein Inhibitors. *Bioorg. Med. Chem. Lett.* **2012**, *22*, 4133.
60. Beckwith, A. L. J.; Schiesser, C. H. Regio- and Stereo-Selectivity of Alkenyl Radical Ring Closure: A Theoretical Study. *Tetrahedron* **1985**, *41*, 3925.

4.8 Experimental Section

4.8.1 General Considerations

Reagents. Commercially available materials were used as received without further purification. Ni(COD)₂ (98% purity) was purchased from Strem, NiCl₂·glyme (97% purity), 2,2'-dipyridyl (bpy, 99% purity), 4,4'-Di-*tert*-butyl-2,2'-dipyridyl (dtbppy, 98% purity), Lithium chloride (LiCl, 99% purity) were purchased from Aldrich, *N,N,N',N'*-Tetramethylethylenediamine (TMEDA, 98% purity) was purchased from Fluorochem, 4,4,5,5-Tetramethyl-2-vinyl-1,3,2-dioxaborolane (Vinyl Bpin, 93% purity, stabilized with Phenothiazine) was purchased from TCI, anhydrous Acetonitrile (99.5% purity) was purchased from Acros or Scharlau. Most of the organic halides utilized in this reaction and other reagents were commercially available.

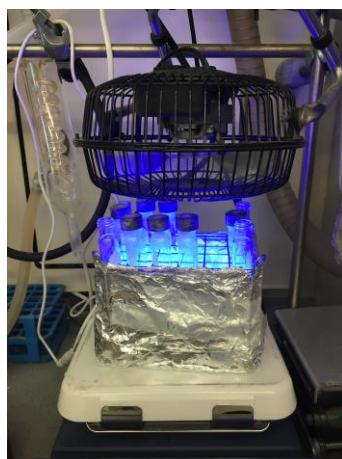
Analytical methods. ¹H and ¹³C NMR spectra were recorded on Bruker 300 MHz, Bruker 400 MHz and Bruker 500 MHz at 20 °C. All ¹H NMR spectra are reported in parts per million (ppm) downfield of TMS and were calibrated using the residual solvent peak of CHCl₃ (7.26 ppm), unless otherwise indicated. All ¹³C NMR spectra are reported in ppm relative to TMS, were calibrated using the signal of residual CHCl₃ (77.16 ppm), ¹¹B NMR and ¹⁹F NMR were obtained with ¹H decoupling unless otherwise indicated. Coupling constants, *J*, are reported in Hertz. Melting points were measured using open glass capillaries in a Büchi B540 apparatus. Gas chromatographic analyses were performed on Hewlett-Packard 6890 gas chromatography instrument with FID detector. Flash chromatography was performed with EM Science silica gel 60 (230-400 mesh). Thin layer chromatography was used to monitor reaction progress and analyze fractions from column chromatography. To this purpose TLC Silica gel 60 F₂₅₄ aluminum sheets from Merck were used and visualization was achieved using UV irradiation and/or staining with Cerium Molybdate Stain (Hanessian's Stain). The procedures described in this section are representative. Thus, the yields may differ slightly from those given in the Schemes of the manuscript. In the cases the High-Resolution Mass Spectra of the molecular ion could not be obtained using ESI and APCI ionization modes the GC-MS of the compound was given.

4.8.2 General Procedure for Optimization of the Reaction Conditions

General procedure: An oven-dried 8 mL screw-cap test tube containing a stirring bar was charged with 4CzIPN (7.9 mg, 5 mol%), the corresponding ligand (7.5 mol%) and methyl 4-benzoate (**4.5.1a**, 86.0 mg, 0.4 mmol, 2.0 equiv). Then the tube was sealed with a Teflon-lined screw cap, and was brought into the glovebox. The corresponding nickel sources (7.5 mol%) was added. Afterwards, the tube was brought out, then Vinyl Bpin (**4.5.2a**, 35 μ L, 0.2 mmol, 1.0 equiv), 2-bromo-2-methylpropane (**4.5.3a**, 56 μ L, 0.5 mmol, 2.5 equiv), TMEDA (90 μ L, 0.6 mmol, 3.0 equiv) and anhydrous MeCN (3.0 mL) were added via syringe. Then, the tube was stirred at 30 °C under irradiation of blue LEDs with a fan for 20 hours. After the reaction was completed, the mixture was diluted with EtOAc, filtered through silica gel and concentrated under vacuum. The yields were determined by ^1H NMR analysis using CH_2Br_2 as internal standard. If needed, the product was purified by column chromatography on silica gel (Hexane/EtOAc = 60:1 to 30:1). **Note:** The reaction gave good yield when it became yellow turbid liquid after 20 hours, if not extend time until the color changed.



Before reaction



During reaction

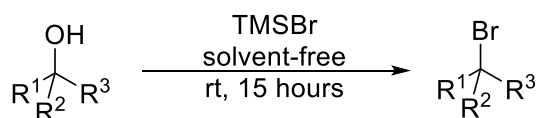


After reaction

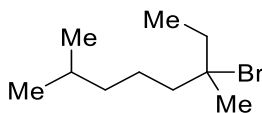
4.8.3 Synthesis of Starting Materials

Commercially available compounds were used as received without further purification. (4-bromo-4-methylcyclohexyl)benzene (**4.5.3c**),¹ 1-bromo-1-methylcyclododecane (**4.5.3d**),² (3-bromo-3-methylbutyl)benzene (**4.5.3e**)³ and ((3-bromo-3-methylbutoxy)methyl) benzene (**4.5.3f**)⁴ were prepared by known procedures, the NMR data matched those reported previously in the literature.

4.8.3.1 Procedure for the Preparation of Tertiary Bromides

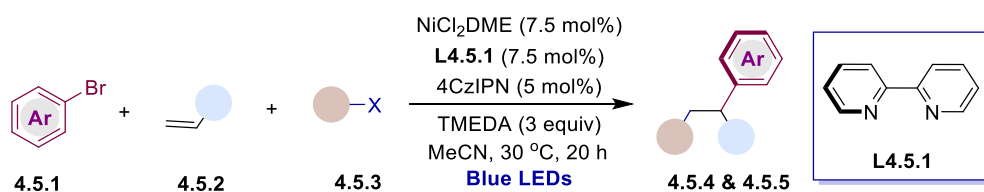


General procedure: To the corresponding tertiary alcohol (5.0 – 10.0 mmol, 1.0 equiv) was added bromotrimethylsilane (5.0 – 10.0 mmol, 1.0 equiv) dropwise under Ar. The reaction mixture was stirring at rt for 15 hours, then diluted with DCM (5 mL) and hexane (5–10 mL according to the polarity of the product). The resulting solution was subjected on a pad of silica gel directly and washed with a mixture of DCM and hexane (1:2 or 1:1). The filtrate was concentrated and dried under vacuum to give the final product in good quality. If not, further purification can be performed by flash column chromatography.

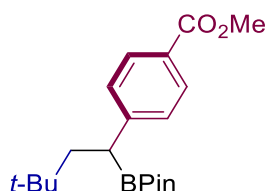


6-Bromo-2,6-dimethyloctane (4.5.3g): To 3,7-Dimethyloctan-3-ol (1.91 mL, 10.0 mmol, 1.0 equiv) was added bromotrimethylsilane (1.32 mL, 10.0 mmol, 1.0 equiv) dropwise under argon. The reaction mixture was stirring at rt for 15 hours, then diluted with DCM (5 mL) and hexane (10 mL). The resulting solution was subjected on a pad of silica gel directly and washed with a mixture of DCM and hexane (1:1, 20 mL). The filtrate was concentrated and dried under vacuum to give the final product **4.5.5g** (2.08 g, 94%) as a colorless liquid, used without further purification. ¹H NMR (400 MHz, CDCl₃): δ 1.96 – 1.73 (m, 4H), 1.70 (s, 3H), 1.59 – 1.42 (m, 3H), 1.19 (q, *J* = 7.4 Hz, 2H), 1.03 (t, *J* = 7.4 Hz, 3H), 0.89 (d, *J* = 6.6 Hz, 6H) ppm. ¹³C NMR (101 MHz, CDCl₃): δ 75.2, 45.3, 39.1, 38.3, 31.2, 28.0, 23.7, 22.7, 10.5 ppm. IR (neat, cm⁻¹): 2952, 1458, 1379, 1139, 844, 794, 735. GC-MS calcd. for (C₁₀H₂₁) [M-Br]: found *t* = 4.540 min, *m/z* = 141.1.

4.8.4 Site-Selective 1,2-Dicarbonylation of Vinyl Boronates

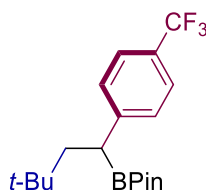


General procedure: An oven-dried 8 mL screw-cap test tube containing a stirring bar was charged with 4CzIPN (7.9 mg, 5 mol%), 2,2'-dipyridyl (**L4.5.1**, 2.3 mg, 7.5 mol%) and aryl bromide (**4.5.1**, 0.4 mmol, 2.0 equiv). Subsequently, the tube was sealed with a Teflon-lined screw cap and the tube was brought into the glovebox. After then $\text{NiCl}_2 \cdot \text{glyme}$ (3.3 mg, 7.5 mol%) was added. Afterwards, the tube was brought out, then Vinyl Bpin (**4.5.2a**, 35 μL , 0.2 mmol, 1.0 equiv), tertiary bromide (**4.5.3**, 0.5 mmol, 2.5 equiv), TMEDA (90 μL , 0.6 mmol, 3.0 equiv) and anhydrous MeCN (3.0 mL) were added via syringe. Then, the tube was stirred at 30 $^\circ\text{C}$ under irradiation of blue LEDs with a fan for 20 – 36 h. After the reaction was completed, the mixture was diluted with EtOAc, filtered through silica gel to remove inorganic salts and concentrated under vacuum. The yields were determined by ^1H NMR analysis using CH_2Br_2 as internal standard. The product was purified by column chromatography on silica gel. **NOTE:** *care must be taken when purifying the products via regular column chromatography. We do recommend that these compounds should be worked up carefully, isolated as soon as possible, and preferably stored in the freezer at low temperatures.*

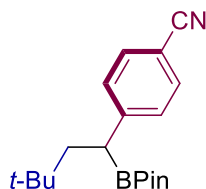


Methyl 4-(3,3-dimethyl-1-(4,4,5,5-tetramethyl-1,3,2-dioxaborolan-2-yl)butyl)benzoate (4.5.4a): Following the general procedure, by using methyl 4-bromobenzoate (85.6 mg, 0.40 mmol), afforded **4.5.1a** (86% NMR yield). After column chromatography purification (Hexane/EtOAc = 30:1) afforded (52 mg, 75%) as white solid. In an independent experiment, 49 mg (71% yield) were obtained, giving an average of 73% yield. **Mp** 92.8 – 93.7 $^\circ\text{C}$. ^1H NMR (400 MHz, CDCl_3) δ 7.90 (d, J = 8.3 Hz, 2H), 7.28 (d, J = 8.3 Hz, 2H), 3.87 (s, 3H), 2.47 (dd, J = 9.4, 4.2 Hz, 1H), 2.02 (dd, J = 13.4, 9.5 Hz, 1H), 1.51 (dd, J = 13.4, 4.2 Hz, 1H), 1.27 – 1.19 (m, 1H), 1.11 (brs, 12H), 0.88 (s, 9H) ppm. ^{13}C NMR (101 MHz, CDCl_3) δ 167.4, 150.9, 129.7, 128.3, 127.1, 83.6, 52.0, 46.1, 31.6, 29.8, 24.6, 24.5 ppm. ^{11}B NMR (128 MHz, CDCl_3) δ 34.09 ppm. **IR** (neat, cm^{-1}): 2976, 2950, 2898, 2868, 1716, 1607,

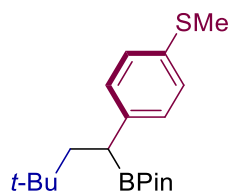
1468, 1436, 1364, 1326, 1275, 1182, 1135, 1106, 1020, 962. **HRMS** calcd. for (C₂₀H₃₂O₄B) [M+H]⁺: 346.2424 found 346.2427.



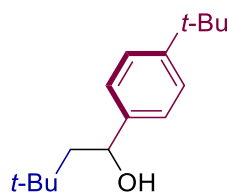
2-(3,3-dimethyl-1-(4-(trifluoromethyl)phenyl)butyl)-4,4,5,5-tetramethyl-1,3,2-dioxaborolane (4.5.4b): Following the general procedure, by using 1-bromo-4-(trifluoromethyl)benzene (56 μ L, 0.40 mmol), afforded **4.5.4b** (81% NMR yield). After column chromatography purification (Hexane/EtOAc = 40:1) afforded (53 mg, 74%) as white solid. In an independent experiment, 53 mg (74% yield) were obtained, giving an average of 74% yield. **Mp.** 93.8 – 94.9 °C. **¹H NMR** (400 MHz, CDCl₃) δ 7.48 (d, J = 8.0 Hz, 2H), 7.33 (d, J = 8.1 Hz, 2H), 2.47 (dd, J = 9.6, 4.0 Hz, 1H), 2.03 (dd, J = 13.4, 9.6 Hz, 1H), 1.50 (dd, J = 13.4, 4.0 Hz, 1H), 1.14 (brs, 12H), 0.90 (s, 9H) ppm. **¹³C NMR** (101 MHz, CDCl₃) δ 149.5 (q, J = 1.6 Hz), 128.5, 127.4 (q, J = 32.2 Hz), 125.3 (q, J = 3.7 Hz), 124.7 (q, J = 272.6 Hz), 83.6, 46.4, 31.6, 29.8, 24.7, 24.6 ppm. **¹⁹F NMR** (376 MHz, CDCl₃) δ -62.3 ppm. **¹¹B NMR** (128 MHz, CDCl₃) δ 33.29 ppm. **IR** (neat, cm⁻¹): 2999, 2860, 2868, 1615, 1470, 1365, 1320, 1257, 1165, 1140, 1109, 1067, 1018, 951. **GC-MS** calcd. for (C₁₉H₂₈O₂BF₃) [M]⁺: found t = 5.992 min, m/z = 356.2.



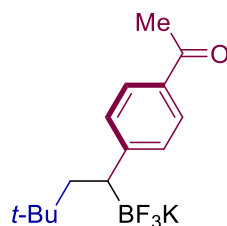
4-(3,3-dimethyl-1-(4,4,5,5-tetramethyl-1,3,2-dioxaborolan-2-yl)butyl)benzotrile (4.5.4c): Following the general procedure, by using 4-bromobenzotrile (72.8 mg, 0.40 mmol), afforded **4.5.4c** (70% NMR yield). After column chromatography purification (Hexane/EtOAc = 25:1) afforded (33 mg, 53%) as white solid. In an independent experiment, 30 mg (48% yield) were obtained, giving an average of 51% yield. **Mp.** 106.1 – 107.6 °C. **¹H NMR** (400 MHz, CDCl₃) δ 7.54 – 7.49 (m, 2H), 7.34 – 7.30 (m, 2H), 2.47 (dd, J = 9.3, 4.3 Hz, 1H), 2.01 (dd, J = 13.4, 9.3 Hz, 1H), 1.49 (dd, J = 13.4, 4.3 Hz, 1H), 1.13 (brs, 12H), 0.88 (s, 9H) ppm. **¹³C NMR** (101 MHz, CDCl₃) δ 151.2, 132.2, 129.0, 119.5, 108.9, 83.8, 46.0, 31.7, 29.8, 24.7, 24.6 ppm. **¹¹B NMR** (128 MHz, CDCl₃) δ 34.44 ppm. **IR** (neat, cm⁻¹): 2975, 2952, 2866, 2228, 1603, 1503, 1471, 1364, 1342, 1328, 1292, 1212, 1138, 962. **HRMS** calcd. for (C₁₉H₂₉NO₂B) [M+H]⁺: 313.2322 found 313.2323.



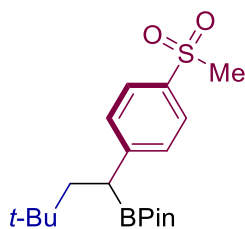
2-(3,3-dimethyl-1-(4-(methylthio)phenyl)butyl)-4,4,5,5-tetramethyl-1,3,2-dioxaborolane (4.5.4d): Following the general procedure, but using Ni(COD)₂ (4.1 mg, 7.5 mol%), **L4.5.2** (4.0 mg, 7.5 mol%), Ir(ppy)₂(bpy)PF₆ (3.2 mg, 2 mol%), LiCl (25.2 mg, 0.6 mmol) and 4-bromothioanisole (81.2 mg, 0.4 mmol), afforded **4.5.4d** (31.0 mg, 46% yield) as a light yellow solid. In another independent experiment, 32.1 mg (48 % yield) were obtained, giving an average of 47 % yield. **Mp.** 71.9 – 72.4 °C. ¹H NMR (400 MHz, CDCl₃) δ 7.15 (s, 4H), 2.45 (s, 3H), 2.35 (dd, *J* = 9.9, 3.9 Hz, 1H), 1.99 (dd, *J* = 13.3, 9.9 Hz, 1H), 1.46 (dd, *J* = 13.3, 3.9 Hz, 1H), 1.14 (d, *J* = 1.4 Hz, 12H), 0.89 (s, 9H) ppm. ¹³C NMR (101 MHz, CDCl₃) δ 142.1, 134.1, 128.7, 127.2, 83.3, 46.5, 31.4, 29.7, 24.6, 24.4, 16.4 ppm. ¹¹B NMR (128 MHz, CDCl₃) δ 33.48 ppm. **IR** (neat, cm⁻¹): 2953, 2862, 1466, 1438, 1362, 1319, 1209, 1139, 1012, 965, 863, 839, 814, 732, 692, 672. **GC-MS** calcd. for (C₁₉H₃₁BO₂S) [M]⁺: found *t* = 7.518 min, *m/z* = 334.2.



1-(4-(tert-Butyl)phenyl)-3,3-dimethylbutan-1-ol (4.5.4e'): Following the general procedure, but using Ni(COD)₂ (4.1 mg, 7.5 mol%), **L4.5.2** (4.0 mg, 7.5 mol%), Ir(ppy)₂(bpy)PF₆ (3.2 mg, 2 mol%), LiCl (25.2 mg, 0.6 mmol) and 1-bromo-4-(tert-butyl)benzene (70.0 μL, 0.40 mmol), afforded **4.5.4e** (71% and 69% NMR yields in two independent experiments) was subjected to the oxidation conditions and the corresponding oxidation product was collected as a white solid **4.5.4e'** (27.0 mg, 58% yield) through column purification (Hexane/EtOAc = 25:1 to 20:1). In an independent experiment, 29 mg (62% yield) were obtained, giving an average of 60% yield. **Mp.** 41.9 – 42.5 °C. ¹H NMR (400 MHz, CDCl₃) δ 7.37 (d, *J* = 8.4 Hz, 2H), 7.28 (d, *J* = 8.4 Hz, 2H), 4.82 (dd, *J* = 8.6, 3.3 Hz, 1H), 1.77 (dd, *J* = 14.5, 8.6 Hz, 1H), 1.64 (s, 1H), 1.60 (dd, *J* = 14.5, 3.3 Hz, 1H), 1.32 (s, 9H), 1.01 (s, 9H) ppm. ¹³C NMR (101 MHz, CDCl₃) δ 150.3, 143.5, 125.5, 125.4, 72.3, 52.8, 34.5, 31.4, 30.5, 30.2 ppm. **IR** (neat, cm⁻¹): 3401, 2948, 2865, 1505, 1464, 1370, 1280, 1081, 1011, 963, 738, 695. **HRMS** calcd. for (C₁₆H₂₆NaO) [M+Na]⁺: 257.1876 found 257.1877.

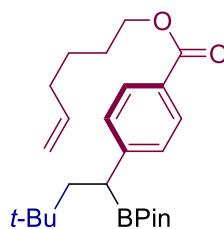


1-(4-(3,3-dimethyl-1-(trifluoroborate)butyl)phenyl)ethan-1-one, potassium salt (4.5.4f'): Following the general procedure, by using 4-bromo-acetophenone (80 mg, 0.40 mmol). After the reaction was completed, the crude reaction through Celite, the solvent was removed. The crude material was added to a round bottom flask equipped with a stirrer bar. MeOH (0.5 M) was added to the flask, and the solution was cooled to 0 °C in an ice-water bath. After cooling for 5 min, aq. KHF_2 (3.5 equiv, 4.5 M) was added dropwise via syringe. The ice-water bath was removed after completion of the addition, and the reaction was allowed to stir at rt overnight. The solvent was removed under vacuum and the resulting crude solid was taken up in boiling acetone (three to five portions), filtered to remove inorganic salts. The filtrate was concentrated via rotary evaporation, and the crude solid was washed with a 1:1 mixture of Pentane/ CH_2Cl_2 then CH_2Cl_2 to afford **4.5.4f'** (44.7 mg, 72% yield) as a colorless solid. In another independent experiment, 37.3 mg (60% yield) were obtained, giving an average of 66% yield. **Mp.** 152.4 – 153.2 °C. **$^1\text{H NMR}$** (400 MHz, d^6 -Acetone): δ 7.72 (d, $J = 8.4$ Hz, 2H), 7.27 (d, $J = 8.3$ Hz, 2H), 2.48 (s, 3H), 1.97 (s, 1H), 1.83 – 1.72 (m, 2H), 0.72 (s, 9H) ppm. **$^{13}\text{C NMR}$** (101 MHz, d^6 -Acetone): δ 196.6, 160.0, 132.1, 128.3, 127.1, 45.0, 32.1, 29.9, 25.5 ppm. **$^{11}\text{B NMR}$** (128 MHz, d^6 -Acetone) δ 4.44 ppm. **IR** (neat, cm^{-1}): 3622, 2950, 2906, 2862, 1668, 1598, 1416, 1363, 1278, 1179, 1165, 1085, 1046, 955. **HRMS** calcd. for $[\text{C}_{14}\text{H}_{19}\text{BF}_3\text{O}]^-$ $[\text{M-K}]^-$: 270.1523 found 270.1530.

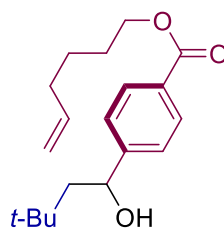


2-(3,3-dimethyl-1-(4-(methylsulfonyl)phenyl)butyl)-4,4,5,5-tetramethyl-1,3,2-dioxaborolane (4.5.4g): Following the general procedure, by using 1-bromo-4-(methylsulfonyl)benzene (94.1 mg, 0.40 mmol), afforded **4.5.4g** (48.4 mg, 66% yield) as a white solid. In another independent experiment, 57.1 mg (78% yield) were obtained, giving an average of 72% yield. **Mp.** 133.9 – 134.5 °C. **$^1\text{H NMR}$** (400 MHz, CDCl_3) δ 7.80 (d, $J = 8.4$ Hz, 2H), 7.41 (d, $J = 8.4$ Hz, 2H), 3.03 (s, 3H), 2.51 (dd, $J = 9.3, 4.1$ Hz, 1H), 2.10 – 1.97 (m, 1H), 1.50 (dd, $J = 13.3, 4.2$ Hz, 1H), 1.13 (s, 12H), 0.89 (s, 9H) ppm. **$^{13}\text{C NMR}$** (101 MHz, CDCl_3) δ 142.1, 134.1, 128.7, 127.2,

83.3, 46.5, 31.4, 29.7, 24.6, 24.4, 16.4 ppm. ^{11}B NMR (128 MHz, CDCl_3) δ 33.31 ppm. IR (neat, cm^{-1}): 2952, 1592, 1472, 1363, 133, 1299, 1136, 1088, 965, 839, 773, 729, 670. HRMS calcd. for $(\text{C}_{19}\text{H}_{31}\text{NaBO}_4\text{S})$ $[\text{M}+\text{Na}]^+$: 388.1965 found 388.1965.

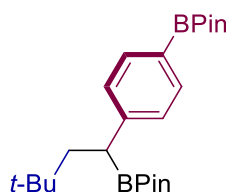


hex-5-en-1-yl 4-(3,3-dimethyl-1-(4,4,5,5-tetramethyl-1,3,2-dioxaborolan-2-yl)butyl)benzoate (4.5.4h): Following the general procedure, by using hex-5-en-1-yl 4-bromobenzoate (118.9 mg, 0.40 mmol), afforded **4.5.4h** (82% NMR yield). After column purification (Hexane/EtOAc = 30:1), afforded **4.5.4h** (49.8 mg, 60% yield) as a colorless oil. In another independent experiment, 48.1 mg (58% yield) were obtained, giving an average of 58% yield. ^1H NMR (400 MHz, CDCl_3) δ 7.91 (d, J = 8.4 Hz, 2H), 7.29 (d, J = 8.3 Hz, 2H), 5.82 (ddt, J = 16.9, 10.2, 6.7 Hz, 1H), 5.03 (ddd, J = 17.1, 3.5, 1.6 Hz, 1H), 4.97 (ddt, J = 10.2, 2.1, 1.2 Hz, 1H), 4.29 (t, J = 6.6 Hz, 2H), 2.47 (dd, J = 9.4, 4.2 Hz, 1H), 2.17 – 2.09 (m, 2H), 2.02 (dd, J = 13.4, 9.4 Hz, 1H), 1.81 – 1.73 (m, 2H), 1.59 – 1.49 (m, 3H), 1.13 (d, J = 1.3 Hz, 12H), 0.89 (s, 9H) ppm. ^{13}C NMR (101 MHz, CDCl_3) δ 166.9, 150.7, 138.4, 129.6, 128.1, 127.3, 114.8, 83.4, 64.6, 46.1, 33.3, 31.5, 29.7, 28.2, 25.3, 24.5, 24.4 ppm. ^{11}B NMR (128 MHz, CDCl_3) δ 32.34 ppm. IR (neat, cm^{-1}): 2977, 2950, 2905, 2866, 1718, 1608, 1365, 1326, 1273, 1143, 1107. HRMS calcd. for $(\text{C}_{25}\text{H}_{39}\text{NaBO}_4)$ $[\text{M}+\text{Na}]^+$: 437.2834 found 437.2828.

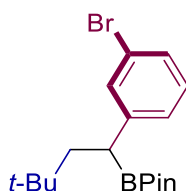


hex-5-en-1-yl 4-(1-hydroxy-3,3-dimethylbutyl)benzoate (4.5.4h'): **4.5.4h** was dissolved in a mixture of THF and H_2O (1:1, 8 mL). Then $\text{NaBO}_3 \cdot 4\text{H}_2\text{O}$ (654 mg, 0.40 mmol) was added portion wise. The reaction mixture was stirred at room temperature for 4 h. After the reaction was completed, water (20 mL) was added. The aqueous phase was extracted with EtOAc (3 x 20 mL), and the combined organic phases were dried over MgSO_4 and concentrated. The residue was purified by column chromatography (Hexane/EtOAc = 20:1), afforded **4.5.4h'** (80.3 mg, 66% yield after two steps) as a colorless oil. ^1H NMR (400 MHz, CDCl_3) δ 8.02 (d, J = 8.2 Hz, 2H), 7.42 (d, J = 8.1 Hz, 2H), 5.84 (ddt, J = 16.9, 10.1, 6.6 Hz, 1H), 5.12 – 4.96 (m, 2H), 4.90 (dt, J = 7.3, 3.2 Hz, 1H), 4.33 (t, J = 6.6 Hz, 2H), 2.15 (q, J = 7.3 Hz, 2H), 1.91

(s, 1H), 1.77 (ddd, $J = 14.6, 10.3, 7.7$ Hz, 3H), 1.63 – 1.49 (m, 3H), 1.02 (s, 9H) ppm. ^{13}C NMR (101 MHz, CDCl_3) δ 166.5, 151.5, 138.4, 129.8, 129.4, 125.6, 114.9, 72.1, 64.9, 53.0, 33.3, 30.6, 30.2, 28.2, 25.3 ppm. IR (neat, cm^{-1}): 3495, 2949, 1698, 1269, 1174, 1111, 1018, 991, 909, 858, 776, 745, 704. HRMS calcd. for $(\text{C}_{19}\text{H}_{28}\text{NaO}_3)$ $[\text{M}+\text{Na}]^+$: 327.1931 found 327.1935.

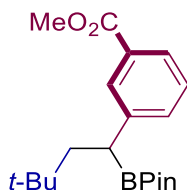


2-(4-(3,3-dimethyl-1-(4,4,5,5-tetramethyl-1,3,2-dioxaborolan-2-yl)butyl)phenyl)-4,4,5,5-tetramethyl-1,3,2-dioxaborolane (4.5.4i): Following the general procedure, by using 2-(4-bromophenyl)-4,4,5,5-tetramethyl-1,3,2-dioxaborolane (113.2 mg, 0.40 mmol), afforded **4.5.4i** (76% NMR yield). After column chromatography purification (Hexane/EtOAc = 30:1) afforded **4.5.4i** (49 mg, 59%) as white solid. In an independent experiment, 45 mg (55% yield) was obtained, giving an average of 57% yield. **Mp.** 134.8 – 136.1 °C. ^1H NMR (400 MHz, CDCl_3) δ 7.68 (d, $J = 8.1$ Hz, 2H), 7.27 – 7.21 (m, 2H), 2.41 (dd, $J = 9.7, 3.9$ Hz, 1H), 2.02 (dd, $J = 13.3, 9.7$ Hz, 1H), 1.50 (dd, $J = 13.4, 3.9$ Hz, 1H), 1.33 (s, 12H), 1.13 (left, s, 6H), 1.13 (right, s, 6H), 0.89 (s, 9H) ppm. ^{13}C NMR (101 MHz, CDCl_3) δ 148.6, 135.0, 127.8, 83.7, 83.4, 46.5, 31.6, 29.8, 25.04, 25.0, 24.7, 24.6 ppm. ^{11}B NMR (128 MHz, CDCl_3) δ 31.77 ppm. IR (neat, cm^{-1}): 2980, 2950, 2866, 1605, 1467, 1390, 1355, 1318, 1271, 1165, 1140, 1089, 1020, 972. HRMS calcd. for $(\text{C}_{24}\text{H}_{41}\text{O}_4\text{B}^{10}\text{B}^{11})$ $[\text{M}+\text{H}]^+$: 414.3222 found 414.3216.

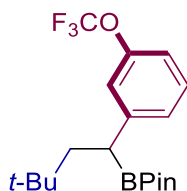


2-(1-(3-bromophenyl)-3,3-dimethylbutyl)-4,4,5,5-tetramethyl-1,3,2-dioxaborolane (4.5.4j): Following the general procedure, but using $\text{Ni}(\text{COD})_2$ (4.1 mg, 7.5 mol%), **L4.5.2** (4.0 mg, 7.5 mol%) and 1,3-dibromobenzene (49 μL , 0.40 mmol), afforded **4.5.4j** (58% NMR yield). After column purification (Hexane/EtOAc = 60:1 to 50:1) afforded **4.5.4j** (35.0 mg, 48% yield) as a light yellow solid. In another independent experiment, 34.8 mg (47% yield) were obtained, giving an average of 47% yield. **Mp.** 63.9 – 64.5 °C. ^1H NMR (400 MHz, CDCl_3) δ 7.42 (t, $J = 1.8$ Hz, 1H), 7.28 – 7.24 (m, 1H), 7.18 (dt, $J = 7.7, 1.3$ Hz, 1H), 7.12 (t, $J = 7.7$ Hz, 1H), 2.38 (dd, $J = 9.9, 3.8$ Hz, 1H), 2.02 (dd, $J = 13.3, 9.9$ Hz, 1H), 1.50 (dd, $J = 13.3, 3.9$ Hz, 1H), 1.18 (s, 12H), 0.93 (s, 9H) ppm. ^{13}C NMR (101 MHz, CDCl_3) δ 147.3, 131.2, 129.7, 128.1, 126.9, 122.3, 83.4, 46.4, 31.4, 29.6, 24.6, 24.4 ppm. ^{11}B NMR (128 MHz, CDCl_3) δ 33.26

ppm. **IR** (neat, cm^{-1}): 2951, 1563, 1472, 1364, 1324, 1207, 1139, 966, 852, 784, 686, 662. **HRMS** calcd. for $(\text{C}_{18}\text{H}_{28}\text{NaBBrO}_2) [\text{M}+\text{Na}]^+$: 389.1258 found 389.1263.

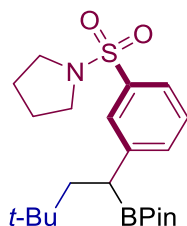


Methyl 3-(3,3-dimethyl-1-(4,4,5,5-tetramethyl-1,3,2-dioxaborolan-2-yl)butyl)benzoate (4.5.4k): Following the general procedure, but using $\text{Ni}(\text{COD})_2$ (4.1 mg, 7.5 mol%), **L4.5.2** (4.0 mg, 7.5 mol%), $\text{Ir}(\text{ppy})_2(\text{bpy})\text{PF}_6$ (3.2 mg, 2 mol%), LiCl (25.2 mg, 0.6 mmol) and methyl 3-bromobenzoate (86.1 mg, 0.40 mmol), afforded **4.5.4k** (78% NMR yield). After column purification (Hexane/EtOAc = 30:1), afforded **4.5.4k** (47.0 mg, 68% yield) as a white solid. In another independent experiment, 47.5 mg (68% yield) were obtained, giving an average of 68% yield. **Mp.** 96.5 – 97.1 °C. **^1H NMR** (400 MHz, CDCl_3) δ 7.94 (t, $J = 1.7$ Hz, 1H), 7.82 (dt, $J = 7.7, 1.4$ Hz, 1H), 7.45 (dt, $J = 7.7, 1.7$ Hz, 1H), 7.32 (t, $J = 7.7$ Hz, 1H), 3.92 (s, 3H), 2.48 (dd, $J = 9.7, 4.0$ Hz, 1H), 2.06 (dd, $J = 13.3, 9.8$ Hz, 1H), 1.53 (dd, $J = 13.4, 4.0$ Hz, 1H), 1.16 (s, 12H), 0.92 (s, 9H) ppm. **^{13}C NMR** (101 MHz, CDCl_3) δ 167.4, 145.3, 132.9, 130.1, 129.3, 128.2, 126.4, 83.4, 52.0, 46.4, 31.4, 29.7, 24.6, 24.4 ppm. **^{11}B NMR** (128 MHz, CDCl_3) δ 33.50 ppm. **IR** (neat, cm^{-1}): 2949, 1718, 1585, 1426, 1363, 1274, 1204, 1139, 1105, 1082, 965, 861, 836, 763, 714, 672. **GC-MS** calcd. for $(\text{C}_{20}\text{H}_{31}\text{BO}_4) [\text{M}]^+$: found $t = 7.359$ min, m/z 346.2.

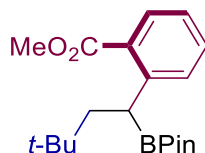


2-(3,3-dimethyl-1-(3-(trifluoromethoxy)phenyl)butyl)-4,4,5,5-tetramethyl-1,3,2-dioxaborolane (4.5.4l): Following the general procedure, but using $\text{Ni}(\text{COD})_2$ (4.1 mg, 7.5 mol%), **L4.5.2** (4.0 mg, 7.5 mol%), $\text{Ir}(\text{ppy})_2(\text{bpy})\text{PF}_6$ (3.2 mg, 2 mol%), LiCl (25.2 mg, 0.6 mmol) and 1-bromo-3-(trifluoromethoxy)benzene (96 mg, 0.40 mmol), afforded **4.5.4l** (78% NMR yield). After column chromatography purification (Hexane/EtOAc = 60:1) afforded **4.5.4l** (48 mg, 64%) as colorless oil. In an independent experiment, 45 mg (60% yield) were obtained, giving an average of 62% yield. **Mp.** 28.1 – 29.1 °C. **^1H NMR** (400 MHz, CDCl_3) δ 7.24 (t, $J = 8.0$ Hz, 1H), 7.19 – 7.09 (m, 2H), 7.00 – 6.94 (m, 1H), 2.42 (dd, $J = 9.8, 4.0$ Hz, 1H), 2.00 (dd, $J = 13.3, 9.8$ Hz, 1H), 1.49 (dd, $J = 13.3, 4.0$ Hz, 1H), 1.14 (brs, 12H), 0.90 (s, 9H) ppm. **^{13}C NMR** (101 MHz, CDCl_3) δ 149.4 (q, $J = 1.5$ Hz), 147.5, 129.5, 126.9, 120.8, 120.7 (q, $J = 280.4$ Hz), 117.7, 83.6, 46.4, 31.5, 29.8, 24.7, 24.5 ppm. **^{19}F NMR** (376 MHz, CDCl_3) δ -57.8 ppm. **^{11}B NMR** (128 MHz, CDCl_3) δ 33.44 ppm. **IR** (neat,

cm⁻¹): 2979, 2955, 2903, 2868, 1608, 1582, 1474, 1366, 1327, 1250, 1225, 1167, 1137, 960. **GC-MS** calcd. for (C₁₉H₂₈O₃BF₃) [M]⁺: found t = 5.915 min, m/z = 372.2.

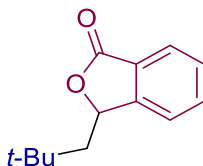


1-((3-(3,3-dimethyl-1-(4,4,5,5-tetramethyl-1,3,2-dioxaborolan-2-yl)butyl)phenyl)sulfonyl)pyrrolidine (4.5.4m): Following general procedure, by using 1-((3-bromophenyl)sulfonyl) pyrrolidine (116.2 mg, 0.40 mmol), afforded **4.5.4m** (78% NMR yield). After column purification (Hexane/DCM = 2:1 to 1:1, then Hexane/EtOAc = 3:1 to 2:1), afforded **4.5.4m** (59.0 mg, 72% yield) as a white solid. In another independent experiment, 54.3 mg (66% yield) were obtained, giving an average of 69% yield. **Mp.** 89.7 – 90.3 °C. **¹H NMR** (400 MHz, CDCl₃) δ 7.71 (t, *J* = 1.7 Hz, 1H), 7.58 (dt, *J* = 7.5, 1.5 Hz, 1H), 7.44 (dt, *J* = 7.6, 1.5 Hz, 1H), 7.37 (t, *J* = 7.6 Hz, 1H), 3.27 – 3.18 (m, 4H), 2.52 – 2.44 (m, 1H), 2.06 – 1.97 (m, 1H), 1.75 – 1.66 (m, 4H), 1.56 – 1.48 (m, 1H), 1.12 (s, 12H), 0.88 (s, 9H) ppm. **¹³C NMR** (101 MHz, CDCl₃) δ 146.4, 136.5, 132.6, 128.7, 127.1, 124.2, 83.5, 47.9, 46.1, 31.5, 29.7, 25.2, 24.5 (left), 24.5 (right) ppm. **¹¹B NMR** (128 MHz, CDCl₃) δ 33.86 ppm. **IR** (neat, cm⁻¹): 2952, 1467, 1364, 1328, 1206, 1139, 1083, 1005, 965, 860, 837, 760, 721, 701, 669. **HRMS** calcd. for (C₂₂H₃₇BNO₄S) [M+H]⁺: 421.2567 found 421.2574.

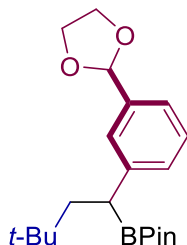


methyl 2-(3-(3,3-dimethyl-1-(4,4,5,5-tetramethyl-1,3,2-dioxaborolan-2-yl)butyl)benzoate (4.5.4n): Following general procedure, but using Ni(COD)₂ (4.1 mg, 7.5 mol%), **L4.5.2** (4.0 mg, 7.5 mol%), Ir(ppy)₂(bpy)PF₆ (3.2 mg, 2 mol%), LiCl (25.2 mg, 0.6 mmol) and methyl-2-bromobenzoate (86.1 mg, 0.40 mmol), afforded **4.5.4n** (70% NMR yield). After column purification (Hexane/EtOAc = 30:1), afforded **4.5.4n** (29.8 mg, 43% yield) as a colorless solid. In another independent experiment, 27.0 mg (39% yield) were obtained, giving an average of 41% yield. **Mp.** 35.6 – 36.3 °C. **¹H NMR** (400 MHz, CDCl₃) δ 7.80 – 7.75 (m, 1H), 7.40 – 7.32 (m, 2H), 7.15 (ddd, *J* = 7.9, 6.0, 2.6 Hz, 1H), 3.88 (s, 3H), 3.05 (t, *J* = 5.7 Hz, 1H), 2.04 (dd, *J* = 13.7, 7.1 Hz, 1H), 1.46 (dd, *J* = 13.7, 5.2 Hz, 1H), 1.15 (d, *J* = 13.9 Hz, 12H), 0.86 (s, 9H) ppm. **¹³C NMR** (101 MHz, CDCl₃) δ 168.6, 147.3, 131.5, 130.6, 130.4, 129.2, 124.8, 83.1, 51.9, 46.2, 31.8, 29.7, 24.8, 24.5 ppm. **¹¹B NMR** (128 MHz, CDCl₃) δ 33.08 ppm. **IR** (neat, cm⁻¹): 2950, 1718, 1474, 1364, 1319, 1267, 1143, 1079, 968,

845, 766, 719, 672. **GC-MS** calcd. for (C₂₀H₃₁BO₄) [M]⁺: found t = 6.918 min, m/z = 346.2.

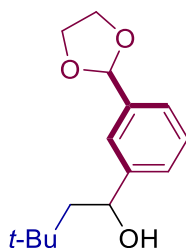


3-neopentylisobenzofuran-1(3H)-one (4.5.4n'): **4.5.4n** was dissolved in a mixture of THF and H₂O (1:1, 8 mL). Then NaBO₃·4H₂O (654 mg, 0.40 mmol) was added portion wise. The reaction mixture was stirred at room temperature for 4 h. After the reaction was completed, water (20 mL) was added. The aqueous phase was extracted with EtOAc (3 x 20 mL), and the combined organic phases were dried over MgSO₄ and concentrated. The residue was purified by column chromatography (Hexane/EtOAc = 20:1 to 10:1), afforded **4.5.4n'** (51.6 mg, 63% yield after two steps) as a white solid. **Mp.** 85.2 – 86.0 °C. **¹H NMR** (400 MHz, CDCl₃) δ 7.87 (d, *J* = 7.9 Hz, 1H), 7.66 (td, *J* = 7.5, 1.1 Hz, 1H), 7.50 (t, *J* = 7.5 Hz, 1H), 7.40 (dd, *J* = 7.7, 1.0 Hz, 1H), 5.52 (d, *J* = 10.4 Hz, 1H), 1.88 (dd, *J* = 15.0, 1.7 Hz, 1H), 1.57 (dd, *J* = 15.0, 10.5 Hz, 1H), 1.10 (s, 9H) ppm. **¹³C NMR** (101 MHz, CDCl₃) δ 170.8, 151.3, 133.9, 128.9, 125.8, 125.6, 121.7, 79.4, 49.5, 30.6, 29.9 ppm. **IR** (neat, cm⁻¹): 3405, 2948, 2866, 1751, 1464, 1367, 1347, 1285, 1214, 1081, 1044, 963, 771, 738, 695. **HRMS** calcd. for (C₁₃H₁₇O₂) [M+H]⁺: 205.1223 found 205.1227.

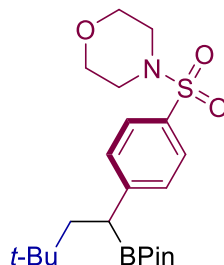


2-(1-(3-(1,3-dioxolan-2-yl)phenyl)-3,3-dimethylbutyl)-4,4,5,5-tetramethyl-1,3,2-dioxaborolane (4.5.4o): Following general procedure, but using Ni(COD)₂ (4.1 mg, 7.5 mol%), **L4.5.2** (4.0 mg, 7.5 mol%), Ir(ppy)₂(bpy)PF₆ (3.2 mg, 2 mol%), LiCl (25.2 mg, 0.6 mmol) and 2-(3-bromophenyl)-1,3-dioxolane (91.6 mg, 0.40 mmol), afforded **4.5.4o** (56% NMR yield). After column purification (Hexane/EtOAc = 20:1), afforded **4.5.4o** (29.5 mg, 41% yield) as a white solid. In another independent experiment, 28.8 mg (40% yield) were obtained, giving an average of 41% yield. **Mp.** 42.7 – 43.5 °C **¹H NMR** (400 MHz, CDCl₃) δ 7.34 (s, 1H), 7.25 – 7.21 (m, 3H), 5.77 (s, 1H), 4.14 – 3.99 (m, 4H), 2.41 (dd, *J* = 10.2, 3.5 Hz, 1H), 2.02 (dd, *J* = 13.3, 10.2 Hz, 1H), 1.49 (dd, *J* = 13.3, 3.6 Hz, 1H), 1.13 (s, 12H), 0.90 (s, 9H) ppm. **¹³C NMR** (101 MHz, CDCl₃) δ 144.9, 137.7, 129.1, 128.3, 126.5, 123.1, 104.0, 83.2, 65.2, 46.6, 31.4, 29.7, 24.6, 24.4 ppm. **¹¹B NMR** (128 MHz, CDCl₃) δ 33.01 ppm. **IR** (neat, cm⁻¹): 2948, 2884, 1472, 1362, 1322, 1140, 1070, 965, 863, 837, 803, 712, 672. **HRMS** calcd. for

(C₂₁H₃₄O₄B) [M+H]⁺: 360.2581 found 360.2587.

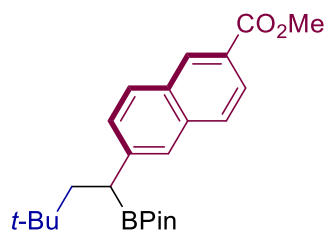


1-(3-(1,3-dioxolan-2-yl)phenyl)-3,3-dimethylbutan-1-ol (4.5.4o): **4.5.4o** was dissolved in a mixture of THF and H₂O (1:1, 8 mL). Then NaBO₃·4H₂O (654 mg, 0.40 mmol) was added portion wise. The reaction mixture was stirred at room temperature for 4 h. After the reaction was completed, water (20 mL) was added. The aqueous phase was extracted with EtOAc (3 x 20 mL), and the combined organic phases were dried over MgSO₄ and concentrated. The residue was purified by column chromatography (Hexane/EtOAc = 20:1 to 10:1), afforded **4.5.4o'** (50.1 mg, 50% yield after two steps) as a light yellow solid. **Mp.** 81.4 – 82.0 °C. **¹H NMR** (400 MHz, CDCl₃) δ 7.46 (d, *J* = 1.4 Hz, 1H), 7.38 – 7.32 (m, 3H), 5.79 (s, 1H), 4.84 (dd, *J* = 8.6, 3.3 Hz, 1H), 4.17 – 3.98 (m, 4H), 1.86 (s, 1H), 1.75 (dd, *J* = 14.6, 8.6 Hz, 1H), 1.58 (dd, *J* = 14.5, 3.3 Hz, 1H), 1.00 (s, 9H) ppm. **¹³C NMR** (101 MHz, CDCl₃) δ 146.8, 138.1, 128.6, 126.7, 125.5, 123.8, 103.7, 72.4, 65.3, 52.9, 30.6, 30.2 ppm. **IR** (neat, cm⁻¹): 3296, 2950, 2893, 1401, 1365, 1150, 1062, 964, 940, 895, 795, 751, 703. **HRMS** calcd. for (C₁₅H₂₂NaO₃) [M+Na]⁺: 273.1461 found 273.1462.

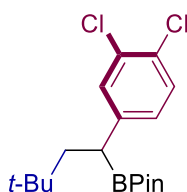


4-((3-(3,3-dimethyl-1-(4,4,5,5-tetramethyl-1,3,2-dioxaborolan-2-yl)butyl)phenyl)sulfonyl)morpholine (4.5.4p): Following the general procedure, but using Ni(COD)₂ (4.1 mg, 7.5 mol%), **L4.5.2** (4.0 mg, 7.5 mol%), Ir(ppy)₂(bpy)PF₆ (3.2 mg, 2 mol%), LiCl (25.2 mg, 0.6 mmol) and 4-((3-bromophenyl)sulfonyl)morpholine (122 mg, 0.40 mmol), afforded **4.5.4p** (68% NMR yield). After column chromatography purification (DCM/Et₂O = 1:2 to Hexane/EtOAc = 2:1) afforded (54 mg, 62%) as white solid. In an independent experiment, 50 mg (57% yield) were obtained, giving an average of 59% yield. **Mp.** 216.6 – 217.9 °C. **¹H NMR** (400 MHz, CDCl₃) δ 7.61 (d, *J* = 8.4 Hz, 2H), 7.39 (d, *J* = 8.4 Hz, 2H), 3.75 – 3.69 (m, 4H), 3.00 – 2.92 (m, 4H), 2.50 (dd, *J* = 9.5, 4.1 Hz, 1H), 2.03 (dd, *J* = 13.4, 9.5 Hz, 1H), 1.51 (dd, *J* = 13.3, 4.1 Hz, 1H), 1.12 (s, 12H), 0.89 (s, 9H) ppm. **¹³C NMR** (101 MHz, CDCl₃) δ 151.5, 131.5, 128.9, 128.0, 83.8, 66.3, 46.2, 46.1, 31.6, 29.7, 24.7, 24.5 ppm. **¹¹B NMR** (128 MHz, CDCl₃) δ

34.18 ppm. **IR** (neat, cm^{-1}): 2978, 2948, 2918, 2860, 1594, 1450, 1362, 1343, 1256, 1209, 1164, 1138, 1114, 1095, 1071, 940. **HRMS** calcd. for $(\text{C}_{22}\text{H}_{36}\text{NNaO}_5\text{SB}^{10})$ $[\text{M}+\text{Na}]^+$: 459.2336 found 459.2336.

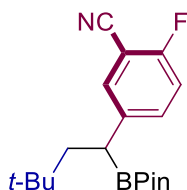


methyl 6-(3,3-dimethyl-1-(4,4,5,5-tetramethyl-1,3,2-dioxaborolan-2-yl)butyl)-2-naphthoate (4.5.4q): Following general procedure, by using methyl 6-bromo-2-naphthoate 106.1 mg, 0.40 mmol), afforded **4.5.4q** (74% NMR yield). After column purification (Hexane/EtOAc = 30:1), afforded **4.5.4q** (46.2 mg, 58% yield) as a white solid. In another independent experiment, 45.3 mg (57% yield) were obtained, giving an average of 57% yield. **Mp.** 103.8 – 104.7 °C. **^1H NMR** (400 MHz, CDCl_3) δ 8.54 (s, 1H), 8.00 (dd, $J = 8.6, 1.6$ Hz, 1H), 7.83 (d, $J = 8.5$ Hz, 1H), 7.78 (d, $J = 8.6$ Hz, 1H), 7.70 (s, 1H), 7.47 (dd, $J = 8.5, 1.6$ Hz, 1H), 3.96 (s, 3H), 2.61 (dd, $J = 9.6, 3.9$ Hz, 1H), 2.13 (dd, $J = 13.3, 9.6$ Hz, 1H), 1.61 (dd, $J = 13.3, 4.0$ Hz, 1H), 1.13 (d, $J = 2.6$ Hz, 12H), 0.93 (s, 9H) ppm. **^{13}C NMR** (101 MHz, CDCl_3) δ 167.4, 145.6, 136.0, 130.8, 130.7, 129.1, 128.3, 127.6, 126.3, 125.8, 125.1, 83.4, 52.1, 46.3, 31.5, 29.7, 24.6, 24.4 ppm. **^{11}B NMR** (128 MHz, CDCl_3) δ 33.29 ppm. **IR** (neat, cm^{-1}): 2950, 1712, 1628, 1474, 1432, 1363, 1322, 1287, 1233, 1192, 1137, 1095, 966, 862, 838, 758, 685, 669. **HRMS** calcd. for $(\text{C}_{24}\text{H}_{33}\text{NaBO}_4)$ $[\text{M}+\text{Na}]^+$: 419.2364 found 419.2357.

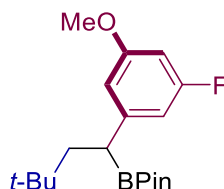


2-(1-(3,4-dichlorophenyl)-3,3-dimethylbutyl)-4,4,5,5-tetramethyl-1,3,2-dioxaborolane (4.5.4r): Following general procedure, by using 4-bromo-1,2-dichlorobenzene 51 μL , 0.40 mmol), afforded **4.5.4r** (91% NMR yield). After column purification (Hexane/EtOAc = 50:1), afforded **4.5.4r** (57.9 mg, 81% yield) as a white solid. In another independent experiment, 58.0 mg (81% yield) were obtained, giving an average of 81% yield. **Mp.** 101.1 – 101.9 °C. **^1H NMR** (400 MHz, CDCl_3) δ 7.34 (d, $J = 2.1$ Hz, 1H), 7.31 (d, $J = 8.3$ Hz, 1H), 7.08 (dd, $J = 8.3, 2.1$ Hz, 1H), 2.36 (dd, $J = 9.6, 4.1$ Hz, 1H), 1.99 (dd, $J = 13.4, 9.6$ Hz, 1H), 1.47 (dd, $J = 13.4, 4.1$ Hz, 1H), 1.17 (s, 12H), 0.91 (s, 9H) ppm. **^{13}C NMR** (101 MHz, CDCl_3) δ 145.4, 132.0, 130.0, 129.99, 128.8, 127.7, 83.5, 46.3, 31.4, 29.6, 24.6, 24.4 ppm. **^{11}B NMR** (128 MHz, CDCl_3) δ 33.00 ppm. **IR** (neat, cm^{-1}): 2965, 1483, 1374, 1309, 1129, 1024, 977, 857,

824, 736, 687. **GC-MS** calcd. for (C₁₈H₂₇BCl₂O₂) [M]⁺: found t = 7.254 min, m/z = 356.2.

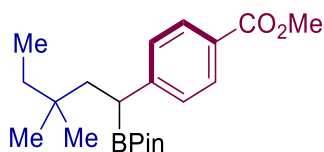


5-(3,3-dimethyl-1-(4,4,5,5-tetramethyl-1,3,2-dioxaborolan-2-yl)butyl)-2-fluorobenzonitrile (4.5.4s): Following general procedure, by using 5-bromo-2-fluorobenzonitrile (80.1 mg, 0.40 mmol), afforded **4.5.4s** (83% NMR yield). After column purification (Hexane/EtOAc = 30:1), afforded **4.5.4s** (47.9 mg, 72% yield) as a white solid. In another independent experiment, 46.0 mg (69% yield) were obtained, giving an average of 71% yield. **Mp.** 102.4 – 102.8 °C. **¹H NMR** (400 MHz, CDCl₃) δ 7.50 – 7.43 (m, 2H), 7.09 (t, *J* = 8.7 Hz, 1H), 2.42 (dd, *J* = 9.4, 4.3 Hz, 1H), 1.99 (dd, *J* = 13.4, 9.4 Hz, 1H), 1.45 (dd, *J* = 13.4, 4.4 Hz, 1H), 1.17 (s, 12H), 0.90 (s, 9H) ppm. **¹³C NMR** (101 MHz, CDCl₃) δ 161.1 (d, *J* = 256.1 Hz), 142.1 (d, *J* = 3.7 Hz), 134.8 (d, *J* = 7.8 Hz), 132.5, 116.0 (d, *J* = 19.3 Hz), 114.3, 101.0 (d, *J* = 15.3 Hz), 83.7, 46.4, 31.5, 29.6, 24.6, 24.4 ppm. **¹¹B NMR** (128 MHz, CDCl₃) δ 32.81 ppm. **¹⁹F NMR** (376 MHz, CDCl₃) δ -112.18 – 112.54 (m, 1F) ppm. **IR** (neat, cm⁻¹): 2953, 2235, 1605, 1496, 1475, 1364, 1324, 1135, 968, 897, 862, 938, 792, 671. **HRMS** calcd. for (C₁₉H₂₈BFNO₂) [M+H]⁺: 331.2228 found 331.2222.

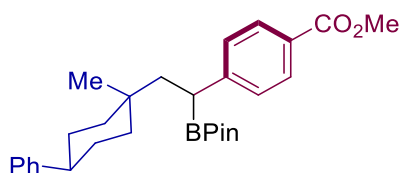


2-(1-(3-fluoro-5-methoxyphenyl)-3,3-dimethylbutyl)-4,4,5,5-tetramethyl-1,3,2-dioxaborolane (4.5.4t): Following general procedure, but using Ni(COD)₂ (4.1 mg, 7.5 mol%), **L4.5.2** (4.0 mg, 7.5 mol%), Ir(ppy)₂(bpy)PF₆ (3.2 mg, 2 mol%), LiCl (25.2 mg, 0.6 mmol) and 1-bromo-3-fluoro-5-methoxybenzene (82.0 mg, 0.40 mmol), afforded **4.5.4t** (74% NMR yield). After column purification (Hexane/EtOAc = 30:1 to 20:1), afforded **4.5.4t** (41.9 mg, 62% yield) as a white solid. In another independent experiment, 43.3 mg (64% yield) were obtained, giving an average of 63% yield. **Mp.** 46.7 – 47.5 °C. **¹H NMR** (400 MHz, CDCl₃) δ 6.59 – 6.53 (m, 2H), 6.37 (dt, *J* = 10.7, 2.3 Hz, 1H), 2.34 (dd, *J* = 9.7, 3.9 Hz, 1H), 1.96 (dd, *J* = 13.3, 9.7 Hz, 1H), 1.47 (dd, *J* = 13.3, 3.9 Hz, 1H), 1.16 (s, 12H), 0.89 (s, 9H) ppm. **¹³C NMR** (101 MHz, CDCl₃) δ 163.5 (d, *J* = 243.7 Hz), 160.6 (d, *J* = 11.8 Hz), 148.1 (d, *J* = 9.1 Hz), 109.5 (d, *J* = 1.7 Hz), 107.3 (d, *J* = 21.6 Hz), 98.4 (d, *J* = 25.3 Hz), 83.4, 55.4, 46.3, 31.4, 29.6, 24.6, 24.4 ppm. **¹¹B NMR** (128 MHz, CDCl₃) δ 33.21 ppm. **¹⁹F NMR** (376 MHz, CDCl₃) δ -112.96 (t, *J* = 10.2 Hz, 1F) ppm. **IR** (neat, cm⁻¹): 2952, 1617, 1583, 1465,

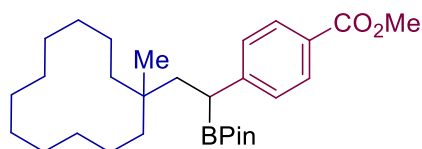
1363, 1319, 1295, 1196, 1136, 1067, 982, 857, 824, 686. **HRMS** calcd. for (C₁₉H₃₀FN₂NaFO₃B¹⁰) [M+Na]⁺: 358.2201 found 358.2202



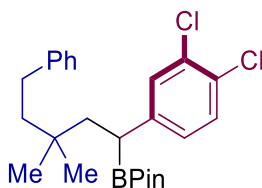
methyl 4-(3,3-dimethyl-1-(4,4,5,5-tetramethyl-1,3,2-dioxaborolan-2-yl)pentyl)benzoate (4.5.5a): Following general procedure, by using 2-bromo-2-methylbutane (65 μ L, 0.5 mmol), afforded **4.5.5a** (68% NMR yield). After column chromatography purification (Hexane/EtOAc = 30:1), afforded **4.5.5a** (41.2 mg, 57% yield) as a white solid. In another independent experiment, 42.0 mg (58% yield) were obtained, giving an average of 57% yield. **Mp.** 74.9 – 75.8 °C. **¹H NMR** (400 MHz, CDCl₃) δ 7.90 (d, J = 8.4 Hz, 2H), 7.29 (d, J = 8.3 Hz, 2H), 3.88 (s, 3H), 2.44 (dd, J = 9.4, 4.0 Hz, 1H), 1.99 (dd, J = 13.5, 9.4 Hz, 1H), 1.51 (dd, J = 13.5, 4.0 Hz, 1H), 1.24 (q, J = 7.5 Hz, 2H), 1.12 (s, 12H), 0.82 (s, 6H), 0.77 (t, J = 7.5 Hz, 3H) ppm. **¹³C NMR** (101 MHz, CDCl₃) δ 167.3, 150.9, 129.6, 128.2, 126.9, 83.4, 51.9, 43.7, 34.3, 33.9, 26.8, 26.7, 24.5, 24.4, 8.4 ppm. **¹¹B NMR** (128 MHz, CDCl₃) δ 33.27 ppm. **IR** (neat, cm⁻¹): 2957, 1715, 1604, 1433, 1332, 1274, 1169, 1135, 1102, 1013, 965, 859, 840, 777, 716, 684. **HRMS** calcd. for (C₂₁H₃₄BO₄) [M+H]⁺: 361.2545 found 361.2553.



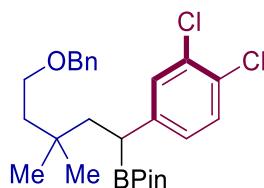
methyl 4-(2-(1-methyl-4-phenylcyclohexyl)-1-(4,4,5,5-tetramethyl-1,3,2-dioxaborolan-2-yl)ethyl)benzoate (4.5.5b): Following general procedure, by using (4-bromo-4-methylcyclohexyl) benzene (126.6 mg, 0.5 mmol), afforded **4.5.5b** (62% NMR yield). After column chromatography purification (Hexane/EtOAc = 30:1), afforded **4.5.5b** (47.4 mg, 51% yield, dr = 2.83:1) as a white solid. In another independent experiment, 47.0 mg (51% yield) were obtained, giving an average of 51% yield. **Mp.** 122.8 – 123.6 °C. **¹H NMR** (400 MHz, CDCl₃) δ 8.00 – 7.93 (m, 2H), 7.40 – 7.34 (m, 1H), 7.32 – 7.27 (m, 2H), 7.26 – 7.16 (m, 3H), 3.92 (s, 3H), 2.63 – 2.38 (m, 2H), 2.30 – 2.06 (m, 1H), 1.83 – 1.27 (m, 11H), 1.17 (d, J = 2.9 Hz, 12H), 0.99 (s, 3H) ppm. **¹³C NMR** (101 MHz, CDCl₃) δ 167.3, 151.0, 150.9, 147.6, 129.7, 129.7, 128.27, 128.25, 128.19, 127.1, 127.0, 126.9, 126.8, 125.84, 125.79, 83.5, 51.9, 48.2, 44.6, 44.4, 38.5, 38.3, 38.2, 38.0, 37.9, 33.5, 33.2, 29.84, 29.80, 29.75, 29.7, 29.5, 24.7, 24.5, 24.4, 24.3, 21.8 ppm. **¹¹B NMR** (128 MHz, CDCl₃) δ 33.27 ppm. **IR** (neat, cm⁻¹): 2929, 2843, 1705, 1601, 1437, 1340, 1281, 1146, 1103, 1008, 996, 879, 763, 698. **HRMS** calcd. for C₂₉H₄₀O₄B¹⁰ [M+H]⁺: 462.3050 found 462.3051.



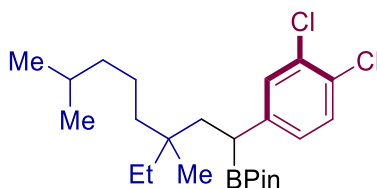
methyl 4-(2-(1-methylcyclododecyl)-1-(4,4,5,5-tetramethyl-1,3,2-dioxaborolan-2-yl)ethyl)benzoate (4.5.5c): Following general procedure, by using 1-bromo-1-methylcyclododecane (130.1 mg, 0.5 mmol), afforded **4.5.5c** (72% NMR yield). After column chromatography purification (Hexane/EtOAc = 30:1), afforded **4.5.5c** (60.2 mg, 64% yield) as a white solid. In another independent experiment, 62.2 mg (66% yield) were obtained, giving an average of 65% yield. **Mp.** 122.8 – 123.6 °C. $^1\text{H NMR}$ (400 MHz, CDCl_3) δ 7.90 (d, $J = 8.4$ Hz, 2H), 7.29 (d, $J = 8.4$ Hz, 2H), 3.88 (s, 3H), 2.46 (dd, $J = 9.7, 3.4$ Hz, 1H), 1.97 (dd, $J = 13.5, 9.7$ Hz, 1H), 1.47 (dd, $J = 13.5, 3.5$ Hz, 1H), 1.34 – 1.16 (m, 22H), 1.12 (s, 12H), 0.78 (s, 3H) ppm. $^{13}\text{C NMR}$ (101 MHz, CDCl_3) δ 167.3, 151.1, 129.6, 128.2, 126.9, 83.4, 51.9, 43.1, 36.4, 35.2, 33.6, 26.9, 26.8, 26.2, 25.4, 24.5, 24.4, 22.7, 22.6, 22.2, 22.1, 19.2 ppm. $^{11}\text{B NMR}$ (128 MHz, CDCl_3) δ 33.00 ppm. **IR** (neat, cm^{-1}): 2930, 2846, 1722, 1607, 1470, 1439, 1335, 1278, 1138, 1110, 1016, 997, 861, 771, 717, 682. **HRMS** calcd. for $\text{C}_{29}\text{H}_{48}\text{O}_4\text{B}$ $[\text{M}+\text{H}]^+$: 470.3676 found 470.3673.



2-(1-(3,4-Dichlorophenyl)-3,3-dimethyl-5-phenylpentyl)-4,4,5,5-tetramethyl-1,3,2-dioxaborolane (4.5.5d): Following general procedure, by using (3-bromo-3-methylbutyl)benzene (136.3 mg, 0.6 mmol) and 4-bromo-1,2-dichlorobenzene (51 μL , 0.40 mmol), afforded **4.5.5d** (53% NMR yield). After column chromatography purification (Hexane/EtOAc = 50:1) afforded **4.5.5d** (40.1 mg, 45% yield) as a white solid. In another independent experiment, 39.8 mg (45% yield) were obtained, giving an average of 45% yield. **Mp.** 59.9 – 61.6 °C. $^1\text{H NMR}$ (400 MHz, CDCl_3) δ 7.36 (d, $J = 2.1$ Hz, 1H), 7.32 (d, $J = 8.3$ Hz, 1H), 7.31 – 7.26 (m, 2H), 7.21 – 7.14 (m, 3H), 7.10 (dd, $J = 8.3, 2.1$ Hz, 1H), 2.62 – 2.46 (m, 2H), 2.39 (dd, $J = 9.5, 3.9$ Hz, 1H), 2.04 (dd, $J = 13.5, 9.5$ Hz, 1H), 1.59 – 1.49 (m, 3H), 1.14 (d, $J = 2.2$ Hz, 12H), 0.97 (d, $J = 2.2$ Hz, 6H) ppm. $^{13}\text{C NMR}$ (101 MHz, CDCl_3) δ 145.3, 143.3, 132.1, 130.1, 130.0, 128.9, 128.3 (left), 128.3 (right), 127.7, 125.6, 83.6, 44.6 (left), 44.6 (right), 34.1, 30.8, 27.3, 27.1, 24.6, 24.4 ppm. $^{11}\text{B NMR}$ (128 MHz, CDCl_3) δ 32.63 ppm. **IR** (neat, cm^{-1}): 2954, 2930, 1706, 1467, 1365, 1324, 1140, 1029, 996, 743, 698, 677. **HRMS** calcd. for $(\text{C}_{25}\text{H}_{34}\text{BCl}_2\text{O}_2)$ $[\text{M}+\text{H}]^+$: 447.2023 found 447.2033.

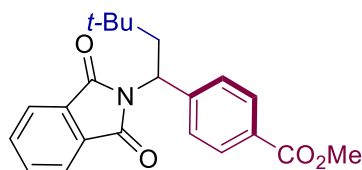


2-(5-(Benzyloxy)-1-(3,4-dichlorophenyl)-3,3-dimethylpentyl)-4,4,5,5-tetraethyl-1,3,2-dioxaborolane (4.5.5e): Following general procedure, by using ((3-bromo-3-methylbutoxy)methyl)benzene (154.3 mg, 0.6 mmol) and 4-bromo-1,2-dichlorobenzene (51 μ L, 0.40 mmol), afforded **4.5.5e** (55% NMR yield). After column chromatography purification (Hexane/EtOAc = 50:1), afforded **4.5.5e** (45.1 mg, 47% yield) as a colorless oil. In another independent experiment 44.8 mg (47% yield) were obtained, giving an average of 47% yield. $^1\text{H NMR}$ (400 MHz, CDCl_3) δ 7.34 – 7.25 (m, 7H), 7.04 (dd, $J = 8.3, 2.1$ Hz, 1H), 4.47 (s, 2H), 3.53 – 3.47 (m, 2H), 2.35 (dd, $J = 9.5, 3.9$ Hz, 1H), 2.00 (dd, $J = 13.5, 9.5$ Hz, 1H), 1.61 (t, $J = 7.3$ Hz, 2H), 1.50 (dd, $J = 13.5, 3.9$ Hz, 1H), 1.16 (s, 12H), 0.91 (d, $J = 1.9$ Hz, 6H) ppm. $^{13}\text{C NMR}$ (101 MHz, CDCl_3) δ 145.2, 138.6, 132.0, 130.1, 130.0, 128.9, 128.4, 127.7, 127.6, 127.5, 83.6, 73.0, 67.4, 44.8, 41.2, 33.3, 27.7, 27.5, 24.6, 24.4 ppm. $^{11}\text{B NMR}$ (128 MHz, CDCl_3) δ 32.38 ppm. **IR** (neat, cm^{-1}): 2955, 2868, 1443, 1369, 1329, 1144, 1093, 1028, 981, 850, 822, 735, 697, 672. **HRMS** calcd. for $(\text{C}_{27}\text{H}_{39}\text{BCl}_2\text{NaO}_4)$ $[\text{M}+\text{Na}+\text{MeOH}]^+$: 531.2211 found 340.2244.

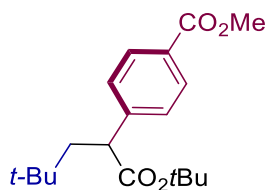


2-(1-(3,4-Dichlorophenyl)-3-ethyl-3,7-dimethyloctyl)-4,4,5,5-tetramethyl-1,3,2-dioxaborolane (4.5.5f): Following general procedure, by using 6-bromo-2,6-dimethyloctane (132.7 mg, 0.6 mmol) and 4-bromo-1,2-dichlorobenzene (51 μ L, 0.40 mmol), afforded **4.5.5f** (56% NMR yield). After column chromatography purification (Hexane/EtOAc = 50:1) afforded **4.5.5f** (40.0 mg, 45% yield, dr = 1:1) as a slightly yellow oil. In another independent experiment 41.5 mg (47% yield) were obtained, giving an average of 46% yield. $^1\text{H NMR}$ (400 MHz, CDCl_3) δ 7.32 (d, $J = 2.1$ Hz, 1H), 7.28 (d, $J = 8.3$ Hz, 1H), 7.06 (dd, $J = 8.3, 2.1$ Hz, 1H), 2.28 (dt, $J = 9.0, 4.5$ Hz, 1H), 1.90 (ddd, $J = 13.6, 9.1, 4.5$ Hz, 1H), 1.53 – 1.41 (m, 2H), 1.28 – 1.19 (m, 3H), 1.15 (d, $J = 2.5$ Hz, 12H), 1.12 – 1.06 (m, 8H), 0.84 (dd, $J = 6.6, 1.6$ Hz, 6H), 0.78 (d, $J = 2.6$ Hz, 3H), 0.74 (td, $J = 7.5, 1.0$ Hz, 3H) ppm. $^{13}\text{C NMR}$ (101 MHz, CDCl_3) δ 145.6, 132.0, 130.1, 130.0, 128.7, 127.8, 83.5, 41.9, 41.6, 40.0, 39.9, 39.3, 38.9, 36.2, 31.6, 31.5, 28.0, 27.9, 24.6, 24.4, 22.71, 22.7, 22.64, 22.6, 21.24, 21.2, 8.1 ppm. $^{11}\text{B NMR}$ (128 MHz, CDCl_3) δ 33.19 ppm. **IR** (neat, cm^{-1}):

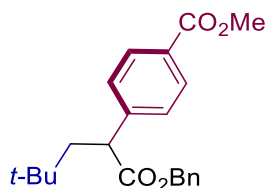
2954, 2929, 1465, 1437, 1379, 1324, 1144, 1029, 980, 851, 820, 751, 727, 670. **HRMS** calcd. for (C₂₄H₄₀BCl₂O₂) [M+H]⁺: 337.2345 found 340.2244.



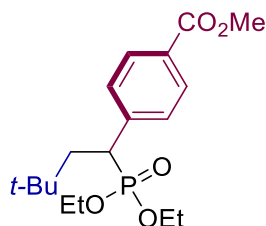
Methyl 4-(1-(1,3-dioxisoindolin-2-yl)-3,3-dimethylbutyl)benzoate (4.5.5g): Following general procedure, but using Ni(COD)₂ (4.1 mg, 7.5 mol%), **L4.5.2** (4.0 mg, 7.5 mol%) and 2-vinylisoindoline-1,3-dione (34.6 mg, 0.2 mmol), afforded **4.5.5g** (73% NMR yield). After column purification (Hexane/EtOAc = 20:1 to 10:1), afforded **4.5.5g** (48.0 mg, 66% yield) as a yellow solid. In another independent experiment, 46.6 mg (64% yield) were obtained, giving an average of 65% yield. **Mp.** 118.5 – 119.4 °C. **¹H NMR** (400 MHz, CDCl₃) δ 7.97 (d, *J* = 8.5 Hz, 2H), 7.79 (dd, *J* = 5.5, 3.0 Hz, 2H), 7.67 (dd, *J* = 5.5, 3.0 Hz, 2H), 7.63 (d, *J* = 8.3 Hz, 2H), 5.54 (dd, *J* = 9.1, 4.5 Hz, 1H), 3.87 (s, 3H), 2.74 (dd, *J* = 14.7, 9.1 Hz, 1H), 2.11 (dd, *J* = 14.7, 4.6 Hz, 1H), 0.93 (s, 9H) ppm. **¹³C NMR** (101 MHz, CDCl₃) δ 168.2, 166.7, 146.1, 134.0, 131.8, 129.9, 129.4, 128.3, 123.3, 52.1, 51.6, 43.7, 30.8, 29.6 ppm. **IR** (neat, cm⁻¹): 2955, 1769, 1700, 1610, 1465, 1384, 1356, 1277, 1098, 1020, 887, 858, 774, 720. **HRMS** calcd. for C₂₂H₂₃NNaO₄ [M+Na]⁺: 388.1519 found 388.1516.



methyl 4-(1-(tert-butoxy)-4,4-dimethyl-1-oxopentan-2-yl)benzoate (4.5.5h): Following the general procedure, but using **L4.5.2** (4.0 mg, 7.5 mol%), 2-bromo-2-methylpropane (**4.5.3a**, 67 μL, 0.60 mmol) and *tert*-butyl acrylate (**4.5.2c**, 29 μL, 0.2 mmol) for 36 h. After column chromatography purification (Hexane/EtOAc = 60:1) afforded **4.5.5h** (39 mg, 60%) as white solid. In an independent experiment, 39 mg (61% yield) were obtained, giving an average of 61% yield. **Mp.** 64.6 – 65.7 °C. **¹H NMR** (400 MHz, CDCl₃) δ 8.03 – 7.92 (m, 2H), 7.43 – 7.33 (m, 2H), 3.90 (s, 3H), 3.58 (dd, *J* = 9.0, 3.7 Hz, 1H), 2.27 (dd, *J* = 14.0, 9.0 Hz, 1H), 1.50 (dd, *J* = 14.0, 3.8 Hz, 1H), 1.36 (s, 9H), 0.90 (s, 9H) ppm. **¹³C NMR** (101 MHz, CDCl₃) δ 173.3, 167.1, 147.0, 130.0, 128.8, 127.9, 80.9, 52.2, 49.6, 47.1, 31.3, 29.6, 27.9 ppm. **IR** (neat, cm⁻¹): 2999, 2950, 2932, 2871, 1718, 1608, 1462, 1439, 1365, 1277, 1220, 1193, 1145, 1105, 1022, 953. **HRMS** calcd. for (C₁₉H₂₈NaO₄) [M+Na]⁺: 343.1880 found 343.1880.



methyl 4-(1-(benzyloxy)-4,4-dimethyl-1-oxopent-2-yl)benzoate (4.5.5i): Following the general procedure, but using **L4.5.2** (4.0 mg, 7.5 mol%), 2-bromo-2-methylpropane (**4.5.3a**, 67 μ L, 0.60 mmol) and benzyl acrylate (**4.5.2d**, 32.4 mg, 0.2 mmol) for 36 h. After column chromatography purification (Hexane/EtOAc = 60:1), afforded **4.5.5h** (34 mg, 58%) as white solid. In an independent experiment, 37 mg (52% yield) were obtained, giving an average of 50% yield. **Mp.** 43.6 – 44.5 °C. **$^1\text{H NMR}$** (400 MHz, CDCl_3) δ 8.02 – 7.93 (m, 2H), 7.43 – 7.39 (m, 2H), 7.34 – 7.27 (m, 3H), 7.26 – 7.21 (m, 2H), 5.17 – 5.00 (m, 2H), 3.91 (s, 3H), 3.78 (dd, $J = 8.9, 4.0$ Hz, 1H), 2.34 (dd, $J = 14.0, 8.9$ Hz, 1H), 1.61 (dd, $J = 14.0, 4.1$ Hz, 1H), 0.89 (s, 9H) ppm. **$^{13}\text{C NMR}$** (101 MHz, CDCl_3) δ 173.9, 166.9, 146.0, 135.7, 130.0, 129.1, 128.56, 128.3, 128.2, 128.0, 66.9, 52.1, 48.4, 47.2, 31.2, 29.5 ppm. **IR** (neat, cm^{-1}): 3421, 2951, 2865, 1721, 1609, 1450, 1436, 1365, 1274, 1254, 1199, 1164, 1141, 1104, 1020, 955. **HRMS** calcd. for $(\text{C}_{22}\text{H}_{27}\text{O}_4)$ $[\text{M}+\text{H}]^+$: 355.1904 found 355.1897.

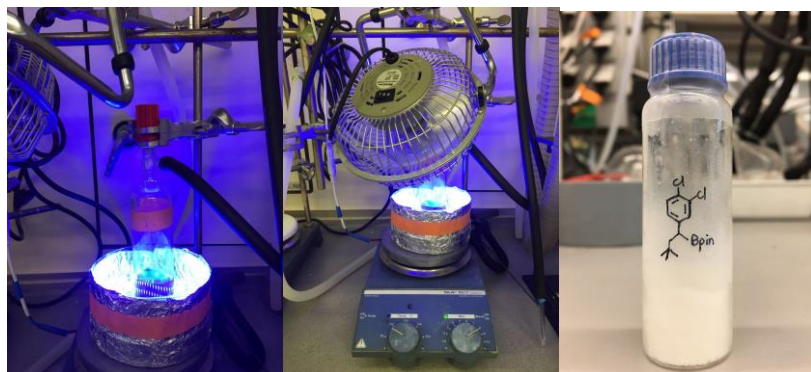
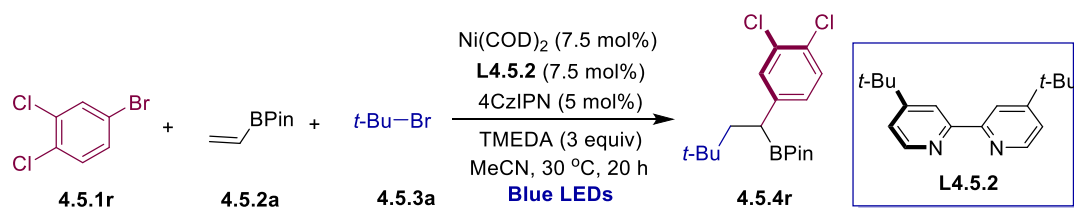


methyl 4-(1-(diethoxyphosphoryl)-3,3-dimethylbutyl)benzoate (4.5.5j): Following the general procedure, but using **L4.5.2** (4.0 mg, 7.5 mol%), 2-bromo-2-methylpropane (**4.5.3a**, 67 μ L, 0.60 mmol) and diethyl vinylphosphonate (**4.5.2e**, 31 μ L, 0.2 mmol) for 36 h. After column chromatography purification (Hexane/EtOAc = 2:1 to 1:1), afforded **4.5.5j** (39 mg, 55%) as colorless oil. In an independent experiment, 36 mg (50% yield) were obtained, giving an average of 52% yield. **$^1\text{H NMR}$** (400 MHz, CDCl_3) δ 8.04 – 7.90 (m, 2H), 7.52 – 7.37 (m, 2H), 4.14 – 3.97 (m, 2H), 3.89 (s, 3H), 3.87 – 3.80 (m, 1H), 3.70 – 3.60 (m, 1H), 3.23 – 3.14 (m, 1H), 2.10 – 1.96 (m, 2H), 1.26 (t, $J = 7.1$ Hz, 3H), 1.06 (td, $J = 7.0, 0.6$ Hz, 3H), 0.75 (s, 9H) ppm. **$^{13}\text{C NMR}$** (101 MHz, CDCl_3) δ 167.1 (d, $J = 1.5$ Hz), 143.9 (d, $J = 8.0$ Hz), 129.7, 129.69 (d, $J = 3.2$ Hz), 128.9 (d, $J = 3.5$ Hz), 62.8 (d, $J = 7.0$ Hz), 62.1 (d, $J = 7.4$ Hz), 52.2, 42.9 (d, $J = 4.0$ Hz), 42.0 (d, $J = 135.3$ Hz), 32.0 (d, $J = 14.8$ Hz), 29.8, 16.5 (d, $J = 6.0$ Hz), 16.4 (d, $J = 5.8$ Hz) ppm. **$^{31}\text{P NMR}$** (162 MHz, CDCl_3) δ 31.87 – 31.33 (m) ppm. **IR** (neat, cm^{-1}): 2975, 2954, 2908, 2867, 1721, 1610, 1475,

Site-Selective 1,2-Dicarbofunctionalization of Vinyl Boronates through Dual Catalysis

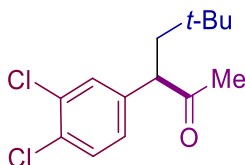
1436, 1367, 1278, 1243, 1182, 1102, 1048, 1020, 939. **HRMS** calcd. for (C₁₈H₃₀O₅P)
[M+H]⁺: 357.1825 found 357.1827.

4.8.5 Gram Scale Reaction

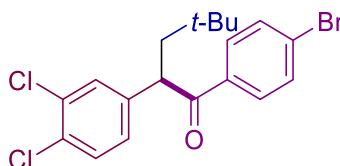


An oven-dried 250 mL Schlenk tube containing a stirring bar was charged with 4CzIPN (197.5 mg, 5 mol%), 4,4'-di-*tert*-butyl-2,2'-bipyridine (**L4.5.2**, 100.7 mg, 7.5 mol%). Subsequently, the tube was evacuated and back-filled with N₂ (3 times) and brought into the glovebox. The corresponding nickel sources: Ni(COD)₂ (103.1 mg, 7.5 mol%) was added. Afterwards, the tube was brought out, then 3,4-dichlorophenyl bromide (**4.5.1r**, 1.275 mL, 10 mmol, 2.0 equiv), Vinyl Bpin (**4.5.2a**, 0.865 mL, 5 mmol, 1.0 equiv), 2-bromo-2-methylpropane (**4.5.3a**, 1.4 mL, 12.5 mmol, 2.5 equiv), TMEDA (2.25 mL, 15 mmol, 3.0 equiv) and anhydrous MeCN (75 mL) were added via syringe under N₂. Then, the tube was stirred at 30 °C under irradiation of blue LEDs with a fan for 48 hours. After the reaction was completed, the mixture was diluted with EtOAc, filtered through silica gel to remove inorganic salts and concentrated under vacuum. ¹H NMR yield (81%) were determined by using CH₂Br₂ as internal standard. The product was purified by column chromatography on silica gel (Hexane/EtOAc = 60:1 to 50:1), obtaining **4.5.4r** (1.302 g, 71% yield) as white solid.

4.8.6 Synthetic Applicability

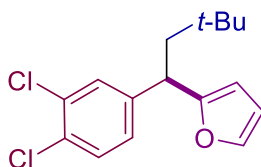


3-(3,4-dichlorophenyl)-5,5-dimethylhexan-2-one (4.5.6): *t*-BuLi (1.7 M in pentane, 0.34 mL, 0.5 mmol) was added dropwise to a solution of ethyl vinyl ether (76 μ L, 0.8 mmol) in THF (2.5 mL) at -78 °C. The resulting solution was stirred at -78 °C for 30 min, allowed to warm up to 0 °C, stirred for 30 min and cooled back to -78 °C. A solution of **4.5.4r** (71.4 mg, 0.2 mmol) in THF (1 mL) was then added dropwise. The resulting solution was stirred at -78 °C for 30 min, allowed to warm up to room temperature, stirred for 5 min and cooled back to -78 °C. A solution of I_2 (206 mg, 0.76 mmol) in THF (2 mL) was then added dropwise. The resulting solution was stirred at -78 °C for 30 min, allowed to warm up to room temperature, stirred for 5 min and cooled back to -78 °C. A suspension of MeONa (80 mg, 1.5 mmol) in MeOH (2.5 mL) was then added dropwise and the resulting mixture was stirred for 1 h at room temperature.⁵ A sat. aq. NH_4Cl solution (2.5 mL) was then added, the resulting mixture was stirred for 4 h before a sat. aq. $Na_2S_2O_3$ solution (2.5 mL) was added. EtOAc (10 mL) was added, the phases were separated and the aqueous layer was extracted with EtOAc (2 x 20 mL). The combined organic layers were washed with water and brine, dried over $MgSO_4$, filtered and concentrated. The residue was purified by column chromatography (Hexane/EtOAc = 50:1), affording **4.5.6** as colorless oil (36.2 mg, 66%). 1H NMR (400 MHz, $CDCl_3$) δ 7.38 (d, J = 8.3 Hz, 1H), 7.33 (d, J = 2.2 Hz, 1H), 7.07 (dd, J = 8.3, 2.2 Hz, 1H), 3.71 (dd, J = 7.4, 4.7 Hz, 1H), 2.29 (dd, J = 14.1, 7.4 Hz, 1H), 2.11 (s, 3H), 1.44 (dd, J = 14.1, 4.7 Hz, 1H), 0.84 (s, 9H) ppm. ^{13}C NMR (101 MHz, $CDCl_3$) δ 207.2, 141.0, 133.0, 131.4, 130.9, 130.3, 127.7, 55.3, 45.6, 31.1, 29.8, 29.4 ppm. IR (neat, cm^{-1}): 2955, 2916, 2867, 1717, 1561, 1467, 1396, 1365, 1151, 1131, 1031, 973. HRMS calcd. for $C_{14}H_{19}Cl_2O$ $[M+H]^+$: 273.0807 found 273.0805.



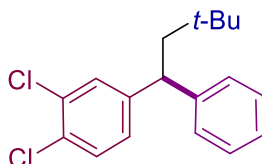
1-(4-bromophenyl)-2-(3,4-dichlorophenyl)-4,4-dimethylpentan-1-one (4.5.7): An oven-dried 8 mL screw-cap test tube containing a stirring bar was charged with **4.5.4r** (71.4 mg, 0.2 mmol, 1 equiv) and was sealed with a Teflon-lined screw cap. The tube was then evacuated and back-filled with argon (3 times), THF (1 mL) and NMP (40

μL , 4 equiv) were added at $-78\text{ }^\circ\text{C}$. Subsequently, *n*-BuLi (40 μL , 2.5 M) was added dropwise and the resulting mixture (solution A) was allowed to stirred at the same temperature for an additional 30 min. Another test tube was charged with 4-bromobenzaldehyde (44.6 mg, 0.24 mmol, 1.2 equiv), evacuated and back-filled with argon (3 times). THF (1 mL) was added, this solution was added to solution A dropwise at $-78\text{ }^\circ\text{C}$. Afterwards, the solution was allowed to warm up to rt and stirred at rt overnight. After the reaction was completed, it was quenched with water, extracted with DCM (10 mL, 3 times). The combined organic layers were dried over anhydrous MgSO_4 and concentrated under vacuum to give a crude product as a mixture of diastereoisomers (dr = 1:1). Dess-Martin reagent (110.3 mg, 0.26 mmol, 1.3 equiv) was used to oxidize the crude product to its ketone derivative in dry DCM (2 mL) at rt overnight.⁶ The final product **4.5.7** (80.1 mg, 97% yield after two steps) was obtained as a white solid after column purification (Hexane/EtOAc = 100:1 to 30:1). **^1H NMR** (400 MHz, CDCl_3) δ 7.82 (d, J = 8.6 Hz, 2H), 7.58 (d, J = 8.6 Hz, 2H), 7.38 (d, J = 2.2 Hz, 1H), 7.34 (d, J = 8.3 Hz, 1H), 7.13 (dd, J = 8.3, 2.2 Hz, 1H), 4.59 (dd, J = 8.7, 3.5 Hz, 1H), 2.54 (dd, J = 14.0, 8.7 Hz, 1H), 1.57 – 1.50 (m, 2H), 0.87 (s, 9H) ppm. **^{13}C NMR** (101 MHz, CDCl_3) δ 198.3, 141.0, 135.3, 133.1, 132.3, 131.3, 131.0, 130.2, 130.1, 128.7, 127.6, 48.7, 47.7, 31.4, 29.9 ppm. **IR** (neat, cm^{-1}): 3066, 2956, 2909, 2866, 1670, 1584, 1567, 1465, 1397, 1365, 1280, 1234, 1215, 1180, 1131, 1071, 1033, 1008, 974. **HRMS** calcd. for $(\text{C}_{19}\text{H}_{19}\text{BrCl}_2\text{NaO})$ $[\text{M}+\text{Na}]^+$: 434.9889 found 434.9887.

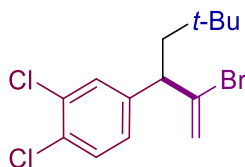


2-(1-(3,4-dichlorophenyl)-3,3-dimethylbutyl)furan (4.5.8): To an oven-dried screw-cap tube containing a stirring bar, furan (1.2 equiv, 0.3 mmol, 22 μL) and THF (1 mL) were added via syringe, and the resulting solution was cooled to $-78\text{ }^\circ\text{C}$. Then *n*-BuLi (1.2 equiv, 2.5 M, 0.3 mmol, 120 μL) was added dropwise under $-78\text{ }^\circ\text{C}$. The resultant mixture was allowed to warm to room temperature and stirred for 1h. Subsequently, the reaction mixture was cooled back to $-78\text{ }^\circ\text{C}$, and a solution of **4.5.4r** (89 mg, 0.25 mmol) in THF (0.5 mL) was added dropwise. The resulting mixture was stirred at the same temperature for 1h and a solution of NBS (1.2 equiv, 0.3 mmol, 54 mg) in THF (1 mL) was added dropwise. After 1h at $-78\text{ }^\circ\text{C}$, sat. aq. $\text{Na}_2\text{S}_2\text{O}_3$ (1 mL) was added and the reaction mixture was allowed to warm to room temperature. The reaction mixture was diluted with EtOAc (10 mL) and water (5 mL). Then the mixture was extracted with EtOAc (3 x 10 mL), dried over MgSO_4 , filtered and concentrated under reduced pressure.⁷ The residue was purified by column

chromatography (Hexane), obtaining **4.5.8** (39 mg, 53%) as yellow oil. $^1\text{H NMR}$ (400 MHz, CDCl_3) δ 7.42 – 7.29 (m, 3H), 7.12 (dd, $J = 8.3, 2.1$ Hz, 1H), 6.28 (dd, $J = 3.2, 1.8$ Hz, 1H), 6.04 (dt, $J = 3.2, 0.8$ Hz, 1H), 4.03 (dd, $J = 7.8, 5.8$ Hz, 1H), 2.16 (dd, $J = 14.1, 7.8$ Hz, 1H), 1.77 (dd, $J = 14.1, 5.9$ Hz, 1H), 0.84 (s, 9H) ppm. $^{13}\text{C NMR}$ (101 MHz, CDCl_3): δ 157.3, 145.1, 141.5, 132.5, 130.5, 130.3, 129.9, 127.3, 110.4, 105.7, 48.4, 41.4, 31.3, 29.8 ppm. **IR** (neat, cm^{-1}): 2955, 2900, 2866, 1796, 1720, 1589, 1562, 1504, 1467, 1396, 1365, 1247, 1131, 1031, 1009. **HRMS** calcd. for $(\text{C}_{16}\text{H}_{19}\text{Cl}_2\text{O})$ $[\text{M}+\text{H}]^+$: 297.0807 found 297.0806.

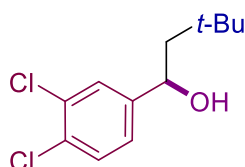


1,2-dichloro-4-(3,3-dimethyl-1-phenylbutyl)benzene (4.5.9): An oven-dried screw-cap tube containing a stirring bar was charged with iodobenzene (22.3 μL , 0.2 mmol), Ag_2O (55.5 mg, 0.3 mmol), $\text{Pd}_2(\text{dba})_3$ (7.4 mg, 8.0 mol% Pd) and PPh_3 (52.4 mg, 0.2 mmol). Then, the tube was sealed, **4.5.4r** (109.2 mg, 0.3 mmol) and THF (5 mL) were added under argon. The mixture was stirred at 70 $^\circ\text{C}$ for 24 h.⁸ The residue was purified by column chromatography (Hexane), afforded **4.5.9** (36 mg, 59%) as colorless oil. $^1\text{H NMR}$ (400 MHz, CDCl_3) δ 7.38 (d, $J = 2.2$ Hz, 1H), 7.34 – 7.23 (m, 5H), 7.20 – 7.11 (m, 2H), 4.01 (t, $J = 6.7$ Hz, 1H), 2.13 – 1.98 (m, 2H), 0.84 (s, 9H) ppm. $^{13}\text{C NMR}$ (101 MHz, CDCl_3): δ 147.3, 145.6, 132.4, 130.5, 129.9, 129.8, 128.8, 127.8, 127.3, 126.5, 49.3, 47.8, 31.7, 30.3 ppm. **IR** (neat, cm^{-1}): 3027, 2954, 2866, 1559, 1468, 1396, 1365, 1246, 1132, 1029, 876. **GC-MS** calcd. for $\text{C}_{18}\text{H}_{20}\text{Cl}_2$ $[\text{M}]^+$: found $t = 7.740$ min, $m/z = 306.1$.



4-(2-bromo-5,5-dimethylhex-1-en-3-yl)-1,2-dichlorobenzene (4.5.10): To an oven-dried round bottom flask containing a stirring bar, **4.5.4r** (0.3 mmol, 109.2 mg), vinyl bromide (0.6 mmol, 1M in THF, 0.6 mL) and diethyl ether (2 mL) were added sequentially. The above solution was stirred at -95 $^\circ\text{C}$, and then freshly prepared LDA (0.86 M, 0.7 mL) was added dropwise over 10 min. The reaction mixture was allowed to stir 1h at -95 $^\circ\text{C}$ followed by dropwise addition of a solution of I_2 (0.66 mmol, 167.4 mg) in methanol (2 mL). After stirring for 5 min, then the mixture was allowed warm to room temperature, stirred for 1h and 20% aqueous solution of $\text{Na}_2\text{S}_2\text{O}_3$ (10 mL) was added. Then, the mixture was extracted with EtOAc (3 x 10 mL), dried over MgSO_4 , filtered and concentrated under reduced pressure.⁹ The mixture was purified by column chromatography (Hexane), afforded **4.5.10** (56 mg, 56% yield) as colorless

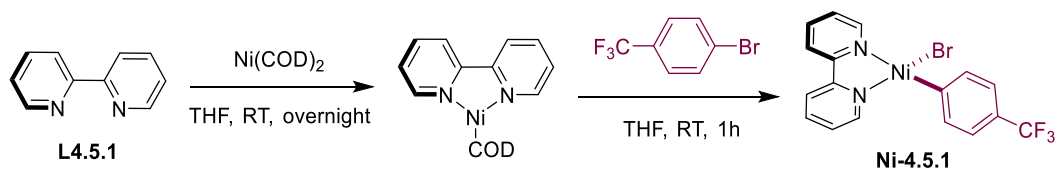
oil. $^1\text{H NMR}$ (400 MHz, CDCl_3) δ 7.44 – 7.35 (m, 2H), 7.15 (dd, $J = 8.3, 2.2$ Hz, 1H), 5.76 – 5.75 (m, 1H), 5.47 (dd, $J = 2.1, 0.8$ Hz, 1H), 3.66 (t, $J = 6.3$ Hz, 1H), 2.01 – 1.96 (m, 1H), 1.76 – 1.71 (m, 1H), 0.89 (s, 9H) ppm. $^{13}\text{C NMR}$ (101 MHz, CDCl_3) δ 143.2, 139.3, 132.5, 131.0, 130.4, 130.2, 127.7, 117.0, 51.7, 46.8, 31.4, 30.1 ppm. **IR** (neat, cm^{-1}): 2955, 2912, 2866, 1729, 1619, 1467, 1396, 1366, 1244, 1131, 1031, 889. **HRMS** calcd. for $\text{C}_{14}\text{H}_{17}\text{Cl}_2$ $[\text{M}-\text{Br}]^+$: 255.0702 found 255.0704.



1-(3,4-dichlorophenyl)-3,3-dimethylbutan-1-ol (4.5.11): **4.5.4r** was dissolved in a mixture of THF and H_2O (1:1, 4 mL). Then $\text{NaBO}_3 \cdot 4\text{H}_2\text{O}$ (327.2 mg, 0.40 mmol) was added portion wise. The reaction mixture was stirred at room temperature for 4 h. After the reaction was completed, water (10 mL) was added. The aqueous phase was extracted with EtOAc (3 x 10 mL), and the combined organic phases were dried over MgSO_4 and concentrated.¹⁰ The residue was purified by column chromatography (Hexane/EtOAc = 30:1 to 20:1), afforded **4.5.11** (69.2 mg, 75% after two steps) as a light-yellow oil. $^1\text{H NMR}$ (300 MHz, CDCl_3) δ 7.43 (d, $J = 2.1$ Hz, 1H), 7.38 (d, $J = 8.2$ Hz, 1H), 7.15 (dd, $J = 8.3, 2.1$ Hz, 1H), 4.78 (dd, $J = 8.6, 3.3$ Hz, 1H), 1.87 (s, 1H), 1.69 (dd, $J = 14.6, 8.6$ Hz, 1H), 1.52 (dd, $J = 14.6, 3.3$ Hz, 1H), 0.99 (s, 10H) ppm. $^{13}\text{C NMR}$ (75 MHz, CDCl_3) δ 146.8, 132.5, 131.0, 130.4, 127.8, 125.1, 71.4, 53.0, 30.6, 30.2 ppm. **IR** (neat, cm^{-1}): 3383, 2951, 2866, 1465, 1394, 1364, 1130, 1068, 1029, 984, 881, 821, 719, 675. **HRMS** calcd. for $(\text{C}_{12}\text{H}_{16}\text{Cl}_2\text{O})$ $[\text{M}+\text{H}]^+$: 246.0573 found 246.0564.

4.8.7 Mechanistic Experiments

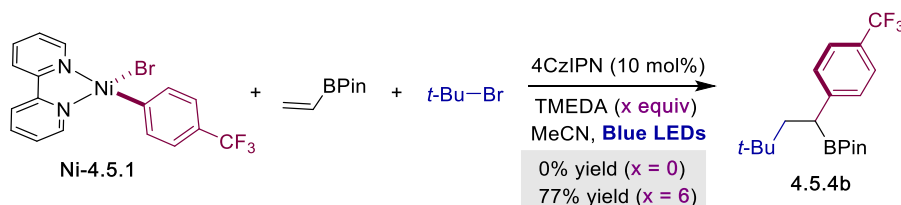
4.8.7.1 Synthesis of Ni-4.5.1



In a nitrogen filled glove box, a 50 mL round bottom flask containing a stirring bar was charged with $\text{Ni}(\text{COD})_2$ (276 mg, 1.0 mmol, 1.0 equiv), 2,2'-dipyridyl (**L4.5.1**, 156 mg, 1.0 mmol, 1.0 equiv) and dry THF (10 mL) giving a dark purple mixture which was stirred overnight at 25 °C. 1-bromo-4-(trifluoromethyl)benzene (1.4 mL, 10 mmol, 10.0 equiv) was added and stirred for additional 1 h. Dry pentane (30 mL) was added to the orange colored mixture and filtered. The resulting precipitate was washed with pentane (3 x 10 mL) and dried under vacuum to afford **Ni-4.5.1** (356 mg,

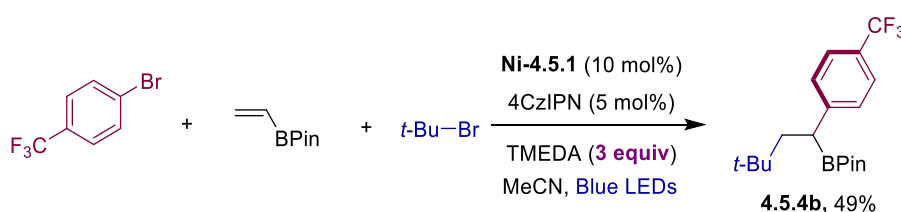
76% yield) as an orange solid. The product was used without further purification. The complex was stored in a nitrogen filled glove box at $-35\text{ }^{\circ}\text{C}$ and showed to be stable in solid form. The product turned out to be highly insoluble in the vast majority of solvents used for NMR spectroscopy, obtaining in all cases broad signals.¹¹ ^1H NMR (400 MHz, CD_2Cl_2) δ 9.40 (s, 1H), 8.05 – 7.87 (m, 4H), 7.76 (d, $J = 7.8$ Hz, 2H), 7.54 (s, 1H), 7.28 – 7.15 (m, 4H) ppm. ^{19}F NMR (376 MHz, CD_2Cl_2) δ -62.1 ppm.

4.8.7.2 Stoichiometric experiments



An oven-dried 8 mL screw-cap test tube containing a stirring bar was charged with 4CzIPN (7.9 mg, 10 mol%). Subsequently, the tube was sealed with a Teflon-lined screw cap and the tube was brought into the glovebox. After then **Ni-4.5.1** (46.8 mg, 0.1 mmol, 1.0 equiv) was added. Afterwards, the tube was brought out, then 2-bromo-2-methylpropane (**4.5.3a**, 56 μL , 0.5 mmol, 5.0 equiv), Vinyl Bpin (**4.5.2a**, 35 μL , 0.2 mmol, 2.0 equiv), TMEDA (90 μL , 0.6 mmol, 6.0 equiv) and anhydrous MeCN (3.0 mL) were added via syringe. Then, the tube was stirred at $30\text{ }^{\circ}\text{C}$ under irradiation of blue LEDs with a fan for 20 h. After the reaction was completed, the mixture was diluted with EtOAc, filtered through silica gel to remove inorganic salts and concentrated under vacuum. The yields were determined by ^1H NMR analysis using CH_2Br_2 as internal standard. As shown from the stoichiometric experiments, no reaction occurred without TMEDA, suggesting that the mechanism might operate via a canonical photocatalytic cycle consisting of a reductive quenching with TMEDA.

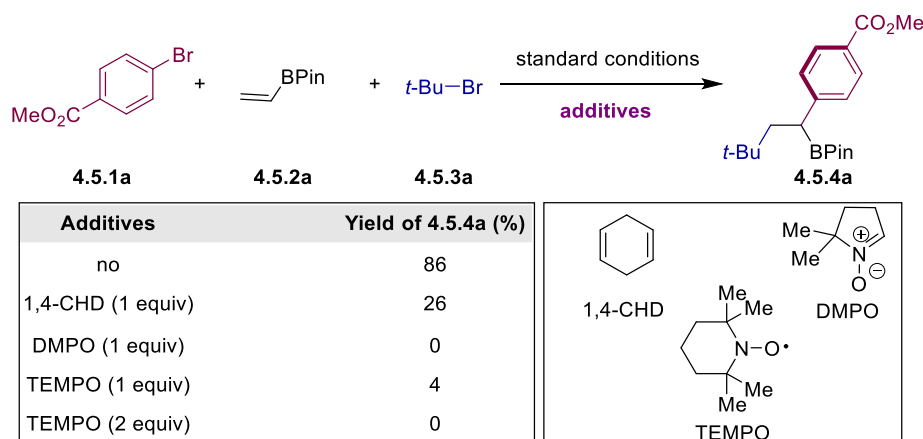
4.8.7.3 Catalytic reaction with Ni-4.5.1



An oven-dried 8 mL screw-cap test tube containing a stirring bar was charged with 4CzIPN (7.9 mg, 5 mol%). Subsequently, the tube was sealed with a Teflon-lined screw cap and the tube was brought into the glovebox. After then **Ni-4.5.1** (6.6 mg, 7.5 mmol%) was added. Afterwards, the tube was brought out, then

1-bromo-4-(trifluoromethyl)benzene (**4.5.1b**, 56 μL , 0.40 mmol), Vinyl Bpin (**4.5.2a**, 35 μL , 0.2 mmol, 2.0 equiv), 2-bromo-2-methylpropane (**4.5.3a**, 56 μL , 0.5 mmol, 5.0 equiv), TMEDA (90 μL , 0.6 mmol, 6.0 equiv) and anhydrous MeCN (3.0 mL) were added via syringe. Then, the tube was stirred at 30 °C under irradiation of blue LEDs with a fan for 20 h. After the reaction was completed, the mixture was diluted with EtOAc, filtered through silica gel to remove inorganic salts and concentrated under vacuum. The yields were determined by ^1H NMR analysis using CH_2Br_2 as internal standard.

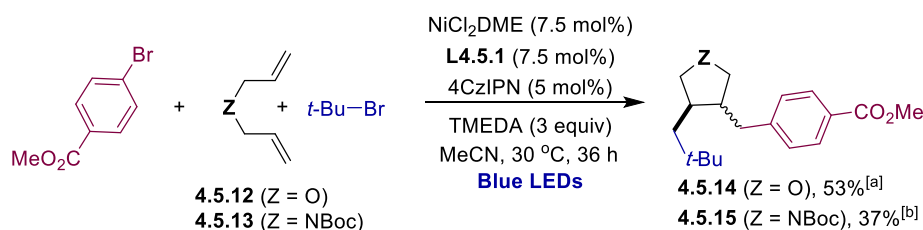
4.8.7.4 Radical trapping Experiments



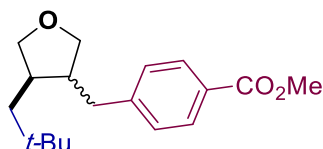
An oven-dried 8 mL screw-cap test tube containing a stirring bar was charged with 4CzIPN (7.9 mg, 5 mol%), 2,2'-dipyridyl (**L4.5.1**, 2.3 mg, 7.5 mol%) and Methyl 4-benzoate (**4.5.1a**, 86.0 mg, 0.4 mmol, 2.0 equiv). The corresponding additives, such as 1,4-CHD and DMPO was added after introducing the tube into glovebox, while TEMPO was added beforewards. Subsequently, the tube was sealed with a Teflon-lined screw cap and the tube was brought into the glovebox. After then $\text{NiCl}_2 \cdot \text{glyme}$ (3.3 mg, 7.5 mol%) was added. Afterwards, the tube was brought out, then Vinyl Bpin (**4.5.2a**, 35 μL , 0.2 mmol, 1.0 equiv), 2-bromo-2-methylpropane (**4.5.3a**, 56 μL , 0.5 mmol, 2.5 equiv), TMEDA (90 μL , 0.6 mmol, 3.0 equiv) and anhydrous MeCN (3.0 mL) were added via syringe. Then, the tube was stirred at 30 °C under irradiation of blue LEDs with a fan for 24 h. After the reaction was completed, the mixture was diluted with EtOAc, filtered through silica gel to remove inorganic salts and concentrated under vacuum. The yields were determined by ^1H NMR analysis using CH_2Br_2 as internal standard.

Note: in the case of 1,4-CHD, it was added 1 hour after the reaction started.

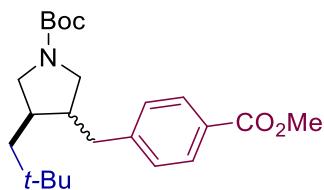
4.8.7.5 Experiments with Radical Probes 12 and 13



An oven-dried 8 mL screw-cap test tube containing a stirring bar was charged with 4CzIPN (7.9 mg, 5 mol%), 2,2'-dipyridyl (**L4.5.1**, 2.3 mg, 7.5 mol%) and methyl 4-bromobenzoate (**4.5.1a**, 85.6 mg, 0.40 mmol). Subsequently, the tube was sealed with a Teflon-lined screw cap and the tube was brought into the glovebox. After then $\text{NiCl}_2 \cdot \text{glyme}$ (3.3 mg, 7.5 mol%) was added. Afterwards, the tube was brought out, then 2-bromo-2-methylpropane (**4.5.3a**, 56 μL , 0.5 mmol, 5.0 equiv), diene (**4.5.17** or **4.5.18**, 0.2 mmol, 1.0 equiv), TMEDA (90 μL , 0.6 mmol, 3.0 equiv) and anhydrous MeCN (3.0 mL) were added via syringe. Then, the tube was stirred at 30 °C under irradiation of blue LEDs with a fan for 36 h. After the reaction was completed, the mixture was diluted with EtOAc, filtered through silica gel to remove inorganic salts and concentrated under vacuum.



Methyl 4-((4-neopentyltetrahydrofuran-3-yl)methyl)benzoate (4.5.19): Following the general procedure, but using allyl ether (35 μL , 0.20 mmol), afforded **5.1.19** (31 mg, 53% yield, dr = 4:1, with the major isomer corresponding to the trans-junction) as white solid. **Mp.** 71.6 – 72.5 °C. $^1\text{H NMR}$ (400 MHz, CDCl_3) δ 7.95 (dd, $J = 8.3, 1.7$ Hz, 2H), 7.27 – 7.20 (m, 2H), 4.13 (t, $J = 7.8$ Hz, 0.2 H), 4.02 (t, $J = 7.8$ Hz, 0.8H), 3.89 (s, 3H), 3.75 – 3.71 (m, 0.79H), 3.66 – 3.57 (m, 0.79H), 3.55 – 3.47 (m, 1.53H), 3.44 – 3.34 (m, 0.37H), 2.97 – 2.82 (m, 1H), 2.59 – 2.54 (m, 0.2H), 2.48 – 2.36 (m, 2.26H), 2.11 – 2.01 (m, 0.21H), 1.94 – 1.85 (m, 0.22H), 1.59 (dd, $J = 13.9, 3.5$ Hz, 0.84H), 1.49 (dd, $J = 14.0, 2.4$ Hz, 0.21H), 1.31 – 1.22 (m, 2.2H), 0.93 (s, 7.23H), 0.85 (s, 1.72H) ppm. $^{13}\text{C NMR}$ (101 MHz, CDCl_3) δ 167.2, 146.7, 146.2, 129.9, 129.89, 129.1, 128.8, 128.2, 75.6, 73.4, 72.4, 71.4, 52.1, 48.3, 47.7, 44.8, 42.2, 41.9, 39.0, 38.7, 33.3, 30.9, 30.8, 30.1, 30.0 ppm. **IR** (neat, cm^{-1}): 2957, 2929, 2868, 1721, 1609, 1438, 1365, 1275, 1185, 1109, 1050, 1020, 957. **HRMS** calcd. for $(\text{C}_{18}\text{H}_{27}\text{O}_3)$ $[\text{M}+\text{H}]^+$: 291.1955 found 291.1958.



tert-butyl 3-(4-(methoxycarbonyl)benzyl)-4-neopentylpyrrolidine-1-carboxylate (5.1.20): Following the general procedure, by using *tert*-butyl diallylcarbamate (39.4 mg, 0.20 mmol), afforded **5.1.20** (29 mg, 37% yield, dr = 1.2:1) as colorless oil. $^1\text{H NMR}$ (400 MHz, CDCl_3) δ 7.99 – 7.91 (m, 2H), 7.21 (dd, $J = 8.2, 6.4$ Hz, 2H), 3.90 (s, 3H), 3.81 – 3.63 (m, 0.44H), 3.53 (t, $J = 9.0$ Hz, 0.56H), 3.32 (t, $J = 9.3$ Hz, 0.43H), 3.20 – 3.02 (m, 1.73H), 2.98 (dd, $J = 13.6, 4.1$ Hz, 0.45H), 2.94 – 2.80 (m, 1.43H), 2.47 – 2.24 (m, 2.16H), 2.04 – 1.91 (m, 0.53H), 1.87 – 1.77 (m, 0.61H), 1.60 – 1.50 (m, 1H), 1.45 (s, 5.17H), 1.41 (s, 3.90H), 1.32 – 1.25 (m, 0.47H), 1.24 – 1.18 (m, 0.59H), 0.94 (s, 5.12H), 0.91 (s, 3.88H) ppm. $^{13}\text{C NMR}$ (101 MHz, CDCl_3) δ 167.2, 167.1, 155.0, 154.5, 146.4, 145.9, 129.94, 129.9, 129.2, 128.8, 128.4, 128.3, 79.3, 79.25, 53.7, 52.2, 51.3, 50.6, 49.3, 47.1, 46.6, 44.2, 42.4, 40.6, 38.3, 38.0, 33.4, 30.9, 30.8, 30.1, 28.7, 28.6 ppm. **IR** (neat, cm^{-1}): 2938, 2899, 2855, 1731, 1698, 1609, 1473, 1406, 1365, 1276, 1248, 1115, 1109, 1023, 957. **HRMS** calcd. for $(\text{C}_{23}\text{H}_{35}\text{NNaO}_4) [\text{M}+\text{Na}]^+$: 412.2458 found 412.246

4.8.7.6 EPR Experiment

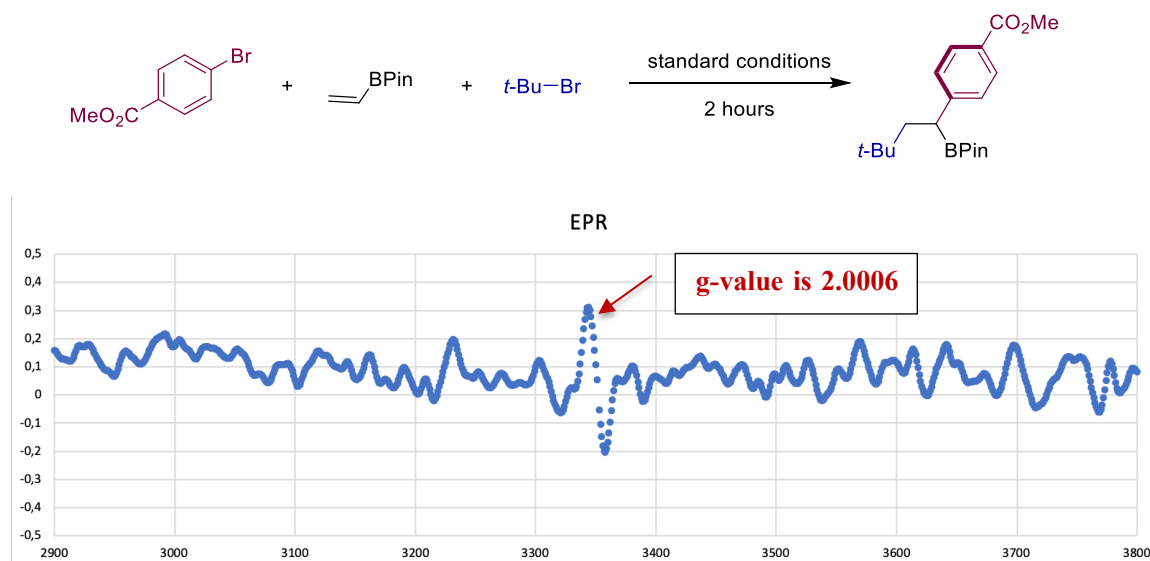


Figure S1. EPR of reaction system under irradiation

Sample preparation: The reaction was run at standard conditions for 2 hours. 0.4 mL of the solution was taken after the tube was introduced into the glovebox. The EPR tube was sealed in the glovebox and took out for irradiation under blue LEDs for an additional 0.5 hour (**Note:** this irradiation step is crucial for the detection of the signal). This sample was immediately cooled down to 77K in liquid nitrogen for the measurement.

The EPR experiment was measured at 77K (liquid nitrogen). The **g-value** is 2.0006. This experiment confirmed the intermediacy of alkyl radicals under our reaction conditions.

4.8.7.7 Stern-Volmer Quenching Experiments

Samples for the quenching experiments were prepared in a 4 mL glass cuvette with a septum screw cap. 4CzIPN was irradiated and the emission intensity at 435 nm was observed. The UV-Vis spectra of 4CzIPN was measured at 0.01 mM and 0.05 mM concentration, no significant change could be observed when adding *t*-BuBr or ArBr or TMEDA.

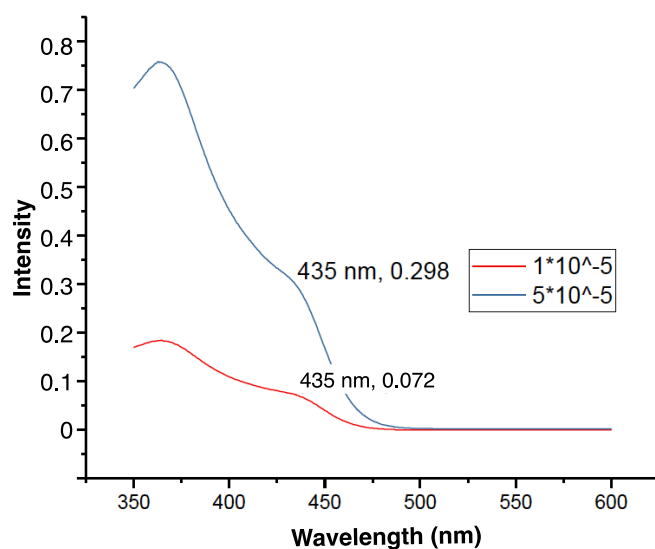


Figure S2. UV-Vis spectra of the photocatalyst

The Stern-Volmer Quenching was measured at 0.01 mM of the photocatalyst.

***t*-BuBr:** No quenching effect was observed when *t*-BuBr was added.

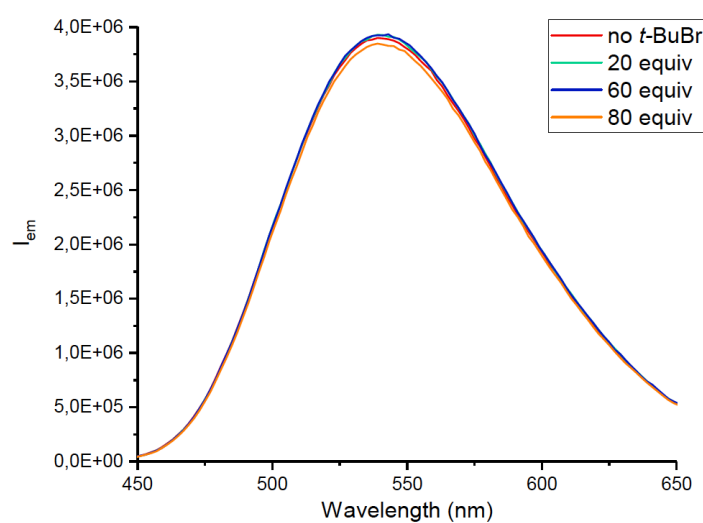


Figure S3. The Stern-Volmer of *t*-BuBr

TMEDA: A stock solution of TMEDA (6 μ L, 0.04 mmol) in 4 ml of MeCN was prepared ($C_0 = 10$ mM). Then, different amounts (5 μ L, 5 μ L, 10 μ L, 10 μ L, 10 μ L, 10 μ L, 30 μ L, 20 μ L) of this stock solution were added to a solution of the photocatalyst 4CzIPN in MeCN (0.01 M). As shown, a significant decrease of 4CzIPN luminescence was observed, suggesting that the mechanism might operate via a canonical photocatalytic cycle consisting of a reductive quenching with TMEDA.

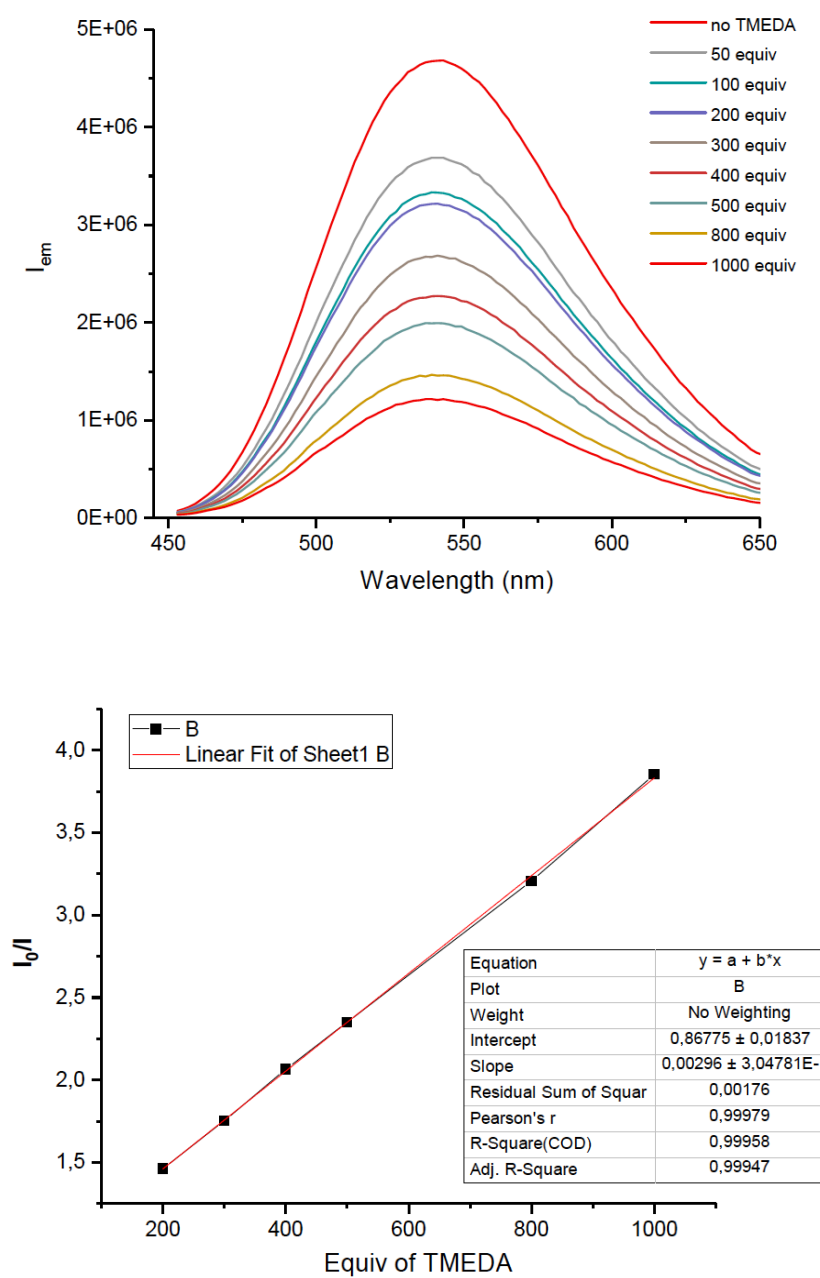


Figure S4. The Stern-Volmer of TMEDA

4.8.7.8 Recovery of the photocatalyst (4CzIPN)

The photocatalyst (4CzIPN) was not decomposed after the reaction complete. The photocatalyst could be recovered in quantitative yield.

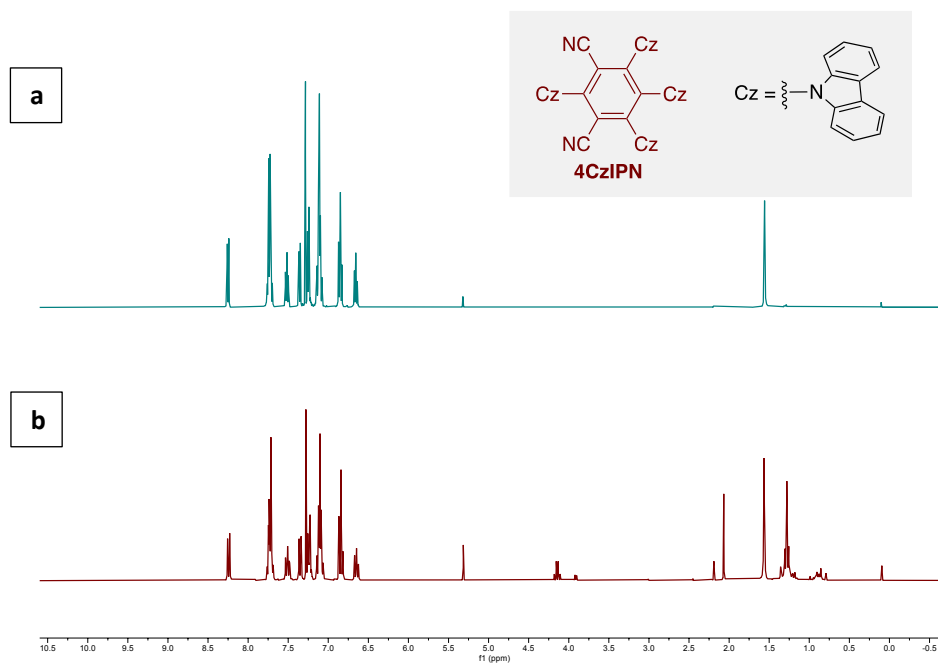
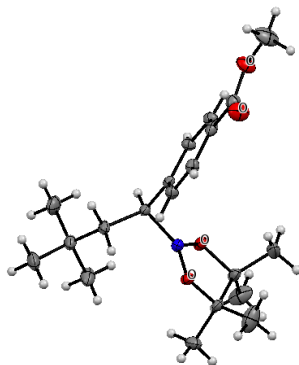


Figure S5. (a) ^1H NMR of 4CzIPN before the reaction. (b) ^1H NMR of 4CzIPN after the reaction.

4.8.8 X-Ray Crystallography Data

4.8.8.1 X-Ray crystallography data of 4.5.4a



X-Ray quality crystals were obtained from a saturated solution of **4.5.4a** in DCM and drops of Et₂O were slowly added, and left few days. A CIF file is available as a separate Supporting Information file.

Table 1. Crystal data and structure refinement for **4.5.4a**.

Identification code	ssun-1	
Empirical formula	C ₂₀ H ₃₁ B O ₄	
Formula weight	346.26	
Temperature	100(2) K	
Wavelength	0.71073 Å	
Crystal system	Monoclinic	
Space group	P2(1)/n	
Unit cell dimensions	a = 6.59530(10) Å	∠ = 90°.
	b = 21.9117(4) Å	⊕ = 97.696(2)°.
	c = 14.3091(3) Å	⊙ = 90°.
Volume	2049.24(7) Å ³	
Z	4	
Density (calculated)	1.122 Mg/m ³	
Absorption coefficient	0.075 mm ⁻¹	
F(000)	752	
Crystal size	0.22 x 0.20 x 0.10 mm ³	
Theta range for data collection	2.349 to 37.316°.	
Index ranges	-10 ≤ h ≤ 11, -37 ≤ k ≤ 36, -24 ≤ l ≤ 23	
Reflections collected	61112	
Independent reflections	10381 [R(int) = 0.0321]	
Completeness to theta = 37.316°	97.399994%	

Chapter 4.

Absorption correction	Multi-scan
Max. and min. transmission	0.993 and 0.764
Refinement method	Full-matrix least-squares on F ²
Data / restraints / parameters	10381/ 379/ 456
Goodness-of-fit on F ²	1.072
Final R indices [I>2sigma(I)]	R1 = 0.0480, wR2 = 0.1266
R indices (all data)	R1 = 0.0636, wR2 = 0.1338
Largest diff. peak and hole	0.467 and -0.240 e.Å ⁻³

Table 2. Bond lengths [Å] and angles [°] for **4.5.4a**.

Bond lengths----

O1-C8	1.344(2)
O1-C9	1.449(3)
O2-C8	1.211(2)
O3-B1	1.3871(15)
O3-C15	1.4651(13)
O4-B1	1.3576(17)
O4-C16	1.452(2)
C1-C2	1.5249(12)
C1-C10	1.5452(11)
C1-B1	1.5769(17)
C1-H1	0.9800
C2-C3	1.3991(12)
C2-C7	1.4029(13)
C3-C4	1.3871(14)
C3-H3	0.9300
C4-C5	1.3936(16)
C4-H4	0.9300
C5-C6	1.3985(12)
C5-C8	1.484(2)
C6-C7	1.3971(12)
C6-H6	0.9300
C7-H7	0.9300
C9-H9A	0.9600
C9-H9B	0.9600
C9-H9C	0.9600
C10-C11	1.5400(11)

Site-Selective 1,2-Dicarbofunctionalization of Vinyl Boronates through Dual Catalysis

C10-H10A	0.9700
C10-H10B	0.9700
C11-C13	1.5313(15)
C11-C12	1.5328(16)
C11-C14	1.5394(13)
C12-H12A	0.9600
C12-H12B	0.9600
C12-H12C	0.9600
C13-H13A	0.9600
C13-H13B	0.9600
C13-H13C	0.9600
C14-H14A	0.9600
C14-H14B	0.9600
C14-H14C	0.9600
C15-C17	1.5203(13)
C15-C18	1.5206(13)
C15-C16	1.5638(15)
C16-C20	1.5180(18)
C16-C19	1.525(2)
C17-H17A	0.9600
C17-H17B	0.9600
C17-H17C	0.9600
C18-H18A	0.9600
C18-H18B	0.9600
C18-H18C	0.9600
C19-H19A	0.9600
C19-H19B	0.9600
C19-H19C	0.9600
C20-H20A	0.9600
C20-H20B	0.9600
C20-H20C	0.9600
O1'-C8'	1.289(13)
O1'-C9'	1.439(16)
O2'-C8'	1.232(15)
O3'-B1'	1.206(17)
O3'-C15'	1.516(14)
O4'-B1'	1.430(17)
O4'-C16'	1.601(17)

Chapter 4.

C1'-C2'	1.513(10)
C1'-C10'	1.527(12)
C1'-B1'	1.654(18)
C1'-H1'	0.9800
C2'-C3'	1.3900
C2'-C7'	1.3900
C3'-C4'	1.3900
C3'-H3'	0.9300
C4'-C5'	1.3900
C4'-H4'	0.9300
C5'-C6'	1.3900
C5'-C8'	1.519(17)
C6'-C7'	1.3900
C6'-H6'	0.9300
C7'-H7'	0.9300
C9'-H9'A	0.9600
C9'-H9'B	0.9600
C9'-H9'C	0.9600
C10'-C11'	1.541(10)
C10'-H10C	0.9700
C10'-H10D	0.9700
C11'-C14'	1.490(15)
C11'-C13'	1.531(14)
C11'-C12'	1.558(14)
C12'-H12D	0.9600
C12'-H12E	0.9600
C12'-H12F	0.9600
C13'-H13D	0.9600
C13'-H13E	0.9600
C13'-H13F	0.9600
C14'-H14D	0.9600
C14'-H14E	0.9600
C14'-H14F	0.9600
C15'-C16'	1.535(5)
C15'-C18'	1.537(5)
C15'-C17'	1.545(5)
C16'-C20'	1.464(15)
C16'-C19'	1.480(16)

Site-Selective 1,2-Dicarbofunctionalization of Vinyl Boronates through Dual Catalysis

C17'-H17D	0.9600
C17'-H17E	0.9600
C17'-H17F	0.9600
C18'-H18D	0.9600
C18'-H18E	0.9600
C18'-H18F	0.9600
C19'-H19D	0.9600
C19'-H19E	0.9600
C19'-H19F	0.9600
C20'-H20D	0.9600
C20'-H20E	0.9600
C20'-H20F	0.9600

Angles-----

C8-O1-C9	115.29(19)
B1-O3-C15	107.10(9)
B1-O4-C16	107.36(10)
C2-C1-C10	111.56(7)
C2-C1-B1	105.64(8)
C10-C1-B1	113.93(8)
C2-C1-H1	108.5
C10-C1-H1	108.5
B1-C1-H1	108.5
C3-C2-C7	118.06(8)
C3-C2-C1	120.96(8)
C7-C2-C1	120.98(8)
C4-C3-C2	121.28(8)
C4-C3-H3	119.4
C2-C3-H3	119.4
C3-C4-C5	120.33(8)
C3-C4-H4	119.8
C5-C4-H4	119.8
C4-C5-C6	119.36(9)
C4-C5-C8	118.74(11)
C6-C5-C8	121.90(13)
C7-C6-C5	119.98(9)
C7-C6-H6	120.0
C5-C6-H6	120.0

Chapter 4.

C6-C7-C2	120.94(9)
C6-C7-H7	119.5
C2-C7-H7	119.5
O2-C8-O1	123.15(19)
O2-C8-C5	124.02(15)
O1-C8-C5	112.81(18)
O1-C9-H9A	109.5
O1-C9-H9B	109.5
H9A-C9-H9B	109.5
O1-C9-H9C	109.5
H9A-C9-H9C	109.5
H9B-C9-H9C	109.5
C11-C10-C1	115.97(7)
C11-C10-H10A	108.3
C1-C10-H10A	108.3
C11-C10-H10B	108.3
C1-C10-H10B	108.3
H10A-C10-H10B	107.4
C13-C11-C12	109.93(10)
C13-C11-C14	108.74(8)
C12-C11-C14	109.00(9)
C13-C11-C10	110.70(8)
C12-C11-C10	110.94(9)
C14-C11-C10	107.45(8)
C11-C12-H12A	109.5
C11-C12-H12B	109.5
H12A-C12-H12B	109.5
C11-C12-H12C	109.5
H12A-C12-H12C	109.5
H12B-C12-H12C	109.5
C11-C13-H13A	109.5
C11-C13-H13B	109.5
H13A-C13-H13B	109.5
C11-C13-H13C	109.5
H13A-C13-H13C	109.5
H13B-C13-H13C	109.5
C11-C14-H14A	109.5
C11-C14-H14B	109.5

H14A-C14-H14B	109.5
C11-C14-H14C	109.5
H14A-C14-H14C	109.5
H14B-C14-H14C	109.5
O4-B1-O3	113.83(12)
O4-B1-C1	123.98(10)
O3-B1-C1	121.94(11)
O3-C15-C17	106.81(9)
O3-C15-C18	107.20(8)
C17-C15-C18	110.43(9)
O3-C15-C16	102.54(9)
C17-C15-C16	113.53(9)
C18-C15-C16	115.45(10)
O4-C16-C20	108.53(11)
O4-C16-C19	106.10(11)
C20-C16-C19	110.36(12)
O4-C16-C15	103.94(10)
C20-C16-C15	114.53(12)
C19-C16-C15	112.76(11)
C15-C17-H17A	109.5
C15-C17-H17B	109.5
H17A-C17-H17B	109.5
C15-C17-H17C	109.5
H17A-C17-H17C	109.5
H17B-C17-H17C	109.5
C15-C18-H18A	109.5
C15-C18-H18B	109.5
H18A-C18-H18B	109.5
C15-C18-H18C	109.5
H18A-C18-H18C	109.5
H18B-C18-H18C	109.5
C16-C19-H19A	109.5
C16-C19-H19B	109.5
H19A-C19-H19B	109.5
C16-C19-H19C	109.5
H19A-C19-H19C	109.5
H19B-C19-H19C	109.5
C16-C20-H20A	109.5

Chapter 4.

C16-C20-H20B	109.5
H20A-C20-H20B	109.5
C16-C20-H20C	109.5
H20A-C20-H20C	109.5
H20B-C20-H20C	109.5
C8'-O1'-C9'	115.7(14)
B1'-O3'-C15'	108.4(10)
B1'-O4'-C16'	108.9(9)
C2'-C1'-C10'	115.8(7)
C2'-C1'-B1'	106.1(8)
C10'-C1'-B1'	116.4(7)
C2'-C1'-H1'	105.9
C10'-C1'-H1'	105.9
B1'-C1'-H1'	105.9
C3'-C2'-C7'	120.0
C3'-C2'-C1'	125.7(5)
C7'-C2'-C1'	114.2(5)
C2'-C3'-C4'	120.0
C2'-C3'-H3'	120.0
C4'-C3'-H3'	120.0
C5'-C4'-C3'	120.0
C5'-C4'-H4'	120.0
C3'-C4'-H4'	120.0
C6'-C5'-C4'	120.0
C6'-C5'-C8'	129.6(7)
C4'-C5'-C8'	110.4(7)
C7'-C6'-C5'	120.0
C7'-C6'-H6'	120.0
C5'-C6'-H6'	120.0
C6'-C7'-C2'	120.0
C6'-C7'-H7'	120.0
C2'-C7'-H7'	120.0
O2'-C8'-O1'	124.9(15)
O2'-C8'-C5'	122.1(12)
O1'-C8'-C5'	112.4(13)
O1'-C9'-H9'A	109.5
O1'-C9'-H9'B	109.5
H9'A-C9'-H9'B	109.5

O1'-C9'-H9'C	109.5
H9'A-C9'-H9'C	109.5
H9'B-C9'-H9'C	109.5
C1'-C10'-C11'	117.7(7)
C1'-C10'-H10C	107.9
C11'-C10'-H10C	107.9
C1'-C10'-H10D	107.9
C11'-C10'-H10D	107.9
H10C-C10'-H10D	107.2
C14'-C11'-C13'	111.6(9)
C14'-C11'-C10'	107.8(7)
C13'-C11'-C10'	109.8(8)
C14'-C11'-C12'	114.8(9)
C13'-C11'-C12'	101.6(10)
C10'-C11'-C12'	111.1(7)
C11'-C12'-H12D	109.5
C11'-C12'-H12E	109.5
H12D-C12'-H12E	109.5
C11'-C12'-H12F	109.5
H12D-C12'-H12F	109.5
H12E-C12'-H12F	109.5
C11'-C13'-H13D	109.5
C11'-C13'-H13E	109.5
H13D-C13'-H13E	109.5
C11'-C13'-H13F	109.5
H13D-C13'-H13F	109.5
H13E-C13'-H13F	109.5
C11'-C14'-H14D	109.5
C11'-C14'-H14E	109.5
H14D-C14'-H14E	109.5
C11'-C14'-H14F	109.5
H14D-C14'-H14F	109.5
H14E-C14'-H14F	109.5
O3'-B1'-O4'	111.9(13)
O3'-B1'-C1'	126.9(12)
O4'-B1'-C1'	120.1(10)
O3'-C15'-C16'	105.8(9)
O3'-C15'-C18'	104.4(7)

Chapter 4.

C16'-C15'-C18'	114.0(9)
O3'-C15'-C17'	103.6(7)
C16'-C15'-C17'	112.1(9)
C18'-C15'-C17'	115.5(10)
C20'-C16'-C19'	112.2(8)
C20'-C16'-C15'	116.3(10)
C19'-C16'-C15'	115.6(10)
C20'-C16'-O4'	108.8(10)
C19'-C16'-O4'	107.9(9)
C15'-C16'-O4'	94.0(8)
C15'-C17'-H17D	109.5
C15'-C17'-H17E	109.5
H17D-C17'-H17E	109.5
C15'-C17'-H17F	109.5
H17D-C17'-H17F	109.5
H17E-C17'-H17F	109.5
C15'-C18'-H18D	109.5
C15'-C18'-H18E	109.5
H18D-C18'-H18E	109.5
C15'-C18'-H18F	109.5
H18D-C18'-H18F	109.5
H18E-C18'-H18F	109.5
C16'-C19'-H19D	109.5
C16'-C19'-H19E	109.5
H19D-C19'-H19E	109.5
C16'-C19'-H19F	109.5
H19D-C19'-H19F	109.5
H19E-C19'-H19F	109.5
C16'-C20'-H20D	109.5
C16'-C20'-H20E	109.5
H20D-C20'-H20E	109.5
C16'-C20'-H20F	109.5
H20D-C20'-H20F	109.5
H20E-C20'-H20F	109.5

Table 3. Torsion angles [°] for **4a**.

C10-C1-C2-C3	40.36(11)
B1-C1-C2-C3	-83.94(11)
C10-C1-C2-C7	-140.73(9)
B1-C1-C2-C7	94.98(11)
C7-C2-C3-C4	2.51(12)
C1-C2-C3-C4	-178.55(10)
C2-C3-C4-C5	-0.99(13)
C3-C4-C5-C6	-1.26(13)
C3-C4-C5-C8	179.46(18)
C4-C5-C6-C7	1.92(13)
C8-C5-C6-C7	-178.83(19)
C5-C6-C7-C2	-0.36(13)
C3-C2-C7-C6	-1.83(13)
C1-C2-C7-C6	179.23(11)
C9-O1-C8-O2	1.4(4)
C9-O1-C8-C5	179.9(3)
C4-C5-C8-O2	6.0(4)
C6-C5-C8-O2	-173.2(2)
C4-C5-C8-O1	-172.5(2)
C6-C5-C8-O1	8.3(3)
C2-C1-C10-C11	158.97(7)
B1-C1-C10-C11	-81.54(10)
C1-C10-C11-C13	-64.74(9)
C1-C10-C11-C12	57.59(12)
C1-C10-C11-C14	176.65(7)
C16-O4-B1-O3	-9.25(16)
C16-O4-B1-C1	165.13(12)
C15-O3-B1-O4	-6.33(15)
C15-O3-B1-C1	179.16(11)
C2-C1-B1-O4	-97.30(14)
C10-C1-B1-O4	139.90(12)
C2-C1-B1-O3	76.64(14)
C10-C1-B1-O3	-46.15(15)
B1-O3-C15-C17	-101.99(11)
B1-O3-C15-C18	139.64(10)
B1-O3-C15-C16	17.65(13)
B1-O4-C16-C20	141.93(12)
B1-O4-C16-C19	-99.48(12)

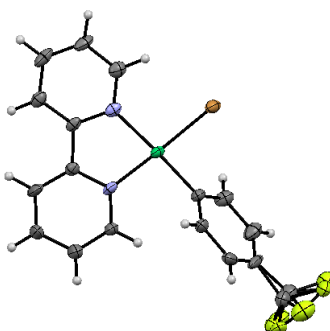
Chapter 4.

B1-O4-C16-C15	19.63(14)
O3-C15-C16-O4	-22.56(12)
C17-C15-C16-O4	92.28(11)
C18-C15-C16-O4	-138.75(10)
O3-C15-C16-C20	-140.79(12)
C17-C15-C16-C20	-25.96(16)
C18-C15-C16-C20	103.01(14)
O3-C15-C16-C19	91.90(12)
C17-C15-C16-C19	-153.26(11)
C18-C15-C16-C19	-24.30(15)
C10'-C1'-C2'-C3'	132.3(8)
B1'-C1'-C2'-C3'	-96.9(9)
C10'-C1'-C2'-C7'	-44.8(9)
B1'-C1'-C2'-C7'	86.0(8)
C7'-C2'-C3'-C4'	0.0
C1'-C2'-C3'-C4'	-177.0(8)
C2'-C3'-C4'-C5'	0.0
C3'-C4'-C5'-C6'	0.0
C3'-C4'-C5'-C8'	178.2(12)
C4'-C5'-C6'-C7'	0.0
C8'-C5'-C6'-C7'	-177.8(15)
C5'-C6'-C7'-C2'	0.0
C3'-C2'-C7'-C6'	0.0
C1'-C2'-C7'-C6'	177.3(8)
C9'-O1'-C8'-O2'	-8(3)
C9'-O1'-C8'-C5'	-179.0(15)
C6'-C5'-C8'-O2'	-169.4(16)
C4'-C5'-C8'-O2'	13(2)
C6'-C5'-C8'-O1'	2(2)
C4'-C5'-C8'-O1'	-176.0(14)
C2'-C1'-C10'-C11'	-151.4(7)
B1'-C1'-C10'-C11'	82.9(10)
C1'-C10'-C11'-C14'	-174.2(8)
C1'-C10'-C11'-C13'	-52.5(12)
C1'-C10'-C11'-C12'	59.1(10)
C15'-O3'-B1'-O4'	24.0(13)
C15'-O3'-B1'-C1'	-167.9(10)
C16'-O4'-B1'-O3'	-4.7(14)

Site-Selective 1,2-Dicarbofunctionalization of Vinyl Boronates through Dual Catalysis

C16'-O4'-B1'-C1'	-173.7(10)
C2'-C1'-B1'-O3'	115.5(13)
C10'-C1'-B1'-O3'	-114.1(12)
C2'-C1'-B1'-O4'	-77.3(12)
C10'-C1'-B1'-O4'	53.2(14)
B1'-O3'-C15'-C16'	-35.2(11)
B1'-O3'-C15'-C18'	85.4(11)
B1'-O3'-C15'-C17'	-153.3(9)
O3'-C15'-C16'-C20'	-86.0(12)
C18'-C15'-C16'-C20'	159.8(10)
C17'-C15'-C16'-C20'	26.3(15)
O3'-C15'-C16'-C19'	139.3(9)
C18'-C15'-C16'-C19'	25.1(15)
C17'-C15'-C16'-C19'	-108.4(11)
O3'-C15'-C16'-O4'	27.3(9)
C18'-C15'-C16'-O4'	-86.9(11)
C17'-C15'-C16'-O4'	139.6(9)
B1'-O4'-C16'-C20'	103.8(10)
B1'-O4'-C16'-C19'	-134.3(9)
B1'-O4'-C16'-C15'	-15.7(11)

4.8.8.2 X-Ray crystallography data of Ni(II) complex Ni-4.5.1



X-Ray quality crystals were obtained from a saturated solution of **Ni-4.5.1** in Toluene and drops of pentane were slowly added, and cooling the solution at $-35\text{ }^{\circ}\text{C}$ overnight. A CIF file is available as a separate Supporting Information file.

Table 1. Crystal data and structure refinement for **Ni-4.5.1**.

Identification code	RJS-834_4t	
Empirical formula	C _{27.50} H _{23.50} Br F ₃ N ₂ Ni	
Formula weight	577.60	
Temperature	100(2)K	
Wavelength	0.71073 \approx	
Crystal system	monoclinic	
Space group	P 21/n	
Unit cell dimensions	a = 10.1360(18) \approx b = 14.018(2) \approx c = 17.441(3) \approx	$\alpha = 90^{\circ}$. $\beta = 98.296(5)^{\circ}$. $\gamma = 90^{\circ}$.
Volume	2452.2(7) \approx^3	
Z	4	
Density (calculated)	1.565 Mg/m ³	
Absorption coefficient	2.462 mm ⁻¹	
F(000)	1170	
Crystal size	0.070 x 0.060 x 0.030 mm ³	
Theta range for data collection	1.872 to 30.629 $^{\circ}$.	
Index ranges	? \leq h \leq ?, ? \leq k \leq ?, ? \leq l \leq ?	
Reflections collected	6875	
Independent reflections	6875 [R(int) = ?]	
Completeness to theta = 30.629 $^{\circ}$	90.9%	
Absorption correction	Multi-scan	
Max. and min. transmission	0.74 and 0.59	
Refinement method	Full-matrix least-squares on F ²	

Data / restraints / parameters	6875/ 331/ 441
Goodness-of-fit on F ²	0.912
Final R indices [I>2sigma(I)]	R1 = 0.0485, wR2 = 0.0952
R indices (all data)	R1 = 0.1574, wR2 = 0.1120
Largest diff. peak and hole	0.874 and -0.536 e. \approx ⁻³

Table 2. Bond lengths [\approx] and angles [∞] for **Ni-4.5.1**.

Bond lengths----

Ni1	C11	1.896(4)
Ni1	N1	1.928(3)
Ni1	N2	1.981(3)
Ni1	Br1	2.3072(7)
N1	C1	1.346(4)
N1	C5	1.358(4)
C1	C2	1.378(5)
C2	C3	1.374(5)
N2	C10	1.334(4)
N2	C6	1.343(4)
C3	C4	1.379(5)
C4	C5	1.389(5)
C5	C6	1.466(5)
C6	C7	1.382(5)
C7	C8	1.383(5)
C8	C9	1.364(6)
C9	C10	1.380(5)
C11	C12'	1.32(3)
C11	C16	1.322(14)
C11	C12	1.436(13)
C11	C16'	1.56(3)
C12	C13	1.393(16)
C13	C14	1.382(11)
C14	C15	1.421(12)
C14	C17	1.483(12)
C15	C16	1.413(17)
C17	F2	1.350(8)
C17	F3	1.378(9)

Chapter 4.

C17	F1	1.412(16)	
C12'	C13'	1.43(3)	
C13'	C14'	1.34(2)	
C14'	C15'	1.32(2)	
C14'	C17'	1.56(3)	
C15'	C16'	1.37(4)	
C17'	F3'	1.22(4)	
C17'	F1'	1.28(2)	
C17'	F2'	1.37(2)	
C1A	C2A	1.376(6)	
C1A	C3A#	1.383(6)	3_667
C2A	C3A	1.390(6)	
C2A	C4A	1.506(9)	
C1B	C2B	1.3900	
C1B	C6B	1.3900	
C1B	C7B	1.511(6)	
C2B	C3B	1.3900	
C3B	C4B	1.3900	
C4B	C5B	1.3900	
C5B	C6B	1.3900	
C1B'	C2B'	1.3900	
C1B'	C6B'	1.3900	
C2B'	C3B'	1.3900	
C2B'	C7B'	1.505(13)	
C3B'	C4B'	1.3900	
C4B'	C5B'	1.3900	
C5B'	C6B'	1.3900	

Angles-----

C11	Ni1	N1	94.64(13)
C11	Ni1	N2	175.70(14)
N1	Ni1	N2	82.69(12)
C11	Ni1	Br1	87.26(10)
N1	Ni1	Br1	176.06(8)
N2	Ni1	Br1	95.62(9)
C1	N1	C5	118.7(3)
C1	N1	Ni1	126.9(3)
C5	N1	Ni1	114.4(2)

Site-Selective 1,2-Dicarbofunctionalization of Vinyl Boronates through Dual Catalysis

N1	C1	C2	121.7(4)
C3	C2	C1	120.1(4)
C10	N2	C6	117.9(3)
C10	N2	Ni1	127.9(3)
C6	N2	Ni1	114.1(2)
C2	C3	C4	118.7(4)
C3	C4	C5	119.5(4)
N1	C5	C4	121.3(3)
N1	C5	C6	115.2(3)
C4	C5	C6	123.5(3)
N2	C6	C7	122.0(3)
N2	C6	C5	113.6(3)
C7	C6	C5	124.3(3)
C6	C7	C8	119.3(4)
C9	C8	C7	118.5(4)
C8	C9	C10	119.3(4)
N2	C10	C9	122.9(4)
C16	C11	C12	119.9(9)
C12'	C11	C16'	111.1(17)
C12'	C11	Ni1	126.9(12)
C16	C11	Ni1	122.4(6)
C12	C11	Ni1	117.7(6)
C16'	C11	Ni1	122.1(12)
C13	C12	C11	120.9(10)
C14	C13	C12	119.2(8)
C13	C14	C15	119.3(9)
C13	C14	C17	122.1(7)
C15	C14	C17	118.6(8)
C16	C15	C14	120.3(9)
C11	C16	C15	120.5(11)
F2	C17	F3	103.5(6)
F2	C17	F1	108.1(8)
F3	C17	F1	105.7(8)
F2	C17	C14	113.5(6)
F3	C17	C14	112.8(6)
F1	C17	C14	112.5(9)
C11	C12'	C13'	122.7(19)
C14'	C13'	C12'	120.9(17)

Chapter 4.

C15'	C14'	C13'	125.0(19)	
C15'	C14'	C17'	114.7(16)	
C13'	C14'	C17'	120.3(16)	
C14'	C15'	C16'	114(2)	
C15'	C16'	C11	126(2)	
F3'	C17'	F1'	114(2)	
F3'	C17'	F2'	97.7(18)	
F1'	C17'	F2'	106.7(18)	
F3'	C17'	C14'	114(2)	
F1'	C17'	C14'	112.8(16)	
F2'	C17'	C14'	109.7(14)	
C2A	C1A	C3A#	121.8(5)	3_667
C1A	C2A	C3A	117.6(4)	
C1A	C2A	C4A	127.0(6)	
C3A	C2A	C4A	115.3(6)	
C1A#	C3A	C2A	120.6(4)	3_667
C2B	C1B	C6B	120.0	
C2B	C1B	C7B	120.0(3)	
C6B	C1B	C7B	120.0(3)	
C3B	C2B	C1B	120.0	
C2B	C3B	C4B	120.0	
C5B	C4B	C3B	120.0	
C4B	C5B	C6B	120.0	
C5B	C6B	C1B	120.0	
C2B'	C1B'	C6B'	120.0	
C3B'	C2B'	C1B'	120.0	
C3B'	C2B'	C7B'	119.4(7)	
C1B'	C2B'	C7B'	120.6(7)	
C4B'	C3B'	C2B'	120.0	
C5B'	C4B'	C3B'	120.0	
C4B'	C5B'	C6B'	120.0	
C5B'	C6B'	C1B'	120.0	

Table 3. Torsion angles [$^{\circ}$] for **Ni-4.5.1**.

C5	N1	C1	C2	0.9(5)
Ni1	N1	C1	C2	178.8(3)
N1	C1	C2	C3	-1.1(6)
C1	C2	C3	C4	0.1(7)
C2	C3	C4	C5	1.0(6)
C1	N1	C5	C4	0.4(5)
Ni1	N1	C5	C4	-177.9(3)
C1	N1	C5	C6	179.4(3)
Ni1	N1	C5	C6	1.2(4)
C3	C4	C5	N1	-1.3(6)
C3	C4	C5	C6	179.7(4)
C10	N2	C6	C7	-0.6(5)
Ni1	N2	C6	C7	-178.6(3)
C10	N2	C6	C5	179.2(3)
Ni1	N2	C6	C5	1.2(4)
N1	C5	C6	N2	-1.6(4)
C4	C5	C6	N2	177.5(3)
N1	C5	C6	C7	178.2(3)
C4	C5	C6	C7	-2.8(6)
N2	C6	C7	C8	-0.2(5)
C5	C6	C7	C8	-179.9(3)
C6	C7	C8	C9	1.2(5)
C7	C8	C9	C10	-1.5(6)
C6	N2	C10	C9	0.3(5)
Ni1	N2	C10	C9	178.0(3)
C8	C9	C10	N2	0.8(6)
N1	Ni1	C11	C12'	65.5(15)
Br1	Ni1	C11	C12'	-118.0(15)
N1	Ni1	C11	C16	-104.0(7)
Br1	Ni1	C11	C16	72.5(7)
N1	Ni1	C11	C12	74.3(7)
Br1	Ni1	C11	C12	-109.2(6)
N1	Ni1	C11	C16'	-113.4(12)
Br1	Ni1	C11	C16'	63.1(12)
C16	C11	C12	C13	1.6(15)
Ni1	C11	C12	C13	-176.7(8)

Chapter 4.

C11	C12	C13	C14	-1.5(16)	
C12	C13	C14	C15	0.1(14)	
C12	C13	C14	C17	177.5(9)	
C13	C14	C15	C16	1.1(14)	
C17	C14	C15	C16	-176.4(9)	
C12	C11	C16	C15	-0.4(14)	
Ni1	C11	C16	C15	177.9(7)	
C14	C15	C16	C11	-1.0(15)	
C13	C14	C17	F2	-6.7(12)	
C15	C14	C17	F2	170.7(7)	
C13	C14	C17	F3	110.7(9)	
C15	C14	C17	F3	-71.9(10)	
C13	C14	C17	F1	-129.9(10)	
C15	C14	C17	F1	47.6(12)	
C16'	C11	C12'	C13'	-1(3)	
Ni1	C11	C12'	C13'	-179.7(14)	
C11	C12'	C13'	C14'	4(3)	
C12'	C13'	C14'	C15'	-3(3)	
C12'	C13'	C14'	C17'	176(2)	
C13'	C14'	C15'	C16'	-1(3)	
C17'	C14'	C15'	C16'	-179.9(19)	
C14'	C15'	C16'	C11	4(3)	
C12'	C11	C16'	C15'	-3(3)	
Ni1	C11	C16'	C15'	175.6(18)	
C15'	C14'	C17'	F3'	99(2)	
C13'	C14'	C17'	F3'	-80(3)	
C15'	C14'	C17'	F1'	-34(2)	
C13'	C14'	C17'	F1'	146.9(18)	
C15'	C14'	C17'	F2'	-152.8(18)	
C13'	C14'	C17'	F2'	28(3)	
C3A#	C1A	C2A	C3A	-1.9(7)	3_667
C3A#	C1A	C2A	C4A	-178.8(5)	3_667
C1A	C2A	C3A	C1A#	1.9(7)	3_667
C4A	C2A	C3A	C1A#	179.2(4)	3_667
C6B	C1B	C2B	C3B	0.0	
C7B	C1B	C2B	C3B	179.9(4)	
C1B	C2B	C3B	C4B	0.0	
C2B	C3B	C4B	C5B	0.0	

C3B	C4B	C5B	C6B	0.0
C4B	C5B	C6B	C1B	0.0
C2B	C1B	C6B	C5B	0.0
C7B	C1B	C6B	C5B	-179.9(4)
C6B'	C1B'	C2B'	C3B'	0.0
C6B'	C1B'	C2B'	C7B'	-178.4(9)
C1B'	C2B'	C3B'	C4B'	0.0
C7B'	C2B'	C3B'	C4B'	178.4(8)
C2B'	C3B'	C4B'	C5B'	0.0
C3B'	C4B'	C5B'	C6B'	0.0
C4B'	C5B'	C6B'	C1B'	0.0
C2B'	C1B'	C6B'	C5B'	0.0

Symetry operations

1 'x, y, z'

2 '-x+1/2, y+1/2, -z+1/2'

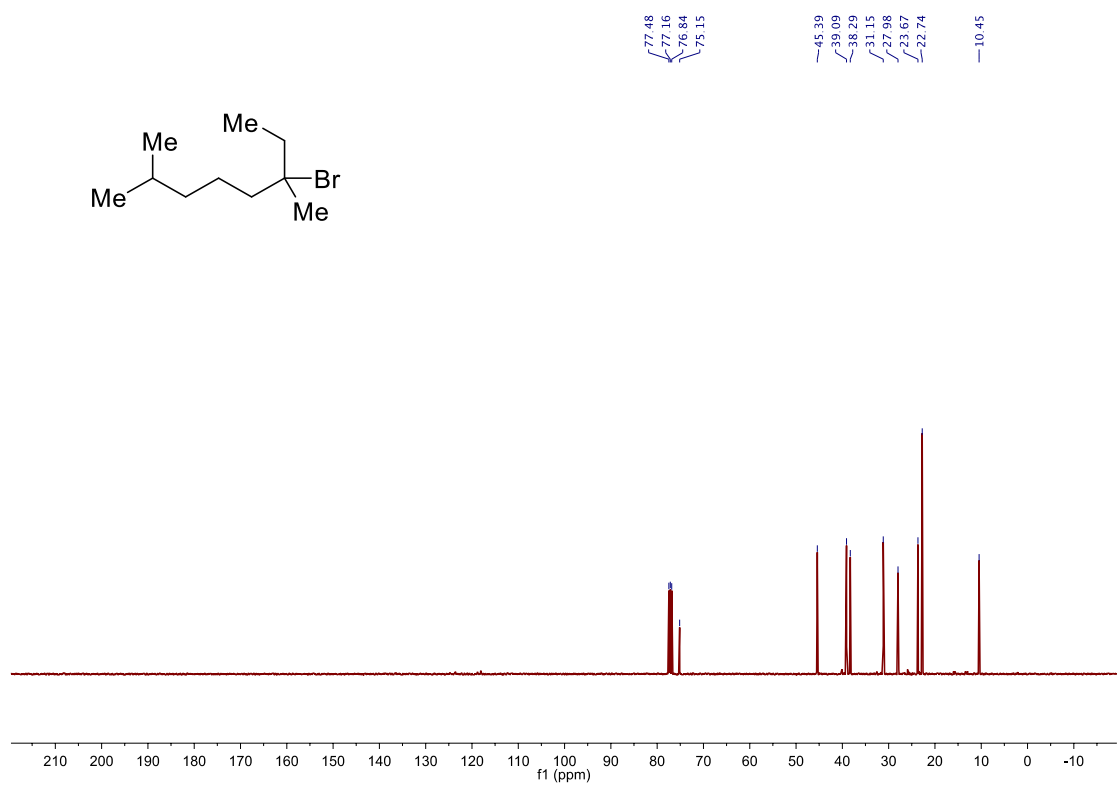
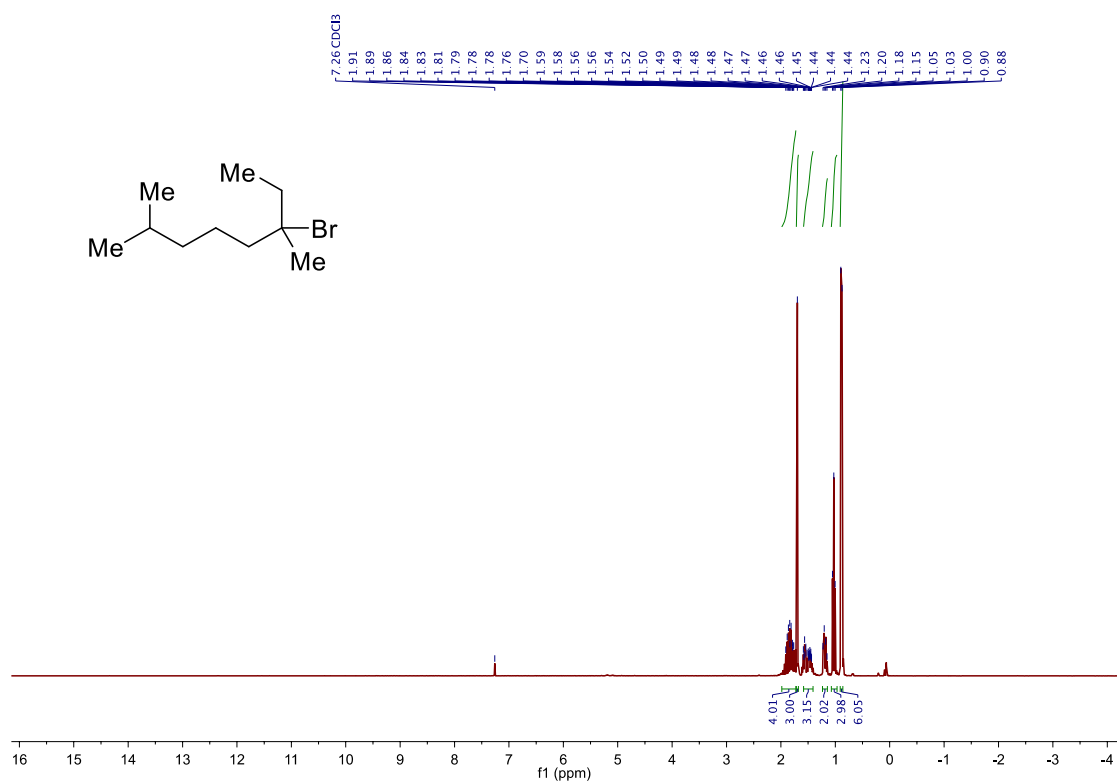
3 '-x, -y, -z'

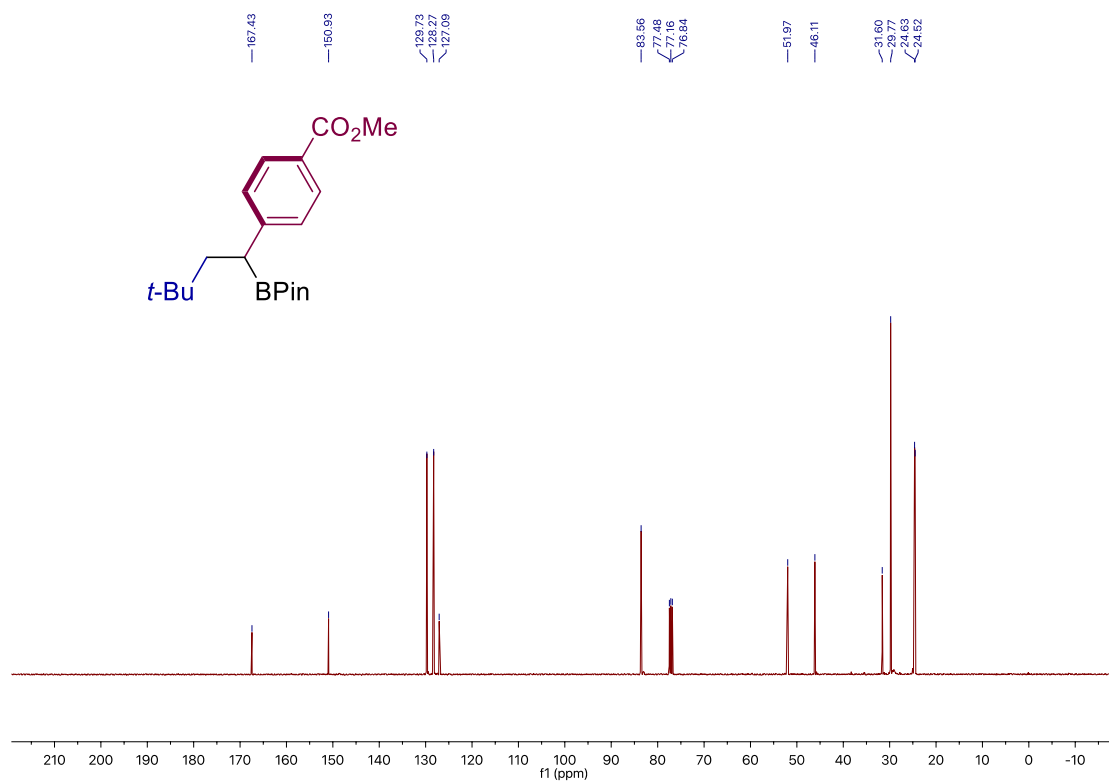
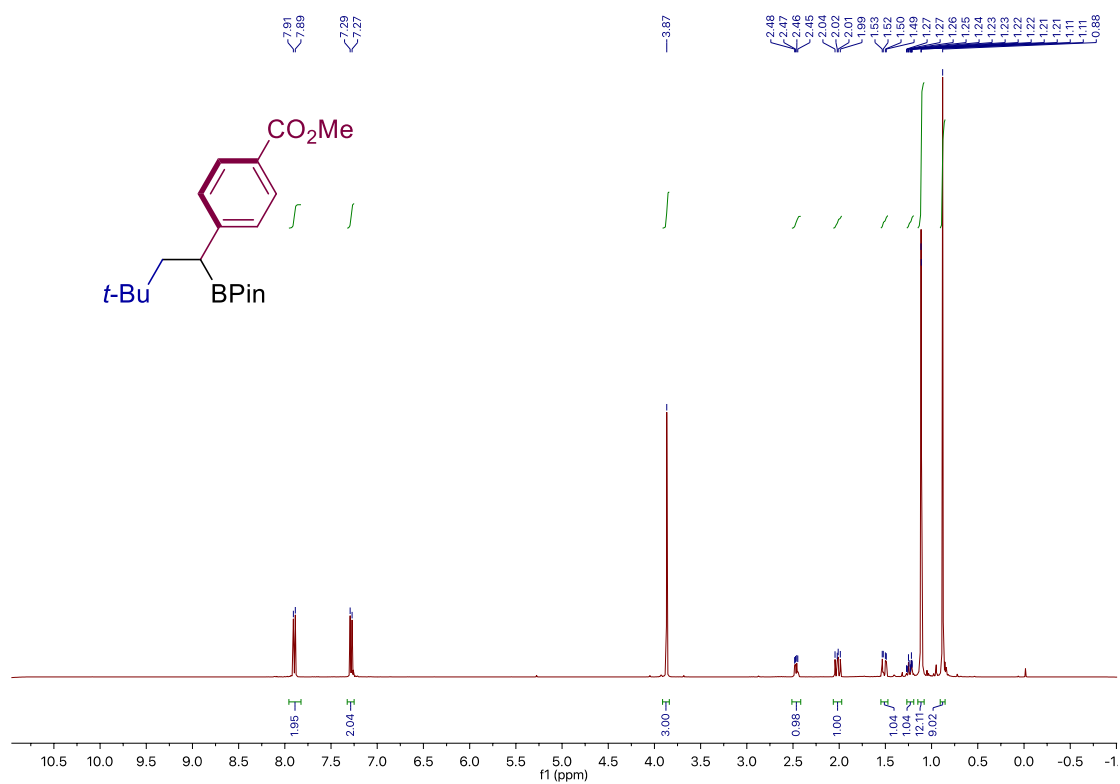
4 'x-1/2, -y-1/2, z-1/2'

4.8.9 Bibliography of Known Compounds

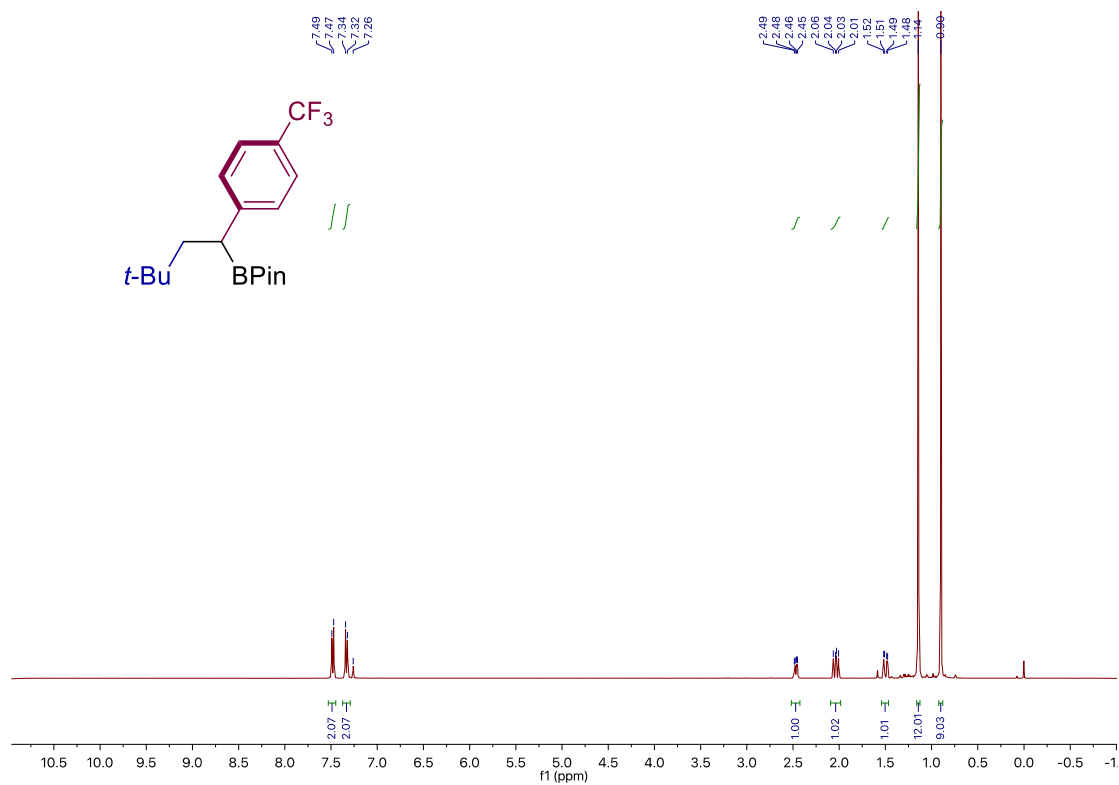
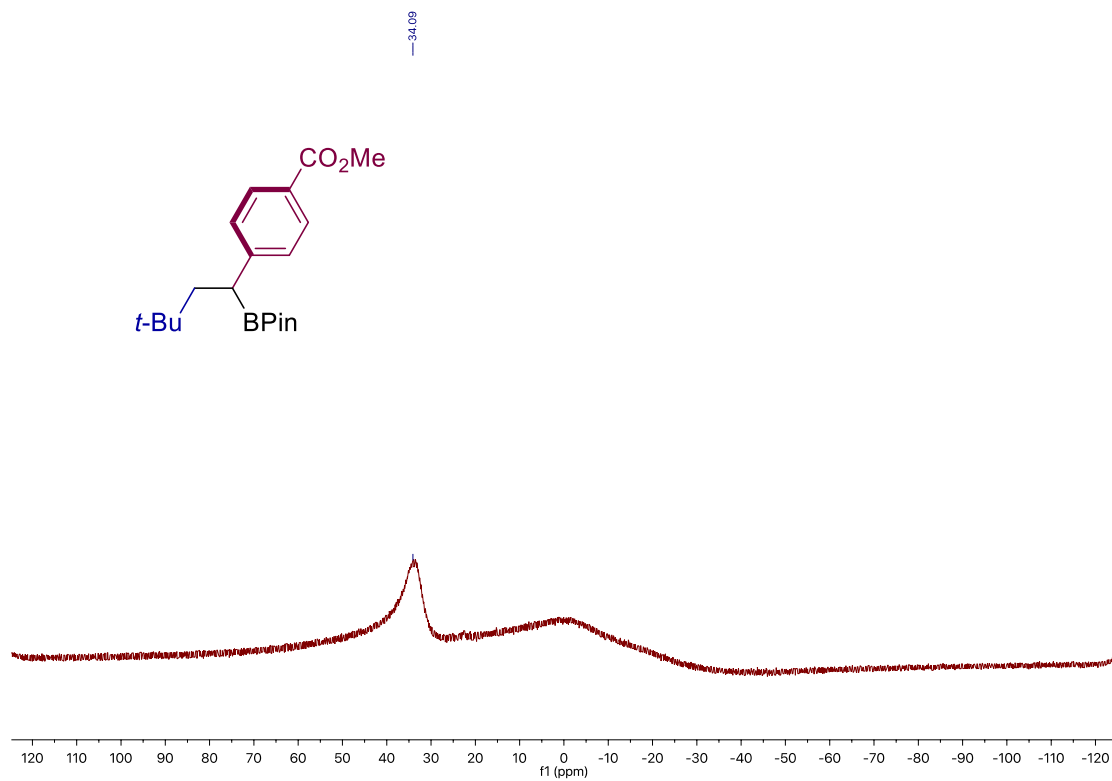
1. T. C. Atack, R. M. Lecker, S. P. Cook, *J. Am. Chem. Soc.* **2014**, *136*, 9521.
2. H. Matsubara, M. Tsukida, D. Ishihara, K. Kuniyoshi, I. Ryu, *Synlett*, **2010**, 13, 2014.
3. N. Ajvazi, S. Stavber, *Tetrahedron Lett.* **2016**, *57*, 2430.
4. F. T. Schevenels, M. Shen, S. A. Snyder, *J. Am. Chem. Soc.* **2017**, *139*, 6329.
5. R. P. Sonawane, V. Jheengut, C. Rabalakos, R. Larouche-Gauthier, H. K. Scott, V. K. Aggarwal, *Angew. Chem., Int. Ed.* **2011**, *50*, 3760.
6. M. R. Hollerbach, T. J. Barker, *Organometallics*, **2018**, *37*, 1425.
7. A. Bonet, M. Odachowski, D. Leonori, S. Essafi, V. K. Aggarwal, *Nat. Chem.* **2014**, *6*, 584.
8. D. Imao, B. W. Glasspole, V. S. Laberge, C. M. Crudden, *J. Am. Chem. Soc.* **2009**, *131*, 5024.
9. Y. Wang, A. Noble, E. L. Myers, V. K. Aggarwal, *Angew. Chem. Int. Ed.* **2016**, *55*, 4270.
10. J. Cossy in *Comprehensive Organic Functional Group Transformations II* (Eds.: A. Katritzky, R. J. K. Taylor), Elsevier, Oxford, 2004.
11. S.-Z. Sun, R. Martin, *Angew. Chem. Int. Ed.* **2018**, *57*, 3622.

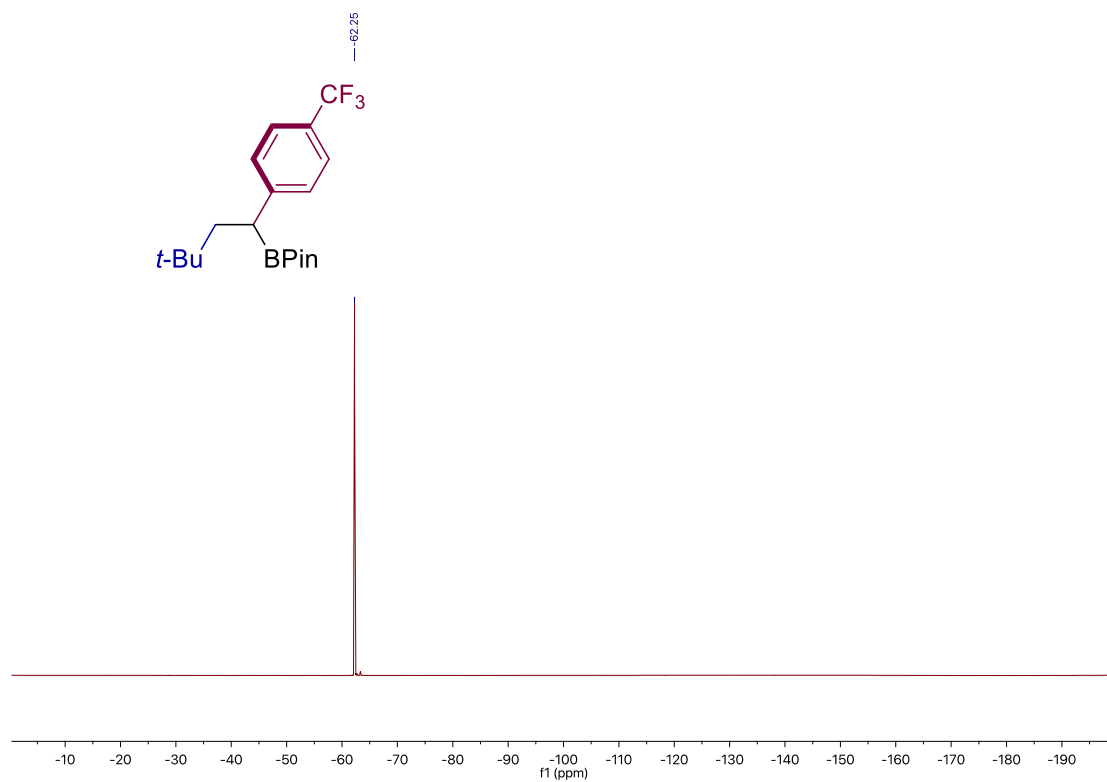
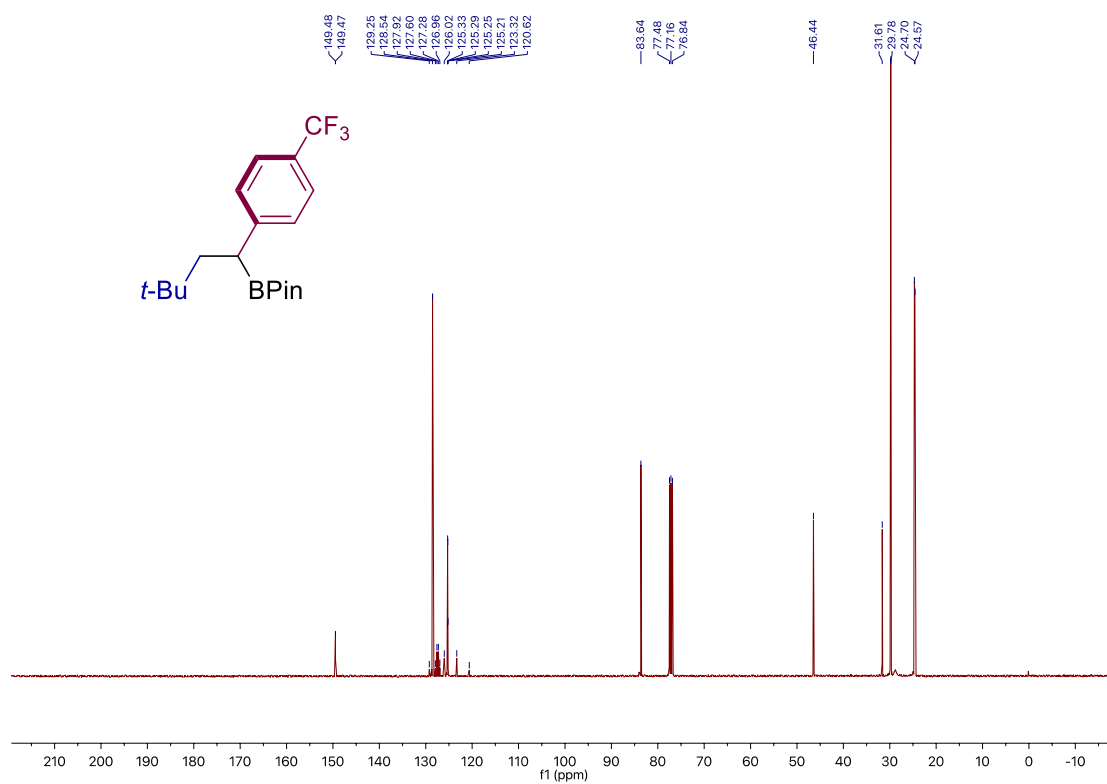
4.8.10 NMR Spectra



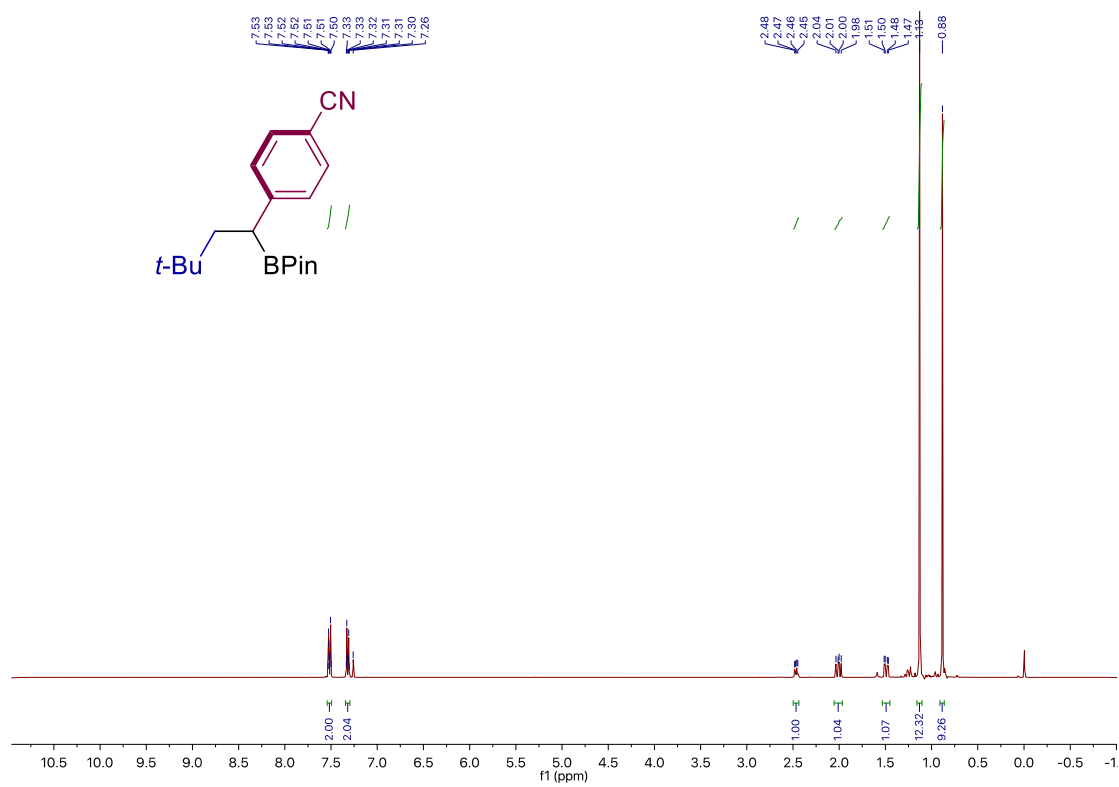
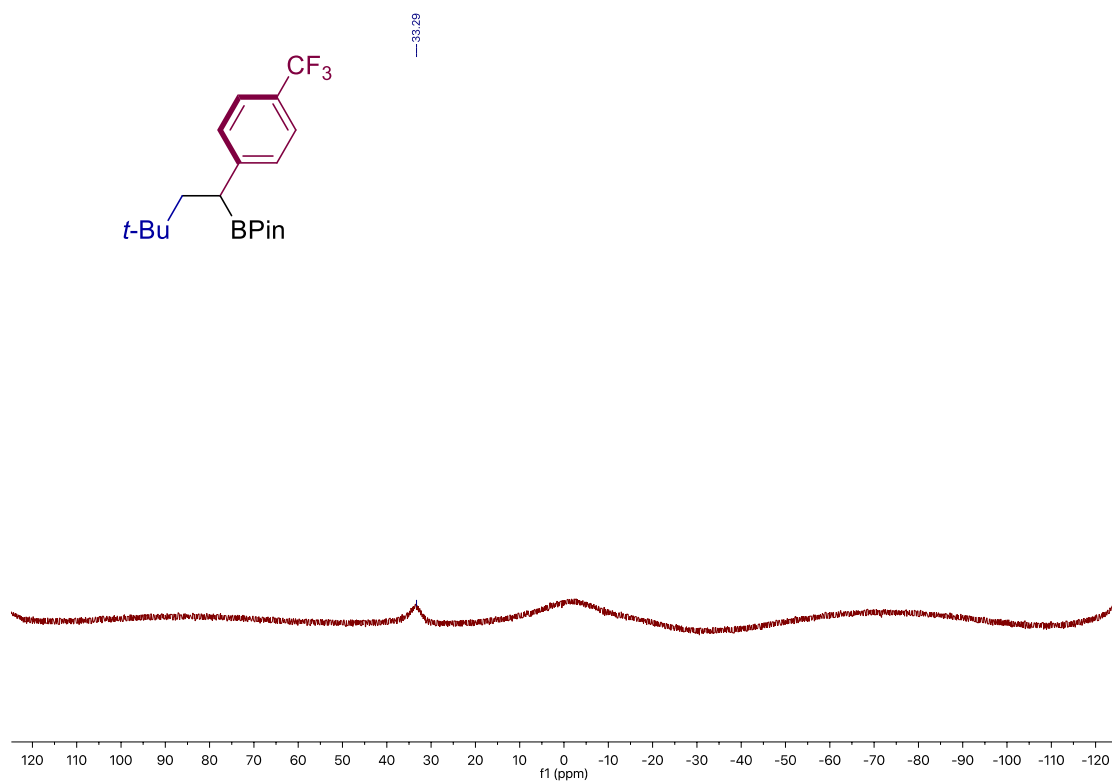


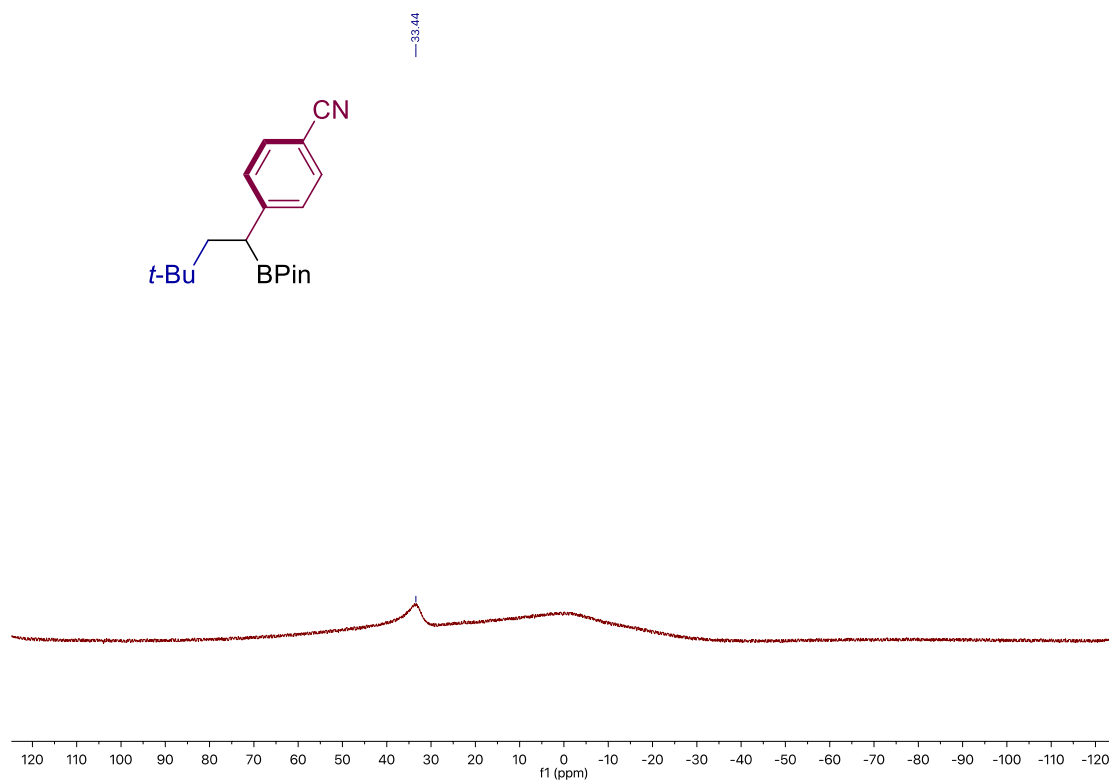
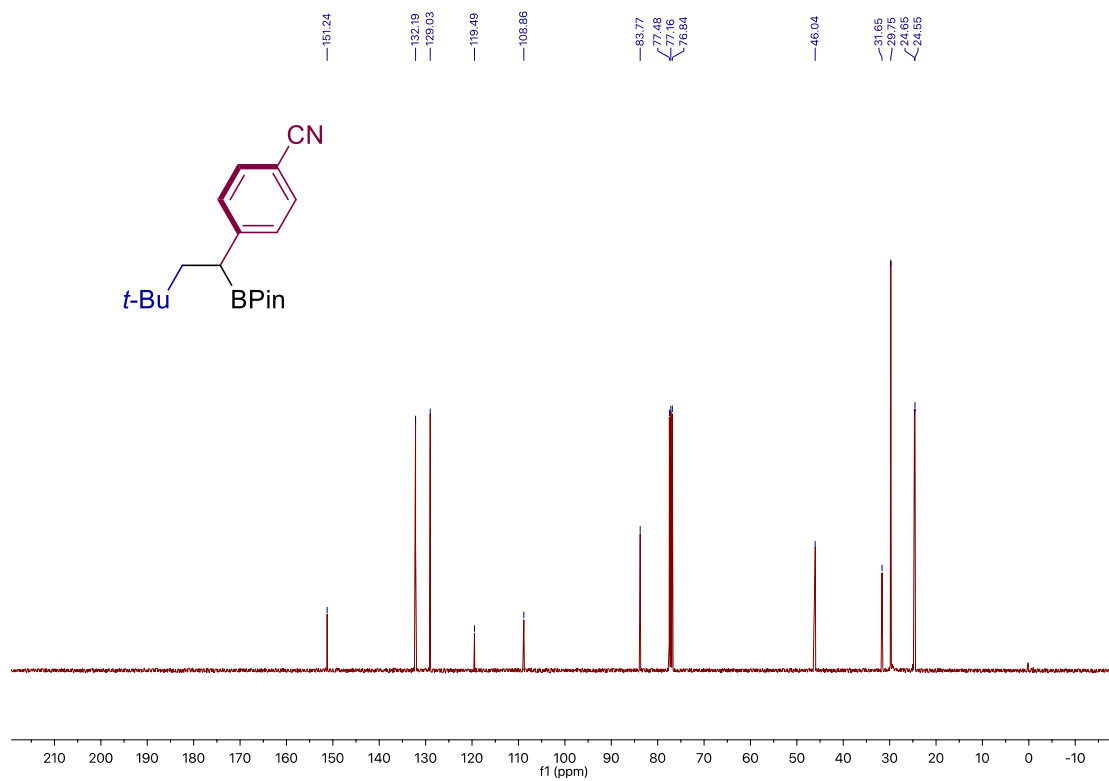
Site-Selective 1,2-Dicarbofunctionalization of Vinyl Boronates through Dual Catalysis



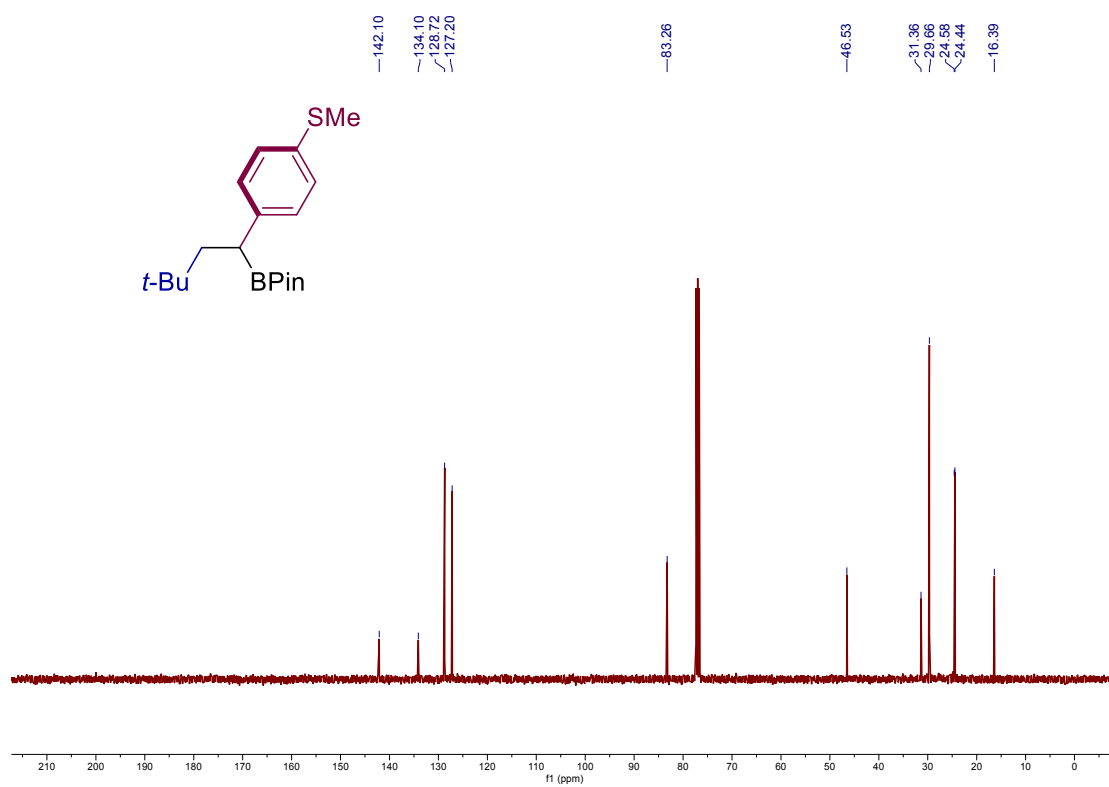
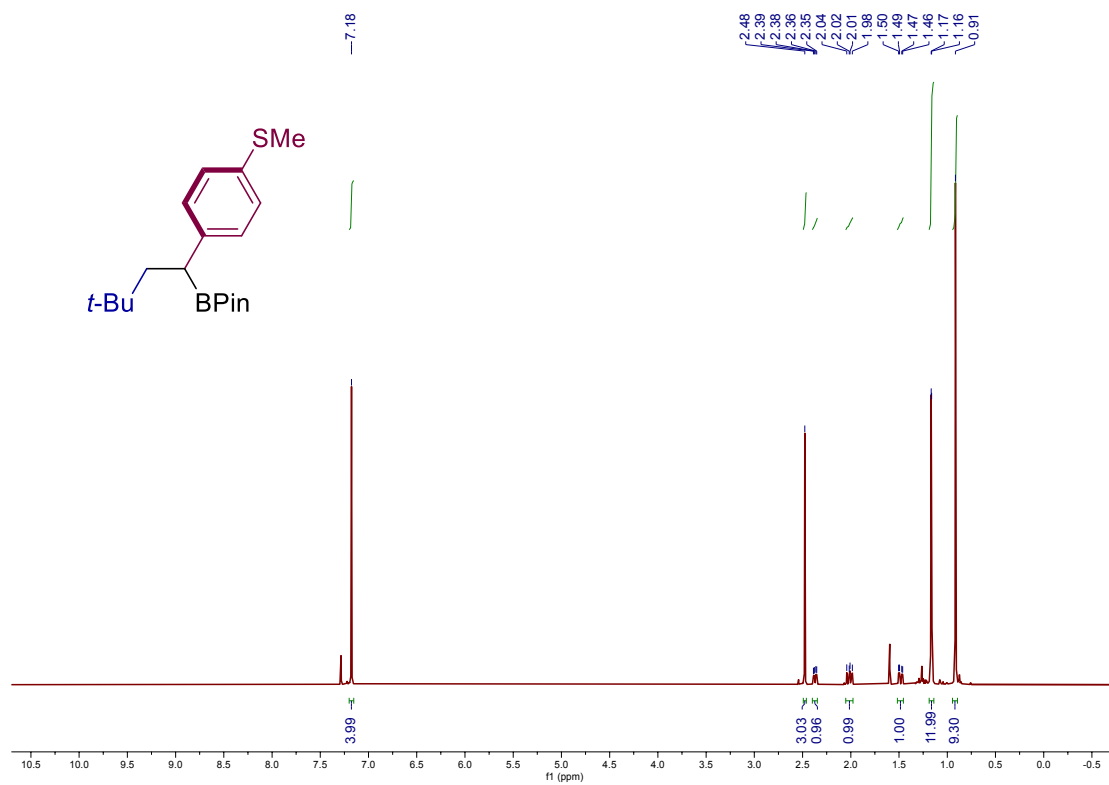


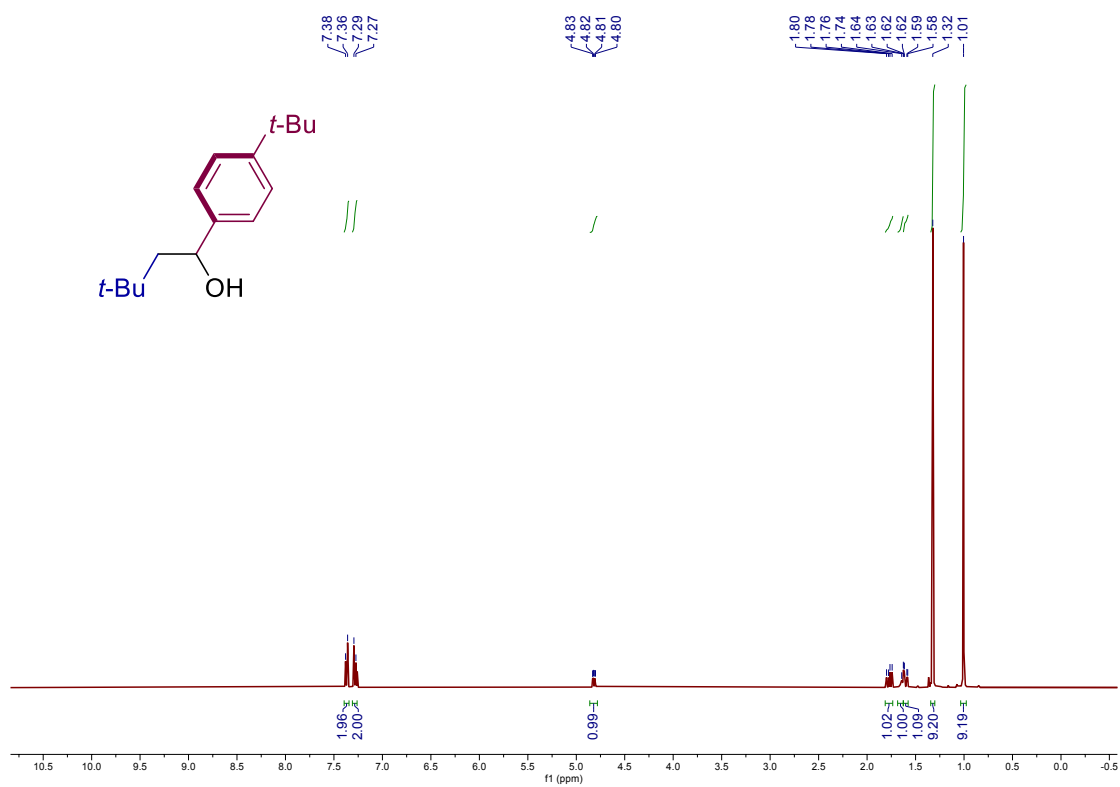
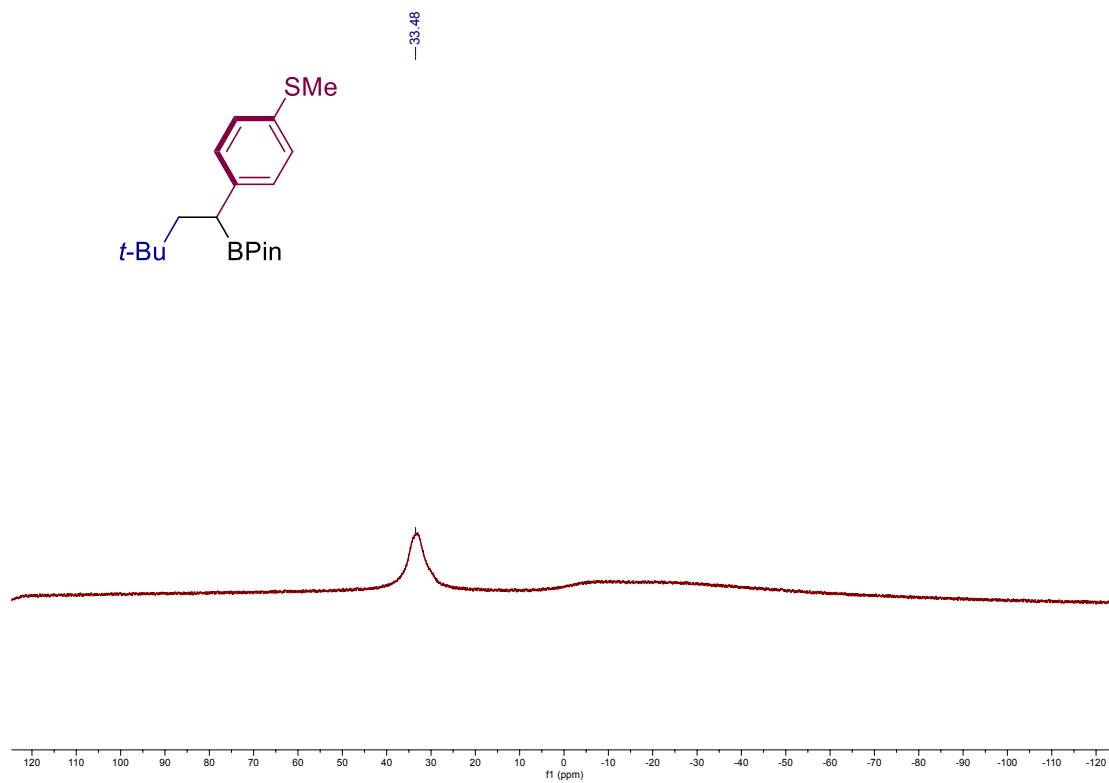
Site-Selective 1,2-Dicarbofunctionalization of Vinyl Boronates through Dual Catalysis



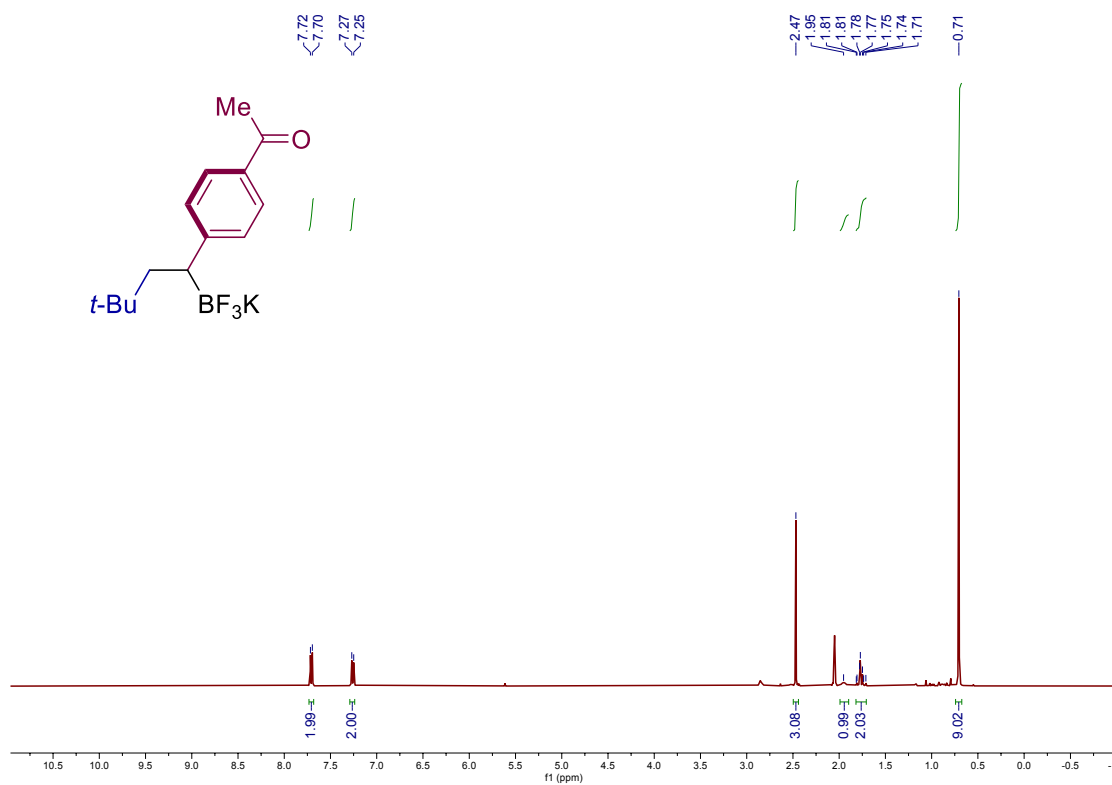
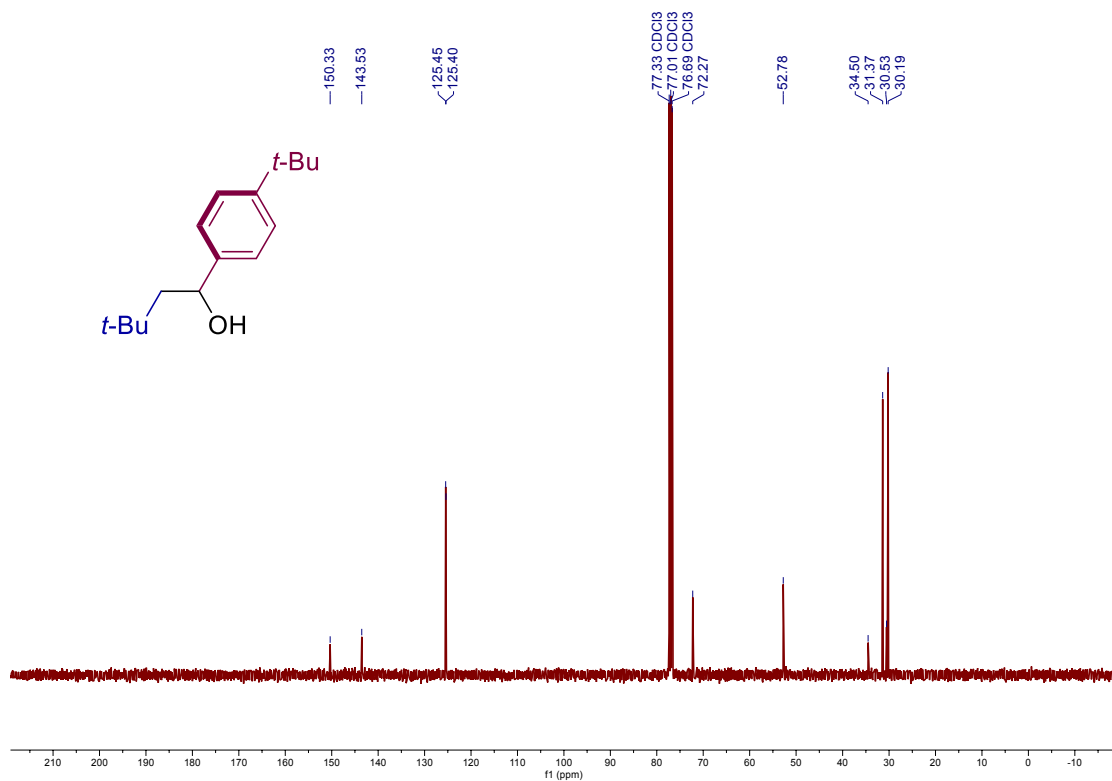


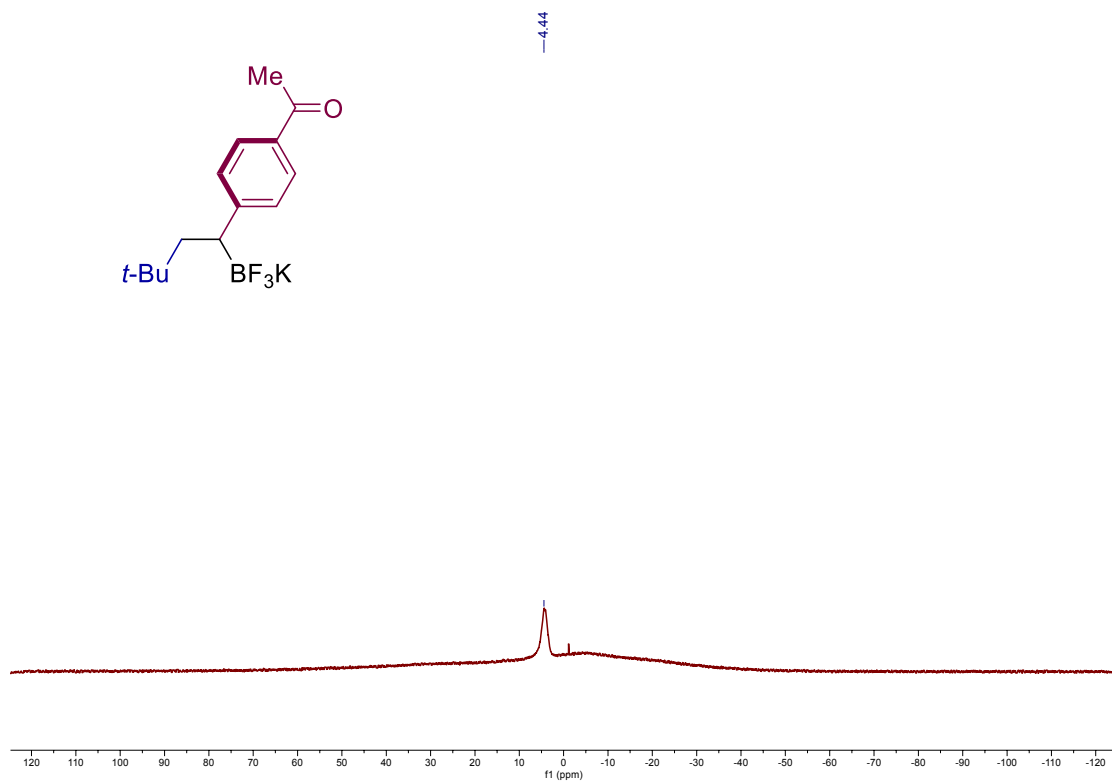
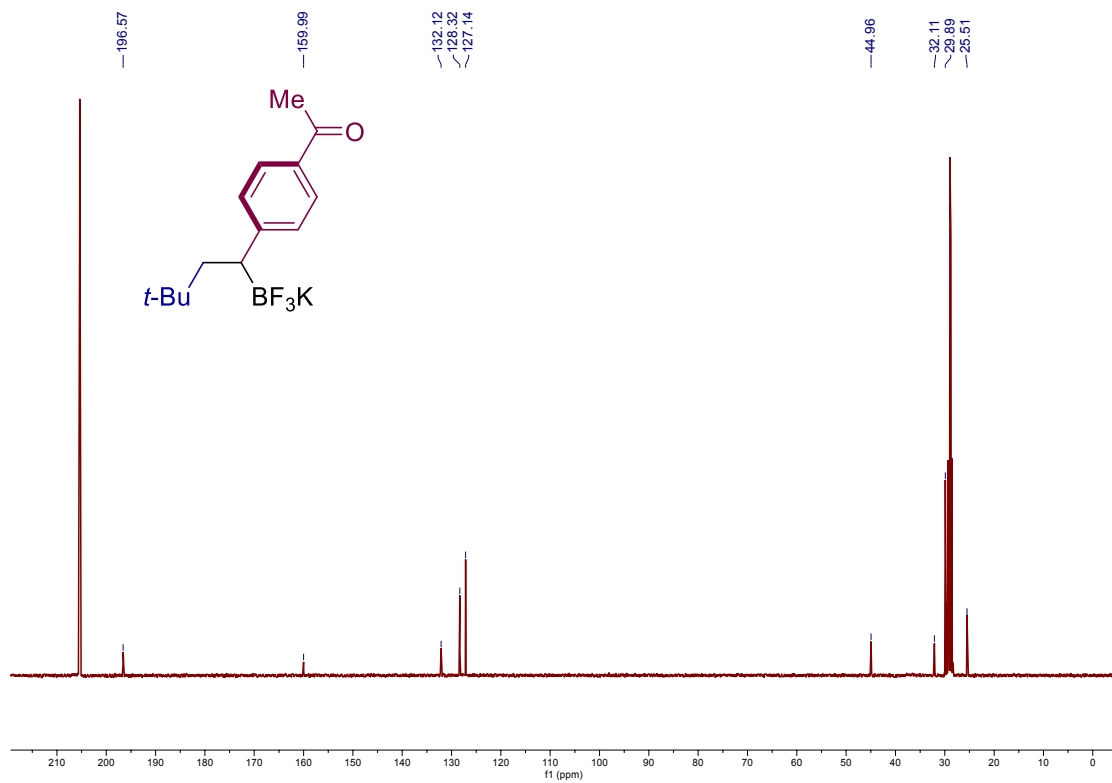
Site-Selective 1,2-Dicarbofunctionalization of Vinyl Boronates through Dual Catalysis



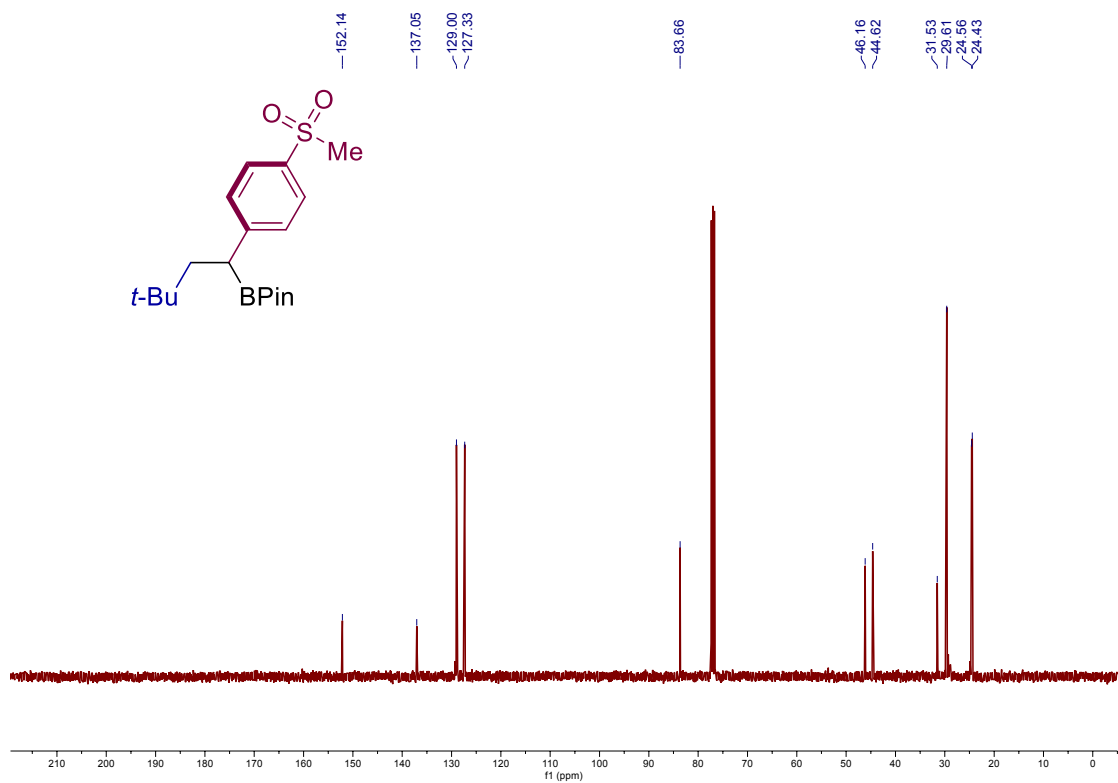
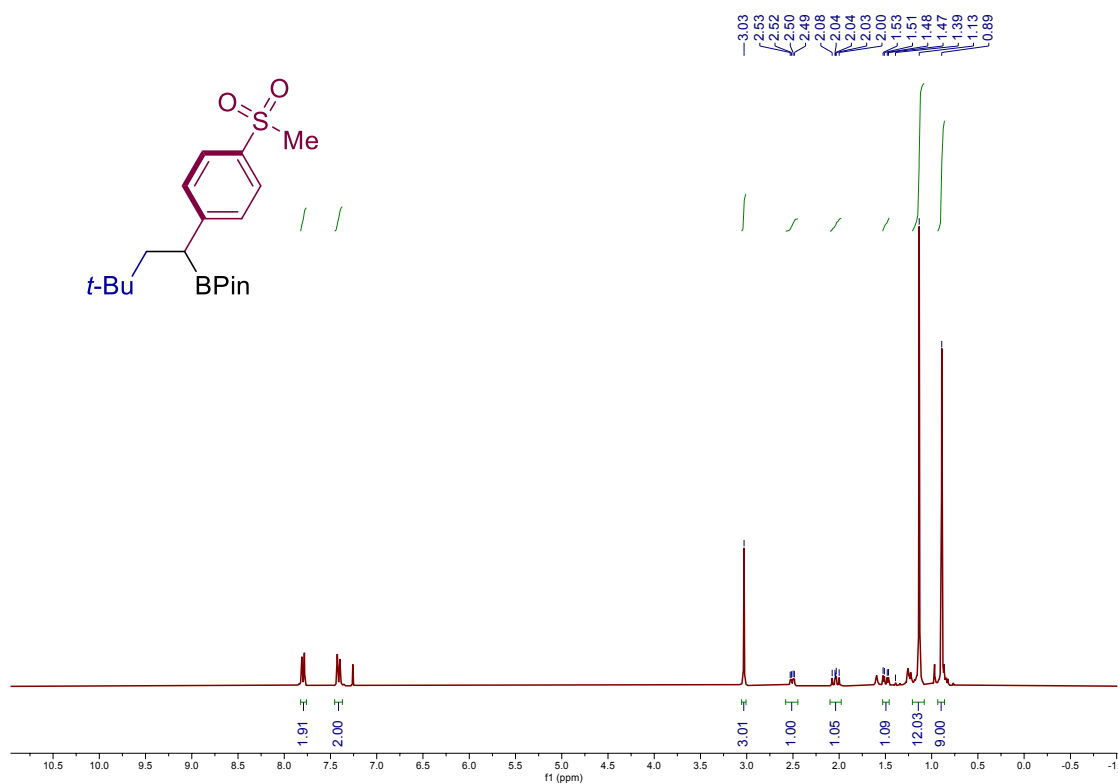


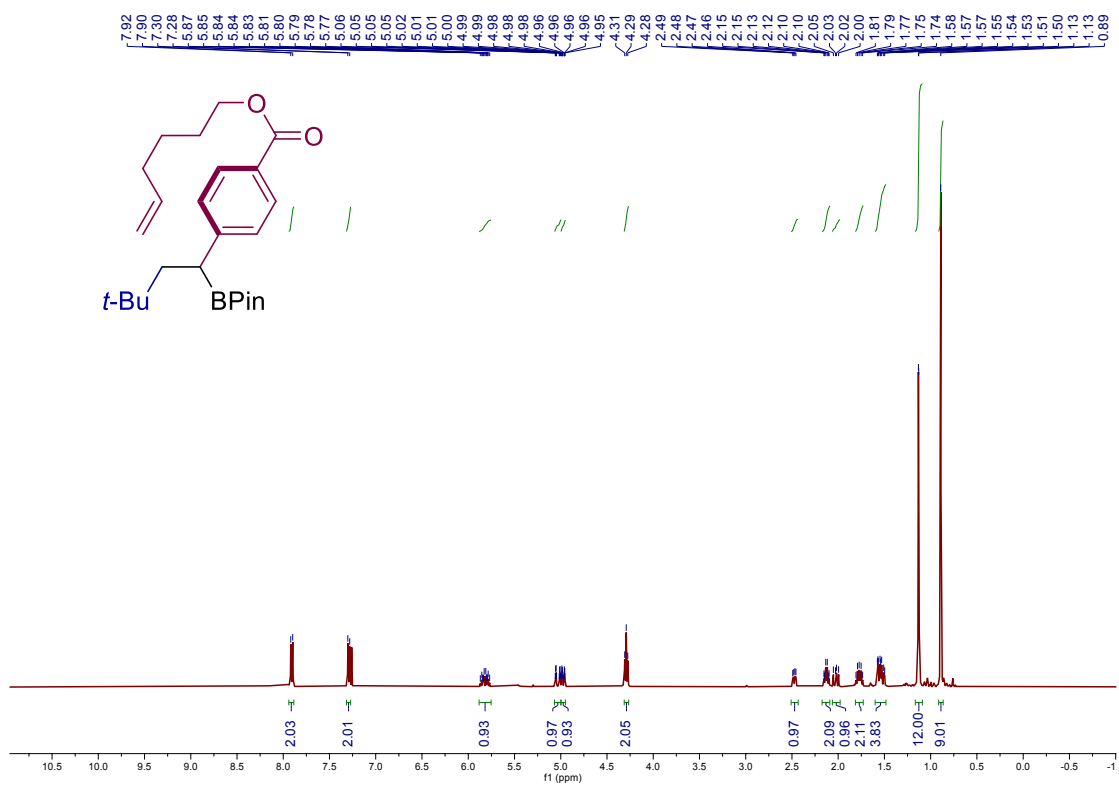
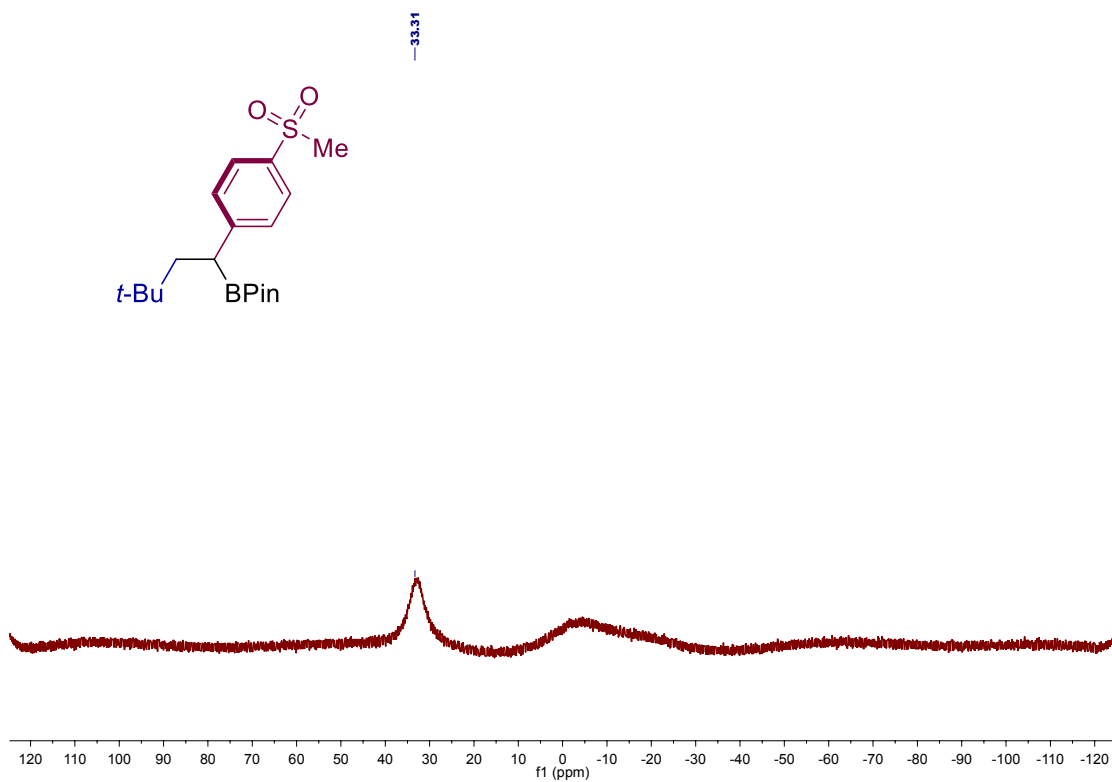
Site-Selective 1,2-Dicarbofunctionalization of Vinyl Boronates through Dual Catalysis



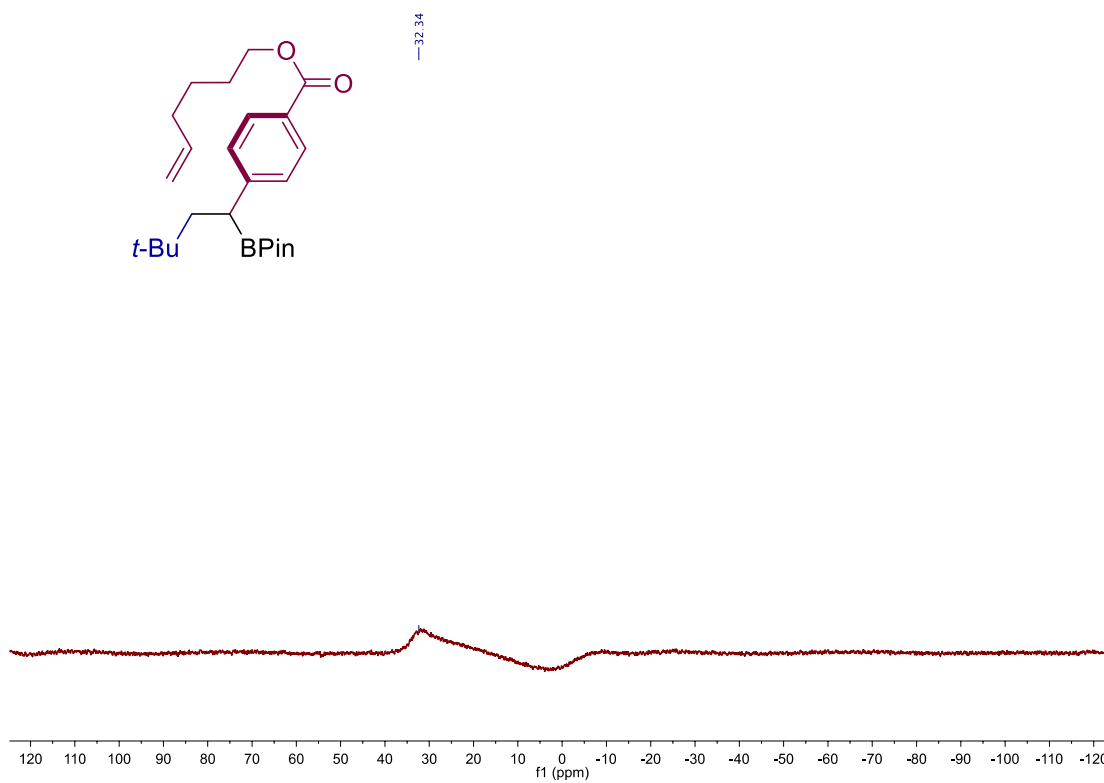
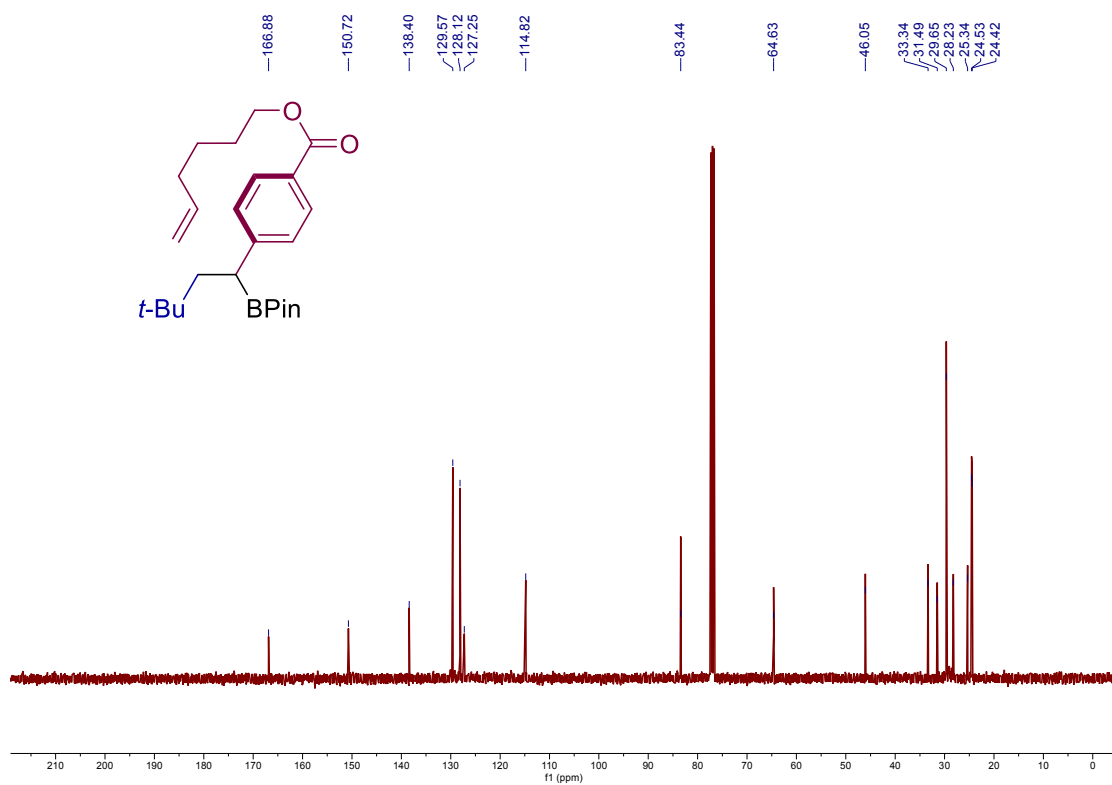


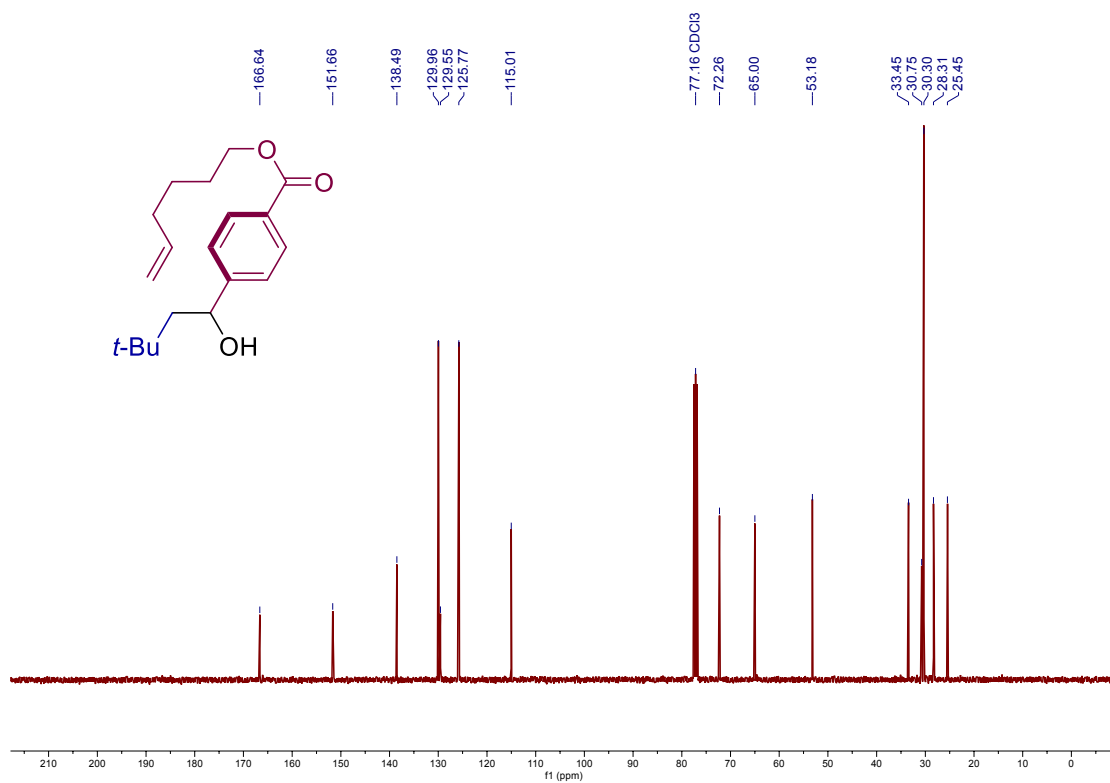
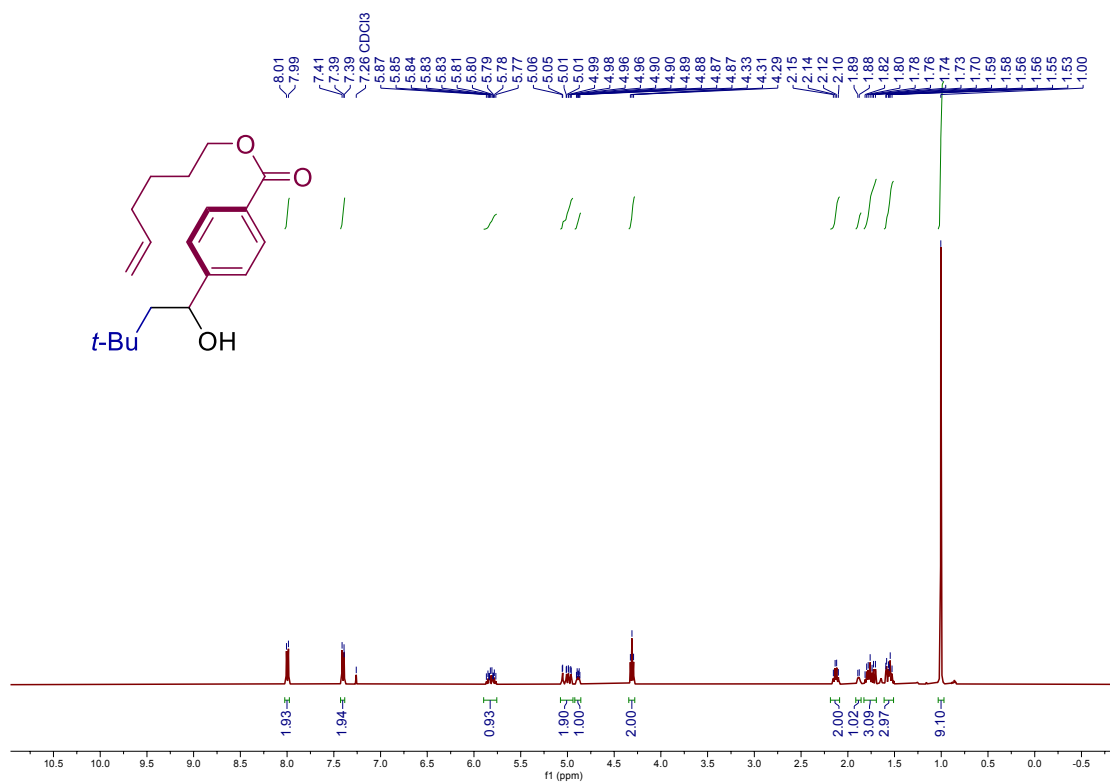
Site-Selective 1,2-Dicarbofunctionalization of Vinyl Boronates through Dual Catalysis



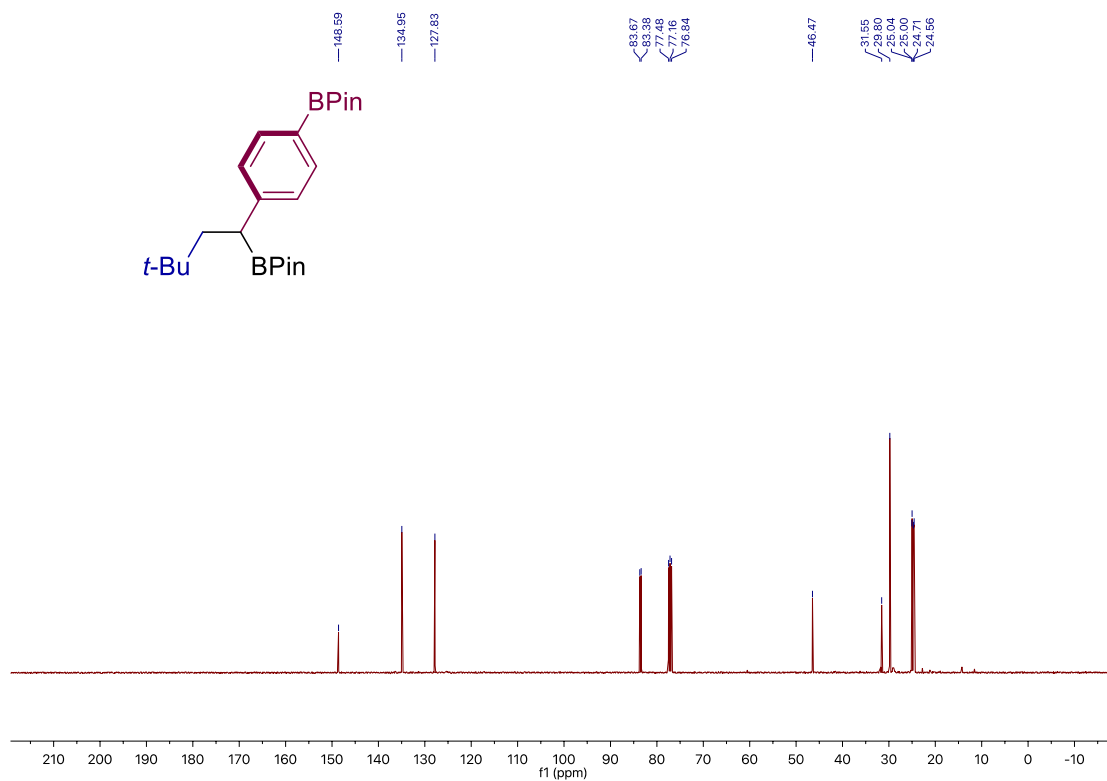
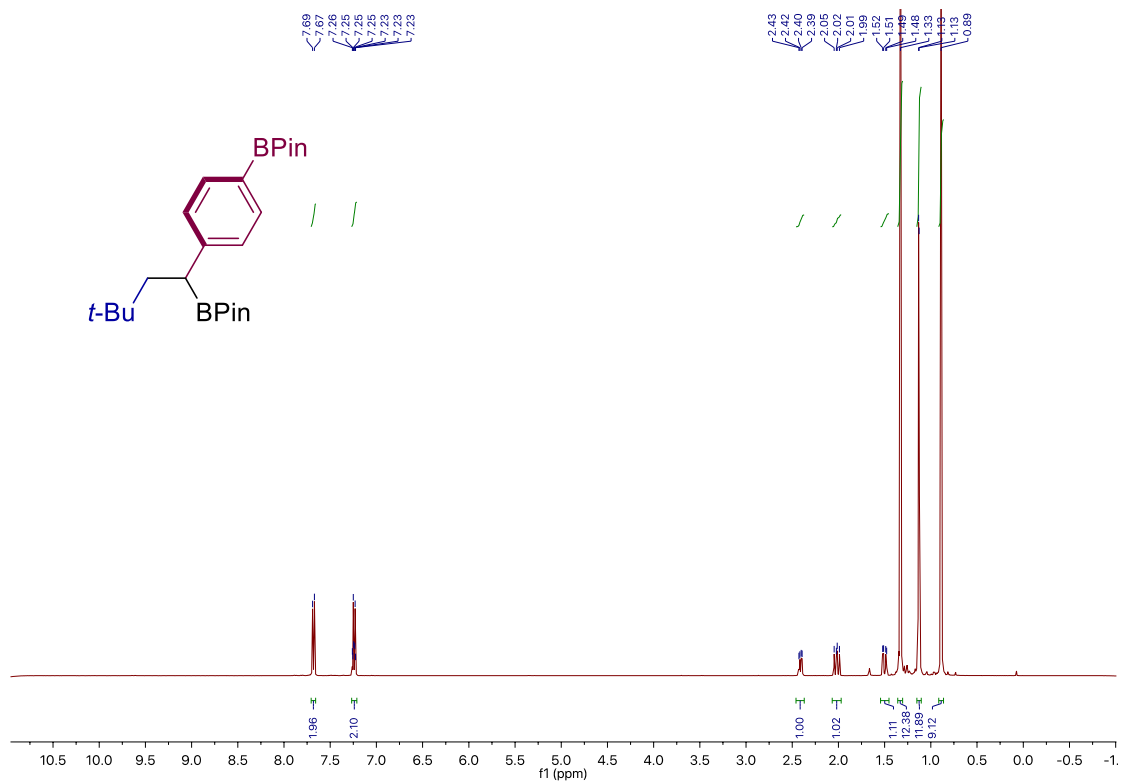


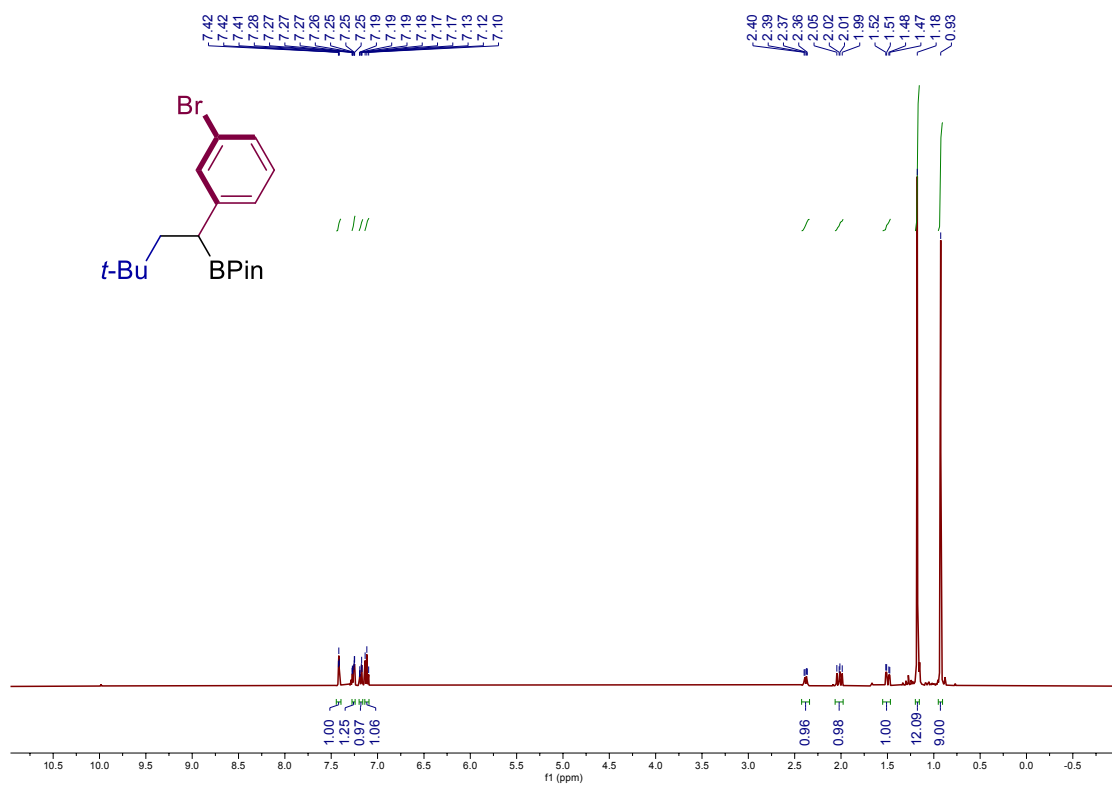
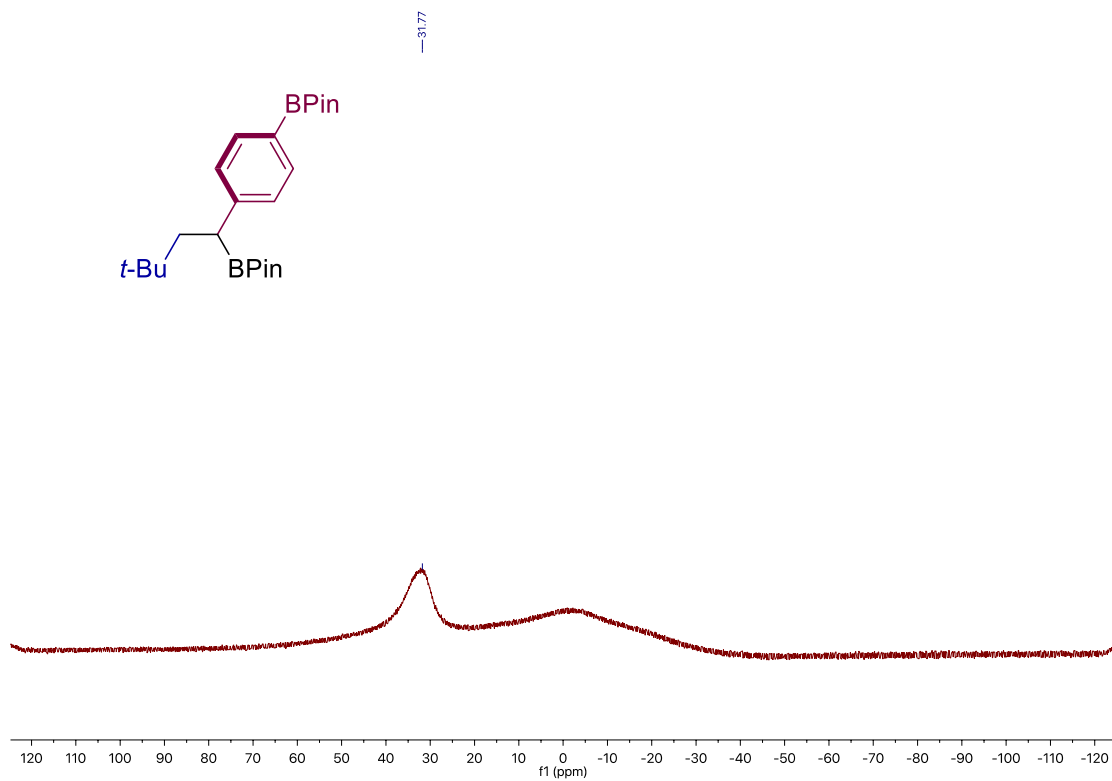
Site-Selective 1,2-Dicarbofunctionalization of Vinyl Boronates through Dual Catalysis



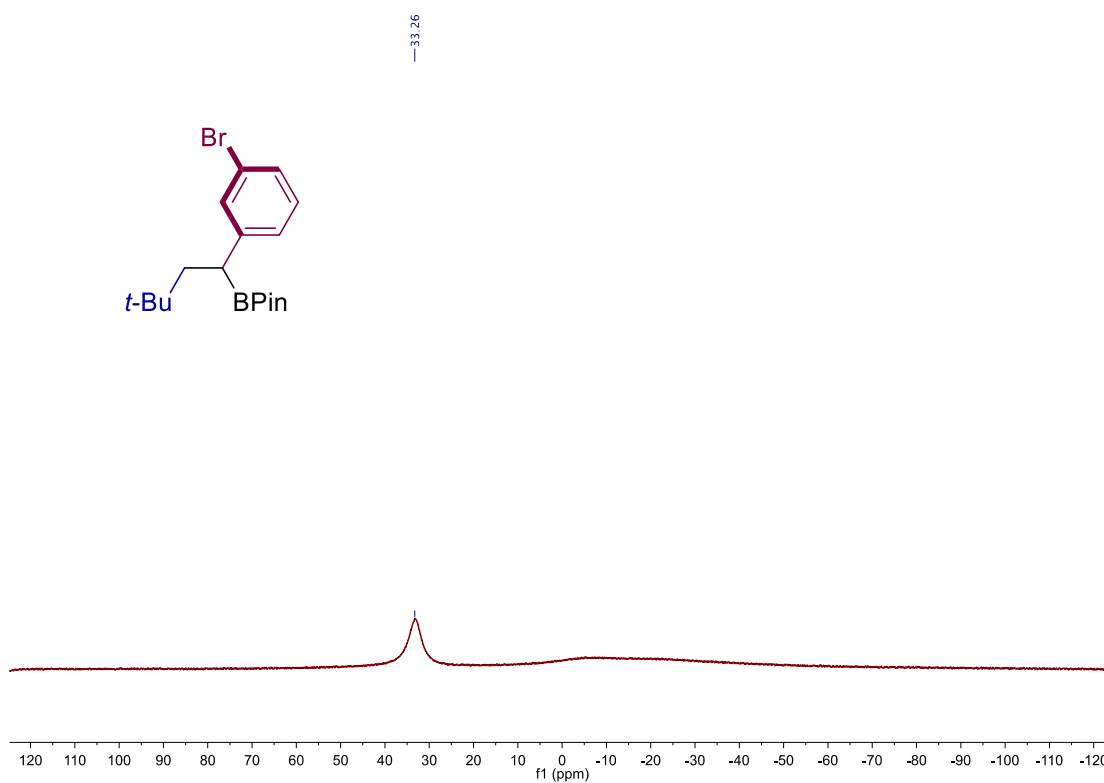
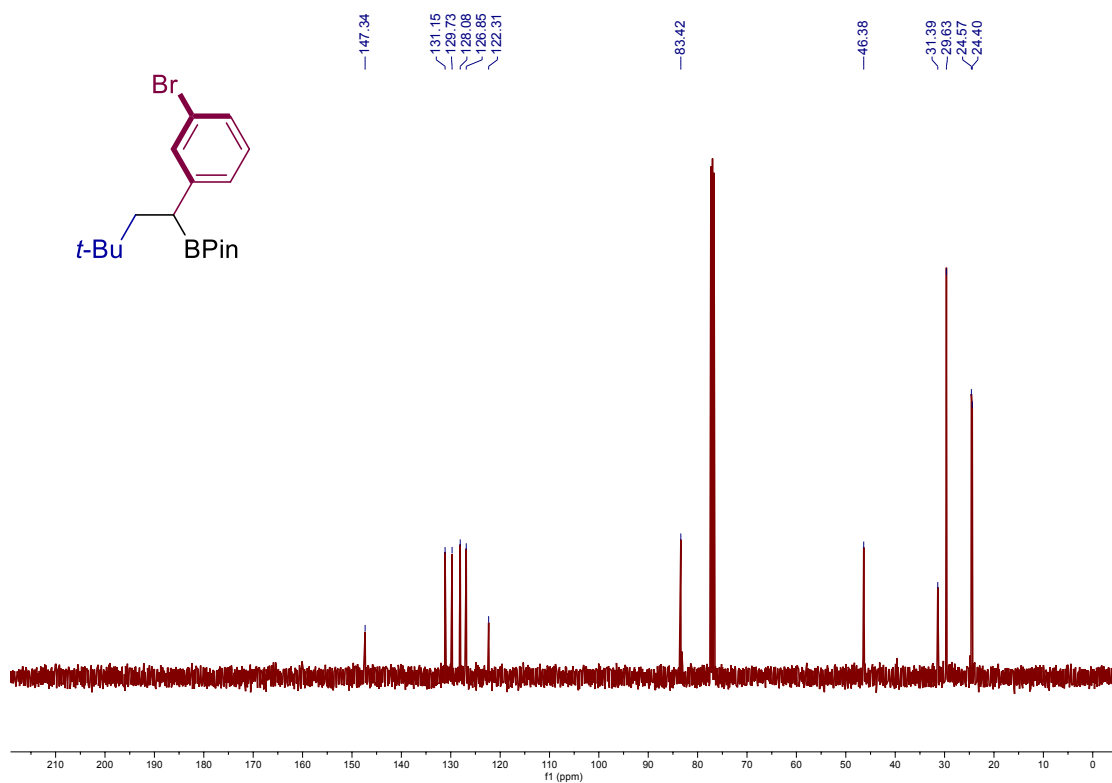


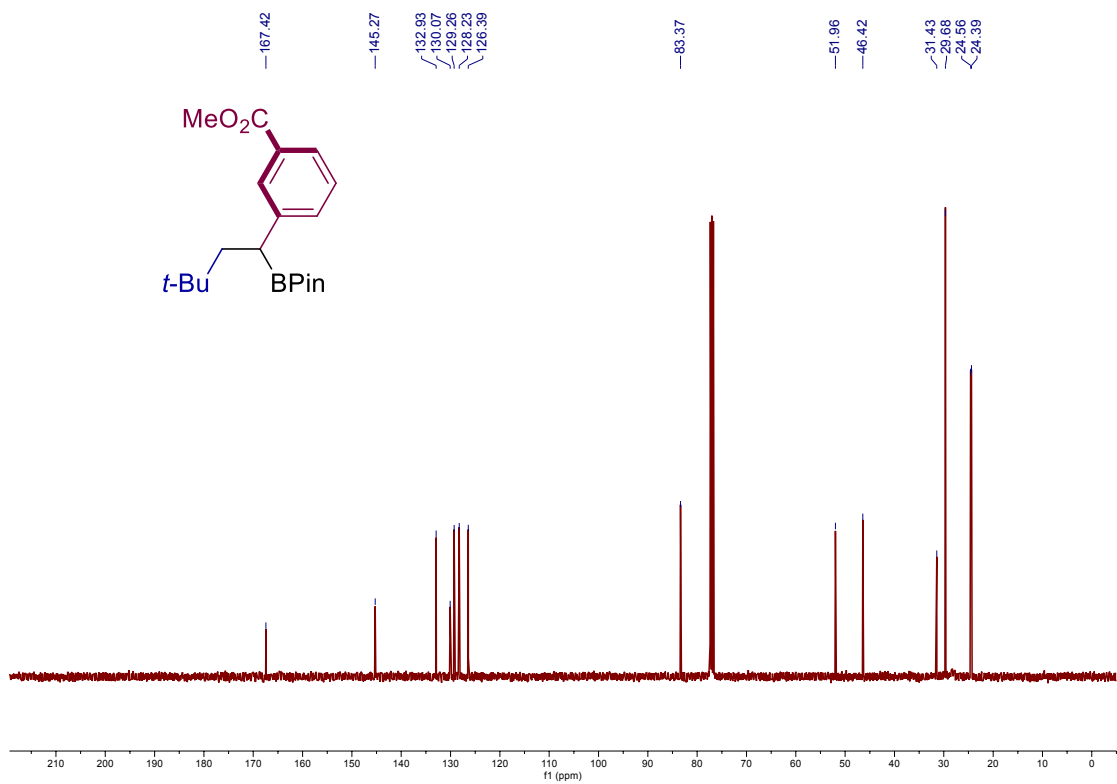
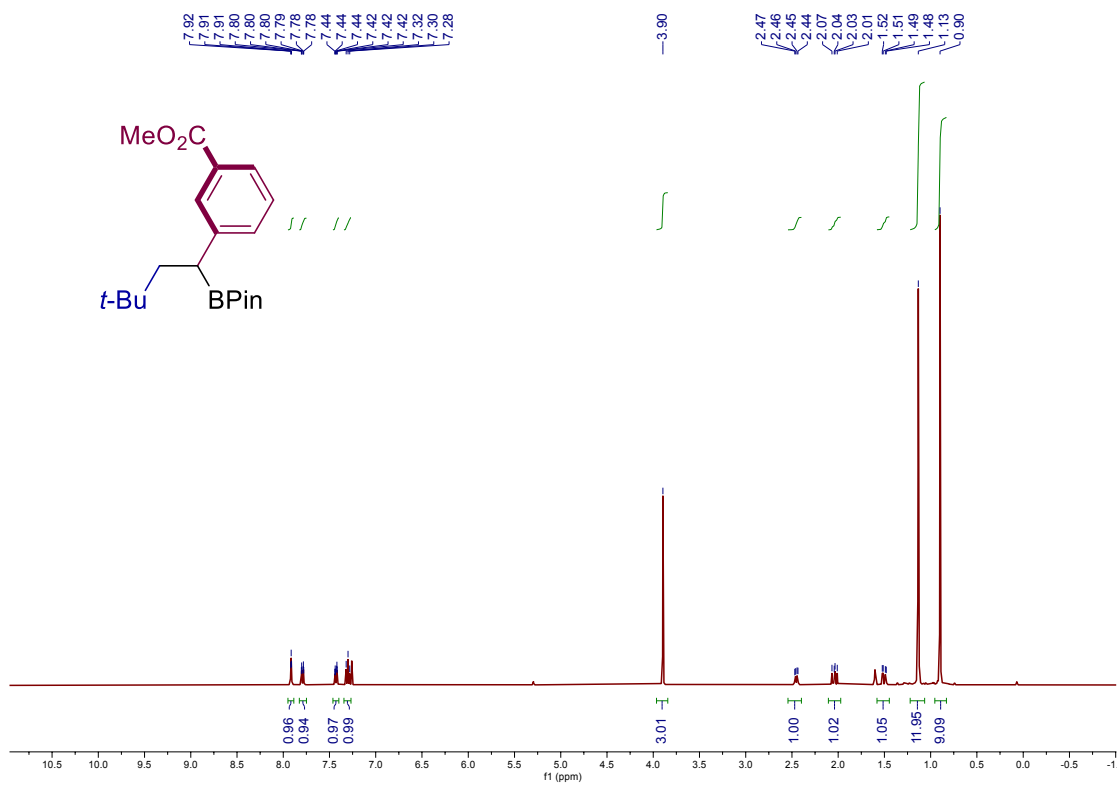
Site-Selective 1,2-Dicarbofunctionalization of Vinyl Boronates through Dual Catalysis



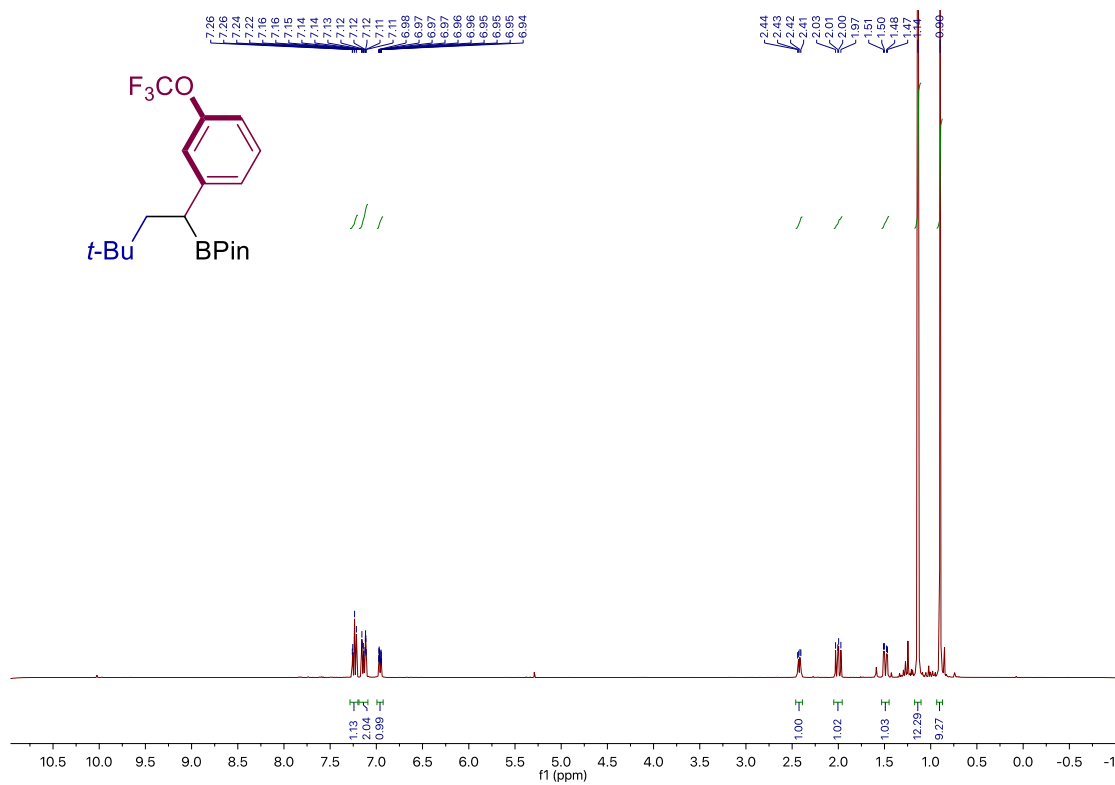
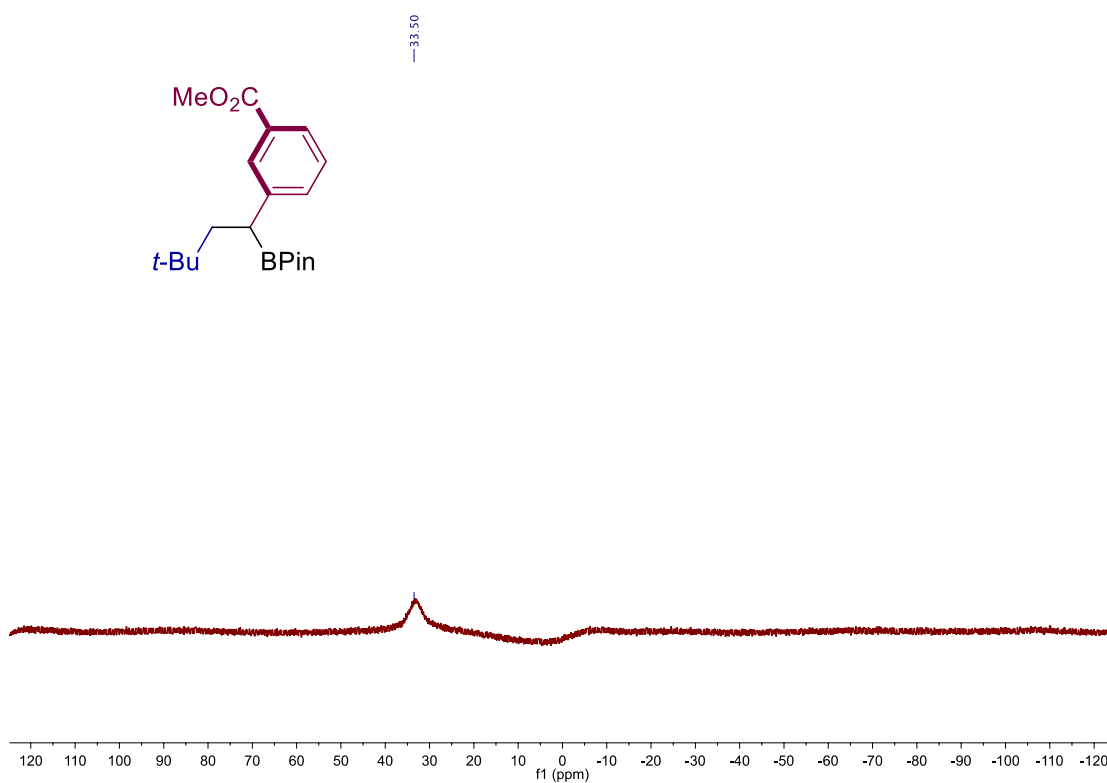


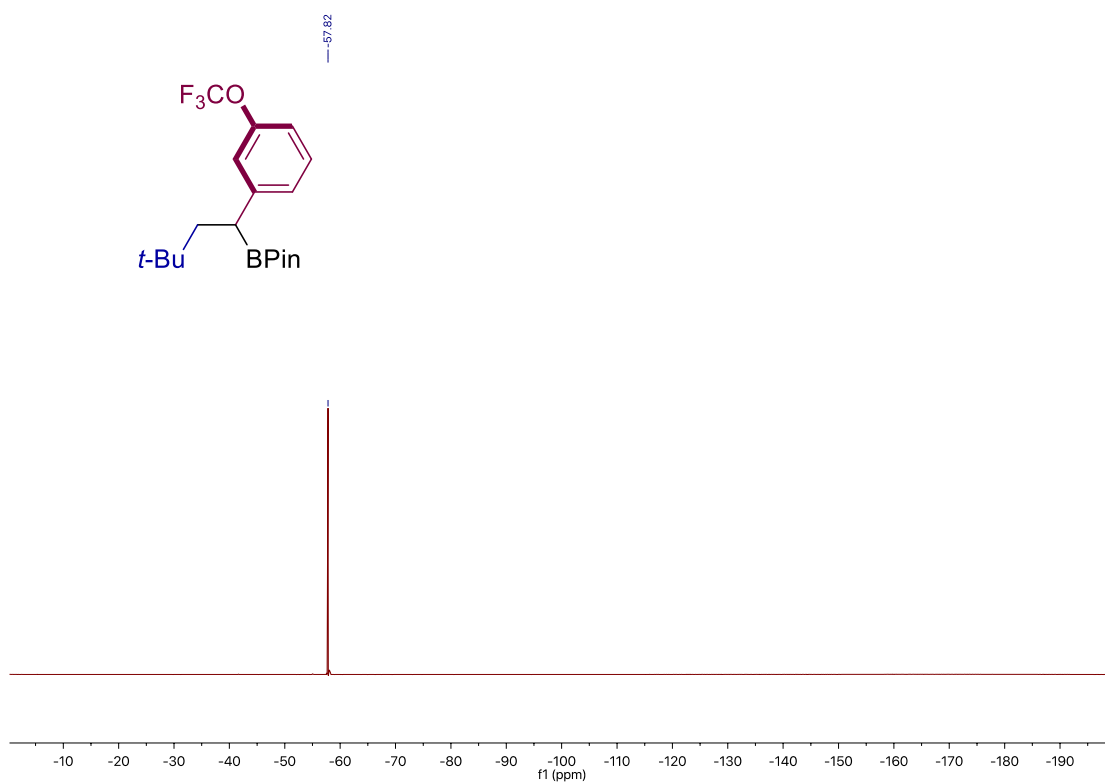
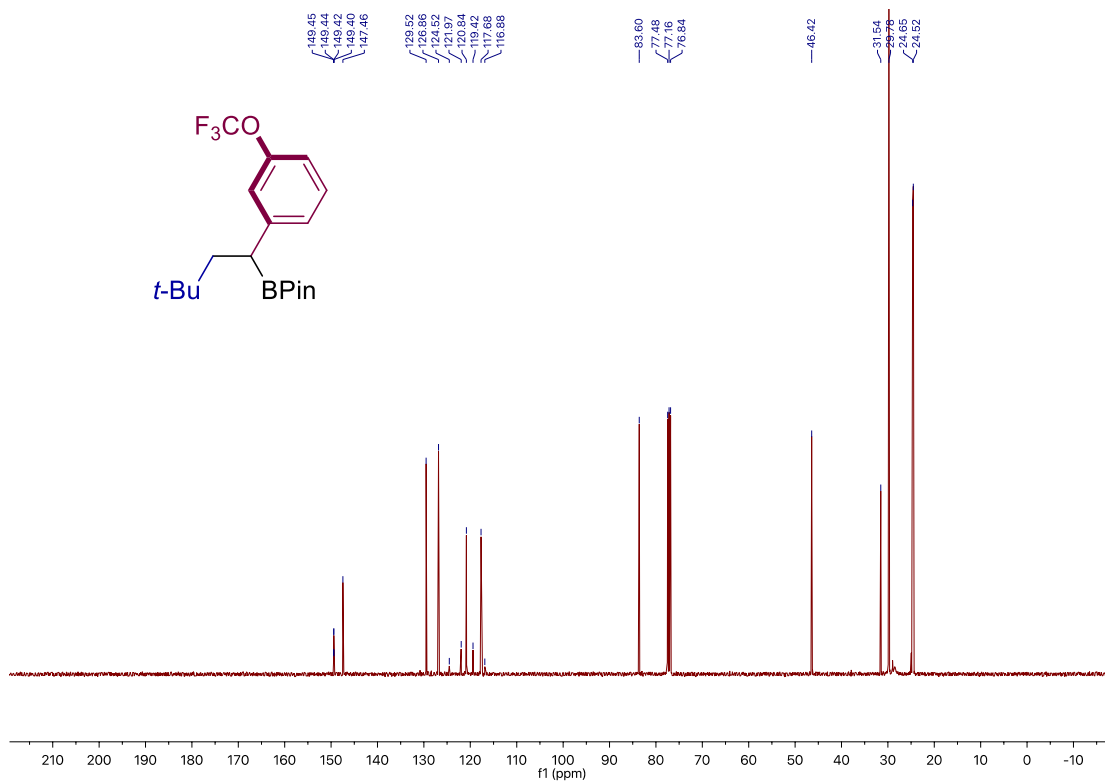
Site-Selective 1,2-Dicarbofunctionalization of Vinyl Boronates through Dual Catalysis



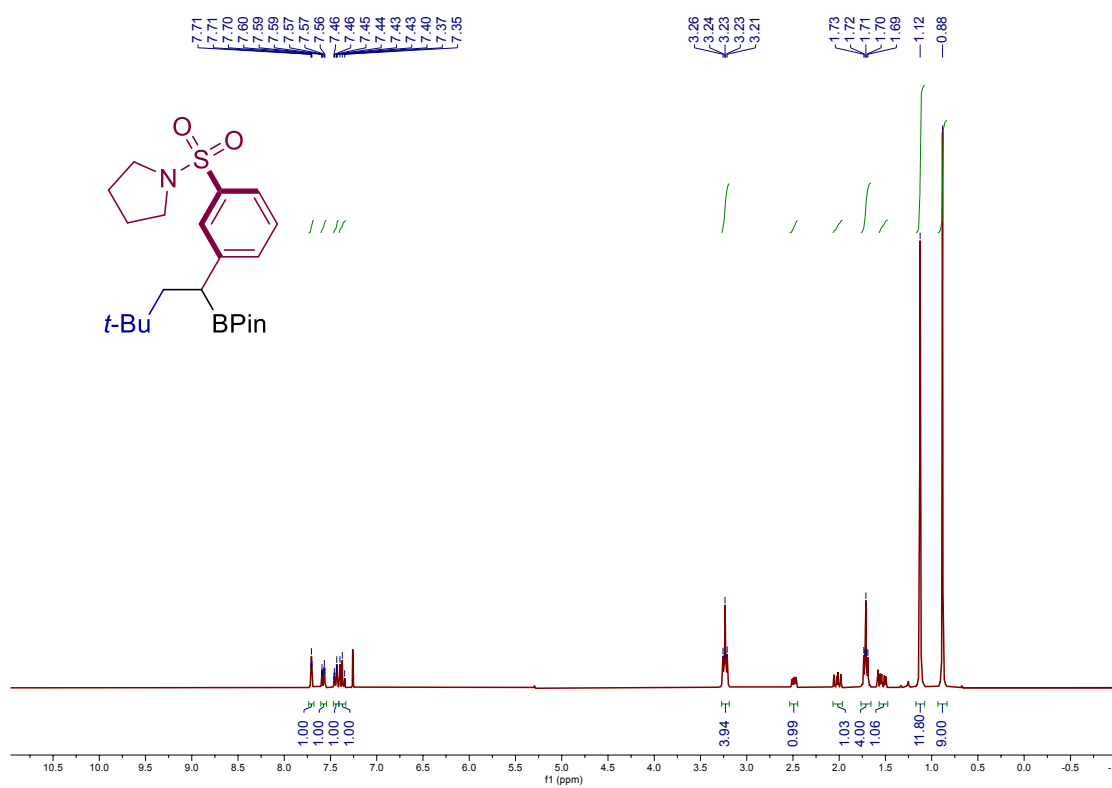
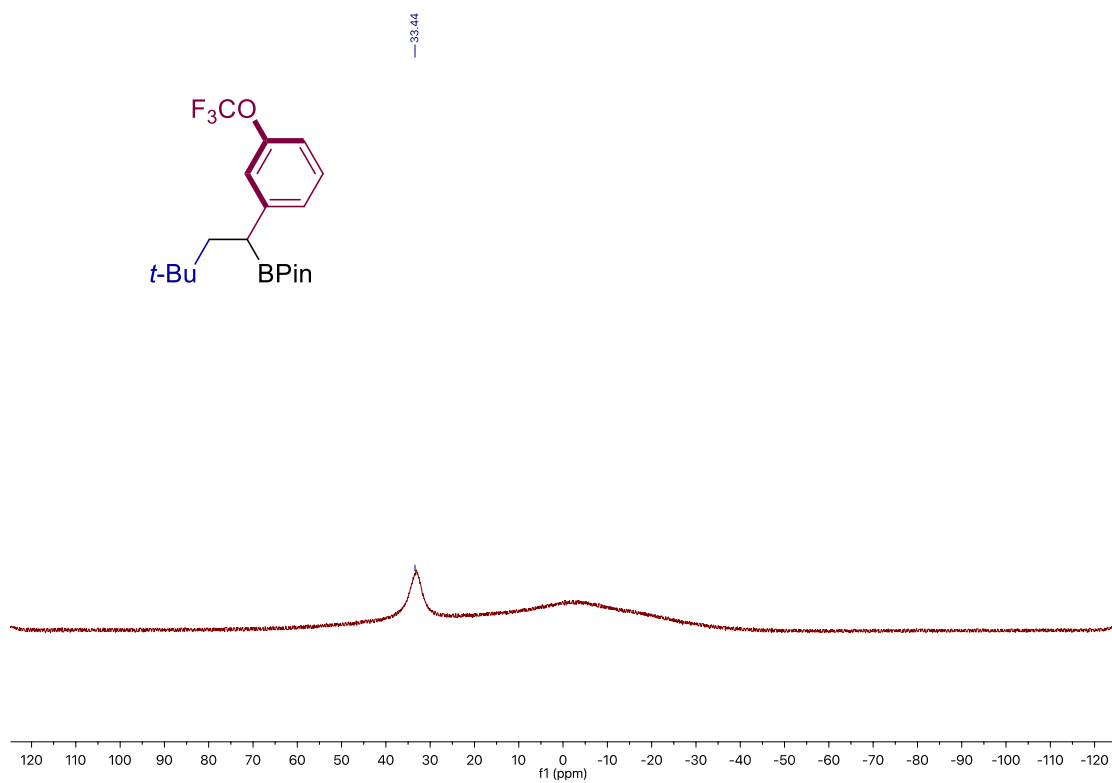


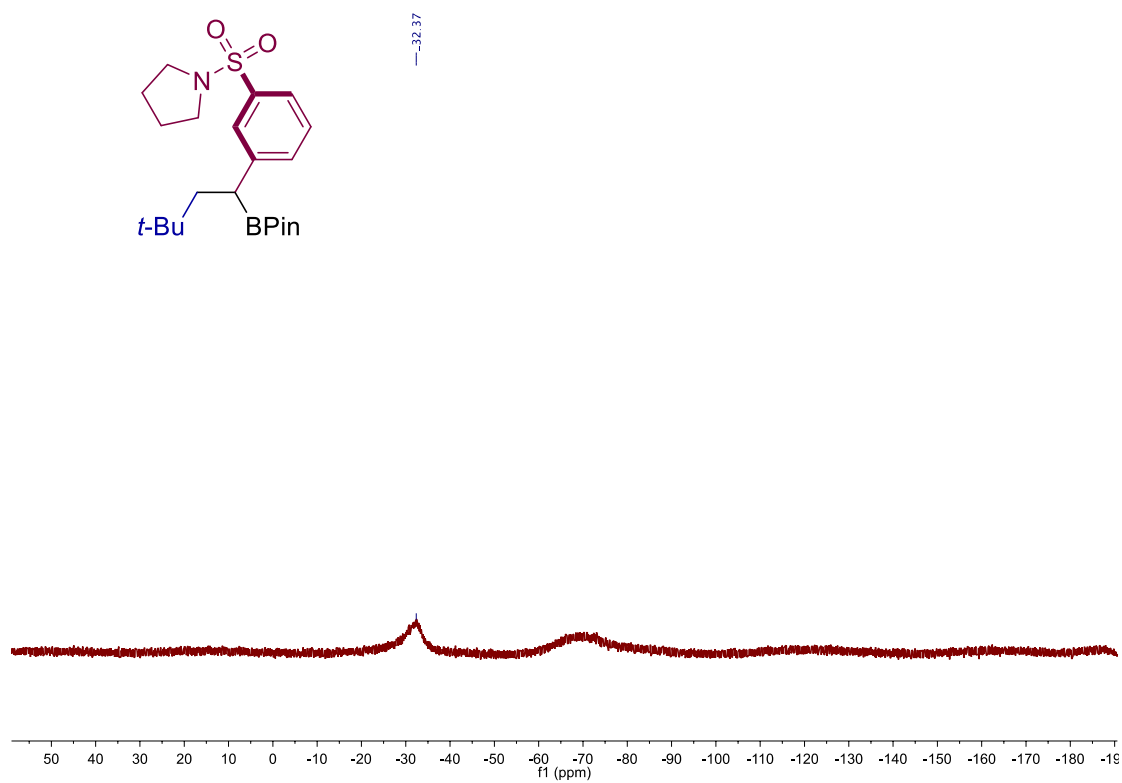
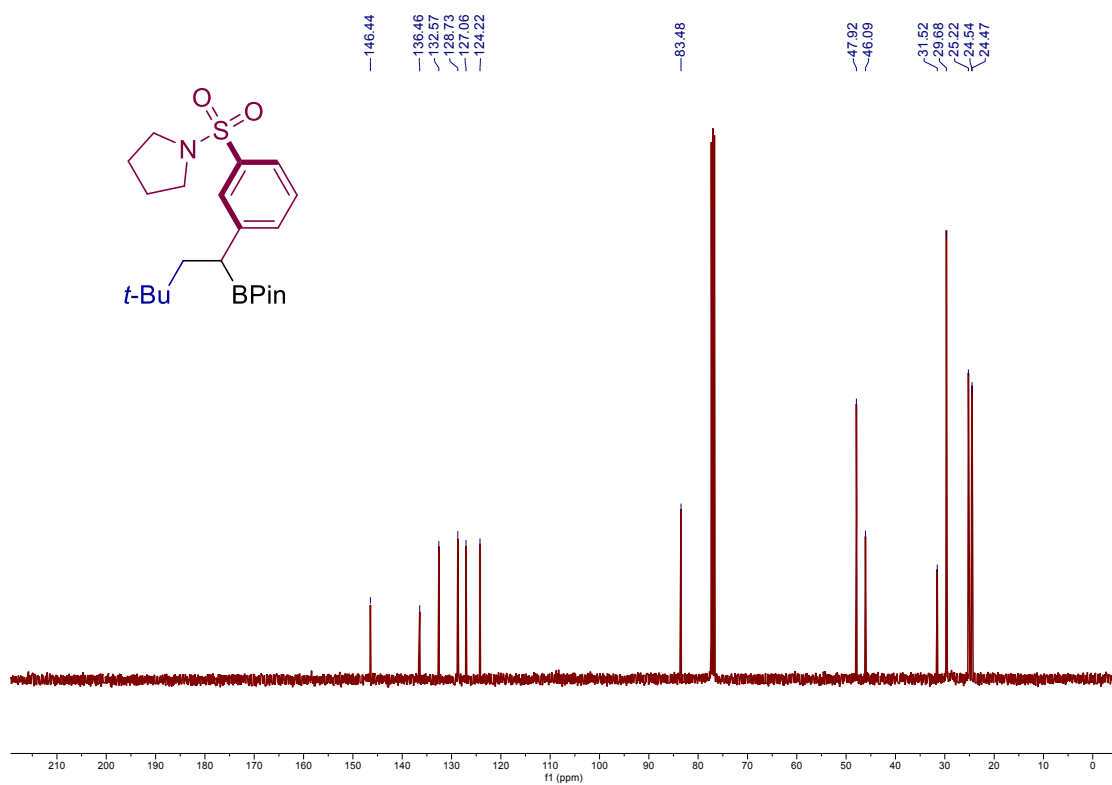
Site-Selective 1,2-Dicarbofunctionalization of Vinyl Boronates through Dual Catalysis



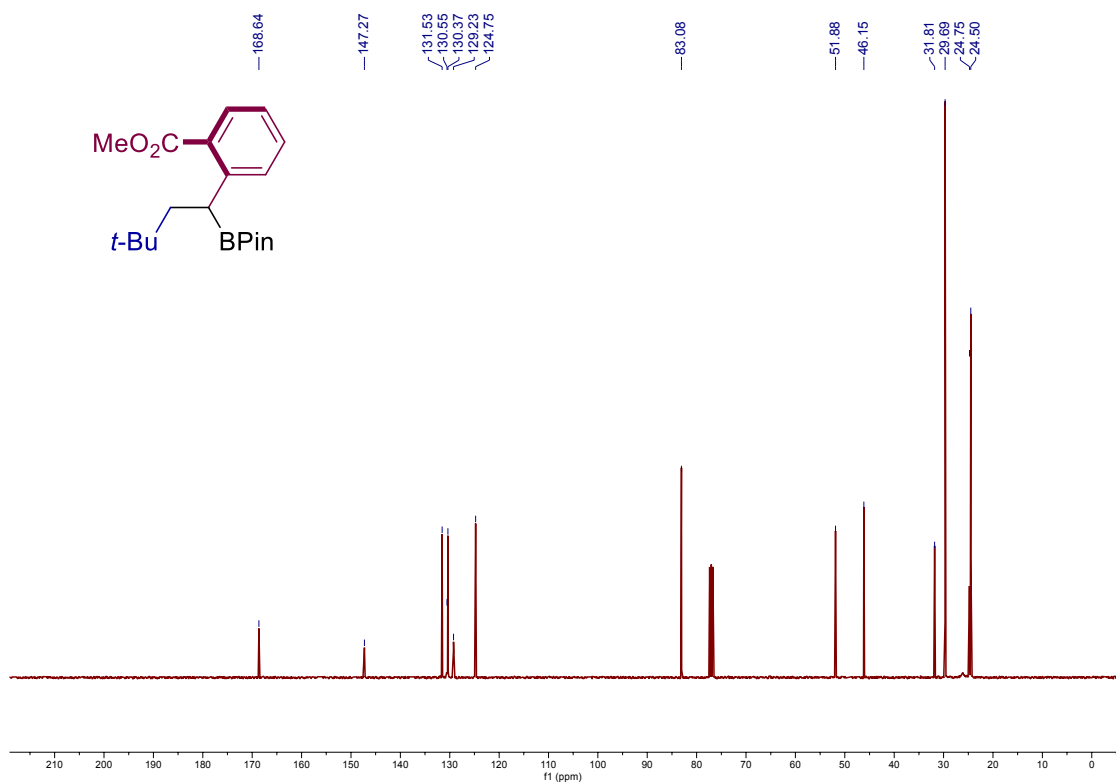
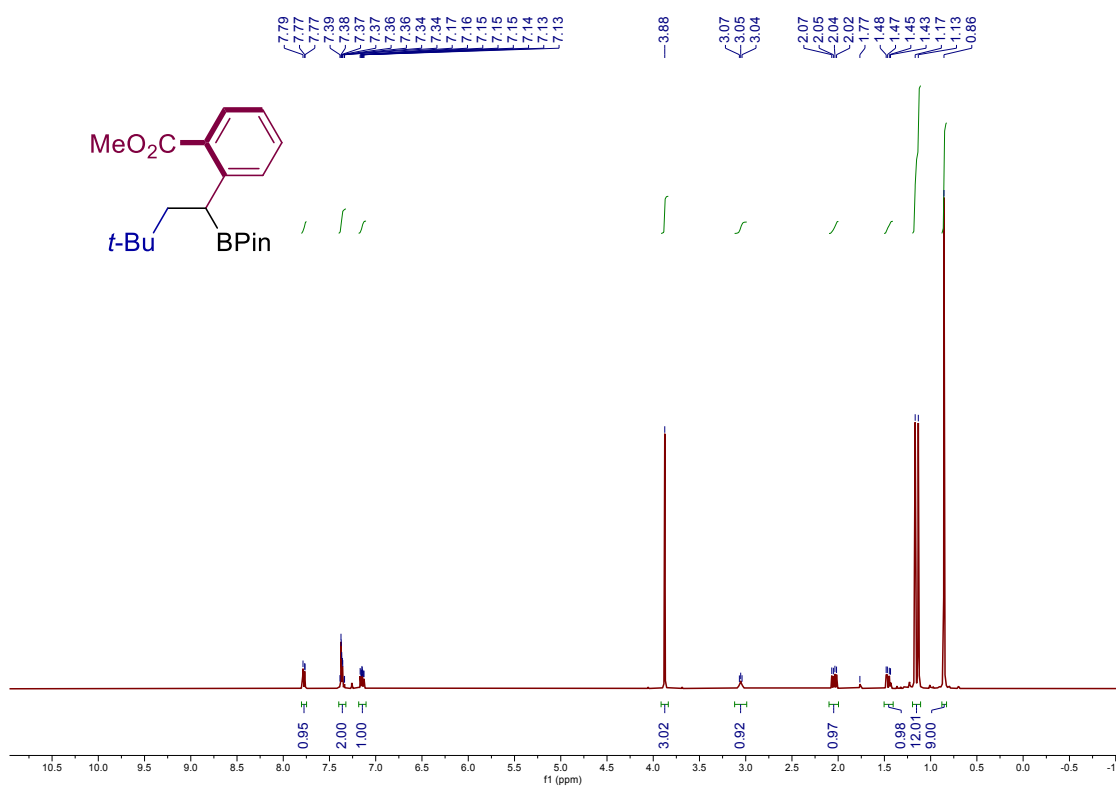


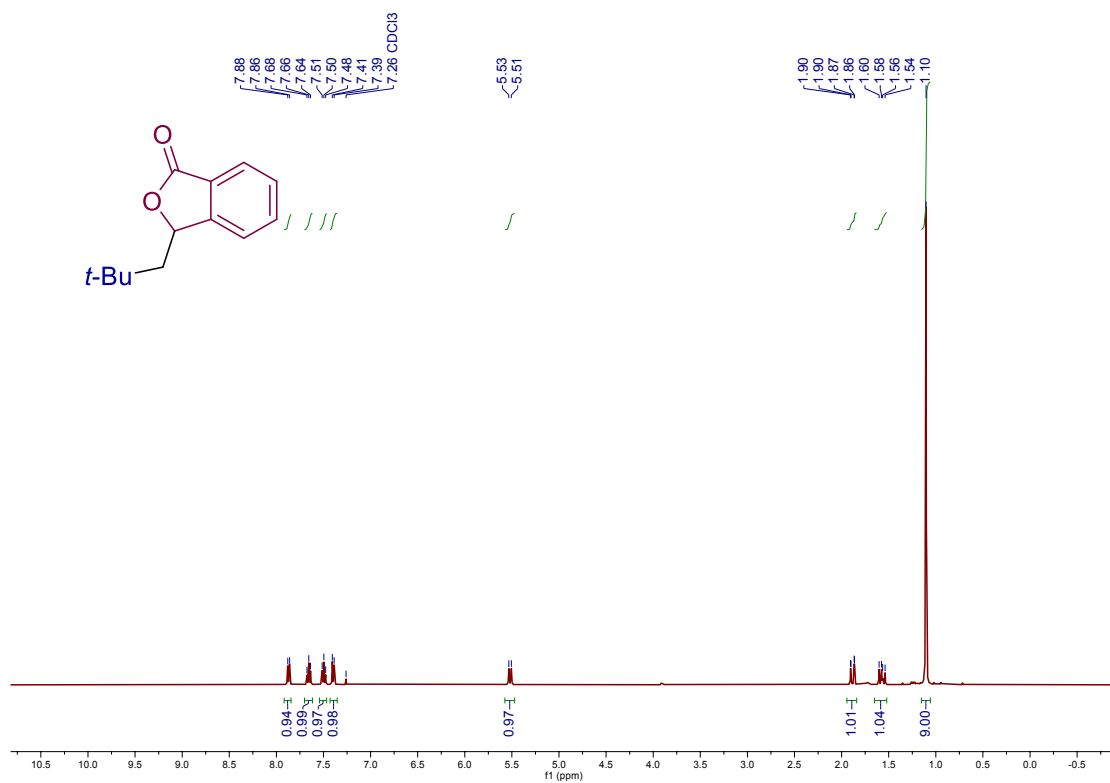
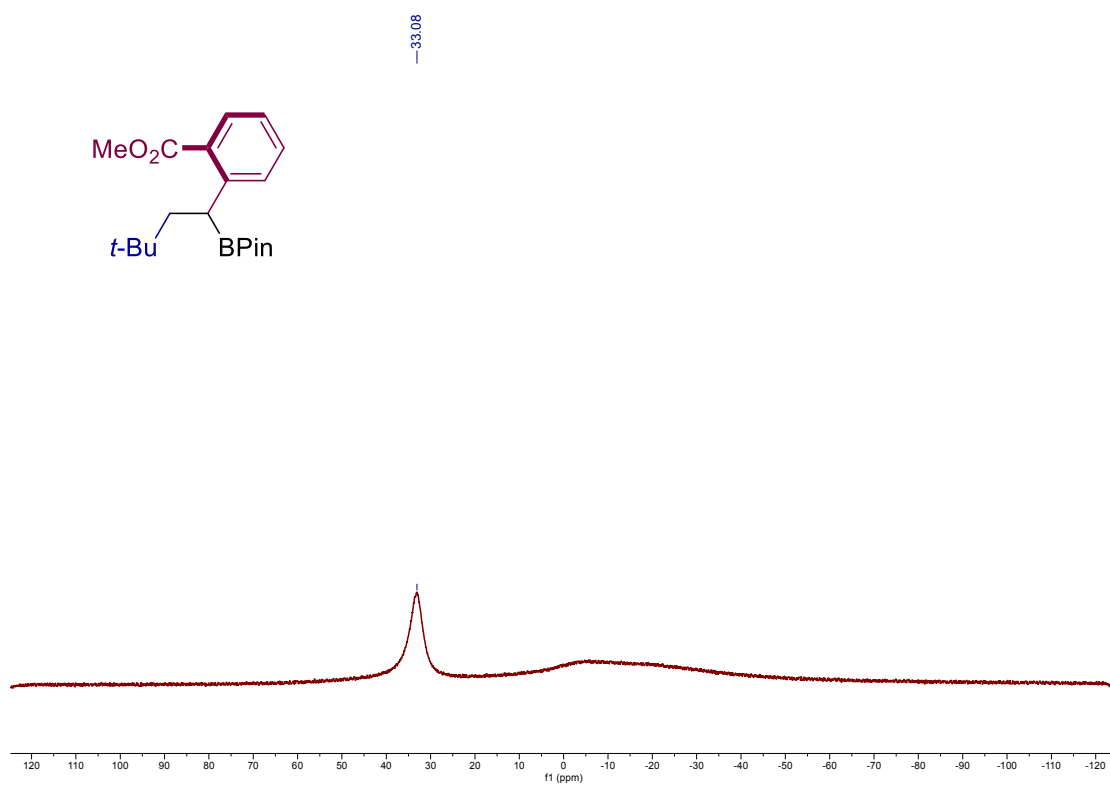
Site-Selective 1,2-Dicarbonylation of Vinyl Boronates through Dual Catalysis



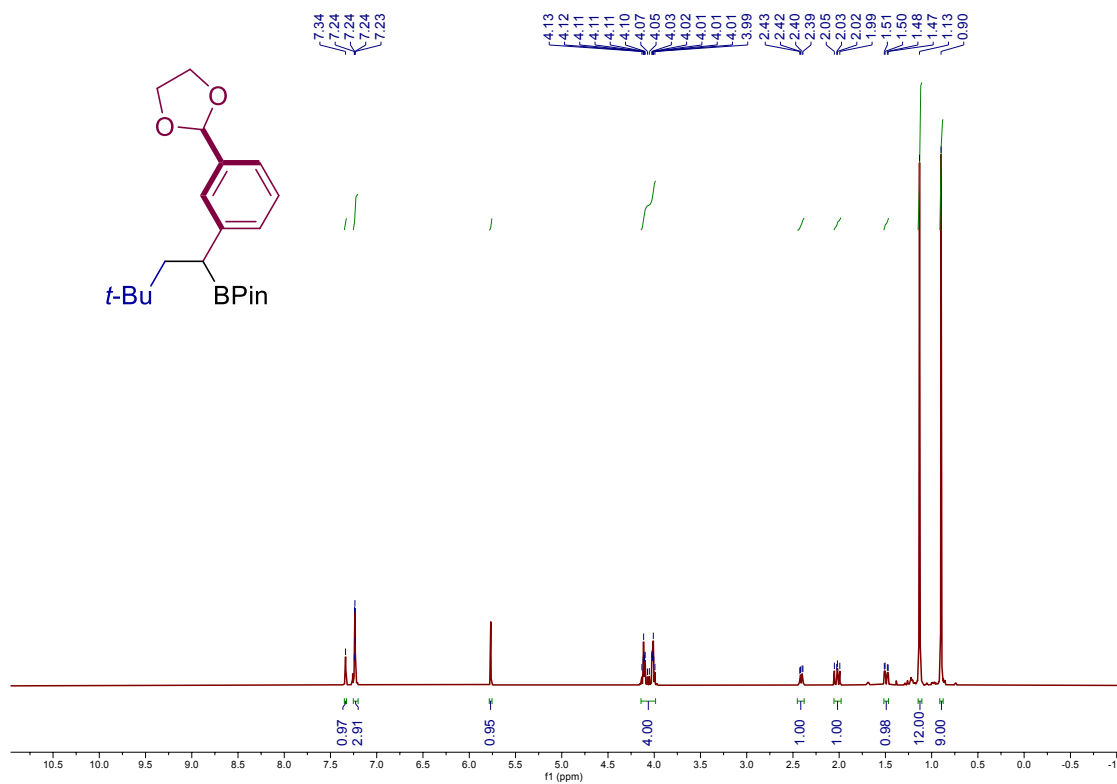
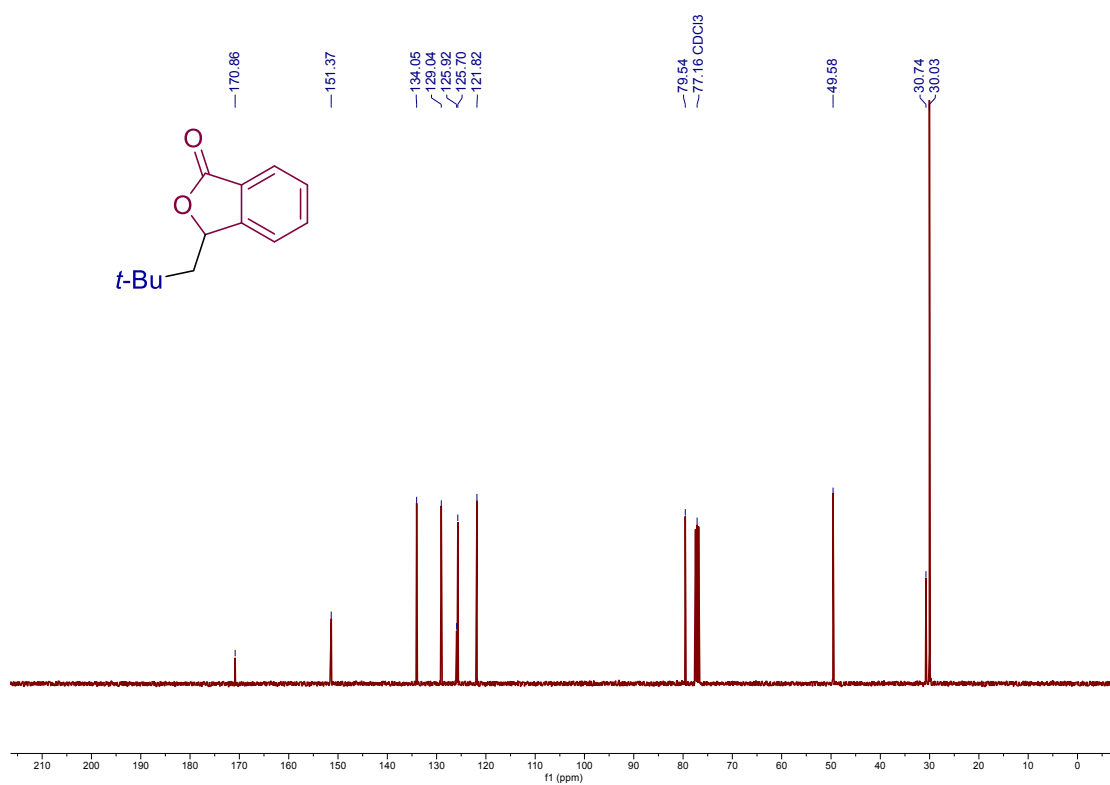


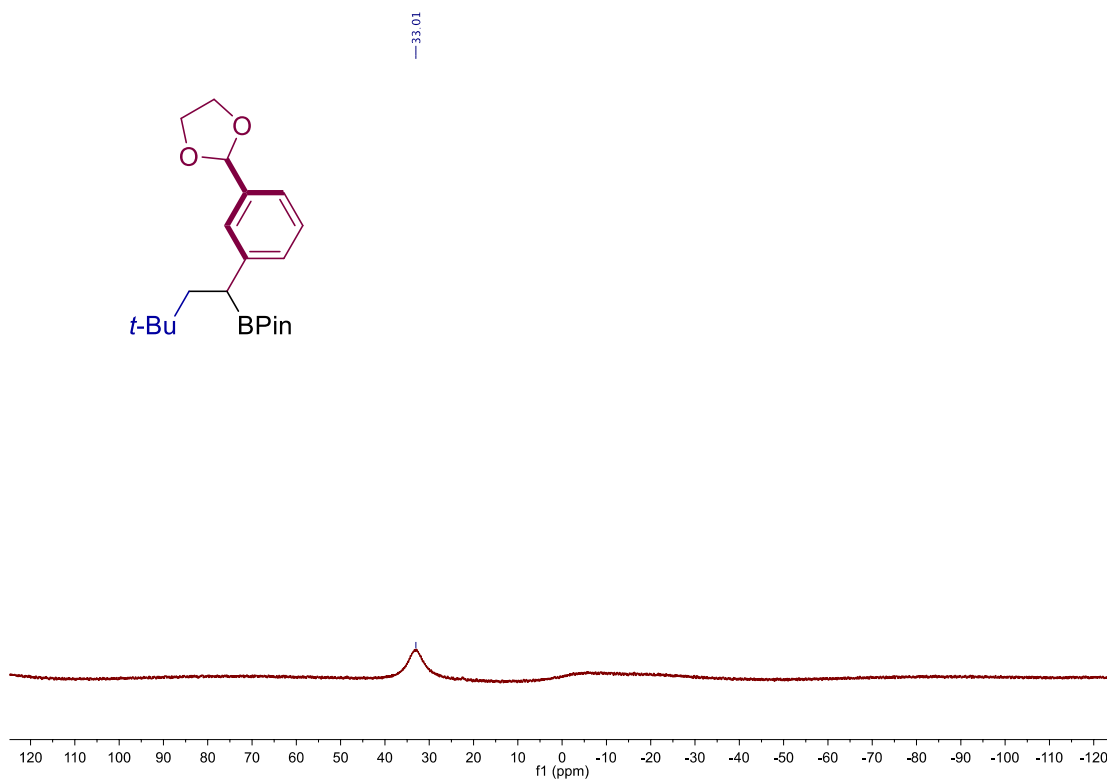
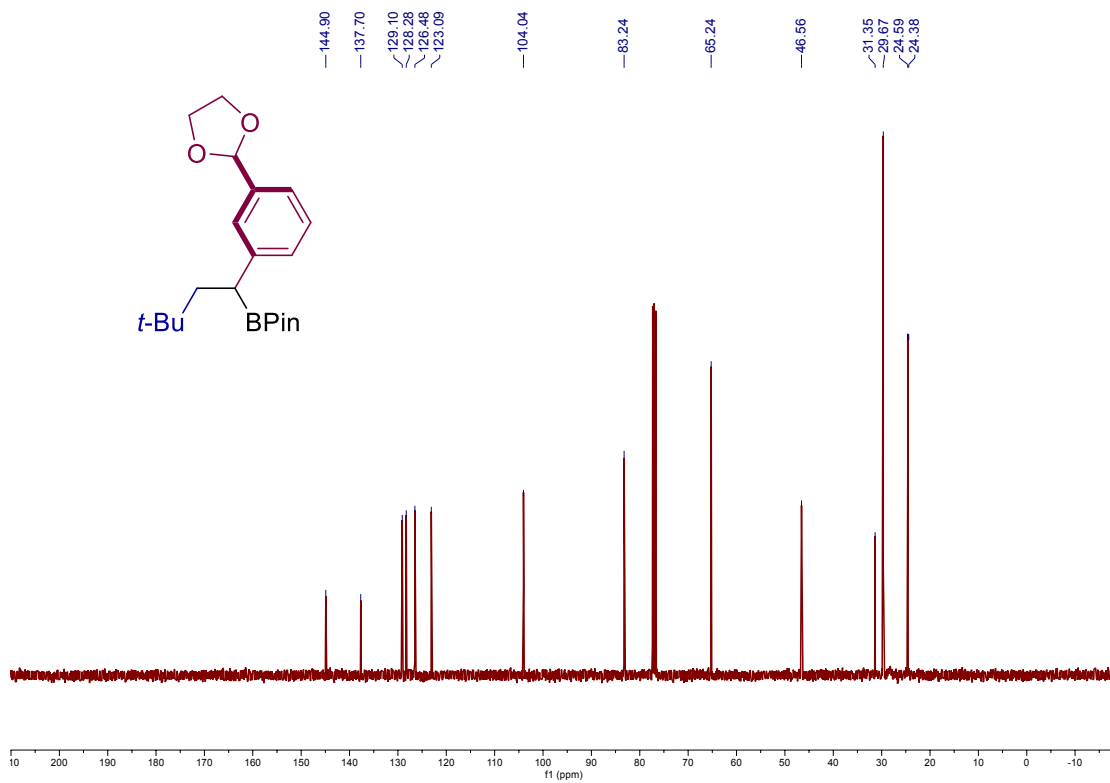
Site-Selective 1,2-Dicarbofunctionalization of Vinyl Boronates through Dual Catalysis



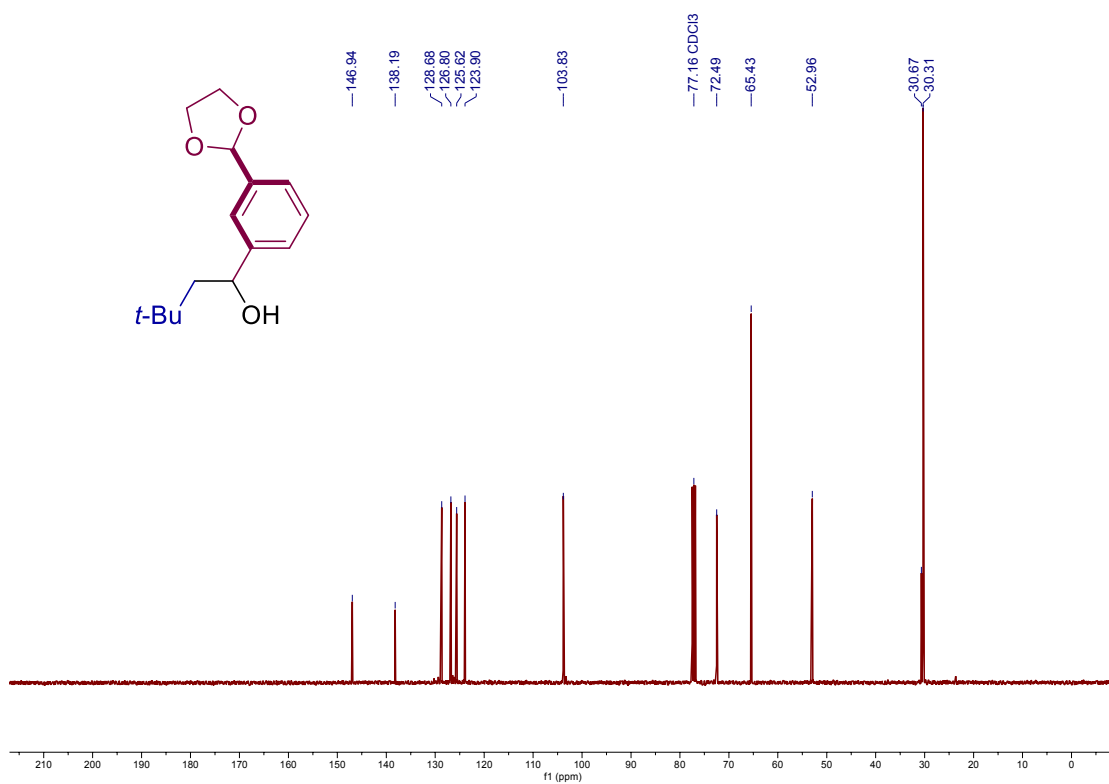
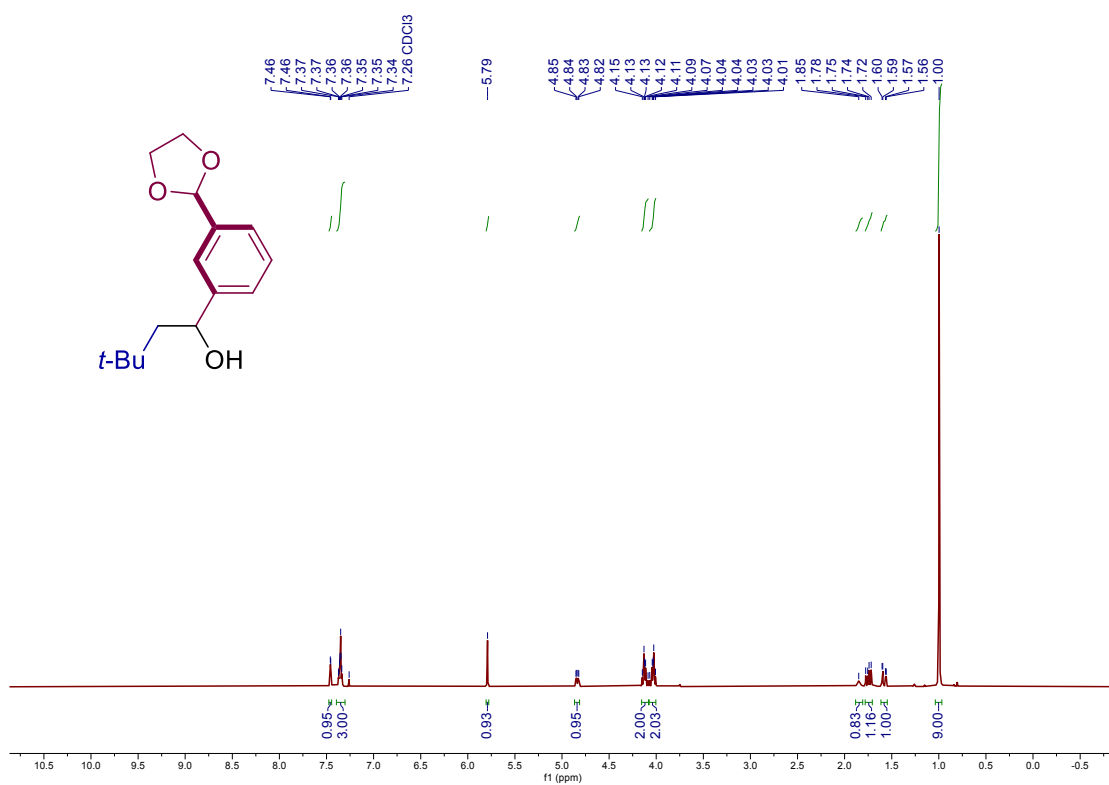


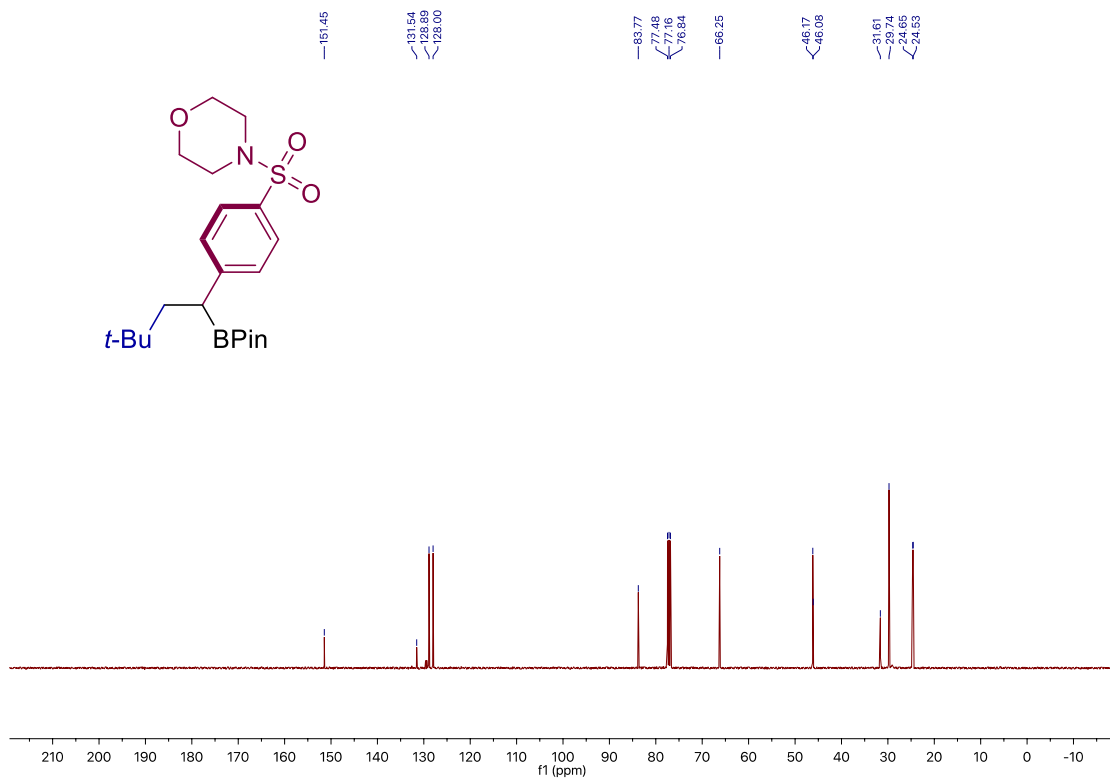
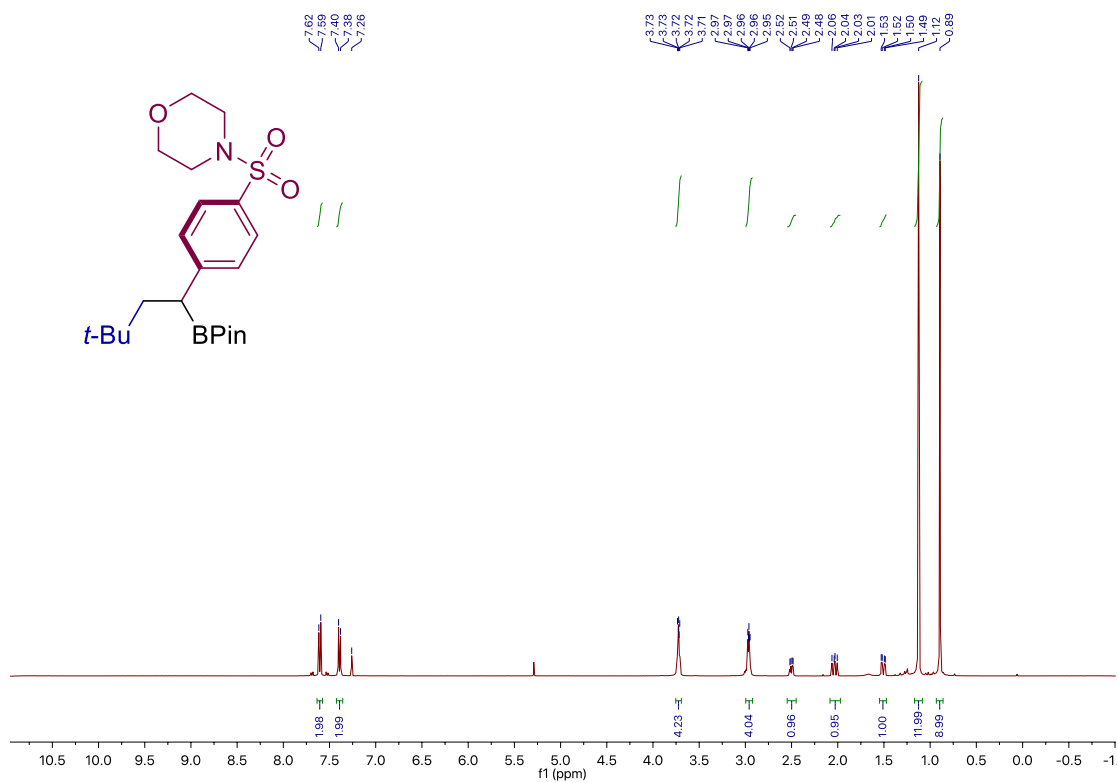
Site-Selective 1,2-Dicarbofunctionalization of Vinyl Boronates through Dual Catalysis





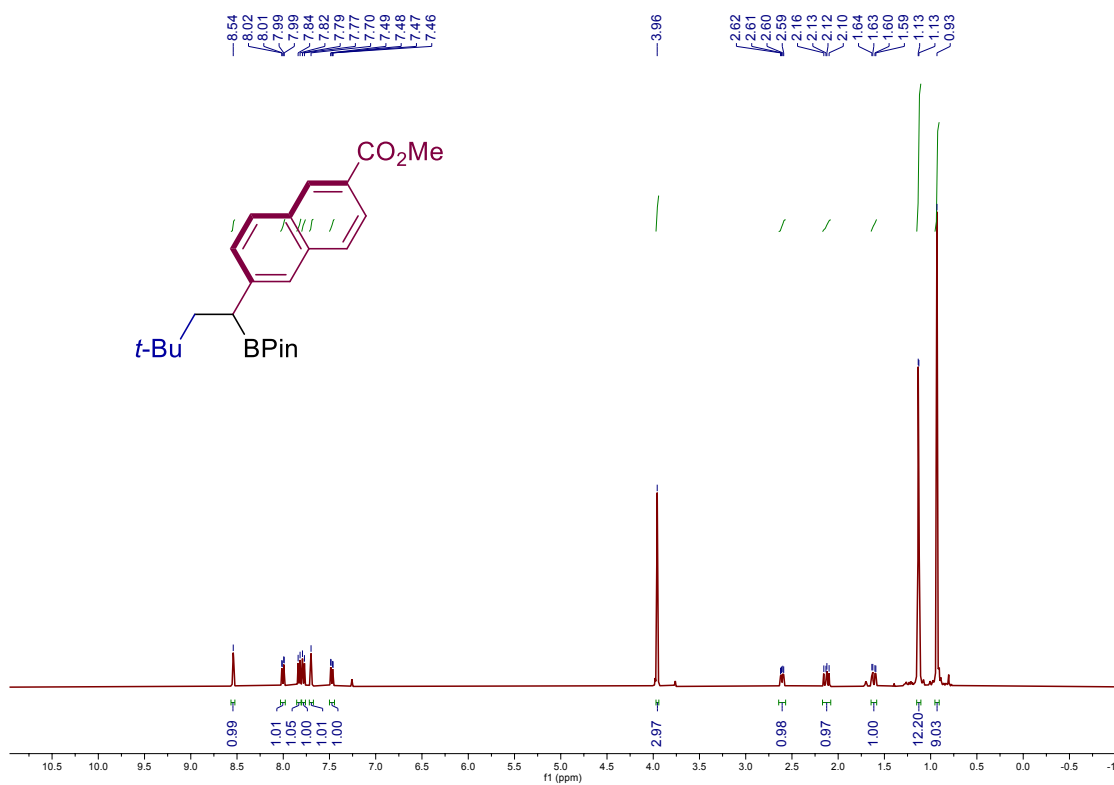
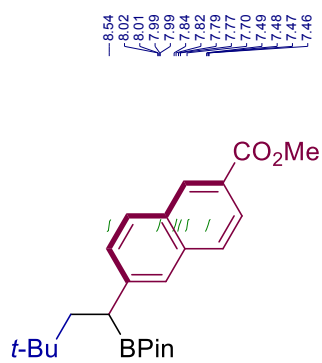
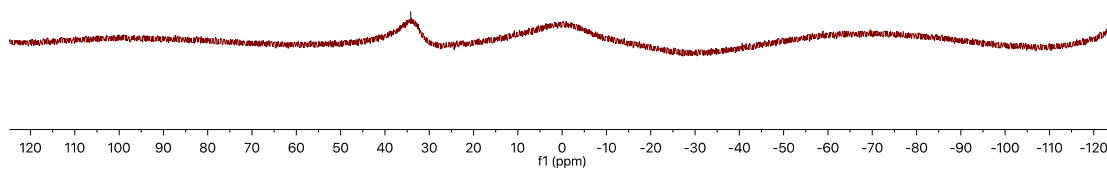
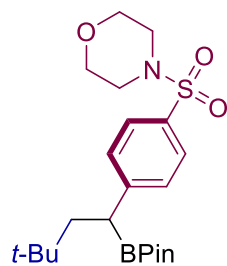
Site-Selective 1,2-Dicarbofunctionalization of Vinyl Boronates through Dual Catalysis

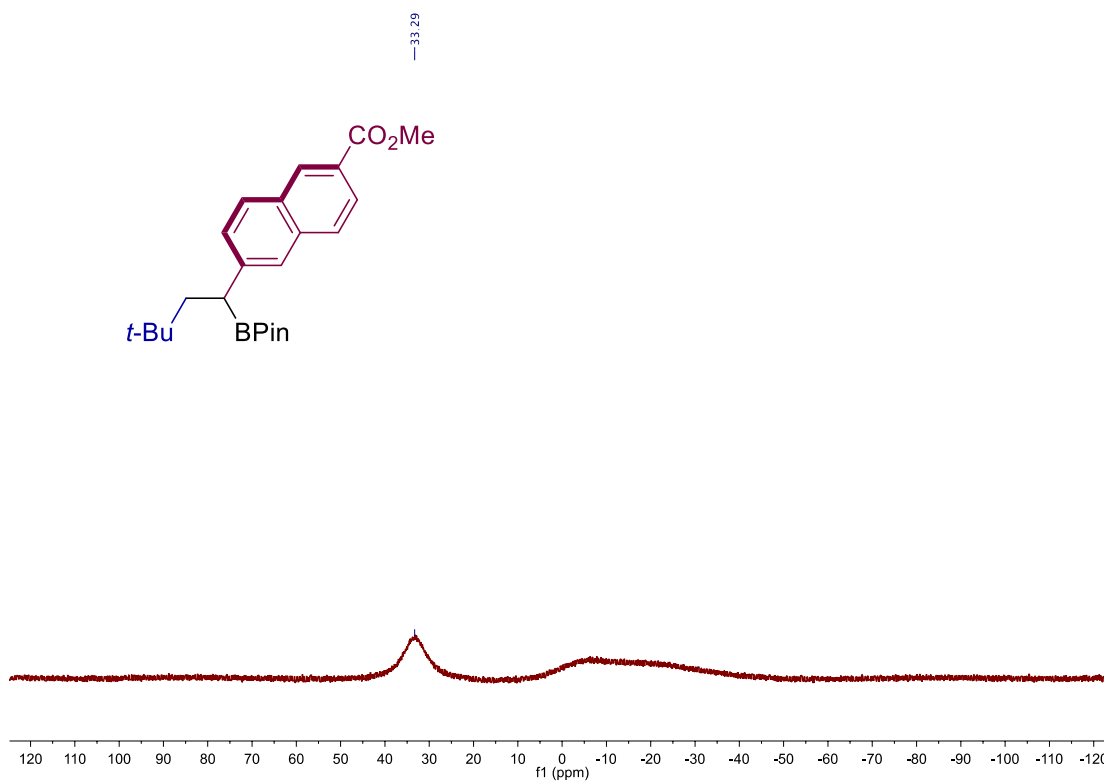
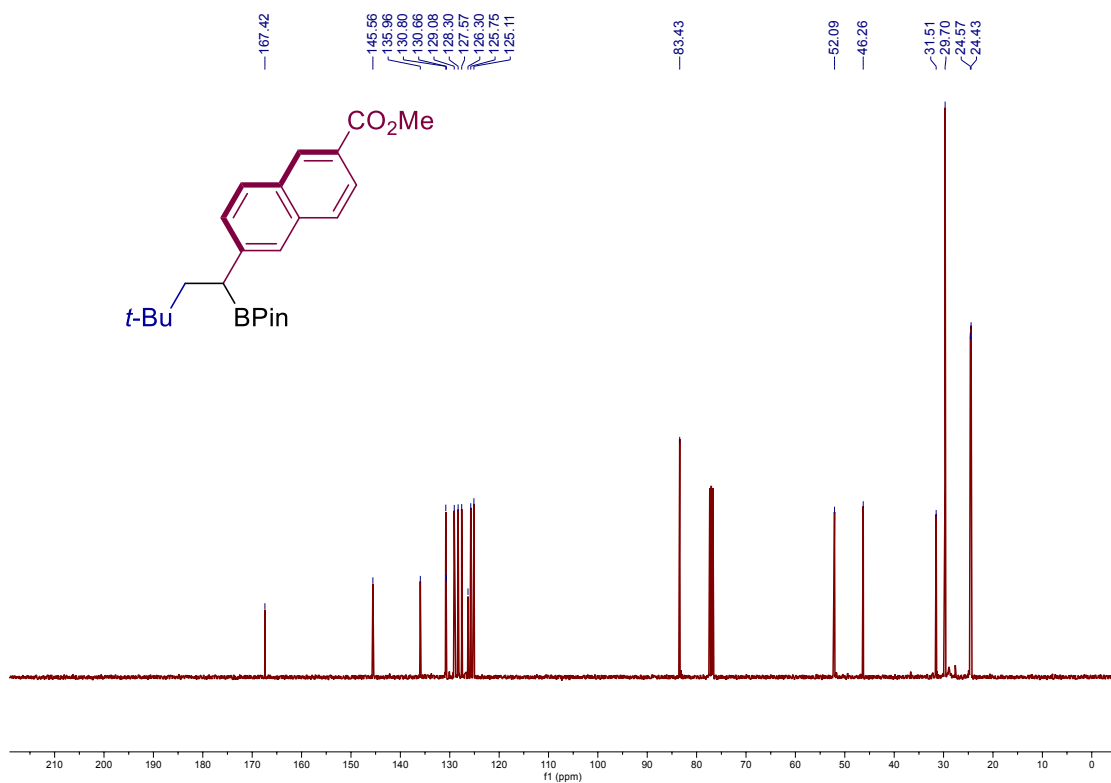




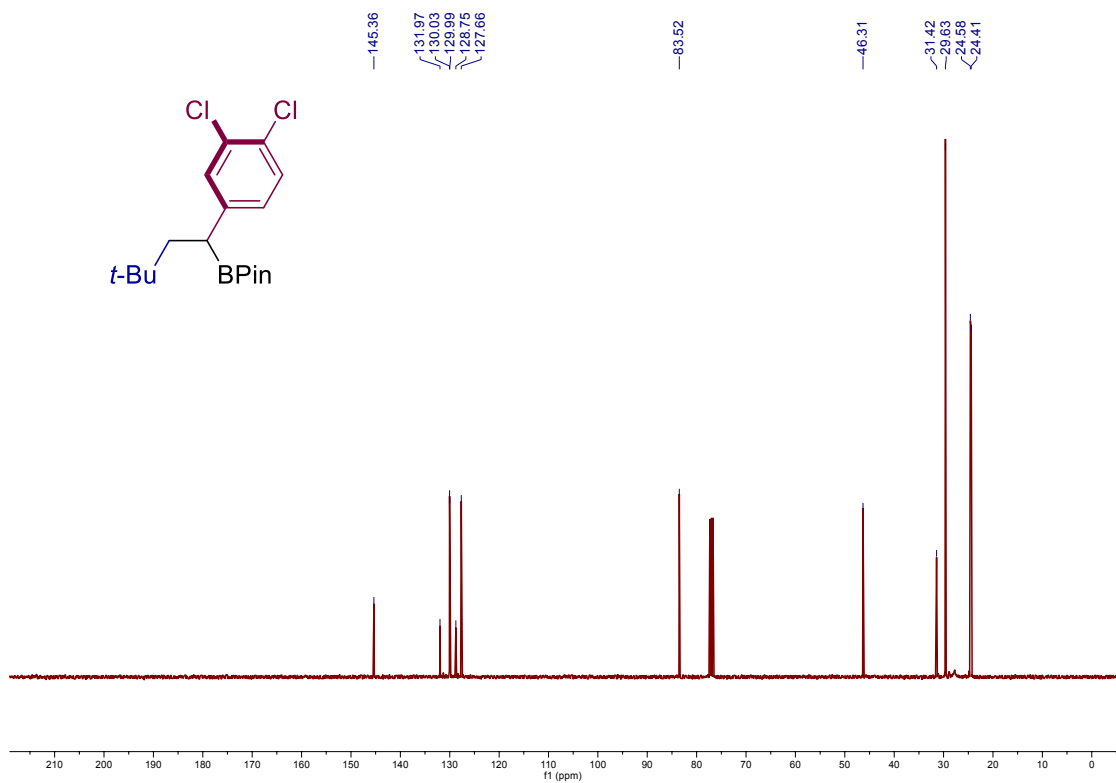
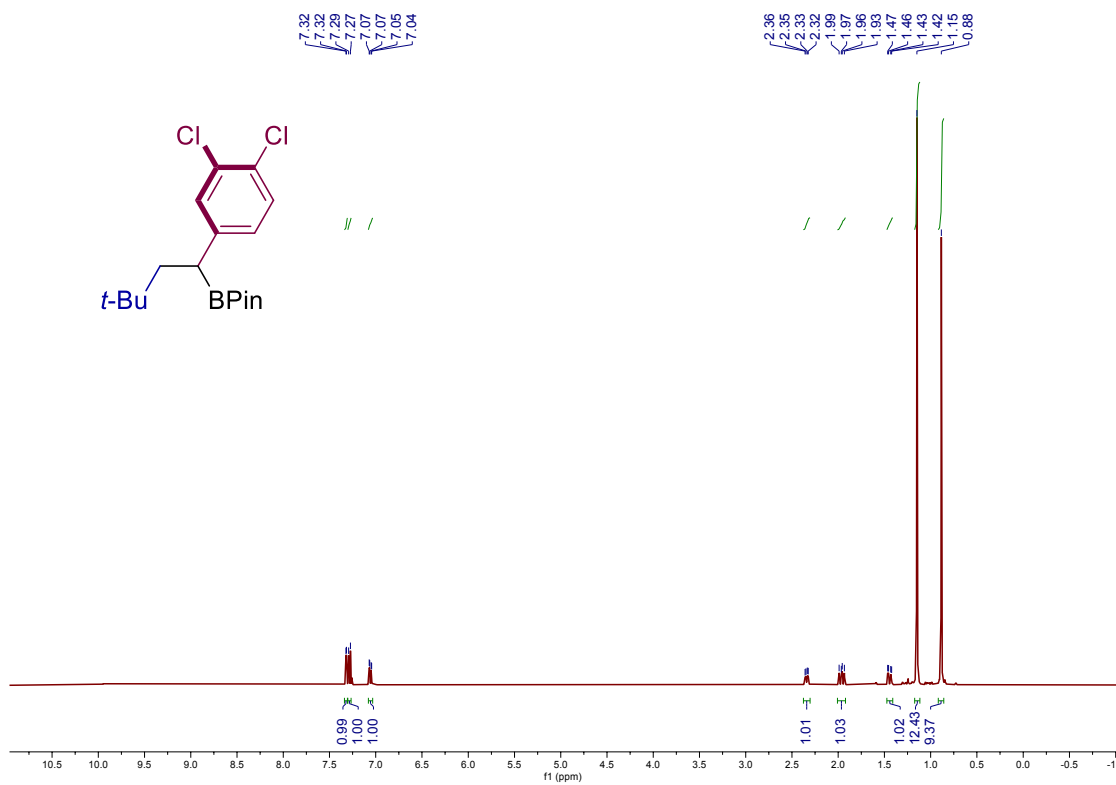
Site-Selective 1,2-Dicarbofunctionalization of Vinyl Boronates through Dual Catalysis

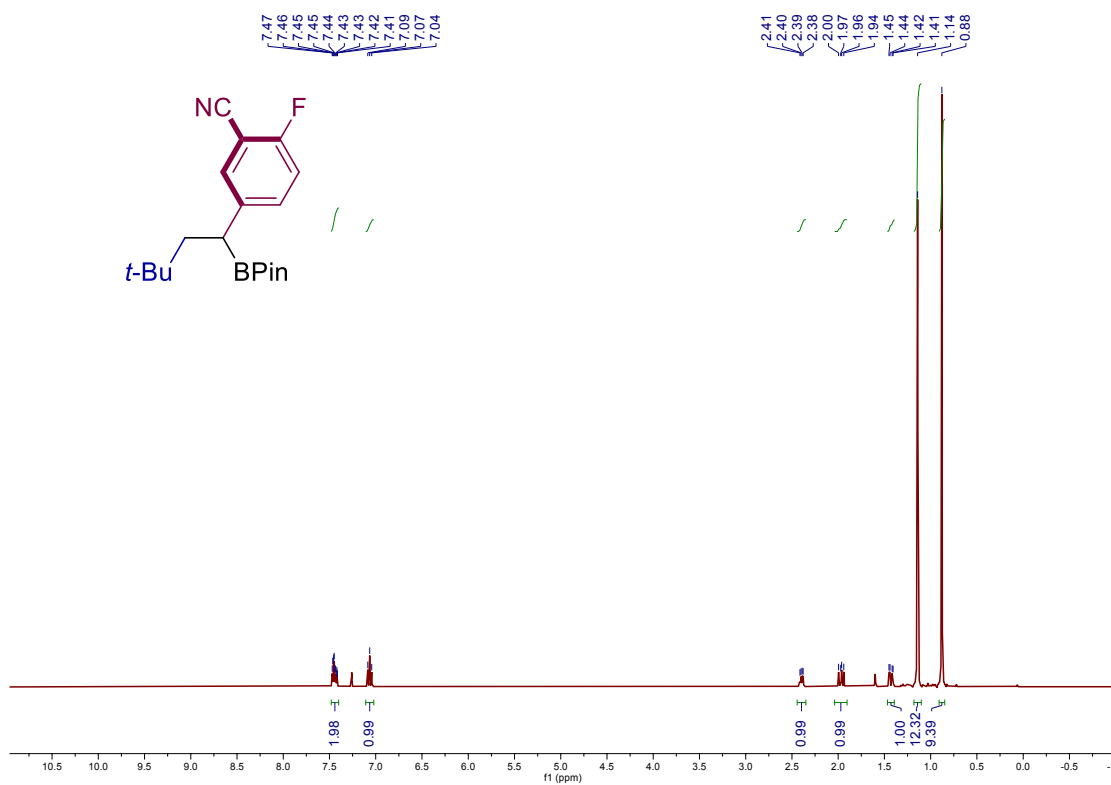
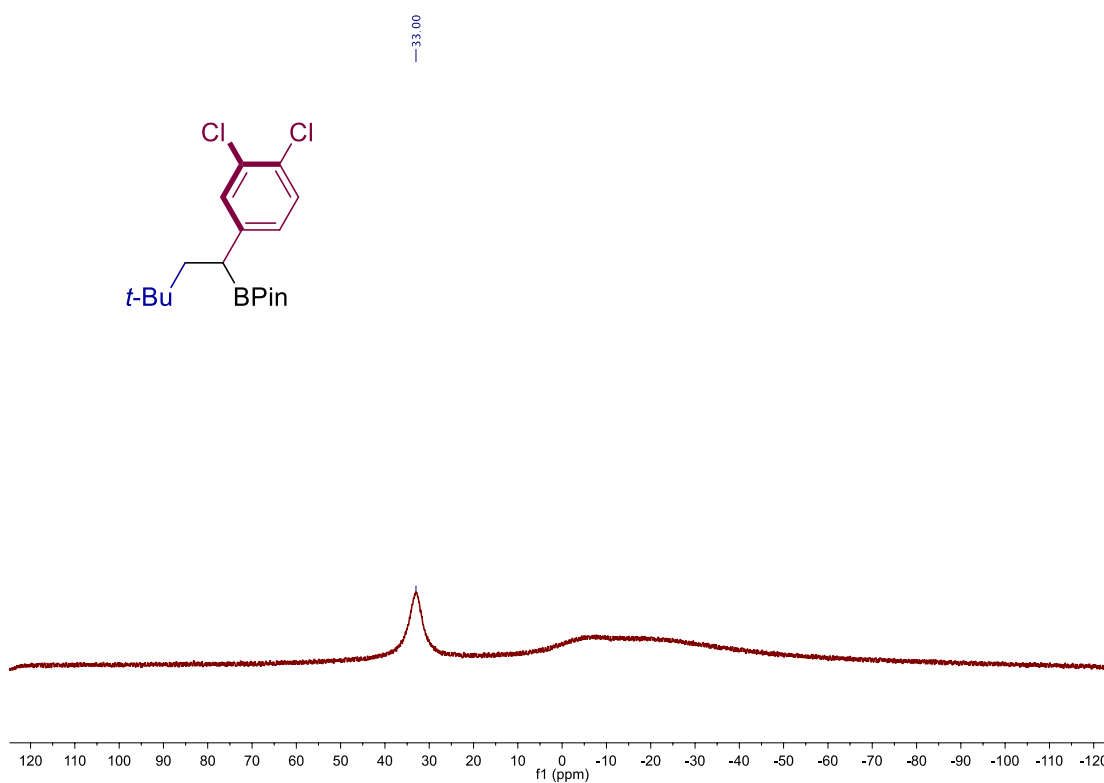
— 34.18



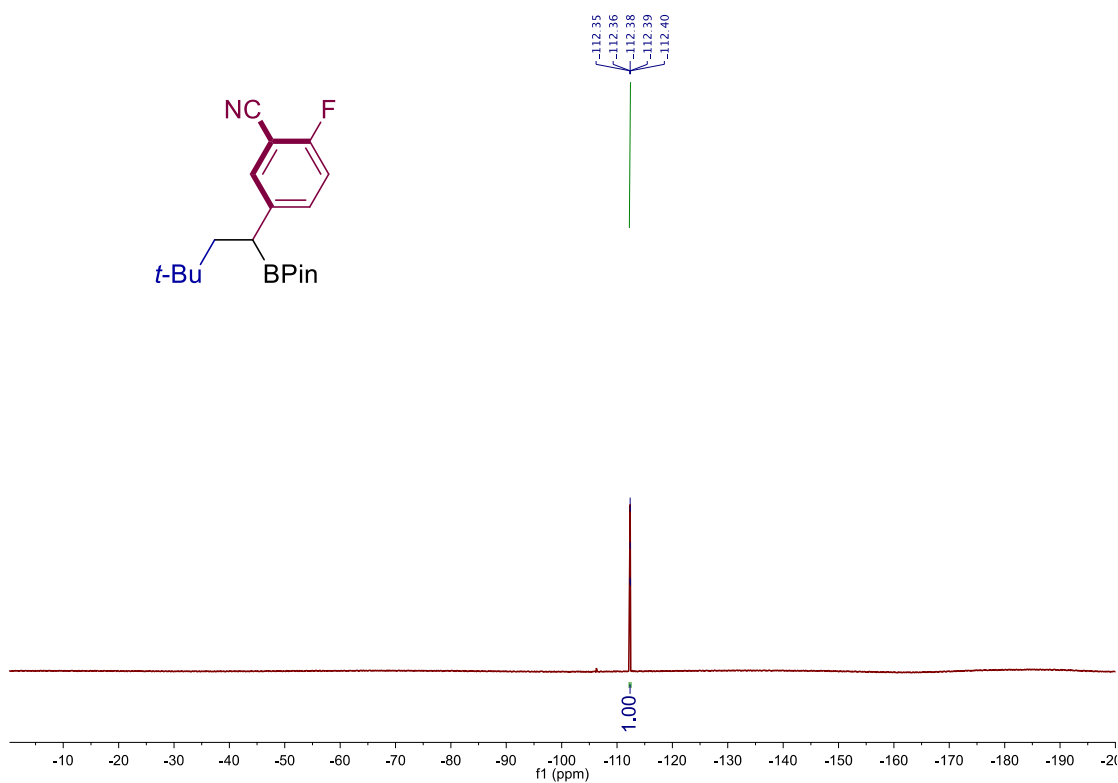
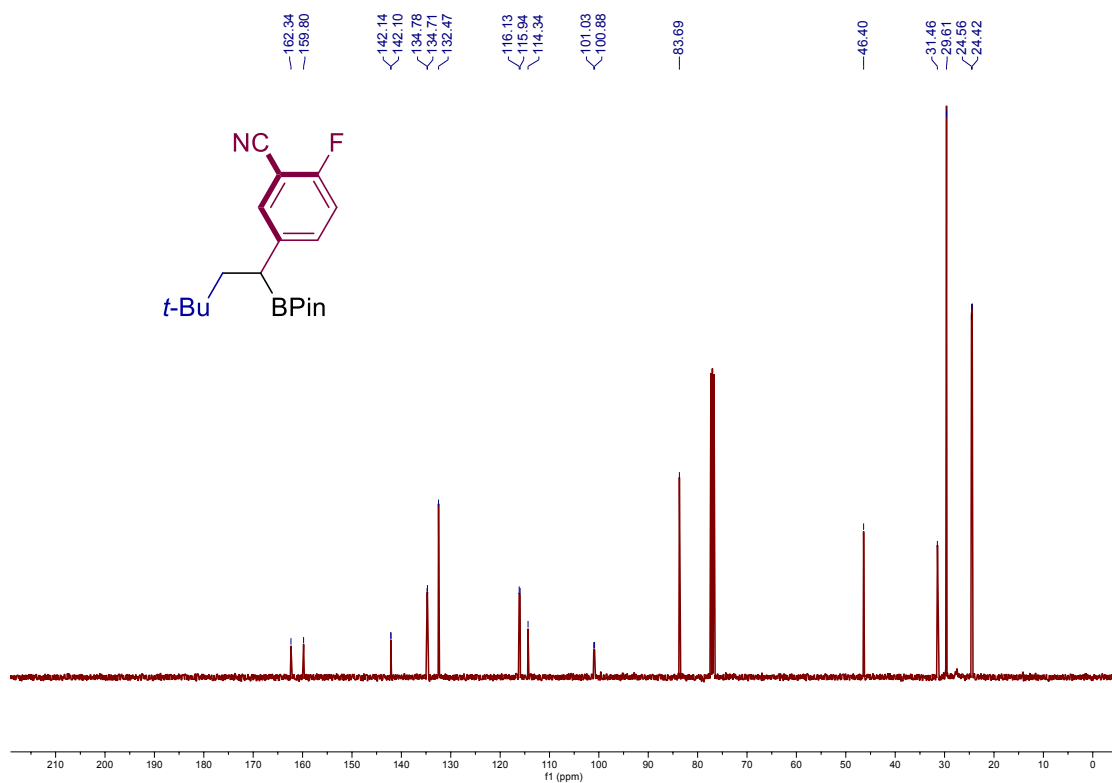


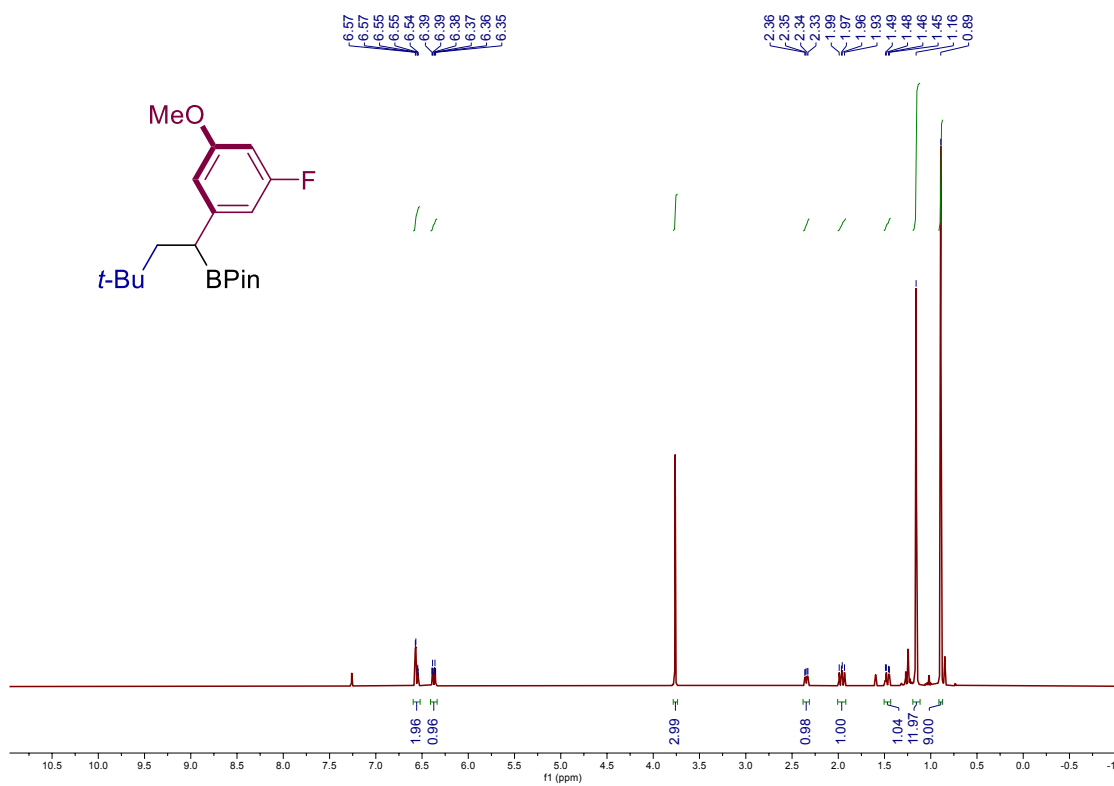
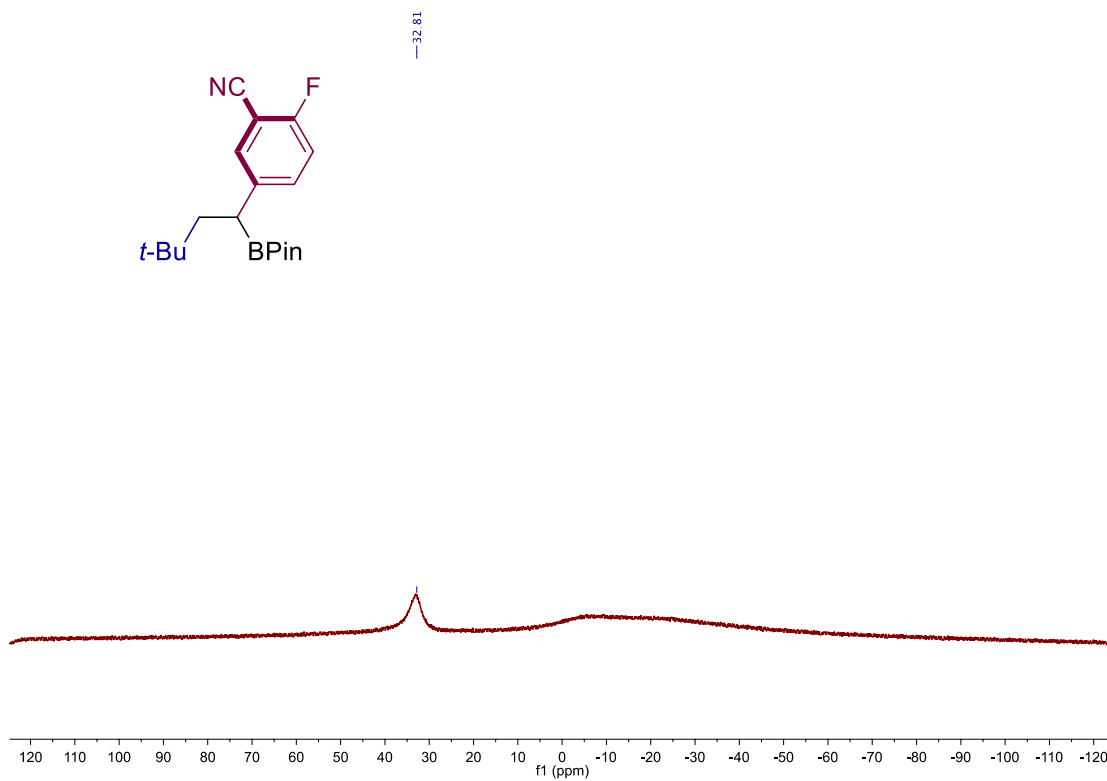
Site-Selective 1,2-Dicarbofunctionalization of Vinyl Boronates through Dual Catalysis



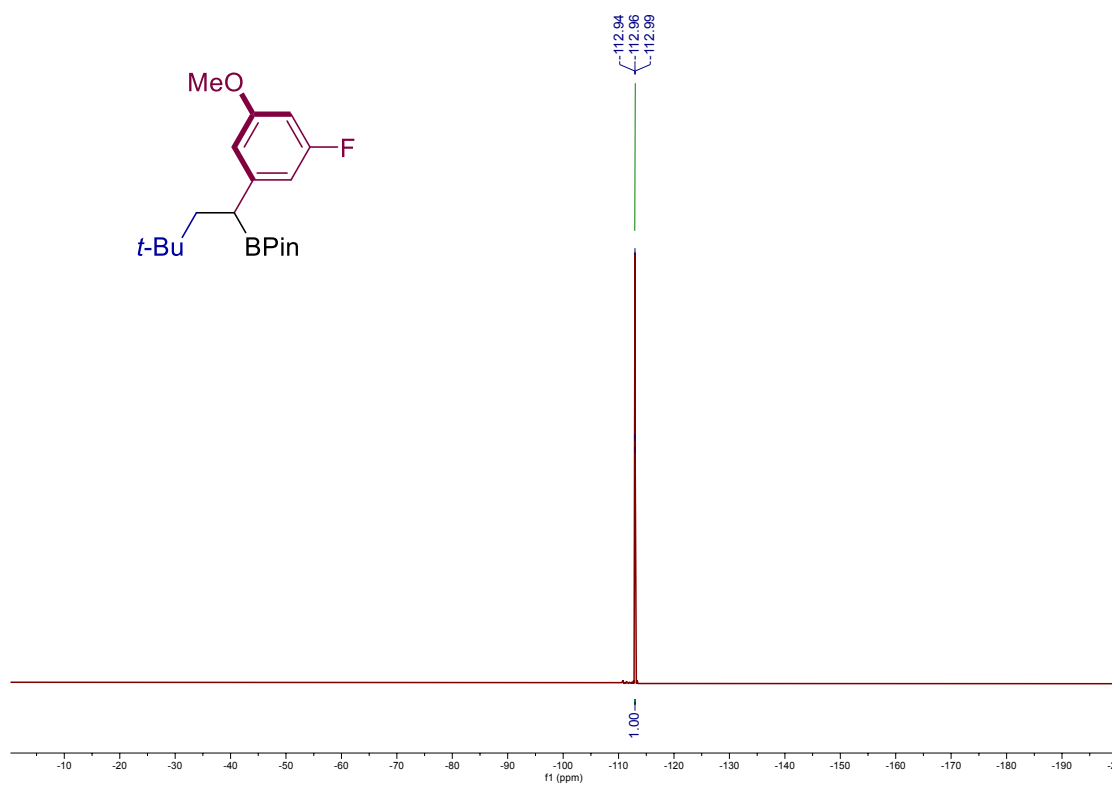
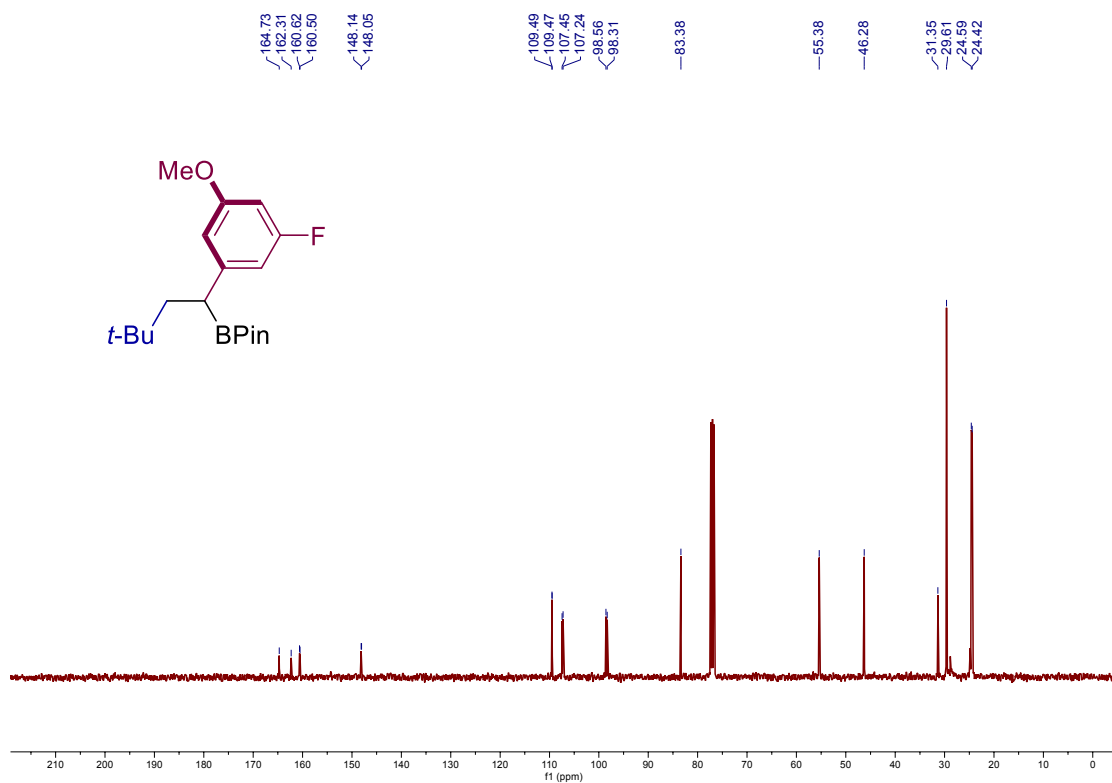


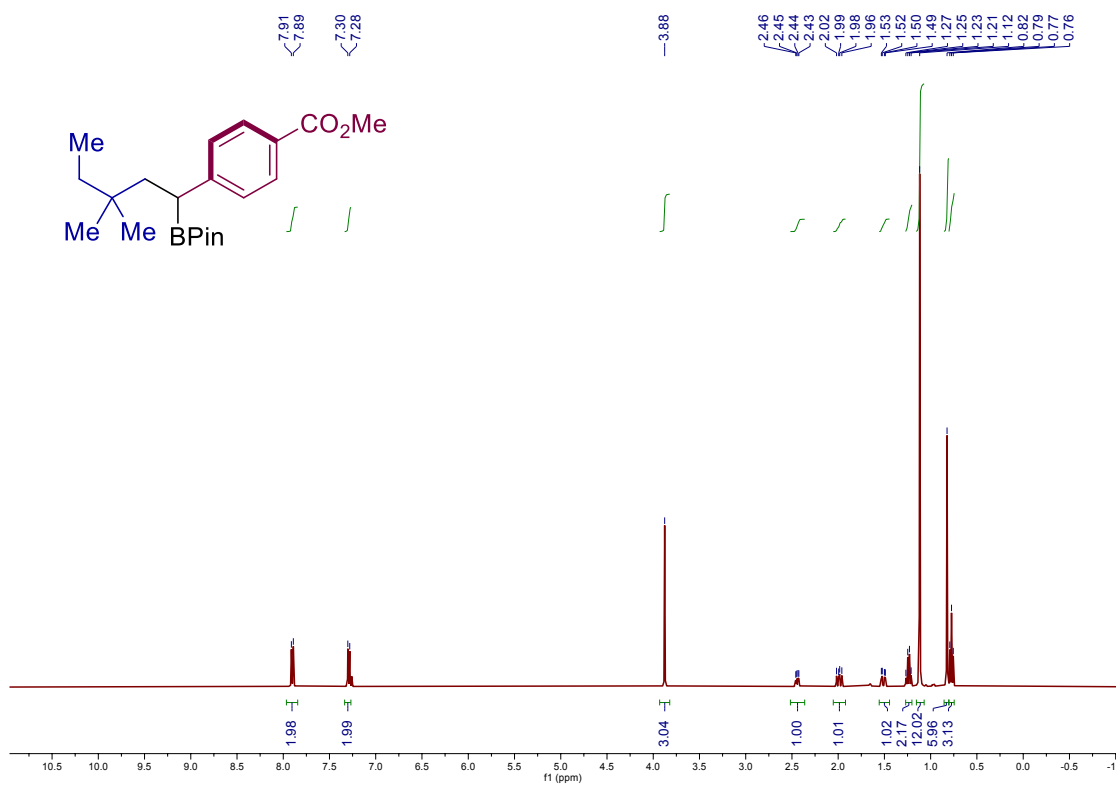
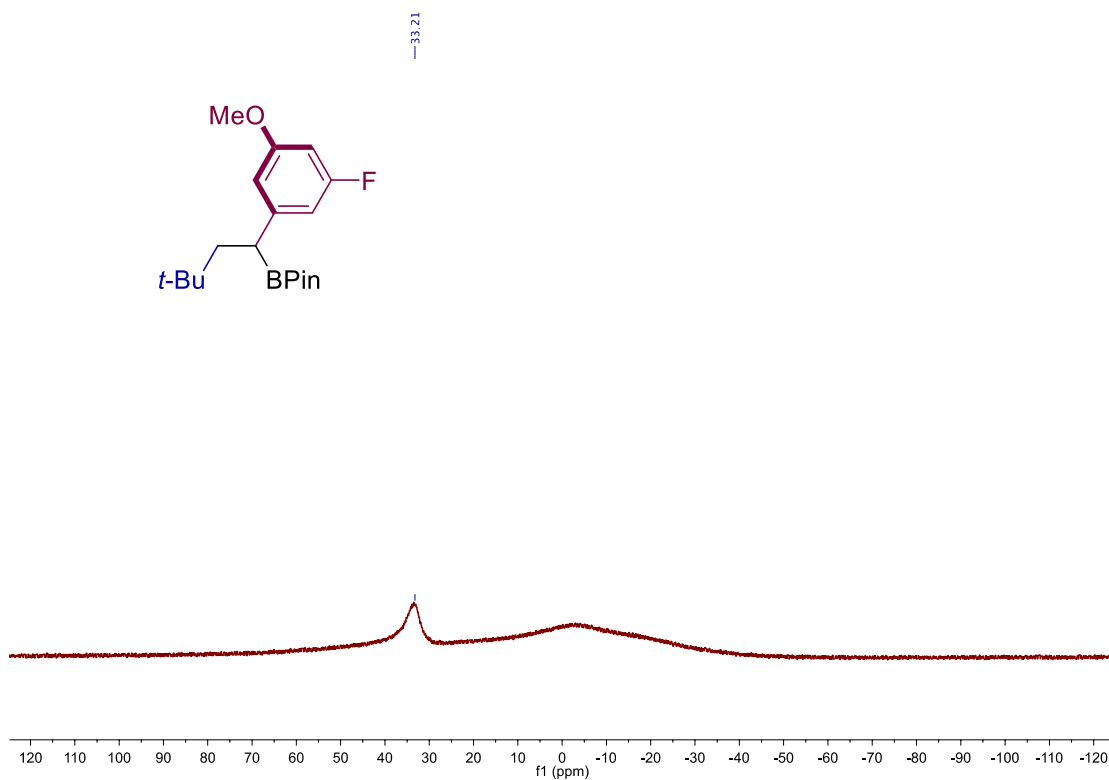
Site-Selective 1,2-Dicarbonylation of Vinyl Boronates through Dual Catalysis



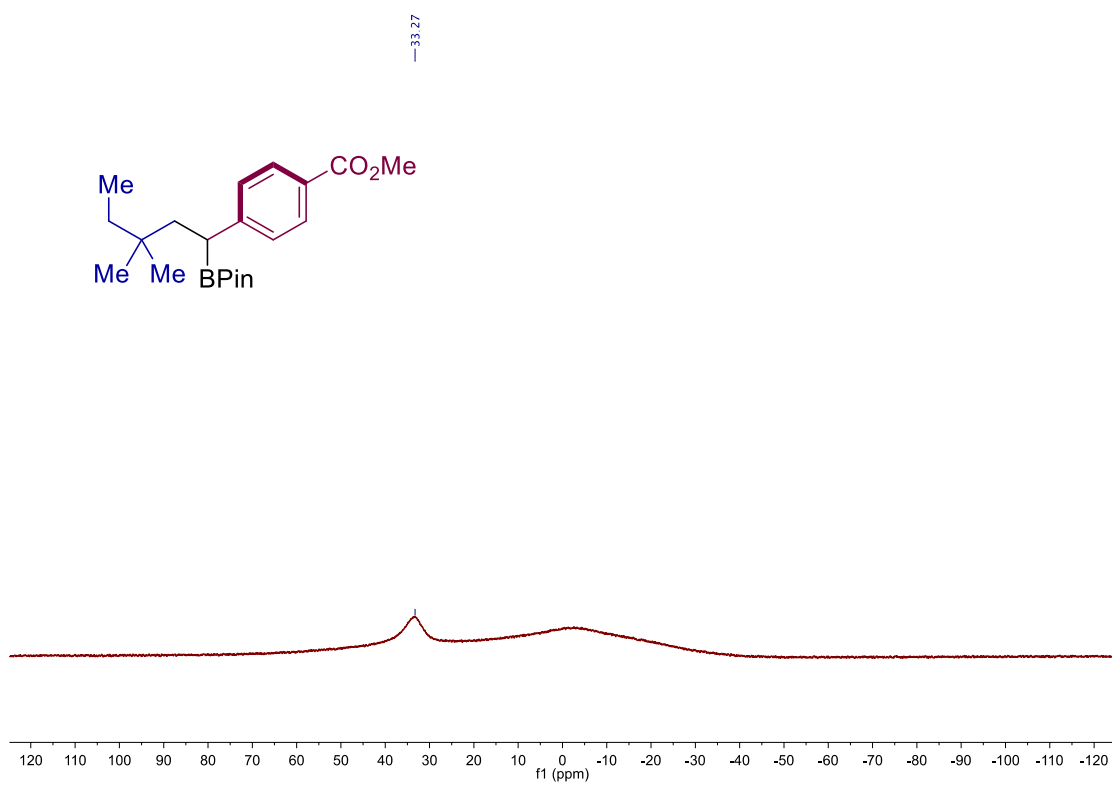
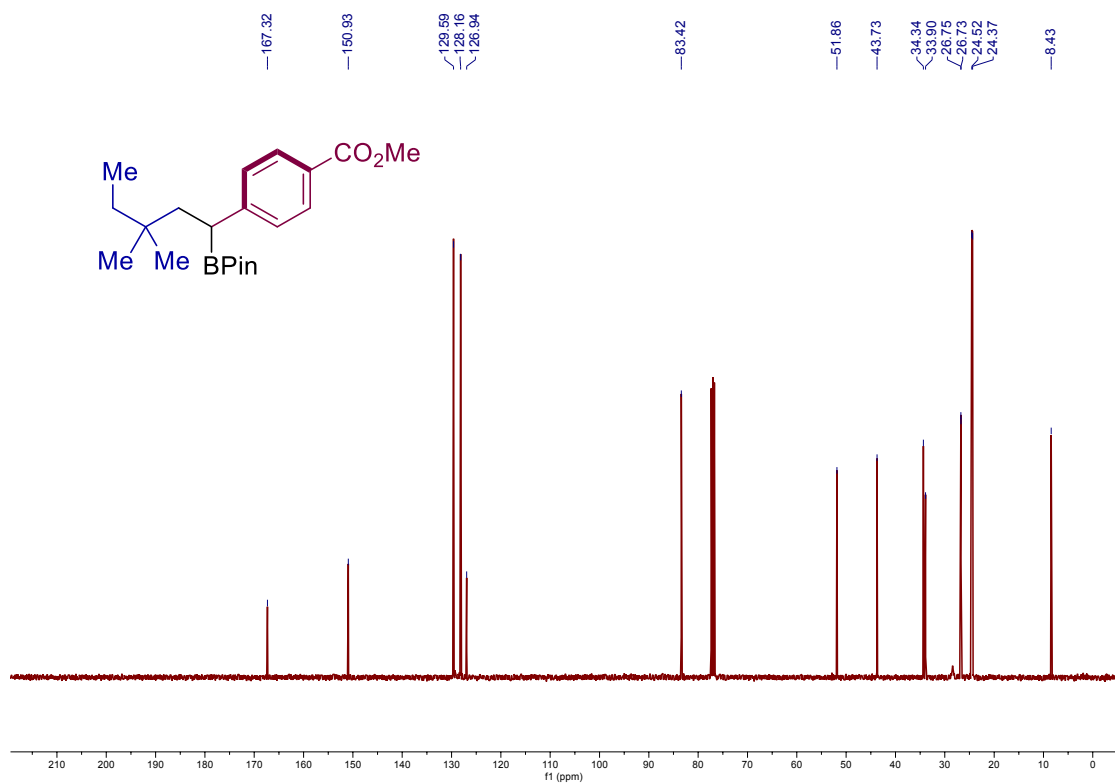


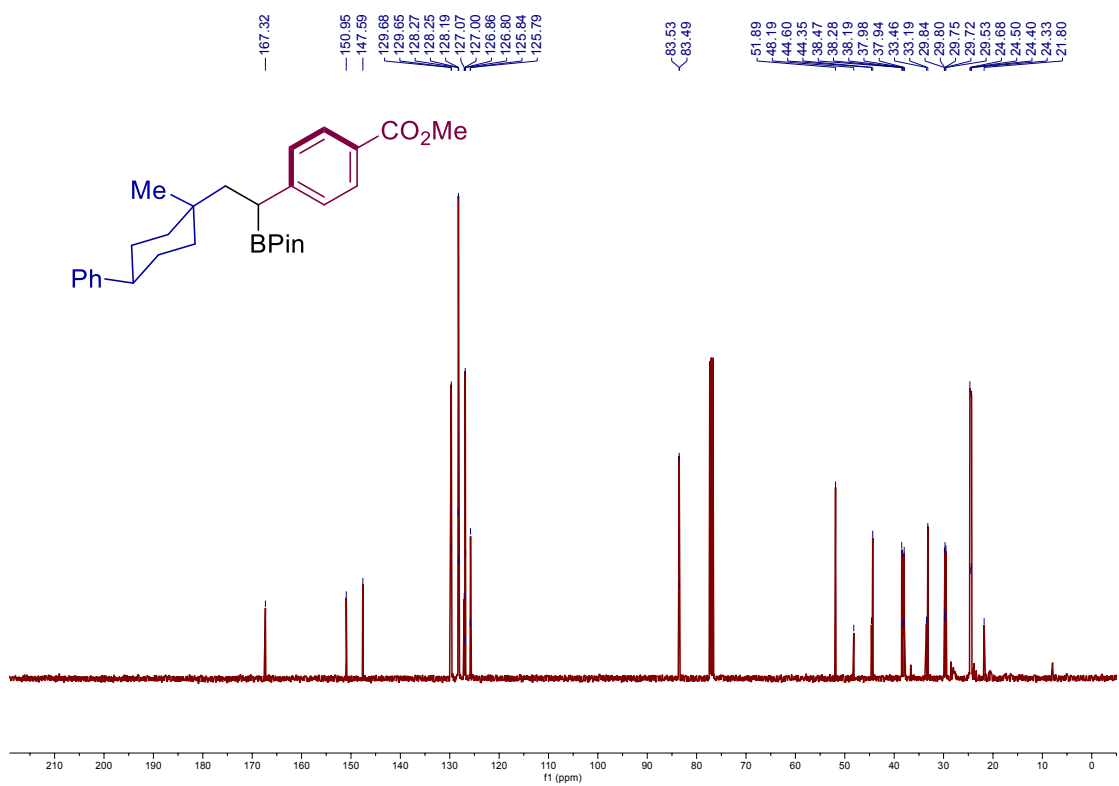
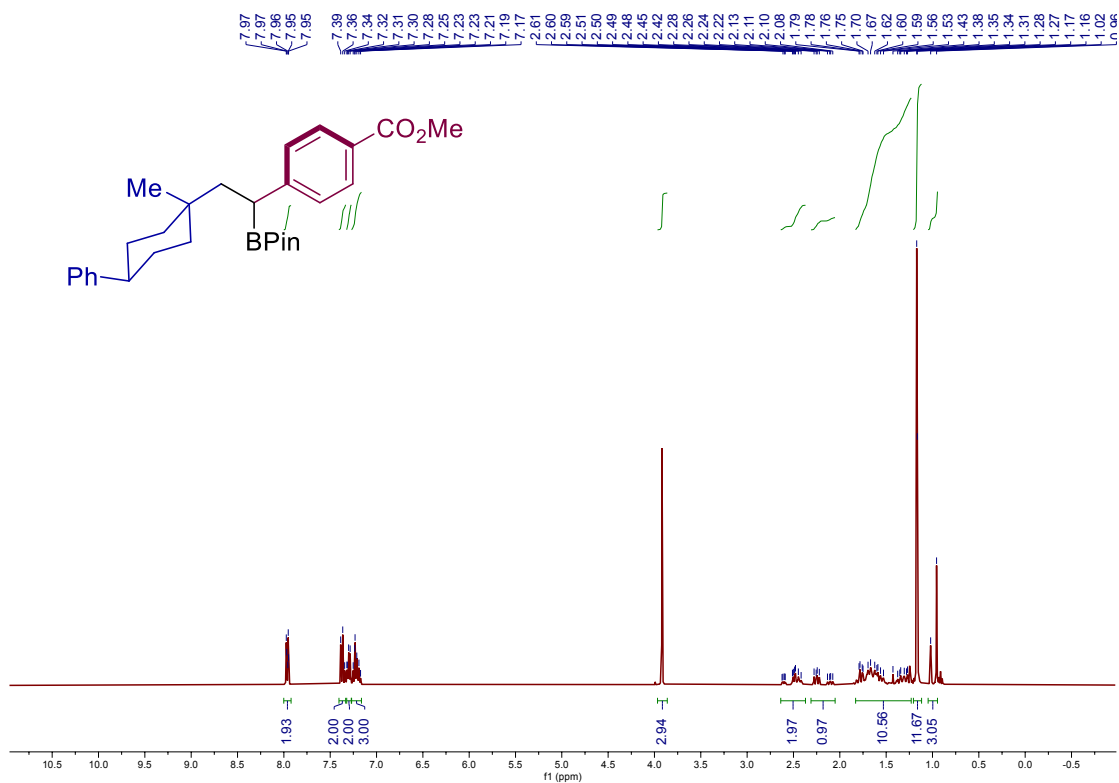
Site-Selective 1,2-Dicarbonylation of Vinyl Boronates through Dual Catalysis



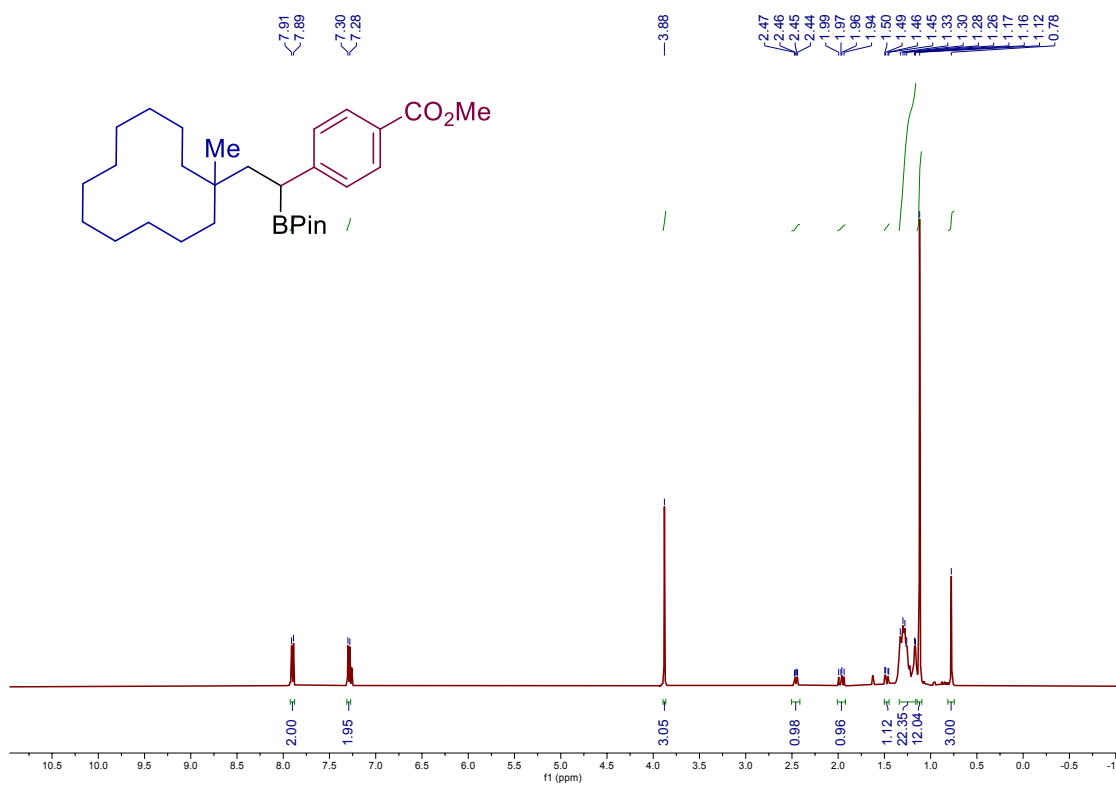
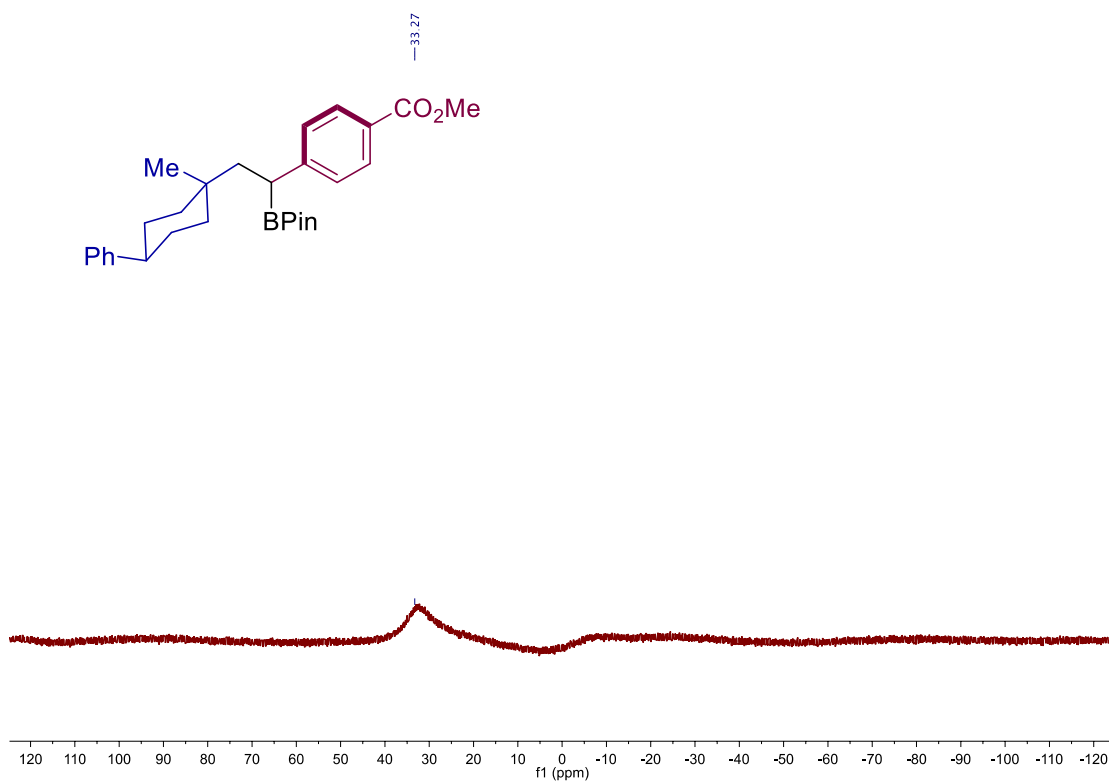


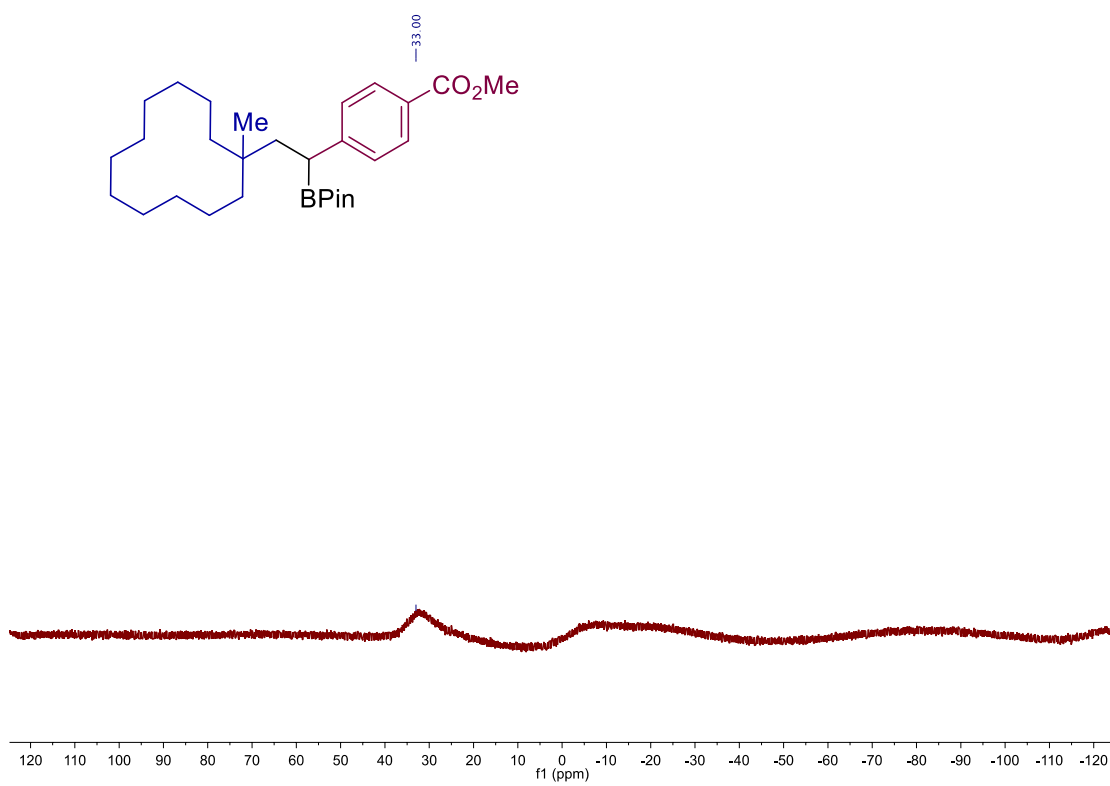
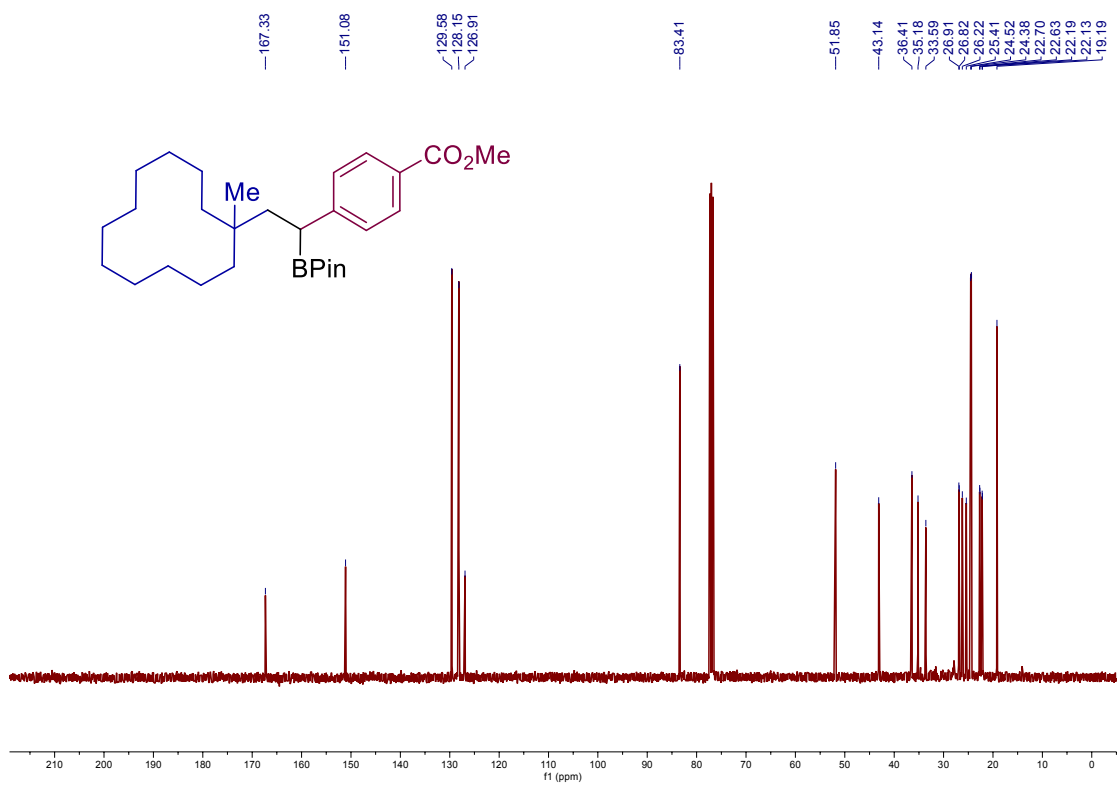
Site-Selective 1,2-Dicarbonylation of Vinyl Boronates through Dual Catalysis



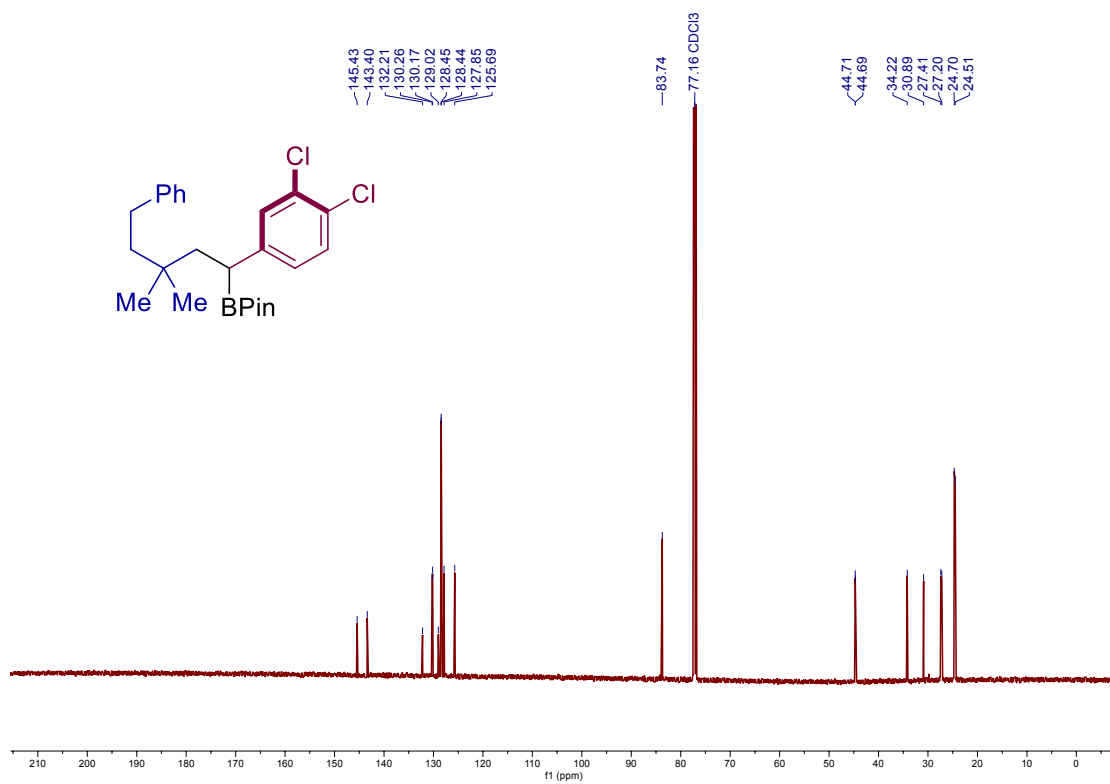
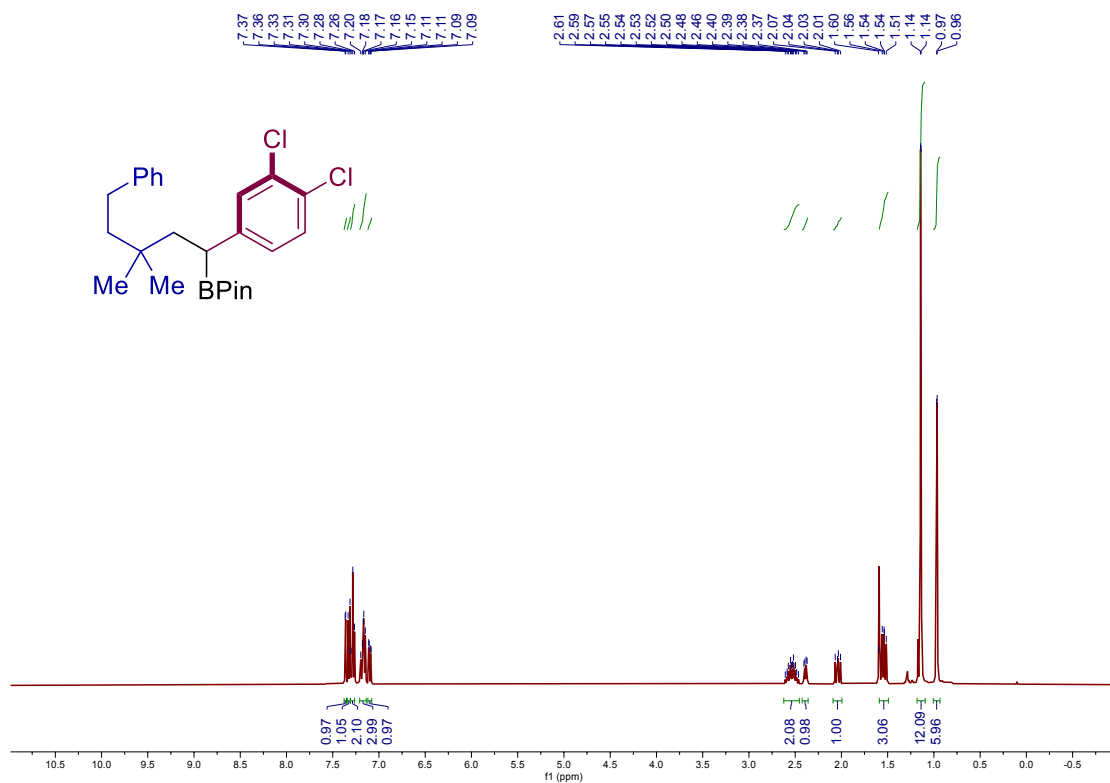


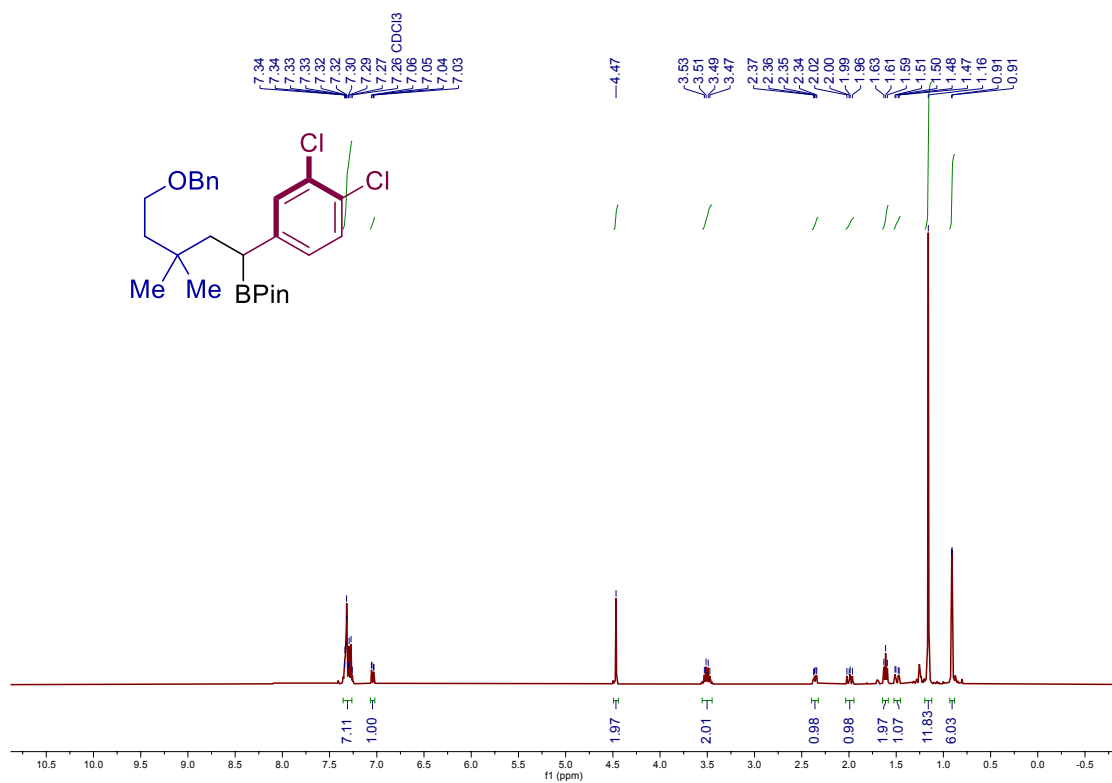
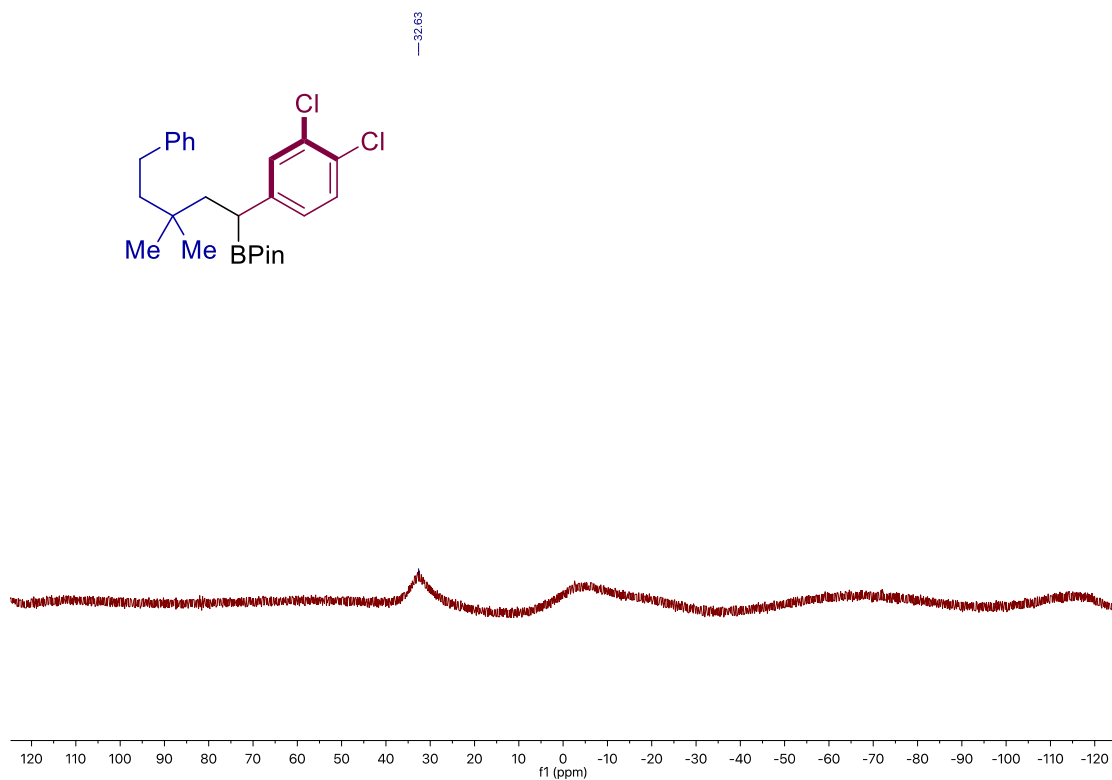
Site-Selective 1,2-Dicarbofunctionalization of Vinyl Boronates through Dual Catalysis



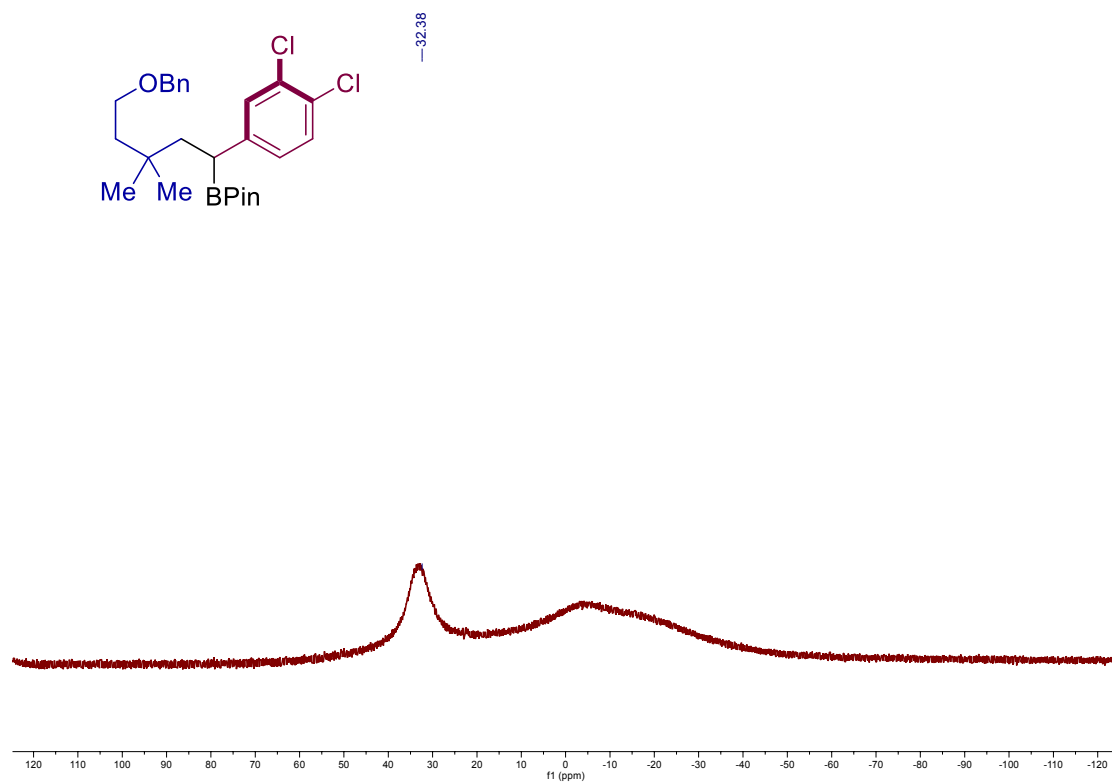
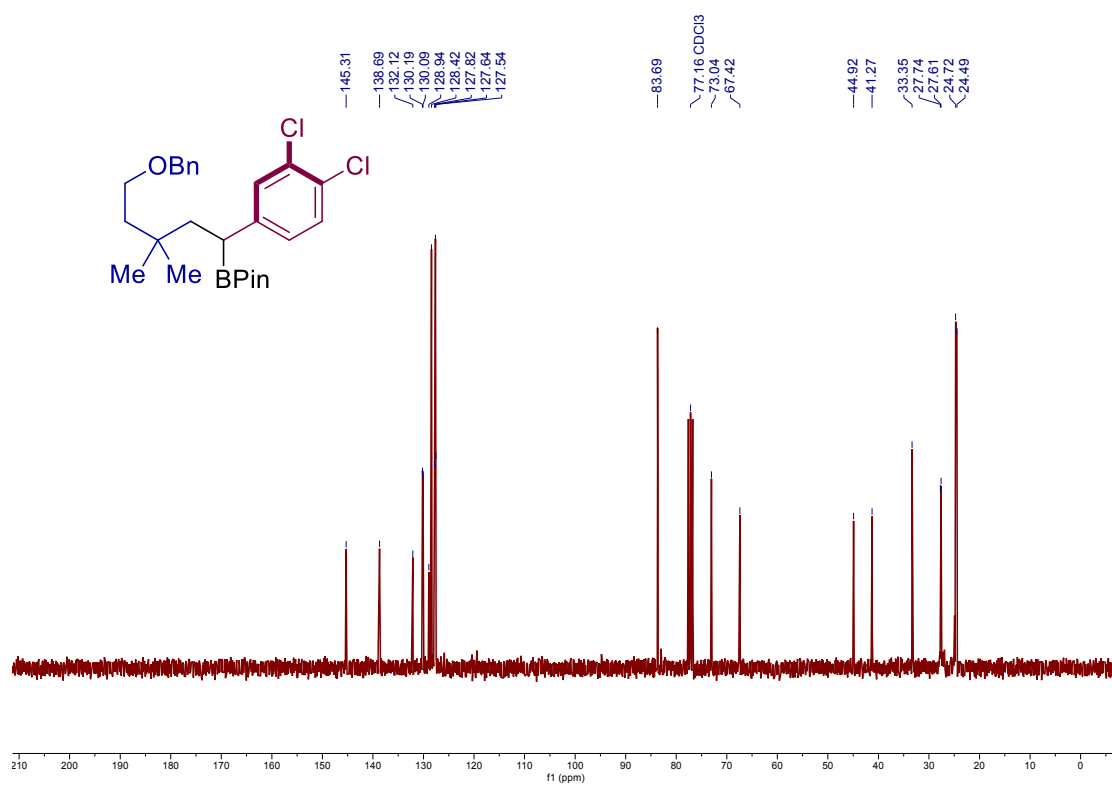


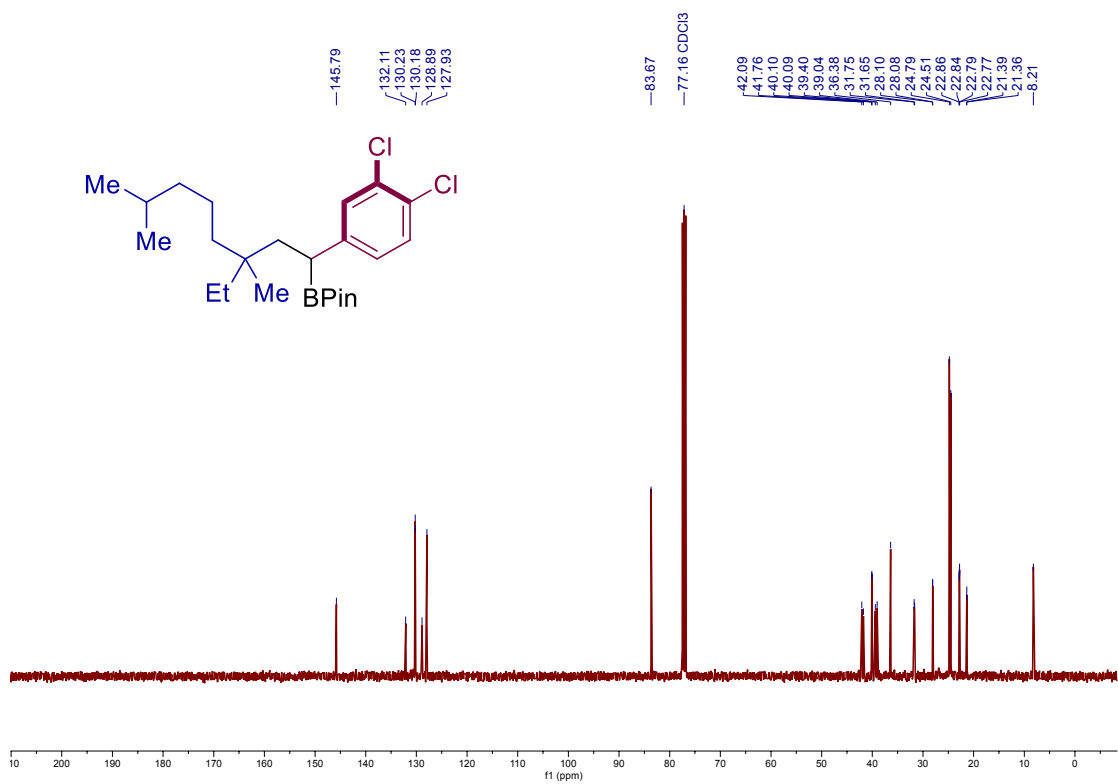
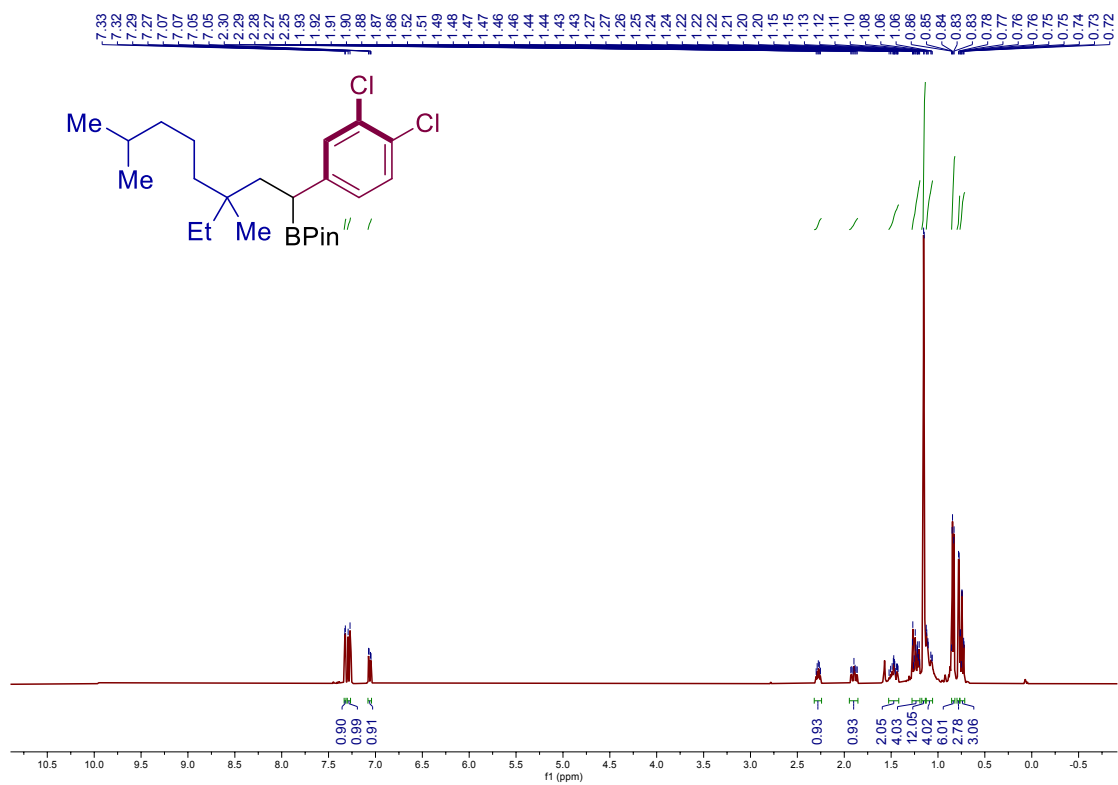
Site-Selective 1,2-Dicarbofunctionalization of Vinyl Boronates through Dual Catalysis



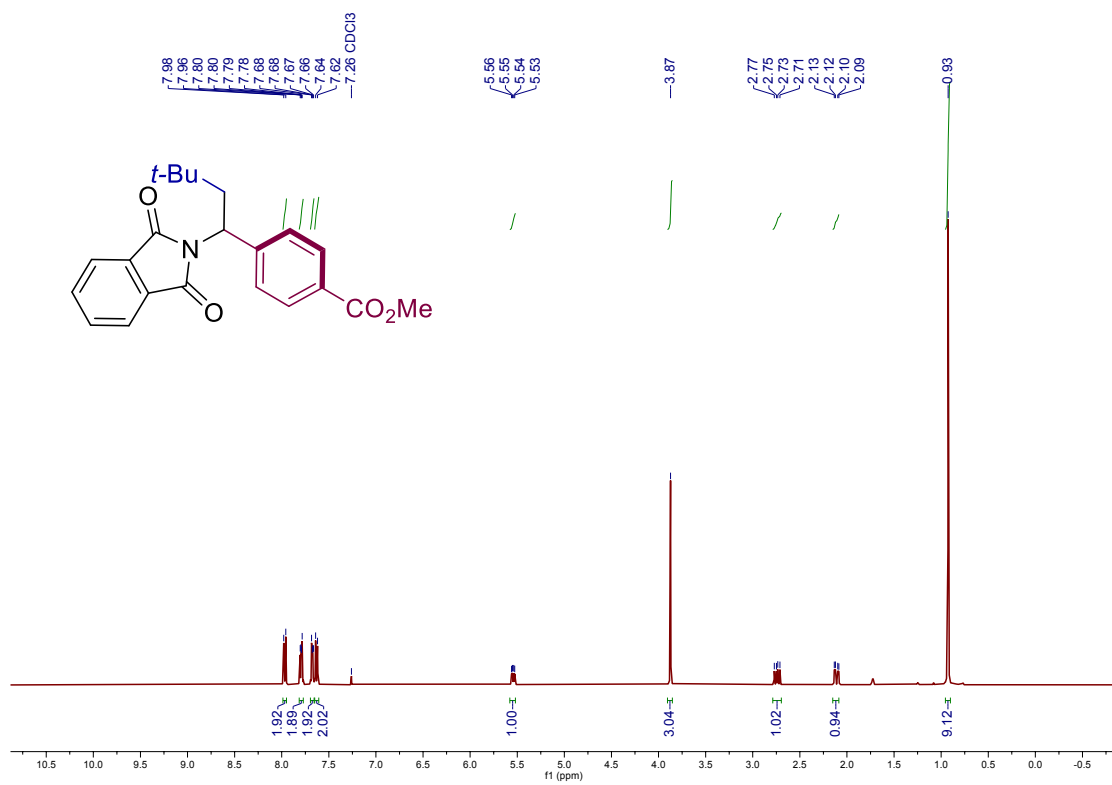
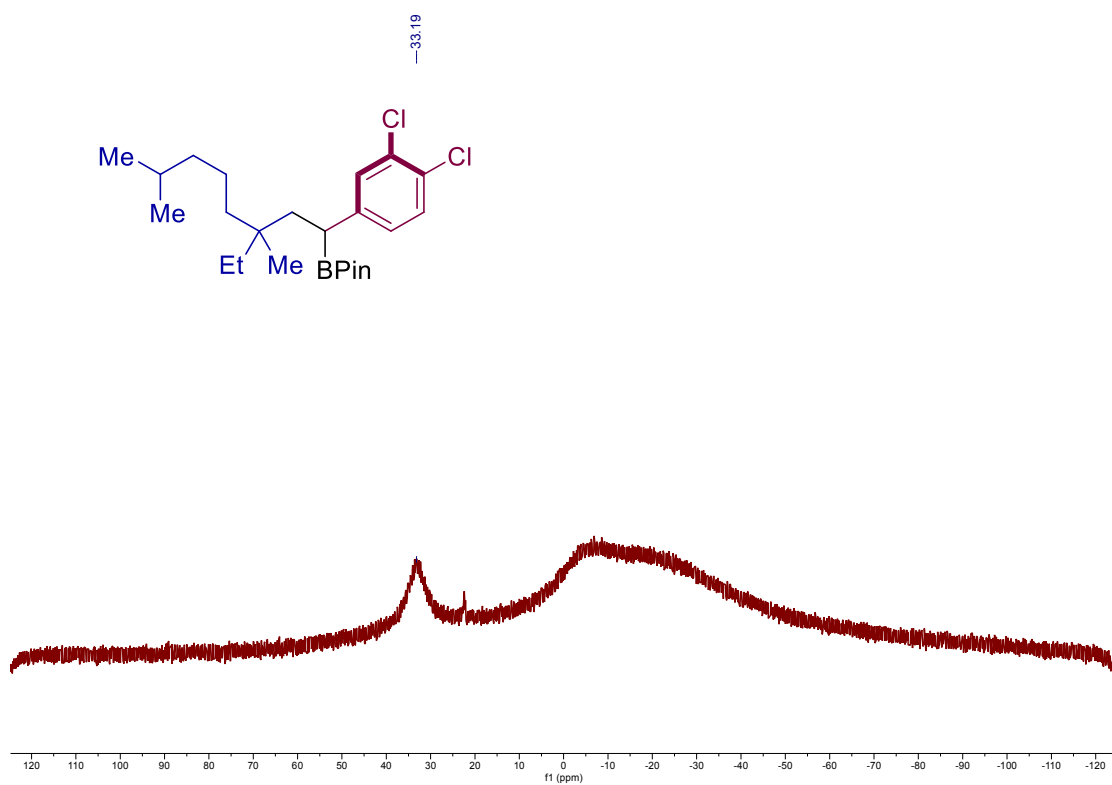


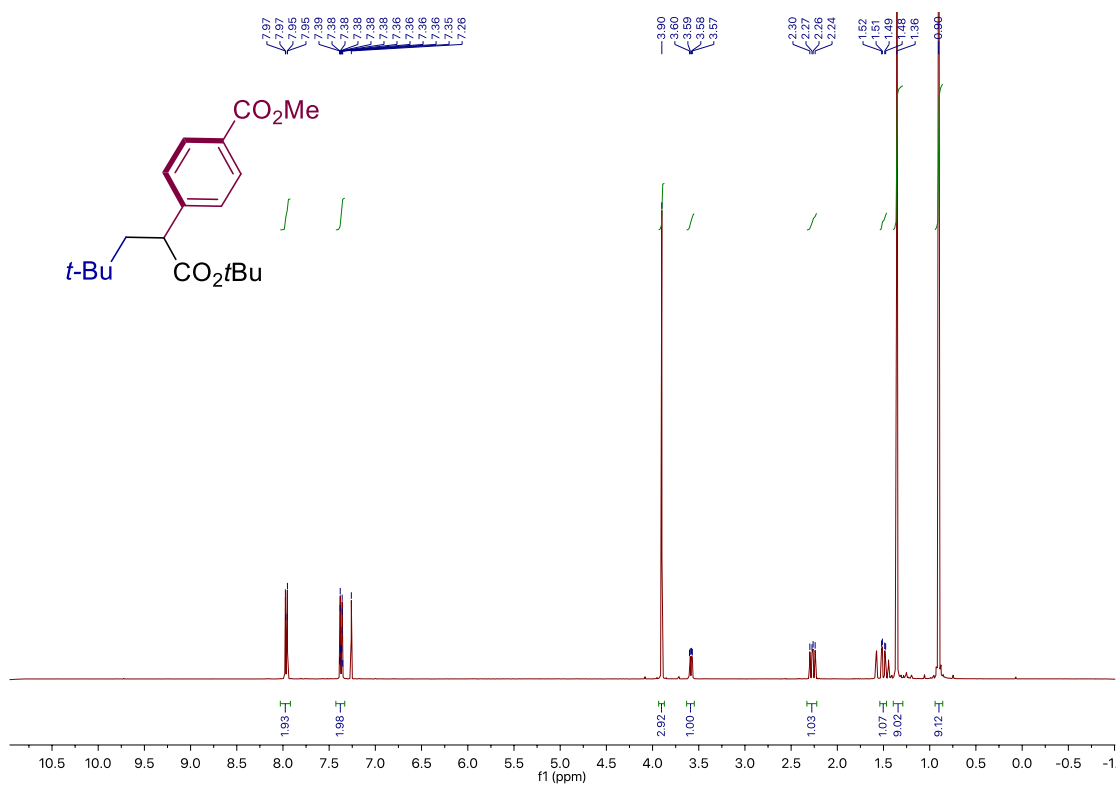
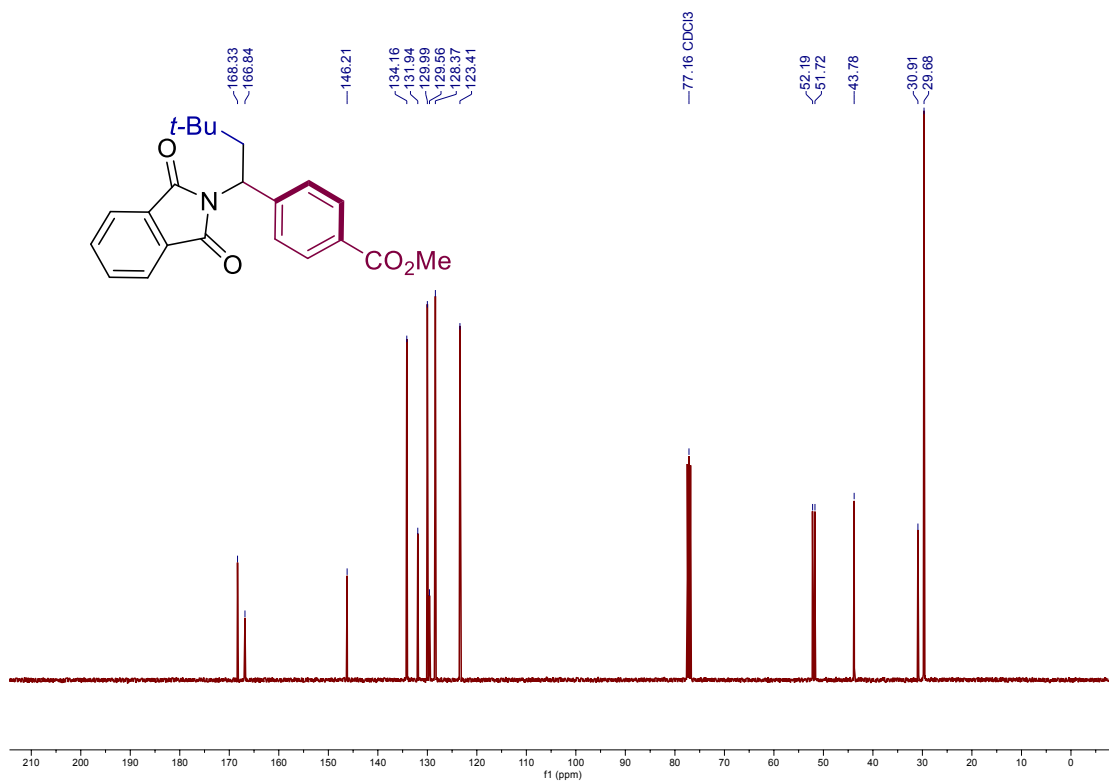
Site-Selective 1,2-Dicarbofunctionalization of Vinyl Boronates through Dual Catalysis



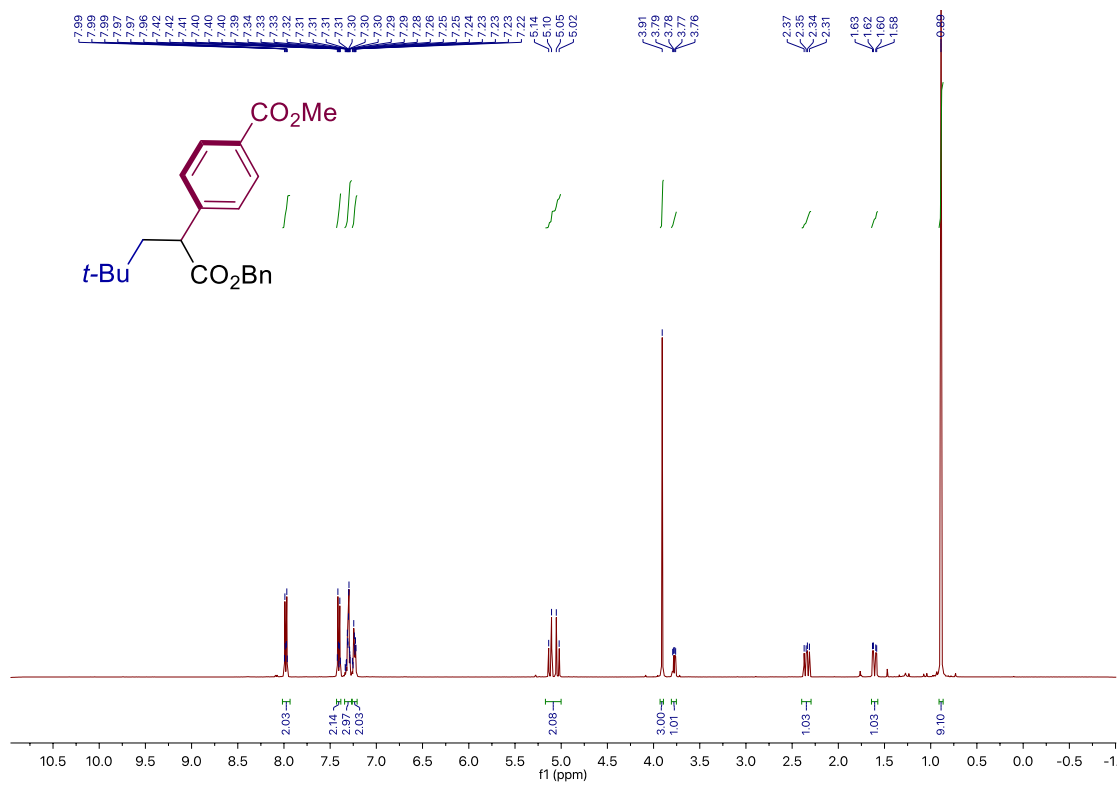
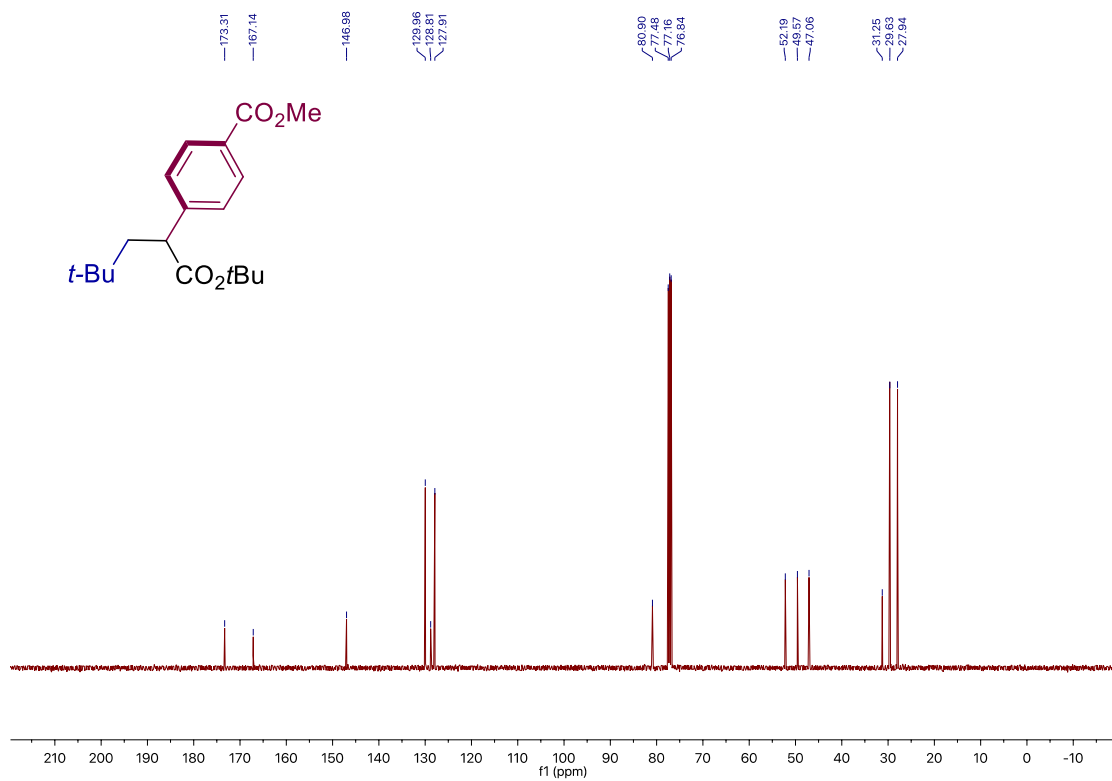


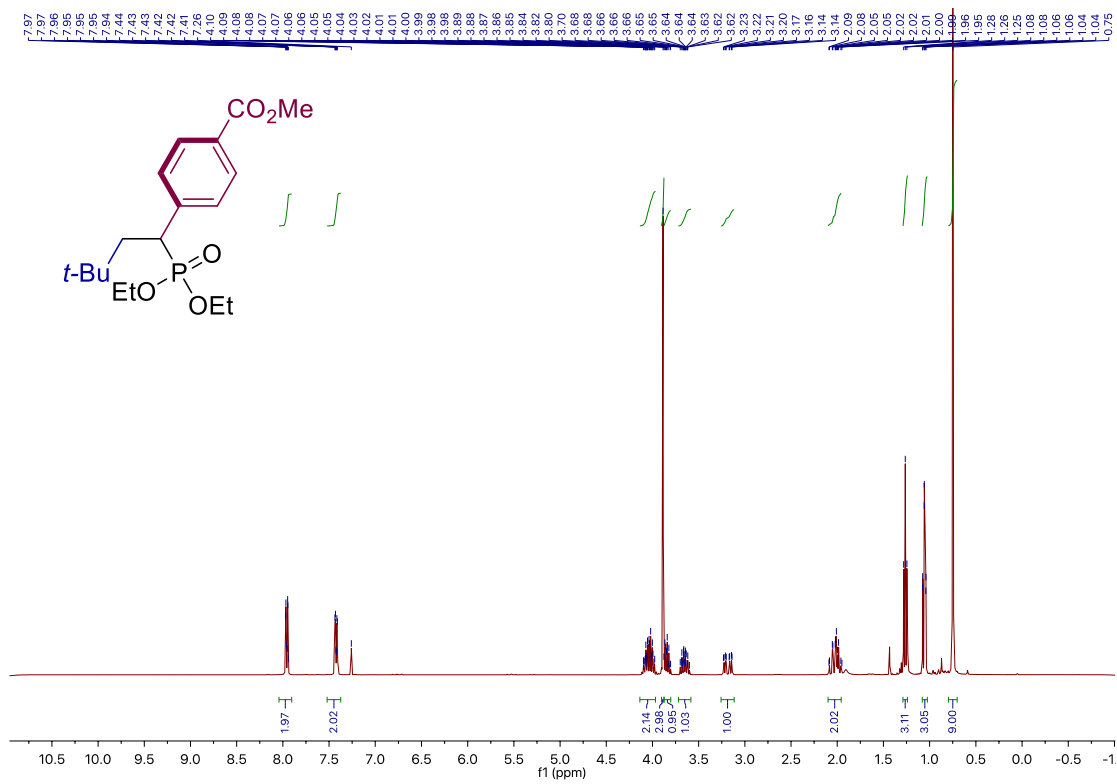
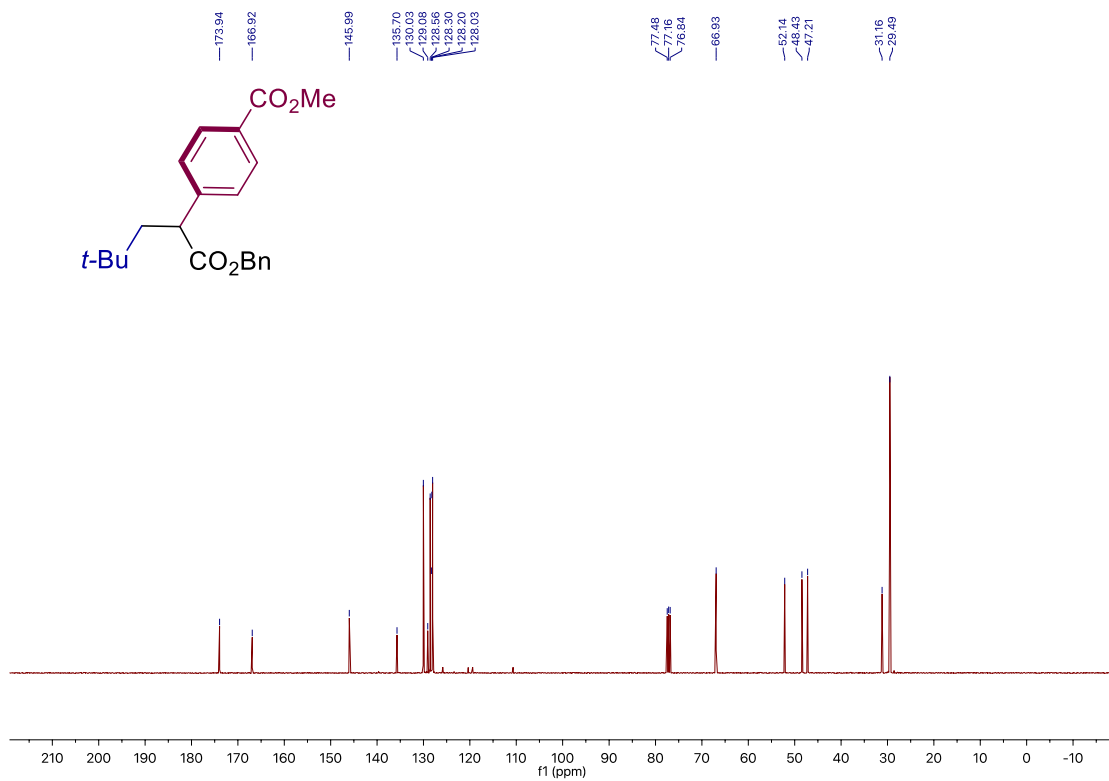
Site-Selective 1,2-Dicarbonylation of Vinyl Boronates through Dual Catalysis



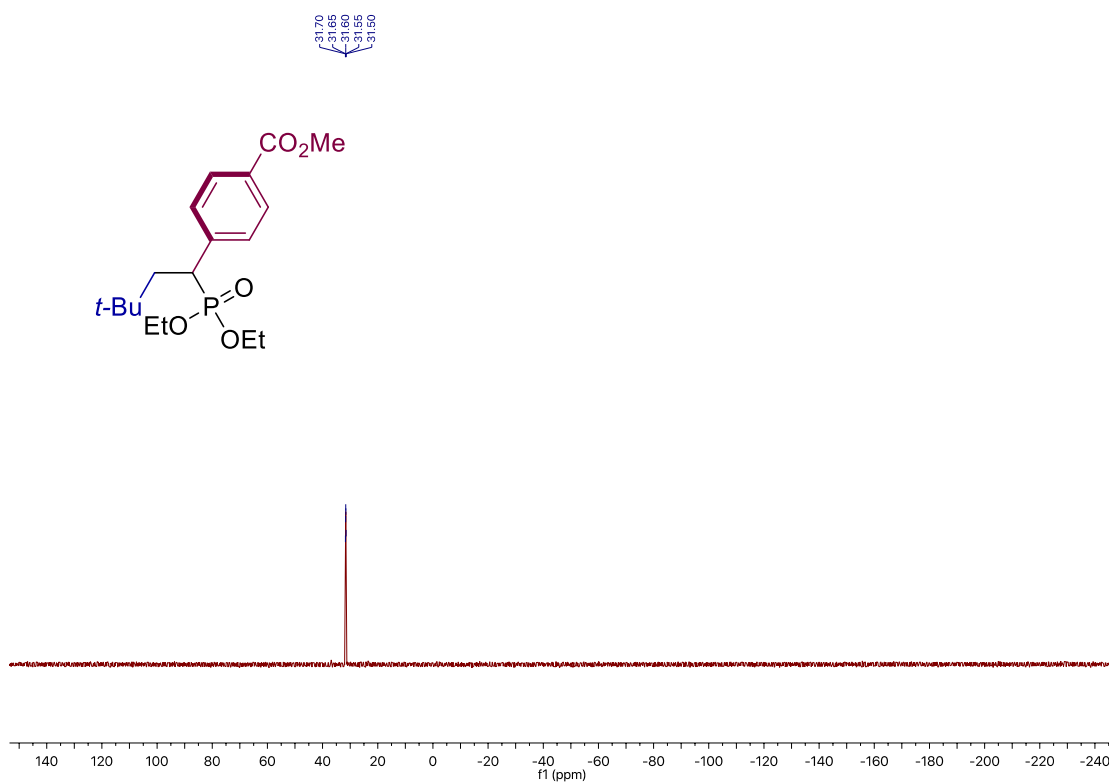
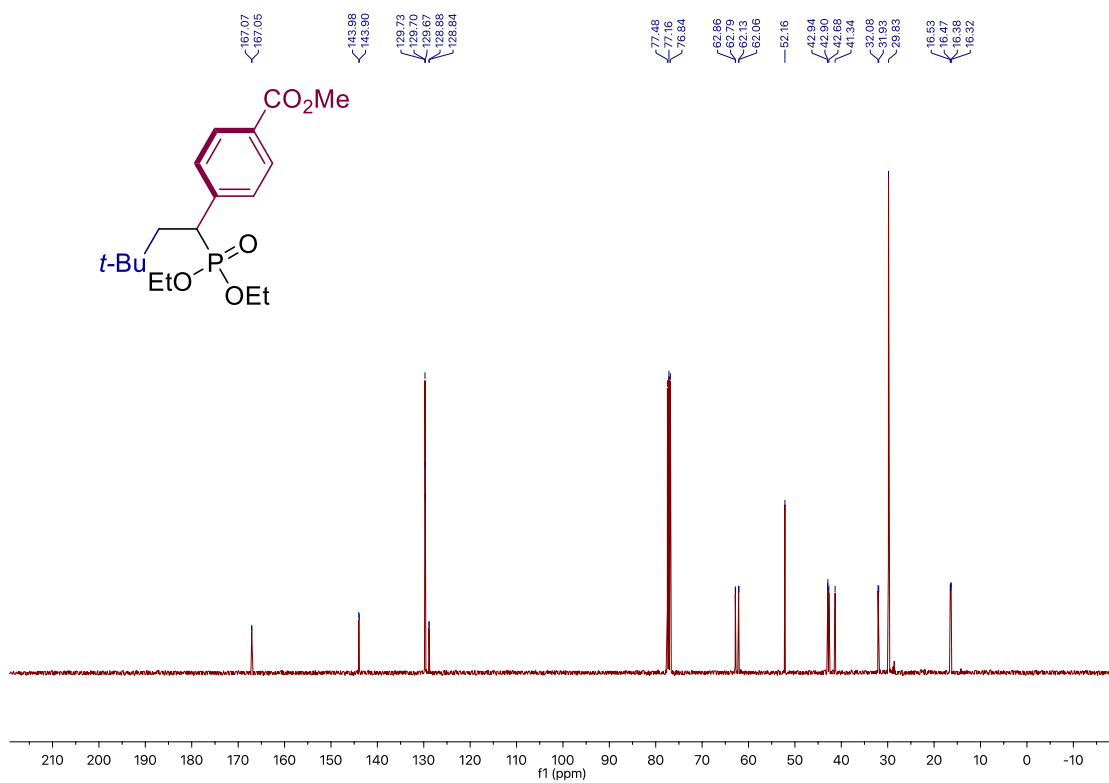


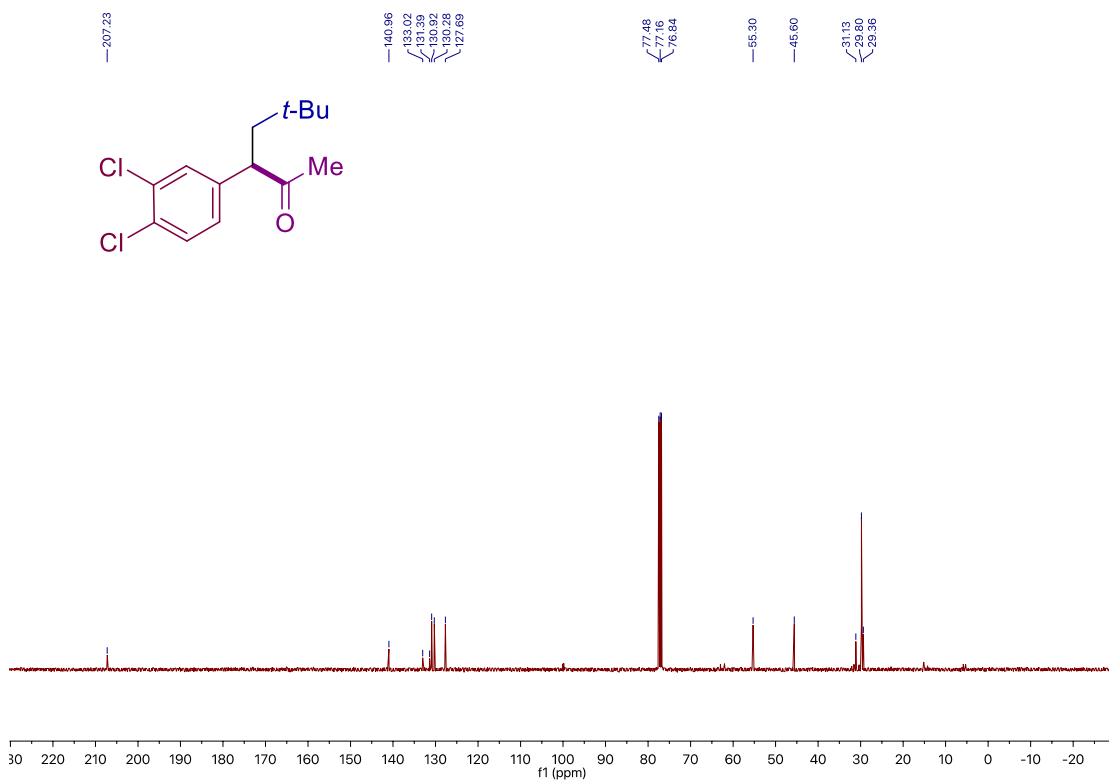
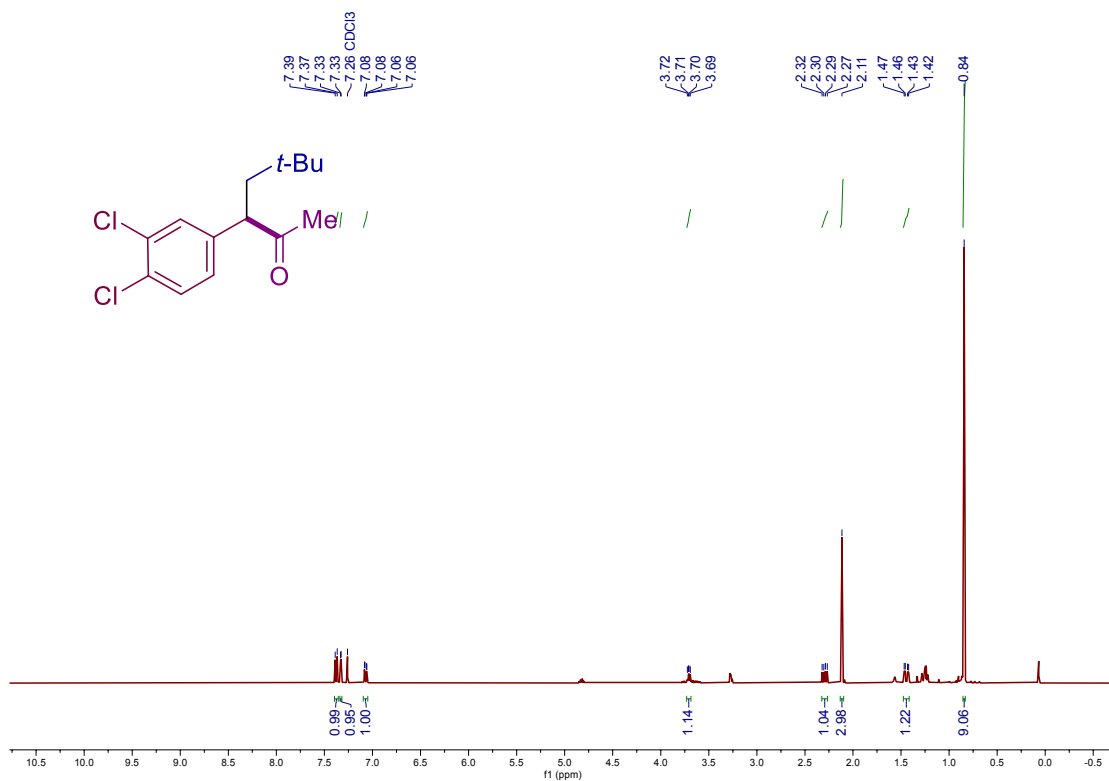
Site-Selective 1,2-Dicarbofunctionalization of Vinyl Boronates through Dual Catalysis



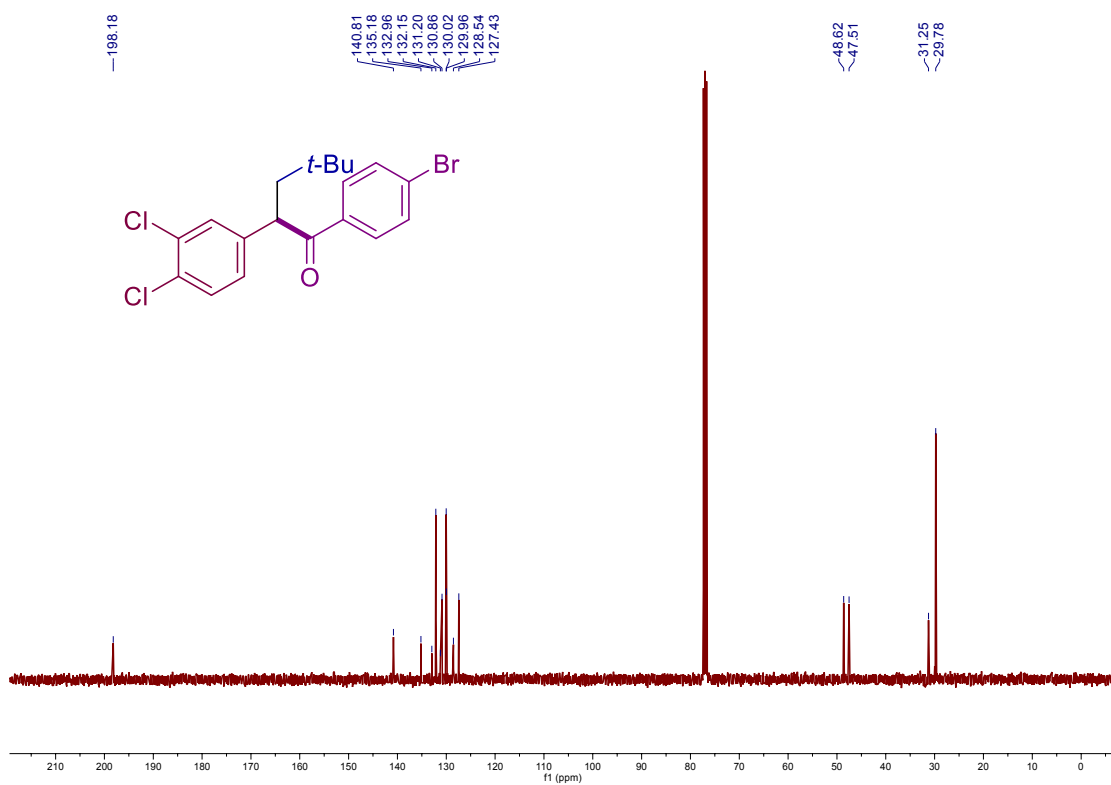
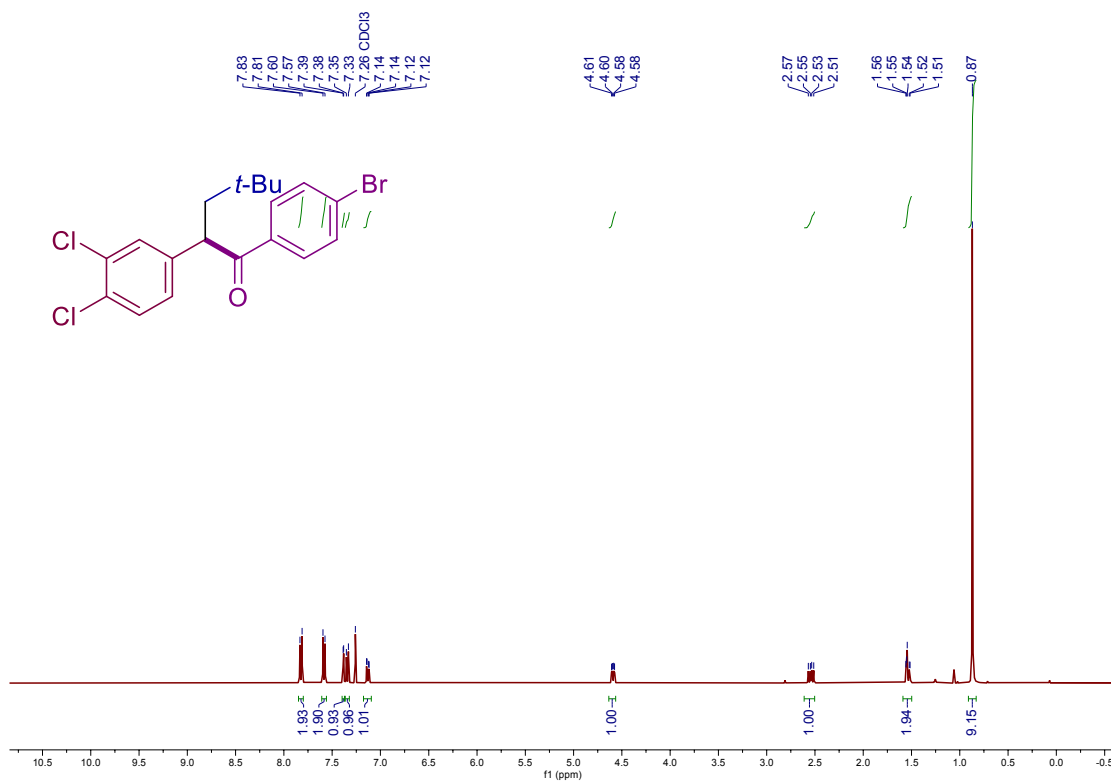


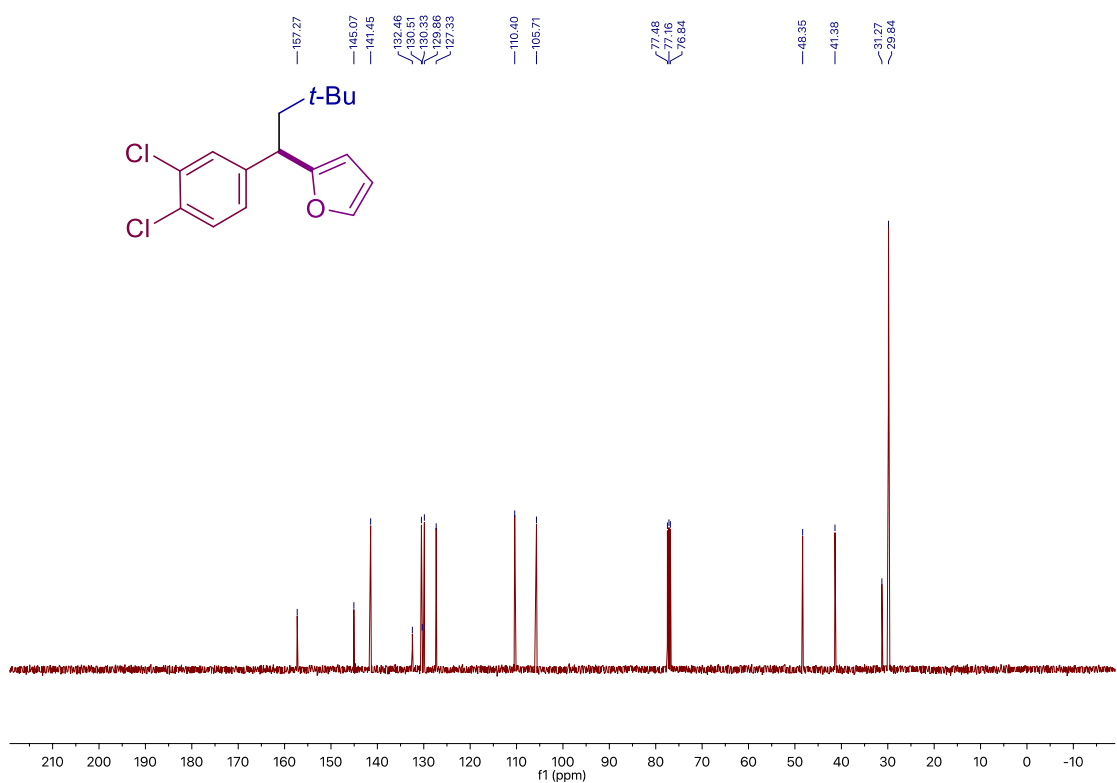
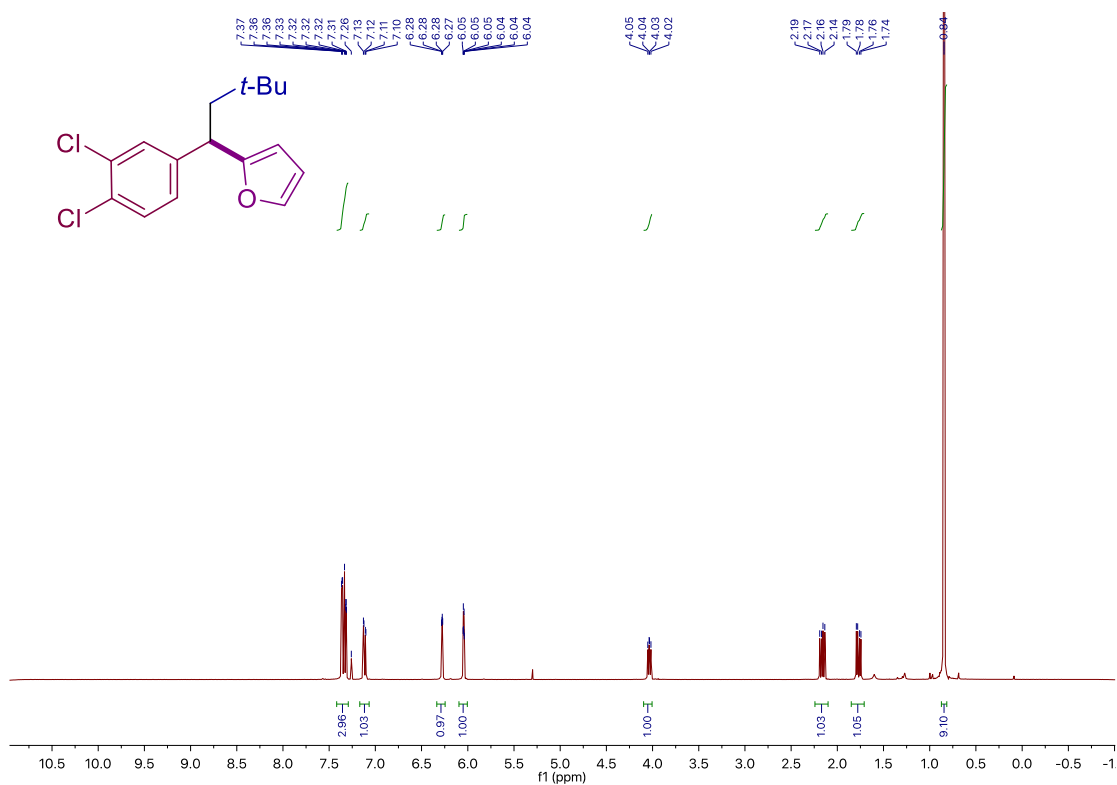
Site-Selective 1,2-Dicarbonylation of Vinyl Boronates through Dual Catalysis



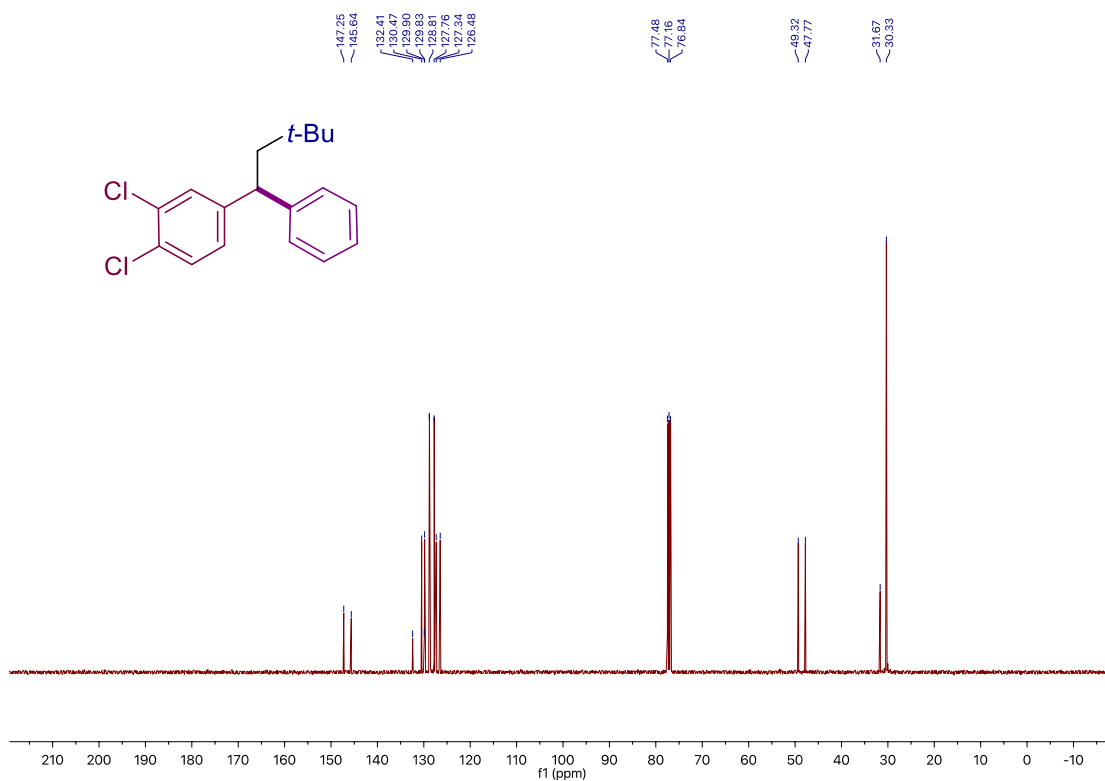
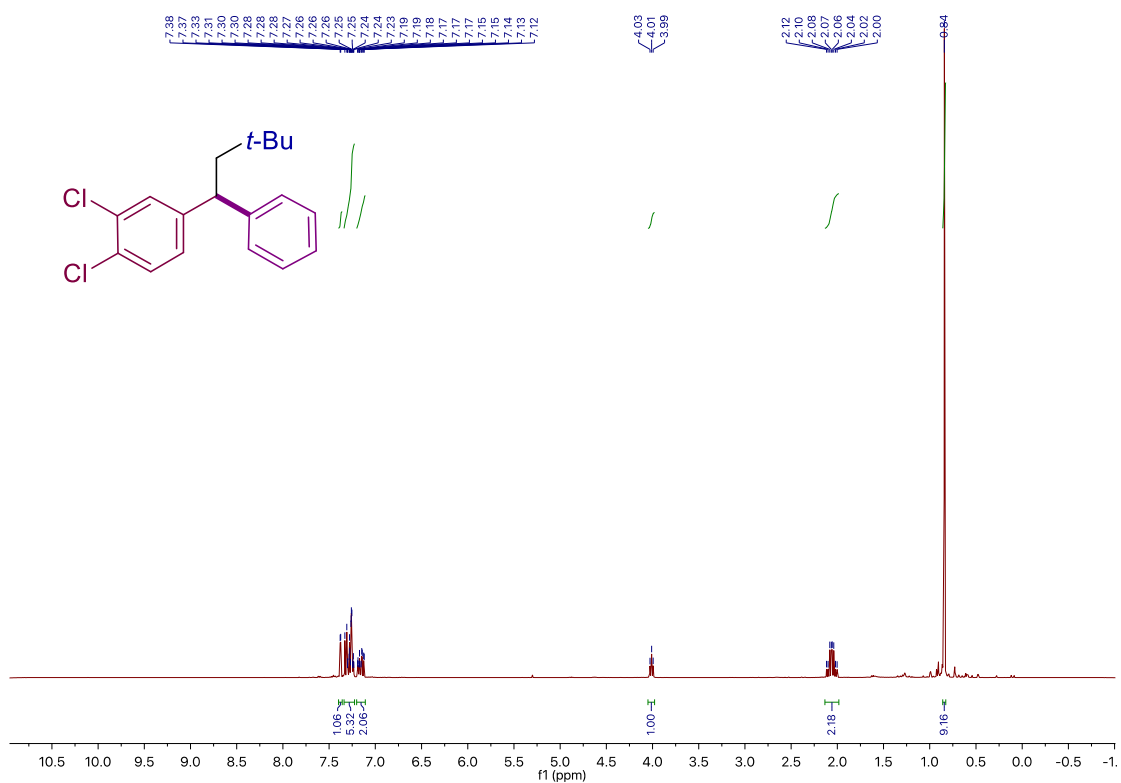


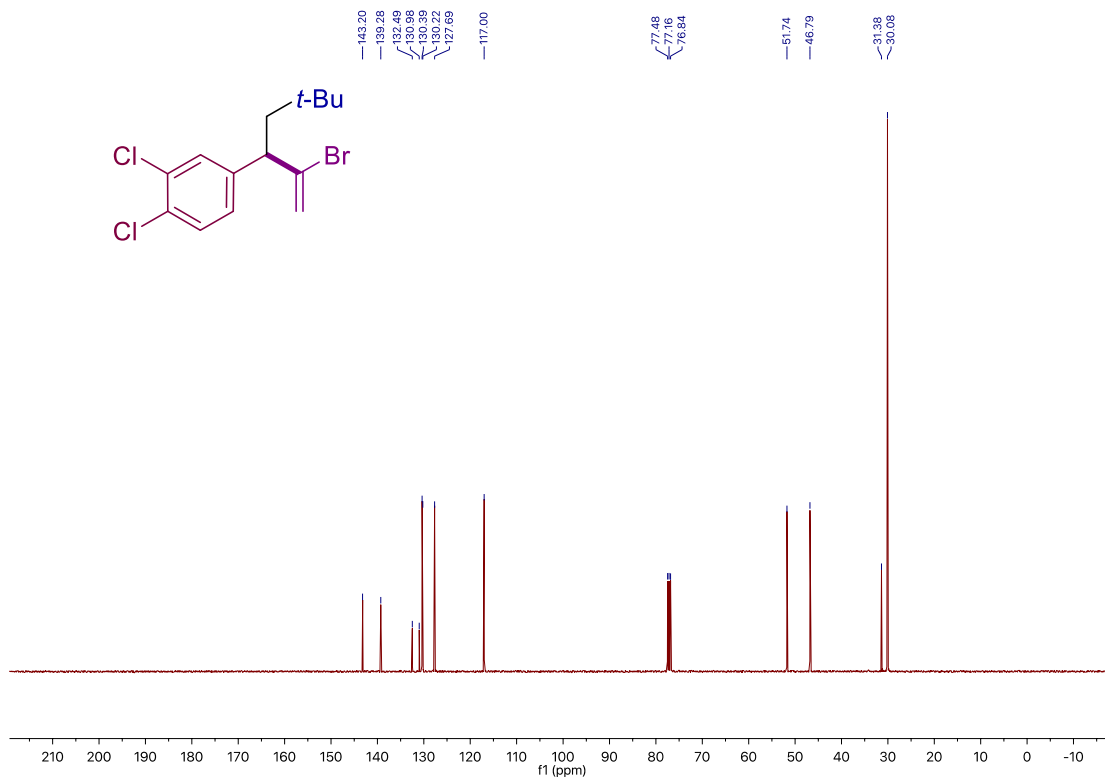
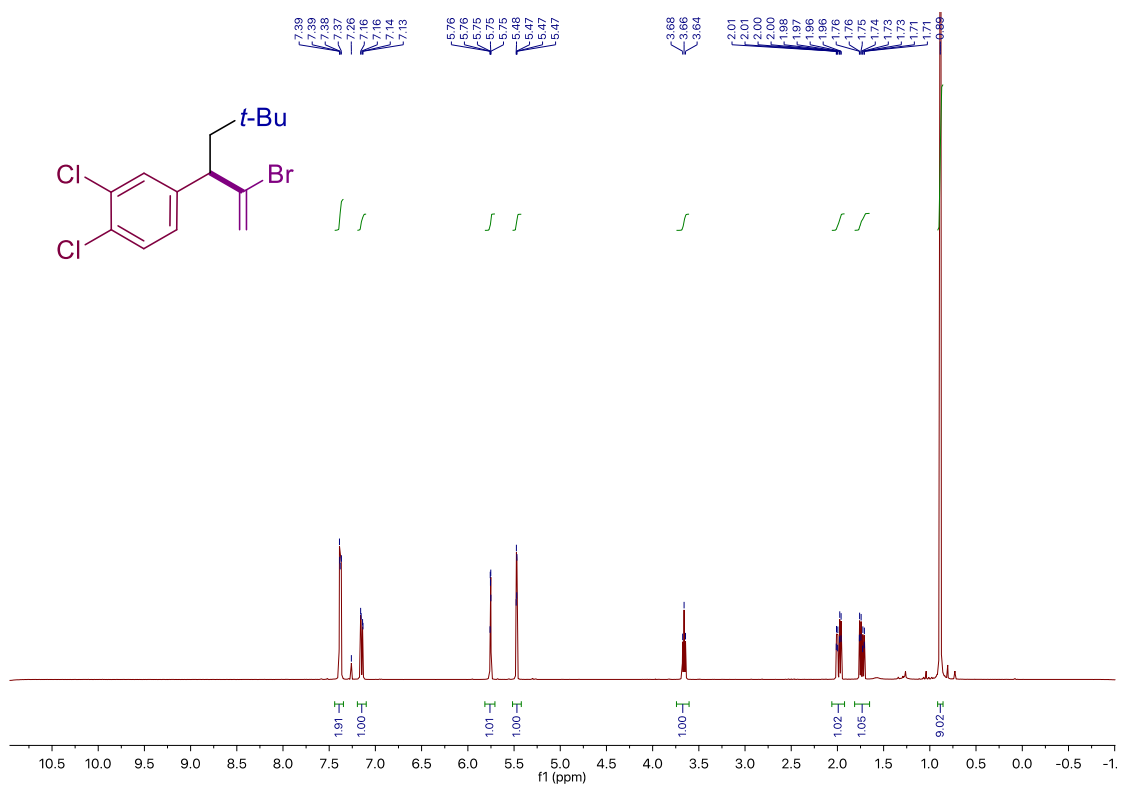
Site-Selective 1,2-Dicarbonylation of Vinyl Boronates through Dual Catalysis



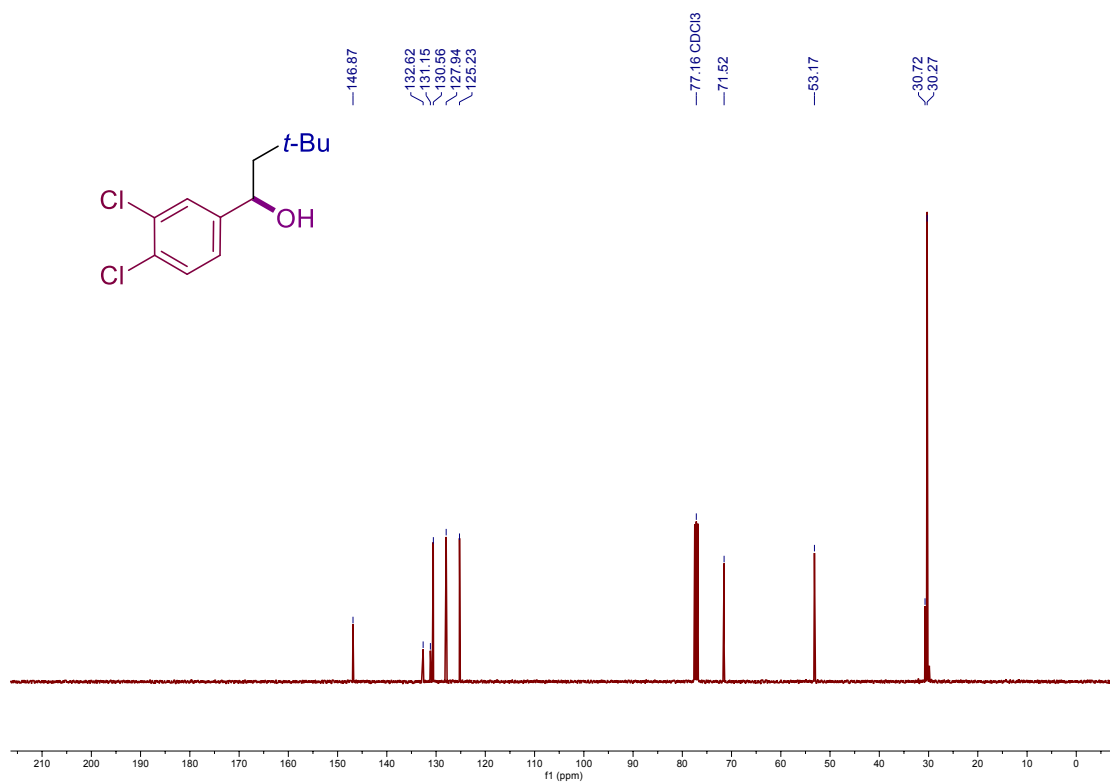
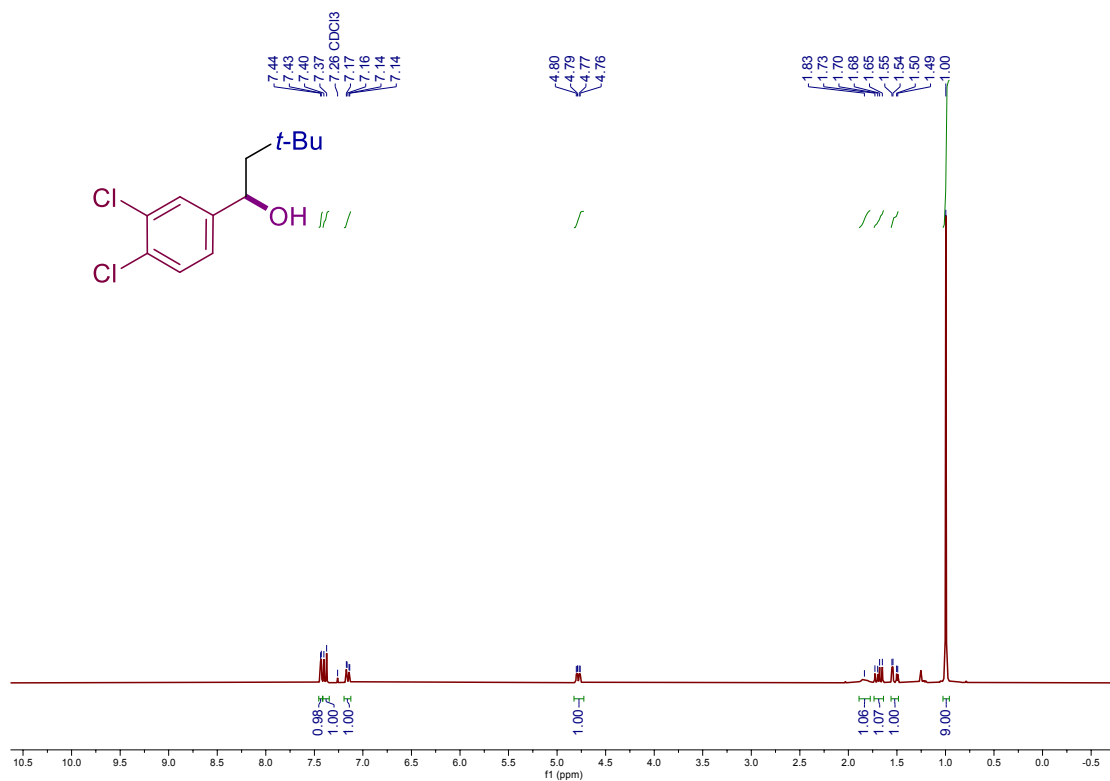


Site-Selective 1,2-Dicarbofunctionalization of Vinyl Boronates through Dual Catalysis

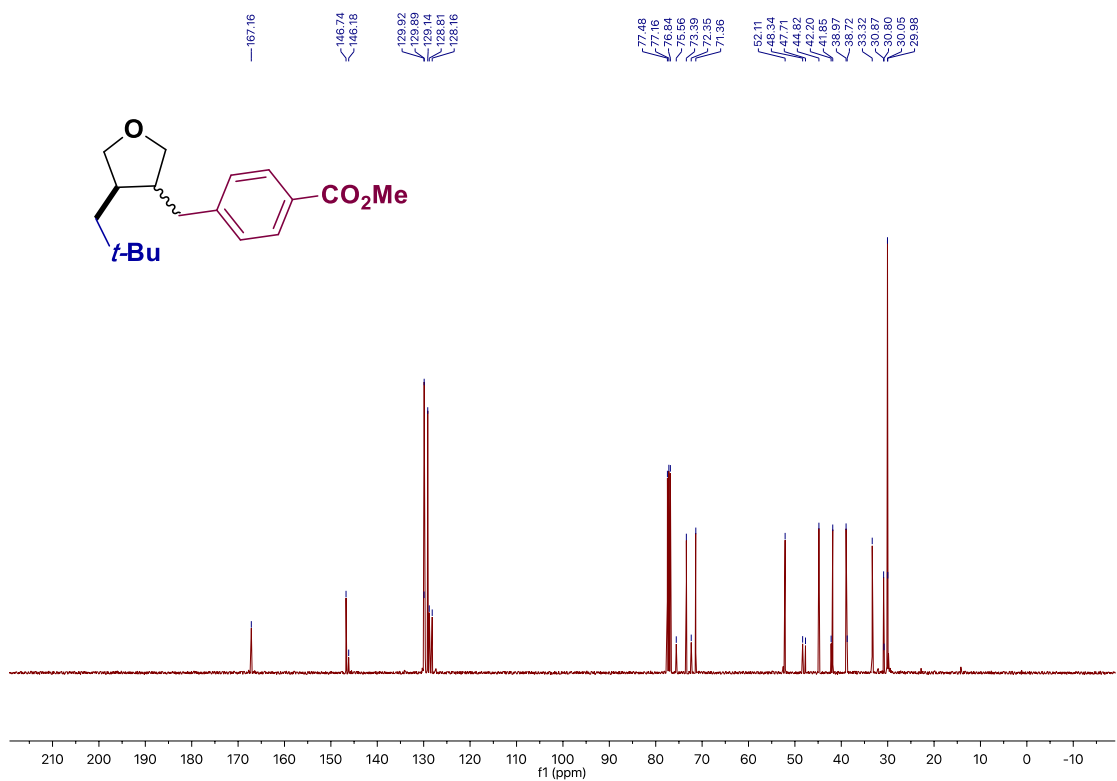
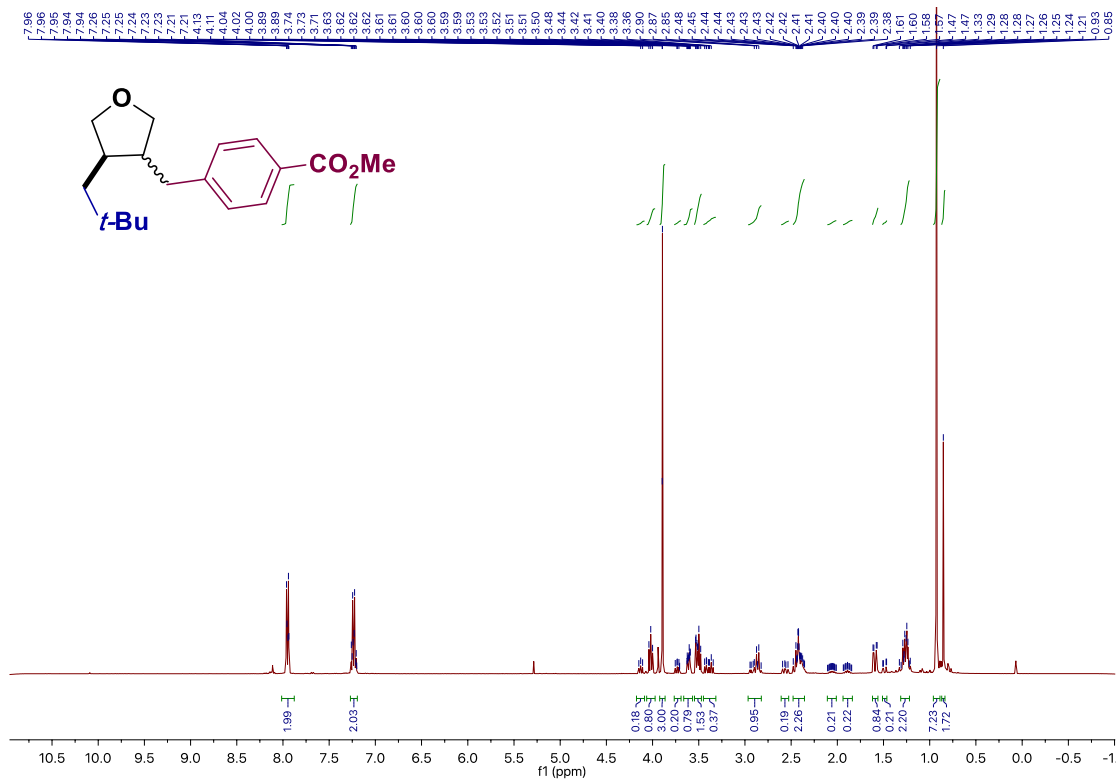




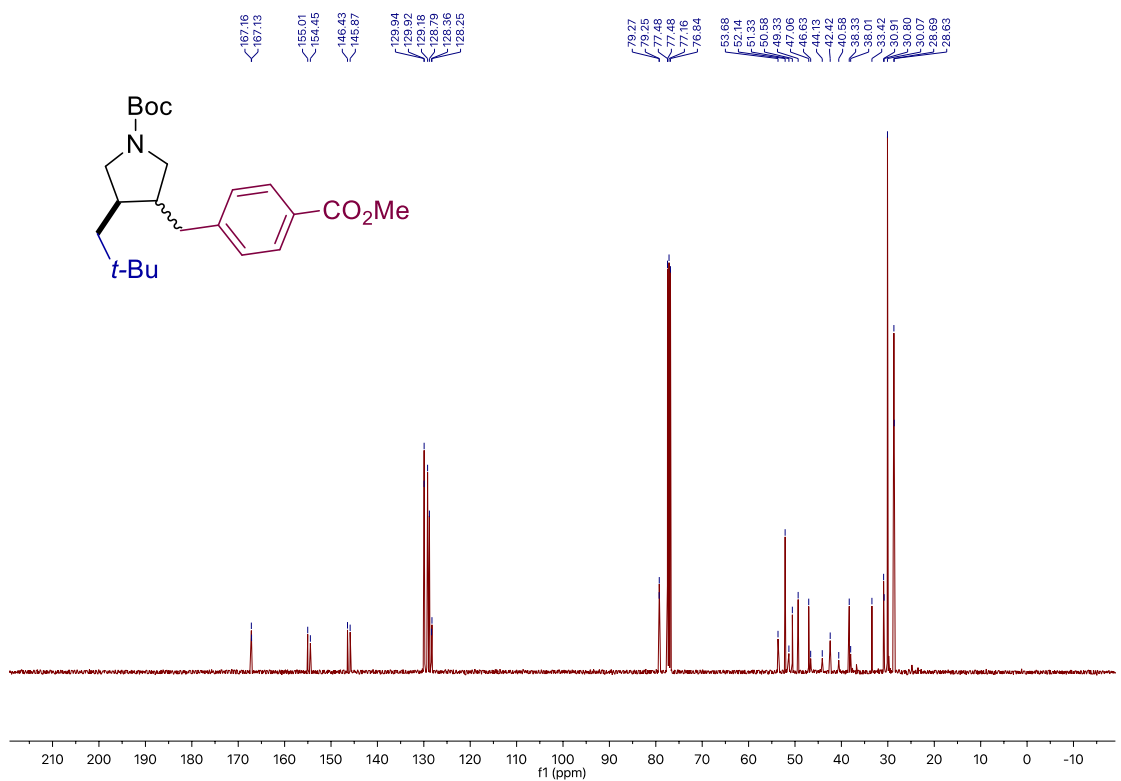
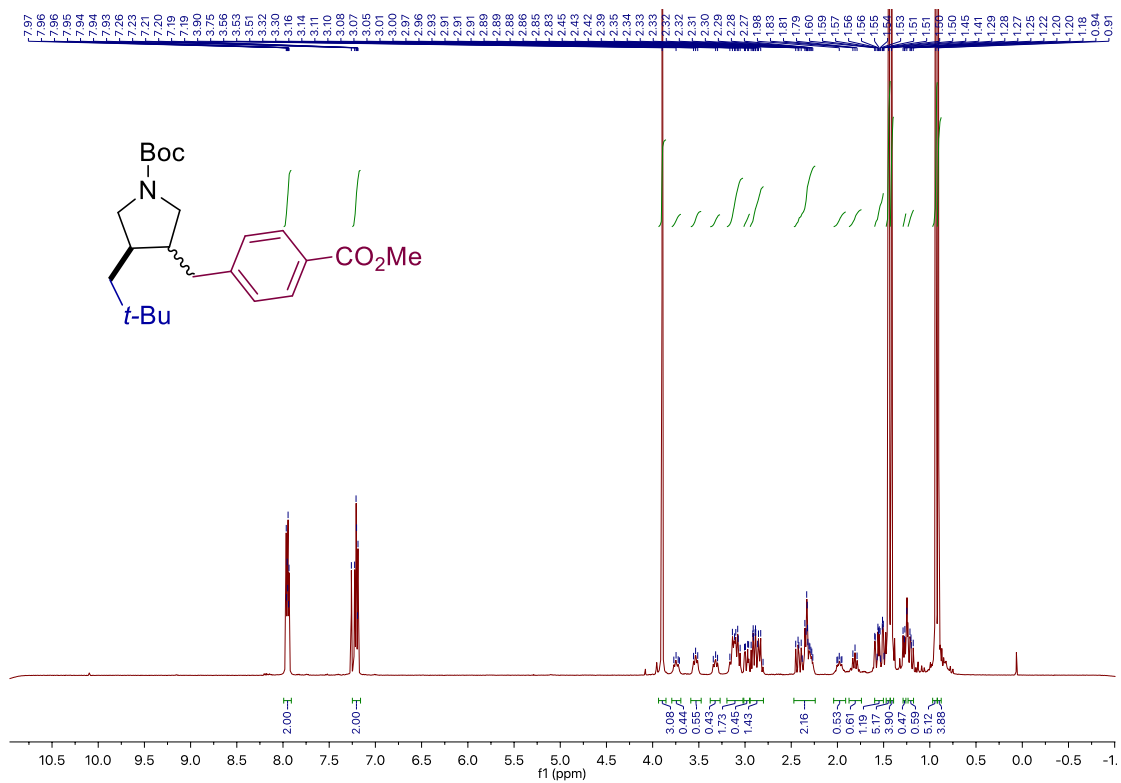
Site-Selective 1,2-Dicarbofunctionalization of Vinyl Boronates through Dual Catalysis



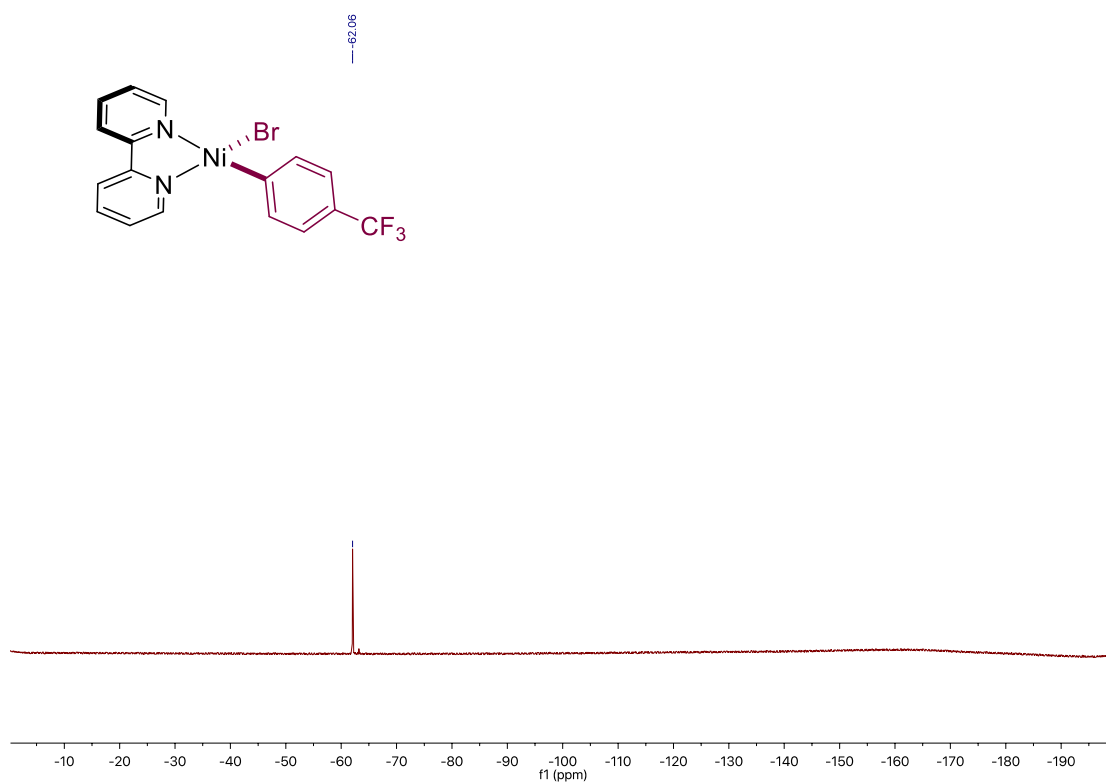
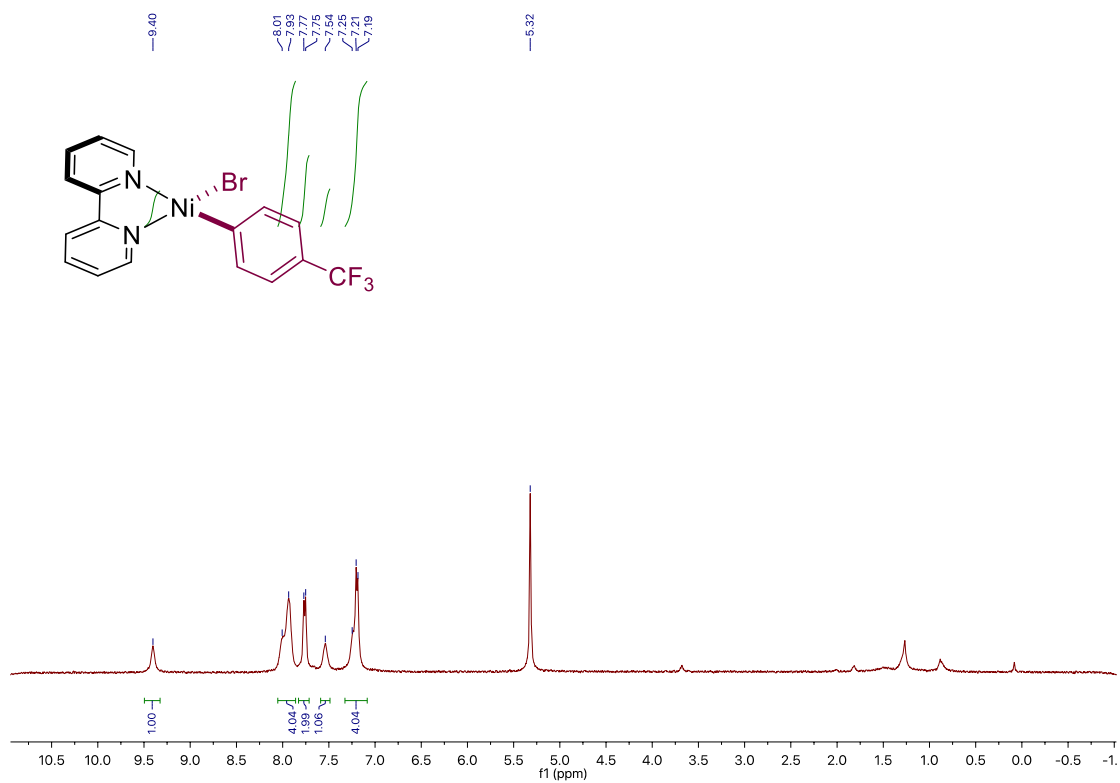
Chapter 4.



Site-Selective 1,2-Dicarbofunctionalization of Vinyl Boronates through Dual Catalysis



Chapter 4.



Chapter 5

Conclusion

The synthetic methods developed during this Doctoral Thesis give access to sp^3 carbon linkages via Ni-catalyzed reductive coupling reactions. It would be useful to highlight what we have achieved in our initial aims.

Chapter 2:

- A site-selective Ni-catalyzed reductive alkylation of unactivated olefins with α -haloboronate have been developed.
- The utilization of internal, unactivated olefins results in a C–C bond-formation at remote unfunctionalized sp^3 C–H sites via Ni-catalyzed chain-walking strategy.
- This mild protocol allowed for incorporating the alkylboron fragment into olefin feedstocks, thus providing a complementary and conceptually different approach to existing borylation techniques.
- The protocol can be applied in an iterative fashion to build up molecular complexity by using simple starting materials.
- Preliminary mechanistic studies ruled out a pathway consisting of an addition of an *in-situ* generated α -boryl radical to the olefin, suggesting that a hydrometallation via nickel hydrides precedes C–C bond-formation with the corresponding α -haloborane.

Chapter 3:

- A site-selective Ni-catalyzed deaminative alkylation of unactivated olefins with alkylamine derived pyridinium salts have been developed.
- The method features as its mild conditions, wide scope and exquisite site-selectivity pattern for both α -olefins and internal olefins, even in the context of ethylene valorization or late-stage functionalization.

Chapter 5.

- This new platform offers new opportunities in both olefin functionalization and deamination events and a complementary activation mode to existing sp^3 - sp^3 bond-forming reactions.

Chapter 4:

- A modular, site-selective 1,2-dicarbofunctionalization via a Ni/Photoredox dual catalyzed reductive coupling of three electrophiles have been described.
- The method presented a complementary new technique for preparing densely functionalized alkyl boron architectures from simple precursors and is characterized by its mild conditions and excellent chemo- and regio-selectivity.
- The applicability of the transformation is demonstrated with further functionalization via C–B bond cleavage.
- Detailed mechanistic studies suggest the initially formation of intermediacy open-shell species and the recombination with an oxidative addition species.



UNIVERSITAT
ROVIRA i VIRGILI